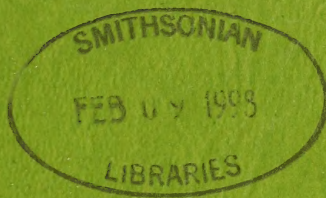


96
1
B716
NH

MORPHOLOGY, PHYLOGENY, BIOGEOGRAPHY
AND SYSTEMATICS OF *PHOXINUS*
(PISCES: CYPRINIDAE)

by

✓ XING-YU CHEN



BONNER ZOOLOGISCHE MONOGRAPHIEN, Nr. 39
1996

Herausgeber:
ZOOLOGISCHES FORSCHUNGSMUSEUM
UND MUSEUM ALEXANDER KOENIG
BONN

BONNER ZOOLOGISCHE MONOGRAPHIEN

Die Serie wird vom Zoologischen Forschungsinstitut und Museum Alexander Koenig herausgegeben und bringt Originalarbeiten, die für eine Unterbringung in den „Bonner zoologischen Beiträgen“ zu lang sind und eine Veröffentlichung als Monographie rechtfertigen.

Anfragen bezüglich der Vorlage von Manuskripten sind an die Schriftleitung zu richten; Bestellungen und Tauschangebote bitte an die Bibliothek des Instituts.

This series of monographs, published by the Zoological Research Institute and Museum Alexander Koenig, has been established for original contributions too long for inclusion in „Bonner zoologische Beiträge“.

Correspondence concerning manuscripts for publication should be addressed to the editor. Purchase orders and requests for exchange please address to the library of the institute.

L'Institut de Recherches Zoologiques et Muséum Alexander Koenig a établi cette série de monographies pour pouvoir publier des travaux zoologiques trop longs pour être inclus dans les „Bonner zoologische Beiträge“.

Toute correspondance concernant des manuscrits pour cette série doit être adressée à l'éditeur. Commandes et demandes pour échanges adresser à la bibliothèque de l'institut, s. v. p.

BONNER ZOOLOGISCHE MONOGRAPHIEN, Nr. 39, 1996

Preis: 57,— DM

Schriftleitung/Editor: G. Rheinwald

Zoologisches Forschungsinstitut und Museum Alexander Koenig

Adenauerallee 150—164, D-53113 Bonn, Germany

Druck: JF.CARTHAUS, Bonn

ISBN 3-925382-42-9

ISSN 0302-671 X

MORPHOLOGY, PHYLOGENY, BIOGEOGRAPHY
AND SYSTEMATICS OF *PHOXINUS*
(PISCES: CYPRINIDAE)

by

XING-YU CHEN

BONNER ZOOLOGISCHE MONOGRAPHIEN, Nr. 39
1996

Herausgeber:
ZOOLOGISCHES FORSCHUNGSMUSEUM
UND MUSEUM ALEXANDER KOENIG
BONN

Chen, Xing-Yu:

Morphology, phylogeny, biogeography and systematics of *Phoxinus* (Pisces: Cyprinidae) / Xing-Yu Chen. Hrsg.: Zoologisches Forschungsinstitut und Museum Alexander Koenig, Bonn. — Bonn: Zoologisches Forschungsinst. und Museum Alexander Koenig, 1996

(Bonner zoologische Monographien ; Nr. 39)

ISBN 3-925382-42-9

NE: GT

*To my mother, father, and Jing,
for their love and encouragement.*

CONTENTS

	Page
Introduction	5
Acknowledgments	5
Methods	6
Material examined	8
Historical review of <i>Phoxinus</i>	12
Phylogenetic relationships of <i>Phoxinus</i> and the related genera	22
Monophyly of the Hemitreman clade and its position in the family Cyprinidae	22
Analysis of transformation series in the Hemitreman clade	26
Phylogenetic relationships of the Hemitreman clade	39
Discussion	43
Non-osteological morphology	44
External morphology	44
Intestine and gas bladder	61
Osteology	67
Neurocranium	67
Viscerocranium	95
Vertebral column	121
Pectoral girdle and fin	131
Phylogenetic relationships of the species of <i>Phoxinus</i>	141
Phylogenetic relationships	141
Discussion on the phylogenetic relationships of the species of <i>Phoxinus</i>	144
Biogeography of <i>Phoxinus</i>	145
Taxonomy of <i>Phoxinus</i>	150
Key to the species of <i>Phoxinus</i>	153
Species accounts	154
<i>Phoxinus phoxinus</i> (Linnaeus)	154
<i>Phoxinus brachyurus</i> Berg	161
<i>Phoxinus issykkulensis</i> Berg	163
<i>Phoxinus neogaeus</i> Cope	166
<i>Phoxinus cumberlandensis</i> Starnes & Starnes	171
<i>Phoxinus tennesseensis</i> Starnes & Starnes	175
<i>Phoxinus oreas</i> (Cope)	179
<i>Phoxinus eos</i> (Cope)	183
<i>Phoxinus erythrogaster</i> (Rafinesque)	188
Abstract	194
Literature Cited	196
Appendices	215
I. Data matrix I (for Hemitremanians)	215
II. Data matrix II (for <i>Phoxinus</i>)	216
III. Transformation series used in the analysis of phylogenetic relationships within <i>Phoxinus</i>	217
IV. List of abbreviations	225

INTRODUCTION

Cyprinidae, the largest freshwater fish family, is divided into two subfamilies (Cavender & Coburn 1992) with 210 genera and 2,010 species (Nelson 1994). *Phoxinus*, belonging to the subfamily Leuciscinae (Chen 1987b, Howes 1991, Cavender & Coburn 1992, Coburn & Cavender 1992), is a small sized genus (less than 100 mm in maximum standard length in most species) with nine species, and is the only minnow genus occurring in both North America and Eurasia. Some species of the genus are widely distributed, others are restricted to small drainage areas. For instance, *P. phoxinus* is widespread in Europe and Asia (Berg 1949, Banarescu 1964), whereas *P. tenesseensis* is found only from the upper Tennessee River drainage of Tennessee and Virginia of USA (Starnes & Jenkins 1988). Since the type species of *Phoxinus*, *phoxinus*, was described by Linnaeus in 1758 (as *Cyprinus phoxinus*), hundreds of papers and books related to the genus have been published. Most of the literature is records of geographical distribution, or brief descriptions of the species of the genus. Only a few of these deal with anatomy and phylogenetic relationships of the species in the genus (e.g., Gasowska 1979, Joswiak 1980, Howes 1985). During the last two centuries, the definition of the genus has been an open question, and its content has changed. For instance, *P. neogaeus* has been placed in four different genera (*Phoxinus*, *Pfille*, *Chrosomus*, and *Leuciscus*) since it was described by Cope (1869) (in Günther 1868). A similar situation is also present in other *Phoxinus* species. The unstable taxonomic status of the *Phoxinus* species resulted from lack of a clear definition of the genus, and lack of comprehensive comparisons among *Phoxinus* species and between *Phoxinus* and other related genera. Joswiak (1980) correctly pointed out that this genus "is a focus of controversy involving the relation between Palearctic and Nearctic cyprinids". The situation has not been improved very much since then.

The present study was designed to review the genus *Phoxinus*, and to provide a hypothesis of its relationships with other genera and among its species. This monograph includes seven sections. A historical review of *Phoxinus* is presented first, followed by a phylogenetic analysis among *Phoxinus* and other genera; then I report the results from the comparative morphological study among the species of the genus. Based on the data from these studies, I analyze the phylogenetic relationships among the species of *Phoxinus* and discuss the biogeography of the genus. Then a classification of the genus is followed by an account of the nine recognized species of the genus.

ACKNOWLEDGMENTS

The following individuals and institutions are acknowledged for their loans or donations of specimens to this project: P. Banarescu (Institute of Biology, Bucharest, Romania), M.-L. Bauchot (Muséum National d'Histoire Naturelle, Paris), N.G. Bogutskaya (Zoological Institute, Academy of Sciences, St.Petersburg, Russia), K. Busse (Zoologisches Forschungsinstitut und Museum A. Koenig, Bonn), B.W. Coad (National Museum of Natural Sciences, Ottawa), F.B. Cross, E.O. Wiley and J.T. Collins (University of Kansas, Lawrence, Kansas), W.N. Eschmeyer and D. Catania (California Academy of Sciences,

San Francisco), D.A. Etnier (University of Tennessee, Knoxville), K.E. Hartel (Museum of Comparative Zoology, Harvard University, Cambridge/USA), G. Howes (British Museum, Natural History, London), S.L. Jewett (Smithsonian Institution, Washington D.C.), E.-J. Kang (Chonbuk National University, Chonbuk, Korea), S. Kimura (Mie University, Japan), J.G. Lundberg (Duke University, Durham, North Carolina), G. Nelson (American Museum of Natural History, New York), T.K. Paaver (Institute of Zoology and Botany, Academia of Sciences, Tartu, Estonia), S. Schaefer (Academy of Natural Sciences, Philadelphia), B. Schatti (Muséum d'Histoire Naturelle, Geneva), K.D. Vasil'eva (Zoological Museum, Moscow Lomonosov State University), H. Wilkens (Zoologisches Institut und zoologisches Museum, Universität Hamburg), Y.-H. Xie (Institute of Freshwater Fishery of Liaoning Province, China).

The Division of Biology and the Museum of Natural History at the University of Kansas are acknowledged for their years of support during the course of this project and my graduate study at the University of Kansas.

I am grateful to Prof. S.-Z. Li (Institute of Zoology, Academia Sinica, Beijing) and Dr. H.-P. Schultze (Paläontologisch-geologisches Institut und Museum, Naturkundemuseum der Humboldt Universität, Berlin) for their helps and suggestions during this project. I am greatly indebted to Drs. G. Arratia (Paläontologisch-geologisches Institut und Museum, Naturkundemuseum der Humboldt Universität, Berlin), E.O. Wiley, F.B. Cross, J.S. Ashe, and L.C. Ferrington, Jr. (University of Kansas), M. Coburn (John Carroll University, Ohio) for their critical review and many suggestions on the draft of the manuscript, and to Drs. G. Arratia and C. R. Robbins (University of Kansas) who reviewed the final version of the manuscript.

I thank many ichthyologists for their help to access the literature. I especially thank E.B. Böhlke (Academy of Natural Science of Philadelphia) for the communication on the date of the original description of *Phoxinus neogaeus*. J. Chorn and K. Shaw (University of Kansas) are acknowledged for preparing the X-ray photographs of *Phoxinus brachyurus*. This project was partially supported by the following scholarship and agencies at the University of Kansas: the International Student Scholarship, the Department of Systematics and Ecology, the Divisions of Ichthyology and Paleontology, the Panorama Society of the Museum of Natural History, and the laboratories of Drs. E.K. Michaelis and M.L. Michaelis.

METHODS

Data Collecting

1. Measurements

Measurements were taken with Dial Calipers reading to 0.1 mm, on the left side of the specimens. Methods for measurements follow Hubbs & Lagler (1947, 1964), except the following which were not defined by those authors:

Prepelvic length is the distance from end of the snout to the base of the left pelvic fin.

Intestine length is the straight length of the intestine. Because the intestine in *Phoxinus* is coiled, it was removed from the body cavity, uncoiled, and then measured.

Length of anterior chamber of gas bladder is the distance between the most anterior point to the most posterior point of the anterior chamber.

Length of posterior chamber of gas bladder is the distance between the most anterior point to the most posterior point of the posterior chamber.

Mouth angle is the angle between the dorsal surface of the head and a plane along the dorsal margin of the lower jaw.

2. Counts

All counts (e.g., branchiostegal rays, fin-rays) were conducted with a Wild Microscope or a Zeiss Microscope. The methods for different counts are described as follows:

Number of rays of paired fins were counted following Hubbs & Lagler (1947, 1964).

Number of rays of the dorsal and anal fins consists of procurent rays (rudimentary unbranched and unsegmented rays) and principal rays of Hubbs & Lagler (1947, 1964).

Hereafter the principal rays are referred to "rays". All procurent rays and rays are counted. Caudal fin-rays were counted as dorsal and ventral procurent, and dorsal and ventral principal rays.

All lateral line scales were counted. Cephalic lateral line pores were divided into six sections following Reno (1969), except the preoperculomandibular canal which is divided into two sections (mandibular and preopercular sections) in the species of *Phoxinus* (see below). All pores in each section were counted.

Following Chen (1988b) and Chen & Arratia (1994), all primary lamellae were counted as the total number of the primary lamella for each olfactory organ. No secondary lamellae are present on the primary lamellae in *Phoxinus*.

Number of gill rakers on the first gill arch were counted and considered as the number of gill rakers of the specimen.

Number of vertebrae includes all vertebrae (from vertebra 1 to preural vertebra 1, ural centra not included), and are divided into precaudal and caudal ones, according to Mayden (1989). The four vertebrae associated with the Weberian apparatus were counted as four and included in the number of precaudal vertebrae. The count of vertebrae was made on cleared and double stained specimens and some radiographs.

3. Non-osteological and osteological morphology

Non-osteological morphology was studied from 75% alcohol preserved specimens with the microscopes mentioned above. Tubercles and scales were studied also with Scanning Electron Microscope (SEM).

Osteological features were studied on cleared and double stained specimens prepared following Dingerkus & Uhler (1977), and from radiographs of some specimens.

All measurements, counts, and non-osteological data were obtained from more than five specimens for most species studied. In most cases, more than 15 specimens for each species were studied. Whenever possible, more than three specimens of each species were studied in order to collect the osteological data. In most *Phoxinus* species, a series of different sex and size was studied.

The illustrations were prepared using microscopes with camera lucida attachment. The photographs were taken with either camera or SEM.

Terminology

Terms for different parts of the fish body follow Cross (1967), except for a few cases mentioned in the text (e.g., breast scales). Terms for different structures of the olfactory organ follow Chen (1988b) and Chen & Arratia (1994). Terms for different structures of the gas bladder follow Bond (1979).

Phylogenetic analyses

The phylogenetic analyses follow the cladistic methodology (Hennig 1966, Wiley 1981). Polarities of the transformation series were determined by outgroups comparison following Maddison et al. (1984). Ontogenetic data were also used to determine the polarities of a few transformation series though some disadvantages might be present in the ontogenetic criterion in the polarity determinations (Mayden & Wiley 1992).

Because no well-supported hypotheses about the sistergroup of *Phoxinus* are available, the relationship among *Phoxinus* and other closely related minnow genera (grouped as Hemitremians herein) are reevaluated using the Exoglossin Clade of Coburn & Cavender (1992) as the outgroups.

According to the result from the analysis of the relationships among *Phoxinus* and other genera (see below), *Lagowskiella*, *Rhynchocypris*, and *Eupallasella* were treated as the outgroups for the polarity determination of the transformation series in the phylogenetic analysis among the species of *Phoxinus*. 210 transformation series including non-osteological and osteological characters were analyzed.

The character states (TS) are identified as 0, 1, 2, 3, or 4, among which 0 represents the plesiomorphic state, whereas 1, 2, 3, and 4 correspond to the apomorphic ones. These numbers are present in square brackets following the transformation series number (e.g., TS 100 [0], TS 100 [1]).

PAUP (version 3.0s) (Phylogenetic Analysis Using Parsimony) program (Swofford 1991) was used to generate the phylogenetic hypotheses presented herein for both the Hemitremian Clade and the species of *Phoxinus*.

Abbreviations

A list of abbreviations used in the figures and text is given in appendix IV at the end of the book.

MATERIAL EXAMINED

Forty-seven species of Cyprinidae were studied. The species are grouped as non-*Phoxinus* species and *Phoxinus* species. The non-*Phoxinus* species are mainly used to evaluate the relationships of *Phoxinus* with other genera, and to compare with the species of *Phoxinus*.

The specimens of non-*Phoxinus* species studied are listed below, whereas the specimens of *Phoxinus* are listed in "Species Accounts". The following information and arrangements are provided for specimens of each species of both non-*Phoxinus* and *Phoxinus*: institution acronym and catalogue number, number of alcohol preserved specimens (**alch.**), number of cleared and stained specimens (**C&S**) (if any), the locality collected, the name(s) of collector(s), and the date of collection.

The abbreviations for the institutions follow Leviton et al. (1985), except the following which are not available in the literature:

- CNUC** Chonbuk National University, Chonju, Korea
IFFL Institute of Freshwater Fishery of Liaoning Province, Dalian, China
NAIJ National Aquacultural Institute, Japan
P Zoological Museum, the Moscow Lomonsov State University, Russia.

Camptostoma anomalum (Rafinesque): KU 3946, 3 C&S, Spring Creek at Big Springs Ranch, Sec 20-21, T32S, R28W, Meade County, Kansas, USA; Cross & Nelson; 13 June 1958. – KU 8889, 6 alch.; Catawba River, McDowell County, North Carolina, USA; F.B. Cross et al.; 5 September 1964. – KU 14127, 1 C&S; Long Creek, 1 mi. NW Holland, Allen County, Kentucky, USA; M.E. Braasch et al.; 1 April 1967. – KU 20365, 5 alch.; Blocker Creek, Rt. 84 bridge at Langley, Pike County, Arkansas, USA; R.L. Mayden et al.; 9 April 1982. – KU 20371, 1 alch., Ouachita River, 6 mi. NE Mena on U.S. Rt 71, Polk County, Arkansas, USA; R.L. Mayden et al.; 9 April 1982.

Camptostoma ornatum Girard: KU 3251, 15 alch.; Cajon Bonita, 6 mi S U.S. border at Arizona-New Mexico State Line, Sonora, Mexico; S.P. Gordon; March 1954.

Carassius auratus (Linnaeus): KU 8673, 2 alch.; Shellrock River, Worth County, Iowa, USA; E. Beetner et al; 9 August 1964.

Clinostomus elongatus (Kirtland): KU 2751, 5 alch.; Big Creek, 2 mi. north of Chardon, Geauga County, Ohio, USA; J.S. Findley; 11 July 1943. – KU 3881, 2 alch.; Cuyahoga County, Ohio, USA; J. Findley & W.B. Quay; 19 September 1944. – KU 11322, 2 alch. and 2 C&S; Monroe Twp., Machochee Creek, Logan County, Ohio, USA; W.L. Pflieger et al.; 26 April 1958. – KU 21401, 15 alch.; Indian Creek, JCT Ohio Rt 84 and Depot Road, Ashtabula County, Ohio, USA; T. Rosseger & M. Coburn; 5 March 1986.

Clinostomus funduloides Girard: KU 3262, 38 alch. and 2 C&S; N. Fork Roanoke River at Route 11 bridge, Montgomery County, Roanoke County line, Virginia, USA; B. Stough, T. Riggins & W.S. Davis; 17 May 1952. – KU 10697, 4 C&S; Carner's Creek, 9 mi. SW Dickson on Tennessee Rt 48, Tennessee, USA; M.E. Braasch; 20 November 1965. – KU 11424, 45 alch.; Stream near Neuse at Camp Durant, Wake County, North Carolina, USA; W.A. Reid; 17 June 1964. – KU 12065, 5 alch.; Blue Spring Creek, 1 mi. W. Hillsboro, on gravel road S. of US 41, Coffee County, Tennessee, USA; M.E. Braasch; 13 August 1966. – KU 20915, 7 alch.; Whites Creek, 4 mi. North Bath Springs, DeCATUR County, Tennessee, USA; M.E. Braasch; 4 April 1978. – KU 22253, 33 alch.; Craig Creek at Va. Rt 621, Montgomery County, Virginia, USA; B.K. Wagner et al.; 9 September 1987. – KU 22268, 9 alch.; Craig Creek at VA Rt 621 bridge, Montgomery County, Virginia, USA; B.K. Wagner et al.; 9 September 1987. – KU 22317, 3 alch.; Ararat River at Rt 739 bridge near North Carolina border, Virginia, USA; B.K. Wagner et al.; 13 September 1987.

Couesius plumbeus (Agassiz): KU 18872, 15 alch.; Pine River, Nigger Creek, Michigan, USA; collector unknown; 1 August 1951. – KU 18881, 8 C&S; Poplar River, 9 mi. S Rockglen, Saskatchewan, Canada; G. Gruchy & T.A. Willock; 7 July 1970. – KU 18965, 15 alch.; Box Elder Creek, South Canyon, Pennington County, South Dakota, USA; Dilger, Robins & Hilton; 30 June 1989.

Ctenopharyngodon idella (Cuvier & Valenciennes): KU 21097, 2 alch.; Butler County, Kansas, USA; bait dealer for K. Brunson; 1984.

Cyprinella callisema (Jordan): KU 8842, 11 C&S; Ogeechee River below mill dam at Mayfield, Hancock-Warren County, Georgia, USA; F.B. Cross et al.; 30 August 1964.

Cyprinella nivea (Cope): KU 18987, 6 C&S; Savannah drainage, SFK Broad River, 1.6 mi. S. Rt 72 in Carlton, Maclison County, Georgia, USA; Denoncourt & Wallace; 15 August 1967.

Cyprinella whipplei Girard: KU 14211, 12 C&S; Elk Creek, SW Tahlequah on Oklahoma Rt 82, Cherokee County, Oklahoma, USA; Cross, Collins & Cavin; 22 April 1970.

Cyprinus carpio Linnaeus: KU 1626, 1 dry skeleton, Douglas County, Kansas, USA. – KU 3739, 1 C&S, Churchill Co., NV, USA. – KU 12440, 1 C&S, Elko Co., NV, USA. – KU 22583, 43 alch.; Walnut Creek at diversion dam, Barton County, Kansas, USA; F.B. Cross et al.; 5 June 1986.

Dionda episcopa Girard: KU 7427, 5 C&S; La Augustura Canal, Coahuila, Mexico; W. Minckley; 18 April 1963. – KU 16891, 5 C&S; Pecos River, 4 mi. S. Pandale, Val Verde County, Texas, USA; B. Stewart et al.; 1 November 1975.

Eupallasea percnurus Pallas: AMNH 10926, 5 alch.; Mai-taichao, Shanxi Province, China; Third Asiatic Expedition, C.H. Pope; late April to July 1922. – MCZ 32369, 3 alch.; Vladivostok, Sedanka River, USSR, Asia; Vlad. Fish. Res. Sta.; date unknown. – NMC 77-0889, 4 alch.; Lake in the infra current of the Tugur River (Basin of Okhotsk Sea), USSR; A.R. Kuznetsov; 25 March 1936. – NMC 73-196, 10 alch.; Pond in Rynarzewo near Bydgoszcz, Poland; J.M. Rembiszewski; date unknown. – USNM 105156, 1 alch.; Middle Amur near Kasatkino, Siberia, Russia; collector unknown; 13 August 1935. – ZIL uncat., 4 alch. and 1 C&S; Lake Khangal, upper Onco, Amur basin, Mongolia; collector and date unknown. – ZIL uncat., 2 alch.; Kolyma River, Russia; collector and date unknown.

Exoglossum laurae (Hubbs): KU 18923, 5 C&S; Little River at National Forest Rt 44 bridge, Pocahontas County, West Virginia, USA; S.A. Pistolis; 11 June 1977.

Exoglossum maxillingua (Lesueur): KU 18924, 10 alch.; Danning Creek at mouth along County Rt. 5042, Bedford County, Pennsylvania, USA; C.H. Hocutt et al.; 19 August 1978.

Gila atraria (Girard): KU 11922, 1 C&S; Park Canyon Creek, 0.3 mi below Lake Enterprise Dam, Washington County, Utah, USA; G. R. Smith; 11 June 1966.

Gila copei (Jordan & Gilbert): KU 11819, 1 C&S; Mammoth Creek above confluence with Sevier River, Garfield County, Utah, USA; Smith & Koehn; 16 April 1966. – KU 11830, 22 alch.; Tributary to Yellow Creek above confluence, T2N, R9E, S4, Summit County, Utah, USA; G.R. Smith & B. Deardon; 24 April 1966.

Hemitremia flammea (Jordan & Gilbert): KU 12066, 1 C&S; Blue spring Creek, 1 mi. W. Hillsboro on gravel road S of US 41, Coffing County, Tennessee, USA; M.E. Braasch; 13 August 1966. – KU 18884, 20 alch.; Dry Branch tributary to Little Cypress Creek, Sec. 4, T15, R11W, Lauderdale County, Alabama, USA; B.R. Wall et al.; 22 March 1969. – KU 18931, 6 alch. and 14 C&S; Crumpton Creek, South of Manchester, Coffee County, Tennessee, USA; Tennessee Valley Authority; 3 October 1972. – KU 20936, 24 alch.; Carrol Creek, 1.5 mi. N. Tullahoma, Coffee County, Tennessee, USA; M.E. Braasch & D. Greaney; 21 April 1988.

Hybognathus hankinsoni Hubbs: KU 2014, 2 C&S; Manganese Lake, Keweenaw County, Michigan, USA; J.M. Lowe; 31 July 1926.

Hybognathus hayi Jordan: KU 9613, 4 C&S; ditch 4 mi. NW Qulin, Sec. 11, T23N, R7E, Butler County, Missouri, USA; W.L. Pflieger et al.; 17 July 1964.

Hybognathus placitus Girard: KU 2020, 24 alch.; North Canadian River, 4 mi. S of Gate, S. 29T4NR28E, Beaver County, Okla, USA; A.B. Leonard; 4 September 1921. – KU 9628, 33 alch.;

Missouri River at Gasconade, T46N, R6W, S5, Gasconade County, Missouri, USA; W.L. Pflieger & party; 26 June 1963. – KU 12597, 3 C&S; Republican River, at Kansas route 148 bridge, 1 mi. W. Norway, Republic County, Kansas, USA; M.E. Braasch; 26 November 1966.

Lagowskiella czekanowskii Dybowski – NMC 77-0884, 5 alch.; small river, Wilyuy district, Eastern Siberia, Knig-Uryah, USSR; Merculov; 20 February 1912.

Lagowskiella lagowskii Dybowski: ANSP 64214, 1 alch.; China; Third Asiatic Expedition; Hsing Lung Shan & E. Tombs; 7 August 1921. – NAIJ 14402-14403, 2 alch. and 2 C&S; Kansong-up, Kosong-gun, Kangwon-do, Pref.; collector unknown; 1 January 1989. – MCZ 3007, 2 alch.; Lake Baikal, Siberia, Russia; J.D.E. Schmeltz, Jr.; 1873. – MCZ 32370, 7 alch.; Chilka River, USSR, Asia; Vlad. Fish. Res. Sta.; 29 April 1929. – USNM 82296-82301, 6 alch.; Hsin Lung Shan District Imperial Hunting Grounds, Northern China, China; A. Sowerby; August 1917. – USNM 179862; 3 alch.; Amur River, Russia; collector and date unknown. – ZIL 15612, 2 alch.; Lake Beloje (Amur River system); collector and date unknown.

Leuciscus leuciscus (Dybowski): KU 10227, 1 C&S; Siberia, Irkutsk; J.F. Aboot; date unknown.

Machyropsis aestivalis (Girard): KU 12103, 5 C&S; Kansas River at Dam in Lawrence, Douglas County, Kansas, USA; G.R. Smith & M.E. Braasch; 9 September 1966.

Margariscus margarita (Cope): KU 1139, 5 alch.; Pond in Wilderness Park, Emmet County, Michigan, USA; U.B.S. Ichthyology class; 24 July 1946. – KU 2393, 1 alch.; Big Stone Bay, Michigan, USA; C. Creaser; 26 August 1938. – KU 3556, 1 alch.; Trant River below Trant Lake on HW 51, 9 mi. SW Boulder JCT, Vilas County, Wisconsin, USA; D. Lang; 1954. – KU 8696, 4 alch.; Isabella River at park area, Sec. 36, T60N, R9W, Lake County, Minnesota, USA; E.G. Beetner & C.E. Judd; 13 August 1964. – KU 8519, 11 alch.; Snake River, Cherry County, Nebraska, USA; R. Peckham; 21 August 1963. – KU 16971, 6 alch.; Kenora, Canada Experimental Lakes Area, Lake 226, Ontario, Canada; D. Kettle & D. Wright; 15 October 1976. – KU 19000, 5 alch. and 7 C&S; Oil Creek, 3/4 mi. S. Rawson, Allegheny County, New York, USA; M.A. Hall & E. C. Raney; 26 July 1937. – KU 21501, 4 alch.; Snake Creek, Sec. 36, T31N, R19E, Blain County, Montana, USA; D. Wannamaker; 16 September 1986.

Nocomis biguttatus (Kirtland): KU 12497, 2 C&S; North Fork White River, Sec. 7, T27N, R11W, Douglas County, Missouri, USA; G.R. Smith; 24 May 1967.

Nocomis leptcephalus (Girard): KU 12740, 1 C&S; Buttahatchie River, 12 mi. E. Hamilton, Marion County, Alabama, USA; collector unknown; 8 September 1964.

Nocomis micropogon (Cope): KU 12018, 7 alch.; Dadd's Creek; Catoosa Wildlife Management area, Cumberland County, Tennessee, USA; M.E. Braasch & A. Gnika; 12 August 1966.

Nocomis platyrhynchus Lachner & Jenkins: KU 18926, 9 C&S; above Wolf Creek on Green Briar river, Summer County, West Virginia, USA; C.H. Hocutt et al.; 29 August 1974.

Notropis buccatus (Cope): KU 18881, 5 alch.; Poplar River, 9 mi. S. Rockglen, Saskatchewan, Canada; C.G. Gruchy & T.A. Willock, USA; 7 July 1970. – KU 22331, 12 alch.; Taylor Branch at Kentucky Rt 478 bridge, McCreary County, Kentucky, USA; B.K. Wagner et al.; 5 March 1988.

Opsariichthys uncirostris Günther: KU 21448, 1 alch.; Hanjian River, China; collector and date unknown. – KU 21949, 1 alch. and 1 C&S; Lake Biwa, Japan; collector unknown; 1 March 1941.

Platygobio gracilis (Richardson): KU 11950, 1 C&S; Jemez River at Jemez, Sandoval County, New Mexico, USA; R.K. Koehn et al.; 27 July 1966. – KU 17257, 6 alch.; Moreau River between Whitehorse and Promise, Dewey County, South Dakota, USA; H.A. Martyn & D. Schooley; 11 October 1974.

Rhynchocypris oxycephalus Mori: CNUC uncat., 4 alch. and 2 C&S; Namgo-dong, Chonju-S, Chollabuk-do, Pref., Korea; collector unknown; 2 April 1988. – FRLM 10769, 1 alch.; Hozumi-cho, Gifu Pref., Japan; collector unknown; 14 April 1990. – FRLM 10776, 1 alch.; Hozumi-cho, Gifu Pref., Ja-

pan; collector unknown; 14 April 1990. – FRLM 10777, 1 alch.; Hozumi-cho, Gifu Pref., Japan; collector unknown; 14 April 1990. – FRLM 10890, 1 alch.; Nigori River, Mie Pref., Japan; collector unknown; 4 May 1990. – FRLM 10891, 1 alch.; Nigori River, Mie Pref., Japan; collector unknown; 4 May 1990. – FRLM 10895, 1 alch.; Nigori River, Mie Pref., Japan; collector unknown; 4 May 1990. – FRLM 10896, 1 alch.; Nigori River, Mie Pref., Japan; collector unknown; 4 May 1990. – FRLM 10898, 1 alch.; Nigori River, Mie Pref., Japan; collector unknown; 4 May 1990. – USNM 105116, 1 alch.; (Siberia) Sedanka River near Vladivostok, USSR; collector unknown; 24 September 1929.

Rutilus rutilus Linnaeus: KU 22430, 1 alch. and 2 C&S; Hessen, Germany; T. Martin, USA; August 1988.

Semotilus atromaculatus (Mitchill): KU 12482, 1 C&S; Hog Creek, Highway 63, Crossing South of Houston, Texas County, Missouri, USA; G.R. Smith; 24 May 1967. – KU 12594, 6 C&S; East Fork Clarks River, 1 mi E. Hardin, Marshall County, Kentucky; M.E. Braasch et al.; 4 April 1967. – KU 13197, 2 C&S; Deep Creek, at HW 70 Cross, Wabaunsee County, Kansas; Roy Irwin, USA; 7 June 1966.

Semotilus corporalis (Mitchill): KU 16915, 5 alch.; S Fork of S Branch of Potomac River, between Moorefield and Fisher, Hardy County, West Virginia, USA; N.H. Douglas et al.; 14 April 1971. – KU 18856, 20 alch.; South Fork of South Branch of Potomac River between Moorefield and Fisher, Hardy County, West Virginia, USA; N.H. Douglas et al.; 14 April 1971. – KU 21770, 12 alch.; Back Creek, Bath County, Virginia, USA; S.M. Smith et al.; 29 October 1986. – KU 21817, 23 alch.; Back Creek, Bath County, Virginia, USA; S.M. Smith et al.; 31 October 1986.

Zacco platypus (Schlegel): KU 12320, 2 alch. and 1 C&S; Siquokaken Inasagun Inasa-Machi Jingu-jigawa River below Misogi Bridge Miyakodagawa River, Japan; Hasegawa Vyeno; 8 July 1964. – KU 12321, 2 alch.; Kusu-gun Kokonoe-Machi Migita, Kusu River (Tributary of Chikugo River), Kyushu, Japan; Villagers; 22 August 1965.

HISTORICAL REVIEW OF *PHOXINUS*

As mentioned in the Introduction, *Phoxinus* is a very interesting group because it is the only minnow genus occurring in North America and Eurasia. Since the first species of *Phoxinus* was described – *Phoxinus phoxinus* (Linnaeus, 1758) – many ichthyologists have been attracted by these fishes to study different aspects of the genus, such as taxonomy, distribution, osteology, behavior, and physiology. Here, I chronologically summarize the literature of the genus, mainly on those related to taxonomy, morphology, and distribution. For sake of convenience, I treat every 10 years as an artificial unit except the parts “up to the 20th century”, including the publications before 1900, and “1980-1994” consisting of a summary of 15 years’ publications.

Up to the 20th century

The first species of *Phoxinus* was described by Linnaeus in his *Systema Naturae* (10th ed., 1758) as *Cyprinus phoxinus*. As for other species described by Linnaeus (1758), the description of this species was very brief. Another species described by Linnaeus (1758), *Cyprinus aphyra*, is generally considered a synonym of *Phoxinus phoxinus* (e.g., Berg 1949, Banarescu 1964, Wheeler 1991).

Rafinesque, one of the most important naturalists in the 19th century, considered the genus *Cyprinus* of Linnaeus being too diverse and thus split it into several genera based on “the position of the dorsal fin and the vent, the number of rays to the abdominal fins” (Rafinesque 1820a, b, 1889). Among these genera, three occur in Europe and one (*Minnilus*) in North America (Rafinesque 1820a, b, 1889).¹ *Phoxinus*, a European genus, differs from the other two European ones, *Dobula* and *Alburnus*², in “ten abdominal rays and no appendage” (Rafinesque 1820a, 1889).

In the same papers, Rafinesque (1820a, b, 1889) described the subgenus *Chrosomus* of *Luxilus* for the “redbelly shiner” from Ohio River, and named the shiner as *Luxilus erythrogaster*. However, Rafinesque also suggested that the subgenus *Chrosomus* might also be considered as a genus. Therefore, the name for this “redbelly shiner” was often cited as *Chrosomus erythrogaster* (Rafinesque) (e.g., Cross 1967) or *Chrosomus erythrogaster* Rafinesque (e.g., Eddy & Underhill 1974). [Both are synonyms of *Phoxinus erythrogaster* (Rafinesque), see below]. This might be an explanation why both *C. erythrogaster* (Rafinesque) and *C. erythrogaster* Rafinesque appear in the literature (cf. species account of *Phoxinus erythrogaster*), though the correct citation should be *Chrosomus erythrogaster* (Rafinesque), not *C. erythrogaster* Rafinesque.

A more complicated and confusing problem was raised by the dates of the publications of Rafinesque (1820a, b; 1889). All of the literature known cited Rafinesque 1820b:45 as the original description of *Phoxinus* Rafinesque, Rafinesque 1820b:47 as the original description of *Chrosomus*, and Rafinesque 1820b:47 as the original description of *Chrosomus erythrogaster* (Rafinesque) (e.g., Starnes & Starnes 1980a, Howes 1985). However, according to the zoological nomenclature rules, the correct citation should be the one published first. Rafinesque’s paper on the fishes of Ohio River, in which *Phoxinus*, *Chrosomus*, and *Chrosomus erythrogaster* were originally described, was published three times under two different titles (i.e., Rafinesque 1820a, b, 1889). Rafinesque (1820a) was published in the journal “The Western Review and Miscellaneous Magazine, a monthly publication” as one of a series of nine papers under the title “Fishes of the River Ohio” published from December 1819 to December 1820 (Eschmeyer 1990). (This magazine was published in Lexington, Kentucky, only from 1818 to 1820.) The paper originally describing *Phoxinus*, *Chrosomus*, and *Chrosomus erythrogaster* (Rafinesque 1820a) was the fourth in the series and was published in May 1820. Rafinesque (1820b) was published on 22 May 1820, as a separate monograph titled “Ichthyologia Ohiensis, or natural history of the fishes inhabiting the River Ohio and its tributary streams, preceded by a physical description of the Ohio and its branches.” The contents of Rafinesque’s papers (1820a, b) are the same. Rafinesque (1889) consists of 250 copies reprinted from Rafinesque (1820b). We do not have any evidence to show whether Rafinesque (1820b) was published earlier than Rafinesque (1820a) because there is no date for Rafinesque (1820a).

¹) *Minnilus*, a synonym of *Notropis* (Eschmeyer 1990: 248), was misspelled as *Minulus* Rafinesque, 1820a:236 and *Minnulus* Rafinesque, 1820a:237.

²) *Alburnus* Catesby, 1771 in Sciaenidae is not an available name because it was published in a rejected work (Eschmeyer 1990:18).

It is possible that the serial papers (at least some of them) were published first, then followed by Rafinesque (1820b) as a collection of these serial papers. (Eschmeyer 1990:605 cited the date of Rafinesque 1820b as December 1820.) If the above argumentation is accepted, we then should cite "Rafinesque 1820a" as the original description of *Phoxinus*, *Chrosomus*, and *Chrosomus erythrogaster*, instead of "Rafinesque 1820b." Based on the above discussion, I therefore cite Rafinesque (1820a) as the original description of *Phoxinus*, *Luxilus erythrogaster*, and *Chrosomus erythrogaster*.

Using *Cyprinus phoxinus* Linnaeus as the type species (as Rafinesque 1820a did), Agassiz (1835:37) established a genus *Phoxinus* for *Cyprinus phoxinus*, and assigned *Cyprinus phoxinus* as *Phoxinus laevis*.

Jordan (1916) demonstrated that the name of the genus *Phoxinus* should be *Phoxinus* Rafinesque, 1820, not *Phoxinus* Agassiz, 1835, because Rafinesque (1820a) was published earlier than Agassiz (1835). Unfortunately, Jordan's papers did not soon get the attention of the active ichthyologists. Many recent publications still cited *Phoxinus* Agassiz as the valid name (e.g., Berg 1949, Yang & Hung 1964, Smith 1979, Heese 1981) without discussion. However, from the above discussion, it is clear that *Phoxinus* Agassiz, 1835 is a synonym of *Phoxinus* Rafinesque, 1820a.

Cope (1862) described another *Chrosomus* species, *C. eos*, from Meshoppen Creek in Susquehanna County of Pennsylvania, USA. He compared *C. eos* with *C. erythrogaster* and indicated as differences between *C. eos* and *C. erythrogaster* the presence or absence of the lateral line and the body shape. Two years later, Cope (1864) compared the two species and found some of the *C. eos* specimens exhibiting a short lateral line, whereas others entirely lacked pored scales. Though Cope (1869) considered the specimens of *C. eos* in Cope (1864) as *Phoxinus neogaeus*, some of these specimens might be indeed *C. eos* because in some specimens the lateral line "is wanting" (Cope 1864). In *P. neogaeus*, there is a short lateral line (Cope 1869). It is necessary to notice that intraspecific variation of the lateral line is present in the species of *Phoxinus*.

Phoxinus neogaeus was described by Cope (1869) from New Hudson, Livingston County, Michigan, in "Synopsis of the Cyprinidae of Pennsylvania." Cope (1869) was the first one to allocate North American species to the European genus *Phoxinus*. He (Cope 1869) distinguished *P. neogaeus* from *P. laevis* (i.e., *P. phoxinus*) by "its scaly vertebral and ventral region, and much shorter lateral line." Three *Phoxinus* species were reported from Pennsylvania (i.e., *P. neogaeus*, *erythrogaster*, and *eos*) (Cope 1869).

The proper date and source for the original description of *Phoxinus neogaeus* is problematic. Cope's paper describing *P. neogaeus* was published in 1869 (Cope 1869). However, it was cited, with a description of the species, by Günther (1868). The date 1869 was widely cited in literature until Gilbert (1971). This confusion might be partially due to the failure of ichthyologists to check the literature thoroughly (Gilbert 1971). The correct date for this species should be cited as *Phoxinus neogaeus* Cope, 1868, as suggested by Robins et al. (1991).

Günther (1868) did not believe *Phoxinus* to be present in Europe, but only in North America, and considered *P. phoxinus* as *Leuciscus phoxinus*. He divided the two North American *Phoxinus* species into two categories: *P. neogaeus* with two rows of pharyngeal teeth,

and *erythrogaster* with one row of pharyngeal teeth, but both bearing an incomplete body lateral line.

The fourth North American *Phoxinus* species, *P. oreas*, was described by Cope (1868) from Roanoke of Montgomery County, Virginia, as *Chrosomus oreas*. This species resembles *Phoxinus eos* (Cope 1868); the most obvious difference is in their coloration pattern (Cope 1868).

Jordan (1885) recognized two species under the genus *Chrosomus*: *C. erythrogaster* and *C. oreas*, and stated *C. eos* identical to *C. erythrogaster*. In the same publication, Jordan recognized 20 species under *Phoxinus* from North America which he split into six subgenera: *Clinostomus*, *Tigoma*, *Siboma*, *Squalius*, *Cheonda*, and *Phoxinus*. Most of these subgenera were raised to genera by Jordan (1924).

Jordan & Evermann (1896), in their four volumes of "The Fishes of North and Middle America", considered *Phoxinus* as one of the eight subgenera included in *Leuciscus*. Three species were assigned under the subgenus *Phoxinus*: *P. neogaeus*, *margarita*, and *orcutti*. They listed three species under *Chrosomus* and pointed out that *Chrosomus* showed many similarities with *Phoxinus* although none of the similarities were listed.

As in other fish groups, research on *Phoxinus* during these years focused mainly on the description of new species and new records of geographical distribution. Detail morphological study was not yet conducted.

1900-1919

Smith (1908) studied the social spawning behavior of *Phoxinus erythrogaster*. This was the first behavioral account of *Phoxinus* species. He also described the morphology of the pearl organ (breeding tubercles) though the author did not recognize the breast tubercles of the breeding males. Sexual dimorphism between the male and female of *P. erythrogaster* was shown by body color, relative size of pectoral fin, and "pearl organs" (Smith 1908).

Cockerell & Callaway (1909) studied the scale morphology of some North American cyprinids and separated the subfamily Chondrostominae of Jordan & Evermann (1896) into four subfamilies. *Chrosomus* was assigned in the subfamily Chrosominae. Cockerell & Callaway (1909) considered *Chrosomus* a very primitive group which "might be an ancient offshoot from the stem which gave rise to Cyprinidae and Catostomidae."

Cockerell (1909) reviewed the nomenclature of North American fishes called "*Leuciscus*" and "*Rutilus*". He demonstrated that the European "*Leuciscus*" and "*Rutilus*" differ from the so-called "*Leuciscus*"- and "*Rutilus*"-species in North America. Cockerell also studied the scales of *Phoxinus* and *Chrosomus*, and pointed out that the scales of both genera were of the same type, minute with radii in all fields. This was the first time that the similarity between European *Phoxinus* and the North American *Chrosomus* was pointed out. (Jordan & Evermann 1896 noticed the two "genera" were similar, but they did not state what was the similarity the "genera" shared. See the above discussion.)

Following Cockerell (1909), Jordan (1916) demonstrated there was no true "*Leuciscus*" in North America and pointed out that the subgenus *Phoxinus* of *Leuciscus* needed to be

raised to generic level. However, Fowler (1918) disagreed with Cockerell (1909) and Jordan (1916). Fowler (1918) studied the cotype of *P. neogaeus* Cope (ANSP 4548) and believed there were *Leuciscus* species in North America. As the result, Fowler (1918) considered *P. neogaeus* Cope as *Leuciscus neogaeus*.

1920-1929

Based mainly on the type material of some cyprinids studied by Baird, Girard and Cope, Fowler (1924) studied the North American cyprinids, and assigned *Chrosomus* with two species, *C. erythrogaster* and *C. oreas*, as a genus of the subfamily Chrodrostominae.

Jordan (1924) reviewed the North American dace allied to *Leuciscus* and proposed a new genus *Pfrille* for *Phoxinus neogaeus* Cope. In the footnotes, Jordan (1924:71) indicated *Pfrille* closely related to *Phoxinus*. *Pfrille* was accepted as a valid genus name until Bailey (1951) considered *Pfrille* a synonym of *Chrosomus*. However, *Pfrille* was used later by some authors (e.g., Stasiak 1972).

Jordan & Hubbs (1925) studied fishes from Japan and proposed a new genus, *Moroco*, based on *Pseudaspius bergi* Jordan & Metz, 1913 as type species. However, *Moroco* was considered a synonym of *Phoxinus* by Berg (1932, 1949) and Banarescu (1964), because *Pseudaspius bergi* was considered a synonym of *Phoxinus lagowskii variegatus* (Berg, 1932), or of *P. lagowskii oxycephalus* (Berg, 1949). (*P. lagowskii variegatus* is a synonym of *P. lagowskii oxycephalus* in Berg 1949.) The synonymy in Berg (1932, 1949) was challenged by several ichthyologists (e.g., Okada 1960, Banarescu 1964, Gasowska 1979). Gasowska (1979) considered *Moroco* a valid genus name, and three species, *Moroco percnurus* (= *P. percnurus* of Berg 1949), *M. lagowskii oxycephalus* (= *P. lagowskii oxycephalus* of Berg 1949), and *M. czekanowskii* (= *P. czekanowskii* of Berg 1949), were included in the genus. Howes (1985) considered *Moroco* a junior synonym of *Lagowskiella*.

Fishes from Ontario of Canada were studied by Hubbs & Brown (1929). Two species of *Phoxinus neogaeus* and *P. erythrogaster* were reported. Hubbs & Brown (1929) noticed the specific breast tuberculation of breeding males of these two species and *P. oreas*. Based on this character, Hubbs & Brown (1929) claimed that these three species share a close relationship. This was the first time that the breast tuberculation of the breeding males was observed in *Phoxinus*.

1930-1939

Berg (1932) published a book on the freshwater fish fauna in Russia, and prepared a synonym list of *Phoxinus*. The list includes *Rhynchocypris* Günther, 1889, *Eulinneella* Dybowski, 1916, *Czekanowskiella* Dybowski, 1916, *?Pfrille* Jordan, 1924, and *Moroco* Jordan & Hubbs, 1925.

The life history of *Clinostomus elongatus* was studied by Koster (1939), who noticed a roughly triangular patch of scales with one to several more or less developed tubercles on each scale present on the breast of this species. Based on the character of this tuberculation and the color pattern, Koster (1939) proposed a close relationship between the *Chrosomus-Pfrille* group and *Margariscus-Clinostomus-Couesius lumbeus* group.

Bullough (1939, 1940) studied the reproductive cycle of *P. phoxinus*. An internal reproductive rhythm able to work without the external seasonal change was reported (Bullough 1939).

1940-1949

During these years, a few studies on the biology of species of *Phoxinus* were conducted. Frost (1943) studied the natural history of *P. phoxinus*, such as habits, age, growth, food, and reproduction. Frost (1946) also demonstrated dietary relationships among *P. phoxinus* and its associated fish species. The lateral line of *P. phoxinus* was studied by Lekander (1949).

Berg (1949) (1964, English translation) reviewed the Eurasian *Phoxinus* species and proposed a synonym list of the genus. This synonymy, in fact, is a modification of that in Berg (1932). The difference between these two synonymies is that *Gila* Baird & Girard of North America was added to the synonymy of Berg (1932) in Berg (1949), as a subgenus of *Phoxinus*. A key was provided for the eight Eurasian species in Berg (1949). However, *Gila* was removed from *Phoxinus*, and considered as a valid genus name by Uyeno (1960).

1950-1959

Bailey (1951) first lumped *Pfrille* into *Chrosomus* though this lumping was challenged by a few ichthyologists (e.g., Gasowska 1979). Underhill (1957) studied the relationships between the distribution of minnows and darters and Pleistocene glaciation in Minnesota, USA. Three species of *Phoxinus* including *P. neogaeus*, *eos*, and *erythrogaster* were found in Minnesota. These species, based on Underhill (1957), had three different origins in Minnesota. *P. eos*, which was common in the state, might have arrived at the earliest time. *P. erythrogaster* was considered as a late migrant from the lower Mississippi basin, and ecologically restricted in the region. *P. neogaeus*, common in Lake Superior and the Hudson Bay drainage system but absent or represented by relicts in other basins, did not enter from the Lower Mississippi basin (Underhill 1957).

1960-1969

Bailey & Allum (1962) suggested that populations of two species of *Phoxinus neogaeus* and *P. eos* in South Dakota are glacial relicts. These authors also found that hybrids of *P. neogaeus* x *P. eos* were common.

Banarescu (1964) reviewed the synonyms of *Phoxinus*. Though I can not agree with some of his synonyms, Banarescu (1964) is one of the most important works in the systematics of *Phoxinus*. At least two contributions to the taxonomic study of the genus were made by Banarescu (1964). He is the first one to consider the North American *Chrosomus Rafinesque* a synonym of *Phoxinus*; he also confirms *Pfrille* Jordan a synonym of *Phoxinus*. The differences between the synonymies of Banarescu (1964) and Berg (1949) are two: (1) Banarescu considered *Chrosomus Rafinesque* as a synonym of *Phoxinus*; and (2) Banarescu deleted *Gila*, *Eulinneella*, *Lagowskiella*, *Eupallasella*, and *Czekanowskiella* from the synonym list of Berg (1949). Banarescu's synonymy, especially his opinion on

Chrosomus as a synonym of *Phoxinus*, was soon accepted by many North American ichthyologists (e.g., Bailey et al. 1970, Mahy 1979c). Under *Phoxinus*, 14 species were listed and a distribution map was provided for *P. phoxinus* (Banarescu 1964).

Starmach (1963) studied the morphological characteristics of *P. phoxinus* from the basin of the Mszanka Stream, Poland. No gender difference among different portions of the body was found for *P. phoxinus*. However, the pharyngeal tooth formulae varied greatly among individuals, even in the same population, as noted by Berinkey (1968). Six different combinations (i.e., 1,4-4,0, 1,4-4,1, 1,4-4,2, 2,4-4,1, 2,4-4,2, and 2,5-4,2) were observed in a small population (17 specimens) from Montenegro, Yugoslavia (Berinkey 1968). It is interesting that the widely used tooth formula, i.e., 2,5-4,2, for *P. phoxinus* presents only a small portion (6%) of the 17 specimens studied by Berinkey (1968).

Yang & Huang (1964) considered *Phoxinus Aggasiz* a valid name and described seven species in the genus from China. A key was provided for the seven species of *Phoxinus*. This was the most comprehensive review of Chinese *Phoxinus* at that time. However, no synonymy of *Phoxinus* was provided by Yang & Huang (1964).

Hill & Jensen (1968) studied numbers of fin rays (pectoral, dorsal, and anal fins) of *Phoxinus erythrogaster* from Big Spring, Johnson County of Oklahoma, USA. They found that variation of the number of rays in the pectoral fin was ontogenetically significant, whereas the number of dorsal and anal fin-rays did not change much in different age groups. They therefore concluded that the number of dorsal and anal fin-rays were less variable than the pectoral fin rays, thus the former two were more useful as taxonomic characters.

Phillips (1968a) studied 24 morphological characters of *Phoxinus erythrogaster* and *eos*. No geographic variation in either species was found. The distribution of the two species in Minnesota was also discussed in Phillips (1968a). Phillips (1969a) compared the morphology of *P. erythrogaster* and *eos* and their geographic variation in Minnesota. The only differences between the two species are the mouth angle and the ratio of snout length to postorbital length. Joswiak & Moore (1982) reanalyzed Phillips' (1969a) data and indicated the two species be distinguishable by these characters.

Besides the taxonomic studies, data on biology of *Phoxinus* were also accumulated in these years. Tyler (1966) studied the lethal temperature of *P. eos* and *neogaeus* in Ontario, Canada. Phillips (1969b) studied the diet of *P. erythrogaster* in Minnesota, USA. Phillips (1969c) also reported the fecundity of *P. erythrogaster*. Hybrids within *Phoxinus* and between *Phoxinus* and other minnows were described, such as *P. eos* x *P. neogaeus* (New 1962), *P. erythrogaster* x *Notropis cornutus frontalis*, *P. erythrogaster* x *Semotilus atromaculatus* (Cross & Minckley 1960), *P. erythrogaster* x *Notropis cornutus*, and *P. erythrogaster* x *Dionda nubila* (Phillips & Etnier 1969).

1970-1979

Although some authors considered *Margariscus margarita* belonging to the same genus as that *Phoxinus neogaeus* was assigned to (e.g., *Leuciscus* in Günther 1868; *Phoxinus* in Jordan 1885), most ichthyologists placed *Margariscus margarita* and *P. neogaeus* in different genera. By studying the hybrids of *Semotilus margarita* (= *Margariscus margari-*

ta) with other *Phoxinus* species (*P. eos* and *P. neogaeus*) and the chromosome number (2N=50), Legendre (1970b) proposed changing the name of this species (*S. margarita*) to *Phoxinus margarita*. However, no other ichthyologists have followed this suggestion.

Stasiak (1972) studied the morphology and life history of *Phoxinus neogaeus*. He supported *Pfrille* as a valid genus for *neogaeus*. However, in a later study Stasiak (1977) changed *Pfrille neogaea* to *Chrosomus neogaeus*.

Mahy (1972) briefly reported his results from an osteological comparison between North American *Phoxinus* species and *P. phoxinus*. Following this, in three serial papers, Mahy (1975a, b, c) studied the osteology of *P. neogaeus*, *erythrogaster*, and *oreas*. It is worthwhile to note that Mahy used the name *Chrosomus neogaeus* in one (Mahy 1975a), and *Phoxinus neogaeus* in the others (Mahy 1975b, c). Mahy (1975c) recognized two groups of nearctic *Phoxinus* species, *P. neogaeus* group and *P. erythrogaster* group. The first group, including one species, *P. neogaeus*, was the closest to *P. phoxinus*. The second group included the rest of the nearctic *Phoxinus* species known by then. Mahy lumped all species of the second group into a single species, *P. erythrogaster*, i.e., all the nearctic *Phoxinus* species (except *P. neogaeus*) were considered different subspecies of *P. erythrogaster*. Thus, three subspecies were proposed in *P. erythrogaster*, i.e., *P. erythrogaster erythrogaster*, *erythrogaster oreas*, and *erythrogaster eos* in North America (Mahy 1975c). However, Mahy's "subspecies view" has not been accepted by other ichthyologists.

Gasowska (1979) accepted neither Banarescu's (1964) synonym list nor Mahy's "subspecies" view. Having studied the osteological characters, Gasowska (1979) considered *Moroco* and *Pfrille* as valid generic names. Gasowska (1979) separated the North American *Phoxinus* species into three groups belonging to different taxonomic levels and considered shape of the pharyngeal process of the pharyngeal bone as the main character to recognize different genera. Gasowska proposed a new genus, *Parchrosomus*, for *Phoxinus oreas* because of the broad pharyngeal process, the shape of the urohyal, and its "lateral head is smaller than the maximal body depth, whereas in the two former species (*P. erythrogaster* and *eos*) the lateral head length is larger than the maximal body depth" (Gasowska 1979). Therefore, according to Gasowska (1979), *P. phoxinus*, *neogaeus*, and *Chrosomus oreas*, and other North American "*Chrosomus*" species belong to three different genera: *Phoxinus*, *Parchrosomus*, and *Chrosomus*. However, I have found no publication citing *Parchrosomus* as a valid genus. One of the major problems in Gasowska (1979) is that the author did not recognize the specific breast tuberculation in his "*Chrosomus*" species though he did notice the presence of the tuberculation in *P. phoxinus* and *neogaeus*. Gosline (1978) proposed four subfamilies for Cyprinidae. Among the subfamilies, Leuciscinae are a very big one including almost all North American minnows and some European cyprinids. According to Gosline (1978), *Phoxinus* is an adaptive form of Leuciscinae.

The fifth North American *Phoxinus* species, *P. cumberlandensis*, was described by Starnes & Starnes (1978) from Kentucky. Starnes & Starnes (1978) proposed two groups of *Phoxinus* species in North America: *P. oreas* group (including *P. oreas* and *cumberlandensis*), and *erythrogaster* group (including *P. eos* and *erythrogaster*) based on the morphology of opercles and intestines, and coloration patterns.

During this period (1970-1979), life history, ecology, and behavior of *Phoxinus phoxinus* attracted many ichthyologists' attention. Wootton & Mills (1979) studied the breeding behavior of *P. phoxinus* in a small lake in Europe. Stott & Buckley (1979) observed *P. phoxinus* avoiding their home range when water was deoxygenated but back home when oxygen was restored. Wootton et al. (1980) studied the relationships between body weight and daily food consumption. Settles & Hoyt (1978) studied the reproductive biology of *P. erythrogaster* from Kentucky.

Some papers describing hybrids were published in these years, such as those by Legendre (1970b) and Stasiak (1972) (*Phoxinus neogaeus* x *P. eos*), and Greenfield et al. (1973) (*P. erythrogaster* x *Notropis cornutus*).

1980-1994

Joswiak (1980) studied the karyotype of five known nearctic *Phoxinus* species and *P. phoxinus*. He demonstrated $2N=50$ for all studied *Phoxinus* species, and his karyotype data supported the lumping of *Phoxinus* and *Chrosomus*. Based on the Nei distance among the *Phoxinus* species, Joswiak (1980) proposed a phylogenetic tree for *Phoxinus*. The tree shows that *P. eos* and *erythrogaster* were derived from *P. oreas*-like ancestor. Joswiak considered his study an evidence supporting the Bering bridge connection for the migration of *Phoxinus* from Eurasia to North America.

Coad (1984) described some *P. phoxinus* specimens with deformed vertebral columns, and Banbura (1985) reported a case of *P. phoxinus* without pectoral fins.

Leuciscinae is a most problematic subfamily in cyprinids to which *Phoxinus* is generally assigned. A few serial papers on the anatomy and relationships of Leuciscinae were published by Howes (1978, 1984, 1985, 1991), though the monophyly of the subfamily is still an open question. Having studied the anatomy and phylogeny of some Chinese carps (e.g., *Ctenopharyngodon* and *Hypophthalmichthys*), Howes (1984) proposed that at least four monophyletic groups could be recognized within Leuciscinae: aspinine, abramine, alburine (raised to subfamily level in Howes 1991), and phoxine with two genera, *Phoxinus* and *Couesius* (Howes 1985, 1991). Howes (1985) reviewed the synonyms of *Phoxinus* and proposed a new synonym list for the genus. This synonym list is a modification of those in Berg (1949) and Banareescu (1964). According to Howes (1985, 1991), *Phoxinus* and *Couesius* share the comb-like tuberculation on the breast scales in breeding males (Howes 1985) and form a sistergroup¹. Howes (1985) is an important contribution to the study of *Phoxinus* because this was the first one to review the synonyms of *Phoxinus* systematically.

Kim & Kang (1986) studied the osteology of *Moroco keumgang* from Korea. Based on the comparison between *Moroco* and *Phoxinus*, the authors claimed *Moroco* as the sistergroup of *Phoxinus*. They proposed the following synapomorphies for the two genera: the presence of the anterior myodome, the lower part of the interorbital septum extended

¹) However, as discussed below and Chen & Arratia (1996), the breast tuberculation of the two genera shows a great difference.

and contacting the parasphenoid, and a relatively straight parasphenoid (Kim & Kang 1986).

Chen et al. (1984) published a hypothesis of phylogenetic relationships among the major groups of Cyprinidae. They proposed ten subfamilies, among which *Phoxinus* belongs to the subfamily Leuciscinae. The content of the subfamily Leuciscinae of Chen et al. (1984) is similar to that of Gosline (1978). However, Howes (1991) complained that the analysis of Chen et al. (1984) was not a cladistic one, although the authors claimed so. Chen et al. (1984) did not provide synapomorphies to support some sistergroup relationships and some subfamilies are recognized by plesiomorphies only.

Cavender & Coburn (1987) studied the evolutionary relationships among eastern North American cyprinids. They stated that *Phoxinus*, *Semotilus*, *Couesius*, *Hemitremia*, and *Clinostomus* share a unique type of anal fin suspension, and the anterior placement of the anal fin pterygiophores. In a later study of the phylogenetic relationships of cyprinids, Cavender & Coburn (1992) recognized two subfamilies, i.e., Cyprininae and Leuciscinae, in the family Cyprinidae. *Phoxinus* was placed in the phoxinin tribe of Leuciscinae.

Chen (1986a, b, 1987a, b) studied the osteology and phylogeny of Chinese leuciscines. He proposed the Chinese leuciscines a monophyletic group and included *Phoxinus* in the subfamily Leuciscinae.

During the study of fish fauna of Huang He (Yellow River) in China, Chen (1988a) described a new *Phoxinus* species, *P. tchangi* from the Huang He tributary. The olfactory organ of *Phoxinus* was studied by Chen (1988b). Chen (1988b) considered the olfactory organ of *Phoxinus* a primitive condition in Cyprinidae because the types of the olfactory organ in *Phoxinus* were commonly found in Cyprinidae.

The sixth North American *Phoxinus* species, *P. tennesseensis*, was described by Starnes & Jenkins (1988) from the Tennessee River drainage, USA. Starnes & Jenkins (1988) also proposed *P. cumberlandensis* the sister species of [*P. oreas* + *tennesseensis*], and *P. eos* the sister species of *P. erythrogaster*.

Banareescu (1989) analyzed the distribution patterns of European freshwater fishes. Two patterns were proposed: vicariant and dispersal. In this paper, Banareescu considered *P. phoxinus* the vicariant sister of *P. neogaeus* though no evidence was discussed (Banareescu 1989).

Bugutskaya (1987, 1988a, b, 1989, 1990, 1991) published several papers on the osteology and classification of Leuciscinae based mainly on the Eurasian genera. She recognized eight tribes in the subfamily: Leuciscini, Alburnini, Phoxini, Abramini, Aspinini, Elopichthyini, Pseudoaspinini, and Hypophthalmichthyini.

The external morphology and biology of *P. phoxinus* from River Skawa of Poland were studied by Heese (1981, 1984). He stated the maximum age of *P. phoxinus* to be more than six years. Sexual dimorphism of the species was shown in the shape of pectoral and ventral fins, the coloration, and the tuberculation (Heese 1981, 1984). Heese's result was similar to that of Frost (1943).

Based on field work in Mongolia in 1984, Travers (1989) described the Mongolian fish fauna. *P. phoxinus* was caught from "Arctic and Pacific basins." Travers (1989) demon-

strated that this species "appears to prefer cold, clear water running over a sand and stone substrate and was often together with *Nemacheilus*, *Misgurnus*, and young salmonids."

Reproductive biology of *Phoxinus phoxinus* was studied by Mills (1987). Mills (1987) reported the reproductive size for *P. phoxinus* at 50 mm length. The behavior of *P. phoxinus* was described by some European ichthyologists. Partridge (1980) and Magurran & Girling (1986) studied the schooling of the species. Kennedy (1981) observed the homing tendency of the species. Legkiy & Popoya (1984) demonstrated that one of the important factors for the downstream migration of *P. phoxinus* was a change in their photoreaction (negative response). Pfeiffer et al. (1985) indicated *P. phoxinus* bear alarm cells through the year. Bioenergetic biology of the species was studied by Cui & Wootton (1988a, b, 1989). Distribution and ecology of *P. cumberlandensis* was studied by O'Bara (1990, 1991).

Wheeler (1991) discussed the status of the type specimens of *P. phoxinus*. The specimens were in very poor condition and Wheeler was not able to identify whether the specimens were the type of the species (see the discussion in the species account of *P. phoxinus*), thus a problem was raised if the specimen is the "real" type of *P. phoxinus*.

Summary

Since the description of *Cyprinus phoxinus* was published (Linnaeus 1758), almost 240 years have passed. In the past more than 200 years, ichthyologists have paid much attention to the genus *Phoxinus*, publishing hundreds of studies related to these fishes. The main contributions during these years can be summarized as follows:

1. Numerous records of the geographic distribution of the genus;
2. Accumulation of data on life history, ecology and behavior of some species, such as *P. phoxinus* and *erythrogaster*;
3. Some knowledge of osteology and external morphology of some species; and
4. Synonyms of some species.

PHYLOGENETIC RELATIONSHIPS OF *PHOXINUS* AND THE RELATED GENERA

Monophyly of the Hemitremanian clade and its position in the family Cyprinidae

According to Chen et al. (1984) and Cavender & Coburn (1992), Cyprinidae comprises two major lineages, the subfamilies Cyprininae and Leuciscinae (Cavender & Coburn 1992) (Fig.1). Phoxinins, defined by the disconnection between temporal and preoperculo-mandibular sensory canals, is one of the eight clades in Leuciscinae. Consisting of Shiner, Chub, and Western clades (Fig.1), phoxinins include almost all North American minnows (excluding *Notemigonus crysoleucas* which belongs to the Eurasian leuciscins) and a few Eurasian genera (Cavender & Coburn 1992; Coburn & Cavender 1992).

The term "phoxinins" used in this publication has different content from that of "phoxinins" of Howes (1985). "Phoxinins" of Howes contains two genera, *Phoxinus* and *Couesius* (Howes 1985, 1991). When I refer to "phoxinins" of Howes, I use "phoxinins of Howes". The term "phoxinins" used herein refers to that of Cavender & Coburn (1992) and Coburn & Cavender (1992).

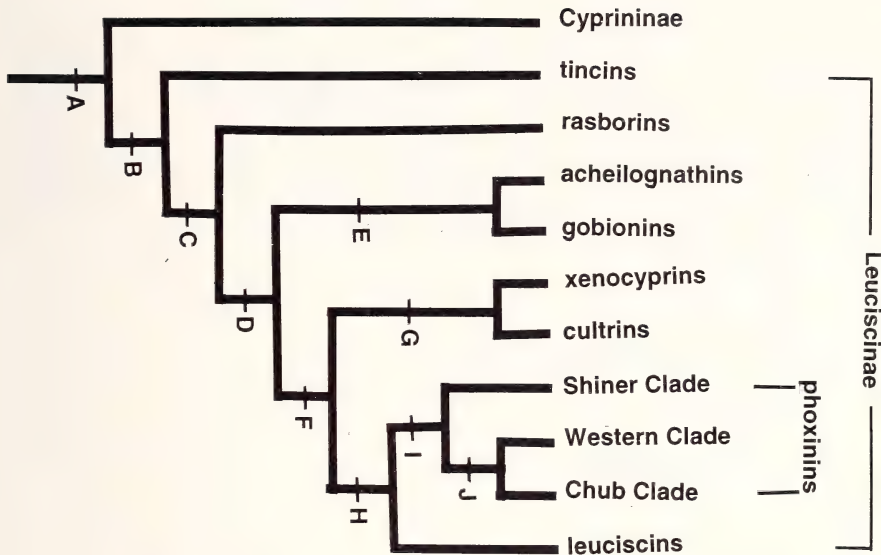


Fig.1: Phylogenetic hypothesis of Cyprinidae, showing the position of phoxinins. The synapomorphies supporting each node are as following. Node A: Absence of uncinate process on epibranchials I and II; subtemporal fossa deep and well-developed; interorbital septum formed by orbitosphenoid and a dorsal component of the parasphenoid. Node B: Rib head and parapophysis of fifth rib modified for greater mobility; origin of dorsal fin behind pelvic insertion; absence of anterior maxillary barbel and accompanying foramen in maxilla. Node C: Crest of neural complex (supraneural) divided dorsally (forked); anterior (free) supraneural in contact with neural complex; three unbranched dorsal fin rays. Node D: Scale without basal radii. Node E: Oval scales with modified circuli in posterior field and apical radii only. Node F: Pterotic elongated, its anterior end reaching in front of the anterior opening of the trigeminal-facial chamber. Node G: Anterior fork of the pelvic bone reduced; 48 diploid chromosomes with longest pair submetacentric. Node H: Supraorbital canal disconnected from the infraorbital canal; pharyngeal teeth in one or two rows. Node I: Phoxinin scale type; basal radii of scale absence; scale with numerous apical radii; infraorbital and preoperculo-mandibular canals not joined; opercular canal absent; preethmoid projecting anteroventrally when viewed anteriorly. Node J: Postorbital cranium elongated; anterior and posterior angles of pharyngeal arch rounded; rib of vertebra 4 with an anterior process (from Chen et al. 1984, Cavender & Coburn 1992, Coburn & Cavender 1992).

The Chub clade within the phoxinins (Fig.1) contains the Exoglossin clade, *Tribolodon*, and some other genera (Fig.2), including *Phoxinus*, defined as Hemitremian clade herein (see below for detail). The Exoglossin clade is well diagnosed by synapomorphies (Coburn & Cavender 1992) such as the shortened mandibular canal terminating posterior to the mental foramen. However, some problems are present in the relationships of other genera in the Chub clade [*Tribolodon* + Hemitremians] as discussed by Coburn & Cavender (1992). First, only two Eurasian genera of phoxinins (*Tribolodon* and *Rhynchocypris*) were studied, obviously, "the examination of additional Eurasian phoxinin genera is clearly required" (Coburn & Cavender 1992:329). Second, all the characters supporting the nodes below the Exoglossin clade in Coburn & Cavender (1992: Fig.13) are either re-

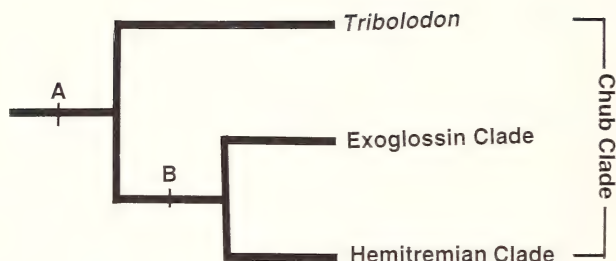


Fig.2: Phylogenetic hypothesis among the Chub Clade. The synapomorphies supporting the nodes are as following. Node A: Scale with apically directed lateral radii; distal lateral ethmoid hooked posteriorly; supraethmoid narrow; supraorbital small with irregular shape; neurocranium depressed with flattened parietal region and reduced orbitosphenoid septum; orbitosphenoid with extended parasphenoid contact. Node B: Postorbital cranium not elongated; weakly developed posttemporal fossa (from Coburn & Cavender 1992).

versed from other clades, reversed at the next few nodes, or vary intragenerically. Thus the phylogenetic relationships of these genera in the Chub clade (Chub clade excluding Exoglossin clade and *Tribolodon*) need to be further evaluated.

According to my results and those of Cavender & Coburn (1987), some North American and Eurasian minnow genera do form a monophyletic group, i.e., the Hemitreman clade, in the Chub clade of Coburn & Cavender (1992), as the sistergroup of the Exoglossin clade (Fig.2); whereas, the Hemitreman clade + Exoglossin clade (including *Platygobio*, *Hybognathus*, *Dionda*, *Campostoma*, *Macrhybopsis*, *Erimystax*, *Nocomis*, *Exoglossum*, *Phenacobius*) form the sistergroup of *Tribolodon* in the Chub clade (Fig.2).

The Hemitreman clade includes eight genera, i.e., *Phoxinus*, *Couesius*, *Semotilus*, *Hemitremia*, *Margariscus*, *Rhynchocypris*, *Eupallasella*, and *Lagowskiella*. All Hemitremians share one synapomorphy: the anterior placement of the anterior pterygiophores of the anal fin. In Hemitremians, the anterior few anal pterygiophores are placed forward to the first haemal spine, at least one anal pterygiophore is positioned anteriorly to the last rib (Fig.3B-C). Having studied all genera of exoglossins, other North America minnow genera, and some Eurasian minnow genera, I could not find this character from outside of the Hemitreman clade. Therefore, I interpret this character as an autapomorphy to support the monophyly of the clade. The anterior position of the anterior anal pterygiophores was first described and interpreted by Cavender & Coburn (1987) to support a monophyletic group including *Phoxinus*, *Margariscus*, *Semotilus*, *Hemitremia*, and *Couesius*. Later, Coburn & Cavender (1992) considered this character an evidence to support a monophyletic group including almost all the Chub clade (only *Tribolodon* excluded); and they interpreted the absence of this character in exoglossins as a reversal of the anterior placement of the anal pterygiophore(s).

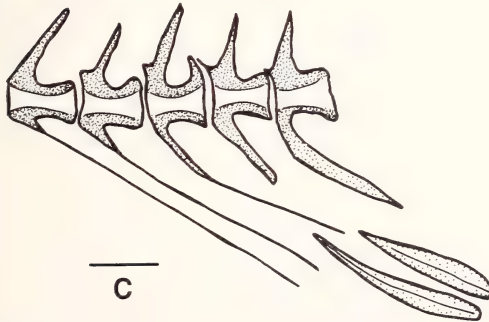
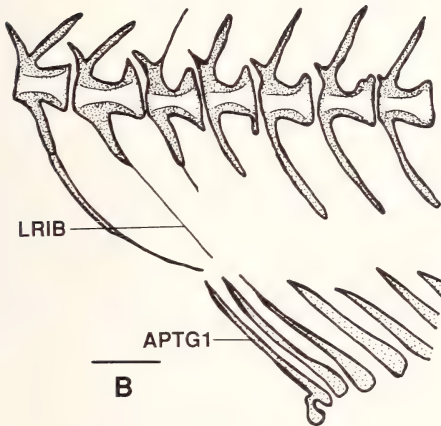
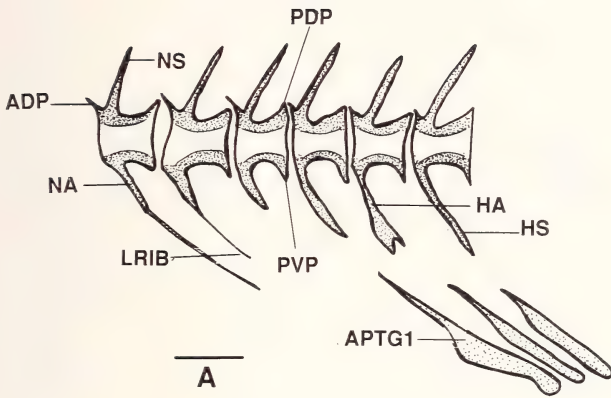


Fig.3: Anterior anal pterygiophores and associated vertebrae in hemitremians and in outgroup. A: *Nocomis platyrhynchus* (KU 18926, SL 46.5 mm); B: *Phoxinus phoxinus* (CNUC, uncat., 76 mm TL); C: *Hemitremia flammea* (KU 18931, 57.4 mm SL). Scale bars = 1 mm (for abbreviations see Appendix IV).

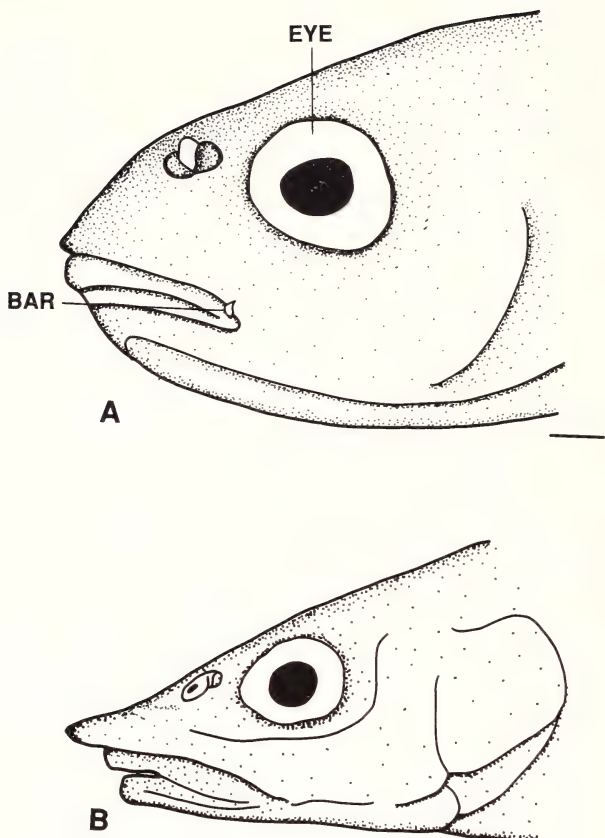


Fig.4: Profiles of lateral view of head of (A) *Couesius plumbeus* (KU 18965, 80.1 mm SL) and (B) *Rhynchocypris oxycephalus* (modified from Howes, 1985). Scale bar = 1 mm.

Analysis of transformation series in the Hemitremian clade

Based on the above discussion and Fig.2, the exoglossins are considered the first outgroup, and *Tribolodon* the second outgroup to polarize characters of the transformation series in the Hemitremian clade.

1. Fleshy rostral process (Fig.4A, B). The fleshy rostral process is an anterior flesh rostral extension. In the ingroups (except *Rhynchocypris*) and the outgroups, the rostral process

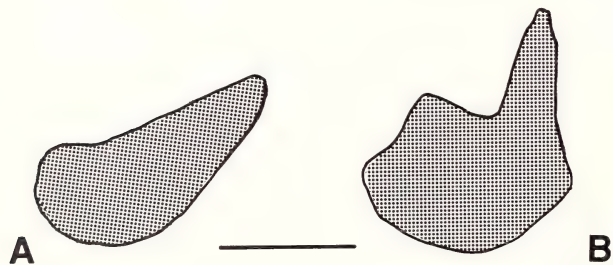


Fig.5: Anterior view of primary lamellae of (A) *Phoxinus phoxinus* (KU 3265, 56.7 mm SL) and (B) *Lagowskiella lagowskii* (NAIJ 14402, 95.8 mm SL). Scale bars = 1 mm.

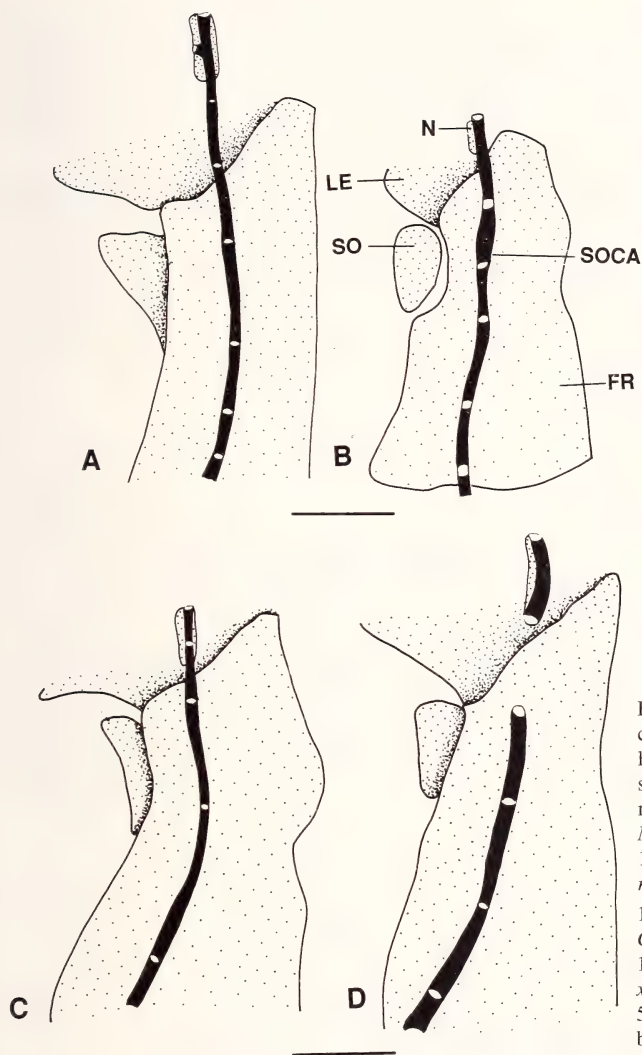


Fig. 6: Part of the supraorbital canal (in black), and nasal, lateral ethmoid, frontal, and supraorbital bones in hemitremians and in the outgroup. A: *Nocomis platyrhynchus* (KU 18926, 46.5 mm SL); B: *Hemimiremia flammea* (KU 18931, 57.4 mm SL); C: *Couesius plumbeus* (KU 18881, 65.0 mm SL); D: *Phoxinus erythrogaster* (KU 5773, 62.0 mm SL). Scale bars = 1 mm.

is very short (Fig. 4A). In *Rhynchocypris*, the rostral process is long and well-developed (Fig. 4B), especially in ripe females (Howes 1985). The process is also present in *Tribolodon hakonensis*, but the process in this species is less developed than that in *Rhynchocypris* (Cavender & Coburn 1992). The long fleshy rostral process was interpreted by Howes (1985) as an apomorphy for the genus *Rhynchocypris*. (This elongated rostral process is also present in *Rhinichthys*, Coburn 1994, pers. comm.). – **TS 1:** Fleshy rostral process very short [0], or long [1].

2. Posterior barbel (Fig.4A-B). The posterior barbel of *Couesius* is a papillate appendage derived from the upper rictal tissue which is not homologous with the barbels of other "barbeled cyprinids" (i.e., cyprinins) (Howes 1985). This posterior barbel is located at the corner of the mouth, and present in *Couesius* only (Fig.4A). – **TS 2:** A posterior barbel absent [0], or present [1].

3. Primary lamellae of the olfactory organ (Fig.5A-B). The primary lamellae of the olfactory organ are arranged at both sides (lateral and medial) of the axis in the olfactory

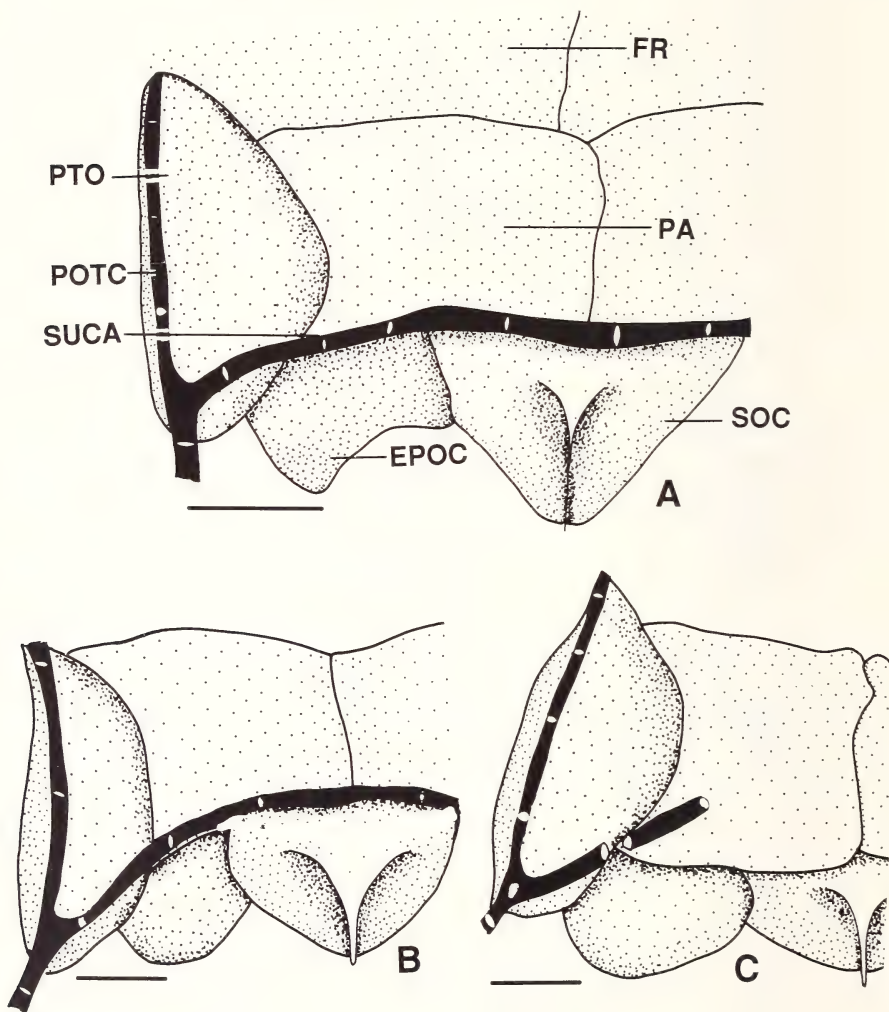


Fig.7: Supratemporal and otic canals (in black), frontal, pterotic, parietal, epioccipital, and supraoccipital bones in hemitremians and in the outgroup. A: *Nocomis platyrhynchus* (KU 18926, 46.5 mm SL); B: *Semotilus corporalis* (KU 18856, 58.0 mm SL); C: *Couesius plumbeus* (KU 18881, 56.6 mm SL). Scale bars = 1 mm.

organ. In *Rhynchocypris* and *Lagowskiella*, the dorsal margin of the primary lamellae bears a deep notch (Fig.5B); in the outgroups and other genera of the ingroups, the margin does not bear the deep notch (Fig.5A). – **TS 3:** A deep notch absent [0] or present [1] on the dorsal margin of the primary lamellae in the olfactory organ.

4. Supraorbital sensory canal (Fig.6A-D). The supraorbital sensory canal runs from the parietal posteriorly to the nasal bone anteriorly. It is interrupted into two portions, though the range of the gap might vary, between the anterior end of the frontal bone and the posterior end of the nasal bone in *Phoxinus* (Fig.6D). The canal is not interrupted at this region in other members of the ingroups and in the outgroups (Fig.6A-C). However, the interrupted canal is also found in *Cyprinus* and *Gila* of Cyprinidae (Cavender & Coburn 1992). – **TS 4:** Supraorbital sensory canal not interrupted [0], or interrupted [1] between the anterior end of the frontal bone and the posterior end of the nasal bone.

5. Supratemporal sensory canal (Fig.7A-C). In the outgroups, in *Rhynchocypris* and *Semotilus*, the left and right portions of the supratemporal sensory canal connect on the parietal (Fig.7A-B). Therefore, the supratemporal canal is continuous between the left and right portions of the canal. In other members of the ingroup, however, the canal is interrupted on the parietal. – **TS 5:** Left and right supratemporal sensory canals connect [0], or not connect [1] each other on the parietal.

6. Preopercular sensory canal (Fig.8 A-C). In the outgroups, in *Hemitremia*, *Rhynchocypris*, *Lagowskiella*, *Margariscus*, *Eupallasella*, and in *Semotilus*, the preopercular sensory canal extends upward and terminates at or near the tip of the ascending arm of the preopercle bone (Fig.8A-B). In *Phoxinus* and *Couesius*, the preopercular canal terminates at about the middle of the ascending arm of the bone (Fig.8C).

Coburn & Cavender (1992) considered the “shortened preopercular canal” an evidence supporting the relationship of *Phoxinus* and other genera of the Chub clade. However, the

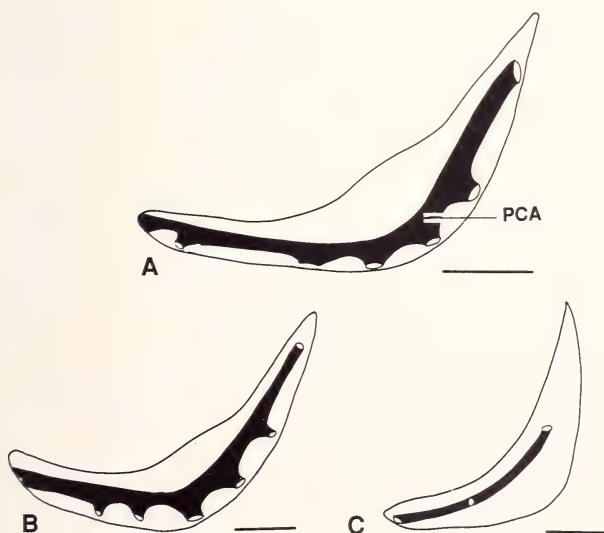


Fig.8: Preopercular canal (in black) and preopercle in hemitremians and in the out-group. A: *Nocomis platyrhynchus* (KU 18926, 46.5 mm SL); B: *Semotilus corporalis* (KU 18856, 58.0 mm SL); C: *Phoxinus erythrogaster* (KU 5773, 62.0 mm SL). Scale bars = 1 mm.

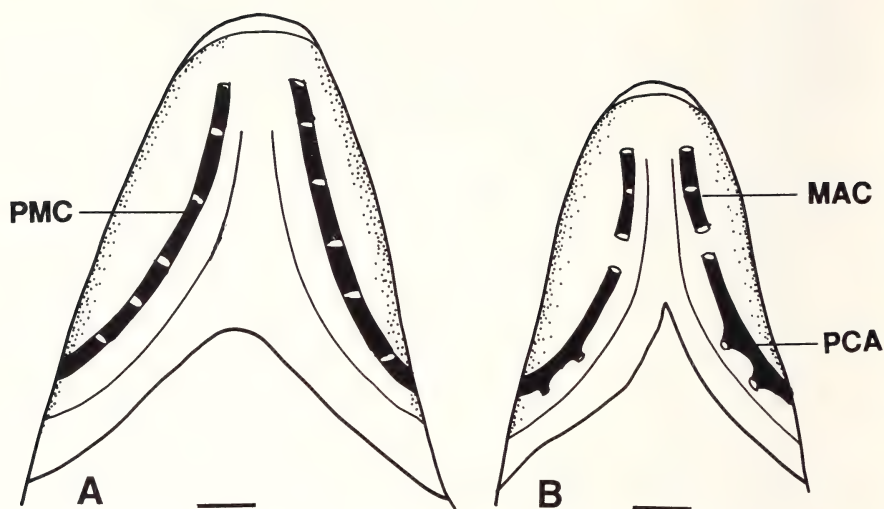


Fig.9: Ventral profile of heads of (A) *Couesius plumbeus* (KU 18965, 73.5 mm SL) and (B) *Phoxinus erythrogaster* (KU 10629, 62.5 mm SL), showing the preoperculomandibular canal (in black). Scale bars = 1 mm.

preopercular canal in *Phoxinus* is much shorter than that in other genera in the Chub clade. In other genera of the Chub clade (e.g., *Nocomis*), the canal ends near the tip of the ascending limb of the preopercle (Coburn & Cavender 1992). In *Phoxinus*, however, the canal terminates at the middle of the preopercle. – **TS 6:** Preopercular sensory canal terminates at or close to the tip [0], or at about the middle [1] of the ascending limb of the preopercle bone.

7. Preoperculomandibular canal (Fig.9A-B). In *Phoxinus*, the preoperculomandibular canal is interrupted between the posterior end of the mandibular portion and the anterior end of preopercular portion, thus the mandibular and the preopercular canals are formed (Fig.9B). This condition is not found in other genera of the ingroup or in the outgroups (Fig.9A). – **TS 7:** Preoperculomandibular canal continuous [0], or interrupted into two portions [1] between the mandibular and the preopercular bones.

8. Basal radii of scales (Fig.10A-C). Generally, scales of most cyprinids bear apical (posterior) radii only (Chu 1935) (Fig.10A). In the exoglossins of the Chub clade, no genus bears basal radii on the scales. Coburn & Cavender (1992) indicated that *Campostoma ornatum* bears basal (anterior) radii on the scale. However, no basal radii were found on the scales in the specimens of *C. ornatum* and *C. anomalum* I studied. In the Hemitreman clade, Coburn & Cavender (1992:352) mentioned the basal radii occurring within the Chub clade only in *Rhynchocypris* and *Phoxinus* of the taxa examined. However, my studies show that four genera in the Hemitreman clade, i.e., *Rhynchocypris*, *Lagowskiella*, *Eupallasella*, and *Phoxinus*, bear both basal and apical radii on their scales (Fig.10C). Basal radii are absent on the scales of *Semotilus*, *Couesius*, *Hemitremia*, and *Margariscus* of Hemitremians (Fig.10B). *Tribolodon* does not have basal radii (Chu 1935, Coburn & Cavender 1992).

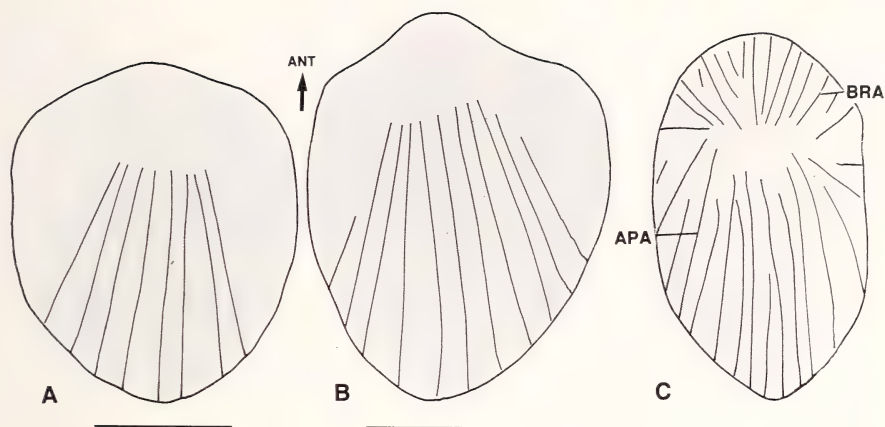


Fig.10: Scales on caudal peduncle in hemitremians and in the outgroup (only showing the general shape of the scale and the radii; circuli not presented). A: *Hybognathus placitus* (KU 2020, 61.6 mm SL); B: *Semotilus corporalis* (KU 16915, 55.4 mm SL); C: *Lagowskiella lagowskii* (MCZ 32370, 103.5 mm TL). Scale bars = 1 mm.

The presence of basal radii was first described by Cockerell & Callaway (1909) as one of the characters of *Phoxinus*. Chu (1935) considered the basal radii a useful character for the identification of some genera and species. In leuciscins [the sistergroup of phoxinins (Cavender & Coburn 1992)], *Rutilus* and *Leuciscus* have basal radii on scales (pers. observ.) that might be an evidence supporting the close relationship of these two genera among the leuciscines proposed by Chen (1987b). However, the arrangement of the radii of these two genera is different from that in the Hemitremian clade having basal and apical radii. In *Leuciscus* and *Rutilus*, the arrangements of both basal and apical radii are fan-shaped, and a large gap is present between the basal and apical radii. In the Hemitremians having basal radii, the radii are present on the entire scali and no gap is present between the apical and basal radii (Fig.10C). – **TS 8:** Scale bearing apical radii only [0], or bearing both apical and basal radii [1].

9. Shape of scales on the caudal peduncle (Fig.10A-C). In *Semotilus*, *Couesius*, *Margariscus*, *Hemitremia*, and in the outgroups, the scales on the caudal peduncle are relatively short, almost round (Fig.10A-B). In other members of the ingroup, the scales are elongated and rectangular-shaped (Fig.10C). – **TS 9:** Scales on caudal peduncle round [0], or elongated [1].

10. Breast scales of breeding male (Fig.11A-C). The term “breast scale” is defined according to Chen & Arratia (1996) as the scales at the region in front of the pectoral fin base, and posterior to the gill cleft. In most members of the ingroup and in the outgroups, the breast scales of breeding males are thin, relatively loose, and not deeply embedded (Fig.11A-B). In *Phoxinus*, however, the breast scales are much thicker and deeply embedded, and the apical (posterior) margins bear tubercles (Fig.11C).

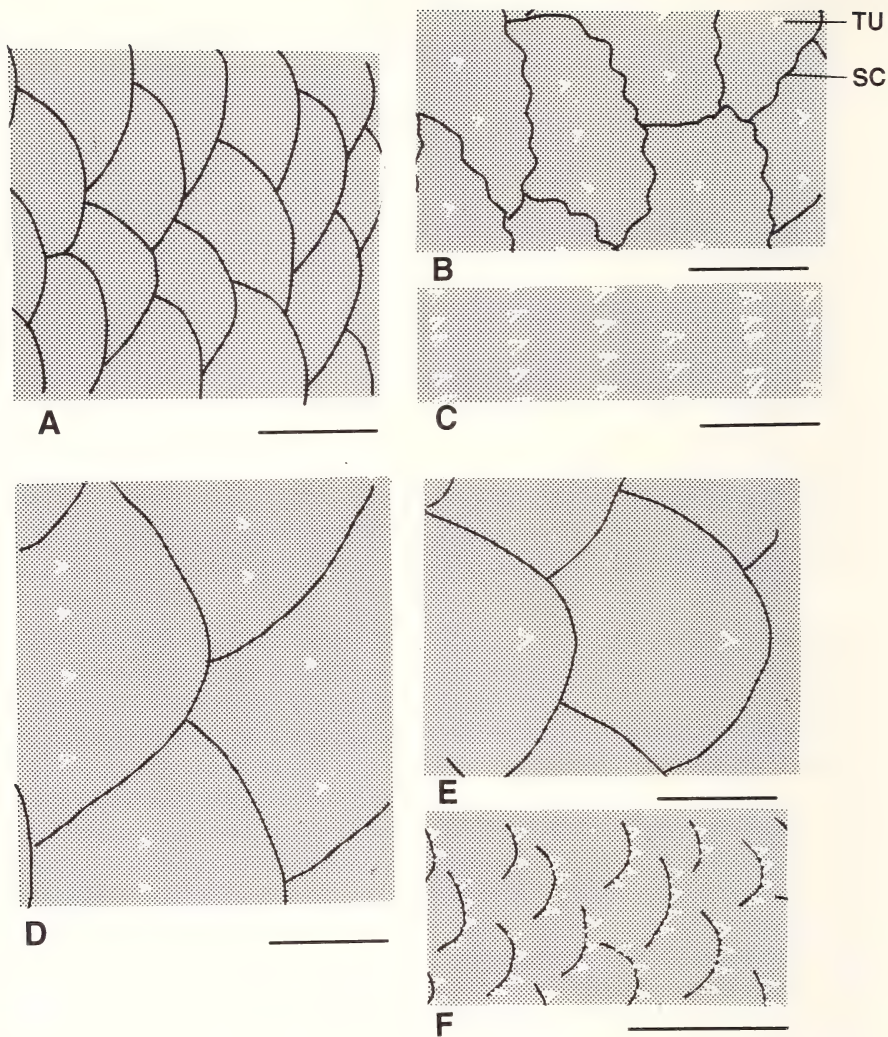


Fig.11: Breast scales and their tubercles (A-C, scale bars = 0.3 mm), and scales on caudal peduncle and their tubercles (D-F, scale bars = 1 mm) in breeding males in hemitremians. A: *Eupallasella percnurus* (MCZ 32369, 99.2 mm SL); B: *Margariscus margarita* (KU 8519, 102.5 mm SL); C: *Phoxinus oreas* (KU 3265, 43.5 mm SL); D: *Campostoma anomalum* (KU 20371, 121.5 mm SL); E: *Clinostomus funduloides* (KU 3262, 62.0 mm SL); F: *Phoxinus erythrogaster* (KU uncat., 47.0 mm SL).

In most members of the ingroup and in the outgroups, the breast scales have a smooth margin (Fig.11A). In *Couesius* and *Margariscus* of the ingroups, the apical (posterior) margin of the breast scales is serrated (Fig.11B). Having studied all genera of the outgroups, I did not find a similar condition on the breast scales in the outgroups. A serra-

ted breast scale was illustrated in Howes (1985: Fig.2) for *Couesius*, but not discussed in his text. Our study also shows the serrated breast scales present in *Couesius* (Chen & Arratia 1996). – **TS 10:** Breast scales not deeply embedded [0], or deeply embedded [1] in breeding males. – **TS 11:** Apical margin of breast scales in breeding male smooth [0], or serrated [1].

11. Tuberculation on breast scales (Fig.11A-C). Based on our observation and published data, all cyprinids, except *Phoxinus*, lack tubercles on the apical margin of breast scales in breeding males (Chen & Arratia 1996). In *Phoxinus*, each breast scale bears a series of sharp tipped tubercles (generally two to six tubercles) on its apical margin (Fig.11C). Males of *Tribolodon hakonensis* also have a tuberculated margin in the breast scales, but the arrangement of the breast scales is different from that in *Phoxinus* (Cavender & Coburn 1992). I interpret the tuberculation in *Tribolodon* homoplastic with that of *Phoxinus* because of the different arrangement of breast scales of the two genera, and the lack of the anteriorly located anal pterygiophores in *Tribolodon* (Coburn & Cavender 1992).

In the outgroups, breeding males do not bear tubercles on the breast scales. In the ingroup, only three genera, *Margariscus*, *Semotilus*, and *Couesius*, bear one or two small tubercles at the middle of each scale, but no tubercles are present at the apical margin (Chen & Arratia 1996). The presence of centrally placed tubercles on the breast scales is interpreted as apomorphic, the absence of the tubercles on this area of scales as plesiomorphic. Chen & Arratia (1996) summarize the history of the study on the tuberculation in *Phoxinus*. They compare the tuberculation on breast scales in *Phoxinus* and *Margariscus-Clinostomus-Couesius*-group of Hubbs & Brown (1929). According to Chen & Arratia (1996), two differences in breast tuberculation between *Phoxinus* and the *Margariscus-Clinostomus-Couesius*-group (defined as *Margariscus*-group hereafter) are present. (1) The breast scales are deeply embedded, and only the apical margin of the scale can be observed in *Phoxinus*; whereas the breast scales are loose, not deeply embedded, and most of a scale can be observed in the *Margariscus*-group. (2) In *Phoxinus*, tubercles are large, tall, sharp, and present at the apical margin of the breast scales, and each scale bears up to six tubercles (even more in some species of the genus); whereas in *Margariscus*-group, the tubercles are small, short, and centrally placed on the scale, and each scale bears only two to three tubercles.

TS 12: The breast scale in breeding males bearing no tubercles on the apical margin [0], or bearing a series of sharp-tipped tubercles at the apical margin [1]. – **TS 13:** Each breast scale of breeding males bearing no tubercle at its center [0], or centrally bearing one to three [1] small tubercles.

12. Tuberculation on scales on caudal peduncle (Fig.11D-F). In breeding males of most members in the ingroup and in the outgroups, each scale on the ventrolateral part of the caudal peduncle bears one or two tubercles on its middle portion, but no tubercles are present on its apical margin (Fig.11D-E). In *Phoxinus*, however, each scale in this region bears a few, up to 12, well-developed and sharp-tipped tubercles at its apical margin (Fig.11F). – **TS 14:** In breeding males, scales on the ventrolateral part of caudal peduncle bearing no tubercles on the apical margin [0]; or bearing two or more tubercles on the apical margin [1].

13. Frontal bone (Fig.6A-D). In *Hemitremia*, the anterolateral margin of the frontal bone bears a deep notch articulating with the supraorbital bone (Fig.6B); the lateral margin of the frontal does not bear the deep notch in other members of the ingroup and in the outgroups (Fig.6A, C, D). – **TS 15:** The anterolateral margin of the frontal articulating with supraorbital bone not forming a deep notch [0], or forming a deep notch [1].

14. Orbital septum (Fig.12A-E). The orbital septum is formed by fusion of the base of the left and right orbitosphenoids. An anterior process is present at the anterior margin of the orbital septum. The process is absent in outgroups and most members of the ingroups (Fig.12A, B, E); the process is present in *Semotilus*, *Hemitremia*, and *Eupallasella* (Fig.12C-D).

The orbital septum is high in most members of the ingroup and in the outgroups (Fig.12B-C), but lower in *Lagowskiella*, *Phoxinus*, and *Couesius* (Fig.12A, E).

In *Semotilus*, *Hemitremia*, *Phoxinus*, *Margariscus*, and in the outgroups, the orbital septum narrowly joins the dorsal side of the parasphenoid (Fig.12C, D-E); in other members of the ingroup, the septum broadly joins the parasphenoid (Fig.12A-B).

In most members of the ingroup and in the outgroups, no cartilage is present in front of the orbital septum in adult individuals (Fig.12A-B, D-E); in *Hemitremia* and *Eupallasella*, a short bar-shaped cartilage is present in front of the orbital septum (Fig.12C).

TS 16: An anterior process at the anterior margin of the orbital septum absent [0], or present [1]. – **TS 17:** Orbital septum high [0], or lower [1]. – **TS 18:** Orbital septum narrowly [0], or widely connecting with the dorsal side of the parasphenoid [1]. – **TS 19:** A cartilage absent [0], or present [1] in front of the orbital septum in adults.

15. Supraorbital bone. In *Hemitremia*, *Lagowskiella*, and in the outgroups, the supraorbital bone is large and well-developed; in other genera of the ingroup, the supraorbital bone is reduced to a narrow and short one.

Howes (1985) proposed presence of the small supraorbital bone as one of the synapomorphies of *Phoxinus*. My study shows that this character is widely distributed in several genera of Hemitremitians. – **TS 20:** Supraorbital bone large [0], or small [1].

16. Basioccipital bone (Fig.13A-C). In *Phoxinus*, *Rhynchocypris*, *Campostoma*, *Dionda*, and *Hybognathus*, the pharyngeal pad of the basioccipital bone bears an anterior process (Fig.13C) (also see Mayden 1989, Schmidt 1989). In other members of the outgroups and ingroups, this process is absent (Fig.13B). However, in *P. neogaeus* and *P. brachyurus*, the process is absent as well. The absence of this anterior process in these two species is interpreted as a reversal of its presence, an apomorphy of these two species (see page 94 for the related discussion). – **TS 21:** The anterior process of the pharyngeal pad of the basioccipital bone absent [0], or present [1].

17. Parasphenoid bone (Fig.13D-E). The anterior part (in front of the ascending wing) of the parasphenoid in Hemitremitians is dorsally bent. The angle α (Fig.13A) is herein defined as the angle between the horizontal line extending from the ventral side of the posterior part (posterior to the ascending wing) of the parasphenoid and the ventral side of the anterior part of the bone (anterior to the ascending wing). The larger this angle is, the greater the bent in the anterior part of the parasphenoid (Fig.13D). In *Hemitremia* and in

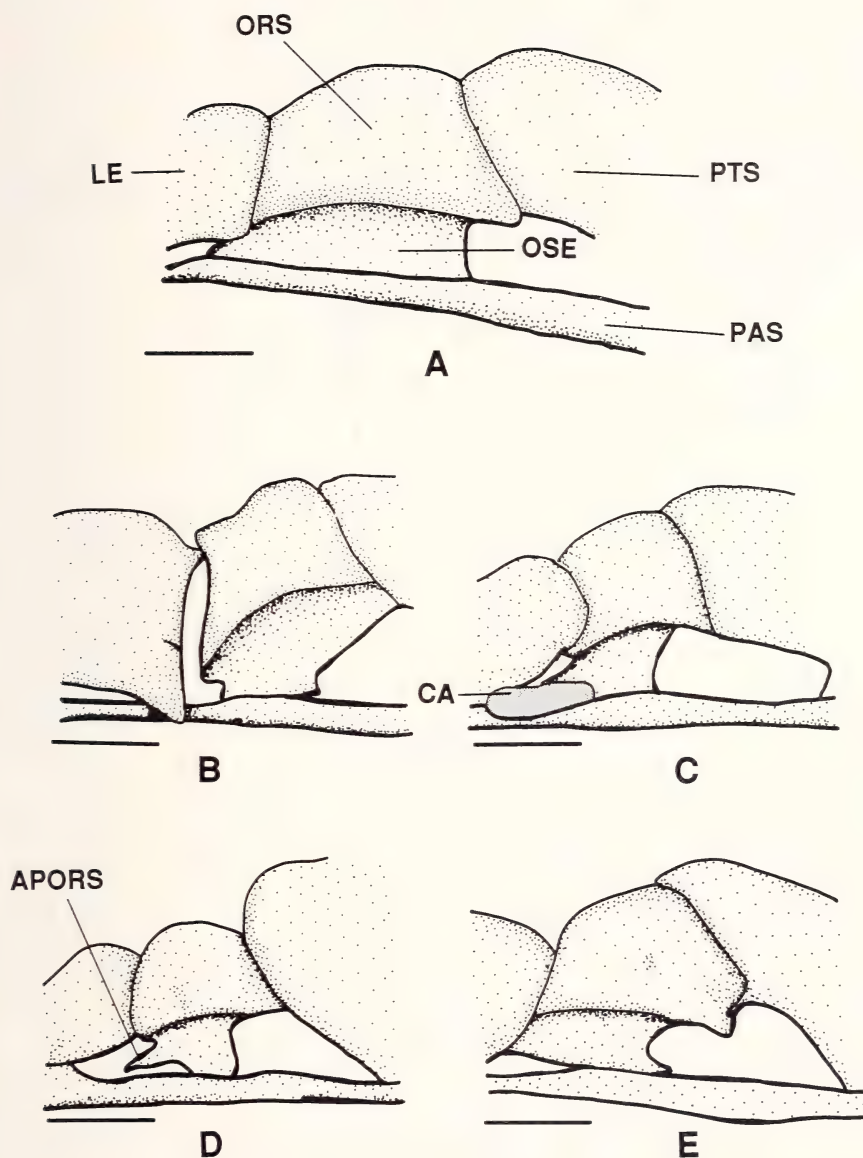


Fig.12: Diagrammatic lateral view of lateral ethmoid, orbitosphenoid, pterosphenoid, and parasphenoid in hemitremians and in the outgroup. A: *Lagowskiella lagowskii* (MCZ 32370, 103.5 mm TL); B: *Campostoma anomalum* (KU 3946, 61.0 mm TL); C: *Hemitremia flammea* (KU 18931, 55.9 mm TL); D: *Semotilus corporalis* (KU 18856, 58.0 mm TL); E: *Phoxinus neogaeus* (KU 8521, 53 mm TL). Scale bars = 1 mm.

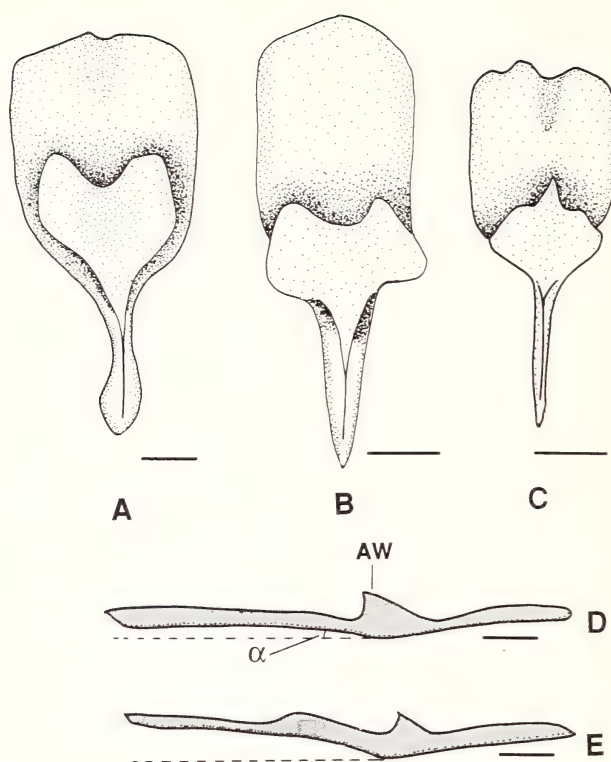


Fig.13: Basioccipital in ventral view (A-C), and parasphenoid in lateral view (D-E) in hemitremians and in the outgroup. A: *Platygobio gracilis* (KU 11950, 101.0 mm SL); B: *Couesius plumbeus* (KU 18881, 56.6 mm SL); C: *Phoxinus phoxinus* (CNUC uncat., 76.0 mm SL); D: *Hemitremia flammea* (KU 18931, 54.8 mm SL); E: *Phoxinus phoxinus* (CNUC uncat., 76.0 mm SL). Scale bars = 1 mm.

the outgroups, this angle is relatively smaller than that in other ingroups. – **TS 22:** Lateral view of the parasphenoid, angle α small [0], or large [1].

18. Quadrate bone (Fig.14A-C). Generally, in most ingroup and in the outgroups, the ventral margin of quadrate bears a very shallow concavity (Fig.14A, C). In *Margariscus*, the concavity is deep and narrow (Fig.14B). – **TS 23:** Ventral margin of the quadrate bearing a shallow and wide concavity [0], or a deep and narrow one [1].

19. Symplectic bone (Fig.14A-C). In most of the ingroup and in the outgroups, the dorsal margin of the symplectic bone bears a poorly developed process (or no process) articulating with the metapterygoid (Fig.14A, C). The process is better developed in *Margariscus* (Fig.14B) than that in other members of the ingroup and in the outgroups. – **TS 24:** Process at dorsal margin of the symplectic poorly [0], or well [1] developed.

20. Metapterygoid bone (Fig.14A-C). In *Couesius*, a deep notch is present at the posterior margin of the metapterygoid (Fig.14C). The notch is not present in other genera of the ingroup and outgroups (Fig.14A, B). – **TS 25:** A deep notch at the posterior margin of the metapterygoid absent [0], or present [1].

21. Opercle bone (Fig.15A-C). In most ingroup and outgroups, the anterodorsal process at the dorsal margin of the opercle is short and blunt (Fig.15A, B). In *Lagowskiella*, the

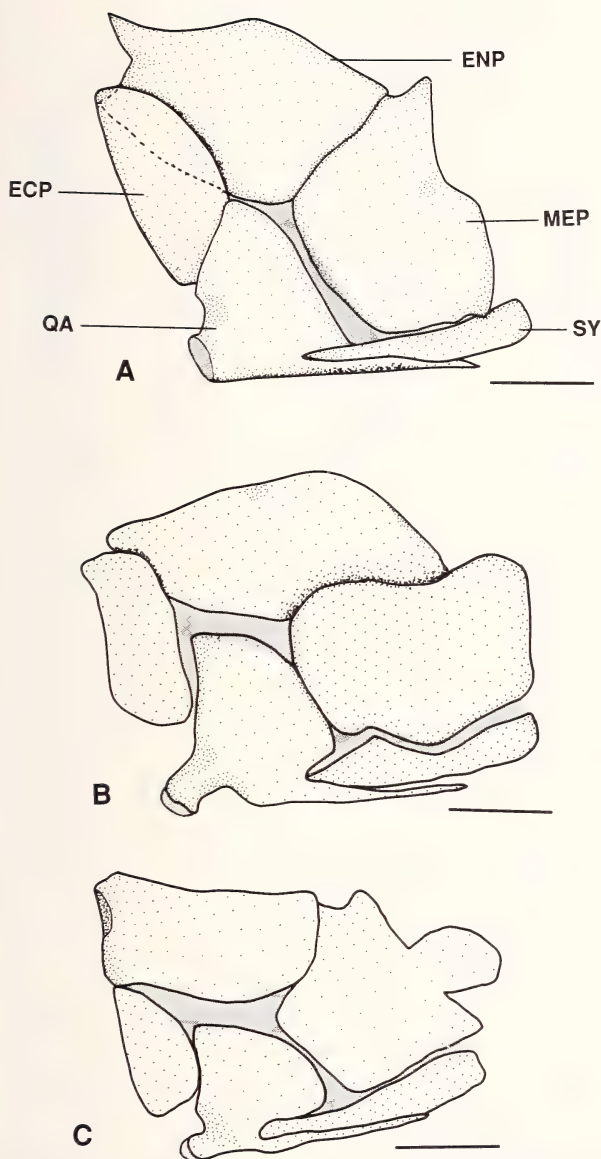


Fig.14: Lateral view of quadrate, symplectic, ectopterygoid, metapterygoid, and entopterygoid of hemitreminans and outgroup. A: *Campostoma anomalum* (KU 3946, 61.0 mm SL); B: *Margariscus margarita* (KU 19000, 70.8 mm SL); C: *Couesius plumbeus* (KU 18881, 56.0 mm SL). Scale bars = 1 mm.

process is long and sharp (Fig.15C). – **TS 26:** Anterodorsal process of the opercle short and blunt [0], or long and sharp [1].

22. Supraneural bones (Fig.16A-C). In the ingroup and the outgroups, the supraneural bones are present in front of the dorsal fin origin. Supraneural bone 4 is the largest of all supraneurals. In *Semotilus*, *Lagowskiella*, and *Couesius* supraneural 4 is very large, and

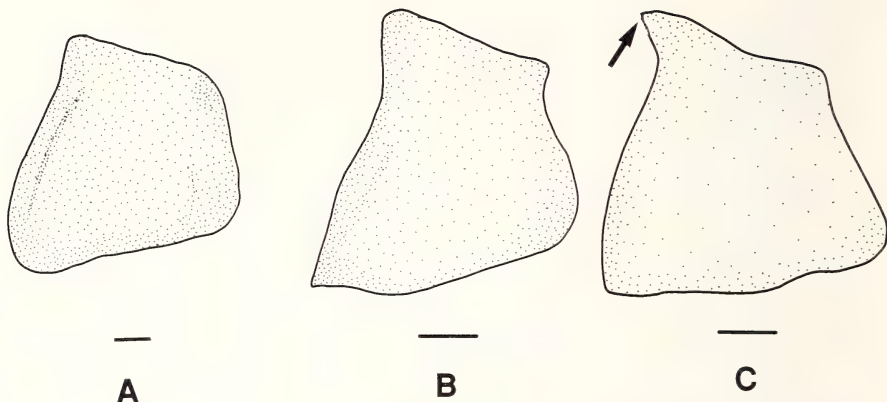


Fig.15: Opercle in lateral view in of hemitremin and in the outgroup. A: *Platygobio gracilis* (KU 11950, 101.0 mm SL); B: *Margariscus margarita* (KU 19000, 77.5 mm SL); C: *Lagowskiella lagowskii* (MCZ 32370, 103.5 mm SL). The arrow shows the anterodorsal process of the opercle. Scale bars = 1 mm.

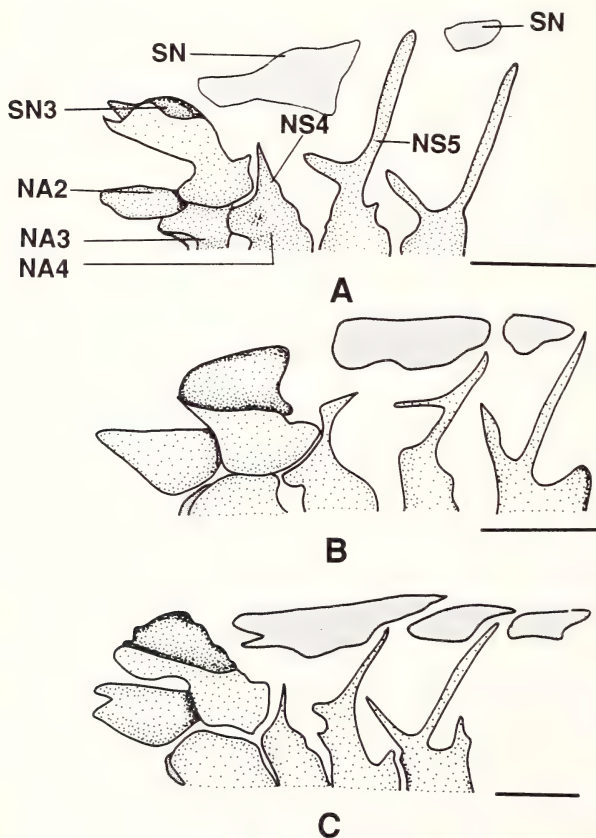


Fig.16: Lateral view of the neural arches and spines of the anterior vertebrae, the neural complex, and supra-neural bones of some species of hemitremin and outgroup. A: *Dionda episcopa* (KU 7427, 38.0 mm SL); B: *Phoxinus issykkulensis* (P-10696, 42.4 mm SL); C: *Couesius plumbeus* (KU 18881, 56.6 mm SL). Scale = 1 mm.

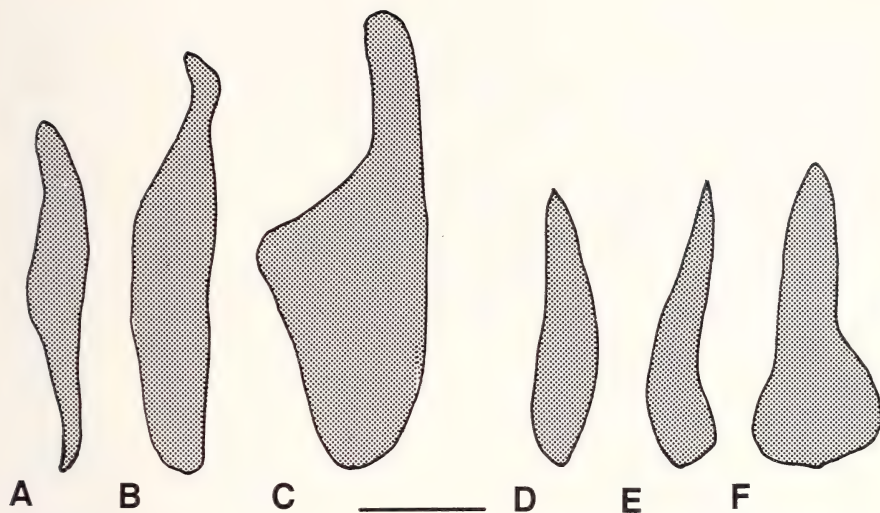


Fig.17: Lateral view of the posttemporal bone (A-C) and supracleithrum (D-F) of hemitremians and outgroup. A: *Campostoma anomalum* (KU 3946, 61.0 mm SL); B: *Couesius plumbeus* (KU 18881, 56.6 mm SL); C: *Hemitremia flammea* (KU 18931, 57.4 mm SL); D: *Dionda episcopa* (KU 16891, 54.1 mm SL); E: *Phoxinus cumberlandensis* (KU 18934, 52.0 mm SL); F: *Hemitremia flammea* (KU 18931, 57.4 mm SL). Scale bars = 1 mm.

extends from the dorsal margin of the neural complex to beyond the neural spine of the fifth vertebra (Fig.16C). In other genera of the ingroups and outgroups, the first supraneural bone is smaller (Fig.16A, B). – **TS 27:** Supraneural 4 small [0], or large [1].

23. Posttemporal bone (Fig.17A-C). Generally, the posttemporal bone is elongated and slender. In the outgroups and in most genera of the ingroup, the ventral portion of the posttemporal is slightly expanded (Fig.17A, B). In *Hemitremia*, however, the ventral portion of the bone is much larger than the dorsal portion of the bone (Fig.17C). – **TS 28:** Ventral portion of posttemporal bone slightly expanded [0], or broadly expanded [1].

24. Supracleithrum (Fig.17D-F). The supracleithrum is expanded at its middle portion. Therefore, the middle portion of the bone is slightly wider than its dorsal and ventral portions (Fig.17D-E). In *Hemitremia*, the supracleithrum is relatively short, the middle portion of the bone is extremely expanded, therefore, the middle portion is much wider than the ventral and dorsal portions of the bone (Fig.17F). – **TS 29:** Middle portion of the supracleithrum slightly expanded [0], or largely expanded [1].

Phylogenetic Relationships of the Hemitremian clade

Appendix I shows distribution of polarities of the 29 transformation series analyzed among the genera of the Hemitremian clade. Based on the matrix of Appendix I, PAUP (version 3.0) generated 135,135 trees with tree length from 43 steps to 57 steps. Two most parsimonious trees were generated with tree length = 43 steps, CI = 0.682 (CI excluding uninformative TS = 0.516), HI = 0.318 (HI excluding uninformative TS = 0.484), as shown

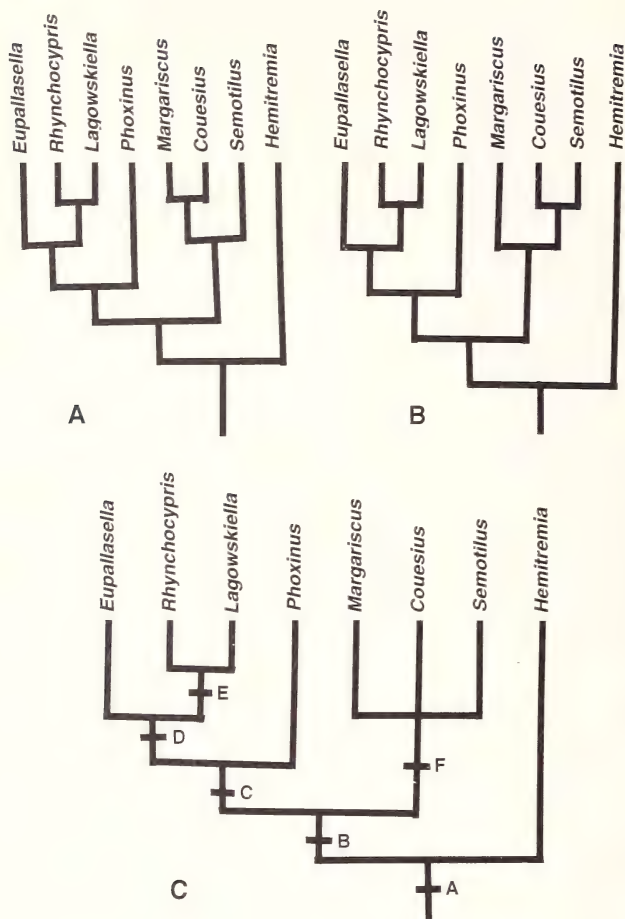


Fig.18: Phylogenetic hypotheses of relationships of the hemitremians. A, B: two equal most parsimonious trees; C: strict consensus tree of A and B. The synapomorphies supporting the nodes of tree C are as following. [The asterisk (*) at the right upper corner of the TS number marks the autapomorphy. The number following nodes A-F correspond to the transformation series (TS) number in page 26-39]: Node A: anterior placement of the anterior anal pterygiophores; Node B: 20, 22*; Node C: 8*, 9*; Node D: 18; Node E: 3; Node F: 13.

in A and B of Fig.18. A strict consensus tree was generated from these two trees (Fig.18C). The only difference between the two equal most parsimonious trees (Fig.18A, B) is the relationships among *Margariscus*, *Couesius*, and *Semotilus*. In tree A, [*Margariscus* + *Couesius*] is the sistergroup of *Semotilus*. In the tree B, *Margariscus* is the sistergroup of [*Couesius* + *Semotilus*]. The strict consensus tree (Fig.18C) shows an unresolved relationship of these three genera. The following discussion is based on the strict consensus tree (Fig.18C).

Two major clades are included in the Hemitremian clade: genus *Hemitremia*, and the *Phoxinus* clade including all the remaining genera of the Hemitremian clade.

The synapomorphies for each node of tree C (Fig.18:C) are given below in telegraphic form and include all changes on the node. The number of the transformation series is in parentheses followed by a brief description of the character. The asterisk (*) marks the

autapomorphy. The apomorphies, the number of species, and the geographic distribution of each genus are briefly discussed under the related node.

Node A: This node unites all eight genera of the Hemitreman clade as a monophyletic group. All genera of the clade share the anteriorly positioned anterior anal pterygiophores.

Hemitremia Cope, 1870 is the sistergroup of the other seven genera of Hemitremians. Five apomorphies are present in the genus *Hemitremia*: (15*) anterolateral margin of frontal bearing a deep notch; (16) anterior margin of orbital septum forming an anteriorly directed sharp process; (19) a cartilage present in front of the orbital septum in adult; (28*) ventral portion of the posttemporal bone expanded; and (29*) middle portion of the supracleithrum expanded.

One species, *Hemitremia flammea* (Jordan & Gilbert), is in the genus which occurs in the tributaries of the middle Cumberland, upper Duke, and middle Tennessee River in Tennessee, Alabama, and Georgia (Boschung 1980).

Node B: This node unites the other seven genera of Hemitremians as a monophyletic group. Two synapomorphies are shared by these seven genera: (20) the supraorbital bone small (reversed in *Lagowskiella* and *Couesius*), and (22*) the parasphenoid relatively bent.

Node C: Four Eurasian genera, *Eupallasella*, *Rhynchocypris*, *Lagowskiella*, and *Phoxinus*, are united by node C. They share two synapomorphies: (8*) scale bearing both apical and basal radii; (9*) scale on caudal peduncle elongated.

These four genera were previously considered one genus, *Phoxinus* (e.g., Berg 1949). Howes (1985) separated *Rhynchocypris*, *Lagowskiella*, and *Eupallasella* from *Phoxinus*, and gave all of them generic status.

Eight synapomorphies are shared by the species of *Phoxinus*: (4*) supraorbital canal interrupted between nasal and frontal bones; (6) preopercular canal ending at middle of the ascending arm of the preopercle; (7*) preoperculomandibular canal interrupted into mandibular and preopercular canals; (10*) breast scales deeply embedded in breeding males; (12*) breast scales bearing a series of tubercles at its apical margin in breeding males; (14*) scales on caudal peduncle bearing three or more tubercles at the scale's apical margin in breeding males; (17) orbital septum lower; (21) pharyngeal pad of occipital bone bearing an anterior process.

Nine species are recognized in *Phoxinus* herein. Species of this genus occur in Eurasia and North America. See below for morphology, phylogenetic relationships, biogeography, and systematics of this genus.

Node D: This node unites three genera, *Eupallasella*, *Rhynchocypris*, and *Lagowskiella*, as a monophyletic group with one synapomorphy: (18) orbital septum widely connected to the dorsal aspect of the parasphenoid.

Eupallasella Dybowski, 1916 bears two synapomorphies: (16) anterior margin of orbital septum bearing an anterior process; (19) a cartilage present in front of the orbital septum in adult.

One species, *Eupallasella percnurus* (Pallas) is recognized by Howes (1985). This species occurs in northeast China (Yang & Huang 1964) and Korea (Berg 1949).

Node E: *Rhynchocypris* and *Lagowskiella* are united at this node by one synapomorphy: (3) dorsal margin of primary lamella of the olfactory organ bearing a deep notch.

Species of *Rhynchocypris* Günther, 1889 share the following three synapomorphies: (1*) long fleshy rostral process; (5) left and right supratemporal canal connecting on the parietal (reversal); (21) pharyngeal pad of basioccipital bearing an anterior process. According to Howes (1985), three species are included in the genus *Rhynchocypris*: *R. oxycephalus* Sauvage & Dabry, 1874, *R. steindachneri* Sauvage, 1883, and *R. costatus* (Fowler, 1899).

R. oxycephalus occurs in the tributaries of Chang Jiang River, northern China, western and Eastern Korea (Berg 1949, Huang & Yang 1964). *R. steindachneri* occurs in Japan and Korea (Jordan & Hubbs 1925). *R. costatus* occurs in Japan (Fowler 1899).

The following four synapomorphies are shared by *Lagowskiella* Dybowski, 1916: (17) orbital septum lower; (20) supraorbital bone large (reversal); (26*) anterodorsal process of the opercle long and sharp; (27) supraneural 4 large.

One species, *Lagowskiella lagowskii* (Dybowski, 1869), is recognized by Howes (1985). This species occurs in east Asia, such as Korea and northeast China (Berg 1949, Yang & Huang 1964).

Node F: This node corresponds to the trichotomy of [*Margariscus* + *Couesius* + *Semotilus*]. The three genera above this node share one synapomorphy: (13) one or two tubercles centrally present on each breast scale in breeding males.

Though the relationship of the three genera is unresolved in the strict consensus tree, the two equal most parsimonious trees (Fig. 21A, B) resolve the relationship. The difference of relationships in Trees A and B (Fig. 21A, B) is due to the different interpretation of two transformation series, TS 11 (shape of apical margin of breast scale) and TS 27 (size of the most anterior supraneural bone). In Tree A, TS 11[1] is considered a synapomorphy of *Couesius* and *Margariscus*, and TS 27[1] a homoplastic character in *Couesius* and *Semotilus*. In Tree B, TS 11[1] is interpreted a homoplastic character in *Margariscus* and *Couesius*, TS 27[1] a synapomorphy of *Couesius* and *Semotilus*.

Two apomorphies are found in the genus *Margariscus* Cockerell, 1909: (23*) presence of a deep notch at the ventral margin of the quadrate; (24*) the symplectic bearing a dorsal process.

A single species, *Margariscus margarita* Cope (in Günther 1868), belongs to *Margariscus* (Robins et al. 1991); it occurs in northern United States and Canada (Lee & Gilbert 1980). *M. margarita* used to be considered a species of *Semotilus* (e.g., Scott & Crossman 1973, Lee & Gilbert 1980). This species was recently separated from *Semotilus* (e.g., Johnston & Ramsey 1990, Coburn & Cavender 1992) because it is likely more closely related to *Couesius*, *Phoxinus*, or perhaps *Hemitremia* than to *Semotilus* (Robins et al. 1991). My study supports separation of the species from *Semotilus*, though the evidence does not support Robins et al. (1991). Neither of the two equal most parsimonious trees, nor the strict consensus tree show the sister group relationship of *Semotilus* and *Margariscus*.

Couesius Jordan, 1878 has seven apomorphies: (2*) presence of a posterior barbel; (6) preopercular canal ending at the middle of the ascending arm of the preopercle; (17) or-

bital septum lower; (18) orbital septum connecting broadly with the dorsal aspect of the parasphenoid; (20) supraorbital bone large (reversal); (25*) metapterygoid bearing a deep notch at its posterior margin; (27) the most anterior supraneural bone large. One species, *C. plumbeus* (Agassiz, 1850), is included in the genus (Robins et al. 1991), which mainly occurs in the western United States and Canada (Well 1980).

Semotilus Rafinesque, 1820a has three apomorphies: (5) the left and right portions of the supratemporal canal connected (reversal); (16) anterior margin of orbital septum forming an anterior process; (27) the most anterior supraneural bone large.

Four species, *Semotilus atromaculatus* (Mitchill, 1818), *S. corporalis* (Mitchill, 1817), *S. lumbee* Snelson & Suttkus, 1978, and *S. thoreauianus* Jordan, 1877 belong to *Semotilus*. The genus occurs mainly in eastern North America (Lee & Platania 1980, Gilbert 1980, Snelson 1980, Johnston & Ramsey 1990, Robins et al. 1991). A phylogenetic hypothesis of relationships among the four species of the genus was proposed by Johnston & Ramsey (1990).

Discussion

The relationships between *Phoxinus* and other minnow genera are an interesting and challenging problem that has attracted many ichthyologists' attention. At least four hypotheses have been proposed by previous authors through different approaches. My hypothesis on the phylogenetic relationships of *Phoxinus* with other genera (Fig.18C) differs from the previous ones. A brief discussion of the previous hypotheses is presented below.

Hypothesis 1: In a study of life history of *Clinostomus elongatus*, Koster (1939) noted that breeding males of *Clinostomus*, *Margariscus*, and *Couesius* had similar breast tuberculation. Koster (1939) therefore proposed a close relationship between *Phoxinus* and the group formed by *Margariscus*, *Clinostomus*, and *Couesius*. Koster (1939) correctly recognized the close relationships of *Margariscus* and *Couesius*. However, the breast tuberculation differs between *Phoxinus* and the group including *Margariscus* and *Couesius*, as discussed above. The breast tuberculation of *Clinostomus elongatus* is similar to that in *Margariscus* and *Couesius*, but this character might be homoplastic because *Margariscus* and *Couesius* are said to belong to the Chub clade, whereas *Clinostomus* belongs to the Shiner clade (Coburn & Cavender 1992).

Hypothesis 2: Like Koster (1939), Howes (1985, 1991) proposed a sistergroup relationship between *Phoxinus* and *Couesius* (forming the phoxinins of Howes) supported by the breast tuberculation. Two problems are present in this hypothesis. First, Howes did not recognize the observation that the breast tuberculation is also present in *Margariscus*, *Semotilus*, and *Clinostomus* (and he also seemed to be not aware of Koster's publication). Therefore, if the "breast tuberculation" of all genera bearing the tuberculation could be evaluated as homologous structures, more genera should be included in the phoxinins of Howes. Secondly, the breast tuberculation patterns of *Phoxinus* and *Couesius* are not similar one another (Chen & Arratia 1996). As discussed above, the breast tuberculation in the two genera should be evaluated as two transformation series. Therefore, the breast tuberculation does not support the sister group relationships of these two genera.

Hypothesis 3: Cavender & Coburn (1987) described the character of anteriorly positioned anal pterygiophores and proposed a monophyletic group including *Phoxinus*, *Semotilus*, *Couesius*, and *Hemitremia* based on this character. All these genera belong to the base of the Chub clade (Coburn & Cavender 1992). See "Monophyly of the Hemitremian clade and its position in the family Cyprinidae" for the discussion about this hypothesis.

Hypothesis 4: Instead of using breast tuberculation, Schmidt (1989) applied the anterior placement of the anterior anal pterygiophores discovered by Cavender & Coburn (1987) and proposed *Phoxinus* the sistergroup of *Semotilus*. However, this character is widely distributed among a few other genera, as discussed by Cavender & Coburn (1987), Coburn & Cavender (1992), and herein.

NON-OSTEOLOGICAL MORPHOLOGY

The morphological description and comparison among the species of *Phoxinus* are presented as two sections, the non-osteological and osteological morphology. In both sections, a brief review of the structure in cyprinids will be presented, followed by a detailed description of the structure in *Phoxinus* and the outgroup taxa (i.e., *Eupallasea*, *Rhynchocypris*, and *Lagowskiella*). Finally, a comparison among *Phoxinus* species and the outgroups, and a discussion on the polarity of the transformation series (TS) are presented. The number of transformation series in the Osteology is continuous with those in this section, and corresponds to the transformation series numbers in Appendices II and III.

Intraspecific variation will be discussed only in a few cases. Because of the ontogenetic variation of certain structures, the description and comparison among the species is based on similar-sized adult specimens. In a few cases young specimens are also used to obtain ontogenetic information.

External Morphology

Mouth (Fig.19A-C)

The mouth in cyprinids shows significant variation, such as mouth shape, width of the mouth opening (mouth gape), relative length of the upper and lower jaws, and morphology of the lower jaw. The mouth can be almost vertical (e.g., *Toxabramis houdemeri*), oblique (e.g., *Erythroculter dabryi*), or horizontal (e.g., *Xenocypris fangi*) (Wu 1964). The shape of the mouth can be partially demonstrated by degree of the mouth angle: the smaller the angle, the more horizontal the mouth; the larger the angle, the more oblique the mouth. The mouth gape can be large enough to reach below the middle of eye (e.g., *P. neogaeus*), or very small only approaching the anterior margin of the nasal opening (e.g., *Plagiognathops microlepis*) (Yang 1964).

In most cyprinids, the lower and upper jaws are almost equal in length (or the lower jaw is slightly shorter or longer than the upper one) (e.g., *Notropis* spp., *Xenocypris yunnanensis*); however, a much longer lower jaw (than the upper one) (e.g., *Luciobrama macrocephalus*), or a much longer upper jaw (e.g., *Varicorhinus tungting*) are also present in some species of the family. In most cyprinids, the structure of the mouth is relatively sim-

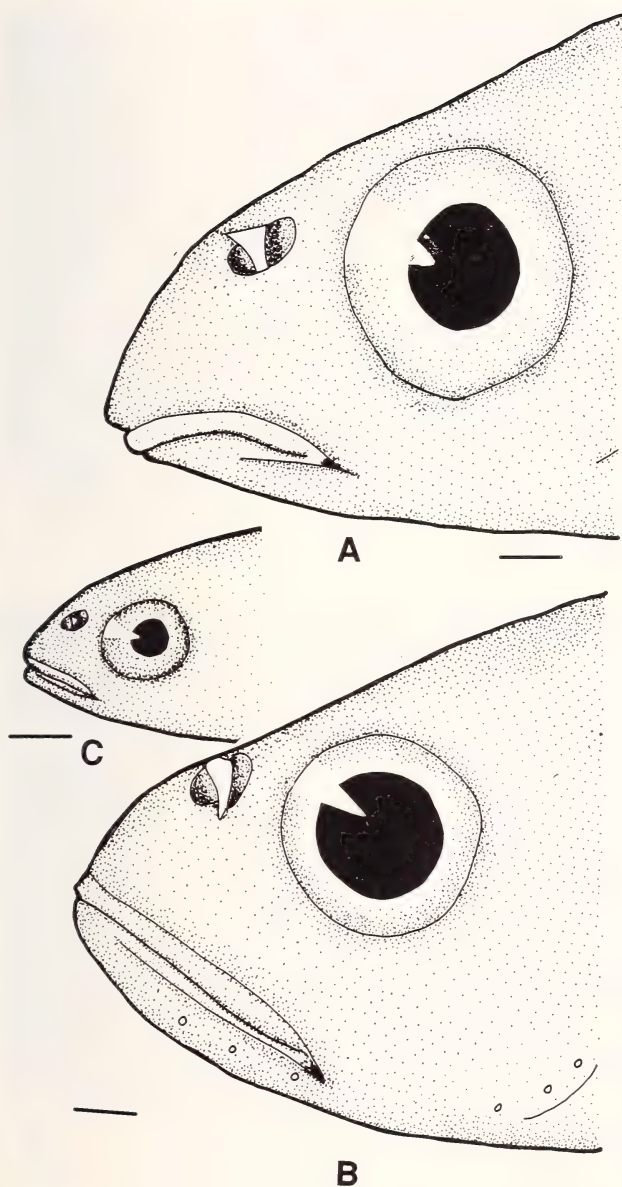


Fig.19: Diagrammatic lateral view of anterior portion of head of some species of *Phoxinus*. A: *P. oreas* (KU 3259, 61.6 mm SL); B: *P. neogaeus* (KU 14254, 55.4 mm SL); C: *P. neogaeus* (ANSP 5408, 20.0 mm SL). Scale bars = 1 mm.

ple (e.g., species of *Phoxinus*), however, in some species, the mouth, especially the lower jaw, presents a very complicated structure, such as a “sucking disk” (e.g., *Garra orientalis* – Nichols 1943).

Morphology of the mouth in *Phoxinus* is relatively simple. All *Phoxinus* species have a terminal or slightly subterminal mouth; the lower jaw is equal to, or slightly shorter than the upper one. No barbel is present (Fig.19 A-C). In *P. oreas* and *tennesseensis*, the mouth angle is small ($\leq 55^\circ$) (TS 1[0]), so the mouth gape is horizontal. In other species, the mouth angle is large ($\geq 60^\circ$) (TS 1[1]) (Fig.19B), and the gape is slightly oblique. In *P. neogaeus*, the mouth gape extends to below the middle of the eye's pupil (TS 2[1]); in other species of the genus, however, the gape never reaches the middle of the pupil (TS 2[0]). In the outgroups, the mouth angle is small ($\leq 55^\circ$), and the mouth gape never extends to below the middle of the eye pupil.

The mouth angle and the gape length increase during growth in species of *Phoxinus*. For instance, in *P. neogaeus*, in a 20 mm standard length specimen, the mouth angle is small and the gape is short (almost reaching the anterior margin of eye); in a 55.4 mm standard length specimen, the angle is much larger and the mouth gape reaches middle of the pupil (Fig.19B, C). Phillips (1969a) showed the mouth of *P. erythrogaster* was less oblique than that of *P. eos*.

Olfactory organ (Figs. 20A-B, 21A-D)

Olfactory organ is a chemical receptor in fish, which can respond to chemical stimuli other than the qualities of sweet, bitter, salty and acid (Harder 1975). In all cyprinids, two nasal openings (anterior and posterior ones) are present on each side of the head. The anterior nasal opening is generally smaller than the posterior one. A nasal bridge is present between the anterior and posterior openings. In *Phoxinus*, the anterior opening is smaller and forms a short ellipse, and the posterior one is an elongated ellipse. No variation in shape of the nasal openings is observed in the genus *Phoxinus*.

A erect structure (nasal septum) is present from dorsal side of the bridge (Fig.20A, B). This nasal septum is an extension of the skin on the bridge. In *P. phoxinus*, *brachyurus*, and *neogaeus*, the dorsal side of the nasal septum is deeply concave (TS 3[1], Fig.20A); whereas, in *P. erythrogaster*, *cumberlandensis*, *tennesseensis*, *oreas*, *eos*, and *issykkulensis*, the nasal septum is not concave on its dorsal side (TS 3[0], Fig.20B) – a similar condition found in the outgroups.

The entire margin of the anterior nasal opening is erect (TS 4[0]) in most *Phoxinus* species and in the outgroups. In *P. erythrogaster*, the middle of the anterior margin is not erect (TS 4[1], Fig.20B).

Similar to the condition in most cyprinids, the olfactory organ in *Phoxinus* is composed of primary lamellae and axis (raphe). No secondary lamellae are present in *Phoxinus*. (In some cyprinids, e.g., *Parabramis pekinensis*, secondary lamellae are present on the primary ones – see Chen 1988b.) Numerous melanophores are present on both primary lamellae and axis.

Morphology of the axis and number of the primary lamellae vary ontogenetically. For instance, in *P. neogaeus*, the axis of the olfactory organ is very short and located at the anterior part of the organ, five primary lamellae are present in a 25 mm standard length individual (Fig.21D). In a 30 mm standard length individual, the axis is more elongated, almost reaching the middle of the organ, six primary lamellae are present. The axis is

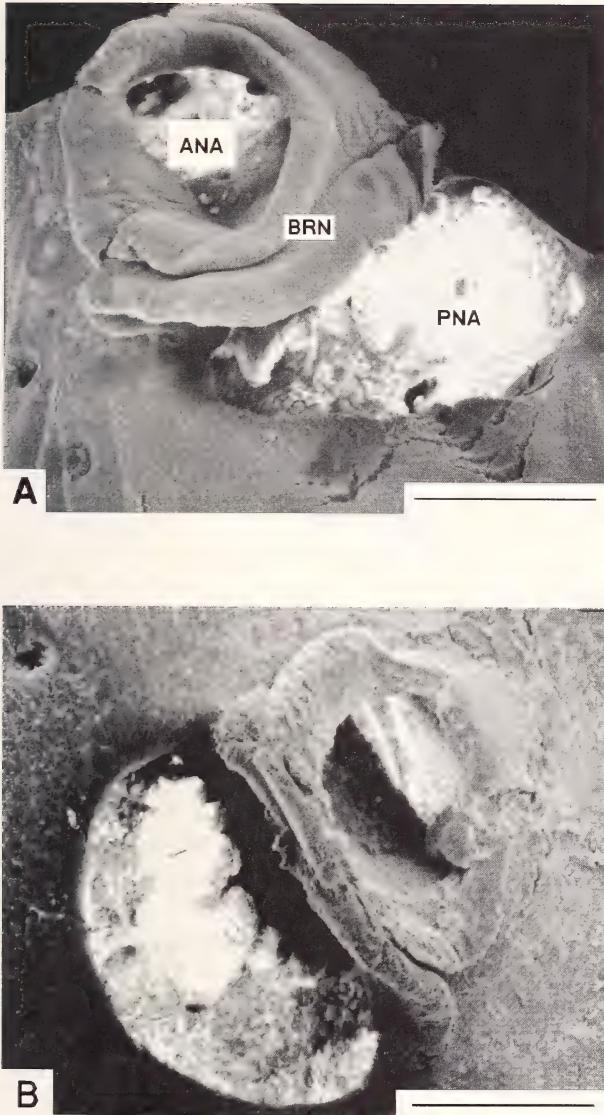


Fig.20: Nasal openings of (A) *Phoxinus phoxinus* (ZFMK, Series b, 80.5 mm SL), and (B) *P. erythrogaster* (KU 10629, 62.2 mm SL). Scale bars = 60 μm.

elongated, reaching middle of the organ, and the primary lamellae increase to eight by 51.8 mm standard length (Fig.21E). As a rule, the number of the primary lamellae increases ontogenetically until adult size is reached (Tab.1; Chen 1988b, Chen & Arratia 1994).

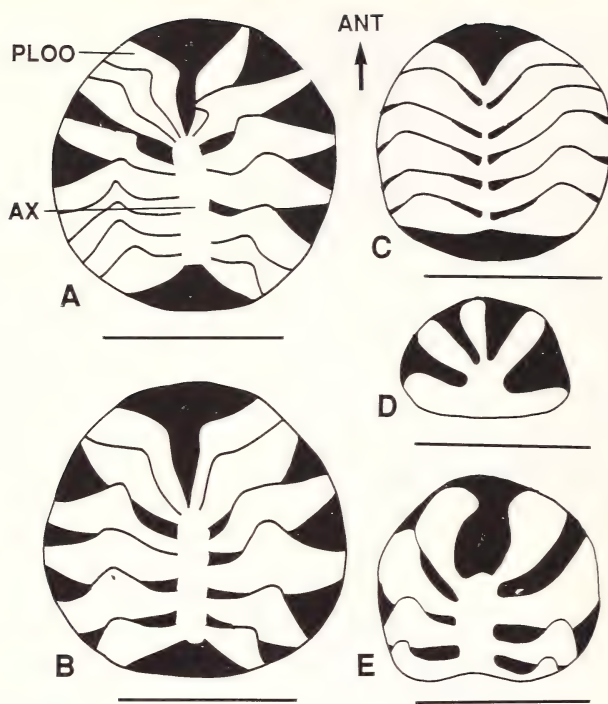


Fig.21: Diagrammatic dorsal view of the olfactory rosette of some species of *Phoxinus*. A: *P. phoxinus* (KU 22853, 56.4 mm SL); B: *P. erythrogaster* (KU 3895, 63.1 mm SL); C: *P. eos* (KU 4578, 41.8 mm SL); D: *P. neogaeus* (UT 44.2894, 25.0 mm SL); E: *P. neogaeus* (KU 14254, 51.8 mm SL). Scale bars = 1 mm.

Primary lamellae (Fig.21A-E): Chen (1988b) reported different shapes of primary lamellae in cyprinids, such as oar-shaped (e.g., *Saurogobio dabryi*), and hooked-shaped (e.g., *Diptychus pachycheilus*). Shape of the primary lamellae varies intra- and intergenerically in cyprinids (Chen 1988b). In adult specimens of *Phoxinus* species, the primary lamellae are oar-shaped and placed at the lateral and medial sides of the axis which is elongated and located at the median of the olfactory organ from the anterior margin to the middle of the organ. Variations of the primary lamellae are present in the shape of its dorsal margin and the number of the primary lamellae.

The dorsal margin of the primary lamellae is convex in the species of *Phoxinus*. Therefore the convex portion is higher than rest of the dorsal margin. In *P. phoxinus* and *erythrogaster*, the highest portion of the dorsal margin of primary lamellae is close to the axis (TS 5[1], Fig.21A-B). In all other species of *Phoxinus*, such as *P. brachyurus*, *neogaeus*, and in the outgroups, the highest portion is positioned off the axis (TS 5[0], Fig.21C).

Number of primary lamellae in adult individuals of the same species does not change significantly within species (Chen 1988b, Chen & Arratia 1994), though the number varies ontogenetically. In cyprinids the number of primary lamellae varies from 10 (e.g., *Phoxinus eos*) to 60 (e.g., *Mylopharyngodon piceus*) (Chen 1988b). In *Phoxinus*, the number of primary lamellae varies from 10 (*P. eos*) to 16 (*P. phoxinus*). In *P. phoxinus*, 16 primary lamellae are present (TS 6[1]); in all other *Phoxinus* species and in the outgroups, the number of the lamellae is 10-13 (TS 6[0]) (Tab.1).

Tab.1: Number (N) of primary lamellae of the olfactory organ in some species of *Phoxinus* with different standard length.

Species	SL(mm)	N	Species	SL(mm)	N
<i>P. cumberlandensis</i>	23.5	4	<i>P. neogaeus</i>	27.0	5
	42.0	10		34.5	8
	48.7	10		48.4	8
	50.9	9			
<i>P. eos</i>	26.4	7		52.0	11
	31.1	7	<i>P. oreas</i>	29.5	9
	41.5	9		33.5	9
	41.8	9		41.8	11
	45.0	10		43.1	10
<i>P. erythrogaster</i>	23.0	4		51.0	12
	26.0	6		53.4	13
	30.1	8			
	40.3	10	<i>P. phoxinus</i>	27.4	8
	46.5	12		46.8	10
	48.5	12		48.0	14
	50.2	12		60.1	16

Axis: Based on the shape of the axis, Chen (1988b) described six patterns of axes in cyprinids; i.e., Y, linear, elongated ellipsoidal, shorted ellipsoidal, bottle, and spindle patterns. Chen (1988b) proposed the elongated ellipsoidal pattern as plesiomorphic in cyprinids because this pattern is the condition present in most cyprinids, from which the shortened ellipsoidal, and linear patterns have derived independently.

Based on the number of primary lamellae and the shape of the axis, Yamamoto (1982) described eight types of olfactory organs in teleosts, lettered from A to H. Types F and G of the olfactory organ (Yomamoto 1982) are present in cyprinids. Chen & Arratia (1994) proposed 11 types (lettered from A to K) of olfactory organs in actinopterygians.

Extending from the anterior margin of the olfactory organ to the posterior portion of the organ, the axis is located at the middle portion of the olfactory organ in *Phoxinus*. Based on the criteria used by Chen (1988b), three morphological types of the axis can be described in *Phoxinus* as the following:

Elongated ellipsoidal type The axis is a narrow and elongated ellipse. This type is present in *Phoxinus phoxinus*, *oreas*, *erythrogaster*, *issykkulensis*, *tennesseensis*, and *brachyurus* (TS 7[0]; Fig.21A, B).

Linear type The axis is elongated, narrow and slender. This type is present in *Phoxinus eos* (TS 7[1]; Fig.21C).

Shorted ellipsoidal type The axis is wider, relatively short and elliptic in shape. This type is present in *P. cumberlandensis* and *neogaeus* (TS 7[2]; Fig.21E).

The elongated ellipsoidal type is present in the outgroups. According to the hypothesis on the relationships among different types of axes in cyprinids proposed by Chen (1988b)

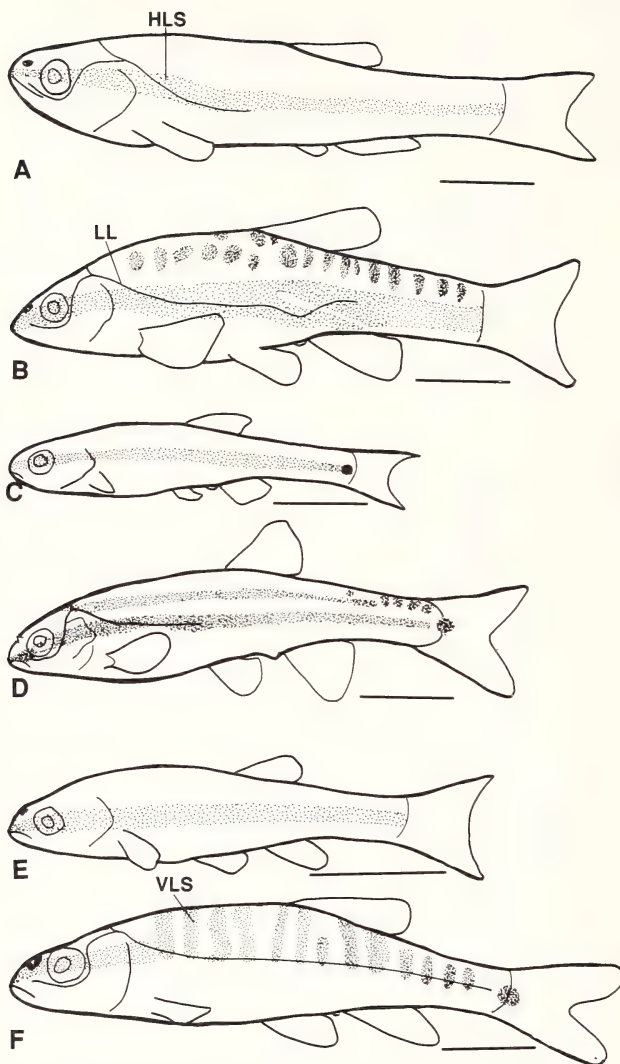


Fig.22: Lateral view of some species of *Phoxinus*, showing body lateral line and stripes. A: *P. neogaeus* (ANSP 48468, 51.0 mm SL); B: *P. oreas* (KU 3254, 47.6 mm SL); C: *P. erythrogaster* (KU uncat., 30.0 mm SL); D: *P. erythrogaster* (KU uncat., 46.0 mm SL); E: *P. phoxinus* (KU 22850, 27.4 mm SL); F: *P. phoxinus* (AMNH 71940, 52.1 mm SL). Scale bars = 1 mm.

and the outgroups comparison, I interpret the elongated ellipsoidal type the plesiomorphic condition, and the linear and the short ellipsoidal types of the axis independently derived from the plesiomorphic condition.

Lateral Line System (Fig.22A-F)

The lateral line system allows the fish to perceive a small pressure change in the surrounding water (Harder 1975). The lateral line system in cyprinids is composed of two sections, the cephalic and body lateral line. In cyprinids, the cephalic lateral line consists

of infraorbital, supraorbital, otic, preoperculomandibular, and supratemporal canals (Reno 1969). The body lateral line can be incomplete (not extending to the base of the caudal fin, e.g., *Rhodeus sinensis*), or complete (terminated at the base of the caudal fin, e.g., *Rutilus rutilus*).

Cephalic lateral line. As discussed in previous section, three characteristics of the cephalic lateral line are present in *Phoxinus*.

1. The supraorbital canal is interrupted between the frontal and nasal bones (Fig.6D).
2. The preopercular canal extends up to the middle of the preopercular's ascending arm only (Fig.8C).
3. The preoperculomandibular canal is divided to the mandibular and the preopercular canals. These two portions do not connect with each other (Fig.9B).

Body lateral line (Fig.22A-F). All *Phoxinus* species bear the body lateral line which is continuous with the cephalic lateral line. The body lateral line in all species is interrupted in different regions and shows individual variations in the interruption.

Length of the body lateral line varies ontogenetically and phylogenetically. The body lateral line is shorter in young than in adults (Fig.22A-F). However, length of the body lateral line in adults has little variation in the same species. In *Phoxinus phoxinus*, *oreas*, *brachyurus*, *erythrogaster*, and in the outgroups, the body lateral line extends posteriorly to the caudal peduncle, even to the base of the caudal fin (TS 8[0]; Fig.22F); in other species of *Phoxinus*, the body lateral line reaches the middle flank between the origins of the pectoral and pelvic fins, or is even shorter (TS 8[1]; Fig.22A-B, D).

Genital Papilla (Fig.23A-D)

The genital papilla is present ventrally just anterior to the origin of the anal fin. Most *Phoxinus* species exhibit sexual dimorphism in the morphology of the genital papillae. Therefore, it is necessary to describe the papillae for the males and females separately.

Males (Fig.23B-C): The ventral surface of the genital papilla is smooth or bears a few skin pleats varying intraspecifically. In *Phoxinus tennesseensis* and *phoxinus*, the papilla bears a fleshy projection which extends beyond the anal orifice. In *P. tennesseensis*, the projection is short and blunt at its posterior end. In *P. phoxinus*, the projection is slender and longer. The projection is absent in other *Phoxinus* species. This projection is also present in *Rhynchocypris*, *Lagowskiella*, but absent in *Eupallasella* (Howes 1985). The projection is present in adult individuals only, not in young ones. Based on the ontogenetic data, I hypothesize presence of the elongated projection the apomorphic (TS 9[1]), and absence the plesiomorphic condition (TS 9[0]).

Females (Fig.23A, D): In all *Phoxinus* species, the ventral surface of the genital papilla bears skin pleats. The shape and number of the pleats vary individually. In *P. phoxinus*, a long and slender projection is present at the posterior end of the papilla (TS 10[1]). The projection is absent in the females of other *Phoxinus* species (TS10[0]). In some genera of the outgroups, e.g., *Rhynchocypris* and *Lagowskiella*, the papilla also bears a short projection, but in *Eupallasella* the projection is absent (Howes 1985). In *P. phoxinus*, the projection is absent in young specimens, and present in adult specimens. Based on the ontogenetic data, the presence of the long projection of the genital papilla in *P. phoxinus*

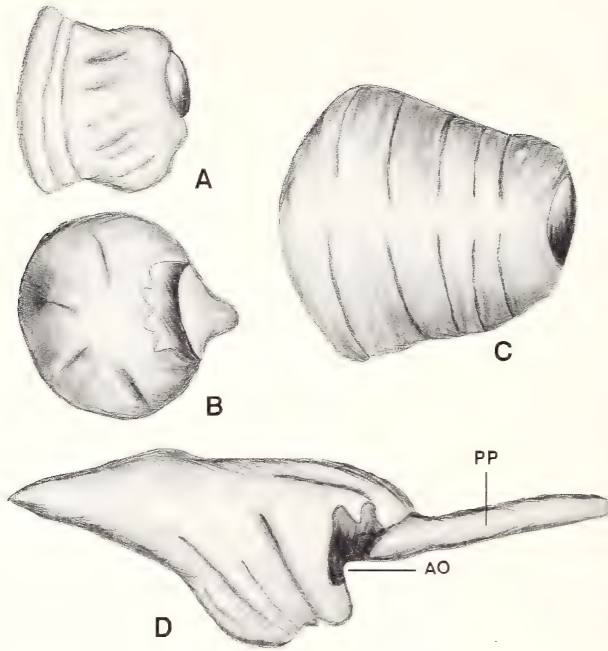


Fig.23: Ventral view of genital papillae of some species of *Phoxinus*. A: *P. cumberlandensis* (UT 44.1366, paratype, 56.8 mm SL, female); B: *P. oreas* (KU 3259, 55.9 mm SL, male); C: *P. tennesseensis* (UT 44.5274, 59.5 mm SL, male); D: *P. phoxinus* (ZFMK 585-586, 81.7 mm SL, female, lateral view). Scale bar = 1 mm.

is interpreted as apomorphic condition. Howes (1985) illustrated *P. phoxinus* as lacking the projection in both males and females. My observation differs from that of Howes (1985) in that a long projection is present in both genders of *P. phoxinus*.

Scales

In cyprinids, generally, scales cover the body, but the head is scaleless. All scales are cycloid and round to oval in shape. The margins of the scales are smooth, except for minor serrations in some species. The size of the scale varies from very large (e.g., *Cyprinus carpio*) to very small (e.g., *Phoxinus erythrogaster*). Similar to other cyprinids, the species of *Phoxinus* bear cycloid scales on the body, but no scale on the head. The scales in *Phoxinus* are very small and deeply embedded. They are more deeply embedded and smaller at the ventral aspect of the body than that at the body's lateral and dorsal sides.

The most distinguishing characteristics of scales in *Phoxinus* are the basal radii, and the elongate shape of the scales on the caudal peduncle. In *Phoxinus*, the radii are present almost evenly on the scale. The scale's focus is eccentric and close to the basal margin. No variation in radii, and shape of the scale is observed among *Phoxinus* species (Fig.10C).

Tuberculation

In cyprinids, breeding tubercles generally appear during the spawning season. Wiley & Collette (1970) studied fish breeding tubercles and listed at least 15 families belonging to

four different orders that have breeding tubercles. Eight of the 15 families are in the order Cypriniformes. Using Scanning Electron Microscope (SEM), Roberts (1982) studied the unculi of ostariophysan fishes and showed the fine surface structure of some breeding tubercles in these fishes. Wiley & Collette (1970) proposed that the breeding tubercles have four primary functions: maintaining the body contact during spawning, defending the nest and/or territories, stimulating females in breeding or spawning periods, and recognizing a mate.

Similar to other cyprinids, both mature males and females of *Phoxinus* species bear breeding tubercles during breeding season. The breeding tubercles are much less developed in females than in males. SEM study demonstrated that the morphology of tubercles is highly diversified among the different regions of the same individual, and in the same region of different species (Chen & Arratia 1996). Based on the observations used SEM, they studied the distribution and fine surface morphology of the tubercles in *Phoxinus*, and recognized nine morphotypes, coded from A to I in *Phoxinus*. The following discussion is based mainly on Chen & Arratia (1996) and only for the transformation series analyzed herein. The readers are suggested to see this paper for details. Because no data on tuberculation are available in the outgroups, the exoglossin clade (Coburn & Cavender 1992) is used as the outgroups to determine the polarity of the transformation series.

Tubercles are present on the dorsal side of the head in all species of *Phoxinus*. *P. phoxinus* has type E tubercles which are large and few (TS 11[1]; Fig.24B). The dorsal side of head in *P. phoxinus* has four or five large tubercles surrounding the dorsal margin of the orbit, and two or three tubercles surrounding the nasal openings (TS 12[1]; Fig.24B). Tuberculation similar to that in *P. phoxinus* is also present in *Campostoma* but not in other minnows studied here. In all other *Phoxinus* species, tubercle type E is not found, but type A and B tubercles are present (TS 11[0]); the tubercles are small and numerous, and randomly present from the posterior margin of the occipital to the anterior end of the snout (Chen & Arratia 1996) (TS 12[0]; Fig.24A).

Type I is present on the pectoral fin in *Phoxinus erythrogaster* only (TS 13[1]), not found in other species (TS 13[0]). In *P. phoxinus*, the whole opercle bears a very high density of tubercles (TS 14[1]); whereas in other species of *Phoxinus* only part of the opercle

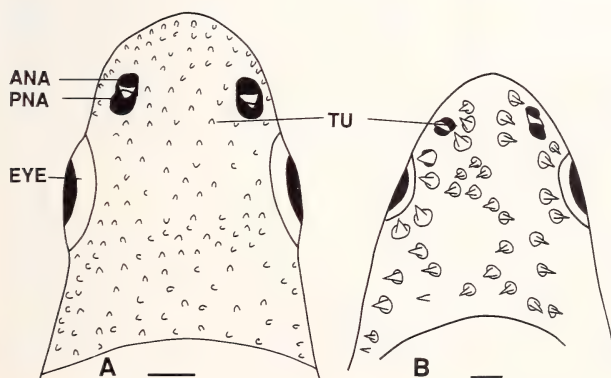


Fig.24: Dorsal view of heads of (A) *Phoxinus oreas* (KU 3259, SL 52.0 mm) and (B) *P. phoxinus* (ZFMK 657-659, 79.6 mm SL), showing distribution of tubercles on the dorsum of head. Scale bars = 1 mm.

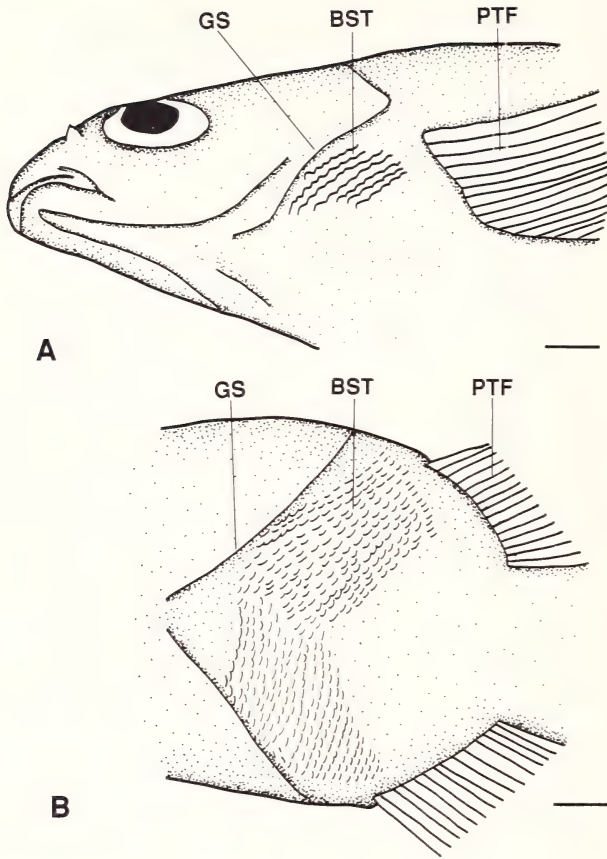


Fig.25: Profile of (A) lateral view of anterior body of *Phoxinus tennesseensis* (UT44.5274, 50.0 mm SL, male), and (B) ventral view of breast of *P. phoxinus* (KU 22859, 55.9 mm SL, female), showing the breast scales bearing tubercles. Scale bars = 1 mm.

bears tubercles at lower density (TS 14[0]) and some regions of the opercle have no tubercles (Chen & Arratia 1996).

On the ventral side of the body, tubercles are present only on the breast scales at the region anterior to the pectoral fin base and posteroventral to the gill cleft. The breast scales with tubercles are deeply embedded in *Phoxinus* species, as discussed previously. The tubercles are arranged as one row on the scale's apical margin. Except *P. cumberlandensis*, all other *Phoxinus* species bear less than 12 tubercles on the apical margin of each breast scale (TS 15[0]); whereas in *P. cumberlandensis*, each breast scale might have up to 16 tubercles (TS15[1]) (Chen & Arratia 1996).

In female *P. phoxinus*, the breast scales bear tubercles at their apical margin (Fig.25B). However, the tuberculation in the females is different with that in males (Fig.25A, B) (Chen & Arratia 1996). In female *P. phoxinus*, the breast scales are not deeply embedded, each scale bears about four small tubercles; in male *P. phoxinus* (and other species of *Phoxinus*), many more tubercles might be present on the apical margin of each breast scale. Tubercle type G is present in female *P. phoxinus* (TS 16[1]) which is not found in other

species (males or females) (TS 16[0]) or male *P. phoxinus*. The breeding female *P. phoxinus* bears tubercles on the scales at the anterior portion (between the left and right breast scales) of the ventral part of the body (TS 17[1]) (Fig.25B). No tubercles are found in this area in other minnows (TS 17[0]) (Fig.25A) (Chen & Arratia 1996).

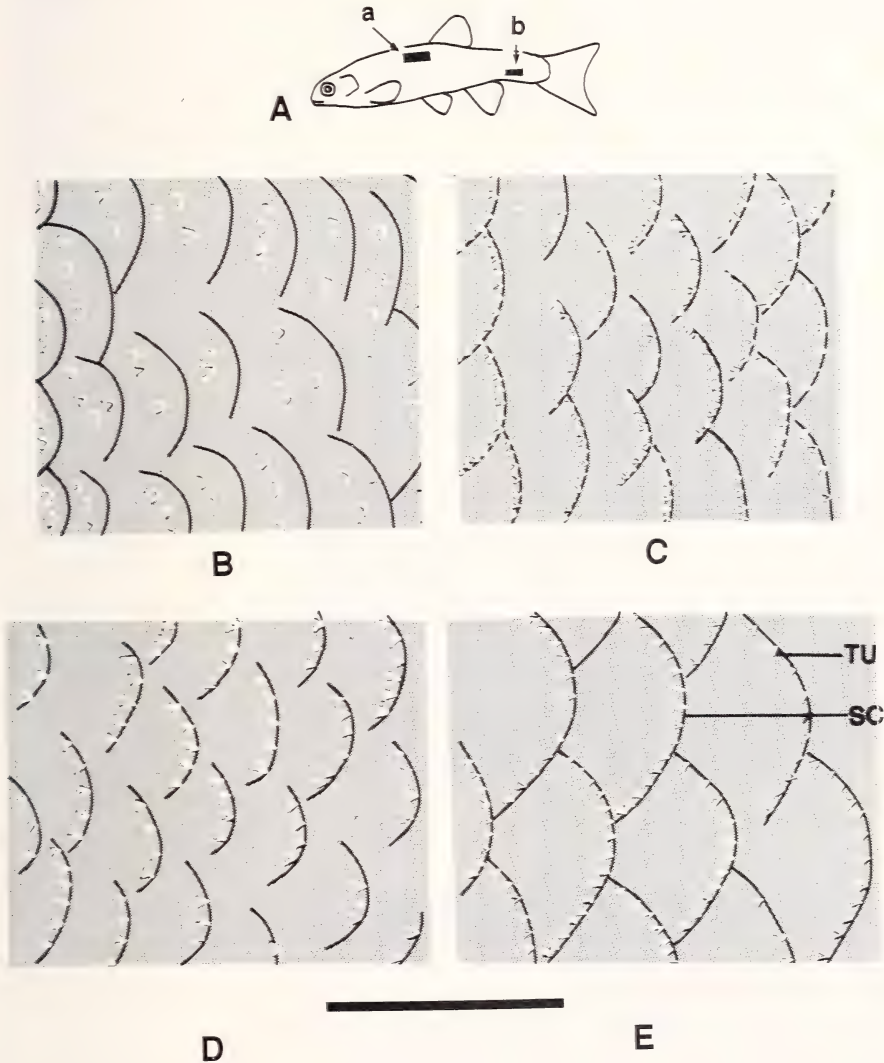


Fig.26: Scales of anterior lateral body (B-C), and of caudal peduncle (D-E) to show the distribution of tubercles on the scales of *Phoxinus*. A: A diagram showing the area presented in B-E (B-C: area a; D-E: area b); B: *P. cumberlandensis* (UT 44.4519, 50.0 mm SL); C: *P. phoxinus* (ZFMK 798, 65.5 mm SL); D: *P. erythrogaster* (KU 7300, 62.5 mm SL); E *P. phoxinus* (ZFMK 585-586, 81.7 mm SL). Scale bars = 1 mm.

In *P. phoxinus*, each scale on the anterior portion of the lateral body bears five to nine tubercles on the apical margin (TS18[1]) (Fig.26C). In other species, each scale bears one to four tubercles forward from the apical margin (TS18[0]) (Fig.26B).

In *P. phoxinus*, each scale on the lateral side of the caudal peduncle (especially at the ventrolateral portion of the caudal peduncle) bears up to 12 tubercles on the apical margin of the scale (TS 19[1]; Fig.26E). In other species of the genus, each scale on the caudal peduncle bears three to six tubercles on the apical margin (TS 19[0]; Fig.26D).

Tubercles on the dorsal side of the pectoral fin-rays are present in rows (Fig.27A, B). In *P. phoxinus*, tubercles are present from the second to sixth rays (total five rays) in three rows on each ray at the distal portion of the fin (TS 20[1]; Fig.27B). In other species, the tubercles are present from the second to fifth ray (total four rays), in two rows at the distal portion of the fin (TS 20[0]; Fig.27A) (Chen & Arratia 1996).

Few tubercles are present on the caudal fin rays in *P. phoxinus* (TS 21[1]), which are not found in other species of the genus (TS21[0]).



Fig.27: Tubercles on the dorsal side of the pectoral fin of (A) *Phoxinus oreas* (KU 3275, 43.5 mm SL, scale bar = 1.0 mm), and (B) *P. phoxinus* (ZFMK 657-659, 79.6 mm SL, scale bar = 176 μ m).

Coloration

Though coloration (or color pattern) of some cyprinids varies intraspecifically, the coloration of other cyprinids is useful for identification of the species (e.g., Yang & Huang 1964) and for phylogenetic analyses of some species or genera (e.g., Howes 1985). Color patterns for identification of the species include bands and stripes (number, shape, and location), speckles (size, shape, number and distribution), and the overall color of the body. However, as discussed by many authors (e.g., Heese 1981) and below, the color pattern might change ontogenetically and/or sexually in some species.

Generally, *Phoxinus* is a very colorful group of fishes. In fact, *P. erythrogaster* is considered by some authors to be the most beautiful North American freshwater fish (e.g., Forbes & Richardson 1920). All *Phoxinus* species bear either horizontal stripes or vertical bands (bars), or both.

The pigmentation described and compared below is based on alcoholic preserved adult specimens. The coloration of juveniles is mentioned in some cases for the ontogenetic change of the coloration in order to determine the polarity of the transformation series.

Numerous melanophores are irregularly present on the lateral body. In addition, all *Phoxinus* species bear vertical bands or horizontal dark stripes on the lateral body, and a dorsal dark stripe on the dorsum of the body extending from nape to in front of caudal fin. Based on the number, size, and shape of the stripes and bands on the lateral body, four types of the color patterns can be recognized on the lateral body in the *Phoxinus* species (Fig.22A-F).

1) *P. neogaeus*-type (Fig.22A): Only one uninterrupted horizontal stripe is present from the anterior end of the snout to the base of the caudal fin along the middle of the lateral body. The stripe is almost equal in width along its length. This type is present in *P. neogaeus*, *cumberlandensis*, *issykkulensis*, and *brachyurus*. In young individuals of *P. cumberlandensis*, the stripe is narrow and almost equal in width along its length (similar to other species in this type), but it is much broader in adults of the species.

2) *P. oreas*-type (Fig.22B): Lateral body bears one horizontal stripe and a few vertical bands. This type is observed in *P. oreas* only. The vertical bands are dorsal to the horizontal stripe which is interrupted into two sections (anterior and posterior section) at about the position of the anal fin. The anterior section of the horizontal stripe gradually curves down to base of the anal fin.

3) *P. erythrogaster*-type (Fig.22D): Lateral body bears two horizontal stripes without vertical bands. This type is present in *P. erythrogaster*, *eos*, and *tennesseensis*. In these species the lower horizontal stripe is broader and longer than the upper one. The lower one extends from the anterior end of the snout to the base of the caudal fin. In *P. erythrogaster* and *eos*, the upper strip is broken into blotches along the caudal peduncle.

4) *P. phoxinus*-type (Fig.22F): Lateral body has about 10 to 15 vertical bands without horizontal stripes. All vertical bands are almost equal in width, as well as the spaces between two bands. This type is present in *P. phoxinus* only.

The dorsal portion of the lateral body (dorsal to the lateral stripe) bears a few big speckles in *P. brachyurus* and *P. oreas*.

One horizontal stripe is present on lateral body in the outgroups. In all members of the ingroup, no matter what pigmentation pattern a species might bear in adults, young specimens (or larvae) always bear one horizontal stripe of equal width along the length of the lateral body (Fig.22C, E). The dorsal horizontal stripe (if any) appears later onto-

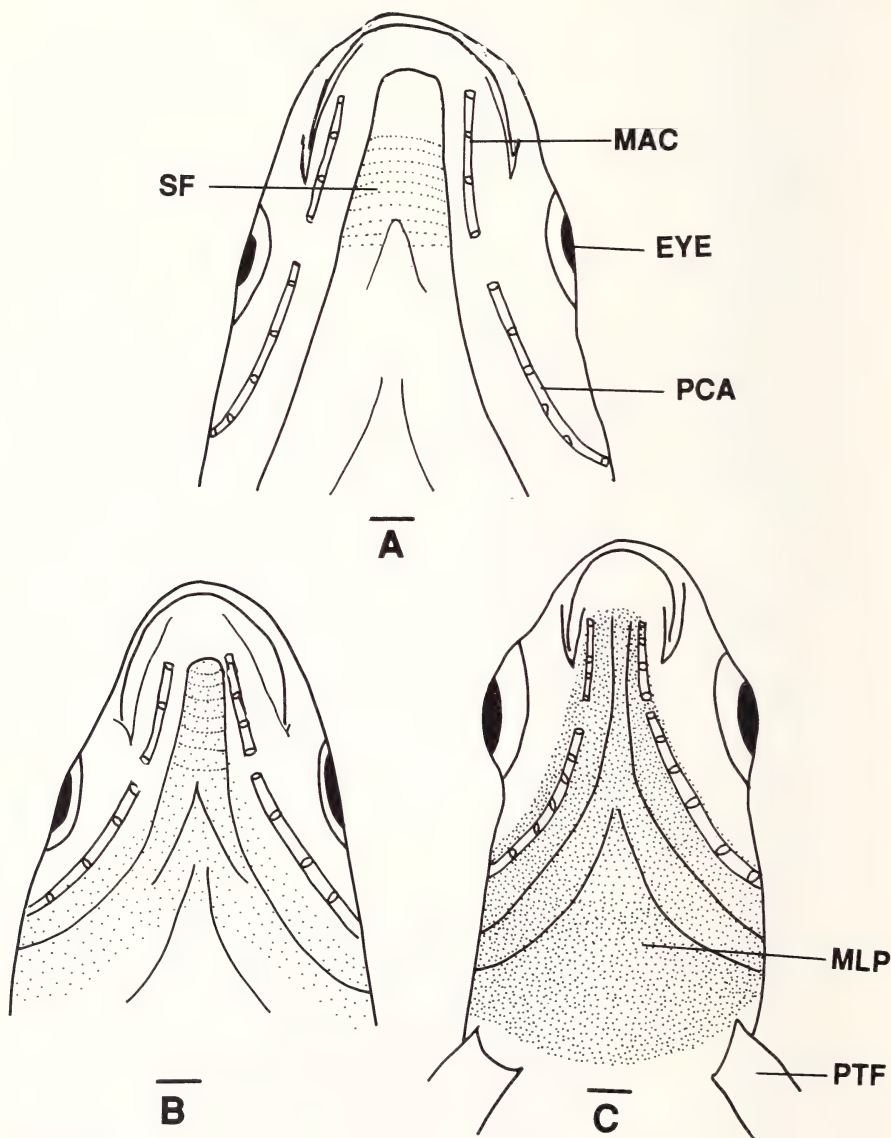


Fig.28: Profiles of ventral view of head, showing the distribution of melanophores. A: *Phoxinus neogaeus* [CA (SU) 09835, 59.5 mm SL]; B: *P. phoxinus* (KU 22860, 57.2 mm SL); C: *P. oreas* (KU 22257, 42.5 mm SL). Scale bars = 1 mm.

genetically. According to Tack (1940a), the vertical bands in *P. phoxinus* are resulted from the interruptions of the horizontal stripe. Therefore, based on the ontogenetic evidence and outgroup comparison, the *P. neogaeus*-type is hypothesized to be plesiomorphic (TS 22[0]), and other types to be apomorphic condition. Because no evidence is found to demonstrate how the apomorphic types are derived, I interpret the apomorphic conditions as independently derived from the *P. neogaeus*-type (*P. erythrogaster*-type: TS 22[1]; *P. phoxinus*-type: TS 22[2]; *P. oreas*-type: TS22 [3]).

The outgroups and most of the ingroup do not bear large speckles at the dorsal region of the lateral body (TS 23[0]). Therefore, the presence of the large speckles in *P. oreas* and *brachyurus* is proposed to be apomorphic (TS 23[1]).

In *P. brachyurus*, *neogaeus*, *issykkulensis*, *eos*, and *erythrogaster*, no (or very few) melanophores are present at the isthmus or the anterior portion of the breast (TS 24[0]; Fig.28A). In *P. phoxinus*, melanophores are present at the isthmus only (TS 24[1])

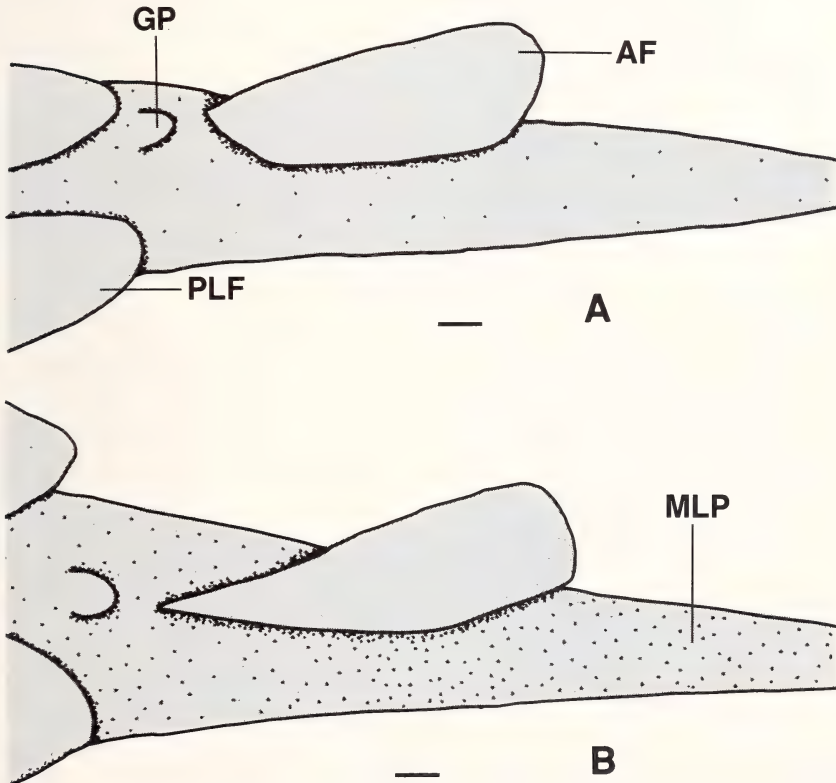


Fig.29: Diagrammatic profiles of ventral view of caudal peduncle of (A) *Phoxinus phoxinus* (KU 22860, 60.0 mm SL), and (B) *P. tennesseensis* (UT 44.5274, 58.5 mm SL), showing the distribution of the melanophores. Scale bars = 1 mm.

(Fig.28B). In *P. oreas*, *tennesseensis*, and *cumberlandensis* melanophores are present on both isthmus and breast (TS 24[2]; Fig.28C).

No melanophore is present on the isthmus and breast in the outgroups. In some young *P. oreas*, melanophores do not extend as far posteriorly as in adults. Thus the absence of melanophores (at both isthmus and breast) is hypothesized to be the plesiomorphic condition, the presence of melanophores at the isthmus, and the presence of melanophores on both isthmus and breast to be the apomorphic conditions.

No (or very few) melanophores are present on the belly in *Phoxinus* species. However, numerous melanophores are present on the ventral surface of the caudal peduncle in *P. brachyurus*, *neogaeus*, *issykkulensis*, and *tennesseensis* (Fig.29B). The presence of these melanophores is apomorphic (TS 25[1]) in comparison with the outgroups which do not bear melanophores in this region (TS 25[0]).

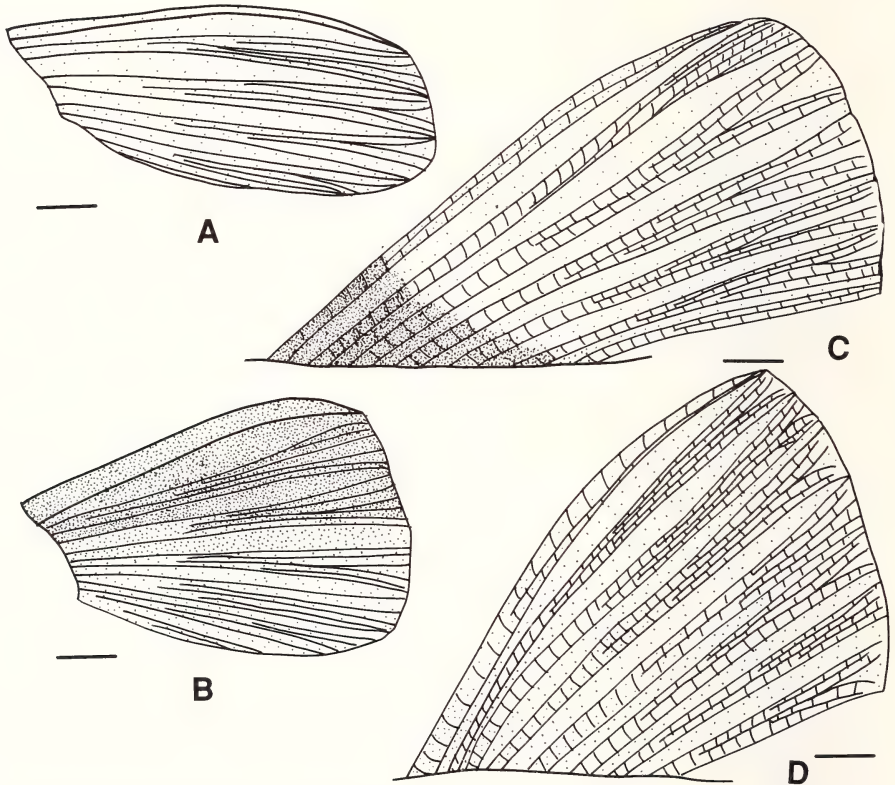


Fig.30: Profiles of dorsal view of pectoral fin (A-B), and lateral view of dorsal fin (C-D) of species of *Phoxinus* showing the distribution of the melanophores on the fins. A: *P. neogaeus*, unbreeding male (ANSP 48468, 59.7 mm SL); B: *P. neogaeus*, breeding male (UT 44.2870, 49.0 mm SL); C: *P. erythrogaster* (KU 7300, 59.5 mm SL); D: *P. tennesseensis* (UT 44.5274, 58.8 mm SL). Scale = 1 mm.

Similar to the outgroups, all *Phoxinus* species have a dark dorsal stripe at the dorsum of the body from the nape to in front of the caudal fin. No significant variation of the stripe is present in *Phoxinus*.

The first to sixth pectoral fin-rays and the interradi al membrane between the rays bear melanophores. The first ray has more melanophores than the remaining (Fig.30A, B). Rays and membrane behind the sixth ray bear few melanophores. Therefore, the first few rays and the membrane are darker than the rest, as in many cyprinids. In most *Phoxinus* species, breeding individuals show slightly darker pectoral fin than nonbreeding ones (TS 26[0]). However, in *P. neogaeus*, the pectoral fin is much darker (TS 26[1]) in breeding males than in nonbreeding males (Fig.30A, B). No variation of the color pattern is present in nonnuptial individuals among the species of *Phoxinus*.

All rays of the pelvic fin and interradi al membranes between rays bear melanophores. The first ray is darker than rest of the fin. No significant variation in color pattern of the pelvic fin is present in the genus.

Melanophores are present on the dorsal fin (Fig.30C, D), and higher density of the melanophores is present on the first ray than on other rays. The highest density of melanophores is at the fin's base. In *P. cumberlandensis* and *tennesseensis*, the melanophores are not much more concentrated at the base than rest of the dorsal fin (TS 27[0]; Fig.30D). In other species of the genus, the melanophores are much more concentrated at the base than rest of the dorsal fin, thus a very dark region is present at the base of the dorsal fin (TS 27[1]; Fig.30C). The latter condition is not present in the outgroups.

All anal fin rays and the interradi al membrane bear melanophores. The first fin ray (unbranched) has slightly more melanophores than the remaining rays. No dark patch is formed at base of the anal fin. No significant variation in anal fin pigmentation is present among the species of *Phoxinus*.

The caudal fin, like the dorsal one, bears melanophores on entire fin. More melanophores are present at the dorsal and ventral part of the caudal fin than the middle of the fin in most species of *Phoxinus*. A round blotch is present at the base of the fin (TS 28[0]) in *P. phoxinus*, *tennesseensis*, *erythrogaster*, *eos*, and *neogaeus*; the blotch is absent in other species of *Phoxinus* (TS 28[1]). In the outgroups, the caudal fin bears a round black blotch at its base.

Intestine and Gas Bladder

Intestine (Figs 31A-G, 32A-D)

The intestine of cyprinids is relatively simple without a stomach and pyloric appendages (caeca) (Harder 1975). However, in some species of cyprinids the most anterior section of the intestine is enlarged, forming a pseudogaster. The length and coiling patterns of the intestine show a lot of variation in cyprinids. Kafuku (1958) studied the intestines of cyprinids and defined six looping types in the family, i.e., (in order of increasing complexity) S-, Zacco-, Gobionidae-, Cyprinus-, Ctenopharyngodon-, and Acheilognathinae-types. Harder (1975) added another, the Screw-type, to the list. The morphology of the intestine is widely used in the identification of species and genera in Cyprinidae (e.g., Cross 1967, Cross & Collins 1975).

The intestine in *Phoxinus* is coiled and the looping pattern varies from very simple patterns to complicated ones. The intestine of the genus can be classified into the *Cyprinus*-type of Kafuku (1958) with different degrees of modifications (simpler or more complicated). The species of *Phoxinus* share the following two characteristics in the coiling pattern of the intestine (Figs.31A-G, 32A-D):

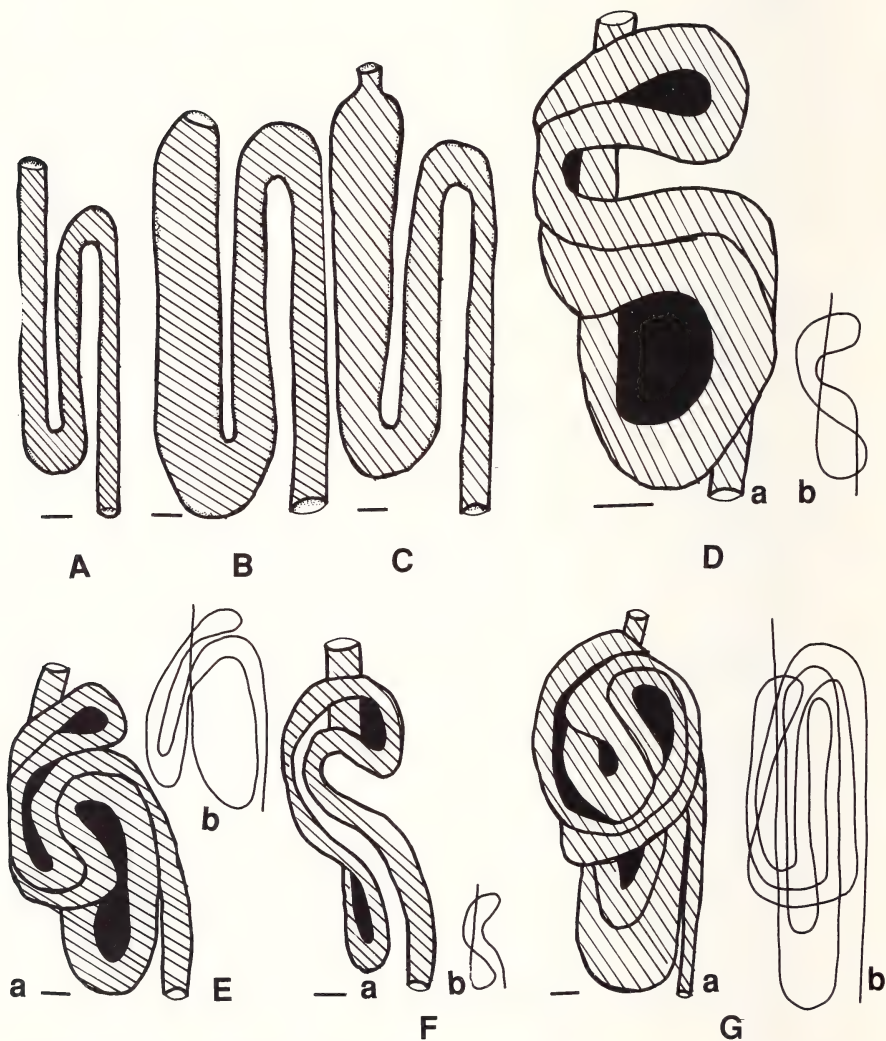


Fig.31: Dorsal view of intestine (a) and its diagrammatic model (b) of *Phoxinus*. A: *P. neogaeus* (KU 14254, 51.8 mm SL); B: *P. issykkulensis* (P-10696, 42.4 mm SL); C: *P. phoxinus* (KU 22853, 56.4 mm SL); D: *P. cumberlandensis* (ANSP 138365, 33.0 mm SL); E: *P. eos* (KU 4578, 41.8 mm SL); F: *P. cumberlandensis* (ANSP 138365, 24 mm SL); G: *P. cumberlandensis* (UT 44.3096, 51.3 mm SL). Scale bars = 1 mm.

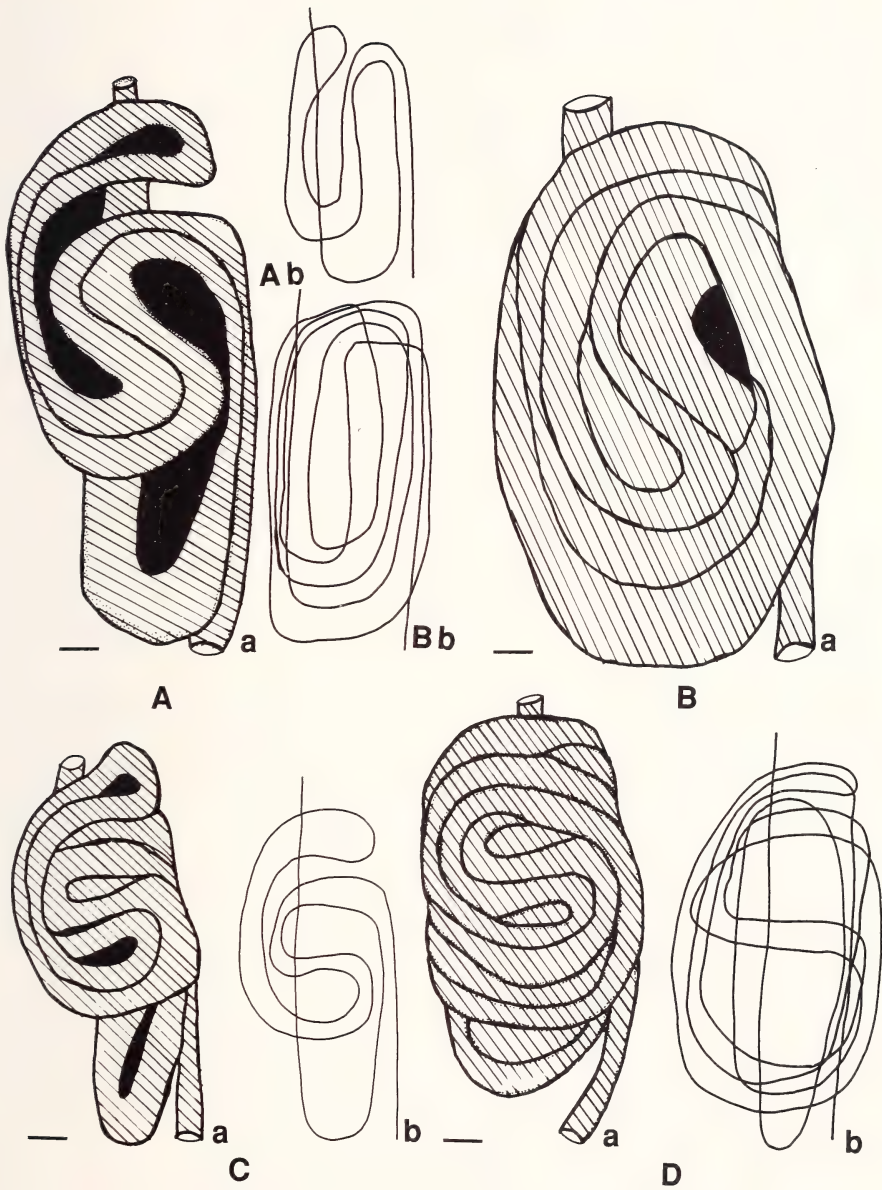


Fig.32: Dorsal view of intestine (a) and diagrammatic model (b) of some species of *Phoxinus*. A: *P. erythrogaster* (KU 3895, 63.1 mm SL); B: *P. tennesseensis* (UT 44.5274, 55.7 mm SL); C: *P. tennesseensis* (ANSP 134735, 47.6 mm SL); D: *P. oreas* (DU field no. B58-3, 59.9 mm SL). Scale bars = 1 mm.

1. The first loop is formed in the following way: the anterior portion of the intestine runs caudally at the left of the body, then turns right, forward then caudally to form the second loop.

2. The beginning of the intestine is located on the left side of the body, whereas the posterior end of the intestine is on the right side of the body.

Significant interspecific variation in *Phoxinus* occurs in the coiling pattern of the intestine. Based on the length, the number and the complexity of loops of the intestine, four types, i.e., *phoxinus*-, *eos*-, *cumberlandensis*-type, and *oreas*-type, can be defined in the genus.

P. phoxinus-type: The intestine is short; its length is shorter than, or equal to standard length of the individual; only 1.5 loops are formed. This type is present in *P. phoxinus*, *brachyurus*, *issykkulensis*, and *neogaeus* (Figs.31A-C).

P. eos-type: The intestine is longer than the *phoxinus*-type; its length is about 200% of standard length. Three loops are present. The third loop encloses most of the first one. This type is present in *P. erythrogaster*, *eos*, and *tennesseensis* (Figs.31E, 32A, C).

P. cumberlandensis-type: The intestine is longer than the *eos*-type. Its length is 230% of the standard length. The coiling pattern of the intestine is more complicated; six loops are present. This type is present in *P. cumberlandensis* only (Fig.31G).

P. oreas-type: This is the most complicated one in the four types. About 10 loops are formed. Its length is about 180% of the standard length. This type is present in *P. oreas* only (Fig.32D).

Ontogenetically, the younger individuals have simpler coiling patterns than the adults in the *Phoxinus* species with a coiled intestine. For instance, *P. cumberlandensis* which bears *cumberlandensis*-type in adults has two loops with a simple coiling in a 24 mm SL individual; two loops with more complicated looping are present in a 33mm SL individual; more complicated looping and more loops are present in a 51.3 mm SL specimen (Fig.31D, F, G). In the outgroups, the intestine is short and the coiling type is simple, similar to the *Phoxinus*-type. Therefore, I hypothesize the polarity of this transformation series is from simple pattern to complicated ones, i.e., *P. phoxinus*-type (TS 29[0]) → *P. eos*-type (TS 29[1]) → *P. cumberlandensis*-type (TS 29[2]) → *P. oreas*-type (TS29[3]).

Gas bladder (Figs.33A-B; 34A-H)

The gas bladder (air-bladder, swim bladder) in cyprinids consists of two chambers (anterior and posterior ones) and a constriction (or isthmus – Harder 1975) between the two chambers¹. A pneumatic duct (*tractus pneumaticus*) originates from the dorsal wall of the esophagus and connects with the posterior chamber or with the constriction at its posterior end.

The anterior chamber in *Phoxinus* is shorter than the posterior one. The anterior end of the anterior chamber is slightly broader than its posterior part. The posterior chamber is

¹ However, three chambers of the gas bladder are also found in some genera of Cyprinidae (e.g., *Megalobrama*, *Erythroculter*, see Yi & Wu 1964).

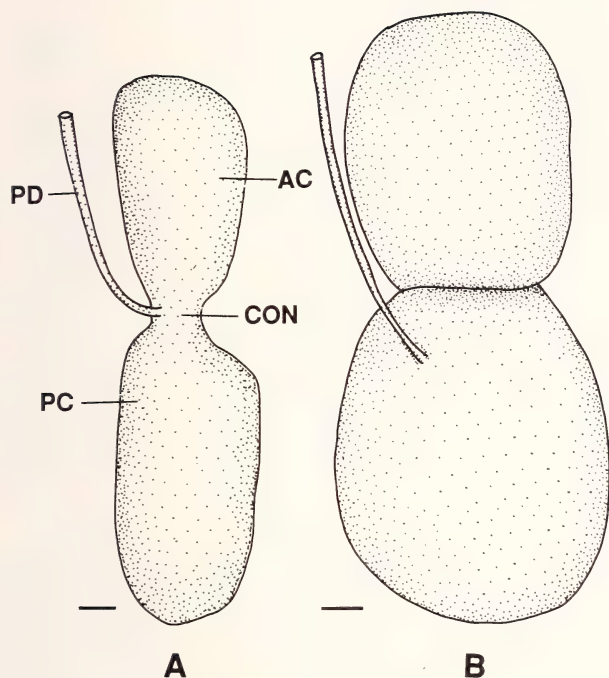


Fig.33: Dorsal view of gas bladder of (A) *Phoxinus erythrogaster* (KU 3895, 63.1 mm SL) and (B) *P. issykkulensis* (P-10696, 42.4 mm SL). Scale bars = 1 mm.

a long tube-like structure; its anterior portion is not broader than its posterior portion in some species of *Phoxinus*.

Morphological variation of the gas bladder among the species of *Phoxinus* is found in the shape of anterior and posterior chambers, the relative length of the two chambers, the length of the constriction, and the position where the pneumatic duct connects with the gas bladder.

The gas bladder is long and slender in *P. phoxinus* (TS 30[1]; Fig.34B). The gas bladder is very short and broad in *P. issykkulensis* (TS 30[2]; Fig.33B). Other species are similar to the outgroups in having a gas bladder that is broader and shorter than that in *P. phoxinus*, but narrower and more slender than that in *P. issykkulensis* (TS 30[0]).

The relative length between the posterior and anterior chambers also varies. Three different conditions can be recognized in the relative length of the two chambers.

(1) The anterior chamber is about 70% of the posterior one in length (TS 31[0]; Fig.34D). In *P. neogaeus* and *erythrogaster*, the anterior chamber is about 75% of the posterior chamber. In *P. tennesseensis*, *oreas*, *cumberlandensis*, *brachyurus*, and *eos*, the anterior chamber is about 70% in length of the posterior one.

(2) In *P. phoxinus*, the anterior chamber is less than 50% in length of the posterior one (TS 31[1]; Fig.34B).

(3) In *P. issykkulensis*, the anterior chamber is almost equal in length to the posterior one (TS 31[2]; Fig.33B).

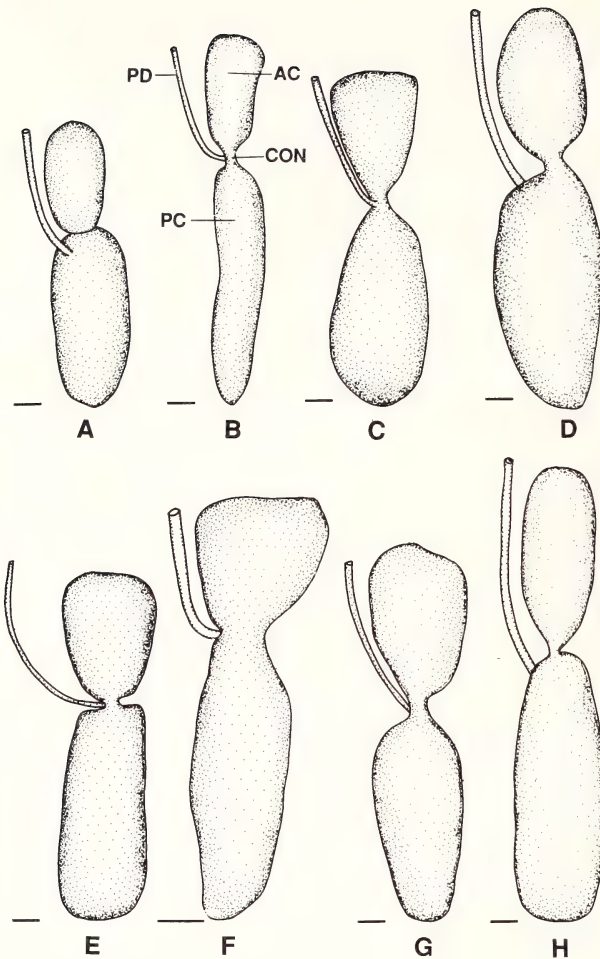


Fig.34: Dorsal view of gas bladder of *Phoxinus*. A: *P. eos* (KU 4578, 41.8 mm SL); B: *P. phoxinus* (KU 22853, 56.3 mm SL); C: *P. oreas* (DU field no. B-58-3, 59.9 mm SL); D: *P. tennesseensis* (UT 5274, 50.0 mm SL); E: *P. cumberlandensis* (UT 44.3096, 51.3 mm SL); F: *P. cumberlandensis* (ANSP 138356, 33 mm SL); G: *P. neogaeus* (KU 14254, 51.8 mm SL); H: *P. brachyurus* (MCZ 3006, 75.9 mm SL). Scale bars = 1 mm.

The condition in *P. erythrogaster* is plesiomorphic because it is similar to that in the outgroups, and other conditions are proposed to be apomorphic.

The constriction of the gas bladder is long and narrow in *P. phoxinus* and *neogaeus* (TS 32[2]; Fig.34B, G). It is shorter and broader in *P. oreas*, *brachyurus*, *erythrogaster*, *cumberlandensis*, and *tennesseensis* (TS32[1]; Fig.34C). It is very short, almost absent in *P. issykkulensis* and *eos* (TS 32[0]; Figs.33B, 34A). A very short constriction is present in the outgroups, and also in young specimens of *Phoxinus* species. Length of the constriction increases ontogenetically, as shown by *P. cumberlandensis* (Fig.34E, F). The polarity of this transformation series (TS 32) is therefore interpreted as very short [0] → short [1] → long [2].

The pneumatic duct connects to the anterior portion of the posterior chamber in *P. eos*, *brachyurus*, *issykkulensis*, and *tennesseensis* (TS 33[1]; Fig.34A). In other species of *Pho-*

xinus and in the outgroups, the duct connects to the constriction of the gas bladder (TS 33[0]; Fig.34C).

Peritoneum

The peritoneum is an epithelial membrane lining the interior of the abdominal cavity which contains the intestine and other organs. The peritoneum in *Phoxinus* varies in color. In *P. phoxinus*, *issykkulensis*, and *brachyurus*, the peritoneum is silver with few melanophores (TS 34[0]; Fig.35A). In all other species of *Phoxinus* (all are North American species), the peritoneum is dark with numerous melanophores (TS 34[1]).

As a rule of thumb, at least in North American cyprinids, species with a long intestine always have a black peritoneum (e.g., *P. erythrogaster*); and species with a short intestine have a silver peritoneum, except that a few species which bear short intestine have a dark peritoneum. *P. neogaeus* is one of the exceptions. I treat a short intestine with silver peritoneum as the plesiomorphic condition.

OSTEOLOGY

For each bone, the general morphology and its relationships with its neighbor elements are described. Then a comparison on shape and size of the bone among the species of *Phoxinus* and the outgroups are conducted, followed by a discussion on the phylogenetic significance and the polarity of the transformation series in the genus *Phoxinus*.

Following Harder (1975), I divide the skeletal system of *Phoxinus* into four sections, i.e., neurocranium, viscerocranium, vertebral column, and appendages.

Neurocranium

Similar to most cyprinids (e.g., Ramaswami 1955a, b), the dorsal aspect of the neurocranium of *Phoxinus* is relatively flat; the posterior portion of the neurocranium is slightly higher and wider than the anterior one. The neurocranium can be divided into five regions, i.e., the ethmoidal, orbital, otic, occipital, and basicranial region.

Ethmoidal Region

This is the most anterior region of the neurocranium. The bones in this region are composed of dermal (e.g., nasal bone) and endochondral (e.g., mesethmoid) elements. Bones included in the region are kinethmoid, supraethmoid, mesethmoid, lateral ethmoid, and preethmoid (cartilage). Among them, the kinethmoid, supraethmoid, and mesethmoid are single, whereas the others are paired elements. The vomer belongs to the basicranial region.

In *Phoxinus*, the supraethmoid, lateral ethmoid, kinethmoid, and preethmoid may be observed in the dorsal view of the ethmoidal region. The lateral ethmoid, preethmoid, and kinethmoid are visible in the ventral view. The mesethmoid can be observed dorsally only after the supraethmoid is removed, or posteriorly after removing the orbital region. The olfactory organ is placed in the olfactory capsule which lies on the ethmoidal region.

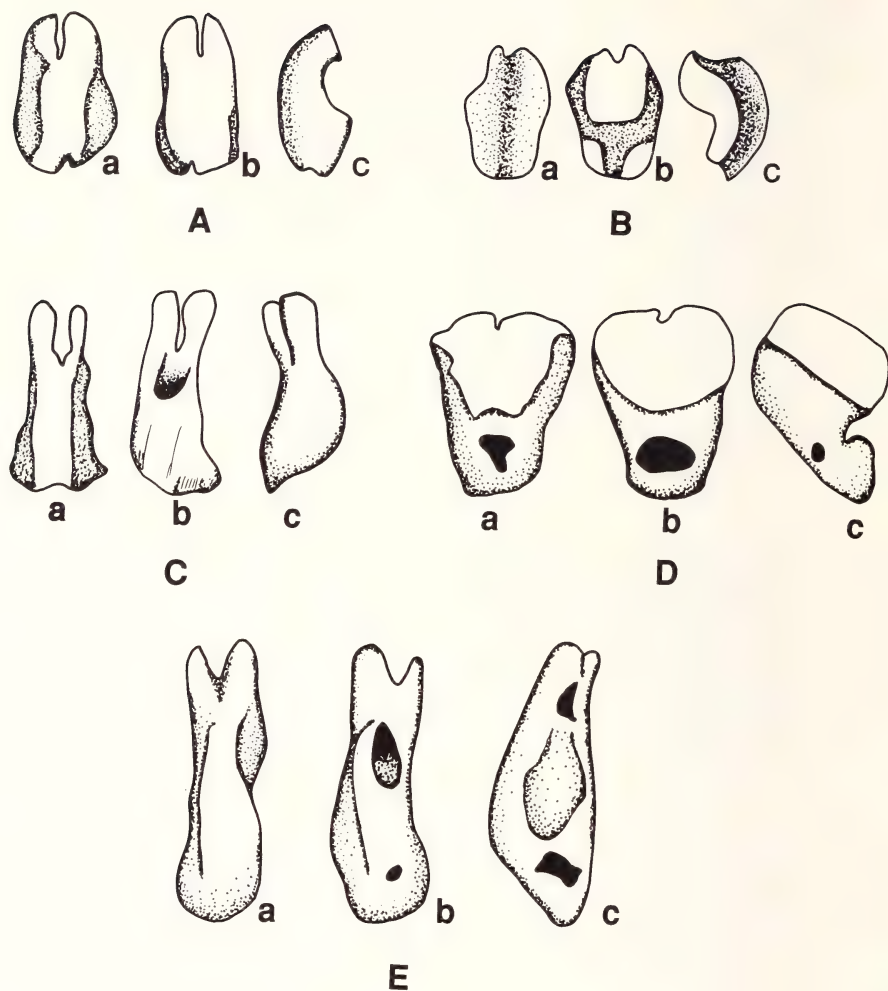


Fig.35: Kinethmoid of *Phoxinus* (a: anterior view; b: posterior view; c: lateral view). A: *P. erythrogaster* (KU 5773, 51.5 mm SL); B: *P. eos* (KU 12255, 43.0 mm SL); C: *P. cumberlandensis* (KU 18934, 52.0 mm SL); D: *P. neogaeus* (KU 8521, 53.0 mm SL); E: *P. phoxinus* (CNUC uncat., 76.0 mm SL). Scale bars = 1 mm.

Kinethmoid (Fig.35A-E). This small median endochondral bone is located at the anterior end of the neurocranium. This bone is bar-like, with numerous modifications on its dorsal and lateral aspects in cyprinids (Ramaswami 1955a, b). Via ligaments, the bone joins with the supraethmoid posteriorly, and maxilla and premaxilla laterally in cyprinids (Ramaswami 1955a, b, Harder 1975, Mayden 1989).

In *Phoxinus*, the kinethmoid-supraethmoidal ligament connects with posterodorsal side of the kinethmoid and with anterior side of the supraethmoid. The kinethmoid-maxillary ligament connects with the dorsolateral side of the kinethmoid and with a anterior process of the maxilla. The kinethmoid-premaxillary ligament connects with the anterior portion of the kinethmoid and with anterior side of the premaxilla. The position of the kinethmoid is flexible. When mouth opens, the kinethmoid moves ventroanteriorly; while mouth is closed, the kinethmoid moves back posterodorsally.

The kinethmoid is slender and crescent in shape. In *P. phoxinus*, *erythrogaster*, *oreas*, *issykkulensis*, *tennesseensis*, and *cumberlandensis*, the distance between its ventral and dorsal margins is longer than the width between its two lateral margins (left and right margins) (TS 35[1]) (Fig.35A, C, E). In *P. neogaeus*, *brachyurus*, and *eos*, however, the bone is short and robust, its dorsal portion is wider than its ventral portion (TS 35[0]; Fig.35B, D).

The dorsal edge of the kinethmoid is forked or notched. In *P. cumberlandensis* and *erythrogaster*, its anterior dorsal edge is deeply forked (TS 36[1]; Fig.35A, C); the fork is deep and narrow, the depth of the fork is about one third of the bone length (dorsal-ventral). In *P. brachyurus*, *phoxinus*, *neogaeus*, *eos*, *tennesseensis*, *issykkulensis*, and *oreas*, the anterior dorsal margin of the bone is shallowly notched, the notch is wider and about one-sixth of the bone length in depth (TS 36[0]; Fig.35B, D, E). In the outgroups, the dorsal margin of the kinethmoid is shallowly notched. Based on the outgroup comparison, a shallowly notched dorsal margin of the kinethmoid is therefore interpreted as plesiomorphic, the deeply forked dorsal margin of the bone as apomorphic condition.

Posteriorly, the kinethmoid is concave at its middle portion in most species of *Phoxinus* (TS 37[0]) except *P. brachyurus* and *eos*. In the latter two species, the kinethmoid is not concave but slightly convex at its middle portion of the posterior side (TS 37[1]). A foramen from the anterior side to the posterior side of the bone is present in *P. neogaeus* and *phoxinus* (TS 38[1]; Fig.35D, E). The foramen is not observed in all other *Phoxinus* species (TS 38[0]) and in the outgroups.

A notch is present at the ventral edge of the kinethmoid in *P. erythrogaster* (TS 39[1]; Fig.35A). The notch is not observed in other species of *Phoxinus* and in the outgroups (TS 39[0]; Fig.35B-E).

Supraethmoid (Fig.36A-E). In cyprinids, the supraethmoid is a single dermal bone located in front of the paired frontals. Its ventral side is sutured to the dorsal side of the mesethmoid. The shape of the supraethmoid is variable in minnows; it might be narrow (e.g., *Barilius*), or "extending so much that it may be visible on the ventral aspect of the skull" (e.g., *Labeo*) (Ramaswami 1955a). In some genera of the family Cyprinidae (e.g., *Aristichthys*), there is a small median fontanelle between the supraethmoid and the frontal (Ramaswami 1955a).

In *Phoxinus*, the supraethmoid is thin and slightly concave at the middle portion of its dorsal aspect, and more or less rectangular-shaped. The lateral portion of the supraethmoid roofs the anterior part of the olfactory capsule. Both the anterolateral and the anterior margins are concave in all *Phoxinus* species, and the posterior margin is concave in most species of *Phoxinus*.

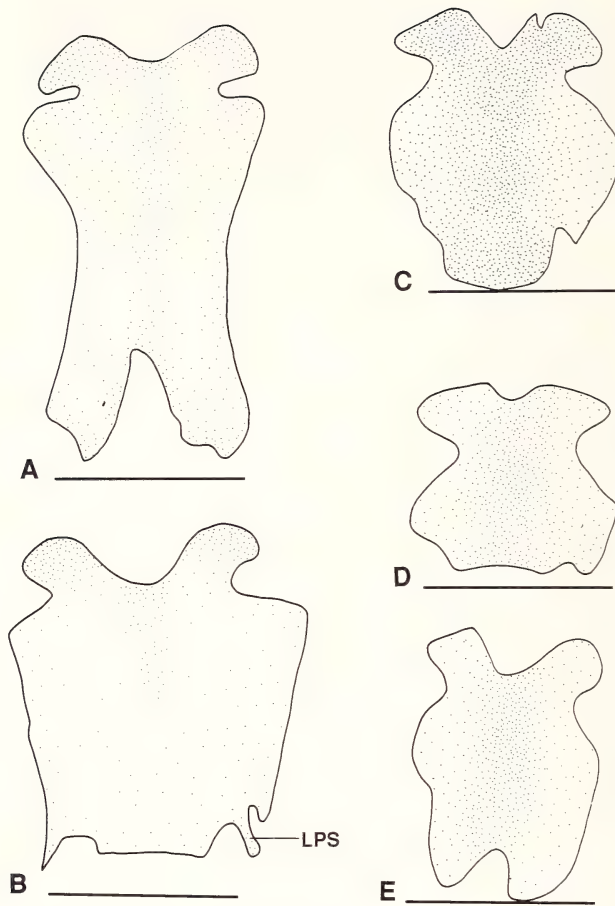


Fig.36: Dorsal view of the supraethmoid of *Phoxinus*. A: *P. phoxinus* (CNUC uncat., 76.0 mm TL); B: *P. neogaeus* (KU 8521, 53.0 mm SL); C: *P. erythrogaster* (KU 5773, 51.5 mm SL); D: *P. oreas* (KU 3259, 55.0 mm SL); E: *P. eos* (KU12255, 43.0 mm SL). Scale bars = 1 mm.

Variation of the supraethmoid among *Phoxinus* species affects its general shape and shape of the lateral and posterior margins. The supraethmoid is short and relatively broad in *P. neogaeus*, *oreas*, *eos*, *erythrogaster*, and *tennesseensis* (TS 40[1]); whereas it is elongated, relatively narrow, and slender in *P. phoxinus*, *brachyurus*, *issykkulensis*, and *cumberlandensis* (TS 40[0]). The middle of the lateral margin of the supraethmoid is convex and forms a small process in *P. oreas*, *eos*, *brachyurus*, and *erythrogaster* (TS 41[0]; Fig.36C, D); the lateral margin is straight in *P. tennesseensis* and *neogaeus*; it is concave and forms a waist-like structure in *P. cumberlandensis*, *issykkulensis*, and *phoxinus* (TS 41[1]; Fig.36A, E). The concavity at the lateral margin is shallow in *P. phoxinus*; it is deeper but narrow in *P. cumberlandensis*. The posterior margin of the supraethmoid is slightly concave in *P. oreas*; deeply concave in *P. phoxinus*, *brachyurus*, *eos*, and *issykkulensis* (TS 42[0]); it is not concave in other species (TS 42[1]), among them the posterior margin of the bone is convex in *P. erythrogaster*, *tennesseensis*, and *neogaeus*; it is almost

straight in *P. cumberlandensis*. Mahy (1975b) stated that the posterior margin of the supraethmoid is concave in *P. neogaeus*. However, my study showed the posterior margin is not concave but bears a lateroposterior process at the posterolateral portion of the bone in *P. neogaeus* (TS 43[1]). The processes were not observed in other species of *Phoxinus* (TS 43[0]).

In the outgroups, the supraethmoid is elongated and relatively narrow; the middle region of the lateral margin is convex, and the posterior margin is deeply concave.

Nasal bone (Fig.37A-G). In cyprinids, the nasal bone is a paired dermal element without direct connection with any other bones. It is placed lateral to the supraethmoid, and anterolateral to the frontal bone and forms part of the dorsal cover of the olfactory capsule. The bone bears part of the supraorbital canal. In *Phoxinus*, the nasal bone is narrow and elongated. The supraorbital canal runs through the middle of the bone in *P. brachyurus*, *oreas*, *phoxinus*, *tennesseensis*, *erythrogaster*, *neogaeus*, and *cumberlandensis* (TS 44[0]; Fig.37A-B); whereas, in *P. issykkulensis* and *eos*, the nasal bone is relatively broad and short and expands mesially; the nasal portion of the supraorbital canal runs on the lateral part of the nasal bone (TS 44[1]; Fig.37G). In *P. brachyurus* and *cumberlandensis*, the nasal portion of the supraorbital canal is broken at its dorsal side (TS 45[1]; Fig.37A); in other species, the nasal portion of the supraorbital canal is complete (not interrupted) (TS 45[0]; Fig.37B). The relative position of the nasal bone to its neighbor bones also varies among the *Phoxinus* species. In *P. neogaeus*, *cumberlandensis*, and *issykkulensis*, the entire nasal bone is over the lateral ethmoid (TS 46[1]). In *P. brachyurus*, *oreas*, *erythrogaster*, *tennesseensis*, *eos*, and *phoxinus*, the nasal bone's posterior portion is placed over the lateral ethmoid, while its anterior portion is positioned over the mesethmoid (TS 46[0]; Fig.37A).

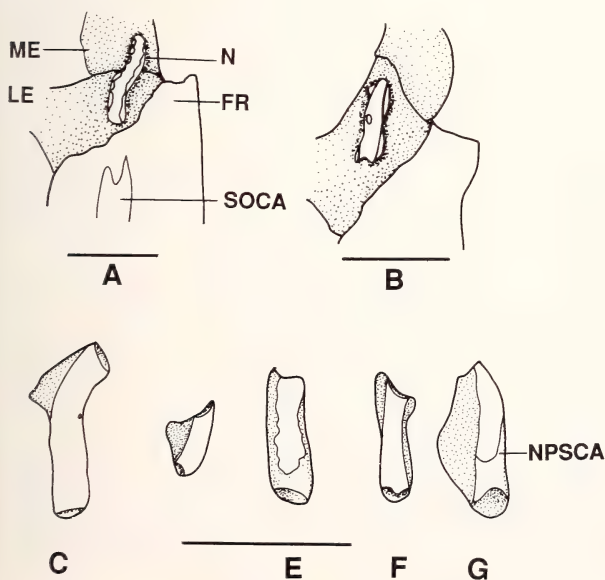


Fig.37: Dorsal view of mesethmoid, lateral ethmoid, frontal, and nasal bones (C-G showing nasal bone only) in *Phoxinus*. A: *P. brachyurus* (MCZ 3006, 75.9 mm SL); B: *P. neogaeus* (KU 8521, 53.0 mm SL); C: *P. tennesseensis* (UT 44.5274, 50.0 mm SL); D: *P. issykkulensis* (P-10696, 42.4 mm SL); E: *P. cumberlandensis* (KU 18934, 52.0 mm SL); F: *P. phoxinus* (KU 22856, 58.0 mm TL); G: *P. eos* (KU 12255, 33.0 mm TL). Scale bars = 1 mm.

In the outgroups, the nasal bone is narrow and elongated, and located over the mesethmoid and lateral ethmoid; the nasal portion of the supraorbital canal is not interrupted.

Preethmoid (Fig.38A, B). In cyprinids, the paired preethmoid is located between the anteroventral side of the mesethmoid and anterolateral side of the vomer. Ramaswami (1955a) stated that *Phoxinus* lacks the preethmoid. This is not the case in the specimens of *Phoxinus* I studied. All species of *Phoxinus* have the preethmoid.

In *Phoxinus*, the preethmoid is semi-spherical in shape. Its position in the skull is similar to that in other cyprinids. The variations of the preethmoid among *Phoxinus* species is in its relative size. The preethmoid is well-developed and large in *P. phoxinus* (TS 47[1]). It is smaller, not well-developed in other species of *Phoxinus* and in the outgroups (TS 47[0]).

Mesethmoid (Figs.38A-B, 39A-B). In cyprinids, the mesethmoid is an endochondral single bone resting on a cartilage (planum ethmoidale) on the vomer, and located at the ventral side of the supraethmoid (Mayden 1989). In *Phoxinus*, the planum ethmoidale is observed in a 33 mm standard length specimen of *P. eos* (Fig.38A). The cartilage is reduced or absent in larger specimens. Dorsally and anteriorly, the mesethmoid shares sutures with the posterior side of the supraethmoid (Fig.38A-B). The mesethmoid sutures with the lateral ethmoid posteriorly.

The mesethmoid is irregular in shape. Anterolaterally, the bone bears two foramina for nerves (Fig.38A-B). Anteriorly, the mesethmoid is concave; the anterior surface of the mesethmoid sutures with the posterior surface of the supraethmoid. Ventrally, the mesethmoid bears one or two conea (Gasowska 1979), the anterior and posterior ones, which are concave and position at the ventral side of the mesethmoid (Fig.39A-B).

Variation in the mesethmoid of *Phoxinus* occurs mainly at its ventral aspect. In *P. phoxinus*, *neogaeus*, and *eos*, the ventral side of the bone is broad and relatively short (TS 48[1]) and bears two conea (TS 49[0]; Fig.39B). In these three species, the anterior conus is broad, short, and surrounded by the arch-like posterior one. In other species of *Phoxinus*, the bone is relatively elongated and narrow (TS 48[0]), only one conus is present (TS 49[1]).

In the outgroups, the ventral side of the mesethmoid is narrow and relatively elongated, but bears two conea. However, the relationships between the two conea in the outgroups

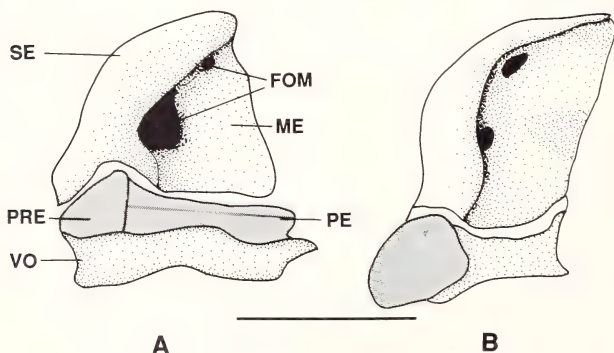


Fig.38: Lateral view of ethmoidal region of (A) *Phoxinus eos* (KU 12255, 33.0 mm SL), and (B) *P. phoxinus* (KU 22856, 58.0 mm SL). Scale bar = 1 mm.

is slightly different from that in *Phoxinus*. In the outgroups, the posterior conus is broad, short, and located posteriorly to the anterior conus.

Lateral Ethmoid (Fig.39C-D). In cyprinids, the lateral ethmoid is located at the anterolateral side of the neurocranium.

Ventrally, the lateral ethmoid sutures with the dorsal aspect of the vomer and of the anterolateral portion of the parasphenoid. The lateral ethmoid sutures posteriorly with the dorsal aspect of the anterior portion of the parasphenoid and the anterior portion of the orbitosphenoid, anteriorly with the mesethmoid and supraethmoid, and dorsally with the ventral side of the frontals. The left and right lateral ethmoids are separated by the parasphenoid and the mesethmoid. The anterior portion of the lateral ethmoid forms part of the bottom of the nasal capsule; the posterior portion of the bone forms the anterior portion of the orbital capsule and the dorsal side of the anterior myodome, and the median portion of the lateral ethmoid forms part of the lateral wall of the braincase. Ventrally, the

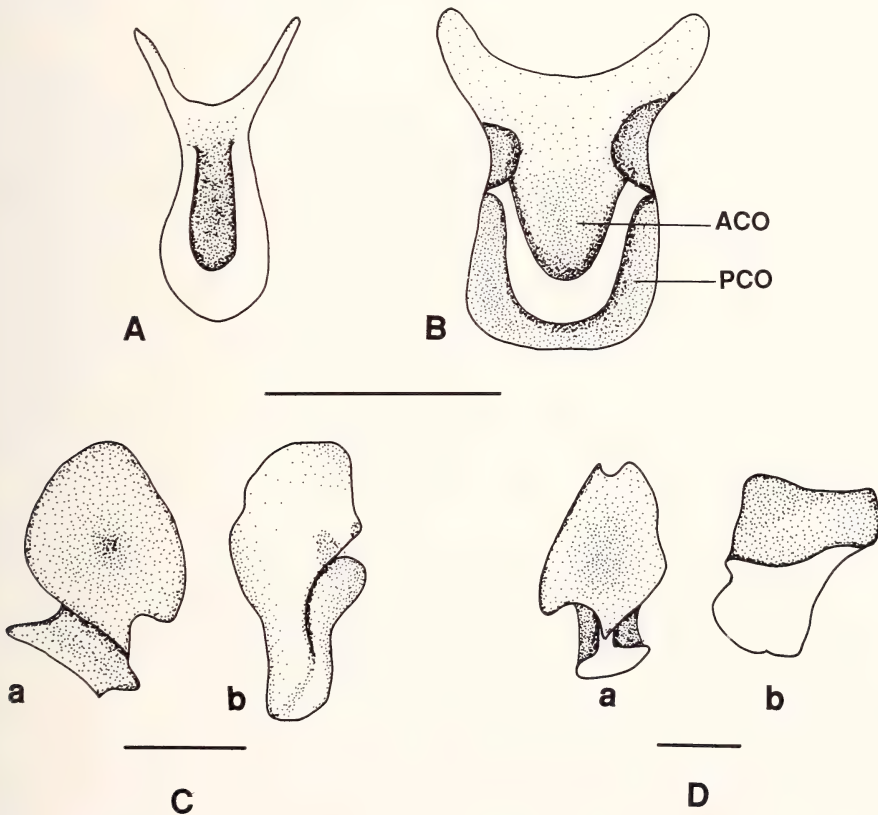


Fig.39: Ventral view of mesethmoid (A-B), and medial (a) and ventral (b) view of lateral ethmoid (C-D) of *Phoxinus*. A: *P. oreas* (KU 3259, 55.0 mm SL); B: *P. neogaeus* (KU 8521, 53.0 mm SL); C: *P. phoxinus* (CNUC uncat., 76.0 mm TL); D: *P. cumberlandensis* (KU 18934; 52.0 mm SL). Scale bars = 1 mm.

lateral ethmoid expands forming a triangular-shaped portion. Posteriorly, the lateral ethmoid is triangular-shaped. Anteriorly, the lateral ethmoid is similar to its posterior view in shape. Medially, the medial side of the bone is concave and bears a notch at its ventral margin. The bone has a T-shaped ridge-like appearance dorsally.

Variation of the lateral ethmoid among *Phoxinus* species affects its shape. Ventrally, the anterior and posterior portions are acute in *P. cumberlandensis* and *erythrogaster* (TS 50[0]; Fig.39D). In *P. erythrogaster*, the anteroventral portion is elongated and forms a process. The anterior and posterior portions of the ventral aspect are blunt in other species of *Phoxinus* (TS 50[1]; Fig.39C).

The concave medial side bears a notch at its dorsal margin in *P. tennesseensis* and *cumberlandensis* (TS 51[1]) (Fig.39D); the notch is not present in other species of *Phoxinus* (TS 51[0]; Fig.39C).

In the outgroups, the anterior and posterior portions of the ventral aspect of the lateral ethmoid are acute; no notch is present at the dorsal margin of the medial aspect of the lateral ethmoid.

Orbital Region

Located posteriorly to the ethmoidal region, the orbital region consists of orbitosphenoid, pterospheneid, frontal, supraorbital, and infraorbital bones.

Frontal (Figs 40A-F). In cyprinids, the frontal is the largest bone in the neurocranium (but in *Aristichthys* the frontal is a small bone – Ramaswami 1955a), and forms the anterodorsal cover of braincase. Shape of the frontal varies from short and broad (e.g., *Rhodeus*) to very slender and elongated (e.g., *Elopichthys bambusa*, *Luciobrama macrocephalus* – Howes 1978, Chen 1987c). Dorsally, it shares a suture with the supraethmoid anteriorly, lateral ethmoid anterolaterally, sphenotic posterolaterally, and parietal posteriorly. In some cyprinids, there is a small fontanel between the anterior margin of the frontal and the posterior margin of the supraethmoid (e.g., species of *Aristichthys*) (Ramaswami 1955a). The left and right frontals meet one another at their mesial margins with slight overlap. Ventrally, the frontal meets the lateral ethmoid anteriorly, orbitosphenoid and pterospheneid laterally. Anteriorly, the frontal roofs the posterior part of the olfactory capsule.

In *Phoxinus*, frontal sutures with other bones similar to that in other cyprinids. The fontanel between frontal and supraethmoid is absent in the genus. The frontal is a rectangular-shaped bone with a posterolateral process at posterior portion of the lateral margin and an anterior process at its anterior margin. The posterior margin of the posterolateral process sutures with the anterior margin of the sphenotic. Shape of the posterolateral process varies among the species of *Phoxinus*. The posterolateral process is sharp and elongated in *P. neogaeus*, *issykkulensis*, *brachyurus*, and *phoxinus* (TS 52[1]); the process is relatively short and broad in other species of *Phoxinus* (TS 52[0]) and in the outgroups. Thus the elongated and sharp posterolateral process is proposed as an apomorphic condition, and the short and broad one a plesiomorphic condition.

The frontal bears the supraorbital canal in *Phoxinus*. The supraorbital canal might be continuous or interrupted. On the ventral side of the frontal bone in *Phoxinus* three concavi-

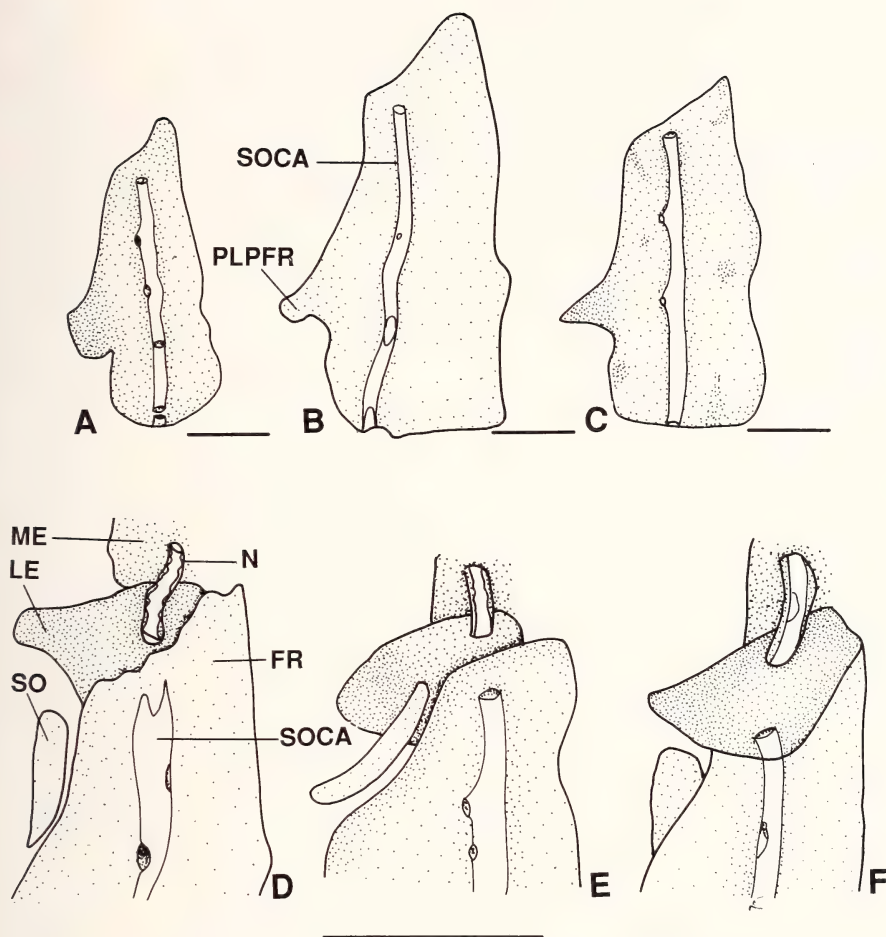


Fig.40: Dorsal view of the frontal bone (A-C), and supraorbital, lateral ethmoid, mesethmoid, frontal, and nasal bones (D-F) of *Phoxinus*. A: *P. cumberlandensis* (KU 18934, 52.0 mm SL); B: *P. erythrogaster* (KU 5773; 51.5 mm SL); C: *P. phoxinus* (CNUC uncat., 76.0 mm TL); D: *P. oreas* (KU 3259, 55.0 mm SL); E: *P. phoxinus* (KU 22856, 58.0 mm SL); F: *P. tennesseensis* (UT 44.5274, 50.0 mm SL). Scale bars = 1 mm.

ties are present, including anterolateral, anteromedial, and posterior ones. The anterolateral and anteromedial concavities are separated by a ridge. The posterior concavity is triangular-shaped and separated by a ridge from the anterolateral and anteromedial concavities.

Supraorbital (Fig.40D-F). In cyprinids, this paired bone is flat plate-shaped with variation in size from broad and short (e.g., *Ctenopharyngodon* and *Hypophthalmichthys* – Howes 1981) to slender and elongated (e.g., *Genghis mongolicus* – Howes 1984). The su-

praorbital bone is placed at anterolateral side of the frontal. The supraorbital sutures with the frontal medially, and might be over the lateral ethmoid anteriorly.

In *Phoxinus*, the supraorbital is a small, elongated crescentic bone. However, it is relatively shorter and broader in *P. oreas* and *tennesseensis* (TS 53[1]; Fig.40F) than that in other species of the genus in which the supraorbital bone is relatively elongated and slender (TS 53[0]; Fig.40D). Its position relative to the supraethmoid, frontal, and lateral ethmoid also varies among the species. In *P. phoxinus*, *neogaeus*, and *cumberlandensis*, the supraorbital bone is placed forward; almost half of the supraorbital bone is above the lateral ethmoid (TS 54[1]; Fig.40E). In other species of *Phoxinus*, however, the supraorbital is placed more posteriorly; it does not overlap the lateral ethmoid, or only a small portion of the supraorbital bone overlaps the lateral ethmoid (TS 54[0]; Fig.40F).

In the outgroups, the supraorbital bone is elongated and slender; only a small portion of the bone overlaps the lateral ethmoid.

Infraorbital series (Fig.41A-H). Four or five paired plate-like bones are included in the infraorbital series: infraorbitals 1, 2, 3, 4, and 5 (Fig.41A-H). In some species of Cyprinidae, infraorbital 5 is present as two small pieces (e.g., *Luciobrama macrocephalus* – Howes 1978); in some species, however, infraorbital 5 is absent (e.g., *Cyprinella* – Mayden 1989).

In cyprinids, infraorbital 1 (lacrymal) is the largest and the most anterior bone of the infraorbital series. It is located lateral to the vomer, and medial to the maxilla. In *Phoxinus*, infraorbital 1 (Fig.41A-H) does not directly articulate with any other bone dorsally and dorsoposteriorly, but with infraorbital 2 ventroposteriorly. Infraorbital 1 bears a concavity at its anterior margin and a process on its dorsal margin. An infraorbital canal runs through the bone. In *P. phoxinus* infraorbital 1 is relatively short and broad, its anterior and posterior margins bear a well-developed notch (TS 55[1]; Fig.41E). In other species of the genus and in the outgroups, infraorbital 1 is relatively elongated and narrow, both the anterior and posterior margins bear no notch or bears a very shallow notch (TS 55[0]; Fig.41H).

Infraorbital 2 (Fig.41A-H) is an elongated rectangular bone. It articulates with infraorbital 1 anteriorly and infraorbital 3 posteriorly. Its anterior portion is slightly broader than its posterior portion in *Phoxinus*. There is variation of the bone among the species of *Phoxinus*. In *P. cumberlandensis*, infraorbital 2 is short and relatively broad, its length (anterior to posterior) is less than two times of its width (ventral to dorsal), and the anterior portion is equal to the posterior one in width (TS 56[1]; Fig.41B). The condition in other species of *Phoxinus* are similar to the condition in the outgroups. The bone is elongated and slender, with the length about three times of the width; its posterior portion is slightly narrower than its anterior portion (TS 56[0]).

Infraorbital 3 (Fig.41A-H) is the longest among all infraorbital bones, and occupies about half of the total length of the infraorbital series. (However, infraorbital 4 is the longest among the infraorbital bones in some cyprinids, such as *Luciobrama macrocephalus* – Howes 1978, Chen 1987c). It is crescent in shape, and articulates with infraorbital 2 anteriorly, and infraorbital 4 posteriorly. In *P. neogaeus*, *cumberlandensis*, *issykkulensis*, and *erythrogaster*, infraorbital 3 is equal in width, i.e., the width of the bone does not change

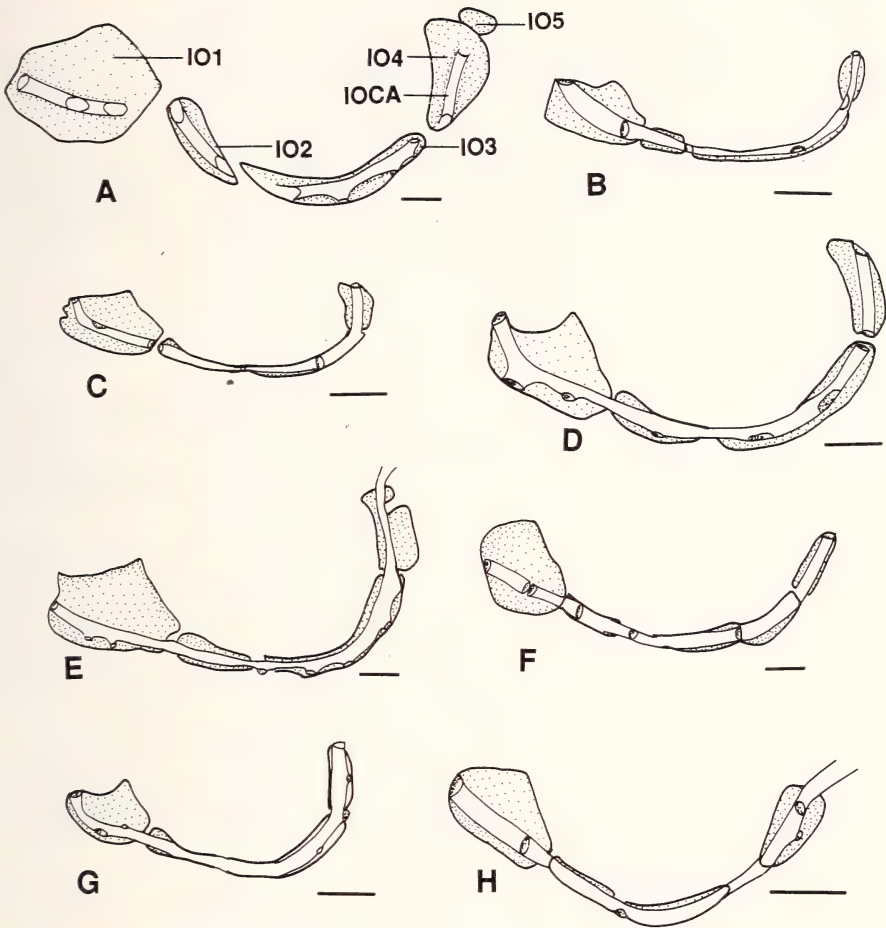


Fig.41: Lateral view of infraorbital bones of *Phoxinus*. A: *P. brachyurus* (MCZ 3006, 75.9 mm SL); B: *P. cumberlandensis* (KU 18934, 52.0 mm SL); C: *P. issykkulensis* (P-10696, 42.4 mm SL); D: *P. erythrogaster* (KU 5773, 62.0 mm SL); E: *P. phoxinus* (CNUC uncat., 76.0 mm TL); F: *P. tennesseensis* (UT 44.5274; 50.0 mm SL); G: *P. oreas* (KU 3259, 52.2 mm SL); H: *P. neogaeus* (KU 8521, 53.0 mm SL). Scale bars = 1 mm.

much from its anterior portion to its posterior portion (TS 57[0]; Fig.41B). The posterior portion of the former is much broader than the anterior portion in *P. oreas*, *phoxinus*, *tennesseensis*, *brachyurus*, and *eos* (TS 57[1]; Fig.41E). In *P. tennesseensis* the anterior margin of infraorbital 3 is far from infraorbital 2 (TS 58[1]; Fig.41F); the anterior margin of the former is close to the latter in other species of *Phoxinus* (TS 58[0]; Fig.41H). In the outgroups, infraorbital 3 does not vary much in width along the length, and the anterior margin of the bone is close to the infraorbital 2.

Infraorbital 4 (Fig.41A-H) is the most posterior bone of the infraorbital series in most species of *Phoxinus*, except *P. brachyurus* (see below). Infraorbital 4 meets infraorbital 3 ventrally and has no direct connection with other bones dorsally in most species. It is crescent in shape and varies in the relative size to infraorbital 2 among the *Phoxinus* species. In *P. eos* and *erythrogaster*, infraorbital 4 is slightly shorter than infraorbital 2. In *P. cumberlandensis*, *issykkulensis*, and *tennesseensis*, it is about the same size as infraorbital 2 (TS 59[0]; Fig.41B). The bone is expanded and much wider than infraorbital 2 in the remaining species of *Phoxinus* (TS 59[1]; Fig.41E). In *P. phoxinus* the bone bears a notch at the dorsal portion of its posterior edge (TS 60[1]; Fig.41E). The notch is absent in other species of *Phoxinus* (TS 60[0]; Fig.41A).

In the outgroups, infraorbital 4 is about same size as the infraorbital 2, and bears no notch at the posterior margin.

Positioned at the dorsal side of infraorbital 4, infraorbital 5 is a small dermal bone and is present in *P. brachyurus* only (TS 61[1]; Fig.41A). The bone is small and irregular-shaped plate-like. It is not observed in the outgroups (TS 61[0]; Fig.41B). Infraorbital 5 articulates with the dorsal margin of infraorbital 4 ventrally, and has no direct connection with other bones on its dorsal side.

Orbitosphenoid (Fig.42A-D). In cyprinids, the orbitosphenoid is a paired chondral bone. The orbitosphenoid is sutured by the lateral ethmoid anteriorly, parasphenoid ventrally, frontal dorsally, and pterospheonoid posteriorly. Gasowska (1979) stated that the orbitosphenoid is a single bone in cyprinids. However, Howes (1978) showed a pair of orbitosphenoids in *Luciobrama macrocephalus*. My study on *Phoxinus* demonstrated that the orbitosphenoid is paired in this genus.

In *Phoxinus*, each orbitosphenoid is a plate-like bone. The ventral portion of the bone is very thin and sutures with the same portion of other orbitosphenoid medially to form the orbital septum. The orbital septum is concave at the middle or dorsal part of its posterior margin, the ventral part of its posterior margin is convex.

The relative position of the ventral part of the posterior margin of the septum (the very thin portion of the orbitosphenoid) to the dorsal portion of the posterior margin of the orbitosphenoids varies among the species of *Phoxinus*. The posterior margin of the septum extends posteriorly beyond the posterior margin of the dorsal portion of the orbitosphenoids in *P. neogaeus*. The septum almost extends to the posterior margin of the dorsal portion of the orbitosphenoids in *P. eos* and *phoxinus* (TS 62[1]); the posterior margin of the septum is far away from the posterior margin of the unfused portion of the orbitosphenoid in other species of *Phoxinus* and in the outgroups (TS 62[0]).

The shape of the posterior edge of the orbital septum varies among the *Phoxinus* species. In *P. cumberlandensis* and *P. erythrogaster*, a process is present on the ventral portion of the posterior margin of the septum (TS 63[1]). This process is not observed in other species of *Phoxinus* and in the outgroups (TS 63[0]).

Pterospheonoid (Fig.42A-D, 43A-B). In cyprinids, the pterospheonoid is a paired bone sutured with the orbitosphenoid anteriorly, frontal anterodorsally, sphenoid posterodorsally, prootic posteriorly, and parasphenoid ventrally. In *Phoxinus*, the posterodorsal edge of the

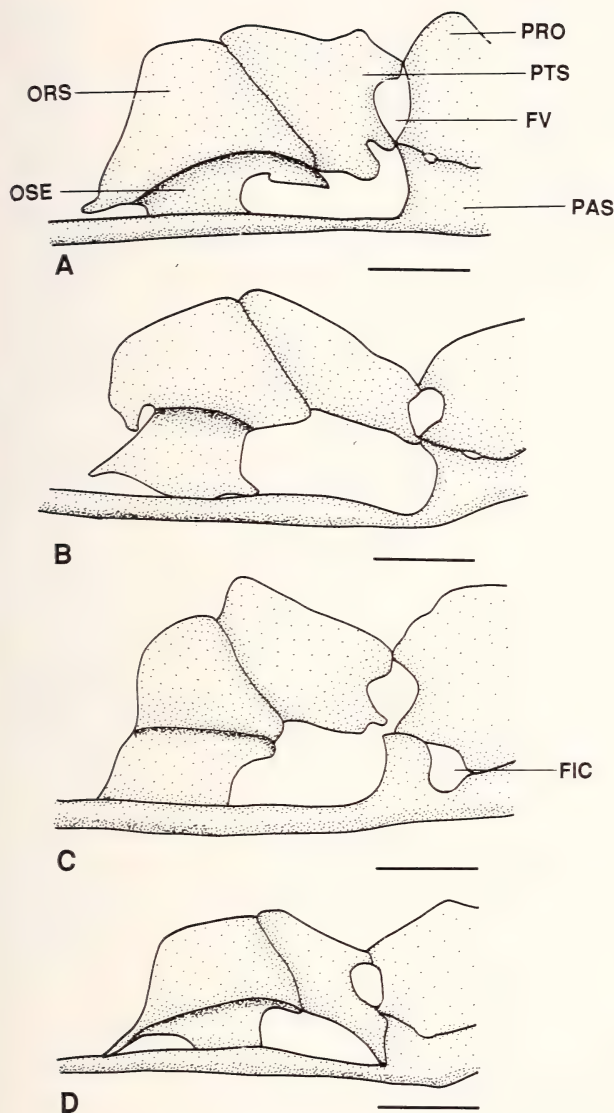


Fig.42: Lateral view of orbitosphenoid, pterosphenoid, prootic, and parasphenoid of *Phoxinus*. A: *P. neogaeus* (KU 8521, SL 53.0 mm); B: *P. erythrogaster* (KU 5773, SL 51.5 mm); C: *P. oreas* (KU 3259, SL 55.0 mm); D: *P. eos* (KU 12255, SL 43.0 mm). Scale bars equal 1 mm.

pterosphenoid forms the anterior part of the hyomandibular fossa, and its posterior margin forms the anterior part of the trigeminal foramen.

The pterosphenoid is irregularly shaped in *Phoxinus*. A process is present at its anterior margin in *P. eos*, *erythrogaster*, and *phoxinus* (TS 64[1]); the process is absent in other species of the genus and in the outgroups (TS 64[0]). The posterior margin of the pterosphenoid bears a notch which forms the anterior part of the trigeminal foramen. The po-

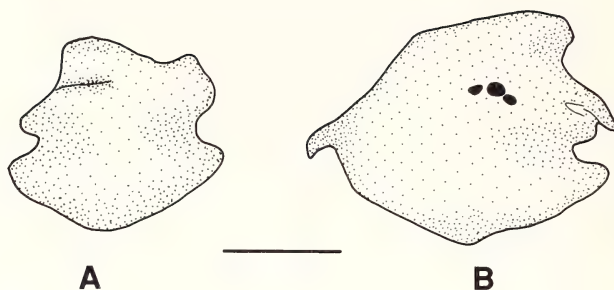


Fig.43: Lateral view of pterosphenoïd of (A) *Phoxinus cumberlandensis* (KU 18934, 52.0 mm SL) and (B) *P. phoxinus* (CNUC uncat., 76.0 mm TL). Scale bar = 1 mm.

sterior portion of the bone bears a process in *P. oreas*, *issykkulensis*, *tennesseensis*, *eos*, *neogaeus*, *brachyurus*, *phoxinus*, and in the outgroups (TS 65[0]), although the process is absent in *P. cumberlandensis* and *erythrogaster* (TS 65[1]).

The pterosphenoïd's ventroposterior margin sutures with anterior edge of the parasphenoid's ascending wing (Fig.42A-D). Variation in *Phoxinus* is present in the extent of the suture between the pterosphenoïd and the ascending wing of the parasphenoid. In *P. neo-*

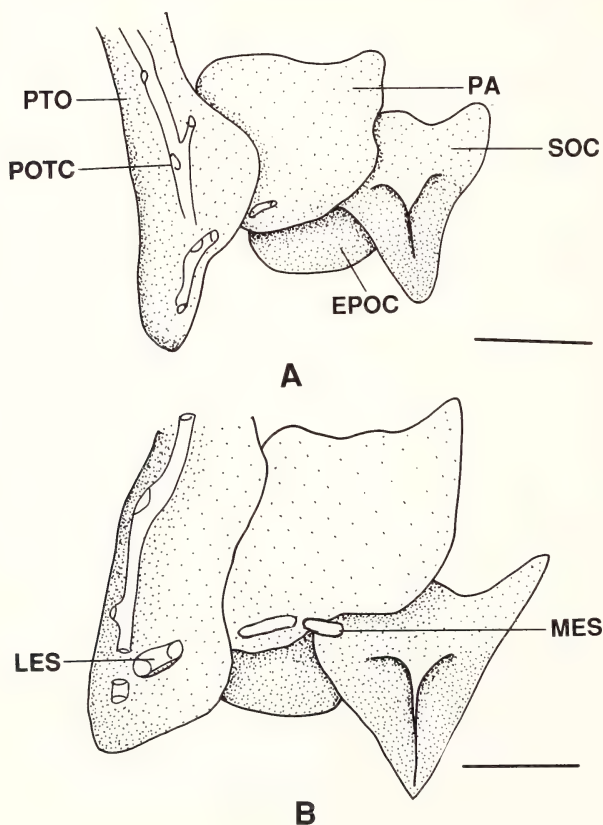


Fig.44: Dorsal view of pterotic, parietal, epioccipital, and supraoccipital (A) *Phoxinus tennesseensis* (UT 44.5274, 50.0 mm SL) and (B) *P. brachyurus* (MCZ 3006, 75.9 mm SL). Scale bars = 1 mm.

gaeus, *erythrogaster*, *brachyurus*, *eos*, and in the outgroups, only a very small portion of the pterosphenoid articulates with the parasphenoid (TS 66[0]). A much larger portion of the pterosphenoid sutures with the wing of the parasphenoid in other species of *Phoxinus* (TS 66[1]).

Otic Region

Located posteriorly to the orbital region, the otic and occipital regions form the otic capsule. Bones in the otic region include parietal, medial extrascapula, sphenotic, prootic, epioccipital, intercalar, pterotic, and lateral extrascapula. All are paired bones.

Parietal and medial extrascapula (Fig.44A-B). In cyprinids, the parietal is a paired dermal bone located at the posterodorsal portion of the neurocranium, and forms the posterodorsal cover of the braincase. The parietal sutures with the frontal anteriorly, sphenotic anterolaterally, pterotic posterolaterally, supraoccipital and epioccipital posteriorly. The left and right parietals suture each other mesially with a small overlap at its middle and posterior portion. Length of the parietal is usually about 30-50% of the frontal length (Howes 1981). A parietal fontanelle exists between the parietal and frontal in some

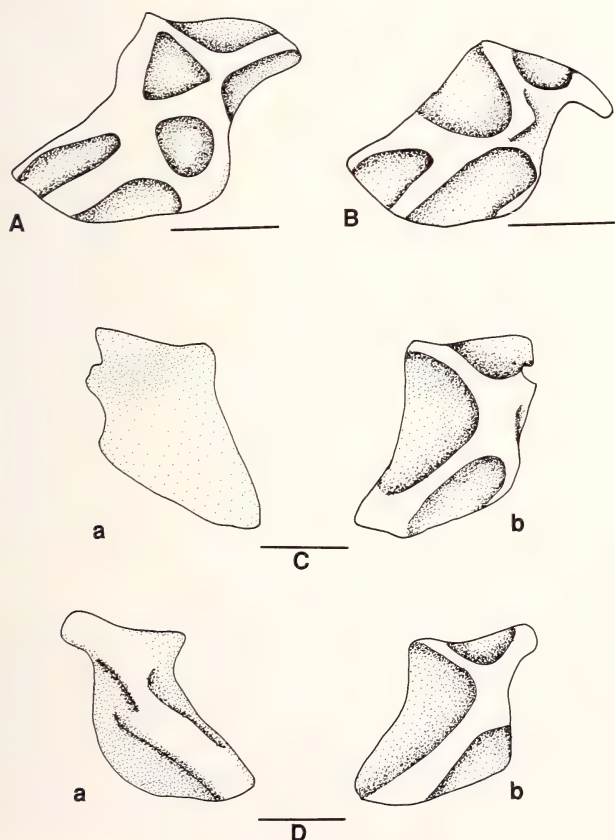


Fig.45: Sphenotic of *Phoxinus*. A: *P. oreas* (KU 3259, SL 55 mm, ventral view); B: *P. eos* (KU12255, 43.0 mm SL, ventral view); C: *P. phoxinus* (CNUC uncat., 76.0 mm TL); D: *P. cumberlandensis* (KU 18934, 52.0 mm SL) (a: dorsal view; b: ventral view). Scale bars = 1 mm.

cyprinids, such as *Cyprinus carpio* (pers. obs.) and some gobions (Ramaswami 1955b). The fontanelle is absent in *Phoxinus*.

In *Phoxinus* the parietal is more or less rectangular plate-like in shape. No variation in shape of the parietal is observed among the *Phoxinus* species.

The medial extrascapula is a small bar-shaped bone carrying the supratemporal canal and is located at the dorsal side of the posterior portion of the parietal. One medial extrascapula is present, partially covering the parietal in *P. neogaeus*, *brachyurus*, and in the out-groups (TS 67[0]); no medial extrascapula is present in other species of *Phoxinus* (TS 67[1]).

Sphenotic (Fig.45A-D). The sphenotic is placed at the dorsolateral side of the neurocranium in cyprinids. Dorsally, the sphenotic sutures the frontal anteromesially, the parietal posteromedially, and the pterotic posteriorly. Ventrally, the sphenotic sutures the pterosphenoid anteriorly and the prootic posteriorly. The bone forms the hyomandibular fossa ventrolaterally.

In *Phoxinus* the sphenotic is irregularly shaped. Generally, its middle portion is broader than its anterior and posterior portion. Dorsally, the anterior portion of the lateral margin of the sphenotic is deeply concave in *P. cumberlandensis* and *neogaeus* (TS 68[1]); the anterior portion of the lateral margin of the bone is shallowly concave in other species of *Phoxinus* (TS 68[0]).

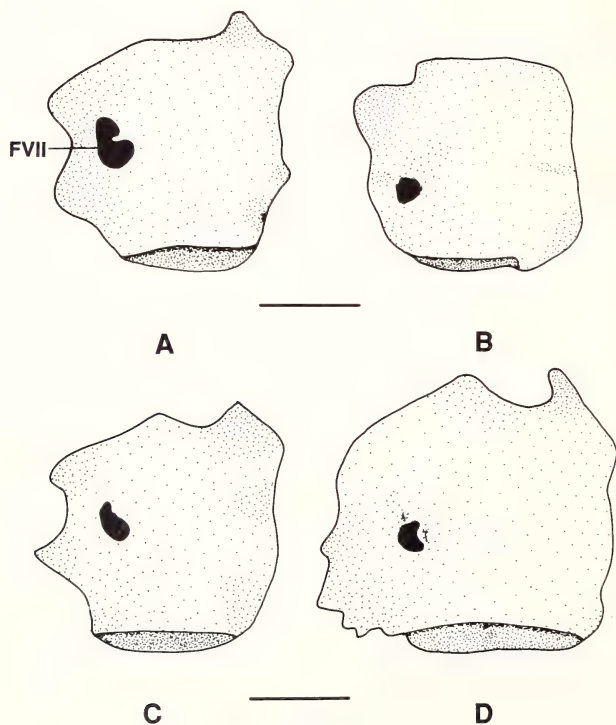


Fig.46: Lateral view of prootic of some species of *Phoxinus*. A: *P. oreas* (KU 3259, 55.0 mm SL); B: *P. eos* (KU 12255, 43.0 mm SL); C: *P. erythrogaster* (KU 5773, 51.5 mm SL); D: *P. neogaeus* (KU 8521, 53.0 mm SL). Scale bars = 1 mm.

Ventrally, the sphenotic bears three to five concavities which are separated from one another by bony ridges. In *P. phoxinus* and *cumberlandensis*, three concavities are present (TS 69[2]). In *P. eos* and *erythrogaster*, there are four concavities (TS 69[0]). Five concavities were found in other species of *Phoxinus* (TS 69[1]).

In the outgroups, the sphenotic is not deeply concave at the anterior portion of the lateral margin, and bears four concavities on its ventral side.

Prootic (Fig.46A-D). In cyprinids, the prootic is placed at the ventral side of the neurocranium. It sutures with sphenotic anterodorsally, pterotic and epioccipital posterodorsally, exoccipital and basioccipital posteriorly, parasphenoid ventrally, and pterosphenoid anteriorly.

In *Phoxinus* the prootic is an irregularly shaped plate-like bone forming a major portion of the posterolateral wall of the braincase. The prootic bears a notch at its anterior margin. This notch and the one at the posterior margin of the pterosphenoid form the trigeminal foramen. The notch on the anterior margin of the prootic is deeper in *P. erythrogaster* and *oreas* (TS 70[1]) than in other species of *Phoxinus* (TS 70[0]). The prootic also bears a facial foramen at its middle portion. A process is present on the dorsal margin of the prootic in some *Phoxinus* species. The process is well-developed in *P. neogaeus*, less developed in *P. oreas*, *erythrogaster*, and *cumberlandensis* (TS 71[0]), and it is absent in other species of the genus (TS 71[1]). Ventrally, the prootic is forked and articulates with the parasphenoid.

In the outgroups, the prootic bears a shallow notch at its anterior margin and a process at its dorsal margin.

Epioccipital (Fig.47A-C). This bone was first named as epiotic by Huxley (1858). Patterson (1975) showed that the bone is an ossification of the occipital arch invading into the otic region, thus he proposed “epioccipital” to replace “epiotic” for the bone. In cyprinids, the epioccipital is a paired endochondral bone, located at the posterior portion of the neurocranium. Dorsally, the epioccipital sutures the supraoccipital mesially, pterotic laterally, and parietal anteriorly. Ventrally, the epioccipital sutures the exoccipital and prootic mesially, the exoccipital and pterotic posteriorly, and pterotic laterally. Posteriorly, the epioccipital sutures the exoccipital ventrally, supraoccipital mesially, and the pterotic laterally.

In cyprinids, a subtemporal fossa is formed by the posterior side of the prootic as the inner wall of the fossa, the dorsoposterior portion of the pterotic, and epioccipital as roof of the fossa. In most cyprinids, including *Phoxinus* and the outgroups, the fossa is relatively deep and circular or oval in shape (Howes 1981).

In *Phoxinus*, the epioccipital is a complicated bone in morphology. Dorsally, the bone is plate-like with a process at its posterior edge. The general shape of the bone in a dorsal view varies among species. In *P. cumberlandensis*, the epioccipital is much narrower at its anterior portion than at its posterior portion and, therefore, is triangular-shaped (TS 72[1]). In other species of the genus, the bone is more or less rectangular (TS 72[0]). In *P. phoxinus*, *brachyurus*, and *issykkulensis*, the process on the posterior margin is large and blunt (TS 73[1]; Fig.47B). In other species of *Phoxinus*, the process is narrow and elongated (TS 73[0]), either sharp (e.g., *P. cumberlandensis*), or blunt (e.g., *P. neogaeus*).

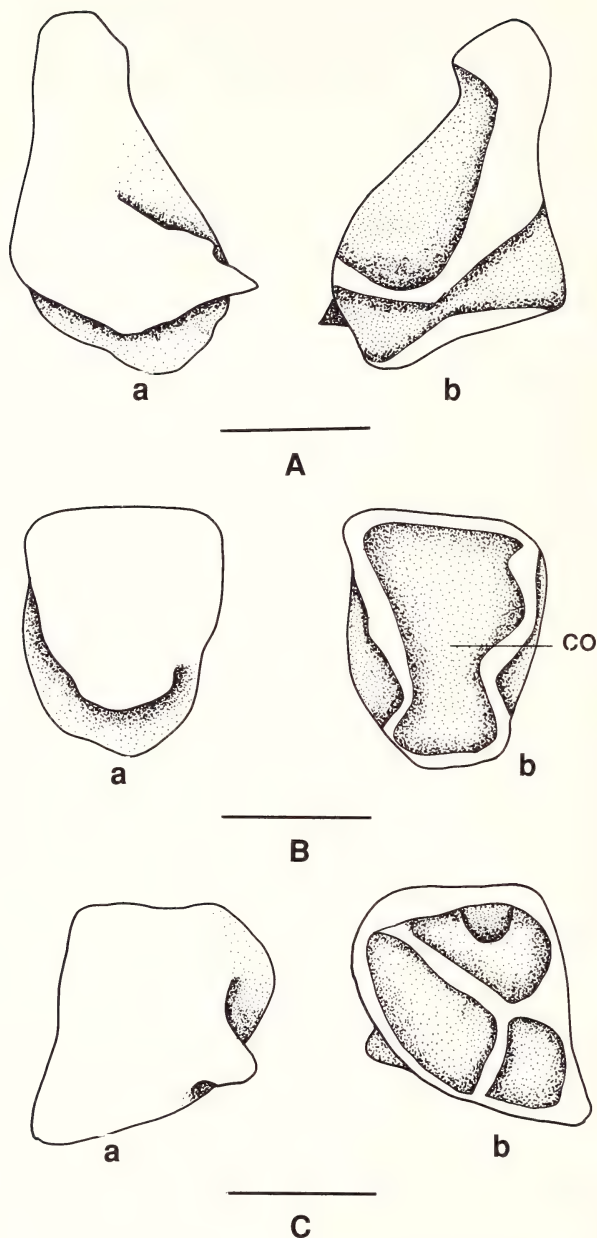


Fig.47: Epioccipital of *Phoxinus* (a: dorsal view; b: ventral view). A: *P. cumberlandensis* (KU 18934; 52.0 mm SL); B: *P. phoxinus* (CNUC uncat., 76.0 mm TL); C: *P. neogaeus* (KU 8521, 53 mm TL). Scale bars = 1 mm.

The epioccipital bears two or three concavities on its ventral aspect. The concavities are separated one another by ridge-like structures. In *P. neogaeus*, the anterior concavity bears another deeper “subconcavity” at its anterior portion (TS 74[1]; Fig.47C). The “subconcavity” is absent in other species of *Phoxinus* (TS 74[0]).

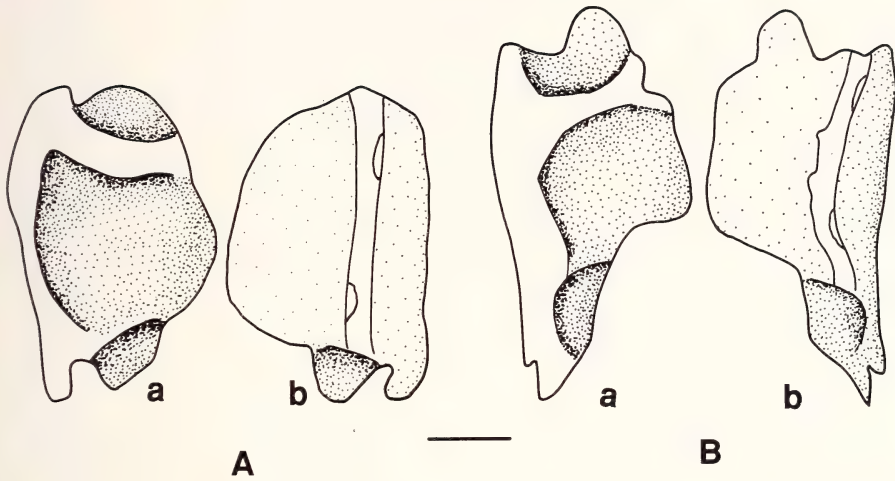


Fig.48: Pterotic of (A) *Phoxinus erythrogaster* (KU 5773, 51.5 mm SL), and (B) *P. cumberlandensis* (KU 18934, 52.0 mm SL) (a: ventral view; b: dorsal view). Scale bars = 1 mm.

In the outgroups, the epioccipital is more or less rectangular; it bears a small sharp process at its posterior margin, and its anterior concavity on the ventral side bears no small deeper "subconcavity".

Intercalar. The intercalar is a small paired endochondral bone placed at the postero-ventral side of the pterotic. It is triangular in shape and does not vary significantly among *Phoxinus* species.

Pterotic and lateral extrascapula (Figs.44A, B; 48A, B). Dorsally, in *Phoxinus*, the pterotic sutures the sphenotic anteriorly and epioccipital posteromedially. Ventrally the pterotic sutures the sphenotic anteriorly, the prootic mesially, and the exoccipital posteriorly. The dorsal aspect of the pterotic is partially overlapped by the lateral extrascapular and the posttemporal in some species of the genus. The posterior portion of the pterotic forms the anterior part of the subtemporal fossa, and the lateral portion of the pterotic forms the dorsolateral portion of hyomandibular fossa.

The pterotic is irregular-shaped in *Phoxinus*. The dorsal aspect (dermopterotic) of the pterotic is plate-like. The otic canal of the cephalic lateral line runs on the dorsal side of the bone. At the anterior part of the bone, an anteriorly directed process is present in most *Phoxinus* species (TS 75[1]), but the process is absent in *P. tennesseensis*, *oreas*, and *erythrogaster* (TS 75[0]). A posteriorly directed process varying among the *Phoxinus* species exists on the posterolateral margin of the pterotic. The process is long and acute in *P. cumberlandensis* (TS 76[1]), but short and blunt in other species of *Phoxinus* and in the outgroups (TS 76[0]).

Ventrally, the pterotic bears two concavities, i.e., the anterior and posterior concavities separated by ridges. The anterior concavity, with the concavity formed by prootic, forms the otic capsule. The medial concavity forms part of subtemporal fossa.

A lateral extrascapular is present on the posterior portion of the pterotic in *P. brachyurus* (TS 77[1]). The lateral extrascapular is a small bar-shaped bone bearing a part of the supratemporal canal of the cephalic lateral line canal. No lateral extrascapular is present in other species of *Phoxinus* and in the outgroups (TS 77[0]).

Occipital Region

The occipital region is the most posterior region of the skull. It forms the posterodorsal cover and the posterior wall of the braincase. Bones in the region include exoccipital and supraoccipital. The former is paired, and the latter is single. The basioccipital will be described in the basicranial region.

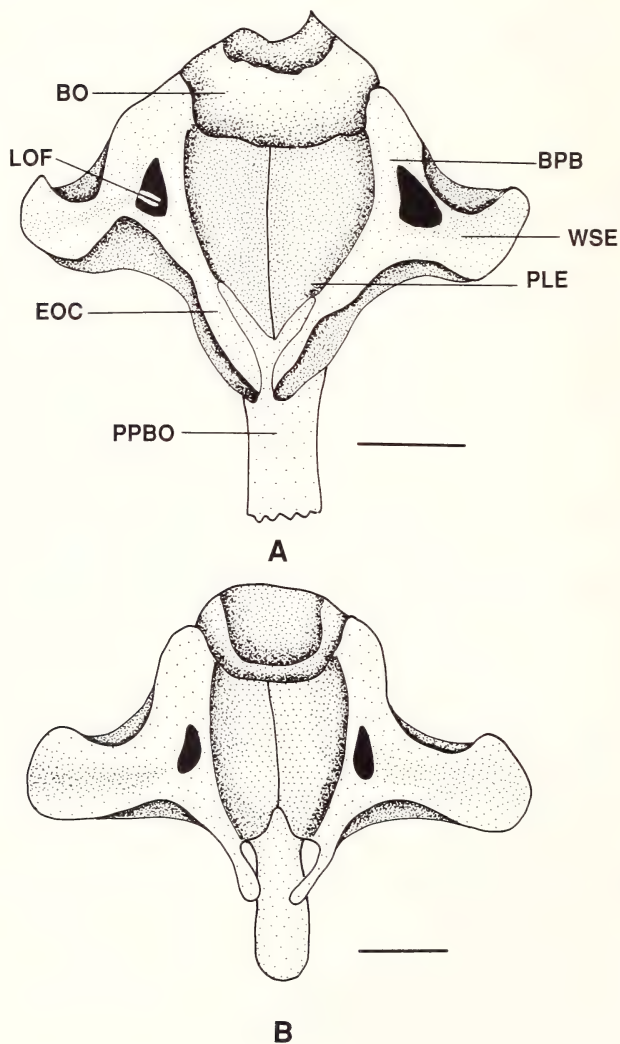


Fig.49: Dorsal view of posterior cranium (parietal removed) of (A) *Phoxinus phoxinus* (CNUC uncat., 76.0 mm TL), and (B) *P. cumberlandensis* (KU 18934, 52.0 mm SL). Scale bars = 1 mm.

Exoccipital (Figs.49A-B, 50). In cyprinids, the exoccipital is a paired endochondral bone placed at the posterior portion of the neurocranium. The exoccipital forms the ventral portion of the braincase's posterior wall and a part of the foramen magnum. The exoccipital sutures with the epioccipital and supraoccipital dorsally and basioccipital ventrally. On the ventral view, it sutures with the prootic anteriorly, basioccipital medially, epioccipital and pterotic anteriorly. The right and left exoccipitals suture one another mesially. A cavum sinus impar is present between the dorsal margin of the basioccipital and the middle portion of the ventral margin of the exoccipital.

Posteriorly, the exoccipital extends laterally and expands medially in *Phoxinus*. The mesial edge of the exoccipital is laterally concave, therefore the foramen magnum is formed between the two exoccipitals laterally and supraoccipital dorsally. A lateral occipital foramen is also formed on the exoccipital at the base near the medial margin. Viewed dorsally (after the supraoccipital and epioccipital removed), the left and right exoccipitals form a butterfly-shaped structure. Each of the two exoccipitals extends laterally to form the "wing" portion of the "butterfly" (Figs.49A-B, 50), and the middle part of the bone forms the "body" (Figs.49A-B, 50). At the median of the exoccipital is a thin and flat plate-like portion (Figs 49A-B, 50) which meets its counter part at the medial side of the exoccipital. The plate-like portion of the basioccipital bears two dorsal crests at the dorsal aspect of the bone (see also the description of basioccipital below). These two dorsal crests of the basioccipital form a canal whereas the plate-like structure of the exoccipital roofs the canal-like structure (Fig.50).

Variation of the exoccipital among the *Phoxinus* species includes shape of the wing portion and the posterior margin of the plate portion. In *P. phoxinus*, *neogaeus*, and *issykku-lensis*, the anterior margin of the wing-like structure is deeply concave (TS 78[1]); the margin is shallowly concave in other species of *Phoxinus* (TS 78[0]). The posterior margin of the plate-like structure is convex in *P. neogaeus*, *issykku-lensis*, and *phoxinus* (TS 79[1]); it is shallowly concave in *P. eos*, and *erythrogaster*, and deeply concave in other species of *Phoxinus* (TS 79[0]).

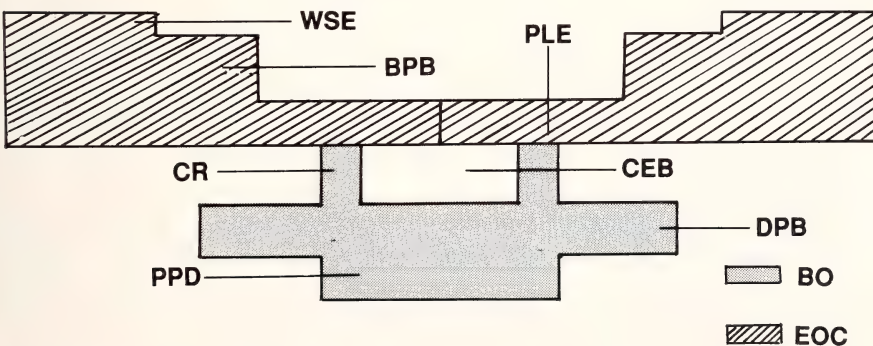


Fig.50: Diagram showing the relationships between basioccipital and exoccipitals (anterior view) of *Phoxinus*.

In the outgroups, the anterior margin of the wing-like structure is shallowly concave, and the posterior margin of the plate-like portion of the exoccipital is concave.

Supraoccipital and medial extrascapula (Figs.44A, B, 51A-C). In cyprinids, the supraoccipital is a medial bone and placed at the most posterior portion of the dorsal side of neurocranium and forms the posterior roof of the braincase. Size of the crest varies greatly in the cyprinids from well-developed (e.g., *Luciobrama macrocephalus*, *Ctenopharyngodon idellus* – Howes 1978, 1981) to poorly developed (e.g., *P. phoxinus*).

Dorsally, the supraoccipital is overlapped by the parietal anteriorly and contacts with the epioccipital laterally in *Phoxinus*. Posteriorly, the supraoccipital sutures with the epioccipital and the exoccipital laterally and exoccipital ventrally. The supraoccipital forms the middle portion of the posterior cover of the braincase and the dorsal edge of the foramen magnum.

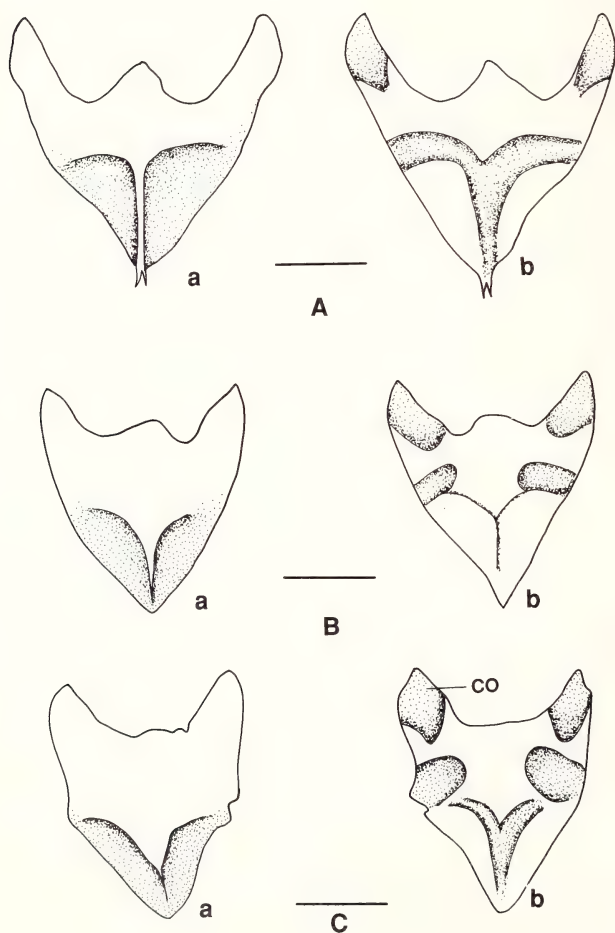


Fig.51: Supraoccipital of *Phoxinus* (a: dorsal view; b: ventral view). A: *P. phoxinus* (CNUC uncat., 76.0 mm TL); B: *P. erythrogaster* (KU 5773, 51.5 mm SL); C: *P. cumberlandensis* (KU 18934; 52.0 mm SL). Scale bars = 1 mm.

In *Phoxinus*, the dorsal portion of the supraoccipital is a flat plate, the posterior portion of the flat plate is bent ventroposteriorly. Viewed dorsally, the middle of the anterior margin of the supraoccipital is deeply concave. Therefore, two anterior processes are present at the lateral portion of the anterior margin of the bone. The crest at the posterior part of the flat plate extends posteriorly. The crest is poorly developed, and is attached by ligaments from the Weberian apparatus and the supraneural bones. Posteriorly, the bone is triangular in shape. The posterior surface of the supraoccipital is attached by epaxial muscles. Four concavities are present on the ventral aspect of the bone (Fig.51A-C).

Variation of the supraoccipital within *Phoxinus* includes the anterior margin and the concavities at the ventral aspect of the bone. In *P. brachyurus*, *issykkulensis*, *phoxinus*, *erythrogaster*, *tennesseensis*, *oreas*, and *neogaeus*, a process is present at the middle of the anterior margin (between the two anterior processes at the anterior margin) (TS 80[1]). The process is well developed in all of the above species, except *P. erythrogaster* in which the process is very short. In *P. cumberlandensis* and *eos*, no process is present at the middle of the anterior margin between the two anterior processes (TS 80[0]). In *P. cumberlandensis*, the four concavities on the ventral side of the supraoccipital are more developed and deeper (TS 81[1]) than that in other species of *Phoxinus* (TS 81[0]).

A small bar-like medial extrascapular (Fig.44B) is present on the supraoccipital in *P. brachyurus* (TS 82[1]). This medial extrascapula is not present in other species of *Phoxinus* (TS 82[0]; Fig.45A).

In the outgroups, the middle of the anterior margin of the supraoccipital bears no process, the concavities on the ventral side of the supraoccipital are small and shallow; the medial extrascapula is absent on the supraoccipital.

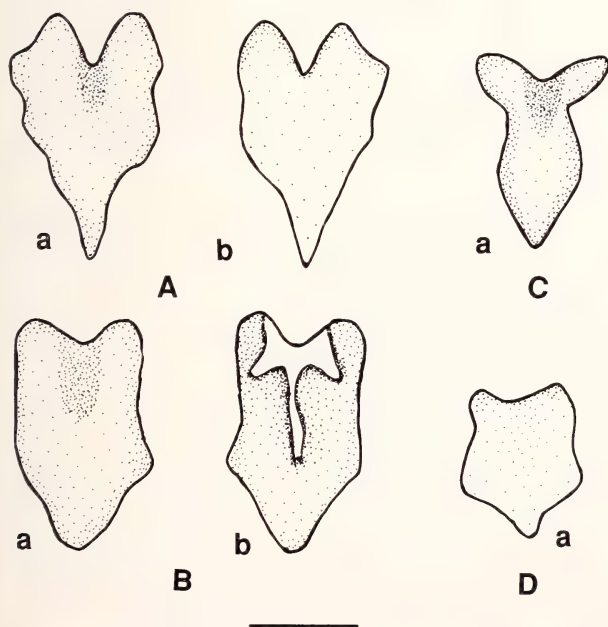


Fig.52: Vomer of *Phoxinus* (a: ventral view; b: dorsal view). A: *P. phoxinus* (CNUC uncat., 76.0 mm TL); B: *P. erythrogaster* (KU 5773; 51.5 mm SL); C: *P. oreas* (KU 3259, 55 mm SL, ventral view); D: *P. eos* (KU 12255, 43.0 mm SL, ventral view). Scale bars = 1 mm.

Basicranial Region

The basicranial region forms the base of the braincase. Three single bones – vomer, parasphenoid, and basioccipital – are included in this region.

Vomer (Fig.52A-D). In cyprinids, the vomer is a single bone, located at the most anteroventral portion of the neurocranium. Dorsally, the vomer connects with the mesethmoid via the planum ethmoidale, as discussed above. Anteriorly, it attaches the kinethmoid via ligaments. The anterolateral edge sutures with the preethmoid.

In *Phoxinus*, the vomer is a plate-like bone bearing a notch at its anterior margin, a constriction at its lateral margin to form a waist, and a process at its posterior margin extending posteriorly and overlapping the ventral side of the parasphenoid.

The process of the posterior margin of the vomer is elongated and sharp in *P. phoxinus* (TS 83[1]); this process is short and blunt in other species of *Phoxinus* and in the outgroups (TS 83[0]). A T-shaped ridge is present at the anterior part of the vomer's dorsal side in *P. erythrogaster* (TS 83[1]); the ridge is not observed in other species of *Phoxinus* and in the outgroups (TS 84[0]).

Parasphenoid (Fig.53A-G). The parasphenoid in cyprinids is a dermal bone and can only be observed in a ventral view of the neurocranium. It is underlaid anteriorly by the vomer.

In cyprinids, the parasphenoid sutures with the lateral ethmoid, orbitosphenoid, pterosphenoid, and prootic dorsally from anterior to posterior. The orbitosphenoid connects with parasphenoid via the orbital septum, as discussed above (however, in some minnows, e.g., *Crossocheilus*, *Labeo*, *Barbus*, the parasphenoid bears a dorsal ridge, via which the parasphenoid contacts with the orbital septum – Ramaswami 1955a, Chen et al. 1984); the pterosphenoid has only a small portion suturing with the ascending wing of the parasphenoid (see below). The posterior part of the parasphenoid overlaps the ventral side of the basioccipital ventrally. The anterior portion of the parasphenoid (anterior to the ascending wing) is generally narrower than the posterior portion (posterior to the ascending wing) in cyprinids.

In *Phoxinus*, the parasphenoid is an elongated plate-like bone; a laterodorsally extending ascending wing is present at the middle of the parasphenoid; the anterior portion of the bone is much narrower than the posterior portion. The anterior portion decreases in size posteriorly. Dorsally, a ridge at the middle of the anterior portion is present which contacts with the orbital septum. The ridge is well-developed in *P. phoxinus* and *eos* (TS 85[1]), and less developed in other *Phoxinus* species (TS 85[0]).

The ascending wing is more or less triangular and bent dorsally. A notch is present on the posterior edge of each ascending wing and, with the prootic, forms the carotid foramen. The notch is well-developed in *P. neogaeus*, *oreas*, *issykkulensis*, *brachyurus*, and *phoxinus* (TS 86[0]); it is less developed in other species of *Phoxinus* (TS 86[1]).

The posterior end of the parasphenoid is forked (Fig.53A-G). The fork is deep and extends to the middle of the posterior part of the parasphenoid in *P. phoxinus* (TS 87[1]); the fork is much shallower in *P. brachyurus*, *erythrogaster*, *eos*, *oreas*, *neogaeus*, *tennes-*

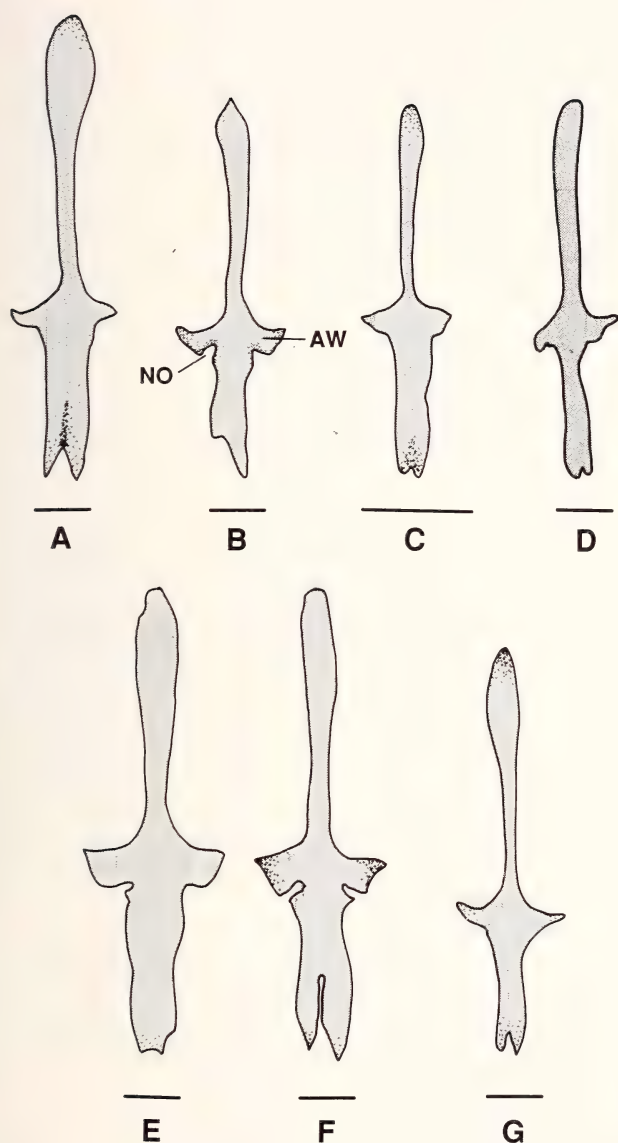


Fig.53: Parasphenoid in ventral view of *Phoxinus*. A: *P. tennesseensis* (UT 44.5274, 50.0 mm SL); B: *P. oreas* (KU 3259, 55.0 mm SL); C: *P. eos* (KU 12255, 43.0 mm SL); D: *P. cumberlandensis* (KU 18934, 52.0 mm SL); E: *P. neogaeus* (KU 8521, 53.0 mm SL); F: *P. phoxinus* (CNUC uncat., 76.0 mm TL); G: *P. erythrogaster* (KU 5773, 51.5 mm SL). Scale bars = 1 mm.

seensis, *issykkulensis*, and *cumberlandensis* (TS 87 [0]); the fork is almost absent in *P. neogaeus*.

The posterior portion of the parasphenoid overlaps the ventral side of the basioccipital. The extent of the overlap varies among species of *Phoxinus*. The posterior end of the parasphenoid extends to the middle of the dorsal part of the basioccipital in *P. neogaeus*,

brachyurus, *issykkulensis*, and *phoxinus* (TS 88 [1]); the posterior end of the bone extends to the posterior portion of the dorsal part of the basioccipital in other *Phoxinus* (TS 88[0]). In the outgroups, the parasphenoid bears a poorly-developed dorsal ridge on its dorsal side, and a well-developed notch on the posterior margin of the ascending wing; the posterior end of the bone is shallowly forked and extends to the posterior portion of the ventral aspect of the basioccipital's dorsal part.

Basioccipital (Figs.49A-B, 50, 54A-B, 55A-D). In cyprinids, the basioccipital is placed at the most posteroventral portion of the neurocranium, and forms the posterior base of the braincase. It sutures with exoccipital dorsally and laterally, prootic anteriorly, and parasphenoid anteroventrally.

The basioccipital is morphologically a complex bone in cyprinids. (It might be the most complicated in all the bones in cyprinids.) Basically, two parts can be recognized from the bone – i.e., dorsal portion, and a pharyngeal process. The dorsal portion appears as a flat plate and is the anterodorsal portion of the basioccipital. The pharyngeal process is the portion located at the posteroventral side of the dorsal portion of the basioccipital (Figs.54A-B, 55A-D). The pharyngeal process consists of a bony plate (pharyngeal pad) for the attachment of a horny pad, a process located at the posterior margin of the pharyngeal pad (posterior process) (Ramaswami 1955a), and an anterior process (in some species). The posterior side of the pharyngeal pad forms the concave condyle articulating with the anterior side of vertebra 1. The dorsal aorta passes the fenestra formed between

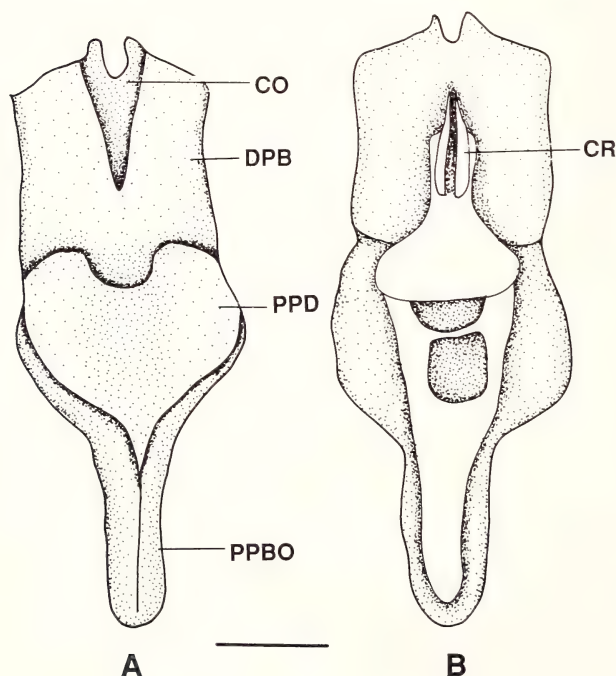


Fig.54: Basioccipital bone of *Phoxinus neogaeus* (KU 8521, 53.0 mm SL) (A: ventral view; B: dorsal view). Scale bar = 1 mm.

the ventral side of the dorsal portion and the dorsal side of the pharyngeal process. The posterior process was formed by the haemal arches of the third vertebral segment assimilated into the skull; the centrum of the vertebral segment was united by the basioccipital to form the condyle (Ramaswami 1955a).

The basic morphology of the basioccipital in *Phoxinus* is similar to that in other cyprinids described above. Variations among the species of *Phoxinus* include the following aspects.

In *P. oreas*, *neogaeus*, and *phoxinus*, a notch is present on the middle of the anterior margin of the basioccipital (TS 89[1]); the notch is absent on the anterior margin in other species of *Phoxinus* (TS 89[0]). In all *Phoxinus* species, a shallow and elongated concavity is present at the anteromiddle portion of the ventral side of the dorsal portion (of the basioccipital) on which the parasphenoid overlaps. In *P. neogaeus*, *phoxinus*, *brachyurus*, and *issykkulensis*, the concavity is triangular and extends to the anterior half of the dorsal portion (TS 90[1]). In other species of *Phoxinus*, however, the concavity is rectangular and extends to the posterior half of the dorsal portion of the basioccipital (TS 90[0]).

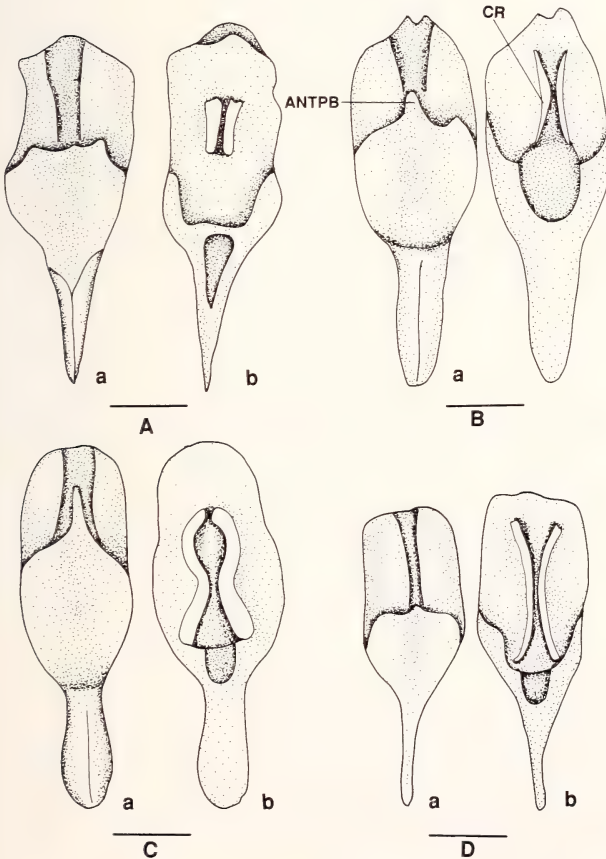


Fig.55: Basioccipital of *Phoxinus* (a: ventral view; b: dorsal view). A: *P. erythrogaster* (KU 5773, 51.5 mm SL); B: *P. oreas* (KU 3259, 55.0 mm SL); C: *P. cumberlandensis* (KU 18934, 52.0 mm SL); D: *P. eos* (KU 12255, 43.0 mm SL). Scale bars = 1 mm.

Dorsally, two anteroposteriorly directed parallel crests (Figs.54B, 55A-D) are present on the mesial portion of the dorsal side of the basioccipital's dorsal portion. These two parallel crests articulate with the ventral side of the exoccipital to form a canal-like structure (see the description of the exoccipital above) (Figs.49A-B, 50). The crests run from the middle to the posterior end of the dorsal portion of the basioccipital. Variation of the crest includes the space between the anterior ends of the left and right crests, and the extent of the development of the crest. The crest is high and the space between the anterior ends of the left and right crests is narrow in *P. cumberlandensis* (TS 91[1]; Fig.55C); whereas the crest is lower and the space is broad in other *Phoxinus* species (TS 91[0]). In *P. erythrogaster*, the crest is short, and placed at the middle of the dorsal side of the dorsal portion (TS 92[1]; Fig.55A). In other *Phoxinus*, the crest is elongated extending from the middle to the posterior margin of the dorsal side of the dorsal portion (TS 92[0]; Fig.55B-D).

As described above, three parts can be recognized for the pharyngeal process in most species of *Phoxinus*, i.e., the pharyngeal pad, the anterior process (lacking in some species, see below) located at the anterior margin of the pharyngeal pad, and the posterior process. The pharyngeal pad is a plate-like structure contacting the masticatory pad at its ventral side. The pharyngeal pad is concave; its margin extends anteriorly forming the anterior process in some species, its posterior margin extends forming the posterior process. Variations were observed in size and shape of the pharyngeal pad, the anterior process, and the posterior process. The pharyngeal pad is well developed, semi-ellipsoidal, elongated and relatively narrow, the length between the anterior and posterior margins (the anterior and posterior processes not included) is longer than the width between the left and right margins of the pad, the ventral concavity is deep in *P. tennesseensis*, *oreas*, and *cumberlandensis* (TS 93[1]). In other *Phoxinus* species, the pharyngeal pad is less developed, semi-round, short and relatively wide, its length is shorter than its width, and the concavity is shallow (TS 93[0]).

The anterior process is long and narrow in *P. cumberlandensis* (Fig.55C), whereas the anterior process is short and broad in *P. oreas*, *tennesseensis*, *issykkulensis*, and *phoxinus*; it is less developed in *P. eos* (Fig.54D) and very small, almost absent in *P. erythrogaster* (TS 94[0]; Fig.55A). In *P. brachyurus* and *neogaeus*, the anterior process is absent, and the anterior margin of the pharyngeal pad is concave (TS 94[1]). Besides the main anterior process mentioned above, two small anterior processes are present at the lateral part of the anterior margin of the pharyngeal pad in *P. phoxinus* (TS 95[1]) (Fig.13C). The lateral processes are absent in other species of *Phoxinus* (TS 95[0]). The posterior process is broader and stout in *P. neogaeus*, *oreas*, *cumberlandensis*, and *tennesseensis* (TS 96[1]). This process is relatively high and narrow in other *Phoxinus* (TS 96[0]).

In the outgroups, the anterior margin of the dorsal portion is straight or slightly convex without concavity; the concavity at the ventral side of the dorsal portion is elongated and rectangular; the crest on the dorsal side of the dorsal portion of the basioccipital is straight, and the space between the anterior ends of the crests is wide; the pharyngeal pad is relatively small and short; the anterior process is not present on the anterior margin of the pharyngeal margin (no lateral process present at the lateral portion of the anterior margin), and the posterior process is narrow.

Presence of the anterior process of the pharyngeal process is previously proposed as an apomorphic character at the genus level for *Phoxinus* (see p. 34). Absence of the process in *Phoxinus* may have resulted from loss or is a reversal of the presence of the process. Therefore, the absence of the process is hypothesized an apomorphic character state within *Phoxinus*.

Viscerocranium

The viscerocranium is located ventrally to the neurocranium. The regions included in the viscerocranium are the upper and lower jaws, hyoid region, suspensorium, opercular region, and branchial region.

Upper jaw

As in all cyprinids, the upper jaw in *Phoxinus* consists of two paired bones: premaxilla and maxilla.

Premaxilla (Fig.56A-E). The premaxilla is an elongated, narrow plate-like bone bearing an ascending process at its anterior portion which contacts with the same process of other premaxilla. The premaxilla tapers posteriorly; therefore, its posterior portion is narrower than its anterior portion. The morphology of the premaxilla varies inter- and intraspecifically.

Maxilla (Figs.57A-C, 58A-E). In cyprinids, the maxilla is a paired elongated plate-like bone. Five processes can be recognized from the maxilla (Ramaswami 1955a). Following Chen (1986b), these five processes were named as the anterior process, anterior ascending process, anteromedial process, posterior ascending process, and posterior process (Fig.57C). These processes show variations among the *Phoxinus* species.

The anterior process (Fig.57C) is the most anterior portion of the maxilla. It is broad and blunt in *P. erythrogaster*, *issykkulensis*, *phoxinus*, *oreas*, and *neogaeus* (TS 97[1]); it is narrow and sharp in *P. brachyurus*, *cumberlandensis*, *tennesseensis*, and in the outgroups (TS 97 [0]).

The anteromedial process is the process located at the medial side of the anterior process (Figs.57A-C, 58A-E). The anteromedial process is broad, blunt, and well developed in *P.*

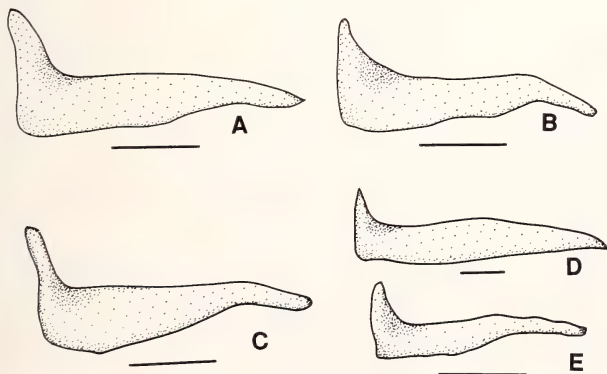


Fig.56: Premaxilla in lateral view of *Phoxinus*. A: *P. phoxinus* (CNUC uncat., 76.0 mm TL); B: *P. cumberlandensis* (KU 18934, 51.5 mm SL); C: *P. oreas* (KU 3259, 55.0 mm SL); D: *P. erythrogaster* (KU 5773, 51.5 mm SL); E: *P. eos* (KU 12255, 43.0 mm SL). Scale bars = 1 mm.

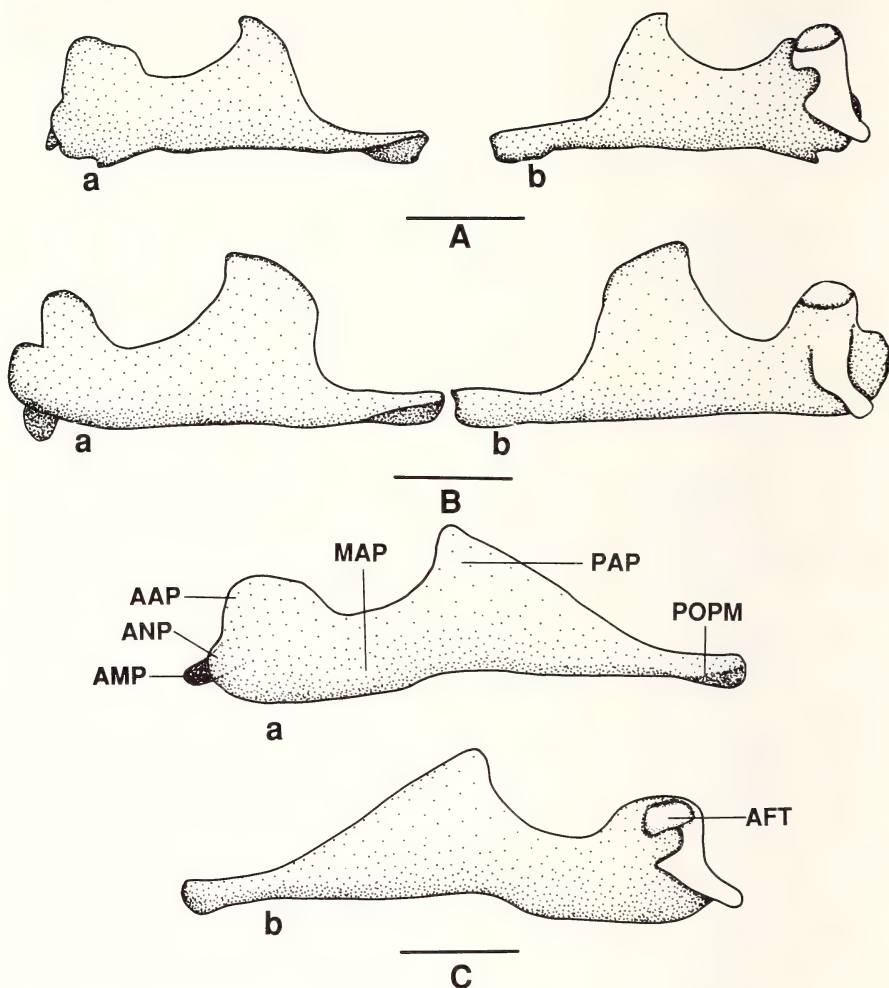


Fig.57: Maxilla of *Phoxinus* (a: lateral view; b: medial view). A: *P. oreas* (KU 3259, 55.0 mm SL); B: *P. phoxinus* (CNUC uncat., 76.0 mm TL); C: *P. neogaeus* (KU 8521, 53.0 mm SL). Scale bars = 1 mm.

oreas, *neogaeus*, *cumberlandensis*, *brachyurus*, *tennesseensis*, *erythrogaster*, and *phoxinus* (TS 98[1]); it is sharp and less developed in *P. eos* (TS 98[0]); it is almost absent in *P. issykkulensis* (TS 98[2]).

In the outgroups, the anteromedial process is sharp. The presence of the blunt process and the very small process are proposed herein to be derived independently.

The anterior ascending process (Fig.57C) was found on the dorsal side of the anteromedial process and extends dorsally. The process is lower, almost absent in *P. erythrogaster*

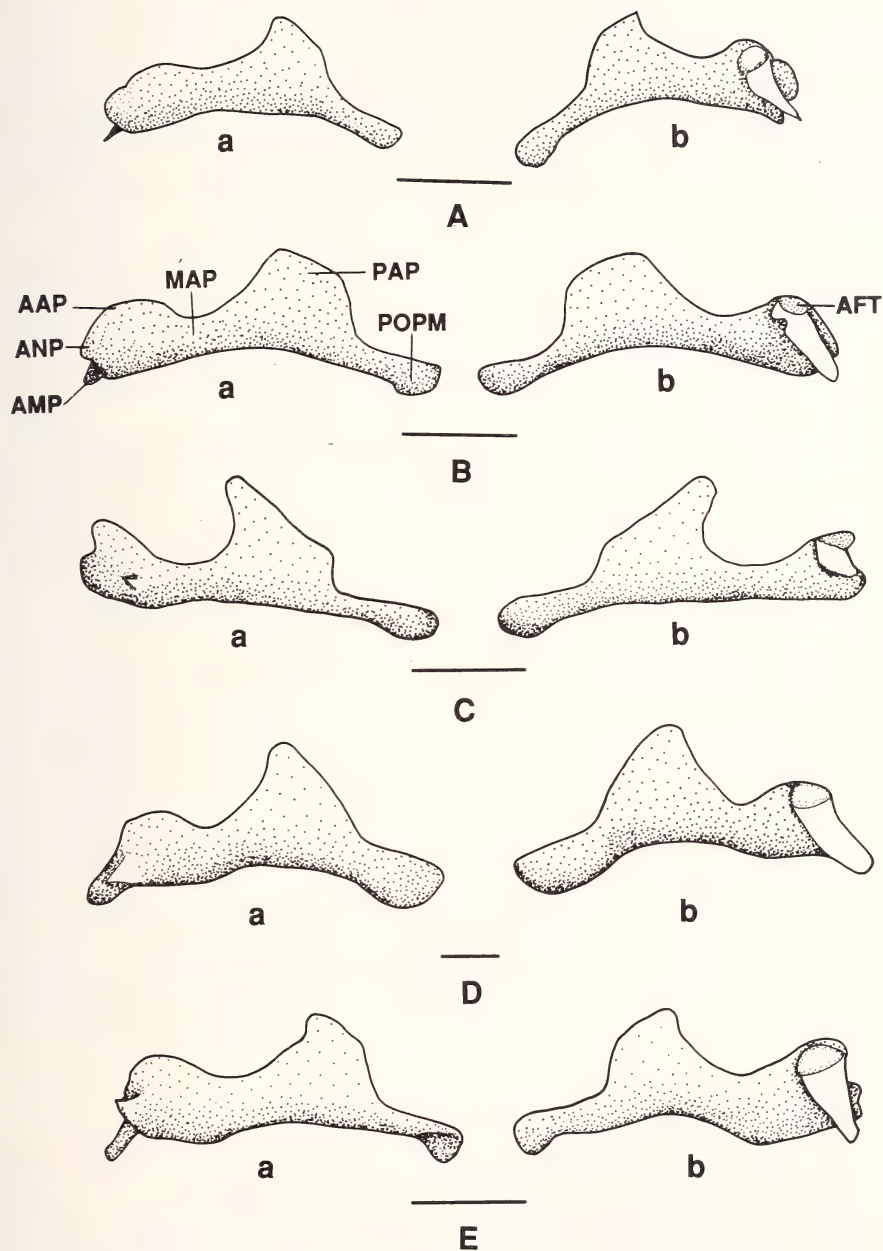


Fig.58: Maxilla of *Phoxinus* (a: lateral view; b: medial view). A: *P. eos* (KU 12255, 43.0 mm SL); B: *P. erythrogaster* (KU 5773, 52.5 mm SL); C: *P. issykkulensis* (P-10696; 42.4 mm SL); D: *P. brachyurus* (MCZ 3006, 75.9 mm SL); E: *P. cumberlandensis* (KU 18934, 52.0 mm SL). Scale bars = 1 mm.

and *P. eos* (TS 99 [1]); whereas it is high in other species of *Phoxinus* and in the outgroups (TS 99 [0]).

Viewed medially, an articularity facet is present (Fig. 57C). The facet is formed by both the dorsal side of the anteromedial process and the base of the anterior ascending process in *P. oreas*, *cumberlandensis*, *erythrogaster*, *tennesseensis*, *brachyurus*, *neogaeus*, and *eos* (TS 100 [1]); whereas the facet is formed only by the anterior ascending process in *P. phoxinus*, *issykkulensis*, and in the outgroups (TS 100[0]).

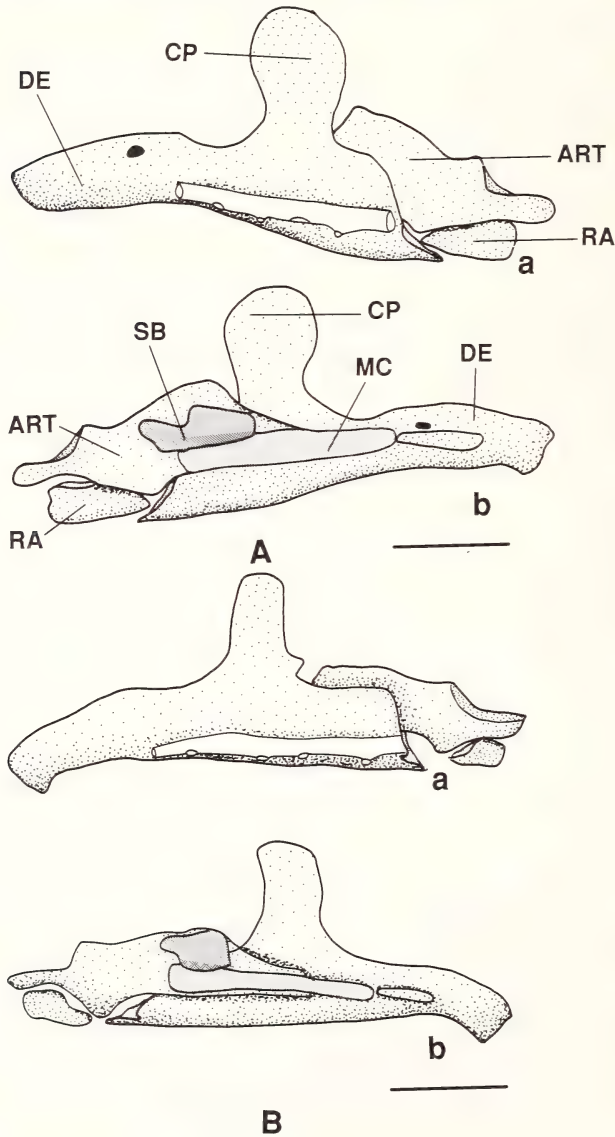


Fig. 59: Lower jaw of *Phoxinus* in lateral (a) and medial (b) views. A: *P. phoxinus* (CNUC uncat.; 76 mm TL); B: *P. oreas* (KU 3259; 55.0 mm SL). Scale bars = 1 mm.

Extending dorsally, the posterior ascending process is located at the posterior portion of the maxilla. It is high and relatively narrow in *P. oreas* and *issykkulensis* (TS101 [1]); it is broad in other species of *Phoxinus* and in the outgroups (TS 101[0]).

The posterior process is the most posterior portion of the maxilla. It extends ventroposteriorly in *P. brachyurus*, *cumberlandensis*, *erythrogaster*, *issykkulensis*, *eos*, and in the outgroups (TS 102[0]); it extends posteriorly in other species of *Phoxinus* (TS 102[1]).

Lower jaw

In cyprinids, the lower jaw is composed of five paired bones and cartilages, i.e., dentary, retroarticular, sesamoid bone, anguloarticular, and Meckel's cartilage. Ramaswami (1955a) did not mention the Meckel's cartilage in the lower jaw of cyprinids, whereas Sarbahi (1932) only described three bones, i.e., dentary, angular (= retroarticular), and articular (= anguloarticular) in *Labeo rohita*.

Dentary (Figs.59A-B, 60A-C, -61A-B). In *Phoxinus*, the dentary is the largest element of the lower jaw; it is L-shaped with a coronoid process at the posterodorsal portion of the bone. Its ventrolateral portion bears the mandibular canal. The anguloarticular, sesamoid bone, and Meckel's cartilage are attached to the medial side of the dentary and the retroarticular to the ventroposterior portion of the dentary.

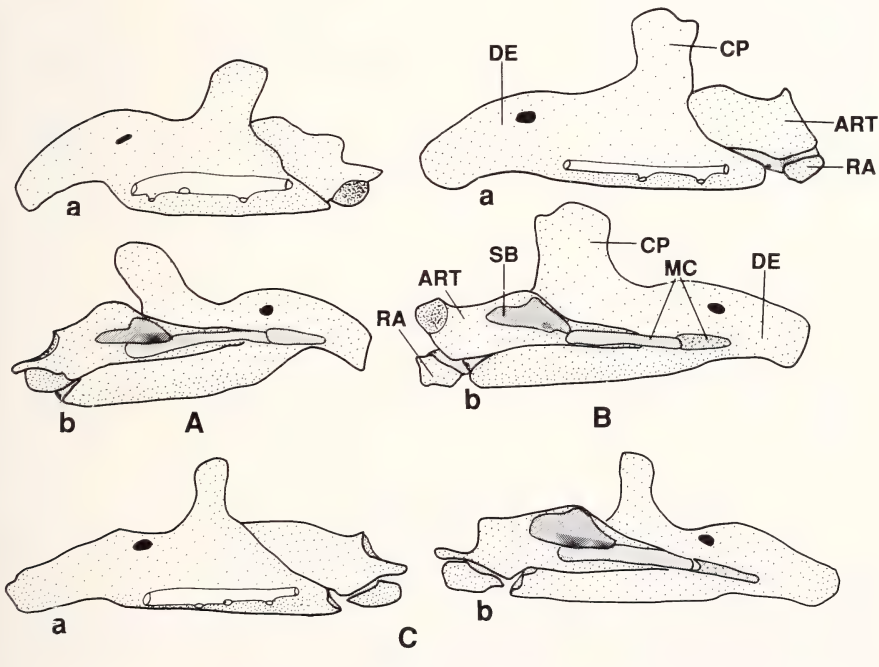


Fig.60: Lower jaw of *Phoxinus* in lateral (a) and medial (b) views. A: *P. eos* (KU 12255, 43.0 mm SL); B: *P. issykkulensis* (P-10696, 42.4 mm SL); C: *P. cumberlandensis* (KU 18934, 52.0 mm SL). Scale bars = 1 mm.

As a whole, the dentary is relatively short and blunt in *P. issykkulensis*, *brachyurus*, and *eos* (TS 103 [1]); it is relatively slender and elongated in other species of *Phoxinus* (TS 103[0]). The coronoid process is perpendicular to the anterior portion of the dentary, and not posteriorly sloped to the dorsal margin of the dentary in *P. cumberlandensis*, *issykkulensis*, *oreas*, and *phoxinus* (TS 104[1]); it is sloped to the dorsal margin of the dentary in other species of the genus (TS 104 [0]). The dentary is slender, and the coronoid process is sloped to the dorsal margin of the dentary in the outgroups.

Retroarticular (Figs.59A-B, 60A-C, 61A-B). The retroarticular is a triangular endochondral bone. It articulates with posteroventral side of the anguloarticular dorsally and ventroposterior portion of the dentary anteriorly. It is well-developed, its length is longer than one-third of the anguloarticular's total length in *P. phoxinus* (TS 105[1]). It is less developed, its length is much less than one-third of the anguloarticular's length in other species of *Phoxinus* and in the outgroups (TS 105[0]).

Sesamoid bone (or sesamoid articular) (Figs.59A-B, 60A-C, 61A-B). The sesamoid bone is a dermal element and located at the medial side of the anguloarticular and of the dentary. It is irregular-shaped with individual variations. The variation of phylogenetic significance is in the relationship between the sesamoid bone and the dentary. In *P. oreas*, *erythrogaster*, and *cumberlandensis*, about one-third of the sesamoid bone overlaps the dentary (TS 106[0]); whereas about half of the sesamoid bone overlaps the dentary in other species of *Phoxinus* (TS 106[1]).

In the outgroups, the sesamoid bone is knife-shaped and only one third of the bone overlaps the dentary.

Anguloarticular (Figs.59A, B, 60A-C, 61A-B). The anguloarticular is placed at posteromedial side of the dentary, and extends to middle of the dentary. The anguloarticular articulates with the retroarticular ventrally and with quadrate ventroposteriorly.

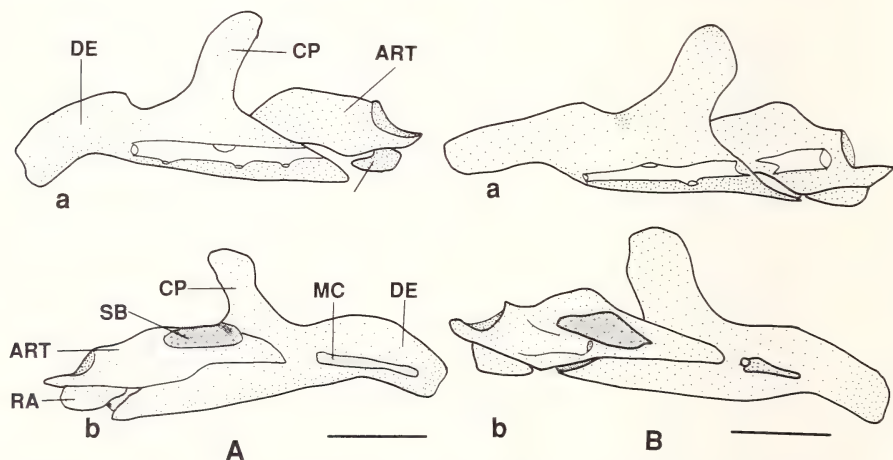


Fig.61: Lower jaw of some species of *Phoxinus* in lateral (a) and medial (b) views. A: *P. tennesseensis* (UT 44.5274, SL 50.0 mm); B: *P. erythrogaster* (KU 5773, SL 52.5 mm SL). Scale bars = 1 mm.

In *Phoxinus*, the anguloarticular is an irregular plate-like bone bearing an articular concavity at its posteroventral portion, a posterior process at the posterior margin, and an anterior process at the anterior margin. The posterior process and the articular concavity of the anguloarticular articulate with the quadrate. The posterior process of the anguloarticular is well-developed and elongated in *P. erythrogaster*, *tennesseensis*, *oreas*, *eos*, *cumberlandensis*, *phoxinus*, and in the outgroups (TS 107[0]); the process is less developed, and short in other species of *Phoxinus* (TS 107[1]).

Meckel's Cartilage (Figs.59A, B, 60A-C, 61A-B). In cyprinids, the Meckel's cartilage is a bar-shaped and partially ossified cartilage in adults; it is placed at the medial side of the middle of the dentary, and the medial anterior portion of anguloarticular. The anterior portion of the cartilage ossifies during ontogeny. This ossified portion, called mento-mecklian, is continuous to the unossified cartilaginous portion and can not be separated from the latter in *Phoxinus*. The shape of the Meckel's cartilage does not vary significantly among *Phoxinus* species. However, the cartilaginous portion is reduced into a very small part in *P. brachyurus* and *erythrogaster* (TS 108[1]); whereas it is not reduced in other species of *Phoxinus* and in the outgroups (TS 108[0]).

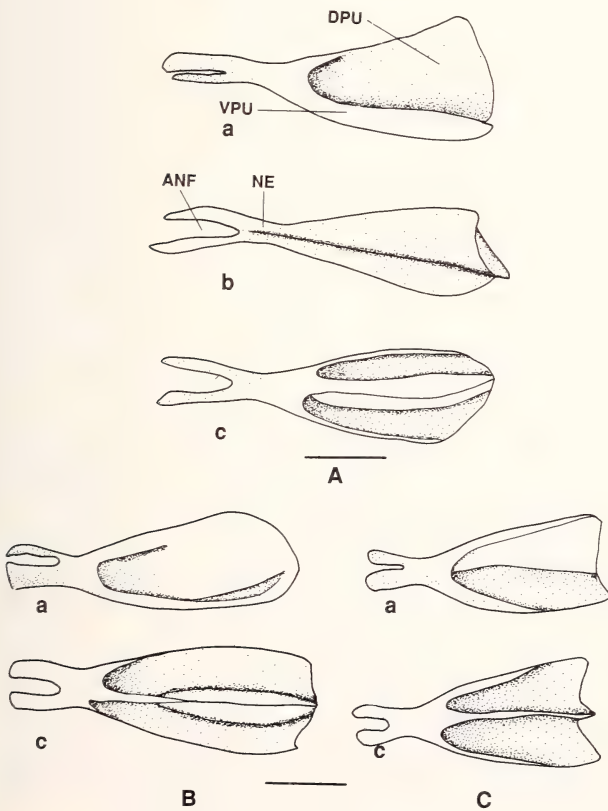


Fig.62: Urohyal of *Phoxinus* (a, lateral, b, ventral and c, dorsal views). A: *P. neogaeus* (KU 8521, 53.0 mm SL); B: *P. brachyurus* (MCZ 3006, 75.9 mm SL); C: *P. tennesseensis* (UT 44,5274, 50.0 mm SL). Scale bars = 1 mm.

Hyoid Region

This region is located posterior to the lower jaw and anterior to the ventral side of the hyomandibular. Via the symplectic and the hyomandibula, this region attaches to the neurocranium. Bones included in the region are the interhyal, posterior ceratohyal, anterior ceratohyal, hypohyal, basihyal, urohyal, and branchiostegals. Among them, the urohyal is formed as an "unpaired ossification of the tendon of the sternohyoideus muscle" (Arratia & Schultze 1990: 247), the branchiostegal rays are dermal elements, and the other are of chondral origin.

Urohyal (Figs.62A-C, 63A-D). In cyprinids, the urohyal is a single bone and placed medially along the ventral portion of the viscerocranium. The urohyal connects to the ventral hypohyal via ligaments anteriorly. The posterior part of the urohyal is attached by the large sternohyoid muscles to the pectoral girdle.

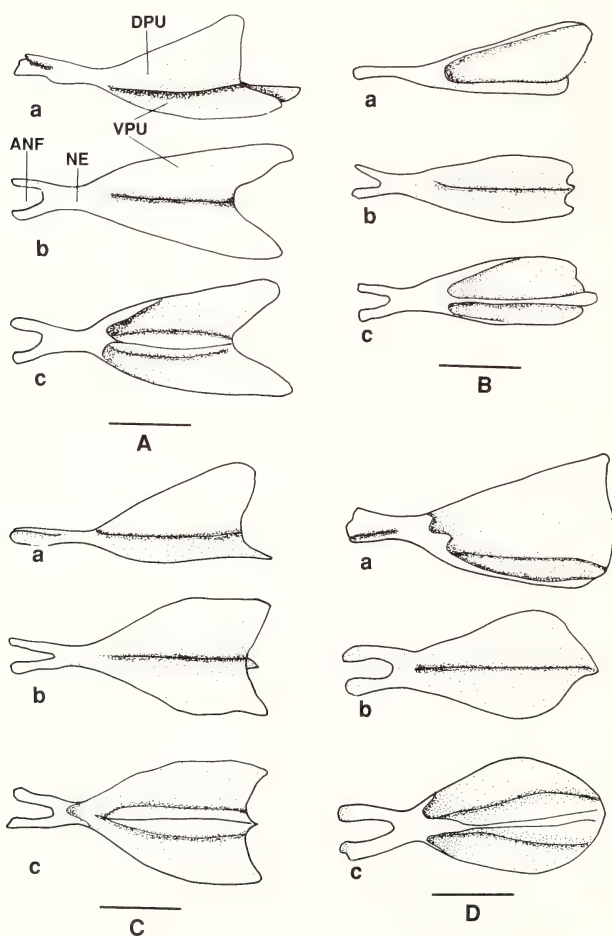


Fig.63: Urohyal of *Phoxinus* (a, lateral, b, ventral and c, dorsal views). A: *P. cumberlandensis* (KU 18934, 52.0 mm SL); B: *P. eos* (KU 12255, 43.0 mm SL); C: *P. erythrogaster* (KU 5773, 51.5 mm SL); D: *P. phoxinus* (CUNC uncat., 76.0 mm TL). Scale bars = 1 mm.

Several parts can be recognized in the urohyal, i.e., the ventral plate (= ventral spread of Kusaka 1974), dorsal plate (= dorsal spread of Kusaka 1974), anterior fork, and neck (Fig.63A). The thin ventral plate of the urohyal is located at the ventral portion of the bone. The bar-shaped neck is at the anterior to the ventral plate. The neck's anterior end is forked, forming the anterior fork of the urohyal. The anterior portion of the dorsal side of the ventral plate bears a concavity. Dorsally, the dorsal plate is present which extends

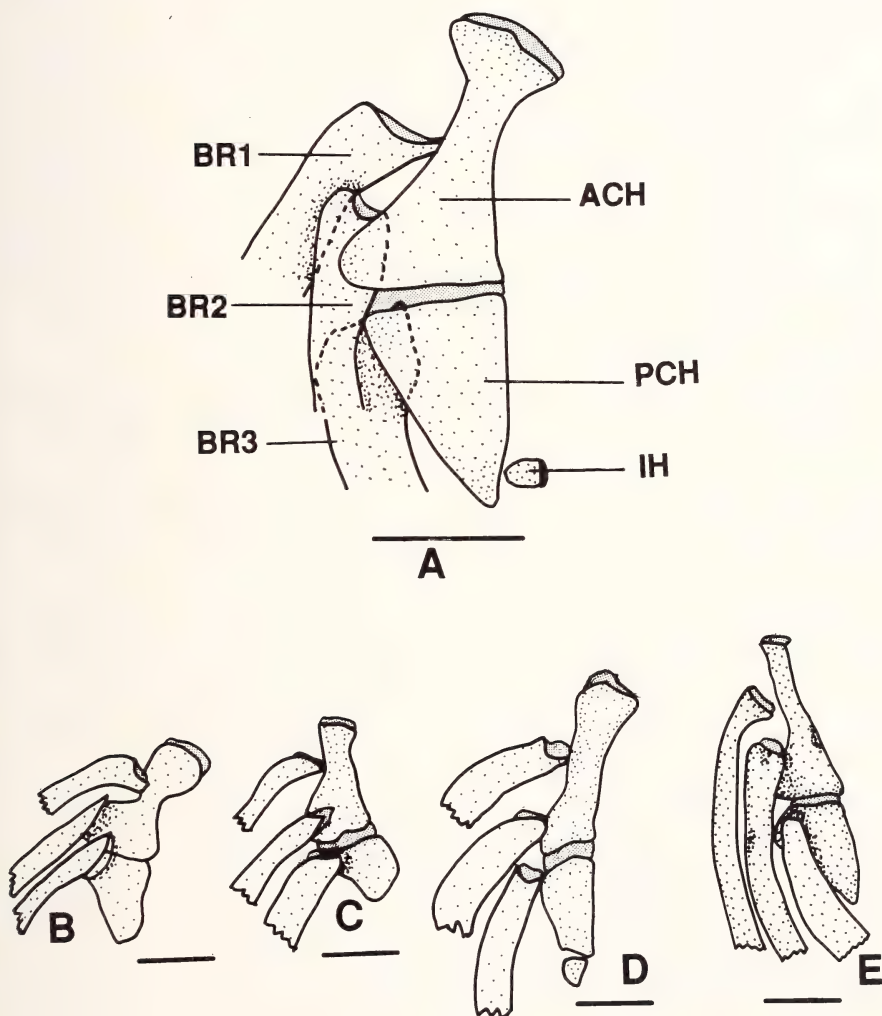


Fig.64: Lateral view of anterior and posterior ceratohyals, branchiostegals, and interhyal of *Phoxinus*. A: *P. oreas* (KU 3259, 55.0 mm SL); B: *P. phoxinus* (KU 22858, 58.0 mm SL); C: *P. eos* (KU 12255, 43.0 mm SL); D: *P. issykkulensis* (P-10696, 42.4 mm SL); E: *P. cumberlandensis* (KU 18934, 45.0 mm SL). Scale bars = 1 mm.

from the mesial line of the dorsal side of the ventral plate. The variations of the urohyal among *Phoxinus* species include the anterior fork, and the ventral and dorsal plates.

The anterior fork is deep in *Phoxinus neogaeus*, *phoxinus*, and *brachyurus* (TS 109[1]), its depth is more than two times of the neck length (from the most posterior point of the anterior fork to the anterior end of the ventral plate). The anterior fork is shallow and equals to (or less than) the neck length in other species of the *Phoxinus* (TS 109[0]).

The ventral plate is the main part of the urohyal. Generally, its posterior portion is broader than its anterior one. In *P. brachyurus*, *neogaeus*, and *phoxinus*, its posterior margin is convex (TS 110[1]). In other species of the *Phoxinus*, however, the posterior margin is concave (TS 110[0]). In *P. eos*, the concave posterior margin bears a process at middle.

The dorsal plate is perpendicular to the dorsal side of the ventral plate. It gradually increases in height posteriorly. Therefore, its posterior portion is higher than its anterior portion and the dorsal plate tends to be triangular in shape. In *P. cumberlandensis*, *oreas*, *erythrogaster*, and *tennesseensis*, the dorsal plate is high and short, its posterior margin is at the level of the most anterior point of the concave posterior margin of the ventral plate (TS 111[1]); in *P. brachyurus*, *issykkulensis*, *phoxinus*, and *neogaeus*, the dorsal plate is lower, its posterior margin is at the level of the most posterior point of the convexed posterior margin (TS 111[0]); in *P. eos*, the dorsal plate is lower and long, its posterior margin extends posterior to the posterior margin of the ventral plate.

In the outgroups, the depth of the anterior fork is less than the elongated neck length, the posterior margin of the ventral plate is shallowly concave; the dorsal plate is low and long, its posterior margin extends beyond the posterior margin of the ventral spread.

Branchiostegals (Fig.64A-E). In cyprinids, the branchiostegals include three pairs of thin, elongated plate-like slender dermal bones, branchiostegals 1, 2, and 3 (from the anterior to the posterior), and are placed at the ventrolateral side of the head.

Branchiostegal 1 (Fig.64A-E) is an elongated bone articulating with the anterior ceratohyal. The anterior end of branchiostegal 1 is concave in *P. neogaeus*, *issykkulensis*, *phoxinus*, *oreas*, *tennesseensis*, and *cumberlandensis* (TS 112[1]); the anterior end is convex in *P. erythrogaster*, *eos*, *brachyurus*, and in the outgroups (TS 112[0]). The relative position of the bone to the anterior ceratohyal does not vary significantly among the *Phoxinus* species.

Branchiostegal 2 (Fig.64A-E) articulates with posterior end of the anterior ceratohyal. The relative position between these two bones does not vary significantly among *Phoxinus* species. The anterior end of the branchiostegal is sharp in *P. phoxinus*, *erythrogaster*, *brachyurus*, and *eos* (TS 113[0]) which is similar to that in the outgroups. The anterior end of the branchiostegal 2 is blunt in other species of *Phoxinus* (TS 113[1]).

Branchiostegal 3 (Fig.64A-E) is the most posterior element of the branchiostegal rays. The position where the branchiostegal contacts the ceratohyals varies among species of *Phoxinus*. In *P. issykkulensis*, *phoxinus*, *erythrogaster*, *neogaeus*, and *brachyurus*, the anterior end of the branchiostegal 3 articulates with both the anterior portion of the posterior ceratohyal and the posterior portion of the anterior ceratohyal (TS 114[1]); branchiostegal 3 articulates with the anterior end of posterior ceratohyal only in other spe-

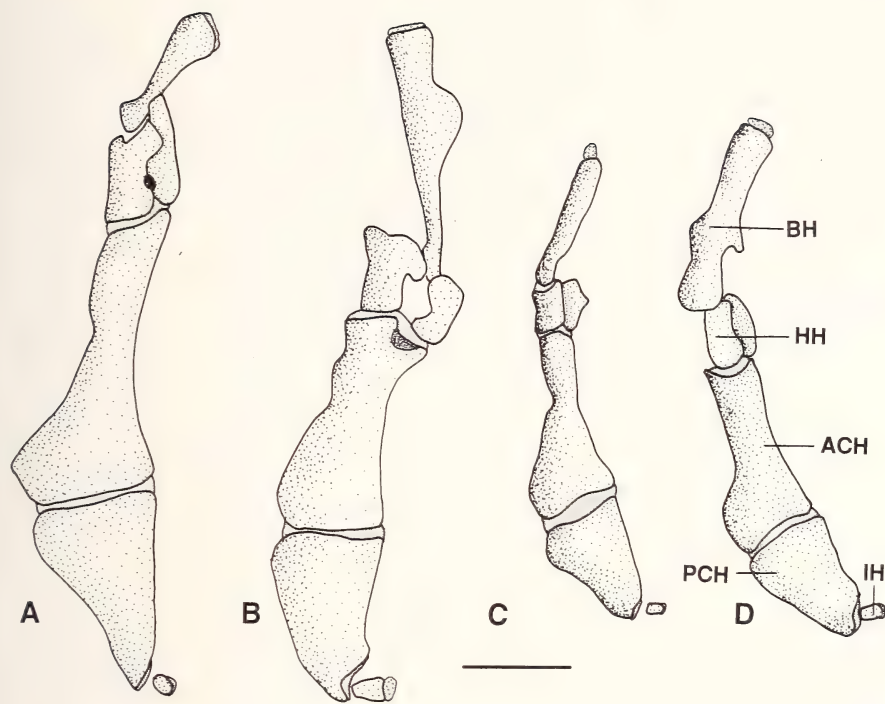


Fig.65: Lateral view of the hyoid arch and basihyal of *Phoxinus*. A: *P. neogaeus* (KU 8521, 53.0 mm SL); B: *P. phoxinus* (CNUC uncat., 76.0 mm TL); C: *P. eos* (KU 12255, 43.0 mm SL); D: *P. cum-berlandensis* (KU 18934, 52.0 mm SL). Scale bars = 1 mm.

cies of the *Phoxinus* and in the outgroups (TS 114[0]). The anterior end of branchiostegal 3 is deeply concave in *P. issykkulensis* (TS 115[1]); the anterior end is not concave in other species of the genus and in the outgroups (TS 115[0]).

Interhyal (Figs.64A-E, 65A-D). The interhyal is a small paired bone located at the most posterior portion of the hyoid region. It articulates with the dorsal side of the posterior ceratohyal, and ventral side of the hyomandibula dorsally via cartilage attaching on the hyomandibula. No variation was found among *Phoxinus* species.

Posterior Ceratohyal (Figs.64A-E, 65A-D). In *Phoxinus*, the posterior ceratohyal is a triangular bone and articulates with the anterior ceratohyal anteriorly, and interhyal posterodorsally. The dorsal side of the posterior ceratohyal bears a notch with which the interhyal articulates. The bone is elongated triangular-shaped in *P. neogaeus*, *issykkulensis*, *brachyurus*, and *phoxinus* (TS 116 [1]), whereas it is short triangular-shaped in other species of *Phoxinus* (TS 116[0]) and in the outgroups.

Anterior Ceratohyal (Figs.64A-E, 66A-D). The anterior ceratohyal is the largest element in the hyoid region, and articulates with the ventral end of the posterior ceratohyal posteriorly, and (the dorsal and ventral) hypophyals anteriorly. The anterior ceratohyal is

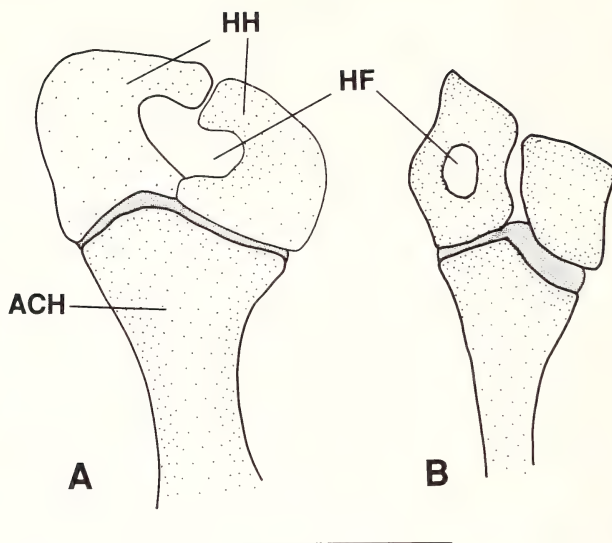


Fig.66: Anterior ceratohyal and hypohyals in lateral view of (A) *Phoxinus oreas* (KU 3259, 55 mm SL), and (B) *P. eos* (KU 12255, 43.0 mm SL). Scale bars = 1 mm.

elongated with a shallow constriction on its anterior portion; its posterior portion is broader than its anterior portion. The anterior margin of the bone is concave in *P. Cumberlandensis* and *tennesseensis* (TS 117[1]); the margin is not concave in other species of *Phoxinus* (TS 117[0]) and in the outgroups. Moreover, a notch is present at the anterior margin of the anterior ceratohyal in *P. phoxinus* and *issykkulensis* (TS 118[1]). This notch is absent in other species of *Phoxinus* and in the outgroups (TS 118[0]).

Hypohyal (Figs.65A-D, 66A-B). In cyprinids, two hypohyals, i.e., dorsal and ventral ones (dorsohyal and ventrohyal in Howes 1978), are present at each side. The dorsal and ventral hypohyals are joined each other by ligaments (Howes 1978). The posterior side of the dorsal hypohyal contacts the dorsoanterior side of anterior ceratohyal, and the ventroposterior side of the ventral hypohyal articulates with the ventroanterior side of the anterior hypohyal. Both hypohyals articulate with the posterior side of the basihyal anteriorly.

In *Phoxinus*, the two hypohyals are not identical in shape. Generally, the bones are rectangular with a notch at the ventral side of the dorsal hypohyal, and a notch at the dorsal side of the ventral hypohyal. The hyoid foramen is usually formed between the two hypohyals (Fig.66A). This condition is present in all species of *Phoxinus*, except *P. eos*, and in the outgroups (TS 119[0]). In *P. eos*, the foramen is formed by the single ventral hypohyal (TS 119[1]) (Fig.66B). In *P. neogaeus*, a concavity is present at the dorsal side of the ventral hypohyal and the ventral side of the dorsal hypohyal (TS 120[1]) – an apomorphic condition found in this species only. In other *Phoxinus* and in the outgroups, the concavity is not present (TS120[0]).

Basihyal (Fig.65A-D). In cyprinids, the basihyal is a single bone located anterior to the hypohyal, and articulates with the left and right hypohyals posteriorly. It is rod- or bar-shaped. In *Phoxinus*, the middle of the lateral side of the basihyal is concave. In *P. cum-*

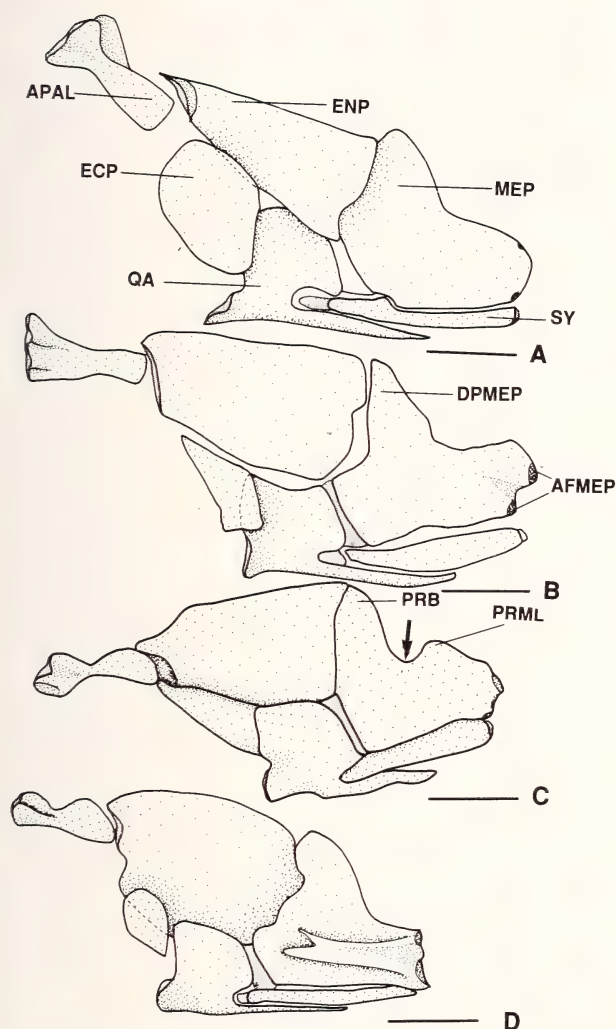


Fig.67: Lateral view of the suspensorium of *Phoxinus*. A: *P. tennesseensis* (UT 44.5274, 50.0 mm SL); B: *P. erythrogaster* (KU 5773, 51.5 mm SL); C: *P. phoxinus* (CNUC uncat., 76.0 mm TL); D: *P. eos* (KU 12255, 43.0 mm SL). The arrow shows notch of the metapterygoid; scale bars = 1 mm.

berlandensis, the anterior portion of the basihyal is bar-shaped, the posterior portion is plate-like with a fork at its lateral margin (TS 121[1]). In other species of *Phoxinus* and in the outgroups, the bone does not bear the fork (TS 121[0]).

Suspensorium

The lower jaw is suspended to the neucranium via the suspensorium. Bones included in the suspensorium are entopterygoid, ectopterygoid, autopalatine, quadrate, symplectic, metapterygoid, and hyomandibula. All are paired bones. Among them, the autopalatine,

metapterygoid, hyomandibular, symplectic and quadrate are chondral bones; whereas, the entopterygoid and ectopterygoid are dermal elements (Arratia & Schultze 1991).

Entopterygoid (Figs.67A-D, 68A-D). In cyprinids, the entopterygoid is an irregularly shaped plate-like dermal bone and located anteriorly to the metapterygoid. It sutures with the anterior margin of the metapterygoid posteriorly, dorsal margin of the quadrate and ectopterygoid ventrally, and posterior end of the autopalatine anteriorly.

In *Phoxinus*, variations of the entopterygoid are in two aspects: the general shape and the articulation with the autopalatine. The entopterygoid is long (anterior-posterior dimension) and relatively narrow (ventral-dorsal dimension) in *P. issykkulensis*, *tennesseensis*, and *cumberlandensis* (TS 122[1]); whereas the bone is short and relatively broad in other species of *Phoxinus* (TS 122[0]). In *P. eos*, *erythrogaster*, and *phoxinus*, the entopterygoid articulates with the posterior end of autopalatine (TS 123[1]); in other species of *Phoxinus* and in the outgroups, it articulates with almost half of the autopalatine (TS 123[0]).

Ectopterygoid (Figs.67A-D, 68A-D). In cyprinids, the ectopterygoid is a small dermal bone placed at the anteroventral side of the entopterygoid. Its posterior side articulates with the anterior margin of the entopterygoid and the quadrate. The ectopterygoid is narrow, slender, and crescent in *P. neogaeus*, *issykkulensis*, *erythrogaster*, and *phoxinus* (TS 124[1]); it is relatively short and broad in other species of *Phoxinus* and in the outgroups (TS 124[0]). The ectopterygoid does not overlap the anterior portion of the entopterygoid in *P. erythrogaster*, *issykkulensis*, *phoxinus*, *tennesseensis*, and *cumberlandensis* (TS 125[1]); the ectopterygoid partially overlaps the entopterygoid in other species of *Phoxinus* and in the outgroups (TS 125[0]). The dorsal margin of the ectopterygoid is far away from the posterior end of the autopalatine in *P. tennesseensis*, *issykkulensis*, *neogaeus*, *erythrogaster*, *oreas*, *eos*, and in the outgroups (TS 126[0]); whereas the two bones are close to each other in other species of *Phoxinus* (TS 126[1]).

Autopalatine (Figs 67A-D, 68A-D). This small endochondral bone is located at the anterior portion of the suspensorium. The anterior portion of the autopalatine articulates with the supraethmoid via a ligament, and connects with the kinethmoid, vomer, maxilla, and infraorbital bone 1 anteriorly. The posterior portion of the autopalatine articulates with the anterior margin of the entopterygoid posteriorly. As discussed under "ectopterygoid," the relative position between the posterior end of the autopalatine and dorsal margin of the entopterygoid varies among the species of *Phoxinus*.

In *Phoxinus*, the autopalatine is a short bar-shaped bone with a forked structure at the anterior end. The shape of this forked structure shows intraspecific variation. Variation with phylogenetic significance includes two aspects. In *P. phoxinus*, *eos*, *cumberlandensis*, and *issykkulensis*, the autopalatine is short, slender, and not well-developed (TS 127[1]) when the similar sized specimens of other *Phoxinus* species and outgroups are compared (TS 127[0]). In *P. phoxinus* and *eos*, the dorsal and ventral margins are concave (TS 128[1]); the margins are almost straight in other species of *Phoxinus* and in the outgroups (TS 128[0]).

Quadrate (Figs.67A-D, 68A-D). In cyprinids, the quadrate is located ventral to the entopterygoid and anterior to the metapterygoid. It articulates with the symplectic dorsally, and with the anguloarticular ventroanteriorly.

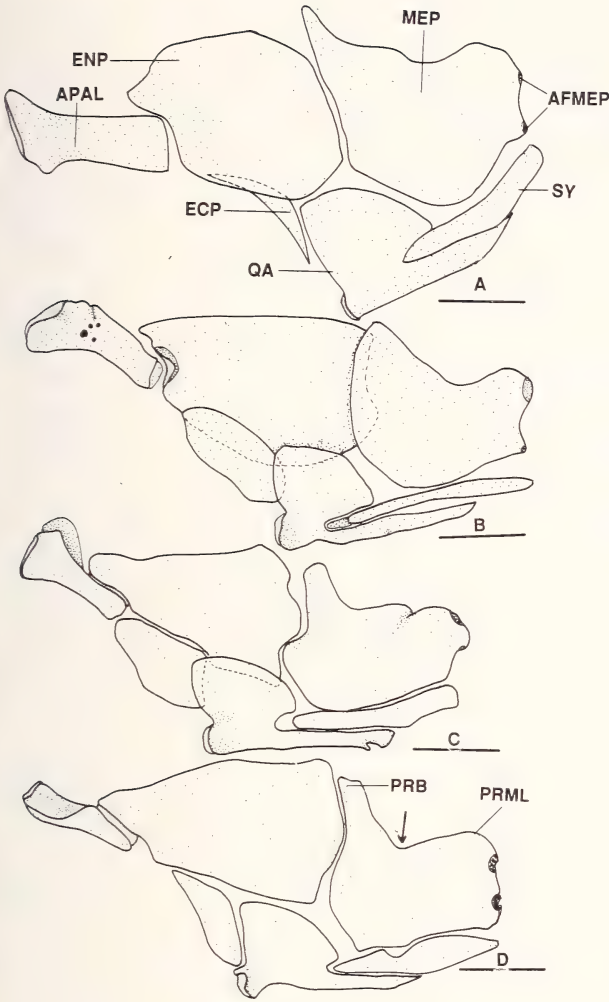


Fig.68: Lateral view of suspensorium *Phoxinus*. A: *P. neogaeus* (KU 8521, 53 mm SL); B: *P. oreas* (KU 3259, 55.0 mm SL); C: *P. cumberlandensis* (KU 18934, 52.0 mm SL); D: *P. issykkulensis* (P-10696, 42.4 mm SL). The arrow shows notch of the metapterygoid; scale bars = 1 mm.

The shape of the quadrate varies greatly in cyprinids. Generally, it is a square-shaped plate bone with a posterior process at its ventral portion, articulating with the symplectic and a condyle (or the articular facet, Arratia & Schultze 1991) at its anteroventral side that articulates with the anguloarticular. The quadrate can be high and short (e.g., *Moroco keumgang* – see Kim & Kang 1986), or low and elongated (e.g., *Luciobrama macrocephalus*, *Elopichthys bambusa* – see Howes 1978, Chen 1987b). The long and elongated condition is generally present in the fish with elongated neurocranium (Howes 1978, Chen 1987b). In *Luciobrama macrocephalus*, a foramen is present at the area posterior to the condyle of the quadrate (Howes 1978, Chen 1987b). Howes (1978:15) indicated that “there appears to be no nerve or vessel of any kind passing through this aperture but only fibers

of the connective tissue which line the floor of the branchial cavity." This foramen has not been reported from other cyprinids.

In *Phoxinus*, the quadrate is high and short. The posteroventral side of the process, articulating with the symplectic, bears a notch in *P. cumberlandensis* (TS 129[1]), which is absent in other species of *Phoxinus* and in the outgroups (TS 129[0]).

Symplectic (Figs.67A-D, 68A-D). In cyprinids, the symplectic is an elongated rod-shaped bone and positioned ventral to the metapterygoid. The symplectic articulates with ventral margin of the metapterygoid dorsally, dorsal margin of the posterior process of quadrate ventrally, and ventral side of the hyomandibular posteriorly.

In *Phoxinus*, the shape and the articulation of the symplectic with other bones are similar to that in most cyprinids. In *P. eos*, *oreas*, and *tennesseensis*, the symplectic is much slender (TS 130[1]) than that in other species of *Phoxinus* and in the outgroups (TS130[0]).

Metapterygoid (Figs.67A-D, 68A-D). In cyprinids, the metapterygoid is a plate-like endochondral bone located anteriorly to the hyomandibula. It articulates with the ventroanterior margin of hyomandibula posteriorly, dorsal margin of the symplectic ventrally, posterior margin of endopterygoid and posterior margin of the quadrate anteriorly.

In *Phoxinus*, the metapterygoid is irregular in shape with two articular facets for the hyomandibula (Figs.67A-D, 68A-D). The dorsal margin of the metapterygoid bears a processus basalis (basal process) on its anterior portion, a processus metapterygoideus lateralis (lateral process) on its posterior portion, and a notch between the two processes. The tri-

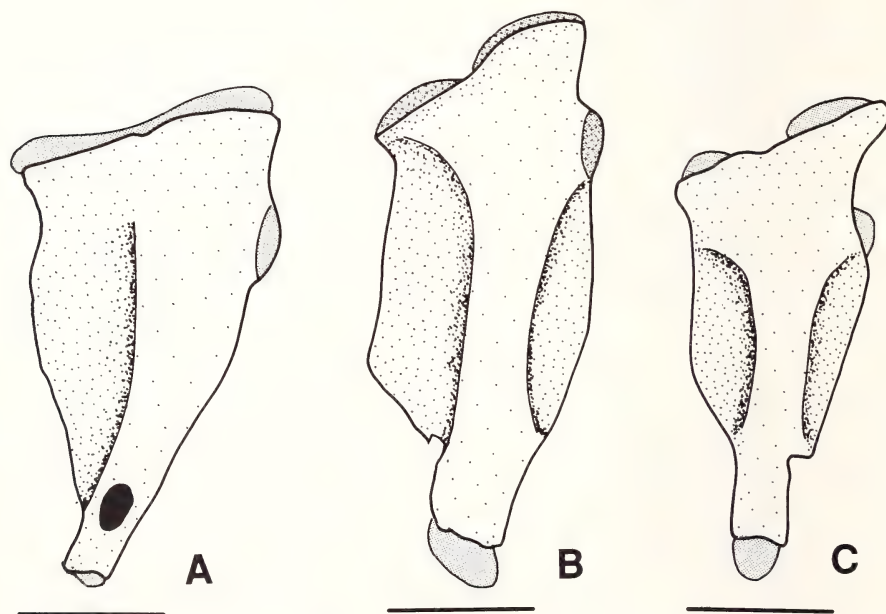


Fig.69: Lateral view of hyomandibula of *Phoxinus*. A: *P. issykkulensis* (P-10696, 42.4 mm SL); B: *P. cumberlandensis* (KU 18934, 52.0 mm SL); C: *P. eos* (KU 12255, 43.0 mm SL). Scale bars = 1 mm.

geminal nerve passes through the notch (Arratia & Schultze 1991). Variations of the metapterygoid include the relative position of the two articular surfaces at the posterior margin, and shape of the two processes.

The two articular surfaces at the posterior margin of the metapterygoid are well-developed and close to each other in *P. eos*, *brachyurus*, *issykkulensis*, *erythrogaster*, and *phoxinus* (TS 131[1]). In other species of *Phoxinus* and in the outgroups, the two surfaces are less developed (TS 131[0]).

The notch at the dorsal margin of the metapterygoid is deep in *P. brachyurus*, *phoxinus*, and in the outgroups (TS 132[0]); it is relatively shallow in other species (TS 132[1]).

The processus basalis of the metapterygoid is narrow and high in *P. erythrogaster*, *phoxinus*, *issykkulensis*, *cumberlandensis*, and in the outgroups (TS 133[0]); the process is broad and relatively lower in other species of *Phoxinus* (TS 133[1]).

Hyomandibular (Figs.69A-C, 70A-F). In cyprinids, the hyomandibular is an endochondral bone and is placed at the posterior portion of the viscerocranium. The dorsal

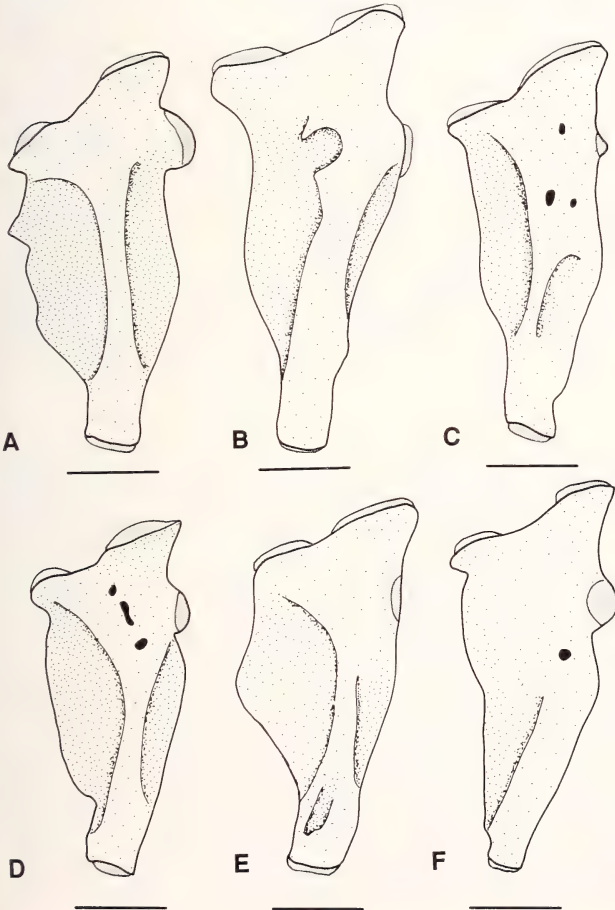


Fig.70: Lateral view of hyomandibula of *Phoxinus*. A: *P. phoxinus* (CNUC uncat., TL 76.0 mm); B: *P. neogaeus* (KU 8521, 53.0 mm SL); C: *P. oreas* (KU 3259, 55.0 mm SL); D: *P. erythrogaster* (KU 5773, 51.5 mm SL); E: *P. brachyurus* (MCZ 3006, 75.9 mm SL); F: *P. tennesseensis* (UT 44.5274, 50.0 mm SL). Scale bars = 1 mm.

portion of the hyomandibula is broader than the rest of the bone. The dorsal margin of the bone is concave and thus forms two articular facets. The anterior facet contacts the hyomandibular fossa which is formed by the sphenotic, pterosphenoid, and the prootic; the posterior one fits into the hyomandibular fossa that is formed by the sphenotic, prootic, and pterotic (Howes 1978, Arratia & Schultze 1991).

The dorsoposterior margin of the hyomandibular bears an articular facet, articulating with the anterior margin of the opercle. The ventral margin of the hyomandibular contacts the dorsoposterior end of the symplectic, and the anterior margin contacts the surfaces at the posterior margin of the metapterygoid.

In *Phoxinus*, the hyomandibular is a plate-like bone. As in other cyprinids, two articulating facets are present on its dorsal margin. The hyomandibular is thick at its dorsal and middle part; it is thin at its anteroventral and posteroventral part. Therefore, three parts can be recognized from the bone, i.e., the body (the thick part), the anterior wing (the anterior thin part), and the posterior wing (the posterior thin part).

The hyomandibular is broad and relatively short in *P. brachyurus*, *phoxinus*, and *issykku-lensis* (TS 134[0]). It is narrow and relative long in other *Phoxinus* species (TS134[1]). The bone bears a notch at the ventroanterior margin in *P. cumberlandensis* and *erythrogaster* (TS 135[1]); the notch is absent in other species of *Phoxinus* (TS 135[0]). In *P. eos*, a notch is present at the ventroposterior margin of the hyomandibular (TS 136[1]); this notch is absent in other *Phoxinus* species (TS 136[0]).

A cartilage is present at the ventral end of the hyomandibula, articulating with the symplectic. The cartilage is large in *P. cumberlandensis*, *erythrogaster*, and *eos* (TS 137[1]); it is much smaller in other species of *Phoxinus* (TS 137[0]).

In the outgroups, the short and relatively broad hyomandibula does not bear notches at its ventroanterior and ventroposterior margins. A small cartilage is attached to the ventral end of the bone.

Opercular Region

In cyprinids, the opercular region is located at the most posterior portion of the viscerocranium, and forms the lateral cover for the gill arches. It is composed of four dermal paired plate bones, i.e., the opercular, subopercular, interopercular, and preopercular bones.

Opercle (Figs.71A-F). The opercle is the largest bone in the opercular region and slightly square-shaped in *Phoxinus*. The opercle articulates with the hyomandibula and preopercle anteriorly, the interopercle ventroanteriorly, and the subopercle ventrally.

The shape of the opercle varies among species of *Phoxinus*. It is elongated and narrow in *P. cumberlandensis* (TS 138[1]); it is short and broad in other *Phoxinus* species (TS 138[0]). The dorsal margin of the bone is almost straight in *P. brachyurus*, *tennesseensis*, and *cumberlandensis* (TS 139[0]); the margin is concave in *P. erythrogaster*, *oreas*, *eos*, *neogaeus*, *issykku-lensis*, and *phoxinus* (TS 139[1]). A narrow and sharp anterodorsal process is present at the anterior end of the dorsal margin in *P. cumberlandensis*, *tennesseensis*, *oreas*, *neogaeus*, and *phoxinus* (TS 140[1]); the process is broad and blunt in *P. erythrogaster*, *eos*, *brachyurus*, and *issykku-lensis* (TS 140[0]).

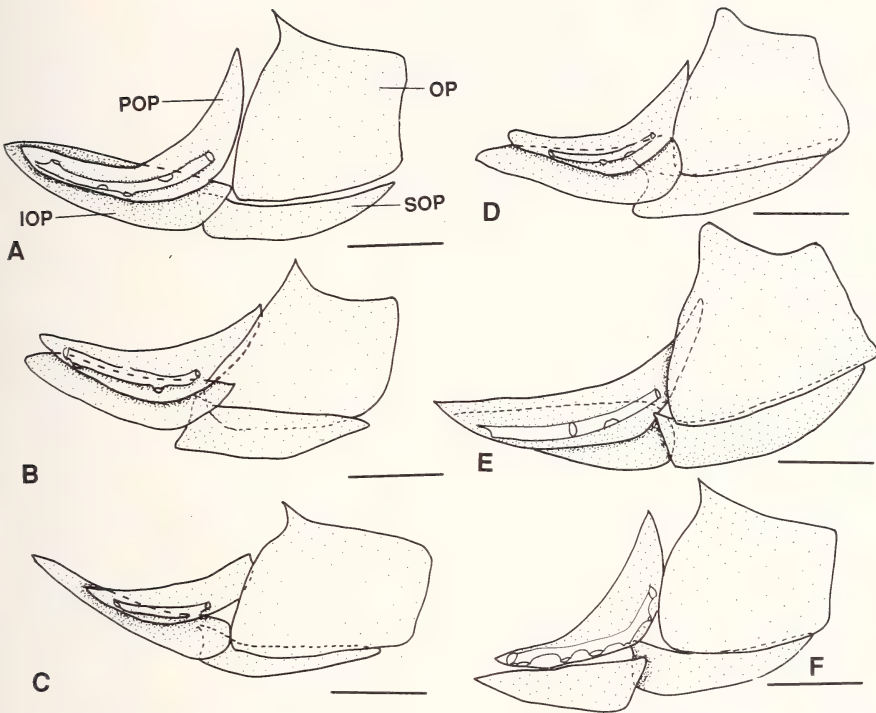


Fig.71: Lateral view of the opercular series of *Phoxinus*. A: *P. tennesseensis* (UT 44.5274, 50.0 mm SL); B: *P. phoxinus* (KU 22856, 56.0 mm SL); C: *P. cumberlandensis* (KU 18934, SL 54.3 mm SL); D: *P. eos* (KU 12255, 43.0 mm SL); E: *P. issykkulensis* (P-10696, 42.4 mm SL); F: *P. oreas* (KU 3259, 52.2 mm SL). Scale bars = 1 mm.

Interopercle (Figs.71A-F). The interopercle is placed at the anteroventral portion of the opercular series. It is partially overlapped by ventral side of the preopercle dorsally, and by anterior portion of the subopercle posteriorly.

The interopercle is elongated triangular plate-like and tapers anteriorly; therefore, its anterior portion is narrower than its posterior portion. The shape of its posterior margin varies individually. The posterior margin can be concave, slope, or round in different specimens of a single species.

Preopercle (Fig.71A-F). The preopercle is a "L"-shaped bone and located anteriorly to the opercle. Its posterior portion contacts the anterior margin of the opercle, its ventral margin contacts with dorsal side of the interopercle. It is crescent in shape, and its middle portion is broader than its anterior and dorsal portions. No variation with phylogenetic significance is observed in *Phoxinus*.

Subopercle (Fig.71A-F). Placed ventrally to the opercle, the subopercle contacts the opercle dorsally and the preopercle anteriorly.

In *Phoxinus* the subopercle is an elongated triangular bone; thus three angles can be recognized, i.e., the anterodorsal, anteroventral, and posterior angles. The subopercle is broader at its anterior portion than at its posterior portion. The dorsal and ventral margins of the bone are much longer than the anterior margin. The posterior angle is elongated and blunt. The anterodorsal angle might be acute or blunt with intraspecific variation. The anteroventral angle is blunt. In *P. neogaeus*, *issykkulensis*, and *tennesseensis*, the anterior margin of the bone is straight (TS 141[1]); in other species of *Phoxinus* and in the outgroups, the margin is concave (TS 141[0]).

Branchial Region

Bones included in the branchial region are pharyngobranchials, epibranchials, ceratobranchials, hypobranchials, basibranchials, and pharyngeal bones. These bones form the gill arch. They can be grouped into two sets, i.e., the dorsal and ventral elements. The dorsal elements include epibranchials and pharyngobranchials, both of which are suspended on the ventral aspect of neurocranium. The ventral elements include rest of the bones.

Pharyngobranchials (PHB, Fig.72A-F). In cyprinids, the pharyngobranchials are placed at the dorsomedial portion of the gill arches and contact the ventral side of the parasphenoid. There are four paired elements, i.e., pharyngobranchials 1, 2, 3, and 4 (from anterior to posterior). Pharyngobranchials 2 and 3 are fused in cyprinids (Chen 1986b, Mayden 1989); whereas the pharyngobranchial 4 is a cartilage present in some species only (e.g., *Luciobrama macrocephalus* – see Howes 1978). Howes (1978) and Kim & Kang (1986) recognized the two pharyngobranchials (PHB 1, and 2+3 herein) in cyprinids (their infrapharyngobranchials) as the pharyngobranchials 2 and 3, the cartilage in front of the first pharyngobranchial was interpreted as the pharyngobranchial 1.

In *Phoxinus*, pharyngobranchial 1 (Fig.72A-F) articulates with epibranchials 1 and 2 laterally, and pharyngobranchial 2+3 posteriorly. The bone is crescent and shallowly concave at its medial margin. The anterior portion of the pharyngobranchial 1 is broader than the posterior portion of the bone, its posterior margin is not forked in *P. brachyurus*, *phoxinus*, *neogaeus*, *eos*, *tennesseensis*, *oreas*, *cumberlandensis*, and *erythrogaster* (TS 142[0]); especially in *P. neogaeus*, the anterior portion of the bone is much broader than its posterior portion, and the bone is wedge-shaped. In *P. issykkulensis*, the posterior portion of the pharyngobranchial 1 is broader than the anterior portion of the bone, its posterior margin is deeply forked (TS 142[1]).

In the outgroups, the pharyngobranchial 1 is crescent, the anterior portion is broader than the posterior portion, its posterior margin is not forked.

Pharyngobranchial 2+3 (Fig.72A-F) is an elongated bone; it is larger than, and located posteriorly to pharyngobranchial 1. It articulates with pharyngobranchial 1 anteriorly, epibranchials 2 and 3 laterally, and pharyngobranchial 4, if any, posteriorly.

Pharyngobranchial 2+3 is crescent-shaped in *P. eos*, *oreas*, *erythrogaster*, *tennesseensis*, and *cumberlandensis* (TS143[1]). The bone bears a concavity at its lateral and medial sides, the posterior portion of the bone is generally broader than the anterior portion in *P. neogaeus*, *phoxinus*, *brachyurus*, *issykkulensis*, and the outgroups (TS 143[0]). In *P. neogaeus*, the concavity is not well developed.

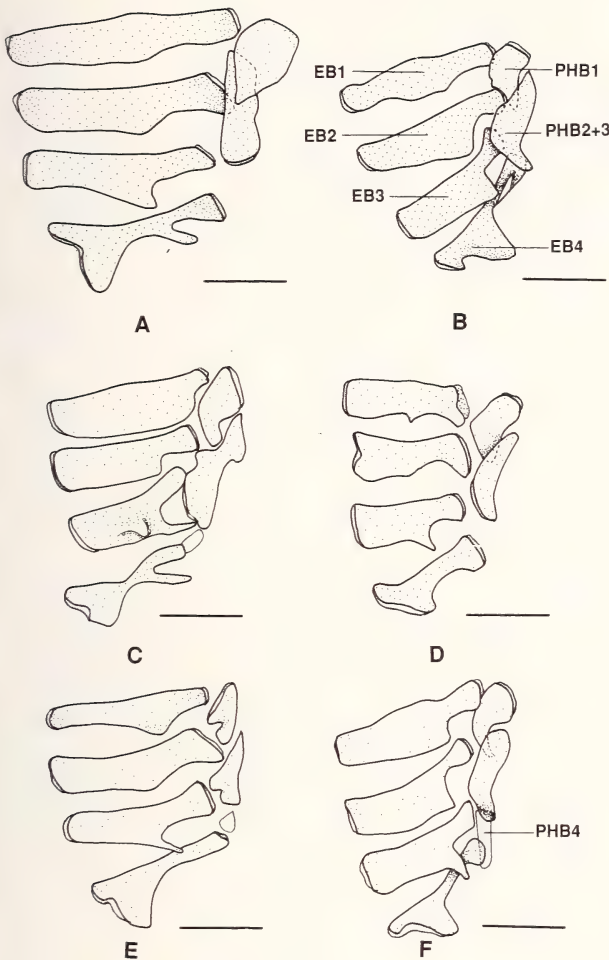


Fig.72: Dorsal view of pharyngobranchials and epibranchials of *Phoxinus*. A: *P. neogaeus* (KU 8521, 53.0 mm SL); B: *P. erythrogaster* (KU 5773, 51.5 mm SL); C: *P. phoxinus* (CNUC uncat., 76.0 mm TL); D: *P. eos* (KU 11335, 49.0 mm SL); E: *P. issykkulensis* (P-10696, 42.4 mm SL); F: *P. oreas* (KU 3259, 55.0 mm SL). Scale bars = 1 mm.

Pharyngobranchial 4 (Fig.72A-F) is a cartilage in *Phoxinus*, and placed at the posterior margin of the pharyngobranchial 2+3. It contacts the pharyngobranchial 2+3 anteriorly, and epibranchial 4 posteriorly. This cartilage is a slender bar in shape. Pharyngobranchial 4 is present in *P. oreas*, *issykkulensis*, and *phoxinus* (TS 144[1]), but absent in other species of *Phoxinus* and in the outgroups (TS 144[0]).

Epibranchials (Fig.72A-F). Four paired bones are included, i.e., epibranchials 1, 2, 3, and 4.

Epibranchial 1 (Fig.72A-F) is a bar-shaped bone articulating with pharyngobranchial 1 dorsally, and ceratobranchial 1 ventrally. The dorsal portion of epibranchial 1 is narrower than the ventral portion. In *P. erythrogaster*, *phoxinus*, *issykkulensis*, and *oreas*, the dorsal portion of epibranchial 1 is constricted, much narrower than the ventral portion of the

bone (TS 145[1]). This condition is not present in other species of *Phoxinus* or the outgroups (TS 145[0]).

Epibranchial 2 (Fig.72A-F) articulates with pharyngobranchials 1 and 2+3 dorsally, and ceratobranchial 2 ventrally. It is short, bar-shaped and has a concavity at its dorsoanterior and dorsoposterior margins. In *P. erythrogaster*, *phoxinus*, and *oreas*, the dorsal portion of the bone is constricted (TS 146[1]). This condition is not present in other species of *Phoxinus* or in the outgroups (TS 146[0]). The ventral margin of the epibranchial 2 is deeply concave in *P. eos* (TS 147[1]); the margin is not concave in other *Phoxinus* species or in the outgroups (TS 147[0]).

Epibranchial 3 (Fig.72A-F) articulates with pharyngobranchial 2+3 dorsally, and ceratobranchial 3 ventrally. It is bar-shaped and forked at its dorsal portion. In *Phoxinus neogaeus*, *eos*, *cumberlandensis*, *erythrogaster*, *tennesseensis*, *brachyurus*, *oreas*, and *issykkulensis*, the posterior process of the dorsal forked structure is much shorter than the anterior branch (TS 148[0]). In *P. phoxinus*, the posterior process is of the same length as the anterior one (TS 148[1]). Therefore, two articular condyles to the pharyngobranchial 2+3 are formed in *P. phoxinus*. Moreover, there is a posterior process at the middle of the bone's lateral side in *P. phoxinus* (TS 149[1]). The process is absent in other species of *Phoxinus* and in the outgroups (TS 149[0]).

Epibranchial 4 (Fig.72A-F) articulates with pharyngobranchial 4 (if any) dorsally, and ceratobranchial 4 ventrally. In *Phoxinus*, this bone is bar-shaped with constriction at the middle of its anterior and posterior margins. The ventral margin of epibranchial 4 is straight in *P. eos*, *tennesseensis*, *oreas*, and *cumberlandensis* (TS 150[0]); it is deeply concave, with two articulating facets contacting the dorsal side of ceratobranchial 4 in *P. erythrogaster*, *neogaeus*, *brachyurus*, *phoxinus*, and *issykkulensis* (TS 150[1]). The dorsal margin of epibranchial 4 is deeply concave in *P. neogaeus* and *phoxinus* (TS 151[1]); the margin is straight without concavity in other species of *Phoxinus* (TS 151[0]) and in the outgroups. The posterior margin of epibranchial 4 bears a wide notch in *P. cumberlandensis*, *issykkulensis*, *oreas*, *erythrogaster*, *tennesseensis*, *brachyurus*, *eos*, and in the outgroups (TS 152[0]); the posterior margin is deeply concave in *P. neogaeus* and *phoxinus* (TS 152[1]).

In *P. erythrogaster* and *P. brachyurus*, a dorsally directed elongated process is present at the lateral side of epibranchial 4 (TS 153[1]). This process is absent in other species of *Phoxinus* and in the outgroups (TS 153[0]).

Ceratobranchials (Fig.73A-F). The ceratobranchials are the longest elements in the branchial region, and consists of four pairs of bones, i.e., ceratobranchials 1, 2, 3, and 4. All ceratobranchials are elongated bar-shaped and bear cartilage at both dorsal and ventral ends. Each ceratobranchial articulates with the same numbered epibranchial dorsally and same numbered hypobranchial ventrally, except ceratobranchial 4 because hypobranchial 4 is absent. No variations with phylogenetic significance are present among the species of *Phoxinus*.

Hypobranchials (Fig.73A-F). Three paired small hypobranchials (1, 2 and 3) are present in *Phoxinus*; they articulates with the same numbered ceratobranchials laterally.

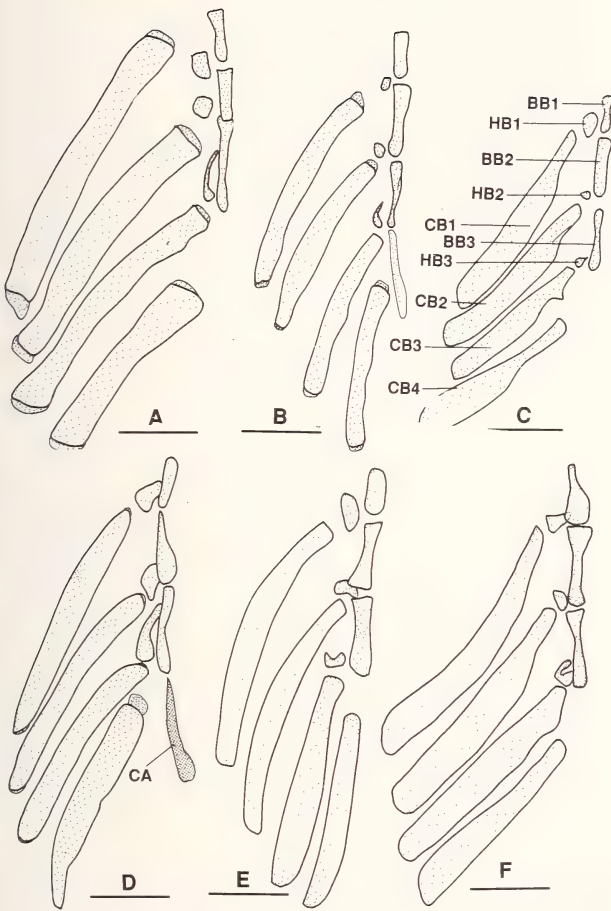


Fig.73: Dorsal view of ceratobranchials, hypobranchials, and basibranchials of *Phoxinus*. A: *P. phoxinus* (CNUC uncat., 76.0 mm TL); B: *P. eos* (KU12255, 43.0 mm SL); C: *P. cumberlandensis* (KU 18934, 52.0 mm SL); D: *P. issykkulensis* (P-10696, 42.4 mm SL); E: *P. oreas* (KU 3259, 55.0 mm SL); F: *P. erythrogaster* (KU 5773, 51.5 mm SL). Scale bars = 1 mm.

Hypobranchials 1 and 2 (Fig.73A-F) are small bones. No variation with phylogenetic significance is present among *Phoxinus* species.

Hypobranchial 3 (Fig.73A-F) is a slender bone tapering ventrally. The left and right hypobranchials 3 are close to each other at their ventral ends, forming an arch-like structure. Basibranchial 3 runs through the arch (Chen 1986b). Variation exists in size of the hypobranchial 3 relative to the basibranchial 2. In *P. phoxinus* and *issykkulensis*, hypobranchial 3 is elongated and its length is almost equal to that of basibranchial 2 (TS 154[1]). In other species of *Phoxinus*, this bone is much shorter than that of basibranchial 2 (TS 154[0]), which is similar to the condition in the outgroups.

Basibranchials (Fig.73A-F). Bones included are three single basibranchials (1, 2 and 3, from anterior to posterior) and placed mesially between the right and left hypobranchials.

In all *Phoxinus* species and in the outgroups, except *P. erythrogaster*, basibranchial 1 (Fig.75A-F) is bar-shaped and slightly concave at the lateral margin (TS 155[0]). In *P. erythrogaster*, the basibranchial 1 is wedge-shaped and its anterior portion is narrower than its posterior portion (TS 155[1]).

Basibranchial 2 (Fig.73A-F) articulates with the posterior margin of basibranchial 1 anteriorly, the anterior margin of the basibranchial 3 posteriorly, and the medial margin of hypobranchial 1 and 2 laterally. It is a slender bar-shaped bone with a slightly concave lateral side. The anterior and posterior ends are broader than the middle of the bone in all *Phoxinus* species and in the outgroups (TS 156[0]), except *P. issykkulensis* in which the bone is tapering anteriorly and sharp at the anterior end (TS 156[1]).

Similar to basibranchials 1 and 2 described above, basibranchial 3 (Fig.73A-F) articulates with the posterior end of basibranchial 2 anteriorly, mesial of hypobranchial 2 and 3 anterolaterally and posteriorly respectively. It is also similar to the basibranchial 2 in shape. It varies in size relative to the basibranchial 2. It is much longer (about two times) than the basibranchial 2 in *P. phoxinus* (TS 157[1]); it is almost of the same length of the basibranchial 2 in other species of *Phoxinus* and the outgroups (TS 157[0]).

In *P. neogaeus*, *eos*, and *issykkulensis*, an elongated cartilage is present at the posterior end of basibranchial 3 which articulates with ventral side of the epibranchial 4 (TS 158[1]). The cartilage is less developed in *P. neogaeus* than that in *P. issykkulensis* and *eos*. The cartilage is very small in other species of *Phoxinus* and the outgroups (TS 158[0]).

Pharyngeal bones and pharyngeal teeth (Fig.74A-C). The pharyngeal bones bearing pharyngeal teeth are located posteriorly to the fourth gill arch. It is the fifth ceratobranchial (Gasowska 1979, Chen 1986b). In cyprinids, the shape of the pharyngeal bones shows a great variation, from very slender (e.g., *Erythroculter ilishaeformis* – Yi & Wu 1964) to very broad (e.g., *Cyprinus carpio*). The pharyngeal teeth on the pharyngeal bone vary in rows and shape in cyprinids. One (e.g., *Rhodeus sericeus*), two (e.g., *P. phoxinus*), three (e.g., *Schizothorax prenanti*), even four rows (*Tetrostichodon* – see Cao 1964) of pharyngeal teeth are present in cyprinids. The teeth vary from slender (e.g., *Acanthorhodeus peihoensis*) to strong (e.g., *Mylopharyngodon piceus*). Almost no book or paper on the taxonomy of cyprinids does not consider the pharyngeal bone and teeth as some of the most useful characters in the identification of genera or species within the family (e.g., Nichols 1943, Wu 1964, 1977). The phylogenetic significance of the pharyngeal bone and the teeth of cyprinids has been discussed by many ichthyologists (e.g., Jurine 1821, Koh 1931, Chu 1935, Girgis 1952, Nikolsky 1963, Peyer 1963, Eastman 1970, Chen 1986a, 1987a, b). Jurine (1821) was the first one describing the pharyngeal bone and teeth of minnows (*Cyprinus carpio*). Chu (1935) was credited as the first known to study the pharyngeal bones and teeth of cyprinid systematically. Eastman & Underhill (1973) studied the intraspecific variation of the pharyngeal tooth formula.

The terms used herein for pharyngeal bones and teeth follow Chu (1935) and Eastman (1970), except the meaning of the posterior angle. The posterior angle (Fig.74) used herein is the angle between the main span of the posterior limb and the posterior edentulous process (Fig.74).

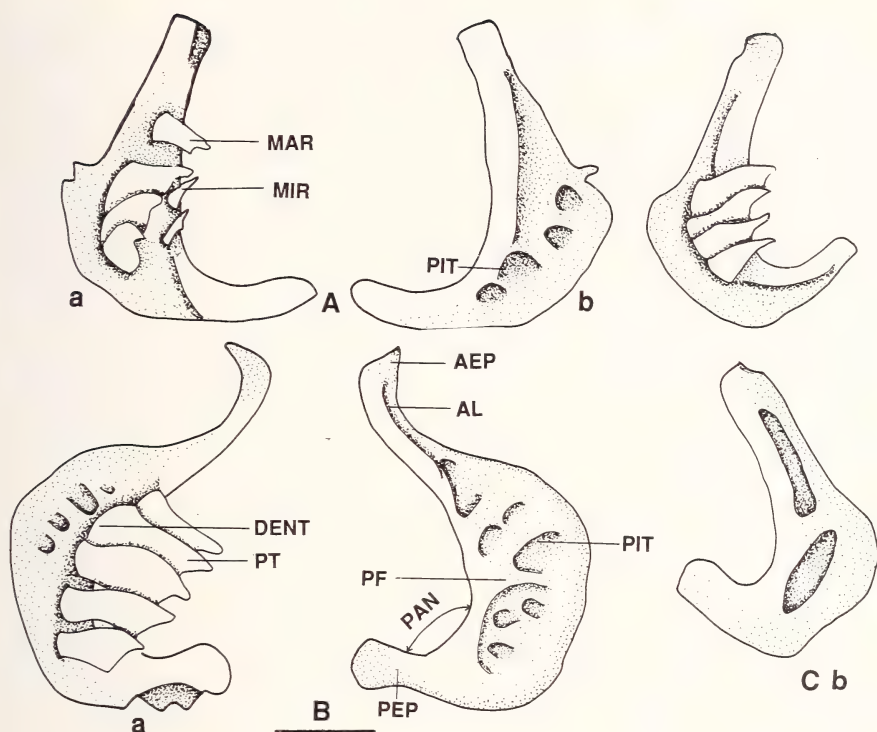


Fig.74: Pharyngeal bone and its teeth of *Phoxinus* in lateral (a) and dorsal (b) views. A: *P. phoxinus* (CNUC uncat. 76.0 mm TL); B: *P. cumberlandensis* (KU 18934, 52.0 mm SL); C: *P. eos* (KU 12255, 43.0 mm SL). Scale bars = 1 mm.

Generally, the pharyngeal bone in *Phoxinus* is “L”-shaped with expansion at the middle of its ventral side. The expanded ventral surface bears several pits, to which masticatory muscles are attached. These pits are well developed in *Phoxinus*. The pharyngeal teeth are located at the dentigerous surface. The teeth are dorsally directed and function to chew food with masticatory pad attached on the pharyngeal pad of the basioccipital bone.

Variations with phylogenetic significance including a few aspects of the pharyngeal bone and teeth among *Phoxinus* species can be described as follows (Fig.74A-C):

1. Posterior angle: This angle partially represents relationship between the posterior edentulous process and the main span of the posterior limb. The smaller the angle, the more anteriorly the posterior edentulous process bends. The angle is smaller in *P. eos*, *tennesseensis*, and *oreas* (TS 159[1]) than in other species of *Phoxinus* and in the outgroups (TS 159[0]).
2. Posterior edentulous process: The posterior edge of the posterior edentulous process bears a flat plate-shaped structure with two small processes in *P. cumberlandensis* (TS 160[1]) (Fig.74B); the structures is not present in other species of *Phoxinus* or in the outgroups (TS 160[0]).

3. Anterior edentulous process: The process is straight in *P. neogaeus*, *erythrogaster*, *phoxinus*, and *eos* (TS 161[1]); it is bent in other species of *Phoxinus* and in the outgroups (TS 161[0]).

4. Tip of the anterior limb: A notch is present at tip of the anterior limb in *P. issykkulensis* and *P. eos* (TS 162[1]); this notch is not present in other species of *Phoxinus* or in the outgroups (TS 162[0]).

5. Pitted surface: Different numbers of pits are present on the surface. Generally, there are a few large and numerous small pits, such as in *P. brachyurus*, *issykkulensis*, *oreas*, *phoxinus*, *neogaeus*, *tennesseensis*, *cumberlandensis*, and in the outgroups (TS 163[0]). In *P. eos*, and *erythrogaster*, however, only two or three large and elongated pits are present with very few or without small ones (TS 163[1]).

6. Pharyngeal teeth: The pharyngeal teeth are present in one row in all North American *Phoxinus* (TS 164[1]) except *P. neogaeus*; the teeth are in two rows in all Eurasian *Phoxinus* (*P. phoxinus*, *brachyurus*, and *issykkulensis*) and the North American *P. neogaeus* (TS 164[0]). If two rows are present, the teeth on the main row are much higher, stronger, and better developed than that in the secondary (minor) row.

Two rows of pharyngeal teeth are present in the outgroups. The presence of one row of the teeth is therefore interpreted as apomorphic, and the presence of two rows of teeth as plesiomorphic in *Phoxinus*.

In the species with two rows of teeth, the formulae of the teeth usually are 5.2(1)-(1)2.5, or 4.2(1)-2(1).4. In the species with one row, the formulae generally are 5-5, or 4-4. However, intraspecific variation of the formulae is very common in *Phoxinus* (e.g., *P. phoxinus*), as indicated in "Species Account".

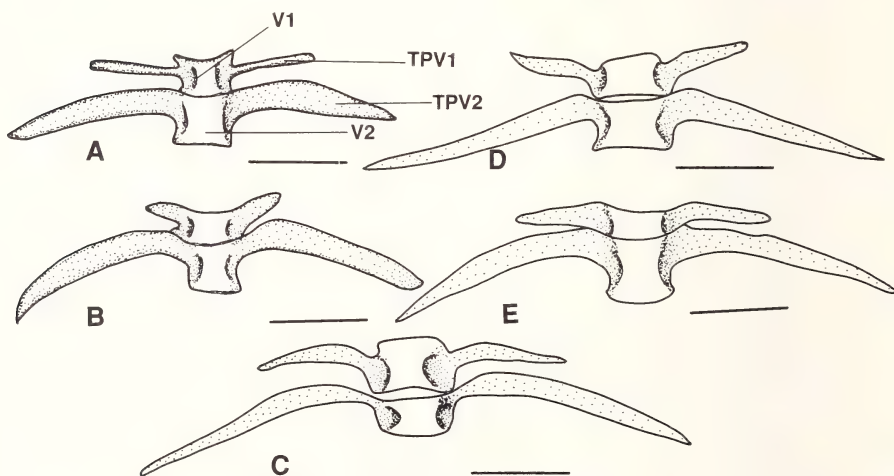


Fig.75: Ventral view of the first and second vertebrae of *Phoxinus*. A: *P. eos* (KU 12255, 43.0 mm SL); B: *P. cumberlandensis* (KU 18934, 52.0 mm SL); C: *P. neogaeus* (KU 8521, 53.0 mm SL); D: *P. oreas* (KU 3259, 55.0 mm SL); E: *P. erythrogaster* (KU 5773, 51.5 mm SL). Scale bars = 1 mm.

Vertebral Column

Weberian Apparatus. In cyprinids, the Weberian apparatus is located at the anterior vertebral column, and function as an otophysic connection between the anterior chamber of gas bladder and inner ear; thus, it can transmit movements of the gas bladder wall to the ear, and aid in hearing and depth perception (Alexander 1962). Two divisions can be recognized from the Weberian apparatus, the pars sustentaculum and the auditum. The pars sustentaculum is composed of the modified first four vertebrae, their arches and gas bladder, and partially function as a supporter for the pars auditum. The pars auditum consists of four paired Weberian ossicles, i.e., claustrum, scaphium, intercalarium, and tripus (from anterior to posterior). The ossicles form a bony chain, connected by ligaments between the ossicles, to connect the gas bladder and inner ear, and to function (with the related ligaments) as a medium to pass the information from the gas bladder to the ear. Numerous papers on the Weberian apparatus in cyprinids have been published. Watson (1939), Alexander (1962), Rosen & Greenwood (1970), and Fink & Fink (1981) are only a few important examples.

The Weberian apparatus in *Phoxinus* is similar to that in other cyprinids. In *Phoxinus*, the vertebral centrum (Figs 75A-E, 76A-D) is short with a short transverse process laterally (transverse process 1). Anteriorly, it articulates with the proatlans of the basioccipital bone. The scaphium and claustrum are placed at the dorsolateral side of the centrum. Variations in *Phoxinus* include the length and relative position of the transverse process. The transverse process is at the anterior margin of the vertebral centrum in *P. cumberlandensis*, *erythrogaster*, *tennesseensis*, and *phoxinus* (TS 165[1]). The transverse process is located at the middle of the lateral side of the vertebral centrum in other species and in the outgroups (TS 165[0]). The transverse process is very short, and extends only to the base of the transverse process of vertebra 2 (transverse process 2) in *P. cumberlandensis* (TS 166[1]). The transverse process is much longer, and almost equals about half of transverse process 2 in length in all other species of *Phoxinus* and in the outgroups (TS 166[0]).

The second vertebral centrum (Figs 75A-E, 76A-D, 77A-C) is more developed than the first one. Its transverse process is elongated. The intercalarium is located at the lateral side of the centrum. A developed neural arch (neural arch 2) is located at the dorsal side of the centrum, and is more or less semi-round. In *P. erythrogaster*, neural arch 2 bears an ascending process at its dorsal portion (TS 167[1]) that is absent in other species of *Phoxinus* and in the outgroups (TS 167[0]).

The third vertebral centrum is more developed than the previous two. No transverse process is present on vertebra 3. Ventrally, a notch is present at the lateral side of the centrum holding the medial ramus of the tripus. A developed neural arch is present at the centrum's dorsal side. Articulating with the ventral portion of neural arch 2 and the neural complex dorsally, neural arch 3 is irregularly shaped and bears an anterior process and a posterior notch. The process is narrow and relatively long in *P. phoxinus* (TS 168[1]; Fig. 77A); the process is broad and relatively short in all other species of *Phoxinus* and in the outgroups (TS 168[0]).

The fourth vertebral centrum (Figs 76A-D, 77A-C, 78A-C) is of similar size to that of the third centrum. A well-developed rib (rib 4) is located at the centrum's lateral side. The

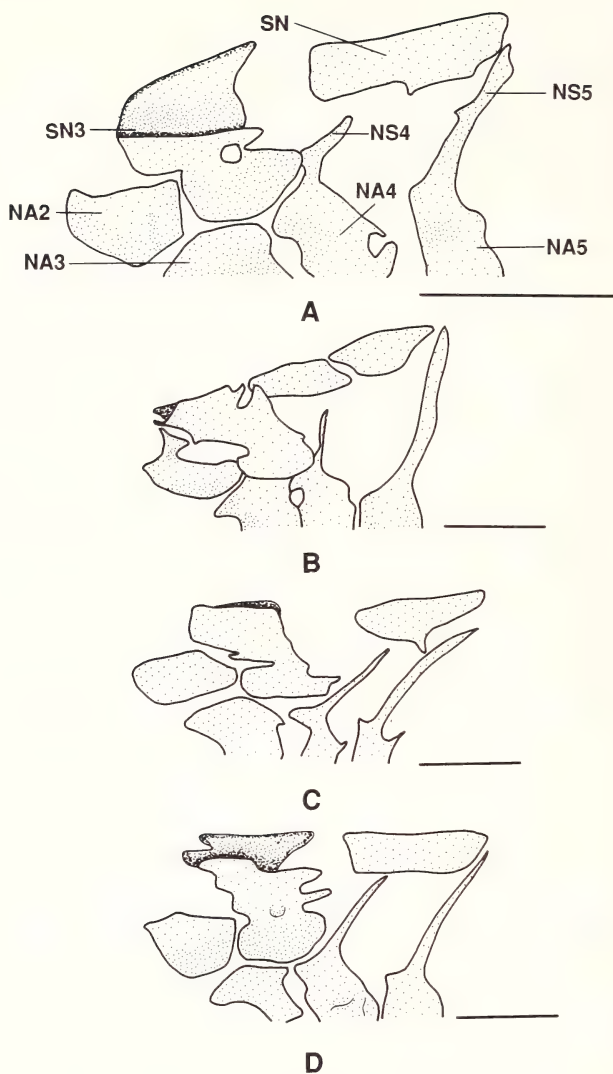


Fig.76: Lateral view of neural arches and spines of anterior vertebrae, neural complex, and supraneural bones of *Phoxinus*. A: *P. issykkulensis* (P-10696, 42.4 mm SL); B: *P. erythrogaster* (KU 5773, 51.5 mm SL); C: *P. neogaeus* (KU 8521, 53.0 mm SL); D: *P. tennesseensis* (UT 44.5274, 50.0 mm SL). Scale bars = 1 mm.

base of the rib is expanded, but the rib's ventral end is sharp. The rib bears a large and shallow notch at its median side in *P. eos* (TS 169[1]; Fig.77A); the notch is absent in other species of *Phoxinus* and in the outgroups (TS 169[0]).

The os suspensorium is developed and plate-like. The left and right os suspensoria are not fused mesially, and a space exists between the dorsal margin of the os suspensorium and the centrum of vertebra 4. The ventral end of the os suspensorium is at the same level of the ventral end of rib 4. Variation occurs in several aspects of the os suspensorium in *Phoxinus*. The os suspensorium is narrow in *P. tennesseensis*, *neogaeus*, *erythrogaster*, *eos*,

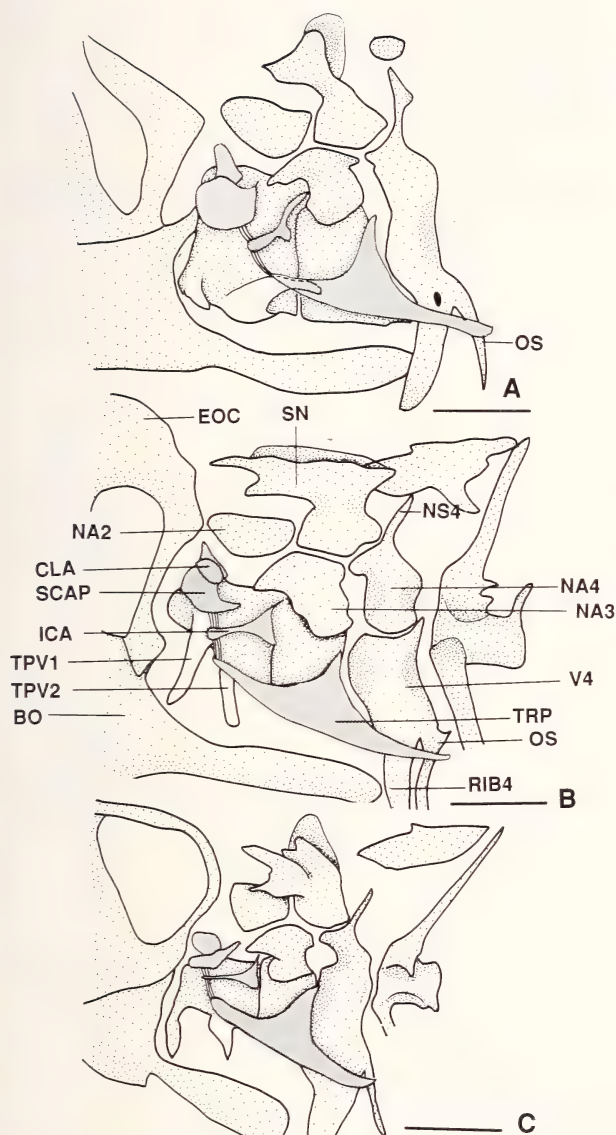


Fig.77: Lateral view of Weberian ossicles, anterior vertebrae and supraneural bones of *Phoxinus*. A: *P. phoxinus* (MCZ 32372, 72.0 mm SL); B: *P. cumberlandensis* (KU 18934, 52.0 mm SL); C: *P. eos* (KU 12255, 43.0 mm SL). Scale bars = 1 mm.

oreas, *issykkulensis*, *brachyurus*, *phoxinus*, and in the outgroups (TS 170[0]); it is broad in *P. cumberlandensis* (TS 170[1]). A notch is present at the medial margin of the suspensorium in *P. erythrogaster* and *P. eos* (TS 171[1]); the notch is absent in other species of *Phoxinus* and in the outgroups. A space from the dorsal margin to the ventral end of the os suspensorium is present between the left and right os suspensoria in *P. tennesseensis*, *neogaeus*, *erythrogaster*, *eos*, *issykkulensis*, *brachyurus*, *oreas*, *cumberlandensis*,

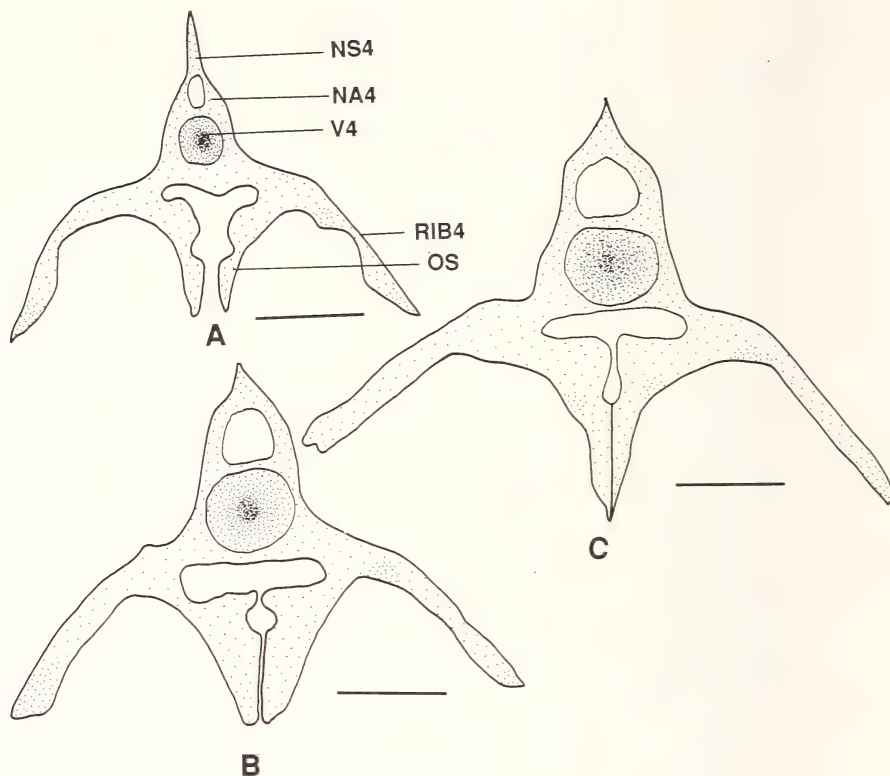


Fig.78: Posterior view of the fourth vertebra, and os suspensorium of *Phoxinus*. A: *P. eos* (KU 12255, 43.0 mm SL); B: *P. cumberlandensis* (KU 18934, 52.0 mm SL); C: *P. phoxinus* (CNUC uncat., 76.0 mm TL). Scale bars = 1 mm.

and in the outgroups (TS 172[0]); the space extends only to the middle of os suspensorium, the left and right parts of the os suspensorium contact each other at the medial from the middle to the ventral end of the os suspensorium in *P. phoxinus* (TS 172[1]).

A neural arch (neural arch 4) and spine are present on dorsal aspect of centrum 4. The anterior edge of neural arch 4 bears a notch. The notch is deep in *P. oreas*, *erythrogaster*, *eos*, and in the outgroups (TS 173[0]), but shallow in other species of *Phoxinus* (TS 173[1]). A space is present between the anterior margin of neural arch 4 and the posterior margin of neural arch 3. This space is partially formed by the notches at the anterior margin of the neural arch 4 and the posterior margin of the neural arch 3. The space extends only to the middle of the anterior margin of neural arch 4 in *P. erythrogaster* (TS 174[1]), but to ventral portion of the anterior margin of neural arch 4 in other species of *Phoxinus* and in the outgroups (TS 174[0]). The neural spine bears a process at its posterior margin of the neural spine 4 in *P. phoxinus* (TS 175[0]) (Fig.80A); the process is absent in other species of *Phoxinus* and in the outgroups (TS 175[0]).

As in other ostariophysans (cf. Fink & Fink 1981), the anteriormost supraneural is absent in *Phoxinus*. Supraneural 3 (neural complex of Chen et al. 1984) is present at dorsal side of the neural arches 3 and 4, and posterior to neural arch 2. Supraneural 3 is a plate-like structure with constriction at the middle of its anterior and posterior margins. Its dorsal

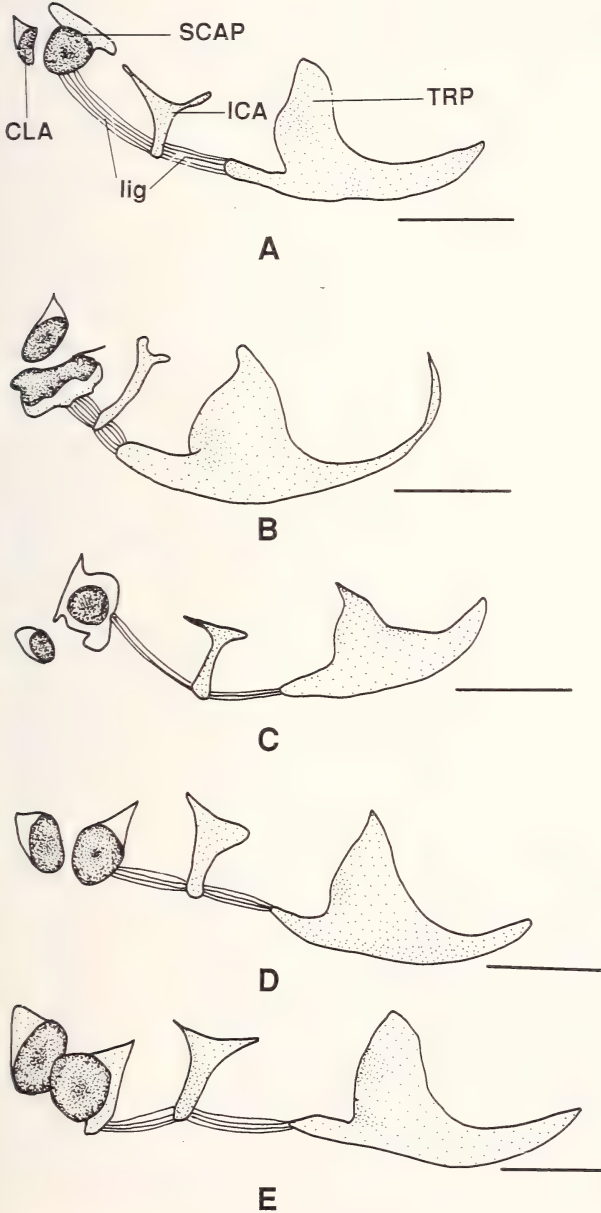


Fig.79: Lateral view of Weberian ossicles of *Phoxinus*. A: *P. oreas* (KU 3259, 55.0 mm SL); B: *P. neogaeus* (KU 8521, 53.0 mm SL); C: *P. eos* (KU 12255, 43.0 mm SL); D: *P. cumberlandensis* (KU 18934, 52.0 mm SL); E: *P. phoxinus* (CNUC uncat., 76.0 mm TL). Scale bars = 1 mm.

part (crest of neural complex – Cavender & Coburn 1992) is deeply grooved. It is narrow and relatively tall in *P. phoxinus*, *erythrogaster*, *brachyurus*, *neogaeus*, and in the outgroups (TS 176[0]); it is broad and relatively short in other species (TS 176[1]). In *P. phoxinus* and *eos*, the grooved portion of the supraneural is narrower (TS 177[1]) than that in other species of *Phoxinus* and in the outgroups (TS 177[0]). In *P. neogaeus*, the anterior portion of the dorsal margin of the supraneural is not grooved (TS 178[1]). In other species of *Phoxinus* and in the outgroups, its entire dorsal margin is grooved (TS 178[0]).

The claustrum (Fig. 77A-C, 79A-E) is located at the anterodorsal side of centrum 1. It covers the atrium sinus impar ventromedially, and the anterior portion of scaphium posteriorly. It is roughly triangular on lateral view, and no variation with phylogenetic significance was observed in *Phoxinus*.

The scaphium (Figs 77A-C, 79A-E) is located posteriorly to the claustrum. Coburn (1982) divided the scaphium into four parts: a cup at mesial, a posterodorsally directed spine, a ventromedial articulating process, and a blunt tubercle posteriorly off the lateral surface of the cup. Intraspecific variation is present in the morphology of different parts of the bone in *Phoxinus*. For instance, in some specimens of *P. phoxinus*, a notch is present on the margin of the cup; the notch is absent in other specimens of the same species; the posterodorsal spine is sharp in some specimens, it is blunt in other specimens of the same species.

The intercalarium (Figs 77A-C, 79A-E, 80B) is a roughly T-shaped bone and placed at the posterior to the scaphium anteriorly and anterior to the tripus. Via ligaments, the intercalarium connects with scaphium and tripus posteriorly. The intercalarium can be divided into three parts, a dorsolateral process, a dorsomedial process, and a main part. Generally, the dorsomedial process is shorter and blunter than the dorsolateral process. The dorsal margin of the bone is deeply concave in *P. neogaeus* and *oreas* (TS 179[1]); it is shallowly concave in other species of *Phoxinus* (TS 179[0]). The main part of the intercalarium is slender and relatively long in *P. erythrogaster* (TS 180[1]); it is broad and relatively short in other species of *Phoxinus* (TS 180[0]). The medial and lateral spines

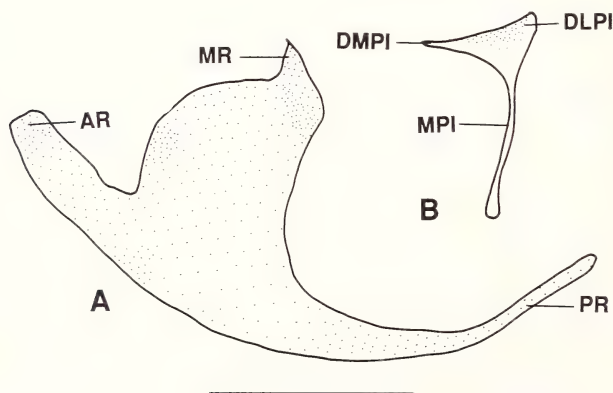


Fig. 80: Lateral view of tripus (A) and intercalarium (B) of *Phoxinus erythrogaster* (KU 5773, 51.5 mm SL). Scale bar = 1 mm.

of the intercalarium are more slender in *P. oreas* (TS 181[1]) than in other species of the genus (TS 181[0]).

In the outgroups, the dorsal margin of the intercalarium is slightly concave, and all three parts of the bone are moderately broad.

The tripus (Figs.77A-C, 79A-E, 80A) is the largest element among the Weberian ossicle, and is located at the posterior portion of the bony chain formed by the ossicle. Three parts can be recognized for this triangular bone: anterior, medial, and posterior ramus. The anterior ramus extends and connects with ventral end of the intercalarium's main part via ligament. The medial ramus extends medially, and is connected with the lateral aspect of



Fig.81: Intermuscular bones of *Phoxinus tennesseensis* (UT 44,5274, 50.0 mm SL) (from caudal peduncle). Scale bar = 1 mm.

the centrum of the third vertebra. The posterior ramus is elongated and extends posteriorly and is concave. The posterior ramus is more slender and elongate in *P. neogaeus* and *erythrogaster* (TS 182[1]) than in other species of *Phoxinus* and in the outgroups (TS 182[0]).

Intermuscular bones. Intermuscular bones (myoseptal or intermyoseptal bones) (Fig.81) are placed in the myoseptum between two myotomes. In epaxial myotomes, the intermuscular bones are present from the first (or second) vertebral segment to the caudal fin base. In hypaxial myotomes, the bones exist from the posterior of the body cavity to the caudal fin base. Generally, intermuscular bones are thin and slender in shape, with or without a fork at the anterior end of the bones in epaxial myotomes or dorsal end of the bones in hypaxial myotomes. Some intermuscular bones are expanded at their posterior ends forming brush-like structures. No variations with phylogenetic significance are present among the species of *Phoxinus*.

Other supraneural bones (Figs.76A-D, 77A-C). Other supraneural bones are located median at the dorsal side of the body, from posterior of the supraneural bone 3 to the anterior of the origin of the dorsal fin in all *Phoxinus* species. The supraneural bones are plate-like, and roughly rectangular in shape.

Supraneural 4 is located between neural spine 5 and the supraneural 3. It is large and extends to the grooved portion of the supraneural 3 in *P. cumberlandensis* (TS 183[1]). It is small and extends to the dorsal of neural spine 4, but not to the grooved portion of supraneural 3 in all other species of the *Phoxinus* and in the outgroups (TS 183[0]). This supraneural bone is poorly developed, very small, and its anterior edge is far away from the posterior margin of neural spine 4 in *P. phoxinus*. In *P. erythrogaster*, supraneural 4 is pieced into two part, the anterior part is located on the dorsal to neural spine 4, and far away from neural spine 5; the posterior part is placed between neural spines 4 and 5 (TS 184[1]). This condition is absent in other species of *Phoxinus* or in the outgroups (TS 184[0]).

A single supraneural is present between two neighbor neural spines from neural spine 5 to the neural spine just anterior to the first dorsal pterygiophore. The supraneurals decrease in size posteriorly. The most posterior few supraneurals are very small. The last one just anterior to the first pterygiophore of the dorsal fin is absent in some specimens of *Phoxinus*.

Vertebrae

The vertebrae of species of *Phoxinus* can be divided into precaudal and caudal elements as defined below. Between the "normal" precaudal and caudal vertebrae two or three vertebrae are present as transitional elements (see below). The total number of the vertebrae, including numbers of the precaudal (the transitional elements included), and caudal elements, is given for each species in the species accounts. Number of vertebrae varies from 37 to 40, of which 18 to 20 are precaudal ones, and 17 to 21 are caudal ones.

Generally, the precaudal vertebrae, except the anterior four elements which were discussed in the "Weberian Apparatus", are almost monomorphic. Dorsally, each vertebra bears a neural arch and spine directed posterodorsally, a pair prezygopophyses, and a pair postzy-

gopophyses. The prezygopophysis is located anteriorly to the neural arch, and decreases in size posteriorly, though the prezygopophysis on vertebra 5 is smaller than that on vertebra 6. The postzygopophysis is located at the posterior margin of the neural arch and articulates with the prezygopophysis of the next vertebra. The postzygopophysis is smaller than the prezygopophysis of the same vertebra; it is posteriorly directed, and slightly increasing in size posteriorly. The neural spines placed ventrally to the dorsal pterygiophores are shorter than those of the neural spines located anteriorly and posteriorly to the dorsal fin. Ribs ventrolaterally articulate with the parapophyses of the vertebrae.

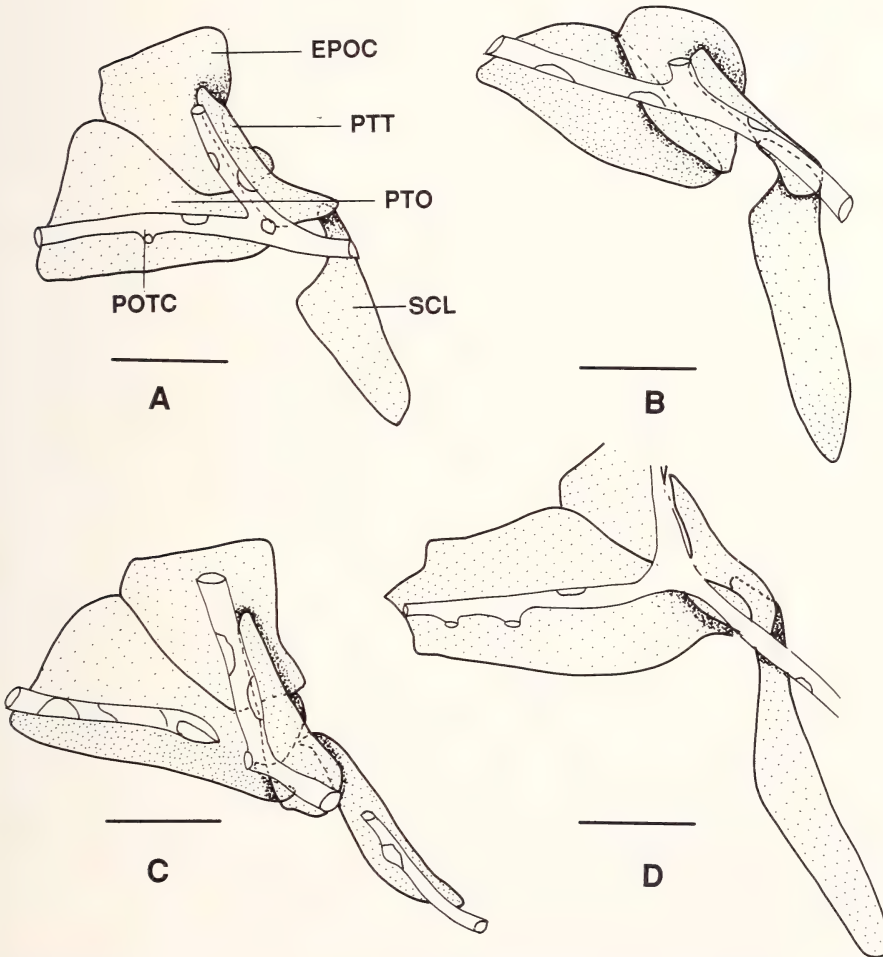


Fig.82: Dorsal view of pterotic, epioccipital, posttemporal, and supracleithrum of *Phoxinus*. A: *P. eos* (KU 12255, 43.0 mm SL); B: *P. phoxinus* (KU 22856, 58.0 mm SL); C: *P. cumberlandensis* (KU 18934, 52.0 mm SL); D: *P. oreas* (KU 3259, 52.2 mm SL). Scale bars = 1 mm.

Each caudal vertebra bears one neural arch and one neural spine, and paired prezygopophyses, postzygopophyses, haemal prezygopophyses, and haemal postzygopophyses. The prezygopophysis of the caudal vertebra is much smaller than that on precaudal vertebrae; however, the postzygopophysis of the caudal vertebrae is larger than that of the precaudal vertebrae.

Each transitional vertebra bears an incomplete haemal arch without haemal spine, and two small free ribs.

No morphological variation with phylogenetic significance is observed in the vertebrae among the species of *Phoxinus*.

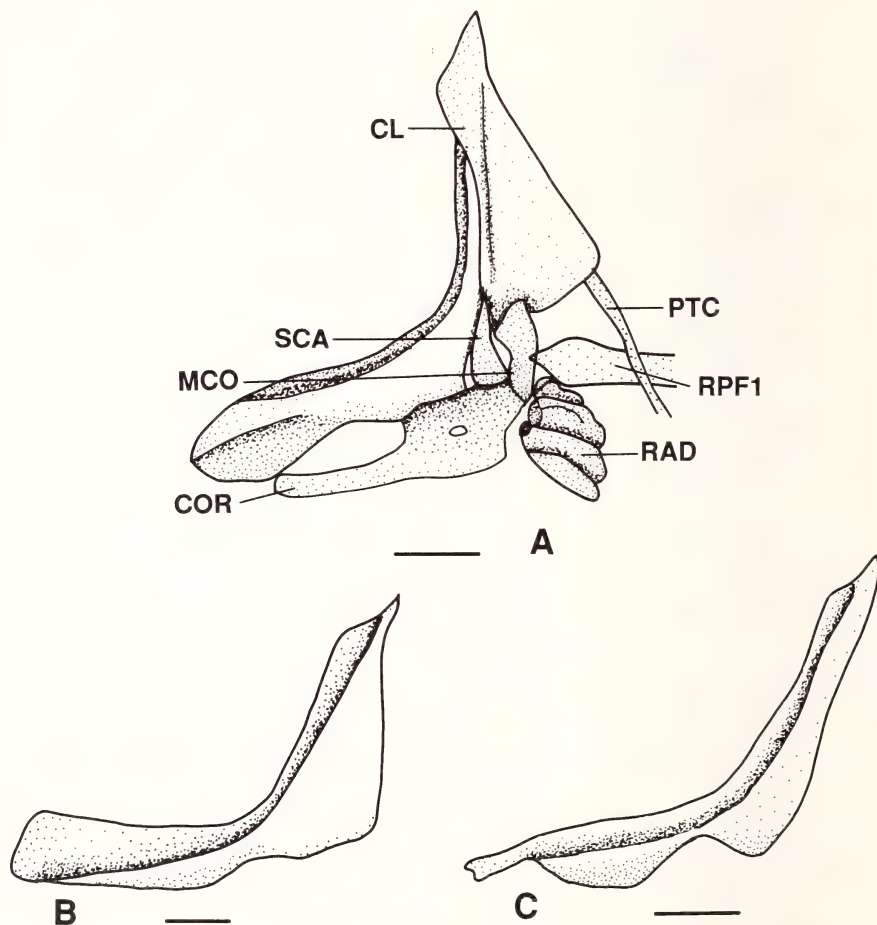


Fig.83: Lateral view of pectoral girdle (A), and cleithrum (B-C) of *Phoxinus*. A. *P. eos* (KU 12255, 43.0 mm SL), supracleithrum and posttemporal not shown; B: *P. phoxinus* (CNUC uncat., 76.0 mm TL); C: *P. issykkulensis* (P-10696, 42.4 mm SL). Scale bars = 1 mm.

Pectoral girdle and fin

In cyprinids, bones in the pectoral girdle include coracoid, mesocoracoid, scapula, posttemporal, supracleithrum, cleithrum, and postcleithrum. The coracoid, mesocoracoid, and scapula are endochondral bones and form the primary pectoral girdle; the remaining are dermal elements and form the secondary pectoral girdle.

Posttemporal (Fig.82A-D). The posttemporal is an elongated bone and located at the posterolateral side of the neurocranium. It overlaps the epioccipital dorsally and supracleithrum ventrally.

Generally, two conditions are present in shape of the posttemporal in *Phoxinus*. The posttemporal expands at its ventral portion in *P. erythrogaster*, *oreas*, *brachyurus*, and *cumberlandensis*, therefore the dorsal portion of the bone is narrower than the ventral one (TS 185[1]). The ventral portion does not expand in other species of *Phoxinus* and in the out-groups (TS 185[0]). The bone partially overlaps the dorsal side of the pterotic in *P. cumberlandensis*, *oreas*, *erythrogaster*, and *eos* (TS 186[1]). In *P. cumberlandensis*, more than half of the bone overlaps the pterotic; in *P. oreas* and *eos*, a small posterior portion of the

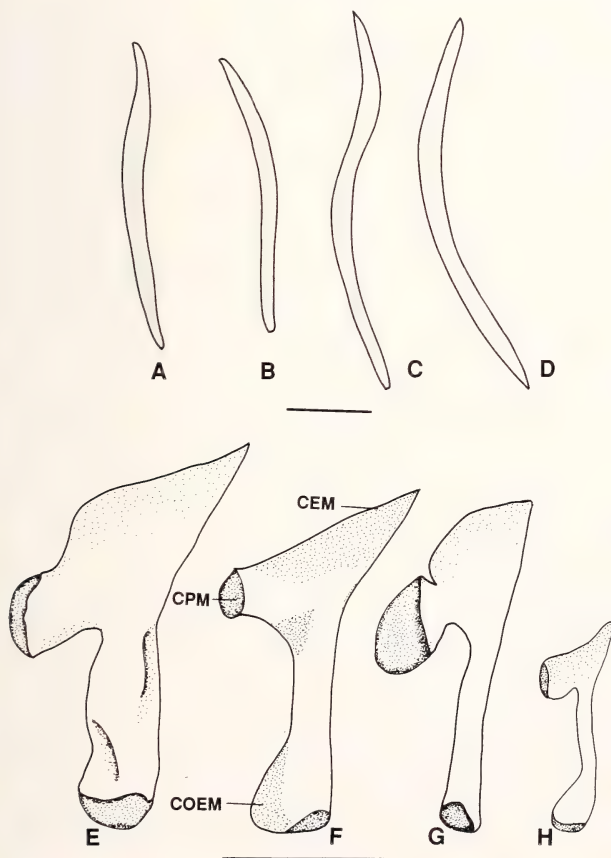


Fig.84: Anterior view of postcleithrum (A-D), and dorsal view of mesocoracoid (E-H) of *Phoxinus*. A: *P. cumberlandensis* (KU 18934, 552.0 mm SL); B: *P. eos* (KU 12255, SL 43.0 mm mm); C: *P. phoxinus* (CNUC uncat., 76.0 mm TL); D: *P. erythrogaster* (KU 5773, 52.0 mm SL); E: *P. erythrogaster* (KU 5773, 51.5 mm SL); F: *P. cumberlandensis* (KU 18934, 52.0 mm SL); G: *P. phoxinus* (CNUC uncat., 76.0 mm TL); H: *P. eos* (KU 12255, 33.0 mm SL). Scale bars = 1 mm.

posttemporal overlaps the pterotic; in *P. erythrogaster*, only a part of the anterior edge of the posttemporal overlaps the pterotic. The posttemporal does not overlap the pterotic in other species of *Phoxinus* or in the outgroups (TS 186[0]).

Supracleithrum (Fig.82A-D). The supracleithrum is an elongated, plate-like bone articulating with the posttemporal dorsomedially, and the cleithrum ventromedially. Its ventral part is slightly expanded. The dorsal portion of the bone is much narrower than its ventral portion in *P. eos* and *phoxinus* (TS 187[1]). The dorsal portion is only slightly narrower than the ventral portion in other species of *Phoxinus* and in the outgroups (TS 187[0]).

Cleithrum (Fig.83A-C). The L-shaped cleithrum is the largest element in the pectoral girdle. It articulates with supracleithrum dorsally, postcleithrum anteriorly, scapula, mesocoracoid, and coracoid posteriorly. Two parts can be recognized from the bone, the horizontal and ascending branches (process). The horizontal branch is the ventral part of the bone and roughly rectangular, with a large notch at the posterior margin. The ascending process is the dorsal part of the bone and roughly perpendicular to the horizontal branch. The ascending process is triangular, and its dorsal tip is sharp.

The notch of the horizontal branch forming the interosseus foramen with the coracoid at the posterior edge is deep in *P. issykkulensis* (TS 188[1]), but shallow in other species of *Phoxinus* and in the outgroups (TS 188[0]). The ventral margin of the ascending process is slightly sloped dorsally in *P. issykkulensis* (TS 189[1]); it is more sloped in other species of *Phoxinus* and in the outgroups (TS 189[0]).

Postcleithrum (Figs.83A, 84A-D). This is an elongated rod-like bone attaching to the mesial surface of the cleithrum's ascending process dorsally; its ventral end is sharp and free. No significant variation is present among the *Phoxinus* species.

Coracoid (Figs.83, 85A-F). The coracoid is a plate-like bone with expansion at the lateral part to form a broad part. It articulates with scapula laterally and with cleithrum posteriorly. The slender part, with the posterior margin of the cleithrum, forms the large interosseus foramen. In *P. cumberlandensis*, *eos*, *neogaeus*, and *erythrogaster*, the slender portion tapers medially; therefore, the posterior portion of the slender part is broader than the medial portion of the slender part in these species (TS 190[1]). In *P. phoxinus*, *brachyurus*, *issykkulensis*, *tennesseensis*, and *oreas*, the entire slender portion is almost equal in width, which is similar to that in the outgroups (TS 190[0]). In *P. cumberlandensis*, the bone bears a forked structure articulating with the scapula (TS 191[1]). The forked structure is absent in other species of *Phoxinus* and in the outgroups (TS 191[0]).

Mesocoracoid (Figs.84E-H). The mesocoracoid is a roughly T-shaped bone and articulates with the cleithrum posteriorly. For sake of description the following terms are given to different parts of the bone. The process articulating with the cleithrum is defined as cleithral process and its anterior end as the cleithral end. The end of the mesocoracoid articulating with coracoid as coracoidal end. The cleithral end is sharp in *P. erythrogaster*, *cumberlandensis* (TS 192[1]); blunt in other species of *Phoxinus* and in the outgroups (TS 192[0]). The cleithral process is straight in *P. cumberlandensis* (TS 193[1]); it is slightly bent in other species of *Phoxinus* and in the outgroups (TS 193[0]). Moreover, a notch is present at the medial margin of the cleithral process in *P. phoxinus* (TS 194[1]); this notch

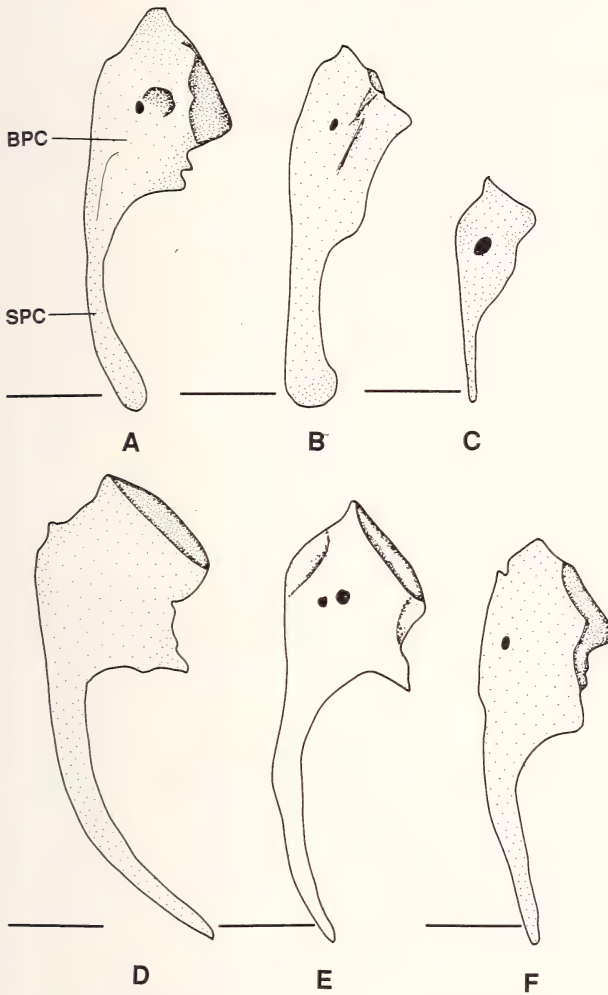


Fig.85: Dorsal view of coracoid of *Phoxinus*. A: *P. oreas* (KU 3259, 55.0 mm SL); B: *P. phoxinus* (CNUC uncat., 76.0 mm TL); C: *P. eos* (KU 12255, 33.0 mm SL); D: *P. neogaeus* (KU 8521, 53.0 mm SL); E: *P. erythrogaster* (KU 5773, 51.5 mm SL); F: *P. cumberlandensis* (KU 18934, 52.0 mm SL). Scale bars = 1 mm.

is absent in other species of *Phoxinus* and in the outgroups (TS 194[0]). The coracoidal end expands in *P. cumberlandensis* and *eos* (TS 195[1]); whereas it does not expand in other species of *Phoxinus* or in the outgroups (TS 195[0]).

Scapula (Fig.83A). The scapula bears a large round foramen at its central, and different facets articulating the cleithrum, mosocoracoid, coracoid, and first pectoral fin-ray. No significant variation is present among the species of *Phoxinus*.

Radials (Figs.83A, 86, 87A-F). Four radials are present in each pectoral fin in *Phoxinus*, namely the radials 1, 2, 3, and 4 (Figs.83A, 87A-F).

The first radial is the shortest among the four. Two articular facets are present at the la-

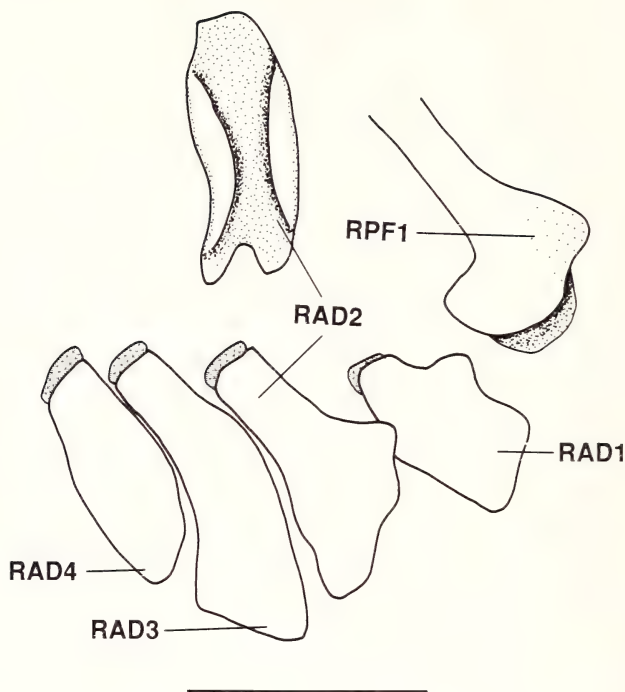


Fig.86: Dorsal view of pectoral radials of *Phoxinus phoxinus* (CNUC uncat., 76.0 mm TL). Scale bars = 1 mm.

teral side of the bone. The two facets articulate with the first pectoral ray and are far away from one another. In *P. eos*, the medial facet is very high and forms a process (TS 196[1]). The facet is much lower in other species of *Phoxinus* and in the outgroups (TS 196[0]). Radial 2 (Figs.86, 87A-F) bears a trough at its lateral side to articulate with the medial side of radial 1. The bone is triangular in *P. cumberlandensis*, *erythrogaster*, *phoxinus*, and *oreas* (TS 197[1]); it is narrow and slender in other species of *Phoxinus* and in the outgroups (TS 197[0]). A process is present at the medial margin of radial 2 in *P. eos* (TS 198[1]); the process is absent in other species of *Phoxinus* and in the outgroups (TS 198[0]).

Radial 3 (Figs.86, 87A-F) is an elongate bone bearing a trough at the lateral side articulating with the medial of radial 2. A process is present at its anteromedial side in *P. cumberlandensis* (TS 199[1]); the process is absent in other species and in the outgroups (TS 199[0]).

Radial 4 (Figs.86, 87A-F) is an elongated bone and does not bear variation with phylogenetic significance in *Phoxinus*.

In *Phoxinus*, 13 to 18 pectoral fin-rays are present with intraspecific variation. See Species Accounts for discussion on variation in the numbers of the pectoral rays for each species. The pectoral rays increase in number with age (Hill & Jenssen 1968). All rays, except the first one, do not bear variation with phylogenetic significance in *Phoxinus*.

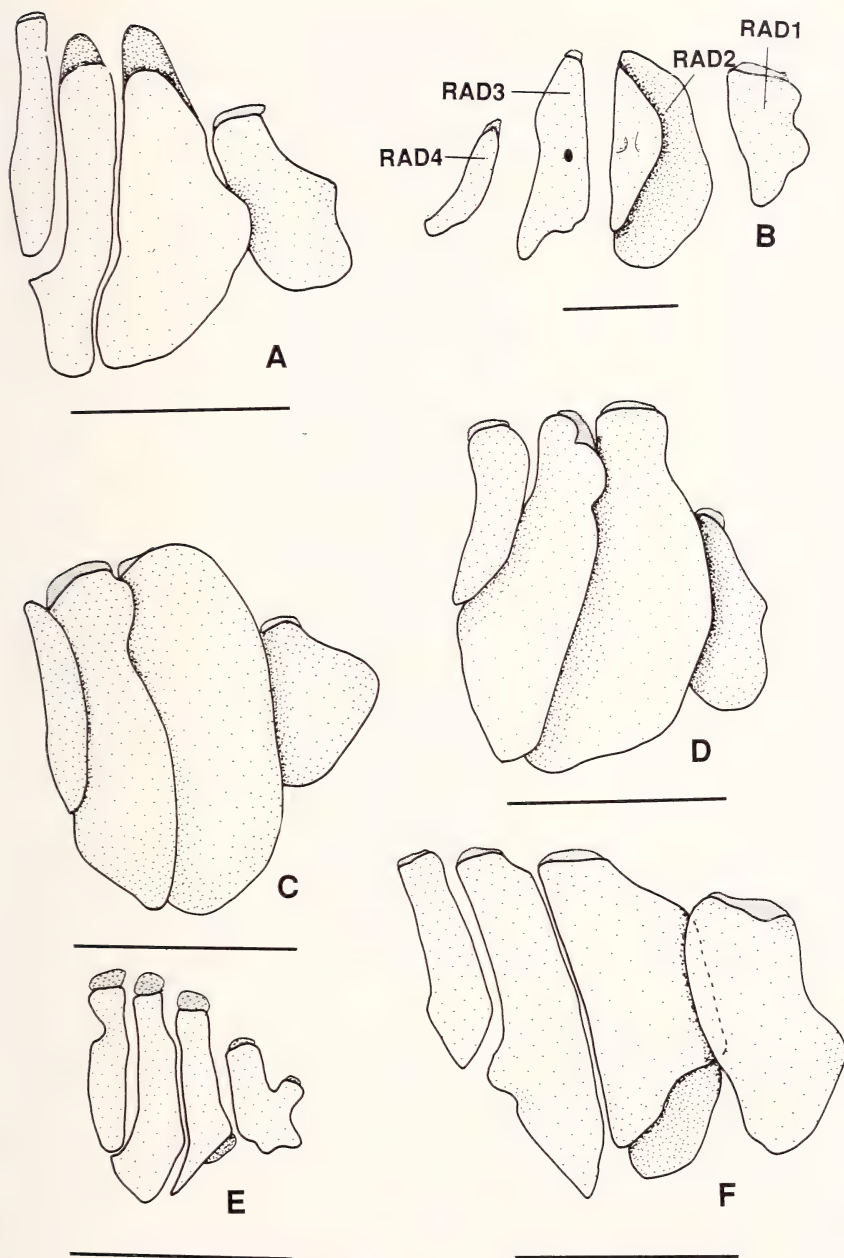


Fig.87: Dorsal view of pectoral radials of *Phoxinus*. A: *P. cumberlandensis* (KU 18934, 52.0 mm SL); B: *P. neogaeus* (KU 8521, 53.0 mm SL); C: *P. erythrogaster* (KU 5773, 51.5 mm SL); D: *P. issykkulensis* (P-10696, 42.4 mm SL); E: *P. eos* (KU 12255, 33.0 mm SL); F: *P. oreas* (KU 3259, 55.0 mm SL). Scale bars = 1 mm.

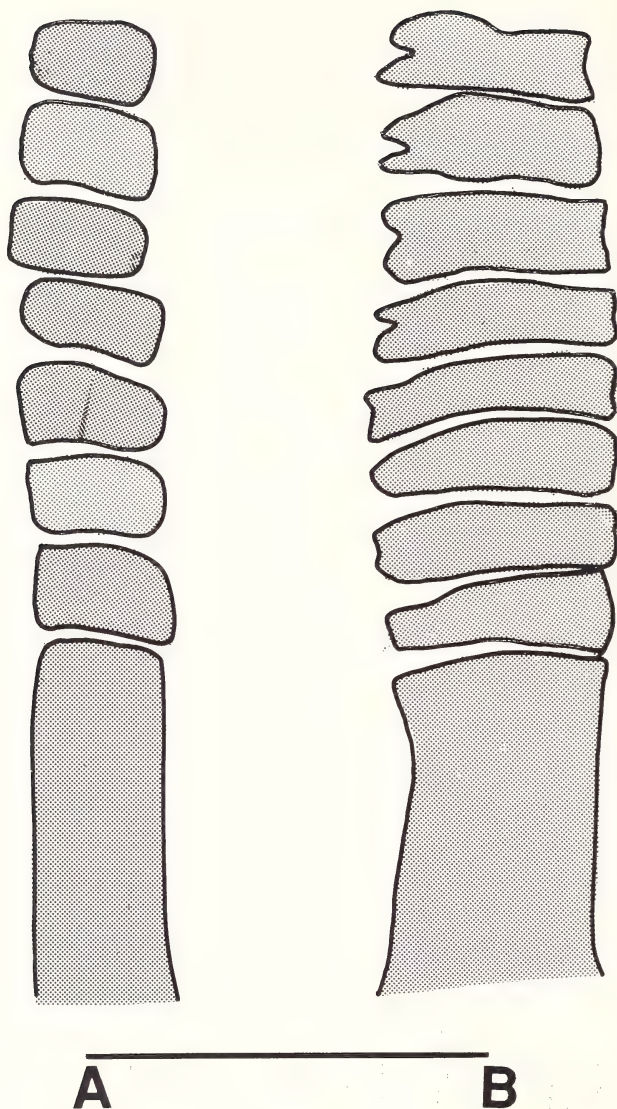


Fig.88: Dorsal view of a portion of the larger hemitrichia of the first pectoral fin ray of breeding males of (A) *Phoxinus erythrogaster* (KU 5773, 51.5 mm SL), and (B) *P. neogaeus* (KU 8521, 53.0 mm SL). Scale bars = 1 mm.

The first pectoral ray is the longest, thickest and strongest in all of the pectoral rays. The two hemitrichia can be easily separated from one another, one is smaller than the other. The base of the larger one is forked and articulates with the scapula; the medial side of the bone is concave and contacts with the smaller one. Variation of the ray is present in its segmentation in breeding males (Fig.88A-B). In breeding male of *P. neogaeus*, the segments are broad and short, most of the segments bear a notch at its lateral margin (TS 200[1]). In other species and in the outgroup, the segments are narrow and relatively high without any notch at the lateral margin (TS 200[0]).

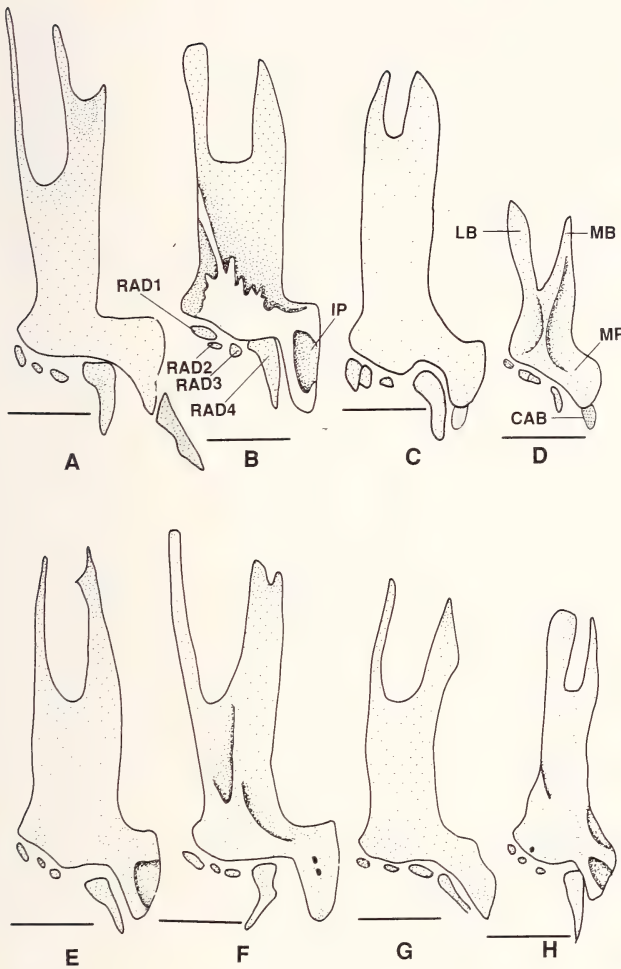


Fig.89: Dorsal view of pelvic girdle of *Phoxinus*. A: *P. phoxinus* (CNUC uncat., 76.0 mm TL); B: *P. erythrogaster* (KU 5773, 51.5 mm SL); C: *P. neogaeus* (KU 8521, 53.0 mm SL); D: *P. issykkulensis* (P-10696, 42.4 mm SL); E: *P. cumberlandensis* (KU 18934, 52.0 mm SL); F: *P. oreas* (KU 3259, 55.0 mm SL); G: *P. tennesseensis* (UT 44,5274, SL 50.0 mm SL); H: *P. eos* (KU 12255, 43.0 mm SL). Scale bars = 1 mm.

Pelvic girdle and fin

The pelvic girdle (Fig.89A-H) is composed of a single, expanded basipterygium. Anteriorly, it is forked, thus two pelvic plates, the medial and lateral plate, are formed. Posterior portion of the basipterygium forms a medial process which bears a posterior ischiac project. One elongated triangular radial and three small ones articulate with the posterior margin of the basipterygium.

Variation is present in the general shape of the basipterygium. In *P. phoxinus*, *oreas*, *issykkulensis*, and *cumberlandensis*, the anterior fork is deep (depth of the fork is equal or longer than the length of the unforked part of the bone, the length of the ischiac project not included) (TS 201[0]); the fork is shallow (depth of the fork is much less than the length of the unforked part of the bone) in other species of *Phoxinus* (TS 201[1]). The

medial pelvic plate is broad and forked in *P. oreas* and *phoxinus* (TS 202[0]); it is narrow and unforked in other species of *Phoxinus* (TS 202[1]). The ischiac process is broad, short triangular in *P. neogaeus*, *issykkulensis*, *cumberlandensis*, and *eos* (TS 203[1]); the process is an elongated triangle in other species of *Phoxinus* (TS 203[0]).

In the outgroups, the anterior fork is deep, the medial branch is broad and forked, and the ischiac process is narrow and elongated triangular-shaped.

A cartilage (Fig.89A, D) exists at the posterior to the ischiac process in *P. issykkulensis*, *neogaeus*, and *phoxinus* (TS 204[1]). The cartilage is small and short rod-like in *P. issykkulensis* and *neogaeus*; whereas it is an elongated triangle in *P. phoxinus*. This cartilage is absent in other species and in the outgroups (TS 204[0]).

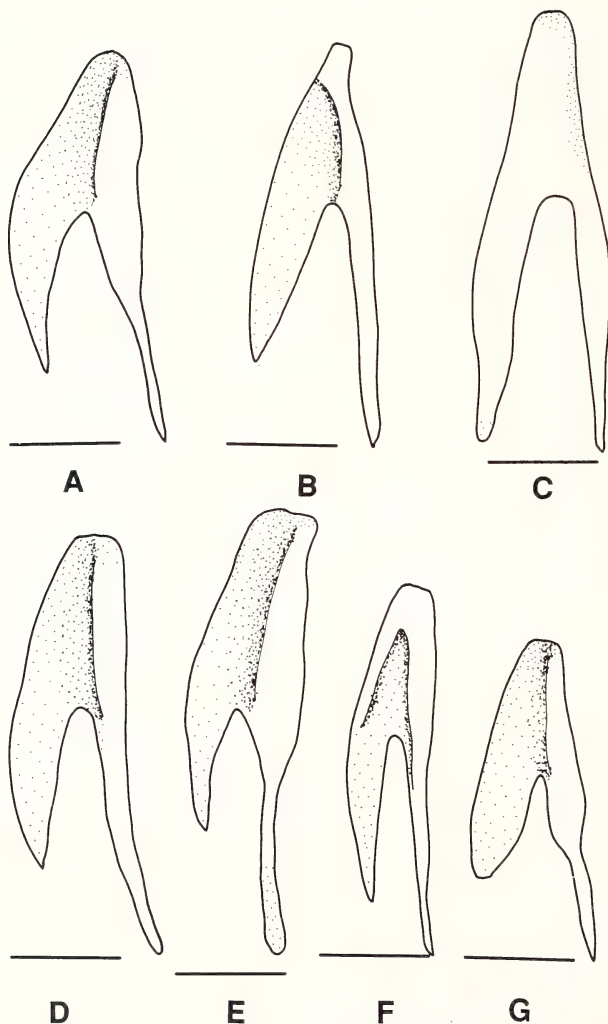


Fig.90: Lateral view of proximal part of the first dorsal pterygiophore of *Phoxinus*. A: *P. cumberlandensis* (KU 18934, 52.0 mm SL); B: *P. neogaeus* (KU 8521, 53.0 mm SL); C: *P. brachyurus* (MCZ 3006, 75.9 mm SL); D: *P. oreas* (KU 3259, 52.2 mm SL); E: *P. phoxinus* (CNUC uncat., 76.0 mm TL); F: *P. tennesseensis* (UT 44.5274, 50.0 mm SL); G: *P. eos* (KU 12255, 43.0 mm SL). Scale bars = 1 mm.

Four radials are present at the posterior margin of the basipterygium. The radials articulate with the basipterygium anteriorly, and the anterior end of the pelvic rays posteriorly. Radials 1 to 3 (from distal to proximal) are small, cubic, or spherical in shape. Significant variation is absent in these bones in *Phoxinus*. Radial 4 is the largest among the four radials. Radial 4 is an elongated triangle in *P. cumberlandensis*, *erythrogaster*, *eos*, *phoxinus*, *neogaeus*, *oreas*, and in the outgroups (TS 205[0]); it is an elongated bar in other species of *Phoxinus* (TS 205[1]).

Seven to eight rays of the pelvic fin are generally present in *Phoxinus*. See below for discussion on variation of the number of fin-rays for each species of *Phoxinus*.

Dorsal Fin

Eight pterygiophores are present in all *Phoxinus* species. In cyprinids, each pterygiophore is composed of three portions: proximal, middle, and distal parts (Harder 1975, Chen 1987a). The proximal part (Fig.90A-G) is elongated and is the main element of pterygiophore. The middle part is short bar-shaped; its dorsal and ventral sides are concave to articulate with the distal and proximal parts of the pterygiophore respectively. The distal part is a small spherical bone. The middle and distal parts in all pterygiophores are similar to one another in shape and without variation among the species of *Phoxinus*. The proximal parts of the second to the eighth pterygiophores are not forked and similar to one another in shape, but decrease in size posteriorly. The proximal part of the first pterygiophore, the largest one, is forked at its ventral portion, and expanded at its middle portion. The proximal part of the first pterygiophore in *P. tennesseensis* is slender (TS 206[1]) than that in other species of *Phoxinus* or in the outgroups (TS 206[0]). In *P. brachyurus*, the fork on the proximal part of the first pterygiophores is deep, the anterior process of the fork is almost equal to the posterior process in length (TS 207[1]). In other species

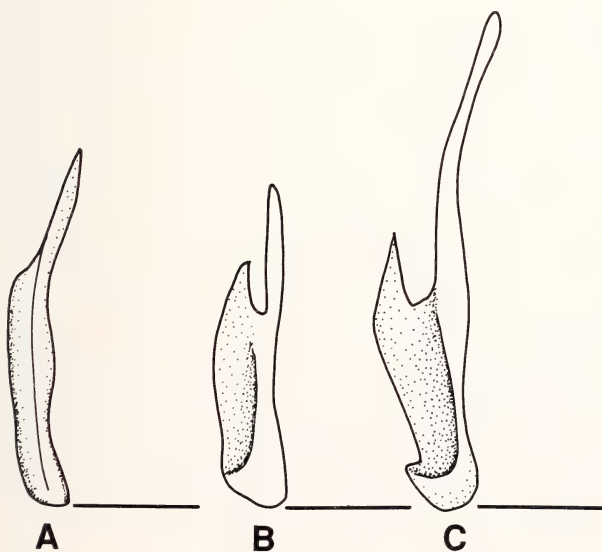


Fig.91: Lateral view of the proximal part of the first pterygiophore of anal fin of *Phoxinus*. A: *P. eos* (KU 12255, 43.0 mm SL); B: *P. tennesseensis* (UT 44.5274, 50.0 mm SL); C: *P. oreas* (KU 3259, 52.2 mm SL). Scale bars = 1 mm.

of *Phoxinus* and in the outgroups, the anterior branch is much shorter than the posterior one (TS 207[0]).

One to three procurent rays, and seven to eight dorsal rays are present in the species of *Phoxinus*. Intraspecific variation of the number of rays is present in the genus; see "Species Account" for discussion on the variation of fin rays for each species.

Anal fin

Eight pterygiophores of the anal fin are present in all *Phoxinus* species; they are similar in shape to dorsal pterygiophores. Each pterygiophore consists of proximal, medial and distal parts. The second to the eighth pterygiophores are similar to each other (though the size decreases posteriorly), not forked, without variation among species of *Phoxinus*. However, the proximal part of the first pterygiophore is forked in *P. oreas* and *P. tennesseensis* (TS 208[1]; Fig.91B-C); it is unforked in other species of *Phoxinus* and in the outgroups (TS 208[0]; Fig.91A).

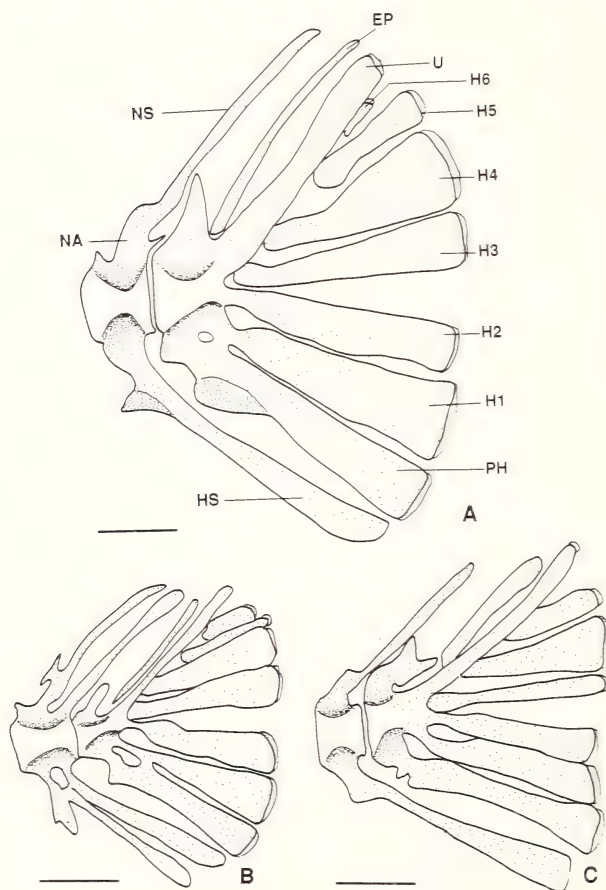


Fig.92: Lateral view of caudal skeleton of *Phoxinus*. A: *P. brachyurus* (MCZ 3006, 75.9 mm SL); B: *P. phoxinus* (KU 22856, 58.0 mm SL); C: *P. cumberlandensis* (KU 18934, 52.0 mm SL). Scale bars = 1 mm.

Similar to the dorsal fin-ray, one or two procurent rays and seven or eight anal fin-rays are present in the species of *Phoxinus*. Intraspecific variation of the number of rays is present; see "Species Account" for discussion on the variation for each species.

Caudal skeleton and fin rays

The general morphology of the caudal skeleton of *Phoxinus* (Fig.92A-C) is similar to that of other cyprinids (c.f. Fink & Fink 1981, Buhan 1972, Mayden 1989). Variation of the caudal skeleton in *Phoxinus* is found in the single epural and hypural 6. The epural is more slender and longer in *P. brachyurus* and *P. erythrogaster* (TS 209[1]) than that in other species of the genus and in the outgroups (TS 209[0]). Hypural 6 is absent in *P. cumberlandensis* and *P. oreas* (TS 210[1]); it is present in other species of the genus or in the outgroups (TS 210[0]).

Two types of caudal rays can be recognized, the principal and procurent rays. Similar to other cyprinids (c.f. Fink & Fink 1981, Schultze & Arratia 1989), principal caudal fin rays in *Phoxinus* are 19 (10+9). The dorsal procurent rays are from four to 12 in number, ventral procurent rays from four to 10, both of which bear intraspecific variations (see "Species Account").

PHYLOGENETIC RELATIONSHIPS OF THE SPECIES OF *PHOXINUS*

Phylogenetic Relationships

Appendix II shows distribution of the polarities of the 210 transformation series among the nine species of *Phoxinus*. Based on the data matrix in Appendix II, PAUP 3.0 (with exhaustive search) generated 2,027,025 trees from 398 steps to 493 steps in tree length. The most parsimonious tree produced by PAUP is shown in Figure 93, with tree length = 398 steps, CI = 0.546 (CI excluding uninformative transformation series = 0.436), HI = 0.454 (HI excluding uninformative transformation series = 0.564).

Two major clades are included in the genus *Phoxinus*, i.e., *brachyurus*-clade, and *erythrogaster*-clade. The *brachyurus*-clade consists of three recognized Eurasian species of the genus and one North American species, *P. neogaeus*. The *erythrogaster*-clade includes the other five North American species of the genus, without *P. neogaeus*.

The synapomorphies for each node (Fig.93) are listed below. The apomorphies of each species are also listed under the appropriate node.

Node A. This node unites the nine species of *Phoxinus* as a monophyletic group. Eight synapomorphies support the monophyly of *Phoxinus*: supraorbital canal interrupted between nasal and frontal bones; preopercular canal ending at the middle of the ascending arm of preopercle; preoperculomandibular canal interrupted into mandibular and preopercular canals; breast scales deeply embedded in breeding males; breast scale bearing a series of tubercles at its apical margin in breeding males; scale on caudal peduncle bearing three or more tubercles at its apical margin in breeding males; orbital septum lower; pharyngeal pad of occipital bone bearing an anterior process.

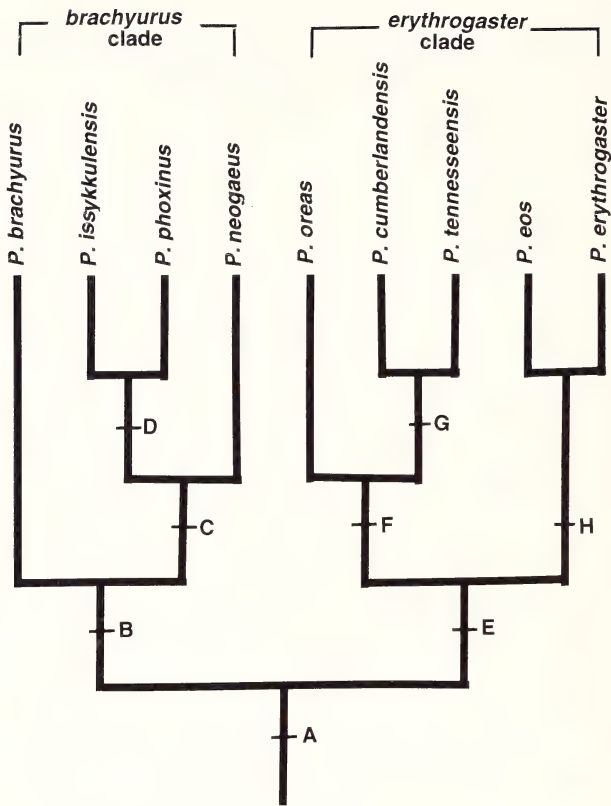


Fig.93: Phylogenetic hypothesis of relationships among species of *Phoxinus* (tree length =398, CI = 0.546, HI = 0.454). See text for the synapomorphies supporting each node.

Node B. This node groups four species of *Phoxinus* as the *brachyurus*-clade, including *P. brachyurus*, *issykkulensis*, *neogaeus*, and *phoxinus*. Nineteen synapomorphies are shared by these species: 1[1], 3[1], 25[1], 46[1], 52[1]* (autapomorphy), 59, 69, 75, 88*[1], 90*[1], 106[1], 107[1], 109[1], 110[1], 114[1], 116[1]*, 150[1], 173[1], and 186[1].

P. brachyurus is the sistergroup of the *Phoxinus* species complex, and bears the following 26 apomorphies: 23[1], 28[1], 30[1], 33[1], 37[1], 45[1], 49[1], 57[1], 61[1], 71[1], 73[1], 77[1], 82[1], 94[1], 103[1], 104[1], 108[1], 126[1], 131[1], 141[1], 153[1], 185[1], 201[1], 205[1], 207[1], and 209[1].

Node C. Species united at Node C are *P. issykkulensis*, *neogaeus*, and *phoxinus*, which form the *phoxinus* species complex. These three species share the following 10 synapomorphies: 41[1], 78[1]*, 79[1]*, 89[1]*, 97[1], 112[1], 118*[1], 124[1], 139[1], and 204[1]*.

P. neogaeus is the sistergroup of the *phoxinus* species pair (*P. phoxinus* + *issykkulensis*) and bears the following 34 apomorphies: 2[1]*, 7[2], 8[1], 26[1], 32[1], 34[1], 38[1], 40[1], 42[1], 43[1]*, 48[1], 54[1], 68[1], 74[1]*, 94[1], 96[1], 102[1], 104[1], 113[1], 120*[1], 132[1], 134[1], 140[1], 151[1], 152[1], 158[1], 161[1], 178[1]*, 179[1], 182[1], 190[1], 200[1], 201[1], and 203[1].

Node D. This node identifies *P. phoxinus* and *issykkulensis* as the *phoxinus* species pair. These two species share the following 13 synapomorphies: 35[1], 66[1], 67[1], 73[1], 100[0] (reversal), 122[1], 125[1], 127[1], 131[1], 133[1], 144[1], 145[1], and 154[1]*.

P. phoxinus bears the 59 following apomorphies: 5[1], 6[1], 9[1], 10[1], 11[1], 12[1], 14[1], 16[1], 17[1], 18[1], 19[1], 20[1], 21[1], 22 [2], 24[1], 25[1], 30[1], 31[1], 32[1], 38[1], 46[1], 47[1], 48[1], 54[1], 55[1], 57[1], 60[1], 62[1], 64[1], 69[1], 83[1], 85[1], 87[1], 95[1], 102[1], 105[1], 107[1], 123[1], 126[1], 128[1], 140[1], 141[1], 146[1], 148[1], 149[1], 151[1], 152[1], 157[1], 161[1], 165[1], 168[1], 172[1], 175[1], 177[1], 187[1], 189[1], 194[1], 197[1], and 202[1].

P. issykkulensis bears the following 25 apomorphies: 3[1], 8[1], 28[1], 31[1], 33[1], 36[1], 42[1], 44[1], 49[1], 59[1], 98[1], 101[1], 103[1], 109[1], 110[1], 113[1], 115[1], 132[1], 142[1], 156[1], 158[1], 176[1], 188[1], 203[1], and 205[1].

Node E. This node groups the five North American species of *Phoxinus* as the *erythrogaster*-clade, including *P. cumberlandensis*, *tennesseensis*, *oreas*, *eos*, and *erythrogaster*. The following nine synapomorphies are shared by these five species: 29[1]*, 34[1], 40[1], 67[1], 132[1], 134[1], 141[1], 143[1]*, and 164[2]*.

Node F. *P. oreas*, *cumberlandensis*, and *tennesseensis* are united at this node as the *oreas* species complex, the sistergroup of the *erythrogaster* species pair (*P. erythrogaster* + *eos*). The following 13 synapomorphies are shared by the *oreas* species complex: 24[1]*, 32[1], 35[1], 49[1], 66[1], 69[1], 93*[1], 96[1], 111[1], 112[1], 113[1], 140[1], and 176[1].

P. oreas is the sistergroup of the two species *P. cumberlandensis* and *tennesseensis*, and bears the following 26 apomorphies: 22[1], 23[1], 28[1], 29[3]*, 53[1], 57[1], 59[1], 65[1], 70[1], 97[1], 101[1], 102[1], 130[1], 139[1], 144[1], 145[1], 146[1], 150[1], 159[1], 179[1], 181[1]*, 185[1], 197[1], 202[1], 208[1], and 210[1].

Node G. *P. cumberlandensis* and *tennesseensis* are grouped at this node. These two species share the following 11 synapomorphies: 8[1], 27[1], 41[1], 42[1], 51[1]*, 86[1], 117[1], 122[1], 125[1], 165[1], and 173[1].

P. cumberlandensis is the sistergroup of *P. tennesseensis*, and bears the following 44 apomorphies: 1[1], 7[1], 15[1]*, 28[1], 29[2]*, 36[1], 40[0] (reversal), 45[1], 46[1], 50[0] (reversal), 54[1], 56[1]*, 63[1]*, 65[1], 68[1], 69[1], 72[1]*, 75[1], 76[1]*, 80[1], 81[1]*, 91[1]*, 121[1]*, 126[1], 127[1], 129[1], 133[1], 135[1], 137[1], 138[1]*, 160[1]*, 166[1]*, 170[1], 183[1], 185[1], 190[1], 191[1]*, 192[1], 193[1]*, 195[1], 197[1], 199[1], 203[1], and 210[1].

P. tennesseensis bears the following 20 apomorphies: 9[1], 22[1], 25[1], 33[1], 53[1], 57[1], 58*[1], 67[0] (reversal), 71[1], 102[1], 104[1], 106[0] (reversal), 130[1], 141[1], 159[1], 186[1], 201[1], 205[1], 206[1]*, and 208[1].

Node H. *P. eos* and *erythrogaster* are grouped at this node as the *erythrogaster* species pair and share the following 17 synapomorphies: 1[1], 22[1], 42[1], 64[1], 86[1], 97[1], 99[1]*, 104[1], 123[1], 131[1], 137[1], 139[1], 161[1], 163[1]*, 171[1], 190[1], and 201[1].

P. eos bears the following 17 apomorphies: 1[1], 22[1], 42[1], 64[1], 86[1], 97[1], 99[1], 104[1], 123[1], 131[1], 137[1], 139[1], 161[1], 163[1], 171[1], 190[1], and 201[1].

P. erythrogaster bears the following 35 apomorphies: 4[1], 5[1], 13[1], 32[1], 35[1], 36[1], 39[1], 49[1], 50[1], 65[1], 70[1], 84[1], 92[1], 108[1], 111[1], 114[1], 124[1], 125[1], 133[1], 135[1], 145[1], 146[1], 150[1], 153[1], 155[1], 165[1], 167[1], 174[1], 180[1], 182[1], 184[1], 185[1], 192[1], 197[1], and 209[1].

Discussion on the phylogenetic relationships of the species of *Phoxinus*

The phylogenetic relationships within *Phoxinus* proposed herein indicate two clades in the genus, the *brachyurus*-clade including all three Eurasian species and *P. neogaeus*, and the *erythrogaster*-clade consisting of the other five North American species (Fig.93). This result supports, in general, the phylogenetic hypotheses among some *Phoxinus* species proposed by Joswiak (1980) based on allozyme data, and Starnes & Starnes (1978) and Starnes & Jenkins (1988) based on external and osteological morphology. However, I disagree with Joswiak's (1980) placement of *Phoxinus* species into three subgenera: *Phoxinus* (including *P. phoxinus*), *Pfrille* (consisting of *P. neogaeus*), and *Chrosomus* (including all other North American species of the genus). If Joswiak's (1980) proposal is followed, the subgenus *Phoxinus* would include all species of the *brachyurus* clade, except *P. neogaeus*, or the subgenus *Pfrille* would consist of all species of the *brachyurus* clade excluding *P. phoxinus*. Either way results in the subgenera *Phoxinus* and *Pfrille* being paraphyletic, which is logically inconsistent with the phylogenetic tree, and not acceptable in the phylogenetic study (Hennig 1966, Wiley 1981, Wiley et al. 1991).

The close relationship between *P. phoxinus* and *P. neogaeus* (both are in the *phoxinus* species complex) has been accepted since the description of *P. neogaeus* was published by Cope (1869), although some authors assigned *P. neogaeus* to another genus (*Pfrille*). However, the close relationship has never been critically reviewed. The characters thought to support this relationship are either plesiomorphic, such as two rows of pharyngeal teeth, short intestine (e.g., Gasowska 1980), or occur in all *Phoxinus* species, such as tuberculation on breast scales in breeding males (e.g., Hubbs & Brown 1929, Gasowska 1979). Ten synapomorphies found in this study support strongly the close relationship between *P. neogaeus* and *P. phoxinus* plus *issykkulensis*.

Mahy (1975c) proposed *P. erythrogaster*, *oreas*, and *eos* as three subspecies of a single species *P. erythrogaster*, and *erythrogaster* as the ancestor of *P. oreas* and *P. eos*. My study does not support Mahy's hypothesis and shows the three "subspecies" as different species. Fig.93 indicates that it is hardly to propose *P. erythrogaster* be the ancestor of *P. eos* and *oreas*. Data from allozymes (Joswiak 1980) also support my phylogenetic hypothesis, not the one of Mahy (1975c). Mahy's failure to recognize the difference of these three species might be "due to his choice of characters" (personal communication of Starnes to Joswiak, cited from Joswiak 1980).

Gasowska (1979) placed *P. neogaeus* in a subgenus *Pfrille* of genus *Phoxinus*, and the other three North American species (*P. eos*, *oreas*, and *erythrogaster*) into two different genera: *P. eos* and *P. erythrogaster* in *Chrosomus*, and *oreas* in a new genus *Parchrosomus*. Gasowska (1979) correctly recognized the close relationship between *P. neogaeus* and *P. phoxinus* based on the breast tuberculation (though it is a plesiomorphic character in the genus of *Phoxinus*). However, she seemed not to recognize that similar breast scale

tuberculation occurs in other North American *Phoxinus* species. If *P. oreas* was considered as a separate genus from *Phoxinus*, the other species of *Phoxinus* would form a paraphyletic group.

Biogeography of *Phoxinus*

Among North American freshwater fishes, the two largest families, Cyprinidae and Percidae, comprise the major part of the primary and secondary Recent freshwater fish community (Patterson 1981, Mayden 1991). These two families are considered by some to have originated in Europe and/or Asia (Banarescu 1972, 1989). Three hypotheses have been proposed to interpret the relationship between the freshwater fish faunas of Eurasia and North America, i.e., "Amphi-Atlantic" hypothesis, "Old Pacific connection" vicariant hypothesis, and "Bering land connection" dispersal hypothesis. These hypotheses can be summarized as following.

1) The Amphi-Atlantic hypothesis implies that the freshwater fish fauna in Europe and in North America bears a closer relationship than either does to the fauna in Asia (see Banarescu & Coad 1991). The trans-Atlantic connection between Europe and North America was present until Early Eocene (Brown & Gibson 1983; Briggs 1986). Patterson (1981) claimed that relationships of *Amia* species indicated North America more closely related to Europe than to Asia. Wiley (1992) proposed that the ancestor of Percidae probably originated in Early Tertiary before the final opening of the North Atlantic, without indicating the place of the ancestral origin. Banarescu (1989) stated that the ancestor of the Percini of Percidae, prevailing in Europe, and the Etheostomatini, endemic to North America, was split by the breaking down of the Atlantic connection between North America and Europe. The above hypotheses might be considered to support an "Amphi-Atlantic" hypothesis. No evidence from Cyprinidae was found supporting this hypothesis because no cyprinid was known from Europe before the Oligocene (Kimmel 1975, Cavender 1986, 1991, Bogutskaya 1991), and no cyprinid fossils have been found in North America until the Oligocene (Cavender 1986, 1991). The Atlantic connection seems too early for the migration (if there was a migration) of the ancestor of cyprinids into North America from Europe, or vice versa.

2) The Old Pacific Connection hypothesis claims that east Asia and North America share a close relationship (see Howes 1984), and the splitting of the ancestor of (at least some) cyprinids in North America and Asia was due to the separation between Asia and North America. A series of collisions among several plates between Siberia and North America happened during the Cretaceous (Fujita 1978). This hypothesis might be supported by the distribution of Polydontidae (Patterson 1981, Grande & Bemis 1991), and the relationships of some insect groups (e.g., caddisflies; see Ross 1974). It may explain the distribution of the monotypic genus *Notemigonus* of eastern North America and its relationship to the genus *Alburnoides* of southwest Asia (Banarescu & Coad 1991). It may also be relevant to the relationship within the aspinine of cyprinids (Howes 1984). However, the earliest cyprinid was found in the Oligocene in North America (Cavender 1986, 1991) which is much younger than the Cretaceous.

3) The "Bering Land Connection" dispersal hypothesis relies on exposure above sea level of Bering land connection between Asia and North America. A Bering land connection existed through most of the Tertiary, and was present again during the Pleistocene (Hopkins 1967, Joswiak 1980, Briggs 1986). "Relatively brief inundations apparently took place in the Late Miocene and Late Pliocene during the interglacial stages" (Briggs 1986:7). The "Bering land connection" dispersal hypothesis implies that the ancestor of the North American cyprinids originated in east Asia, and dispersed into North America from Asia through the Bering land connection (Briggs 1979, 1986, Joswiak 1980). Banareescu (1989) proposed that the ancestor of some North America percids (*Perca*) originated in Europe migrated into Asia and then into North America through the Bering land connection. The "Bering land connection" dispersal hypothesis is accepted by some authors to explain the relationships of (at least) the cyprinid fauna in Asia and North America (e.g., Briggs 1979, Banareescu 1989).

The Bering land connection played an important role in the formation of the North American freshwater fish fauna because the connection provided a possible way for the exchange of the freshwater fishes between North America and Asia, and provided some vicariants for the speciation of the ancestors of (at least) some freshwater fishes on the two continents after the submission of the Bering land connection. As discussed below, I propose the Bering land connection be important for the speciation of *Phoxinus* as well. My interpretation of the role of the connection, however, is based on view of the vicariance biogeography (Wiley 1988), i.e., I propose a "Bering land connection" vicariant hypothesis to interpret the biogeography of *Phoxinus*.

The area cladogram based on the phylogenetic relationship of *Phoxinus* indicates a close relationship between Asia, Europe and North America (Fig.94). However, in order to correctly understand the area cladogram (Fig.94), it is necessary to discuss the geographic distribution of *P. phoxinus*. *P. phoxinus* occurs widely in Europe (whole Europe except southern Spain and Iceland – Sterba 1989), and in central and eastern Asia. The populations of the species in Europe might be interpreted as immigrant from Asia because the European cyprinids had an Asian origin (Banareescu 1960). The east Asian population of *P. phoxinus* was also considered an immigrant by some (Banareescu & Coad 1991). Therefore, *P. phoxinus* might have originated in central Asia, and then dispersed into Europe and East Asia. Thus what the area cladogram (Fig.94) really indicates is that North America bears a closer relationship with Central Asia than with either Europe or East Asia. This implies that the ancestor of the genus *Phoxinus* occurred in North America and Central Asia (not East Asia), and was split by separation of Asia and North America into the ancestor of the *brachyurus* clade in Asia, and the ancestor of the *erythrogaster* clade in North America (cf. Figs.93, 94). This ancestor might have occurred in North America and Asia during (or before) the Miocene when the Bering land connection existed, and was split by submission of the Bering land connection in the Tertiary. Because no fossils of species of *Phoxinus* are known, I am not able to identify the age of the origin for the genus using the fossil record. However, based on the alloelectrophoretic studies on *Phoxinus* allozymes by Joswiak (1980), the separation time of the two clades (*erythrogaster* and *brachyurus* clades) in the genus *Phoxinus* was estimated about 14 million years ago which would conform to the age of the Miocene.

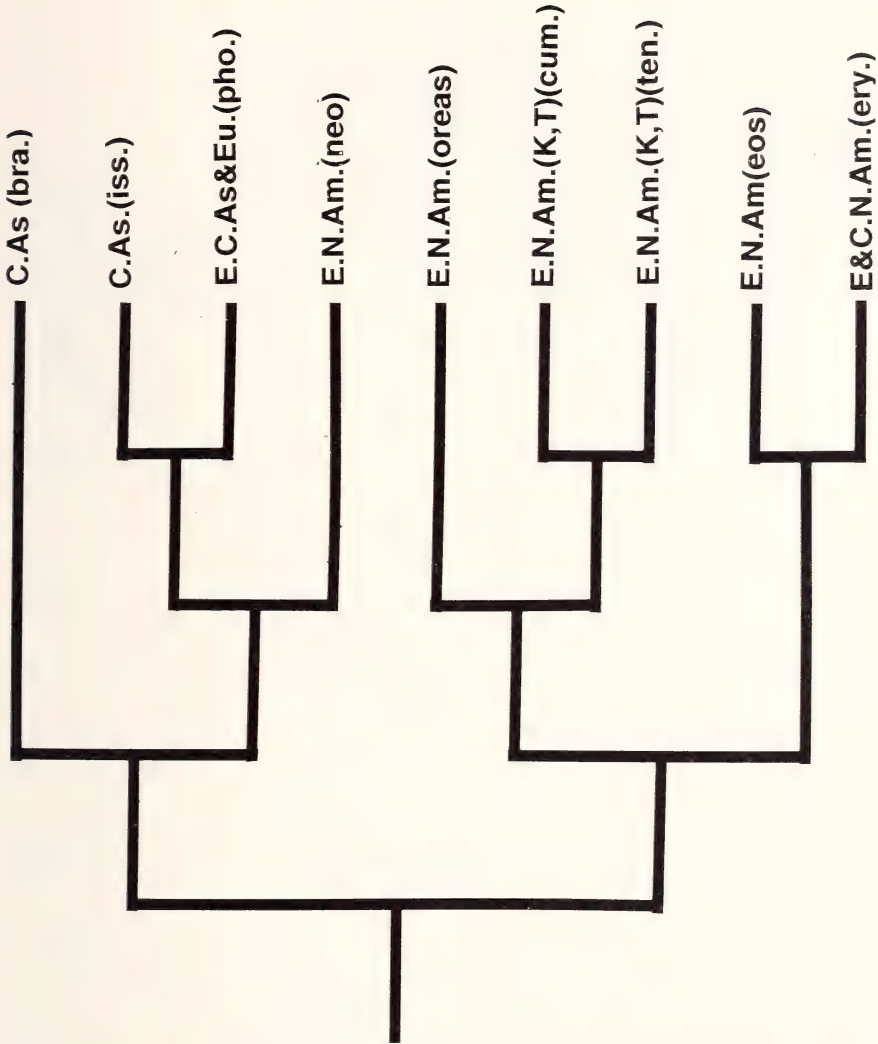


Fig.94: The area diagram of *Phoxinus*, based on the geographic distribution of each species of the genus and the phylogenetic hypothesis of the genus (Fig.93). The abbreviations of the regions are: C.As.: Central Asia; E. & C.N.Am.: east and central North America; E.C.As&Eu.: east and central Asia, and Europe; E.N.Am.: east North America; K,T: states of Kentucky and Tennessee of USA. The name in the parentheses corresponds to the species of *Phoxinus* occurring in the region: bra.: *Phoxinus brachyurus*; cum.: *P. cumberlandensis*; eos: *P. eos*; ery.: *P. erythrogaster*; iss.: *P. issykkulensis*; neo.: *P. neogaeus*; oreas: *P. oreas*; pho.: *P. phoxinus*; ten.: *P. tennesseensis*.

The Asian portion of the ancestor of *Phoxinus* became the ancestor of the *P. phoxinus* clade. This portion was split into *P. brachyurus* and the ancestor of the *P. phoxinus* species complex. How this event happened needs to be better understood. *P. brachyurus* occurs



Fig.95: Composite distribution for the ranges of species of *Phoxinus* in North America. (Data summarized from Lee et al. 1980.)

only in a small area of Illi River of Xinjiang (China) and of Kazakhstan in Asia (Berg 1949, Yang & Huang 1964, Reshetnikoo & Shakirova 1993).

I hypothesize that the ancestor of the *P. phoxinus* complex might have occurred in Asia and dispersed from Asia into North America through the Bering land connection in (or before) the Pliocene, otherwise it would be difficult to interpret the origin of *P. neogaeus*. The ancestor of *Phoxinus* species complex is proposed to have been separated into Asian portion and North American portion, by the submission of the Bering land connection during the Pliocene. The alloelectrophoretic studies on allozymes of *Phoxinus* (Joswiak 1980) showed this separation might have taken place about eight million years ago. The Asian portion of the ancestor was speciated into *P. issykkulensis* which occurs only in Lake Issyk-ku of Kazakhstan, and *phoxinus* which occurs in Asia and Europe. The fish fauna in the Lake Issyk-kul shows that the Lake Issyk-kul was isolated from its surrounding (Reshetnikoo & Shakirova 1993) though when and how the isolation occurred is uncertain. The speciation of the ancestor of "*P. phoxinus* + *P. issykkulensis*" might be related to this vicariant event.

The North American portion of the ancestor of the *Phoxinus* species complex was speciated into *P. neogaeus*, which prefers to live in boggy environment. *P. neogaeus* now oc-



Fig.96: Composite distribution for the ranges of species of *Phoxinus* in Eurasia (data summarized from Berg 1949, Banarescu 1964, Yang & Huang 1964).

curs in the northern portion of North America. Some isolated populations are present in central Wisconsin (Green 1935), South Dakota (Evermann & Cox 1896a, Churchill & Over 1938), Nebraska, Colorado, and Wyoming (Bailey & Allum 1962). (See the species account of *P. neogaeus* below.) The isolated populations indicate *P. neogaeus* used to have a much broader geographic range. These isolated populations might be the descend from glacial populations that failed to expand following the deglaciation (Underhill 1957), or due to the similar causes for the isolated populations of *P. erythrogaster* discussed by Cross (1970) (see below). Mahy (1975c) interpreted the present distribution of *P. neogaeus* as northern dispersal of the species from its refuge.

The Pleistocene glaciation in North America during which ice covered the area to 40° (N. lat.) played an important role in the current geographical distribution of the North American freshwater fishes (Underhill 1957, McPhail 1963, Cross 1970). During the glacial advances, the range of fishes in the area covered by the ice were forced to southward, except some may have persisted in refuge that remained ice-free. The current geographical

distribution of *Phoxinus* in North America exemplifies this. The North American portion of the ancestor of *Phoxinus* became the ancestor of the *erythrogaster* clade after its isolation from Asia in the Tertiary. The *erythrogaster* species pair (*P. eos* and *P. erythrogaster*) speciated from their ancestor probably by the adaptation to different habitats, or by some vicariant event. *P. eos* prefers a boggy environment, whereas *P. erythrogaster* lives in headwater or spring habitats. *P. eos* has a northern distribution not overlapping the range occupied by *P. erythrogaster*, but partially covering the geographic distribution of *P. neogaeus*. *P. erythrogaster* is distributed from Maine and Western Pennsylvania to Arkansas and Alabama, and a few isolated populations are present in Tennessee, Kansas, Colorado, and New Mexico (Koster 1957; Cross 1970). (See the species account of *P. erythrogaster* below).

These isolated populations of *P. erythrogaster* indicate this species once had an extensive southwestern distribution (Cross 1970). Because *P. erythrogaster* usually occurs in headwater or spring habitats, Cross (1970) interpreted the current distribution of this species caused by "(1) southward dispersal (of the species) during glacial advances, due to atmospheric cooling and consequent cooling of streams, probably supplemented by increased moisture and more consistent flow; (2) subsequent extirpation of most southern populations as atmospheric temperatures became warmer, heating the shallower streams and causing many of them to dry, but leaving remnant populations of these species near springs." (Cross 1971:251). The isolated populations of *P. eos* and *P. neogaeus* might be interpreted in a similar manner (Cross 1971).

The ancestor of the *oreas* species complex was hypothesized to have been distributed in the eastern portion of the preglacial Teays River drainage (Starnes & Jenkins 1988). This speciation event might be caused by the "capture of an upper Teays (New River) tributary by an upper Tennessee River (Holston River) tributary" (Starnes & Jenkins 1988:527).

TAXONOMY OF *PHOXINUS* RAFINESQUE, 1820a

Synonymy

Phoxinus Rafinesque, 1820a: 236 (type species: *Cyprinus phoxinus* Linnaeus, 1758: 322; Europe).

Chrosomus Rafinesque, 1820a: 237 (type species: *Luxilus erythrogaster* Rafinesque, 1820a: 237; Kentucky, USA).

Phoxinus Agassiz, 1835: 37 (type species: *Cyprinus phoxinus* Linnaeus, 1758: 322; Europe).

Eulinneella Dybowski, 1916: 101 (type species: *Cyprinus phoxinus* Linnaeus, 1758: 322; Europe).

Pfrrille Jordan, 1924: 71 (Type species: *Phoxinus neogaeus* Cope, 1869: 375, in Günther 1868; New Hudson, Livingston County, Michigan, USA).

? *Achahara* Jordan & Hubbs, 1925: 177 (type species: *Richardsonius semotilus* Jordan & Starks, 1905; Japan).

Parchrosomus Gasowska, 1979: 404 (type species: *Chrosomus oreas* Cope, 1868: 233; Virginia, USA).

Discussion on the Synonymy of *Phoxinus*

The synonymy of *Phoxinus* differs with the views of various authors. Thus the content of the genus changed from time to time. The synonymy used most are those of Berg (1949), Banareescu (1964), and Howes (1985).

Synonymies in Banareescu (1964) and Howes (1985) are modified from those by Berg (1949). *Gila* of North America in the synonymy of Berg (1949) was removed and considered a distinct taxon (Miller 1945; Uyeno 1960). *Eulinneela*, *Lagowskiella*, *Eupallasel-la*, and *Czekanowskiella* were deleted from, and *Chrosomus* was added to, the synonymy in Berg (1949) by Banareescu (1964). Howes (1985) reviewed the synonymy of Berg (1949) and Banareescu (1964), and generally agreed with Banareescu (1964), except for deletion of *Phoxinus* of Agassiz, *Rhynchocyprin*, and *Moroco* from, and adding of *Eulinneela*, *Acahara*, and *Parchrosomus* to the synonymy of Banareescu (1964).

The synonymy of *Phoxinus* proposed herein agrees with those of Howes (1985), except the differences shown in Tab.2. I have not had the opportunity to study the species of *Acahara* (*A. semotilus*), and thus, I follow Howes (1985) in listing this name as a synonym of *Phoxinus* with a question mark (?) indicating the uncertainty.

Tab.2: Differences between the synonymy of *Phoxinus* by Howes (1985) and this study.

Howes (1985)	This Study	Reasons for Change
<i>Chrosomus</i> Rafinesque 1820b:47	<i>Chrosomus</i> Rafinesque 1840a:236	Rafinesque (1820a) might appear earlier than Rafinesque (1820b). See „Historical Review of <i>Phoxinus</i> “ of this study.
Type species of <i>Chrosomus</i> : <i>Chrosomus erythrogaster</i> Raf.	Type species of <i>Chrosomus</i> : <i>Luxilus erythrogaster</i> Rafinesque: 1820a:237	<i>Chrosomus erythrogaster</i> Raf. was originally described as <i>Luxilus erythrogaster</i> Raf.
No <i>Phoxinus</i> Agassiz 1835	With <i>Phoxinus</i> Agassiz 1835	<i>Phoxinus</i> Agassiz 1835 is a synonym of <i>Phoxinus</i> Rafinesque 1820a because both were typed by the same species: <i>Cyprinus phoxinus</i> Linnaeus
Type species of <i>Eulinnella</i> : <i>Phoxinus phoxinus</i> Linn.	Type species of <i>Eulinnella</i> : <i>Cyprinus phoxinus</i> Linnaeus	<i>Phoxinus phoxinus</i> was originally described as <i>Cyprinus phoxinus</i> by Linnaeus (1758)

Diagnosis (emended from Rafinesque 1820a, Berg 1949, Banarescu 1964, and Howes 1985)

Small size, less than 100 mm in SL in most species; body elongate; no barbel; Eurasian species bearing two rows of pharyngeal teeth, and silver peritoneum; North American species bearing one row of pharyngeal teeth (except *Phoxinus neogaeus* with two rows) and dark peritoneum; in young, side with one horizontal dark stripe; in adults, side with at least one longitudinal dark stripe, or about 10 vertical dark bars (*P. phoxinus*); the lateral stripe interrupted or not; supraorbital canal interrupted between nasal and frontal bones; preoperculomandibular canal interrupted into mandibular and preopercular segments; preopercular canal ending at middle of the ascending arm of the preopercle; scales small; in breeding males, breast scales deeply embedded and bearing a series of tubercles at their apical margins; scales on caudal peduncle bearing three or more tubercles at apical margin; orbital septum low; pharyngeal pad of basioccipital bone bearing an anterior process; nasal bone reduced, far from the anterior frontal canal opening; posttemporal fossa small; supraoccipital crest small; supraoccipital anterior margin bearing one anteriorly directed process; vertebrae about 40.

Etymology

Phoxinus is a Greek word for an unknown river fish (Pflieger 1975), meaning tapering (Nelson & Paetz 1992). The name might refer to body shape of the species in the genus.

Composition

Nine species are included in the genus, i.e., *P. brachyurus*, *issykkulensis*, *neogaeus*, *phoxinus*, *erythrogaster*, *eos*, *cumberlandensis*, *oreas*, and *tennesseensis*. I am not certain at the present whether "*P. tchangi* Chen" should be included in the genus because I did not have opportunity to study the specimens of this species during this project. "*P. sedelnikowi* Berg, 1908" was listed as a species of *Phoxinus* by Howes (1985), though he did not study specimens of this species. Whether *P. sedelnikowi* belongs to the genus is an open question because I could not get specimens of the species, and published data about this species are scant.

Distribution

Species of *Phoxinus* occur in North America and Eurasia (Figs.95, 96). See below for the distribution of each species in the genus.

Classification of *Phoxinus*

According to the phylogenetic hypothesis of *Phoxinus* proposed herein (Fig.93) and the phylogenetic listing convention proposed by Wiley (1979, 1981) and Wiley et al. (1991), the classification of *Phoxinus* is arranged as follows:

Genus *Phoxinus**brachyurus* clade*P. brachyurus* Berg*phoxinus* species complex*phoxinus* species pair*P. issykkulensis* Berg*P. phoxinus* (Linnaeus)*P. neogaeus* Cope*erythrogaster* clade*oreas* species complex*P. oreas* (Cope)*cumberlandensis* species pair*P. cumberlandensis* Starnes & Starnes*P. tennesseensis* Starnes & Jenkins*erythrogaster* species pair*P. eos* (Cope)*P. erythrogaster* (Rafinesque)**Key to the species of *Phoxinus***

1. Intestine shorter than standard length, simply coiled; pharyngeal teeth in two rows; most occurring in Eurasia (only *P. neogaeus* in North America) 2.
- Intestine longer than standard length, coils complex; pharyngeal teeth in one row; all occurring in North America 5.
2. Peritoneum dark; mouth opening large, extending to middle of pupil, occurring in North America *P. neogaeus*
- Peritoneum silver, mouth opening small, extending to the anterior margin of orbit, occurring in Eurasian 3.
3. Side with about 10-15 vertical bars; genital papilla well developed with an elongate posterior process in adult of both sexes; dorsal margin of epibranchial 4 deeply forked *P. phoxinus*
- Side with one longitudinal stripe, without vertical bars; genital papilla small, without posterior process; dorsal margin of epibranchial 4 not deeply forked 4.
4. Air bladder short and broad *P. issykkulensis*
- Air bladder slender *P. brachyurus*
5. Opercle narrow and elongate *P. cumberlandensis*
- Opercle broad and short 6.
6. Dentary relatively short and blunt; pharyngeal bone with two large fossae, without small fossae *P. eos*
- Dentary relatively elongate and slender; pharyngeal bone with more than two fossae, both large and small fossae present 7.

7. Sides bearing only one continuous longitudinal stripe (unbroken);
posterior process of basioccipital bone broad and stout *P. tennesseensis*
Side with broken longitudinal stripe(s); posterior process of
basioccipital narrow and slender 8.
8. Side with one longitudinal stripe and a few vertical bars;
isthmus and breast dark; intestine length more than 2.5 times
standard length *P. oreas*
Side with two longitudinal stripes without vertical bars; isthmus
and breast with few or no melanophores; intestine length about
2 times standard length *P. erythrogaster*

SPECIES ACCOUNTS

Phoxinus phoxinus (Linnaeus, 1758)

Synonymy

Cyprinus aphys Linnaeus, 1758 – Linnaeus 1758: 323 (orig. desc.; type locality: Europe)¹;
Tack 1940a: fig.17 (larva); Wheeler 1991: 163 (type specimens in the Zoological Museum of the University of Uppsala).

¹) Abbreviations used in the synonymy are as follows: desc.: description; dist.: distribution; orig.: original; mis.id.: mis-identification.

Cyprinus phoxinus Linnaeus, 1758 – Linnaeus 1758: 322 (orig. desc.; type locality: Europe); Agassiz 1835: 37 (name); Jordan 1890: 50 (name); Jordan 1924: 71 (name); Mahy 1975c: 618 (name); Gasowska 1979: 371 (name).

Phoxinus laevis Agassiz – Agassiz 1835: 37 (orig. desc.; type locality: Europe); Cope 1869: 375 (name); Berg 1905: 196 (name); Nigrelli 1934: 64 (name); Bullough 1940: figs.1-14 (sexual reversal); Harrington 1950: 306, 309 (name); Medlen 1951: 149 (name); Rough 1954: 191 (name); Holz & Weber 1970: 1349, 1350 (nerve fibers in olfactory bulb); Wiley & Collette 1970: 170 (name); Mahy 1975a: 29 (name).

P. phoxinus Linnaeus – Starmach 1963: 367-368, tabs. I, II, IV, figs.1, 1-7, 10 (morphology); Stráskraba et al. 1966: 304 (name); Gentle 1971a: 83, 90, tabs.1-2, figs.1, 2 (color change); Gentle 1971c: 641, tab. 1, figs.2-7 (color change); Gentle 1972a: 701, tabs. 1-2 (physiology, color change); Gentle 1972b: 709, 711 (physiology).

P. phoxinus (Linnaeus) 1758 – Berg 1906: 197, 212 (dist., Russia); Cockerell 1909: 216 (scales); Frost 1943: 139, tabs.1-7, figs.1-9 (life history); Frost 1946: 224 (diet); Jones 1956: 271 (behaviour reaction to light intensity); Banarescu 1964: 333-343, figs.142, 143 (whole body), 144 (dist., Asia, Europe); Berinkey 1968: 275, tabs.I-IV (population variation); Wiley & Collette 1970: 168, 170 (tubercles); Kulamowicz & Korkuc 1971: 299, 301, tabs.1-2 (Morphology); Mann 1971: 155, 166, tabs.13-14 (population); Gentle 1971a: 83, 90, figs.1-4 (color change); Gentle 1971b: 93, 102, figs.1-8 (color change); Mahy 1972: 728 (name); Maitland 1972: 852 (name); Pitcher 1973: 841 (schooling behaviour);

Volkova 1973: 592 (behaviour, Lake Baikal); Kennedy & Pitcher 1975: 454, fig.1 (homing behaviour); Mahy 1975a: 29 (name); Mahy 1975b: 179 (name); Mahy 1975c: 617-641, figs.1-21, 23B (osteology); Howes 1978: 4 (name); Settles & Hoyt 1978: 296 (name); Wheeler 1978: 130, 132, fig.on p.131 (whole body) (Northern Europe); Gasowska 1979: 371, 373, 377, 379, 381, 384-386, 388-390, 392-393, 399-402, figs.1, 9, 16, 22, 28, 35, 41, 47, 53, 57, 66, 74, 78, 87, fig.1 of p.11 (osteology); Stott & Buckley 1979: 135 (behavior); Wootton & Mills 1979: 607, 608, 611, 616, fig.I (physiology); Joswiak et al. 1980: 915 (name); Joswiak 1980: 2, 8, 12, 15, 17, 18, 22, tabs.4-5, fig.2 (chromosomes); Partridge 1980: 68, 69, tab.1, figs.1-9 (schooling behavior); Wootton et al. 1980: 695-697, 704, tab.II, fig.2 (daily food consumption); Heese 1981: 67-75, tabs.1-4, figs 1, 2 (external morphology, Poland); Kennedy 1981: 621, figs.1-3 (homing behavior); Coad 1984: 135, tab.1, figs.1, 2 (specimens with deformed vertebral column); Constantinescu et al. 1984: 267, 284, 286, tab.1, figs.1-10, 12 (breeding coloration, behavior, Romania); Heese 1984: 25, 28, 34, tabs.1-3, figs.2-9, pls. 1-4 (biology, Poland); Legkiy & Popoya 1984: 72-79, tab.1 (behavior); Banbura 1985: 235, fig.2 (two deformed species without pectoral fin); Dauod et al. 1985: 3, figs.2-10 (population structure, diet); Pfeiffer et al. 1985: 553, 555, 558-559, 562-563, 565-567, 569, tabs II-VI, figs.1-12 (alarm substance); Kim & Kang 1986: tabs.1-2, figs.14c, 15b, 16c (osteology); Magurran & Girling 1986: 510 (behavior); Magurran 1986: 159, fig.1 (schooling and shoaling behavior); Pitcher & Turner 1986: 59, 60 (schooling behavior); Pitcher, Green & Magurran 1986: 439 (behavior); Pitcher et al. 1986: 83 (schooling); Cavender & Coburn 1987: 1 (name); Mills 1987: 53, tab.1, figs.1-10 (life history, Dorest, UK); Rasotto et al. 1987: 51, 53, 56, tabs.I-II, figs.1-10 (sexual inversion); Cuvín & Furness 1988: 205, figs.1-4 (toxicology); Doadrio & Garzón 1988: 389, 390, fig.1 (new record, Iberian Peninsula, Spain); Levesley & Magurran 1988: 699, fig.1 (alarm substance reaction); Cui & Wootton 1988a: 749, 750, tabs.I-VI, figs.1-4 (physiology); Cui & Wootton 1988b: 431, tabs.I-III, figs.1-4 (physiology); Banarescu 1989: 92, fig.2 (dist. map Eurasia); Bogutskaya 1989: fig.1a (infraorbital bones); Cui & Wootton 1989: 47-48 (physiology); Jeon 1989: 17, 29, 30, fig.10 (Korea); Travers 1989: 198, fig.18 (whole body) (dist., Mongolia); Chereshevnev 1990: 113 (north-eastern USSR); Banarescu & Coad 1991: 135, 143, 145, 147, 149 (Eurasian); Wheeler 1991: 163 (type specimen).

P. phoxinus (Linné, 1758) – Berg 1949: 123-126, figs.346 (whole body), 347 (whole body) (description, Eurasian).

P. phoxinus colchicus Berg, 1949 – Berg 1949: 126, fig.348 (western Transcaucasia).

P. p. phoxinus Linnaeus – Kulamowicz & Korkuc 1971: 302 (name); Haimovice & Ciuca 1973: 201-202, figs. 1-3. (Karyotype, 2N=52).

P. p. phoxinus (Linnaeus) – Banarescu 1964: 339-343 (Romania).

P. phoxinus ujmoneensis Kaschtschenko – Berg 1949: 127, fig.349 (whole body) (Altai, Lake Teletskoe).

Material studied

AMNH 36873sw, 2 C&S; River Thames and tributary to River Kew, Middlesex County, England; R. P. Vari, and J. Jones; 11 September 1977. – AMNH 71940, 11 alch.; Frame

River, Wareham, Dorset County, England; A. Wheeler; 22 April 1982. – ANSP 6342, 1 alch.; England; collector unknown; date unknown. – ANSP 6343, 8 alch.; Mediterranean, Italy; C. L. Bonaparte; date unknown. – ANSP 82449, 4 alch.; Red Lake, Transilvania, Romania; A. Popescu-Gorj; 20 August 1956. – ANSP 105676, 2 alch.; Chihi, China; collector unknown; August 1932. – ANSP 153914, 10 alch.; Torrenete Stura di Lanzo, Cirie comm., 2 km upstream bridge on the road Cirie-Robassonero, Torino Province, Italy; M. Bani; 27 April 1984. – CAS (SU) 06383, 10 alch.; Herault Dept.-Sete, France; E. Moreau; date unknown. – CAS 48106, 36 alch.; 45 km N of Bucuresti: brook Muciucatu, tributary to Prahova River between villages of Tinosu and Crivina, Romania; P. Banarescu and Damian; 7 April 1981. – CAS 58633, 15 alch.; pond near Torrente Malone, 1 km upstream bridge on road Rivarossa-Argentera, Rivarossa comm., Torino Province, Italy; G. A. C. Balma; 13 November 1985. – FMNH 80685, 12 alch.; River Moldova at Fundul-Moldovei, Bucovina, Romania; P. Banarescu; 6 November 1968. – FRLM, 9508, 1 alch.; Altay, Xinjian, China; collector unknown; 6 June 1989. – FRLM, 9513, 1 alch.; Altay, Xinjian, China; collector unknown; 6 June 1989. – FRLM, 9515, 1 alch.; Altay, Xinjian, China; collector unknown; 6 June 1989. – KU 22850, 16 alch.; upper Maritza River at Kostenetz, Bulgaria, Romania; P. Banarescu; 2 September 1965. – KU 22853, 10 alch.; Taria Brook, tributary to Minis River, 6 km upstream from Bozovici, Romania; P. Banarescu; 23 July 1968. – KU 22854, 10 alch.; Minis River, Banat, Romania; P. Banarescu; 23 July 1968. – KU 22855, 10 alch.; Humorul Brook, Gura Humorului, Romania; P. Banarescu; 7 November 1968. – KU 22856, 4 alch. and 1 C&S; Maciucatul Brook, tributary to Prabhova River, 43 km North Bucuresti, Romania; P. Banarescu; 17 April 1981. – KU 22857, 11 alch.; Aries River at Cimpeni, Transylvania, Romania; P. Banarescu; 2 November 1989. – KU 22858, 86 alch.; Timis River at Carasebes, Romania; P. Banarescu; 11 June 1990. – KU 22859, 5 alch.; Lake Lacul Rosu on 'Bicaz River at Bicaz, Transylvania, Romania; A. Popescu-Gori; date unknown. – KU 22860, 12 alch. and 2 C&S; probably Lake Lacul Rosu, Transylvania, Romania; collector unknown; date unknown. – MCZ 2049, 21 alch.; Lake Neuchatel, Switzerland; L. Agassiz; March 1860. – MCZ 18624, 12 alch.; Europe; C. Gegenbaur; date unknown (recorded in 1864). – MCZ 32372, 25 alch.; Teploje Lake, Bira River, basin of Amur, USSR, Asia; Vlad. Fish. Res. Sta.; 19 April 1927. – MHNG 658.86, 5 alch.; locality unknown; E. Galopin; date unknown. – MHNG 1503.52-55, 4 alch.; département de la Haute-Savoie, rivière des Usses, Près S de Seyssel, France; P. J. Haymoz; 16 November 1974. – MHNG 2012.95-97, 3 alch.; Nery, La Repetance, La Laitre, à Chancy, Genève, Switzerland; Stotz-Régner; 9 May 1979. – MHNG 2082.41-46, 6 alch.; ruisseau Poenari, à tinosu, à 50 km, au Nord de Bucuresti, Romania; P. Banarescu and S. Damian; 7 April 1981. – USNM 204166, 10 alch.; River Mures at Deda, Transylvania, Romania; P. Banarescu; 19 October. – USNM 218523, 21 alch.; Lotru River, tributary to Olt River, at Brezmi, district Vilcea, Romania; P. Banarescu; 16 September 1969. – USNM 271535, 80 alch.; Moraca River and adjacent ponds, the Aluminum Plant, Crana Gora, Czechoslovakia; Knapp and Jacobi; 1 June 1973. – ZFMK 649-653, 656, 7 alch.; 1888. – ZFMK 631, 1 alch.; 8 April 1900. – ZFMK 798, 2 alch. – ZFMK 585-586, 2 alch.; May 1957. – ZFMK 660, 1 alch.; 19 August 1933. – ZFMK 657-659, 3 alch.; 1873. – ZFMK 1780, 1 alch.; 1969. – ZIL uncat. 8 alch.; Kolyma River, Russia; collector unknown; date unknown. – ZMH 15147, 10 alch.; Treen Schleswig-Holstein, Germany;

G. Duncker; 12 July 1926. – ZMH uncat., 3 alch.; Albaum near Altenhundem-Lennestadt, Germany; collector unknown; 16 October 1991. – USNM 276160, 10 alch.; T. stura di Lanzo, Cirie Comm., Toprino Prov., 0.5 KM upstream bridge on the Road Cirio Robassomero, Italy; M. Banio; 27 April 1984.

Diagnosis (amended from Berg 1949, Yang & Huang 1964)

Primary lamellae in olfactory organ 15; no longitudinal lateral stripe; more than 10 vertical bars on side in adults (in young, vertical bars absent, but lateral stripe present on sides); body lateral line complete. Breast scales bearing tubercles in breeding females. Tubercles on dorsum of head large and few; 4 or 5 large tubercles on dorsal rim of orbit; very high density of tubercles on opercle; tubercles present on caudal fin in breeding female; gas bladder slender; intestine short; peritoneum silver; pharyngeal teeth in two rows.

Description (Tab.3)

An Eurasian species of *Phoxinus* with average standard length (adults) about 60 mm, maximum standard length of 125 mm (Berg 1949). Head large, broad, and robust; its length 25% of standard length; its width 51% of its length. Snout elongated, its length 28% of head length, 102% of orbit length. Eye lateral on head; orbit length 27% of head length.

Tab.3: Body proportions (%) of *Phoxinus phoxinus*. (ACGL: anterior chamber of gas bladder length; BD: body depth; BIW: bony interorbital width; CPD: caudal peduncle depth; CPL: caudal peduncle length; HD: head depth; HL: head length; HW: head width; IL: intestine length; Number: number of specimens; OL: orbit length; PCGL: posterior chamber of gas bladder length; PRDL: predorsal fin length; PRPL: prepelvic fin length; S: standard deviation; SL: standard length; SNL: snout length).

	HL/SL	HD/SL	BD/SL	CPL/SL	CPD/SL	PRDL/SL	PRPL/SL	IL/SL	HW/SL	HD/HL
Number	25	26	24	25	25	23	26	4	25	26
	23.2	15.3	18.8	23.3	7.7	52.9	42.5	65.4	11.7	14.1
Range	—	—	—	—	—	—	—	—	—	—
	27.0	21.6	22.8	28.2	10.1	59.0	50.2	76.2	13.9	17.4
Mean	25.3	16.3	20.3	25.6	9.2	55.6	47.1	70.0	12.9	16.3
S(±)	1.0	1.5	1.6	1.6	0.8	1.8	2.1	5.0	0.7	1.5

	OL/HL	HW/HL	SNL/HL	BIW/HL	BIW/OL	SNL/OL	PRDL/PRPL	CPD/CPL	ACGL/PCGL
Number	22	20	25	25	23	22	24	25	3
	23.2	48.2	21.5	26.3	116.7	79.2	115.1	29.0	45.0
Range	—	—	—	—	—	—	—	—	—
	31.8	51.3	34.2	35.2	120.5	121.6	122.1	40.0	54.3
Mean	26.7	49.5	28.1	32.1	118.8	102.3	119.8	36.1	50.0
S(±)	3.3	1.6	2.9	3.4	2.5	14.7	7.3	3.0	4.5

Mouth small, slightly subterminal and oblique; mouth gape not extending to below the anterior margin of the orbit. Lower jaw slightly shorter than the upper one.

Bony interorbital space wide, its width 119% of orbit length and 32% of head length. Anterior nasal opening smaller and shorter than posterior nasal opening, the former about half the size of the latter. Entire margin of anterior nasal opening erect; margin of posterior nasal opening, except its anterior part, not erect.

In young individuals (25.3 mm standard length), axis of olfactory organ very short, oval in shape, and situated in anterior part of olfactory chamber; five primary lamellae present. In larger specimens (60.1 mm standard length), the axis elongated and extending to posterior portion of organ chamber; up to 16 primary lamellae present. Numerous melanophores present on primary lamellae in young, on both primary lamellae and axis in adult. Body slender, not strongly compressed. Maximum body depth 20% of standard length. Caudal peduncle short and high, its length 26% of standard length, its depth 36% of its length.

In male, the genital papilla spheric in shape, and smaller than that in female. Surface of papilla smooth without small skin fold, but one large skin fold present in some specimens. Genital orifice large. Posterior projection of genital papilla well-developed, its posterior end far from origin of anal fin.

In female, genital papilla well-developed, its posterior margin with few well-developed projections; a long projection extending from posterior of papilla, reaching anal fin origin. Surface of papilla bearing developed skin folds.

Pectoral fin fan-like in male, sharper and smaller in female, its posterior margin reaching origin of pelvic fin in adults; 14-16 fin-rays. Origin of pelvic fin farther forward than origin of dorsal fin, and in anterior half of standard length; prepelvic length 47% of standard length; eight rays.

Dorsal fin originating behind pelvic origin, predorsal length 56% of standard length, and 120% of prepelvic length; with two procurent rays, eight fin-rays. Anal fin originating below insertion of dorsal fin; with two procurent rays and eight rays. Caudal fin deeply forked, lobes sharp; with 11 or 12 dorsal procurent, 9-10 ventral procurent rays, and 19 (10+9) principal rays.

Scales covering whole body, weakly embedded on lateral and dorsal surface of body, but deeply embedded on ventral side of the body.

Left and right supratemporal canals separated from each other, with four pores each side. Otic canal with five pores. Supraorbital canal without interruption, except the region between nasal and frontal bones, with nine pores. Infraorbital canal with 10 pores. Preopercular canal with eight pores. Mandibular canal with four pores. Body lateral line complete, extending to caudal fin base, number and positions of the pores varying individually; about 82 lateral line pored scales.

Pharyngeal bone robust; its pitted surface broad with four large fossae. Posterior limb elongate, slender and straight; anterior limb slender, narrowing posteriorly, expanding anteriorly, bearing a notch at anterior end. Pharyngeal teeth very strong, hooked at tip, in two rows, 2,4-5,2, 1,5-5,2, 1,4-5,1. Teeth in main row more developed than those on minor row. Masticatory surface of teeth round and smooth.

Vertebrae 40-43 (three specimens); precaudal vertebrae 22 or 23, caudal vertebrae 18 or 20.

Intestine short, simply looped; its length 70% of standard length. Gas bladder slender and elongated. Anterior chamber of the bladder round at its anterior end, and about 50% of the posterior chamber in length. Both chambers nearly cylindrical, not tapering from anterior to posterior portion, though posterior end narrows slightly. Constriction elongated. Pneumatic duct placed at middle of constriction. Peritoneum silver in color.

Male Tuberculation. Dorsal, lateral and ventral sides of the head bearing tubercles. However, the morphology and density of the tubercles vary with regions. On dorsum of head, tubercles few in number, but large and tall in shape. Three tubercles along the medial margin of nasal opening, two of which are adjacent to tubercles at the medial margin of the other nasal opening. Four tubercles on the dorsal rim of the orbit. The anterior two are close to each other, and posterior two also close together. Five tubercles dorsally between eyes, four of the five forming a square, the remaining one located at center of square. Tips of these tubercles directed left, right, posteriorly, or dorsally. About 14 tubercles arranged in three rows on posterior portion of head: anterior row of three, middle row of four, and posterior row of seven tubercles.

Numerous tubercles present on lateral side of head. Posterior one-third of opercle bearing small, tall, sharp tubercles; anterior area with larger, shorter tubercles. Density of tubercles on the opercle very high, the most dense among all regions in all studied *Phoxinus* species. Branchiostegals and cheek bearing numerous large but short tubercles. No tubercle on anterior end of snout. On ventral side of the head, tubercles mainly present at ventral portion of the lower jaw.

The dorsal, lateral, and most of the ventral sides of body bearing tubercles. About seven rows of scales on breast bearing well-developed tubercles. Each scale in this region bears a few tubercles at its apical margin to form a comb-like edge. Ventral body anterior to anal fin origin not bearing tubercles. Each scale on lateral and dorsal surfaces having four to 12 tubercles at apical margins.

All fins bear sharp tubercles. On ventral side of pectoral fin, membrane between two rays from the first to eighth rays bear four to seven tubercles in one row near the distal margin of the fin; fewer tubercles on fin-rays. On the dorsal side of pectoral fin, each ray from the second to eighth bears three rows of tubercles distally, decreasing to two rows and then to one row proximally. Fewer tubercles present on the membrane. No tubercles present at the proximal part of pectoral fin.

On the dorsal side of the pelvic fin, each of the first five rays bears two rows of tubercles distally, decreasing to one row proximally. The proximal one-third of the fin bears no tubercles. Each of the remaining rays bears one short row of tubercles on the proximal portion. No tubercles on interradial membranes of the fin. Fewer tubercles present on ventral side of fin.

Few tubercles are present on fin rays and membrane of the dorsal, anal, and caudal fins. **Female Tuberculation.** Tubercles are present on dorsal and lateral sides of head, no tubercles on ventral side of head. Tubercles on dorsum of head few, large and sharp. Five large tubercles along dorsal rim of each orbit, two or three of the five at the anterodorsal

side of snout. No tubercles present at anterior end of snout. Numerous small tubercles on lateral side of the head.

Each scale of the 11 rows of breast scales bearing four to eight small tubercles along the apical margin. Scales on the area between the breast scales also bearing tubercles. The remaining ventral area of body bearing no tubercles. No tubercles on all fins.

Coloration. 14-15 parallel and vertical dark bars present on side, from behind the gill cleft to posterior part of caudal peduncle. Bars in front of insertion of dorsal fin longer than those behind insertion. Juveniles (less than 25 mm standard length) lack vertical bars but have one longitudinal stripe from the gill cleft to the caudal fin base. Some specimens also bearing a few large speckles dorsally. A dark dorsal stripe present from nape to base of caudal fin.

Numerous melanophores are present on trunk, except ventral to lateral bars where melanophores are absent or few. Breast region bearing melanophores in male. Dorsum dark, with numerous melanophores, becoming paler on sides in spaces between lateral bars.

Head with numerous melanophores dorsally, laterally, and ventrally. Anterior part of opercle bearing more melanophores than its surrounding.

All fins bearing melanophores on rays and membrane. On pectoral fin, the first ray darker than others. Pelvic fin dark, evenly pigmented. Base of dorsal fin with a black patch, and the rays with more melanophores than the membrane. Anal fin uniformly dark, but base of fin bears very few melanophores. Base of caudal fin bearing more melanophores than rest of the fin.

Biology

P. phoxinus inhabits flowing water, ponds, shallow lakes, and margins of deep lakes, such as Lake Baikal (Berg 1949). It lives on various bottoms, but prefers stony substrates (Frost 1943). Schools of hundreds of individuals sometimes occurs in shoal area (Frost 1943, Partridge 1980). Fish species associated with *P. phoxinus* include freshwater eel [*Anguilla anguilla* (L.)], salmon (*Salmo salar* L.) (Frost 1943), stickleback (*Gasterosteus aculeatus* L.), and *Noemacheilus barbatulus* (L.) (Dauod et al. 1985).

The food mainly consists of copepods, filamentous algae and diatoms. *P. phoxinus* also eats insect larvae (Frost 1943). Dauod et al. (1985) recognized 12 categories of food items for the species: surface insects, mollusca, trichopteran larvae, trichopteran pupae, cladocera, copepoda, chironomid larvae, chironomid pupae, ephemeropteran nymphs, other larvae, *Gammarus* and "chance" food. According to these authors, the diet composition changes seasonally. For instance, the most important food items early in year were chironomid larvae, mollusca, and trichoptern larvae. These foods were replaced by daphnia and surface insects in May.

The species reaches its mature at 35-45 mm standard length in about their second year (Dauod et al. 1985). The breeding season varies from early April to September depending partly on latitude. Prior to spawning, large school of adults migrates to smaller stream having cooler water (Bade 1902, Frost 1943). The school might be concentrated on an approximately circular surface of about 30 cm diameter, and 1.5 cm thick layer. Individuals

in the school form a few breeding centers with the presence of females (Constantinescu et al. 1984). One or two (seldom three) males chase one female spawning (Constantinescu et al. 1984). The male contacted the female then flanked her. Males were also observed rotating two by two. Fecundity ranges from 700 to 1000 eggs. Diameter of a ripe unfertilized egg is about 1.3 mm (Berg 1949), that of an ovum is 1.0 to 1.4 mm (Dauod et al. 1985).

Distribution

P. phoxinus occurs in Europe, and east and central Asia. In Asia, it occurs in northern China to Helong Jiang River, Yalu River and Tumen River (Yang & Huang 1964), Korea (Mori 1928a, b, 1930, 1934, Jeon 1989), and Mongolia (Travers 1989). Banareescu (1964: fig.142) illustrated the geographic distribution of the species.

Comments

Bullough (1940) mentioned that the males were darker than females in *P. phoxinus*. Specimens studied herein, however, show little sexual difference in color. In some populations, females could be slightly darker than males. Frost (1943) showed no difference in color found between females and males.

The type specimen of *P. phoxinus* is problematic. The specimens labeled "*Cyprinus aphyra*" (Catalogue no: ZIU 211) in the Zoological Museum of the University of Uppsala were generally regarded as the type series of *P. phoxinus* because *Cyprinus aphyra* was usually considered a synonym of *P. phoxinus* (Wheeler 1991). However, these specimens are in poor condition and difficult to identify, and no evidence shows whether these specimens are the ones that Linnaeus used to describe *C. aphyra*, or *Cyprinus phoxinus*, or neither (Wheeler 1991).

Etymology

The epithet *Phoxinus* was derived from Greek, means tapering (Nelson & Paetz 1992). It may refer to the body shape of the species.

Phoxinus brachyurus Berg, 1912

Synonymy

Phoxinus brachyurus Berg, 1912 – Berg 1912: 241, fig.16 (orig. desc.; type locality: Chilik River in the Ili basin, Kazakhstan); Berg 1932: 354, 365-366, fig.276; Berg 1949: 107, 121-122, fig.344 (Chilik River, Ili River; Basin of Chu River, Central Asia.); Yang & Huang 1964: 22, 24-25, fig.1-13 (Ili River, Xinjiang, China); Howes 1985: 71 (name).

Material studied

MCZ 3006: 2 alch. and 1 C&S; Siberia, Lake Baikal, USSR; J. D. E. Schmeltz, Jr.; 1873.
– MMSU 3928: 1 alch; Russia; collection date unknown.

Diagnosis (amended from Berg 1949, Yang & Huang 1964)

A *Phoxinus* species with numerous dark blotches on sides of body; left and right supratemporal canal almost joined on the parietal; body lateral line interrupted; two medial extrascapulae on supraoccipital; anterior process of basioccipital absent; epibranchial 4 bearing an elongate dorsally directed process.

Description

An Asian *Phoxinus* species with maximum standard length of 90 mm. Head large, laterally compressed, its length 24% of standard length, its width 13% of its length. Snout moderately elongate, slightly shorter than orbit length in adult, or equal in young; its length 22% of head length, and 92% of orbit length. Eye large. Mouth terminal and moderately large; mouth gape not extending to below anterior margin of the orbit; lower jaw equal to upper in length. Bony interorbital space relatively narrow.

Axis of olfactory organ elongate, elliptical; ten primary lamellae in the olfactory organ. Melanophores present on both primary lamellae and axis. No data available for young individuals.

Body elongate, moderately deep, not strongly compressed; round at abdomen. Dorsal profile slightly arched. Maximum body depth 21% of standard length. Ventral profile nearly horizontal. Caudal peduncle short and high, its length 19% of standard length, its depth 54% of its length.

Genital papilla short and small, without posterior process; much more developed in breeding season than in nonbreeding season (Yang & Huang 1964).

Pectoral fin small and short; its posterior margin forward from base of pelvic fin; fin-rays 13-14. Pelvic fin small, acute at distal end, not reaching the vent; fin-rays eight (two specimens), or seven (one specimen). Dorsal fin round, originating posterior to the pelvic fin base; with one or two procurent rays and eight rays. Anal fin small and round, its origin slightly posterior to insertion of dorsal fin; with one or two procurent rays, eight fin-rays. Caudal fin shallowly forked, its lobes round; dorsal procurent rays six or seven, ventral procurent rays five or six, principal rays 19 (10+9).

Left and right supratemporal canals near to (but not connected) each other at supraoccipital bone, with 5-8 pores. Otic canal with four or five pores. Supraorbital canal interrupted, with 9 or 10 pores. Infraorbital canal interrupted, with 11 (one specimen) or 13 (two specimens) pores. Preopercular canal complete, with 10 pores. Mandibular canal with seven pores. Body lateral line straight, interrupted, extending to base of caudal fin. Entire abdomen scaled.

Pharyngeal bone slender, its posterior limb slightly bent. Pitted surface narrow with four major fossae. Pharyngeal teeth in two rows: 5.2-1.4. Teeth slender, hooked at tip; masticatory surface of teeth round and smooth.

Vertebrae 38-40; precaudal vertebrae 20-21, caudal vertebrae 18-19.

Intestine shorter than standard length, simply looped, its length 75% of standard length (one specimen). Gas bladder relatively slender, anterior chamber 62% of the posterior one

in length (one specimen); pneumatic duct connecting with anterior portion of the posterior chamber. Peritoneum silver in color.

Tuberculation – No data about tuberculation of this species was available at the present.

Coloration – One lateral stripe present at middle of the sides of the body, extending from upper end of gill cleft to caudal fin base; stripe faint anteriorly. Melanophores present on whole body except breast and isthmus, though lighter at ventral portion than at dorsal portion of trunk. Numerous dark speckles (smaller than pupil in diameter) present dorsally on the sides of the body (dorsal of the lateral dark stripe). A mid-dorsal dark stripe present, extending from nape to base of caudal fin.

Biology

Spawning season is in March and April (Berg 1949). No other data available.

Distribution

P. brachyurus is restricted to the drainage of the Ili River in Kazakhstan, and the Xinjiang Uygur Autonomous Region in China.

Comments

Yang & Hung (1964) mentioned that this species lacks scales on the abdomen. Berg (1949) and my observation showed that the entire ventral side of the body is scaled.

Etymology

The epithet “*brachyurus*” might be derived from a combination of “brachy-” meaning “short” and “-urus” meaning “tail” (C.R. Robins 1995; pers. comm.).

***Phoxinus issykkulensis* Berg, 1912**

Synonymy

Phoxinus issykkulensis Berg, 1912 – Berg 1912: 243, fig.7 (orig. desc.; type locality: Lake Issy-kul, Kazakhstan); Berg 1932: 366, fig.27 (desc., Issyk-kul River and tributaries, Kazakhstan); Berg 1949: 122, 123, fig.277 (Lake Issykyl's tributaries, Kazakhstan); Howes 1985: 71 (name).

Material studied

NMC 77-0883 (originally from the Zoological Institute, Academy of Sciences, USSR, Cat. No. 26374), 3 alch.; Brook mouth, Lake Issyk-kul, Jamy-Uguz, USSR; D. Pedashenko; 1909. – MMSU 10696 1 alch. and 1 C&S.. – ZIL 26373 (3), 3 alch; Lake Issyk-kul; collector unknown; date unknown.

Diagnosis (amended from Berg 1949)

Caudal fin deeply forked, its lobes pointed; anteromedial process of maxilla absent; pharyngeal 2+3 triangular in shape; gas bladder broad and short.

Tab.4: Body proportions (%) of *Phoxinus issykkulensis*. (ACGL: anterior chamber of gas bladder length; BD: body depth; BIW: bony interorbital width; CPD: caudal peduncle depth; CPL: caudal peduncle length; HD: head depth; HL: head length; HW: head width; IL: intestine length; number: number of specimens; OL: orbit length; PCGL: posterior chamber of gas bladder length; PRDL: pre-dorsal fin length; PRPL: prepelvic fin length; S: standard deviation; SL: standard length; SNL: snout length).

	HL/SL	HD/SL	BD/SL	CPL/SL	CPD/SL	PRDL/SL	PRPL/SL	IL/SL	HW/SL	HD/HL
Number	7	6	6	7	6	7	6	1	7	6
	26.4	16.6	23.3	18.0	9.0	53.4	48.2	—	12.8	59.3
Range	—	—	—	—	—	—	—	—	—	—
	30.0	18.3	25.5	23.9	10.4	59.7	54.1	—	15.1	63.5
Mean	28.1	17.1	24.4	21.5	9.9	58.0	52.3	89.2	13.8	60.9
S(±)	1.1	0.6	1.1	1.8	0.5	2.7	1.9	—	0.9	1.5

	OL/HL	HW/HL	SNL/HL	BIW/HL	BIW/OL	SNL/OL	PRDL/PRPL	CPD/CPL	ACGL/PCGL
Number	7	7	7	7	5	6	7	7	1
	21.2	47.3	22.2	25.5	104.0	92.0	102.1	40.4	—
Range	—	—	—	—	—	—	—	—	—
	31.9	53.3	27.2	36.1	117.1	116.7	115.8	57.8	—
Mean	25.9	49.2	25.2	30.7	109.2	104.5	110.3	46.4	81.1
S(±)	4.0	2.7	1.8	3.3	6.0	11.6	5.4	6.1	—

Description (Tab.4)

An Eurasian *Phoxinus* species with maximum standard length of 102 mm (Berg 1949). Head large and elongate; laterally compressed, its length 28% of standard length, its width 61% of its length. Snout elongate, its length 25% of head length, and 105% of the orbit length. Eye relatively small, orbit length 26% of head length. Mouth small oblique, sub-terminal, extending to below anterior margin of eyes. Lower jaw slightly shorter than upper one.

Bony interorbital space relatively narrow, its width 109% of orbit length, and 31% of head length.

Axis of olfactory organ a long ellipse in shape. Primary lamellae about 10.

Body elongate, not strongly compressed, round at abdomen. Dorsal profile slightly arched, maximum depth 24% of standard length. Caudal peduncle deep, short and laterally compressed; its length 22% of standard length, its depth 46% of its length.

Genital papilla short, moderately developed, without a projection; its posterior end almost reaching anal fin origin.

Pectoral fin small and short, its posterior margin far away from the pelvic fin base, reaching about half-way between bases of pectoral and pelvic fins; with 14 or 15 fin-rays. Pelvic fin small, not reaching vent, with eight rays.

Dorsal fin round, with one procurent ray and eight rays. Anal fin small and slightly pointed, originated at position slightly posterior the insertion of dorsal fin; with one procurent ray, and eight rays. Caudal fin moderately forked (deeper than in *P. brachyurus*), with four dorsal procurent rays, four ventral procurent rays, and 19 (10+9) principal rays.

Cephalic lateral line well-developed. Supratemporal canal and otic canal not interrupted, each with four pores. Supraorbital canal not interrupted, except the area between the nasal and frontal portions, with 10 pores. Infraorbital canal not interrupted, with 10 pores. Preopercular canal not interrupted, with seven pores. Mandibular canal with three pores. Body lateral line short, the last pored scale about halfway between the posterior margin of pectoral fin and base of pelvic fin; lateral line pored scales often 15. Abdomen anterior to pelvic fin usually scaleless, but some specimens bear scales in posterior portion of region between isthmus and pelvic fin base (Berg 1949).

Pharyngeal bone moderately broad, both the posterior and anterior limbs slightly bent; pitted surface broad, with six major fossae. Pharyngeal teeth in two rows, 5.1-1.5. Teeth slender, hooked at tip in main row; without hooks in minor row.

Vertebrae 37, precaudal vertebrae 21, caudal vertebrae 16.

Intestine short, shorter than standard length, simply looped. Gas bladder short and broad, the anterior chamber almost equal to the posterior one in length, constriction short. Pneumatic duct connecting with the anterior portion of the posterior chamber. Peritoneum slightly brown in color.

Tuberculation. No detailed data about tuberculation of this species are available though the male was hypothesized by Howes (1985) to bear tubercles on breast scales during breeding season. According to Berg (1949), breeding males apparently lack tubercles on the head.

Coloration. A lateral dark stripe present along middle of sides of the body, extending from dorsal end of gill cleft to caudal fin base. Stripe darker posteriorly, darkest on caudal peduncle, and faintest anterior to pectoral fin. Some individuals with a few small dark speckles on sides of body. The mid-dorsal dark stripe extending from nape to caudal fin base. Melanophores present on entire body, except abdomen anterior to anal fin origin and ventral side of the head. Few melanophores present on ventral side of caudal peduncle. All fins bearing melanophores.

Biology

A 45 mm total length female individual was reported to be ripe (Berg 1949). No other data are available at the present time.

Distribution

P. issykkulensis is endemic in Lake Issyk-kul and its tributaries in Kazakhstan (Berg 1949).

Etymology

The epithet "*issykkulensis*" is derived from the combination of "Issykkul" and a Latin suffix "-ensis" to refer the type locality Lake Issyk-kul and its tributary in Central Asia (Kazakhstan) where the species is endemic.

Phoxinus neogaeus Cope, 1868**Synonymy**

Chrosomus eos Cope, 1864 – Cope 1864: 281 (non Cope 1861: 523) (mis. ident., comparison with *Phoxinus erythrogaster*, New Hudson, Livingston County, Michigan).

Chrosomus neogaeus (Cope) – Underhill 1957: 12, 25, 30, map 6 (Minnesota); Bailey & Allum 1962: 40, 120, tab.9, fig.3 (desc., dist., South Dakota); New 1962: 147, 149-151, tab.1, figs.1-5 (external morphology); Tyler 1966: 349-361 (physiology); Roberts 1973: 468 (new record, Albert, Canada); Scott & Crossman 1973 : 393, 396-399, figs. p.396, 398 (desc., dist. Canada); Eddy & Underhill 1974 : 240, 241, fig.5 (whole body); Mahy 1975a: 1, 3, 5, 10, 14, 19, 23, 25-29, figs.1-23 (osteology); Mahy 1975b: 165, 168, 172, 175, figs.1-18 (osteology); Mahy 1975c: 617, 619-634, tab.1. figs.1-3, 6, 8-9, 10-22 (osteology); Stasiak 1977: 771-773, tabs.1-4 (morphology and variation, Mississippi River); Gasowska 1979: 373 (name).

Leuciscus neogaeus (Cope) – Fowler 1918: 16-17, pl.6 [desc. (ANSP 4548, cotype of *P. neogaeus*, New Hudson, Livingston County, Michigan, and other small and poor preserved 37 specimens)].

Pfrille neogaea (Cope) – Jordan 1924: 71 (change of *Phoxinus neogaeus* to *Pfrille neogaea*); Hubbs & Brown 1929: 27, 28 (tubercles; dist., Superior Lake drainage, Lake Huron drainage, Ontario, Canada); Toner 1933: 137(name); Churchill & Over 1938: 54 (desc., dist., Cox Lake, NW Spearfish, Dakota); Lindeborg 1941: 160 (dist., Ontario, Canada); Hubbs & Lagler 1949: 56, 64, fig.130 (Great Lakes region); Scott 1957: 161 (dist., Lonnepine Creek and Loch Leven, Canada); Phillips & Etnier 1969: 96 (name); Eddy & Underhill 1974: 241 (name); Gasowska 1979: 372, 373, 375, 378, 379, 381, 383, 385, 386, 388, 392, 398, 399, figs.3, 10, 17, 23, 29, 37, 42, 48, 69, 67, 75, 79 (osteology); Constantinescu et al. 1984: 286 (name).

Phoxinus neogaeus Cope – Günther 1868: 247 (desc., New Hudson, Michigan); Cope 1869: 375 (original desc.; type locality: New Hudson, Livingston County, Michigan) (in Günther 1868: 247); Jordan 1885: 62 (Wisconsin River, Illinois); Legendre & Steven 1969: 913, tab.I (chromosomes); Legendre 1970a: 325, 329, tabs.1, 2 (vertebrae); Legendre 1970b: 1167-1169, 1171, 1174-1176, tab.I, figs.2, 4, 6, 7 (dist., Quebec, Canada); Gilbert 1971: 476, 477 (name); Mahy 1972: 728 (osteology); Joswiak 1980: 2, 3, 5, 6, 7, 13, 15, 27-22, tabs.2, 4, 5, figs.1B, 2 (chromosome study); Joswiak et al. 1980: 913, tab.1, fig.1B (chromosomes, Wyoming); Stasiak 1980b: 338, fig.on p. 338 (general review); Joswiak, et al. 1982: 968, 969-972, tabs.1, fig.1 (external morphology); Cooper 1983: 112, 114, fig.on p.114 (whole body) (desc., dist., Pennsylvania); Gasowska 1983: 99 (name); Böhlke 1984: 84 (type specimens in ANSP); Constantinescu, Vintilă & Damian 1984: 286, tab.1 (coloration, behavior, and comparison with other *Phoxinus* species); Howes 1985: 71 (name); Coad 1987: 45 (dist., Ottawa, Canada); Dawley et al. 1987: 275-282 (chromosomes); Dawley & Goddard 1988: 649-657, tab. 1 (chromosomes); Harbicht et al. 1988: 475, tab.3, fig.3 (new record, Manitoba, Canada); Starnes & Jenkins 1988: 517 (name); Banarescu 1989: 92, fig.2 (dist. map, North America); Das & Nelson 1989: 579, 583, fig.1A (Albata, Canada); Goddard et al. 1989: 268, 269, 271-277, Appendix, fig.1 (com-

parison on coloration and behavior among species of *Phoxinus*); Mayden 1989: 260 (name); Goddard & Dawley 1990: 1052-1063, tab.1 (New Hampshire); Nelson & Paetz 1992: 155, 157, 158, fig.on p.155 (whole body), map. 12.9 (dist., Alberta, Canada).

Pfrille neogaeus (Cope) – Jordan et al. 1930:21 (name).

Phoxinus (Pfrille) neogaeus (Cope) – Gasowska 1979: 403 (name).

Material studied

Syntypes: ANSP 5408, 7 alch.; New Hudson, from streams flowing into Lake Erie, Oakland County, Michigan, USA; collector unknown; date unknown.

Other specimens. ANSP 48468, 10 alch.; Otter Pond Camps, Caratunk, Maine; W. J. Epling; 1915. – ANSP 50149, 2 alch.; Bay View, Michigan, USA; T. L. Hankinson; date unknown. – CAS (SU) 09835, 41 alch.; Cross Lake Thoroughfare, Eagle Lakes, Aroostock County, Maine, USA; Kendall and Gould; date unknown. – KU 1146, 3 alch.; Pond in Wilderness Park, Emmet County, Michigan, USA; U.B.S Ichthyology class; 24 July 1946. – KU 1148, 2 alch.; Pond in Wilderness Park, Michigan, USA; Biological Survey; 24 July 1946. – KU 8521, 6 alch. and 3 C&S; Snake River, Cherry County, Nebraska, USA; R. Peckham; 21 August 1963. – KU 14254, 2 alch.; Itasca Park, French Park, Beaver Pond, Clearwater County, Minnesota, USA; R. Stasiak; 1 March 1970. – KU 18882, 3 alch. and 12 C&S; Rennie River, Whiteshell Provincial Park, Manitoba, Canada; F.R. Cook & J.C. Cook; 14 August 1964. – UT 44.1506, 2 alch.; Lena Lake, Lake County, Minnesota, USA; Minnesota Department of Conservation; 1964. – UT 44.2870, 41 alch.; Victor Lake near Midiwan Lake, 5 mi. N.W. Isabella, Cook County, Minnesota, USA; D.A. & M.A. Etnier, L.B. & W.C. Starnes; 21 June 1982. – UT 44.2894, 14 alch.; Hill Creek tributary to Midiwan Lake at logging road and above in beaver pond, Kauishiwi system, Cook County, Minnesota, USA; D.A. & M.A. Etnier, W.C. & L.B. Starnes; 21 June 1982.

Diagnosis (amended from Cope 1869)

A *Phoxinus* with one narrow lateral dark stripe almost equal in width from anterior to posterior portion of body; the lateral stripes are continuous onto head and across snout. Mouth large, its opening extending to below anterior margin of pupil of eye. In spawning males, first five (occasionally four) pectoral rays much darker, thicker and stronger than other pectoral rays; segments of these thick rays short and wide. Intestine short with only one loop, its length less than standard length; pneumatic duct dark; pharyngeal teeth in two rows, 2.5-5.2, 2.4-5.1, or 1.5-4.1; pharyngobranchial 4 bearing a median process.

Description (Tab.5)

A North American species of *Phoxinus* with average standard length (adults) about 70 mm. Head large, broad, and robust, its length 27% of standard length, its width 58% of its length. Snout short and blunt; its length 26% of head length, 93% of orbit length. Eye lateral on head and large; orbit length 28% of head length. Mouth large (largest in *Phoxinus*), terminal, and oblique, its opening extending below the anterior margin of eye pupil. Lower jaw slightly shorter than the upper one.

Tab.5: Body proportions (%) of *Phoxinus neogaeus*. (ACGL: anterior chamber of gas bladder length; BD: body depth; BIW: bony interorbital width; CPD: caudal peduncle depth; CPL: caudal peduncle length; HD: head depth; HL: head length; HW: head width; IL: intestine length; Number: number of specimens; OL: orbit length; PCGL: posterior chamber of gas bladder length; PRDL: predorsal fin length; PRPL: prepelvic fin length; S: standard deviation; SL: standard length; SNL: snout length).

	HL/SL	HD/SL	BD/SL	CPL/SL	CPD/SL	PRDL/SL	PRPL/SL	IL/SL	HW/SL	HD/HL
Number	17	18	17	18	18	17	16	3	18	17
	26.0	16.4	18.8	21.5	9.0	54.7	49.1	77.0	14.1	58.6
Range	—	—	—	—	—	—	—	—	—	—
	30.2	22.1	23.5	34.2	27.3	61.6	65.7	85.1	17.3	75.0
Mean	27.4	18.3	21.6	25.2	11.5	57.4	50.1	81.0	16.0	66.1
S(±)	1.4	1.8	1.5	2.8	4.0	2.0	8.3	4.1	1.1	4.5

	OL/HL	HW/HL	SNL/HL	BIW/HL	BIW/OL	SNL/OL	PRDL/PRPL	CPD/CPL	ACGL/PCGL
Number	17	16	17	17	17	17	14	17	3
	23.1	52.4	22.5	29.7	82.2	68.6	107.8	26.4	38.5
Range	—	—	—	—	—	—	—	—	—
	33.7	65.7	29.2	43.5	142.9	100.0	117.1	52.0	75.0
Mean	28.2	58.2	25.9	33.9	116.6	92.9	112.8	43.2	54.5
S(±)	3.4	3.5	2.0	3.2	19.5	10.3	3.0	6.2	18.7

Bony interorbital space wide; its width 117% of orbit length, and 34% of head length.

In young individuals (25 mm standard length), axis of olfactory organ short, not extending to middle of the organ, five primary lamellae present; in adult individuals (52.0 mm standard length), axis extends to posterior portion of the organ, 11 primary lamellae present.

Body not strongly compressed. Its maximum depth 22% of standard length. Caudal peduncle short and high, its length 25% of standard length, its depth 43% of its length.

Genital papillae short and small; longer and more slender in female than in male; its posterior end far forward of anal fin origin.

Pectoral fin fan-like, sharper in female. In breeding male, first four or five rays, especially the first one, thicker, stronger, and darker than rest of pectoral rays; segments of these thick rays shorter and wider; 13-16 fin-rays, usually 14 or 15. Pelvic fin originating in advance of dorsal fin origin, prepelvic length 50% of standard length; fin rays eight, occasionally nine (two of the 17 specimens counted with nine rays).

Dorsal fin originating posterior to pelvic fin origin, predorsal length 57% of standard length, and 113% of prepelvic length; with two procurent rays and eight rays, only one of the 18 specimens with nine rays. Anal fin originating under or slightly behind the insertion of dorsal fin; with one or two procurent rays and eight fin rays. Caudal fin shall-

lowly forked, lobes round; with 7-9 dorsal procurent rays, 5-7 ventral procurent rays and 19 (10+9) principal rays.

Left and right supratemporal canals not connecting with each other; six pores. Otic canal with six pores. Supraorbital canal interrupted in some specimens, 12 pores. Infraorbital canal without interruption, 14 pores. Preopercular canal extending to middle of the preopercle, 10 pores. Mandibular canal without interruption, 6 pores.

Body lateral line extending from dorsal of gill cover, curving down and following lateral stripe, and ending at the level of the pelvic fin; with about 31 pored scales, depending on specimen's size. (Large individuals have more pored scales than juveniles.) Scales well embedded, covering entire body.

Pharyngeal bone somewhat slender; posterior limb straight; pitted surface narrow with four to five major fossae. Pharyngeal teeth in two rows, 2.5-4.2, 2.4-5.2, 2.5-5.2, or 1.5-4.1. Teeth robust, hooked at tip (not hooked for one or two teeth near posterior limb). Masticatory surface of teeth smooth.

37 or 38 vertebrae; 21-22 precaudal vertebrae, 15-17 postcaudal vertebrae.

Intestine short and simply coiled, its length 81% of standard length. Anterior chamber of gas bladder shorter than posterior one; the younger the individual, the more similar the two chambers in length. For instance, anterior chamber length 75% of posterior one's length in a 43.5 mm standard length individual, and 50% of the posterior length in a 60.6 mm standard length individual. Pneumatic duct placed at constriction of gas bladder. Peritoneum dark.

Tuberculation. Tubercles present on entire body (lateral, dorsal, and ventral sides of body; and dorsal and lateral sides of head). Each scale in seven or eight rows on breast bearing three to five tubercles at the apical margins. Ventral side of body with fewer tubercles than sides and dorsum. Each anterolateral scale bearing one or two rows of tubercles; one row close to apical margin, consisting of 4-6 tubercles; second row remote from the margin consisting of 1-3 tubercles. Each scale on the caudal peduncle bearing about 6 tubercles on its apical margin. Tuberculation on fins similar to that in *P. cum-berlandensis* (see below).

Coloration. A distinct lateral black stripe extending from anterior end of snout to caudal fin base, ending in a distinct round black spot at caudal base. Stripe uniformly narrow through its length. The mid-dorsal dark stripe extending from the nape to base of caudal fin, best developed pre-dorsally.

In some specimens, very few melanophores are evident below the lateral stripe and ventral side of body (including chin), except for a small area near base of pectoral fin. In other specimens, melanophores are present on entire body. Melanophores are concentrated along ventral edge of caudal peduncle, forming an elongated dark area on this region. All fins bearing numerous melanophores. On dorsal, anal, pelvic and pectoral fins, melanophores almost evenly distributed though the anterior rays have slightly more melanophores than the posterior rays in all fins. In breeding males, however, first four or five thick rays of pectoral fin bear more melanophores than the rest, so these thick rays look very dark, the other rays almost colorless.

Biology

The biology of *Phoxinus neogaeus* is poorly known. Scott & Crossman (1973) summarized the general biology of the species in Canada. Stasiak (1978) studied reproductive biology in Minnesota. Other data are reported by Hoffman (1967) (parasites), Tyler (1966) (temperature tolerance), and Constantinescu et al. (1984) (behavior).

This minnow prefers cool bog ponds, streams, and small boggy creeks and lakes. Fish species associated include *Phoxinus eos*, *Pimephales promelas*, *Umbra limi*, *Culaea inconstans* in Minnesota (Stasiak 1978); *Phoxinus eos*, *Margariscus margarita*, and *Culaea inconstans* in Canada (Scott & Crossman 1973). Hybrids, *P. neogaeus* \times *eos*, are frequently found at some localities (Hubbs & Brown 1929, New 1962, Legendre 1970b, Stasiak 1978, Joswiak et al. 1982, Joswiak et al. 1985, Das & Nelson 1989, Goddard & Dawley 1990). Few data about food of this species are available. Scott & Crossman (1973) examined a few specimens and found that the summer diet of this species was composed mainly of insects, though some crustaceans and plankton were present. Protozoan parasites were observed in the species' diet, such as *Myxosoma parellipticoides* (Hoffman 1967).

The spawning season begins in late April, reaches its peak in early May, and concludes by end of May in Minnesota (Stasiak 1978). It is later in Canada. Spawning probably occurs in June in northern Ontario (Scott & Crossman 1973). Breeding behavior of *Phoxinus neogaeus* seems complicated: females and males leave a large school, then males stimulate females with pectoral fin placed under belly of females, and with tubercles rubbing against ventral side of the female. Fecundity of this minnow was estimated from 784 to 3060 eggs (Stasiak 1978).

Growth pattern (relationship between length and age) of both sexes was similar when fish were young (≤ 1 year). Females grow faster than males thereafter and have longer life spine. Six-year-old females and five-year-old males have been found (Stasiak 1978).

Distribution

This is one of the northernmost distributed species of *Phoxinus* in North America. It occurs widely in bog ponds, streams and lakes from the Arctic circle in Mackenzie River drainage (Canada) in northwest to St. Lawrence and Atlantic drainage (including New Brunswick, Maine, and New Hampshire) in the east, and Southern Quebec, northern New York State, north of lower Great Lakes to Michigan in the south (Scott & Crossman 1973, Stasiak 1980b). Isolated populations were found in South Dakota (Evermann & Cox 1896, Churchill & Over 1933), Nebraska, Colorado & Wyoming (Bailey & Allum 1962). Scott & Crossman (1973) and Stasiak (1980b) provided maps of the geographic distribution of this species in Canada and North America, respectively.

Comments

The genus name used for this species has had an interesting cycle history. It was originally described by Cope (in Günther 1868) as *Phoxinus neogaeus*. Fowler (1918) called it to *Leuciscus neogaeus*. Jordan (1924) proposed a new genus, *Pfrilles* with *Phoxinus neogaeus* as the type species. No ichthyologists considered it as a species of the *Chrosomus* to which *P. erythrogaster* belonged until Bailey (1951). Although Hubbs and Brown (1929)

discussed a close relationship between *Phoxinus* (*P. phoxinus* and *P. neogaeus*) and *Chrosomus*, Bailey (1951) first merged *P. neogaeus* and other North American *Phoxinus* species into the single genus *Chrosomus*. Banareescu (1964) considered *Chrosomus* a synonym of *Phoxinus*. Thus, through a long way of change, this minnow returned to its original genus *Phoxinus*. After Banareescu (1964), some ichthyologists used the name *Phoxinus neogaeus* (e.g., Mahy 1975c), others used *Pfrille neogaea* (e.g. Gasowska 1979), or *Chrosomus neogaeus* (e.g., Stasiak 1977) for this species. Most ichthyologists seem to agree to use name *Phoxinus neogaeus* for this dace since the early 1980s (e.g., Stasiak 1980). Because hybrids of *P. neogaeus* and *eos* have been found from many places, and hybrids are fertile (Legendre 1970b), some ichthyologists considered these two species sharing a close relationship (e.g., Scott & Crossman 1973), which is not supported by this publication.

Etymology

The epithet name of this species “*neogaeus*” means “new-world” (for neo- and -gaeus) (Nelson & Paetz 1992), referring the species as a New World species of *Phoxinus*.

Phoxinus cumberlandensis Starnes & Starnes, 1978

Synonymy

Chrosomus erythrogaster Rafinesque, 1820 – Jordan & Swain 1883: 248 (mis.id., based on color desc., Whitley County, Kentucky).

Phoxinus cumberlandensis Starnes & Starnes, 1978 – Starnes & Starnes 1978: 508, 509, 512, 513-515, tabs. 1-2, figs.1, 2A, 3A, 4 (orig. desc., Type locality: Cumberland River drainage of Kentucky and Tennessee); Joswiak et al. 1980: 914, tab.1, fig.1A (Chromosomes, Kentucky); Starnes & Starnes 1980a: 335, fig. p.335 (no figure number) (general review); Starnes & Starnes 1981: 360-362, 364-370, tab.1, figs.1-3 (biology, Upper Cumberland River); Warren 1981: 129, 132-133 (new record, eastern Kentucky); Böhlke 1984: 74 (type specimens in ANSP); Constantinescu et al. 1984: tab.1 (coloration and behavior comparison with other *Phoxinus* species); Starnes & Jenkins 1988: 517, 521, 526 (name); O’Bara 1990: 9, 10, 12, 13, tabs.1, 2 (new record and ecology, Upper Cumberland River); O’Bara 1991: (no page number, ecology and behavior).

Phoxinus sp. 1977 Starnes & Starnes 1977: 1-3, figs.1-3 (dist. and population status, Upper Cumberland River).

Material studied

Paratypes: ANSP 138365, 13 alch.; Eagle Creek at Kentucky 896, 3.4 km NE of Kentucky, 90 jct., McCreary County, Kentucky, USA; W.C. & L.B. Starnes; 29 May 1977. – USNM 217810, 85 alch.; Younas Creek at Gravel Road, 0.8 km west of US 25W, 10.7 Air km N W of Williamsburg, Whitley County, Kentucky, USA; W.C. Starnes & L.B. Starnes; 6 September 1976. – UT 44.1366, 5 alch.; Lawson Branch (tributary to Capu-

chin Creek) at gravel road 4.8 km SSW of Scott-Campbell-McCreary County line corner, Scott County, Tennessee, USA; W.C. & L.B. Starnes; 7 May 1977.

Other materials: KU 18934, 8 C&S; Youngs Creek, Whitley County, Kentucky, USA; W.C. Starnes & L.B. Starnes; 25 September 1977. – UT 44.3390, 3 alch.; Davis Branch, tributary to Little Yellow Creek, near US 25E, Cumberland Gap State Park, Bell County, Kentucky, USA; W.L. Pennington & J.R. Shute; 18 November, and 10 December 1985. – UT 44.3905, 3 alch.; Baird and Hatfield Creeks, Cambell County, Tennessee, USA; WAPORA, Inc., project 524; 7 March 1981. – UT 44.4000, 1 alch.; Long Branch, River mile 0.5, Bell County, Kentucky, USA; O'Bara and Swan; 8 November or 11 August 1984. – UT 44.4001, 8 alch.; Young's Creek, County road 204, Whitley County, Kentucky, USA; O'Bara and Swann; 9 October or 10 September 1984. – UT 44.4519, 1 alch.; Straight Creek, 2.9 rd mi. from Tenn. 90 on straight Creek Road, Claiborne County, Tennessee, USA; D.A., E.A., & M.A. Etnier, SE McLain, WW EVE; 23 April 1989.

Diagnosis (amended from Starnes & Starnes 1978)

A *Phoxinus* with one single wide black lateral stripe (two stripes in young) extending from anterior of nasal opening to the caudal fin base; no connection between the left and right stripes at anterior of snout; intestine elongate with six loops in adults; opercle elongated and narrow; epibranchials 2 and 4 bearing an elongate posterior process; epibranchial 5 with a deep broad concavity on its posterior margin; pharyngeal bone with a notch at its posterior limb; anterior process of basioccipital elongate; often displaying a head-down swimming attitude (Starnes & Starnes 1978).

Description (Tab.6)

A North American species of *Phoxinus* reaching about 60 mm standard length. Head short, its length 25% of standard length, its width 51% of its length. Snout short and blunt, its length 17% of head length, 101% of orbit length. Eye lateral on head, moderately large; orbit length 29% of the head length. Mouth small and slightly oblique; its gape not extending to below anterior margin of eye. Lower jaw shorter than upper one, and included by the latter.

Bony interorbital space wide, its length 101% of orbit length, and 32% of head length.

In young individuals (SL \leq 23.5 mm), axis of olfactory organ semi-round and located in anterior portion of organ, four primary lamellae placed around posterior margin of axis. In adults, axis elongate and located mesially extending from anterior to posterior parts of organ; ten primary lamellae present along lateral and mesial margin of axis. Melanophores present on primary lamellae and axis in most specimens.

Body moderately deep and slightly compressed. Maximum body depth 25% of standard length. Caudal peduncle high and relatively short, its depth 35% of its length.

Pectoral fin with 13-18 rays, 15 rays in most specimens. Pectoral fin round, its distal tip close to origin of pelvic fin in male; pectoral fin sharper, shorter, and not approaching to origin of the base of the pelvic fin in females. Pelvic fin with 7-9 rays, eight rays in most specimens; prepelvic length 47% of standard length.

Tab.6: Body proportions (%) of *Phoxinus cumberlandensis*. (ACGL: anterior chamber of gas bladder length; BD: body depth; BIW: bony interorbital width; CPD: caudal peduncle depth; CPL: caudal peduncle length; HD: head depth; HL: head length; HW: head width; IL: intestine length; Number: number of specimens; OL: orbit length; PCGL: posterior chamber of gas bladder length; PRDL: predorsal fin length; PRPL: prepelvic fin length; S: standard deviation; SL: standard length; SNL: snout length).

	HL/SL	HD/SL	BD/SL	CPL/SL	CPD/SL	PRDL/SL	PRPL/SL	IL/SL	HW/SL	HD/HL
Number	33	35	5	33	33	34	32	2	3	5
	24.0	12.0	24.0	22.2	22.0	50.0	39.0	14	2.9	12.0
Range	—	—	—	—	—	—	—	—	—	—
	30.0	17.0	26.5	29.1	29.0	63.0	50.0	31	8.9	16.0
Mean	25.0	15.0	25.2	26.0	26.0	54.0	47	0	230.9	13.0
S(±)	1.0	1.0	2.0	1.9	2.0	3.0	2.0	124.5	1.0	3.3
	OL/HL	HW/HL	SNL/HL	BIW/HL	BIW/OL	SNL/OL	PRDL/ PRPL	CPD/CPL	ACGL/ PCGL	
Number	31	33	33	33	34	34	34	31	4	
	22.1	45.8	14.0	28.0	74.2	76.2	92.9	29.5	55.0	
Range	—	—	—	—	—	—	—	—	—	
	35.3	56.3	20.8	38.0	116.7	133.3	122.3	43.0	70.0	
Mean	29.1	50.6	17.2	32.0	100.9	101.0	113.7	34.6	60.4	
S(±)	3.3	3.6	1.8	3.0	1.64	16.5	7.6	4.6	6.7	

Dorsal fin originating above base of pelvic fin, ending above anal fin origin; predorsal length 54% of standard length, and 114% of prepelvic length; with one or two procurent rays, eight rays. Anal fin small, with one procurent ray, seven or eight fin rays. Anal fin longer in females than in males. Caudal fin deeply forked, lobes nearly acute, with eight or nine dorsal procurent rays, seven or eight ventral procurent rays, and 19 (10+9) principal rays.

Scales small, especially on belly. Scales poorly-embedded or well embedded on sides, deeply embedded ventrally. Scales on the caudal peduncle less embedded than that the remaining body.

No cephalic line pore present in individuals less than 25 mm standard length. Left and right supratemporal canals short and far from each other, with six pores. Supraorbital canal broadly interrupted at different points, with 10 pores. Otic canal with five pores. Infraorbital canal with 13 pores. The preopercular canal with 12 pores. Mandibular canal with four pores.

Body lateral line varying from absent in young to complete in adults. Body lateral line straight in adults and extending from posterior of the opercle to base of the caudal fin. Lateral line interrupted in different places. Pored scales about 62.

Pharyngeal bone developed, pitted surface flat and wide. Pharyngeal teeth in one row, 5-5, occasionally 4-5, or 5-4. Teeth thin, elongate, and hooked at tip.

Vertebrae 37-39; precaudal vertebrae 20-21, caudal vertebrae 17-19.

Intestine long with complex loops, six loops in adults. Relative length of intestine increases as the fish grows, its length about 230% of standard length in adults. Gas bladder short and broad. Anterior chamber broad and round anteriorly, its posterior portion not much narrower than anterior portion; anterior chamber 60% of posterior chamber in length. Constriction elongated, pneumatic duct connecting with middle portion of constriction. Peritoneum dark in color.

Tuberculation. Dorsal, lateral and ventral sides of head bearing scattered small tubercles. Each breast scale bearing 4-5 tubercles at its apical margin (up to 12 on some scales). Each scale on the anterolateral body bearing 2-5 tubercles in one row located near the apical margin of the scale in most specimens; tubercles in two rows in a few specimens. Scales on upper part of the body sides (dorsal to lateral line) bearing better developed tubercles than scales on lower part of sides (ventral to lateral line). Tubercles on apical margin of caudal peduncle scale. Second to fifth pectoral fin rays bearing two rows of tubercles per ray on the dorsal side of the fin, the membrane between the rays also bearing a few tubercles; other fin rays and membrane on the dorsal side, and all rays and membranes on the ventral side, bearing fewer and smaller tubercles. Each pelvic ray bearing one row of tubercles dorsally, and a few tubercles ventrally. Tubercles on dorsal and anal fins small and uniserial. Tubercles absent on caudal fin.

Coloration. The most characteristic color pattern is a broad dark lateral stripe, extending from in front of anterior nasal opening to base of caudal fin. The left and the right lateral stripes are not connecting each other at the end of the snout. Young with two dark stripes that converge into one on the caudal peduncle. Females bearing less developed stripe than males. Body lateral line extends within the stripe. Numerous small black speckles randomly present dorsal to the stripe and on dorsum of body and head. Melanophores absent dorsally on tip of snout. Mid-dorsal stripe present, interrupted once or twice in the predorsal fin region, and the postdorsal fin region. No melanophores present ventral to lateral stripe and silver in color at ventrolateral sides of body and ventral side of head. A few melanophores present on some pectoral and anal rays, and all dorsal and caudal rays. Base of dorsal fin densely pigmented. Caudal fin darker than other fins. The coloration in life was described by Starnes & Starnes (1978).

Biology

The biology of *P. cumberlandensis* was studied by Starnes & Starnes (1978, 1981) and O'Bara (1990, 1991). The following information is abstracted and summarized from those publications.

P. cumberlandensis is restricted to small streams with cold and clear water. In Young's Creek of Kentucky where the dace was found, the water temperature is generally below 23°C. The dace also requires a ratio of riffle area to pool area 60:40 or below. Fish species associated with the *P. cumberlandensis* include *Semotilus atromaculatus*, *Rhinichthys atratulus*, *Camptostoma anomalum*, *Pimephales notatus*, *Catostomus commerso-*

ni, *Etheostoma kennicotti*, *Etheostoma sagitta*, and occasionally *Phoxinus erythrogaster*. Diet of *P. cumberlandensis* varies, mainly including sand (35%), algae (8.4%), invertebrates (4.6%), and some other unidentified organic materials (32.1%). Its diet differs from that of most sympatric species in that invertebrates occupy a very small portion of the whole diet (4.6%); whereas, in other species invertebrates comprise from about 50% (e.g., *Catostomus commersoni*), to almost 100% (e.g., *Etheostoma sagitta*, and *E. kennicotti*). However, its diet is similar to that of *Campostoma anomalum*, *Pimephales notatus*, and *Phoxinus erythrogaster*.

This dace spawns on nest of stoneroller, *Campostoma anomalum*. Its average fecundity is 1540 ova per female. *P. cumberlandensis* grows rapidly the first year, more slowly in the second and third years. Starnes & Starnes (1981) estimated the standard length of the species at the end of the first year as 35.4 mm, end of the second 54.3 mm, and the end of the third 65.5 mm for the dace from the Young's Creek in Kentucky. The life span of the fish was estimated to be 3 years.

Distribution

P. cumberlandensis is restricted to small streams of the upper Cumberland River basin in Kentucky and Tennessee, USA (Starnes & Starnes 1978). It has been found in 30 streams of the Cumberland River drainage (O'Bara 1990).

Comments

Starnes & Starnes (1978) considered *P. cumberlandensis* more closely related to *P. oreas* than to any other *Phoxinus* species, because these two species share similar-shaped opercle, long and complicated looped intestine, and nuptial coloration. Because of its restricted and isolated distribution, and habitat degradation resulting from human activities, mainly from coal mining, this dace is currently listed as a threatened species by the U.S. Fish and Wildlife Service. O'Bara (1990) reported it was apparent absent from eight creeks where it was found from 1979 to 1981.

Etymology

The epithet "*cumberlandensis*" derives from a combination of "Cumberland" and Latin suffix "-ensis" referring to the Cumberland River drainage where the species is endemic (Starnes & Starnes 1978).

Phoxinus tennesseensis Starnes & Jenkins, 1988

Synonymy

Chrosomus erythrogaster (Rafinesque) – Henshall 1889: 31 (Whiteside, Tennessee, mis. id.); Evermann & Hildebrand 1916: 443 (Roaring Fork, Tennessee, mis. id.); Evermann 1918: 339 (mis. id.); Fowler 1923: 9 (Holston, Vagiania, mis. id.); Fowler 1924: 391 (Holston, Vagiania, mis. id.); Fowler 1936: 111 (Hiwassee System, Tennessee, mis. id.).

Chrosomus oreas ssp. – Ross and Carico 1963: 12 (Pigeon System, Tennessee); Jenkins, Lachner & Schwartz 1972: 48, 98 (Tennessee River drainage); Stauffer et al. 1982: 35 (Tennessee River drainage); Starnes & Etnier 1986: 347 (Tennessee River drainage).

Leuciscus erythrogaster (Rafinesque) – Cope 1868: 241, 245, 247 (Middle Fork, Holston System, Vafiania, mis. id.).

Phoxinus erythrogaster (Rafinesque) – Hitch & Etnier 1974: 84 (Hiwassee System, Tennessee, mis. id.).

Phoxinus sp. – Hitch & Etnier 1974: 84 (Hiwassee System, Tennessee).

Phoxinus tennesseensis Starnes & Jenkins, 1988 – Starnes & Jenkins 1988: 517, 519, 523-527, tab.1, figs.1 a-c, 2b, 3 (orig. desc.; type locality: Little River System, Blount County, Tennessee); Schilling & Ryon 1993: 274 (reproductive biology, Tennessee).

Material studied

Paratypes: UT 44.992, 7 alch.; Tributary to Bear Creek at Tenn. 95, Anderson County, Tennessee, USA; D.A. Etnier, W.C. Starnes, G.A. Schuster, W. Scraw, J. Lowa, & Adams; 1 December 1974. – ANSP 134735, 12 alch.; Clinch River system, tributary to east fork Polar Creek at Tenn. 95, 6.2 road mi. N of Clinch River, Roane County, Tennessee, USA; W.C. Starnes & L.B. Starnes; 15 February 1975. – USNM 216212, 15 alch.; Holston River system, Surgoinsville Creek, 1.2 road mi. north of US 11w (Surgoinsville), Hawkins County, Tennessee, USA; W.C. Starnes et al.; 30 November 1975.

Other Materials: UT 44.575, 2 alch.; Chestuee Creek at Nonaburg, McMinn county, Tennessee, USA; R. & S. Hitch; 25 October 1970. – UT 44.98, 2 alch.; Caney Branch, Citico Creek drainage, Nonroe County, Tennessee, USA; R. Tatum & J. Elier; 16 January 1967. – UT 44.5274, 4 alch.. and 2 C&S; Ocoee river system, Polk County, Tennessee, USA; W.L. Pennington et al.; 25 February 1991. – ANSP 22112, 2 alch.; South Fork, Holston River, Virginia, USA; E.D. Cope; date unknown.

Diagnosis (amended from Starnes & Jenkins 1988)

A *Phoxinus* with two lateral dark stripes, the lower one interrupted into two sections; elongate and complex coiled intestine; pneumatic duct connecting with posterior chamber of gas bladder; anterior margin of anterior ceratohyal concave; medial ramus of tripus robust and broad.

Description (Tab.7)

A North American species of *Phoxinus* with maximum standard length of 60 mm. Head large, broad, and robust, its length 25%, its width 61% of standard length. Snout short, its length 27% of head length, 100% of orbit length. Eye lateral on head, moderately large; orbit diameter 30% of head length. Mouth small, subterminal and oblique, its gape not extending below anterior margin of eye. Lower jaw shorter than upper one.

Bony interorbital space wide, its width 112% of orbit length, and 33% of head length. Anterior nasal opening larger than posterior one. Entire margin on anterior nasal opening erect. Posterior, lateral and mesial portions of posterior nasal opening's margin not erect.

Tab.7: Body proportions (%) of *Phoxinus tennesseensis*. (ACGL: anterior chamber of gas bladder length; BD: body depth; BIW: bony interorbital width; CPD: caudal peduncle depth; CPL: caudal peduncle length; HD: head depth; HL: head length; HW: head width; IL: intestine length; Number: number of specimens; OL: orbit length; PCGL: posterior chamber of gas bladder length; PRDL: predorsal fin length; PRPL: prepelvic fin length; S: standard deviation; SL: standard length; SNL: snout length).

	HL/SL	HD/SL	BD/SL	CPL/SL	CPD/SL	PRDL/SL	PRPL/SL	IL/SL	HW/SL	HD/HL
Number	16	16	16	16	16	15	15	3	16	16
	22.5	13.7	17.5	22.5	8.0	51.6	43.3	210.0	11.7	55.2
Range	—	—	—	—	—	—	—	—	—	—
	26.7	17.1	24.1	27.2	11.5	56.2	50.7	22.0	13.7	63.2
Mean	25.3	15.5	20.4	26.1	9.6	54.2	47.9	215.2	13.0	61.3
S(±)	1.2	1.1	2.4	1.5	1.1	1.5	2.2	5.2	0.6	4.0

	OL/HL	HW/HL	SNL/HL	BIW/HL	BIW/OL	SNL/OL	PRDL/PRPL	CPD/CPL	ACGL/PCGL
Number	16	16	16	16	16	14	14	16	2
	26.7	50.5	18.3	28.4	84.4	74.1	109.0	29.5	58.0
Range	—	—	—	—	—	—	—	—	—
	40.0	55.1	33.3	36.8	122.9	115.6	123.2	44.8	62.0
Mean	29.5	51.5	27.3	32.5	111.9	100.3	114.0	37.1	60.0
S(±)	4.9	2.9	4.4	4.4	16.5	13.2	5.7	5.6	2.83

Morphology of olfactory organ changing less ontogenetically than in other *Phoxinus* species. Young individuals (25.6 mm or less standard length) with an elongate axis situated at middle portion of organ, and extending posteriorly; seven or eight primary lamellae present, without melanophores. Large specimens with axis similar to that in young, with about 11 primary lamellae, melanophores present in most primary lamellae, fewer melanophores present on axis.

Body stout, not strongly compressed, though its posterior part more compressed than the anterior part of body. Maximum depth 20% of standard length. Caudal peduncle length 26% of standard length, its depth 37% of its length.

Genital papilla slender and longer in female than in male; its posterior end close to origin of anal fin. Papilla bearing a skin fold, margin of genital orifice serrated in male, but not in female. Both male and female bearing a short process at posterior end of papilla, the process longer and sharper in male than in female.

Pectoral fin fan-like, sharp and elongate, with 15-17 rays. Pelvic fin originating in advance of dorsal fin origin; pelvic fins sharper and longer in female than in male, the posterior tip extending beyond anal fin's origin in female; posterior margin extending to (not beyond) anal origin in male; with eight rays.

Dorsal fin originates farther posteriorly than origin of pelvic fin; predorsal length 54% of standard length, and 114% of prepelvic length; with three procurent fin rays, eight fin

rays. Anal fin originated slightly behind insertion of dorsal fin; with two procurent rays, and eight rays. Caudal fin deeply forked, lobes sharp, with 4-8 dorsal procurent rays, four or five ventral procurent rays, and 19 (10+9) principal rays.

Scales well embedded, covering entire body. Scales at ventral part of body deeply embedded.

Left and right supratemporal canals widely separated from each other; five pores. Otic canal with eight pores. Supraorbital canal with 10 pores. Infraorbital canal with 15 pores. Preopercular canal with eight pores. Mandibular canal with three pores. Body lateral line pored scales 34, last pored scale located at the position of the posterior margin of the pectoral fin; no pored scales found in individuals smaller than 33 mm standard length.

Pharyngeal bone broad, its posterior limb straight; pitted surface broad with four to six major fossae. Pharyngeal teeth in one row, 5-5. Teeth elongate, slender, and hooked at tip (not or very slightly hooked in one or two teeth near the posterior limb).

Vertebrae 38 or 39; precaudal vertebrae 20, caudal vertebrae 18 or 19.

Intestine long, about six complex loops. Its length 215% of standard length.

Anterior chamber of gas bladder shorter than the elliptical posterior one. Former about 60% of the latter in length. Constriction of the gas bladder developed and elongated. Pneumatic duct connected with anterior portion of the posterior chamber. Peritoneum dark.

Tuberculation. Tubercles present on entire body and head, including their lateral, dorsal, and ventral sides. Dorsal part of snout more densely tuberculated than rest of head. Ventral side of head bearing fewer tubercles than rest of head. Each scale in five or six rows on the breast bearing four or five tubercles on its apical margin. Each scale on anterolateral side of body bearing one tubercle near the apical margin. Scales on posterolateral part of body, especially ventral part of the caudal peduncle, bearing four to six tubercles at apical margin; tubercles in this region more developed than that in other parts of body. Tuberculation on all fins similar to that in *Phoxinus phoxinus*.

Coloration. Two lateral stripes present at the sides of body. Lower stripe extending from anterior portion of snout to caudal fin base. In large individuals, lower stripe interrupted at a point dorsal to anal fin origin. In small individuals (less than 30 mm in standard length), the stripe is complete. A dark dorsal stripe extending from nape to caudal fin base without interruption; dorsal stripe more distinct in small individuals than in larger ones.

Numerous melanophores present on sides of body. Region dorsal to the upper lateral stripe darker than region ventral to stripe. Ventral part of body lacking melanophores, except at anal fin base, ventral caudal peduncle and pectoral fin base where few melanophores present. Dorsum and dorsolateral portion of head bearing numerous melanophores. Numerous spots present on area dorsal to the upper lateral stripe in some large individuals, especially in breeding males. Melanophores present on ventral aspect of head. Ventral side of head darker in breeding male than that in breeding female.

Biology

P. tennesseensis occurs in small rivers with fast current and low water temperature (seldom exceeding 20°C), as well as in sluggish ponds with fine gravel, sand and silt sub-

strate. The fish species found associated with *P. tennesseensis* include *Campostoma anomalum* and *Semotilus atromaculatus* (Starnes & Jenkins 1988, Schilling & Ryon 1993). Diet is not well known. The intestine of some contained mainly organic detritus, algae, and diatoms. Starnes & Jenkins (1988) estimated that diet of the species might be similar to that of *P. oreas* and *cumberlandensis* because of the similarity of the intestine in these three species.

P. tennesseensis may spawn over the nest of gravel-nest-building cyprinids, such as *Campostoma* and *Semotilus* which are normally found with this dace and generally in aggregations of eight to more than 100 individuals. The spawning season occurs from late April to middle June (Schilling & Ryon 1993).

Distribution

P. tennesseensis is restricted to small streams of the Upper Tennessee River drainage in Virginia and Tennessee (Starnes & Jenkins 1988; Schilling & Ryon 1993). Starnes & Jenkins (1988: fig.3) mapped the localities where the dace had been found.

Etymology

The epithet “*tennesseensis*” is a combination of Tennessee and the Latin suffix “-ensis” in reference to the type locality and endemism in the Tennessee River drainage (Starnes & Jenkins 1988).

Phoxinus oreas (Cope, 1868)

Synonymy

Chrosomus oreas Cope, 1868 – Cope 1868: 233, 234, pl 23, fig.7 (orig. desc.; type locality; head of Roanoke River, Montgomery County, Virginia); Jordan 1877: 71 (name); Fowler 1924: 391 (desc.); Hubbs & Brown 1929: 28 (tuberculation); Wiley & Collette 1970: 168 (name); Mahy 1975c: 618-634, tab.1, figs.1-3, 6, 8-12, 14-21 (osteology); Goswaska 1979: 373, 374, 379, 381, 383, 392, 399, 403, figs.6, 24, 32, 33, 39, 44, 50, 55, 62, 69, 82, 88 (osteology); Böhlke 1984: 85 (type specimens in ANSP).

Parchrosomus oreas (Cope) – Gasowska 1979: 404 (osteology and taxonomy).

Phoxinus erythrogaster oreas (Cope) – Mahy 1972: 729 (name); Mahy 1975c: 618, 640, fig.22 (osteology, taxonomy).

Phoxinus oreas (Cope) – Mahy 1972: 728 (name); Stauffer et al. 1975: 123, tab. 1 (dist., East River, West Virginia); Mahy 1975c: 617 (name); Hambrick 1977: 238-242, tab.1, fig.1 (Roanoke River, Virginia); Starnes & Starnes 1978 : 509, 513, 514, figs.2B, C (comparison with *Phoxinus cumberlandensis*); Joswiak 1980: 2, 3, 6, 7, 15, 17, 22, tabs 1, 2, 4, 5 , figs.1C, 2 (chromosome study); Joswiak et al. 1980: 914, tab.1, fig.1C (chromosome study, Virginia); Starnes & Starnes 1980c: 339, fig. on p. 339 (general review); Matthews & Styron 1981: 149, 150, 153, 155, tabs.1, 2, 3 (Physiology, Roanoke River, Virginia); Starnes & Starnes 1981: 362, 367 (name); Böhlke 1984: 85 (name); Starnes & Etnier 1986: tab.10.1 (dist., Tennessee River); Starnes & Jenkins 1988: 517, 519, 523-528, tab.1, fig.2a (comparison with *P. tennesseensis*); Mayden 1991: 260 (name).

Material studied

Paralectotypes: ANSP 4552, 14 alch.; Mountain streams forming the head of the Roanoke River, Montgomery County, Virginia, USA; E.D. Cope; August 1867.

Other materials: ANSP 46543, 18 alch.; tributary of James River, Midway Mills, Virginia, USA; E.R. Dunn; 15 November 1915. – KU 3254, 23 alch.; Pine Creek on Route 221, 2.8 mi. N.E. Floyd, Floyd County, Virginia, USA; R. Huffman, M.H. Ross & R.D. Ross; 4 May 1952. – KU 3259, 39 alch. and 8 C&S; Elliot Creek, tributary S. Rogers, Montgomery County, Virginia, USA; W. Davis, M.H. Ross & R.D. Ross; 13 April 1952. – KU 3265, 38 alch.; N. Fork Roanoke River at Route 11 bridge, Montgomery County – Roanoke County line, Virginia, USA; B. Stouth, T. Riggins & W.S. Davis; 17 May 1952. – KU 3275, 14 alch.; Catawa Creek, 6.6 mi. N. W. Salem on Route 311 (James River system), Roanoke county, Virginia, USA; E.C. Raney & R.D. Ross; 14 July 1954. – KU 22257, 22 alch.; Craig Creek at Va. Rout 621, Montgomery County, Virginia, USA; B.K. Wagner et al; 9 September 1987. – KU 22295, 35 alch.; Blackwater River at Rt. 641 bridge, Franklin County, Virginia, USA; B.K. Wagner et al.; 13 September 1987. – UT 44.239, 5 alch.; Elliot Creek at Rogers, Montgomery County, Virginia, USA; Ross; 20 May 1953. – UT 44.3524, 13 alch.; Crab Creek at 18, Alleghany County, North Carolina, USA; 21 May 1986; collector unknown; 1986. – UT 44.526, 45 alch.; Roanoke drainage, Falling River below bridge on Motrosa Farm, Campbell County, Virginia, USA; J. Striegel & S. Robertson; 1970.

Diagnosis (amended from Cope 1868)

A *Phoxinus* with side bearing one longitudinal stripe and 10 to 15 transverse bars. The lateral stripe interrupted or faded at middle of body, the transverse bars present dorsal to the lateral stripe. Ventral side of body from base of pectoral fin to anterior end of isthmus dark; lower jaw shorter than upper one, the former enclosed by the latter; very long intestine with about 10 loops, its length 278% of standard length; epibranchial 3 bearing a large notch and a long posterior process at its dorsoposterior margin; epibranchial 4 bearing a large notch at its posterior margin.

Description (Tab.8)

A North American species of *Phoxinus* with average standard length (adults) about 50 mm, maximum standard length 61 mm. Head moderately large, its length 25% and its width 58% of standard length. Snout length 34% of head length, and 100% of orbit length. Eye large; orbit length 28% of head length. Mouth subterminal, small and almost horizontal; its gape extending below anterior margin of eye. Lower jaw shorter than upper one.

Bony interorbital space wide, its width 119% of orbit length and 32% of head length. Anterior nasal opening elliptical and smaller than the semi-round posterior one.

Young individual (18.1 mm standard length) with axis of olfactory organ short and wide, not extending to middle portion of the organ, seven primary lamellae present; in adult (53.4 mm standard length), axis slender, elongate and extending posteriorly, 13 primary lamellae present. Gill rakers 8, short.

Tab.8: Body proportions (%) of *Phoxinus phoxinus*. (ACGL: anterior chamber of gas bladder length; BD: body depth; BIW: bony interorbital width; CPD: caudal peduncle depth; CPL: caudal peduncle length; HD: head depth; HL: head length; HW: head width; IL: intestine length; Number: number of specimens; OL: orbit length; PCGL: posterior chamber of gas bladder length; PRDL: predorsal fin length; PRPL: prepelvic fin length; S: standard deviation; SL: standard length; SNL: snout length).

	HL/SL	HD/SL	BD/SL	CPL/SL	CPD/SL	PRDL/SL	PRPL/SL	IL/SL	HW/SL	HD/HL
Number	15	15	15	15	15	15	13	2	15	15
	23.3	14.9	19.3	18.9	9.5	53.3	46.8	276.9	12.7	57.5
Range	—	—	—	—	—	—	—	—	—	—
	27.9	18.2	24.8	25.2	13.1	60.1	50.9	279.4	17.8	68.5
Mean	25.4	16.5	22.3	23.3	11.1	56.7	48.8	278.2	14.6	64.9
S(±)	1.2	1.0	3.2	1.8	1.1	2.3	2.1	1.8	1.3	4.1

	OL/HL	HW/HL	SNL/HL	BIW/HL	BIW/OL	SNL/OL	PRDL/PRPL	CPD/CPL	ACGL/PCGL
Number	14	15	15	15	15	15	13	15	4
	25.8	50.4	30.2	27.5	91.1	80.6	109.0	39.1	38.8
Range	—	—	—	—	—	—	—	—	—
	31.2	69.9	39.0	32.3	148.6	121.6	128.5	52.9	85.7
Mean	28.4	57.7	34.2	30.2	118.8	99.7	117.0	47.9	65.5
S(±)	2.6	4.7	2.6	2.7	16.1	12.9	5.2	5.2	5.0

Maximum depth of body 23% of standard length. Caudal peduncle short and high, its length 23%, its depth 48% of standard length.

Genital papilla small. In male, papilla slender with a posterior projection; margin of genital orifice serrated; ventral surface smooth without skin fold. In female, genital papilla short and broad without posterior projection; margin of genital orifice serrated.

Pectoral fin fan-like; sharper in female; with 13-16 rays, usually 14 or 15. Pelvic fin originates in advance of dorsal fin origin; prepelvic length 49% of standard length; pelvic rays usually eight, seven in two of the 16 specimens counted.

Dorsal fin originates posterior to pelvic fin origin, predorsal length 57% of standard length, 117% of prepelvic length; with two procurent rays and eight rays, occasionally seven (two of the 16 specimens counted with seven rays). Anal fin originates under or slightly behind insertion of dorsal fin, with one or two procurent rays and 7-8 rays, mostly eight, only one among 16 specimens with seven rays. Caudal fin shallowly forked, lobes round or somewhat acute; with 9-11 dorsal procurent rays, 7-10 ventral procurent rays, and 19 (10+9) principal rays.

Small individuals (≤ 20 mm standard length) lack cephalic lateral line pores. Left and right supratemporal canals short without connection between each other, with six pores. Otic canal with six pores. Supraorbital canal with an interruption, 10 pores. Infraorbital

canal without interruption, 14 pores. Preopercular canal extending to middle of preopercle, seven pores. Mandibular canal with five pores.

Body lateral line extending from dorsal to gill cover, gradually curving down to horizontal lateral stripe, and ending above the middle region of pectoral fin. Lateral line with one or two interruptions, 15 pored scales present.

Pharyngeal bone slender; pitted surface bearing about seven fossae; anterior limb long and slender, its anterior end flat and expanding; posterior limb straight. Pharyngeal teeth in one row, 5-5; teeth relatively short, hooked at tip.

Vertebrae 38-39; precaudal ones 20 or 21, caudal ones 18.

Intestine long, about 10 loops in adults, the most complex coiling pattern in *Phoxinus*. Its length 278% of standard length. This coiling type formed very early ontogenetically, as observed in specimens at about 18 mm standard length. Anterior chamber of gas bladder short, about 66% of posterior one in length. Pneumatic duct placed at the constriction. Peritoneum dark.

Tuberculation. Entire body, including lateral, dorsal, and ventral sides of body and head, bearing tubercles. Each scale of the six to eight rows of the breast scales (four rows observed in one specimen) bearing 3 or 4 tubercles in one row at apical margin of scale. Each anteroventral scale bearing fewer tubercles than each lateral scale; ventral side of the body between base of pectoral fin and the origin of anal fin lacking tubercles. Each scale at anterolateral body bearing one large tubercle; each scale on the posterior portion of body, especially on ventral side of caudal peduncle, bearing three or four tubercles in one row on its apical margin. Dorsal side of the second to fifth ray of pectoral fin bearing two rows of tubercles; other pectoral rays bearing smaller and fewer tubercles, no tubercles on interradi al membranes. Ventral side of pectoral fin bearing fewer and smaller tubercles than on the dorsal side. Ventral side of the pelvic fin bearing tubercles; fewer tubercles on the dorsal side than on the ventral one of the pelvic fin. Anal and dorsal fins bearing few tubercles. No tubercles present on caudal fin.

Coloration. One lateral dark stripe, and 10-15 transverse bars present on trunk. Lateral stripe ventral to transverse bars (without contacting the stripe). Lateral stripe uniform in width throughout its length. Stripe extends through eye, opercle, and along body, to end at base of caudal fin. No dark spots present at caudal fin base. Transverse bars short, almost evenly present at trunk from posterior to the opercle membrane's posterior margin to the caudal fin base. In some specimens, about 10 dark short bars cross body dorsum, but not connecting the lateral bars. A dorsal stripe from nape to dorsal side of caudal fin not present in these specimens. In other specimens, however, one dark dorsal stripe extending from nape to base of caudal fin, the "crossing stripe" mentioned above not present in these specimens. Numerous melanophores present dorsally to horizontal lateral stripe. No melanophores present ventrally to horizontal stripe, except anteroventral portion of body. Numerous melanophores at anteroventral part of body, from anterior portion of lower jaw to pectoral fin base. Anterior end of the lower jaw bearing more melanophores than rest of ventral side of head. All fins bearing melanophores. First four to five pectoral fin rays bearing more melanophores than other pectoral fin rays. In caudal, anal, and pelvic fins, melanophores almost evenly present on the fins.

Biology

P. oreas occurs in small to medium size rivers. It is present in cool to warm, rapidly to slowly flowing, clear to turbid environments with sandy to rocky bottom (Starnes & Starnes 1980C; Page & Burr 1991). Fish species associated with this dace include *Notropis cerasinus*, *N. ardens* (Raney 1947), *Semotilus atromaculatus*, *Clinostomus funduloides*, *Nocomis leptcephalus*, and *Rhinichthys atratulus* (Maurakis & Woolcott 1992). Hybrids of *P. oreas* x *Semotilus* have been reported (Hamtrick 1977, Maurakis & Woolcott 1992). The diet of *P. oreas* is unknown, but it was thought to be similar to that of *P. erythrogastrus* and *cumberlandensis* by Starnes & Starnes (1980c).

The spawning season of *P. oreas* is in spring and early summer, using the nest of *Nocomis*. Up to 30 males might share one single nest. In most cases, more than one male follows one female during spawning (Raney 1947).

Distribution

P. oreas occurs in a belt-like area in the mountains of eastern North America. It was found from Virginia in the north, to North Carolina in the south. This species is also present in upper Tennessee drainage of Virginia and Tennessee (Stauffer et al. 1975, Starnes & Starnes 1980, Jowswiak et al. 1980).

Etymology

The epithet *oreas* is a Latin word meaning "of the mountains". It probably was chosen to indicate the primary habitat of the species.

Phoxinus eos (Cope, 1862)

Synonymy

Chrosomus eos Cope, 1862 – Cope 1862: 523 (orig desc., type locality: Meshoppen Creek, Susquehanna County, Pennsylvania); Cope 1868: 233 (comparison with *P. oreas*); Cope 1869: 375, 391 (desc., dist., Pennsylvania); Jordan 1877: 71 (name); Jordan & Gilbert 1882: 154 (Susquehanna River, Pennsylvania); Jordan & Swain 1883: 248 (name); Jordan et al. 1930: 113 (east of the Alleghenies, north to the Susquehanna River, Pennsylvania); Toner 1933: 137 (name); Lindeborg 1941: 160 (Ontario, Canada); Hubbs & Lagler 1949: 57, 64, fig.131 (whole body) (Great Lakes region); Scott 1957: 161 (Canada); Underhill 1957: 13, 25, 28, map 7 (dist., Minnesota); Bailey & Allum 1962: 41-42, 120, tab. 9 (dist., South Dakota); New 1962: 147, 149, 151, tab.1, figs. 1-6 (external morphology); Phillips 1969a: 501, 506-509, tab.2B, 3-4, fig.2 (external morphology and variation, Minnesota); Legendre 1970b: 1167, 1172, 1174-1176, tab.I, figs.1-2, 4-6 (Mendelian, Canada); Eddy & Underhill 1974: 239, fig.74 (key); Mahy 1975c: 618-634, tab.1, figs.1-3, 6, 8-12, 14-22 (osteology); Settles & Hoyt 1978: 297 (name); Gaswoska 1979: 373, 381, 383, 392-393, figs.5, 19, 31, 38, 43, 49, 61, 81 (osteology); Böhlke 1984: 75 (type specimens in ANSP).

Chrosomus eos (Cope) – Woronecki 1969: 709-710 (dist., Prince Edward Island, Canada).
Phoxinus eos (Cope) – Legendre & Steven 1969: 913, tabs. 1-2 (chromosome 2N=50); Legendre 1970a: 325, 329, tabs.1-2 (numbers of vertebrae); Mahy 1972: 728 (taxonomic status); Mahy 1975c: 617, 635-639 (taxonomic status); Starnes & Starnes 1978: 509, 513 (name); Joswiak 1980: 2, 3, 5-7, 15, 17-22, tabs.2-5, fig.2 (chromosomes); Joswiak et al. 1980: 913 (name); Stasiak 1980a: 336, figs. p.336 (no figure number) (general review); Starnes & Starnes 1981: 362 (name); Joswiak & Moore 1982: 399-400, fig.1 (discriminant analysis); Joswiak et al. 1982: 968, 972, tab.1 (external morphology); Cooper 1983: 112, 113, fig. p.113 (dist., Pennsylvania); Constantinescu et al. 1984: 286, tab.1 (coloration and behavior comparison with other *Phoxinus* species); Howes 1985: 71 (name); Coad 1987: 45 (dist., Ottawa, Canada); Dawley & Goddard 1988: 649-657, tab.1 (chromosomes); Harbicht et al. 1988: 475, tab.2, fig.2 (new records, Manitoba, Canada); Naud & Magnan 1988: 1249, figs.1, 2 (food and migration); Starnes & Jenkins 1988: 517 (name); Das & Nelson 1989: 579, 581-583, figs.1A, 2 (Alberta, Canada); Goddard et al. 1989: 268, 271-277, fig.1, Appendix (chromosomes); Goddard & Dawley 1990: 1052-1063, tab. 1 (New Hampshire); Dawley et al. 1991: 275-182 (chromosomes); Mayden 1991: 260 (name); Nelson & Paetz 1992: 151, 153, 154, fig. p.151, map. 12.8 (dist., Alberta, Canada).
Phoxinus erythrogaster eos (Cope) – Jordan & Evermann 1896: 244 (name); Fowler 1908: 520 (Pennsylvania); Mahy 1972: 729 (taxonomic status); Mahy 1975c: 618, 839, fig.22 (taxonomic status).

Material studied

Paratypes: ANSP 22117, 2 alch.; Meshoppen Creek, Susquehanna County, Pennsylvania, USA; E.D. Cope; September 1861.

Other Specimens: AMNH 21741sw, 2 C&S; Poce River, Charlie Lake, British Columbia, Canada; Lindsey & Larkin; 12 August 1954. – AMNH 42403, 6 alch.; Mettawee Creek just west of Raceville, Washington County, New York, USA; C.L. Smith et al.; 1 June 1979. – ANSP 70840, 25 alch.; Beaver Pond, Mount Desert, Main, USA; H.W. Fowler; 3 July 1940. – ANSP 71725, 1 alch.; Buffalo Lake, Buffalo, Minnesota, USA; J. Boehlke; 29 September 1945. – CAS (SU) 36992, 23 alch.; near Morse's Line, about on Canada border, Franklin County, Vermont, USA; L. Babbitt & A. Daugherty; 14 September 1941. – KU 1169, 4 alch.; Pond in Wilderness Park, Emmet County, Michigan, USA; U.B.S. Ichthyology Class; 24 July 1946. – KU 2130, 1 alch.; French River, St. Louis County, Minnesota, USA; collector unknown; 26 Aug 1946. – KU 8524, 13 alch.; Snake River, Cherry County, Nebraska, USA; R. Reckham; 21 August 1963. – KU 10316, 16 alch. and 2 C&S; Mississippi River at Itaska State Park, Clearwater County, Minnesota, USA; G.L. Phillips & C.E. Judd; 20 June 1965. – KU 11335, 31 alch. and 2 C&S; Seney National Wildlife Refuge, Schoolcraft County, Michigan, USA; W.L. Pflieger, 31 August 1958. – KU 12255, 30 alch. and 10 C&S; Small stream immediately below outlet of Spring Lake, west side of County road E., Sawyer County, Wisconsin, USA; F.B. Cross & W. Ayers; 25 July 1967. – UT 44.2889, 33 alch.; Crow Wing River, gravel road at outlet of 5th Crow Wing, Hubbard County, Minnesota, USA; D.A. & M.A. Etnier, W.C. & L.B. Starnes; 20 June 1982.

Diagnosis (amended from Cope 1862)

A *Phoxinus* with small mouth, its gape not reaching below anterior margin of eye; two lateral dark stripes present, the lower one more developed than the upper; no dark spots on dorsal part of trunk; axis of olfactory organ long and narrow; nasal bone expanded, triangular in shape; nasal portion of supraorbital canal running along lateral portion of nasal bone; hyoid foramen formed by ventral hypohyal alone; urohyal base bearing a process at the posterior margin; basibranchial 4 present as a cartilage; interopercle with round posterior margin.

Description (Tab.9)

A North American species of *Phoxinus* with average standard length about 50 mm (adults), maximum 61 mm (Stasiak 1980a). Head moderately large, its length 27%, its width 55%, and its depth 22% of standard length. Snout short; its length 24% of head length, 83% of orbit length. Eye large, lateral on head; orbit length 30% of head length. Mouth terminal, small and oblique. Lower jaw slightly shorter than upper one.

Bony interorbital space wide, its width 118% of orbit length, 35% of head length.

Young individual (26.4 mm standard length) with short and broad axis of olfactory organ, the axis not reaching to middle of organ, seven primary lamellae present; adult individu-

Tab.9: Body proportions (%) of *Phoxinus eos*. (ACGL: anterior chamber of gas bladder length; BD: body depth; BIW: bony interorbital width; CPD: caudal peduncle depth; CPL: caudal peduncle length; HD: head depth; HL: head length; HW: head width; IL: intestine length; Number: number of specimens; OL: orbit length; PCGL: posterior chamber of gas bladder length; PRDL: predorsal fin length; PRPL: prepelvic fin length; S: standard deviation; SL: standard length; SNL: snout length).

	HL/SL	HD/SL	BD/SL	CPL/SL	CPD/SL	PRDL/SL	PRPL/SL	IL/SL	HW/SL	HD/HL
Number	16	15	15	15	16	16	16	4	16	16
	25.1	15.5	18.2	22.7	8.2	55.3	47.4	131.0	11.4	55.9
Range	—	—	—	—	—	—	—	—	—	—
	29.3	19.6	26.1	27.9	12.5	61.1	53.0	14.0	17.5	67.6
Mean	26.7	21.5	16.4	25.2	10.6	55.6	51.4	134.8	14.5	61.8
S(±)	1.4	1.1	2.4	1.8	1.1	5.7	2.5	4.4	1.5	5.4
	OL/HL	HW/HL	SNL/HL	BIW/HL	BIW/OL	SNL/OL	PRDL/PRPL	CPD/CPL	ACGL/PCGL	
Number	16	16	16	16	16	15	15	15		4
	28.3	43.4	20.5	30.8	108.0	72.0	98.3	3.6	5	62.5
Range	—	—	—	—	—	—	—	—	—	—
	35.6	62.4	27.6	41.0	146.7	100.0	119.1	51.4		68.3
Mean	29.8	54.7	23.8	34.8	118.3	82.5	111.2	43.2		65.1
S(±)	3.5	6.9	1.9	3.2	14.9	9.9	6.1	5.1		2.55

al (45.0 mm standard length) with a slender, elongated axis extending posteriorly, and 10 primary lamellae.

Body elongate, round in cross section. Maximum depth of body 16% of standard length. Caudal peduncle short and high, its length 25%, its depth 43% of standard length.

Pectoral fin fan-like, sharper in female than in male, 13-16 fin rays, 14 or 15 rays in most specimens studied. Pelvic fin originates in advance of dorsal fin origin; prepelvic length 51% of standard length; rays usually eight, seven in two among 16 specimens counted.

Dorsal fin originates posteriorly to origin of pelvic fin, predorsal length 111% of prepelvic length, with two procurent rays and eight rays, rarely seven (two of the 16 specimens counted). Anal fin originates under or slightly behind the insertion of dorsal fin; with two procurent rays eight, rarely seven (one among 16 specimens counted). Caudal fin shallowly forked, lobes round; with 8-12 dorsal procurent rays, 7-9 ventral procurent rays, 19 (10+9) principal rays.

Supratemporal canal short, without connection between the left and right ones, with six pores. Otic canal, with six pores, connecting with infraorbital canal and body lateral line; however, in a few specimens, no connection between otic canal and body lateral line present. Supraorbital canal with 10 pores. Infraorbital canal without interruption, 14 pores. Preopercular canal extending to middle portion of preopercle; with seven pores. Mandibular canal with interruption, not connecting with preopercular canal, five pores.

Body lateral line extending from dorsal to gill cover, curving down to ventral lateral stripe, and ending at position of middle of pectoral fin. Lateral line interrupted in a few places, most with one or two interruptions. Lateral line pored scales about 17.

Pharyngeal bone short, posterior limb bent; pitted surface bearing two large, elongate fossae; end of anterior limb bearing a notch. Pharyngeal teeth in one row, 5-5, 5-3, or 5-4; teeth elongate, hooked at tip. Gill rakers 8, short.

Vertebrae 37-39; precaudal vertebrae 20-21, caudal vertebrae 17-18.

Intestine long, with complex coils; its length 135% of standard length. Anterior chamber of the gas bladder short, 65% of posterior chamber in length. Pneumatic duct placed at the constriction of the gas bladder. Peritoneum dark.

Tuberculation. Tubercles present on whole body, including lateral, dorsal, and ventral sides, dorsal and lateral sides of head, snout and chin. Each scale in 5-7 rows on breast bearing a few tubercles at its apical margin. Scales on the ventral side other than the breast scales bearing fewer tubercles than scales on sides. Each scale on the anterolateral body bearing one or two rows of tubercles: one row near apical margin, and composed of two or three tubercles; and another row close to center of scale, consisting of one to three tubercles. Tuberculation of pectoral, pelvic, dorsal and anal fins similar to that in *Phoxinus cumberlandensis*. No tubercles on caudal fin.

Coloration. Two dark lateral stripes present on sides. Lower lateral stripe more developed than upper one, and extending from anterior end of snout, through eye, gill cover, and along side to terminate in a black spot at caudal fin base. Stripe almost equal in width throughout its length. Upper lateral stripe shorter than lower one, and interrupted into a series of spots behind dorsal fin origin; or the whole stripe broken down to large speck-

les. Upper lateral stripe beginning dorsally to dorsoposterior margin of opercle, extending almost parallel to lower stripe, and terminating on posterior part of caudal peduncle. A dark mid-dorsal stripe begins at nape and ends at dorsal side of caudal fin base. Dorsal stripe behind insertion of dorsal fin narrower than anterior to dorsal fin origin. Dorsal stripe not evident in specimens less than 25 mm standard length, but lateral stripes occur in these small individuals.

No melanophores present at chin, except on anteroventral side of lower jaw, which bears dense melanophores. Numerous melanophores present dorsal to upper lateral stripe, and on area between upper and lower lateral stripes. No melanophores present ventral to lower lateral stripe, except in a small area near pectoral fin base, and on ventral edge of caudal peduncle.

Numerous melanophores present on fins. First four or five pectoral rays bearing more melanophores than other rays, especially in breeding males. Melanophores almost evenly present on pelvic, anal, and caudal fins. On dorsal fin, base bearing more melanophores than other portions of fin. A black spot present at caudal fin base.

Biology

Biology of *Phoxinus eos* has been studied by numerous ichthyologists from the 1930's to the 1980's though it is still not well known. Cooper (1935) and Hubbs & Cooper (1936) studied the reproductive behavior; Tyler (1966) studied lethal temperature; Scott & Crossman (1973), Stasiak (1978), and Cooper (1983) studied the general biology of the species. The following description is a summary of those publications.

P. eos occurs in bog ponds, lakes and creeks, but prefers quiet water (Cooper 1983). The fish species found associated with *P. eos* include *P. neogaeus*, *Pimephales promelas*, *Umbra limi*, and *Culaea inconstans* (Stasiak 1978). Hybrids of *P. eos* x *P. neogaeus* are common in localities; however, for some reasons, only one parent species was found in these localities (Hubbs & Brown 1929, New 1962, Legendre 1970b, Stasiak 1979, Joswiak, Stasiak & Moore 1982, Das & Nelson 1989, Goddard & Dawley 1990).

Food of *P. eos* is composed of algae, zooplankton and aquatic insects (Scott & Crossman 1973; Cooper 1983). Cooper (1935) reported that the adult dace was observed eating small-mouth bass fry.

Maturity of the species is reached in the second summer of life (Cooper 1983). Spawning begins in spring or early summer. Cooper (1935) and Hubbs & Cooper (1935) described that spawning activity occurs from late May to August in Michigan. Females with large eggs were caught in August by McPhail & Lindsey (1970). Hubbs & Cooper (1935) suggested some females might spawn at least twice in a single summer season. Cooper (1935) described a complicated reproductive behavior of *P. eos*.

Distribution

Stasiak (1980a) compiled the distribution data, indicating the range from Nova Scotia and Prince Edward Island (Canada), the St. Lawrence basin, and Atlantic drainage of New England, west to Peace-Mackenzie drainage in British Columbia and Northwest Territories, South to upper Missouri River drainage in the Great Plains.

Etymology

The epithet “*eos*” is a Latin word, meaning “down”, or “sunrise”. It might refer to the color pattern of the breeding males (Nelson & Paetz 1992).

Phoxinus erythrogaster (Rafinesque, 1820a)

Synonymy

Chrosomus eos (Cope) – Underhill 1957: map 7 (mis.id., Messota; based on Phillips 1968).
Chrosomus erythrogaster (Rafinesque, 1820) – Rafinesque 1820a: 237 (name); Fowler 1904: 244 (dist. Rogers, Arkansas); Fowler 1908: 519 (Pennsylvania); Toner 1933: 137 (name); Koster 1939: 203, 205-206 (behavior); Jennings 1942: 365 (Kansas); Hass 1943: 162 (Illinois); Harlan & Speaker 1951: 75, 192, 216, pl.14 (whole body) (Mississippi River drainage in Iowa); Hubbs & Bailey 1951: 145, 148-151, tabs.I, II (Illinois); Underhill 1957: 13, 25, 29, map 7 (Minnesota); Minckley 1959: 419, 436, tab. 3 (Kansas); Cross & Minckley 1960: 3-4, 6-7, tabs.1-2 (Kansas); Cross 1967: 70, 81-83 (Kansas); Phillips & Etnier 1969: 96, 97, tab.1 (Minnesota); Phillips 1969b: 99, 101, 104, 106-108, tabs.1-3 (diet, Minnesota); Phillips 1969c: 524-525, tab.1 (Fecundity, Dodge County, Minnesota); Stasiak 1972: 3, 34, 43 (name); Mahy 1975c: 617-634, tab.1, figs.1-3, 6, 8-21 (osteology); Freeze & Rayburn 1977: 97 (dist.: Kentucky).

Chrosomus erythrogaster Rafinesque, 1820 – Rafinesque 1820b: 48 (name); Cope 1862: 523 (comparison with *Phoxinus eos*); Cope 1864: 281 (comparison with *P. neogaeus*); Cope 1869: 375, 390-391, fig. (pharyngeal bone and teeth), (desc., dist., Pennsylvania); Jordan & Swain 1883: 248 (Whitley County, Kentucky); Jordan & Evermann 1896: 244 (dist.: New Brunswick to Ohio, Michigan, Iowa, and Northern Alabama); Rafinesque 1899: 102 (name); Smith 1908: 9, figs.1-3 (spawning behavior, Illinois); Cockerell & Callaway 1909: 122 (scales); Forbes & Richardson 1920: 112, 113, 114, fig. (dist., Illinois); Hankinson 1923: 30 (New York); Fowler 1924: 391 (desc., dist., Holston River, Virginia; Illinois; Miami River, Indiana; Delhi, Iowa; Marshfield, Missouri and Rogers, Arkansas); Hubbs & Brown 1929: 28, 29 (dist., Ontario, Canada); Jordan et al. 1930: 113 (dist.: New Brunswick to Ohio, Wisconsin, Colorado and Northern Alabama); Welter 1938: 68 (Kentucky); Hubbs & Lagler 1949: 57, 64, fig. p.132 (whole body) (dist., Great Lakes region); Hill & Jensen 1968: 55, tabs.1, 2, fig.1 (external morphology, Oklahoma); Phillips 1969a: 501, 506-507, tabs.2A, 4, fig.2 (morphology and variation, Minnesota); Wiley & Collette 1970: 168 (name); Hubbs & Echelle 1972: 150 (Arkansas System, New Mexico); Greenfield et al. 1973: 54-59, tabs.1-3, figs.1-5, 7 (morphology); Eddy & Underhill 1974: 238, 239, figs.73 (whole body), 74 (head); Settle & Hoyt 1978: 290, 295, tab.1, figs.1, 2 (reproductive biology, Kentucky); Gasowska 1979: 373-374, 381, 383, 392, 399-400, 402, fig.4, 18, 30, 54, 76, 80, pl.1 fig.5 (osteology).

Chrosomus erythrogaster erythrogaster Rafinesque – 1951 Bailey 1951: 193, 216 (Iowa).

Chrosomus pyrrhogaster Jordan – Jordan 1877a: 71 (North Indiana); Mahy : 618 (name).

Leuciscus erythrogaster (Rafinesque) – Günther 1868: 247 (desc., dist., Ohio, Michigan).

Luxilus erythrogaster Rafinesque, 1820 – Rafinesque 1820a: 237 (orig. desc.; type loca-

lity: Kentucky River, Kentucky). [The Kentucky River might be a small tributary (Starnes & Starnes 1980b).]

Phoxinus erythrogaster (Rafinesque) – Phillips 1968b: 565 (new records, Missouri River, Minnesota); Pflieger 1971: 331, map 33 (dist., Ozark and Lincoln county, Missouri); Mahy 1972: 728 (name); Cross & Collins 1975: 47, fig. p.47, map p.47 (dist., Kansas); Pflieger 1975: 97, 132, map p.132 (dist. Missouri); Mahy 1975c: 635-639, fig.23A (taxonomic status); Frazier & Beadles 1977: 39 (dist., Stone County, Arkansas); Starnes & Starnes 1977: 2 (dist., Upper Cumberland River); Starnes & Starnes 1978: 508, 512-513, 515, figs.2B, 3C (comparison with *P. cumberlandensis*); Smith 1979: 130, 131, figs. p.130 (whole body), and 131 (dist. map) (northern Illinois); Joswiak 1980: ii, 2-3, 5-6, 13, 15-20, 22, tabs.2, 4-5, fig.2 (chromosome); Joswiak et al. 1980: 914 (name); Starnes & Starnes 1980b: 337, fig. and map p.337 (general review); Starnes & Starnes 1981: 362, 365-368 (name); Trautman 1981: 306-308, fig.53 (whole body), map 53 (dist., Ohio); Joswiak & Moore 1982: 398-400, fig.1 (discriminant analysis using Phillips' 1969 data); Cooper 1983: 112-114, fig. and map p.113 (Pennsylvania); Constantinescu et al. 1984: tab.1 (coloration, behavior, and comparison with other *Phoxinus* species); Robinson & Buchanan 1984: 245, 246, figs. p.245, 246 (White, Black, and Illinois Rivers, northern Arkansas); Howes 1985: 57-72, figs.1B and D, 2C, 7D (systematics); Starnes & Etnier 1986: tab.10.1 (Tennessee River, Cumberland River); Cross & Moss 1987: tab. 20.1, 20.3 (Kansas); Starnes & Jenkins 1988: 517, 524, 525, 528 (name); Mayden 1989: 17, 33, 141 (name); Mayden 1991: 260 (name); Hearnald (year unknown): 90 (name).

Phoxinus erythrogaster erythrogaster (Rafinesque) – Mahy 1972: 728 (osteology); Mahy 1975c: 618, 640, fig.22 (taxonomic status).

Material studied

AMNH 21743sw, 3 C&S; White Eyes Creek, Monroe Township, Muskingum County, Ohio, USA; C.L. Smith et al.; 11 August 1963. – AMNH 42937sw, 2C&S; Deep Creek at Rt. I-70, Wabaunsee County, Kansas, USA; R. Irwin; 7 June 1966. – AMNH 52488, 10 alch.; White Eyes Creek, Monroe Township, Muskingum County, Ohio, USA; C.L. Smith et al.; 11 August 1963. – ANSP 4182, 1 alch.; Kiskiminitas River, western Pennsylvania, Pennsylvania; E.D. Cope; date unknown. – ANSP 5479, 4 alch.; Miami River, Indiana, USA; E.D. Cope; date unknown. – ANSP 54567, 6 alch.; Near Bear Creek, Allandale, Ontario, Canada; G. & E. Johns and J.G. Carison; 31 July 1927. – ANSP 83178, 40 alch.; Indian Creek at Walnut Hill, Lee County, Virginia, USA; F.G. Thompson; 27 September 1953. – ANSP 84333, 2 alch.; Franmlin Twp., Tributary North Branch of Salt Creek, 3.5 mi. East of Moreland, Wayne County, Ohio, USA; F.G. Thompson & Maly; 5 January 1953. – ANSP 84345, 13 alch.; Wayne Twp., 1.25 mi. Northeast of Wayne, Ashtabula County, Ohio, USA; F.G. Thompson; 18 October 1953. – ANSP 147537, Red River at mouth of first tributary below Rt. 77 bridge, Powell-Menifee County; Kentucky, USA; R.J. Horwitz; 18 April 1981. – CAS (SU) 05359, 28 alch.; Albany Branch, Clinton County, Kentucky, USA; U.S. fish Commission; date unknown. – KU 5773, 4 C&S; Pigeon Creek, Dent County, Missouri, USA; D.A. Distler; 19 June 1960. – KU 7300, 20 alch.; Pecatonica River, Sec. 13, T5N, R1E, Iowa County, Wisconsin, USA; F.B. Cross & R.

Poff; 14 June 1962. – KU 7606, 1 C&S; Pigeon Creek, Sec. 7-8, T32N R7W, Dent County, Missouri, USA; F.B. Cross et al.; 7 April 1963. – KU 10629, 12 alch. and 2 C&S; Possum Trot Creek, 3.25 mi. NE Dillard, T35N, R2W, S16, Crawford County, Missouri, USA; W.L. Pflieger & S. Cliburn; 18 July 1963. – KU 12495, 3 C&S; North Fork White River, Sec. 7, T27N, R11W, Douglas County, Missouri, USA; G.R. Smith et al.; 24 May 1967. – KU 12496, 5 C&S; North Fork White River, Sec. 7, T27N, R11W, Douglas County, Missouri, USA; G.R. Smith et al.; 24 May 1967. – KU 13198, 1 C&S; Deep Creek at Rt 70 crossing, Wabanusee County, Kansas; R. Irwin; 7 June 1966. – KU 22092, 12 alch.; Tryon Grove Road, Sec. 20, T46N, R8E, McHenry County, Illinois, USA; O.T. Gorman & M.G. Meyer; 26 July 1986. – KU uncat., about 70 alch. and 4 C&S; Barren Fork of Illinois River at Camp Egan (near Proctor), Adair County, Oklahoma, USA; W. Matthews & X. Chen; 27 April 1991.

Diagnosis (amended from Rafinesque 1820a)

A *Phoxinus* with two lateral stripes, the upper one interrupted on caudal peduncle; intestine elongate; pharyngeal teeth in one row; epural bone elongate.

Description (Tab.10)

A North American *Phoxinus* species with average standard length (adults) about 60 mm, maximum standard length up to 90 mm. Head large, broad, and robust, its length 25% and its width 52% of standard length. Eye lateral on head, moderately large, orbit length 26% of head length. Snout moderately elongated, its length 27% of head length, 102% of orbit length. Mouth small, slightly subterminal and oblique, its gape not extending to below anterior margin of eye. Lower jaw slightly shorter than upper one.

Bony interorbital space wide, its width 122% of orbit length, 32% of head length. Anterior nasal opening smaller and shorter than the elongated posterior one. Margin of anterior nasal opening erect, except its anterior portion; margin of posterior nasal opening not erect, except its anterior portion.

Young individuals (18.0 mm standard length or less) with axis of olfactory organ short and located at anterior margin of olfactory chamber, four primary lamellae present; larger individual (46.0 mm standard length or larger) with axis elongate and extending posteriorly, 12 primary lamellae present. Numerous melanophores present on primary lamellae in both young and adult specimens.

Body elongate, stout, not strongly compressed, caudal peduncle more compressed than anterior part of the body. Maximum depth of body 21% of standard length. Caudal peduncle length 24% of standard length, its depth 43% of its length.

In male, genital papilla small, surface smooth without skin fold. In female, genital papilla larger than that in male, its surface bearing a few skin folds. Posterior margin of papilla close to anal fin origin in both male and female.

Pectoral fin fan-like, sharper and smaller in female than in male. The distal tip of pectoral fin never reaching pelvic fin origin; with 13-17 rays, most with 15 or 16 rays. Pelvic fin originates in advance of dorsal fin origin, in anterior half of body, prepelvic fin length

Tab.10: Body proportions (%) of *Phoxinus erythrogaster*. (ACGL: anterior chamber of gas bladder length; BIW: bony interorbital width; CPD: caudal peduncle depth; CPL: caudal peduncle length; HD: body depth; HL: head length; HW: head width; IL: intestine length; Number: number of specimens measured; OL: orbital length; PCGL: posterior chamber of gas bladder length; PRDL: predorsal length; PRPL: prepelvic length; SL: standard length; S: standard deviation; SNL: snout length).

	HL/SL	HD/SL	BD/SL	CPL/SL	CPD/SL	PRDL/SL	PRPL/SL	IL/SL	HW/SL	HD/HL
Number	16	16	16	16	15	16	16	3	16	16
	21.1	14.0	16.8	19.7	8.2	51.7	44.0	170.0	11.1	55.1
Range	—	—	—	—	—	—	—	—	—	—
	26.2	16.5	25.4	25.6	11.3	57.0	49.3	21.0	14.4	72.2
Mean	24.8	15.3	21.1	24.2	10.2	55.1	47.3	193.3	12.6	62.4
S(±)	1.3	0.8	2.1	5.0	0.8	4.8	1.8	20.8	1.0	4.2
	OL/HL	HW/HL	SNL/HL	BIW/HL	BIW/OL	SNL/OL	PRDL/PRPL	CPD/CPL	ACGL/PCGL	
Number	16	16	16	16	16	16	16	16	3	
	20.3	47.1	25.5	26.8	100.0	87.9	107.6	36.4	67.0	
Range	—	—	—	—	—	—	—	—	—	
	30.6	61.1	32.5	34.3	132.3	135.5	117.5	47.2	73.0	
Mean	26.4	51.6	26.7	31.8	122.2	102.3	113.2	43.3	70.0	
S(±)	3.1	5.2	2.1	2.6	14.6	14.0	4.3	4.0	4.32	

47% of standard length; pelvic rays usually eight, one of 16 specimens counted with seven rays.

Dorsal fin originates posterior of origin of pelvic fin, in posterior half of body, predorsal length 55% of standard length, 113% of prepelvic length; procurent rays two, eight rays in all specimens. Anal fin originated slightly behind insertion of dorsal fin; procurent rays two; eight rays. Caudal fin deeply forked, lobes round; with nine or 10 dorsal procurent, nine or 10 ventral procurent rays, and 19 (10+9) principal rays.

Left and right supratemporal canals not connected, but close to each other in adults; with 16 pores. Otic canal connecting with infraorbital canal and lateral line; six pores. Supra-orbital canal with 11 pores. Infraorbital canal without interruption; 18 pores. Preopercular canal extending to middle portion of the preopercle, without branch; 10 pores. Mandibular canal without interruption and branch, and without connection with preopercular canal; with five pores.

In adults, body lateral line extending from dorsal of gill cover, gradually curving down to and following lower lateral stripe, ending near posterior margin of pelvic fin. Lateral line shorter in young than in adults. Lateral line uninterrupted in adults, but with one or two gaps in young individuals. Lateral line scales 43.

Pharyngeal bone well developed and robust, its pitted surface broad with three large fossae. Posterior limb short, strong, and bent anteriorly. Anterior limb slender, narrower posteriorly, and expanding at anterior end. Pharyngeal teeth in one row, 5-5. Teeth strong, hooked at tip.

Vertebrae 37; precaudal vertebrae 20, caudal vertebrae 17.

Intestine long, with about 3.5 loops. Its length 193% of standard length. Gas bladder broad and relatively short. Anterior chamber round at anterior end, and almost equal in width for whole chamber. Posterior chamber almost equal in width from anterior to posterior ends. Anterior chamber 70% of posterior chamber in length. Constriction short and broad. Pneumatic duct placed at middle of the constriction. Peritoneum dark.

Tuberculation. **Male** Whole head, including its dorsal, lateral, and ventral sides, bearing tubercles. Tubercles on head small and short. Dorsum of head bearing higher density of tubercles than rest of body. Each scale in 10 or 11 rows on the breast bearing two to four tubercles on its apical margin, forming comb-like edge. All tubercles in this region similar in size and shape. Dorsal, lateral, and ventral sides of the body bearing tubercles. Each scale bearing one or two small, short tubercles near center of the scale, except in ventrolateral portion of the caudal peduncle. Every scale on the ventrolateral part of the caudal peduncle bearing one row of four to six well-developed tubercles on apical margin.

All fins except caudal fin bearing tubercles. Pelvic, dorsal, and anal fins, and ventral side of the pectoral fin have few small, short tubercles on fin rays and membrane. On pectoral fin, dorsal side of the second to seventh fin rays bearing two rows of well developed, sharp tubercles on its distal portion, decreasing to one row proximally. Proximal one-third of pectoral fin without tubercles. Few small tubercles on interradial membrane of pectoral fin.

Female Females bearing very small tubercles, hardly descendible with naked eye. Anterior end of snout tuberculated. Entire lateral and ventral sides of body bearing tubercles. Each scale in these regions bearing one or two small tubercles near center of scale. Pectoral, pelvic, dorsal, and anal fins bearing few small tubercles on both membrane and rays.

Coloration. Two distinct lateral black stripes present on the flank. Lower one longer and broader than upper one. Lower lateral stripe extending uninterrupted from anterior end of snout to base of caudal fin; the stripe broader at middle portion of body. Upper lateral stripe originates dorsal to posterior margin of opercle, and extends to posterior portion of caudal peduncle, but not reaching caudal fin base. Upper lateral stripe almost equal in width along its length, but interrupted in its posterior portion, forming a series of dots. A few small speckles (smaller than pupil of eye) occur dorsal to the upper lateral stripe. In females, the lateral stripes narrower and fainter than that in males, especially upper lateral stripe. Body dorsum darker than flank, bearing a mid-dorsal dark stripe. Dorsal stripe originating at nape and extending to posterior end of body. In most specimens studied, the dorsal stripe is continuous posterior to dorsal fin, but is interrupted in three specimens. No melanophores on ventral side of the body, except the breast area in males bearing some melanophores. In female, lateral body, as a whole, paler than in male.

Head with numerous melanophores dorsally, diminishing laterally. Anterior end of snout bearing melanophores. Lower portion of lateral side of head without melanophores. Numerous melanophores along margin of lower jaw. Therefore, left and right lower lateral stripe on the body continuous as a black band crossing the anterior end of the snout and lower jaw. Numerous melanophores present on sides of body, except ventral to the lower lateral stripe. Area between upper and lower lateral stripes pale.

Melanophores present on all fins. On pectoral fin, rays bearing more melanophores than the membranes, the first ray darkest. The posterior three or four rays and membranes almost lacking melanophores. As a whole, distal part with more melanophores than proximal part. Pelvic fin-rays bearing more melanophores than membrane, and distal part bearing more melanophores than proximal part. Dorsal fin-rays and membrane bearing melanophores; all rays equally pigmented. Base of dorsal fin bearing more melanophores than rest of the fin, forming a black basal patch. All anal fin-rays and membrane, except the most posterior two rays and membrane, bearing melanophores. Caudal fin darkest of all fins. High density of melanophores on middle portion of caudal fin forms a slightly darker patch. A dark spot about size of pupil present at caudal fin base.

Biology

Phoxinus erythrogaster occurs in small, clear, and spring-fed streams (Cross 1967, Smith 1979, pers. obs.). This species prefers headwaters, and scarcity of the permanent springs might limit the distribution of the species in the Plains region (Cross 1967, Smith 1979). This dace can be in schools of a dozen to a few hundred individuals (Smith 1908). The fish species associated with *P. erythrogaster* include *Semotilus atromaculatus*, *Notropis cornutus*, *Campostoma anomalum*, *Rhinichthys* sp. and *Cottus* sp. (Smith 1908, Cross 1967). A few hybrids of *P. erythrogaster* with other species have been described, including *P. erythrogaster* \times *Luxilus cornutus* (Hubbs & Bailey 1951, Minckley 1959, Cross & Minckley 1960, Greenfield et al. 1973), *P. erythrogaster* \times *Campostoma anomalum* (Hubbs & Bailey 1951), *P. erythrogaster* \times *Notropis nubilus* (Phillips & Etnier 1969), *P. erythrogaster* \times *Semotilus atromaculatus* (Cross & Minckley 1960), and *P. erythrogaster* \times *Notropis pilsbryi* (Robinson & Miller 1972).

The diet of *P. erythrogaster* includes diatoms, algae, bits of macrophytes, and small aquatic insects (Forbes & Richardson 1920, Phillips 1969b, Cooper 1983). The dace obtains food by nibbling or sucking the surface slime from stone and other objects (Forbes & Richardson 1920).

The spawning season varies from April to June, depending on the locality: in northern population from late May to the mid-June, in southern population from April to June (Eddy & Underhill 1974, Settles & Hoyt 1978, Starnes & Starnes 1981). The fecundity was estimated from less than 700 (Settle & Hoyt 1978) to about 20,000 eggs (Phillips 1969c). The dace can be mature during the first year (Settles & Hoyt 1978, Smith 1979). According to Smith (1908), this species has a complex breeding behavior.

Distribution

P. erythrogaster occurs widely from Minnesota and western Pennsylvania, southward to Arkansas and Alabama (Starnes & Starnes 1980). Isolated populations occur on Crowley

Ridge in the Mississippi Embayment, and along the eastern rim of Mississippi floodplain in Mississippi (Hemphill 1957), and near Reelfoot Lake, Tennessee (Starnes & Starnes 1980). These are considered the relic populations (Starnes & Starnes 1980). In New Mexico and Colorado, isolated populations are present in the Arkansas River drainage (Koster 1957, Cross, pers. comm.). Starnes & Starnes (1980) summarized the distribution data and prepared a map showing the geographical distribution of the species.

Comments

No subspecies of this widely distributed species has been reported. Some local and regional intraspecific variation of the species was studied in Oklahoma by Hill & Jensen (1969), and elsewhere by Phillips (1968a, 1969a). The intraspecific variation seems not to be significant.

Smith (1979) considered *Oxygeneum pulverulentum* Forbes a synonym of *P. erythrogaster*. However, *O. pulverulentum* is a hybrid of *P. erythrogaster* x *Campostoma anomalum* (Hubbs & Bailey 1952).

Etymology

The epithet *erythrogaster* is a Greek word, meaning "red belly" (Pflieger 1975), referring to the ventral color of the breeding male.

ABSTRACT

Key Words: Cyprinidae, *Phoxinus*, Morphology, Osteology, Phylogeny, Taxonomy, Biogeography.

Phoxinus is a small sized genus of Cyprinidae and occurs in both North America and Eurasia. A detailed review on major literature related to *Phoxinus* showed that the definition, taxonomy, and composition of *Phoxinus* have changed since its first description by Rafinesque (1820a), due to the unclear phylogenetic relationships among *Phoxinus* and between *Phoxinus* and other minnow genera.

The phylogenetic relationships of *Phoxinus* and other related minnow genera at the base of the Chub clade were reevaluated based on 29 transformation series. The Hemitreman clade was recognized as a monophyletic group and supported by the anterior placement of the anterior anal pterygiophores. Eight genera are included in the Hemitreman clade, i.e., *Margariscus*, *Couesius*, *Semotilus*, *Hemitremia*, *Phoxinus*, *Eupallasella*, *Rhynchocypris*, and *Lagowskiella*, among which *Hemitremia* is the sistergroup of all other seven genera.

The non-osteological and osteological morphology and their variations were described and compared among *Phoxinus*, and between *Phoxinus* and the outgroups (i.e., *Eupallasella*, *Rhynchocypris*, and *Lagowskiella*). The monophyly of *Phoxinus* was supported by eight transformation series, such as the specific tuberculation on the breast scales in breeding

males, the presence of an anterior process of the basioccipital bone, and division of the preoperculomandibular canal. Nine species were recognized in *Phoxinus*, including *P. brachyurus*, *phoxinus*, *issykkulensis*, *neogaeus*, *tennesseensis*, *cumberlandensis*, *oreas*, *eos*, and *erythrogaster*.

Two-hundred and ten transformation series were analyzed and polarized based mainly on outgroup comparison to evaluate the phylogenetic relationships among species of *Phoxinus*. The phylogenetic relationships of the species within the genus *Phoxinus* were resolved based on the 210 transformation series by PAUP (v.3.0). In *Phoxinus*, two major groups were recognized as the *brachyurus*- and the *erythrogaster*-clade. The *brachyurus*-clade consists of the three Eurasian and one North American species: *P. brachyurus*, *issykkulensis*, *phoxinus*, and *neogaeus*. Members of the *erythrogaster*-clade are the other five North American species, i.e., *P. cumberlandensis*, *tennesseensis*, *oreas*, *eos*, and *erythrogaster*.

Three hypotheses on the geographic relationships of the freshwater fish faunae in North America and Eurasia were reviewed and compared. These are the "trans-Atlantic", the "old Pacific connection", and the "Bering land connection" dispersal hypotheses. None of these hypotheses could explain the geographic distribution of *Phoxinus*. A "Bering land connection" vicariant hypothesis was proposed here to interpret the genus' geographic distribution. The Bering land connection vicariant hypothesis proposed that the submergence of the Bering land bridge during the Miocene caused the speciation of the ancestor of *Phoxinus*, while the interruption of the bridge during the Pliocene split the ancestor of the *Phoxinus* species complex. This hypothesis was well supported by the alloelectrophoretic studies of Joswiak (1980). The speciation within the *erythrogaster*-clade and the *phoxinus* species pair might be due to some vicariant events and/or adaptation to the habitats.

LITERATURE CITED

- Agassiz, L. (1835): Description de quelques espèces de cyprins du lac de Neuchâtel, qui sont encore inconnues aux naturalistes. – Mém. Soc. Neuchâtel Sci. Nat. 1:33-48.
- (1850): Lake Superior: its physical character, vegetation, and animals, compared with those of other similar regions. Boston. 428 pp.
- (1854): Notices of a collection of fishes from the southern band of the Tennessee River, Alabama. – Amer. J. Sci. Arts., ser 2(17):353-365.
- Alexander, R.M. (1962): The structure of the Weberian apparatus in the Cyprini. – Proc. Zool. Soc. Lond. 139:451-473.
- (1966): The functions and mechanisms of the protrusile upper jaws of two species of cyprinid fish. – J. Zool. Lond. 149:188-296.
- Arratia, G., & H.-P. Schultze (1990): The urohyal: development and homology within Osteichthyans. – J. Morph. 203:247-282.
- (1991): Palatoquadrate and its ossification: development and homology within Osteichthyans. – J. Morph. 208:1-81.
- Bailey, R.M. (1951): A check-list of the fishes of Iowa, with keys for identification. In: J.R. Harlan & E.B. Speaker (eds.): Iowa Fish and Fishing: 186-237. State Conservation Commission, State of Iowa.
- Bailey, R.M., & M.O. Allum (1962): Fishes of South Dakota. – Misc. Pub. Univ. Mich. Mus. Zool. 119:1-125.
- Bailey, R.M., J.E. Fitch, E.S. Herald, E.A. Lachner, C.C. Lindey, C.R. Robins, & W.B. Scott (1970): A List of Common and Scientific Names of Fishes from the United States and Canada. – Amer. Fish. Soc. Spec. Publ. 6, Washington, D.C. (3rd ed.).
- Banarescu, P. (1960): Einige Fragen zur Herkunft und Verbreitung der Süßwasserfisch-Fauna der europäisch-mediterranen Unterregion. – Arch. Hydrobiol. 57:16-34.
- (1964): Fauna Republicii Populare Romine. Pisces -Osteichthyes. Bucuresti, Romine. – Editura Academiei Republicii Populare Romine.
- (1973): Some reconsideration on the zoogeography of the Euro-Mediterranean fresh-water fish fauna. – Rev. Rom. Biol. Zool. 18(4):257-264.
- (1989): Vicariant patterns and dispersal in European freshwater fishes. – Spixiana 12:91-103.
- Banarescu, P., & B.W. Coad (1991): Cyprinids of Eurasia. In: I.J. Winfield & J.S. Nelson (eds.): Cyprinid Fishes. Systematics, biology and exploitation: 127-155. – Chapman & Hall, London, New York, Tokyo, Melbourne, Madras.
- Banbura, J. (1985): The roach *Rutilus rutilus* (L.) and the minnow *Phoxinus phoxinus* (L.) without pectoral fins. – Przegląd Zool. 29:235-237.
- Beer, G.R. de. (1937): The Development of the Vertebrate Skull. – Oxford: Clarendon Press.
- Berg, L.S. (1906): Notes sur quelques espèces paléarctiques du genre *Phoxinus*. – St. Petersburg Ann. Mus. Zool. Acad. Sci. 11:196-213.
- (1908): (title unknown.) – Ezhegodnik Zoologicheskogo muzeya Akademi Nauk, XIII. 226 pp.

- (1912): Fauna de la Russie et des pays limitrophes. Poissons (Marsipobranchii et Pisces). Vol. III, Ostariophsi. Part I. – St. Petersburg.
- (1932): Les Poissons des Eaux Douces de L'U.R.S.S. et des Pays Limitrophes, 3rd ed., revue et augmentée. Part. I – Leningrad.
- (1949): Freshwater Fishes of the U.S.S.R and Adjacent Countries II. – Izdatel'stvo Akademii Nauk USSR, Moskva-Leningrad. (in Russian) (1964, English version, Smithsonian Instit. by Israel Program for Scientific Translations, Jerusalem).
- Berinke, L. (1968): The variance of *Phoxinus* population. – Ann. Hist. Nat. Mus. Hung., Budapest 60:275-284.
- Bogutskaya, N.G. (1987): Morphological characters of some groups of genera of the subfamily Leuciscinae. – J. Ichthyology 28(3):26-34.
- (1988a): The limits and morphological features of cyprinid subfamily Leuciscinae. – Proc. Zool. Inst. Leningrad, Syst. Morph. Ecol. Fishes 181:96-113.
- (1988b): Topography of the canals of the sensory system of cyprinoid fishes of the subfamilies of Leuciscinae, Xenocyprininae, and Cultrinae. – J. Ichthyology 28(3):367-382.
- (1989): Cyprinid infraorbital bones and the problems of "dermosphenoticum". – Proc. Zool. Institute, Leningrad, 201:29-43.
- (1990): Morphological principles of Leuciscinae, Cyprinidae: Communication I. – Vopr. Ikhtiol. 30(3):355-367.
- (1991): The morphological basis for the classification of cyprinid fishes (Leuciscinae, Cyprinidae). Communication 2. – J. Ichthyology 31:66-82.
- Böhlke, E.B. (1984): Catalog of type specimens in the ichthyological collection of the Academy of Natural Sciences of Philadelphia. – Acad. Nat. Sci. Philad. Spec. Publ. 14: i-viii + 1-246.
- Bond, C.E. (1979): Biology of Fishes. – W. B. Saunders Co. Philadelphia, London, Toronto.
- Boschung, H.T. (1980): *Hemitemia flammea* (Jordan & Gilbert). In: D.S. Lee, C.R. Gilbert, C.H. Hocutt, R.E. Jenkins, D.E. McAllister, & J.R. Stauffer, Jr. (eds.): Atlas of North American Freshwater Fishes: 173.. – North Carolina State Museum of Natural History, Raleigh, North Carolina.
- Briggs, J.C. (1979): Ostariophysian zoogeography: an alternative hypothesis. – Copeia 1:111-118.
- (1986): Introduction to the zoogeography of North American fishes. In: C.H. Hocutt & E.O. Wiley (eds.): The Zoogeography of North American Freshwater Fishes: 1-16. – John Wiley & Sons., New York, Chichester, Brisbane, Toronto, Singapore.
- Brown, J.H., & A.C. Gibson (1983): Biogeography. – The C. V. Mosby Company. St. Louis. Toronto. London.
- Buhan, P.J. (1972): The comparative osteology of the caudal skeleton of some North American minnows (Cyprinidae). – Amer. Midl. Nat. 88(2):484-490.
- Bullough, W.S. (1939): A study of the reproductive cycle of the minnow in relation to environment. – Proc. Zool. Soc. London A109:79-102.
- (1940): A study of sexual reversal in the minnow (*Phoxinus laevis* L.). – J. Exp. Zool. 85:475-501.

- Burr, B.M., & M.L. Warren, Jr. (1986): A distributional atlas of Kentucky fishes. – Kentucky Nat. Pres. Comm. Sci. Tech. Ser. (4):1-398. Frankfort, Kentucky.
- Cateshy, M. (1771): The natural history of Carolina, Florida and the Bahama Islands; containing the figures of birds, beasts, fishes, serpents, with their descriptions in English and French, etc. 3rd. ed. – London.
- Cao, W.-X. (1964): Schizothoracine. In: H. Wu (ed.): The Chinese Cyprinidae 1:137-197. – Shanghai Science and Technology Press, Shanghai (in Chinese).
- Cavender, T.M. (1986): Review of the fossil history of North American freshwater fishes. In: C.H. Hocutt & E.O. Wiley (eds): The Zoogeography of North American Freshwater Fishes: 699-724. – John Wiley & Sons., New York, Chichester, Brisbane, Toronto, Singapore.
- (1991): The fossil record of the Cyprinidae. In: I.J. Winfield & J.S. Nelson (eds.): Cyprinid Fishes. Systematics, Biology and Exploitation: 34-54. – Chapman & Hall, London, New York, Tokyo, Melbourne. Madras.
- Cavender, T.M., & M.M. Coburn (1987): Evolutionary relationships among eastern North American cyprinids. Part III (Abstract). – Ohio J. Sci. 87(2), 1pp.
- (1992) Phylogenetic relationships of North American Cyprinidae. In: R.L. Mayden (ed.): Systematics, Historical Ecology, and North American Freshwater Fishes: 293-327. – Stanford University Press, Stanford.
- Chen, X.-L., P.-Q. Yue & R.-D. Lin (1984): Major groups within the family Cyprinidae and their phylogenetic relationships. – Acta Zootax. Sinica 9(4):424-440 (in Chinese with English summary).
- Chen, X.-Y. (1986a): On the pharyngeal bones and teeth of leuciscine fishes (Cyprinidae). – Zool. Research. (Kunming, China) 7(2):193-196 (in Chinese with English summary).
- (1986b): Studies on the branchocranium of Chinese leuciscine fishes (Cypriniformes, Cyprinidae). – J. Graduate School, Academia Sinica, Beijing 3(2):138-147 (in Chinese with English summary).
- (1987a): Studies of the skeleton of leuciscine fishes of China, with particular reference of its significance in taxonomy. – Acta Zootax. Sinica 12(3):311-322 (in Chinese with English summary).
- (1987b): Studies on the phylogenetic relationships of Chinese leuciscine fishes (Pisces: Cypriniformes). – Acta Zootax. Sinica 12(4):427-439 (in Chinese with English summary).
- (1987c): The skeleton system of *Esox reicheri* Dabowski, with special reference to the adaptation of feeding behavior. – J. Henan Normal Univ. (Natural Sciences) (Henan, China) (4):95-101 (in Chinese with English summary).
- (1988a): A new species of *Phoxinus* from China (Pisces: Cypriniformes). – Sinozoologia (Beijing) 6:35-38 (in Chinese with English summary).
- (1988b): Studies on the olfactory organs of Cyprinidae in China (Pisces, Cypriniformes). – Acta Zootax. Sinica 13(2):182-194 (in Chinese with English summary).
- Chen, X.-Y., & G. Arratia (1994): The olfactory organs of Acipenseriformes and comparison with other Actinopterygians: Patterns of diversity. – J. Morph. 222:241-267.

- (1996): Breeding tubercles of *Phoxinus* (Teleostei: Cyprinidae). Morphology, distribution, and phylogenetic implications. – J. Morph. 228:127-144.
- Chereshnev, I.A. (1990): Ichthyofauna composition and features of freshwater fish distribution in the Northeastern USSR. – J. Ichthyology 30(5):836-884.
- Chu, Y.T. (1935): Comparative study on the scales and on the pharyngeals and their teeth in Chinese cyprinids, with particular reference to taxonomy and evolution. – Biol. Bull. St. John's Univ., Shanghai (2):10-210.
- Churchill, E.P., & W.H. Over (1938): Fishes of South Dakota. – S. Dakota Dept. Game and Fish.
- Coad, B.W. (1984): Osteology of deformed vertebral columns in the cyprinid fish *Phoxinus phoxinus* L. of Lake Windermere. – Naturalist (England) 931:135-137.
- (1987): Checklist of the fishes of the Ottawa district. – Trail. Landscape. 21:40-60.
- Coburn, M.M. (1982): Anatomy and relationships of the cyprinid *Notropis atherinoides*. – Ph.D. dissertation, Ohio State Univ., Columbus, Ohio.
- Coburn, M.M., & T.M. Cavender (1992): Interrelationships of North American cyprinid fishes. In: R.L. Mayden (ed.): Systematics, Historical Ecology, and North American Freshwater Fishes: 328-373. – Stanford University Press, Stanford.
- Cockerell, T.D.A. (1909): The nomenclature of the American fishes usually called *Leuciscus* and *Rutilus*. – Proc. Biol. Soc. Washington 22:215-218.
- Cockerell, T.D.A., & O. Callaway (1909): Notes on the scales of fishes, the herbivorous Cyprinidae. – Proc. Biol. Soc. Washington 22:121-124.
- Constantinescu, V., C. Vintilă, & S. Damian (1984): Contribution to the knowledge of the breeding coloration and behavior in *Phoxinus phoxinus* (Pisces, Cyprinidae). – Travaux Mus. Hist. nat. "Gr. Antipa" 25:267-289.
- Cooper, E.L. (1983): Fishes of Pennsylvania and Northeastern United States. – Pennsylvania State Univ. Press, University Park and London.
- Cooper, G.P. (1935): Some results of forage fish investigation in Michigan. – Trans. Amer. Fish. Soc. 76:132-142.
- Cope, E.D. (1862): Observation upon certain cyprinid fish in Pennsylvania. – Proc. Acad. Nat. Sci. Philad. (1862):522-524.
- (1864): Partial catalogue of the cold-blooded Vertebrata of Michigan. Part I. – Proc. Acad. Nat. Sci. Philad. (1864):276-285.
- (1868): On the distribution of fresh-water fishes in the Allegheny region of Southwestern Virginia. – J. Acad. Nat. Sci. Philad., ser. 2,6:207-247.
- (1869): Synopsis of the Cyprinidae of Pennsylvania. – Trans. Amer. Philos. Soc. 13:351-410.
- Cross, F.B. (1967): Handbook of fishes of Kansas. – Miss. Pub. Mus. Nat. Hist., Univ. Kansas 45:1-357.
- (1970): Fishes as indicators of Pleistocene and recent environments in the Central Plains. In: Pleistocene and Recent Environments of the Central Great Plains. – Dept. Geology, Univ. Kansas; Spec. Publ. Univ. Kansas Press, Lawrence, Kansas 3:241-257.
- Cross, F.B., & J.T. Collins (1975): Fishes in Kansas. – Public. Educ. Ser. 3:1-189. Mus. Nat. Hist. Univ. Kansas, Lawrence, Kansas.

- Cross, F.B. & W.L. Minckley (1960): Five natural hybrid combinations in minnows (Cyprinidae). – Univ. Kansas Mus. Nat. Hist. Publ. 13:1-18.
- Cross, F.B., & R.E. Moss (1987): Historic changes in fish communities and aquatic habitats in plain streams of Kansas. In: W.J. Matthews & D.C. Heins (eds): Community and Evolution Ecology of North American Stream Fishes: 155-165. – Univ. Oklahoma Press, Norman, Oklahoma.
- Cui, Y., & R.J. Wootton (1988a): Effects of ration, temperature and body size on the body composition, energy content and condition of the minnow, *Phoxinus phoxinus* (L.). – J. Fish. Biol. 32:749-764.
- (1988b): Bioenergetics of growth of a cyprinid, *Phoxinus phoxinus*: the effect of ration, temperature and body size on food consumption, fecal production and nitrogenous excretion. – J. Fish. Biol. 33:431-433.
- (1988c): The metabolic rate of the minnow, *Phoxinus phoxinus* (L.) (Pisces: Cyprinidae), in relation to ration, body size and temperature. – Functional Ecol. 2:157-161.
- (1989): Bioenergetics of growth of a cyprinid, *Phoxinus phoxinus* (L.): development and testing of a growth model. – J. Fish. Biol. 34:47-67.
- Cuvin, M.L.A., & R.W. Furness (1988): Uptake and elimination of inorganic mercury and selenium by minnows *Phoxinus phoxinus*. – Aquat. Toxicol. 13:205-215.
- Das, M.K., & J.S. Nelson (1989): Hybridization between northern redbelly dace (*Phoxinus eos*) and finescale dace (*Phoxinus neogaeus*) (Osteichthyes: Cyprinidae) in Alberta. – Canad. J. Zool. 67:579-584.
- Dauod, H.A., T. Bolger & J.J. Bracken (1985): Studies on the minnow *Phoxinus phoxinus* (L.) from an upland Irish reservoir system. – Irish Fish. Invest. (Ser. A.) 26:3-22.
- Dawley, R.M., & K.A. Goddard (1988): Diploid-triploid mosaics among unisexual hybrids of the minnows *Phoxinus eos* and *Phoxinus neogaeus*. – Evolution 42:649-659.
- Dawley, R.M., R.J. Schultz & K.A. Goddard (1987): Clonal reproduction and polyploid in unisexual hybrids of *Phoxinus eos* and *Phoxinus neogaeus* (Pisces: Cyprinidae). – Copeia 2:275-283.
- Dingerkus, G., & L.D. Uhler (1977): Enzyme clearing of alkane blue stained whole small vertebrates for demonstration of cartilage. – Stain. Tech. 52:229-232.
- Doadrio, I., & P. Garzón (1988): Nuevas localidades de *Phoxinus phoxinus* (L., 1758) (Ostariophysi, Cyprinidae) en la Península Iberica. – Misc. Zool. 10:389-390.
- Dybowski, B.I. (1869): Vorläufige Mitteilungen über die Fischfauna des Ononflusses und des Ingoda in Transbaikalien. – Verh. K.-K. Zool.-Bot. Ver. Ges. Wien. 19:945-958.
- (1916): (title unknown). – Pamietnik Fizyograficzny, Warsaw. V. 23:100-102.
- Eastman, J.T. (1970): The Pharyngeal Bones and Teeth of Minnesota Cyprinid and Catostomid Fishes: Functional Morphology, Variation and Taxonomic Significance. – Ph.D. thesis, Univ. Minnesota, Minneapolis, Minnesota.
- Eastman, J.T., & J.C. Underhill (1973): Intraspecific variation in the pharyngeal tooth formulae of some cyprinid fishes. – Copeia 1:45-53.
- Eddy, S., & J.C. Underhill (1974): Northern Fishes. 3rd ed. – Univ. Minn. Press, Minneapolis.

- Eschmeyer, W.N. (1990): Catalog of the Genera of Recent Fishes. – California Academy of Sciences, San Francisco.
- Evermann, B.W. (1918): The Fishes of Kentucky and Tennessee: a distributional catalog of the known species. – Bull. Bur. Fish. 35:295-368.
- Evermann, B.W., & O. Cox (1896a): Fishes of the Missouri River basin. – Rep. U.S. Comm. Fish. for 1894 (1895-6). Bureau of Fisheries Document 424, Washington, D.C.
- (1896b): A report upon the fishes of the Missouri River basin. Rep. U.S. Comm. Fish. 20:325-429.
- Evermann, B.W., & S.F. Hilderbrand (1916): Notes of the fishes of east Tennessee. – Bull. Bur. Fish. 34:433-451.
- Fink, S.V., & W.L. Fink (1981): Interrelationships of the ostariophysan fishes (Teleostei). – Zool. J. Linn. Soc. 72:297-353.
- Forbes, S.A., & R.E. Richardson (1920): The Fishes of Illinois. 2nd ed. – Dept. Registration and Education, Natural History Survey Division, State of Illinois, Springfield, Illinois.
- Fowler, H.W. (1899): Notes on a small collection of Chinese fishes. – Proc. Acad. Nat. Sci. Philad. (1899):179-182.
- (1904): Notes on the fishes from Arkansas, Indian territory and Texas. – Proc. Acad. Nat. Sci. Philad. 56:242-249.
- (1908): A synopsis of the Cyprinidae of Pennsylvania. – Proc. Acad. Nat. Sci. Philad. 60:517-553.
- (1918): A review of the fishes described in Cope's partial catalogue of the cold-blooded vertebrates of Michigan. – Occ. Pap. Mus. Zool., Univ. Mich. 60:1-51.
- (1923): Records of fishes for the southern states. – Proc. Biol. Soc., Washington 36:7-34.
- (1924): Notes on North American cyprinoid fishes. – Proc. Acad. Nat. Sci. Philad. 76:389-416.
- (1936): Notes on some Tennessee fishes. – Fish Culturist 15(6):111.
- Frazier, G.C., & J.K. Beadles (1977): The fishes of Sylamore Creek, Stone County, Arkansas. – Arkansas Acad. Sci. Proc. 31:38-41.
- Freeze, T.M., & K.J. Rayburn (1977): A note on the distribution of *Chrosomus erythrogaster* (Cyprinidae) in Kentucky. – Trans. Kentucky Acad. Sci. 38:97.
- Frost, W.E. (1943): The natural history of the minnow, *Phoxinus phoxinus*. – J. Anim. Ecol. 12:139-162.
- (1946): On the food relationships of fish in Windermere. – Biol. Jarboek 13:216-231.
- Fujita, K. (1978): Pre-Cenozoic tectonic evolution of northeast Siberia. – J. Geol. 86:159-172.
- Gasowska, M. (1979): Osteological revision of the genus *Phoxinus* Raf., sensu Banarescu 1964, with description of a new genus, *Parchrosomus* gen.nov. (Pisces, Cyprinidae). – Ann. Zool. Polska Akad. Nauk, Warszawa 34:371-413.
- (1983): Revision of the systematic status of *Phoxinus phoxinus* (L.) and *Ph. percnurus* (Pall.) = *Moroco percnurus* (Pall.) (Pisces, cyprinidae) on the basis of osteological investigation. – Roczniki Nau. Roln. (Ser. H.) 100:99-111.

- Gentle, M.J. (1971a): The central nervous control of colour change in the minnow (*Phoxinus phoxinus* L.). I. Blinding and the effects of tectal removal on normal and blind fish. – J. Exp. Biol. 54:83-91.
- (1971b): The central nervous control of colour change in the minnow (*Phoxinus phoxinus* L.). II. Tectal ablations in normal fish. – J. Exp. Biol. 54:93-102.
- (1971c): Electrical activity in the optic tectum and colour change in the minnow (*Phoxinus phoxinus* L.). – J. Exp. Biol. 55:641-649.
- (1972a): The eye and color change in the minnow (*Phoxinus phoxinus* L.) – J. Exp. Biol. 57:701-707.
- (1972b): A note on the paling centra of the minnow (*Phoxinus phoxinus* L.). – J. Exp. Biol. 57:709-711.
- Gilbert, C.R. (1971): Emended publication dates for certain fish species described by E.D. Cope, with notes on the type materials of *Notropis photogenis* (Cope). – Copeia 3:474-479.
- (1980): *Semotilus corporalis* (Mitchill). In: D.S. Lee, C.R. Gilbert, C.H. Hocutt, R.E. Jenkins, D.E. McAllister, & J.R. Stauffer, Jr. (eds.): Atlas of North American Freshwater Fishes: 362. – North Carolina State Museum of Natural History, Raleigh, North Carolina.
- Girgis, S. (1952): The bucco-pharyngeal feeding mechanism in a herbivorous bottom-feeding cyprinoid, *Labeo horie* (Cuvier). – J. Morph. 90:281-315.
- Goddard, K.A., & R.M. Dawley (1990): Clonal inheritance of a diploid nuclear genome by a hybrid freshwater minnow (*Phoxinus eos* x *neogaeus*, Pisces: Cyprinidae). – Evolution 44:1052-1065.
- Goddard, K.A., R.M. Dawley, & T.E. Dowling (1989): Origin and genetic relationships of diploid, triploid, and diploid-triploid mosaic biotypes in the *Phoxinus eos* x *neogaeus* unisexual complex. In: R.M. Dawley & J.P. Bogart (eds.): Evolution and Ecology of Unisexual Vertebrates 6:268-280. – Bull. New York State Museum, Albany, New York.
- Gosline, W.A. (1978): Unbranched dorsal-fin rays and subfamily classification in the fish family Cyprinidae. – Occ. Pap., Mus. Zool., Univ. Mich. 684:1-21.
- Grande, L., & W.E. Bemis (1991): Osteology and phylogenetic relationships of fossil and Recent paddlefishes (Polyodontidae) with comments on the interrelationships of Acipenseriformes. – J. Vert. Paleont. 11 (Suppl. to no. 1): 1-121.
- Greene, C.W. (1935): The Distribution of Wisconsin Fishes. – Wisconsin Conserv. Comm., Wisconsin.
- Greenfield, D.W., F. Abdel-Hameed, G.D. Deckert, & R.R. Flinn (1973): Hybridization between *Chrosomus erythrogaster* and *Notropis cornutus* (Pisces: Cyprinidae). – Copeia 1:54-60.
- Günther, A. (1868): Catalogue of the Fishes in the British Museum 7. – London.
- (1889): Reports on the pelagic fishes collected by H. M. S. Challenger during the years 1873-76. In: Report on the Scientific Results of the Voyage of H. M. S. Challenger during the years 1873-76. 31 (pt. 78) :1-47.
- Haimovice, S., & L. Ciuca (1973): L'étude du caryotype au vairon *Phoxinus phoxi-*

- nus phoxinus* L. (Ostariophysi, Cyprinidae). – Ann. Stiintifice ale Univ., “al I. Cuza” din Iasi 19:201-202.
- Hambrick, P.S. (1977): The intergeneric hybrid, *Notropis cerasinus* x *Phoxinus oreas* (Pisces: Cyprinidae) in the upper Roanoke River drainage, Virginia. – Amer. Midl. Nat. 98:238-243.
- Hankinson, T.L. (1923) The creek fish of Western New York. – Copeia 1923 (115):20-34.
- Harbicht, S.M., W.G. Franzin, & K.W. Stewart (1988): New distributional records for the minnows *Hybognathus hankinsoni*, new record, *Phoxinus eos*, and *Phoxinus neogaeus* in Manitoba. – Canad. Field-Nat. 102:475-484.
- Harder, W. (1975): Anatomy of Fishes. Parts I & II (1-132). – E. Schweizerbart'sche Verlagsbuchhandlung (Nägele & Obermiller).
- Harlan, J.R., & E.B. Speaker (1951): Iowa Fish and Fishing. – State of Iowa.
- Harrington, R.W. Jr. (1950): Preseasonal breeding of the bridled shiner, *Notropis bifrenatus*, induced under light-temperature control. – Copeia 4:304-311.
- (1955): The osteocranium of the American cyprinid fish, *Notropis bifrenatus*, with an annotated synonymy of teleost skull bones. – Copeia 3:267-290.
- Hass, R.L. (1943): A list of the fishes of McHenry County, Illinois. – Copeia 3:160-164.
- Hearald, E.S. (year unknown): Fishes of North America. – Doubleday & Company, Inc., New York.
- Heese, T. (1981): Morphology of *Phoxinus phoxinus* (L. 1758) (Pisces, Cyprinidae) from the River Skawa. – Acta Ichthyol. Piscatoria 11:67-77.
- (1984): On some problems in biology of minnow, *Phoxinus phoxinus* (L.) (Cyprinidae) in the River Skawa. – Acta Ichthyol. Piscatoria 14:25-42.
- Hennig, W. (1966): Phylogenetic Systematics. – Univ. Illinois Press, Urbana.
- Henshall, J.A. (1889): On a collection of fishes from east Tennessee, Alabama, and Escambia Rivers. – Bull. U.S. Fish Comm. 12:31-33.
- Hill, L.G., & T.A. Jenssen (1968): A meristic study of the redbelly dace, *Chrosomus erythrogaster* (Cyprinidae), from a stream in southern Oklahoma. – Southwest Naturalist 13:55-60.
- Hitch, R.K. & D.A. Etnier (1974): Fishes of the Hiwassee River system – Ecological and taxonomic considerations. – J. Tennessee Acad. Sci. 49(3):81-87.
- Hoffman, G.L. (1967): Parasites of North America Fishes. – Univ. Calif. Press, Los Angeles, California.
- Holz, A. & W. Weber (1970): Periodisch auftretende Querstrukturen in Nervenfasern des Bulbus olfactorius der Elritze *Phoxinus laevis*. – Experientia 26:1349-1350.
- Hopkins, D.M. (1967): The Bering Land. – Stanford Univ. Press, Stanford, California.
- Howes, G.J. (1978): The anatomy and relationships of the cyprinid fish *Luciobrama macrocephalus* (Lacépède). – Bull. Brit. Mus. Nat. Hist. (Zool.) 34:1-64.
- (1981): Anatomy and phylogeny of the Chinese major carps *Ctenopharyngodon* Steind., 1866 and *Hypophthalmichthys* Blkr., 1860. – Bull. Brit. Mus. Nat. Hist. (Zool.) 41:1-52.

- (1984) Phyletics and biogeography of the aspinine cyprinid fishes. – Bull. Brit. Mus. Nat. Hist. (Zool.) 47:283-303.
- (1985) A revised synonymy of the minnow genus *Phoxinus* Rafinesque, 1820 (Teleostei: Cyprinidae) with comments on its relationships and distribution. – Bull. Brit. Mus. Nat. Hist. (Zool.) 48:57-74.
- (1991): Systematics and biogeography: an overview. In: I.J. Winfield & J.S. Nelson (eds.): Cyprinid Fishes. Systematics, Biology and Exploitation: 1-33. – Chapman & Hall, London, New York, Tokyo, Melbourne. Madras.
- Hubbs, C.L., & A.A. Echelle (1972): Endangered nongame fishes of the upper Rio Grande basin. In: Symposium on Rare and Endangered Wildlife of the Southwestern United States: 147-167. – New Mexico Dept. Game and Fish., Santa Fe.
- Hubbs, C.L., & D.E. Brown (1929): Materials for a distributional study of Ontario fishes. – Trans. Royal Canad. Inst. 17:1-56.
- Hubbs, C.L., & G.P. Cooper (1936): Minnows of Michigan. – Bull. Cranbrook Inst. Sci. 8:1-95.
- Hubbs, C.L., & K.F. Lagler (1947): Fishes of the Great Lakes Region. – Cranbrook Inst. Sci. Bull. 26:1-186.
- (1964): Fishes of the Great Lake Region. – Univ. Mich. Press., Ann Arbor, Michigan.
- Hubbs, C.L., & R.M. Bailey (1951): Identification of *Oxygeneum pulverulentum* Forbes, from Illinois, as a hybrid cyprinid fish. – Pap. Mich. Acad. Sci. Arts. Lett. 37:143-152.
- Huxley, T.H. (1858): Theory of the vertebrate skull. – Proc. Roy. Soc. London 9:381-433.
- Jenkins, R.E., E.A. Lachner, & F.J. Schwartz (1972): Fishes of the central Appalachian drainages: their distribution and dispersal. In: P.C. Holt (ed.): The Distributional History of the Biota of the Southern Appalachians. Part III: The Vertebrates: 43-117. – Virginia Polytech. Inst. State Univ., Res. Div. Monogr. 4.
- Jennings, D. (1942): Kansas fish in the Kansas State College Museum at Manhattan. – Trans. Kansas Acad. Sci. 45:363-366.
- Jeon, S.R. (1989) Studies on the key and distribution of the genera *Tribolodon*, *Phoxinus* and *Moroco* (Pisces: Leuciscine) from Korea. – J. Basic. Sci., Sang Myung Women's University 3:17-36.
- Johnston, C.E. & J.S. Ramsey (1990): Redescription of *Semotilus thoreauianus* Jordan, 1877, a cyprinid fishes of southeastern United States. – Copeia 1990 :119-130.
- Jones, F.R.H. (1956): The behaviour of minnows in relation to light density. – J. Exp. Biol. 33(2):271-281.
- Jordan, D.S., (1877a): On the fishes of Northern Indiana. – Proc. Acad. Nat. Sci. Philad. 1877:42-82.
- (1877b): Notes on a collection of fishes from the Rio Grande, at Brownsville, Texas. – Bull. U.S. Geol. Geogr. Surv. Terr. 4 (no.2, part 17): 397-406.
- (1885): A catalogue of the fishes known to inhabit the waters of North America, north of the Tropic of Cancer, with notes on species discovered in 1883 and 1884. – Rep. U.S. Fish Comm. 13:789-973.

- (1890): On the fishes described in Müller's supplement volumn to the Systema Naturae of Linnaeus. – Proc. Acad. Nat. Sci. Philad. 1890:48-50.
- (1905): On a collection of fishes made in Korea, by Pierre Louis Jouy, with description of new species. – Proc. U.S. Nat. Mus. 28:193-212.
- (1916): The nomenclature of American fishes as affected by the opinion of the international commission on zoological nomenclature. – Copeia 1:25-28.
- (1917): Changes in names of American fishes. – Copeia 1:85-89.
- (1924): Concerning the American dace allied to the genus *Leuciscus*. – Copeia 1:70-72.
- Jordan, D.S., & C.H. Gilbert (1877): On the genera of North American fresh-water fishes. – Proc. Acad. Nat. Sci. Philad. 1877:83-104.
- Jordan, D.S. & B.W. Evermann (1896): The Fishes of North and Middle America: A Descriptive Catalogue of the Species of Fish-like Vertebrates Found in the Waters of North America, North of the Isthmus of Panama. – Bull. U.S. Nat. Mus. 47:i-ix + 1-1240.
- Jordan, D.S., & J. Swain (1883): List of fishes collected in the clear fork of the Cumberland, Whitley County, Kentucky, with description of three new species. – Proc. U.S. Nat. Mus. 6:248-251.
- Jordan, D.S., & C.W. Metz (1913): A catalog of the fishes known from the waters of Korea. – Mem. Carnegie Mus., Pittsburgh 6:1-65.
- Jordan, D.S., & C.L. Hubbs (1925): Record of fishes obtained by David Starr Jordan in Japan, 1922. – Mem. Carnegie Mus., Pittsburg 10(2):92-346.
- Jordan, D.S., B.W. Evermann & H.W. Clark (1930): Checklist of the Fishes and Fishlike Vertebrates of North and Middle America, North of the Northern Boundary of Venezuela and Colombia. Part. II. Report of the United States Commission of Fisheries for the Fiscal Year 1928 (1930). – Bur. Fish. Doc. Washington No. 1055:1-670.
- Joswiak, G.R. (1980): Genetic Divergence within a Genus of Cyprinid Fish (*Phoxinus*: Cyprinidae). – Ph.D. Dissertation (unpublished), Wayne State University, Detroit, Michigan.
- Joswiak, G.R., & W.S. Moore (1982): Discriminated analysis of two cyprinid fishes *Phoxinus eos* and *Phoxinus erythrogaster* (Pisces: Cyprinidae). – Amer. Midl. Nat. 108:398-401.
- Joswiak, G.R., R.H. Stasiak, & B.F. Koop (1985): Diploid and triploid in the hybrid minnow, *Phoxinus eos* x *Phoxinus neogaeus* (Pisces: Cyprinidae). – Experientia 41:505-507.
- Joswiak, G.R., W.C. Starnes & W.S. Moore (1980): Karyotypes of three species of the genus *Phoxinus* (Pisces, Cyprinidae). – Copeia 4:913-916.
- (1982): Allozyme analysis of the hybrid *Phoxinus eos* x *Phoxinus neogaeus* (Pisces, Cyprinidae) in Nebraska. – Canad. J. Zool. 60:968-973.
- Jurine, L. (1821): Sur les dents et la mastication des poissons appeles cyprins. – Mém. Soc. Physi. Hist. Nat. Geneve 1:19-24.
- Kafuku, T. (1958): Speciation in cyprinid fishes on the basis on intestinal differentiation, with some reference to that among catostomids. – Bull. Fresh. Fish Res. Lab., Tokyo. 8:45-78.

- Kennedy, G.J.A. (1981): Individual variation in homing tendency in the European minnow, *Phoxinus phoxinus* (L.). – *Anim. Behav.* 29:621-625.
- Kennedy, G.J.A., & J.T. Pitcher (1975): Experiments on homing in shoals of the European minnow *Phoxinus phoxinus* (L.). – *Trans. Amer. Fish. Soc.* 104:454-457.
- Kim, I.S., & G.Y. Lee (1985): Systematics study of the subfamily Leuciscinae (Cyprinidae) from Korea. – *Bull. Korean Fish Soc.* 18:381-400.
- Kim, I.-S., & E.-J. Kang (1986): The osteology of *Moroco keumgang* Uchida (Pisces, Cyprinidae) in Korea. – *Bull. N. Univ. (Nat. Sci.)* 1986:319-337.
- Kimmel, P.G. (1975): Fishes of the Miocene-Pliocene Deer Butte Formation, Southeast Oregon. – *Univ. Michigan Paleontol. Pap. Paleontol.* 14:69-87.
- Koh, T.P. (1931): Osteology of *Carassius auratus*. – *The Science Reports of the National Tsing Hua University. Ser. B* 1(12):61-82 (Beijing).
- Koster, W.J. (1939): Some phases of the life history and relationships of the cyprinid, *Clinostomus elongatus* (Kirtland). – *Copeia* 4:201-208.
- (1957): Guide to the Fishes of New Mexico. – Univ. New Mexico Press, Albuquerque.
- Kulamowicz, A., & M. Korkuc (1971): Morfologia *Phoxinus phoxinus* (L. 1758) – Cyprinidae, Osteichthyes – z rz. Sufraganca w dorzeczu srodkowej Wisly. – *Prz. Zool., Wroclaw* 15:299-303.
- Kusaka, T. (1974): The Urohyal of Fishes. – Univ. Tokyo Press, Tokyo.
- Lee, D.S., & S.P. Platania (1980): *Semotilus atromaculatus* (Mitchill). In: D.S. Lee, C.R. Gilbert, C.H. Hocutt, R.E. Jenkins, D.E. McAllister, & J.R. Stauffer, Jr. (eds.): *Atlas of North American Freshwater Fishes*: 361. – North Carolina State Museum of Natural History, Raleigh, North Carolina.
- Lee, D.S., & C.R. Gilbert (1980): *Semotilus margarita* (Cope). In: D.S. Lee, C.R. Gilbert, C.H. Hocutt, R.E. Jenkins, D.E. McAllister, & J.R. Stauffer, Jr. (eds.): *Atlas of North American Freshwater Fishes*: 364. – North Carolina State Museum of Natural History, Raleigh, North Carolina.
- Lee, D.S., C.R. Gilbert, C.H. Hocutt, R.E. Jenkins, D.E. McAllister, & J.R. Stauffer, Jr. (eds.) (1980): *Atlas of North American Freshwater Fishes*. – North Carolina State Museum of Natural History, Raleigh, North Carolina.
- Legendre, P. (1970a): Comptage de vertebres chez quelques cyprinidae du Quebec et l'Ontario. – *Nat. Canad.* 97:325-329.
- (1970b): The bearing of *Phoxinus* (Cyprinidae) hybridity on the classification of its North American species. – *Canad. J. Zool.* 48:1167-1177.
- Legendre, P., & D.M. Steven (1969): Denombrement des chromosomes chez quelques cyprins. – *Nat. Canad.* 96:913-918.
- Legkiy, B.P., & I.K. Popoya (1984): Development of photoreaction in juvenile roach, *Rutilus rutilus*, and minnow, *Phoxinus phoxinus* (Cyprinidae), in relation to downstream migration. – *J. Ichthyol.* 24:72-79.
- Lekander, B. (1949): The sensory line system and the canal bones in the head of some ostariophysi. – *Acta Zool. (Stockholm)* 30:1-131.
- Levesley, P.B., & A.E. Magurran (1988): Population differences in the reaction of minnows to alarm substance. – *J. Fish. Biol.* 32:699-706.

- Leviton, A.E., R.H. Gibbs, Jr., E. Heal, & C.E. Dawson (1985): Standards in herpetology and ichthyology: Part I. Standard symbolic codes for institutional resource collections in herpetology and ichthyology. – *Copeia* 3:802-832.
- Lindeborg, R.G. (1941): Records of fishes from the Quetico Provincial Park of Ontario, with comments on the growth of the yellow pike-perch. – *Copeia* 3:159-161.
- Linnaeus, C. (1758): *Systema Naturae*. ed. X. (*Systema naturae per regna tria naturae, secundum classes, ordines, genera, species, cum Characteribus, Differentiis, synonymis, locis*. Tomus I. Editio decima, reformata.). – Holmiae.
- Maddison, W.P., D.J. Donoghue, & D.R. Maddison (1984): Outgroups analysis and parsimony. – *Syst. Zool.* 33:83-103.
- Magurran, A.E. (1986): The development of shoaling behavior in the European minnow, *Phoxinus phoxinus*. – *J. Fish Biol.* 29 (Suppl. A):159-169.
- Magurran, A.E., & S.L. Girling (1986): Predator model recognition and response habit in shoaling minnows. – *Anim. Behav.* 34:510-518.
- Mahy, G. (1972): Osteology of the North American species of the genus *Chrosomus*, compared with their Eurasian relative *Phoxinus phoxinus* (Pisces, Cyprinidae). – *Amer. Zool.* 12:728-729.
- (1975a): Ostéologie comparée et phylogénie des Poissons Cyprinoïdes. I. Osteologie crânienne du goujon à fines écailles, *Chrosomus neogaeus* (Cope). – *Nat. Canad.* 102:1-31.
- (1975b): Ostéologie comparée et phylogénie des Poissons Cyprinoïdes. II. L'Appareil de Weber, le squelette axial et les ceintures du goujon à fines écailles *Chrosomus neogaeus* (Cope). – *Nat. Canad.* 102:165-180.
- (1975c): Ostéologie comparée et phylogénie des Poissons Cyprinoïdes. III. Ostéologie comparée de *C. erythrogaster* Rafinesque, *C. eos* Cope, *C. oreas* Cope, *C. neogaeus* (Cope), et *P. phoxinus* (Linné) et phylogénie du genre *Chrosomus*. – *Nat. Canad.* 102:617-642.
- Maitland, P.S. (1972): Loch lomond: man's effects on the salmonid community. – *J. Fish. Res. Bd., Canada* 29:849-860.
- Mann, R.H.K. (1971): The populations, growth and production of fish in four small streams in southern England. – *J. Anim. Ecol.* 40:155.
- Matthews, W.J. (1990): Spatial and temporal variation in fishes of riffle habitats: a comparison of analytical approaches for the Roanoke River. – *Amer. Midl. Nat.* 124:31-45.
- Matthews, W.J., & J.T. Styron, Jr. (1981): Tolerance of headwater vs mainstream fishes for abrupt physiochemical change. – *Amer. Midl. Nat.* 105:149-158.
- Maurakis, E.G., & W.S. Woolcott (1992): An intergeneric hybrid, *Phoxinus oreas* x *Semotilus atromaculatus*, from the James River Drainage, Virginia. – *Copeia* 2:548-553.
- Mayden, R.L. (1989): Phylogenetic studies of North American minnows, with emphasis on the genus *Cyprinella* (Teleostei: Cypriniformes). – *Misc. Publ. Mus. Nat. Hist. Univ. Kansas* 80:1-187.
- (1991): Cyprinids of the New World. In: I.J. Winfield, & J.S. Nelson (eds.): *Cypr-*

- nid Fishes. Systematics, biology and exploitation: 240-263. – Chapman & Hall, London. New York, Tokyo, Melbourne, Madras.
- Mayden, R.L., & E.O. Wiley (1992): The fundamentals of phylogenetic systematics. In: R.L. Mayden (ed.): Systematics, Historical Ecology, and North American Freshwater Fishes: 114-185. – Stanford Univ. Press, Stanford, California.
- McPhail, J.D. (1963): The Postglacial Dispersal of Freshwater Fishes in Northern North America. – Ph.D. Dissertation (unpublished), McGill University, Montreal, Canada.
- McPhail, J.D., & C.C. Lindsey (1970): Freshwater Fishes of Northwestern Canada and Alaska. – Bull. Fish. Res. Bd. Can. Ottawa 173:1-381.
- Medlen, A.B. (1951): Preliminary observations of the effects of temperature and light upon reproduction in *Gambusia affinis*. – Copeia 2:148-152.
- Miller, R.R. (1945): A new cyprinid fish from southern Arizona and Sonora, Mexico, with the description of a new subgenus of *Gila* and a review of related species. – Copeia 2:104-110.
- Mills, C.A. (1987): The life history of the minnow *Phoxinus phoxinus* (L.) in a productive stream. – Freshwater Biol. 17:53-67.
- Minckley, W.L. (1959): Fishes of the Big Blue River basin, Kansas. – Univ. Kansas Publ., Mus. Nat. Hist. 11:401-442.
- Mori, T. (1928a): A catalogue of the fishes of Korea. – J. Pan-Pacific Res. Inst. Honolulu 3(3):3-8.
- (1928b): On the fresh water fishes from the Yalu River, Korea, with description of new species. – J. Chosen nat. Hist. Soc. (Korea) 11:1-24.
- (1930): On the freshwater fishes of the Tumen River, Korea, with descriptions of new species. – J. Chosen Nat. Hist. Soc. 6:1-24.
- (1934): The Freshwater Fishes of Jehol. Report of the First Scientific Expedition to Manchoukuo. Sec. V, pt. 1. – Waseda Univ., Tokyo.
- Naud, M., & P. Magnan (1988): Diel onshore-offshore migration in northern redbelly dace, *Phoxinus eos* (Cope), in relation to prey distribution in a small oligotrophic lake. – Canad. J. Zool. 66:1249-1253.
- Nelson, J.S. (1994): Fishes of the World. 3rd edition. – John Wiley & Sons, New York.
- Nelson, J.S., & M.J. Paetz (1992): The Fishes of Alberta (2nd ed.). – Univ. Alberta Press. Edmonton, & Univ. Calgary Press, Calgary.
- New, J.G. (1962): Hybridization between two cyprinids, *Chrosomus eos* and *Chrosomus neogaeus*. – Copeia 1:147-152.
- Nichols, J.T. (1943): The Fresh-water Fishes of China. Natural History of Central Asia 9. – Amer. Mus. Nat. Hist., New York.
- Nigrelli, R.F. (1934): Pseudo-melanosis in the tail of trout and salmon. – Copeia 2:61-66.
- Nikolsky, G.V. (1963): The Ecology of Fishes. – Academic Press, New York.
- O'Bara, C.J. (1990): Distribution and ecology of the blackside dace, *Phoxinus cumberlandensis* (Osteichthyes: Cyprinidae). – Brimileyana 16:9-15.
- (1991): Ecological and behavioral characteristics of the black dace *Phoxinus cumberlandensis*. – Program and Abst., Combined Meetings of 75th Ann. and 71st Ann. Mee-

- ting of Amer. Soc. of Ichthyol. Herpetol. and the 7th Ann. Meeting Amer. Elasmobranch Soc. 1991. New York.
- Okada, Y. (1960): Studies on the freshwater fishes of Japan. II. Sp. Part. – J. Facul. Fish. Univ. Mie. Otanimachi 4:368-497.
- Page, L.M., & B.M. Burr (1991): A Field Guide to Freshwater Fishes, North America, North of Mexico. – Houghton Mifflin Co., Boston.
- Parker, W.K. (1874): On the structure and development of the skull in the salmon (*Salmo salar*). – Phil. Trans. Royal Soc. London, Part I, 163:95-145.
- Partridge, B.L. (1980): The effect of school size on the structure and dynamics of minnow schools. – Anim. Behav. 28:68-77.
- Patterson, C. (1975): The braincase of pholidophorid and leptolepid fishes, with a review of the actinopterygian braincase. – Phil. Trans. Royal Soc. London. Series B. 269:275-579.
- (1981): The development of the North American fish fauna – a problem of historical biogeography. In: P.L. Forey (ed.): The Evolving Biosphere: 265-281. – Brit. Mus. (Nat. Hist.) and Cambridge Univ. Press, London.
- Peyer, B. (1963): Die Zähne: Ihr Ursprung, ihre Geschichte und ihre Aufgabe. – Springer-Verlag, Berlin.
- Pflieger, W.L. (1971): A distributional study of Missouri fishes. – Mus. Nat. Hist. Univ. Kansas Publ. 20:225-570.
- (1975): The Fishes of Missouri. – Missouri Department of Conservation, State of Missouri.
- Pfeiffer, W., U. Walz, R. Wolf, & U. Mangol-Wernado (1985): Effects of steroid hormones and other substances on alarm substance cells and mucous cells in the epidermis of the European minnow, *Phoxinus phoxinus* (L.), and other Ostariophysi (Pisces). – J. Fish Biol. 27:553-570.
- Phillips, G.L. (1968a): *Chrosomus erythrogaster* and *C. eos* (Osteichthyes, Cyprinidae): Taxonomy, Distribution, Ecology. – Ph.D. Dissertation (unpublished). Univ. Minnesota, Minneapolis, Minnesota.
- (1968b): A note on the distribution of *Chrosomus erythrogaster* (Cyprinidae) in the Missouri River system. – Amer. Midl. Nat. 80:564-565.
- (1969a): Morphology and variation of the American cyprinid fishes *Chrosomus erythrogaster* and *Chrosomus eos*. – Copeia 3:501-509.
- (1969b): Diet of minnow *Chrosomus erythrogaster* (Cyprinidae) in a Minnesota stream. – Amer. Midl. Nat. 82:99-109.
- (1969c): Accuracy of fecundity estimate for the minnows *Chrosomus erythrogaster* (Cyprinidae). – Trans. Amer. Fish. Soc. 98:524-526.
- Phillips, G.L., & D.A. Etnier (1969): A 'new' hybrid minnow. – J. Minnesota Acad. Sci. 35:96-97.
- Pitcher, T.J. (1973): Some field measurements on minnow schools. – Trans. Amer. Fish. Soc. 102:840-843.
- Pitcher, T.J., A.E. Maguran, & J.R. Allan (1986): Size-segregative behavior in minnow shoals. – J. Fish Biol. 29 (Suppl. A): 83-95.

- Pitcher, T.J., & J.R. Turner (1986): Danger at dawn: experimental support for the twilight hypothesis in shoaling minnows. – J. Fish Biol. 29 (Suppl. A.): 59-70.
- Pitcher, T.J., D.A. Green, & A.E. Magurran (1986): Dicing with death: predator inspection behavior in minnow shoals. – J. Fish Biol. 28:439-448.
- Rafinesque, C.S. (1820a): Fishes of the River Ohio. – Western Rev. Misc. Mag. 2(4):235-242.
- (1820b): Ichthyologia Ohiensis, or Natural History of the Fishes Inhabiting the River Ohio and its Tributary Streams, Preceded by a Physical Description of the Ohio and Its Branches. – Lexington, Kentucky.
- (1889): Ichthyologia Ohiensis, or Natural History of the Fishes Inhabiting the River Ohio and Its Tributary Streams, Preceded by a Physical Description of the Ohio and Its Branches. – The Burrows Brothers Co., Lexington, Kentucky. Cleveland. [This is a reprint of Rafinesque (1820b).]
- Ramaswami, L.S. (1955a): Skeleton of cyprinoid fishes in relation to phylogenetic studies. 6. The skull and Weberian apparatus in the subfamily Gobioninae (Cyprinidae). – Acta Zool. 36:127-158.
- (1955b): Skeleton of cyprinoid fishes in relation to phylogenetic studies. 7. The skull and Weberian apparatus of Cyprininae (Cyprinidae). – Acta Zool. 36:199-242.
- Raney, E.C. (1947): *Nocomis* nests used by other breeding cyprinid fishes in Virginia. – Zoologica (New York) 32(3):125-132.
- Rasotto, M.B., P. Cardellini & E. Marconato (1987): The problem of sexual inversion in the minnow, *Phoxinus phoxinus* (L.). – J. Fish Biol. 30:51-57.
- Reno, H.W. (1969): Cephalic lateral-line systems of the cyprinid genus *Hybopsis*. – Copeia 4:736-773.
- Reshetnikov, Y.S. & F.M. Shakirova (1993): A zoogeographical analysis of the ichthyofauna of central Asia including a list of freshwater fishes. – J. Ichthyol. 33:99-110.
- Roberts, T.R. (1982): Unculi (horny projections arising from single cells), an adaptive feature of the epidermis of Ostariophysan fishes. – Zool. Scripta 11:55-76.
- Roberts, W.E. (1973): *Percina caprodes semifasciata*, the logperch, newly recorded in Alberta, and new distribution records for *Chrosomus neogaeus* and *Semotilus margarita*. – Canad. Field-Nat. 87:467-468.
- Robins, C.R., R.M. Bailey, C.E. Bond, J.R. Brooker, E.A. Lachner, R.N. Lea & W.B. Scott (1980): A list of common and scientific names of fishes from the United States and Canada (4th ed.). – Amer. Fish. Soc. Spec. Publ. 12:1-174. Bethesda, Maryland.
- (1991): A list of common and scientific names of fishes from the United States and Canada (5th ed.). – Amer. Fish. Soc. Spec. Publ. 20:1-183. Bethesda, Maryland.
- Robison, H.W., & R.J. Miller (1972): A new intergeneric cyprinid hybrid (*Notropis pilsbryi* x *Chrosomus erythrogaster*) from Oklahoma. – Southwestern Nat. 16:442-444.
- Robison, H.W., & T.M. Buchanan (1984): Fishes of Arkansas. – The Univ. Arkansas Press, Fayetteville.
- Rojo, A.L. (1991): Dictionary of Evolutionary Fish Osteology. – CRC Press, Boca Raton, Ann Arbor, Boston, London.

- Rosen, D.E., & P.H. Greenwood (1970): Origin of the Weberian apparatus and the relationships of the ostariophysan and gonorhynchiform fishes. – *Amer. Mus. Novitates* (2428):1-25.
- Ross, H.H. (1974): *Biological Systematics*. – Addison-Wesley Publication Co., Inc., Reading, Massachusetts.
- Ross, R.D., & J.E. Carico (1963): Records and distribution problems of fishes of the North Middle, and South Forks of the Holston River, Virginia. – *Virginia Agric. Exper. Station. Virginia Polytech. Inst., Techn. Bull.* 161:5-23.
- Rough, G.E. (1954): The frequency range of mechanical vibrations perceived of three species of freshwater fish. – *Copeia* 3:191-194.
- Sarbahi, D.S. (1932): The endoskeleton of *Labeo rohita* (Ham. Buch.). – *J. Proc. Asiatic Soc. Bengal.* 28:295.
- Schilling, E.M., & M.G. Ryon (1993): Reproductive biology of the Tennessee dace (*Phoxinus tennesseensis*) on the DOE Oak Ridge Reservation. – *Programs and Abst., Meet. Amer. Soc. Ichthyol. Herpetol., Herpetol. League, Amer. Elasmobranch Soc.* 1993, Austin: 274.
- Schmidt, T.R. (1989): The Phylogenetic Relationships of *Hybognathus* (Actinopterygii: Cyprinidae). – M.S. Thesis (unpublished), Univ. Kansas, Lawrence, Kansas.
- Schultze, H.-P., & G. Arratia (1989): The composition of the caudal skeleton of teleosts (Actinopterygii: Osteichthys). – *Zool. J. Linn. Soc.* 97:187-231.
- Scott, W.B. (1957): Distributional records of fishes in Western Canada. – *Copeia* 2:160-161.
- Scott, W.B., & E.J. Crossman (1973): *Freshwater Fishes of Canada*. – *Bull. Fish. Res. Bd. Canada, Ottawa* 184:1-196.
- Settles, W.H., & R.D. Hoyt (1978): The reproductive biology of the southern redbelly dace, *Chrosomus erythrogaster* Rafinesque, in a spring-fed stream in Kentucky. – *Amer. Midl. Nat.* 99:290-298.
- Smith, B.G. (1908): The spawning habits of *Chrosomus erythrogaster* Rafinesque. – *Biol. Bull.* 14(6):9-18.
- Smith, P.W. (1979): *The Fishes of Illinois*. – Univ. Illinois Press, Urbana, Chicago, London.
- Snelson, F.F. Jr. (1980): *Semotilus lumbee* Snelson & Suttkus. In: D.S. Lee, C.R. Gilbert, C.H. Hocutt, R.E. Jenkins, D.E. McAllister & J.R. Stauffer, Jr. (eds.): *Atlas of North American Freshwater Fishes*: 363. – North Carolina State Museum of Natural History, Raleigh, North Carolina.
- Starmach, J. (1963): The appearance and characteristics of the minnow (*Phoxinus phoxinus* L.) in the basin of the Mszanka Stream. – *Acta Hydrobiol. (Krakow)* 5:367-381.
- Starnes, L.B., & W.C. Starnes (1981): Biology of the blackside dace *Phoxinus cumberlandensis*. – *Amer. Midl. Nat.* 106:360-371.
- Starnes, W.C., & L.B. Starnes (1977): Status report on a new and threatened species of *Phoxinus* from the upper Cumberland drainage. – *Proc. Southeast. Fish. Council* 2:1-3.
- (1978): A new cyprinid of the genus *Phoxinus* endemic to the upper Cumberland River drainage. – *Copeia* 3:508-516.

- (1980a): *Phoxinus cumberlandensis* Starnes & Starnes. In: D.S. Lee, C.R. Gilbert, C.H. Hocutt, R.E. Jenkins, D.E. McAllister, & J.R. Stauffer, Jr. (eds.): Atlas of North American Freshwater Fishes: 335. – North Carolina State Museum of Natural History, Raleigh, North Carolina.
- (1980b): *Phoxinus erythrogaster* (Rafinesque). In: D.S. Lee, C.R. Gilbert, C.H. Hocutt, R.E. Jenkins, D.E. McAllister & J.R. Stauffer, Jr. (eds.): Atlas of North American Freshwater Fishes: 337. – North Carolina State Museum of Natural History, Raleigh, North Carolina.
- Starnes, W.C., & L.B. Starnes (1980c): *Phoxinus oreas* (Cope). In: D.S. Lee, C.R. Gilbert, C.H. Hocutt, R.E. Jenkins, D.E. McAllister & J.R. Stauffer, Jr. (eds.): Atlas of North American Freshwater Fishes: 339. – North Carolina State Museum of Natural History, Raleigh, North Carolina.
- Starnes, W.C., & D.A. Etnier (1986): Drainage evolution and fish biogeography of the Tennessee and Cumberland Rivers drainage stream. In: D.S. Lee, C.R. Gilbert, C.H. Hocutt, R.E. Jenkins, D.E. McAllister & J.R. Stauffer, Jr. (eds.): The Zoogeography of North American Freshwater Fishes: 325-361. – John Wiley and Sons, Inc., New York.
- Starnes, W.C., & R.E. Jenkins (1988): A new cyprinid fish of the genus *Phoxinus* (Pisces: Cypriniformes) from the Tennessee River drainage with comments on relationships and biogeography. – Proc. Biol. Soc. Wash. 101:517-529.
- Stasiak, R.H. (1972): The Morphology and Life History of the Fine Scale Dace, *Pfritle neogaea*, in Itasca State Park, Minnesota. – Ph.D. Dissertation (unpublished), Univ. Minn., Minneapolis, Minnesota.
- (1977): Morphology and variation in the finescale dace, *Chrosomus neogaeus*. – Copeia 4:771-774.
- (1978): Reproduction, age, and growth of the finescale dace, *Chrosomus neogaeus*, in Minnesota. – Trans. Amer. Fish. Soc. 107:720-723.
- (1980a): *Phoxinus eos* (Cope). In: D.S. Lee, C.R. Gilbert, C.H. Hocutt, R.E. Jenkins, D.E. McAllister & J.R. Stauffer, Jr. (eds.): Atlas of North American Freshwater Fishes: 336. – North Carolina State Museum of Natural History, Raleigh, North Carolina.
- (1980b): *Phoxinus neogaeus* Cope. In: D.S. Lee, C.R. Gilbert, C.H. Hocutt, R.E. Jenkins, D.E. McAllister & J.R. Stauffer, Jr. (eds.): Atlas of North American Freshwater Fishes: 338. – North Carolina State Museum of Natural History, Raleigh, North Carolina.
- Stauffer, J.R., Jr., C.H. Hocutt, M.T. Masnik & J.E. Reed, Jr. (1975): The longitudinal distribution of the fishes of the East River, West Virginia - Virginia. – Virginia J. Sci. 26(3):121-125.
- Stauffer, J.R., B.M. Burr, C.H. Hocutt & R.E. Jenkins (1982): Checklist of the fishes of the central and northern Appalachian mountains. – Proc. Biol. Soc. Wash. 95:27-47.
- Sterba, G. (1989): Freshwater Fishes of the World. Vol. 1. – Cosmo Publications, New Delhi, India.

- Stott, B., & B.R. Buckley (1979): Avoidance experiment with homing shoals of minnows *Phoxinus phoxinus* in a laboratory stream channel. – J. Fish. Biol. 14:135-146.
- Stráskraba, M., J. Čihák, S. Frank & V. Hruška (1966): Contribution to the problem of food competition among the sculpin, minnow and brown trout. – J. Anim. Ecol. 35:303-311.
- Swofford, D.L. (1991): PAUP: Phylogenetic Analysis Using Parsimony, Version 3.0. – Illinois Nat. Hist. Sur., Champaign, Illinois.
- Tack, E. (1940a): Die Dressur der Ellritze und ihre Abhängigkeit vom Wetter. – Z. Vergl. Physiol. Berlin 29:146-171.
- (1940b): Die Ellritze (*Phoxinus laevis* Ag.), eine monographische Bearbeitung. – Arch. Hydrobiol. 37:321-425.
- Toner, G.C. (1933): Annotated list of fishes of Georgian Bay. – Copeia 3:133-140.
- Trautman, M.B. (1981): The Fishes of Ohio, with Illustrated Keys (revised edition). – Ohio State Univ. Press, Columbus.
- Travers, R.A. (1989): Systematic account of a collection of fishes from the Mongolian People's Republic: with a review of the hydrobiology of the major Mongolian drainage basins. – Bull. Brit. Mus. Nat. Hist. (Zool.) 55:173-207.
- Tyler, A.V. (1966): Some lethal temperature relations of two minnows of the genus *Chrosomus*. – Can. J. Zool. 44:349-364.
- Ueno, K., & Y. Ojima (1984): A chromosome study of nine species of Korean cyprinid fish. – Jap. J. Ichthyol. 31:338-344.
- Underhill, J.C. (1957): The distribution of Minnesota minnows and darters in relation to Pleistocene glaciation. – Univ. Minn. Mus. Nat. Hist. Occ. Pap. 7.
- Uyeno, T. (1960): Osteology and Phylogeny of the American Cyprinid Fishes Allied to the Genus *Gila*. – Univ. Mich., Ann Arbor.
- Volkova, L.A. (1973): The effect of light intensity on the availability of food organisms to some Lake Baikal fishes. – J. Ichthyol. 13:591-602.
- Warren, M.L. Jr. (1981): New distribution records of eastern Kentucky fishes. – Brimleyana 6:129-140.
- Watson, J.M. (1939): The development of the Weberian ossicles and anterior vertebrae in the goldfish. – Proc. Royal Soc. London. (B) 127:452-472.
- Well, A.W. (1980): *Couesius plumbeus* (Agassiz). In: D.S. Lee, C.R. Gilbert, C.H. Hocutt, R.E. Jenkins, D.E. McAllister & J.R. Stauffer, Jr. (eds.): Atlas of North American Freshwater Fishes: 150. – North Carolina State Museum of Natural History, Raleigh, North Carolina.
- Welter, W.A. (1938): A list of the fishes of the Licking River Drainage in Eastern Kentucky. – Copeia 2:64-68.
- Wheeler, A. (1978): Key to the Fishes of Northern Europe. – Frederick Warne, London.
- (1991): The Linnaean fish collection in the Zoological Museum of the University of Uppsala. – Zool. J. Linn. Soc. 103:145-195.
- Wiley, E.O. (1979): An annotated Linnaean hierarchy, with comments on natural taxa and competing systems. – Syst. Zool. 28:308-337.

- (1981): *Phylogenetics: The Theory and Practices of Phylogenetic Systematics*. – John Wiley and sons, New York.
- (1988): Vicariance biogeography. – *Ann. Rev. Ecol. Syst.* 19:513-542.
- (1992): Phylogenetic relationships of the Percidae (Teleost.: Perciformes): a preliminary hypothesis. In: R.L. Mayden (ed.): *Systematics, Historical Ecology, and North American Freshwater Fishes*: 247-267. – Stanford Univ. Press, Stanford, California.
- Wiley, E.O., D. Siegel-Causey, D.R. Brooks & V.A. Funk (1991): The complete cladist. – *Spec. Publ. Mus. Nat. Hist. Univ. Kansas* 19:1-158.
- Wiley, M.L., & B.B. Collette (1970): Breeding tubercles and contact organs in fishes: their occurrence, structure, and significance. – *Bull. Amer. Mus. Nat. Hist.* 143:147-216.
- Wootton, R.J., T.R.M. Allen & S.J. Cole (1980): Effect of body weight and temperature on the maximum daily food consumption of *Gasterosteus aculeatus* L. and *Phoxinus phoxinus* (L.): selecting an appropriate model. – *J. Fish Biol.* 17:695-705.
- Wootton, R.J. & L.A. Mills (1979): Annual cycle in female minnows *Phoxinus phoxinus* (L.) from an upland Welsh lake. – *J. Fish Biol.* 14:607-618.
- Woronecki, D.E. (1969): First record of occurrence of the northern redbelly dace, *Chrosomus eos*, within Prince Edward Island. – *J. Fish. Res. Boar. Can.* 26:709-710.
- Wu, H.W. (ed.) (1964): *The Chinese Cyprinidae 1*. – Shanghai Science and Technology Press, Shanghai (in Chinese).
- (ed.) (1977): *The Chinese Cyprinidae 2*. – Shanghai Science and Technology Press, Shanghai (in Chinese).
- Yamamoto, M. (1982): Comparative morphology of the peripheral olfactory organ in teleosts. In: T.J. Hara (ed.): *Chemoreception in Fishes*: 39-60. – Elsevier Scientific Publishing Company, Amsterdam, Oxford, New York.
- Yang, G. (1964): Xenocyprininae (= Chondrostominae). In: H.W. Wu (ed.): *The Chinese Cyprinidae 1*:121-136. – Shanghai Science and Technology Press, Shanghai (in Chinese).
- Yang, G., & H. Hung (1964): Leuciscinae. In: H.W. Wu (ed.): *The Chinese Cyprinidae 1*:7-62. – Shanghai Science and Technology Press, Shanghai (in Chinese).
- Yi, B. & Q. Wu (1964): Abramidinae. In: H.W. Wu (ed.): *The Chinese Cyprinidae 1*:63-102. – Shanghai Science and Technology Press, Shanghai (in Chinese).

Author's address:

Xing-yu Chen, Ph.D., Department of Pharmacology and Toxicology, Malott Hall, the University of Kansas, Lawrence, Kansas 66045, USA

Appendix III

The transformation series used in the analysis of the phylogenetic relationship within the genus *Phoxinus*. The transformation series numbers corresponding to the TS numbers in the text (page 44-141) and Appendix II. [0] = plesiomorphic, [1], [2], [3] = apomorphic character.

- 1) Mouth angle small ($\leq 55^\circ$) [0] (Fig.19A), or large ($\leq 60^\circ$) [1] (Fig.19B).
- 2) Mouth gape not extending to [0] (Fig.19A), or extending to [1] (Fig.19B) below the middle of eye pupil.
- 3) Dorsal side of nasal septum on the bridge between the anterior and posterior nasal openings smooth [0] (Fig.20B), or concave [1] (Fig.20A).
- 4) Middle portion of the anterior margin of anterior nasal opening erect [0] (Fig.20A), or unerect [1] (Fig.20B).
- 5) The highest portion of the dorsal margin of primary lamellae of the olfactory organ distant from the axis [0] (Fig.21C), or close to the axis [1] (Fig.21A, B).
- 6) Fewer (about 10) [0], or more (about 16) [1] primary lamellae in the olfactory organ present (Tab.1).
- 7) Elongated ellipsoidal type [0] (Fig.21A, B), or linear type [1] (Fig.21C), or shorted ellipsoidal type [2] (Fig.21E) of axes of the olfactory organ.
- 8) Body lateral line extending to the caudal peduncle [0] (Fig.22F), or not [1] (Fig.22A, B, D).
- 9) Absence [0] (Fig.23C), or presence [1] (Fig.23B) of a fleshy projection at the posterior end of the genital papillae in male.
- 10) Absence [0] (Fig.23A), or presence [1] (Fig.23D) of a fleshy projection at the posterior end of the papilla in female.
- 11) Type E tubercles absent [0] (Fig.24A), or present [1] (Fig.24B) on dorsal aspect of head (Chen & Arratia 1996).
- 12) Tubercles on dorsal aspect of head occurring randomly [0] (Fig.24A), or unrandomly [1] (Fig.24B) (Chen & Arratia 1996).
- 13) Type I of tubercles absent [0], or present [1] on pectoral fin (Chen & Arratia 1996).
- 14) Tubercles on opercle with low density [0], or high density [1] (Chen & Arratia 1996).
- 15) In breeding male, each breast scale bearing less than 12 [0], or up to 16 [1] tubercles on its apical margin (Chen & Arratia 1996).
- 16) In females, Type G tubercle absent [0], or present [1] on the breast scales (Chen & Arratia 1996).
- 17) Tubercles absent [0] (Fig.25A), or present [1] (Fig.25B) on the scales between the left and right breast scales of breeding females.
- 18) On anterior part of lateral body, tubercles present off from [0] (Fig.26B) or on [1] the apical margin of the scale (Fig.26C).
- 19) Fewer (upto six) [0] (Fig.26D), or more (upto 12) [1] (Fig.26E) tubercles present on the apical margin of each scale on caudal peduncle.
- 20) Two [0] (Fig.27A), or three [1] (Fig.27B) rows of tubercles on the distal portion of each pectoral fin-ray.
- 21) Tubercles absent [0], or present [1] on the caudal fin.

- 22) Presence of one horizontal stripe (*Phoxinus neogaeus*-type) [0] (Fig.22A), or two horizontal stripes (*P. erythrogaster*-type) [1] (Fig.22D), or only vertical bands (*P. phoxinus*-type) [2] (Fig.22F), or one horizontal stripe and a few vertical bands (*P. oreas*-type) [3] (Fig.22B) on the lateral body.
- 23) Large dark blotches absent [0] (Fig.22A), or present [1] (Fig.22B) on the dorsolateral body.
- 24) Few melanophores present at the isthmus [0] (Fig.28A), or more melanophores present only on isthmus [1] (Fig.28B), or much more melanophores present on both isthmus and the anterior portion of the breast [2] (Fig.28C).
- 25) Melanophores absent [0] (Fig.29A), or present [1] (Fig.29B) at ventral side of caudal peduncle.
- 26) Pectoral fin slightly dark [0], or much darker [1] in breeding male than in nonbreeding one.
- 27) A dark region absent [0] (Fig.30C), or present [1] (Fig.30D) at base of dorsal fin.
- 28) A black patch present [0], or absent [1] at base of caudal fin.
- 29) Intestine *Phoxinus phoxinus*-type [0] (Fig.31A-C), or *P. eos*-type [1] (Fig.32A, C), or *P. cum-berlandensis*-type [2] (Fig.31G), or *P. oreas*-type [3] (Fig.32D).
- 30) Gas bladder neither slender nor broad ("normal shape") [0], or very slender [1], or very broad [2].
- 31) Anterior chamber of gas bladder about 70% [0] (Fig.33B), or about 50% [1] (Fig.34B) or almost equal to [2] (Fig.33C) length of the anterior chamber.
- 32) Constriction of gas bladder very short [0] (Fig.33B), or short [1] (Fig.34C), or long [2] (Fig.34B).
- 33) Pneumatic duct connecting with constriction of gas bladder [0] (Fig.34B), or with anterior portion of the posterior chamber of the gas bladder [1] (Fig.34H).
- 34) Peritoneum silver [0], or dark [1] in color.
- 35) Kinethmoid short [0] (Fig.35B, D), or elongated [1] (Fig.35A, C, E).
- 36) Dorsal margin of kinethmoid slightly notched [0] (Fig.35D), or deeply forked [1] (Fig.35C).
- 37) Posterior side of kinethmoid concave [0], or not concave [1].
- 38) A foramen absent [0] (Fig.35A-C), or present [1] (Fig.35D, E) through anterior and posterior surfaces of kinethmoid.
- 39) A notch absent [0] (Fig.35B), or present [1] (Fig.35A) at ventral margin of kinethmoid.
- 40) Supraethmoid elongated and narrow [0] (Fig.36A), or short and broad [1] (Fig.36C).
- 41) Middle of lateral margin of supraethmoid convex [0] (Fig.36C, D), or not convex [1] (Fig.36A).
- 42) Posterior margin of supraethmoid concave [0] (Fig.36A), or unconvex [1] (Fig.36B).
- 43) Two small, sharp processes at anterior part of posterior margin of supraethmoid absent [0] (Fig.36A), or present [1] (Fig.36B).
- 44) Nasal bone narrow and elongated [0] (Fig.37E), or broad and relatively short [1] (Fig.37D).
- 45) Supraorbital canal on nasal bone complete [0] (Fig.37B), or interrupted [1] (Fig.37A, E).
- 46) Nasal bone placed over mesethmoid and lateral ethmoid [0] (Fig.37A), or over the lateral ethmoid alone [1] (Fig.37B).
- 47) Preethmoid small [0] (Fig.38A), or large [1] (Fig.38B).
- 48) Ventral side of mesethmoid elongated and narrow [0] (Fig.39A), or broad and short [1] (Fig.39B).
- 49) Mesethmoid bearing two [0] (Fig.39B), or one [1] (Fig.39A) conus.
- 50) Anterior and posterior portions of ventral side of lateral ethmoid acute [0] (Fig.39D), or blunt [1] (Fig.39C).
- 51) A notch absent [0] (Fig.39C), or present [1] (Fig.39D) on dorsal margin of the medial side of lateral ethmoid.

- 52) Posterolateral process of frontal bone short and blunt [0] (Fig.40A), or long and sharp [1] (Fig.40C).
- 53) Supraorbital bone slender [0] (Fig.40D), or short and broad [1] (Fig.40F).
- 54) Only a small portion (or none) [0] (Fig.40F), or almost half [1] (Fig.40E) of supraorbital located over lateral ethmoid.
- 55) Absence [0] (Fig.41A), or presence [1] (Fig.41E) of a well-developed notch at anterior and posterior margin of infraorbital bone 1.
- 56) Infraorbital 2 long [0] (Fig.41A), or short [1] (Fig.41B).
- 57) Infraorbital 3 almost equal in width for the entire bone [0] (Fig.41B), or its posterior portion broader than its anterior portion [1] (Fig.41E).
- 58) Anterior end of infraorbital 3 close to [0] (Fig.41H), or far from [1] (Fig.41F) the posterior end of infraorbital 2.
- 59) Infraorbital 4 similar to [0] (Fig.41F), or larger than [1] (Fig.41A) infraorbital 2 in size.
- 60) A notch absent [0] (Fig.41A), or present [1] (Fig.41E) on posterior margin of infraorbital 4.
- 61) Infraorbital 5 absent [0] (Fig.41B), or present [1] (Fig.41A).
- 62) Posterior margin of the orbital septum not extending beyond [0] (Fig.42B), or extending beyond [1] (Fig.42A) the posterior margin of the unfused portion of the orbitosphenoid.
- 63) A process at the ventroposterior margin of the orbital septum absent [0] (Fig.42A), or present [1] (Fig.42B).
- 64) A process at anterior margin of the pterosphenoid absent [0], or present [1].
- 65) A process on the posterior margin of pterosphenoid present [0] (Fig.43B), or absent [1] (Fig.43A).
- 66) A small [0] or large [1] portion of the pterosphenoid connecting with parasphenoid.
- 67) Medial extrascapular present [0], or absent [1] on parietal.
- 68) Dorsally, the lateral and medial margins of sphenoid shallowly [0] (Fig.45C), or deeply [1] (Fig.45D) concave.
- 69) Ventral side of sphenoid bearing four [0] (Fig.45B), or five [1] (Fig.45A), or three [2] (Fig.45D) concavities.
- 70) Prootic bearing a shallow [0] (Fig.46B), or a deep [1] (Fig.46C) notch on its anterior margin.
- 71) A process at dorsal margin present [0] (Fig.47A), or absent [1] (Fig.47B) on prootic.
- 72) Epioccipital rectangular [0] (Fig.46B), or triangular [1] (Fig.46A) in shape from the dorsal view.
- 73) A process at posterior margin of the epioccipital narrow and elongated [0] (Fig.47A), or broad and short [1] (Fig.47B).
- 74) Anterior concavity on the ventral aspect of epioccipital without [0] (Fig.47A), or with [1] (Fig.47C) a deeper concavity.
- 75) A process on the anterior margin of pterotic absent [0] (Fig.48A), or present [1] (Fig.48B).
- 76) Posterior process of pterotic short and blunt [0] (Fig.48A), or elongated and sharp [1] (Fig.48B).
- 77) Absence [0] or presence [1] of a lateral extrascapula.
- 78) The anterior margin of the wing-like structure of exoccipital shallowly [0] (Fig.49B), or deeply [1] (Fig.49A) concave.
- 79) Posterior margin of the plate-like portion of the exoccipital concave [0] (Fig.49B), or convex [1] (Fig.49A).
- 80) A mesial process at anterior margin of supraoccipital absent [0] (Fig.51C), or present [1] (Fig.51A).
- 81) Ventral side of supraoccipital bearing shallow [0] (Fig.51A), or deep [1] (Fig.51C) concavities.

- 82) A medial extrascapula absent [0] (Fig.44A), or present [1] (Fig.44B) on supraoccipital.
- 83) Vomer's posterior process short and blunt [0] (Fig.52B), or elongated and sharp [1] (Fig.52A).
- 84) A T-shaped ridge at dorsal side of vomer absent [0] (Fig.52A), or present [1] (Fig.52B).
- 85) A ridge on the dorsal side of parasphenoid poorly [0], or well [1] developed.
- 86) A notch at the posterior margin of ascending wing of parasphenoid large [0] (Fig.53E), or small [1] (Fig.53A).
- 87) Fork on the posterior end of parasphenoid broad and shallow [0] (Fig.53A), or narrow and deep [1] (Fig.53F).
- 88) Posterior portion of parasphenoid reaching to the posterior [0], or middle [1] portion of the dorsal part of basioccipital.
- 89) A notch absent [0] (Fig.55A), or present [1] (Fig.55B) at the anterior margin of basioccipital.
- 90) A concavity at the ventral side of the dorsal portion of basioccipital elongate and rectangular [0], or short and triangular [1].
- 91) Space between the anterior end of crest at the dorsal side of basioccipital broad [0] (Fig.55B), or narrow [1] (Fig.55C).
- 92) The crest at the dorsal side of the dorsal portion of basioccipital elongated [0] (Fig.55B), or short [1] (Fig.55A).
- 93) Pharyngeal pad of basioccipital poorly [0] (Fig.55A), or well [1] (Fig.55C) developed.
- 94) The anterior process of the pharyngeal pad of basioccipital bone present [0] (Fig.55B), or absent [1] (Fig.55A).
- 95) The lateral process at the anterior margin of the pharyngeal pad of basioccipital absent [0] (Fig.55A), or present [1] (Fig.13C).
- 96) The posterior process of basioccipital narrow [0] (Fig.55A), or broad [1] (Fig.55C).
- 97) The anterior process of maxilla narrow [0] (Fig.58C), or broad [1] (Fig.58C).
- 98) Anteromedial process of maxilla sharp [0] (Fig.58A), or blunt [1] (Fig.58B), or very small (almost absent) [2] (Fig.58C).
- 99) Anterior ascending process of maxilla high [0] (Fig.58E), or lower, almost absent [1] (Fig.58B).
- 100) The articulatory facet of maxilla formed by base of the anterior ascending process [0] (Fig.58C), or by both of the anteromedial process and the anterior ascending process [1] (Fig.58B).
- 101) Posterior ascending process of maxilla broad [0] (Fig.58B), or narrow [1] (Fig.58C).
- 102) Posterior process of maxilla extending ventroposteriorly [0] (Fig.58D), or posteriorly [1] (Fig.58B).
- 103) Dentary slender [0] (Fig.60C), or blunt [1] (Fig.60B).
- 104) Coronoid process of dentary not perpendicular to [0] (Fig.60A), or perpendicular [1] (Fig.60C) to the dorsal margin of the dentary.
- 105) Retroarticular short [0], or elongated [1].
- 106) About one third [0] (Fig.60C), or about half [1] (Fig.59A) of sesamoid bone overlapping the dentary.
- 107) Posterior process of anguloarticular long and blunt [0], or short and sharp [1].
- 108) Meckel's cartilage "normal" [0] (Fig.61A), or reduced [1] (Fig.61B) in size.
- 109) The anterior fork of urohyal shallow, shorter than the neck length [0] (Fig.62C), or deep, longer than the neck length [1] (Fig.62A).
- 110) Posterior margin of the ventral plate of urohyal concave [0], or convex [1].

- 111) Dorsal plate of urohyal low and elongated [0] (Fig.62A), or relatively high and short [1] (Fig.62C).
- 112) Anterior end of branchiostegal 1 not concave [0] (Fig.64C), or concave [1] (Fig.64B).
- 113) Anterior end of branchiostegal 2 sharp [0] (Fig.64B), or blunt [1] (Fig.64A).
- 114) Branchiostegal 3 connects with posterior ceratohyal only [0] (Fig.64A), or with both posterior and anterior ceratohyals [1] (Fig.64B).
- 115) Anterior end of branchiostegal 3 not concave [0] (Fig.64B), or deeply concave [1] (Fig.64D).
- 116) Posterior ceratohyal short-triangular [0] (Fig.65A), or long-triangular [1] (Fig.65D) in shape.
- 117) Anterior margin of anterior ceratohyal not concave [0] (Fig.65B), or concave [1] (Fig.65A).
- 118) A notch on the anterior margin of anterior ceratohyal absent [0] (Fig.65D), or present [1] (Fig.65C).
- 119) Hyoid foramen formed by both dorsal and ventral hypophyals [0] (Fig.66A), or by ventral hypophyal alone [1] (Fig.66B).
- 120) A shallow concavity absent [0], or present [1] at the dorsal side of the ventral hypophyal and the ventral side of dorsal hypophyal.
- 121) A concavity at the lateral margin of basihyal absent [0] (Fig.65B), or present [1] (Fig.65A).
- 122) Entopterygoid broad and relatively short [0] (Fig.68A), or narrow and relatively long [1] (Fig.68D).
- 123) Entopterygoid connecting with one half of the autopalatine [0], or with the posterior end of autopalatine only [1].
- 124) Ectopterygoid relatively short and broad [0], or narrow and slender [1].
- 125) Ectopterygoid partially overlapping [0] (Fig.68B), or not overlapping [1] (Fig.68D) the entopterygoid.
- 126) Dorsal margin of ectopterygoid far from [0] (Fig.68D), or close to [1] (Fig.68C) the posterior end of the autopalatine.
- 127) Autopalatine well [0] (Fig.68B) or poorly [1] (Fig.68D) developed.
- 128) Laterally, dorsal and ventral margins of autopalatine not concave [0], or concave [1].
- 129) A notch at posteroventral margin of quadrate absent [0] (Fig.68A), or present [1] (Fig.68C).
- 130) Symplectic broad [0] (Fig.68A), or slender [1] (Fig.68B).
- 131) The two articulating facets at posterior margin of metapterygoid for the hyomandibula small [0], or large [1].
- 132) Notch on the dorsal margin of metapterygoid deep [0], or shallow [1].
- 133) Processus basalis (basal process) of metapterygoid narrow and high [0] (Fig.67C), or broad and low [1] (Fig.67A).
- 134) Hyomandibula broad and relatively short [0], or narrow and relatively long [1].
- 135) A notch at the ventroanterior margin of hyomandibula absent [0] (Fig.69A), or present [1] (Fig.69B).
- 136) A posterior notch at ventroposterior margin of hyomandibula absent [0] (Fig.69A), or present [1] (Fig.69C).
- 137) A small [0] (Fig.69A), or large [1] (Fig.69C) cartilage present at ventral side of hyomandibula.
- 138) Opercle short and broad [0], or long and narrow [1].
- 139) Dorsal margin of opercle straight [0], or shallowly concave [1].
- 140) Anterodorsal process of opercle broad and round [0], or narrow and sharp [1].

- 141) Anterior margin of subopercle concave [0], or straight [1].
- 142) Posterior margin of pharyngobranchial 1 not forked [0] (Fig.72A), or forked [1] (Fig.72E).
- 143) Pharyngobranchial 2+3 unrescent [0] (Fig.72A), or crescent [1] (Fig.72B) in shape.
- 144) Pharyngobranchial 4 absent [0] (Fig.74A), or present as a cartilage [1] (Fig.74E).
- 145) Dorsal portion of epibranchial 1 not constricted [0] (Fig.72A), or constricted [1] (Fig.72E).
- 146) Dorsal portion of epibranchial 2 slightly constricted [0] (Fig.72C), or well-constricted [1] (Fig.72D).
- 147) Ventral margin of epibranchial 2 not concave [0] (Fig.72A), or deeply concave [1] (Fig.72D).
- 148) Posterior process of the forked portion of epibranchial 3 much shorter than [0] (Fig.72A), or almost equal to [1] (Fig.72C) the anterior process of the structure in length.
- 149) A process absent [0] (Fig.72A), or present [1] (Fig.72C) on the lateral side of epibranchial 3.
- 150) Ventral margin of epibranchial 4 straight [0] (Fig.72D), or deeply concave [1] (Fig.72A).
- 151) Dorsal margin of epibranchial 4 not concave [0] (Fig.72B), or deeply concave [1] (Fig.72A).
- 152) Posterior margin of epibranchial 4 shallowly concave [0], or deeply concave [1].
- 153) A process absent [0] (Fig.72A), or present [1] (Fig.72B) at the lateral side of epibranchial 4.
- 154) Hypobranchial 3 short [0] (Fig.73B), or elongated [1] (Fig.73A).
- 155) Basibranchial 1 short bar-shaped [0] (Fig.73A) or wedge-shaped [1] (Fig.73F).
- 156) Basibranchial 2 bar-shaped [0] (Fig.73A), or wedge-shaped [1] (Fig.73D).
- 157) Basibranchial 3 similar to [0] (Fig.73B), or much longer than [1] (Fig.73A) basibranchial 2 in size.
- 158) A cartilage at the posterior end of basibranchial 3 very small [0] (Fig.73A), or elongated [1] (Fig.73D).
- 159) Posterior angle of the pharyngeal bone large [0], or small [1].
- 160) A small flat plate-like structure with two small processes absent [0], or present [1] at the posterior edentulous process of the pharyngeal bone.
- 161) Anterior edentulous process of pharyngeal bone curved [0], or straight [1].
- 162) A notch absent [0], or present [1] at the anterior limb's tip of pharyngeal bone.
- 163) Pitted surface of pharyngeal bone bearing large and small pits [0] or large pits only [1].
- 164) Pharyngeal teeth on pharyngeal bone in two rows [0], or one row [1].
- 165) Transverse process 1 located at middle [0] (Fig.75A), or anterior portion [1] (Fig.75B) of the centrum of the vertebra 1.
- 166) Transverse process of vertebra 1 long [0] (Fig.75A), or short [1] (Fig.75B).
- 167) Neural arch 2 not bearing [0] (Fig.76A), or bearing [1] (Fig.76B) an ascending process.
- 168) Anterior process of neural arch 3 short and broad [0] (Fig.77B), or long and narrow [1] (Fig.77A).
- 169) A shallow notch absent [0] (Fig.78B), or present [1] (Fig.78A) at medial side of rib 4.
- 170) Os suspensorium narrow [0] (Fig.78C), or broad [1] (Fig.78B).
- 171) A notch absent [0] (Fig.78B), or present [1] (Fig.78A) at the medial edge of os suspensorium.
- 172) The space between the left and right os suspensorium extending to the ventral margin [0] (Fig.78A), or to the middle [1] (Fig.78C) of os suspensorium.
- 173) Notch at the anterior margin of neural arch 4 deep [0], or shallow [1].
- 174) Space between the neural arch 4 and neural arch 3 extending to the ventral portion [0] (Fig.76A), or to the middle [1] (Fig.76B) of the anterior margin of neural arch 4.

- 175) A process absent [0] (Fig.77B), or present [1] (Fig. 77A) at the dorsoposterior margin of neural spine 4.
- 176) Supraneural 3 narrow and tall [0] (Fig.77A), or broad and short [1] (Fig.77B).
- 177) Grooved portion of supraneural 3 broad [0] (Fig.77B), or narrow [1] (Fig.77A).
- 178) The entire dorsal margin of supraneural 3 grooved [0] (Fig.76A), or only the posterior part of the margin grooved [1] (Fig.76C).
- 179) Dorsal margin of the intercalarium shallowly [0] (Fig.79C), or deeply [1] (Fig.79B) concave.
- 180) Main part of the intercalarium short [0], or slender [1].
- 181) Lateral spine of the intercalarium short [0] (Fig.79B), or elongate [1] (Fig.79A).
- 182) Posterior ramus of the tripus broad and short [0], or elongated and slender [1].
- 183) Supraneural 4 small [0] (Fig.77C), or large [1] (Fig.77B).
- 184) Supraneural 4 a single bone [0] (Fig.76A), or pieced into two parts [1] (Fig.76B).
- 185) Ventral portion of the posttemporal not expanded [0] (Fig.82A), or expanded [1] (Fig.82C).
- 186) Posttemporal not overlapping [0] (Fig.82B), or overlapping [1] (Fig.82C) pterotic.
- 187) Dorsal portion of supracleithrum slightly narrower [0] (Fig.82C), or much narrower [1] (Fig.82A) than the ventral portion of the bone.
- 188) Notch at posterior margin of the horizontal branch of cleithrum shallow [0] (Fig.83B), or deep [1] (Fig.83C).
- 189) Ventral margin of the ascending process of cleithrum slope [0] (Fig.83B), or almost vertical [1] (Fig.83C).
- 190) Anterior portion of the slender part of coracoid not narrower [0] (Fig.85B), or narrower [1] (Fig.85E) than the posterior portion of the slender part.
- 191) A forked structure absent [0] (Fig.85B), or present [1] (Fig.85F) at the broad part of coracoid.
- 192) Cleithral end of mesocoracoid blunt [0] or sharp [1].
- 193) Cleithral process of mesocoracoid curved [0], or straight [1].
- 194) A notch absent (0) (Fig.84E), or present (1) (Fig.84G) at cleithral process of mesocoracoid.
- 195) Coracoidal end of mesocoracoid expanding [0] (Fig.84E), or not expanding [1] (Fig.84F).
- 196) Articular facets on the lateral side of radial 1 of the pectoral fin low [0] (Fig.87A), or high [1] (Fig.87E).
- 197) Pectoral radial 2 slender [0] (Fig.87E), or triangular [1] (Fig.87A).
- 198) A process at the medial margin of pectoral radial 2 absent [0] (Fig.87C), or present [1] (Fig.87E).
- 199) A process absent [0] (Fig.87B), or present [1] (Fig.87A) on pectoral radial 3.
- 200) Segments of the first pectoral fin ray high and narrow [0] (Fig.88A), or short and broad [1] (Fig.88B).
- 201) Anterior fork of pelvic basipterygium deep [0] (Fig.89D), or shallow [1] (Fig.89C).
- 202) Medial process of pelvic basipterygium broad and forked [0] (Fig.89A), or narrow and unforked [1] (Fig.89B).
- 203) Ischiac process of pelvic basipterygium narrow and elongated triangular [0] (Fig.89G), or broad and short triangular [1] (Fig.89C) in shape.
- 204) A cartilage at the posterior end of the ischiac process of pelvic basipterygium absent [0] (Fig.89B), or present [1] (Fig.89D).
- 205) Pelvic radial 4 triangular [0] (Fig.89B), or bar-shaped [1] (Fig.89D).
- 206) Proximal part of the first dorsal pterygiophore broad [0] (Fig.90A), or slender [1] (Fig.90F).

- 207) Anterior process of the proximal part of dorsal fin's first pterygiophore much shorter than [0] (Fig.90A), or equal to [1] (Fig.90C) its posterior process in length.
- 208) Proximal part of the first anal pterygiophore unforked [0] (Fig.91A), or forked [1] (Fig.91B).
- 209) Epural short [0] (Fig.95B), or elongated [1] (Fig.92A).
- 210) Hypural 6 present [0] (Fig.95A), or absent [1] (Fig.92C).

Appendix IV

List of abbreviations used in figures and text

AAP	Anterior ascending process of maxilla	CLA	Claustrum
AC	Anterior chamber of gas bladder	CO	Cavity
ACH	Anterior ceratohyal	COEM	Coracoidal end of mesocoracoid
ACO	Anterior conus of mesethmoid	CON	Constriction of gas bladder
ADP	Anterior dorsal vertebral postzygapophysis	COR	Coracoid
AEP	Anterior edentulous process of the pharyngeal bone	CP	Coronoid process
AF	Anal fin	CPM	Cleithral process of mesocoracoid
AFMEP	Articular surface of metapterygoid for hyomandibular	CR	Crest
AFT	Articular surface of maxilla	DE	Dentary
AL	Anterior limb of pharyngeal bone	DENT	Dentigerous surface of pharyngeal bone
AMP	Anteromedial process of maxilla	DLPI	Dorsolateral process of intercalarium
ANA	Anterior nasal opening	DMPI	Dorsomedial process of intercalarium
ANF	Anterior fork of urohyal	DPB	Dorsal portion of basioccipital
ANP	Anterior process of maxilla	DPU	Dorsal plate of urohyal
ANT	Anterior	EB	Epibranchial
ANTPB	Anterior process of basioccipital	ECP	Ectopterygoid
APA	Apical radial of scale	ENP	Entopterygoid
APAL	Autopalatine	EOC	Exoccipital
APORS	Anterior process of orbital septum	EP	Epural
APTG	Anal pterygiophore	EPOC	Epioccipital
AR	Anterior ramus of tripus	EYE	Eye
ART	Anguloarticular	FIC	Carotid foramen
AW	Ascending wing of parasphenoid	FOM	Foramen
AX	Axis of olfactory organ	FR	Frontal
BAR	Barbel	FV	Trigeminal foramen
BB	Basibranchial	FVII	Facial foramen
BH	Basihyal	GP	Genital papilla
BO	Basioccipital	GS	Gill cleft
BPB	Body portion of exoccipital	H	Hypural
BPC	Broader part of coracoid bone	HA	Haemal arch
BR	Branchiostegal ray	HB	Hypobranchial
BRA	Basal radial of scale	HF	Hyoid foramen
BST	Breast scale with tubercles	HH	Hypohyal
CA	Cartilage	HLS	Horizontal lateral strip on the flank
CAB	Cartilage at posterior end of ischiac process of basipterygium	HS	Haemal spine
CB	Ceratobranchial	ICA	Intercalarium
CEB	Canal formed by exoccipital and basioccipital	IH	Interhyal
CEM	Cleithral end of mesocoracoid	IO	Infraorbital bone
CL	Cleithrum	IOP	Interopercle
		IP	Ischiac project of basipterygium
		LB	Lateral pelvic plate of basipterygium
		LE	Lateral ethmoid
		LES	Lateral extrascapula
		Lig	Ligament

LL	Body lateral line	PH	Parhypural
LOF	Lateral occipital foramen	PHB	Pharyngobranchial
LPS	Lateroposterior process of supraethmoid	PIT	Pit of pharyngeal bones
LRIB	Last rib	PLE	Plate-like structure of exoccipital
MAC	Mandibular canal	PLF	Pelvic fin
MAP	Main part of maxilla	PLOO	Primary lamella of olfactory organ
MAR	Main row of pharyngeal teeth	PLPFR	Posterolateral process of frontal
MB	Medial pelvic plate of basiptyergium of the pelvic girdle	PMC	Preoperculomandibular canal
MC	Meckel's cartilage	PNA	Posterior nasal opening
MCO	Mesocoracoid	POP	Preopercle
ME	Mesethmoid	POPM	Posterior process of maxilla
MEP	Metapterygoid	PP	Posterior projection of genital papilla
MES	Medial extrascapula	PPBO	Posterior process of basioccipital
MIR	Minor row of pharyngeal teeth	PPD	Pharyngeal pad of the basioccipital
MLP	Melanophore	PR	Posterior ramus of tripus
MP	Medial process of basiptyergium	PRB	Processus basalis of the metapterygoid
MPI	Main part of intercalarium	PRE	Preethmoid
MR	Medial ramus of tripus	PRML	Processus metapterygoideus lateralis of metapterygoid
N	Nasal bone	PRO	Prootic
NA	Neural arch	PT	Pharyngeal tooth
NE	Neck portion of urohyal	PTC	Postcleithrum
NO	Notch	PTF	Pectoral fin
NOR	North	PTG	Anal pterygiophore
NPSCA	Nasal portion of supraorbital sensory canal	PTO	Pterotic
NS	Neural spine	PTS	Pterosphenoid
OP	Opercle	PTT	Posttemporal
ORS	Orbitsphenoid	PU	Preural centrum
OS	Os suspensorium	PVP	Posterior ventral postzygopophysis of vertebra
OSE	Orbital septum	QA	Quadrate
OTC	Otic canal of cephalic lateral line	RA	Retroarticular
PA	Parietal	RAD	Radial
PAN	Posterior angle of pharyngeal bone	RIB	Rib
PAP	Posterior ascending process of maxilla	RPF	Pectoral fin ray
PAS	Parasphenoid	SB	Sesamoid bone (sesamoid articular)
PC	Posterior chamber of gas bladder	SC	Scale
PCA	Preopercular sensory canal	SCA	Scapula
PCH	Posterior ceratohyal	SCAP	Scaphium
PCO	Posterior conus of mesethmoid	SCL	Supracleithrum
PD	Pneumatic duct	SE	Supraethmoid
PDP	Posterior dorsal vertebral postzygopophysis	SF	Skin fold
PE	Planum ethmoidale	SN	Supraneural bone
PEP	Posterior edentulous process of pharyngeal bone	SO	Supraorbital
PF	Pitted surface of pharyngeal bone	SOC	Supraoccipital
		SOCA	Supraorbital canal
		SOP	Subopercle

SPC Slender part of coracoid
SUCA Supratemporal canal of cephalic lateral line
SY Symplectic
TPV Transverse process of vertebra
TRP Tripus
TU Tubercle

U Urostyle
V Vertebra
VLS Vertical lateral strip of the flank
VO Vomer
VPU Ventral plate of urohyal
WSE Wing-like structure of exoccipital

In der Serie BONNER ZOOLOGISCHE MONOGRAPHIEN sind erschienen:

1. Naumann, C.M.: Untersuchungen zur Systematik und Phylogenese der holarktischen Sesiiden (Insecta, Lepidoptera), 1971, 190 S., DM 48,—
2. Ziswiler, V., H.R. Güttinger & H. Bregulla: Monographie der Gattung *Erythrura* Swainson, 1837 (Aves, Passeres, Estrildidae). 1972, 158 S., 2 Tafeln, DM 40,—
3. Eisentraut, M.: Die Wirbeltierfauna von Fernando Poo und Westkamerun. Unter besonderer Berücksichtigung der Bedeutung der pleistozänen Klimaschwankungen für die heutige Faunenverteilung. 1973, 428 S., 5 Tafeln, DM 106,—
4. Herrlinger, E.: Die Wiedereinbürgerung des Uhus *Bubo bubo* in der Bundesrepublik Deutschland. 1973, 151 S., DM 38,—
5. Ulrich, H.: Das Hypopygium der Dolichopodiden (Diptera): Homologie und Grundplanmerkmale. 1974, 60 S., DM 15,—
6. Jost, O.: Zur Ökologie der Wasseramsel (*Cinclus cinclus*) mit besonderer Berücksichtigung ihrer Ernährung. 1975, 183 S., DM 46,—
7. Haffer, J.: Avifauna of northwestern Colombia, South America. 1975, 182 S., DM 46,—
8. Eisentraut, M.: Das Gaumenfaltenmuster der Säugetiere und seine Bedeutung für stammesgeschichtliche und taxonomische Untersuchungen. 1976, 214 S., DM 54,—
9. Rath, P., & E. Kulzer: Physiology of hibernation and related lethargic states in mammals and birds. 1976, 93 S., 1 Tafel, DM 23,—
10. Haffer, J.: Secondary contact zones of birds in northern Iran. 1977, 64 S., 1 Faltafel, DM 16,—
11. Guibé, J.: Les batraciens de Madagascar. 1978, 144 S., 82 Tafeln, DM 36,—
12. Thaler, E.: Das Aktionssystem von Winter- und Sommergoldhähnchen (*Regulus regulus*, *R. ignicapillus*) und deren ethologische Differenzierung. 1979, 151 S., DM 38,—
13. Homberger, D.G.: Funktionell-morphologische Untersuchungen zur Radiation der Ernährungs- und Trinkmethoden der Papageien (Psittaci). 1980, 192 S., DM 48,—
14. Kullander, S.O.: A taxonomical study of the genus *Apistogramma* Regan, with a revision of Brazilian and Peruvian species (Teleostei: Percoidei: Cichlidae). 1980, 152 S., DM 38,—
15. Scherzinger, W.: Zur Ethologie der Fortpflanzung und Jugendentwicklung des Habichtskauzes (*Strix uralensis*) mit Vergleichen zum Waldkauz (*Strix aluco*). 1980, 66 S., DM 17,—
16. Salvador, A.: A revision of the lizards of the genus *Acanthodactylus* (Sauria: Lacertidae). 1982, 167 S., DM 42,—
17. Marsch, E.: Experimentelle Analyse des Verhaltens von *Scarabaeus sacer* L. beim Nahrungserwerb. 1982, 79 S., DM 20,—
18. Hutterer, R., & D.C.D. Happold: The shrews of Nigeria (Mammalia: Soricidae). 1983, 79 S., DM 20,—
19. Rheinwald, G. (Hrsg.): Die Wirbeltiersammlungen des Museums Alexander Koenig. 1984, 239 S., DM 60,—
20. Nilson, G., & C. Andrén: The Mountain Vipers of the Middle East — the *Vipera xanthina* complex (Reptilia, Viperidae). 1986, 90 S., DM 23,—
21. Kumerloeve, H.: Bibliographie der Säugetiere und Vögel der Türkei. 1986, 132 S., DM 33,—
22. Klaver, C., & W. Böhme: Phylogeny and Classification of the Chamaeleonidae (Sauria) with Special Reference to Hemipenis Morphology. 1986, 64 S., DM 16,—

23. Bublitz, J.: Untersuchungen zur Systematik der rezenten Caenolestidae Trouessart, 1898 — unter Verwendung craniometrischer Methoden. 1987, 96 S., DM 24,—
24. Arratia, G.: Description of the primitive family Diplomystidae (Siluriformes, Teleostei, Pisces): Morphology, taxonomy and phylogenetic implications. 1987, 120 S., DM 30,—
25. Nikolaus, G.: Distribution atlas of Sudan's birds with notes on habitat and status. 1987, 322 S., DM 81,—
26. Löhrl, H.: Echo-ökologische Untersuchungen an verschiedenen Kleiberarten (Sittidae) — eine vergleichende Zusammenstellung. 1988, 208 S., DM 52,—
27. Böhme, W.: Zur Genitalmorphologie der Sauria: Funktionelle und stammesgeschichtliche Aspekte. 1988, 175 S., DM 44,—
28. Lang, M.: Phylogenetic and biogeographic patterns of Basiliscine Iguanians (Reptilia: Squamata: "Iguanidae"). 1989, 172 S., DM 43,—
29. Hoi-Leitner, M.: Zur Veränderung der Säugetierfauna des Neusiedlersee-Gebietes im Verlauf der letzten drei Jahrzehnte. 1989, 104 S., DM 26,—
30. Bauer, A. M.: Phylogenetic systematics and Biogeography of the Carphodactylini (Reptilia: Gekkonidae). 1990, 220 S., DM 55,—
31. Fiedler, K.: Systematic, evolutionary, and ecological implications of myrmecophily within the Lycaenidae (Insecta: Lepidoptera: Papilionoidea). 1991, 210 S., DM 53,—
32. Arratia, G.: Development and variation of the suspensorium of primitive Catfishes (Teleostei: Ostariophysi) and their phylogenetic relationships. 1992, 148 S., DM 37,—
33. Kotrba, M.: Das Reproduktionssystem von *Cyrtodiopsis whitei* Curran (Diopsidae, Diptera) unter besonderer Berücksichtigung der inneren weiblichen Geschlechtsorgane. 1993, 115 S., DM 32,—
34. Blaschke-Berthold, U.: Anatomie und Phylogenie der Bibionomorpha (Insecta, Diptera). 1993, 206 S., DM 52,—
35. Hallermann, J.: Zur Morphologie der Ethmoidalregion der Iguania (Squamata) — eine vergleichend-anatomische Untersuchung. 1994, 133 Seiten, DM 33,—
36. Arratia, G., & L. Huaquin: Morphology of the lateral line system and of the skin of Diplomystid and certain primitive Loricarioid Catfishes and systematic and ecological considerations. 1995, 110 Seiten, DM 28,—
37. Hille, A.: Enzymelektrophoretische Untersuchung zur genetischen Populationsstruktur und geographischen Variation im *Zygaena-transalpina*-Superspezies-Komplex (Insecta, Lepidoptera, Zygaenidae). 1995, 224 Seiten, DM 56,—
38. Martens, J., & S. Eck: Towards an Ornithology of the Himalayas: Systematics, ecology and vocalizations of Nepal birds. 1995, 448 Seiten, 3 Farbtafeln, DM 112,—
39. Chen, X.: Morphology, phylogeny, biogeography and systematics of *Phoxinus* (Pisces: Cyprinidae). 1996, 227 Seiten, DM 57,—

Seit Nr. 30 werden die Monographien ausschließlich über die Konvertierung von Disketten-texten hergestellt. Dies ergibt neben einer Kosten- und Zeitersparnis auch eine deutlich geringere Fehlquote im Endprodukt. Dazu müssen einige Voraussetzungen erfüllt sein: IBM-kompatibel, Betriebssystem MS-DOS, 3,5- oder 5,25-Zoll-Diskette, „endlos“ beschrieben, ASCII oder wordperfect. Wer sich für Einzelheiten interessiert, wende sich bitte an den Schriftleiter.

Wegen der Gestaltung der Manuskripte, insbesondere des Literaturverzeichnisses, werden die Autoren auf die letzten erschienenen Monographien verwiesen.

QL
1
B716
NH

THE MORPHOLOGY OF THE HIND WING
ARTICULATION AND WING BASE OF THE
SCARABAEOIDEA (COLEOPTERA) WITH SOME
PHYLOGENETIC IMPLICATIONS

by

D. J. BROWNE & C. H. SCHOLTZ

BONNER ZOOLOGISCHE MONOGRAPHIEN, Nr. 40
1996

Herausgeber:
ZOOLOGISCHES FORSCHUNGSMUSEUM
UND MUSEUM ALEXANDER KOENIG
BONN

SMITHSONIAN
MAY 25 1997
LIBRARIES

BONNER ZOOLOGISCHE MONOGRAPHIEN

Die Serie wird vom Zoologischen Forschungsinstitut und Museum Alexander Koenig herausgegeben und bringt Originalarbeiten, die für eine Unterbringung in den „Bonner zoologischen Beiträgen“ zu lang sind und eine Veröffentlichung als Monographie rechtfertigen.

Anfragen bezüglich der Vorlage von Manuskripten sind an die Schriftleitung zu richten; Bestellungen und Tauschangebote bitte an die Bibliothek des Instituts.

This series of monographs, published by the Zoological Research Institute and Museum Alexander Koenig, has been established for original contributions too long for inclusion in „Bonner zoologische Beiträge“.

Correspondence concerning manuscripts for publication should be addressed to the editor. Purchase orders and requests for exchange please address to the library of the institute.

L'Institut de Recherches Zoologiques et Muséum Alexander Koenig a établi cette série de monographies pour pouvoir publier des travaux zoologiques trop longs pour être inclus dans les „Bonner zoologische Beiträge“.

Toute correspondance concernant des manuscrits pour cette série doit être adressée à l'éditeur. Commandes et demandes pour échanges adresser à la bibliothèque de l'institut, s. v. p.

BONNER ZOOLOGISCHE MONOGRAPHIEN, Nr. 40, 1996

Preis: 50,— DM

Schriftleitung/Editor: G. Rheinwald

Zoologisches Forschungsinstitut und Museum Alexander Koenig

Adenauerallee 150—164, D-53113 Bonn, Germany

Druck: JF. CARTHAUS, Bonn

ISBN 3-925382-43-7

ISSN 0302-671 X

THE MORPHOLOGY OF THE HIND WING
ARTICULATION AND WING BASE OF THE
SCARABAEOIDEA (COLEOPTERA) WITH SOME
PHYLOGENETIC IMPLICATIONS

by

D. J. BROWNE & C. H. SCHOLTZ

BONNER ZOOLOGISCHE MONOGRAPHIEN, Nr. 40
1996

Herausgeber:
ZOOLOGISCHES FORSCHUNGSMUSEUM
UND MUSEUM ALEXANDER KOENIG
BONN

Die Deutsche Bibliothek — CIP-Einheitsaufnahme

Browne, D. J.:

The morphology of the hind wing articulation and wing base of the Scarabaeoidea (Coleoptera) with some phylogenetic implications / D. J. Browne; C. H. Scholtz. Hrsg.: Zoologisches Forschungsinstitut und Museum Alexander Koenig, Bonn. — Bonn: Zoologisches Forschungsinst. und Museum Alexander Koenig, 1996 (Bonner zoologische Monographien ; Nr. 40)

ISBN 3-925382-43-7

NE: Scholtz, C. H.;; GT

CONTENTS

	Page
Abstract	5
Introduction	5
Acknowledgements	6
Material and Methods	6
Specimen preparation and examination	6
Taxa studied	7
The morphology and terminology of the wing articulation and wing base of Scarabaeoidea	9
General structure of the wing	9
The wing articulation	10
First axillary	10
Second axillary	11
Median plate	12
Third axillary	12
The wing base	12
First basal plate	12
Second basal plate	13
Basalare	14
Additional structures	14
Results and discussion	15
Description format	15
Glaresidae	15
Passalidae	19
Diphyllostomatidae	23
Lucanidae	26
Glaphyridae	30
Trogidae	34
Bolboceratidae	38
Pleocomidae	43
Geotrupidae	47
Hybosoridae	51
Ceratocanthidae	55
Ochodaeidae	59
Scarabaeidae	63
Aphodiinae	64
Aegialiinae	68
Aulonocneminae	72
Scarabaeinae	76
Orphninae	81
Melolonthinae	85
Acoma	89
Chasmatopterinae	93

Hopliinae	97
Oncerinae	101
Ruteliinae	105
Dynastinae	109
Cetoniinae	113
Trichiinae	117
Valginae	121
Literature cited	126
Appendix	130
List of abbreviations	130
Figures	132

ABSTRACT

Two character suites, the hind wing articulation, comprised of the first, second and third axillaries and the median plate, and the hind wing base, comprised of the first and second basal plates, are described for Glaresidae, Passalidae, Diphylostomatidae, Lucanidae, Glaphyridae, Trogidae, Bolboceratidae, Pleocomidae, Geotrupidae, Hybosoridae, Ochodaeidae, Ceratocanthidae and Scarabaeidae (Aphodiinae, Aegialiinae, Aulonocneminae, Orphninae, Melolonthinae, *Acoma*, Oncerinae, Chasmatopterinae, Hopliinae, Rutelinae, Dynastinae, Cetoniinae, Trichiinae and Valginae). Due to the magnitude of this study, large number of characters and high degree of variability of the structures, it was not possible, at this early stage, to adequately analyse the phylogenetic content of the various character states. However, some notes concerning genealogical relationships among the major taxa are given.

INTRODUCTION

The Scarabaeoidea are one of the largest and most variable superfamilies of Coleoptera. Members of the superfamily vary tremendously in size, facies and habits but are united by several unique characters (Lawrence & Britton 1991). Most adults are robust, short-legged beetles with a typically lamellate antennal club, highly modified prothorax with large coxae, usually dentate tibiae, strong intrinsic wing-folding mechanism, the second abdominal sternite represented only by a lateral portion, the eighth tergite forming a true pygidium and four Malpighian tubules. Hind coxal plates are absent. Larvae are grub-like and usually C-shaped, with well-developed antennae and legs. They are without urogomphi. Scarabaeoids feed on a wide range of plant and animal matter and dung. This varies from detritus and most types of dung through lower plants to virtually all higher plant tissues and carrion to predation on other insects. Their habits range from free-living through fairly sophisticated forms of brood care to sub-social behaviour.

The Scarabaeoidea are morphologically one of the best-studied beetle groups. There have been many broadly based comparative studies covering most major structures. These include: antennae (Iablokoff-Khnzorian 1977), antennal sensilla (Meinecke 1975), eye (Caveney 1986), mouthparts (Nel & Scholtz 1990), prothorax (Hlavac 1975), coxae (Ritcher 1969c; Hlavac 1975), spiracles (Richer 1969a,b), wing venation (Crowson 1967; Iablokoff-Khnzorian 1977), alimentary canal (unpublished), metendosternite (Crowson 1938; Iablokoff-Khnzorian 1977), male genitalia (d'Hotman & Scholtz 1990a,b), female genitalia (Tanner 1927; Holloway 1972; Lawrence & Newton 1982; unpublished), ovarioles (Ritcher & Baker 1974), karyotype (Smith & Virkki 1978; Yadav & Pillai 1979), central nervous system (Iablokoff-Khnzorian 1977; unpublished), spermatozoan number (Virkki 1969), malpighian tubules (Caveney 1986) and larvae (Areekull 1957; Ritcher 1966; Hinton 1967; Costa et al. 1988) to name a few. These character suites were recently reviewed and phylogenetically assessed by Scholtz (1990).

The current project is one of a series by members of our research team in which various morphological structures of the major groups of Scarabaeoidea are being studied to

determine phylogenetic trends in them as an indication of possible relationships between the groups (d'Hotman & Scholtz 1990a,b; Nel & Scholtz 1990; Scholtz 1990; Browne et al. 1993; Browne & Scholtz 1994, 1995; Scholtz & Browne in press; Scholtz et al. 1994, submitted). These studies are complementary to the ones undertaken by various authors over the past 20 years (see above). However, because of the magnitude of this project and because of the lack of published data on comparative morphology of scarabaeoid hind wing articulation and wing base and the difficulty of interpreting phylogenetic trends, it was decided to separate the comparison of the morphological structures from the analysis of phylogenetic trends in hind wing articulation and wing base structure. The former is reported here and the latter will be dealt with in a separate communication to be published later.

ACKNOWLEDGEMENTS

We are very grateful to Dr. J. Kukalová-Peck (Carleton University, Ottawa) who contributed significantly to this project, and also for critical comments on various drafts of this manuscript.

For loan of material we thank Dr. S. Endrödi-Younga (Transvaal Museum, Pretoria), Dr. D. Carlson (California), Prof. J. Doyen (University of California, Berkeley), Dr. A. Hardy (Department of Food and Agriculture, California), Prof. E. Holm (University of Pretoria), Prof. H. Howden (Carleton University, Ottawa), Mr. M. Kerley (The Natural History Museum, London), Mrs. J. McNamara (Biosystematics Research Institute, Ottawa), Dr. O. Merkl (Hungarian Museum of Natural History, Budapest) and Prof. S. Peck (Carleton University, Ottawa).

The senior author is especially grateful to the following people for extending their courtesies throughout the duration of this project: Mary and Ronald Browne (Ottawa), Catherine Yarymowich (Toronto), Gustav Prackelt, Marianne and Clarke Scholtz (Pretoria), Ron Boyd, Henry Howden, Glen Kit, Jarmila Kukalová-Peck, Stewart Peck and Mike Weber (Carleton University, Ottawa).

This work was funded by grants from the Foundation for Research Development of South Africa and The University of Pretoria.

MATERIAL AND METHODS

In this contribution we present the database of a major report of the cladistic relationships of the families of Scarabaeoidea based on characters of the hind wing articulation and hind wing base (Browne 1993). More than 250 genera, representing all of the major scarabaeoid taxa from most geographical regions, were examined.

Specimen preparation and examination

All material examined was either dried museum specimens or prepared slides. Besides material from our own collection, dried museum material was also obtained from Prof. J.

Doyen (University of California, Berkeley); Prof. E. Holm (University of Pretoria); Mr. M. Kerley (The Natural History Museum, London); Mrs. J. McNamara (Biosystematics Research Centre, Ottawa); and Dr. O. Merkl (Hungarian Museum of Natural History, Budapest). Prepared slides were obtained from Dr. A. Hardy (Department of Food and Agriculture, California) and Dr. D. Carlson (Orangeville, California).

In order to relax the specimens, they were boiled for approximately five minutes in distilled water. The specimens were then pinned to a styrofoam platform and further prepared in one of two methods. The first consisted of using fine forceps to remove the wings at the tergum, keeping the wing articulation intact. The right wing was placed on a clean slide with several drops of absolute alcohol. The wing was spread, and held until the alcohol had evaporated. No mounting medium was used, but in many instances putty was used to fix the wing in an outstretched position (especially large wings). The first, second and third axillaries, of the left wing, were dissected and mounted on paper points. The second method involved pinning the just-boiled specimen to a spreading board, securing the right elytron by either excising it or pinning it away from the anterior margin of the wing, and securing the wing in an outstretched position for drying. Softening and clearing the wings in either hot or cold KOH did not prove to be useful and was attempted only a few times before this method was abandoned.

High contrast photographs which clearly indicated veins and degree of sclerotization were produced by placing the wing and slide into a Durst 609 enlarging camera and exposing directly onto Ilford Ilfospeed Multigrade II photographic paper. Exposure times varied from 2 seconds for poorly sclerotized, small wings, to 60 seconds for well sclerotized, large wings. The exposed paper was developed using Ilford PQ Universal developer and Amfex high speed developer. Developing times were gauged by eye and feature contrast. The wing articulation, wing base and fine veinal features, such as the radial cell and hinges, were poorly reproduced using this method. For these a Hitachi Model S-450 scanning electron microscope was used for both viewing and photographing.

Illustrations of the hind wing articulation, wing base and wing venation were completed using a Zeiss dissecting binocular microscope and a Zeiss 1,8 Camera Lucida. Finer features, from small species, were drawn directly from SE micrographs. Correction of drawings was completed with a Zeiss compound microscope. Photographing directly through a Zeiss dissecting microscope produced poor photographs, with uneven glare due to strong wing fluting and poor resolution.

Taxa studied

Hind wings of the following genera were examined during the course of this study. Family and subfamily concepts are from Scholtz (1990), Browne (1993), and Scholtz & Browne (Bolboceratidae, in press).

Superfamily Scarabaeoidea

Glaresidae: *Glaresis*

Passalidae: *Aceraius*, *Aulacocyclus*, *Ceracupes*, *Didimus*, *Odontotaenius*, *Oileus*, *Passalus*, *Proculejus*, *Verres*, *Veturius*

Diphyllostomatidae: *Diphyllostoma*

Lucanidae: *Aegus*, *Aesalus*, *Ceruchus*, *Chiasognathus*, *Dorcus*, *Figulus*, *Lamprima*, *Neolucanus*, *Nicagus*, *Nigidius*, *Penichrolucanus*, *Platycerus*, *Prosopocoilus*, *Sinodendron*, *Syndesus*

Glaphyridae: *Amphicoma*, *Lichnanthe*

Trogidae: *Trox*, *Omorgus*, *Polynoncus*

Bolboceratidae: *Athyreus*, *Australobolbus*, *Blackbolbus*, *Blackburnium*, *Bolbaineus*, *Bolbapium*, *Bolboceras*, *Bolbocerastes*, *Bolbocerosoma*, *bolbocerosum*, *Bolbochromus*, *Bolbogonium*, *Bolbohamatum*, *Bolbelasmus*, *Bolboleus*, *Bolborhachium*, *Bolborhinum*, *Bolborhombus*, *Bradycinetulus*, *Elephastomus*, *Eucanthus*, *Gilletinus*, *Neoathyreus*, *Pereirabolbus*, *Stenaspidius*

Pleocomidae: *Pleocoma*

Geotrupidae: *Anoplotrupes*, *Ceratophyus*, *Ceratotrupes*, *Chromogeotrupes*, *Cnemotrupes*, *Enoplotrupes*, *Epigeotrupes*, *Frickius*, *Geohowdenius*, *Geotrupes*, *Haplogeotrupes*, *Megatrupes*, *Mycotrupes*, *Odontotrupes*, *Onthotrupes*, *Phelotrupes*, *Sericotrupes*, *Thorectes*, *Typhoeus*

Hybosoridae: *Anaides*, *Araeotanopus*, *Brenskea*, *Chaetodus*, *Dalmothoracodes*, *Hapalonychus*, *Hybochaetodus*, *Hybosorus*, *Liparochnus*, *Microphaeochroops*, *Phaeochridius*, *Phaeochroops*, *Phaeochrous*, *Trichops*

Ceratocanthidae: *Astaenomoechus*, *Ceratocanthus*, *Cloeotus*, *Cyphopisthes*, *Eubrittoniella*, *Eusphaeropeltis*, *Madrasostes*, *Perignamptus*, *Philharmostes*, *Pterorthochaetes*, *Synarmostes*

Ochodaecidae: *Chaetocanthus*, *Ochodaeus*, *Pseudochodaeus*, *Synochodaeus*

Scarabaeidae: *Acognatha*, *Acoma*, *Aegialia*, *Agamopus*, *Alaberoides*, *Allokotarsa*, *Amphimallon*, *Anachalcos*, *Anatochilus*, *Anisonyx*, *Anomala*, *Anomalura*, *Aphodius*, *Aphonides*, *Apogonia*, *Archophileurus*, *Asthenopholis*, *Ataenius*, *Aulonocnemis*, *Bolax*, *Brachymacroma*, *Callirhinus*, *Camenta*, *Camentoserica*, *Campilipus*, *Campsiura*, *Catharsius*, *Canthidium*, *Canthon*, *Cartwrightia*, *Chironitis*, *Chlorocala*, *Chnaunanthus*, *Circellium*, *Coenochilus*, *Colobopterus*, *Comythovalgus*, *Copris*, *Coprophaeus*, *Coptorhina*, *Cotinus*, *Cyclocephala*, *Cyclomera*, *Cymophorus*, *Cyphonistes*, *Cyptochirus*, *Cyrioperta*, *Deltotrichum*, *Deltorrhinum*, *Diastictus*, *Dichelonyx*, *Dichelus*, *Dichotomius*, *Dinacoma*, *Diplognatha*, *Diplotaxis*, *Drepanocanthus*, *Drepanocerus*, *Drepanopodus*, *Dynastes*, *Dyscinetus*, *Eriesthis*, *Euoniticellus*, *Euparia*, *Eurysternus*, *Eutheola*, *Garetta*, *Geniates*, *Genuchus*, *Gnorimella*, *Golofa*, *Gymnoloma*, *Gymnopleurus*, *Heliocopris*, *Heteronychus*, *Hoplia*, *Hybaloides*, *Hybalus*, *Hyboscherna*, *Hypselogenia*, *Kheper*, *Larupea*, *Lepidota*, *Lepithrix*, *Leptohoplia*, *Leucothyreus*, *Liatongus*, *Macroductylus*, *Melimesthes*, *Milichus*, *Neoserica*, *Nyassinus*, *Olaberoides*, *Oncerus*, *Oniticellus*, *Onitis*, *Onthophagus*, *Oplostomus*, *Orizabus*, *Orphnidus*, *Orphnus*, *Osmoderma*, *Oxygryllus*, *Oxysternon*, *Pachynema*, *Paracotalpa*, *Parathyce*, *Pedaria*, *Pedaridium*, *Pelidnota*, *Peritrichia*, *Phacosoma*, *Phalogogonia*, *Phalops*, *Phanaeus*, *Phileurus*, *Philoscaptus*, *Phobetus*, *Phyllopertha*, *Phyllophaga*, *Popillia*, *Proagoderus*, *Pseudachloa*, *Pseudataenius*, *Pseudorphnus*, *Pycnoschema*, *Raceloma*, *Rhinocoeta*, *Rhyssemus*, *Sarophorus*, *Scarabaeus*, *Scatimus*, *Sceliages*, *Scelophysa*, *Schizonycha*

Serica, Sisyphus, Sparmannia, Spilophorina, Stethpseudincta, Strategus, Strigodermella, Sulcophanaeus, Syrichthodontus, Tephraea, Tragiscus, Trichiorhyssemus, Trochalus, Trogodes, Uroxys, Valgus, Xinidium, Xyloryctes

The figures occur together at the end of this book. The abbreviations used in the descriptions and figures are given in the Appendix.

THE MORPHOLOGY AND TERMINOLOGY OF THE HIND WING ARTICULATION AND WING BASE OF SCARABAEOIDEA (COLEOPTERA)

General structure of the wing

The wing is divided into three main sections: (1) the wing articulation; (2) the wing base, and (3) the membranous wing and veins. The wing articulation and wing base are separated by a hinge line (Kukalová-Peck 1983) (Figs.1, 2b). Muscles attached to the wing articulation mobilize the sclerites, while the wing base conveys the movement of the wing articulation to the wing blade.

We are in agreement with Kukalová-Peck (1983) that there were eight veinal pairs in the ancestral protowing (Fig.1). From leading edge to trailing edge, the primary veins are as follows (abbreviations to be used in the text are in brackets): Precosta (PC), Costa (C), Subcosta (Sc), Radius (R), Media (M), Cubitus (Cu), Anal (A) and Jugal (J). Each primary vein was primitively composed of two fluted sectors, a convex anterior (A+) and a concave posterior (P-). Thus, ScA denotes the anterior subcostal sector while CuP denotes the posterior cubital sector. Branching of veins was primitively even (=dichotomous). For example, MP branched into MP1+2 and MP3+4 then branched again into MP1, MP2, MP3, and MP4. Each primary veinal sector branched about three times in the primitive condition.

The ancestral articulation was a simple, broad band extending between the wing and the tergum and continuing ventrally under the wing. Dorsally, the band was fissured into eight rows of four sclerites, aligned with eight veinal pairs, giving 32 sclerites (Fig.1). The articular sclerites serve as channels which keep the blood passages between the wing veins and the body cavity open.

The nomenclature of the articular band is based on the articulation of Palaeodictyoptera: Homiopteridae. Abbreviations given in brackets will be used in the remainder of the text. The basivenalia (B) are the most distal column of sclerites and are the sclerites which are continuous with or hinged to the veinal pair. They are followed proximally by fulcalaria (F) which primitively have musculature and provide the hinges for wings of the Pterygota, axalaria (AX), and proxalaria (P) which are the most varied in shape, length and width. Each row of sclerites is named by using the primary vein with which it is aligned as an adjective. For example, PCu denotes the cubital proxalare while BJ denotes the jugal basivenale.

The primitively separated proxalaria, axalaria and fulcalaria are, in Neoptera, fused together to form several typical clusters (= strongest neopterous synapomorphy; Kukalová-Peck 1983, 1991): the humeral plate (HP), the first axillary (1Ax), the second axillary (2Ax), the median plate (MED), the third axillary (3Ax), and sometimes the fourth axillary (4Ax) (not illustrated) (Figs.2a-b, 3) (for additional details see Snodgrass 1935 and Kukalová-Peck 1983, 1991). In the Coleoptera the basivenalia have fused together to form the *first basal plate (1BP)* and the *second basal plate (2BP)* (Fig.3) (Browne & Scholtz 1994).

The Wing Articulation

First Axillary (1Ax).

The first axillary is composed of four fused sclerites (Figs.2b, 4): subcostal fulcalare, subcostal axalare, radial axalare and medial proxalare (FSc + AXSc + AXR + PRM). Recent evidence from Neuroptera clearly shows that the head is composed of only one sclerite (FSc), the neck by two sclerites (AXSc and AXR) and the tail by a single sclerite (PRM) (J.Kukalová-Peck, personal communication 1993; the interpretation proposed by Kukalová-Peck & Lawrence (1993:203) that the head is composed of FSc + AXSc, the neck by AXM and the tail by PRM should be replaced by this new interpretation). Proximally 1Ax articulates with the subcostal proxalare (PRSc) and the radial proxalare (PRR), which are fused together (Fig.2b), anteriorly with the anterior subcostal basivenale (BScA) (Figs.2b, 3) and distally with the second axillary (2Ax) (Figs.2a, 3).

Dorsal view (Figs.2a-b, 3, 4): 1Ax, as mentioned above, articulates with PRSc + PRR proximally (Fig.2b), BScA anteriorly (Figs.2b, 3) and 2Ax distally (Figs.2a, 3). The distal margin of the neck articulates with 2Ax (Figs.2a, 3). In all Polyphaga this articulation takes the form of a concavity, termed the *distal embayment* (Fig.4).

The deltoid-shaped tail is divided into two main sections the *proximal arch* and the *distal arch* (Fig.4). In Coleoptera PRR is enlarged posteriorly. The proximal arch of 1Ax is recurved along the entire length (Fig.4) and articulates just below the distal margin of the more proximal PRR (which is fused to the tergum - Fig.2b). This junction is termed the *PRR articulation*. The distal arch articulates with 2Ax (Figs.2a, 3). Both articulations are mediated by tough membranes.

Ventral view (Fig.5): Ventrally, the distal margin of the neck folds proximad to form a very broad, crescent-shaped ridge, termed the *distal neck ridge*. The proximal margins of the head and neck are curved ventrad to form a second, slender ridge, termed the *proximal neck ridge*. Medially the head and neck are deeply concave.

The proximal and distal arches of the tail are each often margined by a ridge extending along the entire length of each arch. Often these ridges extend posteriad and fuse to a third ridge which extends along the posterior margin of the tail, forming a triangle with an open top. These ridges are termed the *proximal tail ridge*, *posterior tail ridge* and *distal tail ridge* and are of variable width and length. The ridges and the concavities accommodate the proximal ridge and lobe of 2Ax.

Anterior view (Fig.6): The head is armed with one or two teeth and a long concave projection which surrounds the postero-proximal corner of BScA. The ventral tooth is referred to as *FSc1* and the dorsal as *FSc2*. The teeth are usually separated by a *ventral projection* and an *embayment*.

FSc1 is formed as a convex tooth which extends along the ventral margin of the ventral projection. *FSc1* articulates in a groove formed between two large convexities on the proximal margin of BScA and is prevented from pivoting anteriorly by the dorsal margin of BScA.

The ventral projection, a slender, concave structure, articulates with the inner surface of the posterior convexity on the proximal margin of BScA. A concavity, which is of variable length, runs the length of the ventral projection. The embayment separates *FSc1*/ventral projection from *FSc2*, and surrounds the most posterior convexity on the proximal margin of BScA. *FSc2* is formed as a slender, convex tooth. It articulates in a deep concavity formed along the posterior margin of BScA.

Second Axillary (2Ax).

The second axillary is composed of the medial axalare and radial fulcalare (AXM + FR) (Figs.2b, 3b, 7a). The bulk of 2Ax is formed by AXM (Fig.7a).

Dorsal view (Figs.2b, 3, 7): FR, the arm, connects with the posterior radial basivenale (BRP) (Figs.2b, 3) anteriorly and AXM posteriorly (Figs.2b, 3, 16). FR may be very large and strongly sclerotized (Figs.2b, 3, 16), slender (Fig.7a) or absent.

AXM is a bi-lobed structure (Fig.7). It is composed of a *dorso-proximal lobe* (*d-pl*), a *dorso-distal lobe* (*d-dl*), a *dorso-proximal ridge* (*d-pr*) and a *dorso-distal ridge* (*d-dr*) (Fig.7b). The ridges and lobes are collectively termed the arm and body respectively. Each lobe is generally either deltoid- or harp-shaped. The ridges extend between and separate the lobes. Anteriorly and posteriorly, one ridge may conceal another. Medially the ridges are often separated by a *medial groove* (*mg*) (Fig.7c) which articulates with the 1Ax distal embayment and arch. Anteriorly the ridges may be very long or short, strongly or weakly elevated, but they always articulate with the 1Ax distal embayment and arch. Posteriorly the ridges are broadly separated from their ventral components to form a concavity to accommodate a tendon (see below). The proximal lobe and ridge are concealed under 1Ax in intact specimens leaving only the distal ridge and lobe visible (compare Fig.3, an intact wing articulation, with Fig.7, a dissected 2Ax). The proximal lobe articulates with the 1Ax ridges. Distally, the distal lobe is broadly fused to the medial plate (MED) (Fig.3b). The distal ridge and lobe articulate with FR (Fig.7a).

Ventral view (Fig.8): Both lobes and ridges have ventral components. For convenience the prefix ventro- is added. It is composed of a *ventro-proximal lobe* (*v-pl*), a *ventro-distal lobe* (*v-dl*), a *ventro-proximal ridge* (*v-pr*) and a *ventro-distal ridge* (*v-dr*).

The proximal lobe is equipped with a convexity. This convexity is termed the *posterior wing process junction* (*PWP*) and articulates with the posterior wing process by a short section of tough membrane.

The ventro-distal ridge terminus, here termed the *subalare tendon attachment point (STAP)* is generally spatulate and broadly separated from its dorsal components. This section forms a very large attachment point for a long section of very stiff membrane or tendon which is connected to PRA+PRJ. It is the latter which is joined to the subalare and finally the M79 muscle.

Median Plate (MED).

The median plate is composed of FM1 proximally and FM2 distally (Fig.3). Anteriorly, FM1 is fused to the proximal margin of the anterior medial basivenale (BMA), while FM2 is fused to the proximal margin of the posterior medial basivenale (BMP). The proximal margin of FM1 is fused to 2Ax, the postero-proximal margin is loosely associated with 1Ax distal arch terminus and the postero-distal margin is fused to the third axillary (3Ax). Therefore, the junction between 1Ax+2Ax and 3Ax is mediated by FM1. FM1 and FM2 may be separated, or partially or fully fused. FM1 is generally very large. Although FM1 can be greatly reduced, a small remnant always remains to mediate the junction between 1Ax+2Ax and 3Ax.

Third Axillary (3Ax).

The third axillary is composed of the cubital, anal and jugal axalaria and fulcalaria (AXCu + AXA + AXJ + FCu + FA + FJ) (Fig.9).

The head of 3Ax is composed of AXCu proximally, FCu medially and FA distally. The neck is composed of AXCu proximally and FA distally. The prong lies at the proximal margin of the neck and articulates with the detached AXCu fragment. The prong is often extended posteriorly and proximally to form a ridge. In some scarabaeoids FA and/or AXCu is greatly enlarged, forming a distinct arm.

The tail is composed of AXA proximally and FJ distally. These two sclerites are often separated by a medial weakening which is termed the window. The detached AXCu fragment is a small, separated piece of 3Ax, specifically AXCu (Figs.3b, 9). The M71 muscle inserts into this fragment, which, when contracted, pulls it down causing the proximal part of 3Ax to sink down and the distal part to lift and slightly rotate. This allows 3Ax to fold upon itself. The folding is mediated by the detached AXCu fragment and the 3Ax neck prong.

The Wing Base

First Basal Plate (1BP).

The first basal plate is composed of the precostal and costal fulcalaria and basivenalia (FPC + BPC + FC + BC collectively known as the humeral plate (HP)), the anterior subcostal basivenale (BSca), the posterior subcostal basivenale (BScP hidden beneath BSca), the subcosta anterior vein base (ScA bulge) and the radial basivenale (BR) (Figs.3, 10). 1BP is articulated to 1Ax, 2Ax and MED (Fig.3).

Dorsal view (Figs.3, 10-11, 17): HP distally is continuous with PC and C and folds posteriorly along its whole length (Figs.3b, 10-11). The membranous gap between HP and BScA + ScA can be of varying width (compare Fig.10 with Fig.11).

BScA is usually deltoid and separated into a *proximal section* and a *distal section* (Figs.10-11). The postero-proximal and posterior margins of BScA articulate with the 1Ax head via deep grooves and convexities mediated by tough membranous strips (Fig.3). Two convexities separated by a narrow groove are located proximally and a very deep concavity extends along the posterior margin of BScA.

The ScA bulge lies distal to BScA and is partially separated from the latter by a concavity of varying width and depth (compare Fig.3b with Fig.11). Posteriorly, the ScA bulge is adjacent to, and may be fused with, the anterior margin of BR. In some taxa a small convexity, an extension of the postero-proximal margin of the ScA bulge, overlaps the antero-distal margin of BR. This is termed the *ScA-BRP brace* (found only in Geotrupidae).

BRP is an arch-shaped structure curving anteriorly (Figs.3, 10, 13). The proximal and distal sections are termed the *proximal arch* and *distal arch* (Fig.13). Medially BRP forms a membranous embayment (Fig.13). If the embayment is wider anteriorly than posteriorly, then BRP is termed *closed* (Fig.13b). If not then BRP is termed *open* (Fig.13a). The proximal arch is usually secondarily divided into a large main arch and a small, proximal sub-arch termed *brp* (Fig.13a). The posterior margins of both *brp* and the proximal arch articulate with FR (Fig.3). Anteriorly, *brp* gives rise to a long extension which fuses with the posterior margin of BScA, forming part of the concavity which articulates with FSc2 (Fig.3b). This extension is termed the *brp projection* (Fig.13a). Distally, the distal arch gives rise to, and is fused with, RP (Figs.3b, 13).

Anterior view (Fig.12): HP is a slender structure which is usually clavate proximally and slender apically. The apex is continuous with PC and C (Fig.3b). The proximal section of HP folds dorsally and ventrally.

Ventral view (Fig.15): HP forms an eyelet which surrounds the small, proximal section of the basalare (see Fig.72 in Kukalová-Peck & Lawrence 1993:245). This junction is strengthened by a short section of tough membrane.

BScP (Fig.15) is a polished, smooth, usually deltoid structure which articulates with the distal section of the basalare when the wing is extended. No membrane mediates this junction. Distally BScP is continuous with ScP.

Second Basal Plate (2BP).

The second basal plate is a large central plate composed of the anterior and posterior medial basivenale, the anterior and posterior cubital basivenale and the base of the cubitus anterior vein (BMA + BMP + BCuA + BCuP + CuA) (Figs.3b, 13). 2BP is articulated to MED and 3Ax (Fig.3).

BMA has a similar shape to BR, an arch-shaped structure curving posteriorly (Fig.13a). It too is separated into a *proximal arch* and a *distal arch* (Fig.13b). The posterior margins of the BRP arches meet, but do not fuse with, the anterior margins of the BMA arches (Fig.13b). The BMA proximal arch is often extended ventrad below the BRP proximal

arch terminus (Fig.17). Posteriorly BMA is fused with BMP. This fusion may be incomplete (Figs.13a, 18) or complete (Fig.13b). Distally BMA is primitively continuous with MA.

BMP is a rectangular sclerite, which narrows proximally and broadens distally (Fig.13a). It is composed of a postero-proximal section, which lies posterior of BMA, and a distal section, which lies distal to BMA. The distal margin is continuous with MP and gives rise to one, or rarely two, tube-like braces, depending on the taxon concerned. These braces extend from BMP and fuse with either the base of BCuA or with CuA. They are termed the *BMP-BCuA brace* (Figs.3b, 13a, 19) and the *BMP-CuA brace* (Fig.13b) respectively. Browne (1991b:223) incorrectly termed these braces the *bma1+bmp1-BCuA brace* and the *bma1+bmp1-CuA brace* having erroneously concluded that BMA also shared in the formation of the brace with BMP. BCuA is either adjacent to or fused with BCuP (Figs.3b, 13b). The fusion can be deep and broad or secondarily reduced as a distal concavity, termed the *distal embayment* (Fig.13b).

Basalare (BAS).

The basalare is composed of a *head*, *neck*, and *tail*. It is not strictly part of the dorsal wing articulation but it serves an important function in the depression and elevation of the wing.

The head is clavate and bi-lobed, and articulates with HP and BScP. The proximal lobe articulates with the eyelet formed by HP ventrally and is termed the *HP lobe* (Fig.14). When the wing is closed, the distal lobe fits in an eyelet between the postero-ventral margin of HP and the antero-ventral margin of BScA. When the wing is extended the distal lobe articulates with BScP and is termed the *BScP lobe* (Fig.14).

Anteriorly the neck separates the two lobes and posteriorly it extends ventrad as a long tube-like structure which terminates at the tail. The tail is embedded in the proximal margin of the tergum, anterior of the posterior wing process (see Fig.72 in Kukalová-Peck & Lawrence 1993:245). It is broad and scaphoid.

Additional Structures.

The subcostal and radial proxalaria (PRSc + PRR) are fused together (Fig.2b). Their proximal margins are fused to the tergum while their distal margins are stiffly hinged to the proximal margin of 1Ax.

The cubital, anal and jugal proxalaria (PRCu, PRA, PRJ) are also fused to the tergum (Fig.2b). PRCu medially extends distad as a projection termed the medial extension. It can be of variable length and is associated with the proximal margin of the detached AXCu fragment of 3Ax.

PRA and PRJ are fused together and the antero-distal margin articulates weakly with the proximal margin of the 3Ax tail (Fig.2b). The ventral side of the postero-distal margin is stiffly connected to 2Ax by a very strong strip of membrane. Ventrally it is connected to the subalare which is attached to the M79 muscle. Posteriorly the subalare is connected to the lateral process of the epimeron by the short M70 muscle.

The anal basivenalia (BAA + BAP) are of variable size and degree of sclerotization (Fig.2b). Distally they are continuous with AA and AP respectively. The anterior margin of BAA is often closely associated with, or fused to, BCuP. The jugal basivenalia (BJA + BJP) are very small to absent (Fig.2b). Distally they are continuous with JA and JP respectively.

RESULTS AND DISCUSSION

Description format

Descriptions of scarabaeoid families and scarab subfamilies, and most other taxa of uncertain phylogenetic status were constructed based on a broad examination of many scarabaeoid taxa. To avoid undue repetition a hierarchical system of italic and plain font styles are employed. An hypothetical example of a 2Ax description format is as follows:

“Body - Dorsal View: Proximal lobe deltoid; long; arises medially from arm. *Base* very broad. *Apex* narrowly rounded; weakly curved anteriad. Antero-proximal margin with a concavity. Distal lobe deltoid ...”

This indicates that the structure being described is 2Ax body (one dash) in the dorsal view (full colon). More specifically, the description details the dorsal view of the proximal lobe including observations about its base and apex (italics). An additional note concerning the antero-proximal margin of the apex is also given. A description of the distal lobe follows and the hierarchical system is repeated.

The descriptions which follow are groundplans. Therefore, any modification of those states can be considered as derived.

Glaresidae

Introduction

Glaresidae are a small (about 50 species), virtually cosmopolitan monotypic family (Scholtz 1990) accommodating the genus *Glaresis* Erichson. It has wide geographical distribution which includes Africa, southern and eastern Europe, and North- and South America. It is absent from Australia. Approximately 50 species are included in the genus. Glaresidae biology and phylogeny were dealt with by Scholtz et al. (1987).

Glaresis was originally placed in the Trogidae based on a few generalized characters. The lack of any demonstrable apomorphies led Scholtz et al. (1987) to propose the family Glaresidae. Based on the non-chiasmate Xyp sex chromosome, Smith & Virkki (1978) concluded that *Glaresis* is the most archaic living scarabaeoid genus. This view was reiterated by Scholtz et al. (1994) in a review of all characters suites, including those of the hind wing articulation and wing base.

Hind Wing Articulation Description

First Axillary (Fig.20)

Head - Dorsal surface normal size. *Antero-dorsal margin* oriented weakly postero-distad; normal width; planate. *Antero-proximal margin* strongly enlarged ventrally. *Postero-proximal margin* weakly and narrowly enlarged proximally. *FSc2* base normal width. *Apex* oriented postero-distad; rounded. Anterior surface broad; very long; not waisted medially. *FSc1* absent. *Ventral projection* short but of normal width; tapers from base to apex; oriented disto-ventrad and curved posteriad; deeply concave. Apex narrow. Concavity located in the preapical area; surrounded by three unequally strong ridges. *Distal embayment* oriented dorsad. *FSc2* oriented distad and weakly dorsad; deltoid; extremely short and broad. Dorsal surface not enlarged. Head and neck dorsal surface weakly curved proximad.

Neck normal width and length; weakly oriented antero-distad; broadly articulated with 2Ax; discontinuous with tail. Proximal margin entire; curved ventrad; convex. Distal margin concave. *Distal embayment* weakly concave; shallow but broad.

Tail - Dorsal view: Proximal arch normal size; weakly concave. *Antero-proximal margin* concave. *Postero-proximal margin* convex. Articulation with PRR very weak. Posterior margin moderately concave. Distal arch normal size. *Apex* weakly curved ventrad and posteriad; acuminate. *Distal margin* straight. - Ventral view: Proximal, distal and posterior margins with very weak ridges.

Second Axillary (Figs.16, 21)

Radial Fulcalare strikingly broadly ovoid and extremely large; very strongly sclerotized; fused to the entire anterior margin of 2Ax distal lobe and ridge; almost indistinct from 2Ax.

Ridge - Dorsal view: Proximal ridge only very weakly differentiated from the body. *Apex to postero-median section* absent. *Postero-median to terminus* extremely narrow along the entire length; straight; very short; weakly distinct from lobe; strongly depressed below the distal ridge; weakly extended past the posterior margin of lobe; straight; oriented posteriad. Distal ridge only very weakly differentiated from the body. *Apex* oriented ventro-proximad; convex and broadly falcate; extremely short. *Anterior section* arises from the anterior margin of the distal lobe; extremely short; very broad; curves proximad. *Anterior to terminus* absent. Articulation with 1Ax weak; anteriorly 1Ax distal arch articulates below the proximal margin of the distal lobe; posteriorly 1Ax distal arch articulates between the proximal ridge and distal lobe. - Ventral view: Proximal and distal ridges are only weakly differentiated from each other; proximal ridge completely conceals the distal ridge. *Apex* broadly truncate. *Anterior to antero-median section* stout; curved distad. *Median to posterior section* not visible; obscured by the distal lobe. *Subalare tendon attachment point* moderately long and narrow; extends posteriad from the median; visible dorsally along the postero-proximal and postero-distal margins of the body; the postero-dorsal section of the proximal ridge is extended past the terminus of the subalare tendon attachment point. Terminus narrowly rounded; not curved ventrad; oriented posteriad.

Body - Dorsal view: about as long as broad. Proximal lobe oriented proximad; arises ventrally from the postero-medial section of the distal lobe and ridge; short; clavate;

strongly sclerotized; convex. *Base* narrow. *Apex* very broadly rounded; straight. *Anterior margin* concave. *Posterior margin* weakly enlarged; concave. Distal lobe large; deltoid; much larger than proximal lobe; strongly sclerotized; planate; not sloped ventrad. *Anterior margin* normal length; straight; oriented postero-distad. *Base* extremely broad; extends from the apex to the terminus of the ridge. *Apex* very broadly rounded. *Posterior margin* straight; not reduced. - Ventral view: Proximal lobe short; convex. *Posterior wing process junction* ovoid; occupies the posterior margin of the lobe. Distal lobe extremely large; continuous with ridge; weakly concave.

Median Plate (Fig.3)

FM1 oriented posteriad. *Anterior to posterior section* extremely broad. *Proximal margin* convex. Articulation with 2Ax extends from the antero-distal margin of the distal lobe to the posterior section over the posterior section of the ventral ridge. *Distal margin* very broadly and strongly fused to 3Ax. FM2 moderately long; oriented posteriad; very broadly acerose; separated from FM1 by a short, extremely narrow section of membrane.

Third Axillary (Fig.22)

Head weakly convex; normal length. Proximal margin weakly convex. Anterior margin weakly convex; not enlarged ventrally. *Antero-proximal and antero-distal margins* not extended anteriorly. AXCu present as a very slender, anterior extension along the proximal margin of head. FCu normal size; occupies most of the head; weakly ovoid to deltoid. FA moderately narrow; occupies the distal margin of head. *Anterior margin* entire. Suture line between FCu and FA present. Suture line between FCu and AXCu present. Suture line between FA and FJ present.

Neck very weakly elevated proximally but not distally. FCu section of neck absent. AXCu forms entire neck; extremely long. Proximal margin elevated as a weakly distinct ridge. *Ridge* does not curve distad; very long. Dorsal surface of ridge is weakly curved proximad. Posterior section absent. Prong armed with a single extremely narrow and short tooth; oriented postero-proximad. Detached AXCu fragment slenderly ovoid; moderately sclerotized.

Tail long; narrow; convex. Dorsal surface oriented laterad. Proximal margin strongly elevated dorsad to the dorsal plane of the neck; slopes distad along its entire length. Anterior to antero-median section very weakly concave. Antero-median to posterior section convex; oriented dorso-distad. *Window* absent. AXA straight. FJ+AXJ and AXA equally narrow. Suture line between FJ and AXJ present. Suture line between FA+AXJ and AXA present. Suture line between AXA and AXCu present.

Hind Wing Base Description

First Basal Plate (Fig.10)

Humeral Plate extremely narrow; long. Anterior margin convex; lies very distant from BScA and ScA. Apex very weakly deltoid; extremely narrow; not curved ventrad. Dorsal margin sinuate. Proximal margin convex; very weakly curved ventrad. Ventral margin sinuate. Suture line between FPC+BPC and FC+BC present. *FC+BC* present as a very long and narrow sclerite posterior to FPC+BPC.

Anterior Subcostal Basivenale oriented antero-distad; slenderly ovoid; convex; weakly elevated dorsad. Proximal section indistinct from the distal section. *Distal margin* discontinuous from the ScA bulge; separated by a shallow concavity. Apex broadly rounded. – Subcosta Anterior moderately convex. Bulge very broad.

Radial Basivenale extremely broadly open; broadly convex but extremely narrow; continuous with radial stem; angled antero-proximad. Proximal arch slenderly deltoid; continuous with the anterior margin of BR; extensions absent; angled postero-proximad. *Posterior margin* rounded. *Anterior margin* strongly elevated above the posterior margin of the ScA bulge; very broad; straight; angled antero-proximad. Embayment broad but extremely shallow; broadly deltoid. Distal arch absent. *br* absent. *br projection* narrow; convex; fused to the postero-distal margin of BScA.

Second Basal Plate (Figs.23, 17-19)

MA-BMA Junction present. – MP-BMP Junction: MP broadly continuous with BMP along all margins and surfaces. – Crimp Patterns absent. – BMP-CuA Brace absent. – BMP-BCuA Brace present; very strong but slender; extends posteriad; distinct from BMP; much more strongly convex than BMP. Posterior fused within a deep concavity on the antero-proximal margin of BCuA.

Medial Basivenalia massive; BMA and BMP incompletely fused. BMA extremely broad and very long; scaphoid; lies antieriad of BMP. *Postero-medial section* gives rise to FM2. *Proximal, medial and distal surfaces* very strongly convex. *Anterior margin* broadly concave. *Proximal arch* planate and straight; extremely long; extremely broad; oriented antero-proximad. Apex terminates below BR proximal arch apex. Postero-proximal section gives rise to FM1. *Distal arch* Dorsal view: weakly differentiated from the posterior section of BMA but distinct; weakly extended distad. – Ventral view: strongly extended distad and continuous with BMA remnant. BMP *proximal and distal sections* undifferentiated; broadly fused to both IBP and BCu. *Anterior section* weakly rectangular; convex; curves antieriad; incompletely fused to BMA, separated by a very deep groove; discontinuous with the posterior section of BMP. *Posterior section* present; broadly deltoid; flat; strongly depressed below BMA and BMP anterior section; weakly sclerotized; fused to BMA. *Distal section* distinct from the BMP-BCuA brace; long; broad; rectangular; strongly convex.

Cubital Basivenalia narrowly fused. Posterior margin of BCuA fused with the anterior margin of BCuP. *Suture line* present. BCuA deltoid; small; convex; oriented postero-distad; strongly sclerotized; lies posteriad of BMP and antieriad of the CuA base. *Anterior margin* with a moderately broad but shallow concavity. *Posterior margin* continuous with CuA. BCuP very large; ovoid; convex; oriented postero-distad; moderately sclerotized. Distal embayment absent. – Cubitus Anterior fused to BCuA. Junction marked by a distinct suture.

Basalare

Head - HP lobe very small; continuous with neck. Apex broadly truncate. *Dorsal surface* weakly elevated from neck; not polished. BScP lobe claviform; weakly projects dorsad.

Dorsal surface ovoid; weakly convex; polished; not depressed from neck. *Ventral surface* polished. – Posterior Subcostal Basivenale deltoid, polished.

Discussion

Glaresidae exhibit the generalized scarabaeoid state of all characters, including those of the wing articulation and wing base which leaves no doubt that Glaresidae are the most archaic family in the Scarabaeoidea, quite likely very close in structure to the ancestral scarabaeoid (Scholtz et al. 1994), and the sister group of all other scarabaeoids (Browne & Scholtz 1995). This family does not display any autapomorphic characters of the hind wing articulation or wing base (Browne 1991a, 1993; Scholtz et al. 1994; Browne & Scholtz 1995).

Passalidae

Introduction

The Passalidae are a virtually cosmopolitan family with approximately 40 genera and 500 species which are most abundant in tropical regions (Reyes-Castillo 1970).

The Passalidae are a well-defined family whose monophyly is supported by numerous derived characters and there is little doubt that it is one of the more archaic scarabaeoid families (Reyes-Castillo 1970). The numerous and unusual derived features exhibited by Passalidae have led some workers to suggest that they be excluded completely from the Scarabaeoidea (Reyes-Castillo pers. comm. 1990). This family is comprised of two subfamilies, Aulacocyclinae and Passalinae (Reyes-Castillo 1970).

Hind Wing Articulation Description

First Axillary (Fig.24)

Head - Dorsal surface normal size. *Antero-dorsal margin* normal width; weakly deplanate; oriented weakly postero-distad. *Antero-proximal margin* very strongly enlarged ventrally. *Postero-proximal margin* weakly enlarged proximally. *FSc2* base normal width. Apex rounded; oriented postero-distad. Anterior surface broad; very long; not waisted medially. *FSc1* very weak. *Ventral projection* tapers from the base to apex; short but of average width; deeply concave; oriented disto-ventrad and curved posteriad. Apex narrow. Concavity located in the preapical area; surrounded by three unequally strong ridges. *Distal embayment* oriented dorsad. *FSc2* deltoid; broad; very convex; oriented distad and weakly dorsad. *Dorsal margin* not enlarged. Head and neck dorsal surface weakly curved proximad.

Neck normal width and length; weakly oriented antero-distad; broadly articulated with 2Ax. Proximal margin straight. Distal margin weakly concave. *Distal embayment* concave; moderately narrow.

Tail - Dorsal view: Proximal arch strongly reduced along all margins. *Antero-proximal margin* concave. *Dorsal surface* weakly concave. *Postero-proximal margin* weakly convex; weakly recurved. Articulation with PRR strong. Posterior margin concave. Distal arch

strongly expanded anteriorly and distally. *Distal margin* very weakly convex. *Apex* very weakly curved ventrad and posteriad; acuminate. - Ventral view: Proximal arch margined by a broad ridge. Posterior margin with a long ridge; entire but weak. Distal margin with a broad ridge.

Second Axillary (Fig.25)

Radial Fulcalare moderately broad. Terminus fused to the 2Ax ridge-body junction. *Point of fusion* moderately broad; weakly extended along the anterior margin of 2Ax.

Ridges - Dorsal view: Proximal ridge entire; weakly distinct from lobe. *Apex* narrow. *Anterior section* partially concealed by the distal ridge. *Antero-median to postero-median section* extremely narrow; partially enlarged above the distal ridge. *Posterior section* strikingly enlarged above the distal ridge; oriented posteriad. *Apex* narrow. Distal ridge very weakly distinct from lobe. *Apex* narrow but broadly falcate; convex; moderately short; oriented ventro-proximad; not fused to the proximal ridge apex. *Anterior section* moderately short; moderately narrow; strongly curved proximad. *Median to posterior section* slender; oriented posteriad. - Ventral view: Proximal ridge moderately narrow; distinct from lobe. *Anterior to median section* conceals the proximal section of the distal ridge; curved proximad. *Postero-median to posterior section* partially obscured by the distal ridge; visible proximally as a slender, concave piece. Distal ridge moderately broad; very long. *Postero-median to posterior section* rectangular; moderately broad. *Proximal and posterior sections* arise from the posterior margin of the distal lobe. *Subalare tendon attachment point* extends posteriad from the median; strikingly lengthened; slender.

Body - Dorsal view: about as long as broad. Proximal lobe small; deltoid; arises antero-medially from ridge but depressed below the ridge; strongly sclerotized; convex; oriented proximad. *Base* very narrow. *Apex* truncate; weakly curved anteriad. *Anterior margin* deeply concave. *Posterior margin* weakly concave; weakly enlarged. Distal lobe strikingly reduced posteriorly and apically; longer and broader than the proximal lobe; strongly sclerotized; weakly concave; arises from the extreme anterior section of the ridge. *Proximal half* very thick; strongly sclerotized. *Distal half* thin; strongly sclerotized; weakly concave. *Anterior margin* strongly sclerotized; weakly sinuate; normal length. *Base* broad. *Apex* reduced; rounded. *Posterior margin* concave; reduced. - Ventral view: Proximal lobe partially concealed by the distal ridge; slender; cylindrical; convex; distinct from proximal ridge; oriented weakly antero-proximad. *Posterior wing process junction* weakly ovoid; occupies the posterior margin of the lobe. *Base* narrow. *Apex* round. Distal lobe deltoid; flat; small; distinct from distal ridge.

Median Plate (Fig.26)

FM1 large. *Anterior section* very narrow. *Antero-median section* abruptly broad. *Antero-distal margin* fused with FM2; a small membranous gap separates the two anteriorly. *Proximal margin* broadly fused with 2Ax from a point just posterior of the apex to the terminus. *Distal margin* broadly fused to 3Ax along the antero-proximal margin to the median. FM2 weakly distinct from FM1; short; deltoid.

Third Axillary (Fig.27)

Head moderately broad; normal length; weakly convex. Proximal margin straight. Anterior margin straight; not enlarged ventrally. AXCu absent. FCu normal size; weakly convex to concave. FA large; long; rectangular; extends far ventrad along the entire length of the head and dorsally occupies about one fourth of the head. Suture line between FCu and AXCu present. Suture line between FCu and FA present. Suture line between FA and AXCu present.

Neck not elevated dorsad; oriented postero-proximad. FCu section of neck absent. Neck comprised of AXCu proximally and medially, and FA distally. AXCu weakly elevated; broad; extended proximally and posteriorly. *Proximal embayment* oriented postero-proximad; extremely broad; deeply concave. *Distal margin* extended ventrad; large. Prong very broad. Ridge enlarged dorsally relative to AXA. *Apex* armed with two very weak teeth; extremely broad. Apices broadly rounded. Detached AXCu fragment deltoid; very large; slender. *Proximal margin* broadly but weakly concave. *Distal margin* convex; aciculate.

Tail long and narrow; weakly convex; very weakly sclerotized; oriented posteriad; lies ventrad to the head+neck. *Dorsal surface* oriented laterad. AXA and AXJ indistinct; slender and very weakly sclerotized; straight. *Suture line* absent. FJ deltoid; moderately sclerotized. *Posterior* separates AXJ from AXA. *Apex* recurved to form a "stem" connecting the more dorsal FA with the tail. Anterior margin of the tail extends anteriorly below the head+neck. Proximal and distal margins straight.

Hind Wing Base Description

First Basal Plate (Fig.28)

Humeral Plate extremely narrow and very long; distant from BScA. Anterior margin not curved posteriad. Dorsal and ventral margins nearly straight. *Apex* weakly curved ventrad. Suture lines between FPC+BPC and FC+BC absent.

Anterior Subcostal Basivenale broadly deltoid; weakly bi-lobed; weakly convex; oriented distad. Proximal margin with two embayments separated by a long ridge. *Embayments and ridge* oriented proximad. Posterior embayment margined posteriorly by a small ridge. Proximal and distal sections indistinct from each other. BScA ventrally deeply concave. BR, br and the br projection broadly fused to BScA. *Suture lines* absent. – Subcosta Anterior weakly convex. Bulge not prominent.

Radial Basivenale open; long; convex; slenderly deltoid; oriented proximad. Proximal arch extremely broad; very long; rectangular; continuous with the anterior margin of BR; oriented posteriad. *Postero-distal section* rounded. Anterior margin convex; moderately narrow. Embayment normal size. Distal arch absent. br very broad; strongly sclerotized. *br projection* extremely broad; fused to the distal and posterior margins of BScA.

Second Basal Plate (Fig.29)

MA-BMA Junction absent. – MP-BMP Junction entire; MP continuous with BMP. – Crimp Patterns absent. – BMP-CuA Brace – slender; convex; adjacent to, but more convex and

distinct from, the distal margin of 2BP; intervening membrane sclerotized. Anterior section continuous with MP. Posterior section continuous with CuA. – BMP-BCuA Brace absent.

Medial Basivenalia massive; strongly sclerotized. BMA broadly scaphoid; very large; angled postero-proximad; flat but elevated above and separated from BMP by a deep groove; lies anteriad, but not proximad, of BMP; fully fused to BMP. *Anterior margin* concave. *Proximal arch* planate; straight; broad; enlarged antero-proximally. *Distal arch* extremely long; allantoid; extends far distad. BMP planate; large; broadly fused to 1BP and BCuA; very weakly separated into anterior and posterior sections; discontinuous with brace. *Anterior margin* concave; fused to 1BP. *Proximal margin* deeply concave. *Posterior margin* fused to BCuA and CuA; indistinct. *Distal margin* discontinuous with brace.

Cubital Basivenalia large; ovoid or weakly deltoid; narrowly fused. Postero-distal margin of BCuA fused to antero-proximal margin of BCuP. *Suture line* very weak but present. BCuA about the same size as BCuP; oriented postero-distad. Distal margin with a very deep embayment. *Embayment* strongly sclerotized. BCuP oriented antero-distad. – Cubitus Anterior basally connected to BCuA along the postero-proximal margin. Anterior interrupted by the BMP-CuA Brace.

Basalare (Fig.30)

Head - HP lobe short; broad; weakly elevated. *Dorsal surface* truncate; weakly polished. BScP lobe large; broad; oriented disto-ventrad; laterally ovoid. *Dorsal surface* broadly ovoid; polished. *Ventral surface* polished. – Posterior Subcostal Basivenale ovoid; long; polished; oriented proximo-ventrad.

Discussion

As with other morphological characters (see Scholtz 1990), passalids exhibit numerous autapomorphic wing articulation and wing base character states. Monophyly of the Passalidae is supported by the fact that all of the taxa in this family share the following 13 apomorphic character states of the wing articulation and wing base:

1. 1Ax: the proximal arch is very strongly reduced along all margins,
2. the distal arch strongly expanded anteriorly and distally;
3. 2Ax: the distal lobe is strikingly reduced posteriorly and apically,
4. arises from the extreme anterior section of the ridge;
5. 3Ax: the tail is very weakly sclerotized,
6. the demarcation between sclerites absent.
7. the tail extends anteriad below the posterior margin of the neck,
8. is separated from the head+neck by a tube-shaped stem;
9. 1BP: the proximal margin of BScA is interrupted by a deep and broad groove, giving it a bi-lobed appearance which provides additional support for the 1Ax head teeth,
10. the proximal and distal sections of BScA are indistinct from each other,
11. the proximal arch of BR is extremely broad, very long and rectangular,
- 12/13. BR, br and the br projection apices are fused to, and indistinguishable from BScA.

Passalidae share six apomorphic character states of the wing articulation and wing base with Diphylostomatidae, Lucanidae, Glaphyridae, Trogidae, Bolboceratidae and Pleocomidae (Browne & Scholtz 1995).

Diphylostomatidae

Introduction

The Diphylostomatidae are a monotypical family with three species endemic to the western USA. Males and females are dimorphic. Males are smaller and long-winged and females are larger, with reduced wings, eyes and antennae. Nothing is known about their biology and the larvae are unknown.

Diphylostoma was described as a member of Aesalinae (Lucanidae) but since it apparently has little in common with Lucanidae, Holloway (1972) elevated *Diphylostoma* to family status. She based this on the presence of exposed protrochantin, exposed second abdominal segment, reduced female genitalia in *Diphylostoma* and differences in wing venation, male genitalia and leg structure between *Diphylostoma* and Lucanidae. This system is currently accepted by other workers in the field (Scholtz 1990).

Holloway (1972) suggested that Diphylostomatidae are closely related to Geotrupidae. Recently, Caveney (1986) suggested, based on synapomorphic ommatidium structure, that Diphylostomatidae are probably more closely related to Lucanidae. This relationship is supported by wing articulation and wing base characters (Browne & Scholtz 1995).

Hind Wing Articulation Description

First Axillary (Fig.31)

Head - Dorsal surface normal size. *Antero-dorsal margin* normal width; weakly deplanate; oriented weakly postero-distad. *Postero-proximal margin* weakly enlarged proximally. *Proximal margin* strongly enlarged ventrally. *FSc2* base normal width. Apex rounded; oriented postero-distad. Anterior surface broad; very long; not waisted medially. *FSc1* very weak. *Ventral projection* tapers from base to apex; short but of normal width; deeply concave; oriented disto-ventrad and curved posteriad. Apex narrow; rounded. Concavity located in the preapical area; surrounded by three unequally strong ridges of unequal length. *Distal embayment* oriented dorsad. *FSc2* deltoid; broad; very convex; oriented distad and weakly dorsad; not enlarged dorsally. Head and neck dorsal surface weakly curved proximad.

Neck normal width and length; strongly curved proximad; weakly oriented antero-distad. Proximal margin moderately convex. Distal margin deeply but narrowly concave; broadly articulated with 2Ax. *Distal embayment* concave.

Tail - Dorsal view: Proximal arch normal size. *Dorsal surface* weakly concave. *Antero-proximal margin* concave. *Postero-proximal margin* convex; weakly recurved. Articulation with PRR strong but short. Distal arch normal size; slightly longer than the proximal arch; weakly oriented postero-proximad. Apex aciculate; weakly curved ventrad and posteriad. *Distal margin* straight. - Ventral view: Proximal arch margined by very weak ridges.

Posterior margin with a long ridge; entire but very weak. Distal arch with a very broad, but weakly elevated ridge.

Second Axillary (Fig.32)

Radial Fulcalare very narrow; virgate; poorly sclerotized. Terminus fuses to the 2Ax ridge. *Point of fusion* very narrow; restricted to the medial section of the 2Ax ridge; absent from body.

Ridges - Dorsal view: Proximal ridge entire; distinct from lobe. *Anterior to antero-medial section* concealed distally by distal ridge. *Antero-medial to posterior section* moderately broad; partially elevated above the distal ridge. *Posterior section* acerose; strikingly enlarged above the distal ridge; oriented posteriad. Distal ridge distinct from lobe. *Apex* narrowly falcate; moderately short; convex; curved; oriented ventro-proximad. *Anterior section* slender; moderately short; curved proximad. Fuses with the anterior margin of the distal lobe. *Median section* curved distad. *Posterior section* obscured by the proximal ridge. - Ventral view: Proximal ridge broad; indistinct from the proximal lobe. *Apex* aciculate. *Anterior section* broadly acerose; weakly curved proximad; conceals the distal ridge proximally. *Median to posterior section* concealed by the distal ridge. Distal ridge moderately broad. *Median and posterior sections* arise from the proximal and posterior margins of the distal lobe; indistinct from lobe. *Median section* convex. *Subalare tendon attachment point* moderately long and narrow; extends posteriad from the median; not curved ventrad. Posterior margin rounded. Distal separated from the dorsal surface of the ventro-distal lobe.

Body - Dorsal view: Proximal lobe narrow but long; deltoid; arises postero-medially from ridge; moderately sclerotized; flat; depressed below the ridge; oriented proximad. *Base* enlarged anteriorly and posteriorly. *Anterior and posterior margins* greatly enlarged; concave. *Median to apex* reduced. *Apex* narrowly rounded. Distal lobe roundly deltoid; small; reduced distally; shorter but broader than proximal lobe; weakly sclerotized; weakly concave. *Anterior margin* normal length; weakly concave. *Posterior margin* weakly concave. - Ventral view: Proximal lobe distally concealed by the distal ridge; slender; weakly convex. *Posterior wing process junction* ovoid; occupies the posterior margin of the lobe. Distal lobe weakly concave; continuous with ridge.

Median Plate (Fig.33)

FM1 and FM2 fused as a single plate; weakly sclerotized. *Anterior, median and posterior margins* about equally broad. *Proximal margin* broadly fused to 2Ax. *Distal margin* broadly fused to 3Ax.

Third Axillary (Fig.34)

Head narrow; normal length; weakly convex. Proximal margin straight. Anterior margin narrow; not enlarged ventrally; weakly convex. FCu normal size. *Distal margin* reduced by FA. FA broad; weakly sclerotized; only visible laterally. AXCu large; occupies the proximal margin of the head. *Anterior margin* weakly enlarged anteriad. Suture line

between FCu and FA present. Suture line between FCu and AXCu present. Suture line between AXCu and FA present. Suture line between FA and FJ present.

Neck weakly elevated dorsad. FCu section of neck absent. Neck comprised of AXCu. *Proximal embayment* oriented proximad; small; shallowly concave. Ridge posterior section present. Prong armed with a single tooth. *Tooth* short; deltoid. Apex weakly rounded. Detached AXCu fragment very small; slender; weakly sclerotized.

Tail long; moderately broad. Dorsal surface oriented laterad. Anterior section only weakly concave. Median and posterior section very weakly convex to planate. *Window* absent. FJ and AXJ equally broad; moderately sclerotized. *Suture line* present. FJ occupies an equal amount of the tail as FJ+AXJ. AXA moderately long; straight. Suture line between FJ+AXJ and AXA present. Suture line between AXA and AXCu strong.

Hind Wing Base Description

First Basal Plate (Fig.35)

Humeral Plate slender. Anterior margin convex sinuate. Apex curved ventrad. Dorsal margin weakly sinuate; slender; distant from BScA. Ventral margin weakly sinuate. Suture lines between FPC+BPC and FC+BC absent.

Anterior Subcostal Basivenale broadly deltoid; weakly convex; oriented distad. Proximal section separated from the distal section by a prominent suture; as large as the distal section. Antero-median section oriented anteriad; weakly convex; terminus adjacent to HP. Apex broadly rounded; oriented distad. – Subcosta Anterior convex. Bulge not prominent; narrow; separated from BScA by a weak concavity.

Radial Basivenale strongly open; straight; slender; oriented proximad; continuous with radial stem. Proximal arch slenderly deltoid; oriented posteriad. *Anterior section* present. *Postero-distal margin* rounded. Anterior margin weakly convex to straight; narrow. Embayment normal size. Distal arch absent. *br* weak. *br projection* moderately narrow; strongly convex; extends anteriad from the antero-proximal margin of *br*; distinct from BScA.

Second Basal Plate (Fig.36)

MA-BMA Junction absent. – MP-BMP Junction not entire. Anterior margin continuous with BMP. – Crimp Patterns absent. – BMP-CuA Brace slender; convex; entire; adjacent to, but distinct from, the distal margin of 2BP. Anterior section continuous with MP. Point of fusion discontinuous. Posterior section continuous with CuA. – BMP-BCuA Brace absent.

Medial Basivenalia very large; rectangular. Anterior and posterior margins weakly convex. Anterior margin separated from BR by membrane. Posterior margin separated from BCuA by a sclerotized, concave groove. BMA broadly scaphoid; weakly convex; separated from BMP by a broad, shallow groove; lies anteriad, but not proximad of BMP; fully fused to BMP. *Proximal arch* planate; straight; enlarged antero-proximally; slightly shorter than the distal arch. *Distal arch* distinct; oriented antero-distad. BMP rectangular; convex; discontinuous with brace; distinct from 1BP and BCu. *Anterior section* rectangular; weakly

convex; separated from the posterior section by a weak impression. *Posterior section* present; weakly convex; depressed below the anterior section.

Cubital Basivenalia large; ovoid to deltoid; broadly fused. Posterior margin of BCuA fused with anterior margin of BCuP. *Suture line* weak. BCuA about the same size as BCuP; deltoid; convex; oriented weakly postero-distad; strongly sclerotized; an extension enters CuA along the anterior margin, just proximal of the brace-vein junction; curved anteriad. BCuP large; oriented distad; weakly sclerotized. *Proximal margin* forms a convex ridge. Embayment shallow. – Cubitus Anterior fused to BCuA; only partially separated by a weak sclerotized groove. Anterior section interrupted by the BMP-CuA Brace.

Basalare (Fig.37)

Head - HP lobe digitate; very thin; small. *Apex* clavate; weakly curved ventrad. *Base* adjacent to, but separated from, BScP lobe. BScP lobe claviform; convex; bulbous; obscures neck: much larger than HP lobe. *Dorsal surface* moderately polished. *Ventral surface* rough. – Posterior Subcostal Basivenale deltoid; polished.

Discussion

Monophyly of the Diphyllostomatidae is supported by the fact that all of the taxa in this family share the following five apomorphic character states of the wing articulation and wing base:

1. 1Ax: the distal margin of the neck is deeply, but narrowly concave;
2. 2Ax: the dorso-proximal lobe base is greatly enlarged anteriorly and posteriorly,
3. but medially to apically reduced,
4. the distal margin of the subalare tendon attachment point is strongly separated from the dorsal surface of the ventro-distal lobe, the latter extends posteriad beneath the former;
5. 2BP: BCuA curves anteriad.

Analysis of wing articulation and wing base characters indicates that Diphyllostomatidae are a distinctive family warranting familial status and the sister group of Lucanidae (Browne & Scholtz 1995). Diphyllostomatidae share six apomorphic character states of the wing articulation and wing base with Passalidae, Lucanidae, Glaphyridae, Trogidae, Bolboceratidae and Pleocomidae (Browne & Scholtz 1995).

Lucanidae

Introduction

The Lucanidae are a large family with five large subfamilies and several small ones which include approximately 100 genera and 750 species with virtually world-wide distribution. Lucanidae are a well defined family whose monophyly is supported by many derived characters (Crowson 1967, 1981; Howden 1982; Scholtz 1990). Caveney (1986) suggested, based on synapomorphic ommatidium structure, that Lucanidae are probably more closely related to Diphyllostomatidae. This relationship was reiterated by Scholtz (1990) and is supported by wing articulation and wing base characters (Browne & Scholtz 1995).

Hind Wing Articulation Description

First Axillary (Fig.38)

Head - Dorsal surface normal size. *Antero-dorsal margin* normal width; weakly deplanate; oriented weakly postero-distad. *Postero-proximal margin* weakly enlarged proximally. *Proximal margin* strongly enlarged ventrally. *FSc2* base normal width. Apex rounded; oriented postero-distad. Anterior surface broad; very long; not waisted medially. *FSc1* very weak. *Ventral projection* tapers from base to apex; short but of normal width; deeply concave; oriented disto-ventrad and curved posteriad. Apex narrow. Concavity located in the preapical area; surrounded by three unequally strong ridges of unequal length. *Distal embayment* oriented dorsad. *FSc2* deltoid; broad; very convex; oriented distad and weakly dorsad; not enlarged dorsally. Head and neck dorsal surface weakly curved proximad.

Neck normal width and length; weakly oriented antero-distad; recurved relative to tail. Proximal margin convex. Distal margin weakly concave; broadly articulated with 2Ax. *Distal embayment* shallow; broad.

Tail - Dorsal view: weakly concave. Proximal arch normal size. *Dorsal surface* weakly concave. *Antero-proximal margin* concave. *Postero-proximal margin* weakly convex. Articulation with PRR strong but short. Posterior margin weakly concave. Distal arch normal size; slightly larger than the proximal arch; weakly oriented postero-proximad. *Apex* aciculate; weakly curved ventrad and posteriad. *Distal margin* very weakly concave. - Ventral view: Proximal and distal arches with ridges. Posterior margin with a prominent ridge.

Second Axillary (Fig.39)

Radial Fulcalare present as re-enforced membrane.

Ridges - Dorsal view: Proximal ridge entire; distinct from lobe. *Apex* lengthened anteriorly, beyond the ventro-distal ridge apex. *Anterior to antero-median section* partially concealed distally by distal ridge; strongly curved ventro-distad beneath the distal ridge; separated from the distal ridge by a broad gap which extends to the mid-line of 2Ax. *Antero-median to posterior section* moderately broad; elevated above the distal ridge. *Posterior section* acerose; strikingly enlarged above the distal ridge; oriented posteriad. Distal ridge distinct from lobe. *Apex* narrowly falcate; moderately short; convex; very strongly curved distad; reduced distally and anteriorly, revealing the distal and apical sections of the dorso-proximal ridge. *Anterior section* slender; moderately short; shorter than the proximal ridge; strongly curved proximad; recurved, but curves abruptly ventrad towards the apex. Fuses with the anterior margin of the distal lobe. *Subapical to antero-median section* strongly oriented postero-distad. *Median to posterior section* strongly depressed ventrad, curving beneath the antero-median section of the dorso-proximal ridge, giving the appearance that the dorso-distal ridge and lobe twists around the dorso-proximal ridge and lobe. - Ventral view: Proximal ridge moderately broad; indistinct from the proximal lobe. *Apex* aciculate. *Anterior section* broadly acerose; weakly curved proximad; conceals the distal ridge proximally. *Median to posterior section* concealed by the distal ridge. Distal ridge moderately broad. *Median and posterior sections* arise from the proximal and posterior

margins of the distal lobe; indistinct from lobe; short; narrow. *Median section* convex. *Subalare tendon attachment point* moderately long and narrow; extends posteriad from the median; not curved ventrad; weakly visible dorsally. Posterior margin rounded.

Body - Dorsal view: Proximal lobe short; narrow; deltoid; arises postero-medially from ridge; moderately sclerotized; flat; depressed below the ridge; oriented proximad. *Base* weakly enlarged. *Anterior and posterior margins* greatly enlarged; concave. *Apex* narrowly rounded; curved anteriad. Distal lobe large and broad; roundly deltoid; not reduced distally; much larger than proximal lobe; weakly sclerotized; convex; slopes strongly ventrad from the ridge giving the appearance that the distal ridge and lobe are curving and twisting around the proximal ridge and lobe. *Base* very broad. *Apex* broadly rounded. *Anterior margin* normal length; weakly concave. *Posterior margin* weakly concave. - Ventral view: Proximal lobe narrow and long; weakly convex. *Posterior wing process junction* ovoid; occupies the posterior margin of the lobe. Distal lobe weakly concave; continuous with ridge; planate.

Median Plate (Fig.40)

FM1 oriented proximad anteriorly and postero-proximad medially and posteriorly; rectangular. *Anterior, median and posterior sections* extremely broad. *Proximal margin* straight. Articulation with 2Ax extends from apical angle of the distal lobe over the posterior section of the ventral ridge. *Distal margin* broadly fused to 3Ax. FM2 oriented proximad and weakly posteriad; rectangular; separated from FM1 by a moderately wide section of membrane; very small; acerose.

Third Axillary (Fig.41)

Head narrow; normal length; weakly convex. Proximal margin straight. Anterior margin narrow; not enlarged ventrally; weakly convex. FCu normal size. *Distal margin* strongly reduced by FA and AXCu. FA broad; weakly sclerotized; only visible laterally. AXCu large; occupies half of the head. *Anterior margin* enlarged anteriad. Suture line between FCu and FA present. Suture line between FCu and AXCu present. Suture line between AXCu and FA present. Suture line between FA and FJ present.

Neck very weakly elevated dorsad. FCu section of neck absent. Neck comprised of AXCu. *Proximal embayment* oriented proximad; small; shallowly concave. Ridge posterior section present. Prong armed with a single tooth. *Tooth* short; weakly deltoid. Apex moderately broadly rounded. Detached AXCu fragment very small; slender; weakly sclerotized.

Tail long; aciculate; convex. Dorsal surface oriented laterad. Anterior only weakly convex. Median and posterior very weakly convex to planate. *Window* absent. FJ and AXJ equally broad; moderately strongly sclerotized. *Suture line* present. FJ occupies an equal amount of the tail as FJ+AXJ. AXA moderately long; straight. Suture line between FJ+AXJ and AXA present. Suture line between AXA and AXCu strong.

Hind Wing Base Description

First Basal Plate (Fig.42)

Humeral Plate moderately long. Anterior margin weakly sinuate. Apex deltoid; curved ventrad. Dorsal margin weakly sinuate; distant from BScA. Ventral margin weakly sinuate. Suture lines between FPC+BPC and FC+BC present.

Anterior Subcostal Basivenale broadly deltoid; weakly convex; oriented distad. Proximal section long; separated from the distal section by a prominent suture; as large as the distal section. Antero-median oriented anteriorly; weakly convex; terminus distant from HP. Apex broadly rounded; oriented distad. – Subcosta Anterior weakly convex. Bulge narrow.

Radial Basivenale convex; strongly open; slender; oriented antero-proximad; continuous with radial stem. Proximal arch narrow; short; oriented postero-proximad. *Anterior section* present. *Postero-distal margin* rounded. Anterior margin elevated above BScA; narrow. Embayment normal size. Distal arch absent. br moderately sclerotized; large; discontinuous with BR. *br projection* apically broad; distinct from BSc.

Second Basal Plate (Fig.43)

MA-BMA Junction absent. – MP-BMP Junction entire. MP almost continuous with BMP; enters below the distal plate. – Crimp Patterns absent. – BMP-CuA Brace moderately broad; convex; entire; adjacent to, but distinct from, the distal margin of 2BP. Anterior continuous with MP. Point of fusion discontinuous. Posterior continuous with CuA. – BMP-BCuA Brace absent.

Medial Basivenalia very large; rectangular. Anterior and posterior margins concave. Anterior margin separated from BR by membrane. Posterior margin separated from BCuA by a sclerotized, concave groove. BMA broadly scaphoid; weakly convex; separated from BMP by a broad, shallow groove; lies anteriorly, but not proximad of BMP; fully fused to BMP. *Proximal arch* allantoid; long; weakly convex; straight; enlarged antero-proximally. *Distal arch* distinct; oriented distad. BMP rectangular; convex; discontinuous with brace; distinct from 1BP and BCu. *Anterior section* rectangular; weakly convex; separated from the posterior section by a weak impression. *Posterior section* present; weakly convex; depressed below the anterior section.

Cubital Basivenalia broadly fused. Posterior margin of BCuA fused with anterior margin of BCuP. *Suture line* weak. BCuA about the same size as BCuP; deltoid; strongly convex; oriented weakly distad. BCuP deltoid; weakly convex; oriented postero-distad; weakly sclerotized. *Proximal margin* forms a convex ridge. Embayment very shallow. – Cubitus Anterior fused to BCuA. Anterior interrupted by the BMP-CuA Brace.

Basalare (Fig.44)

Head - HP lobe weakly claviform; convex; dorsally elevated from neck; continuous with neck. *Apex* curved ventrad. *Dorsal surface* polished. *Ventral surface* rough. BScP lobe claviform; weakly concave; not elevated from neck. *Dorsal surface* lenticular; polished; lies below the ventral margin of the HP lobe. *Ventral surface* rough. – Posterior Subcostal Basivenale weakly deltoid to ovoid; polished.

Discussion

Monophyly of the Lucanidae is supported by the fact that all of the taxa in this family share the following six apomorphic character states of the wing articulation, all confined to 2Ax:

1. the apex of the dorso-distal ridge is very strongly curved distad,
2. reduced distally and anteriorly,
3. revealing the distal and apical sections of the dorso-proximal ridge, the anterior section of the dorso-distal ridge is recurved with the apex assuming a ventral orientation (in addition to the distal curvature discussed above),
4. the subapical to antero-median section of the dorso-distal ridge is strongly oriented postero-distad,
5. the median to posterior section of the dorso-distal ridge and lobe is strongly depressed ventrad, curving beneath the antero-median section of the dorso-proximal ridge, giving the appearance that the dorso-distal ridge and lobe twists around the dorso-proximal ridge and lobe,
6. the dorso-proximal ridge apex is lengthened anteriorly, beyond the ventro-distal ridge apex.

Lucanidae share six apomorphic character states of the wing articulation and wing base with Passalidae, Diphylostomatidae, Glaphyridae, Trogidae, Bolboceratidae and Pleocomidae (Browne & Scholtz 1995).

Howden (1982) considered lucanids to be most closely related to Passalidae. Caveney (1986) suggested, based on synapomorphic acone ommatidium structure between all diphylostomatids and many lucanids, that Lucanidae are probably more closely related to Diphylostomatidae, a view which is supported here (Browne & Scholtz 1995).

The Lucanidae do not exhibit any wing articulation and wing base character states which support Howden's (1982) proposal that it branched off early from other members of the Scarabaeoidea and subsequently followed a separate evolutionary pathway, as do Passalidae.

Glaphyridae

Introduction

Glaphyridae are represented in the Holarctic Region by Glaphyrinae (with *Amphicoma* and *Lichnanthe* the largest genera) and in South America by Lichniinae (*Lichnia* and *Cratoscelis*). Adults are long-legged, hairy and brightly coloured.

The males of *Amphicoma* spp. are pollen feeders and visit flowers (Crowson 1967), whereas, according to Ritcher (1958), adults of *Lichnanthe* never feed. Ritcher (1958) noted that larvae of *Lichnanthe vulpina* (Hertz) feed on cranberry roots and those of *L. rathvoni* Le Conte on decaying leaves and other plant debris. The length of the life cycle is 3-4 years (Ritcher 1966).

Hind Wing Articulation Description

First Axillary (Fig.45)

Head - Dorsal surface normal size. *Antero-dorsal margin* normal width; weakly deplanate; oriented weakly postero-distad. *Antero-proximal margin* extended anteriorly as a large convexity. *Postero-proximal margin* weakly enlarged proximally. *Proximal margin* strongly enlarged ventrally; convex. *FSc2* base normal width. Apex rounded; oriented postero-distad. Anterior surface broad; very long; not waisted medially. *FSc1* very weak. *Ventral projection* tapers from base to apex; short but of normal width; shorter than *FSc2*; deeply concave; oriented disto-ventrad and curved posteriad. Apex narrow. Dorsal surface concave. - Ventral surface flattened. Concavity located in the preapical area; surrounded by three unequally strong ridges of unequal length. *Distal embayment* oriented dorsad. *FSc2* deltoid; broad; very convex; oriented distad and weakly dorsad; not enlarged dorsally. Proximal margin broadly fused to the ventrad projection. Dorsal surface convex. Ventral surface concave. Head and neck dorsal surface weakly curved proximad.

Neck normal width and length; narrower than head; recurved relative to tail; weakly oriented antero-distad. Proximal margin straight. Distal margin concave; broadly articulated with 2Ax. *Distal embayment* concave; moderately deep; broad.

Tail - Dorsal view: concave. Proximal arch normal size; extended postero-proximad and weakly so postero-distad. *Dorsal surface* weakly concave. *Antero-proximal margin* convex. *Postero-proximal margin* convex. Articulation with PRR strong but short. Posterior margin weakly concave. Distal arch normal size; weakly curved ventrad; extended postero-distad. *Apex* aciculate; strongly curved ventrad and posteriad. *Distal margin* very weakly concave. - Ventral view: Proximal arch with a broad ridge. Posterior margin with a narrow but prominent ridge. Distal arch with a very small ridge.

Second Axillary (Fig.46)

Radial Fulcalare not sclerotized; present only as re-enforced membrane.

Ridges - Dorsal view: Proximal ridge entire; distinct from lobe. *Anterior to antero-median section* concealed by the distal ridge. *Antero-median to posterior section* moderately broad; strongly elevated above the distal ridge; extends adjacent to the distal ridge. *Posterior section* acerose; strikingly enlarged above the distal ridge; oriented posteriad. Distal ridge distinct from lobe; extends anteriorly and curves very weakly proximally from the dorso-distal lobe base. *Apex* extremely broad; falcate; moderately short; convex; oriented weakly ventro-proximad. *Anterior section* broad; moderately short; curved proximad. *Median section* abruptly curved ventrad. *Posterior section* extends adjacent to, but lies below, the proximal ridge. - Ventral view: Proximal ridge very broad; indistinct from lobe. *Apex* very broadly rounded; curved distad. *Anterior section* very broad; sinuate; conceals the distal ridge proximally. *Median to posterior section* concealed by the distal ridge. Distal ridge extremely broad. *Anterior to median section* concealed by the proximal ridge. *Median and posterior sections* arise from the proximal, posterior and postero-distal margins of the distal lobe; indistinct from lobe; short; extremely broad. *Median section* convex. *Postero-median section* waisted. *Subalare tendon attachment point* moderately long and narrow; extends posteriad from the median; not curved ventrad; spatulate; moderately visible dorsally.

Body - Dorsal view: Proximal lobe short; broad; arises ventrally and postero-medially from the ridge; moderately sclerotized; flat; oriented proximad. *Base* strongly enlarged anteriorly and posteriorly; broad. *Anterior and posterior margins* greatly enlarged; concave. *Apex* broadly rounded; curved anteriad. Distal lobe small and broad; roundly deltoid; reduced distally; broader but shorter than the proximal lobe; moderately sclerotized; convex. *Base* very broad. *Apex* broadly rounded. *Anterior margin* normal length; weakly concave. *Posterior margin* weakly concave. - Ventral view: Proximal lobe extremely small; weakly convex; nearly completely obscured by the distal ridge. *Posterior wing process junction* small; ovoid; occupies the posterior margin of the lobe. Distal lobe weakly concave; continuous with ridge; small.

Median Plate (Fig.47)

FM1 oriented proximad anteriorly and postero-proximad medially and posteriorly; rectangular. *Anterior section* narrow. *Median and posterior section* extremely broad. *Proximal margin* straight. Articulation with 2Ax extends from apical angle of the distal lobe over the posterior section of the ventral ridge. *Distal margin* moderately narrowly fused to 3Ax. FM2 oriented proximad and weakly posteriad; rectangular; separated from FM1 by a moderately wide section of membrane; very small; acerose.

Third Axillary (Fig.48)

Head strikingly convex; moderately broad; normal length. Anterior margin narrow; not enlarged ventrally; weakly convex. FCu normal size; occupies the anterior to antero-medial section of head. *Posterior and proximal margins* reduced by a greatly enlarged AXCu. *Distal margin* strongly reduced by FA and AXCu. FA broad; convex; extended distad along its entire length. AXCu large; occupies about half of the head. *Anterior margin* extended anteriad. Suture line between FCu and FA present. Suture line between FCu and AXCu present. Suture line between AXCu and FA present. Suture line between FA and FJ present. Neck elevated dorsad. FCu section of neck absent. Neck comprised by AXCu. *Proximal embayment* oriented proximad; small; shallowly concave. Ridge posterior section present. Prong armed with a single tooth. *Tooth* very broad; long; deltoid. Apex broadly rounded. Detached AXCu fragment large; broad; moderately sclerotized.

Tail long; acuminate; dorsal surface is recurved. Dorsal surface oriented laterad. Anterior section only weakly convex. Median and posterior section very weakly convex to flat. Window absent. Distal margin straight. FJ and AXJ equally broad; moderately strongly sclerotized. *Suture line* present. AXA occupies an equal amount of the tail as FJ+AXJ; straight. Suture line between FJ+AXJ and AXA present. Suture line between AXA and AXCu strong.

Hind Wing Base Description

First Basal Plate (Fig.49)

Humeral Plate moderately broad and short. Anterior margin sinuate. Apex broadly rounded; curved ventrad. Dorsal margin convex; distant from BScA. Distal margin reduced. Ventral

margin concave. Suture line between FPC+BPC and FC+BC present. FPC+BPC small; rectangular; much shorter than FC+BC; distinct.

Anterior Subcostal Basivenale broadly deltoid; weakly convex; oriented distad. Proximal section extended as a short, narrow rectangle; separated from the distal section by a prominent suture; as large as the distal section. Distal section continuous with the ScA bulge. Apex broadly rounded; oriented distad. – Subcosta Anterior weakly convex. Bulge narrow.

Radial Basivenale convex; open; slender; oriented antero-proximad; continuous with the radial stem. Proximal arch moderately narrow; short; directed strongly postero-proximad. *Anterior section* present. *Posterior margin* extended proximad. Postero-distal margin rounded. Anterior margin elevated above BScA; narrow. Embayment of normal size; very strongly deltoid; surrounding margins are straight. Distal arch extremely weak; oriented posteriad. *br* moderately sclerotized; very small; discontinuous with BR. *br projection* dove-tail shaped; apically broad; arises from the antero-proximal margin of BR; distinct from BScA.

Second Basal Plate (Fig.50)

MA-BMA Junction absent. – MP-BMP Junction entire. MP continuous with BMP. – Crimp Patterns absent. – BMP-CuA Brace moderately broad and convex; adjacent to, but distinct from, the distal margin of 2BP. Anterior margin slightly reduced; appears to arise from below MP; oriented postero-distad. Point of fusion discontinuous with MP. Posterior margin continuous with CuA; curved postero-distad. – BMP-BCuA Brace absent. – False BMP-BCuA Brace present as a very strongly convex tube; formed from the median section of BMP. Posterior margin distant from CuA and BCuA.

Medial Basivenalia very large. Anterior and posterior margins concave. Anterior margin adjacent to BR. Posterior margin separated from BCuA by a sclerotized concave groove and membrane. BMA broadly scaphoid; completely fused with but distinct from BMP. *Anterior margin* concave. *Median* convex. *Posterior margin* reduced. *Proximal arch* allantoid; planate; straight; enlarged antero-proximally. *Distal arch* distinct; oriented antero-distad; very small. BMP extremely narrow and short; discontinuous with the BMP-CuA brace; indistinct from the False BMP-BCuA brace; distinct from 1BP and BCu. *Proximal section* extremely small; weakly convex. *Medial section* distinct; tube-shaped; separated from the proximal and distal sections by deep grooves. *Distal section* slender; more weakly convex than the medial section. Antero-distal section separated from the posterior section by a weak impression. Postero-distal section present; very weakly depressed below the anterior section. *Distal margin* strongly elevated from the surrounding membrane.

Cubital Basivenalia fused. Postero-proximal margin of BCuA fused with the antero-distal margin of BCuP. *Suture line* present. BCuA slightly smaller than BCuP; deltoid; convex; oriented distad; strongly sclerotized. BCuP weakly ovoid and convex; oriented posteriad; weakly sclerotized. Embayment shallow. – Cubitus Anterior adjacent to, but not fused with BCuA. Junction formed as a deep groove.

Basalare (Fig.51)

Head - HP lobe convex; dorsally elevated from neck; continuous with neck. *Apex* not curved. *Dorsal and ventral surfaces* rough. BScP lobe claviform; convex; weakly elevated from neck. *Dorsal surface* lenticular; slender; polished; lies below the ventral margin of the HP lobe. *Ventral surface* polished. – Posterior Subcostal Basivenale weakly square-shaped; polished.

Discussion

Monophyly of the Glaphyridae is supported by the fact that all of the taxa in this family share the following five apomorphic character states of the wing articulation and wing base:

1. 1Ax: the distal arch apex of the tail is strongly curved ventrad;
2. 2Ax: the apex of the dorso-distal ridge is extremely broad along its entire length, extends anteriorly, and curves very weakly proximally from the dorso-distal lobe base,
3. the subalare tendon attachment point is very short, very broad, and apically shallowly and narrowly concave;
4. 1BP: the BR embayment is of normal size, but is more strongly deltoid, with all margins straight;
5. 2BP: the medial section of BMP is distinct from the remainder of BMP as an elevated tube-shaped structure.

The phylogenetic position of Glaphyridae within the Scarabaeoidea has been an issue of some debate. This family was once accorded superfamily status due to its unusual distinctiveness, but Hinton (1967) more realistically accorded family status. Based on male and female genitalia, Zunino (1988) claimed that glaphyrids occupy an intermediate position between Melolonthinae and Scarabaeidae. Holloway (1972) noted that, according to Crowson's (1967) key, glaphyrids occupy a position close to Diphyllostomatidae. d'Hotman & Scholtz (1990a,b) and Scholtz (1990) presented convincing evidence, from numerous adult and larval characters, which suggests that glaphyrids are archaic. More importantly, they found that the basal piece of the male genitalia is very similar to some lucanid genera.

Analysis of wing articulation and wing base characters indicates that Glaphyridae are the sister group of Trogidae + Bolboceratidae + Pleocomidae, with whom they share a single derived state of the hind wing base (Browne & Scholtz 1995).

Trogidae

Introduction

The Trogidae are a monophyletic, cosmopolitan family, consisting of three genera and about 300 species. Trogids have wide distribution, but occur mainly on the southern continents in sandy arid regions (Scholtz 1986). *Trox* Fabricius occurs naturally in Europe, North America and Africa. *Omorgus* Erichson occurs in South and North America,

Australia and Africa, whereas *Polynoncus* Burmeister occurs only in South America. Adults and larvae are keratin-feeders.

The Trogidae are a well-defined family whose monophyly is supported by numerous derived characters (Scholtz 1986; Scholtz 1990; Scholtz & Peck 1990; Browne et al. 1993). Their phylogenetic position within the Scarabaeoidea as one of the most archaic families has been proposed by Crowson (1967, 1981) and Scholtz (1986). Howden (1982) concluded that trogids are highly apomorphic and probably closely related to the Hybosoridae. The wings of Trogidae have previously been well-studied (Browne et al. 1993).

Hind Wing Articulation Description

First Axillary (Fig.52)

Head - Dorsal surface normal size weakly convex; moderately broad. *Antero-dorsal margin* normal width; weakly deplanate; oriented postero-distad. *Antero-proximal margin* very strongly enlarged ventrally. *Postero-proximal margin* weakly enlarged proximally. *FSc2* base normal width. Apex rounded; oriented postero-distad. Anterior surface broad; very long; not waisted medially. *FSc1* very weak. *Ventral projection* tapers from base to apex; short but of normal width; deeply concave; oriented disto-ventrad and curved posteriad. Apex narrow. Concavity located in the preapical area; surrounded by three unequally strong ridges. *Distal embayment* moderately broad; oriented dorsad. *FSc2* deltoid; broad; very convex; oriented distad and weakly dorsad. Dorsal surface concave. Ventral surface convex. Apex blunt. *Dorsal margin* not enlarged. Head and neck dorsal surface weakly curved proximad.

Neck moderately broad; moderately long; oriented weakly antero-distad; broadly articulated with 2Ax. Proximal margin weakly convex. Distal margin concave. *Distal embayment* moderately concave. Embayment re-enforcement moderately strong.

Tail - Dorsal view: Proximal arch normal size; weakly concave. *Postero-proximal margin* convex. Articulation with PRR strong. Posterior margin weakly concave. Distal arch normal size. Apex weakly curved postero-ventrad; aciculate. -Ventral view: Proximal arch with a slender ridge. Posterior margin with a prominent ridge. Distal margin with a slender ridge.

Second Axillary (Fig.53)

Radial Fulcalare slender; weakly sclerotized.

Ridges - Dorsal view: Proximal ridge distinct from lobe; entire. *Anterior to antero-median section* partially concealed by the distal ridge. *Antero-median to posterior section* strongly enlarged above the distal ridge; demarcated from body by an impression. *Posterior section* incorporated into lobe; distinct from lobe but only weakly extended past the posterior margin of lobe; moderately enlarged above the distal ridge; extends posteriad. Distal ridge weakly distinct from lobe. Apex oriented ventro-proximad; convex and broadly falcate; moderately short. *Anterior section* slender; moderately short; curved proximad and weakly ventrad. *Median to posterior section* extends below the proximal ridge; very weakly

demarcated from body by an impression. *Posterior section* strongly acerose; extends far past the posterior margin of lobe. - Ventral view: Proximal ridge moderately broad; long; curved distad; distinct from lobe. *Apex* aciculate. *Anterior to antero-median section* digitate; slender; obscures distal ridge. *Median to posterior section* obscured by the distal ridge. Distal ridge broad but short. *Anterior to median section* concealed by the proximal ridge. *Median and posterior sections* arise from the proximal and posterior margins of the distal lobe; weakly distinct from lobe; broad but short. *Median section* convex. *Postero-median section* waisted. *Subalare tendon attachment point* very long and narrow; apically not curved ventrad; posterior margin rounded; extends posteriad from the median; weakly visible dorsally.

Body - Dorsal view: about as long as broad. Proximal lobe oriented proximad; long; moderately small; weakly deltoid; arises from the postero-medial section of ridge; strongly sclerotized; convex. *Base* broad. *Posterior margin* weakly enlarged; concave. *Apex* weakly curved antero-proximad; narrowly truncate. Distal lobe large and broad; roundly deltoid; much larger than proximal lobe; moderately sclerotized; planate. *Base* moderately broad. *Apex* broadly rounded. *Anterior margin* normal length; straight. *Posterior margin* very weakly concave; very weakly reduced. - Ventral view: Proximal lobe narrow and long; convex. *Posterior wing process junction* formed as an ovoid convexity which extends antero-proximally from the postero-distal corner of the lobe; long. Distal lobe discontinuous with ridge; planate.

Median Plate (Fig.54)

FM1 narrow; oriented proximad anteriorly and postero-proximad medially and posteriorly. *Anterior section* broad narrow. *Median and posterior section* extremely broad. *Proximal margin* convex. Articulation with 2Ax extends along the posterior third of the distal lobe over the posterior section of the ventral ridge. *Distal margin* weakly and narrowly fused to 3Ax. FM2 very long; oriented posteriad; acerose. *Apex* separated from FM1; separated by a membranous gap.

Third Axillary (Fig.55)

Head broad and truncate; strikingly convex; normal length. Proximal margin straight. Anterior margin weakly convex; not enlarged ventrally. FCu normal size; occupies two-thirds of the head; weakly ovoid. FA moderately large; occupies the distal third of head, broadening posteriorly; narrowly deltoid. Suture line between FCu and FA present. Suture line between FCu and AXCu present. Suture line between FA and FJ present.

Neck moderately elevated dorsad. FCu forms the anterior portion of neck. FA forms the distal portion of neck. AXCu section of neck extremely narrow; moderately elevated. Prong armed with two teeth. *Anterior tooth* very small; fastigate. *Apex* rounded. *Posterior tooth* moderately short; fastigate. *Apex* rounded. Ridge enlarged dorsally relative to AXA. Detached AXCu fragment pectinate; thin. *Apex* aciculate; armed with one long posterior tooth, and two short anterior teeth.

Tail narrow, long and convex; acerose. Dorsal surface oriented mesad. Anterior section concave. Median section concave. Posterior section convex. *Window* absent. FJ antero-

distal margin strongly curved ventrad. FJ+AXJ slender; weakly concave. AXA strongly sclerotized; occupies about two-thirds of the tail area; straight. Suture line between FJ and AXJ absent. Suture line between FJ+AXJ and AXA present. Suture line between AXA and AXCu present.

Hind Wing Base Description

First Basal Plate (Fig.56)

Humeral Plate slender; lies distant from BScA. Anterior margin weakly sinuate; moderately sclerotized. *Apex* weakly curved ventrad. Dorsal margin weakly sinuate. *Apex* concave. Ventral margin weakly sinuate. Suture line between FPC+BPC and FC+BC present.

Anterior Subcostal Basivenale deltoid; convex; oriented distad. Proximal and distal sections separated by a distinct suture. *Proximal section* as large as the distal section. *Apex* broadly rounded. Postero-proximal margin with an embayment. Distal margin separated from ScA bulge by a deep concavity. – Subcosta Anterior weakly convex. Bulge very broad.

Radial Basivenale very weakly convex; broadly open; oriented antero-proximad; continuous with radial stem. Proximal arch slenderly deltoid; small; straight; continuous with the anterior section of BR; directed posteriad. *Postero-distal section* rounded. Anterior margin straight; very narrow; only medially weakly elevated dorsad. Embayment normal size. Distal arch absent. *br* weak but present; very slender; moderately sclerotized; continuous with BR. *br projection* apically broad; distinct from BSc.

Second Basal Plate (Fig.57)

MA-BMA Junction absent. – MP-BMP Junction entire. MP almost continuous with BMP; arises from below the distal plate. – Crimp Patterns weak to moderately strong; found on MP and the antero-distal section of 2BP. Crimps are weakly convex; margined by impressions; dense proximally, sparse distally. – BMP-CuA Brace present; moderately thin; convex; distant from distal margin of 2BP; extends postero-proximad from 2BP. Anterior entire; fused to the postero-proximal corner of MP and the antero-distal corner of BMP. Point of fusion continuous. Posterior discontinuous with CuA; fused to the antero-proximal angle of CuA. *Point of fusion* marked by a suture line. – BMP-BCuA Brace absent. – False BMP-BCuA Brace present as a moderately broad and strongly convex tube extending along the distal margin of 2BP. Anterior margin with overlapping plates. Posterior margin terminates adjacent to, but not touching or fused with, BCuA.

Medial Basivenalia - General habitus: very large; broad and long. Anterior and posterior margins distally weakly concave. BMA broadly scaphoid; completely fused to BMP. *Proximal and medial surfaces* flat. *Distal surface* convex. *Anterior margin* weakly concave. *Proximal arch* weakly convex and straight; enlarged antero-proximally; deltoid to weakly allantoid. *Distal arch* weakly distinct. BMP rectangular; convex; distinct from brace; separated from both 1BP and BCu. *Proximal section* weakly convex; separated from BMA by a shallow concavity. *Postero-median section* concave. *Antero-distal section* formed as a large, rectangular convexity; distinct from the postero-distal section. Distal

margin forms the anterior half of the BMP-BCuA brace; elevated from surrounding membrane. Antero-distal margin aquiline; with many overlapping plates. *Postero-distal section* forms the posterior half of the BMP-BCuA brace; as equally elevated as the antero-distal section.

Cubital Basivenalia broadly fused. Posterior margin of BCuA fused with anterior margin of BCuP. *Suture line* present. BCuA slightly smaller than BCuP; deltoid; strongly convex; oriented distad; strongly sclerotized; lies proximal to the base of CuA. BCuP weakly rectangular; less convex than BCuA; oriented distad; moderately sclerotized. Distal embayment weak. – Cubitus Anterior arises from within a toroid concavity in BCuA.

Basalare (Fig.58)

Head - HP lobe weakly claviform; convex; elevated from neck; continuous with neck. *Dorsal surface* polished. BScP lobe moderately claviform; concave; weakly elevated from neck. *Dorsal surface* lenticular; polished. *Ventral surface* rough. – Posterior Subcostal Basivenale deltoid; polished.

Discussion

Monophyly of the Trogidae is supported by the fact that all of the taxa in this family share the following four apomorphic character states of the wing articulation and wing base (Browne et al. 1993 only recorded three, autapomorphy no. 1 is new):

1. 2Ax: the subalare tendon attachment point is short, narrow and apically rounded;
2. 2BP: with transverse crimps on the medial vein, mesal of the medial bridge and distal of 2BP,
3. the BMP-CuA brace is either reduced or modified (both are autapomorphic) depending on the genus;
4. RP3+4 is lost.

Trogidae share six apomorphic character states of the wing articulation and wing base with Passalidae, Diphyllotomatidae, Lucanidae, Glaphyridae, Bolboceratidae and Pleocomidae (Browne & Scholtz 1995). Analysis of wing articulation and wing base characters indicates that Trogidae occupy an intermediate position between Glaphyridae and Bolboceratidae + Pleocomidae, more closely related to the latter (Browne & Scholtz 1995).

Bolboceratidae

Introduction

The Bolboceratidae are a large, well-defined family whose monophyly is supported by numerous derived characters (Scholtz 1990; Browne 1991a,b; Scholtz & Browne, in press).

Bolboceratidae, previously classified as one of four subfamilies of Geotrupidae, have recently been elevated to family status since there is little evidence for the traditional view that Geotrupidae constitute a monophyletic assemblage (Ritcher 1969a,b; Scholtz 1990;

Browne 1991a; Scholtz & Browne, in press). Bolboceratid wings are well known (Browne 1991a,b; Browne & Scholtz 1995). The following is a summary of those findings.

Hind Wing Articulation Description

First Axillary (Fig.66)

Head - Dorsal surface normal size; convex. *Antero-dorsal margin* normal width; weakly deplanate; very strongly oriented ventro-distad. *Antero-proximal margin* very strongly enlarged ventrally. *Postero-proximal margin* weakly enlarged proximally. *FSc2* convex. Base normal width. Apex rounded; oriented postero-distad. Anterior surface broad; very long; not waisted medially. *FSc1* very weak; small; slender; fused to the proximal margin of the ventrad projection. Dorsal and ventral surfaces convex. *Apex* acute. *Ventral projection* weakly tapered from the base to apex; short but of average width; deeply concave; oriented disto-ventrad and curved posteriad. Apex narrower than the base; rounded. Concavity located in the preapical area; surrounded by three unequally strong ridges. Dorso-medial surface concave. Ventral surface convex. *Distal embayment* oriented dorsad. *FSc2* weakly deltoid to digitate; moderately broad; oriented distad and weakly dorsad. Dorsal surface very convex; not enlarged. Ventral surface convex. Apex truncate. Head and neck dorsal surface weakly curved proximad. Ventral re-enforcing ridge prominent.

Neck normal width but extremely short; weakly oriented antero-distad; broadly articulated with 2Ax; discontinuous with tail. Proximal margin curved ventrad. Distal margin concave. *Distal embayment* concave; with an extremely strong secondary embayment supported posteriorly by a sclerotized plate; extremely deep but very narrow.

Tail - Dorsal view: Proximal arch strongly but narrowly expanded postero-distally; falcate; strongly curved postero-distad. *Antero-proximal margin* deeply concave. *Dorsal surface* weakly concave. *Postero-proximal margin* extremely convex; strikingly recurved; strongly enlarged proximad. Articulation with PRR posteriorly extremely strong; very weak anteriorly; markedly enlarged posteriorly and distally; with a broad and strong connection along the medial groove and recurved arch. Posterior margin moderately concave. Distal arch normal size. Apex very weakly curved ventrad and posteriad; acuminate. Distal margin straight. - Ventral view: Proximal arch with a slender ridge. Posterior margin with a prominent ridge. Distal arch with an extremely slender ridge.

Second Axillary (Fig.67)

Radial Fulcalare extremely slender; moderately sclerotized; articulation with 2Ax ridge extremely narrow.

Ridges - Dorsal view: Proximal ridge entire; distinct from lobe. *Apex* not spatulate. *Anterior to antero-median section* partially concealed by the distal ridge. *Antero-median to postero-median section* strongly elevated above the distal ridge; demarcated from body by an impression. *Posterior section* moderately enlarged above the dorso-distal ridge; slender; incorporated into lobe; distinct from lobe but only weakly extended past the posterior margin of lobe; extends posteriad from the median. Distal ridge weakly distinct from lobe. *Apex* oriented ventro-proximad; convex and broadly falcate; moderately short.

Anterior section moderately short; curved proximad and very weakly ventrad. *Median to posterior section* extends adjacent but below the proximal ridge; very weakly demarcated from body by an impression. *Posterior section* acerose; very weakly extended past the posterior margin of lobe. - Ventral view: Proximal ridge slender; long; curved distad; distinct from lobe. *Apex* aciculate. *Anterior to antero-median section* digitate; slender; conceals the distal margin of the distal ridge. *Median to posterior section* obscured by the distal ridge. Distal ridge slender; long. *Anterior to median section* partially concealed by the proximal ridge; curves proximad. *Median and posterior sections* arise from the posterior margin of the distal lobe; distinct from lobe; broad and moderately long. *Median section* convex. *Postero-median section* not waisted. *Subalare tendon attachment point* moderately long and narrow; apically not curved ventrad; posterior margin rounded; extends posteriad from the median reversal; broadly visible dorsally.

Body - Dorsal view: about as long as broad. Proximal lobe oriented proximad; arises from the postero-medial section of the ridge, depressed below the ridge; short and small; deltoid; strongly sclerotized; concave. *Posterior margin* weakly enlarged; concave. *Base* moderately broad. *Apex* narrowly rounded; weakly curved anteriad. Distal lobe moderately large and broad; deltoid; much larger than proximal lobe; moderately sclerotized; very strongly convex. *Anterior margin* normal length; concave. *Apex* narrowly rounded. *Posterior margin* straight; weakly reduced. - Ventral view: Proximal lobe extremely small; convex. *Posterior wing process junction* nearly completely conceals the proximal lobe; formed as a prominent ovoid convexity which extends anteriorly from the posterior margin of the distal ridge. Distal lobe moderately large and broad; discontinuous with ridge; weakly concave.

Median Plate (Fig.68)

FM1 oriented strongly postero-distad. *Anterior section* very narrow. *Median section* narrow. *Postero-median to posterior section* very broad; convex. *Proximal margin* convex. Articulation with 2Ax extends from the postero-medial margin of the distal lobe to the posterior section over the posterior section of the ventral ridge. *Distal margin* very weakly and narrowly fused to 3Ax. FM2 very short; oriented posteriad; acerose; separated from FM1 by a long, broad section of membrane.

Third Axillary (Fig.69)

Head planate; moderately broad; normal length. Proximal margin straight. Anterior margin weakly convex; not enlarged ventrally; from the proximal angle it slopes sharply postero-distad. *Antero-proximal margin* extended anteriad; very broadly rounded. *Antero-distal margin* extended ventrad; broadly but shallowly concave. Posterior section enlarged dorsally to form an arm; proximally continuous with the neck. FCu normal size; distinct; occupies most of the head; broadly deltoid. FA extremely small. *Anterior margin* strongly reduced by a much enlarged FCu. AXCu reduced proximally; very narrowly margins the postero-proximal margin of FCu. Suture line between FCu and FA present. Suture line between FCu and AXCu present. Suture line between FA and FJ present.

Neck proximally moderately elevated; distally weakly elevated as an arm. FCu section of neck absent. AXCu forms entire neck. Proximal margin elevated as a very narrow ridge. *Ridge* extends to antero-median of the proximal margin of tail; moderately short; enlarged dorsally relative to AXA. Dorsal surface of ridge is curved distad. Medial and distal margins weakly convex; formed by FCu anteriorly and FA posteriorly. Prong armed with a single short tooth; oriented proximo-dorsad; narrow. Detached AXCu fragment saddle-shaped; strongly curved ventrad both anteriorly and posteriorly; slender; moderately sclerotized.

Tail narrowly deltoid; long; planate. *Dorsal surface* oriented mesad. Anterior and median section weakly calceolate. Posterior section planate. *Window* present; weak; occupies most of the tail. FJ+AXJ very slender; occupies distal fifth of tail; moderately sclerotized. Suture line between FJ and AXJ present. Suture line between FA+AXJ and AXA present. AXA more weakly sclerotized than FA+AXJ; the former occupies less than a fifth of the tail; straight. Suture line between AXA and AXCu present.

Hind Wing Base Description

First Basal Plate (Fig.70)

Humeral Plate moderately broad and short. Anterior margin sinuate; strongly sclerotized; lies distant from BScA. Apex very narrow; weakly curved ventrad. Dorsal margin strongly sinuate; distant from BScA. Proximal margin weakly sinuate; curved proximo-ventrad. Ventral margin strongly sinuate. Suture line between FPC+BPC and FC+BC absent.

Anterior Subcostal Basivenale oriented distad; broadly deltoid; weakly convex. Proximal and distal sections separated by a prominent suture. *Proximal section* about the same size as the distal section. Apex broadly rounded. Proximal margin extended as a long, narrow rectangle curving postero-ventrad. Distal section continuous with ScA bulge; separated by a weak concavity. – Subcosta Anterior moderately convex. Bulge moderately broad.

Radial Basivenale convex; open; very weakly discontinuous with radial stem; angled antero-proximad; rectangular. Proximal arch slenderly deltoid; moderately long; angled posteriad; continuous with the anterior margin of BR. *Postero-distal section* rounded. Anterior margin not elevated above the posterior margin of ScA bulge; broad; straight; angled antero-proximad. Embayment normal size. Distal arch very weakly discontinuous with radial stem; oriented posteriad. br strongly sclerotized; occupies more than half of the proximal arch; discontinuous with BR. *br projection* small.

Second Basal Plate (Fig.71)

MA-BMA Junction absent. – MP-BMP Junction: MP discontinuous with BMP; arises from below the distal plate. – Crimp Patterns absent. – BMP-CuA Brace present; slender; convex; extends postero-distad from 2BP. Anterior section reduced; fused to the postero-distal corner of 2BP; not fused with BMP or the MP-BMP junction. Posterior section continuous with CuA; fused to the antero-proximal angle of CuA. – BMP-BCuA Brace absent.

Medial Basivenalia moderately reduced on all margins; narrow and long; rectangular but narrowing proximally. Anterior and posterior margins concave. BMA narrow; completely fused to BMP. *Proximal and medial surfaces* flat. *Distal surface* convex. *Anterior margin* concave. *Proximal arch* broadly deltoid; planate; enlarged antero-proximally. *Distal arch* distinct; very long; slender; convex. BMP junction with BMA discontinuous and very broad; rectangular; very weakly separated from BMA by a shallow concavity; flat; distinct from brace; separated from 1BP and BCu. *Postero-median, antero-distal and postero-distal sections* indistinguishable from each other. Distal margin strongly elevated above the surrounding membrane.

Cubital Basivenalia narrowly fused; slender and long. Postero-proximal margin of BCuA fused with the antero-proximal margin of BCuP. *Suture line* present. BCuA very narrow and long; convex; oriented postero-distad; strongly sclerotized; lies proximal of CuA. BCuP very narrow and long; convex; oriented postero-distad; weakly sclerotized. Distal embayment narrow but deep. – Cubitus Anterior adjacent to, but discontinuous with, BCuA. Junction separated by a concavity. Base strongly shifted distad.

Basalare (Fig.72)

Head - HP lobe small; continuous with neck. *Apex* broadly rounded. *Dorsal surface* elevated from neck; not polished. BScP lobe claviform; projects posteriad from neck. *Dorsal surface* ovoid; weakly convex; polished; not elevated from neck. *Ventral surface* polished. – Posterior Subcostal Basivenale broadly deltoid; polished.

Discussion

Monophyly of the Bolboceratidae is supported by the fact that all of the taxa in this family share the following 12 apomorphic character states of the wing articulation and wing base:

1. 1Ax: the ventral surface of the head has a prominent ridge,
2. the dorsal surface of the head is very strongly oriented ventro-distad,
3. the neck is extremely short,
4. the distal embayment is secondarily extremely deep, but very narrow,
5. posteriorly strengthened by a sclerotized plate;
6. 2Ax: the anterior margin of the dorso-distal lobe is concave,
7. the dorsal surface of this lobe is very strongly convex,
8. the subalare tendon attachment point is very short, very broad, and apically shallowly and narrowly concave;
9. 3Ax: the posterior section of the head is enlarged dorsally to form an arm, which is proximally continuous with the neck;
10. 2BP: the postero-distal section of BMP is continuous with the BMP-CuA brace,
11. the latter is very strongly convex, broad and oriented more strongly distad than posteriad,
12. the base of CuA is shifted distad.

Bolboceratidae share six apomorphic character states of the wing articulation and wing base with Passalidae, Diphyllostomatidae, Lucanidae, Glaphyridae, Trogidae and Pleocomidae (Browne & Scholtz 1995). Analysis of wing articulation and wing base characters

indicates that Bolboceratidae are the sister group of Pleocomidae (Browne & Scholtz 1995).

Pleocomidae

Introduction

The Pleocomidae are a monotypic family. The genus *Pleocoma* Le Conte consists of 33 described species and three subspecies (Hovore 1977). *Pleocoma* has a very restricted distribution, occurring in the western USA., especially Oregon, California and Utah. Crowson (1981), Virkki (1967) and Ritcher (1966) treated Pleocomidae as a family and it is regarded as such in this study. Males are winged and females flightless.

Hind Wing Articulation Description

First Axillary (Fig.59)

Head - Dorsal surface large; convex; enlarged posteriorly; convex. *Antero-dorsal margin* normal width; weakly deplanate; oriented weakly postero-distad. *Antero-proximal margin* very strongly enlarged ventrally. *Postero-proximal margin* weakly enlarged proximally. *FSc2* convex. Base normal width. Apex rounded; oriented postero-distad. Anterior surface broad; very long; not waisted medially. *FSc1* very weak; very small and narrow; fused to the ventral projection. Dorsal surface convex. Ventral surface planate. *Ventral projection* weakly tapered from the base to apex; short but of average width; deeply concave; oriented disto-ventrad and curved posteriad. Apex narrower than the base but truncate. Concavity located in the preapical area; surrounded by three unequally strong ridges. Dorso-medial surface concave. Ventral surface convex. *Distal embayment* oriented dorsad. *FSc2* weakly deltoid to digitate; moderately broad; oriented distad and weakly dorsad. Dorsal surface very convex; not enlarged. Ventral surface weakly concave. Apex acute. Head and neck dorsal surface weakly curved proximad.

Neck normal width and length; weakly oriented antero-distad; broadly articulated with 2Ax. Proximal margin weakly convex; curved ventrad. Distal margin concave. *Distal embayment* shallow and broad.

Tail - Dorsal view: Proximal arch strongly but narrowly expanded postero-distally; falcate; strongly curved postero-distad. *Antero-proximal margin* concave. *Dorsal surface* weakly concave. *Postero-proximal margin* convex; strikingly recurved. Articulation with PRR posteriorly extremely strong; very weak anteriorly; markedly enlarged posteriorly and distally. Posterior margin straight. Distal arch normal size. Apex very weakly curved ventrad and posteriad; aciculate. -Ventral view: Proximal arch with a narrow but prominent ridge. Posterior margin with a narrow but prominent ridge. Distal arch with an extremely slender but long ridge.

Second Axillary (Fig.60)

Radial Fulcalare moderately broad; articulation with 2Ax ridge moderately broad.

Ridges - Dorsal view: Proximal ridge entire; distinct from lobe. *Anterior to antero-median section* partially concealed by the distal ridge. *Antero-median to postero-median section* strongly elevated above the distal ridge; demarcated from body by an impression. *Posterior section* moderately enlarged above the dorso-distal ridge; extremely long; not incorporated into lobe; distinct from lobe and extremely strongly extended past the posterior margin of lobe; extends posteriad from the median. Distal ridge weakly distinct from lobe. *Apex* oriented ventro-proximad; convex and broadly falcate; moderately short. *Anterior section* moderately short; curved proximad. *Median to posterior section* extends below the proximal ridge; very weakly demarcated from body by an impression. *Posterior section* strongly acerose; weakly extended past the posterior margin of lobe. - Ventral view: Proximal ridge broad; moderately long; straight; distinct from lobe. *Apex* acuminate. *Anterior to antero-median section* digitate; broad; obscures distal ridge except the apex. *Median to posterior section* obscured by the distal ridge. Distal ridge broad but short. *Apex* narrow. *Anterior to median section* concealed by the proximal ridge. *Median and posterior sections* arise from the proximal and posterior margins of the distal lobe; distinct from lobe; slender. *Median section* concave. *Postero-median section* convex and waisted. *Subalare tendon attachment point* extremely long and slender; apically not curved ventrad; posterior margin rounded; extends posteriad from the median; strongly visible dorsally.

Body - Dorsal view: about as long as broad. Proximal lobe oriented proximad; arises from the postero-medial section of the ridge, depressed below the ridge; strikingly small; deltoid; strongly sclerotized; convex. *Posterior margin* weakly enlarged; concave. *Base* extremely narrow. *Apex* narrowly rounded; very weakly curved anteriad. Distal lobe moderately long and broad; roundly deltoid; larger than proximal lobe; moderately sclerotized; markedly convex. *Anterior margin* normal length; straight. *Apex* narrowly rounded. *Posterior margin* very weakly concave; reduced. - Ventral view: Proximal lobe extremely small; only the apex is visible; convex. *Posterior wing process junction* obscures most of the proximal lobe; formed as a prominent ovoid convexity which extends anteriorly from the posterior margin of the distal ridge. *Base* ridge-like; convex. *Apex* small; ovoid. Distal lobe discontinuous with ridge; weakly concave.

Median Plate (Fig.61)

FM1 oriented strongly postero-distad. *Anterior to posterior section* very broad. *Proximal margin* convex. Articulation with 2Ax extends along the entire margin of the distal lobe over the posterior section of the ventral ridge. *Distal margin* fused to the proximal margin of 3Ax from the antero-distal corner to just anterior to the neck of 3Ax. FM2 very short; oriented posteriad; acerose; separated from FM1 by a long slender section of membrane.

Third Axillary (Fig.62)

Head strikingly convex; moderately broad; normal length. Proximal margin straight. Anterior margin weakly convex; not enlarged ventrally. Antero-proximal margin rounded; very weakly cleft. Antero-distal margin rounded. FCu normal size; distinct; ovoid. FA narrow; short; displaced anteriorly by FCu. AXCu does not form part of the head. Suture

line between FCu and FA present. Suture line between FCu and AXCu present. Suture line between FA and FJ present.

Neck moderately elevated proximally; distally very weakly so. FCu section of neck absent. AXCu forms entire neck. Proximal margin elevated as a weak ridge; extends to mid-line of proximal margin of tail; short. Prong armed with a single slender tooth. Ridge enlarged dorsally relative to AXA. Detached AXCu fragment deltoid; moderately sclerotized.

Tail broadly deltoid; long; planate. *Dorsal surface* oriented mesad. Anterior section broad; concave; weakly calceolate. Posterior section concave to flat. *Window* weak. FJ+AXJ slender; occupies distal third of tail; strongly sclerotized. Suture line between FJ and AXJ present. Suture line between FA+AXJ and AXA present. AXA more weakly sclerotized than FA+AXJ; occupies more than half of the tail; straight. Suture line between AXA and AXCu present.

Hind Wing Base Description

First Basal Plate (Fig.63)

Humeral Plate slender; apically weakly clavate. Anterior margin sinuate; strongly sclerotized. Apex very broad; clavate; curved ventrad. Dorsal margin slender; distant from BScA; strongly sinuate. Proximal margin J-shaped; curved proximo-ventrad. Ventral margin strongly sinuate. Distal section narrow. Suture line between FPC+BPC and FC+BC absent.

Anterior Subcostal Basivenale oriented distad; very broadly deltoid; very weakly convex. Proximal and distal sections separated by a prominent suture. *Proximal section* about the same size as the distal section. Apex broadly rounded. *Distal section* extremely broad; separated from ScA by a shallow concavity. – Subcosta Anterior weakly convex. Bulge extremely broad.

Radial Basivenale very small; convex; narrowly open; weakly angled antero-proximad; continuous with radial stem. Proximal arch slenderly deltoid; long; curved postero-proximad; continuous with the anterior margin of BR. *Postero-distal section* rounded. Anterior margin convex; moderately narrow; weakly elevated dorsad. Embayment normal size. Distal arch extremely weak; oriented posteriad. br strongly sclerotized; occupies the antero-proximal corner of BR; weakly discontinuous with BR. *br projection* apically broad; medially concave; indistinct from BSc.

Second Basal Plate (Fig.64)

MA-BMA Junction absent. – MP-BMP Junction: MP discontinuous with BMP; arises from below the distal margin. – Crimp Patterns absent. – BMP-CuA Brace present; slender; strongly convex; entire; distant from the distal margin of 2BP; extends postero-proximad. Anterior section reduced; not fused with BMP or the MP-BMP junction; arises from below the antero-distal margin of 2BP; more strongly convex than BMP. Posterior section continuous with CuA; fused to the antero-proximal angle of CuA. Point of fusion not marked by a suture line. – BMP-BCuA Brace absent.

Medial Basivenalia moderately reduced on all margins. Anterior and posterior margins isolated from surrounding sclerites. BMA broadly scaphoid; completely fused to BMP. *Proximal surface* flat. *Distal surface* convex. *Anterior margin* concave. *Proximal arch* short; broad; straight; planate; enlarged antero-proximally. *Distal arch* distinct; slender; strongly convex. BMP junction with BMA discontinuous and very broad; extremely small; rectangular; strongly convex to flat; distinct from brace; separated from 1BP and BCu. *Proximal section* extremely small; flat to weakly convex; very weakly distinguishable from BMA. Antero-distal and postero-distal margins sharply aquiline. *Median section* deeply concave. *Distal section* formed as a very large, rectangular convexity; strongly convex; prominent. Distal margin deeply concave; very strongly elevated above the surrounding membrane. Antero-distal and postero-distal sections continuous and equally elevated.

Cubital Basivenalia partially fused. Postero-proximal margin of BCuA fused with antero-proximal margin of BCuP. *Suture line* present. BCuA larger than BCuP; ovoid to weakly deltoid; strongly convex; oriented postero-distad; strongly sclerotized; lies proximal of CuA. *Median section* concave. BCuP C-shaped; smaller than BCuA; moderately convex proximally; weakly so distally; oriented postero-distad; weakly sclerotized especially distally. Distal embayment very deep. – Cubitus Anterior continuous with BCuA.

Basalare (Fig.65)

Head - HP lobe broad; continuous with neck; smaller than BScP lobe; very thin in cross-section. *Apex* broadly rounded. *Dorsal surface* weakly curved posteriad; elevated from neck; not polished. BScP lobe claviform; projects posteriad from neck. *Dorsal surface* ovoid; convex; polished; equally elevated as the HP lobe. *Ventral surface* polished. – Posterior Subcostal Basivenale deltoid; polished.

Discussion

Monophyly of the Pleocomidae is supported by the fact that all of the taxa in this family share the following three apomorphic character states of the wing articulation and wing base:

1. 2Ax: the dorso-proximal lobe is strikingly small and basally extremely narrow,
2. the subalare tendon attachment point is extremely long and narrow;
3. 2BP: BMP is very strongly convex and extremely small.

Pleocomidae share six apomorphic character states of the wing articulation and wing base with Passalidae, Diphylostomatidae, Lucanidae, Glaphyridae, Trogidae and Bolboceratidae (Browne & Scholtz 1995; Scholtz et al., submitted).

Pleocomidae have long been considered the sister group of Geotrupidae (Bolboceratini-Athyreini-Lethrini, Howden 1982) based on doubtful synapomorphies (Scholtz 1990). However, it has been suggested that this family may be related to Melolonthinae due to the highly modified club with 4-7 annuli (Howden has subsequently favoured the latter relationship over the former, pers. comm. 1991). Browne's analyses (1991a, 1993), based on synapomorphic wing structure and a subsequent analysis examining all character suites (Scholtz et al., submitted), supported Howden (1982). Pleocomidae and Geotrupidae have similar spiracle (Ritcher 1969a,b) and eye structure (Caveney 1986). Some genitalic and

mouthpart character states are similar to those of Diphyllostomatidae, but Pleocomidae share more derived character states with Geotrupidae (d'Hotman & Scholtz 1990b; Nel & Scholtz 1990; Scholtz 1990). Analysis of hind wing articulation and wing base characters indicates that Pleocomidae are the sister group of Bolboceratidae (Browne & Scholtz 1995).

Geotrupidae

Introduction

The Geotrupidae are a large widespread family which comprises three subfamilies: Geotrupinae, Lethrinae and Taurocerastinae (*Frickius* and *Taurocerastes*). The wingless Lethrinae were not examined here.

Hind Wing Articulation Description

First Axillary (Fig.73)

Head - Dorsal surface normal size; convex. *Antero-dorsal margin* oriented moderately postero-distad; normal width; weakly deplanate. *Antero-proximal margin* very strongly enlarged ventrally. *Postero-proximal margin* weakly enlarged proximally. *FSc2* base normal width. Apex oriented postero-distad; moderately narrow. Anterior surface broad; very long; not waisted medially. *FSc1* very weak; slender; fused to the proximal margin of the ventrad projection. Dorsal and ventral surfaces convex. Apex acute. *Ventral projection* tapers from base to apex; short but of average width; deeply concave; oriented disto-ventrad and curved posteriad. Dorsal surface concave. Ventral surface convex. Apex narrow but truncate. Concavity located in the preapical area; surrounded by three unequally strong ridges. *Distal embayment* oriented dorsad; narrow. *FSc2* oriented strongly dorsad and weakly distad; deltoid; very convex; broad. Dorsal surface convex. Ventral surface convex. Apex narrowly truncate. *Dorsal margin* not enlarged. Head and neck dorsal surface strongly curved proximad.

Neck normal width and length; weakly oriented antero-distad; broadly articulated with 2Ax; continuous with tail. Proximal margin moderately curved ventrad. Distal margin sinuate. *Distal embayment* very weakly concave; narrow.

Tail - Dorsal view: Proximal arch normal size; not extended posteriad and only very weakly so proximad; straight. *Dorsal surface* weakly concave. *Antero-proximal margin* convex. *Postero-proximal margin* straight. Articulation with PRR strong along the entire length of the proximal arch; strong; long but narrow; weakly recurved. Antero-dorsal surface concave. Postero-dorsal surface weakly concave. Posterior margin straight. Distal arch normal size; weakly extended posteriad. *Apex* very weakly curved ventrad and posteriad; acuminate. *Distal margin* straight. - Ventral view: Proximal arch with a broad ridge. Posterior margin with a prominent but narrow ridge. Distal arch with a slender ridge.

Second Axillary (Fig.74)

Radial Fulcalare weakly sclerotized; slender.

Ridges - Dorsal view: Proximal ridge entire; distinct from lobe. *Apex* narrow. *Anterior section* distally obscured by the distal ridge. *Anterior to antero-median section* depressed below the distal ridge. *Antero-median to postero-median section* strongly enlarged above the distal ridge. *Posterior section* moderately enlarged above the distal ridge; oriented posteriad; slender; very long; incorporated into lobe; distinct from lobe and strongly extended past the posterior margin of lobe. Distal ridge weakly distinct from lobe. *Apex* not fused to the proximal ridge apex; oriented ventrad; broadly spatulate; slender. *Anterior section* extremely short; curved proximad. *Median to posterior section* extends adjacent to, but lies below, the proximal ridge; very weakly demarcated from body by an impression. *Posterior section* acerose; very weakly extended past the posterior margin of lobe. - Ventral view: Proximal ridge slender; curved distad; distinct from lobe. *Apex* acuminate. *Anterior to antero-median section* digitate; slender; conceals the proximal margin of the distal ridge. *Median to posterior section* obscured by the distal ridge. Distal ridge slender. *Anterior to median section* partially concealed by the proximal ridge; straight. *Median and posterior sections* arise from the posterior and proximal margins of the distal lobe; distinct from lobe; very broad but short. *Median section* convex. *Postero-median section* waisted. *Subalare tendon attachment point* short and broad; apically not curved ventrad; posterior margin rounded; extends posteriad from the median; spatulate; visible dorsally.

Body - Dorsal view: about as long as broad. Proximal lobe short and moderately small; deltoid; arises medially from ridge, but depressed below the ridge; strongly sclerotized; convex; oriented proximad. *Base* moderately broad. *Apex* broadly rounded. *Anterior margin* very weakly concave. *Posterior margin* very weakly enlarged; very weakly concave. Distal lobe large and broad; deltoid; much larger than proximal lobe; moderately sclerotized; convex. *Apex* acute. *Anterior margin* straight. *Posterior margin* straight; weakly reduced. - Ventral view: Proximal lobe small; convex. *Posterior wing process junction* formed as a large ovoid convexity which conceals the base of the proximal lobe; extends anteriad from the posterior corner of the lobe base. *Base* moderately narrow. *Apex* round. Distal lobe deltoid; moderately large and broad; discontinuous with ridge; weakly concave.

Median Plate (Fig.75)

FM1 oriented strongly postero-distad. *Anterior section* moderately narrow. *Median to posterior section* very broad. *Proximal margin* convex. Articulation with 2Ax extends from the antero-distal margin of the distal lobe to the posterior section of the ventral ridge. *Distal margin* very broadly and strongly fused to 3Ax. FM2 very short; oriented posteriad; acerose; separated from FM1 by a long, broad section of membrane.

Third Axillary (Fig.76)

Head very broad; dorso-ventrally flattened; dorsal surface moderately and extensively concave. Proximal margin convex. Anterior margin dorsally weakly convex; anteriorly weakly concave; not enlarged ventrally; from the proximal angle it slopes abruptly antero-distad. *Antero-proximal margin* not extended anteriad. *Antero-distal margin* not extended

ventrad; narrow; straight. FCu reduced distally; large; broadly ovoid; weakly convex. FA small. *Anterior margin* entire; not reduced by FCu. AXCu absent. Suture line between FCu and FA present. Suture line between FCu and AXCu present. Suture line between FA and FJ absent.

Neck elevated proximally; depressed distally. FCu section of neck absent. AXCu forms entire neck. Proximal margin elevated as a broad ridge. *Ridge* extends to postero-median of the proximal margin of tail; moderately long; enlarged dorsally relative to tail. Dorsal surface of the ridge curves distad. Prong armed with a single short tooth; oriented proximo-dorsad; narrow. Detached AXCu fragment saddle-shaped; strongly curved ventrad both anteriorly and posteriorly; slender; moderately sclerotized.

Tail deltoid; very broad; short; planate. *Dorsal surface* oriented mesad. *Window* absent. FJ+AXJ narrow; occupies the distal half of the tail; moderately sclerotized. Suture line between FJ and AXJ absent. Suture line between FA+AXJ and AXA present. AXA equally sclerotized as FA+AXJ; the former occupies the postero-proximal half of the tail; straight. Suture line between AXA and AXCu present.

Hind Wing Base Description

First Basal Plate (Fig.77)

Humeral Plate moderately broad and long. Anterior margin convex; strongly sclerotized; distant from BScA. Apex moderately narrow; curved ventrad. Dorsal margin concave. Proximal margin weakly concave; curved proximo-ventrad. Ventral margin strongly sinuate. Suture line between FPC+BPC and FC+BC present.

Anterior Subcostal Basivenale broadly deltoid; strongly convex. Proximal and distal sections separated by a prominent suture. *Proximal section* extends postero-ventrad as a broad convexity; about as large as the distal section. *Distal section* continuous with ScA bulge; separated by a weak concavity. Apex broadly rounded; oriented distad. – Subcosta Anterior strongly convex. Bulge broad. *Postero-proximal margin* with a distinct ScA-BR Brace.

Radial Basivenale convex; closed; continuous with radial stem; angled proximad; extremely broadly rectangular. Proximal arch strikingly broad; deltoid; continuous with the anterior margin of BR; angled posteriad. *Postero-distal section* rounded. Anterior margin strongly depressed below the posterior margin of ScA bulge; not visible dorsally; weakly convex; angled proximad. Embayment normal sized. Distal arch very weak; continuous with radial stem; oriented posteriad. br strongly sclerotized; occupies less than half of the proximal arch; discontinuous with BR. *br projection* weakly distinct from BSc as a long, dove-tail shaped extension.

Second Basal Plate (Fig.78)

MA-BMA Junction absent. – MP-BMP Junction: MP only very weakly continuous with the anterior margin of BMP; arises from below the distal plate. – Crimp Patterns absent. – BMP-CuA Brace absent.

BMP-BCuA Brace partially reduced; weakly distinct; short; moderately narrow; formed as a tube-like convexity from the distal margin of 2BP; extends posteriad from 2BP antero-distal section; equally broad along the entire length. Anterior to postero-median section partially reduced. Posterior section continuous with BCuA. Terminus not prominent; weakly fused to the anterior section of BCuA, just mesad of the distal margin.

Medial Basivenalia - General habitus: broad and moderately long; rectangular. Anterior and posterior margins straight. Distal margin deeply concave; strongly elevated from surrounding membrane. BMA broadly scaphoid; short; completely fused to BMP. *Proximal surface* weakly convex. *Medial and distal surfaces* strongly convex. *Anterior margin* straight. *Proximal arch* weakly distinct; planate and straight; enlarged antero-proximally; extremely small; slender; acerose. *Distal arch* weakly distinct; extremely broad but short; strongly convex. BMP rectangular; markedly convex; very weakly separated from BMA by a shallow concavity; brace fused to BMP; separated from both 1BP and BCu by membrane. *Proximal section* weakly separated from BMA; convex; slopes ventro-distad. *Antero-distal section* long; narrow; rectangular; strongly convex; discontinuous from the postero-distal section. *Postero-distal section* similar to the latter, but less convex.

Cubital Basivenalia moderately narrowly fused. Postero-proximal margin of BCuA fused with the antero-proximal margin of BCuP. *Suture line* present. BCuA narrow; moderately long; convex; oriented distad; strongly sclerotized. *Anterior margin* with a moderately broad, but shallow, concavity. *Distal margin* strongly extended posteriad as a slender convexity; weakly sinuate. BCuP broad; convex; oriented posteriad; moderately sclerotized. Distal embayment broad but moderately shallow. – Cubitus Anterior continuous with BCuA. Junction marked by a narrow concave groove.

Basalare (Fig.79)

Head - HP lobe large; continuous with neck. *Apex* broadly truncate. *Dorsal surface* very strongly elevated from neck; not polished. BScP lobe claviform; short; projects posteriad from neck. *Dorsal surface* ovoid; weakly convex; polished; elevated from neck but not as strongly as the HP lobe. *Ventral surface* not polished. – Posterior Subcostal Basivenale broadly deltoid; polished.

Discussion

Monophyly of the Geotrupidae is supported by the fact that all of the taxa in this group share the following three apomorphic character states of the wing articulation and wing base:

1. 2Ax: the dorso-distal ridge apex is long and curved
2. the anterior section is strikingly elongate
3. 1BP: ScA-BR brace present.

Geotrupidae share 12 apomorphic character states of the wing articulation and wing base with Hybosoridae, Ochodaeidae and Ceratocanthidae (Browne & Scholtz 1995). Analysis of wing articulation and wing base characters indicates that Geotrupidae are the sister group of Hybosoridae + Ochodaeidae + Ceratocanthidae (Browne & Scholtz 1995).

Hybosoridae

Introduction

The Hybosoridae are a large variable cosmopolitan family which is best represented in the tropics (Scholtz 1990). This family contains 28 genera and 275 species (Allsop 1984; Kuijten 1986).

Hind Wing Articulation Description

First Axillary (Fig.80)

Head - Dorsal surface normal size; convex; clavate. *Antero-dorsal margin* oriented moderately postero-distad; normal width; weakly deplanate. *Antero-proximal margin* very strongly enlarged ventrally. *Postero-proximal margin* weakly enlarged proximally. *FSc2* base normal width; long. Apex oriented anteriorly; moderately narrow. Anterior surface broad; very long; not waisted medially. *FSc1* very weak; very small; slender; fused to the proximal margin of the ventrad projection. Dorsal and ventral surfaces convex. Apex acute. *Ventral projection* tapers from base to apex; short but of average width; deeply concave; oriented disto-ventrad and curved posteriad. Dorsal surface concave. Ventral surface convex. Apex narrow and broadly truncate. Concavity located in the preapical area; surrounded by three unequally strong ridges. *Distal embayment* oriented dorsad; narrow; concave. *FSc2* oriented strongly dorsad and weakly distad; deltoid; very convex; broad. Dorsal surface convex. Ventral surface convex. Apex acuminate. Dorsal margin not enlarged. Head and neck dorsal surface strongly curved dorsad.

Neck normal width and length; weakly oriented antero-distad; broadly articulated with 2Ax; continuous with tail. Proximal margin moderately curved ventrad. Distal margin concave. *Distal embayment* concave; moderately broad.

Tail - Dorsal view: Proximal arch normal size; weakly extended posteriad and proximad; weakly convex. Apex very weakly curved ventrad. *Dorsal surface* weakly concave. *Antero-proximal margin* concave. *Postero-proximal margin* convex. Articulation with PRR extends along the entire length of the proximal arch; strong; long and moderately broad; moderately recurved. Antero-dorsal and postero-dorsal surfaces concave. Posterior margin concave. Distal arch normal size. Apex very weakly curved ventrad and posteriad; acuminate. *Distal margin* straight. - Ventral view: Proximal arch with a weak ridge. Distal arch with a very small ridge. Posterior margin with a prominent but slender ridge.

Second Axillary (Fig.81)

Radial Fulcalare weakly sclerotized; slender.

Ridges - Dorsal view: Proximal ridge entire; distinct from lobe. Apex narrow. *Anterior to median section* obscured by the distal ridge. *Median to posterior section* strongly enlarged above the distal ridge. *Posterior section* moderately enlarged above the distal ridge; oriented posteriad; slender; moderately long; distinct from lobe and moderately extended past the posterior margin of lobe. Distal ridge distinct from lobe. Apex not fused to the proximal ridge apex; oriented ventrad; convex; spatulate; moderately short. *Anterior*

section moderately short; curved antero-ventrad, basally abruptly, and strongly, curved distad. *Median to posterior section* extends adjacent to, but lies below, the proximal ridge; very weakly demarcated from the body by an impression. *Posterior section* acerose; very weakly extended past the posterior margin of lobe. - Ventral view: Proximal ridge slender; short; curved distad; distinct from lobe. *Apex* aciculate. *Anterior to antero-median section* digitate; slender; conceals the distal ridge. *Median to posterior section* obscured by the distal ridge. Distal ridge slender; short. *Anterior to median section* concealed by the proximal ridge. *Median and posterior sections* arise from the posterior and proximal margins of the distal lobe; distinct from lobe; broad but short. *Median section* convex. *Postero-median section* waisted. *Subalare tendon attachment point* short and broad; apically not curved ventrad; posterior margin rounded, but truncate; extends posteriad from the median; spatulate; weakly visible dorsally.

Body - Dorsal view: about as long as broad. Proximal lobe moderately long and broad; deltoid; arises medially from the ridge, but depressed below the ridge; strongly sclerotized; convex; oriented proximad. *Base* moderately broad. *Apex* broadly rounded; weakly curved anteriad. *Anterior margin* very weakly concave. *Posterior margin* very weakly enlarged; very weakly concave. Distal lobe moderately small and broad; deltoid; shorter but broader than the proximal lobe; moderately sclerotized; concave. *Anterior margin* convex. *Apex* aciculate; oriented proximad. *Posterior margin* straight; very weakly reduced. - Ventral view: Proximal lobe moderately large; convex. *Posterior wing process junction* formed as a large, slenderly ovoid convexity which conceals the posterior section of the proximal lobe from the base to the apex; occupies the posterior section of the lobe. Distal lobe large and broad; discontinuous with ridge; deeply concave.

Median Plate (Fig.82)

FM1 oriented strongly postero-distad. *Anterior section* narrow. *Median to posterior section* moderately narrow. *Proximal margin* convex. Articulation with 2Ax extends from the antero-distal margin of the distal lobe to the posterior section, over the posterior section of the ventral ridge. *Distal margin* narrowly and weakly fused to 3Ax. FM2 moderately long and slender; oriented postero-distad; acerose. *Anterior to postero-median section* separated from FM1 by a long, narrow section of membrane. *Postero-median to posterior section* fused to FM1.

Third Axillary (Fig.83)

Head very broad; dorso-ventrally flattened. Dorsal surface deeply and extensively concave. Proximal margin convex. Anterior margin dorsally weakly convex; not enlarged ventrally; from proximal angle it is oriented antero-distad. *Antero-proximal margin* not extended anteriad. *Antero-distal margin* not extended ventrad; narrow. *Posterior margin* with a weak concavity which extends to the tail. FCu strongly reduced distally; moderately large; distinct; occupies about half of the head; broadly ovoid. FA moderately large; occupies about half of the head; smaller than FCu. *Anterior margin* entire; not reduced by FCu. AXCu absent. Suture line between FCu and FA present. Suture line between FCu and AXCu present. Suture line between FA and FJ absent.

Neck elevated proximally; depressed distally. FCu section of neck absent. AXCu forms the entire neck. Proximal margin elevated as a broad ridge. Ridge extends to postero-median of the proximal margin of the tail; moderately long; enlarged dorsally relative to tail. Dorsal surface of the ridge is curved distad. *Embayment* deep; extends to the medial margin of the tail. Prong armed with a single tooth; oriented proximo-dorsad. Detached AXCu fragment slender; deltoid; moderately sclerotized.

Tail deltoid; broad; short; planate. *Dorsal surface* oriented mesad. *Window* absent. FJ+AXJ narrow; occupies the distal half of the tail; weakly sclerotized. Suture line between FJ and AXJ absent. Suture line between FA+AXJ and AXA present. AXA as equally sclerotized as FA+AXJ; the former occupies the postero-proximal half of the tail; straight. Suture line between AXA and AXCu present.

Hind Wing Base Description

First Basal Plate (Fig.84)

Humeral Plate slender. Anterior margin convex; lies distant from BScA. Apex slender; ovoid; oriented proximad. Dorsal margin convex. Proximal margin convex; curved proximo-ventrad. Ventral margin concave. Suture line between FPC+BPC and FC+BC present. FPC+BPC formed as a moderately large sclerite below the ventro-proximal margin of FC+BC.

Anterior Subcostal Basivenale broadly deltoid; convex; moderately elevated. Proximal and distal sections separated by a prominent suture. Proximal section extended postero-ventrad as a very broad convexity; about as large as the distal section. Distal section discontinuous with the ScA bulge; separated by a narrow but deep concavity. Apex broadly rounded; oriented distad. – Subcosta Anterior convex. Bulge moderately broad; distinct.

Radial Basivenale large; strongly convex; open; discontinuous with the radial stem; angled proximad; very strongly recurved; moderately broadly rectangular. Arises from the radial stem and curves very strongly dorsad away from both ScA and BScA. Proximal arch strikingly broad; angled posteriad; deltoid; posteriorly strongly extended proximad and distad; continuous with the anterior margin of BR. *Postero-distal section* rounded. *Posterior margin* extremely broad; deeply concave; surrounds the terminus of BMA proximal arch. Anterior margin strongly elevated above the posterior margin of the ScA bulge and BScA; narrow; convex; angled antero-distad; continuous with the distal arch. Embayment normal size. Distal arch very weak; discontinuous with the radial stem; very narrow; strongly recurved; oriented posteriad. *br* strongly sclerotized; large; rectangular; occupies one-half of the proximal arch; discontinuous with BR; posteriorly extended postero-proximad. *br projection* distinct from BSc as a slender extension; oriented antero-ventrad.

Second Basal Plate (Fig.85)

MA-BMA Junction absent. – MP-BMP Junction: MP only very weakly continuous with the anterior margin of BMP; arises from below the distal plate. – Crimp Patterns absent. – BMP-CuA Brace absent.

BMP-BCuA Brace partially reduced; weakly distinct; moderately narrow; formed as a secondary tube-like convexity from the postero-distal margin of 2BP; curves postero-proximad from 2BP postero-distal section; equally broad along the entire length. Anterior section weakly reduced. Posterior section continuous with BCuA. Terminus fused to the anterior section of BCuA, just mesad of the distal margin.

Medial Basivenalia broad and moderately long; rectangular. Anterior and posterior margins straight. Distal margin concave; strongly elevated from the surrounding membrane. BMA broadly scaphoid; moderately short but broad; completely fused to BMP. *Proximal surface* weakly convex. *Medial and distal surfaces* concave. *Anterior margin* moderately concave. *Proximal arch* moderately long; planate and falcate; moderately broad; enlarged antero-proximally. *Distal arch* weakly distinct; moderately broad; extremely short; convex. BMP rectangular; convex; separated from BMA by a shallow concavity; brace fused to BMP. *Proximal section* moderately broad; rectangular; very weakly separated from BMA; deeply concave. *Distal section* very weakly separated into anterior and posterior sections; indistinct from MP; rectangular; broad; strongly convex. Postero-distal section less convex than the antero-distal section.

Cubital Basivenalia moderately narrowly fused; moderately broad and short. Postero-proximal margin of BCuA fused with the antero-proximal margin of BCuP. *Suture line* present. BCuA moderately broad and short; convex; oriented distad; moderately sclerotized. *Anterior margin* with a moderately broad, but shallow, concavity. *Distal margin* extended posteriad as a moderately strong, broad convexity. BCuP slender; very weakly convex; oriented posteriad; very weakly sclerotized. Distal embayment broad but moderately shallow. – Cubitus Anterior continuous with BCuA. Junction marked by a shallow groove.

Basalare (Fig.86)

Head - HP lobe moderately long and very narrow; continuous with neck. *Apex* narrowly rounded. *Dorsal surface* elevated from BScP lobe; not polished. BScP lobe claviform; moderately broad; reduced; projects dorsally from neck. *Dorsal surface* ovoid; convex; polished; elevated from neck. *Ventral surface* polished. – Posterior Subcostal Basivenale deltoid; polished.

Discussion

This family displays the following two autapomorphic character states of the wing articulation:

1. 1Ax: FSc2 is falcate
2. and broad.

Hybosorids are thought to occupy an intermediate position between Ochodaeidae and Ceratocanthidae (d'Hotman & Scholtz 1990b; Nel & Scholtz 1990; Scholtz 1990). Analysis of wing articulation and wing base characters supports this position (Browne & Scholtz 1995). Howden & Gill (1988) placed hybosorids between Trogidae and Ceratocanthidae. Analysis of wing articulation and wing base characters does not support such a relationship. Ceratocanthidae are generally considered to be the sister group of

Hybosoridae (Howden & Gill 1988; d'Hotman & Scholtz 1990b; Nel & Scholtz 1990; Scholtz 1990). Analysis of wing articulation and wing base characters supports such a relationship (Browne & Scholtz 1995).

Hybosoridae share 12 apomorphic character states of the wing articulation and wing base with Geotrupidae, Ochodaeidae and Ceratocanthidae (Browne & Scholtz 1995).

Ceratocanthidae

Introduction

The Ceratocanthidae are a small family with pantropical distribution. Species occur mainly in forests in Asia (three genera; 58 species), Africa (11 genera, 41 species) and America (three genera; unknown number of species, Paulian 1977a; 1978), as well as on various islands. The southern African and Australian ceratocanthids were recently revised by Paulian (1977a,b, 1978).

Hind Wing Articulation Description

First Axillary (Fig.87)

Head - Dorsal surface normal size; convex. *Antero-dorsal margin* oriented moderately postero-distad; normal width; weakly deplanate. *Antero-proximal margin* very strongly enlarged ventrally. *Postero-proximal margin* weakly enlarged proximally. *FSc2* base normal width; long. Apex oriented anteriad; moderately narrow. Anterior surface broad; very long; not waisted medially. *FSc1* very weak; very small; slender; fused to the proximal margin of the ventral projection. Dorsal and ventral surfaces convex. Apex acute. *Ventral projection* tapers from base to apex; short but of average width; deeply concave; oriented disto-ventrad and curved posteriad. Dorsal surface concave. Ventral surface convex. Apex narrow and broadly truncate. Concavity located in the preapical area; surrounded by three unequally strong ridges. *Distal embayment* oriented dorsad; narrow; concave. *FSc2* oriented strongly dorsad and weakly distad; falcate; very convex; narrow. Dorsal surface convex. Ventral surface convex. Apex aciculate. Dorsal margin not enlarged. Head and neck dorsal surface strongly curved dorsad. Apex aciculate.

Neck normal width and length; weakly oriented antero-distad; broadly articulated with 2Ax; continuous with tail. Proximal margin moderately curved ventrad. Distal margin concave. *Distal embayment* moderately concave; broad.

Tail - Dorsal view: Proximal arch normal size; extended posteriad and proximad; convex. Apex very weakly curved ventrad. *Dorsal surface* weakly concave. *Antero-proximal margin* concave. *Postero-proximal margin* convex. Articulation with PRR extends along the entire length of the proximal arch; strong; long and moderately broad; moderately recurved. Antero-dorsal and postero-dorsal surfaces concave. Posterior margin concave. Distal arch normal size. Apex very weakly curved ventrad and posteriad; aciculate. *Distal margin* straight. - Ventral view: Proximal arch with a small ridge. Posterior margin with a prominent ridge. Distal margin with a very small ridge.

Second Axillary (Fig.88)

Radial Fulcalare weakly sclerotized; slender.

Ridges - Dorsal view: Proximal ridge entire; distinct from the lobe. *Apex* narrow. *Anterior to median section* obscured by the distal ridge. *Median to posterior section* strongly enlarged above the distal ridge. *Posterior section* moderately enlarged above the distal ridge; oriented posteriad; slender; moderately long; distinct from lobe and moderately extended past the posterior margin of lobe. Distal ridge distinct from lobe. *Apex* not fused to the proximal ridge apex; oriented ventrad; convex; spatulate; moderately short. *Anterior section* moderately short; curved antero-ventrad, basally abruptly, but weakly, curved distad. *Median to posterior section* extends adjacent to, but lies below, the proximal ridge; very weakly demarcated from the body by an impression. *Posterior section* acerose; very weakly extended past the posterior margin of the lobe. - Ventral view: Proximal ridge slender; short; curved proximad; distinct from lobe. *Apex* acuminate. *Anterior to antero-median section* digitate; slender; conceals the distal ridge. *Median to posterior section* digitate; slender; conceals the distal ridge. Distal ridge slender; short. *Anterior to median section* concealed by the proximal ridge. *Median and posterior sections* arise from the posterior and proximal margins of the distal lobe; distinct from the lobe; broad but short. *Median section* convex. *Postero-median section* waisted. *Subalare tendon attachment point* short and broad; apically not curved ventrad; posterior margin rounded, but truncate; extends posteriad from the median; spatulate; weakly visible dorsally.

Body - Dorsal view: about as long as broad. Proximal lobe moderately long and broad; deltoid; arises medially from the ridge, but depressed below the ridge; strongly sclerotized; convex. *Base* broad. *Apex* broadly rounded; straight. *Anterior margin* very weakly concave. *Posterior margin* very weakly enlarged; very weakly concave. Distal lobe moderately large and broad; deltoid; shorter but broader than the proximal lobe; moderately sclerotized; concave. *Anterior margin* convex. *Apex* broadly rounded. *Posterior margin* convex; very weakly reduced. - Ventral view: Proximal lobe large; convex. *Posterior wing process junction* formed as a large, slenderly ovoid convexity; arises from the postero-distal margin of the lobe and extends antero-proximad to the lobe mid-line. Distal lobe moderately large and broad; discontinuous with ridge; deeply concave.

Median Plate (Fig.89)

FM1 oriented strongly postero-distad. *Anterior section* very narrow. *Median to posterior section* moderately narrow. *Proximal margin* convex. Articulation with 2Ax extends from the antero-distal margin of the distal lobe to the posterior section, over the posterior section of the ventral ridge. *Distal margin* narrowly and weakly fused to 3Ax. FM2 moderately long and slender; oriented postero-distad; acerose. *Anterior to posterior section* separated from FM1 by a long, narrow section of membrane.

Third Axillary (Fig.90)

Head very broad and convex; dorso-ventrally flattened. Dorsal surface deeply and extensively concave. Anterior margin dorsally weakly convex; not enlarged ventrally; from proximal angle it is oriented antero-distad. *Antero-proximal margin* not extended anteriad.

Antero-distal margin not extended ventrad; narrow. *Posterior margin* with a narrow concavity which extends to the tail. FCu strongly reduced distally; large; distinct; occupies most of the head; broadly ovoid. FA small. *Anterior margin* entire; not reduced by FCu. AXCu present; moderately narrow; extends to the antero-proximal margin. Suture line between FCu and FA present. Suture line between FCu and AXCu present. Suture line between FA and FJ absent.

Neck elevated proximally; depressed distally. FCu section of neck absent. AXCu forms the entire neck. Proximal margin elevated as a broad ridge. Ridge extends to postero-median of the proximal margin of tail; moderately long; enlarged dorsally relative to tail. Dorsal surface of ridge is curved distad. *Embayment* very deep; extends past the medial margin of tail. Prong armed with a single very long and broad tooth; oriented proximo-dorsad. Detached AXCu fragment slender; ovoid; moderately sclerotized.

Tail deltoid; broad; short; planate. *Dorsal surface* oriented mesad. *Window* absent. FJ+AXJ narrow; occupies the distal half of the tail; weakly sclerotized. Suture line between FJ and AXJ absent. Suture line between FA+AXJ and AXA present. AXA as equally sclerotized as FA+AXJ; the former occupies the postero-proximal half of the tail; straight. Suture line between AXA and AXCu present.

Hind Wing Base Description

First Basal Plate (Fig.91)

Humeral Plate moderately broad and long. Anterior margin weakly sinuate; lies distant from BScA. Apex moderately broad; deltoid; oriented proximad. Dorsal margin convex. Proximal margin convex; oriented proximad; straight. Ventral margin concave. Suture line between FPC+BPC and FC+BC present. FPC+BPC formed as a small sclerite below the ventro-proximal margin of FC+BC.

Anterior Subcostal Basivenale broadly deltoid; convex; moderately elevated. Proximal and distal sections separated by a prominent suture. *Proximal section* extended postero-ventrad as a very broad convexity; about as large as the distal section. *Distal section* discontinuous with the ScA bulge; separated by a very broad and extremely deep concavity. Apex broadly rounded; oriented distad.

Subcosta Anterior strongly convex. Bulge moderately broad; distinct. *Median section* deeply concave; all other margins strongly convex.

Radial Basivenale large; strongly convex; open; discontinuous with the radial stem; angled antero-proximad; very strongly recurved; moderately broadly rectangular. Arises from the radial stem and curves very strongly antero-proximad and dorsad away from both ScA and BScA. Proximal arch strikingly broad; angled posteriad; deltoid; posteriorly strongly extended proximad and distad; continuous with the anterior margin of BR. *Postero-distal section* rounded. *Posterior margin* extremely broad; deeply concave; surrounds the terminus of BMA proximal arch. Anterior margin strongly elevated above the posterior margin of the ScA bulge and BScA; moderately broad; convex; angled antero-distad; continuous with the distal arch. Embayment normal size. Distal arch very weak; discontinuous with the radial stem; very broad; strongly recurved; oriented posteriad. br

strongly sclerotized; extremely large; deltoid; occupies one-half of the proximal arch; discontinuous with BR; posteriorly strongly extended proximad and posteriad as a broad sclerite. *br projection* distinct from BSc as an long and slender extension; oriented antero-ventrad.

Second Basal Plate (Fig.92)

MA-BMA Junction absent. – MP-BMP Junction: MP continuous with BMP along all margins. – Crimp Patterns absent. – BMP-CuA Brace absent. – BMP-BCuA Brace partially reduced; weakly distinct; moderately narrow; formed as a secondary tube-like convexity from the posterior margin of 2BP; extends posteriad from 2BP postero-distal section; oriented posteriad; equally broad along the entire length. Anterior section weakly reduced. Posterior section continuous with BCuA; fused to the antero-distal angle of BCuA. Terminus fused to the anterior section of BCuA, just mesad of the distal margin.

Medial Basivenalia broad and moderately long; rectangular. Anterior and posterior margins straight. Distal margin extremely deeply concave; strongly elevated from the surrounding membrane. BMA broadly scaphoid; short but broad; completely fused to BMP. *Proximal surface* weakly convex. *Medial and distal surfaces* flat. *Anterior margin* deeply concave. *Proximal arch* moderately long; planate and falcate; moderately broad; enlarged antero-proximally. *Distal arch* weakly distinct; moderately broad; extremely short; convex. BMP separated from BMA by a shallow concavity; brace fused to BMP. *Proximal section* extremely narrow; almost absent; rectangular; very weakly separated from BMA; convex. *Distal section* very weakly separated into anterior and posterior sections; indistinct from MP; formed as a reversed C-shape; slender; strongly convex. Postero-distal section less convex than the antero-distal section.

Cubital Basivenalia broadly fused. Postero-proximal margin of BCuA fused with the antero-proximal margin of BCuP. *Suture line* present. BCuA moderately broad and short; convex; oriented distad; strongly sclerotized. *Anterior margin* with a moderately broad, but shallow, concavity. *Distal margin* extended posteriad as a moderately strong, broad convexity. BCuP stout; weakly convex; oriented posteriad; weakly sclerotized especially posteriorly. Distal embayment broad but moderately shallow. – Cubitus Anterior continuous with BCuA. Junction marked by a shallow groove.

Basalare (Fig.93)

Head - HP lobe long; discontinuous with neck; appears to arise from the anterior margin of a greatly enlarged BScP lobe; curves posteriad. *Apex* rounded. *Dorsal surface* very weakly elevated above the BScP lobe; not polished. BScP lobe claviform; broad and extended distad and anteriad; projects posteriad and strongly distad from neck. *Dorsal surface* ovoid; strongly convex; polished; elevated from neck. *Ventral surface* polished. – Posterior Subcostal Basivenale deltoid; polished.

Discussion

Monophyly of the Ceratocanthidae is supported by the fact that all of the taxa in this family share the following two apomorphic character states of the wing articulation:

1. 1Ax: FSc2 strongly oriented anteriad
2. strikingly long and narrow.

Ceratocanthidae share 12 apomorphic character states of the wing articulation and wing base with Geotrupidae, Ochodaeidae and Hybosoridae (Browne & Scholtz 1995). Ceratocanthids are closely related to Ochodaeidae and Hybosoridae. Hybosoridae are generally considered to be the sister group of Ceratocanthidae (Howden & Gill 1988; d'Hotman & Scholtz 1990b; Nel & Scholtz 1990; Scholtz 1990). Analysis of wing articulation and wing base characters supports such a relationship (Browne & Scholtz 1995).

Ochodaeidae

Introduction

The Ochodaeidae consist of two subfamilies, eight genera and approximately 80 species. The family has a virtually cosmopolitan distribution, with the genus *Ochodaeus* Serville occurring in Africa, North and South America, Madagascar, Europe, the Orient and on Oriental and Palaearctic Islands. *Pseudochodaeus* Carlson & Ritcher occurs in the western USA, *Namibiotalpa* Scholtz & Evans is restricted to sandy areas of the Namib Desert, *Codocera* Eschscholtz is widespread in eastern Europe and *Enodognathus* Benderitter occurs on Madagascar. The latter four genera are monotypic. *Chaetocanthus* Pringuey and *Synochodaeus* Kolbe are endemic to southern Africa, as is *Odontochodaeus* Paulian to Madagascar (Scholtz et al. 1988). Other important works on the Ochodaeidae are those of Carlson (1975) and Carlson & Ritcher (1974).

Hind Wing Articulation Description

First Axillary (Fig.94)

Head - Dorsal surface normal size; convex. *Antero-dorsal margin* oriented moderately postero-distad; normal width; weakly deplanate. *Antero-proximal margin* very strongly enlarged ventrally. *Postero-proximal margin* weakly enlarged proximally. *FSc2* base normal width. Apex oriented anteriad; moderately narrow. Anterior surface broad; very long; not waisted medially. *FSc1* very weak; very small; slender; fused to the proximal margin of the ventrad projection. Dorsal and ventral surfaces convex. Apex acute. *Ventral projection* tapers from base to apex; short but of average width; deeply concave; oriented disto-ventrad and curved posteriad. Dorsal surface concave. Ventral surface convex. Apex narrow and rounded. Concavity located in the preapical area; surrounded by three unequally strong ridges. *Distal embayment* oriented dorsad; narrow; concave. *FSc2* oriented strongly dorsad and weakly distad; falcate; very convex; extremely narrow. Dorsal surface very convex; not enlarged. Ventral surface convex. Apex acuminate. Head and neck dorsal surface strongly curved dorsad.

Neck normal width and length; weakly oriented antero-distad; broadly articulated with 2Ax; continuous with tail. Proximal margin moderately curved ventrad. Distal margin concave. *Distal embayment* moderately concave; broad.

Tail - Dorsal view: Proximal arch normal size; not extended posteriad and only very weakly so proximad; weakly convex. *Apex* very weakly curved ventrad. *Dorsal surface* weakly concave. *Antero-proximal margin* concave. *Postero-proximal margin* weakly convex. Articulation with PRR extends along the entire length of the proximal arch; strong; long but narrow; weakly recurved. Antero-dorsal surface concave. Postero-dorsal surface weakly concave. Posterior margin very weakly concave. Distal arch normal size. *Apex* very weakly curved ventrad and posteriad; aciculate. *Distal margin* straight. - Ventral view: Proximal arch with a tapering ridge. Distal arch with an extremely small ridge. Posterior margin with a prominent ridge.

Second Axillary (Fig.95)

Radial Fulcalare very weakly sclerotized; very slender.

Ridges - Dorsal view: Proximal ridge entire; distinct from lobe. *Apex* narrow. *Anterior to median section* obscured by the distal ridge. *Median to posterior section* strongly enlarged above the distal ridge. *Posterior section* moderately enlarged above the distal ridge; oriented posteriad; slender; moderately long; distinct from lobe and moderately extended past the posterior margin of lobe. Distal ridge very weakly distinct from lobe. *Apex* not fused to the proximal ridge apex; oriented ventrad; convex; narrowly spatulate; moderately short. *Anterior section* moderately short; straight; curved antero-ventrad, basally abruptly curved distad. *Median to posterior section* extends adjacent to, but lies below, the proximal ridge; very weakly demarcated from body by an impression. *Posterior section* acerose; very weakly extended past the posterior margin of lobe. - Ventral view: Proximal ridge slender; short; curved distad; distinct from lobe. *Apex* aciculate. *Anterior to antero-median section* digitate; slender; very weakly conceals the proximal margin of the distal ridge. *Median to posterior section* obscured by the distal ridge. Distal ridge slender; short. *Anterior to median section* partially concealed by the proximal ridge; curved proximad. *Median and posterior sections* arise from the posterior and proximal margins of the distal lobe; distinct from lobe; broad but short. *Median section* convex. *Postero-median section* waisted. *Subalare tendon attachment point* short and broad; apically not curved ventrad; posterior margin weakly rounded; extends posteriad from the median; spatulate; weakly visible dorsally.

Body - Dorsal view: about as long as broad. Proximal lobe long and broad; deltoid; arises medially from ridge, but depressed below the ridge; strongly sclerotized; convex; oriented proximad. *Base* broad. *Apex* broadly rounded to truncate; weakly curved anteriad. *Anterior margin* very weakly concave. *Posterior margin* very weakly enlarged; very weakly concave. Distal lobe weakly reduced; large and broad; deltoid; much larger than the proximal lobe; weakly sclerotized; concave. *Anterior margin* straight. *Apex* acute. *Posterior margin* straight; very weakly reduced. - Ventral view: Proximal lobe extremely small; convex. *Posterior wing process junction* formed as a large ovoid convexity which conceals the posterior section of the proximal lobe from the base to the apex; occupies the posterior section of the lobe. Distal lobe large and broad; discontinuous with ridge; flat.

Median Plate (Fig.96)

FM1 oriented strongly postero-distad. *Anterior section* narrow. *Median to posterior section* moderately narrow. *Proximal margin* convex. Articulation with 2Ax extends from the antero-distal margin of the distal lobe to the posterior section, over the posterior section of the ventral ridge. *Distal margin* narrowly and weakly fused to 3Ax. FM2 moderately long and slender; oriented postero-distad; acerose. *Anterior to postero-median section* separated from FM1 by a long, narrow section of membrane. *Postero-median to posterior section* fused to FM1.

Third Axillary (Fig.97)

Head large; dorso-ventrally flattened. Dorsal surface moderately and extensively concave. Proximal margin convex. Anterior margin dorsally weakly convex; not enlarged ventrally; from the proximal angle it is oriented distad. *Antero-proximal margin* not extended anteriad. *Antero-distal margin* not extended ventrad; narrow. *Posterior margin* with a narrow concavity which extends to the tail. FCu reduced distally; distinct; broadly ovoid. FA large. *Anterior margin* entire; not reduced by FCu. AXCu absent. Suture line between FCu and FA present. Suture line between FCu and AXCu present. Suture line between FA and FJ absent.

Neck elevated proximally; depressed distally. FCu section of neck absent. AXCu forms entire neck. Proximal margin elevated as a broad ridge. Ridge large; moderately long; extends to postero-median of the proximal margin of tail; enlarged dorsally relative to tail. Dorsal surface of ridge is curved distad; concavity absent. *Embayment* very deep; extends past the medial margin of tail. Prong armed with a single short tooth; oriented proximo-dorsad; narrow. Detached AXCu fragment slender; rectangular; weakly sclerotized.

Tail deltoid; very broad; short; planate. *Dorsal surface* oriented mesad. *Window* absent. FJ+AXJ narrow; occupies distal half; weakly sclerotized. Suture line between FJ and AXJ absent. Suture line between FA+AXJ and AXA present. AXA as equally sclerotized as FA+AXJ; the former occupies the postero-proximal half of the tail; straight. Suture line between AXA and AXCu present.

Hind Wing Base Description

First Basal Plate (Fig.98)

Humeral Plate slender. Anterior margin moderately convex; weakly sclerotized; lies distant from BScA. Apex narrow; curved ventrad. Dorsal margin convex. Proximal margin convex; curved proximo-ventrad. Ventral margin concave. Suture line between FPC+BPC and FC+BC present. FPC+BPC formed as a small sclerite below the ventro-proximal margin of FC+BC.

Anterior Subcostal Basivenale broadly deltoid; convex. Proximal and distal sections separated by a prominent suture. *Proximal section* extended postero-ventrad as a moderately broad convexity; about as large as the distal section. *Distal section* continuous with the ScA bulge; separated by a weak concavity. Apex broadly rounded; oriented distad. – Subcosta Anterior weakly convex. Bulge broad.

Radial Basivenale large; convex; broadly open; discontinuous with the radial stem; angled antero-proximad; broadly rectangular. Proximal arch strikingly broad; angled postero-proximad; deltoid; posteriorly weakly extended proximad and distad; continuous with the anterior margin of BR. *Postero-distal section* rounded. *Posterior margin* concave; surrounds the terminus of BMA proximal arch. Anterior margin elevated above the posterior margin of ScA bulge; extremely narrow; convex; angled antero-proximad; continuous with the distal arch. Embayment normal size. Distal arch very weak; discontinuous with the radial stem; extremely narrow; recurved; oriented posteriad. br strongly sclerotized; extremely large; deltoid; occupies over three-quarters of the proximal arch; discontinuous with BR; posteriorly strongly extended proximad and posteriad as a broad sclerite. *br projection* distinct from BSc as a slender, deltoid extension; oriented antero-ventrad.

Second Basal Plate (Fig.99)

MA-BMA Junction absent. – MP-BMP Junction: MP only very weakly continuous with the anterior margin of BMP; arises from below the distal plate. – Crimp Patterns absent. – BMP-CuA Brace absent. – BMP-BCuA Brace partially reduced; weakly distinct; moderately narrow; formed as a secondary tube-like convexity from the distal margin of 2BP; extends posteriad from 2BP antero-distal section; equally broad along the entire length. Anterior section weakly reduced. Posterior section continuous with BCuA. Terminus prominent; fused to the anterior section of BCuA, just mesad of the distal margin.

Medial Basivenalia broad and moderately long; rectangular. Anterior and posterior margins straight. Distal margin deeply concave; strongly elevated from the surrounding membrane. BMA broadly scaphoid; very short but broad; completely fused to BMP. *Proximal surface* weakly convex. *Medial and distal surfaces* flat. *Anterior margin* concave. *Proximal arch* long; planate and falcate; very narrow; enlarged antero-proximally. *Distal arch* weakly distinct; moderately broad; extremely short; strongly convex. BMP rectangular; convex; separated from BMA by a shallow concavity; brace fused to BMP; separated from both 1BP and BCu by membrane. *Proximal section* narrow; deltoid; weakly separated from BMA; convex. *Antero-distal section* long; narrow; rectangular; strongly convex; discontinuous from the postero-distal section. *Postero-distal section* similar to the latter but less convex.

Cubital Basivenalia completely fused. Posterior margin of BCuA fused with the anterior margin of BCuP. *Suture line* present. BCuA very narrow and long; convex; oriented distad; strongly sclerotized. *Anterior margin* with a moderately broad, but shallow, concavity. *Distal margin* strongly extended posteriad as a moderately strong, slender convexity. BCuP very broad; ovoid; convex; oriented posteriad; moderately sclerotized. Distal embayment absent. – Cubitus Anterior continuous with BCuA. Junction marked by a narrow concave groove.

Basalare (Fig.100)

Head - HP lobe moderately small; continuous with neck. *Apex* narrowly truncate. *Dorsal surface* very strongly elevated from neck; not polished. BScP lobe claviform; stout;

projects posteriad from neck. *Dorsal surface* ovoid; strongly convex; polished; elevated from neck, but lies below the HP lobe. *Ventral surface* not polished. – Posterior Subcostal Basivenale deltoid; polished.

Discussion

Ochodaeidae do not display any autapomorphic character states of the wing articulation or wing base (Browne & Scholtz 1995). They share 12 apomorphic character states of the wing articulation and wing base with Geotrupidae, Hybosoridae and Ceratocanthidae (Browne & Scholtz 1995).

Carlson & Ritcher (1974) implied that close relationship exists between Ochodaeidae and Hybosoridae, Iablokoff-Khnzorian (1977) suggested that Aclopidae are more closely related to Ochodaeidae, Crowson (1981) implied relationship between Ochodaeidae, Hybosoridae and Geotrupidae, and Lawrence & Newton (1982) concluded that Ochodaeidae, Hybosoridae and Ceratocanthidae appear to be closely related. Scholtz et al. (1988) corroborated Lawrence & Newton (1982) and proposed that ochodaeids are the sister group of Hybosoridae-Ceratocanthidae, a view confirmed by Browne (1993) and reiterated here.

Scarabaeidae

The Scarabaeidae are a large family consisting of the following taxa: Aphodiinae, Aegialiinae, Aulonocneminae, Orphninae, Melolonthinae, *Acoma*, Oncerinae, Chasmatopterinae, Hopliinae, Rutelinae, Dynastinae, Cetoniinae, Trichiinae and Valginae (Browne 1993). The family is characterized by the loss of functional spiracles, membranization of pregenital segments, the loss of one of the free anal veins in the wing, and by larvae with 4-jointed antennae and the absence of stridulatory organs on the legs (Lawrence & Newton 1982).

All scarabaeids share the following 23 apomorphic character states of the wing articulation:

1. 1Ax: head proximal margin reduced,
2. dorsal surface posteriorly reduced,
3. anterior surface narrow,
4. ventral projection long and narrow,
5. embayment mesad,
6. neck long;
7. 2Ax: dorso-proximal and dorso-distal margins of dorso-proximal enlarged proximally and distally,
- 8./9. antero-median to posterior sections of the dorso-proximal ridge enlarged laterad over dorso-distal ridge,
10. anterior section of dorso-distal ridge basally curved distad,
11. posterior wing process ridge-shaped, enlarged to occupy both the anterior margin of the ventro-proximal lobe to the postero-proximal corner of subalare tendon attachment point,

12. subalare tendon attachment point very short, very broad, and apically deeply and broadly concave
13. with the base arising from the distal section of 2Ax and extends postero-proximad;
14. 3Ax: distorted, moderately long to very short,
- 15./16. tail curved, very short and very broad;
17. 1BP: anterior section of proximal arch of BR reduced by a greatly enlarged br,
18. distal arch of BR large and convex,
19. HP curves postero-dorsad close to, or even over, BScA;
20. 2BP: strongly reduced proximally,
21. proximal arch of BMA strongly oriented antero-proximad and ventrad,
22. BMP convex and very narrow,
23. the BMP-BCuA brace greatly enlarged, very broad and very convex.

Aphodiinae

Introduction

The Aphodiinae are a large subfamily with some 1 200 species representing numerous genera in five tribes. Their distribution is world wide. Adults are characterized by 8/9-jointed antennae and tarsi with distinct claws (Arnett 1968). The mouthparts are usually concealed by the clypeus. Seven pairs of spiracles are present, all situated in the pleural membrane and the pygidium is covered (in dorsal view).

The adults of most species are dung feeders, although some have been found feeding on decaying fungi, in decaying organic matter, or in the soil (Ritcher 1966). A few species are associated with ants. Larvae live on dung, organic matter, or may be root feeders (Ritcher 1966).

Hind Wing Articulation Description

First Axillary (Fig.101)

Head - Dorsal surface strikingly reduced posteriorly; convex; all margins are equally extremely narrow and very long. *Antero-dorsal margin* oriented weakly postero-distad; reduced in width; planate. *Antero-proximal margin* with ventral enlargement reduced. *Postero-proximal margin* enlargement reduced and absent. *FSc2* base normal width. Apex oriented postero-distad; rounded. Anterior surface strikingly narrow; strikingly short; not waisted medially. *FSc1* distinct; short but broad. Dorsal and ventral surfaces convex. Apex acute. *Ventral projection* long and narrow; enlarged mesally; deeply concave; strongly oriented postero-distad, weakly ventrad and not curved posteriad. Dorsal surface concave. Ventral surface convex. Apex narrow; rounded. Concavity located in the preapical area; surrounded by three unequally strong ridges. *Distal embayment* oriented mesad. *FSc2* fused to the distal margin of the ventral projection; oriented distad and weakly dorsad; reduced; small; round; planate; broad. Dorsal surface not enlarged; convex. Ventral surface convex. Apex rounded. Head and neck dorsal surface extended anteriad.

Neck strikingly narrow; strikingly long; strongly oriented distad and ventrad; articulation with 2Ax narrow, reduced anteriorly; continuous with tail. Proximal margin not curved ventrad. Distal margin straight. *Distal embayment* very weakly concave; narrow.

Tail - Dorsal view: Proximal arch strikingly reduced anteriorly and posteriorly; expanded proximally; strongly convex. *Dorsal surface* weakly concave. *Antero-proximal margin* concavity absent. *Postero-proximal margin* strongly convex. Articulation with PRR strong along the entire length of the proximal arch; long and broad; strongly recurved. Antero-dorsal surface concave. Postero-dorsal surface weakly concave. Posterior margin deeply concave. Distal arch markedly reduced anteriorly and posteriorly; strikingly elongated distally; curved ventrad along its entire length. *Apex* strongly curved ventrad and posteriad; aciculate. *Distal margin* weakly convex; appears twisted. - Ventral view: Proximal arch with a very broad ridge. Distal arch with a small ridge. Posterior margin with a broad ridge; medially narrow.

Second Axillary (Fig.102)

Radial Fulcalare absent.

Ridges - Dorsal view: Proximal ridge entire; indistinct from lobe; strongly sinuate. *Anterior section* completely concealed by the distal ridge. *Antero-median to postero-median section* strikingly enlarged above and laterad over the distal ridge; extremely slender; curves abruptly postero-proximad from the antero-median to postero-median. *Postero-median section* moderately broad and long; moderately extended past the posterior margin of the lobe; curves abruptly postero-distad and ventrad over, and conceals, the distal ridge posterior. *Posterior section* weakly enlarged above the distal ridge; oriented posteriad. Distal ridge weakly distinct from lobe. *Apex* enlarged; strongly curved ventro-proximad; convex; strikingly narrowly falcate; short. *Anterior section* moderately short; extended antero-proximad; strongly recurved. *Anterior to median section* extends adjacent to, but lies below, the proximal ridge. *Posterior section* concealed by the proximal ridge. - Ventral view: Proximal ridge stout; curved distad; distinct from lobe. *Apex* broad and truncate. *Anterior to antero-median section* broadly digitate; lies adjacent to the distal ridge. *Median to posterior section* obscured by the distal ridge. Distal ridge broad; short. *Anterior to median section* moderately broad; curved proximad. *Median and posterior sections* arise from the posterior and proximal margins of the distal lobe; distinct from lobe; narrow and short. *Median section* strongly convex. *Postero-median section* not waisted. *Subalare tendon attachment point* weakly spatulate; moderately long and narrow; apically strongly curved ventrad around the dorso-proximal ridge terminus; posterior margin rounded; extends weakly postero-distad from the median; strongly recurved; visible dorsally.

Body - Dorsal view: extremely short. Proximal lobe very long and narrow; lingulate; oriented postero-proximad; arises posteriorly from the ridge; enlarged to the same dorsal plane as the ridge; weakly sclerotized; concave. *Base* narrow. *Apex* narrowly rounded; weakly curved anteriad. *Anterior margin* concave. *Posterior margin* strikingly enlarged; broadly convex. Distal lobe very long and narrow; lingulate; longer than the proximal lobe; arises anteriorly from the ridge; weakly sclerotized; planate. *Apex* rounded. *Anterior margin* normal length; weakly concave. *Posterior margin* straight; reduced. - Ventral view:

Proximal lobe moderately large; convex. *Posterior wing process junction* formed as an extremely long, ridge-like convexity; shifted posteriad to occupy the extreme postero-proximal corner of the subalare tendon attachment point. Distal lobe moderately long and narrow; discontinuous with ridge; planate.

Median Plate (Fig.103)

FM1 oriented strongly postero-distad. *Anterior section* narrow. *Median to posterior section* moderately narrow. *Proximal margin* convex. Articulation with 2Ax extends from the antero-distal margin of the distal lobe to the posterior section, over the posterior section of the ventral ridge. *Distal margin* broadly but and weakly fused to 3Ax. FM2 absent.

Third Axillary (Fig.104)

Head weakly convex; strikingly reduced posteriorly. Proximal margin shallowly concave. Anterior margin weakly concave; broad; enlarged ventrally. *Antero-proximal margin* not extended anteriorly. *Antero-distal margin* extended distad. FCu normal size; distinct; occupies two-thirds of the head; ovoid. *Proximal margin* not reduced by AXCu. *Posterior margin* weakly reduced by an enlarged AXCu. *Distal margin* reduced by an enlarged FA. FA moderately small; extended proximad. *Anterior margin* entire. AXCu weakly extended anteriorly onto head. Suture line between FCu and FA present. Suture line between FCu and AXCu present. Suture line between FA and FJ present.

Neck elevated proximally; distally depressed. FCu section of neck absent. AXCu forms entire neck. Proximal margin very strongly and extensively elevated as a narrow ridge. *Ridge* extends close to the postero-proximal margin of the tail; very long. Dorsal surface of ridge is weakly curved distad; enlarged dorsally relative to AXA. *Embayment* moderately deep. Prong armed with a single short tooth; oriented proximo-dorsad; narrow. Detached AXCu fragment slender; rectangular; weakly sclerotized.

Tail reduced; moderately deltoid; short. *Dorsal surface* oriented mesad. Anterior to posterior section concave. *Window* absent. FJ+AXJ narrow; occupies the distal half of the tail; weakly sclerotized. Suture line between FJ and AXJ absent. Suture line between FA+AXJ and AXA present. AXA as equally sclerotized as FA+AXJ; the former occupies the postero-proximal half of the tail; straight. Suture line between AXA and AXCu present.

Hind Wing Base Description

First Basal Plate (Fig.105)

Humeral Plate broad. Anterior margin weakly sinuate; weakly sclerotized; lies adjacent to BScA. Apex moderately narrow; curved ventrad. Dorsal margin sinuate. Proximal margin convex; curved proximo-ventrad. Ventral margin weakly concave. Suture line between FPC+BPC and FC+BC absent.

Anterior Subcostal Basivenale oriented distad; slenderly ovoid; convex; strongly elevated dorsad. Proximal and distal sections separated by a prominent suture. *Proximal section* extended as a very narrow convexity; about as large as the distal section. *Distal section* continuous with ScA bulge; separated by a deep concavity. Apex broadly spatulate;

strongly curved ventrad beneath the postero-proximal margin of the ScA bulge. – Subcosta Anterior weakly convex. Bulge narrow.

Radial Basivenale extremely broad but very short; convex; narrowly open; discontinuous with the radial stem; angled proximad; slenderly ovoid. Proximal arch strikingly broad; with proximal and distal extensions; angled posteriad; broadly deltoid. *Anterior section* strikingly reduced by a greatly enlarged br; discontinuous with the anterior margin of BR. *Median section* narrow. *Posterior section* extremely broad; moderately extended proximad and very strongly extended distad. Posterior margin concave; surrounds the terminus of the BMA proximal arch. *Postero-distal margin* rounded. Anterior margin elevated above the posterior margin of the ScA bulge; extremely narrow; convex; angled proximad; continuous with the distal arch. Embayment extremely narrow. Distal arch present; convex; broadly curved proximad; discontinuous with the radial stem; recurved. br strongly sclerotized; large; occupies one-half of the proximal arch; discontinuous with BR; posteriorly extended proximad. *br projection* distinct from BSc as a very short extension; oriented antero-ventrad.

Second Basal Plate (Fig.106)

MA-BMA Junction absent. – MP-BMP Junction: MP continuous with BMP on all margins. – Crimp Patterns absent. – BMP-CuA Brace absent. – BMP-BCuA Brace present but modified; broadly continuous with BMP; entire but only moderately strong; strongly shifted distad; slender; equally broad along the entire length; convex; arises and extends postero-distad from the MP-BMP junction. Terminus appears fused with the base of BCuA but actually fuses with the distal margin of BCuA. *Point of fusion* continuous.

Medial Basivenalia very strongly reduced on all margins; extremely narrow and long; tube-shaped. BMA very narrowly scaphoid; long; strongly convex along all margins; completely fused to BMP. *Anterior margin* moderately concave. *Proximal arch* planate; straight but strongly curved ventrad; long; moderately broad. Apex spatulate; curved antero-ventrad beneath the BR proximal arch. *Distal arch* indistinct; continuous with the anterior margins of both BMP and the BMP-BCuA brace. BMP junction with BMA continuous and narrowly tubular; fused to the BMP-BCuA brace to form a narrow, looping tube; separated from both IBP and BCu by membrane; anterior margin strongly convex; extremely narrow; strongly elevated dorsad. *Postero-distal section* absent.

Cubital Basivenalia moderately narrowly fused; small and ovoid. Postero-proximal margin of BCuA fused with the antero-proximal margin of BCuP. *Suture line* present. BCuA small and ovoid; convex; oriented antero-distad; strongly shifted anteriad to occupy the postero-distal section of 2BP; moderately sclerotized. *Distal margin* anteriad of the antero-proximal margin of CuA. BCuP moderately small; ovoid; long; convex; oriented postero-distad; weakly sclerotized. Distal embayment narrow but deep. – Cubitus Anterior discontinuous with BCuA.

Basalare (Fig.107)

Head - HP lobe slender; continuous with neck. *Apex* narrowly rounded. *Dorsal surface* strongly elevated from neck; not polished. BScP lobe broad; claviform; projects posteriad

from the neck. *Dorsal surface* ovoid; strongly convex; polished; elevated from the neck but not as strongly as the HP lobe. *Ventral surface* not polished. – Posterior Subcostal Basivenale broadly deltoid; polished.

Discussion

Although aphodiines do not exhibit any autapomorphic wing articulation and wing base characters, they do share seven derived states of the wing articulation and wing base with Aulonocneminae and Aegialiinae, which together form a monophyletic group (Browne 1993). It is likely that these three taxa together form Aphodiinae, as has been implied by other workers (Koshantschikov 1913; Scholtz 1990). Aphodiinae share 46 apomorphic character states of the wing articulation and wing base with Aegialiinae, Aulonocneminae and Scarabaeinae (Browne 1993).

Aegialiinae

Introduction

Aegialiines are usually small and resemble aphodiines. They have been reported from North America, Europe, India and Tasmania (Arnett 1968). The Aegialiinae was divided by Iablokoff-Khnzorian (1977) into three tribes, the Chironini, Aegialiini, Eremazini. Representatives of the latter two tribes will be discussed. Adults are thought to be saprophagous and larvae feed on decaying organic matter (Iablokoff-Khnzorian 1977).

Hind Wing Articulation Description

First Axillary (Fig.108)

Head - Dorsal surface strikingly reduced posteriorly; convex; all margins are equally extremely narrow and very long. *Antero-dorsal margin* oriented weakly postero-distad; reduced in width; planate. *Antero-proximal margin* with ventral enlargement reduced. *Postero-proximal margin* enlargement reduced and absent. *FSc2* base normal width. Apex oriented postero-distad; rounded. Anterior surface strikingly narrow; strikingly short; not waisted medially. *FSc1* distinct; short but broad. Dorsal and ventral surfaces convex. Apex acute. *Ventral projection* long and narrow; enlarged mesally; deeply concave; strongly oriented postero-distad, weakly ventrad and not curved posteriad. Dorsal surface concave. Ventral surface convex. Concavity located in the preapical area; surrounded by three unequally strong ridges. *Distal embayment* oriented mesad. *FSc2* fused to the distal margin of the ventral projection; oriented distad and weakly dorsad; reduced; small; round; planate; broad. Dorsal surface not enlarged; convex. Ventral surface convex. Apex rounded. Head and neck dorsal surface extended anteriorly.

Neck strikingly narrow; strikingly long; strongly oriented distad and ventrad; articulation with 2Ax narrow, reduced anteriorly; continuous with tail. Proximal margin not curved ventrad. Distal margin straight. *Distal embayment* shallow.

Tail - Dorsal view: Proximal arch strikingly reduced anteriorly and posteriorly; expanded proximally; strongly convex. *Dorsal surface* weakly concave. *Antero-proximal margin*

concavity absent. *Postero-proximal margin* strongly convex. Articulation with PRR strong along the entire length of the proximal arch; long and broad; strongly recurved. Antero-dorsal surface concave. Postero-dorsal surface weakly concave. Posterior margin deeply concave. Distal arch markedly reduced anteriorly and posteriorly; strikingly elongated distally; curved ventrad along its entire length. *Apex* strongly curved ventrad and posteriad; aciculate. *Distal margin* weakly convex; appears twisted. - Ventral view: Proximal arch with a very broad ridge. Distal arch with a small ridge. Posterior margin with a broad ridge; medially narrow.

Second Axillary (Fig.109)

Radial Fulcalare absent.

Ridges - Dorsal view: Proximal ridge entire; indistinct from lobe; strongly sinuate. *Anterior section* completely concealed by the distal ridge. *Antero-median to postero-median section* strikingly enlarged above and laterad over the distal ridge; extremely slender; curves abruptly postero-proximad from the antero-median to postero-median. *Postero-median section* moderately broad and long; moderately extended past the posterior margin of the lobe; curves abruptly postero-distad and ventrad over, and conceals, the distal ridge posterior. *Posterior section* weakly enlarged above the distal ridge; oriented posteriad. Distal ridge weakly distinct from lobe. *Apex* enlarged; strongly curved ventro-proximad; convex; strikingly narrowly falcate; short. *Anterior section* moderately short; extended antero-proximad; strongly recurved. *Anterior to median section* extends adjacent to, but lies below, the proximal ridge. *Posterior section* concealed by the proximal ridge. - Ventral view: Proximal ridge stout; curved distad; distinct from lobe. *Apex* broad and truncate. *Anterior to antero-median section* broadly digitate; lies adjacent to the distal ridge. *Median to posterior section* obscured by the distal ridge. Distal ridge broad; short. *Anterior to median section* moderately broad; curved proximad. *Median and posterior sections* arise from the posterior and proximal margins of the distal lobe; distinct from lobe; narrow and short. *Median section* strongly convex. *Postero-median section* not waisted. *Subalare tendon attachment point* weakly spatulate; moderately long and narrow; apically strongly curved ventrad around the dorso-proximal ridge terminus; posterior margin rounded; extends weakly postero-distad from the median; strongly recurved; visible dorsally.

Body - Dorsal view: extremely short. Proximal lobe very long and narrow; lingulate; oriented postero-proximad; arises posteriorly from the ridge; enlarged to the same dorsal plane as the ridge; weakly sclerotized; concave. *Base* narrow. *Apex* narrowly rounded; weakly curved anteriorly. *Anterior margin* concave. *Posterior margin* strikingly enlarged; broadly convex. Distal lobe very long and narrow; lingulate; longer than the proximal lobe; arises anteriorly from the ridge; weakly sclerotized; planate. *Apex* rounded. *Anterior margin* normal length; weakly concave. *Posterior margin* straight; reduced. - Ventral view: Proximal lobe moderately large; convex. *Posterior wing process junction* formed as an extremely long, ridge-like convexity; shifted posteriad to occupy the extreme postero-proximal corner of the subalare tendon attachment point. Distal lobe moderately long and narrow; discontinuous with ridge; planate.

Median Plate (Fig.110)

FM1 oriented strongly postero-distad. *Anterior section* narrow. *Median to posterior section* moderately narrow. *Proximal margin* convex. Articulation with 2Ax extends from the antero-distal margin of the distal lobe to the posterior section over the posterior section of the ventral ridge. *Distal margin* broadly but weakly fused to 3Ax. FM2 absent.

Third Axillary (Fig.111)

Head weakly convex; strikingly reduced posteriorly. Proximal margin shallowly concave. Anterior margin weakly concave; broad; enlarged ventrally. *Antero-proximal margin* not extended anteriad. *Antero-distal margin* extended distad. FCu normal size; distinct; occupies two-thirds of the head; ovoid. *Proximal margin* not reduced by AXCu. *Posterior margin* weakly reduced by an enlarged AXCu. *Distal margin* reduced by an enlarged FA. FA moderately small; extended proximad. *Anterior margin* entire. AXCu weakly extended anteriad onto head. Suture line between FCu and FA present. Suture line between FCu and AXCu present. Suture line between FA and FJ present.

Neck elevated proximally; distally depressed. FCu section of neck absent. AXCu forms entire neck. Proximal margin very strongly and extensively elevated as a narrow ridge. *Ridge* extends close to the postero-proximal margin of the tail; very long. Dorsal surface of ridge is weakly curved distad; enlarged dorsally relative to AXA. *Embayment* moderately deep. Prong armed with a single short tooth; oriented proximo-dorsad; narrow. Detached AXCu fragment slender; rectangular; weakly sclerotized.

Tail reduced; moderately deltoid; short. *Dorsal surface* oriented mesad. Anterior to posterior section concave. *Window* absent. FJ+AXJ narrow; occupies the distal half of the tail; weakly sclerotized. Suture line between FJ and AXJ absent. Suture line between FA+AXJ and AXA present. AXA as equally sclerotized as FA+AXJ; the former occupies the postero-proximal half of the tail; straight. Suture line between AXA and AXCu present.

Hind Wing Base Description

First Basal Plate (Fig.112)

Humeral Plate extremely broad. Anterior margin convex; weakly sclerotized; lies adjacent to BScA. Apex broad; curved ventrad. Dorsal margin deeply concave. Proximal margin convex; curved proximo-ventrad; clavate. Ventral margin concave. Suture line between FPC+BPC and FC+BC absent.

Anterior Subcostal Basivenale oriented distad; slenderly ovoid; convex; strongly elevated dorsad. Proximal and distal sections separated by a prominent suture. *Proximal section* extended as a moderately narrow convexity; about as large as the distal section. *Distal section* continuous with ScA bulge; separated by a deep concavity. Apex broadly spatulate; strongly curved ventrad beneath the postero-proximal margin of the ScA bulge. – Subcosta Anterior weakly convex. Bulge broad.

Radial Basivenale extremely broad but very short; convex; narrowly open; discontinuous with the radial stem; angled proximad; slenderly ovoid. Proximal arch strikingly broad;

with proximal and distal extensions; angled posteriad; broadly deltoid. *Anterior section* strikingly reduced by a greatly enlarged br; discontinuous with the anterior margin of BR. *Median section* narrow. *Posterior section* extremely broad; moderately extended proximad and very strongly extended distad. Posterior margin concave; surrounds the terminus of the BMA proximal arch. *Postero-distal margin* rounded. Anterior margin elevated above the posterior margin of the ScA bulge; extremely narrow; convex; angled proximad; continuous with the distal arch. Embayment extremely narrow. Distal arch present; convex; broadly curved proximad; discontinuous with the radial stem; recurved. br strongly sclerotized; large; occupies one-half of the proximal arch; discontinuous with BR; posteriorly extended proximad. *br projection* distinct from BSc as a slender, dove-tail shaped extension; oriented antero-ventrad.

Second Basal Plate (Fig.113)

MA-BMA Junction absent. – MP-BMP Junction: MP continuous with BMP on all margins. – Crimp Patterns absent. – BMP-CuA Brace absent. – BMP-BCuA Brace present but modified; broadly continuous with BMP; entire but only moderately strong; strongly shifted distad; slender; equally broad along the entire length; convex; arises and extends postero-distad from the MP-BMP junction. Terminus appears fused with the base of BCuA but actually fuses with the distal margin of BCuA. *Point of fusion* continuous.

Medial Basivenalia very strongly reduced on all margins; extremely narrow and long; tube-shaped. BMA very narrowly scaphoid; long; strongly convex along all margins; completely fused to BMP. *Anterior margin* moderately concave. *Proximal arch* planate; straight but strongly curved ventrad; long; moderately broad. Apex spatulate; curved antero-ventrad beneath the BR proximal arch. *Distal arch* indistinct; continuous with the anterior margins of both BMP and the BMP-BCuA brace. BMP junction with BMA continuous and narrowly tubular; fused to the BMP-BCuA brace to form a narrow, looping tube; separated from both IBP and BCu by membrane; anterior margin strongly convex; extremely narrow; strongly elevated dorsad. *Postero-distal section* very weakly sclerotized; nearly absent.

Cubital Basivenalia moderately narrowly fused; small and ovoid. Postero-proximal margin of BCuA fused with the antero-proximal margin of BCuP. *Suture line* present. BCuA small and ovoid; convex; oriented antero-distad; strongly shifted anteriorly to occupy the postero-distal section of 2BP; moderately sclerotized. *Distal margin* anteriorly of the antero-proximal margin of CuA. BCuP moderately small; ovoid; long; convex; oriented postero-distad; weakly sclerotized. Distal embayment very weak. – Cubitus Anterior continuous with BCuA.

Basalare (Fig.114)

Head - HP lobe slender; continuous with neck. *Apex* narrowly rounded. *Dorsal surface* strongly elevated from neck; not polished. BScP lobe narrow; claviform; projects dorsad from neck. *Dorsal surface* narrowly ovoid; strongly convex; polished; elevated from neck but not as elevated as the HP lobe. *Ventral surface* not polished. – Posterior Subcostal Basivenale broadly deltoid; polished.

Discussion

Although Aegialiinae do not exhibit any autapomorphic wing articulation and wing base characters, they do share seven derived character states of the wing articulation and wing base with Aulonocneminae and Aphodiinae, which together form a monophyletic group (Browne 1993). It is likely that these three taxa together form Aphodiinae, as has been implied by other workers (Koshantschikov 1913; Scholtz 1990).

Many workers have suggested that aegialiines are most closely related to Aphodiinae (Stebnicka 1985; Cambefort 1987; Nel & Scholtz 1990; d'Hotman & Scholtz 1990a). Many primitive morphological characters support this relationship, including those of the mouthparts (Nel & Scholtz 1990), male genitalia (d'Hotman & Scholtz 1990a), spiracles (Ritcher 1969a,b), and chromosomes (Virkki 1967). This view is reiterated here. Aegialiinae share 46 apomorphic character states of the wing articulation and wing base with Aphodiinae, Aulonocneminae and Scarabaeinae (Browne 1993).

Aulonocneminae

Introduction

This is a small subfamily comprising four genera and about 50 species, which occur mainly on Madagascar but also on other Indian Ocean Islands, and in southern Africa. An *Aulonocnemis* larva was described by Paulian & Lumaret (1974). Adult characters include those of mouthparts that are not covered by the labrum or clypeus, a covered pygidium, and eyes that are visible in ventral view. They are thought to be sapro-xylophagous (Cambefort 1987).

Hind Wing Articulation Description

First Axillary (Fig.115)

Head - Dorsal surface strikingly reduced posteriorly; convex; all margins are equally extremely narrow and very long. *Antero-dorsal margin* oriented weakly postero-distad; reduced in width; planate. *Antero-proximal margin* with ventral enlargement reduced. *Postero-proximal margin* enlargement reduced and absent. *FSc2* base normal width. Apex oriented postero-distad; rounded. Anterior surface strikingly narrow; strikingly short; not waisted medially. *FSc1* distinct; short but broad. Dorsal and ventral surfaces convex. Apex acute. *Ventral projection* moderately short and narrow; enlarged mesally; deeply concave; strongly oriented postero-distad, weakly ventrad and not curved posteriad. Dorsal surface concave. Ventral surface convex. Apex narrow; truncate. Concavity located in the preapical area; surrounded by three unequally strong ridges. *Distal embayment* oriented mesad. *FSc2* fused to the distal margin of the ventral projection; oriented distad and weakly dorsad; reduced; small; round; planate. Dorsal surface not enlarged; convex. Ventral surface convex. Apex rounded. Head and neck dorsal surface extended anteriad.

Neck strikingly narrow; strikingly long; strongly oriented distad and ventrad; articulation with 2Ax narrow, reduced anteriorly; continuous with tail. Proximal margin not curved ventrad. Distal margin straight. *Distal embayment* very weakly concave.

Tail - Dorsal view: Proximal arch strikingly reduced anteriorly and posteriorly; expanded proximally; strongly convex; strongly curved posteriad. *Dorsal surface* weakly concave. *Antero-proximal margin* concavity absent. *Postero-proximal margin* strongly convex. Articulation with PRR strong along the entire length of the proximal arch; long and broad; strongly recurved. Antero-dorsal surface concave. Postero-dorsal surface weakly concave. Posterior margin deeply concave. Distal arch markedly reduced anteriorly and posteriorly; strikingly elongated distally; extremely long; curved ventrad along its entire length. *Apex* strongly curved ventrad and posteriad; acuminate. *Distal margin* weakly convex; appears twisted. - Ventral view: Proximal arch with an extremely broad ridge. Distal arch with a small ridge. Posterior margin with a very broad ridge; medially narrow.

Second Axillary (Fig.116)

Radial Fulcalare absent.

Ridges - Dorsal view: Proximal ridge entire; indistinct from lobe; strongly sinuate. *Anterior* completely concealed by the distal ridge. *Antero-median to postero-median* strikingly enlarged above and laterad over the distal ridge; extremely slender; curves abruptly postero-proximad from the antero-median to postero-median. *Postero-median* moderately broad and long; moderately extended past the posterior margin of the lobe; curves abruptly postero-distad and ventrad over, and conceals, the distal ridge posterior. *Posterior* weakly enlarged above the distal ridge; oriented posteriad. Distal ridge weakly distinct from lobe. *Apex* enlarged; strongly curved ventro-proximad; convex; strikingly narrowly falcate; short. *Anterior* moderately short; extended antero-proximad; strongly recurved. *Anterior to median* extends adjacent to, but lies below, the proximal ridge. *Posterior* concealed by the proximal ridge. - Ventral view: Proximal ridge stout; curved distad; distinct from lobe. *Apex* broad and truncate. *Anterior to antero-median* broadly digitate; lies adjacent to the distal ridge. *Median to posterior* obscured by the distal ridge. Distal ridge broad; short. *Anterior to median* moderately broad; curved proximad. *Median and posterior sections* arise from the posterior and proximal margins of the distal lobe; distinct from lobe; narrow and short. *Median* strongly convex. *Postero-median* not waisted. *Subalare tendon attachment point* weakly spatulate; moderately long and narrow; apically strongly curved ventrad around the dorso-proximal ridge terminus; posterior margin rounded; extends weakly postero-distad from the median; strongly recurved; visible dorsally.

Body - Dorsal view: extremely short. Proximal lobe very long and narrow; lingulate; oriented postero-proximad; arises posteriorly from the ridge; enlarged to the same dorsal plane as the ridge; weakly sclerotized; concave. *Base* narrow. *Apex* narrowly rounded; curved anteriorly. *Anterior margin* concave. *Posterior margin* strikingly enlarged; broadly convex. Distal lobe moderately short and narrow; shorter than the proximal lobe; arises anteriorly from the ridge; weakly sclerotized; planate. *Apex* rounded. *Anterior margin* normal length; weakly concave. *Posterior margin* straight; entire. - Ventral view: Proximal lobe moderately large; convex. *Posterior wing process junction* formed as an extremely long, ridge-like convexity; shifted posteriad to occupy the extreme postero-proximal corner of the subalare tendon attachment point. Distal lobe small; discontinuous with ridge; planate.

Median Plate (Fig.117)

FM1 oriented strongly postero-distad. *Anterior* narrow. *Median to posterior* moderately narrow. *Proximal margin* convex. Articulation with 2Ax extends from the antero-distal margin of the distal lobe to the posterior section over the posterior section of the ventral ridge. *Distal margin* broadly but weakly fused to 3Ax. FM2 absent.

Third Axillary (Fig.118)

Head weakly convex; strikingly reduced posteriorly. Proximal margin shallowly concave. Anterior margin weakly concave; broad; enlarged ventrally. *Antero-proximal margin* not extended anteriad. *Antero-distal margin* extended distad. FCu normal size; distinct; occupies two-thirds of the head; ovoid. *Proximal margin* not reduced by AXCu. *Posterior margin* weakly reduced by an enlarged AXCu. *Distal margin* reduced by an enlarged FA. FA moderately small; extended proximad. *Anterior margin* entire. AXCu weakly extended anteriad onto head. Suture line between FCu and FA present. Suture line between FCu and AXCu present. Suture line between FA and FJ present.

Neck elevated proximally; distally depressed. FCu section of neck absent. AXCu forms entire neck. Proximal margin very strongly and extensively elevated as a narrow ridge. *Ridge* extends close to the postero-proximal margin of the tail; very long. Dorsal surface of ridge is weakly curved distad; enlarged dorsally relative to AXA. *Embayment* moderately deep. Prong armed with a single short tooth; oriented proximo-dorsad; narrow. Detached AXCu fragment slender; rectangular; weakly sclerotized.

Tail reduced; moderately deltoid; short. *Dorsal surface* oriented mesad. Anterior to posterior concave. *Window* absent. FJ+AXJ narrow; occupies the distal half of the tail; weakly sclerotized. Suture line between FJ and AXJ absent. Suture line between FA+AXJ and AXA present. AXA as equally sclerotized as FA+AXJ; the former occupies the postero-proximal half of the tail; straight. Suture line between AXA and AXCu present.

Hind Wing Base Description

First Basal Plate (Fig.119)

Humeral Plate very broad. Anterior margin sinuate; weakly sclerotized; lies adjacent to BScA. Apex clavate; curved ventrad. Dorsal margin sinuate. Proximal margin convex; curved proximo-ventrad. Ventral margin weakly concave. Suture line between FPC+BPC and FC+BC absent.

Anterior Subcostal Basivenale oriented distad; slenderly ovoid; convex; strongly elevated dorsad. Proximal and distal sections separated by a prominent suture. *Proximal section* extended as a very narrow convexity; about as large as the distal section. *Distal section* continuous with ScA bulge; separated by a deep concavity. Apex broadly spatulate; strongly curved ventrad beneath the postero-proximal margin of the ScA bulge. – Subcosta Anterior weakly convex. Bulge narrow.

Radial Basivenale extremely broad but very short; convex; narrowly open; discontinuous with the radial stem; angled proximad; slenderly ovoid. Proximal arch strikingly broad; with proximal and distal extensions; angled posteriad; broadly deltoid. *Anterior* strikingly

reduced by a greatly enlarged br; discontinuous with the anterior margin of BR. *Median* narrow. *Posterior* extremely broad; moderately extended proximad and very strongly extended distad. Posterior margin concave; surrounds the terminus of the BMA proximal arch. *Postero-distal margin* rounded. Anterior margin elevated above the posterior margin of the ScA bulge; extremely narrow; convex; angled proximad; continuous with the distal arch. Embayment extremely narrow. Distal arch present; convex; broadly curved proximad; discontinuous with the radial stem; recurved. br strongly sclerotized; large; occupies one-half of the proximal arch; discontinuous with BR; posteriorly extended proximad. *br projection* distinct from BSc as a small, deltoid extension; oriented antero-ventrad.

Second Basal Plate (Fig.120)

MA-BMA Junction absent. – MP-BMP Junction: MP continuous with BMP on all margins. – Crimp Patterns absent. – BMP-CuA Brace absent. – BMP-BCuA Brace present but modified; broadly continuous with BMP; entire but only moderately strong; strongly shifted distad; slender; equally broad along the entire length; convex; arises and extends postero-distad from the MP-BMP junction. Terminus appears fused with the base of BCuA but actually fuses with the distal margin of BCuA. *Point of fusion* continuous.

Medial Basivenalia very strongly reduced on all margins; extremely narrow and long; tube-shaped. BMA very narrowly scaphoid; long; strongly convex along all margins; completely fused to BMP. *Anterior margin* moderately concave. *Proximal arch* planate; straight but strongly curved ventrad; long; moderately broad. Apex spatulate; curved antero-ventrad beneath the BR proximal arch. *Distal arch* indistinct; continuous with the anterior margins of both BMP and the BMP-BCuA brace. BMP junction with BMA continuous and narrowly tubular; fused to the BMP-BCuA brace to form a narrow, looping tube; separated from both IBP and BCu by membrane; anterior margin strongly convex; extremely narrow; strongly elevated dorsad. *Postero-distal section* absent.

Cubital Basivenalia moderately narrowly fused; small and ovoid. Postero-proximal margin of BCuA fused with the antero-proximal margin of BCuP. *Suture line* present. BCuA small and ovoid; convex; oriented antero-distad; strongly shifted anteriorad to occupy the postero-distal section of 2BP; moderately sclerotized. *Distal margin* anteriorad of the antero-proximal margin of CuA. BCuP moderately small; ovoid; long; convex; oriented postero-distad; weakly sclerotized. Distal embayment small. – Cubitus Anterior discontinuous with BCuA.

Basalare (Fig.121)

Head - HP lobe slender; continuous with neck. *Apex* narrowly rounded. *Dorsal surface* strongly elevated from neck; not polished. BScP lobe broad; claviform; projects posteriorad from neck. *Dorsal surface* ovoid; strongly convex; polished; elevated from neck but not as elevated as the HP lobe. *Ventral surface* not polished. – Posterior Subcostal Basivenale broadly deltoid; polished.

Discussion

Although Aulonocneminae do not exhibit any autapomorphic character states of the wing articulation and wing base, they do share seven derived character states of the wing

articulation and wing base with Aegialiinae and Aphodiinae, which together form a monophyletic group (Browne 1993). It is likely that these three taxa together form Aphodiinae, as has been implied by other workers (Koshantschikov 1913; Scholtz 1990). Aulonocneminae share 46 apomorphic character states of the wing articulation and wing base with Aphodiinae, Aegialiinae and Scarabaeinae (Browne 1993). This relationship has been suggested previously (Stebnicka 1985; Cambefort 1987; Nel & Scholtz 1990; d'Hotman & Scholtz 1990a). Many morphological characters support this relationship, including those of the mouthparts (Nel & Scholtz 1990), male genitalia (d'Hotman & Scholtz 1990a), and others from the head, thorax and abdomen (Stebnicka 1985). Only a single diagnostic character separates aulonocnemines from Aphodiinae (Stebnicka 1985).

Scarabaeinae

Introduction

The Scarabaeinae are a large subfamily of approximately 4500 species and 200 genera (Halffter & Edmonds 1982). Members of the subfamily are generally known as the true dung beetles. The Scarabaeinae include six tribes, Onthophagini, Coprini, Eurysternini, Oniticellini, Onitini and Scarabaeini.

The adults and larvae of most Scarabaeinae utilize subliquid and liquid contents of dung and decaying vegetation, described by Stebnicka (1985) as coprophagy or soft saprophagy. For further information on biology, the reader is referred to the recent work by Halffter & Matthews (1966) and Halffter & Edmonds (1982).

Hind Wing Articulation Description

First Axillary (Fig.122)

Head - Dorsal surface strikingly reduced posteriorly; convex; all margins are equally extremely narrow and very long. *Antero-dorsal margin* oriented weakly postero-distad; reduced in width; planate. *Antero-proximal margin* with ventral enlargement reduced. *Postero-proximal margin* enlargement reduced and absent. *FSc2* base normal width. Apex oriented postero-distad; rounded. Anterior surface strikingly narrow; strikingly short; not waisted medially. *FSc1* distinct; long and broad; oriented antero-dorsad; very strongly elevated over the base of the ventrad projection. Dorsal and ventral surfaces convex. Apex acute. *Ventral projection* long and narrow; enlarged mesally; deeply concave; strongly oriented postero-distad, weakly ventrad and not curved posteriad. Dorsal surface concave. Ventral surface convex. Apex narrow; rounded; weakly recurved. Concavity located in the preapical area; surrounded by three unequally strong ridges. *Distal embayment* moderately shallow; oriented mesad. *FSc2* fused to the distal margin of the ventral projection; oriented distad and weakly dorsad; reduced; small; round; completely planate; broad. Dorsal surface not enlarged; convex. Ventral surface convex. Apex aciculate. Head and neck dorsal surface extended anteriad.

Neck very narrow; strikingly long; strongly oriented distad and ventrad; articulation with 2Ax narrow, reduced anteriorly; medially convex; discontinuous with tail. Proximal margin

very weakly sinuate; weakly curved ventrad. Distal margin very weakly sinuate. *Distal embayment* very weakly concave; narrow.

Tail - Dorsal view: perpendicular to neck. Proximal arch strikingly reduced anteriorly and posteriorly; expanded proximally; extremely small; convex. *Dorsal surface* weakly concave. *Antero-proximal margin* concavity present. *Postero-proximal margin* strongly convex. Articulation with PRR strong along the entire length of the proximal arch; very short but broad; strongly recurved. Antero-dorsal surface concave. Postero-dorsal surface weakly concave. Posterior margin straight. Distal arch very strongly reduced anteriorly and posteriorly; very strikingly expanded and elongated distally; strongly curved ventrad along its entire length; oriented distad. *Apex* strongly curved ventrad and weakly so posteriad; aciculate. *Distal margin* straight. - Ventral view: Proximal and distal margins each with prominent ridges.

Second Axillary (Fig.123)

Radial Fulcalare absent.

Ridges - Dorsal view: Proximal ridge entire; distinct from lobe; strongly sinuate. *Anterior section* completely concealed by the distal ridge. *Antero-median to postero-median section* strikingly enlarged above and laterad over the distal ridge; extremely slender; curves abruptly postero-proximad from the antero-median to postero-median. *Postero-median section* moderately broad and long; moderately extended past the posterior margin of the lobe; curves abruptly postero-distad and ventrad over, and conceals, the distal ridge posterior. *Posterior section* strongly reduced posteriorly; does not extend past the posterior margin of the lobe; strikingly enlarged laterad over the distal ridge; oriented posteriad; does not curve ventrad. Distal ridge weakly distinct from lobe. *Apex* enlarged; strongly curved ventro-proximad; convex; strikingly narrowly falcate; short. *Anterior section* moderately short; extended antero-proximad; not recurved. *Antero-median to posterior section* concealed by the proximal ridge. - Ventral view: Proximal ridge moderately long; broadly acerose; curved distad; distinct from the lobe. *Apex* narrow and rounded. *Anterior to antero-median section* broadly acerose; lies adjacent to the distal ridge. *Median to posterior section* obscured by the distal ridge. Distal ridge broad; short. *Apex* narrow and rounded. *Anterior to median section* moderately long; broadly acerose; curved proximad. *Median and posterior sections* arise from the posterior and proximal margins of the distal lobe; distinct from the lobe; moderately narrow and very short. *Median section* strongly convex. *Postero-median section* waisted. *Subalare tendon attachment point* weakly spatulate; moderately long and narrow; apically strongly curved ventrad around the dorso-proximal ridge terminus; posterior margin rounded; extends weakly postero-distad from the median; extremely strongly recurved; visible dorsally.

Body - Dorsal view: extremely short. Proximal lobe very long and narrow; lingulate; oriented postero-proximad; arises posteriorly from the ridge; enlarged to the same dorsal plane as the ridge; strongly sclerotized; weakly concave. *Base* very broad. *Apex* rounded; straight. *Anterior margin* concave. *Posterior margin* strikingly enlarged; concave. Distal lobe moderately short but very broad; broadly deltoid; as long as the proximal lobe; arises posteriorly from the ridge; weakly sclerotized; planate. *Apex* aciculate. *Anterior margin*

normal length; concave. *Posterior margin* straight; reduced. - Ventral view: Proximal lobe moderately large; convex. *Posterior wing process junction* formed as an extremely long, ridge-like convexity; shifted posteriad to occupy the extreme postero-proximal corner of the subalare tendon attachment point. Distal lobe moderately small and broad; continuous with ridge; planate.

Median Plate (Fig.124)

FM1 oriented strongly postero-distad. *Anterior section* narrow. *Median to posterior section* moderately narrow. *Proximal margin* convex. Articulation with 2Ax extends from the antero-distal margin of the distal lobe to the posterior section, over the posterior section of the ventral ridge. *Distal margin* broadly and strongly fused to 3Ax; suture line indistinct. FM2 slender; fused to the distal margin of FM1 along its entire length; separated by a very weak suture line. *Postero-distal section* forms a strongly sclerotized convexity which extends over a complimentary concavity on the antero-proximal extension of the 3Ax head; posteriorly deeply concave.

Third Axillary (Fig.125)

Head moderately broad; weakly convex; strikingly reduced posteriorly. Proximal margin shallowly concave. Anterior margin weakly concave; broad; enlarged ventrally as a broad plate with a deep concavity. *Antero-proximal margin* weakly extended proximad; very strongly sclerotized; forms a ball and socket joint with FM2. Anterior margin of extension convex; articulates within the FM2 concavity. Posterior margin of extension concave; articulates with the FM2 convexity. *Proximal margin* deeply concave; strongly fused with FM1. *Antero-distal margin* strongly extended distad. FCu normal size; distinct; occupies two-thirds of the head; deltoid. *Posterior margin* not reduced by AXCu. *Distal margin* reduced by an enlarged FA and AXCu. AXCu strongly extended anteriad along the distal margin of FCu. *Distal section* almost extending to the antero-distal corner of the head; lies between FCu and FA. FA moderately large; extended proximad. *Anterior margin* entire. Suture line between FCu and FA present. Suture line between FCu and AXCu present. Suture line between FA and FJ present.

Neck elevated proximally and distally along most of its length. FCu section of neck absent. AXCu forms entire neck. Proximal margin very strongly and extensively elevated as a very broad ridge. *Ridge* extends close to the postero-proximal margin of the tail; very long. Dorsal surface of ridge is very strongly curved distad over the distal margin of the tail; enlarged dorsally relative to AXA. Antero-distal margin not elevated. *Embayment* moderately shallow. Prong armed with a single tooth; oriented proximo-dorsad; narrow. *Proximal margin* fused to AXCu. Detached AXCu fragment slender; deltoid; weakly sclerotized.

Tail reduced; broadly deltoid; short. *Dorsal surface* oriented mesad. Anterior to posterior section concave. *Window* absent. FJ+AXJ narrow; occupies the most of the tail area; moderately sclerotized. Suture line between FJ and AXJ absent. Suture line between FA+AXJ and AXA present. AXA as equally sclerotized as FA+AXJ; the former occupies

the postero-proximal section of the tail; strongly reduced; extremely small; straight. Suture line between AXA and AXCu present.

Hind Wing Base Description

First Basal Plate (Fig.126)

Humeral Plate very broad. Anterior margin weakly sinuate; weakly sclerotized; lies adjacent to BScA. Apex broad; curved ventrad. Dorsal margin sinuate. Proximal margin straight; strongly curved proximo-ventrad. Ventral margin weakly concave. Suture line between FPC+BPC and FC+BC absent.

Anterior Subcostal Basivenale oriented distad; slenderly ovoid; convex; strongly elevated dorsad. Proximal and distal sections separated by a prominent suture. *Proximal section* extended as a very narrow convexity; about as large as the distal section. *Posterior margin* deeply concave. *Distal section* extremely narrow and long; continuous with ScA bulge; separated by a deep concavity. Antero-distal to medio-distal margin separated from ScA by a deep concavity. Apex broadly spatulate; deeply concave; strongly curved ventrad beneath the postero-proximal margin of the ScA bulge. – Subcosta Anterior very strongly convex. Bulge extremely broad.

Radial Basivenale extremely broad but very short; convex; open; discontinuous with the radial stem; angled proximad; slenderly ovoid. Proximal arch strikingly enlarged; with proximal and distal extensions; angled posteriad; broadly deltoid. Distal extension strikingly enlarged antero- to postero-distally. *Anterior section* strikingly reduced by a greatly enlarged br; discontinuous with the anterior margin of BR. *Median section* narrow. *Posterior section* extremely broad; moderately extended proximad and very strongly extended distad. Posterior margin concave; surrounds the terminus of the BMA proximal arch. *Postero-distal margin* rounded. Anterior margin not elevated above the posterior margin of the ScA bulge; extremely narrow; convex; angled proximad; continuous with the distal arch. Embayment strikingly narrow and falcate. Distal arch present; convex; broadly curved proximad; discontinuous with the radial stem; recurved. br strongly sclerotized; large; occupies one-half of the proximal arch; discontinuous with BR; posteriorly extended proximad. *br projection* distinct from BSc as a slender, dove-tail shaped extension; oriented antero-ventrad.

Second Basal Plate (Fig.127)

MA-BMA Junction absent. – MP-BMP Junction: MP continuous with BMP on all margins. – Crimp Patterns absent. – BMP-CuA Brace absent. – BMP-BCuA Brace present but modified; broadly continuous with BMP; entire but only moderately strong; shifted distad; slender; equally broad along the entire length; convex; arises and extends postero-distad from the MP-BMP junction. Terminus fused with the distal margin of BCuA. *Point of fusion* discontinuous.

Medial Basivenalia very strongly reduced on all margins; extremely short and narrow; tube-shaped. BMA very narrowly scaphoid; long; strongly convex along all margins; completely fused to BMP. *Anterior margin* moderately concave. *Proximal arch* planate; straight but strongly curved ventrad; long; moderately narrow. Apex narrowly spatulate;

curved antero-ventrad beneath the BR proximal arch. *Distal arch* reduced; indistinct; continuous with the anterior margins of both BMP and the BMP-BCuA brace. BMP junction with BMA continuous and narrowly tubular; fused to the BMP-BCuA brace to form a narrow, looping tube; separated from both 1BP and BCu by membrane; anterior margin strongly convex; extremely narrow; strongly elevated dorsad. *Postero-distal section* reduced.

Cubital Basivenalia broadly fused. Posterior margin of BCuA fused with the anterior margin of BCuP. *Suture line* present. BCuA very small and ovoid; convex; oriented antero-distad; moderately shifted anteriad to occupy the postero-distal section of 2BP; weakly sclerotized. *Proximal margin* proximad of CuA antero-proximal margin. BCuP large; deltoid; moderately short; very weakly convex; oriented postero-distad; very weakly sclerotized. Distal embayment absent. – Cubitus Anterior continuous with BCuA.

Basalare (Fig.128)

Head - HP lobe slender; continuous with neck. *Apex* narrowly rounded. *Dorsal surface* strongly elevated from neck; polished. BScP lobe moderately broad; claviform; projects dorsad and posteriad from neck. *Dorsal surface* ovoid; convex; polished; elevated from neck but not as strongly as the HP lobe. *Ventral surface* not polished. – Posterior Subcostal Basivenale deltoid; polished.

Discussion

Monophyly of the Scarabaeinae is supported by the fact that all of the taxa in this subfamily share the following 12 apomorphic character states of the wing articulation and wing base:

1. 1Ax: FSc1 is very strongly elevated, long and oriented antero-dorsad over the base of the ventral projection,
2. FSc2 is completely planate,
3. the neck is medially convex,
4. the distal arch of the tail is strongly reduced anteriorly, strongly elongated distally,
5. strongly reduced posteriorly;
6. 2Ax: the posterior section of the dorso-proximal ridge is strikingly enlarged laterad;
7. FM1+FM2 – together with the proximal extension of the 3Ax head are highly modified to form a ball-and-socket joint;
8. 3Ax: the antero-proximal section of the head is narrowly enlarged proximally to form a long extension;
9. 1BP: the proximal arch of BR is strikingly enlarged,
10. the distal extension of the proximal arch is strikingly enlarged antero- to postero-distally,
11. the BR embayment is strikingly narrow and falcate;
12. 2BP: extremely short and narrow.

Many workers have suggested that scarabaeines occupy an intermediate position between Aphodiinae and Melolonthinae, most closely related to the former (Howden 1982; Scholtz 1990). Many larval and adult characters support this relationship (Howden 1982)

including those of the mouthparts (Nel & Scholtz 1990) and male genitalia (d'Hotman & Scholtz 1990a). Scarabaeinae share 46 apomorphic character states of the wing articulation and wing base with Aegialiinae, Aulonocneminae and Aphodiinae (Browne 1993).

Orphninae

Introduction.

The Orphninae are a small Old World group with a few genera. Most species are in *Orphnus* and *Hybalus*. Adults and larvae have been recorded feeding on potatoes and sugar cane (Paulian & Lumaret 1982). The larvae of two species of *Hybalus* were also described in that paper.

Adults are short and convex, with a broad clypeus (similar to the Coprinae). Mouthparts are seldom visible in dorsal view (exposed). Antennae are 10-jointed and seven pairs of spiracles are present, all situated in the pleural membrane. The pygidium is visible in dorsal view and wing venation resembles that of *Brenskea* (Hybosoridae) (Iablokoff-Khnzorian 1977). Little is known about their biology.

Hind Wing Articulation Description

First Axillary (Fig.129)

Head Dorsal surface strongly reduced posteriorly; broad; clavate; convex. *Antero-dorsal margin* oriented weakly postero-distad; normal width; planate. *Antero-proximal margin* with ventral enlargement reduced. *Postero-proximal margin* enlargement moderate and broad. *FSc2* base normal width; deeply concave. Apex oriented postero-distad; rounded but weakly truncate. Anterior surface narrow; long; not waisted medially. *FSc1* absent. *Ventral projection* long and narrow; deeply concave; oriented ventrad and weakly postero-distad. Dorsal surface base to median concave. Ventral surface convex. Concavity located in the preapical area; surrounded by three unequally strong ridges. *Distal embayment* oriented ventro-mesad. *FSc2* oriented distad and weakly dorsad; weakly deltoid; convex; broad; moderately short. Dorsal surface enlarged dorsally; convex; appears twisted. Ventral surface convex. Base proximally with a convexity. Apex acuminate. Head and neck dorsal surface extended antierad.

Neck normal width; long; weakly oriented antero-distad; articulation with 2Ax extends along the distal margin of the neck and tail; continuous with tail. Proximal margin reduced; sinuate; not curved ventrad. Distal margin concave. *Distal embayment* moderately concave; moderately shallow but broad.

Tail - Dorsal view: Proximal arch normal size. *Dorsal surface* weakly concave. *Antero-proximal margin* weakly convex. *Postero-proximal margin* straight. Articulation with PRR strong along the entire length of the proximal arch; long and broad; strongly recurved. Antero-dorsal surface concave. Postero-dorsal surface concave. Posterior margin weakly concave. Distal arch normal size; curved ventrad along its entire length. *Apex* weakly curved posteriad; acuminate. *Distal margin* weakly concave. - Ventral view: Proximal arch

with a weak ridge. Posterior margin with a prominent ridge. Distal arch with a very slender ridge.

Second Axillary (Fig.130)

Radial Fulcalare present; moderately sclerotized; slender.

Ridges - Dorsal view: Proximal ridge entire; distinct from lobe. *Apex* partially obscured by the distal ridge; waisted. *Anterior section* distal margin exposed. *Antero-median to postero-median section* moderately enlarged above and laterad over the distal ridge. *Posterior section* weakly enlarged above the distal ridge; broadly curved postero-proximad; slender; long; distinct from lobe; extended past the posterior margin of lobe. Distal ridge weakly distinct from lobe. *Apex* narrow; convex; strikingly elongate; aciculate; strongly curved ventro-proximad; the distal margin is reduced revealing the ventral section of the distal lobe. *Anterior section* slender and strikingly elongate; straight and anteriad. *Median to posterior section* dorsally concealed by the proximal ridge. *Posterior section* extended past the posterior margin of lobe. - Ventral view: Proximal ridge anteriorly completely conceals the distal ridge. *Apex* aciculate. *Anterior to antero-median section* moderately narrow and very long; curved distad. *Median to posterior section* obscured by the distal ridge. Distal ridge *median and posterior sections* arise from the posterior and proximal margins of the distal lobe; distinct from lobe; broad; moderately long. *Antero-median section* weakly waisted. *Median section* convex. *Postero-proximal angle* not reduced. *Postero-distal angle* not extended postero-distad. *Subalare tendon attachment point* short and moderately broad; apically not curved ventrad; posterior margin medially concave; extends posteriad from the median; weakly visible dorsally.

Body - Dorsal view: about as long as broad. Proximal lobe long; deltoid; oriented proximad; arises from the postero-medial section of the ridge; depressed below the ridge; strongly sclerotized; weakly concave. *Base* moderately broad. *Apex* rounded; weakly curved anteriad. *Anterior margin* concave. *Posterior margin* weakly enlarged; concave. Distal lobe moderately long and broad; deltoid; shorter than proximal lobe; moderately sclerotized; planate; very weakly sloped ventrad. *Anterior margin* weakly convex; oriented postero-distad; moderately reduced. *Apex* aciculate. *Posterior margin* straight; weakly reduced. - Ventral view: Proximal lobe short; convex. *Posterior wing process junction* formed as a slender, ridge-like convexity; occupies the postero-proximal section of the lobe and is greatly lengthened anteriorly, extending to, and partially running along the anterior margin of the lobe. Distal lobe moderately large; discontinuous with ridge; weakly concave.

Median Plate (Fig.131)

FM1 oriented strongly postero-proximad. *Anterior to posterior section* moderately broad. *Proximal margin* convex. Articulation with 2Ax extends from the antero-distal margin of the distal lobe to the posterior section over the posterior section of the ventral ridge. *Distal margin* extremely narrowly and weakly fused to 3Ax. FM2 moderately short; oriented proximad; acerose; separated from FM1 by a short and narrow section of membrane.

Third Axillary (Fig.132)

Head weakly convex; normal length. Proximal margin shallowly concave. Anterior margin weakly concave; broad; narrow, not enlarged ventrally; from the proximal angle it slopes antero-distad. *Antero-proximal margin* not extended anteriad. *Antero-distal margin* very weakly extended anteriad. AXCu occupies the proximal one-fifth of head; convex. FCu normal size; distinct; occupies the central three-fifths of the head; deltoid. FA moderately narrow; occupies the distal one-fifth of head. *Anterior margin* entire. Suture line between FCu and FA present. Suture line between FCu and AXCu present. Suture line between FA and FJ absent.

Neck elevated proximally and weakly so distally. FCu section of neck absent. AXCu forms entire neck; extremely small. Proximal margin elevated as a very narrow and short ridge. *Ridge* extends to median of the proximal margin of tail; very short. Dorsal surface of ridge is weakly curved proximad; enlarged dorsally relative to AXA. Prong armed with a single very broad but short tooth; oriented postero-dorsad. Detached AXCu fragment saddle-shaped; strongly curved ventrad both anteriorly and posteriorly; slender; moderately sclerotized.

Tail reduced; deltoid; short. *Dorsal surface* oriented laterad. Proximal margin weakly elevated dorsad to the dorsal plane of the neck; slopes distad along its entire length. Anterior to antero-median section deeply concave. Antero-median to posterior section convex; oriented dorso-distad. *Window* absent. FJ+AXJ broad; extends close to the dorsal plane of the neck; occupies the anterior half of the tail; moderately sclerotized; curved distad. Suture line between FJ and AXJ absent. Suture line between FA+AXJ and AXA present. AXA extremely short and narrow; more strongly sclerotized than FA+AXJ; occupies the posterior half of the tail; curved postero-distad. Suture line between AXA and AXCu present.

Hind Wing Base Description

First Basal Plate (Fig.133)

Humeral Plate moderately broad and long. Anterior margin concave; strongly sclerotized; adjacent to BScA. Apex rounded; moderately broad; curved ventrad. Dorsal margin sinuate. Proximal margin weakly convex; curved ventrad. Ventral margin very strongly sinuate. Suture line between FPC+BPC and FC+BC present.

Anterior Subcostal Basivenale oriented distad; broadly ovoid; convex; moderately elevated dorsad. Proximal and distal sections separated by a prominent suture. *Proximal section* extended postero-proximad as a very broad convexity; larger than the distal section. *Distal section* discontinuous with the ScA bulge; separated by a moderately deep concavity. Apex broadly rounded; oriented distad. – Subcosta Anterior moderately convex; moderately extended posteriad. Bulge broad.

Radial Basivenale convex; open; discontinuous with radial stem; angled antero-proximad; broadly rectangular. Proximal arch slenderly deltoid; curved postero-distad. *Anterior* strikingly reduced by a greatly enlarged br; discontinuous with the anterior margin of BR. *Posterior margin* weakly concave; does not surround the BMA arch apex. *Postero-distal*

margin rounded. Anterior margin depressed below the posterior margin of ScA bulge; extremely narrow; convex; angled antero-proximad. Embayment normal size. Distal arch discontinuous with radial stem; moderately broad; convex; broadly curved proximad; oriented postero-proximad. *br* strongly sclerotized; occupies about one-third of the proximal arch; discontinuous with BR. *br projection* slenderly deltoid; concave; distinct from BScA.

Second Basal Plate (Fig.134)

MA-BMA Junction absent. – MP-BMP Junction: MP broadly continuous with BMP; arises from below the BMP-BCuA brace. – Crimp Patterns absent. – BMP-CuA Brace absent. – BMP-BCuA Brace present but modified; discontinuous with BMP; entire and greatly strengthened; extends posteriad; slender; equally broad along the entire length; convex; distinct from BMP. Terminus fused to the disto-medial section of BCuA. *Point of fusion* continuous.

Medial Basivenalia reduced proximally. BMA broadly scaphoid; completely fused to BMP. *Proximal surface* convex. *Medial and distal surfaces* flat. *Anterior margin* weakly concave. *Proximal arch* moderately long; planate and straight; oriented antero-proximad; strongly curved ventrad. Apex terminates below distal section of the BR proximal arch apex. *Distal arch* indistinct; fused to the proximal section of BMP. BMP junction with BMA discontinuous and very broad; fused to brace; markedly convex; separated from both 1BP and BCu by membrane. *Proximal section* moderately broadly deltoid; planate; slopes ventro-distad. *Distal section* indistinguishable from BMP-BCuA brace; long; broad; rectangular; strongly convex.

Cubital Basivenalia broadly fused. Postero-proximal margin of BCuA fused with the medial margin of BCuP. *Suture line* present. BCuA moderately large; convex; oriented postero-distad; lies posteriad of BMP; moderately sclerotized. *Anterior margin* with a moderately broad, shallow concavity. *Distal margin* continuous with CuA. BCuP large; ovoid; convex; oriented postero-distad; very weakly sclerotized. Distal embayment small. – Cubitus Anterior fused to BCuA. Junction marked by a distinct groove.

Basalare (Fig.135)

Head - HP lobe slender; continuous with neck. *Apex* narrowly truncate. *Dorsal surface* weakly elevated from neck; ovoid not polished. BScP lobe claviform; projects posteriad from neck. *Dorsal surface* weakly deltoid; convex; polished; weakly elevated from neck; slopes ventrad. *Ventral surface* polished. – Posterior Subcostal Basivenale weakly rectangular; polished.

Discussion

Orphninae do not display any apomorphic character states of the wing articulation and wing base but rather are characterized by a plethora of primitive character states of the wing articulation and wing base relative to other members of the orphnine line (Browne 1993).

Orphninae have been related to Hybosoridae (Iablokoff-Khnzorian 1977; Paulian 1984), Ochodaeidae (Blackwelder 1944; Paulian 1984) and Aphodiinae + Melolonthinae (Chalumeau & Gruner 1974). d'Hotman & Scholtz (1990a) proposed that orphnines lie phylogenetically near Scarabaeinae and Melolonthinae. They found that the aedeagus resembles those of Hopliinae and several Melolonthinae genera.

Orphninae share 22 apomorphic character states of the wing articulation and wing base with Melolonthinae, Rutelinae, Dynastinae, Cetoniinae, Oncerinae, Chasmatopterinae, *Acoma*, Hopliinae, Trichiinae and Valginae (Browne 1993).

Melolonthinae

Introduction

The Melolonthinae are a very large, diverse group with cosmopolitan distribution. According to Ritcher (1958), adults do not feed or they are strictly phytophagous, feeding on leaves, flowers or young fruits. Larvae feed on plant roots or humus.

Hind Wing Articulation Description

First Axillary (Fig.136)

Head - Dorsal surface strongly reduced posteriorly; broad; weakly clavate; convex. *Antero-dorsal margin* oriented weakly postero-distad; normal width; very convex. *Antero-proximal margin* with ventral enlargement reduced. *Postero-proximal margin* enlargement moderate and broad. *FSc2* base weakly enlarged; deeply concave. Apex oriented postero-distad; rounded but narrowly so. Anterior surface narrow; long; waisted medially. *FSc1* absent. *Ventral projection* long and narrow; enlarged mesally; deeply concave; oriented ventrad and weakly postero-distad. Dorsal surface base to median concave. Ventral surface convex. Apex wider than base; strongly flared; truncate. Concavity basad and moderately extended apicad from the base of the ventral projection; surrounded by three unequally strong ridges. *Distal embayment* oriented ventro-mesad. *FSc2* oriented distad and weakly dorsad; square; convex; broad; moderately short. Dorsal surface enlarged dorsally; convex; appears twisted. Ventral surface convex. Base proximally with a large convexity. Apex aciculate. Head and neck dorsal surface extended anteriad.

Neck normal width; long; weakly oriented antero-distad; articulation with 2Ax extends along the distal margin of the neck and tail; continuous with tail. Proximal margin reduced; sinuate; not curved ventrad. Distal margin concave. *Distal embayment* moderately concave; moderately shallow but broad.

Tail - Dorsal view: Proximal arch normal size. *Dorsal surface* weakly concave. *Antero-proximal margin* weakly convex. *Postero-proximal margin* straight. Articulation with PRR strong along the entire length of the proximal arch; very long but narrow; weakly recurved. Antero-dorsal surface concave. Postero-dorsal surface concave. Posterior margin weakly concave. Distal arch normal size. *Apex* weakly curved posteriad and ventrad; aciculate. *Distal margin* weakly concave. - Ventral view: Proximal arch with a weak ridge. Distal arch with a very small ridge. Posterior margin with a prominent but slender ridge.

Second Axillary (Fig.137)

Radial Fulcalare absent.

Ridges - Dorsal view: Proximal ridge entire; distinct from lobe. *Apex* nearly completely obscured by the distal ridge; waisted. *Anterior section* distal margin exposed. *Antero-medial to postero-medial section* moderately enlarged above and laterad over the distal ridge. *Posterior section* weakly enlarged above the distal ridge; broadly curved postero-proximad; slender; long; distinct from lobe; strongly extended past the posterior margin of lobe. Distal ridge weakly distinct from lobe. *Apex* narrow; convex; strikingly elongate; acuminate; strongly curved ventro-proximad; the distal margin is reduced revealing the ventral section of the distal lobe. *Anterior section* slender and strikingly elongate; straight and anteriad. *Median to posterior section* dorsally concealed by the proximal ridge. *Posterior section* very strongly extended past the posterior margin of lobe. - Ventral view: Proximal ridge anteriorly completely conceals the distal ridge. *Apex* acuminate. *Anterior to antero-medial section* moderately narrow and very long; curved distad. *Median to posterior section* obscured by the distal ridge. Distal ridge *median and posterior sections* arise from the posterior and proximal margins of the distal lobe; distinct from lobe; moderately broad; moderately long. *Antero-medial section* weakly waisted. *Median section* convex. *Postero-proximal angle* weakly reduced. *Postero-distal angle* not extended postero-distad. *Subalare tendon attachment point* short and moderately broad; apically not curved ventrad; posterior margin medially concave; extends posteriad from the median; the postero-dorsal section of the proximal ridge is moderately extended past the terminus of the subalare tendon attachment point; moderately visible dorsally.

Body - Dorsal view: slender and strikingly elongate. Proximal lobe long; deltoid; oriented proximad; arises from the postero-medial section of the ridge; depressed below the ridge; strongly sclerotized; weakly concave. *Base* moderately broad. *Apex* rounded; weakly curved posteriad. *Anterior margin* concave. *Posterior margin* weakly enlarged; concave. Distal lobe short and moderately broad; deltoid; shorter than proximal lobe; moderately sclerotized; planate; moderately sloped ventrad. *Anterior margin* weakly convex; oriented antero-distad; moderately reduced. *Apex* broadly rounded. *Posterior margin* straight; moderately reduced. - Ventral view: Proximal lobe short; convex. *Posterior wing process junction* formed as a slender, ridge-like convexity; occupies the postero-proximal section of the lobe and is greatly lengthened anteriorly, extending to, and running along the anterior margin of the lobe. Distal lobe small; discontinuous with ridge; concave.

Median Plate (Fig.138)

FM1 oriented strongly postero-proximad. *Anterior to posterior section* moderately narrow. *Proximal margin* convex. Articulation with 2Ax extends from the antero-distal margin of the distal lobe to the posterior section, over the posterior section of the ventral ridge. *Distal margin* extremely narrowly and weakly fused to 3Ax. FM2 moderately short; oriented proximad; acerose; separated from FM1 by a long, narrow section of membrane.

Third Axillary (Fig.139)

Head weakly convex; normal length. Proximal margin shallowly concave. Anterior margin weakly concave; broad; narrow, not enlarged ventrally; from the proximal angle it slopes antero-distad. *Antero-proximal margin* not extended anteriad. *Antero-distal margin* weakly extended anteriad. AXCu occupies the proximal one-fifth of head; convex. FCu normal size; distinct; occupies the central three-fifths of the head; deltoid. FA moderately narrow; occupies the distal one-fifth of head. *Anterior margin* entire. Suture line between FCu and FA present. Suture line between FCu and AXCu present. Suture line between FA and FJ absent.

Neck elevated proximally and weakly so distally. FCu section of neck absent. AXCu forms entire neck; extremely small. Proximal margin elevated as a very narrow and short ridge. *Ridge* extends to median of the proximal margin of tail; very short. Dorsal surface of ridge is weakly curved proximad; enlarged dorsally relative to AXA. Prong armed with a single broad but short tooth; oriented postero-dorsad. Detached AXCu fragment saddle-shaped; strongly curved ventrad both anteriorly and posteriorly; slender; moderately sclerotized.

Tail reduced; deltoid; short. *Dorsal surface* oriented laterad. Proximal margin strongly elevated dorsad to the dorsal plane of the neck; slopes distad along its entire length. Anterior to antero-median section concave. Antero-median to posterior section convex; oriented dorso-distad. *Window* absent. FJ+AXJ broad; extends close to the dorsal plane of the neck; occupies the anterior half of the tail; moderately sclerotized; curved distad. Suture line between FJ and AXJ absent. Suture line between FA+AXJ and AXA present. AXA extremely short and narrow; more strongly sclerotized than FA+AXJ; occupies the posterior half of the tail; curved postero-distad. Suture line between AXA and AXCu present.

Hind Wing Base Description

First Basal Plate (Fig.140)

Humeral Plate moderately narrow; long. Anterior margin sinuate; strongly sclerotized; adjacent to BScA. Apex deltoid; moderately narrow; curved ventrad. Dorsal margin sinuate. Proximal margin straight; curved ventrad. Ventral margin sinuate. Suture line between FPC+BPC and FC+BC absent.

Anterior Subcostal Basivenale oriented distad; broadly ovoid; convex; moderately elevated dorsad. Proximal and distal sections separated by a prominent suture. *Proximal section* extended anteriorly and postero-proximally as a very broad convexity; larger than the distal section. *Distal section* discontinuous with the ScA bulge; separated by a moderately deep concavity. Apex broadly rounded; oriented distad.

Subcosta Anterior moderately convex; moderately extended posteriorly. Bulge moderately broad. – Radial Basivenale convex; open; discontinuous with radial stem; angled antero-proximad; broadly rectangular. Proximal arch slenderly deltoid; curved postero-distad. *Anterior section* strikingly reduced by a greatly enlarged br; discontinuous with the anterior margin of BR. *Posterior margin* weakly concave; surrounds the BMA arch apex. *Postero-distal margin* weakly truncate; very weakly extended distad. Anterior margin depressed

below the posterior margin of ScA bulge; extremely narrow; convex; angled antero-proximad. Embayment normal size. Distal arch discontinuous with radial stem; moderately broad; convex; broadly curved proximad; oriented postero-proximad. *br* strongly sclerotized; occupies about one-third of the proximal arch; discontinuous with BR. *br projection* broad along its entire length; concave; distinct from BScA.

Second Basal Plate (Fig.141)

MA-BMA Junction absent. – MP-BMP Junction: MP broadly continuous with BMP; arises from below the BMP-BCuA brace. – Crimp Patterns absent. – BMP-CuA Brace absent. – BMP-BCuA Brace present but modified; discontinuous with BMP; entire and greatly strengthened; extends posteriad; moderately enlarged; equally broad along the entire length; convex; distinct from BMP. Terminus fused to the disto-medial section of BCuA. *Point of fusion* continuous.

Medial Basivenalia reduced proximally. BMA broadly scaphoid; completely fused to BMP. *Proximal surface* convex. *Medial and distal surfaces* planate. *Anterior margin* weakly concave. *Proximal arch* moderately long; planate and straight; oriented proximad; strongly curved ventrad. Apex terminates below BR proximal arch apex. *Distal arch* indistinct; fused to the proximal section of BMP. BMP junction with BMA discontinuous and very broad; fused to brace; markedly convex; separated from both 1BP and BCu by membrane. *Proximal section* broadly deltoid; planate; slopes ventro-distad. *Distal section* indistinguishable from BMP-BCuA brace; long; broad; rectangular; strongly convex.

Cubital Basivenalia narrowly fused; slender and long. Postero-proximal margin of BCuA fused with the antero-proximal margin of BCuP. *Suture line* present. BCuA moderately narrow and long; convex; oriented distad; lies posteriad of BMP; strongly sclerotized. *Anterior margin* with a broad shallow concavity. *Distal margin* continuous with CuA. BCuP ovoid; convex; oriented posteriad; moderately sclerotized. Distal embayment very broad and deep. – Cubitus Anterior fused to BCuA. Junction marked by a distinct suture.

Basalare (Fig.142)

Head - HP lobe large; continuous with neck. *Apex* broadly truncate. *Dorsal surface* weakly elevated from neck; not polished. BScP lobe claviform; weakly projects posteriad from neck. *Dorsal surface* rectangular; weakly convex; polished; depressed from neck; slopes ventrad. *Ventral surface* polished. – Posterior Subcostal Basivenale rectangular; polished.

Discussion

Although Melolonthinae, as it is currently recognized, do not display any autapomorphic character states of the wing articulation and wing base, they do share two apomorphic character states of the wing articulation and wing base with *Acoma*, Hopliinae, Oncerinae and Chasmatopterinae. It is likely that these taxa together form Melolonthinae (Browne 1993).

Melolonthinae have been associated with Glaphyridae and Oncerinae (Fowler 1912, in Yadav & Pillai 1979), Aphodiinae (Yadav 1973) and Dynastinae (Howden 1982). However, Melolonthinae are most commonly considered to be the sister group of Rutelinae or

Rutelinae + Dynastinae (Ritcher 1969a,b; Yadav & Pillai 1979; Meinecke 1975; Caveney 1986; Scholtz 1990; Lawrence & Britton 1991).

Melolonthinae share 22 apomorphic character states of the wing articulation and wing base with Orphninae, Rutelinae, Dynastinae, Cetoniinae, Oncerinae, Chasmatopterinae, *Acoma*, Hopliinae, Trichiinae and Valginae (Browne 1993).

Acoma

Introduction

Acoma is a small genus which occurs in the western United States (Howden 1958; Ritcher 1969a,b). *Acoma* is a well defined genus of uncertain phylogenetic status (Ritcher 1969a,b). Both Arrow (1912, in Ritcher 1969a,b) and Leng (1920) placed *Acoma* in Pleocomidae. Davis (1924, in Howden 1958) thought *Acoma* belonged near *Podolasia* while Blackwelder (1944) listed it in the tribe Chasmatopterini of the subfamily Melolonthinae. Howden (1958) stated that the phylogenetic placement of the genus is likely to remain in doubt until the morphology of the female is known. Ritcher (1969a,b) has suggested that *Acoma* is related to one of the scarab subfamilies, but he does not elaborate.

Hind Wing Articulation Description

First Axillary (Fig.143)

Head - Dorsal surface strongly reduced posteriorly; broad; clavate; convex. *Antero-dorsal margin* oriented weakly postero-distad; normal width; very convex. *Antero-proximal margin* with ventral enlargement reduced. *Postero-proximal margin* enlargement moderate and broad. *FSc2* base weakly enlarged; deeply concave. Apex oriented postero-distad; rounded but narrowly so. Anterior surface narrow; long; waisted medially. *FSc1* absent. *Ventral projection* long and narrow; enlarged mesally; deeply concave; oriented ventrad and weakly postero-distad. Dorsal surface base to median concave. Ventral surface convex. Apex wider than base; strongly flared; truncate. Concavity basad and moderately extended apicad from the base of the ventral projection; surrounded by three unequally strong ridges. *Distal embayment* oriented ventro-mesad. *FSc2* oriented distad and weakly dorsad; deltoid; convex; broad; moderately short. Dorsal surface enlarged dorsally; convex; appears twisted. Ventral surface convex. Base proximally with a large convexity. Apex aciculate. Head and neck dorsal surface extended antieriad.

Neck normal width; long; weakly oriented antero-distad; articulation with 2Ax extends along the distal margin of the neck and tail; continuous with tail. Proximal margin reduced; sinuate; not curved ventrad. Distal margin concave. *Distal embayment* moderately concave; moderately shallow but broad.

Tail - Dorsal view: Proximal arch normal size. *Dorsal surface* weakly concave. *Antero-proximal margin* weakly convex. *Postero-proximal margin* straight. Articulation with PRR strong along the entire length of the proximal arch; very long but narrow; weakly recurved. Antero-dorsal surface concave. Postero-dorsal surface concave. Posterior margin weakly

concave. Distal arch normal size. *Apex* weakly curved posteriad and ventrad; acuminate. *Distal margin* weakly concave. - Ventral view: Proximal arch with a prominent ridge. Distal arch with a narrow and short ridge. Posterior margin with a prominent ridge.

Second Axillary (Fig.144)

Radial Fulcrum absent.

Ridges - Dorsal view: Proximal ridge entire; distinct from lobe. *Apex* nearly completely obscured by the distal ridge; waisted. *Anterior section* distal margin exposed. *Antero-median to postero-median section* moderately enlarged above and laterad over the distal ridge. *Posterior section* weakly enlarged above the distal ridge; broadly curved postero-proximad; slender; long; distinct from lobe; strongly extended past the posterior margin of lobe. Distal ridge weakly distinct from lobe. *Apex* narrow; convex; strikingly elongate; acuminate; strongly curved ventro-proximad; the distal margin is reduced revealing the ventral section of the distal lobe. *Anterior section* slender and strikingly elongate; straight and anteriorad. *Median to posterior section* dorsally concealed by the proximal ridge. *Posterior section* very strongly extended past the posterior margin of lobe. - Ventral view: Proximal ridge anteriorly completely conceals the distal ridge. *Apex* acuminate. *Anterior to antero-median section* moderately narrow and very long; curved distad. *Median to posterior section* obscured by the distal ridge. Distal ridge *median and posterior sections* arise from the posterior and proximal margins of the distal lobe; distinct from lobe; moderately broad; moderately long. *Antero-median section* weakly waisted. *Median section* convex. *Postero-proximal angle* enlarged. *Postero-distal angle* reduced. *Subalare tendon attachment point* short and moderately broad; apically not curved ventrad; posterior margin medially concave; extends posteriad from the median; the postero-dorsal section of the proximal ridge is strongly extended past the terminus of the subalare tendon attachment point; moderately visible dorsally.

Body - Dorsal view: slender and strikingly elongate. Proximal lobe long; deltoid; oriented proximad; arises from the postero-medial section of the ridge; depressed below the ridge; strongly sclerotized; concave. *Base* moderately broad. *Apex* rounded; weakly curved anteriorad. *Anterior margin* concave. *Posterior margin* weakly enlarged; concave. Distal lobe short and moderately broad; deltoid; shorter than proximal lobe; moderately sclerotized; planate; strongly sloped ventrad. *Anterior margin* weakly convex; oriented antero-distad; moderately reduced. *Apex* broadly rounded; moderately reduced. *Posterior margin* straight; moderately reduced. - Ventral view: Proximal lobe moderately short; convex. *Posterior wing process junction* formed as a slender, ridge-like convexity; occupies the postero-proximal section of the lobe and is greatly lengthened anteriorly, extending to, and running along the anterior margin of the lobe. Distal lobe small; weakly discontinuous with ridge; concave.

Median Plate (Fig.145)

FM1 oriented strongly postero-proximad. *Anterior to posterior section* moderately narrow. *Proximal margin* convex. Articulation with 2Ax extends from the antero-distal margin of the distal lobe to the posterior section over the posterior section of the ventral ridge. *Distal*

margin extremely narrowly and weakly fused to 3Ax. FM2 moderately short; oriented proximad; acerose; separated from FM1 by a long, narrow section of membrane.

Third Axillary (Fig.146)

Head weakly convex; normal length. Proximal margin shallowly concave. Anterior margin weakly concave; broad; narrow, not enlarged ventrally; from the proximal angle it slopes antero-distad. *Antero-proximal margin* not extended anteriad. *Antero-distal margin* weakly extended anteriad. AXCu occupies the proximal one-fifth of head; convex. FCu normal size; distinct; occupies the central three-fifths of the head; deltoid. FA moderately narrow; occupies the distal one-fifth of head. *Anterior margin* entire. Suture line between FCu and FA present. Suture line between FCu and AXCu present. Suture line between FA and FJ absent.

Neck elevated proximally and weakly so distally. FCu section of neck absent. AXCu forms entire neck; extremely small. Proximal margin elevated as a very narrow and short ridge. *Ridge* extends to median of the proximal margin of tail; very short. Dorsal surface of ridge is weakly curved proximad; enlarged dorsally relative to AXA. Prong armed with a single broad but short tooth; oriented postero-dorsad. Detached AXCu fragment saddle-shaped; strongly curved ventrad both anteriorly and posteriorly; slender; moderately sclerotized.

Tail reduced; deltoid. *Dorsal surface* oriented laterad. Proximal margin strongly elevated dorsad to the dorsal plane of the neck; slopes distad along its entire length. Anterior to antero-median concave. Antero-median to posterior convex; oriented dorso-distad. *Window* absent. FJ+AXJ broad; extends close to the dorsal plane of the neck; occupies the anterior half of the tail; moderately sclerotized; curved distad. Suture line between FJ and AXJ absent. Suture line between FA+AXJ and AXA present. AXA extremely short and narrow; more strongly sclerotized than FA+AXJ; occupies the posterior half of the tail; curved postero-distad. Suture line between AXA and AXCu present.

Hind Wing Base Description

First Basal Plate (Fig.147)

Humeral Plate moderately broad and long. Anterior margin concave; strongly sclerotized; adjacent to BScA. Apex rounded; moderately broad; curved ventrad. Dorsal margin convex. Proximal margin convex; curved ventrad. Ventral margin concave. Suture line between FPC+BPC and FC+BC absent.

Anterior Subcostal Basivenale oriented distad; broadly ovoid; convex; strongly elevated dorsad. Proximal and distal sections separated by a prominent suture. *Proximal section* extended anteriorly and postero-proximally as a moderately broad convexity; larger than the distal section. *Distal section* discontinuous with the ScA bulge; separated by a moderately deep concavity. Apex broadly rounded; oriented distad.

Subcosta Anterior moderately convex; moderately extended posteriorly. Bulge moderately broad. – Radial Basivenale convex; open; discontinuous with radial stem; angled antero-proximad; broadly rectangular. Proximal arch slenderly deltoid; curved postero-distad. *Anterior section* strikingly reduced by a greatly enlarged br; discontinuous with the anterior

margin of BR. *Posterior margin* weakly concave; surrounds the BMA arch apex. *Postero-distal margin* truncate. Anterior margin depressed below the posterior margin of ScA bulge; extremely narrow; convex; angled antero-proximad. Embayment normal size. Distal arch discontinuous with radial stem; moderately broad; convex; broadly curved proximad; oriented postero-proximad. *br* strongly sclerotized; occupies about one-third of the proximal arch; discontinuous with BR. *br projection* deltoid; slender; concave; distinct from BScA.

Second Basal Plate (Fig.148)

MA-BMA Junction absent. – MP-BMP Junction: MP broadly continuous with BMP; arises from below the BMP-BCuA brace. – Crimp Patterns absent. – BMP-CuA Brace absent. – BMP-BCuA Brace present but modified; discontinuous with BMP; entire and greatly strengthened; extends posteriad; moderately enlarged; equally broad along the entire length; convex; distinct from BMP. Terminus fused to the disto-medial section of BCuA. *Point of fusion* continuous.

Medial Basivenalia reduced proximally. BMA broadly scaphoid; completely fused to BMP. *Proximal surface* convex. *Medial and distal surfaces* planate. *Anterior margin* weakly concave. *Proximal arch* moderately long; planate and straight; oriented proximad; strongly curved ventrad. Apex terminates below BR proximal arch apex. *Distal arch* indistinct; fused to the proximal section of BMP. BMP junction with BMA discontinuous and very broad; fused to brace; markedly convex; separated from both IBP and BCu by membrane. *Proximal section* broadly deltoid; planate; slopes ventro-distad. *Distal section* indistinguishable from BMP-BCuA brace; long; broad; rectangular; strongly convex.

Cubital Basivenalia narrowly fused; slender and long. Postero-proximal margin of BCuA fused with the antero-proximal margin of BCuP. *Suture line* present. BCuA very narrow and long; convex; oriented distad; lies posteriad of BMP; strongly sclerotized. *Anterior margin* with a broad shallow concavity. *Distal margin* continuous with CuA. BCuP weakly ovoid; convex; oriented postero-distad; moderately sclerotized. Distal embayment slender and moderately deep. – Cubitus Anterior fused to BCuA Junction marked by a distinct suture.

Basalare (Fig.149)

Head - HP lobe large; continuous with neck. *Apex* broadly truncate. *Dorsal surface* weakly elevated from neck; not polished. BScP lobe claviform; weakly projects posteriad from neck. *Dorsal surface* ovoid; weakly convex; polished; depressed from neck; slopes ventrad. *Ventral surface* polished. – Posterior Subcostal Basivenale deltoid; polished.

Discussion

Although *Acoma* does not display any autapomorphic character states of the wing articulation and wing base, it does share two apomorphic character states of the wing articulation and wing base with Melolonthinae, Hopliinae, Oncerinae and Chasmatopterinae. It is likely that these taxa together form Melolonthinae (Browne 1993).

Acoma shares 22 apomorphic character states of the wing articulation and wing base with Orphninae, Melolonthinae, Rutelinae, Dynastinae, Cetoniinae, Oncerinae, Chasmatopterinae, Hopliinae, Trichiinae and Valginae (Browne 1993).

Chasmatopterinae

Introduction

Chasmatopterinae is a poorly defined subfamily but there is little doubt that it is one of the more transformed scarab subfamilies closely related to Melolonthinae (Horn 1867; Saylor 1937; d'Hotman & Scholtz 1990a,b). Chasmatopterines were removed from Melolonthinae and elevated to subfamily status based on the position of the adult abdominal spiracles of the 7th and 8th segments in the pleural membrane (Saylor 1938), but Ritcher (1969a,b) found that these spiracles are situated in the lower parts of the tergites. However, chasmatopterines are more commonly considered to belong to either Chasmatopterini (Leng 1920; d'Hotman & Scholtz 1990a) or Melolonthini (Nel & Scholtz 1990).

Hind Wing Articulation Description

First Axillary (Fig.150)

Head - Dorsal surface strongly reduced posteriorly; broad; weakly clavate; convex. *Antero-dorsal margin* oriented weakly postero-distad; normal width; very convex. *Antero-proximal margin* with ventral enlargement reduced. *Postero-proximal margin* enlargement moderate and broad. *FSc2* base weakly enlarged; deeply concave. Apex oriented postero-distad; rounded but narrowly so. Anterior surface narrow; long; waisted medially. *FSc1* absent. *Ventral projection* long and narrow; enlarged mesally; deeply concave; oriented ventrad and weakly postero-distad. Dorsal surface base to median concave. Ventral surface convex. Apex wider than base; strongly flared; truncate. Concavity basad and moderately extended apicad from the base of the ventral projection; surrounded by three unequally strong ridges. *Distal embayment* oriented ventro-mesad. *FSc2* oriented distad and weakly dorsad; deltoid; convex; broad; moderately short. Dorsal surface enlarged dorsally; convex; appears twisted. Ventral surface convex. Base proximally with a large convexity. Apex acuminate. Head and neck dorsal surface extended anteriad.

Neck normal width; long; weakly oriented antero-distad; articulation with 2Ax extends along the distal margin of the neck and tail; continuous with tail. Proximal margin reduced; sinuate; not curved ventrad. Distal margin concave. *Distal embayment* moderately concave; moderately shallow but broad.

Tail - Dorsal view: Proximal arch normal size. *Dorsal surface* weakly concave. *Antero-proximal margin* weakly convex. *Postero-proximal margin* straight. Articulation with PRR strong along the entire length of the proximal arch; very long but narrow; weakly recurved. Antero-dorsal surface concave. Postero-dorsal surface concave. Posterior margin weakly concave. Distal arch normal size. *Apex* weakly curved posteriad and ventrad; acuminate. *Distal margin* weakly concave. - Ventral view: Proximal arch with a weak and very slender

ridge. Posterior margin with a prominent but very slender ridge. Distal arch with a small ridge.

Second Axillary (Fig.151)

Radial Fulcalare absent.

Ridges - Dorsal view: Proximal ridge entire; distinct from lobe. *Apex* nearly completely obscured by the distal ridge; waisted. *Anterior section* distal margin exposed. *Antero-median to postero-median section* moderately enlarged above and laterad over the distal ridge. *Posterior section* weakly enlarged above the distal ridge; broadly curved postero-proximad; slender; long; distinct from lobe; strongly extended past the posterior margin of lobe. Distal ridge weakly distinct from lobe. *Apex* narrow; convex; strikingly elongate; aciculate; strongly curved ventro-proximad; the distal margin is reduced revealing the ventral section of the distal lobe. *Anterior section* slender and strikingly elongate; straight and anteriad. *Median to posterior section* dorsally concealed by the proximal ridge. *Posterior section* very strongly extended past the posterior margin of lobe. - Ventral view: Proximal ridge anteriorly completely conceals the distal ridge. *Apex* aciculate. *Anterior to antero-median section* moderately narrow and very long; curved distad. *Median to posterior section* obscured by the distal ridge. Distal ridge *median and posterior sections* arise from the posterior and proximal margins of the distal lobe; distinct from lobe; moderately broad; moderately long. *Antero-median section* not waisted. *Median section* convex. *Postero-proximal angle* not reduced. *Postero-distal angle* reduced. *Subalare tendon attachment point* short and moderately broad; apically not curved ventrad; posterior margin medially concave; extends posteriad from the median; the postero-dorsal section of the proximal ridge is very moderately extended past the terminus of the subalare tendon attachment point; moderately visible dorsally.

Body - Dorsal view: slender and strikingly elongate. Proximal lobe long; deltoid; oriented proximad; arises from the postero-medial section of the ridge; depressed below the ridge; strongly sclerotized; weakly concave. *Base* moderately broad. *Apex* rounded; curved anteriad. *Anterior margin* concave. *Posterior margin* weakly enlarged; concave. Distal lobe short and moderately broad; deltoid; longer than proximal lobe; moderately sclerotized; planate; weakly sloped ventrad. *Anterior margin* weakly convex; oriented antero-distad; moderately reduced. *Apex* broadly rounded. *Posterior margin* straight; moderately reduced. - Ventral view: Proximal lobe short; convex. *Posterior wing process junction* formed as a slender, ridge-like convexity; occupies the postero-proximal section of the lobe and is greatly lengthened anteriorly, extending to, and running along the anterior margin of the lobe. Distal lobe small; weakly discontinuous with ridge; concave.

Median Plate (Fig.152)

FM1 oriented strongly postero-proximad. *Anterior to posterior section* moderately narrow. *Proximal margin* convex. Articulation with 2Ax extends from the antero-distal margin of the distal lobe to the posterior section over the posterior section of the ventral ridge. *Distal margin* extremely narrowly and weakly fused to 3Ax. FM2 moderately short; oriented proximad; acerose; separated from FM1 by a long, narrow section of membrane.

Third Axillary (Fig.153)

Head weakly convex; normal length. Proximal margin shallowly concave. Anterior margin weakly concave; broad; narrow, not enlarged ventrally; from the proximal angle it slopes antero-distad. *Antero-proximal margin* not extended anteriad. *Antero-distal margin* weakly extended anteriad. AXCu occupies the proximal one-fifth of head; convex. FCu normal size; distinct; occupies the central three-fifths of the head; deltoid. FA moderately narrow; occupies the distal one-fifth of head. *Anterior margin* entire. Suture line between FCu and FA present. Suture line between FCu and AXCu present. Suture line between FA and FJ absent.

Neck elevated proximally and weakly so distally. FCu section of neck absent. AXCu forms entire neck; extremely small. Proximal margin elevated as a very narrow and short ridge. *Ridge* extends to median of the proximal margin of tail; very short. Dorsal surface of ridge is weakly curved proximad; enlarged dorsally relative to AXA. Prong armed with a single broad but short tooth; oriented postero-dorsad. Detached AXCu fragment saddle-shaped; strongly curved ventrad both anteriorly and posteriorly; slender; moderately sclerotized.

Tail reduced; deltoid; short. *Dorsal surface* oriented laterad. Proximal margin strongly elevated dorsad to the dorsal plane of the neck; slopes distad along its entire length. Anterior to antero-median section concave. Antero-median to posterior section convex; oriented dorso-distad. *Window* absent. FJ+AXJ broad; extends close to the dorsal plane of the neck; occupies the anterior half of the tail; moderately sclerotized; curved distad. Suture line between FJ and AXJ absent. Suture line between FA+AXJ and AXA present. AXA extremely short and narrow; more strongly sclerotized than FA+AXJ; occupies the posterior half of the tail; curved postero-distad. Suture line between AXA and AXCu present.

Hind Wing Base Description

First Basal Plate (Fig.154)

Humeral Plate moderately broad and long. Anterior margin convex; strongly sclerotized; adjacent to BScA. Apex rounded; moderately narrow; weakly curved ventrad. Dorsal margin concave. Proximal margin weakly convex; curved ventrad. Ventral margin sinuate. Suture line between FPC+BPC and FC+BC absent.

Anterior Subcostal Basivenale oriented distad; broadly ovoid; convex; moderately dorsad. Proximal and distal sections separated by a prominent suture. *Proximal section* extended anteriorly and postero-proximally as a moderately broad convexity; larger than the distal section. *Distal section* discontinuous with the ScA bulge; separated by a moderately deep concavity. Apex broadly rounded; oriented distad. – Subcosta Anterior moderately convex; moderately extended posteriorly. Bulge moderately broad.

Radial Basivenale convex; open; discontinuous with radial stem; angled antero-proximad; broadly rectangular. Proximal arch slenderly deltoid; curved postero-distad. *Anterior section* strikingly reduced by a greatly enlarged br; discontinuous with the anterior margin of BR. *Posterior margin* weakly concave; surrounds the BMA arch apex. *Postero-distal margin* truncate. Anterior margin depressed below the posterior margin of ScA bulge;

extremely narrow; convex; angled antero-proximad. Embayment normal size. Distal arch discontinuous with radial stem; moderately broad; convex; broadly curved proximad; oriented postero-proximad. *br* strongly sclerotized; occupies about one-third of the proximal arch; discontinuous with BR. *br projection* deltoid; slender; concave; distinct from BScA.

Second Basal Plate (Fig.155)

MA-BMA Junction absent. – MP-BMP Junction: MP broadly continuous with BMP; arises from below the BMP-BCuA brace. – Crimp Patterns absent. – BMP-CuA Brace absent. – BMP-BCuA Brace present but modified; discontinuous with BMP; entire and greatly strengthened; extends posteriad; moderately enlarged; equally broad along the entire length; convex; distinct from BMP. Terminus fused to the disto-medial section of BCuA. *Point of fusion* continuous.

Medial Basivenalia reduced proximally. BMA broadly scaphoid; completely fused to BMP. *Proximal surface* convex. *Medial and distal surfaces* planate. *Anterior margin* weakly concave. *Proximal arch* moderately long; planate and straight; oriented proximad; strongly curved ventrad. Apex terminates below BR proximal arch apex. *Distal arch* indistinct; fused to the proximal section of BMP. BMP junction with BMA discontinuous and very broad; fused to brace; markedly convex; separated from both IBP and BCu by membrane. *Proximal section* broadly deltoid; planate; slopes ventro-distad. *Distal section* indistinguishable from BMP-BCuA brace; long; broad; rectangular; strongly convex.

Cubital Basivenalia broadly fused. Posterior margin of BCuA fused with the anterior margin of BCuP. *Suture line* present. BCuA small; convex; very weakly oriented postero-distad; lies posteriad of BMP; weakly sclerotized. *Anterior margin* with a broad shallow concavity. *Distal margin* partially continuous with CuA. BCuP deltoid; small; convex; oriented postero-distad; weakly sclerotized. Distal embayment absent. – Cubitus Anterior partially fused to BCuA. Junction marked by a distinct suture.

Basalare (Fig.156)

Head - HP lobe slender; continuous with neck. *Apex* narrowly truncate. *Dorsal surface* elevated from neck; not polished. BScP lobe claviform; weakly projects posteriad from neck. *Dorsal surface* ovoid; weakly convex; polished; depressed from neck; slopes ventrad. *Ventral surface* polished. – Posterior Subcostal Basivenale deltoid; polished.

Discussion

Although Chasmatopterinae do not display any autapomorphic character states of the wing articulation and wing base, they do share two apomorphic character states of the wing articulation and wing base with Melolonthinae, Hopliinae, Oncerinae and *Acoma*. The evidence indicates that neither subfamilial nor tribal status is warranted, and it should be returned to Melolonthinae as *Chnaunanthus* (Browne 1993).

Chasmatopterinae share 22 apomorphic character states of the wing articulation and wing base with Orphninae, Melolonthinae, Rutelinae, Dynastinae, Cetoniinae, Oncerinae, *Acoma*, Hopliinae, Trichiinae and Valginae (Browne 1993).

Hopliinae

Introduction

The Hopliinae have wide distribution. Most adults feed on flowers, but they have also been recorded feeding on young leaves and fruit. Larvae develop in the ground and are either rhizophagous or saprophagous (Iablokoff-Khnzorian 1977). This ill-defined subfamily of uncertain phylogenetic status contains two tribes, Hopliini and Pachynemini (d'Hotman & Scholtz 1990a,b).

Hind Wing Articulation Description

First Axillary (Fig.157)

Head - Dorsal surface strongly reduced posteriorly; broad; weakly clavate; convex. *Antero-dorsal margin* oriented weakly postero-distad; normal width; very convex. *Antero-proximal margin* with ventral enlargement reduced. *Postero-proximal margin* enlargement moderate and broad. *FSc2* base weakly enlarged; deeply concave. Apex oriented postero-distad; rounded but narrowly so. Anterior surface narrow; long; waisted medially. *FSc1* absent. *Ventral projection* long and narrow; enlarged mesally; deeply concave; oriented ventrad and weakly postero-distad. Dorsal surface base to median concave. Ventral surface convex. Apex wider than base; strongly flared; truncate. Concavity basad and moderately extended apicad from the base of the ventral projection; surrounded by three unequally strong ridges. *Distal embayment* oriented ventro-mesad. *FSc2* oriented distad and weakly dorsad; deltoid; convex; broad; moderately short. Dorsal surface enlarged dorsally; convex; appears twisted. Ventral surface convex. Base proximally with a large convexity. Apex acuminate. Head and neck dorsal surface extended anteriad.

Neck normal width; long; weakly oriented antero-distad; articulation with 2Ax extends along the distal margin of the neck and tail; continuous with tail. Proximal margin reduced; sinuate; not curved ventrad. Distal margin concave. *Distal embayment* moderately concave; moderately shallow but broad.

Tail - Dorsal view: Proximal arch normal size. *Dorsal surface* weakly concave. *Antero-proximal margin* weakly convex. *Postero-proximal margin* straight. Articulation with PRR strong along the entire length of the proximal arch; very long but narrow; weakly recurved. Antero-dorsal surface concave. Postero-dorsal surface concave. Posterior margin concave. Distal arch normal size. *Apex* weakly curved posteriad and ventrad; acuminate. *Distal margin* weakly concave. - Ventral view: Proximal arch with a prominent and broad ridge. Distal arch with a moderately broad, but short ridge. Posterior margin with a prominent ridge.

Second Axillary (Fig.158)

Radial Fulcalare absent.

Ridges - Dorsal view: Proximal ridge entire; distinct from lobe. *Apex* nearly completely obscured by the distal ridge; waisted. *Anterior section* distal margin exposed. *Antero-median to postero-median section* moderately enlarged above and laterad over the distal

ridge. *Posterior section* weakly enlarged above the distal ridge; broadly curved postero-proximad; slender; long; distinct from lobe; strongly extended past the posterior margin of lobe. Distal ridge weakly distinct from lobe. *Apex* narrow; convex; strikingly elongate; aciculate; strongly curved ventro-proximad; the distal margin is reduced revealing the ventral section of the distal lobe. *Anterior section* slender and strikingly elongate; straight and anteriad. *Median to posterior section* dorsally concealed by the proximal ridge. *Posterior section* very strongly extended past the posterior margin of lobe. - Ventral view: Proximal ridge anteriorly completely conceals the distal ridge. *Apex* weakly aciculate. *Anterior to antero-median section* moderately narrow and very long; curved distad. *Median to posterior section* obscured by the distal ridge. Distal ridge *median and posterior sections* arise from the posterior and proximal margins of the distal lobe; distinct from lobe; moderately broad; moderately long. *Antero-median section* not waisted. *Median section* convex. *Postero-proximal angle* not reduced. *Postero-distal angle* not extended postero-distad. *Subalare tendon attachment point* short and moderately broad; apically not curved ventrad; posterior margin medially concave; extends posteriad from the median; the postero-dorsal section of the proximal ridge is moderately extended past the terminus of the subalare tendon attachment point; strongly visible dorsally.

Body - Dorsal view: slender and strikingly elongate. Proximal lobe long; deltoid; oriented proximad; arises from the postero-medial section of the ridge; depressed below the ridge; strongly sclerotized; weakly concave. *Base* moderately broad. *Apex* rounded; curved anteriad. *Anterior margin* concave. *Posterior margin* weakly enlarged; concave. Distal lobe short and moderately broad; deltoid; slightly shorter than proximal lobe; moderately sclerotized; planate; moderately sloped ventrad. *Anterior margin* weakly convex; oriented antero-distad; moderately reduced. *Apex* broadly rounded; strongly reduced. *Posterior margin* straight. - Ventral view: Proximal lobe moderately short; convex. *Posterior wing process junction* formed as a slender, ridge-like convexity; occupies the postero-proximal section of the lobe and is greatly lengthened anteriorly, extending to, and running along the anterior margin of the lobe. Distal lobe moderately small; weakly discontinuous with ridge; concave.

Median Plate (Fig.159)

FM1 oriented strongly postero-proximad. *Anterior to posterior section* moderately narrow. *Proximal margin* convex. Articulation with 2Ax extends from the antero-distal margin of the distal lobe to the posterior section over the posterior section of the ventral ridge. *Distal margin* extremely narrowly and weakly fused to 3Ax. FM2 moderately short; oriented proximad; acerose; separated from FM1 by a long, narrow section of membrane.

Third Axillary (Fig.160)

Head weakly convex; normal length; very weakly bi-lobed. Proximal margin shallowly concave. Anterior margin weakly concave; broad; narrow, not enlarged ventrally; from the proximal angle it slopes antero-distad. *Antero-proximal margin* not extended anteriad. *Antero-distal margin* weakly extended anteriad. AXCu occupies the proximal one-fifth of head; convex. FCu normal size; distinct; occupies the central three-fifths of the head;

deltoid. FA moderately narrow; occupies the distal one-fifth of head. *Anterior margin* entire. Suture line between FCu and FA present. Suture line between FCu and AXCu present. Suture line between FA and FJ absent.

Neck elevated proximally and weakly so distally. FCu section of neck absent. AXCu forms entire neck; extremely small. Proximal margin elevated as a very narrow and short ridge. *Ridge* extends to median of the proximal margin of tail; very short. Dorsal surface of ridge is weakly curved proximad; enlarged dorsally relative to AXA. Prong armed with a single broad but short tooth; oriented postero-dorsad. Detached AXCu fragment saddle-shaped; strongly curved ventrad both anteriorly and posteriorly; slender; moderately sclerotized.

Tail reduced; deltoid; short. *Dorsal surface* oriented laterad. Proximal margin strongly elevated dorsad to the dorsal plane of the neck; slopes distad along its entire length. Anterior to antero-median section concave. Antero-median to posterior section convex; oriented dorso-distad. *Window* absent. FJ+AXJ broad; extends close to the dorsal plane of the neck; occupies the anterior half of the tail; moderately sclerotized; curved distad. Suture line between FJ and AXJ absent. Suture line between FA+AXJ and AXA present. AXA extremely short and narrow; more strongly sclerotized than FA+AXJ; occupies the posterior half of the tail; curved postero-distad. Suture line between AXA and AXCu present.

Hind Wing Base Description

First Basal Plate (Fig.161)

Humeral Plate moderately broad and long. Anterior margin weakly sinuate; strongly sclerotized; adjacent to BScA. Apex very weakly deltoid; moderately narrow; curved ventro-proximad. Dorsal margin sinuate. Proximal margin weakly concave; curved ventrad. Ventral margin sinuate. Suture line between FPC+BPC and FC+BC absent.

Anterior Subcostal Basivenale oriented distad; broadly ovoid; convex; moderately dorsad. Proximal and distal sections separated by a prominent suture. *Proximal section* extended anteriorly and postero-proximally as a moderately broad convexity; larger than the distal section. *Distal section* discontinuous with the ScA bulge; separated by a moderately deep concavity. Apex broadly rounded; oriented distad. – Subcosta Anterior moderately convex; moderately extended posteriorly. Bulge narrow.

Radial Basivenale convex; open; discontinuous with radial stem; angled antero-proximad; rectangular. Proximal arch slenderly deltoid; oriented posteriad. *Anterior section* strikingly reduced by a greatly enlarged br; discontinuous with the anterior margin of BR. *Posterior margin* concave; surrounds the BMA arch apex. *Postero-distal margin* truncate. Anterior margin depressed below the posterior margin of ScA bulge; extremely narrow; convex; angled antero-proximad. Embayment normal size. Distal arch discontinuous with radial stem; moderately broad; convex; broadly curved proximad; oriented postero-proximad. br strongly sclerotized; occupies about one-third of the proximal arch; discontinuous with BR. *br projection* very slender; concave; distinct from BScA.

Second Basal Plate (Fig.162)

MA-BMA Junction absent. – MP-BMP Junction: MP broadly continuous with BMP; arises from below the BMP-BCuA brace. – Crimp Patterns absent. – BMP-CuA Brace absent. – BMP-BCuA Brace present but modified; discontinuous with BMP; entire and greatly strengthened; extends posteriad; moderately enlarged; equally broad along the entire length; convex; distinct from BMP. Terminus fused to the disto-medial section of BCuA. *Point of fusion* continuous.

Medial Basivenalia reduced proximally. BMA broadly scaphoid; completely fused to BMP. *Proximal surface* convex. *Medial and distal surfaces* planate. *Anterior margin* weakly concave. *Proximal arch* moderately long; planate and straight; oriented proximad; strongly curved ventrad. Apex terminates below BR proximal arch apex. *Distal arch* indistinct; fused to the proximal section of BMP. BMP junction with BMA discontinuous and very broad; fused to brace; markedly convex; separated from both IBP and BCu by membrane. *Proximal section* broadly deltoid; planate; slopes ventro-distad. *Distal section* indistinguishable from BMP-BCuA brace; long; broad; rectangular; strongly convex.

Cubital Basivenalia broadly fused. Posterior margin of BCuA fused with the anterior margin of BCuP. *Suture line* present. BCuA very narrow and long; convex; oriented distad; lies posteriad of BMP; strongly sclerotized; very weakly distinguishable from CuA. *Anterior margin* with a broad shallow concavity. *Distal margin* continuous with CuA. BCuP weakly deltoid; convex; oriented postero-distad; moderately sclerotized. Distal embayment absent. – Cubitus Anterior fused to BCuA. Junction very weakly distinct.

Basalare (Fig.163)

Head - HP lobe large; continuous with neck. Apex broadly truncate. *Dorsal surface* weakly elevated from neck; not polished. BScP lobe claviform; weakly projects posteriad from neck. *Dorsal surface* rectangular; weakly convex; polished; depressed from neck; slopes ventrad. *Ventral surface* polished. – Posterior Subcostal Basivenale weakly rectangular; polished.

Discussion

Hopliinae is one of the more transformed scarab subfamilies closely related to Melolonthinae (d'Hotman & Scholtz 1990a,b). Hopliines are sometimes considered to be rutelines (Scholtz & Holm 1985), "oncerines" (Leng 1920) but are more often treated as a melolonthine tribe (Blackwelder 1944; Ritcher 1969ab; Howden & Hardy 1971; Hardy 1977). Caveney (1986) found that the structure of the eye is similar to that of *Macroductylus*.

Although Hopliinae do not display any autapomorphic character states of the wing articulation and wing base, they do share two apomorphic character states of the wing articulation and wing base with Melolonthinae, Hopliinae, Oncerinae, Chasmatopterinae and *Acoma*. The lack of autapomorphic character states of the wing articulation and wing base in hopliines does not warrant subfamilial status and it is more likely that it is a Melolonthinae tribe, Hopliini, as it was previously treated by Scholtz (1990).

Hopliinae share 22 apomorphic character states of the wing articulation and wing base with Orphninae, Melolonthinae, Rutelinae, Dynastinae, Cetoniinae, Oncerinae, Chasmatopterinae, *Acoma*, Trichiinae and Valginae (Browne 1993).

Oncerinae

Introduction

Oncerines are generally quite small and their distribution is rather localized in Southern and Lower California (Saylor 1938). They are a very small, poorly defined subfamily but there is little doubt that it is one of the more transformed scarab subfamilies closely related to Melolonthinae (Horn, 1867; Saylor 1938). Oncerines have commonly been treated as a separate subfamily based on the non-melolonthine position of the abdominal spiracles (Horn, 1867). Leng (1920) placed oncerines in a separate subfamily with *Chnaunanthus* (currently Chasmatopterinae) and many genera which are currently placed in Melolonthinae.

Hind Wing Articulation Description

First Axillary (Fig.164)

Head - Dorsal surface strongly reduced posteriorly; broad; weakly clavate; convex. *Antero-dorsal margin* oriented weakly postero-distad; normal width; very convex. *Antero-proximal margin* with ventral enlargement reduced. *Postero-proximal margin* enlargement moderate and broad. *FSc2* base weakly enlarged; deeply concave. Apex oriented postero-distad; rounded but narrowly so. Anterior surface narrow; long; waisted medially. *FSc1* absent. *Ventral projection* long and narrow; enlarged mesally; deeply concave; oriented ventrad and weakly postero-distad. Dorsal surface base to median concave. Ventral surface convex. Apex wider than base; strongly flared; truncate. Concavity basad and moderately extended apicad from the base of the ventral projection; surrounded by three unequally strong ridges. *Distal embayment* oriented ventro-mesad. *FSc2* oriented distad and weakly dorsad; deltoid; convex; broad; moderately short. Dorsal surface enlarged dorsally; convex; appears twisted. Ventral surface convex. Base proximally with a large convexity. Apex aciculate. Head and neck dorsal surface extended anteriad.

Neck normal width; long; weakly oriented antero-distad; articulation with 2Ax extends along the distal margin of the neck and tail; continuous with tail. Proximal margin reduced; sinuate; not curved ventrad. Distal margin concave. *Distal embayment* moderately concave; moderately shallow but broad.

Tail - Dorsal view: Proximal arch normal size. *Dorsal surface* weakly concave. *Antero-proximal margin* weakly convex. *Postero-proximal margin* straight. Articulation with PRR strong along the entire length of the proximal arch; very long but narrow; weakly recurved. Antero-dorsal surface concave. Postero-dorsal surface concave. Posterior margin weakly concave. Distal arch normal size. *Apex* weakly curved posteriad and ventrad; aciculate. *Distal margin* weakly concave. - Ventral view: Proximal arch with a weak ridge. Posterior margin with a prominent ridge. Distal arch with a slender ridge.

Second Axillary (Fig.165)

Radial Fulcalare absent.

Ridges - Dorsal view: Proximal ridge entire; distinct from lobe. *Apex* nearly completely obscured by the distal ridge; waisted. *Anterior section* distal margin exposed. *Antero-medial to postero-medial section* moderately enlarged above and laterad over the distal ridge. *Posterior section* weakly enlarged above the distal ridge; broadly curved postero-proximad; slender; long; distinct from lobe; strongly extended past the posterior margin of lobe. Distal ridge weakly distinct from lobe. *Apex* narrow; convex; strikingly elongate; acuminate; strongly curved ventro-proximad; the distal margin is reduced revealing the ventral section of the distal lobe. *Anterior section* slender and strikingly elongate; straight and anteriad. *Median to posterior section* dorsally concealed by the proximal ridge. *Posterior section* very strongly extended past the posterior margin of lobe. - Ventral view: Proximal ridge anteriorly completely conceals the distal ridge. *Apex* acuminate. *Anterior to antero-medial section* moderately narrow and very long; curved distad. *Median to posterior section* obscured by the distal ridge. Distal ridge *median and posterior sections* arise from the posterior and proximal margins of the distal lobe; distinct from lobe; moderately broad; moderately long. *Antero-medial section* not waisted. *Median section* convex. *Postero-proximal angle* not reduced. *Postero-distal angle* reduced. *Subalare tendon attachment point* short and moderately broad; apically not curved ventrad; posterior margin medially concave; extends posteriad from the median; the postero-dorsal section of the proximal ridge is very moderately extended past the terminus of the subalare tendon attachment point; moderately visible dorsally.

Body - Dorsal view: slender and strikingly elongate. Proximal lobe long; deltoid; oriented proximad; arises from the postero-medial section of the ridge; depressed below the ridge; strongly sclerotized; weakly concave. *Base* moderately broad. *Apex* rounded; weakly curved anteriad. *Anterior margin* concave. *Posterior margin* weakly enlarged; concave. Distal lobe short and moderately broad; deltoid; shorter than the proximal lobe; moderately sclerotized; planate; moderately sloped ventrad. *Anterior margin* weakly convex; oriented antero-distad; moderately reduced. *Apex* acuminate. *Posterior margin* straight; moderately reduced. - Ventral view: Proximal lobe short; convex. *Posterior wing process junction* formed as a slender, ridge-like convexity; occupies the postero-proximal section of the lobe and is greatly lengthened anteriorly, extending to, and running along the anterior margin of the lobe. Distal lobe small; weakly discontinuous with ridge; concave.

Median Plate (Fig.166)

FM1 oriented strongly postero-proximad. *Anterior to posterior section* moderately narrow. *Proximal margin section* convex. Articulation with 2Ax extends from the antero-distal margin of the distal lobe to the posterior section over the posterior section of the ventral ridge. *Distal margin* extremely narrowly and weakly fused to 3Ax. FM2 moderately short; oriented proximad; acerose; separated from FM1 by a long, narrow section of membrane.

Third Axillary (Fig.167)

Head weakly convex; normal length. Proximal margin shallowly concave. Anterior margin weakly concave; broad; narrow, not enlarged ventrally; from the proximal angle it slopes antero-distad. *Antero-proximal margin* not extended anteriad. *Antero-distal margin* weakly extended anteriad. AXCu occupies the proximal one-fifth of head; convex. FCu normal size; distinct; occupies the central three-fifths of the head; deltoid. FA moderately narrow; occupies the distal one-fifth of head. *Anterior margin* entire. Suture line between FCu and FA present. Suture line between FCu and AXCu present. Suture line between FA and FJ absent.

Neck elevated proximally and weakly so distally. FCu section of neck absent. AXCu forms entire neck; extremely small. Proximal margin elevated as a very narrow and short ridge. *Ridge* extends to median of the proximal margin of tail; very short. Dorsal surface of ridge is weakly curved proximad; enlarged dorsally relative to AXA. Prong armed with a single broad but short tooth; oriented postero-dorsad. Detached AXCu fragment saddle-shaped; strongly curved ventrad both anteriorly and posteriorly; slender; moderately sclerotized.

Tail reduced; deltoid; short. *Dorsal surface* oriented laterad. Proximal margin strongly elevated dorsad to the dorsal plane of the neck; slopes distad along its entire length. Anterior to antero-median section concave. Antero-median to posterior section convex; oriented dorso-distad. *Window* absent. FJ+AXJ broad; extends close to the dorsal plane of the neck; occupies the anterior half of the tail; moderately sclerotized; curved distad. Suture line between FJ and AXJ absent. Suture line between FA+AXJ and AXA present. AXA extremely short and narrow; more strongly sclerotized than FA+AXJ; occupies the posterior half of the tail; curved postero-distad. Suture line between AXA and AXCu present.

Hind Wing Base Description

First Basal Plate (Fig.168)

Humeral Plate moderately broad; long. Anterior margin convex; strongly sclerotized; adjacent to BScA. Apex deltoid; moderately narrow; curved ventrad. Dorsal margin concave. Proximal margin weakly convex; curved ventrad. Ventral margin sinuate. Suture line between FPC+BPC and FC+BC absent.

Anterior Subcostal Basivenale oriented distad; broadly ovoid; convex; moderately dorsad. Proximal and distal sections separated by a prominent suture. *Proximal section* weakly extended anteriorly and postero-proximally as a moderately broad convexity; larger than the distal section. *Distal section* discontinuous with the ScA bulge; separated by a moderately deep concavity. Apex broadly rounded; oriented distad. – Subcosta Anterior moderately convex; moderately extended posteriorly. Bulge moderately broad.

Radial Basivenale convex; open; discontinuous with radial stem; angled antero-proximad; broadly rectangular. Proximal arch slenderly deltoid; curved postero-distad. *Anterior* strikingly reduced by a greatly enlarged br; discontinuous with the anterior margin of BR. *Posterior margin* weakly concave; surrounds the BMA arch apex. *Postero-distal margin* truncate. Anterior margin depressed below the posterior margin of ScA bulge; extremely

narrow; convex; angled antero-proximad. Embayment normal size. Distal arch discontinuous with radial stem; moderately broad; convex; broadly curved proximad; oriented postero-proximad. *br* strongly sclerotized; occupies about one-third of the proximal arch; discontinuous with BR. *br projection* slenderly deltoid; concave; distinct from BScA.

Second Basal Plate (Fig.169)

MA-BMA Junction absent. – MP-BMP Junction: MP broadly continuous with BMP; arises from below the BMP-BCuA brace. – Crimp Patterns absent. – BMP-CuA Brace absent. – BMP-BCuA Brace present but modified; discontinuous with BMP; entire and greatly strengthened; extends posteriad; moderately enlarged; equally broad along the entire length; convex; distinct from BMP. Terminus fused to the disto-medial section of BCuA. *Point of fusion* continuous.

Medial Basivenalia reduced proximally. BMA broadly scaphoid; completely fused to BMP. *Proximal surface* convex. *Medial and distal surfaces* planate. *Anterior margin* weakly concave. *Proximal arch* moderately long; planate and straight; oriented proximad; strongly curved ventrad. Apex terminates below BR proximal arch apex. *Distal arch* indistinct; fused to the proximal section of BMP. BMP junction with BMA discontinuous and very broad; fused to brace; markedly convex; separated from both IBP and BCu by membrane. *Proximal section* broadly deltoid; planate; slopes ventro-distad. *Distal section* indistinguishable from BMP-BCuA brace; long; broad; rectangular; strongly convex.

Cubital Basivenalia narrowly fused; small. Postero-proximal margin of BCuA fused with the antero-proximal margin of BCuP. *Suture line* present. BCuA very small; convex; oriented postero-distad; lies posteriad of BMP; weakly sclerotized. *Anterior margin* with a broad shallow concavity. *Distal margin* continuous with CuA. BCuP narrowly ovoid; convex; oriented postero-distad; weakly sclerotized. Distal embayment narrow but deep. – Cubitus Anterior fused to BCuA. Junction marked by a distinct suture.

Basalare (Fig.170)

Head - HP lobe slender; continuous with neck. Apex narrowly truncate. *Dorsal surface* elevated from neck; not polished. BScP lobe claviform; weakly projects posteriad from neck. *Dorsal surface* ovoid; weakly convex; polished; depressed from neck; slopes ventrad. *Ventral surface* polished. – Posterior Subcostal Basivenale ovoid; polished.

Discussion

Although Oncerinae do not display any autapomorphic character states of the wing articulation and wing base, they do share two apomorphic character states of the wing articulation and wing base with Melolonthinae, Hopliinae, Chasmatopterinae and *Acoma*. The evidence indicates that neither subfamilial nor tribal status is warranted, and it should be placed in Melolonthinae as *Oncerus* (Browne 1993).

Oncerinae share 22 apomorphic character states of the wing articulation and wing base with Orphninae, Melolonthinae, Rutelinae, Dynastinae, Cetoniinae, Chasmatopterinae, *Acoma*, Hopliinae, Trichiinae and Valginae (Browne 1993).

Rutelinae

Introduction

The Rutelinae are a very large, diverse cosmopolitan group. Adults either do not feed or they feed on leaves, fruits and flowers (Ritcher 1958). Larvae feed on humus, plant litter or plant roots (Ritcher 1966).

Hind Wing Articulation Description

First Axillary (Fig.171)

Head - Dorsal surface strongly reduced posteriorly; broad; not clavate; convex. *Antero-dorsal margin* oriented strikingly postero-distad; very broad; weakly deplanate. *Antero-proximal margin* with ventral enlargement reduced. *Postero-proximal margin* enlargement strong and very broad. *FSc2* base moderately enlarged; deeply concave. Apex oriented postero-distad; rounded but narrowly so. Anterior surface narrow; long; not waisted medially. *FSc1* absent. *Ventral projection* long and narrow; enlarged mesally; convex; strongly oriented ventrad and posteriad. Dorsal surface base to subapical area convex. Ventral surface convex. Apex concave; wider than base; strongly flared; truncate. Concavity strongly shifted mesad just past the base of the ventral projection onto the anterior surface of the head, and not extended apicad; surrounded by three equally strong ridges of equal length. *Distal embayment* oriented ventro-mesad. *FSc2* oriented distad and weakly dorsad; deltoid; convex; broad; short. Dorsal surface not enlarged dorsally; convex; not twisted. Ventral surface convex. Base proximally with a large convexity. Apex aciculate. Head and neck dorsal surface extended anteriad.

Neck normal width; long; weakly oriented antero-distad; articulation with 2Ax extends along the distal margin of the neck and tail; continuous with tail. Proximal margin not reduced; convex; curved ventrad. Distal margin concave. *Distal embayment* concave; moderately deep and broad.

Tail - Dorsal view: Proximal arch moderately expanded posteriorly and proximally. *Dorsal surface* moderately concave. *Antero-proximal margin* very weakly convex. *Postero-proximal margin* straight. Articulation with PRR strong along the entire length of the proximal arch; very long but narrow; weakly recurved. Antero-dorsal surface moderately concave. Postero-dorsal surface moderately concave. Posterior margin weakly concave. Distal arch strikingly reduced anteriorly, distally and posteriorly. *Apex* weakly curved posteriad and ventrad; very broadly rounded. *Distal margin* straight. - Ventral view: Proximal and posterior margins with very prominent ridges. Distal arch with a very slender ridge.

Second Axillary (Fig.172)

Radial Fulcalare absent.

Ridges - Dorsal view: Proximal ridge entire; distinct from lobe. *Apex* obscured by the distal ridge; waisted. *Anterior section* distal margin exposed. *Antero-median to postero-median section* moderately enlarged above and laterad over the distal ridge. *Posterior*

section weakly enlarged above the distal ridge; broadly curved postero-proximad; slender; moderately long; distinct from lobe; weakly extended past the posterior margin of lobe. Distal ridge weakly distinct from lobe. *Apex* narrow; partially planate; slender; strikingly elongate; aciculate; strongly curved ventro-proximad; the distal margin is reduced revealing the ventral section of the distal lobe. *Anterior section* slender and strikingly elongate; straight and antieriad. *Median to posterior section* dorsally concealed by the proximal ridge. *Posterior section* weakly extended past the posterior margin of lobe. - Ventral view: Proximal ridge anteriorly completely concealed by the distal ridge. *Median to posterior section* obscured by the distal ridge. Distal ridge *apex* aciculate. *Anterior section* moderately narrow and very long; curved distad. *Median and posterior sections* arise from the posterior and proximal margins of the distal lobe; distinct from lobe; moderately broad; long. *Antero-median section* weakly waisted. *Median section* convex. *Postero-proximal angle* strongly extended postero-proximad. *Postero-distal angle* not extended postero-distad. *Subalare tendon attachment point* long and moderately broad; apically not curved ventrad; posterior margin narrowly rounded; postero-distal margin reduced; dorsally concave; surrounds the dorso-proximal ridge posterior within the concavity; extends postero-proximad from the median; postero-dorsal section of the proximal ridge is very weakly extended past the terminus of the subalare tendon attachment point; strongly visible dorsally.

Body - Dorsal view: slender and strikingly elongate. Proximal lobe long; deltoid; oriented proximad; arises from the postero-medial section of the ridge; depressed below the ridge; strongly sclerotized; weakly concave. *Base* moderately broad. *Apex* rounded; weakly curved posteriad. *Anterior margin* concave. *Posterior margin* weakly enlarged; concave. Distal lobe very short and moderately broad; deltoid; shorter than proximal lobe; moderately sclerotized; planate; very strongly sloped ventrad. *Anterior margin* weakly convex; oriented postero-distad; strikingly reduced. *Apex* broadly rounded; strongly reduced. *Posterior margin* straight; moderately reduced. - Ventral view: Proximal lobe moderately short; convex. *Posterior wing process junction* formed as a slender, ridge-like convexity; occupies the postero-proximal section of the lobe and is greatly lengthened anteriorly, extending to, and running along the anterior margin of the lobe. Distal lobe extremely small; weakly discontinuous with ridge; concave.

Median Plate (Fig.173)

FM1 oriented strongly postero-proximad. *Anterior to posterior section* moderately narrow. *Proximal margin* convex. Articulation with 2Ax extends from the antero-distal margin of the distal lobe to the posterior section over the posterior section of the ventral ridge. *Distal margin* extremely narrowly and weakly fused to 3Ax. FM2 moderately short; oriented proximad; acerose; separated from FM1 by a long, narrow section of membrane.

Third Axillary (Fig.174)

Head weakly convex; normal length; very weakly bi-lobed. Proximal margin shallowly concave. Anterior margin weakly concave; broad; narrow, not enlarged ventrally; from the proximal angle it slopes antero-distad. *Antero-proximal margin* not extended antieriad.

Antero-distal margin weakly extended anteriad. AXCu occupies the proximal one-seventh of head; convex. FCu normal size; distinct; occupies the central three-sevenths of the head; deltoid. FA moderately broad; occupies the distal three-sevenths of head. *Anterior margin* entire. Suture line between FCu and FA present. Suture line between FCu and AXCu present. Suture line between FA and FJ absent.

Neck elevated proximally and weakly so distally. FCu section of neck absent. AXCu forms entire neck; extremely small. Proximal margin elevated as a very narrow and short ridge. *Ridge* extends to median of the proximal margin of tail; very short. Dorsal surface of ridge is weakly curved proximad; enlarged dorsally relative to AXA. Prong armed with a single moderately broad and long tooth; oriented postero-dorsad. Detached AXCu fragment saddle-shaped; strongly curved ventrad both anteriorly and posteriorly; slender; moderately sclerotized.

Tail reduced; deltoid; short. *Dorsal surface* oriented laterad. Proximal margin strongly elevated dorsad to the dorsal plane of the neck; slopes distad along its entire length. Anterior to antero-median section concave. Antero-median to posterior section convex; oriented dorso-distad. *Window* absent. FJ+AXJ broad; extends close to the dorsal plane of the neck; occupies the anterior half of the tail; moderately sclerotized; curved distad. Suture line between FJ and AXJ absent. Suture line between FA+AXJ and AXA present. AXA extremely short and narrow; more strongly sclerotized than FA+AXJ; occupies the posterior half of the tail; curved postero-distad. Suture line between AXA and AXCu present.

Hind Wing Base Description

First Basal Plate (Fig.175)

Humeral Plate broad. Anterior margin convex; strongly sclerotized; very broadly adjacent to, and almost fused with BScA. Apex clavate; broad; very weakly curved ventrad. Dorsal margin concave. Proximal margin weakly convex; curved ventrad. Ventral margin sinuate. Suture line between FPC+BPC and FC+BC absent.

Anterior Subcostal Basivenale oriented distad; very broadly ovoid; moderately convex; moderately curved anteriad. Proximal and distal sections separated by a prominent suture. *Proximal section* strongly and extremely broadly extended anteriorly and postero-proximally as a moderately broad convexity; larger than the distal section. *Distal section* weakly discontinuous with the ScA bulge; separated by a very shallow concavity. Apex broadly rounded; oriented distad. – Subcosta Anterior convex; extended posteriorly. Bulge moderately broad.

Radial Basivenale convex; moderately broadly open; discontinuous with radial stem; angled antero-proximad; rectangular. Proximal arch slenderly deltoid; curved postero-distad. *Anterior section* strikingly reduced by a greatly enlarged br; discontinuous with the anterior margin of BR. *Posterior margin* weakly concave; surrounds the BMA arch apex. *Postero-distal margin* truncate. Anterior margin depressed below the posterior margin of ScA bulge; narrow; convex; angled antero-proximad. Embayment normal size. Distal arch discontinuous with radial stem; moderately broad; convex; broadly curved

proximad; oriented postero-proximad. *br* strongly sclerotized; occupies about one-third of the proximal arch; discontinuous with BR. *br projection* narrow along its entire length; concave; distinct from BScA.

Second Basal Plate (Fig.176)

MA-BMA Junction absent. – MP-BMP Junction: MP broadly continuous with BMP; arises from below the BMP-BCuA brace. – Crimp Patterns absent. – BMP-CuA Brace absent. – BMP-BCuA Brace present but modified; discontinuous with BMP; entire and greatly strengthened; extends posteriad; anteriorly enlarged; convex; distinct from BMP. Terminus fused to a deep concavity on the disto-medial section of BCuA. *Point of fusion* discontinuous.

Medial Basivenalia reduced proximally. BMA broadly scaphoid; completely fused to BMP. *Proximal surface* convex. *Medial and distal surfaces* planate. *Anterior margin* weakly concave. *Proximal arch* moderately long; planate and straight; oriented proximad; strongly curved ventrad. Apex terminates below BR proximal arch apex. *Distal arch* indistinct; fused to the proximal section of BMP. BMP junction with BMA discontinuous and very broad; fused to brace; markedly convex; separated from both 1BP and BCu by membrane. *Proximal section* broadly deltoid; planate; slopes ventro-distad. *Distal section* indistinguishable from BMP-BCuA brace; long; broad; rectangular; strongly convex.

Cubital Basivenalia moderately broadly fused. Postero-proximal margin of BCuA fused with the anterior margin of BCuP. *Suture line* present. BCuA narrow and long; convex; oriented distad; lies posteriad of BMP; strongly sclerotized. *Anterior margin* with a moderately broad extremely deep concavity. *Distal margin* continuous with CuA. BCuP deltoid; convex; oriented postero-distad; moderately sclerotized. Distal embayment moderately deep and broad. – Cubitus Anterior fused to BCuA. Junction marked by a distinct suture.

Basalare (Fig.177)

Head - HP lobe large; continuous with neck. *Apex* broadly truncate. *Dorsal surface* elevated from neck; not polished. BScP lobe claviform; weakly projects posteriad from neck. *Dorsal surface* weakly rectangular; weakly convex; polished; depressed from neck; slopes ventrad. *Ventral surface* polished. – Posterior Subcostal Basivenale weakly deltoid; polished.

Discussion

Although Rutelinae do not display any autapomorphic character states of the wing articulation and wing base, they do share 19 apomorphic character states of the wing articulation and wing base with Dynastinae, Cetoniinae, Trichiinae and Valginae, and four apomorphic character states of the wing articulation and wing base with Dynastinae, its sister group (Howden 1982; Scholtz 1990; Browne 1993).

Rutelinae have usually been associated with both Melolonthinae and Dynastinae (Ritcher 1969a,b; Howden 1982; d'Hotman & Scholtz 1990a; Nel & Scholtz 1990; Scholtz 1990).

However, Rutelinae are considered to be more closely related to Dynastinae, and Melolonthinae being the sister group of this lineage (Meinecke 1975; Howden 1982).

Rutelinae share 22 apomorphic character states of the wing articulation and wing base with Orphninae, Melolonthinae, Dynastinae, Cetoniinae, Oncerinae, Chasmatopterinae, *Acoma*, Hopliinae, Trichiinae and Valginae (Browne 1993).

Dynastinae

Introduction

The Dynastinae are a large cosmopolitan group, which may or may not feed as adults (Ritcher 1958). Ritcher also mentioned that those that do feed probably feed on plant juices obtained from underground stems, shoots or roots. Larval feeding habits are very diverse, and vary from dung, humus and other organic matter, to plant roots.

Hind Wing Articulation Description

First Axillary (Fig.178)

Head - Dorsal surface strongly reduced posteriorly; broad; not clavate; convex. *Antero-dorsal margin* oriented strikingly postero-distad; very broad; weakly deplanate. *Antero-proximal margin* with ventral enlargement reduced. *Postero-proximal margin* enlargement strong and very broad. *FSc2* base moderately enlarged; deeply concave. Apex oriented postero-distad; rounded but narrowly so. Anterior surface narrow; long; not waisted medially. *FSc1* absent. *Ventral projection* long and narrow; enlarged mesally; convex; strongly oriented ventrad and posteriad. Dorsal surface base to subapical area convex. Ventral surface convex. Apex concave; wider than base; strongly flared; truncate. Concavity strongly shifted mesad just past the base of the ventral projection onto the anterior surface of the head, and not extended apicad; surrounded by three equally strong ridges of equal length. *Distal embayment* oriented ventro-mesad. *FSc2* oriented distad and weakly dorsad; deltoid; convex; broad; short. Dorsal surface not enlarged dorsally; convex; not twisted. Ventral surface convex. Base proximally with a large convexity. Apex aciculate. Head and neck dorsal surface extended anteriad.

Neck normal width; long; weakly oriented antero-distad; articulation with 2Ax extends along the distal margin of the neck and tail; continuous with tail. Proximal margin not reduced; convex; curved ventrad. Distal margin concave. *Distal embayment* concave; moderately deep and broad.

Tail - Dorsal view: Proximal arch moderately expanded posteriorly and proximally. *Dorsal surface* moderately concave. *Antero-proximal margin* very weakly convex. *Postero-proximal margin* straight. Articulation with PRR strong along the entire length of the proximal arch; very long but narrow; weakly recurved. Antero-dorsal surface moderately concave. Postero-dorsal surface moderately concave. Posterior margin weakly concave. Distal arch strikingly reduced anteriorly, distally and posteriorly. *Apex* weakly curved posteriad and ventrad; very broadly rounded. *Distal margin* straight. - Ventral view: Proximal posterior and distal margins with slender ridges.

Second Axillary (Fig.179)

Radial Fulcalare absent.

Ridges - Dorsal view: Proximal ridge entire; distinct from lobe. *Apex* obscured by the distal ridge; waisted. *Anterior section* distal margin exposed. *Antero-median to postero-median section* moderately enlarged above and laterad over the distal ridge. *Posterior section* weakly enlarged above the distal ridge; broadly curved postero-proximad; slender; moderately long; distinct from lobe; weakly extended past the posterior margin of lobe. Distal ridge weakly distinct from lobe. *Apex* narrow; partially planate; slender; strikingly elongate; aciculate; strongly curved ventro-proximad; the distal margin is reduced revealing the ventral section of the distal lobe. *Anterior section* slender and strikingly elongate; straight and anteriad. *Median to posterior section* dorsally concealed by the proximal ridge. *Posterior section* weakly extended past the posterior margin of lobe. - Ventral view: Proximal ridge anteriorly completely concealed by the distal ridge. *Median to posterior section* obscured by the distal ridge. Distal ridge *apex* aciculate. *Anterior section* moderately narrow and very long; curved distad. *Median and posterior sections* arise from the posterior and proximal margins of the distal lobe; distinct from lobe; moderately broad; long. *Antero-median section* weakly waisted. *Median section* convex. *Postero-proximal angle* strongly extended postero-proximad. *Postero-distal angle* not extended postero-distad. *Subalare tendon attachment point* long and moderately broad; apically not curved ventrad; posterior margin narrowly rounded; postero-distal margin reduced; dorsally concave; surrounds the dorso-proximal ridge posterior within the concavity; extends postero-proximad from the median; postero-dorsal section of the proximal ridge is very weakly extended past the terminus of the subalare tendon attachment point; strongly visible dorsally.

Body - Dorsal view: slender and strikingly elongate. Proximal lobe long; deltoid; oriented proximad; arises from the postero-medial section of the ridge; depressed below the ridge; strongly sclerotized; weakly concave. *Base* moderately broad. *Apex* rounded; weakly curved posteriad. *Anterior margin* concave. *Posterior margin* weakly enlarged; concave. Distal lobe very short and moderately broad; deltoid; shorter than proximal lobe; moderately sclerotized; planate; very strongly sloped ventrad. *Anterior margin* weakly convex; oriented postero-distad; strikingly reduced. *Apex* broadly rounded; strongly reduced. *Posterior margin* straight; moderately reduced. - Ventral view: Proximal lobe moderately short; convex. *Posterior wing process junction* formed as a slender, ridge-like convexity; occupies the postero-proximal section of the lobe and is greatly lengthened anteriorly, extending to, and running along the anterior margin of the lobe. Distal lobe extremely small; weakly discontinuous with ridge; concave.

Median Plate (Fig.180)

FM1 oriented strongly postero-proximad. *Anterior to posterior section* moderately narrow. *Proximal margin* convex. Articulation with 2Ax extends from the antero-distal margin of the distal lobe to the posterior section over the posterior section of the ventral ridge. *Distal*

margin extremely narrowly and weakly fused to 3Ax. FM2 moderately short; oriented proximad; acerose; separated from FM1 by a long, narrow section of membrane.

Third Axillary (Fig.181)

Head weakly convex; normal length; very weakly bi-lobed. Proximal margin shallowly concave. Anterior margin weakly convex; broad; narrow, not enlarged ventrally; from the proximal angle it slopes antero-distad. *Antero-proximal margin* not extended anteriad. *Antero-distal margin* weakly extended anteriad. AXCu occupies the proximal one-seventh of head; convex. FCu normal size; distinct; occupies the central three-sevenths of the head; deltoid. FA moderately broad; occupies the distal three-sevenths of head. *Anterior margin* entire. Suture line between FCu and FA present. Suture line between FCu and AXCu present. Suture line between FA and FJ absent.

Neck elevated proximally and weakly so distally. FCu section of neck absent. AXCu forms entire neck; extremely small. Proximal margin elevated as a very narrow and short ridge. *Ridge* extends to median of the proximal margin of tail; very short. Dorsal surface of ridge is weakly curved proximad; enlarged dorsally relative to AXA. Prong armed with a single moderately broad and long tooth; oriented postero-dorsad. Detached AXCu fragment saddle-shaped; strongly curved ventrad both anteriorly and posteriorly; slender; moderately sclerotized.

Tail reduced; deltoid; short. *Dorsal surface* oriented laterad. Proximal margin strongly elevated dorsad to the dorsal plane of the neck; slopes distad along its entire length. Anterior to antero-median section concave. Antero-median to posterior section convex; oriented dorso-distad. *Window* absent. FJ+AXJ broad; extends close to the dorsal plane of the neck; occupies the anterior half of the tail; moderately sclerotized; curved distad. Suture line between FJ and AXJ absent. Suture line between FA+AXJ and AXA present. AXA extremely short and narrow; more strongly sclerotized than FA+AXJ; occupies the posterior half of the tail; curved postero-distad. Suture line between AXA and AXCu present.

Hind Wing Base Description

First Basal Plate (Fig.182)

Humeral Plate moderately broad but short. Anterior margin convex; strongly sclerotized; very broadly adjacent to, and almost fused with BScA. Apex deltoid; moderately narrow; curved ventrad. Dorsal margin concave. Proximal margin weakly convex; curved ventrad. Ventral margin sinuate. Suture line between FPC+BPC and FC+BC absent.

Anterior Subcostal Basivenale oriented distad; very broadly ovoid; moderately convex; moderately curved anteriad. Proximal and distal sections separated by a prominent suture. *Proximal section* strongly and extremely broadly extended anteriorly and postero-proximally as a moderately broad convexity; larger than the distal section. *Distal section* weakly discontinuous with the ScA bulge; separated by a very shallow concavity. Apex broadly rounded; oriented distad. – Subcosta Anterior convex; extended posteriorly. Bulge moderately broad.

Radial Basivenale convex; moderately broadly open; discontinuous with radial stem; angled antero-proximad; rectangular. Proximal arch slenderly deltoid; curved postero-distad. *Anterior section* strikingly reduced by a greatly enlarged br; discontinuous with the anterior margin of BR. *Posterior margin* weakly concave; surrounds the BMA arch apex. *Postero-distal margin* truncate. Anterior margin depressed below the posterior margin of ScA bulge; narrow; convex; angled antero-proximad. Embayment normal size. Distal arch discontinuous with radial stem; moderately broad; convex; broadly curved proximad; oriented postero-proximad. br strongly sclerotized; occupies about one-third of the proximal arch; discontinuous with BR. *br projection* moderately narrow; concave; distinct from BScA.

Second Basal Plate (Fig.183)

MA-BMA Junction absent. – MP-BMP Junction: MP broadly continuous with BMP; arises from below the BMP-BCuA brace. – Crimp Patterns absent. – BMP-CuA Brace absent. – BMP-BCuA Brace present but modified; discontinuous with BMP; entire and greatly strengthened; extends posteriad; anteriorly enlarged; convex; distinct from BMP. Terminus fused to a deep concavity on the disto-medial section of BCuA. *Point of fusion* discontinuous.

Medial Basivenalia reduced proximally. BMA broadly scaphoid; completely fused to BMP. *Proximal surface* convex. *Medial and distal surfaces* planate. *Anterior margin* weakly concave. *Proximal arch* moderately long; planate and straight; oriented proximad; strongly curved ventrad. Apex terminates below BR proximal arch apex. *Distal arch* indistinct; fused to the proximal section of BMP. BMP junction with BMA discontinuous and very broad; fused to brace; markedly convex; separated from both 1BP and BCu by membrane. *Proximal section* broadly deltoid; planate; slopes ventro-distad. *Distal section* indistinguishable from BMP-BCuA brace; long; broad; rectangular; strongly convex.

Cubital Basivenalia moderately broadly fused. Postero-proximal margin of BCuA fused with the anterior margin of BCuP. *Suture line* present. BCuA narrow and long; convex; oriented distad; lies posteriad of BMP; strongly sclerotized. *Anterior margin* with a moderately broad extremely deep concavity. *Distal margin* continuous with CuA. BCuP very weakly deltoid; convex; oriented postero-distad; moderately sclerotized. Distal embayment moderately broad and deep. – Cubitus Anterior fused to BCuA. Junction marked by a distinct suture.

Basalare (Fig.184)

Head - HP lobe large; continuous with neck. Apex broadly truncate. *Dorsal surface* weakly elevated from neck; not polished. BScP lobe claviform; weakly projects posteriad from neck. *Dorsal surface* weakly rectangular; weakly convex; polished; depressed from neck; slopes ventrad. *Ventral surface* polished. – Posterior Subcostal Basivenale weakly deltoid; polished.

Discussion

Although Dynastinae do not display any autapomorphic character states of the wing articulation and wing base, they do share 19 apomorphic character states of the wing articulation and wing base with Rutelinae, Cetoniinae, Trichiinae and Valginae, and four apomorphic character states of the wing articulation and wing base with Rutelinae, their sister group (Howden 1982; Scholtz 1990; see Browne 1993).

Dynastinae have usually been associated with Rutelinae by the presence of unequal tarsal claws and similar abdominal spiracle pattern, mouthparts and male genitalia (Ritcher 1969a,b; Howden 1982; d'Hotman & Scholtz 1990a; Nel & Scholtz 1990; Scholtz 1990).

Dynastinae share 22 apomorphic character states of the wing articulation and wing base with Orphninae, Melolonthinae, Rutelinae, Cetoniinae, Oncerinae, Chasmatopterinae, *Acoma*, Hopliinae, Trichiinae and Valginae (Browne 1993).

Cetoniinae

Introduction

The Cetoniinae are a large and diverse cosmopolitan subfamily (Scholtz 1990) consisting of several ill-defined tribes (E. Holm pers. comm. 1993).

Hind Wing Articulation Description

First Axillary (Fig.185)

Head - Dorsal surface strongly reduced posteriorly; extremely broad; clavate; convex. *Antero-dorsal margin* oriented strikingly postero-distad; very broad; weakly deplanate. *Antero-proximal margin* with ventral enlargement reduced. *Postero-proximal margin* enlargement strong but very narrow. *FSc2* base moderately enlarged; deeply concave. Apex oriented postero-distad; rounded but narrowly so. Anterior surface narrow; long; not waisted medially. *FSc1* absent. *Ventral projection* extremely long and narrow; enlarged mesally; base to terminus; straight to weakly curved anteriad. Dorsal surface base to terminus convex. - Ventral surface convex. Apex convex; wider than base; flare reduced; truncate. Concavity strongly shifted dorso-mesad past the base of the ventral projection far onto the anterior surface of the head, and not extended apicad; surrounded by three ridges of equal length; the apical ridge is strongly reduced. *Distal embayment* oriented ventro-mesad. *FSc2* oriented distad and weakly dorsad; deltoid; convex; broad; long. Dorsal surface not enlarged dorsally; convex; not twisted. Ventral surface convex. Base proximally with a convexity. Apex aciculate. Head and neck dorsal surface extended anteriad.

Neck strikingly broad; long; weakly oriented antero-distad; articulation with 2Ax extends along the distal margin of the neck and tail; continuous with tail. Proximal margin sinuate; curved ventrad. Distal margin concave. *Distal embayment* broadly but shallowly concave.

Tail - Dorsal view: Proximal arch strikingly expanded posteriorly and proximally. *Dorsal surface* deeply concave. *Antero-proximal margin* weakly concave. *Postero-proximal margin* convex. Articulation with PRR strong along the entire length of the proximal arch;

very long but narrow; weakly recurved. Antero-dorsal surface concave. Postero-dorsal surface concave. Posterior margin weakly concave; angled strongly antero-distad. Distal arch moderately reduced anteriorly, distally and posteriorly. *Apex* very weakly curved postero-distad. *Distal margin* straight. - Ventral view: Proximal, posterior and distal margins with very prominent, broad ridges.

Second Axillary (Fig.186)

Radial Fulcalare absent.

Ridges - Dorsal view: Proximal ridge entire; weakly distinct from lobe. *Apex* obscured by the distal ridge; waisted. *Anterior section* distal margin exposed. *Antero-median to postero-median section* moderately enlarged above and laterad over the distal ridge. *Posterior section* weakly enlarged above the distal ridge; broadly curved postero-proximad; extremely short; distinct from lobe; weakly extended past the posterior margin of lobe. Distal ridge distinct from lobe. *Apex* narrow; completely planate; slender; strikingly elongate; aciculate; strongly curved ventro-proximad; the distal margin is reduced revealing the ventral section of the distal lobe. *Anterior section* slender and strikingly elongate; straight and anteriad. *Median to posterior section* dorsally concealed by the proximal ridge. *Posterior section* weakly extended past the posterior margin of lobe. - Ventral view: Proximal ridge anteriorly completely concealed by the distal ridge. *Median to posterior section* obscured by the distal ridge. Distal ridge *apex* broadly rounded. *Anterior section* very broad and short; curved distad. *Median and posterior sections* moderately broad; long. *Antero-median section* weakly waisted. *Median section* very strongly convex to form a ridge. *Postero-proximal angle* strongly extended postero-proximad. *Postero-distal angle* not extended postero-distad. *Subalare tendon attachment point* long and moderately broad; apically not curved ventrad; posterior margin narrowly rounded; postero-distal margin reduced; dorsally concave; surrounds the dorso-proximal ridge posterior within the concavity; extends postero-proximad from the median; postero-dorsal section of the proximal ridge is very weakly extended past the terminus of the subalare tendon attachment point; strongly visible dorsally.

Body - Dorsal view: slender and strikingly elongate. Proximal lobe moderately long; deltoid; oriented proximad; arises from the postero-medial section of the ridge; depressed below the ridge; strongly sclerotized; weakly concave. *Base* broad. *Apex* rounded; curved anteriad. *Anterior margin* concave. *Posterior margin* weakly enlarged; concave. Distal lobe very short and moderately broad; deltoid; shorter than proximal lobe; moderately sclerotized; planate; very strongly sloped ventrad. *Anterior margin* weakly convex; oriented postero-distad; strikingly reduced. *Apex* broadly rounded; strongly reduced. *Posterior margin* straight; moderately reduced. - Ventral view: Proximal lobe short; convex. *Posterior wing process junction* formed as a slender, ridge-like convexity; occupies the postero-proximal section of the lobe and is greatly lengthened anteriorly, extending to, and running along the anterior margin of the lobe. Distal lobe extremely small; weakly discontinuous with ridge; concave.

Median Plate (Fig.187)

FM1 oriented strongly postero-proximad. *Anterior to posterior section* extremely narrow and very long. *Proximal margin* straight. Articulation with 2Ax extends along the distal margin of the distal ridge over the posterior section of the ventral ridge. *Distal margin* extremely narrowly and weakly fused to 3Ax. FM2 absent.

Third Axillary (Fig.188)

Head weakly convex; normal length; strikingly bi-lobed, embayment strong. Proximal margin strikingly deeply concave. Anterior margin very deeply concave; broad; narrow, not enlarged ventrally; from the proximal angle it slopes very strongly antero-distad. *Embayment* curves postero-distad. *Antero-proximal margin* strongly extended proximad as a lobe. Proximal lobe weakly convex; long; moderately narrow. *Antero-distal margin* strongly extended anteriad as a lobe. Distal lobe very strongly convex; moderately broad and long. AXCu occupies the proximal one-third of the proximal lobe; convex. FCu strikingly reduced distally; moderately large; distinct; occupies distal two-thirds of the proximal lobe and the proximal one-half of the distal lobe. FA moderately narrow; occupies the distal one-half of the distal lobe. *Anterior margin* entire. Suture line between FCu and FA present. Suture line between FCu and AXCu present. Suture line between FA and FJ absent. Head and neck junction strikingly reduced, extremely narrow.

Neck elevated proximally and weakly so distally. FCu section of neck absent. AXCu forms entire neck; extremely small. Proximal margin elevated as a very narrow and short ridge. *Ridge* extends to median of the proximal margin of tail; very short. Dorsal surface of ridge is strongly curved distad over the distal margin of the tail and strongly curved ventrad reducing the width of the tail; enlarged dorsally relative to AXA. Prong armed with a single broad but short tooth; oriented postero-dorsad. Detached AXCu fragment saddle-shaped; strongly curved ventrad both anteriorly and posteriorly; slender; moderately sclerotized.

Tail reduced; extremely narrow; very short. *Dorsal surface* oriented laterad. *Window* absent. FJ+AXJ extremely narrow and short; occupies the anterior half of the tail; moderately sclerotized; curved ventrad. Suture line between FJ and AXJ absent. Suture line between FA+AXJ and AXA present. AXA extremely short and narrow; more strongly sclerotized than FA+AXJ; occupies the posterior half of the tail; curved postero-distad. Suture line between AXA and AXCu present.

Hind Wing Base Description

First Basal Plate (Fig.189)

Humeral Plate very broad and moderately short. Anterior margin convex; strongly sclerotized; adjacent to BScA. Apex clavate; moderately broad; weakly curved ventrad. Dorsal margin convex. Proximal margin deeply concave; strongly curved ventro-proximad. Ventral margin concave. Suture line between FPC+BPC and FC+BC absent.

Anterior Subcostal Basivenale oriented distad; rectangular; convex; moderately elevated dorsad. Proximal and distal sections separated by a prominent suture. *Proximal section*

strongly and extremely broadly extended anteriorly and postero-proximally as a very broad convexity; much larger than the distal section. *Distal section* discontinuous with the ScA bulge; separated by a moderately deep concavity. Apex broadly rounded; oriented distad. – Subcosta Anterior moderately convex; moderately extended posteriad. Bulge moderately broad.

Radial Basivenale convex; open; discontinuous with radial stem; angled proximad; rectangular. Proximal arch slenderly deltoid; curved postero-distad. *Anterior section* strikingly reduced by a greatly enlarged br; discontinuous with the anterior margin of BR. *Posterior margin* weakly concave; surrounds the BMA arch apex. *Postero-distal margin* truncate. Anterior margin depressed below the posterior margin of ScA bulge; moderately broad; straight; angled proximad. Embayment normal size. Distal arch discontinuous with radial stem; moderately broad; convex; broadly curved proximad; oriented postero-proximad. br strongly sclerotized; occupies about one-third of the proximal arch; discontinuous with BR. *br projection* deltoid; short; concave; weakly distinct from BScA.

Second Basal Plate (Fig.190)

MA-BMA Junction absent. – MP-BMP Junction: MP broadly continuous with BMP; arises from below the BMP-BCuA brace. – Crimp Patterns absent. – BMP-CuA Brace absent. – BMP-BCuA Brace present but modified; discontinuous with BMP; entire and greatly strengthened; extends posteriad; posteriorly enlarged; convex; distinct from BMP. Terminus fused to a deep concavity on the disto-medial section of BCuA. *Point of fusion* discontinuous.

Medial Basivenalia reduced proximally. BMA broadly scaphoid; completely fused to BMP. *Proximal surface* convex. *Medial and distal surfaces* planate. *Anterior margin* concave. *Proximal arch* very short; planate and straight; oriented antero-proximad; strongly curved ventrad. Apex terminates below BR proximal arch apex. *Distal arch* indistinct; fused to the proximal section of BMP. BMP junction with BMA discontinuous and very broad; fused to brace; markedly convex; separated from both IBP and BCu by membrane. *Proximal section* broadly deltoid; planate; slopes ventro-distad. *Distal section* indistinguishable from BMP-BCuA brace; long; broad; rectangular; strongly convex.

Cubital Basivenalia completely fused. Posterior margin of BCuA fused with the anterior margin of BCuP. *Suture line* present. BCuA very narrow and long; convex; oriented distad; lies posteriad of BMP; strongly sclerotized. *Anterior margin* with an extremely broad extremely deep concavity. *Distal margin* continuous with CuA. BCuP large; weakly deltoid; convex; oriented posteriad; moderately sclerotized. Distal embayment absent. – Cubitus Anterior fused to BCuA. Junction indistinct.

Basalare (Fig.191)

Head - HP lobe large; continuous with neck. Apex broadly truncate. *Dorsal surface* weakly elevated from neck; not polished. BScP lobe claviform; weakly projects posteriad from neck. *Dorsal surface* weakly rectangular; weakly convex; polished; depressed from neck; slopes ventrad. *Ventral surface* polished. – Posterior Subcostal Basivenale weakly deltoid; polished.

Discussion

Analysis of wing articulation and wing base characters indicates that this subfamily is paraphyletic since it does not display any autapomorphic wing articulation and wing base characters but does share two apomorphic character states of the wing articulation and wing base with Trichiinae (excluding *Osmoderma*) (Browne 1993). It is likely that these taxa together form Cetoniinae (Browne 1993).

Cetoniines were once placed in Rutelinae (Leng 1920) but are now most commonly considered to be the sister group of Rutelinae and/or Dynastinae (Ritcher 1969a,b; Meinecke 1975; Howden 1982; Caveney 1986; d'Hotman & Scholtz 1990a; Nel & Scholtz 1990; Scholtz 1990). Krikken (1984) considers Trichiinae + Valginae to be the sister group of Cetoniinae, and Rutelinae and/or Dynastinae the sister group of Trichiinae + Valginae + Cetoniinae.

Cetoniinae share 22 apomorphic character states of the wing articulation and wing base with Orphninae, Melolonthinae, Rutelinae, Dynastinae, Oncerinae, Chasmatopterinae, *Acoma*, Hopliinae, Trichiinae and Valginae (Browne 1993).

Trichiinae

Introduction

The Trichiinae are a medium-sized group with cosmopolitan distribution. Adults of several species have been collected on flowers while others feed on sap that flows from bark. Larvae feed on decaying plant material (Ritcher 1966).

Hind Wing Articulation Description

First Axillary (Fig.192)

Head - Dorsal surface strongly reduced posteriorly; extremely broad; clavate; convex. *Antero-dorsal margin* oriented strikingly postero-distad; very broad; weakly deplanate. *Antero-proximal margin* with ventral enlargement reduced. *Postero-proximal margin* enlargement strong but very narrow. *FSc2* base moderately enlarged; deeply concave. Apex oriented postero-distad; rounded but narrowly so. Anterior surface narrow; long; not waisted medially. *FSc1* absent. *Ventral projection* extremely long and narrow; enlarged mesally; base to terminus; straight to weakly curved anteriad. Dorsal surface base to terminus convex. - Ventral surface convex. Apex convex; wider than base; flare reduced; truncate. Concavity strongly shifted dorso-mesad past the base of the ventral projection onto the anterior surface of the head, and not extended apicad; surrounded by three ridges of equal length; the apical ridge is weakly reduced. *Distal embayment* oriented ventro-mesad. *FSc2* oriented distad and weakly dorsad; deltoid; convex; broad; long. Dorsal surface not enlarged dorsally; convex; not twisted. Ventral surface convex. Base proximally with a convexity. Apex acuminate. Head and neck dorsal surface extended anteriad.

Neck strikingly broad; long; weakly oriented antero-distad; articulation with 2Ax extends along the distal margin of the neck and tail; continuous with tail. Proximal margin sinuate; curved ventrad. Distal margin concave. *Distal embayment* broadly but shallowly concave.

Tail - Dorsal view: Proximal arch strikingly expanded posteriorly and proximally. *Dorsal surface* deeply concave. *Antero-proximal margin* weakly concave. *Postero-proximal margin* convex. Articulation with PRR strong along the entire length of the proximal arch; very long but narrow; weakly recurved. Antero-dorsal surface concave. Postero-dorsal surface concave. Posterior margin weakly concave; angled strongly antero-distad. Distal arch moderately reduced anteriorly, distally and posteriorly. *Apex* moderately narrowly digitate; weakly curved postero-distad. *Distal margin* straight. - Ventral view: Proximal margin with a very strong ridge. Distal margin with a weak ridge. Posterior margin with a prominent ridge.

Second Axillary (Fig.193)

Radial Fulcalare absent.

Ridges - Dorsal view: Proximal ridge entire; weakly distinct from lobe. *Apex* obscured by the distal ridge; waisted. *Anterior section* distal margin exposed. *Antero-median to postero-median section* moderately enlarged above and laterad over the distal ridge. *Posterior section* weakly enlarged above the distal ridge; broadly curved postero-proximad; extremely short; distinct from lobe; weakly extended past the posterior margin of lobe. Distal ridge distinct from lobe. *Apex* narrow; completely planate; slender; strikingly elongate; acuminate; strongly curved ventro-proximad; the distal margin is reduced revealing the ventral section of the distal lobe. *Anterior section* slender and strikingly elongate; straight and anteriad. *Median to posterior section* dorsally concealed by the proximal ridge. *Posterior section* weakly extended past the posterior margin of lobe. - Ventral view: Proximal ridge anteriorly completely concealed by the distal ridge. *Median to posterior section* obscured by the distal ridge. Distal ridge *apex* broadly rounded. *Anterior section* very broad and short; curved distad. *Median and posterior sections* moderately broad; long. *Antero-median section* weakly waisted. *Median section* very strongly convex to form a ridge. *Postero-proximal angle* strongly extended postero-proximad. *Postero-distal angle* not extended postero-distad. *Subalare tendon attachment point* long and moderately broad; apically not curved ventrad; posterior margin narrowly rounded; postero-distal margin reduced; dorsally concave; surrounds the dorso-proximal ridge posterior within the concavity; extends postero-proximad from the median; postero-dorsal section of the proximal ridge is very weakly extended past the terminus of the subalare tendon attachment point; strongly visible dorsally.

Body - Dorsal view: slender and strikingly elongate. Proximal lobe moderately; deltoid; oriented proximad; arises from the postero-medial section of the ridge; depressed below the ridge; strongly sclerotized; weakly concave. *Base* broad. *Apex* rounded; curved anteriad. *Anterior margin* concave. *Posterior margin* weakly enlarged; concave. Distal lobe very short and moderately broad; deltoid; shorter than proximal lobe; moderately sclerotized; planate; very strongly sloped ventrad. *Anterior margin* weakly convex; oriented postero-distad; strikingly reduced. *Apex* broadly rounded; strongly reduced. *Posterior margin* straight; moderately reduced. - Ventral view: Proximal lobe short; convex. *Posterior wing process junction* formed as a slender, ridge-like convexity; occupies the postero-proximal section of the lobe and is greatly lengthened anteriorly,

extending to, and running along the anterior margin of the lobe. Distal lobe extremely small; weakly discontinuous with ridge; concave.

Median Plate (Fig.194)

FM1 oriented strongly postero-proximad. *Anterior to posterior section* extremely narrow and very long. *Proximal margin* straight. Articulation with 2Ax extends along the distal margin of the distal ridge over the posterior section of the ventral ridge. *Distal margin* extremely narrowly and weakly fused to 3Ax. FM2 absent.

Third Axillary (Fig.195)

Head weakly convex; normal length; strikingly bi-lobed, embayment weak. Proximal margin moderately deeply concave. Anterior margin convex; broad; narrow, not enlarged ventrally; from the proximal angle it slopes very strongly antero-distad. *Antero-proximal margin* broadly extended proximad as a lobe. Proximal lobe weakly convex; short. *Antero-distal margin* broadly extended anteriorly as a lobe. Distal lobe very strongly convex; short. AXCu occupies the proximal one-third of the proximal lobe; convex. FCu strikingly reduced distally; moderately large; distinct; occupies distal two-thirds of the proximal lobe and the proximal one-half of the distal lobe. FA moderately narrow; occupies the distal one-half of the distal lobe. *Anterior margin* entire. Suture line between FCu and FA present. Suture line between FCu and AXCu present. Suture line between FA and FJ absent. Head and neck junction strikingly reduced, extremely narrow.

Neck elevated proximally and weakly so distally. FCu section of neck absent. AXCu forms entire neck; extremely small. Proximal margin elevated as a very narrow and short ridge. *Ridge* extends to median of the proximal margin of tail; very short. Dorsal surface of ridge is strongly curved distad over the distal margin of the tail and strongly curved ventrad reducing the width of the tail; enlarged dorsally relative to AXA. Prong armed with a single broad but short tooth; oriented postero-dorsad. Detached AXCu fragment saddle-shaped; strongly curved ventrad both anteriorly and posteriorly; slender; moderately sclerotized.

Tail reduced; extremely narrow; very short. *Dorsal surface* oriented laterad. *Window* absent. FJ+AXJ extremely narrow and short; occupies the anterior half of the tail; moderately sclerotized; curved ventrad. Suture line between FJ and AXJ absent. Suture line between FA+AXJ and AXA present. AXA extremely short and narrow; more strongly sclerotized than FA+AXJ; occupies the posterior half of the tail; curved postero-distad. Suture line between AXA and AXCu present.

Hind Wing Base Description

First Basal Plate (Fig.196)

Humeral Plate moderately broad and long. Anterior margin strongly sinuate; strongly sclerotized; adjacent to BScA. Apex broadly rounded; clavate; curved ventrad. Dorsal margin convex. Proximal margin convex; strongly curved ventro-proximad. Ventral margin concave. Suture line between FPC+BPC and FC+BC absent.

Anterior Subcostal Basivenale oriented distad; broadly ovoid; convex; moderately elevated dorsad. Proximal and distal sections separated by a prominent suture. *Proximal section* strongly and extremely broadly extended anteriorly and postero-proximally as a very broad convexity; much larger than the distal section. *Distal section* discontinuous with the ScA bulge; separated by a moderately deep concavity. Apex broadly rounded; oriented distad. – Subcosta Anterior moderately convex; moderately extended posteriad. Bulge moderately broad.

Radial Basivenale convex; open; discontinuous with radial stem; angled proximad; rectangular. Proximal arch slenderly deltoid; curved postero-distad. *Anterior section* strikingly reduced by a greatly enlarged br; discontinuous with the anterior margin of BR. *Posterior margin* weakly concave; surrounds the BMA arch apex. *Postero-distal margin* truncate. Anterior margin depressed below the posterior margin of ScA bulge; moderately broad; straight; angled proximad. Embayment normal size. Distal arch discontinuous with radial stem; moderately broad; convex; broadly curved proximad; oriented postero-proximad. br strongly sclerotized; occupies about one-third of the proximal arch; discontinuous with BR. *br projection* slender; short; concave; weakly distinct from BScA.

Second Basal Plate (Fig.197)

MA-BMA Junction absent. – MP-BMP Junction: MP broadly continuous with BMP; arises from below the BMP-BCuA brace. – Crimp Patterns absent. – BMP-CuA Brace absent. – BMP-BCuA Brace present but modified; discontinuous with BMP; entire and greatly strengthened; extends posteriad; posteriorly enlarged; convex; distinct from BMP. Terminus fused to a deep concavity on the disto-medial section of BCuA. *Point of fusion* discontinuous.

Medial Basivenalia reduced proximally. BMA broadly scaphoid; completely fused to BMP. *Proximal surface* convex. *Medial and distal surfaces* planate. *Anterior margin* concave. *Proximal arch* very short; planate and straight; oriented antero-proximad; strongly curved ventrad. Apex terminates below BR proximal arch apex. *Distal arch* indistinct; fused to the proximal section of BMP. BMP junction with BMA discontinuous and very broad; fused to brace; markedly convex; separated from both 1BP and BCu by membrane. *Proximal section* broadly deltoid; planate; slopes ventro-distad. *Distal section* indistinguishable from BMP-BCuA brace; long; broad; rectangular; strongly convex.

Cubital Basivenalia broadly fused. Posterior margin of BCuA fused with the anterior margin of BCuP. *Suture line* present. BCuA very narrow and long; convex; oriented distad; lies posteriad of BMP; strongly sclerotized. *Anterior margin* with an extremely broad extremely deep concavity. *Distal margin* continuous with CuA. BCuP weakly deltoid; convex; oriented posteriad; moderately sclerotized. Distal embayment very narrow but deep. – Cubitus Anterior fused to BCuA. Junction indistinct.

Basalare (Fig.198)

Head - HP lobe large; continuous with neck. *Apex* broadly truncate. *Dorsal surface* weakly elevated from neck; not polished. BScP lobe claviform; weakly projects posteriad from neck. *Dorsal surface* rectangular; weakly convex; polished; depressed from neck; slopes

ventrad. *Ventral surface* polished. – Posterior Subcostal Basivenale weakly rectangular; polished.

Discussion

Trichiinae do not display any apomorphic character states of the wing articulation and wing base. In addition, it is quite likely that this subfamily is polyphyletic and comprised by at least two distinct lineages (E. Holm pers. comm. 1992), formed by *Osmoderma* and all other Trichiinae (Browne 1993). The latter share two autapomorphic character states of the wing articulation and wing base with Cetoniinae.

Trichiines are most commonly associated with Cetoniinae and Valginae, as either a cetoniine tribe (Leng 1920; Ritcher 1969ab; Caveney 1986) or a separate subfamily (Blackwelder 1944; Howden 1968; d'Hotman & Scholtz 1990a; Nel & Scholtz 1990; Scholtz 1990). Trichiinae, together with their sister group Valginae, are considered to be more archaic than Cetoniinae (Krikken 1984). Krikken (1984) suggested that Trichiinae are the sister group of Valginae and that together they are the sister group of Cetoniinae.

Trichiinae share 22 apomorphic character states of the wing articulation and wing base with Orphninae, Melolonthinae, Rutelinae, Dynastinae, Oncerinae, Chasmatopterinae, *Acoma*, Hopliinae, Cetoniinae and Valginae (Browne 1993)

Valginae

Introduction

This subfamily consists of about 200 species world wide. Adults are usually associated with flowers. In North America all stages of *Valgus* have been found beneath loose bark at the base of trees in damp, rotten wood, in association with termites (Ritcher 1966), and in Australia large numbers of *Microvalgus* have been reared from termite mound material (Britton 1970). The relationship between the valgines and termites is unknown. In central Europe, *Valgus hemipterus* is common where termites are absent.

Hind Wing Articulation Description

First Axillary (Fig.199)

Head - Dorsal surface strongly reduced posteriorly; broad; clavate; convex. *Antero-dorsal margin* oriented strikingly postero-distad; very broad; weakly deplanate. *Antero-proximal margin* with ventral enlargement reduced. *Postero-proximal margin* enlargement strong and very broad. *FSc2* base moderately enlarged. Apex oriented postero-distad; rounded but narrowly so. Anterior surface narrow; long; not waisted medially. *FSc1* absent. *Ventral projection* extremely long and narrow; enlarged mesally; basally to subapically curved anteriad; apically curved posteriad. Dorsal surface base to terminus convex. - Ventral surface convex. Apex convex; wider than base; flare reduced; truncate. Concavity strongly shifted dorso-mesad past the base of the ventral projection far onto the anterior surface of the head, and not extended apicad; surrounded by three ridges of equal length; the apical ridge is absent. *Distal embayment* oriented ventro-mesad. *FSc2* oriented distad and

weakly dorsad; deltoid; convex; broad; long. Dorsal surface not enlarged dorsally; convex; not twisted. Ventral surface convex. Base proximally with a convexity. Apex aciculate. Head and neck dorsal surface extended antieriad.

Neck strikingly broad; long; weakly oriented antero-distad; articulation with 2Ax extends along the distal margin of the neck and tail; continuous with tail. Proximal margin sinuate; curved ventrad; only the anterior is very weakly reduced. Distal margin concave. *Distal embayment* broadly but very shallowly concave.

Tail - Dorsal view: Proximal arch strikingly enlarged posteriorly. *Dorsal surface* deeply concave. *Antero-proximal margin* weakly concave. *Postero-proximal margin* convex. *Postero-proximal angle* very broadly rounded. Articulation with PRR extremely strong along the entire length of the proximal arch; very long but narrow; very strongly recurved. Antero-dorsal surface deeply concave. Postero-dorsal surface deeply concave. Posterior margin deeply concave; angled antero-distad. Distal arch moderately reduced anteriorly, distally and posteriorly. *Apex* very narrow; digitate; weakly oriented postero-distad; weakly curved ventrad. *Distal margin* convex. - Ventral view: Proximal, distal and posterior ridges indistinct; form a single very broad ridge.

Second Axillary (Fig.200)

Radial Fulcalare absent.

Ridges - Dorsal view: Proximal ridge entire; weakly distinct from lobe. *Apex* obscured by the distal ridge. *Anterior section* distal margin exposed. *Antero-median to postero-median section* moderately enlarged above and laterad over the distal ridge. *Posterior section* weakly enlarged above the distal ridge; broadly curved postero-proximad; moderately short; weakly extended past the posterior margin of lobe. Distal ridge distinct from lobe. *Apex* narrow; completely planate; slender; strikingly elongate; aciculate; strongly curved ventro-proximad; the distal margin is reduced revealing the ventral section of the distal lobe. *Anterior section* slender and strikingly elongate; straight and antieriad. *Median to posterior section* dorsally concealed by the proximal ridge. *Posterior section* weakly extended past the posterior margin of lobe. - Ventral view: Proximal ridge anteriorly completely concealed by the distal ridge. *Median to postero-median section* obscured by the distal ridge. *Postero-median to terminus* acerose; extremely long; extends ventro-distad from the proximal lobe; much longer than the subalare tendon attachment point. Distal ridge *apex* broadly rounded. *Anterior section* broad and short; curved distad. *Median and posterior sections* extremely narrow; acerose; long. *Antero-median section* not waisted. *Median section* very strongly convex to form a ridge. *Postero-proximal angle* very strongly extended postero-proximad. *Postero-distal angle* not extended postero-distad. *Subalare tendon attachment point* strikingly long, narrow and acerose; apically not curved ventrad; posterior margin aciculate; extends postero-proximad from the median; postero-dorsal section of the proximal ridge is strongly extended past the terminus of the subalare tendon attachment point; strongly visible dorsally.

Body - Dorsal view: slender and strikingly elongate. Proximal lobe moderately; deltoid; oriented proximad; arises from the postero-medial section of the ridge; depressed below the ridge; strongly sclerotized; weakly concave. *Base* broad. *Apex* rounded; curved

anteriad. *Anterior margin* concave. *Posterior margin* weakly enlarged; concave. Distal lobe extremely small; deltoid; shorter than proximal lobe; moderately sclerotized; planate. *Anterior margin* straight; oriented distad; strikingly reduced. *Apex* broadly rounded. *Posterior margin* convex; strongly reduced. - Ventral view: Proximal lobe short; convex. *Posterior wing process junction* formed as a slender, ridge-like convexity; occupies the postero-proximal section of the lobe and is greatly lengthened anteriorly, extending to, and running along the anterior margin of the lobe. Distal lobe extremely small; weakly discontinuous with ridge; concave.

Median Plate (Fig.201)

FM1 oriented strongly postero-proximad. *Anterior to posterior section* extremely narrow and very long. *Proximal margin* straight. Articulation with 2Ax extends along the distal margin of the distal ridge over the posterior section of the ventral ridge. *Distal margin* extremely narrowly and weakly fused to 3Ax. FM2 absent.

Third Axillary (Fig.202)

Head weakly convex; normal length; strikingly bi-lobed; lobes exceedingly narrow and very long. Proximal margin strikingly deeply concave. Anterior margin very deeply concave; broad; narrow, not enlarged ventrally; from the proximal angle it slopes very strongly antero-distad. *Embayment* extremely deep and extends posteriorly to the head-neck junction; deltoid. *Antero-proximal margin* very strongly extended proximad as a lobe. Proximal lobe convex; strikingly long; narrow; acerose. *Antero-distal margin* very strongly extended anteriad as a lobe. Distal lobe convex; strikingly long; narrow; acerose. AXCu occupies the proximal one-third of the proximal lobe; convex. FCu strikingly reduced distally; distinct; occupies distal two-thirds of the proximal lobe and the proximal one-half of the distal lobe. FA moderately narrow; occupies the distal one-half of the distal lobe. *Anterior margin* entire. Suture line between FCu and FA present. Suture line between FCu and AXCu present. Suture line between FA and FJ absent. Head and neck junction extremely narrow.

Neck strongly elevated, extremely long and narrow; curved postero-distad. FCu section of neck absent. AXCu forms entire neck; extremely small. Posterior section elevated as a very narrow and short ridge. *Ridge* extends to median of the proximal margin of tail; very short. Dorsal surface of ridge is strongly curved distad over the distal margin of the tail; enlarged dorsally relative to AXA. Prong armed with a single broad but short tooth; oriented postero-dorsad. Detached AXCu fragment saddle-shaped; strongly curved ventrad both anteriorly and posteriorly; slender; moderately sclerotized.

Tail reduced; extremely narrow; very short. *Dorsal surface* oriented laterad. *Window* absent. FJ+AXJ extremely narrow and short; occupies the anterior half of the tail; moderately sclerotized; curved ventrad. Suture line between FJ and AXJ absent. Suture line between FA+AXJ and AXA present. AXA extremely short and narrow; more strongly sclerotized than FA+AXJ; occupies the posterior half of the tail; curved postero-distad. Suture line between AXA and AXCu present.

Hind Wing Base Description

First Basal Plate (Fig.203)

Humeral Plate strongly lengthened distally as an extremely slender, sinuate sclerite. Anterior margin sinuate; strongly sclerotized; adjacent to, and almost fused with BScA. *Antero-distal surface* membranous. Apex broadly deltoid; curved ventrad. Dorsal margin sinuate. Proximal margin deeply concave; strongly curved ventro-proximad. Ventral margin sinuate. Suture line between FPC+BPC and FC+BC absent.

Anterior Subcostal Basivenale oriented distad; rectangular; small; convex. Proximal and distal sections separated by a prominent suture. *Proximal section* strongly and extremely broadly extended anteriorly and postero-proximally as a broad convexity; much larger than the distal section. *Distal section* extremely narrow; discontinuous with the ScA bulge; separated by a moderately deep concavity. Apex broadly rounded; oriented distad. – Subcosta Anterior extremely broad; both concave and convex; extended posteriorly. Bulge moderately broad; fused to BR.

Radial Basivenale very strongly convex; open; discontinuous with radial stem; angled proximad; rectangular to ovoid. Proximal arch slenderly deltoid; curved postero-distad. *Anterior section* strikingly reduced by a greatly enlarged br; discontinuous with the anterior margin of BR. *Posterior margin* weakly concave; surrounds the BMA arch apex. *Postero-distal margin* truncate. Anterior margin fused to the posterior margin of ScA; extremely narrow; strongly convex; angled antero-proximad. Embayment normal size. Distal arch discontinuous with radial stem; moderately broad; convex; broadly curved proximad; oriented postero-proximad. br strongly sclerotized; occupies about one-third of the proximal arch; discontinuous with BR. *br projection* slender; short; weakly distinct from BScA.

Second Basal Plate (Fig.204)

MA-BMA Junction absent. – MP-BMP Junction: MP broadly continuous with BMP; arises from below the BMP-BCuA brace. – Crimp Patterns absent. – BMP-CuA Brace absent. – BMP-BCuA Brace present but modified; discontinuous with BMP; entire and greatly strengthened; extends posteriad; posteriorly enlarged; convex; distinct from BMP. Terminus fused to a deep concavity on the disto-medial section of BCuA. *Point of fusion* discontinuous.

Medial Basivenalia reduced proximally. BMA broadly scaphoid; completely fused to BMP. *Proximal surface* convex. *Medial and distal surfaces* weakly convex. *Anterior margin* weakly concave. *Proximal arch* extremely short; planate and straight; oriented antero-proximad; strongly curved ventrad. Apex terminates below BR proximal arch apex. *Distal arch* indistinct; fused to the proximal section of BMP. BMP junction with BMA discontinuous and very broad; fused to brace; markedly convex; separated from both 1BP and BCu by membrane. *Proximal section* broadly deltoid; planate; slopes ventro-distad. *Distal section* indistinguishable from BMP-BCuA brace; long; broad; rectangular; strongly convex.

Cubital Basivenalia narrowly fused. Postero-proximal margin of BCuA fused with the antero-proximal margin of BCuP. *Suture line* present. BCuA very narrow and long; convex; oriented distad; lies posteriad of BMP; strongly sclerotized. *Anterior margin* with an extremely broad extremely deep concavity. *Distal margin* continuous with CuA. BCuP ovoid; convex; oriented posteriad; moderately sclerotized. Distal embayment very narrow but deep. – Cubitus Anterior fused to BCuA. Junction indistinct.

Basalare (Fig.205)

Head - HP lobe large; continuous with neck. *Apex* broadly truncate. *Dorsal surface* weakly elevated from neck; not polished. BScP lobe claviform; weakly projects posteriad from neck. *Dorsal surface* rectangular; weakly convex; polished; depressed from neck; slopes ventrad. *Ventral surface* polished. – Posterior Subcostal Basivenale weakly deltoid; polished.

Discussion

Monophyly of the Valginae is supported by the fact that all members of this subfamily display 10 apomorphic character states of the wing articulation and wing base:

1. 1Ax: the postero-proximal margin of the head displays a strong and very broad proximal enlargement,
2. the anterior surface of the ventral projection is basally to subapically curved anteriorly and apically curved posteriad,
3. the proximal arch is strikingly enlarged posteriorly;
4. 2Ax: the subalare tendon attachment point is strikingly long, narrow and acerose;
5. 3Ax: the proximal and distal lobes of the head are exceedingly narrow and very long,
6. the embayment is extremely deep and extends posteriorly to the head-neck junction,
7. the FCu-neck junction is extremely narrow;
8. 1BP: HP is strongly lengthened distally as an extremely slender, sinuate sclerite,
9. the sclerotized section of ScA which lies between HP anteriorly, and BScA posteriorly and proximally, is completely reduced and membranous,
10. the BScA distal section is extremely slender and the proximal section very broad.

Krikken (1984) considers Valginae to be the sister group of "Trichiinae" and together the sister group of Cetoniinae. d'Hotman & Scholtz (1990a) consider Valginae to be the most transformed scarabaeoid subfamily.

Valginae share 22 apomorphic character states of the wing articulation and wing base with Orphninae, Melolonthinae, Rutelinae, Dynastinae, Oncerinae, Chasmatopterinae, Acoma, Hopliini, Cetoniinae and Trichiinae (Browne 1993).

LITERATURE CITED

- Allsop, P.G. (1984): Checklist of the Hybosoridae (Coleoptera: Scarabaeoidea). – *Coleopt. Bull.* 38:105-117.
- Areekull, S. (1957): The comparative internal larval anatomy of several genera of Scarabaeidae (Coleoptera). – *Ann. Entomol. Soc. Amer.* 50:562-577.
- Arnett, R.H. (1968): The beetles of the United States. Ann Arbor, Michigan.
- Blackwelder, R.E. (1944): Checklist of the coleopterous insects of North America, Mexico, Central America, the West Indies, and South America. – *Unit. Stat. Nation. Mus. Bull.* 185:197-265.
- Britton, E.B. (1970): Coleoptera. In: *Insects of Australia*. 1st ed. CSIRO, Canberra, pp 495-621.
- Browne, D.J. (1991a): The phylogenetic significance of wing characters in the Geotrupidae (Coleoptera: Scarabaeoidea). M.Sc. Thesis (University of Pretoria).
- (1991b): Wing structure of the genus *Eucanthus* Westwood; confirmation of the primitive nature of the genus (Scarabaeoidea: Geotrupidae: Bolboceratinae). – *J. Entomol. Soc. South. Afr.* 54:221-230.
- (1993): Phylogenetic significance of the hind wing basal articulation characters of the Scarabaeoidea (Coleoptera). Ph.D. Thesis (University of Pretoria).
- Browne, D.J., & C.H. Scholtz (1994): The morphology of the hind wing articulation of Scarabaeoidea, with implications for the rest of the Coleoptera. – *Syst. Entomol.* 19:133-143.
- & – (1995): The phylogeny of the families of Scarabaeoidea (Coleoptera) based on characters of the hind wing articulation, wing base and wing venation. – *Syst. Entomol.* 23:145-173.
- Browne, D.J., C.H. Scholtz & J. Kukalová-Peck (1993): Phylogenetic significance of wing characters in the Trogidae (Coleoptera: Scarabaeoidea). – *Afr. Entomol.* 1:195-206.
- Cambefort, Y. (1987): Insectes Coléoptères Aulonocnemidae. – *Faune de Madagascar* 69:3-86.
- Carlson, D.C. (1975): Taxonomic characters of the genus *Ochodaeus* Serville with description of two new species in the *O. pectoralis* Le Conte species complex (Coleoptera: Scarabaeoidea). – *Bull. South. Calif. Acad. Sci.* 74:49-65.
- Carlson, D.C., & P.O. Ritcher (1974): A new genus of Ochodaeinae and a description of the larva of *Pseudochodaeus estriatus* (Schaeffer). – *Pan-Pacif. Entomol.* 50:99-110.
- Caveney, S. (1986): The phylogenetic significance of ommatidium structure in the compound eyes of polyphagan beetles. – *Can. J. Zool.* 64:1787-1819.
- Chalumeau, F., & L. Gruner (1974): Scarabaeoidea des Antilles Françaises. – *Ann. Soc. Entomol. France* 10:781-819.
- Costa, C., S.A. Vanin & S.A. Casari-Chen (1988): Larvas de Coleoptera do Brasil. São Paulo (Museu de Zoologia).
- Crowson, R.A. (1938): The met-endosternite in Coleoptera: a comparative study. – *Trans. Roy. Entomol. Soc., London* 87:397-416.

- (1967): The natural classification of the families of Coleoptera. Hampton (Classey).
- (1981): The biology of the Coleoptera. London (Academic Press).
- d'Hotman, D., & C.H. Scholtz (1990a): Comparative morphology of the male genitalia of derived groups of Scarabaeoidea (Coleoptera). – *Elytron* 4:3-39.
- & – (1990b): Phylogenetic significance of the structure of the external male genitalia in the Scarabaeoidea (Coleoptera). – *Entomol. Mem.* 77:1-51.
- Halffter, G., & W.D. Edmonds (1982): The nesting behaviour of dung beetles (Scarabaeinae). Mexico (Instituto de Ecologia).
- Halffter, G., & E.G. Matthews (1966): The natural history of dung beetles of the subfamily Scarabaeinae (Coleoptera, Scarabaeoidea). – *Folia Entomol. Mexicana* 12-14:3-312.
- Hardy, A.R. (1977): A revision of the *Hoplia* of the Nearctic realm (Coleoptera: Scarabaeidae). – *Occ. Pap. Entomol.* 23:1-48.
- Hinton, H.E. (1967): Structure and ecdysial process of the larval spiracles of the Scarabaeoidea, with special reference to those of *Lepidoderma*. – *Austr. J. Zool.* 15:947-953.
- Ilavac, T.F. (1975): The prothorax of Coleoptera (except Bostrichiformia-Cucujiformia). – *Bull. Mus. Comp. Zool.* 147:137-183.
- Holloway, B.A. (1972): The systematic position of the genus *Diphylostoma* Fall (Coleoptera: Scarabaeoidea). – *New Zealand J. Sci.* 15:31-38.
- Horn, G.H. (1867): Descriptions of new genera and species of western Scarabaeidae, with note on others already known. – *Trans. Amer. Entomol. Soc.* 22:163-169.
- Hovore, F.T. (1977): New synonymy and status changes in the genus *Pleocoma* Le Conte (Coleoptera: Scarabaeoidea). – *Coleopt. Bull.* 31:229-237.
- Howden, H.F. (1968): A review of the Trichiinae of North and Central America (Coleoptera: Scarabaeidae). – *Entomol. Soc. Can.* 54:1-75.
- (1958): Species of *Acoma* having a three-segmented antennal club (Coleoptera: Scarabaeidae). – *Can. Entomol.* 95:377-401.
- (1982): Larval and adult characters of *Frickius* Germain, its relationship to the Geotrupini, and a phylogeny of some major taxa in the Scarabaeoidea (Insecta: Coleoptera). – *Can. J. Zool.* 60:2713-2724.
- Howden, H.F., & B.D. Gill (1988): *Xenocanthus*, a new genus of inquiline Scarabaeidae from southeastern Venezuela (Coleoptera). – *Can. J. Zool.* 66:2071-2076.
- Howden, H.F., & A.R. Hardy (1971): Generic placement and adult behavior of the genus *Leptohoplia* Saylor. – *Proc. Entomol. Soc. Washington* 73:337-341.
- Iablokoff-Khnzorian, S.M. (1977): Über die Phylogenie der Lamellicornia. – *Entomol. Abh. Staatl. Mus. Tierkde. Dresden* 41:135-199.
- Koshantschikov, W. (1913): Sechster Beitrag zur Kenntnis der Aphodiini (Coleoptera, Lamellicornia). – *Arch. Nat.gesch.* 79A,(11):186-203.
- Krikken, J. (1984): A new key to the suprageneric taxa in the beetle family Cetoniidae, with annotated lists of the known genera. – *Zool. Verh.* 210:3-75.
- Kuijten, P.J. (1986): Revision of the African and Madagascan species of *Phaeochrous* Castelnau, 1940 (Coleoptera: Scarabaeidae, Hybosorinae). – *Zool. Wetensch. Annz.* 249:1-50.

- Kukalová-Peck, J. (1983): Origin of the insect wing and wing articulation from the arthropodan leg. – *Can. J. Zool.* 61:1618-1669.
- (1991): Fossil history and the evolution of hexapod structures. In: *Insects of Australia*, 2nd ed. CSIRO, Canberra, pp 141-179.
- Kukalová-Peck, J., & J.F. Lawrence (1993): Evolution of the hind wing in Coleoptera. – *Can. Entomol.* 125:181-258.
- Lawrence, J.F., & A.F. Newton (1982): Evolution and classification of beetles. – *Ann. Rev. Ecol. Syst.* 13:261-290.
- Lawrence, J.F., E.S. Nielsen & I.M. Mackerras (1991): Skeletal anatomy and key to orders. In: *Insects of Australia*, 2nd ed. CSIRO, Canberra, pp 3-32.
- Leng, C.W. (1920): Catalogue of the Coleoptera of America, north of Mexico. New York (John D. Sherman).
- Meinecke, C.C. (1975): Reichsensillen und Systematik der Lamellicornia (Insecta, Coleoptera). – *Zoomorphol.* 82:1-42.
- Nel, A., & C.H. Scholtz (1990): Comparative morphology of the mouthparts of adult Scarabaeoidea (Coleoptera). – *Entomol. Mem.* 80:1-84.
- Paulian, R. (1977a): Révision des Ceratocanthidae. – *Rev. Zool. Afr.* 91:223-316.
- (1977b): The Australian Ceratocanthidae (Coleoptera: Scarabaeoidea). – *J. Austr. Entomol. Soc.* 16:261-265.
- (1978): Révision des Ceratocanthidae (Coleoptera: Scarabaeoidea) II.-Les Especies orientales et Australiennes. – *Ann. Soc. Entomol. France (N.S.)* 14:479-514.
- (1984): Les Orphninae américains (Coléoptères, Scarabaeoidea). – *Ann. Soc. Entomol. France* 20:65-92.
- Paulian, R., & J.-P. Lumaret (1974): Les larves des Scarabaeidae: 4. Le genre *Aulonocnemis* Schaufuss. – *Bull. Soc. Entomol. France* 79:233-240.
- & – (1982): Le larve des Orphnidae (Col. Scarabaeoidea). – *Bull. Soc. Entomol. France* 87:263-272.
- Reyes-Castillo, P. (1970): Coleoptera Passalidae: Morfologia y division en grandes grupos generos americanos. – *Folia Entomol. Mexicana* 20-22:1-236.
- Ritcher, P.O. (1958): Biology of the Scarabaeidae. – *Ann. Rev. Entomol.* 3:311-329.
- (1966): White grubs and their allies. A study of North American scarabaeoid larvae. Corvallis (Oregon State University Press).
- (1969a): Spiracles of adult Scarabaeoidea (Coleoptera) and their phylogenetic significance. I. The abdominal spiracles. – *Ann. Entomol. Soc. Amer.* 62:869-880.
- (1969b): Spiracles of adult Scarabaeoidea (Coleoptera) and their phylogenetic significance. II. Thoracic spiracles and adjacent sclerites. – *Ann. Entomol. Soc. Amer.* 62:1388-1398.
- (1969c): Morphology of the posterior procoxal bridges in Scarabaeoidea (Coleoptera). – *Coleopt. Bull.* 23:89-92.
- Ritcher, P.O., & C.W. Baker (1974): Ovariole numbers in Scarabaeoidea (Coleoptera: Lucanidae, Passalidae, Scarabaeidae). – *Proc. Entomol. Soc. Washington* 76:480-494.

- Saylor, L.W. (1938): Revision of the subfamily Oncerinae with description of a new genus (Coleoptera: Scarabaeidae). – Proc. Entomol. Soc. Washington 40:99-103.
- Scholtz, C.H. (1986): Phylogeny and systematics of the Trogidae (Coleoptera: Scarabaeoidea). – Syst. Entomol. 11:355-363.
- (1990): Phylogenetic trends in the Scarabaeoidea (Coleoptera). – J. Nat. Hist. 24:1027-1066.
- Scholtz, C.H., & D.J. Browne (in press): Polyphyly in the Geotrupidae (Scarabaeoidea: Coleoptera): A case for a new family. – J. Nat. Hist. (accepted Nov. 1995).
- Scholtz, C.H., D.J. Browne & J. Kukalová-Peck (1994): Glaresidae, archaopteryx of the Scarabaeoidea (Coleoptera). – Syst. Entomol. 19:259-277.
- Scholtz, C.H., D.J. Browne, J. Kukalová-Peck & E. Pretorius (submitted, Nov. 1995): The structure and affinities of the Plecomidae (Insecta: Coleoptera: Scarabaeoidea). – Afr. Entomol.
- Scholtz, C.H., D. d'Hotman & A. Nel (1987): Glaresidae, a new family of Scarabaeoidea (Coleoptera) to accommodate the genus *Glaresis* Erichson. – Syst. Entomol. 12:343-354.
- Scholtz, C.H., D. d'Hotman, A.V. Evans & A. Nel (1988): Phylogeny and systematics of the Ochodaeidae (Coleoptera: Scarabaeoidea). – J. Entomol. Soc. South. Afr. 51:207-240.
- Scholtz, C.H., & E. Holm (1985): Insects of southern Africa. Durban (Butterworths).
- Scholtz, C.H., & S. Peck (1990): Description of a *Polynoncus* Burmeister larva, with implications for phylogeny of the Trogidae (Coleoptera: Scarabaeoidea). – Syst. Entomol. 15:383-389.
- Smith, S.G., & N. Virkki (1978): Animal cytogenetics Vol. 3. Insecta 5. Berlin (Gebrüder Borntraeger).
- Snodgrass, R.E. (1935): Principles of insect morphology. New York (McGraw-Hill).
- Stebnicka, A.Z. (1985): A new genus and species of Aulonocneminae from India with notes on comparative morphology (Coleoptera: Scarabaeidae). – Rev. Suisse Zool. 92:649-658.
- Tanner, V.M. (1927): The female genitalia of Coleoptera. – Trans. Amer. Entomol. Soc. 53:3-50.
- Virkki, N. (1967): Chromosome relationships in some North America scarabaeoid beetles, with special reference to *Pleocoma* and *Trox*. – Can. J. Genet. Cytol. 9:107-125.
- (1969): Sperm bundles and phylogenesis. – Z. Zellphysiol. 101:13-27.
- Yadav, J.S. (1973): Chromosome number and sex-determining mechanism in fourteen species of Coleoptera. – Current Sci. 42:514.
- Yadav, J.S., & R.K. Pillai (1979): Karyotypic studies on five species of Melolonthinae (Scarabaeidae: Coleoptera). – Nucleus 19:195-200.
- Zunino, M. (1988): I Glaphyridae e la filogenesi delgi Scarabaeoidea (Coleoptera). – Atti XV Congr. Nazion. Ital. Entomol., L'Aquila 1988:329-333.

APPENDIX

List of abbreviations

1Ax – first axillary	BCuP – posterior cubital basivenale
1BP – first basal plate	BJ – jugal basivenale
2Ax – second axillary	BJA – anterior jugal basivenale
2BP – second basal plate	BJP – posterior jugal basivenale
3Ax – third axillary	BM – medial basivenale
4Ax – fourth axillary	BMA – anterior medial basivenale
A – anal vein	BMP – posterior medial basivenale
AA – anterior anal vein	BPC – precostal basivenale
AP – posterior anal vein	BPCA – anterior precostal basivenale
AX – axalare	BPCP – posterior precostal basivenale
AXA – anal axalare	br – proximal sub-section of proximal arch of BR
AXAA – anterior anal axalare	BR – radial basivenale
AXAP – posterior anal axalare	BRA – anterior radial basivenale
AXC – costal axalare	BRP – posterior radial basivenale
AXCA – anterior costal axalare	BSc – subcostal basivenale
AXCP – posterior costal axalare	BScA – anterior subcostal basivenale
AXCu – cubital axalare	BScP – posterior subcostal basivenale
AXCuA – anterior cubital axalare	C – costal vein
AXCuP – posterior cubital axalare	CA – anterior costal vein
AXJ – jugal axalare	CP – posterior costal vein
AXJA – anterior jugal axalare	Cu – cubital vein
AXJP – posterior jugal axalare	CuA – anterior cubital vein
AXM – medial axalare	CuP – posterior cubital vein
AXMA – anterior medial axalare	d-dl – dorso-distal lobe
AXMP – posterior medial axalare	d-dr – dorso-distal ridge
AXPC – precostal axalare	d-nr – distal neck ridge
AXPCA – anterior precostal axalare	d-pl – dorso-proximal lobe
AXPCP – posterior precostal axalare	d-pr – dorso-proximal ridge
AXR – radial axalare	d-tr – distal tail ridge
AXRA – anterior radial axalare	F – fulcalare
AXRP – posterior radial axalare	FA – anal fulcalare
AXSc – subcostal axalare	FAA – anterior anal fulcalare
AXScA – anterior subcostal axalare	FAP – posterior anal fulcalare
AXScP – posterior subcostal axalare	FC – costal fulcalare
B – basivenale	FCA – anterior costal fulcalare
BA – anal basivenale	FCP – posterior costal fulcalare
BAA – anterior anal basivenale	FCu – cubital fulcalare
BAP – posterior anal basivenale	FCuA – anterior cubital fulcalare
BAS – basalare	FCuP – posterior cubital fulcalare
BC – costal basivenale	FJ – jugal fulcalare
BCA – anterior costal basivenale	FJA – anterior jugal fulcalare
BCP – posterior costal basivenale	FJP – posterior jugal fulcalare
BCu – cubital basivenale	FM – medial fulcalare
BCuA – anterior cubital basivenale	

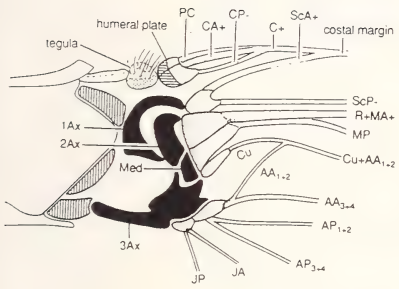
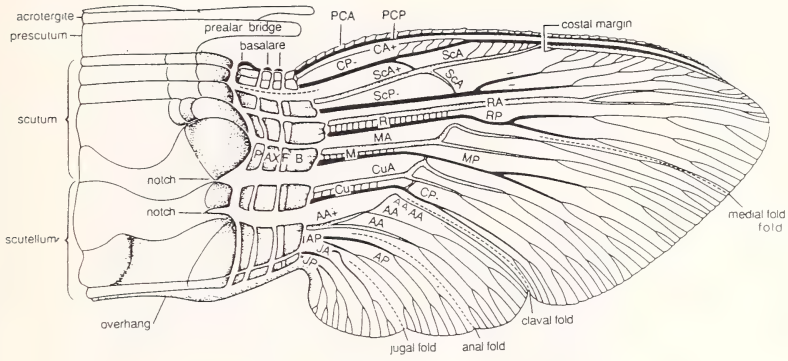
- FM1 – the distal portion of FM which articulates with BMA
 FM2 – the proximal portion of FM which articulates with BMP
 FMA – anterior medial fulcalare
 FMP – posterior medial fulcalare
 FPC – precostal fulcalare
 FPCA – anterior precostal fulcalare
 FPCP – posterior precostal fulcalare
 FR – radial fulcalare
 FRA – anterior radial fulcalare
 FRP – posterior radial fulcalare
 FSc – subcostal fulcalare
 FSc1 – ventral tooth of 1Ax head
 FSc2 – dorsal tooth of 1Ax head
 FScA – anterior subcostal fulcalare
 FScP – posterior subcostal fulcalare
 HP – humeral plate
 J – jugal vein
 JA – anterior jugal vein
 JP – posterior jugal vein
 M – medial vein
 MA – anterior medial vein
 MED – medial plate
 mg – medial groove
 MP – posterior medial vein
 p-nr – proximal neck ridge
 p-tr – proximal tail ridge
 PC – precostal vein
 PCA – anterior precostal vein
 PCP – posterior precostal vein
 post-tr – posterior tail ridge
 PR – proxalare
 PRA – anal proxalare
 PRAP – posterior anal proxalare
 PRC – costal proxalare
 PRCA – anterior costal proxalare
 PRCP – posterior costal proxalare
 PRCu – cubital proxalare
 PRCuA – anterior cubital proxalare
 PRCuP – posterior cubital proxalare
 PRJ – jugal proxalare
 PRJA – anterior jugal proxalare
 PRJP – posterior jugal proxalare
 PRM – medial proxalare
 PRMA – anterior medial proxalare
 PRMP – posterior medial proxalare
 PRPC – precostal proxalare
 PRPCA – anterior medial proxalare
 PRPCP – posterior medial proxalare
 PRR – radial proxalare
 PRRA – anterior radial proxalare
 PRRP – posterior radial proxalare
 PRSc – subcostal proxalare
 PRScA – anterior subcostal proxalare
 PRScP – posterior subcostal proxalare
 PWP – posterior wing process junction
 R – radial vein
 RA – anterior radial vein
 RP – posterior radial vein
 Sc – subcostal vein
 ScA – anterior subcostal vein
 ScP – posterior subcostal vein
 STAP – subalare tendon attachment point
 v-dl – ventro-distal lobe
 v-dr – ventro-distal ridge
 v-pl – ventro-proximal lobe
 v-pr – ventro-proximal ridge

Authors' address:

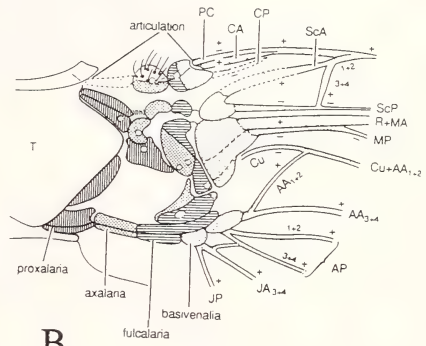
D.J. Browne and C.H. Scholtz, Department of Entomology, University of Pretoria, Pretoria 0002, South Africa.

Figs.1-2: **1:** Scheme of ancestral Pterygote wing articulation, wing base and wing venation; the ancestral band of unfused sclerites (P=proxalare, AX=axalare, F=fulcalare, B=basivenale) gave rise to all Recent types of wing articulation and wing base (from Kukalová-Peck 1983). – **2:** Wing articulation and wing base of Neoptera (diagrammatic): a, showing the three axillary sclerites and median plate and their associations with basivenalia; b, showing homologies with the original band sclerites illustrated in Figure 1; c, showing the position of the axillary sclerites in relation to the wing venation (a from Lawrence et al. 1991; b from Kukalová-Peck 1991; c from Kukalová-Peck & Lawrence 1993).

1

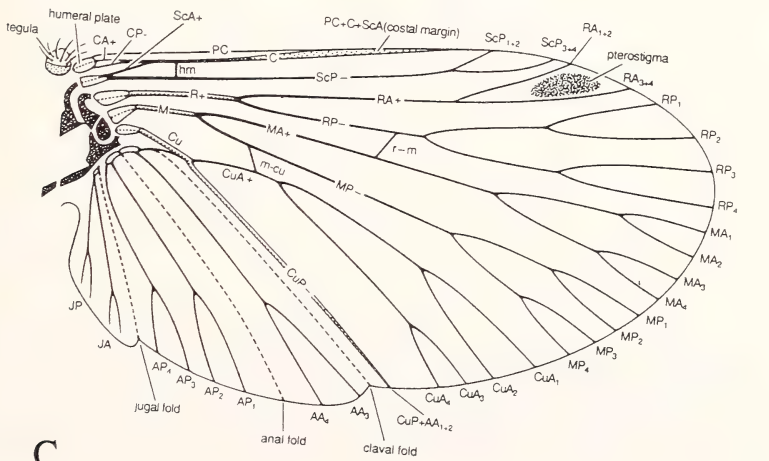


A



B

2



C

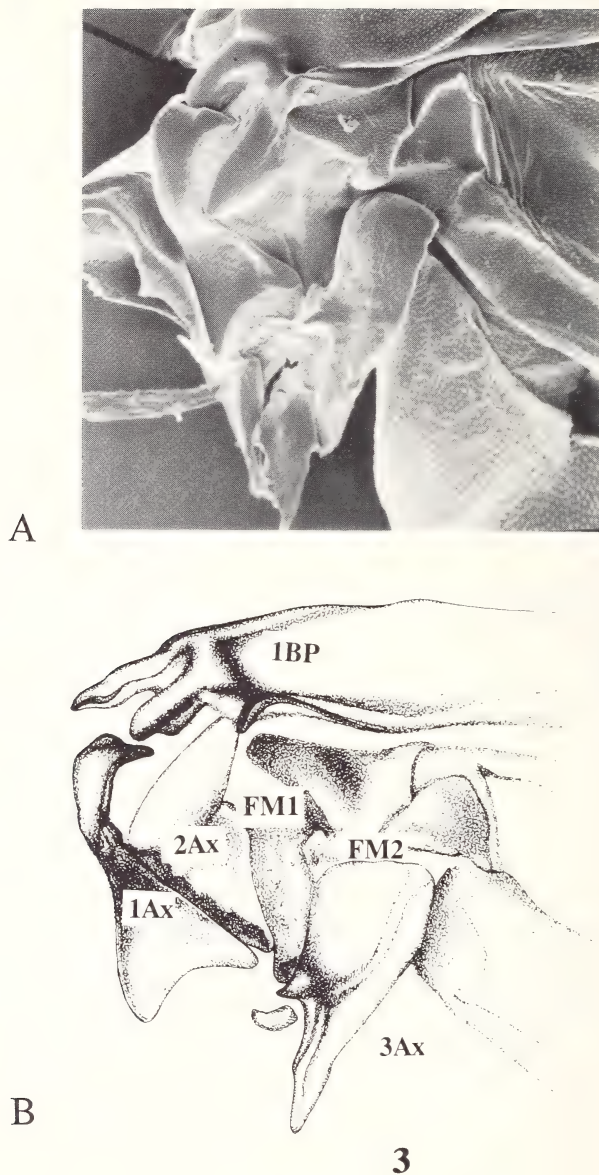
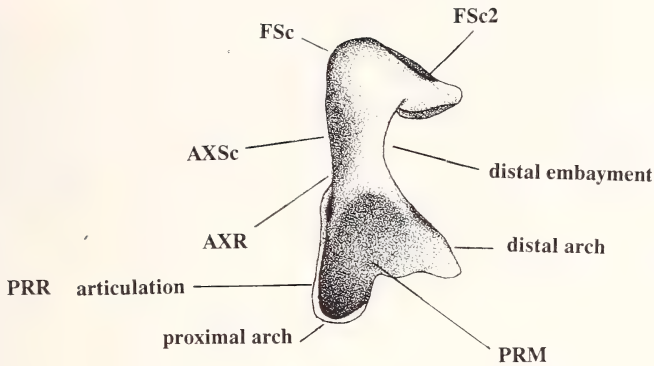
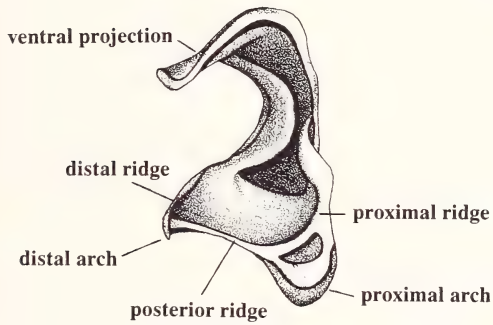


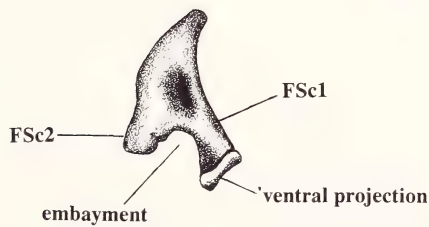
Fig.3: Hind wing articulation and wing base of *Glaresis walzlae* (Glaresidae): a, scanning electron micrograph (1000x); b, showing relative positions of axillaries and basal plates, first axillary (1Ax), second axillary (2Ax), FR, AXM, the position of the 2Ax proximal lobe beneath 1Ax (stippled region on the distal arch of the 1Ax tail), third axillary (3Ax), detached AXCu fragment of 3Ax, first basal plate (1BP), HP, PC+C, BScA, ScA, BRP, second basal plate (2BP), BMA, BMP, MP, BMP-BCuA brace, BCuA, BCuP, and median plate (MED=FM1+FM2) (slightly diagrammatic).



4



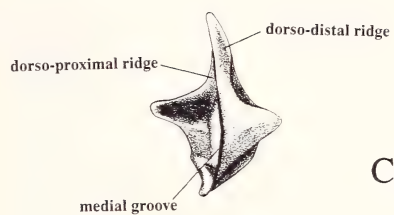
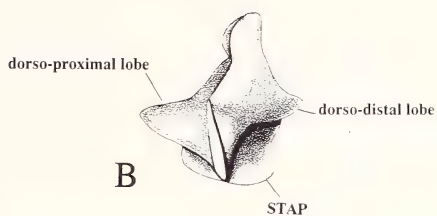
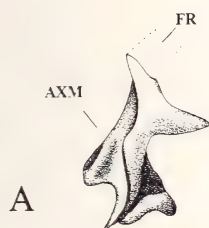
5



6

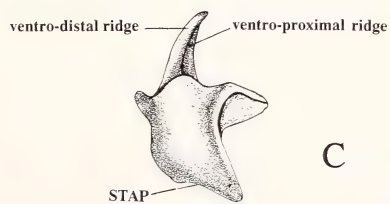
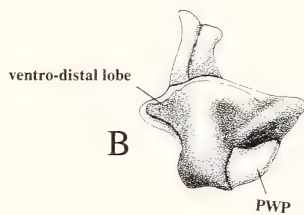
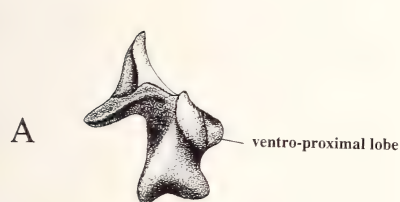
Figs.4-6: First axillary of Rutelinae (Scarabaeidae) showing the position of the original band sclerites: **4:** dorsal, showing FSc1, FSc2, AXSc, AXR, PRM, head, neck, distal embayment, tail, PRR articulation, proximal arch, distal arch and posterior margin of the tail. – **5:** ventral, showing ventral projection, distal neck ridge, proximal neck ridge, distal tail ridge, distal arch, posterior tail ridge, posterior margin of the tail, proximal arch, and proximal tail ridge. – **6:** anterior, showing FSc1, FSc2, ventral projection and embayment. Not to scale. Originals Browne (1993).

Figs.7-8: Second axillary of Scarabaeoidea: **7:** dorsal; a, Bolboceratidae showing the position of FR and AXM; b, Scarabaeinae (Scarabaeidae), showing dorso-proximal ridge (d-pr), dorso-distal ridge (d-dr), dorso-proximal lobe (d-pl), dorso-distal lobe (d-dl) and the part of the subalare tendon attachment point (STAP); c, Rutelinae (Scarabaeidae), showing the dorso-proximal ridge (d-pr), dorsal distal ridge (d-dr), and the apex of the dorsal distal ridge, anterior section of the dorsal distal ridge, medial section of the dorso-proximal and dorso-distal ridges, and terminus of the dorso-proximal and dorso-distal ridges, medial groove (mg) and part of the subalare tendon attachment point (STAP). – **8:** ventral; a, Bolboceratidae, showing the ventral proximal lobe (v-pl), ventro-distal lobe (v-dl), ventro-proximal ridge (v-pr), ventro-distal ridge (v-dr), posterior wing process (PWP) and the subalare tendon attachment point (STAP); b, Scarabaeinae (Scarabaeidae), showing the ventro-proximal lobe (v-pl), ventro-distal lobe (v-dl), ventro-proximal ridge (v-pr), ventro-distal ridge (v-dr), posterior wing process (PWP) and the subalare tendon attachment point (STAP); c, Rutelinae (Scarabaeidae), showing the ventro-proximal lobe (v-pl), ventro-distal lobe (v-dl), ventro-proximal ridge (v-pr), ventro-distal ridge (v-dr), posterior wing process (PWP) and subalare tendon attachment point (STAP). Not to scale. Originals Browne (1993).



C

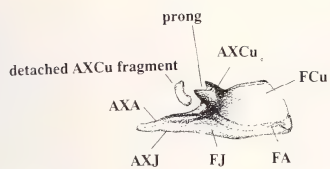
7



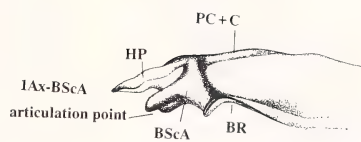
C

8

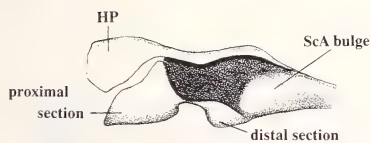
Figs.9-15: **9:** Dorso-lateral view of the third axillary of *Glaresis waltzlae* (Glaresidae) showing original band sclerites and detached AXCu fragment of 3Ax. – **10:** Dorsal view of the first basal plate of *Glaresis waltzlae* (Glaresidae) showing HP, PC+C, 1Ax-BScA articulation point, BScA, ScA and BRP. – **11:** Dorsal view of the first basal plate (excluding BRP) of Scarabaeinae (Scarabaeidae) showing the humeral plate (HP); the proximal and distal sections of BScA, and ScA bulge. – **12:** Anterior view of the humeral plate of Scarabaeinae (Scarabaeidae) showing the proximal, dorsal, ventral and distal margins. – **13:** Second basal plate (including BRP) of Scarabaeoidea: a, *Glaresis waltzlae* (Glaresidae) showing BRP, proximal and distal arches of BRP, embayment (open), RP, brp, brp projection, BMA, BMP, BMP-BCuA brace and BCuA; b, Bolboceratidae showing BRP, embayment (closed), RP, BMA, the proximal and distal arches of BMA, BMP, MP, BMP-CuA brace, BCuA, BCuP, distal embayment and CuA. – **14:** Dorso-lateral view of the basalare of Bolboceratidae (Geotrupidae) showing the HP lobe and BScP lobe. – **15:** Dorso-lateral view of BScP of Bolboceratidae, showing BScP and ScP. Not to scale. Originals Browne (1993).



9



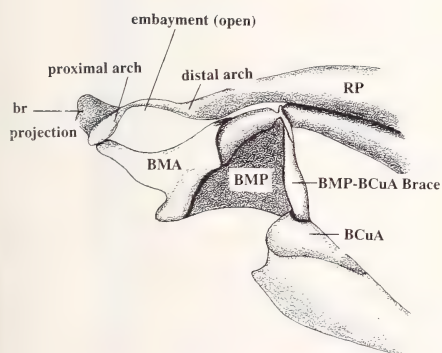
10



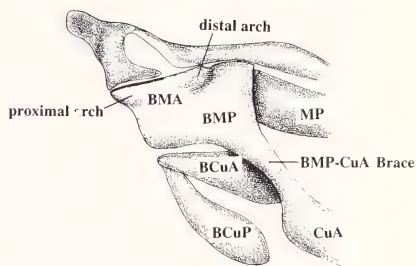
11



12



A



B

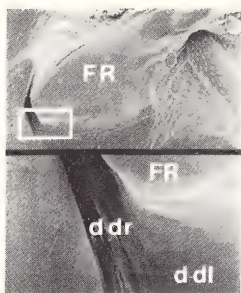
13



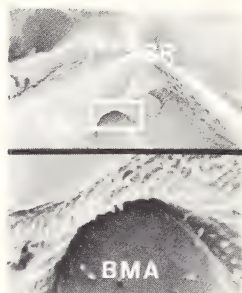
14



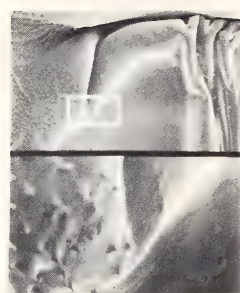
15



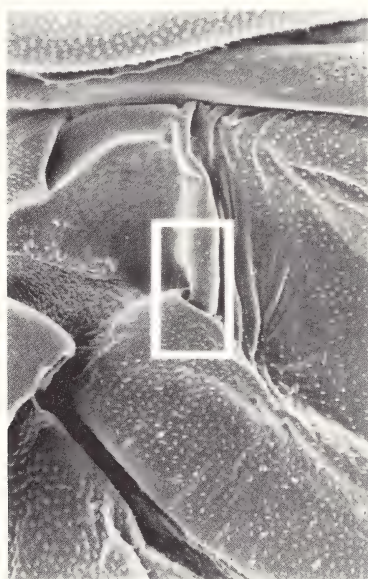
16



17

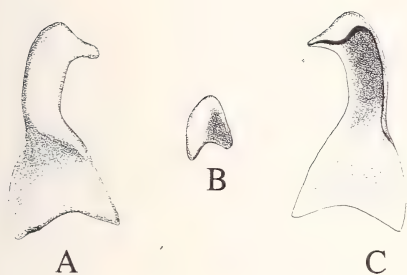


18

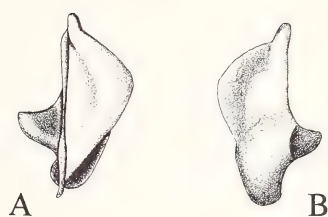


19

Figs.16-19: Scanning electron micrographs of some basal articulation structures of *Glaresis walzlae* (Glaresidae). – **16**: Second axillary showing the anterior section of the distal lobe and ridge of 2Ax and FR. – **17**: First and second basal plates showing the relative positions of BRP, brp, FR, and apex of the proximal arch of BMA. – **18**: Second basal plate showing the incomplete junction between BMA and BMP. – **19**: Second basal plate showing the BMP-BCuA brace. Not to scale. Originals Browne (1993).



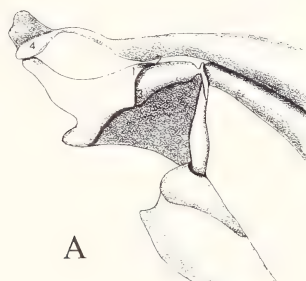
20



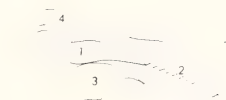
21



22



23



B

Figs.20-23: Hind wing articulation and wing base of *Glareis waltzlae* (Glareidae). – **20**: First axillary: a, dorsal; b, ventral; c, anterior. – **21**: Second axillary: a, dorsal; b, ventral. – **22**: Dorsolateral view of the third axillary. – **23**: Second basal plate (including BR); a, dorsal; b, ventral showing RA (serrated line); 1, BMA, 2, RA, 3, BMP, 4, BR. Not to scale. Originals Browne (1993).

Figs.24-25: Hind wing articulation and wing base of Passalidae. – **24**: First axillary: a, dorsal; b, ventral; c, anterior: 1, *Veturius tuberculifrons* (Proculini: Passalinae); 2, *Passalus punctatostratus* (Passalini: Passalinae); 3, *Ceracupes arrowi* (Aulacocyclinae). – **25**: Second axillary: a, dorsal; b, ventral: 1, *Oileus sargi* (Proculini: Passalinae); 2, *Passalus punctatostratus* (Passalini: Passalinae); 3, *Ceracupes arrowi* (Aulacocyclinae). Not to scale. Originals Browne (1993).

A



1



2



3

24

B



1



2



3

C



1



2



3

A



1



2



3

25

B



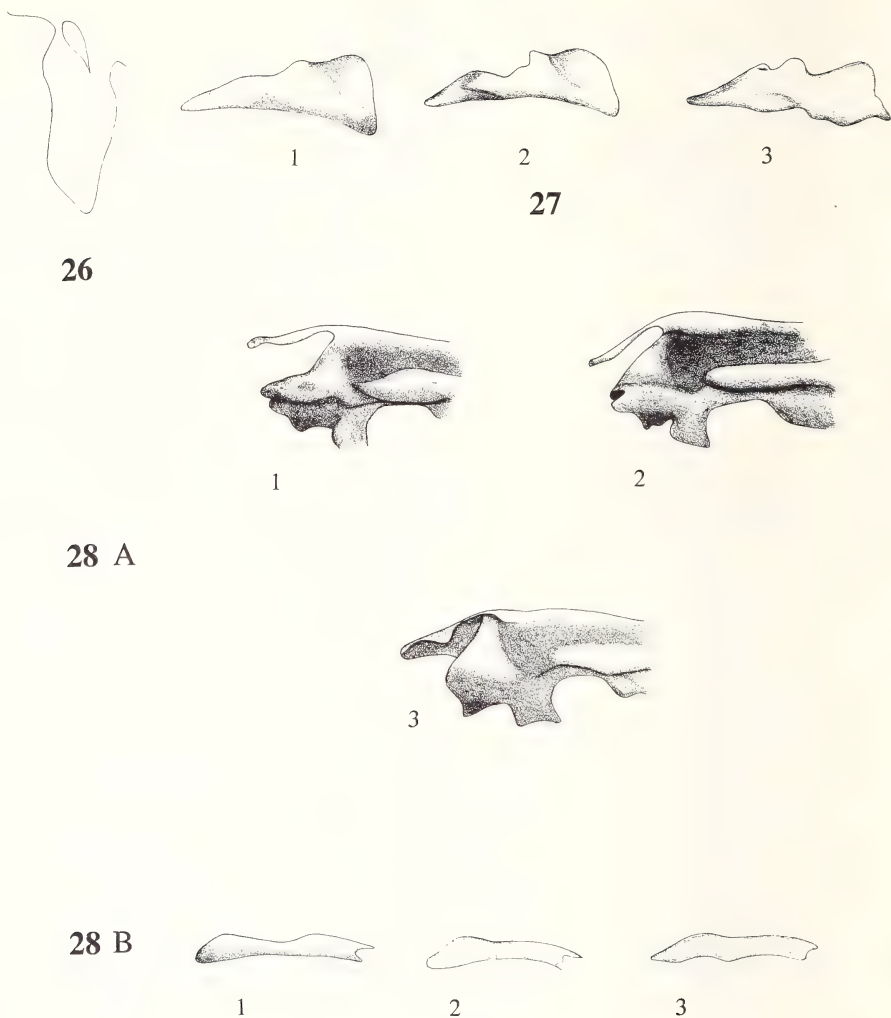
1



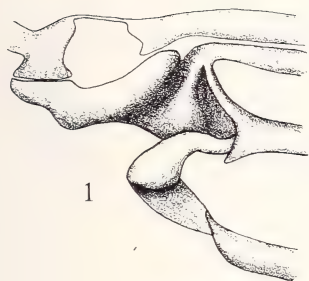
2



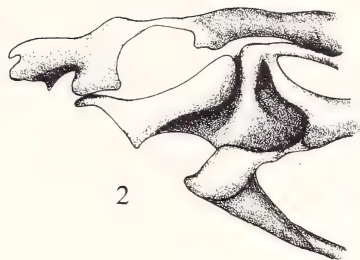
3



Figs. 26-28: Hind wing articulation and wing base of Passalidae. – **26**: Outline of the median plate of *Ceracupes arrowi* (Aulacocyclinae). – **27**: Dorso-lateral view of the third axillary of Passalidae: 1, *Oileus sargi* (Proculini: Passalinae); 2, *Aceraius grandis hirsutus* (Passalini: Passalinae); 3, *Aulacocyclus errans* (Aulacocyclinae). – **28**: First basal plate: a, dorsal; b, anterior: 1, *Odontotaenius disjunctus* (Proculini: Passalinae); 2, *Passalus punctatostriatus* (Passalini: Passalinae); 3, *Aulacocyclus errans* (Aulacocyclinae). Not to scale. Originals Browne (1993).

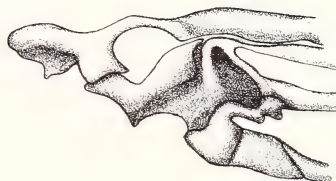


1



2

29



3

A



1



2



3

30

B



1



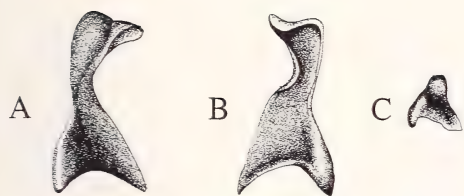
2



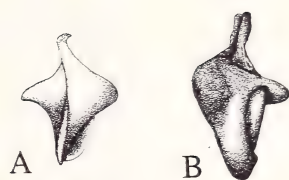
3

Figs.29-30: Hind wing articulation and wing base of Passalidae. – **29**: Dorsal view of the second basal plate (including BR): 1, *Odontotaenius disjunctus* (Proculini: Passalinae); 2, *Passalus punctatostrigatus* (Passalini: Passalinae); 3, *Aulacocyclus errans* (Aulacocyclusinae). – **30**: Dorso-lateral view of the basalare and BScP: a, basalare; b, BScP: 1, *Odontotaenius disjunctus* (Proculini: Passalinae); 2, *Aceraius grandis hirsutus* (Passalini: Passalinae); 3, *Aulacocyclus errans* (Aulacocyclusinae). Not to scale. Originals Browne (1993).

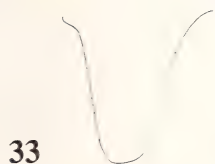
Figs.31-37: Hind wing articulation and wing base of Diphyllotomatidae. – **31:** First axillary: a, dorsal; b, ventral; c, anterior. – **32:** Second axillary: a, dorsal; b, ventral. – **33:** Outline of the median plate. – **34:** Outline of the dorso-lateral view of the third axillary. – **35:** Dorsal view of the first basal plate (excluding BR): a, dorsal; b, anterior view of HP. – **36:** Dorsal view of the second basal plate (including BR). – **37:** Dorso-lateral view of the basalare and BScP: a, basalare; b, BScP. Not to scale. Originals Browne (1993).



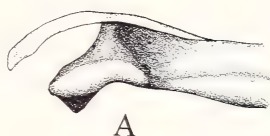
31



32



33



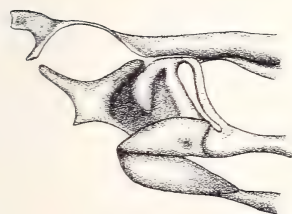
35



34



B



36



A



B

37



1



2



3



4



5



6

38 A



7



8



9



10



11



12



13

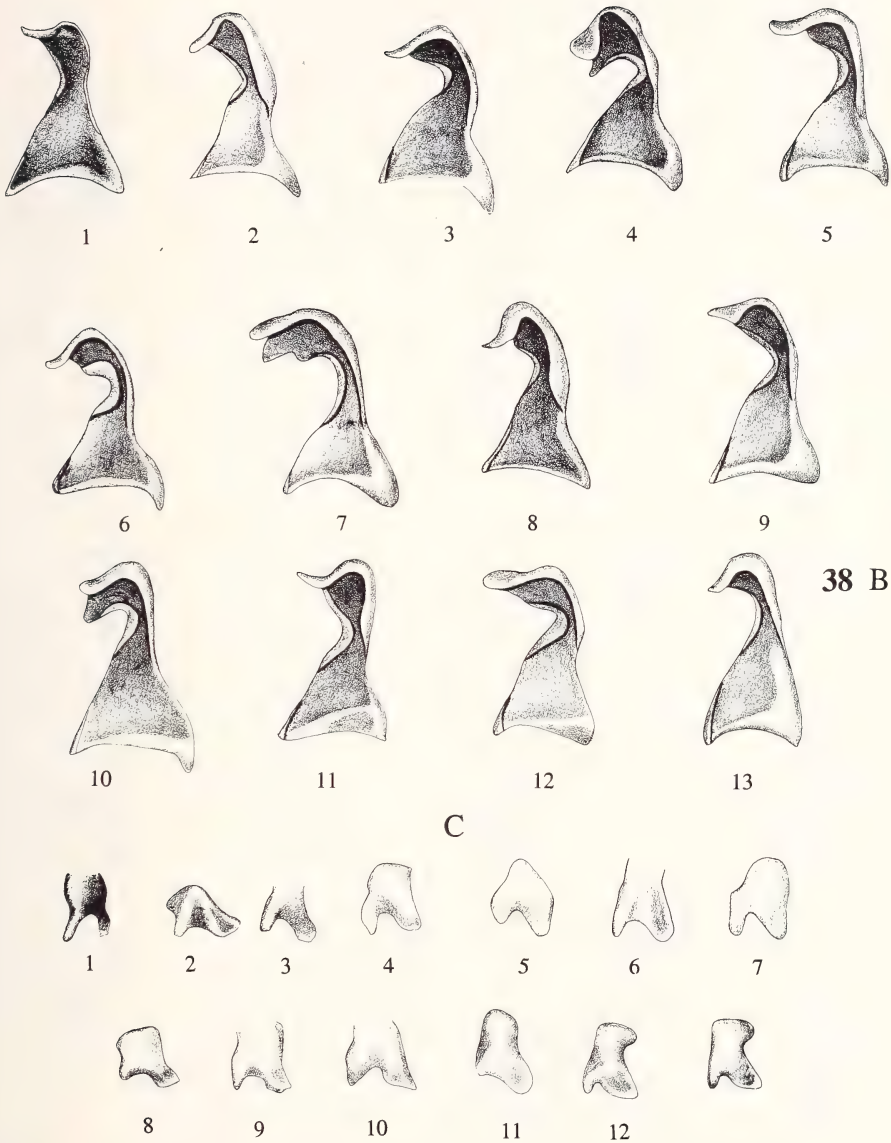
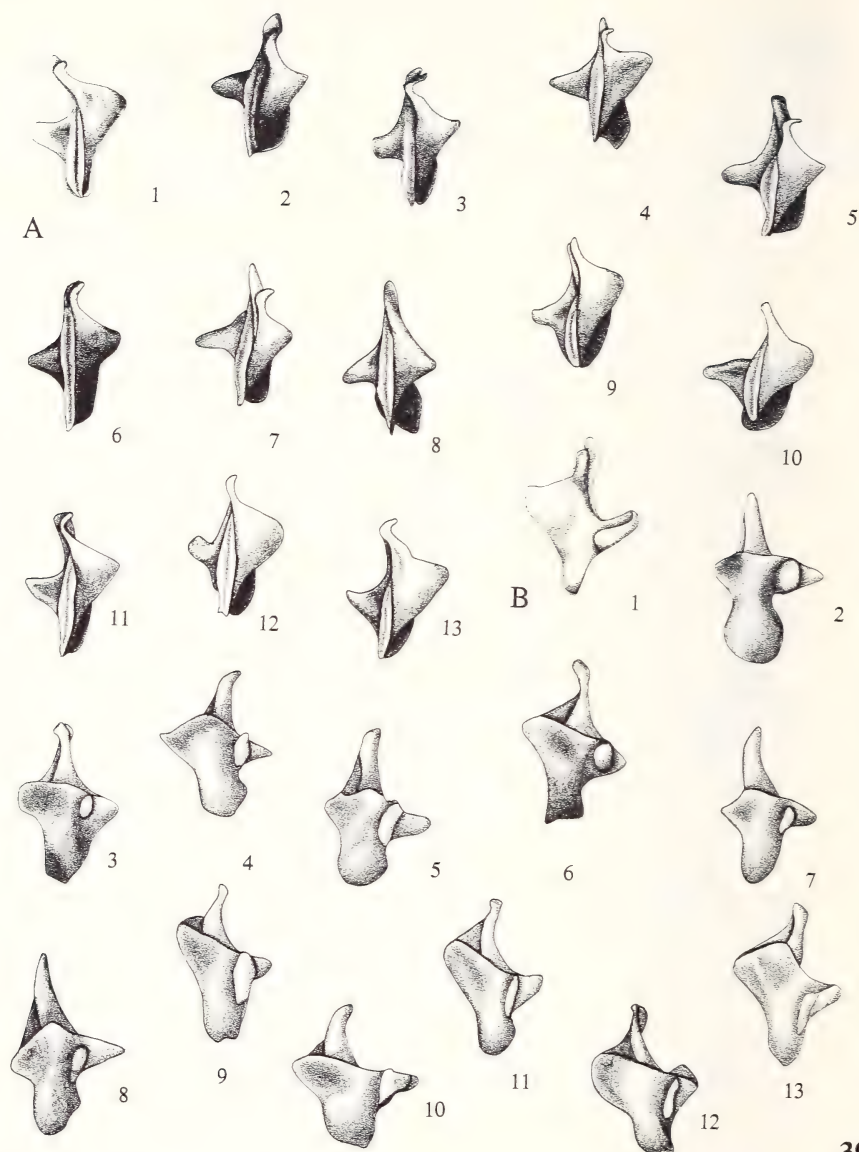
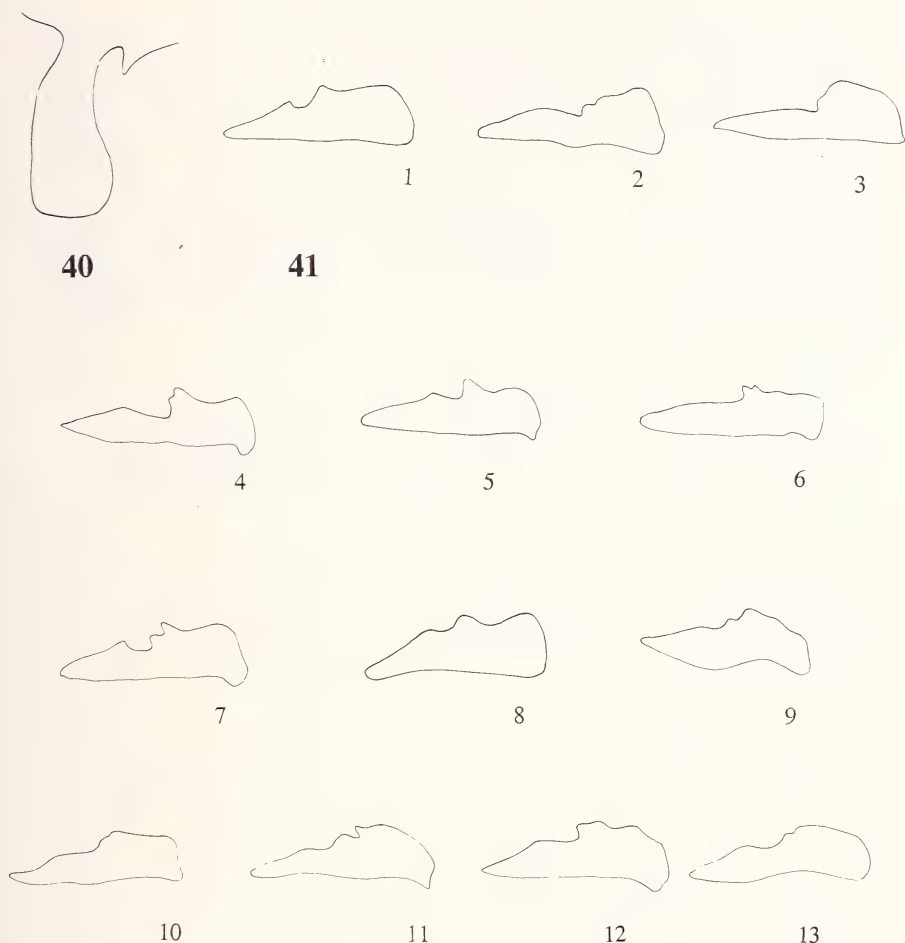


Fig.38: Hind wing articulation and wing base of Lucanidae. First axillary: a, dorsal; b, ventral; c, anterior 1, *Aesalus asiaticus* (Aesalinae); 2, *Lamprima aurata* (Lampriminae); 3, *Platycerus* spec. (Platycerini: Lucaninae); 4, *Aegus formosa* (Dorcini: Lucaninae); 5, *Neolucanus castanopterus* (Lucanini: Lucaninae); 6, *Nigidius bubalus* (Figulini: Lucaninae); 7, *Prosopocoilus savagei* (Cladognathini: Lucaninae); 8, *Chiasognathus* spec. (Chiasognathini: Lucaninae); 9, *Nicagus japonicus* (Nicaginae); 10, *Penichrolucanus leveri* (Penichrolucaninae); 11, *Sinodendron cylindricum* (Sinodendrini: Syndesinae); 12, *Syndesus cornutus* (Syndesini: Syndesinae); 13, *Ceruchus* spec. (Ceruchini: Syndesinae): a, dorsal; b, ventral; c, anterior. Not to scale. Originals Browne (1993).



39

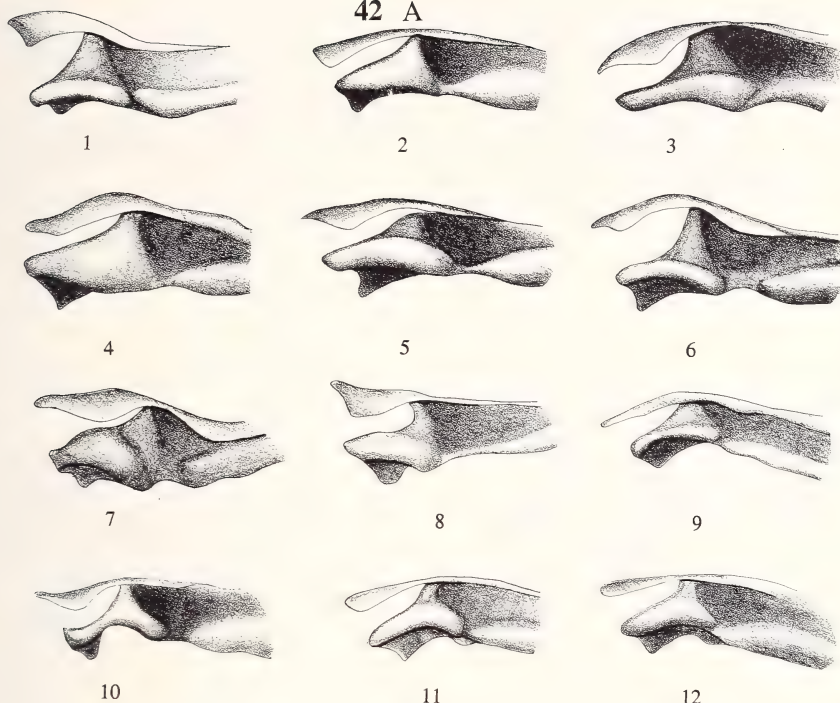
Fig.39: Hind wing articulation and wing base of Lucanidae. Second axillary: a, dorsal; b, ventral: 1, *Aesalus asiaticus* (Aesalinae); 2, *Lamprima aurata* (Lampriminae); 3, *Platycerus* spec. (Platycerini: Lucaninae); 4, *Dorcus parallelipedus* (Dorcini: Lucaninae); 5, *Neolucanus castanopterus* (Lucanini: Lucaninae); 6, *Figulus binodulus* (Figulini: Lucaninae); 7, *Prosopocoilus savagei* (Cladognathini: Lucaninae); 8, *Chiasognathus* spec. (Chiasognathini: Lucaninae); 9, *Nicagus japonicus* (Nicaginae); 10, *Penichrolucanus leveri* (Penichrolucaninae); 11, *Sinodendron cylindricum* (Sinodendrini: Syndesinae); 12, *Syndesus cornutus* (Syndesini: Syndesinae); 13, *Ceruchus* spec. (Ceruchini: Syndesinae). Not to scale. Originals Browne (1993).



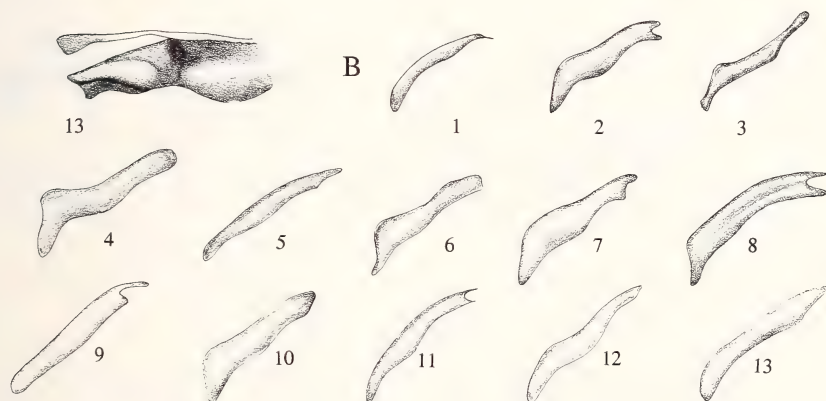
Figs.40-41: Hind wing articulation and wing base of Lucanidae. – **40:** Outline of the median plate. – **41:** Outline of the dorso-lateral view of the third axillary: 1, *Aesalus asiaticus* (Aesalinae); 2, *Lamprima latreillei* (Lampriminae); 3, *Platycerus* spec. (Platycerini: Lucaninae); 4, *Aegus formosa* (Dorcini: Lucaninae); 5, *Neolucanus castanopterus* (Lucanini: Lucaninae); 6, *Figulus binodulus* (Figulini: Lucaninae); 7, *Prosopocoilus savagei* (Cladognathini: Lucaninae); 8, *Chiasognathus* spec. (Chiasognathini: Lucaninae); 9, *Nicagus japonicus* (Nicaginae); 10, *Penichrolucanus leverii* (Penichrolucaninae); 11, *Sinodendron cylindricum* (Sinodendrini: Syndesinae); 12, *Syndesus cornutus* (Syndesini: Syndesinae); 13, *Ceruchus* spec. (Ceruchini: Syndesinae). Not to scale. Originals Browne (1993).

Fig.42: Hind wing articulation and wing base of Lucanidae. First basal plate (excluding BR): a, dorsal; b, anterior: 1, *Aesalus asiaticus* (Aesalinae); 2, *Lamprima latreillei* (Lampriminae); 3, *Platycerus* spec. (Platycerini: Lucaninae); 4, *Dorcus parallelipipedus* (Dorcini: Lucaninae); 5, *Neolucanus castanopterus* (Lucanini: Lucaninae); 6, *Nigidius bubalus* (Figulini: Lucaninae); 7, *Prosopocoilus fabre* (Cladognathini: Lucaninae); 8, *Chiasognathus* spec. (Chiasognathini: Lucaninae); 9, *Nicagus japonicus* (Nicaginae); 10, *Penichrolucanus leveri* (Penichrolucaninae); 11, *Sinodendron cylindricum* (Sinodendrini: Syndesinae); 12, *Syndesus cornutus* (Syndesini: Syndesinae); 13, *Ceruchus* spec. (Ceruchini: Syndesinae). Not to scale. Originals Browne (1993).

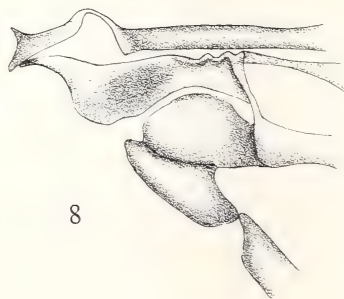
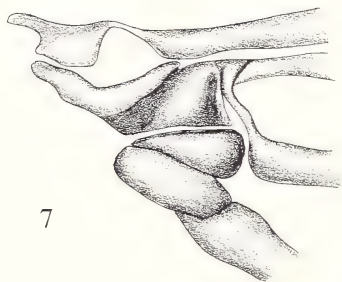
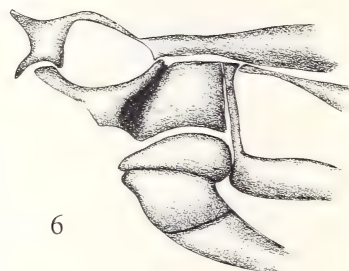
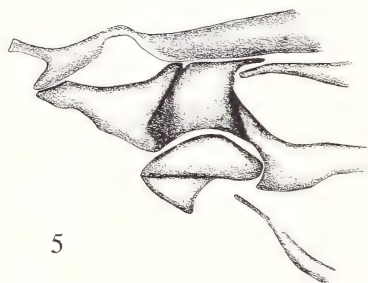
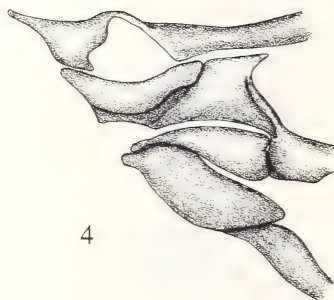
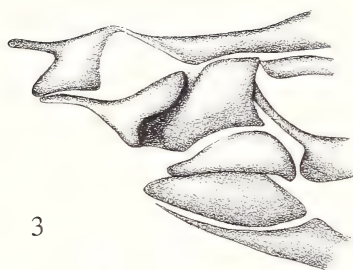
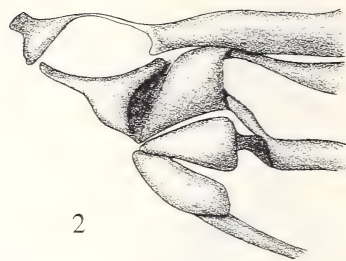
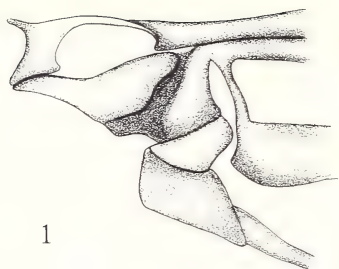
42 A



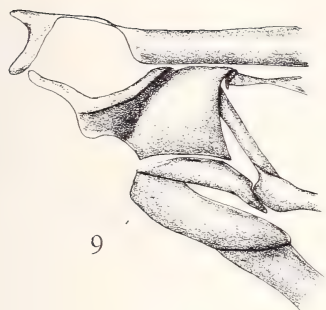
B



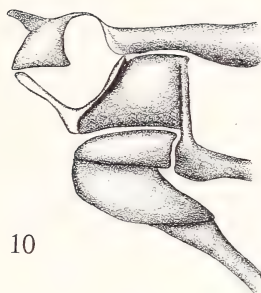
43



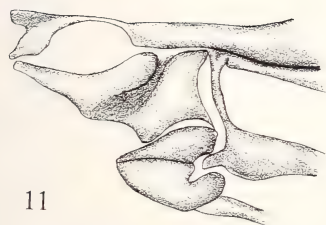
43



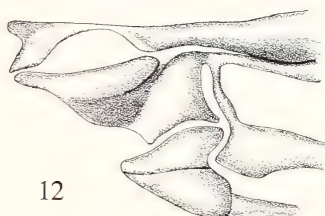
9



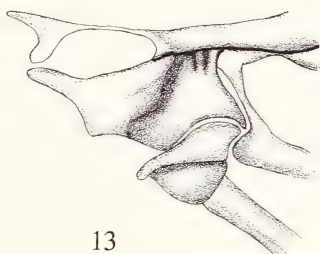
10



11



12

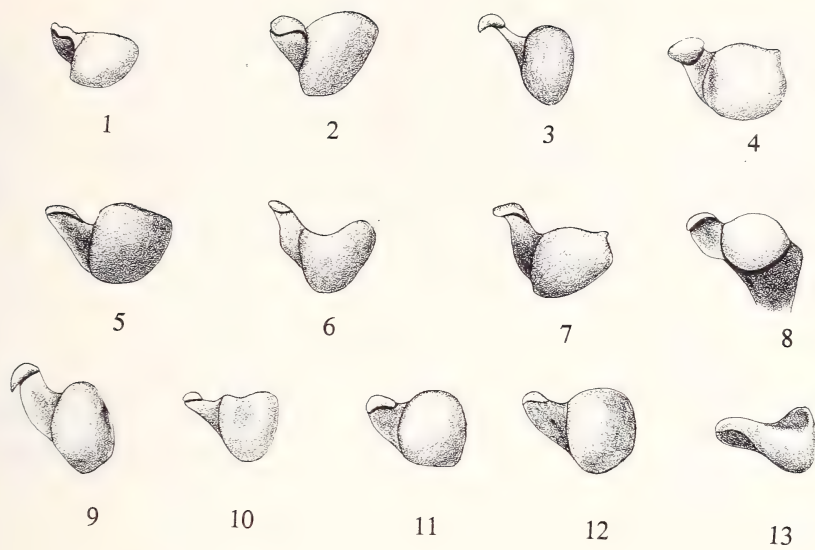


13

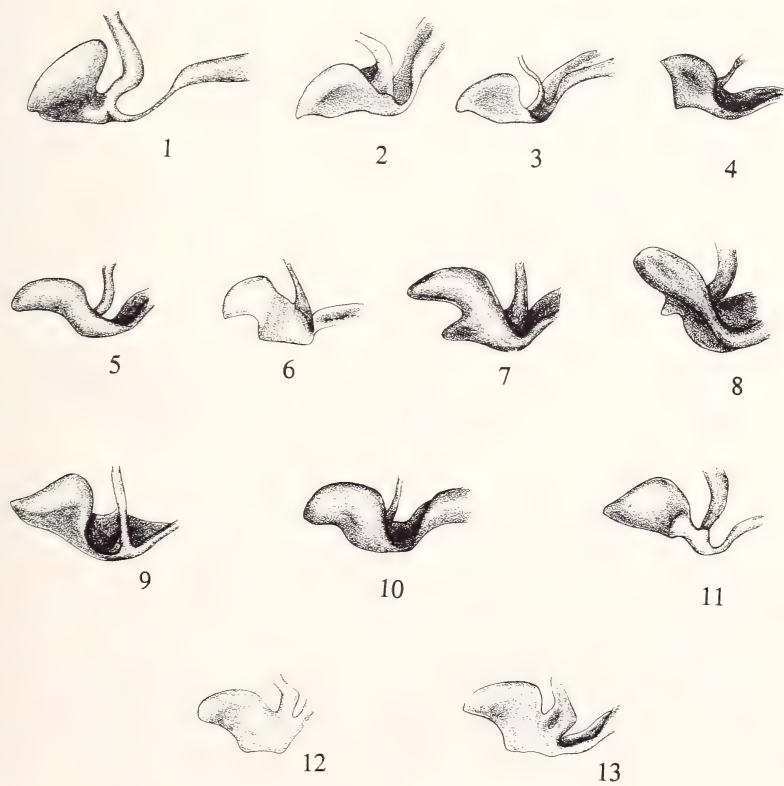
Fig.43: Hind wing articulation and wing base of Lucanidae. Dorsal view of the second basal plate (including BR): 1, *Aesalus asiaticus* (Aesalinae); 2, *Lamprima latreillei* (Lampriminae); 3, *Platycerus* spec. (Platycerini: Lucaninae); 4, *Dorcus parallelipipedus* (Dorcini: Lucaninae); 5, *Neolucanus castanopterus* (Lucanini: Lucaninae); 6, *Nigidius bubalus* (Figulini: Lucaninae); 7, *Prosopocoilus fabre* (Cladognathini: Lucaninae); 8, *Chiasognathus* spec. (Chiasognathini: Lucaninae); 9, *Nicagus japonicus* (Nicaginae); 10, *Penichrolucanus leverii* (Penichrolucaninae); 11, *Sinodendron cylindricum* (Sinodendrini: Syndesinae); 12, *Syndesus cornutus* (Syndesini: Syndesinae); 13, *Ceruchus* spec. (Ceruchini: Syndesinae). Not to scale. Originals Browne (1993).

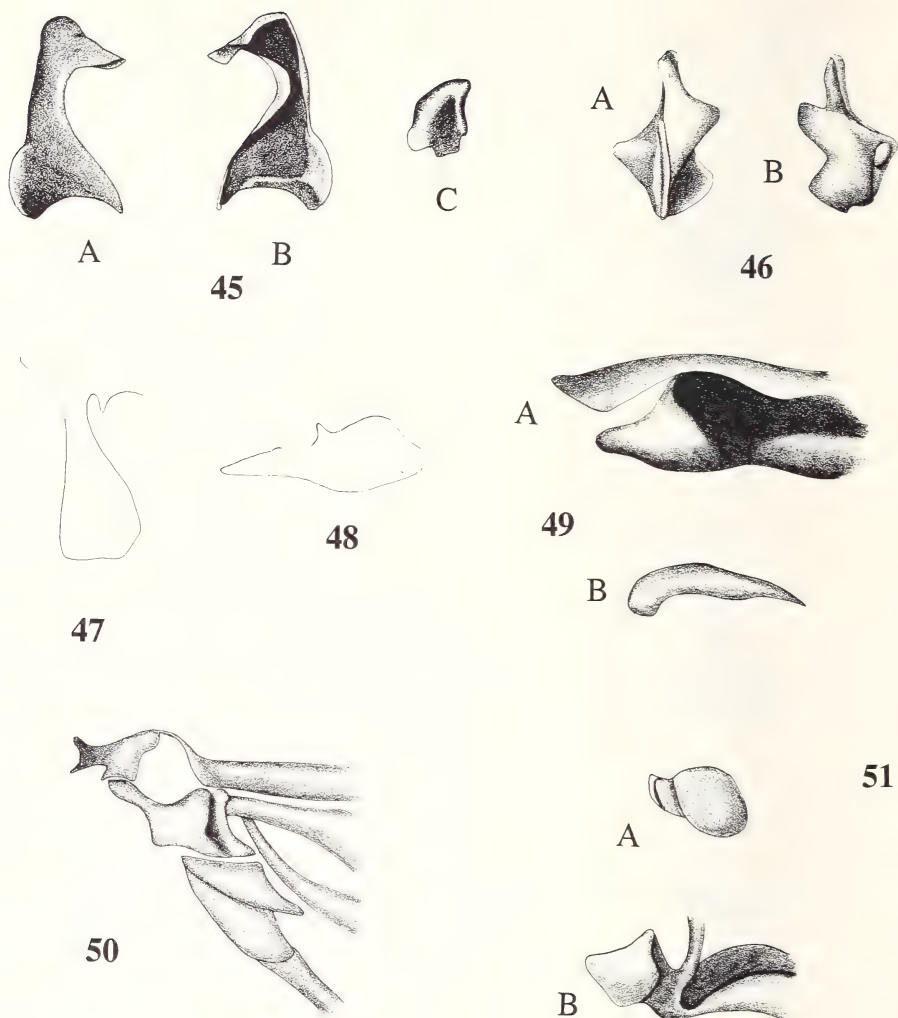
Fig.44: Hind wing articulation and wing base of Lucanidae. Dorso-lateral view of the basalare and BScP: a, basalare; b, BScP: 1, *Aesalus asiaticus* (Aesalinae); 2, *Lamprima latreillei* (Lampriminae); 3, *Platycerus* spec. (Platycerini: Lucaninae); 4, *Dorcus parallelipipedus* (Dorcini: Lucaninae); 5, *Neolucanus castanopterus* (Lucanini: Lucaninae); 6, *Nigidius bubalus* (Figulini: Lucaninae); 7, *Prosopocoilus fabre* (Cladognathini: Lucaninae); 8, *Chiasognathus* spec. (Chiasognathini: Lucaninae); 9, *Nicagus japonicus* (Nicaginae); 10, *Penichrolucanus leverii* (Penichrolucaninae); 11, *Sinodendron cylindricum* (Sinodendrini: Syndesinae); 12, *Syndesus cornutus* (Syndesini: Syndesinae); 13, *Ceruchus* spec. (Ceruchini: Syndesinae) with the basalare in the dorsal view. Not to scale. Originals Browne (1993).

A



B





Figs.45-51: Hind wing articulation and wing base of *Lichnanthe apina* (Glaphyridae). – **45**: First axillary: a, dorsal; b, ventral; c, anterior. – **46**: Second axillary: a, dorsal; b, ventral. – **47**: Outline of the median plate. – **48**: Outline of the dorso-lateral view of the third axillary. – **49**: Dorsal view of the first basal plate (excluding BR): a, dorsal; b, anterior view of HP. – **50**: Dorsal view of the second basal plate (including BR). – **51**: Dorso-lateral view of the basalare and BScP: a, basalare; b, BScP. Not to scale. Originals Browne (1993).

Figs.52-53: Hind wing articulation and wing base of Trogidae. – **52**: First axillary: a, dorsal; b, ventral; c, anterior: 1, *Trox montanus*; 2, *Polynoncus longitarsus*; 3, *Omorgus villosus*. – **53**: Second axillary: a, dorsal; b, ventral: 1, *Trox montanus*; 2, *Polynoncus longitarsus*; 3, *Omorgus villosus*. Not to scale. Originals Browne (1993).

52

A



1



2



3

B



1



2



3

C



1



2



3

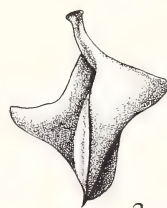
A



1



2



3

53

B



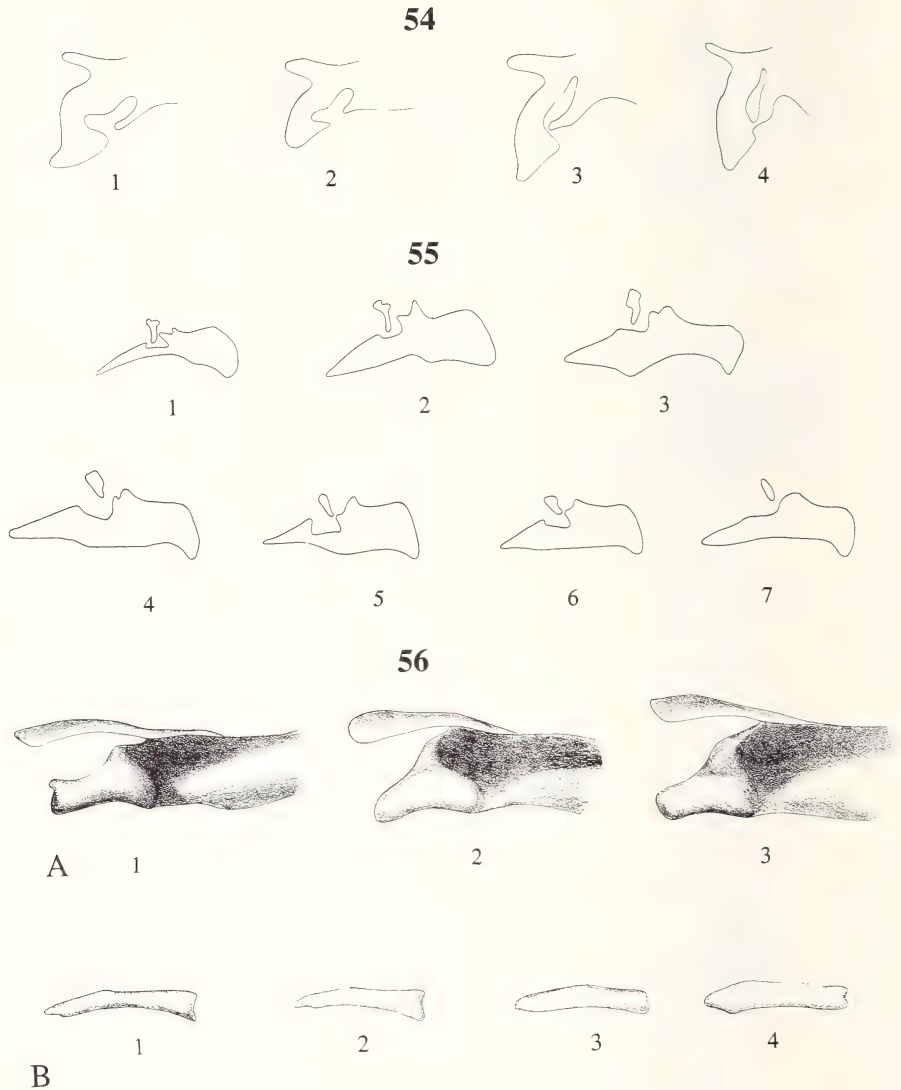
1



2

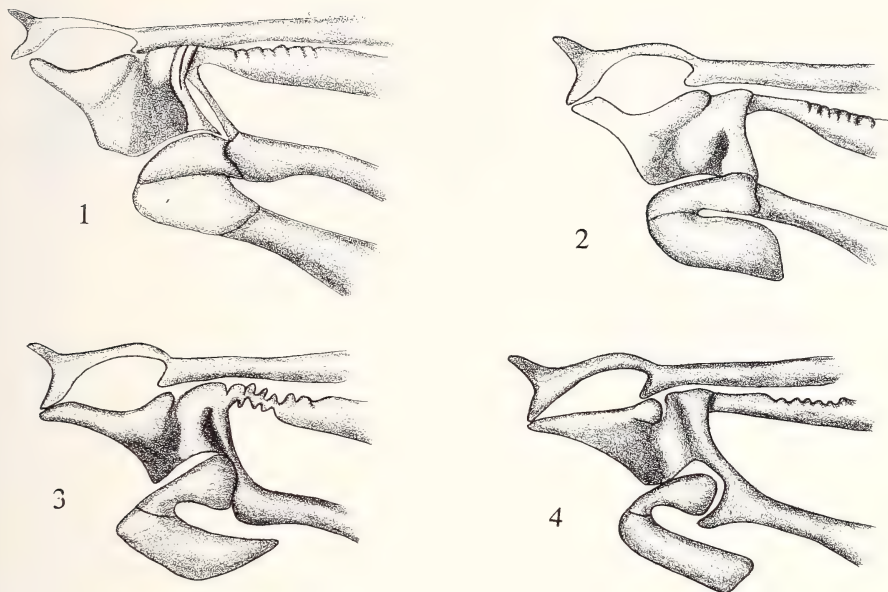


3

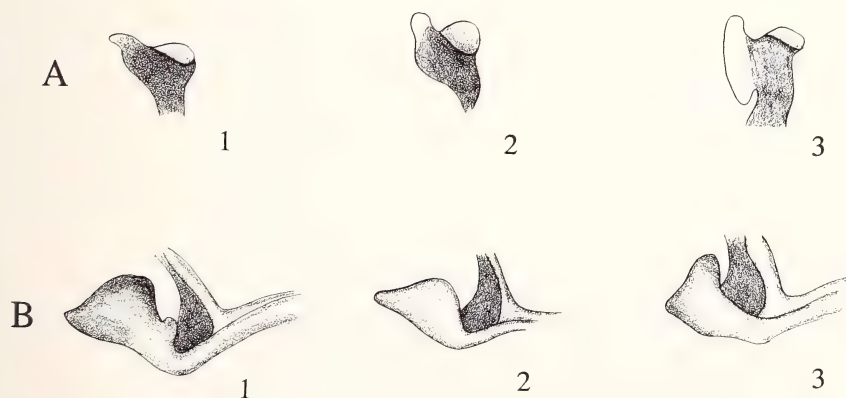


Figs. 54-56: Hind wing articulation and wing base of Trogidae. – **54:** Outline of the median plate: 1, *Trox plicatus*; 2, *Trox sulcatus*; 3, *Polynoncus longitarsus*; 4, *Omorgus quadridens*. – **55:** Outline of the dorso-lateral view of the third axillary: 1, *Trox plicatus*; 2, *Trox luridus*; 3, *Polynoncus gemmingeri*; 4, *Omorgus euclensis*; 5, *Omorgus suberosus*; 6, *Omorgus squalidus*; 7, *Omorgus (Haroldomorgus) batesi*. – **56:** First basal plate (excluding BR): a, dorsal; b, anterior: 1, *Trox plicatus*; 2, *Trox sulcatus*; 3, *Polynoncus longitarsus*. Not to scale. Originals Browne (1993).

57

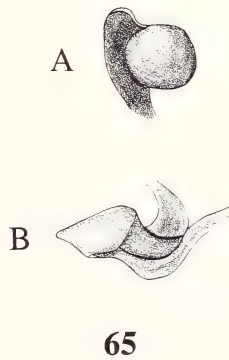
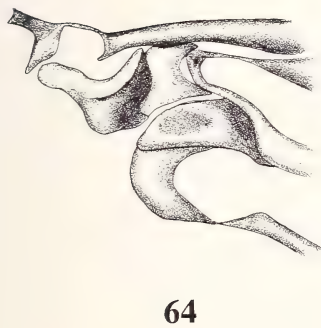
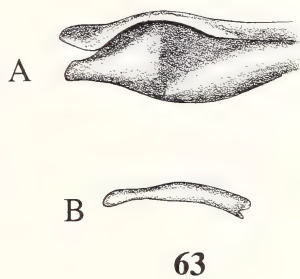
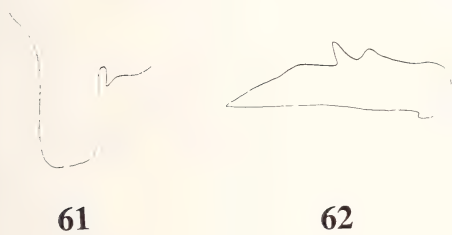
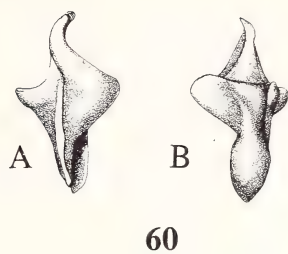
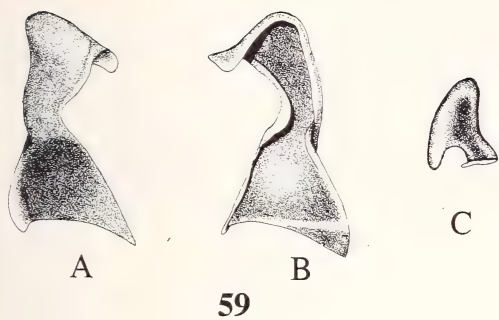


58



Figs. 57-58: Hind wing articulation and wing base of Trogidae. – **57**: Dorsal view of the second basal plate (including BR): 1, *Trox plicatus*; 2, *Trox sulcatus*; 3, *Polynoncus longitarsus*; 4, *Omorgus quadridens*. – **58**: Lateral view of the basalare and BScP: a, basalare; b, BScP: 1, *Trox montanus*; 2, *Polynoncus longitarsus*; 3, *Omorgus squalidus*. Not to scale. Originals Browne (1993).

Figs.59-65: Hind wing articulation and wing base of *Pleocoma linsleyi* (Pleocomidae). – **59**: First axillary: a, dorsal; b, ventral; c, anterior. – **60**: Second axillary: a, dorsal; b, ventral. – **61**: Outline of the median plate. – **62**: Outline of the dorso-lateral view of the third axillary. – **63**: Dorsal view of the first basal plate (excluding BR): a, dorsal; b, anterior view of HP. – **64**: Dorsal view of the second basal plate (including BR). – **65**: Dorso-lateral view of the basalare and BScP: a, basalare; b, BScP. Not to scale. Originals Browne (1993).



Figs.66-67: Hind wing articulation and wing base of Bolboceratidae. – **66**: First axillary: a, dorsal; b, ventral; c, anterior: 1, *Eucanthus felschei* (Bolboceratini); 2, *Bolborhinum binasutum* (Bolboceratini); 3, *Neoathyreus panamaensis* (Athyreini). – **67**: Second axillary: a, dorsal; b, ventral: 1, *Eucanthus felschei* (Bolboceratini); 2, *Bolborhinum binasutum* (Bolboceratini); 3, *Neoathyreus panamaensis* (Athyreini). Not to scale. Originals Browne (1993).

66

A



1



2



3

B



1



2



3

C



67

A



1



2



3

B



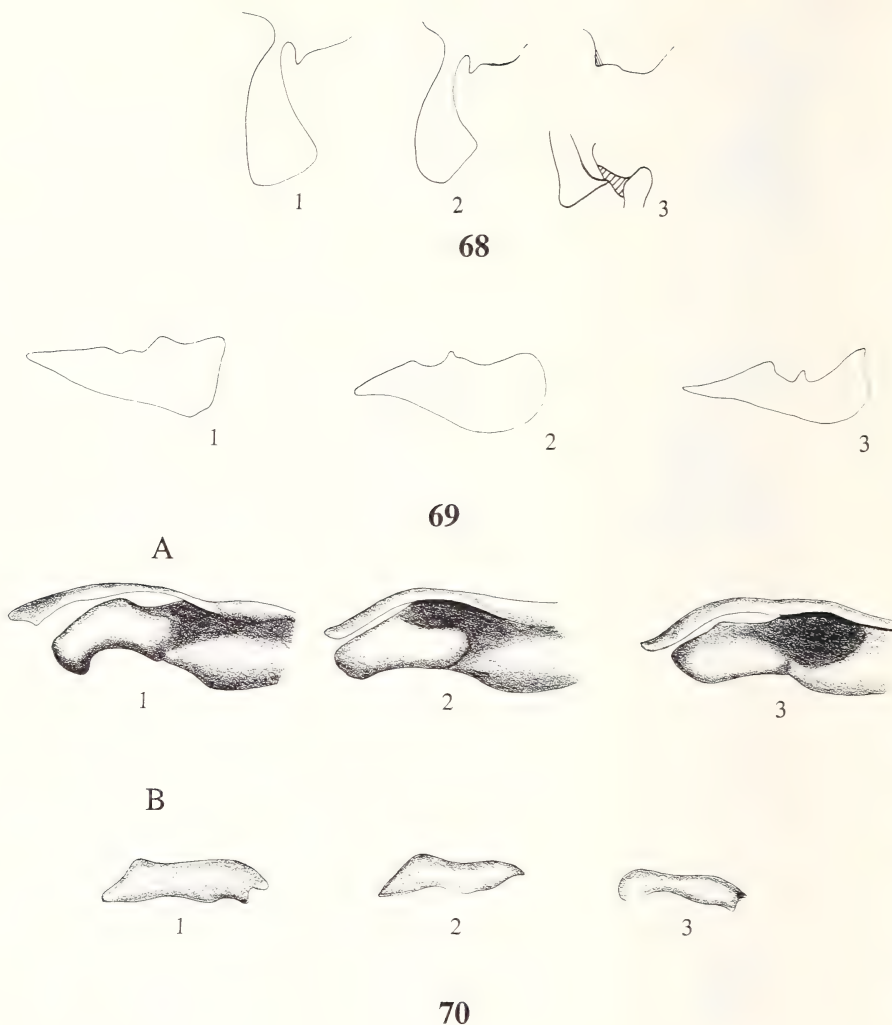
1



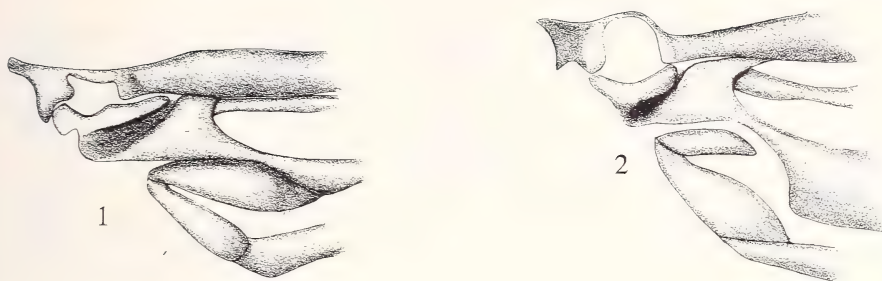
2



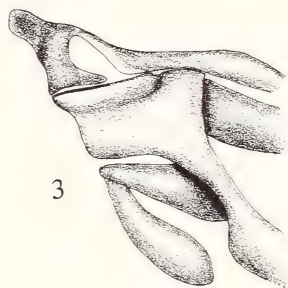
3



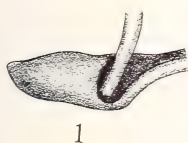
Figs. 68-70: Hind wing articulation and wing base of Bolboceratidae. – **68**: Outline of the median plate: 1, *Eucanthus felschei* (Bolboceratini); 2, *Bolborhinum binasutum* (Bolboceratini); 3, *Neoathyreus panamaensis* (Athyreini) showing the relative positions of 1Ax+2Ax, the anterior and posterior remnants of MED (shaded areas) and 3Ax. – **69**: Outline of the dorso-lateral view of the third axillary: 1, *Eucanthus subtropicus* (Bolboceratini); 2, *Bolborhinum binasutum* (Bolboceratini); 3, *Neoathyreus panamaensis* (Athyreini). – **70**: First basal plate (excluding BR) of Bolboceratidae: a, dorsal; b, anterior: 1, *Eucanthus felschei* (Bolboceratini); 2, *Bolborhinum binasutum* (Bolboceratini); 3, *Neoathyreus panamaensis* (Athyreini). Not to scale. Originals Browne (1993).



71



A

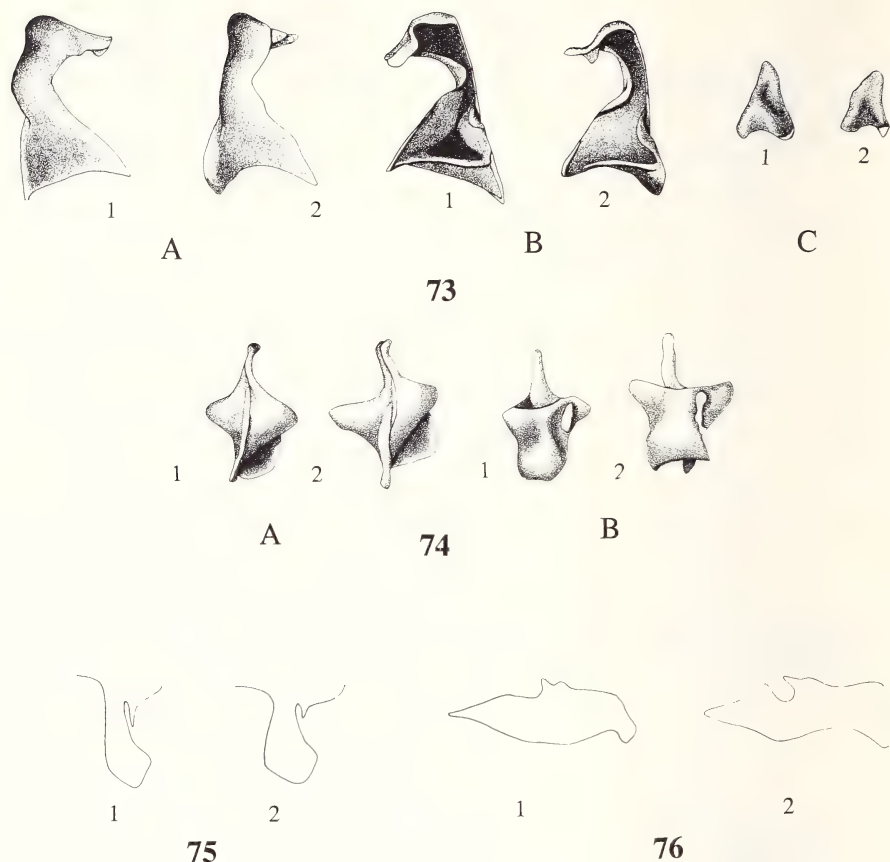


B

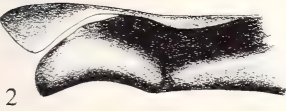
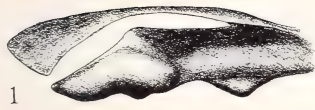


72

Figs.71-72: Hind wing articulation and wing base of Bolboceratidae. – **71**: Dorsal view of the second basal plate (including BR): 1, *Eucanthus felschei* (Bolboceratini); 2, *Bolborhinum binasutum* (Bolboceratini); 3, *Neoathyreus panamaensis* (Athyreini). – **72**: Dorso-lateral view of the basalare and BScP: a, basalare; b, BScP: 1, *Eucanthus felschei* (Bolboceratini); 2, *Bolborhinum binasutum* (Bolboceratini); 3, *Neoathyreus panamaensis* (Athyreini). Not to scale. Originals Browne (1993).



Figs. 73-76: Hind wing articulation and wing base of Geotrupidae. – **73**: First axillary: a, dorsal; b, ventral; c, anterior: 1, *Cnemotrupes splendidus* (Geotrupinae: Geotrupidae); 2, *Frickius* spec. (Taurocerastinae: Geotrupidae). – **74**: Second axillary: a, dorsal; b, ventral: 1, *Cnemotrupes splendidus* (Geotrupinae: Geotrupidae); 2, *Frickius* spec. (Taurocerastinae: Geotrupidae). – **75**: Outline of the median plate: 1, *Cnemotrupes splendidus* (Geotrupinae: Geotrupidae); 2, *Frickius* spec. (Taurocerastinae: Geotrupidae). – **76**: Outline of the dorso-lateral view of the third axillary: 1, *Cnemotrupes splendidus* (Geotrupinae: Geotrupidae); 2, *Frickius* spec. (Taurocerastinae: Geotrupidae). Not to scale. Originals Browne (1993)



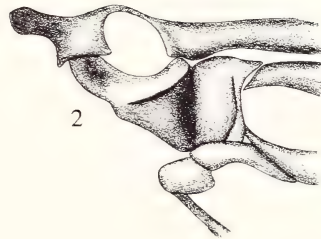
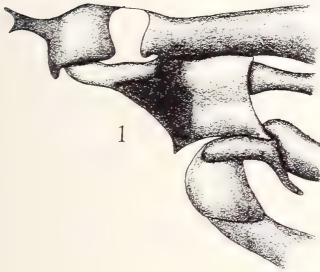
A

77



2

B



78



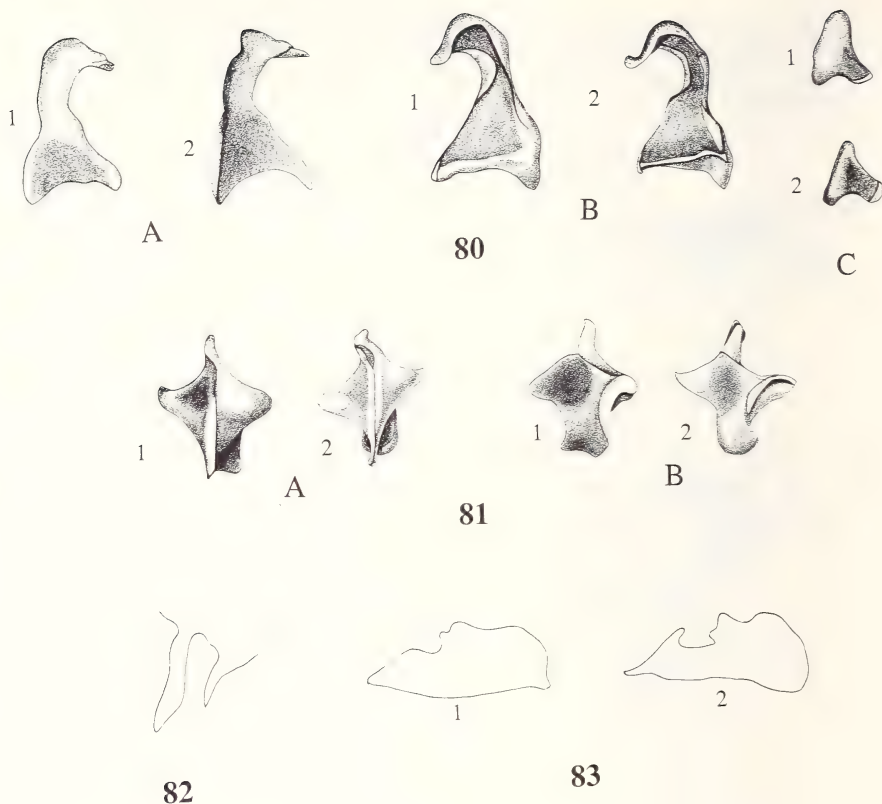
A



B

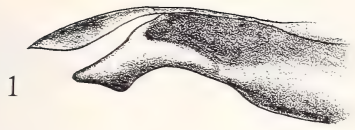
79

Figs. 77-79: Hind wing articulation and wing base of Geotrupidae. – **77**: First basal plate (excluding BR): a, dorsal; b, anterior: 1, *Cnemotrupes splendidus* (Geotrupinae: Geotrupidae); 2, *Frickius* spec. (Taurocerastinae: Geotrupidae). – **78**: Dorsal view of the second basal plate (including BR): 1, *Cnemotrupes splendidus* (Geotrupinae: Geotrupidae); 2, *Frickius* spec. (Taurocerastinae: Geotrupidae). – **79**: Dorso-lateral view of the basalare and BScP: a, basalare; b, BScP: 1, *Cnemotrupes splendidus* (Geotrupinae: Geotrupidae); 2, *Frickius* spec. (Taurocerastinae: Geotrupidae). Not to scale. Originals Browne (1993).



Figs.80-83: Hind wing articulation and wing base of Hybosoridae. – **80**: First axillary: a, dorsal; b, ventral; c, anterior: 1, *Hybosorus ruficornis* (Old World); 2, *Anaides simplicicollis* (New World). – **81**: Second axillary: a, dorsal; b, ventral: 1, *Hybosorus ruficornis* (Old World); 2, *Anaides simplicicollis* (New World). – **82**: Outline of the median plate. – **83**: Outline of the dorso-lateral view of the third axillary: 1, *Hybosorus ruficornis* (Old World); 2, *Anaides simplicicollis* (New World). Not to scale. Originals Browne (1993).

Figs.84-86: Hind wing articulation and wing base of Hybosoridae. – **84**: First basal plate (excluding BR): a, dorsal; b, anterior: 1, *Phaeochrous mashunus* (Old World); 2, *Anaides simplicicollis* (New World). – **85**: Dorsal view of the second basal plate (including BR): 1, *Phaeochrous mashunus* (Old World); 2, *Anaides simplicicollis* (New World). – **86**: Dorso-lateral view of the basalare and BScP: a, basalare; b, BScP: 1, *Phaeochrous mashunus* (Old World); 2, *Anaides simplicicollis* (New World). Not to scale. Originals Browne (1993).

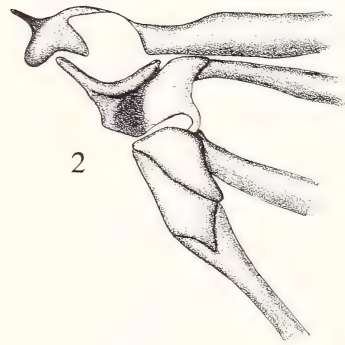
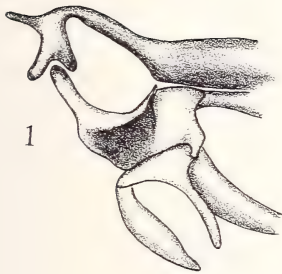


A

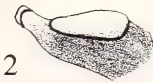


B

84



85

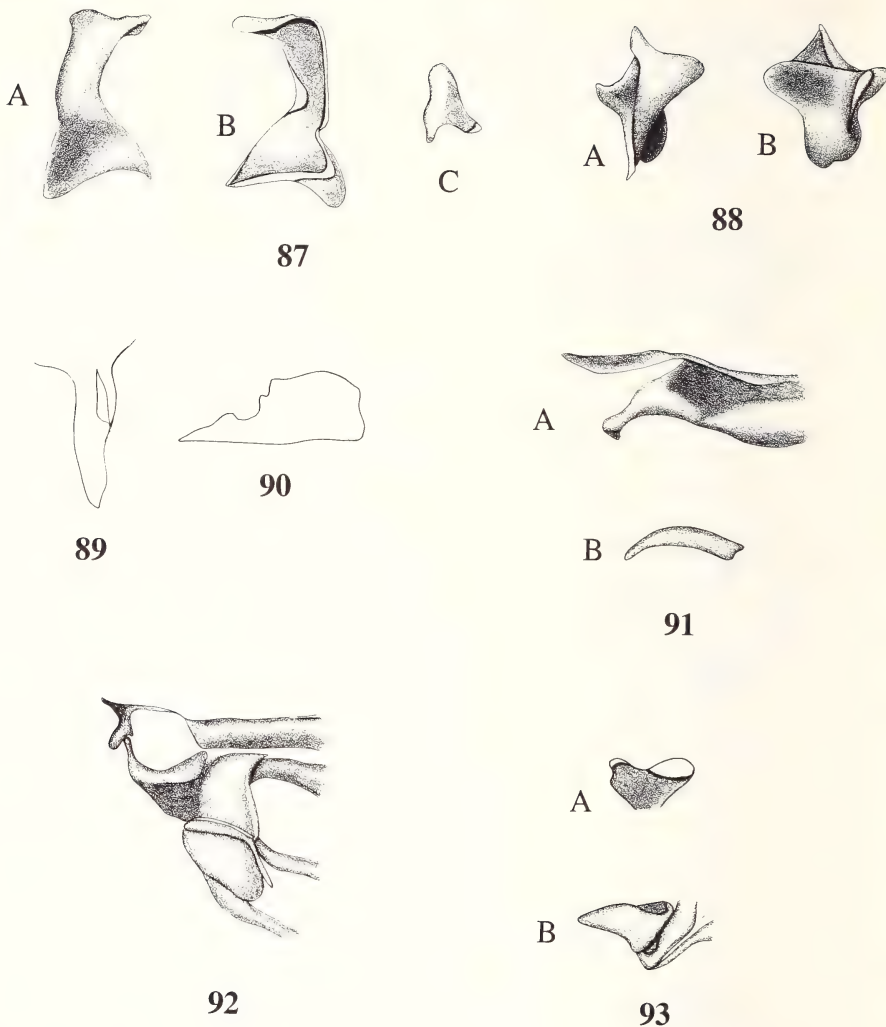


A

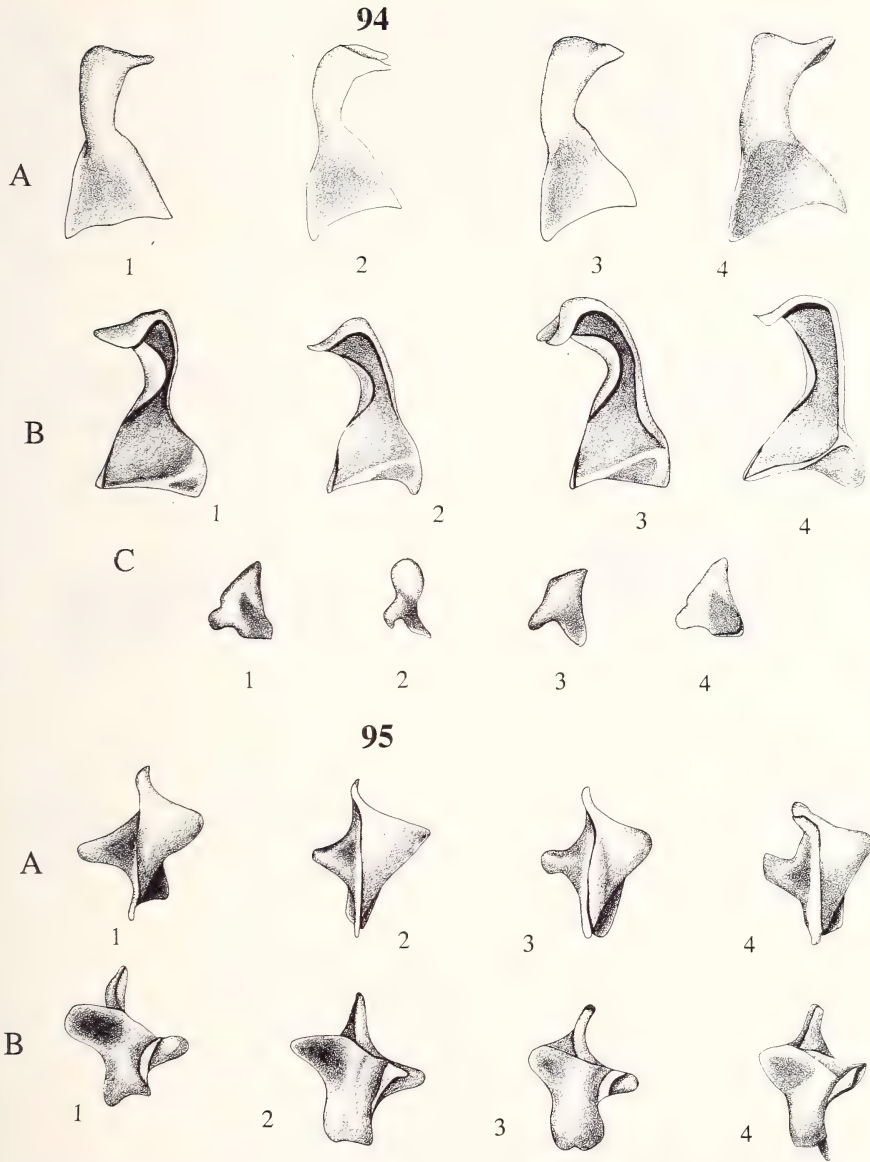


B

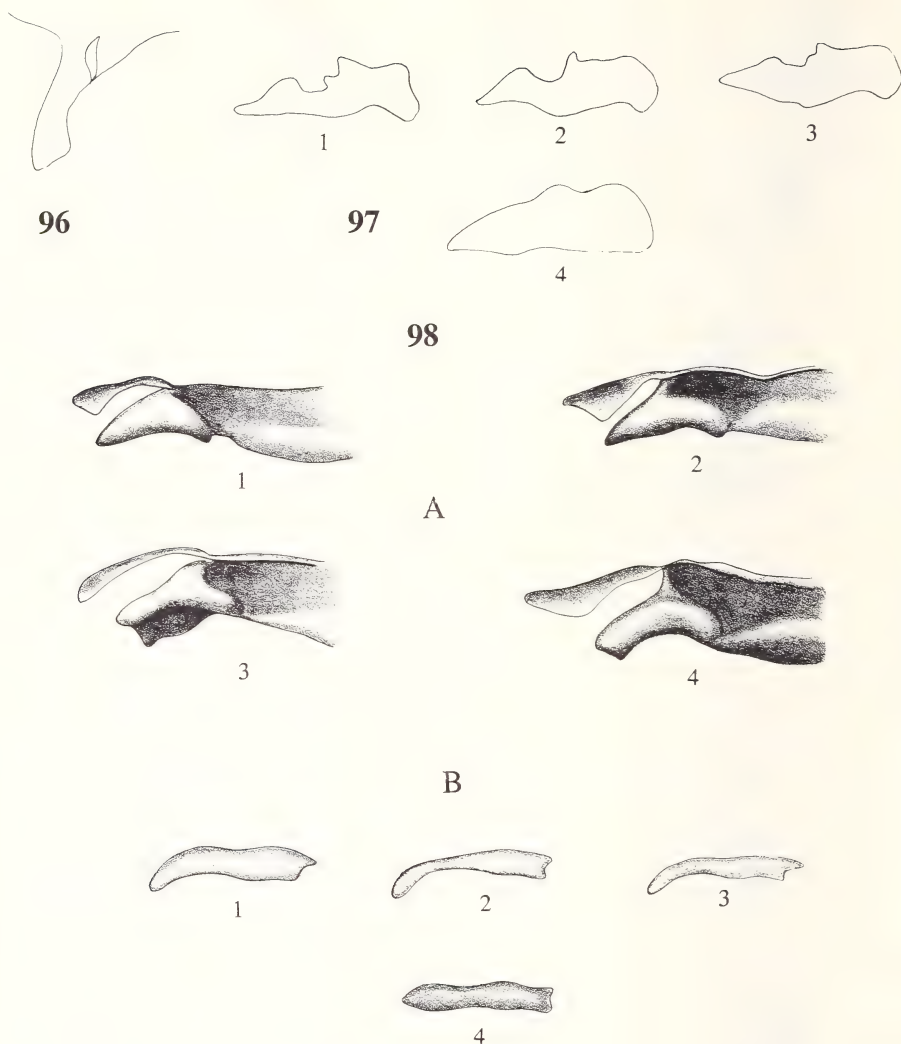
86



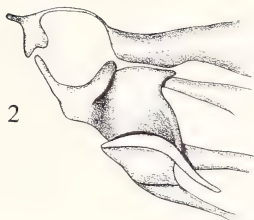
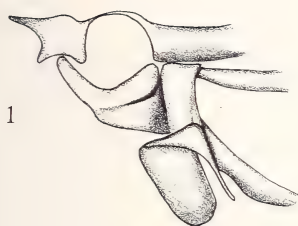
Figs.87-93: Hind wing articulation and wing base of *Ceratocanthus nitidus* (Ceratocanthidae). – **87**: First axillary: a, dorsal; b, ventral; c, anterior. – **88**: Second axillary: a, dorsal; b, ventral. – **89**: Outline of the median plate. – **90**: Outline of the dorso-lateral view of the third axillary. – **91**: Dorsal view of the first basal plate (excluding BR): a, dorsal; b, anterior view of HP. – **92**: Dorsal view of the second basal plate (including BR). – **93**: Dorso-lateral view of the basalare and BScP: a, basalare; b, BScP. Not to scale. Originals Browne (1993).



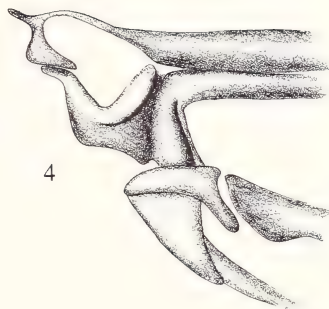
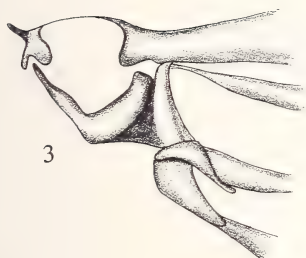
Figs.94-95: Hind wing articulation and wing base of Ochodaeidae. – **94**: First axillary: a, dorsal; b, ventral; c, anterior; 1, *Ochodaeus* spec. (Ochodainae); 2, *Chaetocanthus insuetus* (Chaetocanthini: Chaetocanthinae); 3, *Pseudochodaeus estriatus* (Pseudochodaeini: Chaetocanthinae); 4, *Synochodaeus modestus* (Synochodaeini: Chaetocanthinae). – **95**: Second axillary: a, dorsal; b, ventral: 1, *Ochodaeus* spec. (Ochodainae); 2, *Chaetocanthus insuetus* (Chaetocanthini: Chaetocanthinae); 3, *Pseudochodaeus estriatus* (Pseudochodaeini: Chaetocanthinae); 4, *Synochodaeus modestus* (Synochodaeini: Chaetocanthinae). Not to scale. Originals Browne (1993).



Figs.96-98: Hind wing articulation and wing base of Ochodaeidae. – **96**: Outline of the median plate. – **97**: Outline of the dorso-lateral view of the third axillary: 1, *Ochodaeus* spec. (Ochodainae); 2, *Chaetocanthus insuetus* (Chaetocanthini: Chaetocanthinae); 3, *Pseudochodaeus estriatus* (Pseudochodaeini: Chaetocanthinae); 4, *Synochodaeus modestus* (Synochodaeini: Chaetocanthinae). – **98**: First basal plate (excluding BR): a, dorsal; b, anterior: 1, *Ochodaeus* spec. (Ochodainae); 2, *Chaetocanthus insuetus* (Chaetocanthini: Chaetocanthinae); 3, *Pseudochodaeus estriatus* (Pseudochodaeini: Chaetocanthinae); 4, *Synochodaeus modestus* (Synochodaeini: Chaetocanthinae). Not to scale. Originals Browne (1993).



99



B



1



2



3

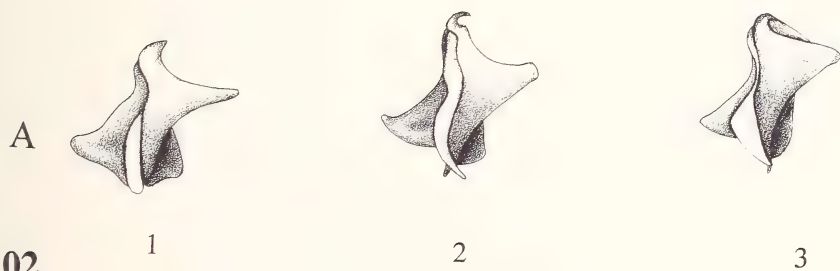
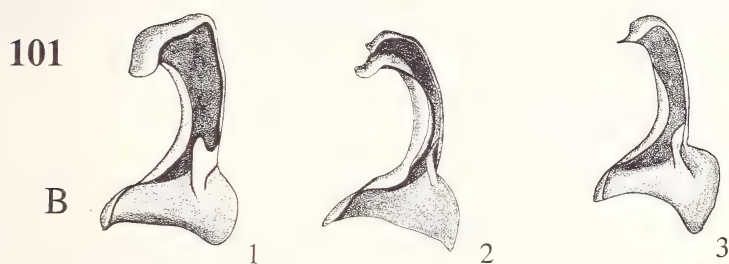
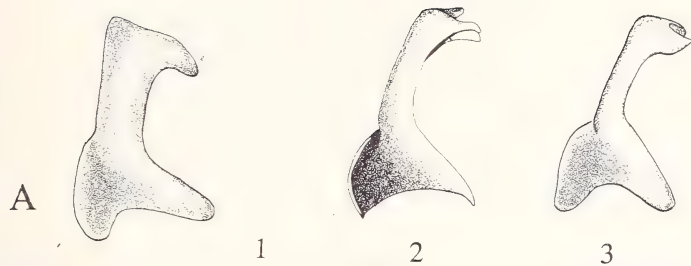
100



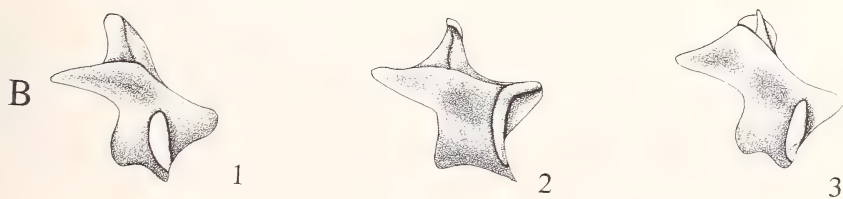
4

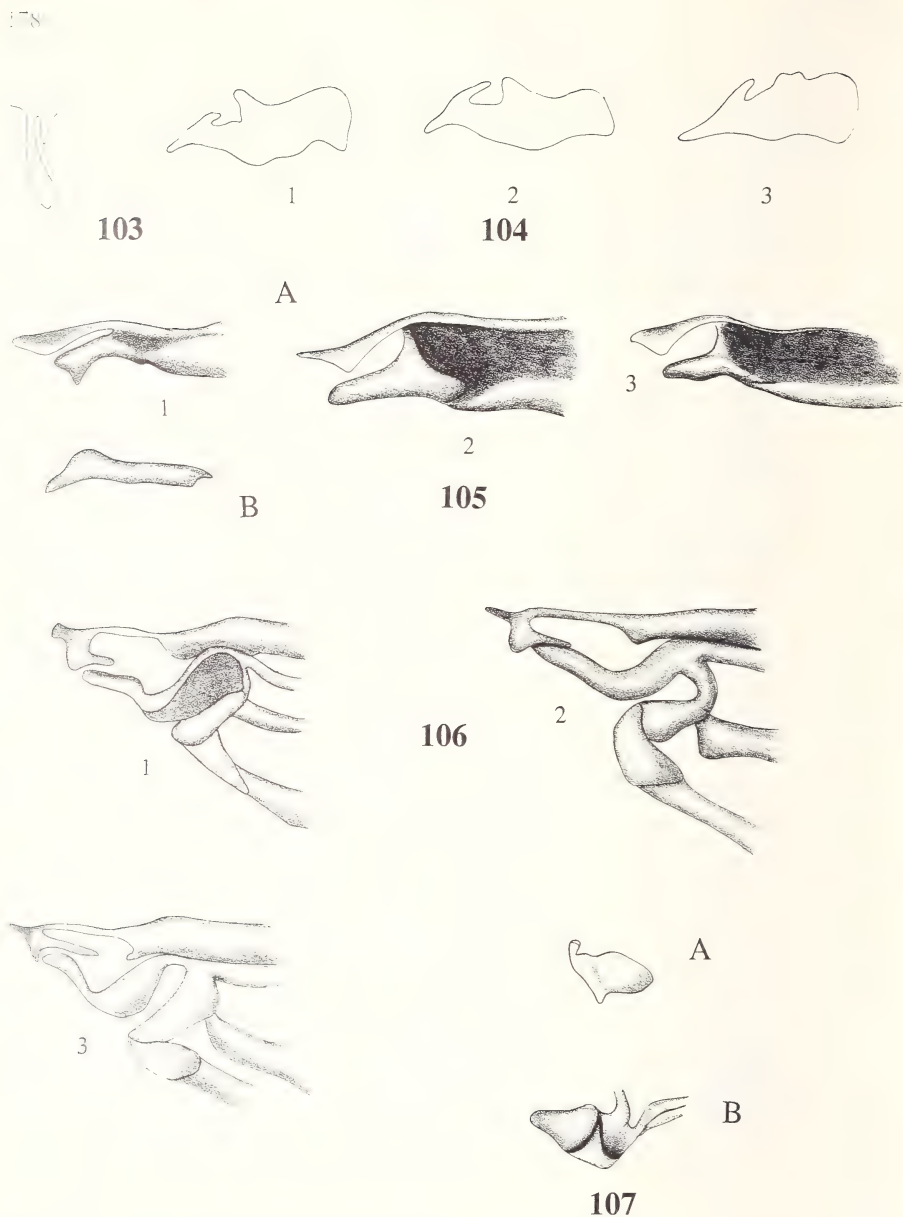
Figs.99-100: Hind wing articulation and wing base of Ochodaidae. – **99**: Dorsal view of the second basal plate (including BR): 1, *Ochodaes* spec. (Ochodainae); 2, *Chaetocanthus insuetus* (Chaetocanthini: Chaetocanthinae); 3, *Pseudochodaes estriatus* (Pseudochodaeni: Chaetocanthinae); 4, *Synochodaes modestus* (Synochodaeni: Chaetocanthinae). – **100**: Dorso-lateral view of the basalare and BScP: a, basalare; b, BScP: 1, *Ochodaes* spec. (Ochodainae); 2, *Chaetocanthus insuetus* (Chaetocanthini: Chaetocanthinae); 3, *Pseudochodaes estriatus* (Pseudochodaeni: Chaetocanthinae); 4, *Synochodaes modestus* (Synochodaeni: Chaetocanthinae). Not to scale. Originals Browne (1993).

Figs.101-102: Hind wing articulation and wing base of Aphodiinae (Scarabaeidae). – **101:** First axillary of Aphodiinae (Scarabaeidae): a, dorsal; b, ventral; c, anterior: 1, *Colobopterus* spec. (Aphodiini); 2, *Ataenius desertus* (Eupariini); 3, *Rhyssemus hamatus* (Psammodiini). – **102:** Second axillary of Aphodiinae (Scarabaeidae): a, dorsal; b, ventral: 1, *Colobopterus* spec. (Aphodiini); 2, *Ataenius desertus* (Eupariini); 3, *Rhyssemus hamatus* (Psammodiini). Not to scale. Originals Browne (1993).

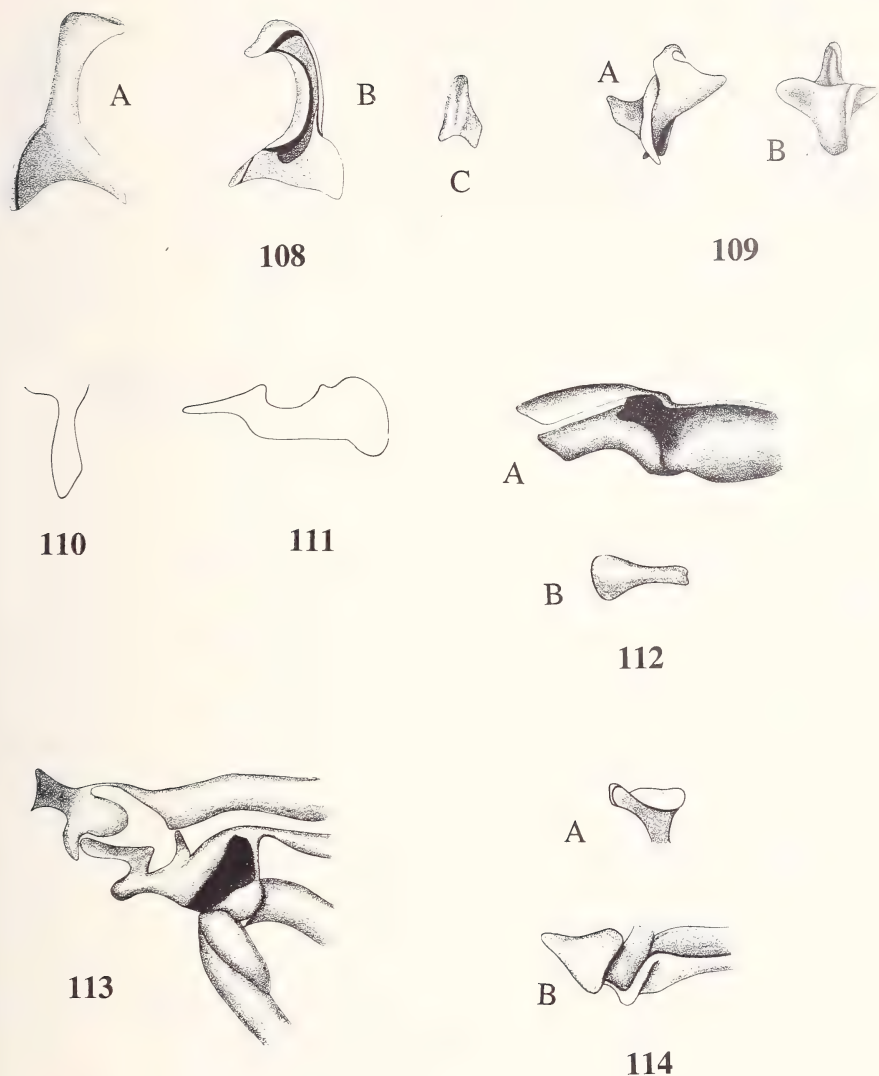


102

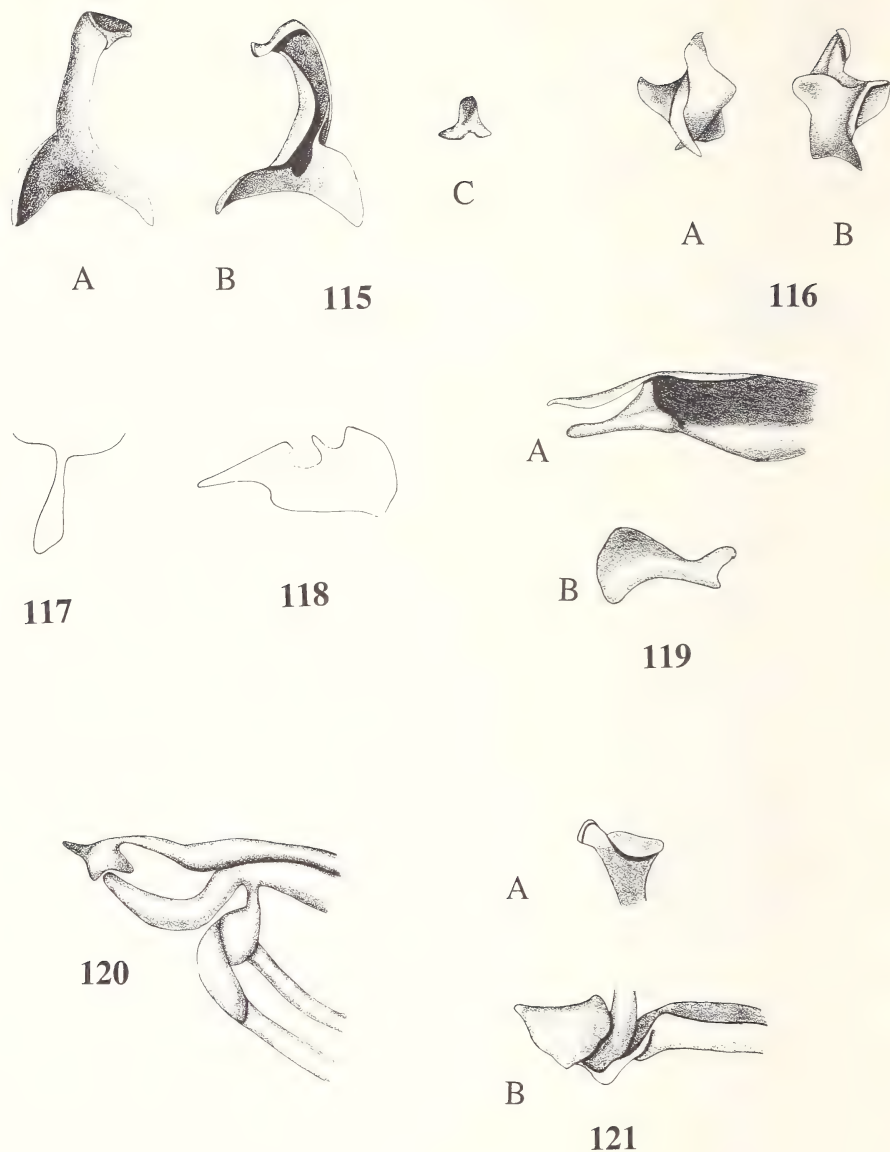




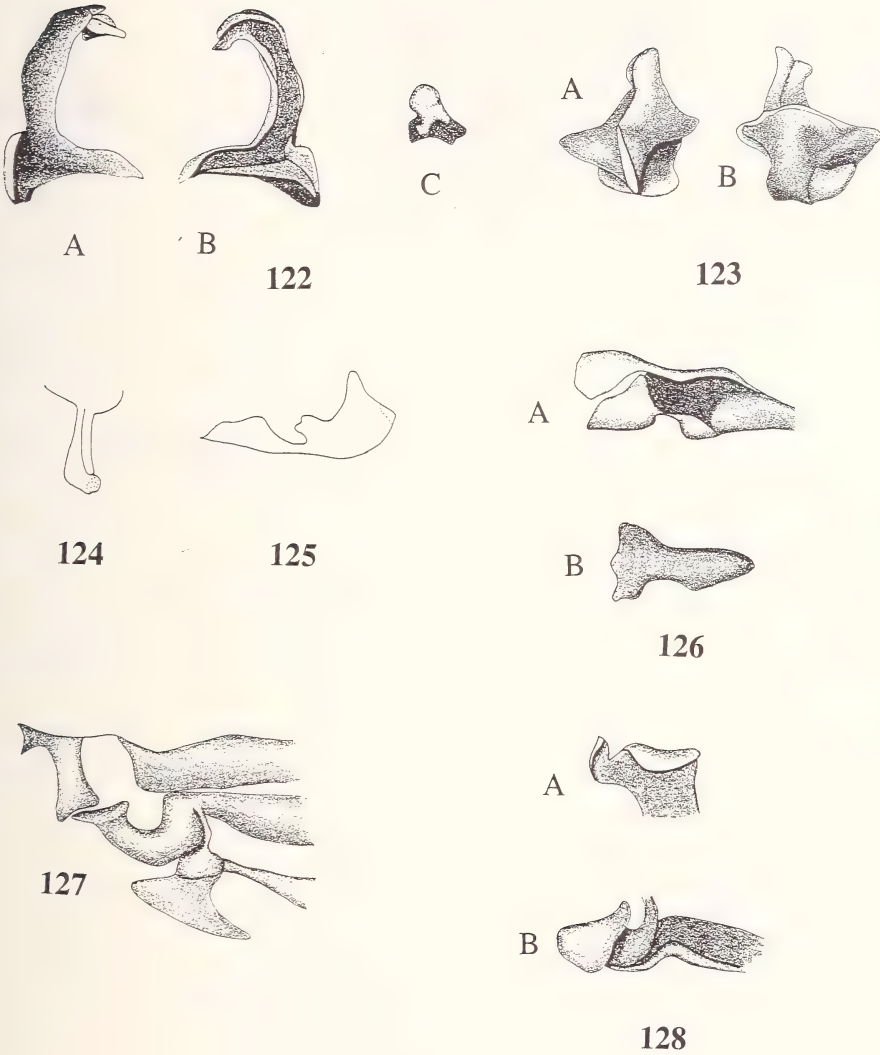
Figs.103-107: Hind wing articulation and wing base of Aphodiinae (Scarabaeidae). – **103:** Outline of the median plate. – **104:** Outline of the dorso-lateral view of the third axillary: 1, *Colobopterius* spec. (Aphodiini); 2, *Ataenius desertus* (Eupariini); 3, *Rhyssemus hamatus* (Psammodiini). – **105:** First basal plate (excluding BR): a, dorsal; b, anterior: 1, *Colobopterius* spec. (Aphodiini); 2, *Ataenius desertus* (Eupariini); 3, *Rhyssemus hamatus* (Psammodiini). – **106:** Dorsal view of the second basal plate (including BR): 1, *Colobopterius* spec. (Aphodiini); 2, *Ataenius desertus* (Eupariini); 3, *Rhyssemus hamatus* (Psammodiini). – **107:** Dorso-lateral view of the basalare and BScP of Aphodiinae (Scarabaeidae): a, basalare; b, BScP. Not to scale. Originals Browne (1993).



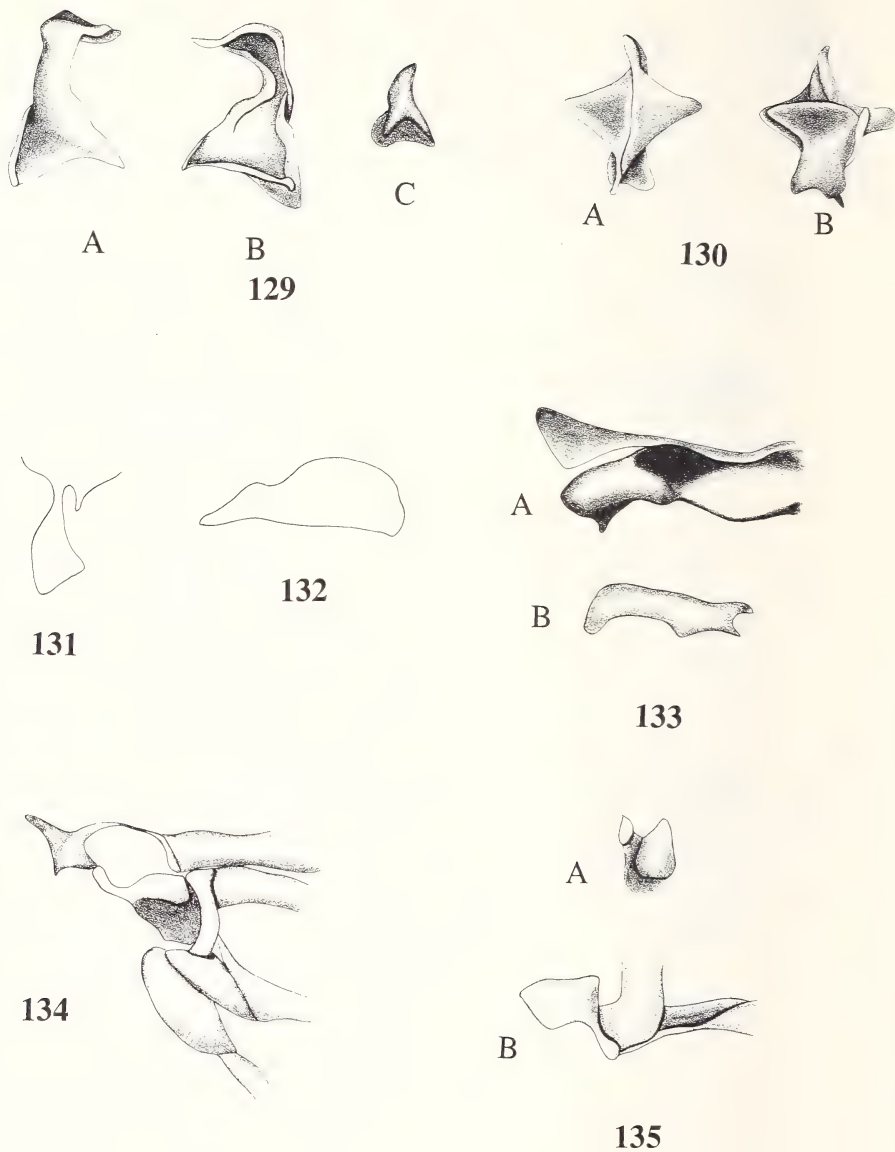
Figs.108-114: Hind wing articulation and wing base of *Aegialia crossa* (Aegialiinae: Scarabaeidae). – **108**: First axillary: a, dorsal; b, ventral; c, anterior. – **109**: Second axillary: a, dorsal; b, ventral. – **110**: Outline of the median plate. – **111**: Outline of the dorso-lateral view of the third axillary. – **112**: Dorsal view of the first basal plate (excluding BR): a, dorsal; b, anterior view of HP. – **113**: Dorsal view of the second basal plate (including BR). – **114**: Dorso-lateral view of the basalare and BScP: a, basalare; b, BScP. Not to scale. Originals Browne (1993).



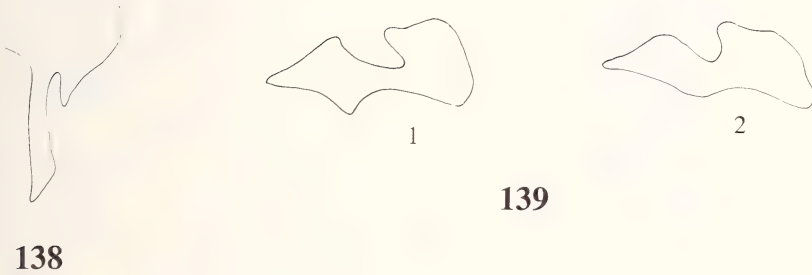
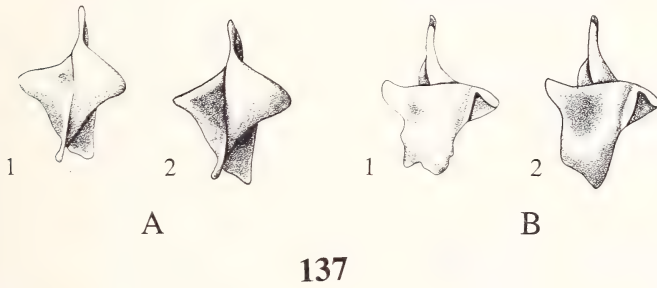
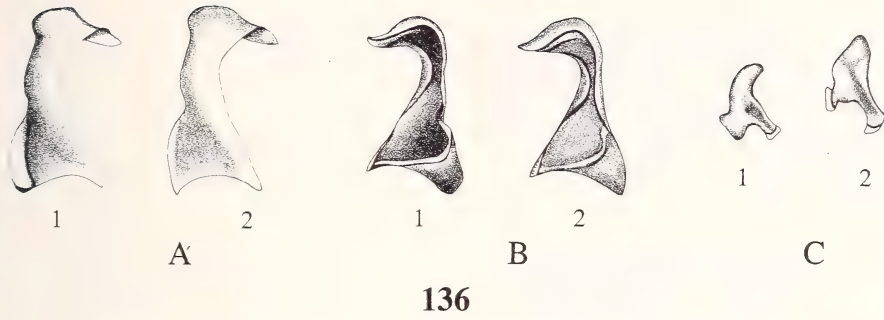
Figs.115-121: Hind wing articulation and wing base of *Aulonocnemis vulgaris* (Aulonocneminae: Scarabaeidae). – **115**: First axillary: a, dorsal; b, ventral; c, anterior. – **116**: Second axillary: a, dorsal; b, ventral. – **117**: Outline of the median plate. – **118**: Outline of the dorso-lateral view of the third axillary. – **119**: Dorsal view of the first basal plate (excluding BR): a, dorsal; b, anterior view of HP. – **120**: Dorsal view of the second basal plate (including BR). – **121**: Dorso-lateral view of the basalare and BScP: a, basalare; b, BScP. Not to scale. Originals Browne (1993).



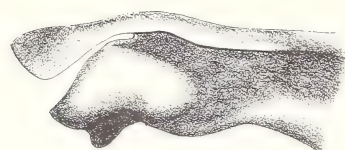
Figs.122-128: Hind wing articulation and wing base of *Eurysternus caribaeus* (Scarabaeinae: Scarabaeidae). – **122**: First axillary: a, dorsal; b, ventral; c, anterior. – **123**: Second axillary: a, dorsal; b, ventral. – **124**: Outline of the median plate. – **125**: Outline of the dorso-lateral view of the third axillary. – **126**: Dorsal view of the first basal plate (excluding BR): a, dorsal; b, anterior view of HP. – **127**: Dorsal view of the second basal plate (including BR). – **128**: Dorso-lateral view of the basalare and BScP: a, basalare; b, BScP. Not to scale. Originals Browne (1993).



Figs.129-135: Hind wing articulation and wing base of *Orphnidus capensis* (Orphninae: Scarabaeidae). – **129**: First axillary: a, dorsal; b, ventral; c, anterior. – **130**: Second axillary: a, dorsal; b, ventral. – **131**: Outline of the median plate. – **132**: Outline of the dorso-lateral view of the third axillary. – **133**: Dorsal view of the first basal plate (excluding BR): a, dorsal; b, anterior view of HP. – **134**: Dorsal view of the second basal plate (including BR). – **135**: Dorso-lateral view of the basalare and BScP: a, basalare; b, BScP. Not to scale. Originals Browne (1993).

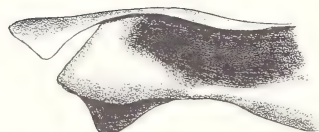


Figs.136-139: Hind wing articulation and wing base of Melolonthinae (Scarabaeidae). – **136:** First axillary: a, dorsal; b, ventral; c, anterior: 1, *Macroductylus subspinosus*; 2, *Phyllophaga cribrosa*. – **137:** Second axillary: a, dorsal; b, ventral: 1, *Macroductylus subspinosus*; 2, *Phyllophaga cribrosa*. – **138:** Outline of the median plate. – **139:** Outline of the dorso-lateral view of the third axillary: 1, *Macroductylus subspinosus*; 2, *Phyllophaga cribrosa*. Not to scale. Originals Browne (1993).



1

A



2



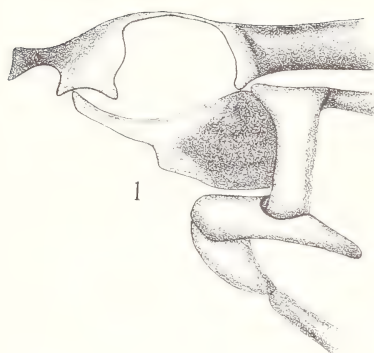
1

B

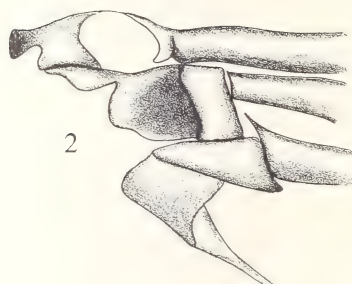


2

140



1



2

141



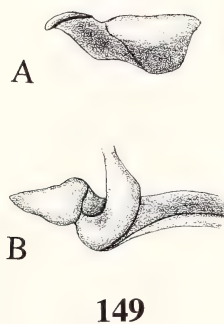
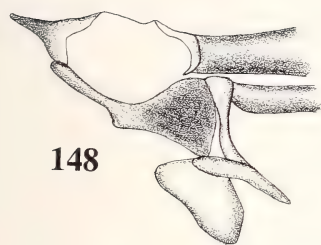
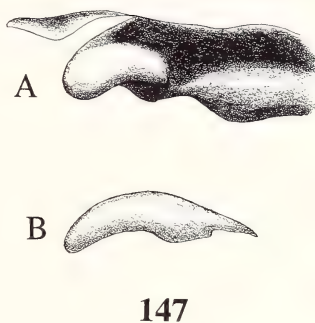
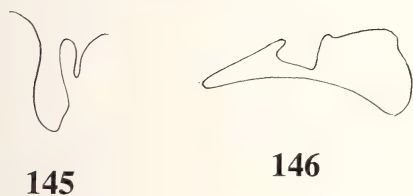
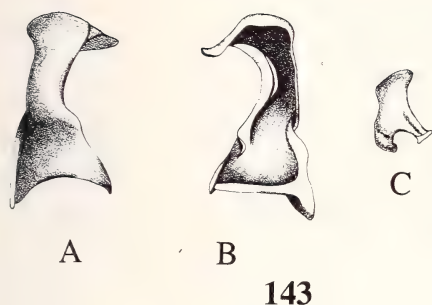
A



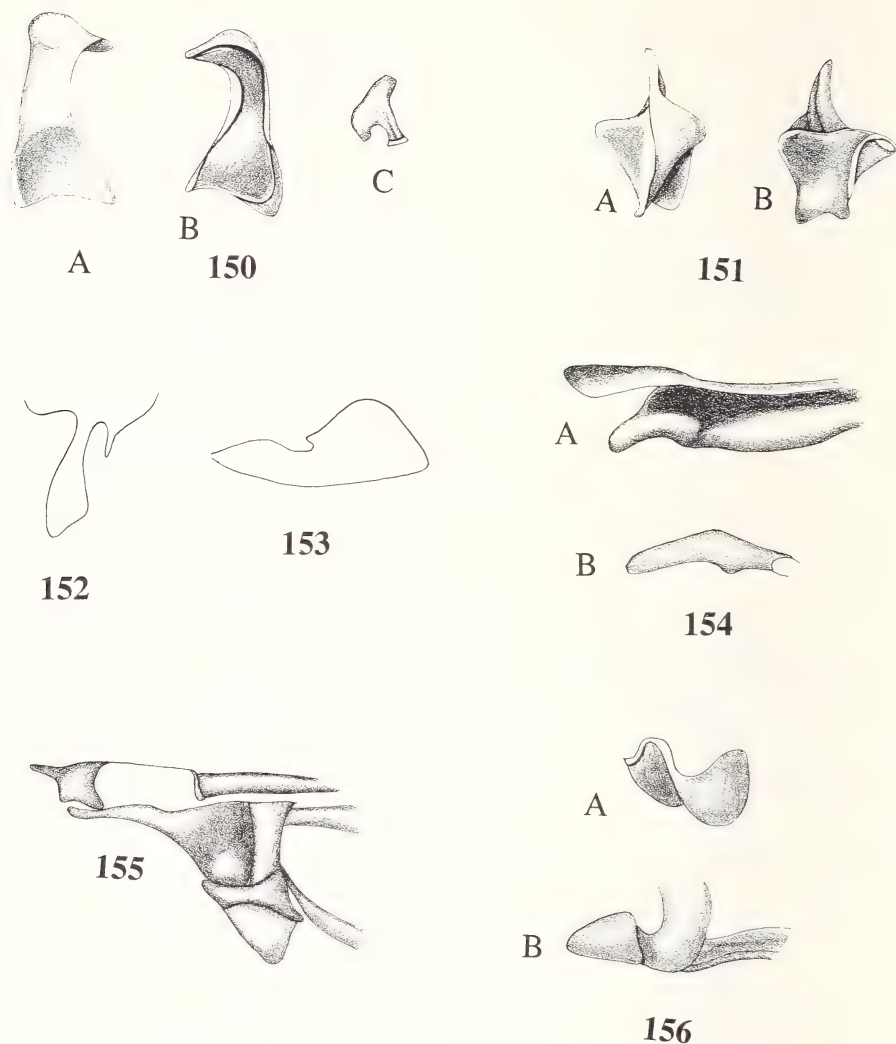
B

142

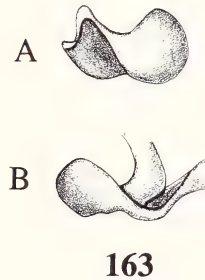
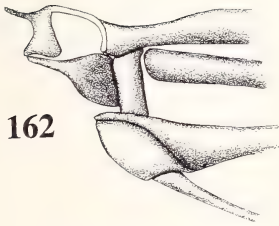
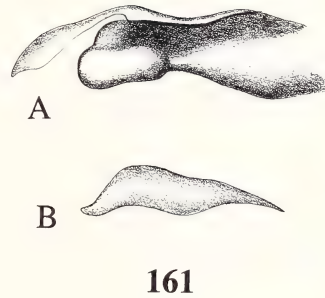
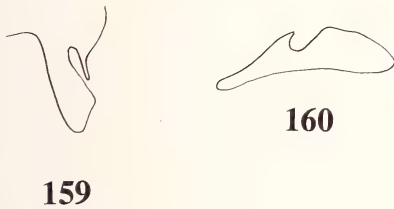
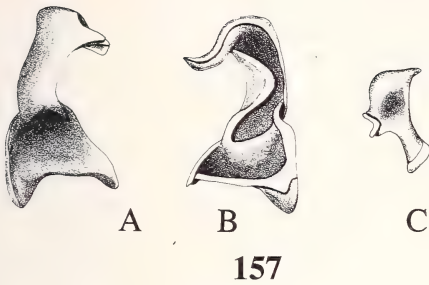
Figs.140-142: Hind wing articulation and wing base of Melolonthinae (Scarabaeidae). – **140**: First basal plate (excluding BR): a, dorsal; b, anterior: 1, *Macrodactylus subspinosus*; 2, *Phyllophaga cribrosa*. – **141**: Dorsal view of the second basal plate (including BR): 1, *Macrodactylus subspinosus*; 2, *Phyllophaga cribrosa*. – **142**: Basalare and BScP of Melolonthinae (Scarabaeidae): a, dorsal view of basalare; b, dorso-lateral view of BScP. Not to scale. Originals Browne (1993).



Figs.143-149: Hind wing articulation and wing base of *Acoma glabrata* (Scarabaeidae). – **143**: First axillary: a, dorsal; b, ventral; c, anterior. – **144**: Second axillary: a, dorsal; b, ventral. – **145**: Outline of the median plate. – **146**: Outline of the dorso-lateral view of the third axillary. – **147**: Dorsal view of the first basal plate (excluding BR): a, dorsal; b, anterior view of HP. – **148**: Dorsal view of the second basal plate (including BR). – **149**: Dorso-lateral view of the basalare and BScP: a, basalare; b, BScP. Not to scale. Originals Browne (1993).

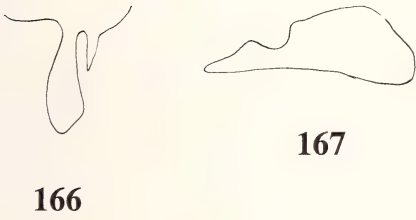
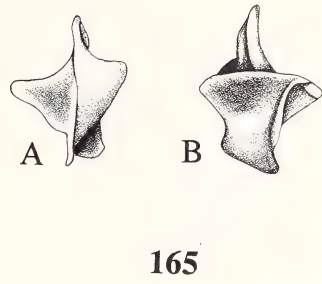
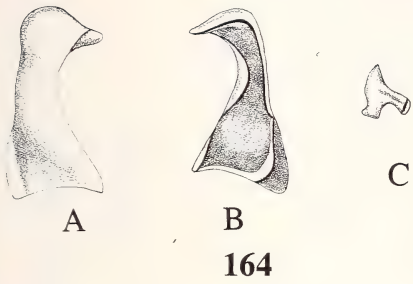


Figs.150-156: Hind wing articulation and wing base of *Chnaunanthus chapini* (Scarabaeidae). – **150**: First axillary: a, dorsal; b, ventral; c, anterior. – **151**: Second axillary: a, dorsal; b, ventral. – **152**: Outline of the median plate. – **153**: Outline of the dorso-lateral view of the third axillary. – **154**: Dorsal view of the first basal plate (excluding BR): a, dorsal; b, anterior view of HP. – **155**: Dorsal view of the second basal plate (including BR). – **156**: Dorso-lateral view of the basalare and BScP: a, basalare; b, BScP. Not to scale. Originals Browne (1993).

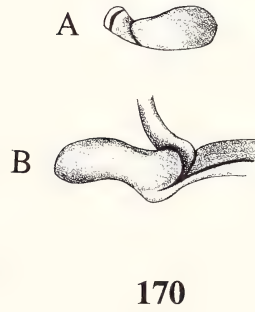
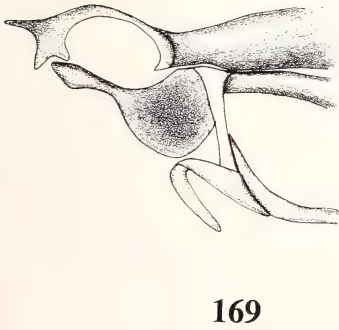
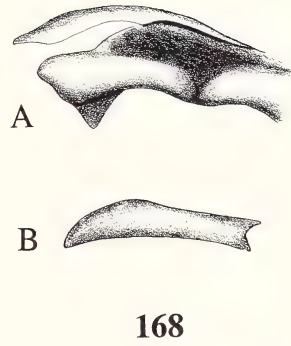


Figs.157-163: Hind wing articulation and wing base of *Lepithrix lineata* (Scarabaeidae). – **157**: First axillary: a, dorsal; b, ventral; c, anterior. – **158**: Second axillary: a, dorsal; b, ventral. – **159**: Outline of the median plate. – **160**: Outline of the dorso-lateral view of the third axillary. – **161**: Dorsal view of the first basal plate (excluding BR): a, dorsal; b, anterior view of HP. – **162**: Dorsal view of the second basal plate (including BR). – **163**: Dorso-lateral view of the basalare and BScP: a, basalare; b, BScP. Not to scale. Originals Browne (1993).

Figs.164-170: Hind wing articulation and wing base of *Oncerus floralis* (Scarabaeidae). – **164**: First axillary: a, dorsal; b, ventral; c, anterior. – **165**: Second axillary: a, dorsal; b, ventral. – **166**: Outline of the median plate. – **167**: Outline of the dorso-lateral view of the third axillary. – **168**: Dorsal view of the first basal plate (excluding BR): a, dorsal; b, anterior view of HP. – **169**: Dorsal view of the second basal plate (including BR). – **170**: Dorso-lateral view of the basalare and BScP: a, basalare; b, BScP. Not to scale. Originals Browne (1993).

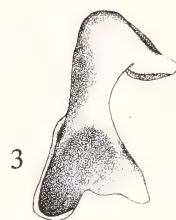


167

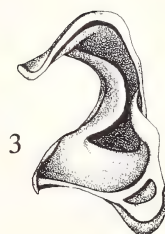
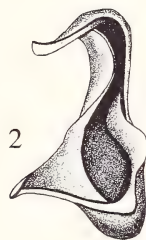


Figs.171-172: Hind wing articulation and wing base of Rutelinae (Scarabaeidae). – **171:** First axillary: a, dorsal; b, ventral; c, anterior: 1, *Leptohoplia testacepennis*; 2, *Popillia basalis*; 3, *Pelidnota punctulata*. – **172:** Second axillary: a, dorsal; b, ventral: 1, *Leptohoplia testacepennis*; 2, *Popillia basalis*; 3, *Pelidnota punctulata*. Not to scale. Originals Browne (1993).

171



B

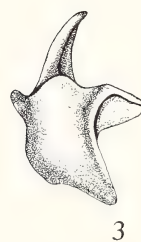
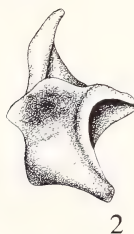


C



172

A



B





173



1

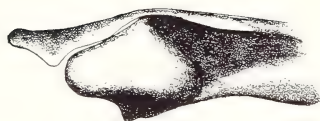


2

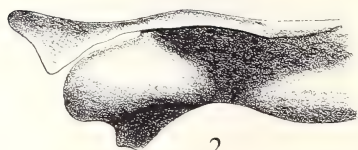


3

174



1



2

A



3

B



1



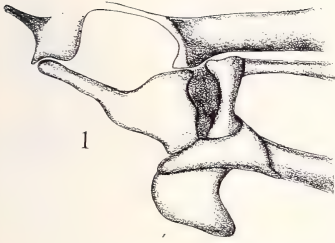
2



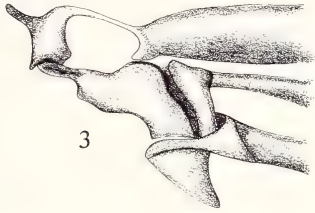
3

175

Figs.173-175: Hind wing articulation and wing base of Rutelinae (Scarabaeidae). – **173**: Outline of the median plate. – **174**: Outline of the dorso-lateral view of the third axillary: 1, *Leptohoplia testaceipennis*; 2, *Popillia basalis*; 3, *Pelidnota punctulata*. – **175**: First basal plate (excluding BR): a, dorsal; b, anterior: 1, *Leptohoplia testaceipennis*; 2, *Popillia basalis*; 3, *Pelidnota punctulata*. Not to scale. Originals Browne (1993).



176



A



1



2



3

B



1



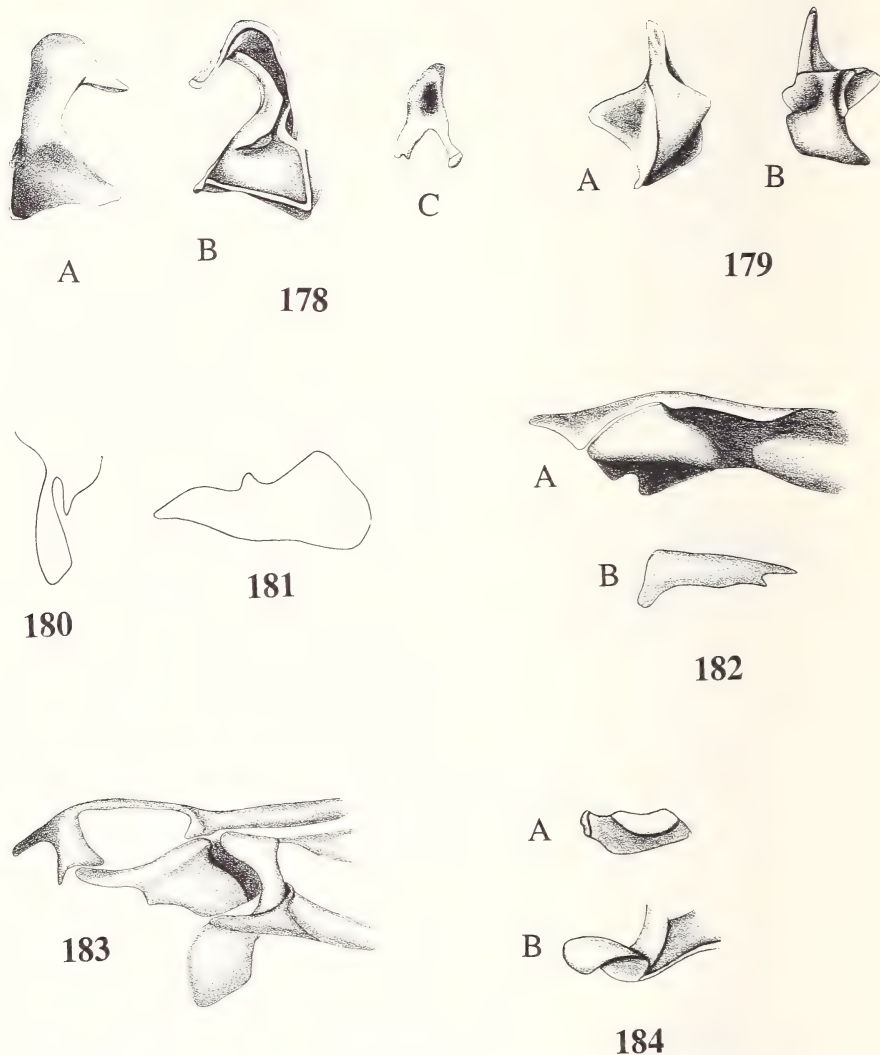
2



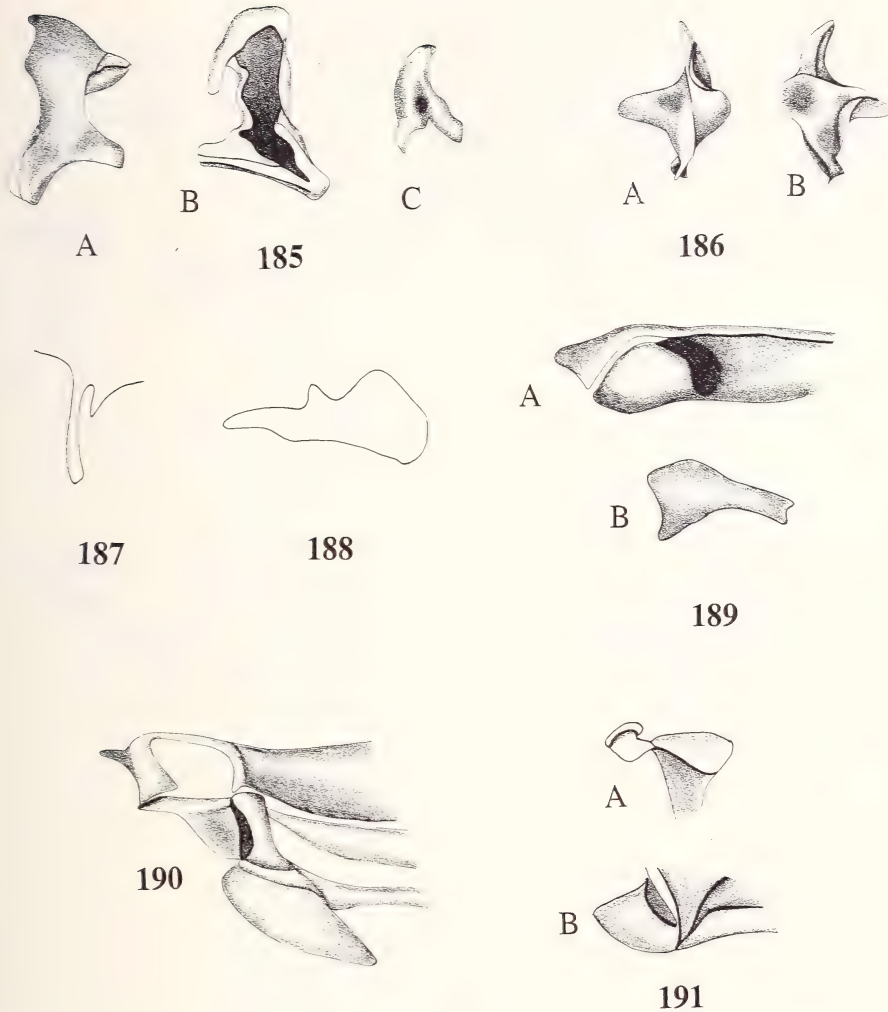
3

177

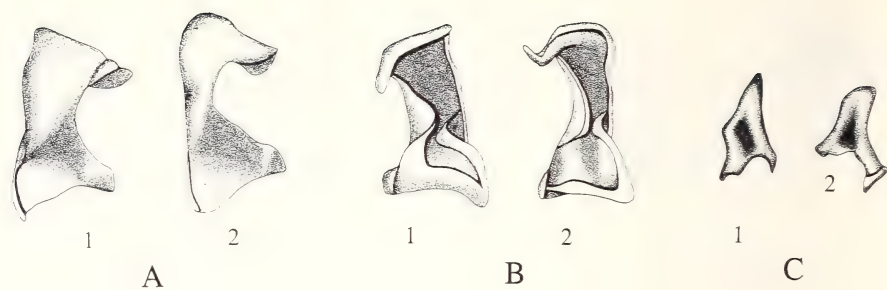
Figs.176-177: Hind wing articulation and wing base of Rutelinae (Scarabaeidae). – **176**: Dorsal view of the second basal plate (including BR): 1, *Leptohoplia testacepennis*; 2, *Popillia basalis*; 3, *Pelidnota punctulata*. – **177**: Dorso-lateral view of the basalare and BScP: a, basalare; b, BScP: 1, *Leptohoplia testacepennis*; 2, *Popillia basalis*; 3, *Pelidnota punctulata*. Not to scale. Originals Browne (1993).



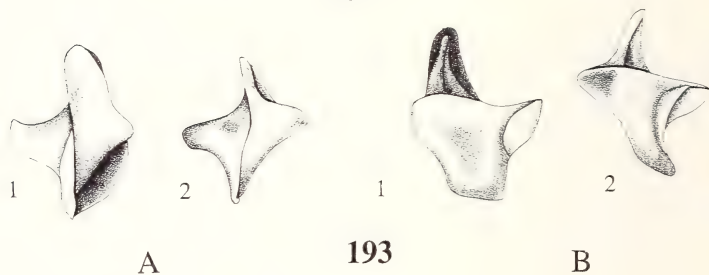
Figs.178-184: Hind wing articulation and wing base of *Philoscaptus boarensis* (Dynastinae: Scarabaeidae). – **178**: First axillary: a, dorsal; b, ventral; c, anterior. – **179**: Second axillary: a, dorsal; b, ventral. – **180**: Outline of the median plate. – **181**: Outline of the dorso-lateral view of the third axillary. – **182**: Dorsal view of the first basal plate (excluding BR): a, dorsal; b, anterior view of HP. – **183**: Dorsal view of the second basal plate (including BR). – **184**: Dorso-lateral view of the basalare and BScP: a, basalare; b, BScP. Not to scale. Originals Browne (1993).



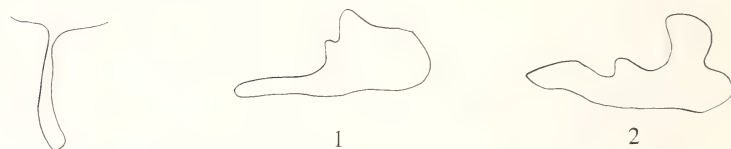
Figs.185-191: Hind wing articulation and wing base of *Rhinocoeta minor* (Cetoniinae: Scarabaeidae).
 – **185**: First axillary: a, dorsal; b, ventral; c, anterior. – **186**: Second axillary: a, dorsal; b, ventral. –
187: Outline of the median plate. – **188**: Outline of the dorso-lateral view of the third axillary. – **189**:
 Dorsal view of the first basal plate (excluding BR): a, dorsal; b, anterior view of HP. – **190**: Dorsal
 view of the second basal plate (including BR). – **191**: Dorso-lateral view of the basalare and BScP:
 a, basalare; b, BScP. Not to scale. Originals Browne (1993).



192



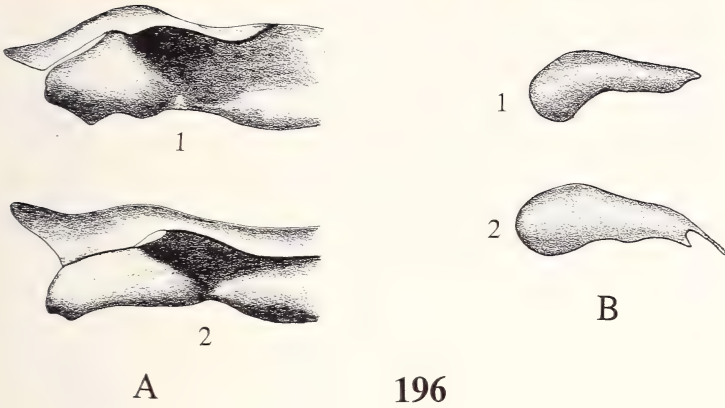
193



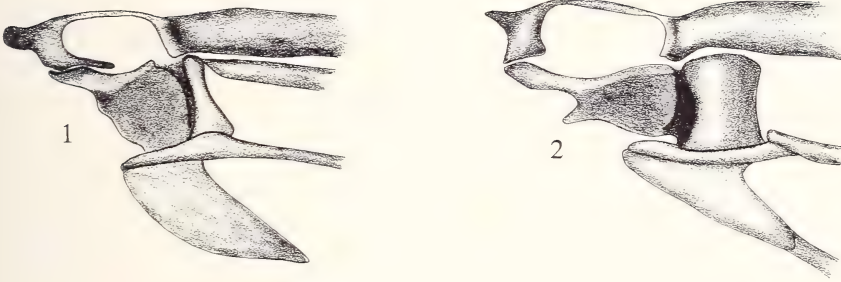
195

194

Figs. 192-195: Hind wing articulation and wing base of Trichiinae (Scarabaeidae). – **192**: First axillary: a, dorsal; b, ventral; c, anterior: 1, *Osmoderma scabrum*; 2, *Campilipus* spec. – **193**: Second axillary: a, dorsal; b, ventral: 1, *Osmoderma scabrum*; 2, *Campilipus* spec. – **194**: Outline of the median plate of Trichiinae (Scarabaeidae). – **195**: Outline of the dorso-lateral view of the third axillary: 1, *Osmoderma scabrum*; 2, *Campilipus* spec. Not to scale. Originals Browne (1993).



196

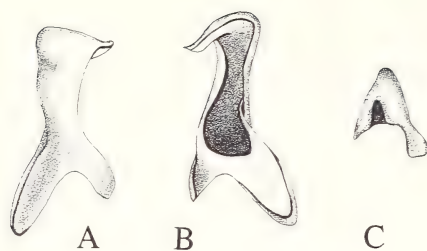


197

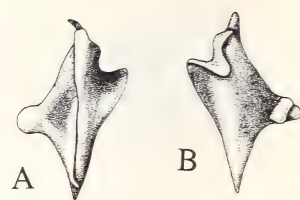


198

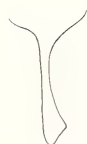
Figs.196-198: Hind wing articulation and wing base of Trichiinae (Scarabaeidae). – **196**: First basal plate (excluding BR): a, dorsal; b, ventral: 1, *Osmoderma scabrum*; 2, *Campilipus* spec. – **197**: Dorsal view of the second basal plate (including BR): 1, *Osmoderma scabrum*; 2, *Campilipus* spec. – **198**: Dorso-lateral view of the basalare and BScP: a, basalare of Trichiinae; b, BScP of *Osmoderma scabrum*; c, BScP of *Campilipus* spec. Not to scale. Originals Browne (1993).



199



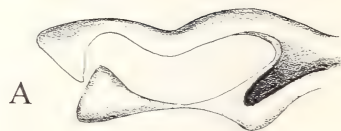
200



201



202

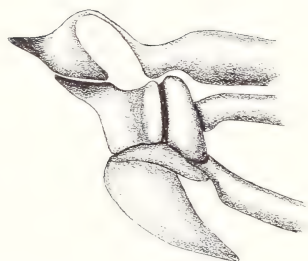


A



B

203



204



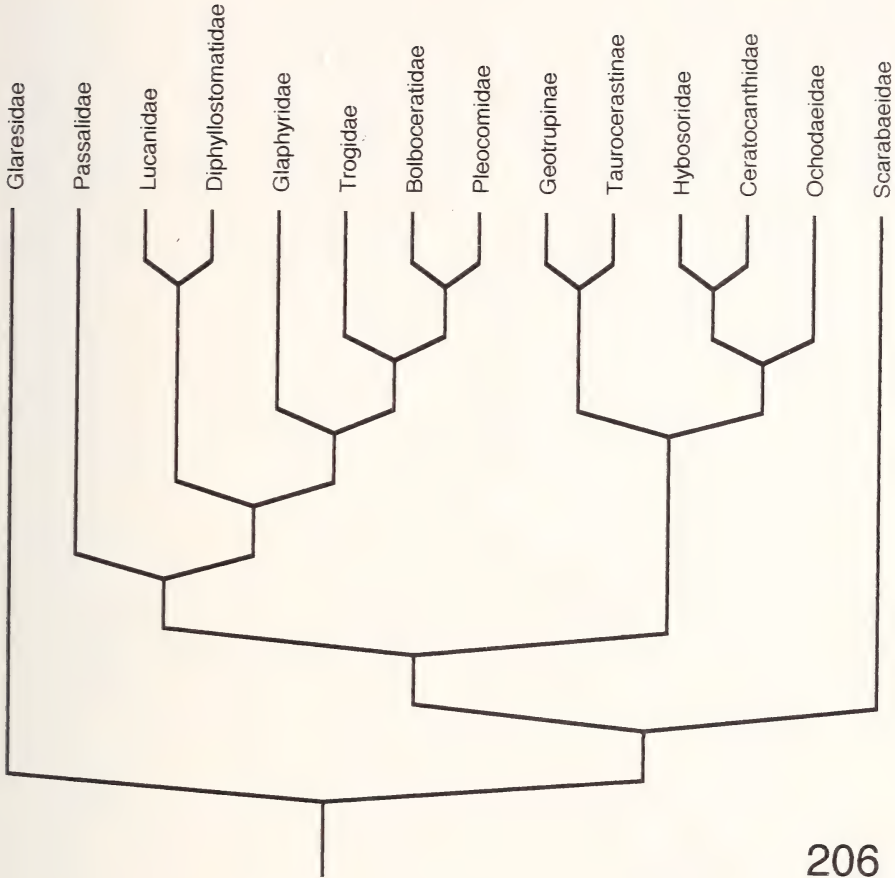
A



B

205

Figs.199-205: Hind wing articulation and wing base of *Comythovalgus* spec. (Valginae: Scarabaeidae). – **199**: First axillary: a, dorsal; b, ventral; c, anterior. – **200**: Second axillary: a, dorsal; b, ventral. – **201**: Outline of the median plate. – **202**: Outline of the dorso-lateral view of the third axillary. – **203**: Dorsal view of the first basal plate (excluding BR): a, dorsal; b, anterior view of HP. – **204**: Dorsal view of the second basal plate (including BR). – **205**: Dorso-lateral view of the basalare and BScP: a, basalare; b, BScP. Not to scale. Originals Browne (1993).



206

Fig.206: Hypothesised branching patterns among members of Scarabaeoidea based on characters of the hind wing articulation, wing base and wing venation (Browne 1993; Browne & Scholtz 1995).

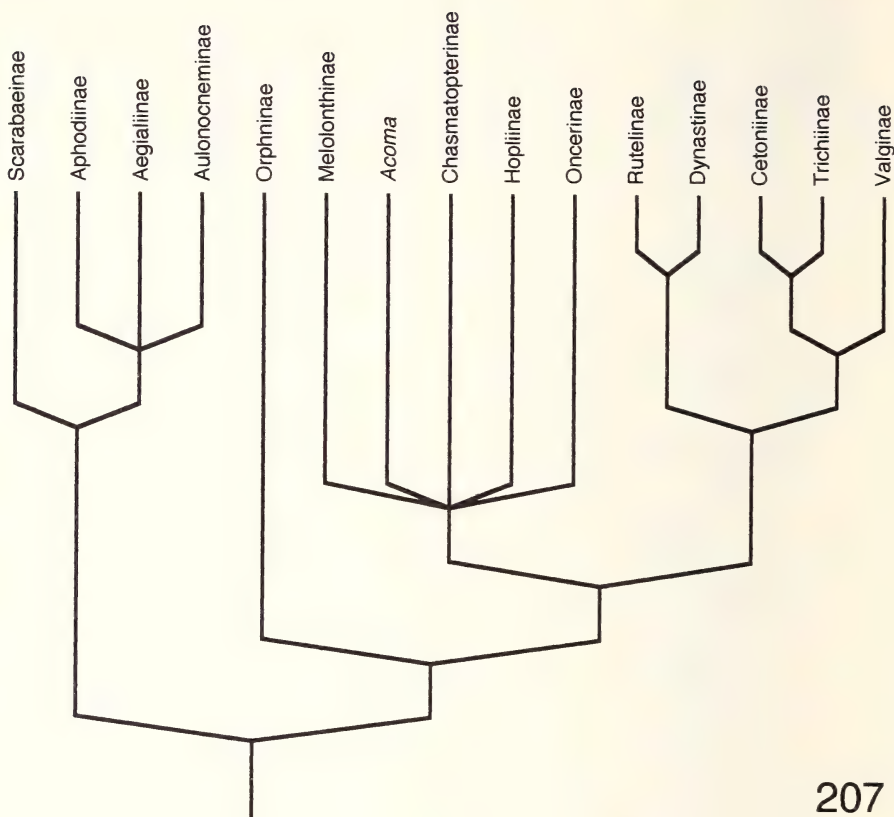


Fig.207: Hypothesised branching patterns among members of Scarabaeidae based on characters of the hind wing articulation and wing base (Browne 1993).

In der Serie BONNER ZOOLOGISCHE MONOGRAPHIEN sind erschienen:

1. Naumann, C.M.: Untersuchungen zur Systematik und Phylogenese der holarktischen Sesiiden (Insecta, Lepidoptera), 1971, 190 S., DM 48,—
2. Ziswiler, V., H.R. Güttinger & H. Bregulla: Monographie der Gattung *Erythrura* Swainson, 1837 (Aves, Passeres, Estrildidae). 1972, 158 S., 2 Tafeln, DM 40,—
3. Eisentraut, M.: Die Wirbeltierfauna von Fernando Poo und Westkamerun. Unter besonderer Berücksichtigung der Bedeutung der pleistozänen Klimaschwankungen für die heutige Faunenverteilung. 1973, 428 S., 5 Tafeln, DM 106,—
4. Herrlinger, E.: Die Wiedereinbürgerung des Uhus *Bubo bubo* in der Bundesrepublik Deutschland. 1973, 151 S., DM 38,—
5. Ulrich, H.: Das Hypopygium der Dolichopodiden (Diptera): Homologie und Grundplanmerkmale. 1974, 60 S., DM 15,—
6. Jost, O.: Zur Ökologie der Wasseramsel (*Cinclus cinclus*) mit besonderer Berücksichtigung ihrer Ernährung. 1975, 183 S., DM 46,—
7. Haffer, J.: Avifauna of northwestern Colombia, South America. 1975, 182 S., DM 46,—
8. Eisentraut, M.: Das Gaumenfaltenmuster der Säugetiere und seine Bedeutung für stammesgeschichtliche und taxonomische Untersuchungen. 1976, 214 S., DM 54,—
9. Rath, P., & E. Kulzer: Physiology of hibernation and related lethargic states in mammals and birds. 1976, 93 S., 1 Tafel, DM 23,—
10. Haffer, J.: Secondary contact zones of birds in northern Iran. 1977, 64 S., 1 Tafel, DM 16,—
11. Guibé, J.: Les batraciens de Madagascar. 1978, 144 S., 82 Tafeln, DM 36,—
12. Thaler, E.: Das Aktionssystem von Winter- und Sommergoldhähnchen (*Regulus regulus*, *R. ignicapillus*) und deren ethologische Differenzierung. 1979, 151 S., DM 38,—
13. Homberger, D.G.: Funktionell-morphologische Untersuchungen zur Radiation der Ernährungs- und Trinkmethoden der Papageien (Psittaci). 1980, 192 S., DM 48,—
14. Kullander, S.O.: A taxonomical study of the genus *Apistogramma* Regan, with a revision of Brazilian and Peruvian species (Teleostei: Percoidei: Cichlidae). 1980, 152 S., DM 38,—
15. Scherzinger, W.: Zur Ethologie der Fortpflanzung und Jugendentwicklung des Habichtskauzes (*Strix uralensis*) mit Vergleichen zum Waldkauz (*Strix aluco*). 1980, 66 S., DM 17,—
16. Salvador, A.: A revision of the lizards of the genus *Acanthodactylus* (Sauria: Lacertidae). 1982, 167 S., DM 42,—
17. Marsch, E.: Experimentelle Analyse des Verhaltens von *Scarabaeus sacer* L. beim Nahrungserwerb. 1982, 79 S., DM 20,—
18. Hutterer, R., & D.C.D. Happold: The shrews of Nigeria (Mammalia: Soricidae). 1983, 79 S., DM 20,—
19. Rheinwald, G. (Hrsg.): Die Wirbeltiersammlungen des Museums Alexander Koenig. 1984, 239 S., DM 60,—
20. Nilson, G., & C. Andrén: The Mountain Vipers of the Middle East — the *Vipera xanthina* complex (Reptilia, Viperidae). 1986, 90 S., DM 23,—
21. Kumerloewe, H.: Bibliographie der Säugetiere und Vögel der Türkei. 1986, 132 S., DM 33,—
22. Klaver, C., & W. Böhme: Phylogeny and Classification of the Chamaeleonidae (Sauria) with Special Reference to Hemipenis Morphology. 1986, 64 S., DM 16,—

23. Bublitz, J.: Untersuchungen zur Systematik der rezenten Caenolestidae Trouessart, 1898 — unter Verwendung craniometrischer Methoden. 1987, 96 S., DM 24,—
24. Arratia, G.: Description of the primitive family Diplomystidae (Siluriformes, Teleostei, Pisces): Morphology, taxonomy and phylogenetic implications. 1987, 120 S., DM 30,—
25. Nikolaus, G.: Distribution atlas of Sudan's birds with notes on habitat and status. 1987, 322 S., DM 81,—
26. Löhrl, H.: Etho-ökologische Untersuchungen an verschiedenen Kleiberarten (Sitidae) — eine vergleichende Zusammenstellung. 1988, 208 S., DM 52,—
27. Böhme, W.: Zur Genitalmorphologie der Sauria: Funktionelle und stammesgeschichtliche Aspekte. 1988, 175 S., DM 44,—
28. Lang, M.: Phylogenetic and biogeographic patterns of Basiliscine Iguanians (Reptilia: Squamata: "Iguanidae"). 1989, 172 S., DM 43,—
29. Hoi-Leitner, M.: Zur Veränderung der Säugetierfauna des Neusiedlersee-Gebietes im Verlauf der letzten drei Jahrzehnte. 1989, 104 S., DM 26,—
30. Bauer, A. M.: Phylogenetic systematics and Biogeography of the Carphodactylini (Reptilia: Gekkonidae). 1990, 220 S., DM 55,—
31. Fiedler, K.: Systematic, evolutionary, and ecological implications of myrmecophily within the Lycaenidae (Insecta: Lepidoptera: Papilionoidea). 1991, 210 S., DM 53,—
32. Arratia, G.: Development and variation of the suspensorium of primitive Catfishes (Teleostei: Ostariophysi) and their phylogenetic relationships. 1992, 148 S., DM 37,—
33. Kotrba, M.: Das Reproduktionssystem von *Cyrtodiopsis whitei* Curran (Diopsidae, Diptera) unter besonderer Berücksichtigung der inneren weiblichen Geschlechtsorgane. 1993, 115 S., DM 32,—
34. Blaschke-Berthold, U.: Anatomie und Phylogenie der Bibionomorpha (Insecta, Diptera). 1993, 206 S., DM 52,—
35. Hallermann, J.: Zur Morphologie der Ethmoidalregion der Iguania (Squamata) — eine vergleichend-anatomische Untersuchung. 1994, 133 S., DM 33,—
36. Arratia, G., & L. Huaquin: Morphology of the lateral line system and of the skin of Diplomystid and certain primitive Loricarioid Catfishes and systematic and ecological considerations. 1995, 110 S., DM 28,—
37. Hille, A.: Enzymelektrophoretische Untersuchung zur genetischen Populationsstruktur und geographischen Variation im *Zygaena-transalpina*-Superspezies-Komplex (Insecta, Lepidoptera, Zygaenidae). 1995, 224 S., DM 56,—
38. Martens, J., & S. Eck: Towards an Ornithology of the Himalayas: Systematics, ecology and vocalizations of Nepal birds. 1995, 448 S., 3 Farbtafeln, DM 112,—
39. Chen, X.: Morphology, phylogeny, biogeography and systematics of *Phoxinus* (Pisces: Cyprinidae). 1996, 227 S., DM 57,—
40. Browne, D. J., & C. H. Scholtz: The morphology of the hind wing articulation and wing base of the Scarabaeoidea (Coleoptera) with some phylogenetic implications. 1996, 200 S., DM 50,—

Seit Nr. 30 werden die Monographien ausschließlich über die Konvertierung von Disketten-texten hergestellt. Dies ergibt neben einer Kosten- und Zeitersparnis auch eine deutlich geringere Fehlerquote im Endprodukt. Dazu müssen einige Voraussetzungen erfüllt sein: IBM-kompatibel, Betriebssystem MS-DOS, 3,5- oder 5,25-Zoll-Diskette, „endlos“ beschrieben, ASCII oder wordperfect. Wer sich für Einzelheiten interessiert, wende sich bitte an den Schriftleiter.

Wegen der Gestaltung der Manuskripte, insbesondere des Literaturverzeichnisses, werden die Autoren auf die letzten erschienenen Monographien verwiesen.

716
H

A MORPHOLOGICAL PERSPECTIVE ON THE
PHYLOGENETIC RELATIONSHIPS
OF THE EXTANT PHOCID SEALS
(MAMMALIA: CARNIVORA: PHOCIDAE)



by

O. R. P. BININDA-EMONDS & A. P. RUSSELL

BONNER ZOOLOGISCHE MONOGRAPHIEN, Nr. 41

1996

Herausgeber:
ZOOLOGISCHES FORSCHUNGSMUSEUM
UND MUSEUM ALEXANDER KOENIG
BONN

BONNER ZOOLOGISCHE MONOGRAPHIEN

Die Serie wird vom Zoologischen Forschungsinstitut und Museum Alexander Koenig herausgegeben und bringt Originalarbeiten, die für eine Unterbringung in den „Bonner zoologischen Beiträgen“ zu lang sind und eine Veröffentlichung als Monographie rechtfertigen.

Anfragen bezüglich der Vorlage von Manuskripten sind an die Schriftleitung zu richten; Bestellungen und Tauschangebote bitte an die Bibliothek des Instituts.

This series of monographs, published by the Zoological Research Institute and Museum Alexander Koenig, has been established for original contributions too long for inclusion in „Bonner zoologische Beiträge“.

Correspondence concerning manuscripts for publication should be addressed to the editor. Purchase orders and requests for exchange please address to the library of the institute.

L'Institut de Recherches Zoologiques et Muséum Alexander Koenig a établi cette série de monographies pour pouvoir publier des travaux zoologiques trop longs pour être inclus dans les „Bonner zoologische Beiträge“.

Toute correspondance concernant des manuscrits pour cette série doit être adressée à l'éditeur. Commandes et demandes pour échanges adresser à la bibliothèque de l'institut, s. v. p.

BONNER ZOOLOGISCHE MONOGRAPHIEN, Nr. 41, 1996

Preis: 64,— DM

Schriftleitung/Editor: G. Rheinwald

Zoologisches Forschungsinstitut und Museum Alexander Koenig

Adenauerallee 150—164, D-53113 Bonn, Germany

Druck: JF•CARTHAUS, Bonn

ISBN 3-925382-44-5

ISSN 0302-671 X

A MORPHOLOGICAL PERSPECTIVE ON THE
PHYLOGENETIC RELATIONSHIPS
OF THE EXTANT PHOCID SEALS
(MAMMALIA: CARNIVORA: PHOCIDAE)

by

O. R. P. BININDA-EMONDS & A. P. RUSSELL

BONNER ZOOLOGISCHE MONOGRAPHIEN, Nr. 41
1996

Herausgeber:
ZOOLOGISCHES FORSCHUNGSMUSEUM
UND MUSEUM ALEXANDER KOENIG
BONN

Die Deutsche Bibliothek — CIP-Einheitsaufnahme

Bininda-Emonds, O. R. P.:

A morphological perspective on the phylogenetic relationships of the extant phocid seals (Mammalia: Carnivora: Phocidae) / by O. R. P. Bininda-Emonds & A. P. Russell. Hrsg.: Zoologisches Forschungsinstitut und Museum Alexander Koenig, Bonn. — Bonn: Zoologisches Forschungsinst. und Museum Alexander Koenig, 1996

(Bonner zoologische Monographien ; Nr. 41)

ISBN 3-925382-44-5

NE: Russell, A. P.; GT

CONTENTS

	Page
Introduction	5
Characterization of the Phocidae	5
Taxonomic and systematic history	6
Points of contention	7
The systematic status and interrelationships of the monk seals (genus <i>Monachus</i>) . .	7
The taxonomic status of the genera within the Phocini	8
The systematic status of the Monachinae	9
Phocid phylogeny at the species level	10
Ancestral affinities of the phocids	11
Goals of this project	14
Acknowledgements	16
Methods and materials	17
Data sources	17
Specimens	17
Characters	18
Data collation	19
Cladistic analysis	20
Assumptions concerning characters	20
Assumptions concerning taxa	22
Search criteria and summarizing output	23
Statistical tests	23
Goodness-of-fit statistics	23
The bootstrap	24
Permutation tail probabilities	25
Skewness	26
Successive approximations	28
Support analyses	28
Comparative tools	29
Constraint analyses	29
Missing taxa	33
Condensed analysis	33
Unweighted analysis	38
Taxonomic conventions	38
Overall parsimony analysis	39
Incidence of polymorphism	39
Overall solution	39
Outgroup relations	42
Ingroup relations	43
Relationships within the Monachinae	43
Relationships within the Phocinae	44
Summary of ingroup relationships	46
Support for the overall solution	47
Statistical tests	48
Interpreting statistical results	48
Character covariation within the data set	54

Regional support within the overall solution	54
Bootstrap analysis	54
Successive approximations	58
Support analysis	58
Overall conclusions	58
Comparative tools	66
Constraint analysis	66
Outgroup constraints	66
Internal constraints	71
Overall conclusions – possible effects of polymorphic data	76
Missing taxa	77
Unweighted solution	81
Condensed analysis	83
Character analysis	85
Snout	86
Orbit and zygomatic arch	95
Palate and ventral side of snout	108
Basicranial region	115
Bony tentorium and bony falx	133
Dorsal braincase	135
Teeth	137
Mandible	147
Forelimb	148
Pelvis	154
Hind Limb	158
Miscellaneous	162
Summary	165
Discussion and conclusions	175
Summary of results	175
Potential sources of error	177
Taxonomic implications	180
Biogeography and fossil evidence	181
Future directions	185
Abstract	187
Literature cited	188
Appendices:	198
A: Specimen list	198
B: List of characters	202
C: Character matrix	210
D: Branch lengths and linkages	212
E: Apomorphy lists (unweighted)	214
F: Character diagnostics (unweighted)	252

INTRODUCTION

As a group, the true or earless seals (Mammalia: Carnivora: Phocidae) present one of the more interesting puzzles in mammalian systematics. The roughly century-old debate on the position of the phocids within the carnivores (and especially their placement relative to the remaining pinnipeds) has attracted consistent attention, but the internal relationships of the group remain reasonably poorly studied to this day. About the only point of universal agreement is that the phocids are a natural, distinct group. It remains for an all-encompassing study employing a suitably rigorous methodology (such as cladistic analysis) to attempt to resolve the points of contention or uncertainty in phocid systematics.

Characterization of the Phocidae

The phocid seals have been referred to as being among the most specialized of carnivores (Wyss 1988a). Like all pinnipeds, the phocids are amphibious and are characterized by many features that can be interpreted as adaptations to an aquatic environment. These range from a fusiform, streamlined body shape and flippers that enhance aquatic locomotion, to the many specializations of the inner ear required for efficient underwater hearing (see Repenning 1972; de Muizon 1982a), to a simplified homodont dentition to help capture their slippery aquatic prey (see Chapskii 1955a). However, they are clearly distinguished from the remaining pinnipeds (and especially the sea lions and fur seals) by features denoting a greater adaptation to the aquatic environment: the lack of a protruding external pinna (as in the walrus as well), their generally superior diving ability (Costa 1993), and their reliance on the hind limbs for aquatic locomotion. In fact, the modifications associated with this last point are so great as to define perhaps the most definitive phocid characteristic, the inability to turn the hind limbs forward to support the weight of the body on land. Thus, the phocids are restricted on land to some form of crawling locomotion: inchworm-like movements (with or without assistance from the flippers), a modified "swimming" type of locomotion, and/or rolling and sliding (O'Gorman 1963; Ridgway 1972; King 1983).

The phocids inhabit both the northern and southern hemispheres, although they are largely restricted to the polar and sub-polar regions. The limits of their distribution seem to be marked by the 20°C summer isotherm, with only the monk seals (*Monachus* spp.) breaking this rule of thumb to inhabit tropical climes (Davies 1958a; McLaren 1960a; King 1964). The phocids are the only pinnipeds to inhabit Antarctica year-round, with several species being largely tied to the ice along the continent (see King 1968). One curiosity of phocids among pinnipeds is their ability to survive in estuarine and freshwater habitats (King 1983), allowing for the existence of many populations or entire species in land-locked lakes (Doutt 1942; Davies 1958b; King 1983).

The phocids show a tremendous diversity in size, spanning from the largest to among the smallest of all pinnipeds. Smallest of all phocids are the ringed seals (*Pusa* spp.) which average about 1.4 m nose-to-tail length, while the largest is the male southern elephant seal (*Mirounga leonina*) which spans four to five metres in length and can weigh up to 3.6 tonnes (King 1983).

Taxonomic and systematic history

The distinctiveness of the phocids has long been recognized. They were first accorded familial status by Brookes (1828) and, except for minor transient alterations, the membership of the family has remained the same ever since (although species assignments are contentious in some cases; see Appendix A for the list of species recognized here). Monophyly of this group has never been seriously challenged and appears to be universally accepted today (de Muizon 1982a; Wyss 1988a).

The higher level taxonomy of the phocids has been surprisingly stable in view of how historically contentious their placement within the carnivores has been (see below). The phocids are the only extant members of the superfamily Phocoidea (Smirnov 1908), or those pinnipeds that are unable to turn the hind limbs forward on land. Together with the Otarioidea (Smirnov 1908; sea lions, fur seals, walrus, and allied fossil forms), they constitute the Pinnipedia (Illiger 1811). Although their arctoid affinities are readily accepted (Flynn et al. 1988), the distinctiveness of all pinnipeds from the remaining fissiped carnivores has led them to be viewed as a separate order (e.g., Scheffer 1958; Ewer 1973; Corbet & Hill 1991), or, more commonly, as a suborder within the carnivores (e.g., Turner 1848; Flower 1869; Mivart 1885; Simpson 1945; King 1983). However, the possibility of a diphyletic origin of the pinnipeds has led some workers to abandon a distinct Pinnipedia altogether (e.g., McKenna 1969; Mitchell & Tedford 1973).

Taxonomy within the phocids largely reflects the historically poorly described and largely unresolved internal relationships of the phocids. Early taxonomies generally divided the phocids into four main subfamilies [but see Allen (1880) for a more complete review]: the Cystophorinae (Gill 1866; hooded and elephant seals), Lobodontinae (Gill 1866; Antarctic seals), Monachinae (Trouessart 1897; *Monachus* spp.), and Phocinae (Gill 1866; remaining northern hemisphere seals). Although this taxonomy is generally representative of the major phocid types, the granting of equal taxonomic status to each group does not appear to be justified.

Throughout much of their taxonomic history, the Lobodontinae and Monachinae have been alternately separated and rejoined, a fact indicating the general lack of distinctiveness between the two taxa. Scheffer (1958), holding that the only real distinction between the two taxa was one of geography, subsumed the two as tribes (Lobodontini and Monachini respectively) within a newly defined Monachinae.

The next major step involved the dismantling of the Cystophorinae by King (1966). The Cystophorinae were erected largely on the basis of two features: a 2/1 incisor formula and the possession of some form of inflatable nasal proboscis in the adult males [but see King (1966) and Ridgway (1972) for additional minor similarities]. It continued to be recognized despite numerous obvious differences between its two constituent genera (*Cystophora* and *Mirounga*), including the morphology of the nasal sac and manner in which it is inflated (Reeves & Ling 1981; King 1983; Kovacs & Lavigne 1986). Finally, King (1966) argued that the two diagnostic cystophorine features likely arose via convergence and pointed to a suite of 17 other cranial and post-cranial features that allied *Cystophora* with the "northern" seals and *Mirounga* spp. with the "southern" seals. McLaren (1975) later ascribed the convergent cystophorine features [also found in the fossil pinniped *Allodesmus*

(Mitchell 1975)] as being due to feeding specializations and sexual selection. Both genera were later established as members of monotypic tribes within their respective subfamilies (Burns & Fay 1970; de Muizon 1982a).

Thus, two subfamilies are typically recognized today – the Monachinae and Phocinae, corresponding roughly to the seals of the southern (plus *Monachus* spp.) and northern hemispheres respectively – with the previously recognized subfamilies mentioned above largely relegated as tribes within this scheme. Although generally accepted as being paraphyletic, the Cystophorinae are still occasionally referred to, primarily in catalogues of mammalian species (e.g., Ridgway 1972; Hall 1981; Stains 1984; Wilson & Reeder 1993). Considerably less attention has been focused below the tribal level, and the work that has been done possesses numerous shortcomings. As well, the utility of the tribal designations within the Monachinae has recently been questioned (Hendey and Repenning 1972; King 1983), as has the status of the Monachinae as a whole (Wyss 1988a; see below).

Points of contention

Thus, within the taxonomic framework laid out above, we identified five outstanding major problems concerning the systematics of the phocid seals, representing either points of contention or areas that have not been adequately studied. The various opinions expressed by previous workers for each problem may be regarded as hypotheses to be tested here.

The systematic status and interrelationships of the monk seals (genus *Monachus*)

Monachus spp. are nearly universally regarded as the most primitive of the extant phocids, being considerably more primitive morphologically than many fossil forms (Repenning & Ray 1977; Repenning et al. 1979; de Muizon 1982a; King 1983; Wyss 1988a). The three constituent species – *M. monachus*, *M. schauinslandi*, and *M. tropicalis* – are widely separated geographically, being found in and around the Mediterranean, in the vicinity of Hawaii, and in the Caribbean respectively [although *M. tropicalis* is believed to have been extinct since the early 1950s (Kenyon 1977)]. All three species are poorly known and insufficiently described, especially with respect to their soft anatomy.

The distinctly primitive nature of *Monachus* appears to have contributed to the long standing view that the genus is monophyletic. As well, the differences between the species are apparently so slight that if it were not for their far-flung distribution, all three might be viewed as subspecies of a single species (Scheffer 1958). However, Wyss (1988a) recently put forth the novel suggestion that the genus might be paraphyletic and recognized largely on the basis of the possession of phocid symplesiomorphies. *M. schauinslandi* was held to be the most primitive of the monk seals (and of all phocids), largely on the basis of the anatomy of the ear region (Wyss 1988a). However, this is a relatively recent view [originating with Repenning & Ray (1972)], with earlier researchers, while recognizing the primitive nature of *M. schauinslandi*, regarding it as sharing a common ancestor with *M. tropicalis* to the exclusion of *M. monachus* (King 1956, 1983; Davies 1958b; Kenyon & Rice 1959; King & Harrison 1961; de Muizon 1982a). Altogether, further description and phylogenetic treatment of this genus would be valuable.

The taxonomic status of the genera within the Phocini

The tribe Phocini is comprised of the genera *Halichoerus*, *Histriophoca*, *Pagophilus*, *Phoca*, and *Pusa*. Together, they are apparently clearly distinguished from the remaining phocids by the presence of a white natal coat (lanugo) (McLaren 1960a, 1966, 1975), a reduced karyotype of $2N = 32$ (Arnason 1974, 1977), and numerous morphological characters (King 1966; Burns & Fay 1970). Of the five constituent genera, the distinctive nature of *Halichoerus* has long been recognized, it being the first seal to be separated from the original, all-encompassing seal genus *Phoca* (see Chapskii 1955a; Scheffer 1958). *Halichoerus* is the largest of the phocines, and is typified by a long, high, and wide snout which gives it a "Roman nose" in profile (King 1972, 1983; Bonner 1981). Modifications of the nasal region parallel those in *Cystophora* and *Mirounga*, and to such a degree that it is often considered that *Halichoerus* should also possess some form of nasal appendage (King 1972).

Differences between the remaining members of the Phocini are slight. Despite being individually recognizable, the features of the skulls of each genus overlap to such a degree that Burns & Fay (1970) subsumed the four taxa as subgenera within a newly defined *Phoca* (also Doult 1942). *Halichoerus*, although closely related to the remaining Phocini, was not included in the newly defined *Phoca* due to an insufficient sample size to allow proper re-designation, coupled with sufficient cranial differentiation to allow it to be clearly set apart (Burns & Fay 1970).

However, this exclusion of *Halichoerus* does not appear to be justified. Arnason et al. (1995) note that the cranial characters used to distinguish *Halichoerus* would not merit generic distinction within the terrestrial carnivores, a point conceded by Burns & Fay (1970). In addition, most biomolecular studies indicate either no or equal difference between all the constituent genera of the Phocini (e.g., McDermid & Bonner 1975; Baram et al. 1991; Arnason et al. 1993; Arnason et al. 1995). Perhaps of more importance is the contention that *Halichoerus* is more closely related to the clade of *Phoca* (sensu stricto) and *Pusa* than either genus is to *Histriophoca* and *Pagophilus* (Chapskii 1955a; McLaren 1975; de Muizon 1982a; Mouchaty et al. 1995; Perry et al. 1995), thus rendering *Phoca* (sensu Burns & Fay) paraphyletic. A similar arrangement, with similar consequences for *Phoca* (sensu Burns & Fay), has been suggested infrequently between *Cystophora* and the clade of *Histriophoca* plus *Pagophilus* (de Muizon 1982a; Perry et al. 1995). [In any case, the close morphological similarity of *Histriophoca* and *Pagophilus* has been noted on many occasions (Chapskii 1955a; Davies 1958b; McLaren 1975), but may be based on symplesiomorphies (de Muizon 1982a).] As well, there are reports of interbreeding between *Halichoerus* and either *Pusa hispida* or *Phoca vitulina* in captivity (Chapskii 1955a; Scheffer 1958). In view of recent statements that the generic distinction afforded *Halichoerus* is inappropriate unless it is also applied to the subgenera of *Phoca* (sensu Burns & Fay) (Arnason et al. 1993, 1995), we will use *Phoca* in the strict sense and continue to recognize *Histriophoca*, *Pagophilus*, and *Pusa* as distinct genera.

In any case, phylogenetic resolution among the Phocini is generally poor. Most authors advocate two roughly equally derived main clades falling along *Halichoerus-Phoca-Pusa* and *Histriophoca-Pagophilus* lines (Chapskii 1955a; de Muizon 1982a; Arnason et al.

1995; Mouchaty et al. 1995; Perry et al. 1995). However, a primitive or ancestral status for either *Pagophilus* or *Pusa* within the Phocini has been suggested by some authors [Burns & Fay (1970) and Shaughnessy & Fay (1977), and McLaren (1966, 1975) respectively].

Altogether, these systematic difficulties within the Phocini likely stem from the relatively recent major radiation of the group [latest Miocene (Arnason et al. 1995) or post-early Pliocene and/or Pleistocene (Ray 1976a)], so that its members are not clearly differentiated from one another. This is especially true for *Phoca vitulina*, a species that has been described as being in the midst of a rapidly evolving “species swarm” (Ray 1976a: 402). Individuals of this species from the Atlantic and Pacific Oceans are readily distinguishable from one another (Allen 1902; Doult 1942; Chapskii 1955a, 1967; Davies 1958b; Arnason et al. 1995), but there is much debate as to the exact subspecific make-up of the Pacific subgroup [for summaries, see Shaughnessy & Fay (1977) or Bigg (1981)]. This impacts here primarily on the larga seal, a taxon distinguishable from other Pacific *P. vitulina* based on geographical, ecological, behavioural, and morphological grounds (Shaughnessy 1975), but of uncertain taxonomic status. It has variously been regarded as an unnatural, “garbage” taxon (Allen 1902), as a subspecies of *P. vitulina* (Scheffer 1958; Burns 1970; Shaughnessy 1975; Baram et al. 1991), as the species *Phoca largha* (Chapskii 1955a, 1967; McLaren 1966, 1975; Shaughnessy & Fay 1977; Bigg 1981; King 1983; Arnason et al. 1995), or of uncertain status (Allen 1880). As well, the population boundaries of the larga seal are highly contentious, ranging from encompassing all Pacific harbour seals (Chapskii 1955a), to only those inhabiting the western Cis-Asiatic region (roughly from the Chukchi Sea to the coast of China) (Scheffer 1958; Chapskii 1967), to only those in this latter region that breed on the pack ice (Shaughnessy & Fay 1977). For our purposes, we will accept the larga seal as the species *Phoca largha* [species description given in Chapskii (1967)] in order to establish its systematic relationship with *Phoca vitulina*. As well, we will recognize this species as inhabiting the entire western Cis-Asiatic region, a distribution that has become increasingly accepted.

The systematic status of the Monachinae

Since its inception, membership of the subfamily Monachinae has fluctuated from including only *Monachus* spp., to its present status of encompassing all southern hemisphere seals (lobodontines plus *Mirounga* spp.) plus *Monachus* spp. This instability appears to be due simply to an increasing refinement of phocid taxonomy with time, although it may relate to the suggestion of Wyss (1988a) that the subfamily is paraphyletic. This novel suggestion is apparently connected with the paraphyly of *Monachus*, and with the recognition of *M. schauinslandi* as the sister taxon of the remaining phocids in particular (Berta & Wyss 1994; see above). Although a strongly divergent adaptive radiation has been noted for the monachines (Ray 1976b), paraphyly of the subfamily would contradict a number of apparent synapomorphies, particularly among postcranial elements (see King 1966; Hendey & Repenning 1972; de Muizon 1982a), which would have to be re-interpreted as phocid symplesiomorphies. It also clashes with biomolecular evidence (Sarich 1975, 1976), and the finding that the monachines and phocines are equally ancient lineages with distinct representatives of each being found among the first

fossil phocids (Ray 1976a; de Muizon 1982a). The possible paraphyly of the monachines has not been adequately tested since Wyss's (1988a) analysis – studies conducted since have only examined a subset of all monachines, and the only study which corroborates paraphyly for the subfamily (Arnason et al. 1995) does so very weakly – and requires further confirmation.

Phocid phylogeny at the species level

The previous three points are specific, and somewhat contentious, instances of a much more pervasive problem. Overall, the species level relationships for all phocids remain to be fully and adequately elucidated. Much of this can be traced to the paucity of studies performed below the tribal level in phocids, where, of those studies that do, most concentrate on the Phocini at the expense of the monachine tribes. Another hindrance revolves around a similar lack of studies employing a rigorous methodology, and hence some form of testability. Such studies are limited to the morphometric analysis of Burns & Fay (1970); the cladistic studies of King (1966), de Muizon (1982), Wyss (1988a), and Berta & Wyss (1994); and the molecular studies of Arnason et al. (1995), Mouchaty et al. (1995) and Perry et al. (1995). However, these studies all possess one of the two shortcomings mentioned above. Burns & Fay (1970), Mouchaty et al. (1995) and Perry et al. (1995) only examined the phocines or a subset thereof in detail, Arnason et al. (1995) included only half of all monachines, while the resolution is limited in the four cladistic studies as each was essentially performed at the subfamily, generic, generic to tribal, and tribal levels respectively.

Beyond a possible lack of resolution, there is a real danger in performing cladistic analyses above the species level. Such studies tacitly assume the monophyly of the higher level taxa [with monophyly defined here sensu Hennig (1966): all and only the descendants of a common ancestor], something that with the lack of low level systematic studies has not been adequately demonstrated for most phocid taxa. Thus, we may be forcing a less than optimal phylogeny of the phocids as the potential for some taxa to be paraphyletic has not been allowed historically. This is classically demonstrated in the study of Berta & Wyss (1994). Despite their agreement with the earlier findings of Wyss (1988a), they reluctantly took *Monachus* to be monophyletic, causing them to question the validity of their indicated phylogeny for the whole of the monachines (Berta & Wyss 1994: 43). As well, studies assuming the monophyly of higher level taxa tend to make sweeping generalizations concerning character states, often obscuring important, and potentially informative variation within that taxon.

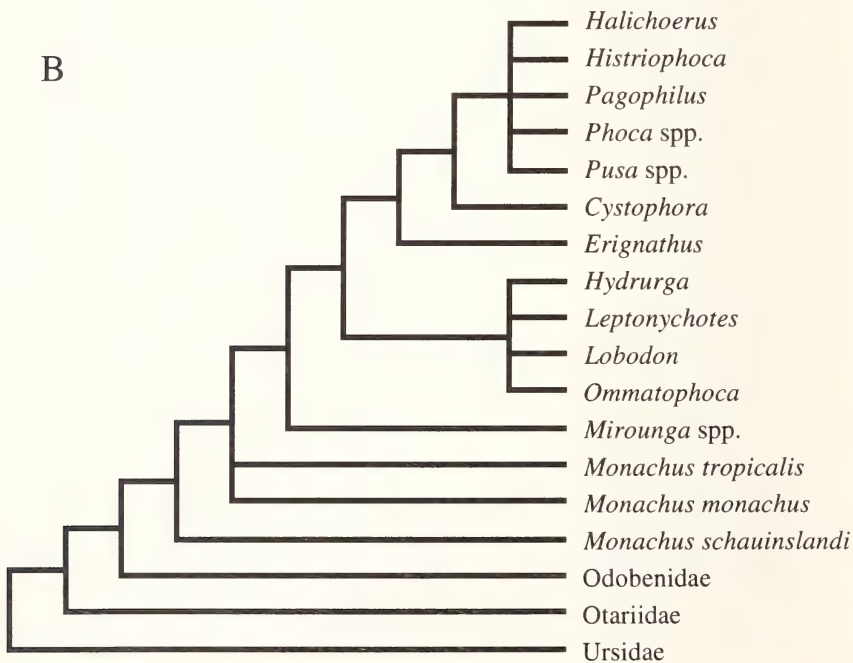
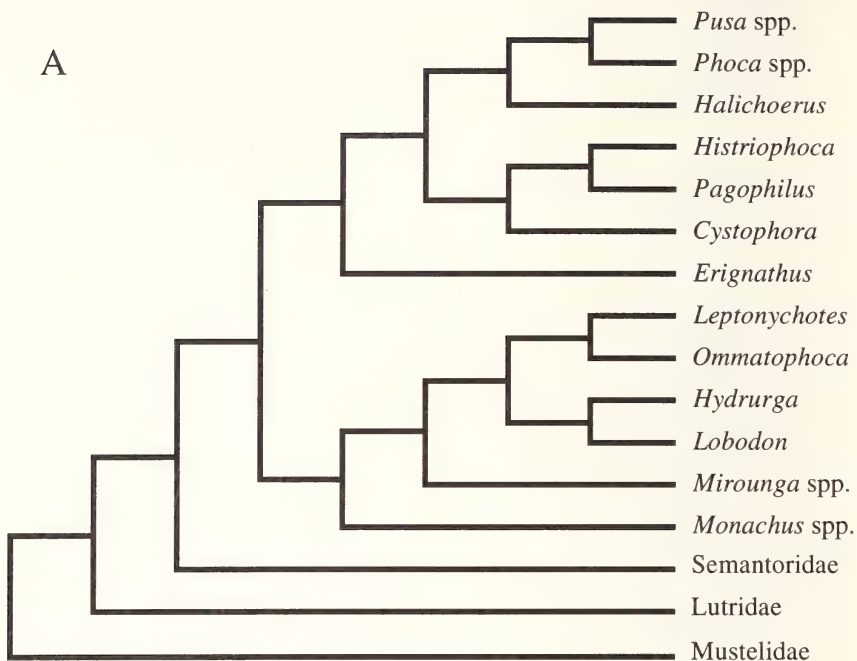
Although cladistic analysis is increasingly the method of choice in phylogenetic analysis (and will be used here), a cladistic solution for a species level phylogeny of the phocids may prove difficult. There is some suggestion that cladistic methodology has a functional lower limit around the species level, based on philosophical considerations of the species and of evolution in general [de Queiroz & Donoghue (1990); Wheeler & Nixon (1990); but see Vrana & Wheeler (1992) for a contrasting viewpoint]. More importantly, however, there may be more immediate methodological problems threatening to impede any potential cladistic solution (Arnold 1981). In any cladistic study, the exclusion of any taxa (whether by choice or through circumstance) may drastically alter the resultant phylogeny.

Although this problem potentially exists at all taxonomic levels, Arnold (1981) holds that it may become more detrimental at the lower levels. As well, as exemplified in the study of de Muizon (1982a), it may be difficult to identify enough shared derived features to adequately establish any species level relationships; Arnold (1981) has suggested that the frequency of synapomorphies likely decreases with decreasing taxonomic level (although molecular data may be more immune to this problem). These practical problems may be offset somewhat as most phocid genera are monotypic. Thus, except for the polytypic genera *Mirounga*, *Monachus*, *Phoca*, and *Pusa*, any species differences will essentially translate into generic differences.

Compounding all these problems is evidence for one or more relatively recent adaptive radiations among phocids. The case for the Phocini has been mentioned above, but Ray (1976a) also indicates that the full modernization of the lobodontines and of the phocines as a whole could have occurred no more than four million years ago, in response to climatic deterioration and adaptation to high latitudes (see also Repenning et al. 1979). With such a comparatively short time for differentiation, achieving full resolution within these groups might be difficult.

Ancestral affinities of the phocids

An important historical problem influencing phocid phylogeny is the uncertainty regarding phocid ancestry, a debate that underlies the controversy over whether the pinnipeds have a single or a dual origin. With regard to this latter question, a clear dichotomy is evident in the literature. Although the arctoid affinities of all pinnipeds are not in doubt (Flynn et al. 1988), most morphological, biogeographical, and paleontological studies historically favour a diphyletic origin for the pinnipeds, whereby the phocids are accorded a mustelid (possibly lutrine) ancestry, while the remaining pinnipeds (the otarioids) display ursid affinities (e.g., Flower 1869; Mivart 1885; McLaren 1960b; Hunt 1974; Ray 1976a; Tedford 1976; de Muizon 1982a, Wozencraft 1989; Nojima 1990). In contrast, most biomolecular and karyological studies support a monophyletic Pinnipedia of ursid ancestry, with the phocids and otarioids being sister taxa (e.g., Sarich 1969a, 1969b, 1975, 1976; Arnason 1974, 1977; Haslewood 1978; de Jong 1982; de Jong & Goodman 1982; Wayne et al. 1989; Vrana et al. 1994; Arnason et al. 1995; Lento et al. 1995). The monophyly hypothesis rests on the overall similarity between all pinnipeds in all aspects, including those features representing adaptations to an aquatic existence. Proponents of the diphyly hypothesis dismiss these latter features as being convergent [see especially Mitchell (1967) and Repenning (1990); but see Wyss (1989) for a contrasting viewpoint], and emphasize other, non-aquatically related, similarities between the appropriate taxa. An especially strong argument for the diphyly camp rests with the different centres and timing of the first appearance of the otarioids [North Pacific about 22 million years before present (MYBP)] versus the phocids (North Atlantic about 15 MYBP) in the fossil record (Repenning et al. 1979). The case for diphyly is also strengthened by the suggestion of the fossil taxa *Potamotherium*, and possibly *Semantor*, as putative intermediates between the phocids and their musteloid ancestors (Ray 1976a; Tedford 1976; de Muizon 1982a). Recently, however, there has been increasing acceptance of a monophyletic Pinnipedia, due not only to molecular work (see above), but also to numerous morphological studies



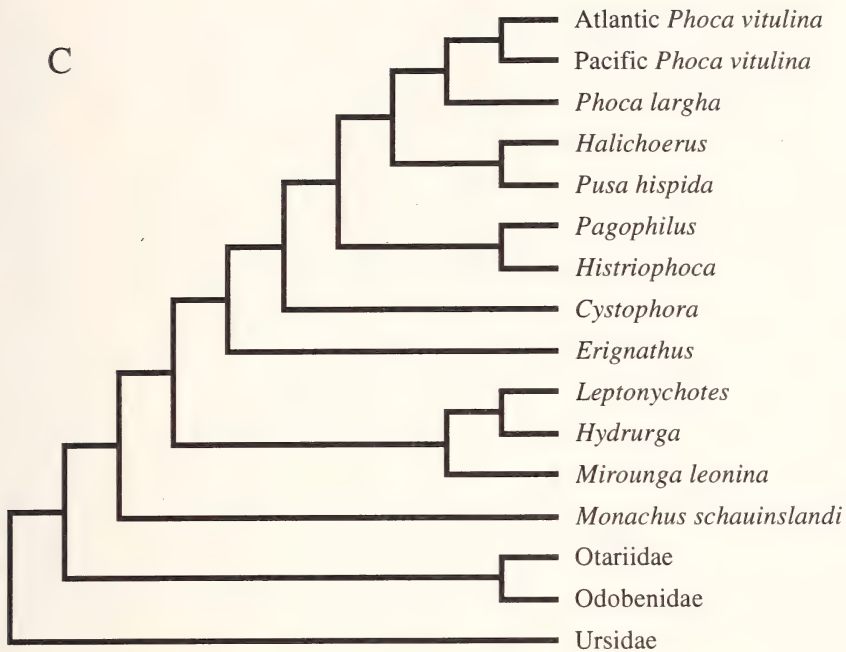


Fig.1: Phylogeny of the Phocidae according to (A) de Muizon (1982a), (B) Wyss (1988a), and (C) Arnason et al. (1995). Adapted from de Muizon (1982a), Wyss (1987, 1988a), and Arnason et al. (1995).

supporting such a scenario (e.g., Wyss 1987; Wolsan 1993; Wyss & Flynn 1993; Berta & Wyss 1994; Hunt & Barnes 1994). But within such a framework, Wyss (1987) held the Otarioidea to be related by symplesiomorphies only, and instead proposed an *Odobenus*-phocid clade with an otariid sister group. This arrangement has since become the dominant view of pinniped phylogeny (e.g., Flynn 1988; Berta 1991; Cozzuol 1992; Wyss & Flynn 1993; Berta & Wyss 1994; Vrana et al. 1994).

Similarly, most workers in this area now also accept the ursids to be the sister group of the pinnipeds, although several morphological or immunological studies persist in proposing a mustelid, and not ursid, ancestry (e.g., Arnason & Widegren 1986; Miyamoto & Goodman 1986; Wolsan 1993). However, much of this discussion may be moot. As Repenning & Tedford (1977) note, considerations of polyphyly are largely dependent on the definitions employed. Additionally, both fossil and molecular evidence indicate that the mustelid, ursid, and pinniped lineages were all diverging at about the same time from the primitive arctoid stock (Sarich 1976; Wayne et al. 1989; C.A. Repenning pers. comm.). Hence, any discussion of mustelid or ursid affinities for the pinnipeds may be irrelevant as these two groups may not have truly existed at the time of pinniped divergence. Thus, the whole question of pinniped ancestry may form part of

an unresolvable polytomy. This was one option put forth by Flynn et al. (1988), the other being an ursid sister group to the pinnipeds. Taken together, this discussion demonstrates that the question of phocid affinities (and those of the remaining pinnipeds) within the Arctoidea should still be regarded as being uncertain, if they are even resolvable to begin with.

Yet, the question of phocid ancestry still bears critical importance to the determination of the internal relationships of the phocids. In cladistic analysis, the accepted method of determining character polarities is through outgroup analysis (Hennig 1966; Arnold 1981; Wiley 1981; Maddison et al. 1984). Normally, this procedure is reasonably straightforward, with the most closely related taxon to the ingroup designated as the outgroup, and thus serving to identify the primitive states for the various characters examined. However, with respect to phocid phylogeny, the uncertainty regarding the ancestral affinities of the phocids complicates the question of designating an outgroup taxon. Yet, rather than employing multiple outgroups and allowing the analysis to dictate the most closely related outgroup taxon (and thus character polarities), most studies examining internal phocid relationships have, to date, either not stated an explicit outgroup, or have assumed either an ursid or mustelid (and occasionally lutrine) outgroup, thus potentially biasing the resultant character polarities [see Maddison et al. (1984) for some of the errors inherent in selecting outgroups and how they can, in turn, affect an analysis using outgroups].

Goals of this project

Currently, most of our knowledge concerning phocid phylogeny derives from the studies of de Muizon (1982a), Wyss (1988a), and, recently, Arnason et al. (1995) (Fig.1). However, each study possesses important shortcomings. All three phylogenies are dependent upon the supposition of a particular arctoid outgroup (lutrine, ursid, and ursid respectively). In the case of Wyss (1988a), we feel that such an assumption was not adequately tested in a prior analysis (Wyss 1987; see also Wozencraft 1989). In de Muizon's (1982a) study, some of the characters used deserve closer scrutiny (e.g., aquatic, high snout, "important" sexual dimorphism), several clades are supported by only a single character, and conflicting (i.e., homoplasious) characters are not mentioned. Yet, despite their limitations and conflicts with each other, these three studies provide the best resolved cladograms of the phocids to date.

Using these three studies as a guide, and bearing the five outstanding problems we have identified above in mind, we present the current state of knowledge regarding phocid phylogeny in Fig.2. The cladogram is characterized by large regions of uncertainty and poor resolution, primarily within the Lobodontini and Phocini, within the polytypic genera, and for the ancestral affinities of the phocids as a whole. One area of strong, almost universal, agreement concerns the most primitive members of each phocid subfamily: *Erignathus* for the phocines (Chapksii 1955a; King 1966, 1983; Burns & Fay 1970; McLaren 1975; Ray 1976a; Wyss 1988a; Berta & Wyss 1994; Arnason et al. 1995; Mouchaty et al. 1995; Perry et al. 1995) and *Monachus* spp. for the monachines (Hendey 1972; Repenning and Ray 1977; Repenning et al. 1979; de Muizon 1982a; King 1983; Wyss 1988a; Arnason et al. 1995; Lento et al. 1995).

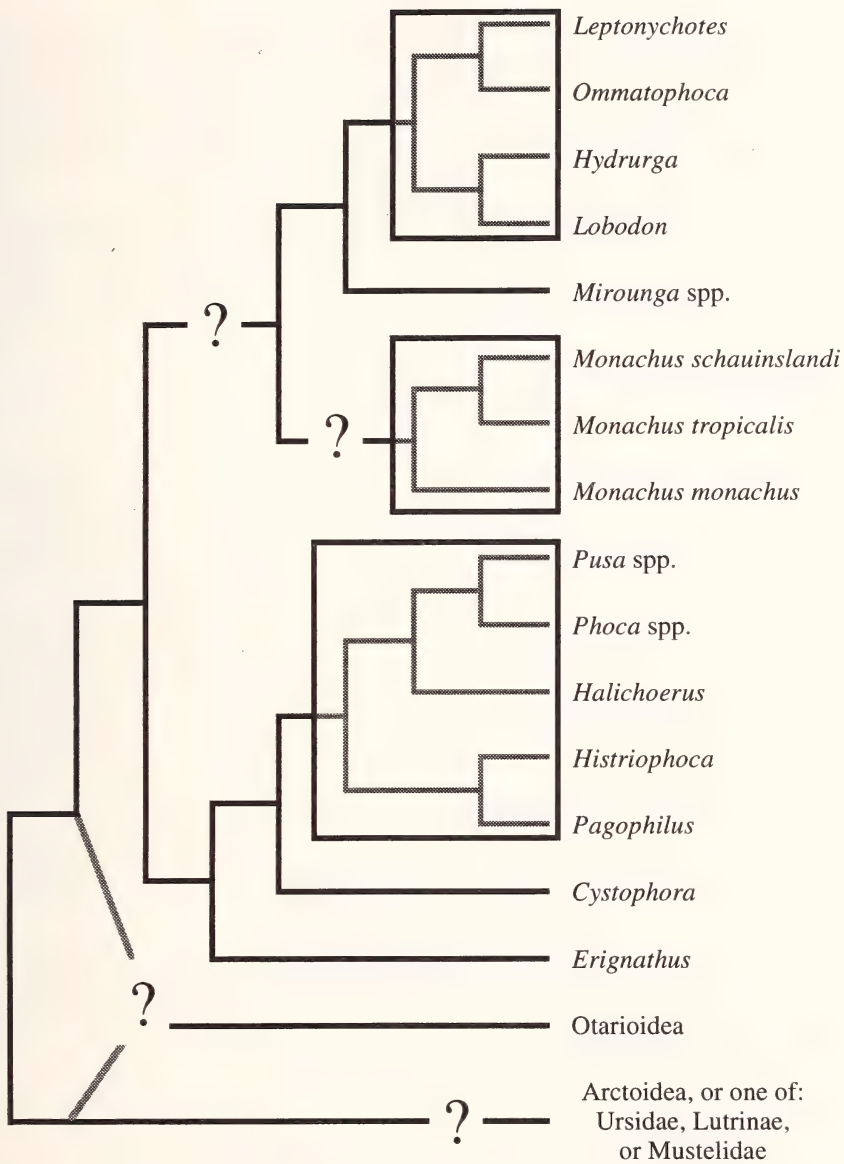


Fig.2: Diagrammatic representation of the current state of knowledge regarding phocid phylogeny. Rectangles indicate monophyletic groups with uncertain internal phylogeny (with the most commonly suggested pattern filled in when possible). Question marks refer to either general uncertainty (outgroup relationships) or to possible instances of paraphyly (ingroup relationships).

The overall goal of this study is to attempt to answer the five outstanding questions regarding phocid phylogeny that we have identified above. This is done via a cladistic analysis (sensu Hennig 1966) based on parsimony, using the outgroup method to determine character polarities. Morphological data are used exclusively. Further assumptions and details concerning this analysis are found in the **Methods and Materials** section, with the results being presented in the **Overall Parsimony** section.

The remainder of this study deals largely with the various means available to judge the robustness of the indicated solution. Attempts to place confidence intervals on phylogenies/taxonomies have been difficult, and thus have only rarely been carried out. One advantage of cladistic analysis in this regard is its ability to roughly indicate the support for a solution (or any portion thereof) by the number of synapomorphies supporting various nodes of the cladogram. However, this measure of support is still somewhat subjective, as it is dependent upon the characteristics of the data set (e.g., the number and type of characters examined) and therefore does not allow for easy comparison between data sets. Cladistics has recently seen the development of statistical and other comparative tools that seemingly allow an even more objective assessment of the quality of a solution, as well as facilitating comparisons between different phylogenetic hypotheses. Again, the tests and assumptions behind them are described in the **Methods and Materials** section, with the results presented in **Statistical Tests** and **Comparative Tools** sections.

With the rise of the use of statistics in cladistics, the realization that any cladistic hypothesis is only as good as the data it is based upon seems to have been forgotten. This point becomes even more crucial when one realizes that the outcomes of most of the newly-developed statistical procedures seem to be consistently misinterpreted (see **Statistical Tests**). Thus, we are left with one real, but increasingly rarely used "test" as to the quality of a solution: an in-depth examination of the characters that were used. This is to be found in the **Character Analysis** section, in which descriptions and historical notes are presented for all the characters examined in this study, together with a description of the evolutionary pathway implied for each character by the overall solution that was found.

Finally, this study concludes by examining such broad-ranging topics as potential sources of error, future lines of research, miscellaneous corroborating evidence (biogeography and timing of parturition), and the taxonomic implications of the proposed phylogeny of the phocid seals advocated herein.

ACKNOWLEDGEMENTS

This contribution grew from the M.Sc. thesis work of the senior author. For comments and suggestions throughout that process, the assistance of Marc Ereshefsky, Larry Linton, Gordon Pritchard, Herb Rosenberg, and especially Harold Bryant are gratefully acknowledged. Late hints by Andy Purvis helped to round things out. We also thank the many people involved in loaning us specimens, or providing access to collections in their care: Dr. G.G. Musser and W.K.-H. Fuchs (American Museum of Natural History, New York); Dr. Ted Daeschler and Fred Ulmer (Academy of Natural Sciences of Philadelphia);

Miss Paula Jenkins, Richard Sabin, Mary Sheridan, Daphne Hills, and Richard Harbord [British Museum (Natural History)]; Dr. Maria E. Rutzmoser and Judy Chupasko (Museum of Comparative Zoology, Harvard); Dr. Harold N. Bryant (Provincial Museum of Alberta); Dr. Wayne Roberts (University of Alberta Museum of Zoology); Warren Fitch (University of Calgary Museum of Zoology); Drs. James G. Mead, Charles W. Potter, Clayton E. Ray, and Dave J. Bohaska (United States National Museum, Washington, D.C.); and Mr. John Rozdilsky (University of Washington Burke Museum). Funding for this project was provided by an NSERC postgraduate A scholarship, a University of Calgary Thesis Research Grant, the Jake Duerksen Memorial Scholarship from the Department of Biological Sciences (OBE), and by an NSERC operating grant (APR).

METHODS AND MATERIALS

Data sources

Specimens

For this study, all extant species of phocid seal plus extant representatives of all major caniform lineages, with an emphasis on putative phocid or pinniped sister groups, were examined (see Appendix A). Although the Caribbean monk seal, *Monachus tropicalis*, is believed to have been extinct since the early 1950s (Kenyon 1977), its persistence well into historical times, its potentially critical role in the resolution of the systematic status of the monk seals (genus *Monachus*) as a whole, and that fact that it is as well-represented in museum collections as any other extant phocid species caused it to be included in this study. Specimens were examined either while they were on loan from or in their respective institutions.

A conscious decision was made to exclude fossil taxa from this study. This was largely due to a lack of available specimens, with most being on loan to other institutions at the time of the museum visits. This is unfortunate as the inclusion of fossil specimens can serve to bridge large gaps between highly divergent extant taxa (Gauthier et al. 1988) such as exist here between the pinnipeds and other arctoid carnivores. Selected fossil forms may also reveal much concerning phocid and/or pinniped ancestry. For example, the advocacy of the lutrine-like fossil *Potamotherium* as an intermediate between the mustelids and phocids is a key argument supporting the hypothesis of a diphyletic Pinnipedia (Ray 1976a; Tedford 1976), or at least a mustelid affinity for all pinnipeds (Wolsan 1993). Likewise, the previously regarded otarioid-like fossil desmatophocids (= *Allodesmus*, *Desmatophoca*, and *Pinnarctidion*) are now regarded as the putative phocid sister group within a monophyletic Pinnipedia (Wyss 1987; Berta 1991; Wyss & Flynn 1993; Berta & Wyss 1994). Finally, the exclusion of any taxa, whether extant or fossil, from such a low level analysis may have deleterious effects on the resulting cladogram (Arnold 1981). These points are countered somewhat by the admittedly poor fossil record of pinnipeds (Davies 1958b; Hendey 1972; Hendey & Repenning 1972; Ray 1976a), and the generally high preponderance of missing features (and hence data) in fossil specimens. As well, the inclusion of fossil pinnipeds does not seem to alter the phylogenetic relationships of the pinnipeds as determined from the analysis of extant forms alone (Flynn et al. 1988; Berta &

Wyss 1994), although it may alter the implied evolutionary pathway of selected characters. However, given a reasonable degree of completeness (see Huelsenbeck 1991b), the overall potential advantages of including fossil evidence cannot be discounted.

Although there are suggestions in the literature that molecular data may operate more effectively than morphological data at lower taxonomic levels (e.g., Novacek 1993), morphological data were used exclusively. This largely reflects the availability of such data for all the desired species. Among phocids, both *Mirounga* spp. and *Monachus* spp. are CITES-listed animals (Anonymous 1992), and all pinnipeds are subject to the Marine Mammal Protection Act, making the acquisition of fresh samples as a source of molecular data difficult. As well, the full potential of morphological data at low taxonomic levels may not have been properly exploited yet, with the use of non-traditional or multistate characters (see **Character Analysis** and Bryant 1989), possibly derived from techniques such as morphometric analysis (see **Discussion** and **Conclusion**), hopefully improving the effectiveness of this type of data in such cases.

Data were obtained primarily from osteological specimens (see also **Characters** below). This was necessitated by the tendency of museums to preserve mammals as skulls, skeletons, and study skins. Furthermore, as phocids are fairly large mammals, many specimens are represented by skulls alone. Generally, the best available (i.e., most complete and undamaged) specimens for a given species were selected for study while attempting to maintain an equal sex ratio. This latter point was especially important for such grossly sexually dimorphic taxa as *Zalophus californianus* and *Mirounga* spp. Damaged specimens were occasionally employed to view various internal characters of the skull. Missing data were substituted by literature values wherever possible.

Numerous specimens of each taxon were examined in order to take account of intraspecific variation. This was especially important for the pinnipeds, as they apparently display an inordinate amount of intraspecific variation, primarily in their cranial characters (Mivart 1885; Doult 1942; Davies 1958b; Ray 1976b). With respect to phocids, King (1966) has also commented on how the large intergeneric differences of the skull confound comparisons between the genera, and on the potential problems resulting from the high intraspecific variability of the teeth. (She does add, however, that the tympanic region seems to be relatively stable.) Unfortunately, however, postcranial material, and especially the distal elements of the limbs, were typically only obtainable from a restricted number of specimens. An extreme case is for *Pusa caspica*, where all postcranial observations were derived from a single individual.

Although Hennig (1966) notes that characters can be taken from any life stage of an organism (i.e., any semaphoront), juvenile individuals were also largely excluded from this study. This primarily reflects the very poor representation of juvenile specimens in museum collections. However, this decision secondarily served to minimize the already high intraspecific variation observed in phocids (see above) by avoiding comparisons between vastly different age classes.

Characters

A total of 196 characters were examined in this study (see Appendix B). Characters were selected so that they were at least theoretically observable from the material typically

present in museum collections. The vast majority (191 characters) were osteological, originating from both the cranial (153 characters) and post-cranial skeleton (38 characters). This disposition towards osteological cranial characters reflects both the high information content of the skull in mammals, and the tendency of museums to preserve large mammals as skulls only. The osteological characters were divided according to their general region as follows: snout, 21; orbit and zygomatic arch, 35; palate and ventral side of snout (excluding teeth), 18; basicranial region, 43; bony tentorium and bony falx, 5; dorsal braincase, 4; teeth, 23; mandible (excluding teeth), 3; miscellaneous skull, 1; forelimb, 17; pelvis, 8; hind limb, 12; and miscellaneous post-cranial, 1. Twenty-eight of the originally selected and recorded characters were excluded from the analysis for various reasons (see **Character Analysis**), leaving a functional total of 168 characters. The fact that a character was autapomorphic (including those multistate characters with autapomorphic states) was not considered sufficient grounds for its exclusion (see Yeates 1992). Although such characters do not provide grouping information, their inclusion here reveals cases of unusual and previously undocumented morphologies, or of when our observations do not accord with those of the literature, calling the value of the particular character into doubt. Specific descriptions of all individual characters, including those deleted from the analysis, are found in the **Character Analysis** section.

Data collation

For the 27 taxa used in this study, a total of 286 specimens were examined (see Appendix A). The data editor of MacClade 3.0 (Maddison & Maddison 1992) was used to input the character states for each individual specimen and to generate a consensus set of character states for each species. Polymorphic data (i.e., when a specimen simultaneously possessed two or more states or, more commonly, was intermediate between two supposedly discrete morphologies) were maintained.

Although all variation is important and potentially informative, the large amount of intraspecific variation, primarily among the phocids, required some manner of resolution. Retention of every state indicated for a species by its representative specimens would unnecessarily clutter the analysis (and thereby possibly decrease resolution) with what amount to statistical outliers. Clearly, some states were more predominant than others within a species, and it was these presumably more informative states that needed to be retained. We accomplished this with a modified majority rule algorithm which would hopefully maintain only the more predominant character state(s). For a given taxon and a given character, the consensus state was ordinarily the most frequent state among all specimens for that taxon. Note that polymorphic data, such as when a specimen possessed both states 0 and 1, were treated as a discrete state (the state "01"), rather than independent occurrences of the singular states. However, if the next most frequent state(s) possessed the same frequency, or the same frequency minus one observation (i.e., highest frequency -1), then the consensus state was a combination of these "equally" most frequent states (i.e., the taxon was counted as being polymorphic for that character).

The only exception to the above formula occurred if one or more of the "equally" most frequent states was polymorphic to begin with. In this case, the specimen polymorphisms were "broken", the frequencies for each singular state were counted, and the above

algorithm was reapplied. This was necessitated as the normal polymorphic consensus between the "equally" most frequent states 0 and 01, for instance, is meaningless (i.e., the state "001"), and probably reflects a greater preponderance of state 0 in that particular taxon. However, note that a polymorphic consensus could still result if two or more singular states happened to be "equally" frequent.

The overall effect of this algorithm was to produce many polymorphic taxa, something fairly uncommon in phylogenetic analysis. It is unclear to us exactly why this is the case, but it is likely done (whether through the selection of characters that yield monomorphic taxa, through the algorithms employed to arrive at consensus states for the taxa, or by simply coding polymorphic data as missing) to simplify the overall analysis. However, we believe that the large amount of polymorphism that we observed to be natural and important, with its undue restriction resulting in the loss of a great deal of potential information. This same procedure was employed to collapse species into a higher level taxon for the condensed analysis (see below). The final data matrix appears in Appendix C.

Cladistic analysis

A cladistic analysis (*sensu* Hennig 1966) of the final data matrix was conducted using the parsimony program PAUP 3.1.1 (Swofford 1993). PAUP was also used to conduct the many statistical tests and comparative tools employed in this study to judge the robustness of the overall solution (see below).

Despite its supposed increased objectivity over other systematic methods, a cladistic analysis still entails a large number of assumptions, both about how the data are to be treated and how the actual analysis is to be conducted. The numerous assumptions we have made concerning the data (both characters and taxa), the implications thereof, and their apparent advantages over alternative assumptions are described first. This is followed by an explanation of both the search criteria and methods of summarizing the output that were used.

Assumptions concerning characters

All characters were assumed to be of equal weight, and multistate ones were held to be unordered. Although either case requires assumptions equal in magnitude to weighted or ordered characters (Sober 1988; Barrett et al. 1991), they were resorted to out of simplicity and/or ignorance. In the first case, equally weighted characters typically imply independence among characters (as co-dependent characters are accordingly down-weighted), and/or characters of roughly equal importance, reliability, or quality [see Underwood (1982) and Bryant (1989) for other uses of weighting]. However, this is not implied here. As we could not objectively determine the degree of character independence, nor relative character importance *a priori*, we adopted the simplest solution, that of equally weighted characters.

Indeed, we make no pretense as to the independence of our characters. By all being drawn from the same organism, all characters will be correlated with one another to some degree. However, to our knowledge, there has never been a test devised that quantifies the level of character independence or correlation, nor has it ever been explicitly stated what level

of independence is sufficient for a cladistic analysis. As well, mere word play can apparently increase the degree of independence of a group of otherwise highly correlated features. For example, we examined four features of the incisive foramina in this study (roughly size, shape, location, and number; see **Character Analysis**). But, by redefining these characters in terms of other variables (e.g., size of the nasopalatine nerve passing through the foramina, presence of a down-growth of the premaxilla or not, ...), they cease being incisive foramina characters at first glance. Finally, recent evidence indicates that character independence for a single structure may, in some cases, be greater than previously presumed. Atchley & Hall (1991) suggest that the single mammalian dentary bone (as evidenced by the mouse) may, in fact, be composed of up to six separate centres of ossification or condensation, one for each of the ramal, incisor, molar, condyloid process, coronoid process, and angular process regions. Thus, there is at least the potential for each to be acted upon independently during ontogeny, and thus phylogeny. In other words, the mammalian mandible could justifiably be represented by up to six characters (one from each of the regions above) and not violate the independence criterion. Therefore, in selecting a set of characters, the best solution is likely to represent all body regions as much as possible (within the constraints of their relative information content), and not to over-represent any one region or feature to any great extent.

One clarification is required with respect to the phrase “equal weighting”. PAUP’s algorithms essentially weight characters in proportion to the number of states they possess, thereby artificially attaching greater importance to multistate characters (Swofford 1993). To correct for this, all characters were inversely weighted (base weight = 100) according to the number of states each possessed. So, “equally” weighted will, hereafter, be taken to mean inversely weighted, and not unweighted (i.e., where all characters share some identical weight “x”). Unfortunately, inverse weighting creates rather unwieldy tree lengths, obfuscating discussion and comparison of less than most parsimonious solutions. To compensate for this, discussion is directed towards the number of character state changes (or, equivalently, the number of synapomorphies, both of which equal the number of unweighted steps) along a branch, and not the branch lengths derived from inverse weighting. When this is not possible, “corrected steps” were devised and are referred to. These are simply the absolute number of inversely weighted steps divided by the average character weight of the inversely weighted character set (= 69), rounded up to the next whole number. Both methods appear to be roughly equivalent (i.e., corrected steps appear to be a reasonable estimator of the number of character state changes), based on preliminary comparisons when both were available.

Unordered characters (i.e., Fitch parsimony) were likewise used, as we could not conclusively identify the exact sequence of character transformations based on criteria set out by Hauser & Presch (1991). Thus, all possible transformations were allowed and were considered to be equally probable. In any case, the supposed advantages of ordered characters (e.g., increased resolution and stability, and fewer equally most parsimonious solutions) may be overstated. While ordering may be advantageous for a single character, such is not necessarily the case over an entire matrix due to the interaction of all characters (Hauser & Presch 1991).

Although some authors indicate that both missing data and inapplicable characters (e.g., feather size for mammalian taxa) be coded as "missing" (represented by a question mark) (e.g., Swofford 1993), a distinction was made here between these two cases. Inapplicable characters were instead assigned to a discrete state (state 9), as advocated by Maddison (1993). Largely, this ties in with how PAUP (and other computer algorithms) treat missing data. PAUP will initially treat the missing datum as if it were almost entirely absent from the tree (at least with respect to that character), and then later attempt to infer an appropriate state for any missing data based on parsimony (Maddison 1993). While this latter step is valuable when the state is unknown due to ignorance (creating a valuable hypothesis to be tested in the future), it is clearly inappropriate for inapplicable characters in that PAUP may infer a state that clearly does not apply to the taxon in question (e.g., "large feathers" in mammals when it should really be "feathers absent") (Platnick et al. 1991).

Assumptions concerning taxa

In dealing with the large number of polymorphic taxa, PAUP's multistate taxa option was set at "polymorphism", forcing PAUP to account for all but one of a polymorphic taxon's states in the most parsimonious way possible by invoking changes within this terminal taxon (Swofford 1993). Although the underlying assumption of this setting is that the multistate taxon is a heterogeneous group (i.e., a higher level cluster of morphologically variable taxa), this setting comes the closest to treating the indicated polymorphisms as real and important. The alternative setting, "uncertainty", selects only the most parsimonious state out of the set provided, ignoring the remaining states, and thus the polymorphism, altogether. However, one limitation of "polymorphism" is that PAUP will not form a polymorphic ancestral taxon, even if all of its descendants are identically polymorphic (Swofford 1993). Although this results in the loss of much potential grouping information, it should be noted that the other major phylogeny inference packages (i.e., Hennig86 v1.5 and PHYLIP v3.5) will not handle polymorphic data at all (Sanderson 1990).

The taxa *Canis lupus*, *Enhydra lutris*, *Lutra canadensis*, *Martes americana*, *Odobenus rosmarus*, *Procyon lotor*, *Ursus americanus*, and *Zalophus californianus* (hereafter referred to solely by their generic appellations, as are the monotypic phocid genera) were assigned as outgroup taxa. In so doing, we assumed that each taxon is a representative member of a higher level taxon: canids, lutrines, mustelids minus lutrines, odobenids, procyonids, ursids, and otariids respectively. This is almost certainly not the case, but we deemed the alternative, using the presumed ancestral state for each higher level taxon, as less desirable. Such an assessment requires at least some tacit assumptions about both the internal phylogeny and ancestral affinities of the higher taxon. As well, the use of ancestral states may conceal the presence of some potentially important derived subgroups with which the true affinities of the ingroup may lie. In any case, trees were rooted such that the collective outgroup used here was forced to be paraphyletic with respect to the phocids (which were forced to be monophyletic) in accordance with the current views on caniform phylogeny (see Tedford 1976; Flynn et al. 1988; Wyss & Flynn 1993; Vrana et al. 1994).

Search criteria and summarizing output

The number of taxa examined here prevented an exact solution from being found (via exhaustive or branch and bound algorithms). Therefore, PAUP's heuristic search option was used, which although highly effective, cannot guarantee an optimal solution (Swofford 1993). Unless otherwise indicated, all searches were heuristic and used a random addition sequence (with 25 repetitions), TBR branch-swapping on minimal trees only (with steepest descent on), collapsed zero-length branches, and an unlimited number of MAXTREES. This combination of options seemed to be the most effective in finding an optimal solution, and should minimize the analysis becoming trapped in local optima or on islands of less than optimal trees (Maddison 1991; Swofford 1993).

In those cases where multiple equally most parsimonious solutions were found, the rival results were summarized through the use of both strict and majority rule consensus trees. These two methods provide different types of information. By retaining only those groups that are found in all rival solutions, strict consensus trees will identify regions with multiple, conflicting solutions as polytomies. However, within these regions, some groups may occur with a greater frequency than others. The majority rule consensus algorithm, by retaining those groups found in greater than 50% of the rival solutions, will tend to preserve these more frequent groups that are ignored by the strict algorithm.

Character state assignments for internal nodes (see **Character Analysis**) were reconstructed using both accelerated and delayed transformation optimization criteria (ACCTRAN and DELTRAN respectively). With no ambiguity in the reconstruction of a character, both methods will yield identical results. For equally parsimonious reconstructions of a homoplastic character, ACCTRAN optimization will tend to favour an early origin of the derived state, followed by a reversal back to the more primitive state, while DELTRAN optimization will tend to favour later parallel derivations of the derived state (but note that these are not hard and fast rules) (Wiley et al. 1991; Swofford 1993). Thus, the repeated claims of a predisposition towards reversals in phocid (and especially phocine) evolution (e.g., Wyss 1988; Berta & Wyss 1994) may reflect the singular use of ACCTRAN optimization (the default choice in PAUP). A third optimization criterion available in PAUP, MINE, was not employed as its output is often identical to that of DELTRAN optimization (Swofford 1993).

Statistical tests

One of the more active areas in theoretical cladistics in recent years has been the development, and subsequent dissection, of various statistical tests designed to objectively quantify the robustness of a given cladogram. In this section, each of the tests used in this study are described in turn, including their objectives, their shortcomings and/or criticisms, and how they were implemented here.

Goodness-of-fit statistics

The most basic method used to judge the quality of a solution is the use of one or more goodness-of-fit statistics: consistency index (CI), homoplasy index (HI), retention index (RI), and rescaled consistency index (RC) [see Farris (1989), Wiley et al. (1991), and

Swofford (1993) for definitions and descriptions of each]. These indices can refer either to the fit of individual characters or of the data matrix as a whole (where they are referred to as ensemble indices) to a given tree topology. Unless specified otherwise, the goodness-of-fit statistics quoted herein always refer to the optimal, and not consensus solutions of an analysis.

The utility of the CI (and presumably the HI) is limited by it being inflated by autapomorphic features (which can be corrected for as is done herein), as well as being dependent on both the number of states a character possesses and the size of the data set (Farris 1989; Wiley et al. 1991; Swofford 1993). Both the RI and the RC have been designed to avoid these shortcomings; however, this latter property does allow the calculation of expected CIs for data sets of various sizes (see Sanderson & Donoghue 1989), and hence a means to more objectively judge the quality of a solution.

Although Swofford (1993) indicates that the HI behaves slightly differently when multistate taxa are interpreted with the "polymorphic" option (as change is now allowed within the taxon terminals), this appears to be true for the other three indices as well. Presumably, this derives in part from PAUP's failure to designate multistate ancestral nodes under this option (see above). Therefore, identically polymorphic taxa within a clade will each gain their identical second states by convergence within their respective terminals, rather than via inheritance from a similarly polymorphic common ancestor. However, as this scenario is the proper interpretation for distantly related taxa, the overall effect on a given index will be dependent on the distribution of polymorphisms among the taxa.

It should be pointed out that these indices are merely different ways to indicate levels of homoplasy in a solution. Unfortunately, the tendency in phylogenetic studies based on a parsimony criterion is to automatically equate increased homoplasy with a poorer solution. However, it is reasonable to expect that different groups will be characterized by different levels of homoplasy, so that a high level of homoplasy may be diagnostic of the group under study, rather than of a poor solution. Therefore, these indices should really be limited to comparing different solutions for the same group.

The bootstrap (Felsenstein 1985)

The bootstrap is a non-parametric statistical procedure adopted for use in phylogenetic analysis by Felsenstein (1985). It aims to infer the variability of an unknown distribution (the true phylogeny) from which data were taken (the characters) by resampling with replacement from the data. By taking a large number of replicates, one can estimate the confidence interval of the original unknown distribution. Groups that are supported by a large number of characters will be found in most solutions. The bootstrap frequency indicates the proportion of all solutions that a particular clade was found in.

Despite its widespread use, the bootstrap has shown some problems in its adaptation to phylogenetic analysis. [It apparently has a larger problem in that, despite concerted effort, it has never been demonstrated to be a valid technique for those applications in which it is supposed to be used (L.R. Linton pers. comm.).] These problems derive largely from the key assumption that the data be independently drawn and identically distributed (i.e., a representative, random sample of all possible characters) (Felsenstein 1985; Sanderson

1989). Sanderson (1989) has indicated that this is not likely the case for most systematic studies, so bootstrap frequencies are probably not estimates of the true confidence intervals. The use of replacement during sampling may also artificially increase character non-independence by allowing the same character to be sampled more than once (L.R. Linton pers. comm.). As well, the bootstrap can become problematic when parsimony is used to estimate phylogeny and rates of evolution in the various lineages are greatly unequal (Felsenstein 1985). Thus, the bootstrap solution may differ from the most parsimonious one, a difference that arises from the fact that the bootstrap represents a phylogeny estimated from repeated samplings and not the real one (Felsenstein 1985), and from the properties of consensus trees, of which the bootstrap solution is one (Swofford 1993).

These problems seem to become detrimental to the analysis when more than two topologies are possible (as is usually the case in phylogenetic studies), prompting some algorithmic or procedural corrections (Hall & Martin 1988; Rodrigo 1993; Li & Zharkikh 1994, 1995). However, the only "correction" that we have heeded is Hedges's (1992) suggestion that most studies involving the bootstrap do not use enough replications, with at least 500 replications being required to ensure that the bootstrap frequency is within one percent of the 95% confidence interval. In recognition of all of these difficulties and the varying opinions as to the utility of the bootstrap (see Felsenstein & Kishino 1993; Hillis & Bull 1993), bootstrap frequencies are interpreted here as rough indicators of support for the various nodes of the cladogram, and not as true confidence intervals.

Herein, 1,000 bootstrap replicates were conducted using the heuristic search option of PAUP. Heuristic searches were identical to that detailed above except that taxa were added with the CLOSE algorithm with HOLD = 10, and with only 100 MAXTREES allowed for each replication. Only the 168 included characters were sampled, and with equal probability (i.e., their inverse weights were not used to designate repeat counts of a character). "Irrelevant" characters (primarily autapomorphies here) were retained with the suggestion that they do not adversely affect bootstrap results (Harshman 1994).

Permutation tail probabilities (PTP) (Archie 1989; Faith & Cranston 1991)

The PTP test seeks to assess the degree of phylogenetic structure in a data set based on the amount of cladistic covariation between its characters, as compared to a matrix that possesses random covariation. A data set with an associated solution that is shorter than a statistically significant proportion of those derived from a number of random data sets (e.g., by being within the lower fifth percentile of tree length) is said to possess "significant cladistic structure" (Faith & Cranston 1991). Random data sets are constructed from the original by randomly permutating character states between the included taxa within each character. Outgroup taxa are excluded from this process to maintain polarity assessments. Thus, each random data set maintains most of the characteristics of the original.

Several methods exist to assess the level of significance of a PTP test. The simplest is the PTP statistic which is defined as the proportion of all data sets (original and random) that produce a tree as short or shorter than that derived from the original data set (Faith & Cranston 1991). A critical length value corresponding to the desired level of significance

can also be determined by simply arranging the lengths derived from the random data sets in ascending order and counting off to the appropriate percentile (L.R. Linton pers. comm.).

A serious limitation of the PTP statistic is that it will consistently underestimate the departure of the data from randomness with the low number of randomizations typically employed in phylogenetic PTP analyses (Källersjö et al. 1992). Therefore, Källersjö et al. (1992) have derived two more accurate, albeit slightly conservative measures (α' and α^*) for such instances from the standardized Z-scores of the sample of random solutions. However, bearing the conservative natures of all these statistics in mind, Källersjö et al. (1992) recommend using the smallest value obtained from any of the PTP statistic (which they refer to as α' , α'' , or α^*).

Strictly speaking, a PTP test is not sensitive to hierarchical structure in the data set, but merely to patterns of association (Alroy 1994). The tacit assumption then is that the character covariation that the PTP test is sensitive to is due solely to common ancestry, and not to other correlative factors such as character non-independence. Together, this leads to the PTP test being an extremely forgiving and occasionally erroneous test (Källersjö et al. 1992; Novacek 1993). Therefore, it appears that a significant result is not so telling with respect to the PTP test as opposed to a non-significant result.

Another limitation of the PTP test is that it only operates at the level of the solution as a whole, and not for subgroups of interest within it. Although Faith (1991) has suggested an analogous procedure for this latter goal, this topology-dependent PTP test (T-PTP test) is limited to very small data sets for practical reasons. This is because the idea behind a posteriori T-PTP tests for the monophyly of a given clade is to determine how likely it is to form any clade with a similar number of members, and not how likely it is to form that one particular clade of interest. Thus, in order to a posteriori determine whether there is statistical support for a monophyletic Monachinae for instance, we need test not only the monachines, but all clades of nine taxa, for which, for the 19 phocids examined here, there are 92,378 such combinations. It is possible to correct for, rather than test all these possible combinations (see Faith 1991), but for the example given here, a significant result (at the 0.05 level) would still require a P value on the order of 10^{-7} .

The lack of a PTP subroutine in any computer package to date makes use of the PTP test rather labour intensive. Thus, only the minimally suggested number of data sets, 100 (99 permuted plus the original), were analyzed. The permuted data sets were created using the SEQBOOT program of PHYLIP (version 3.52c) (Felsenstein 1993), and subsequently converted to PAUP's NEXUS format to be analyzed using the heuristic search option as detailed above. All three measures of significance – α' , α'' , and α^* – were determined for this analysis. As we make no pretense as to the independence of our characters, we will interpret the results of this analysis in terms of character covariation only, and not hierarchical structure.

Skewness (Fitch 1979)

Skewness tests derive from Fitch's (1979) simple observation that distributions of tree length for most phylogenetic data sets possess long left-hand tails (i.e., are left-skewed).

Hillis & Huelsenbeck (1992) suggest that this phenomenon, which indicates the presence of relatively few solutions around the most parsimonious solution, derives from an increased amount of correlation between characters. Therefore, like the PTP test, interpreting a significant left-hand skew to mean significant phylogenetic signal requires the assumption that the indicated correlation derives primarily from common ancestry. So, once again, a non-significant result is more revealing than a significant one (Hillis & Huelsenbeck 1992), although a distribution with a significant left-hand skew does apparently increase the probability that parsimony will correctly identify the actual phylogeny (Huelsenbeck 1991a).

Hillis & Huelsenbeck (1992) also suggested that a significant left-skew for the whole solution may only be an artifact of a particularly strongly indicated subgroup. Therefore, a tree length distribution of all solutions, but with the relationships of this one subgroup constrained, should produce a non-significant skew. Presumably, this is due to the left-hand tail of a left-skewed distribution being composed primarily of solutions containing the indicated subgroup as a clade (but with different combinations of relationships internally).

Despite the work of Huelsenbeck (1991a) and Hillis & Huelsenbeck (1992), the use of skewness (as measured by the g_1 statistic) as an indicator of phylogenetic signal is also not without its problems. Skewness analyses will occasionally give an erroneous outcome due to being influenced more strongly by character state frequency (which in turn affects the pattern of branching) than by correlation between characters, as well as being insensitive to character number (Källersjö et al. 1992). However, this last point is countered by the question of whether support should be measured by the absolute [as in simply tallying the number of synapomorphies, and as Källersjö et al. (1992) apparently feel it should be] or the relative number of characters (as in the bootstrap) supporting a node. Källersjö et al. (1992) also question whether the limited random sample of all possible solutions that skewness statistics are based on for studies with more than 10 taxa can accurately estimate the distribution of all possible solutions, or even sufficiently sample from the attenuated left-hand tail of the distribution. However, Hillis & Huelsenbeck (1992) demonstrate that a random sample of only 10,000 trees does produce a statistically accurate sample, regardless of the number of taxa.

In all but two cases (see below), skewness statistics, g_1 , were obtained from a random sample of 1,000,000 trees generated using the RANDOM TREES subroutine of PAUP, and all were compared to critical values published for a given number of taxa and characters (both binary and four-state) by Hillis & Huelsenbeck (1992). Although molecular simulations were used to achieve these critical values, they should, at the very least, give a rough indicator of the level of significance. For those cases when the exact values for either taxa or character number were not present, the next higher category was used, producing a more conservative estimate of the level of significance. However, all skewness results here should be regarded as extremely tenuous as the RANDOM TREES subroutine of PAUP (version 3.1.1) contains major bugs that inhibit the analysis of (inversely) weighted data matrices.

For the "constrained" skewness analysis, the strongly supported subgroup in question (hereafter referred to as the "anti-Phocini" clade) was held to be all taxa excluding

Erignathus, *Histiophoca*, *Pagophilus*, *Phoca* spp., and *Pusa* spp. (hereafter, the “E-Phocini” clade) based on the results of other tests. However, as PAUP cannot produce distributions of truly constrained topologies, distributions were estimated by collapsing the constrained subgroup to its ancestral node. As well, as constrained skewness has not been tested before, reciprocal constraints were analyzed in which the strongly and weakly supported subgroups were alternately collapsed (to nodes 34 and 33 respectively; see Fig.5B) to test whether the collapsing resorted to here had some effect on skewness. If Hillis & Huelsenbeck’s (1992) conjecture is accurate, then one would expect the distribution with a collapsed (weaker) “E-Phocini” clade to maintain a significant skew, while that with a collapsed (stronger) “anti-Phocini” clade should possess a non-significant skew. Tests were paired to account for both ACCTRAN and DELTRAN reconstructions of the ancestral node. For the case when the “anti-Phocini” were collapsed only, it was possible to derive the skewness statistic from an exhaustive search of all 135,135 possible trees rather than invoke PAUP’s RANDOM TREES subroutine.

Successive approximations (Farris 1969)

Successive approximations is an a posteriori weighting technique that seeks to arrive at a more robust solution (i.e., fewer and more resolved equally most parsimonious solutions) by differentially weighting characters in proportion to how well they have performed in a previous analysis. This procedure is typically recursive, and continues until no further change is observed in either tree topology or character weights (Swofford 1993).

Although the use of successive approximations has increased resolution and decreased ambiguity when applied to some data sets (Novacek 1993), its use is also somewhat problematic. First and foremost, it is not clear how to determine a character’s quality. Typically, one of three goodness-of-fit statistics – CI, RI, or RC (see above) – is used, but there appears to be no reason to favour one over another. As well, characters do not fit equally well to all equally most parsimonious solutions, and a decision must be reached whether to reweight characters according to their maximum, minimum, or average value of the goodness-of-fit statistic chosen (Swofford 1993). Other problems include the tendency of missing data to artificially make their characters less homoplastic (thereby contributing more to future analyses), and the obvious circularity of the procedure as a whole (Novacek 1993).

Here characters were reweighted (base weight = 1,000) using all combinations of CI, RI, and RC, and their maximum, minimum, and average values. Fractional weights were rounded off to the nearest whole number. All searches used the heuristic search option as detailed above.

Support analyses (Källersjö et al. 1992)

The general concept of support tests (also known as decay analyses) is to view trees (or their summaries in the form of consensus trees) of increasingly greater length, and thus homoplasy, so as to determine when a clade of interest disappears or is contradicted. Clades that withstand the intrusion of increasing levels of homoplasy to the greatest extent are judged to have the strongest support (Novacek 1991; Swofford 1993). This basic procedure (termed Bremer support by Källersjö et al. 1992) suffers from being dependent on the

different properties of each data set. No objective benchmark has yet been able to delineate strong from weak support [although the confidence intervals may be surprisingly large (see Cavender 1978, 1981)], so all results can only be stated in relative terms (e.g., a clade has stronger support than another, not strong support *per se*), and only for the data set in question (Novacek 1991). Through the use of permutation, Källersjö et al. (1992) have refined the concept of support to give it a more objective, statistical basis; however, as the calculation of this total support is prohibitive using PAUP, it was unfortunately not examined here.

All trees in increasing increments of 69 steps (= one corrected step; see above) from the most parsimonious tree length were retained using the KEEP command of PAUP in conjunction with the heuristic search procedure described above. As a heuristic search pattern was used, the number of trees retained at each step should be viewed only as a rough estimate of the total number of trees of that length or shorter, rather than an exact figure. Summaries at each length were viewed using both strict and majority rule consensus algorithms (see above for advantages of each). Unfortunately, with the large number of taxa examined here (and concomitant large number of possible trees), PAUP quickly ran into memory limitations, and the support analysis could only be performed for solutions up to and including four corrected steps longer than the most parsimonious length.

All these statistical tests are dependent on the power of the computer and/or the search algorithm employed. In the case of all but skewness, it is important to minimally maintain the searches as robust as the original so that the results will be roughly comparable. For the PTP test, this is especially critical given that any less than optimal solution for the random data sets will increase the probability of generating a significant result (Källersjö et al. 1992). Similar errors can be anticipated for the remaining procedures as well.

Comparative tools

Relatively less attention has been paid to the various non-statistical means of inferring the robustness of a cladogram. Of the comparative techniques described below, only the constraint analyses really qualify as a (non-statistical) means of inferring the robustness of a cladistic hypothesis. Although the remaining four "analyses" do indirectly indicate the strength of the pattern of phocid phylogeny obtained herein, they are, more properly, specific, interesting questions that arose in the course of this study. Each analysis is again described in turn.

Constraint analyses

One invaluable feature of PAUP allows the user to constrain searches to satisfy (or not satisfy) a given topology or range of topologies. Of its many possible uses (see Swofford 1993), topological constraints were used here to view how much less parsimonious a desired set of alternative relationships forced the overall solution to be. In many ways, this procedure is akin to support analyses, except that the shortest solution containing a set of relationships not found in the most parsimonious solution(s) is desired here.

Major competing hypotheses of phocid phylogeny were identified from the literature and tested here. These hypotheses apply to both outgroup and ingroup relations and the

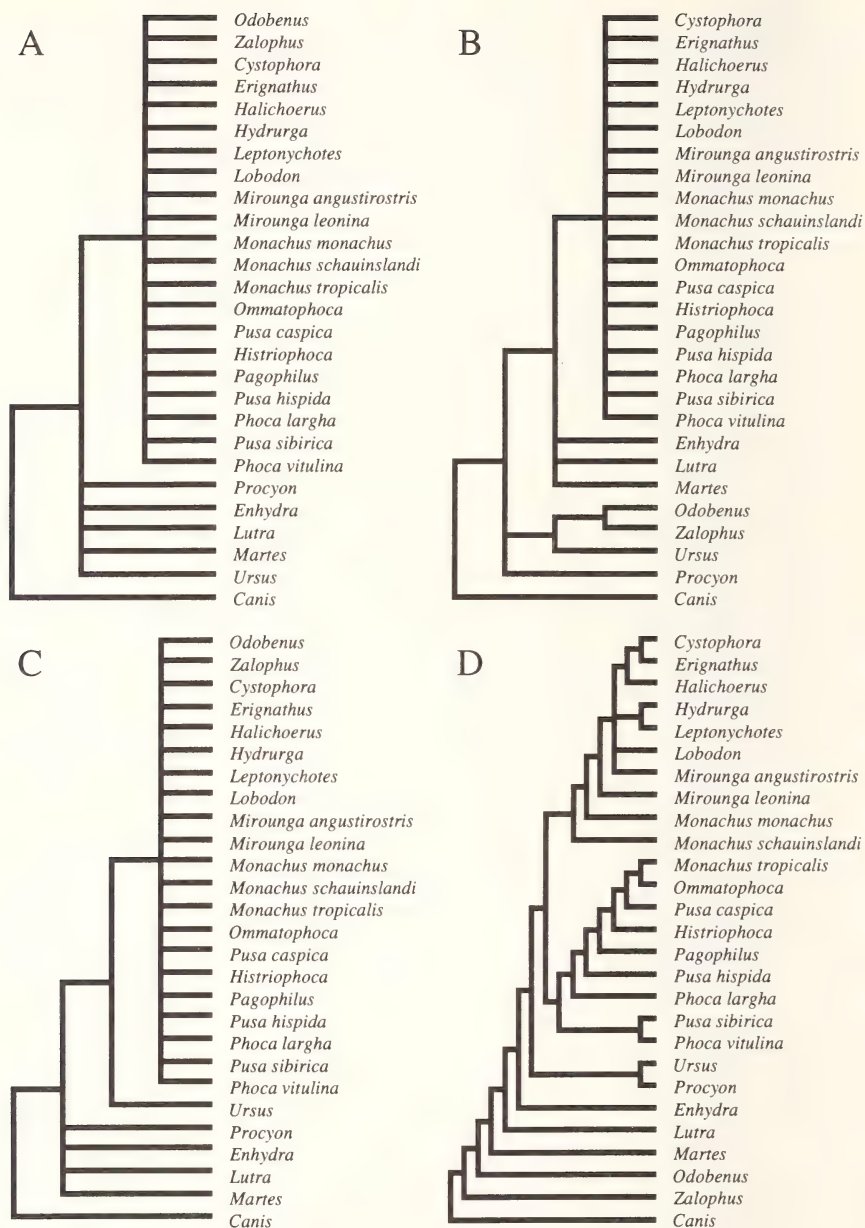


Fig.3A–D: Monophyly constraint trees used to examine various alternative hypotheses of outgroup relationships: (A) (not) monophyly, (B) diphyly, (C) ursid – monophyly, and (D) ursid – diphyly.

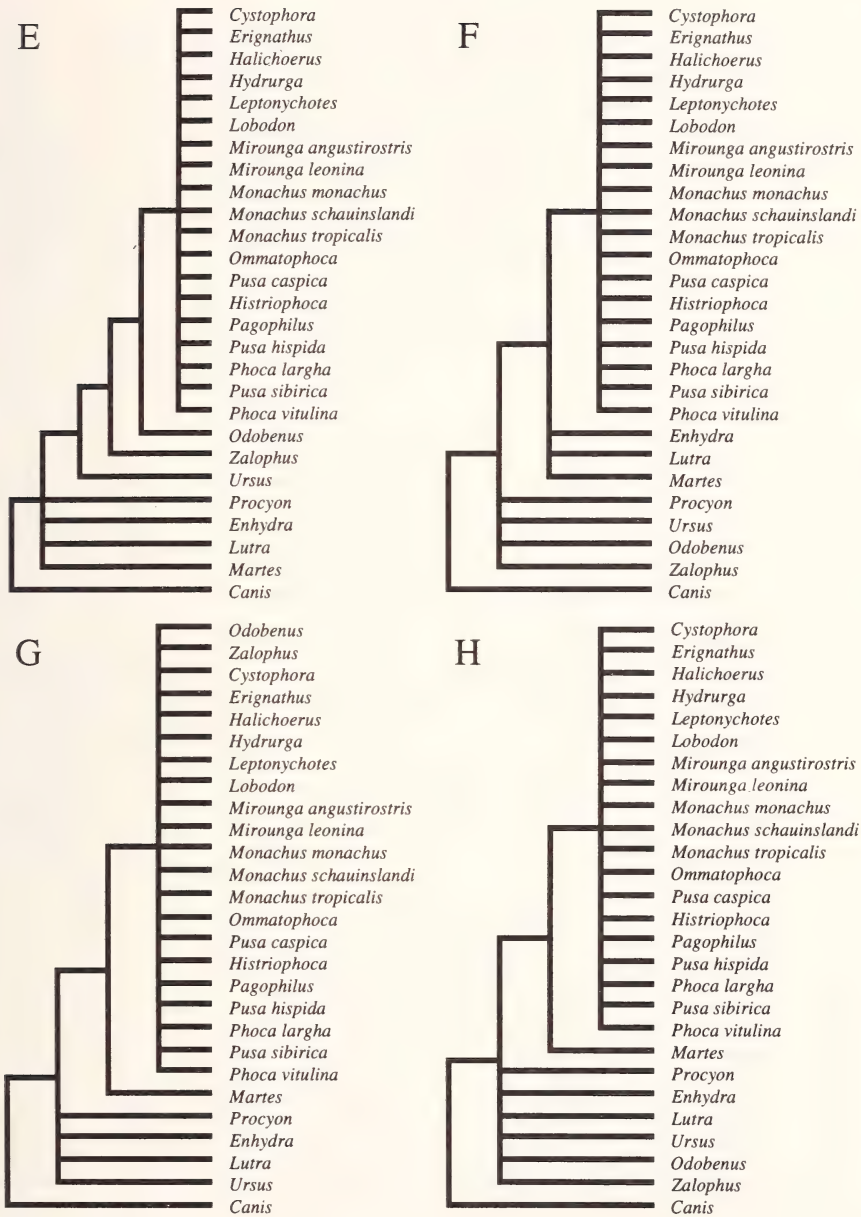


Fig.3E–H: Monophyly constraint trees used to examine various alternative hypotheses of outgroup relationships: (E) ursid – odobenid, (F) mustelid – diphyly, (G) musteline – monophyly, and (H) musteline – diphyly.

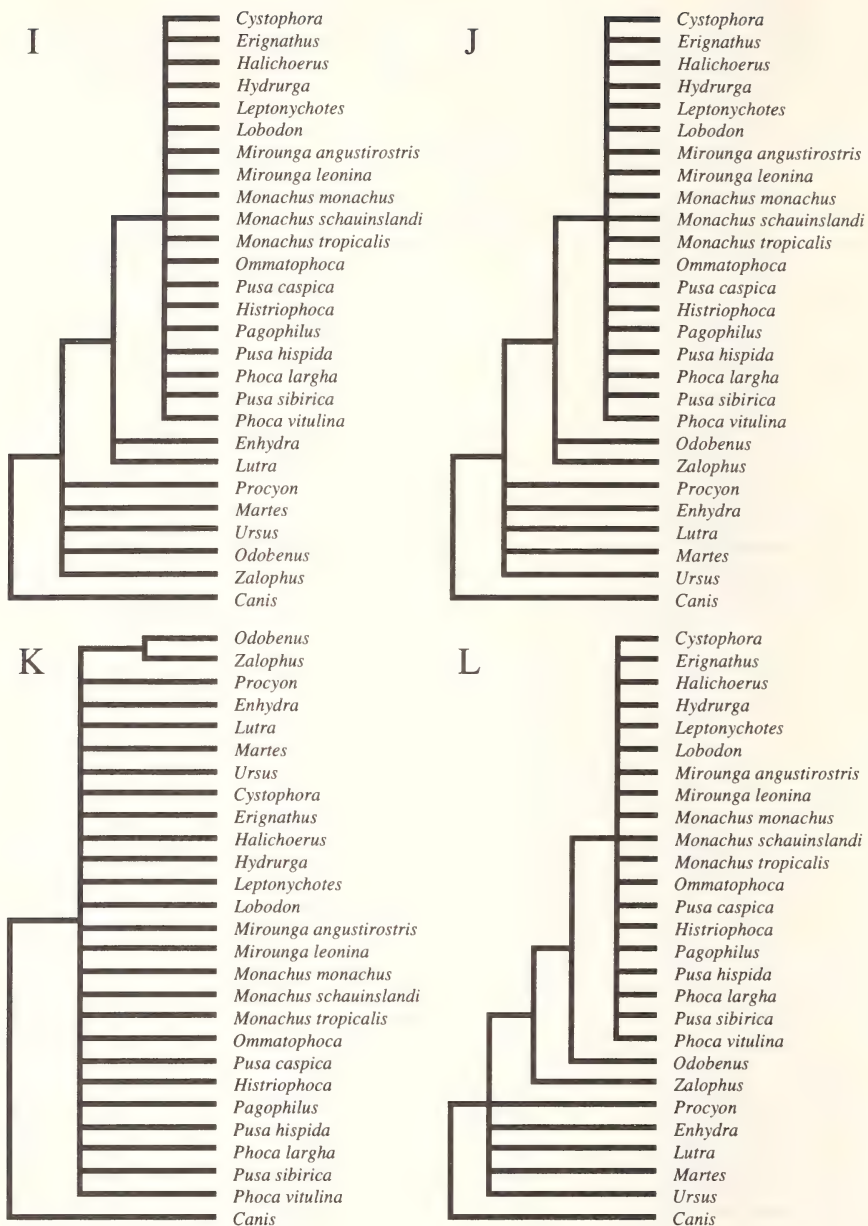


Fig.3I-L: Monophyly constraint trees used to examine various alternative hypotheses of outgroup relationships: (I) lutrine – diphyly, (J) (not) otarioid, (K) (not) otarioidea, and (L) odobenid.

constraint trees as tested are presented in Figs.3 and 4 respectively. Two additional ingroup trees, corresponding to the solutions of the unweighted and condensed analyses (see below), were also tested (Fig.4O and P).

As with Bremer support, constraint analyses suffer from a lack of any explicit statement on how much longer a tree must be for it to be rejected on statistical or other grounds [but again, see Cavender (1978, 1981)]. Thus, we again employ this analysis more in a relative fashion, using it to distinguish between more weakly and more strongly supported solutions. Whenever possible, bootstrap frequencies for the clade being examined were also added as a second, albeit similarly approximate, line of evidence.

All searches employed the heuristic search pattern described above, except for the ingroup constraint trees “de muizon” and “condense”, which were analyzed using exhaustive and branch and bound search algorithms respectively (both collapsing zero-length branches), both of which guarantee an optimal solution.

Missing taxa

On the suggestion of Arnold (1981) that missing taxa may have a detrimental effect on low level cladistic analyses, five phocid taxa (*Cystophora*, *Erignathus*, *Lobodon*, *Ommatophoca*, and *Phoca largha*) were selectively deleted and the analysis re-run in order to view the effects of their individual removal, if any. These taxa were selected on the basis of their topological position, various tendencies elucidated by other analyses, or for historical considerations (see **Comparative Tools** section for full details). As the removal of these taxa alters the intrinsic properties of the data matrix, comparisons with other results are primarily limited to comparisons of gross topological changes and various goodness-of-fit-statistics. All searches were conducted using the heuristic search pattern described above.

Condensed analysis

Historical considerations of phocid phylogeny show a strong tendency to assume the monophyly of some higher taxa. However, as this is the first species-level cladistic analysis of the entire family to be performed, some of these assumptions of monophyly will not have been rigorously tested before now. Thus, in order to view the possible historical effects of assumed monophyly on phocid phylogeny, we re-ran the analysis with several species collapsed into one of four higher taxa: the genera *Mirounga*, *Monachus*, and *Phoca* (sensu Burns & Fay 1970), and the tribe Lobodontini.

Although the paraphyly of three of these four taxa has been suggested, it has not been widely accepted in each case. Certainly, the strongest and almost indisputable case is for *Phoca* (sensu Burns & Fay); however, this taxon is almost universally recognized today. Only Wyss (1988a) has provided evidence for a paraphyletic *Monachus*, something that has not been re-examined to date [although it is endorsed by Berta & Wyss (1994)]. It has been hinted that the Lobodontini may be polyphyletic, or even paraphyletic, but only with the inclusion of fossil taxa (Hendey 1972; McLaren 1975; Ray 1976a; Berta & Wyss

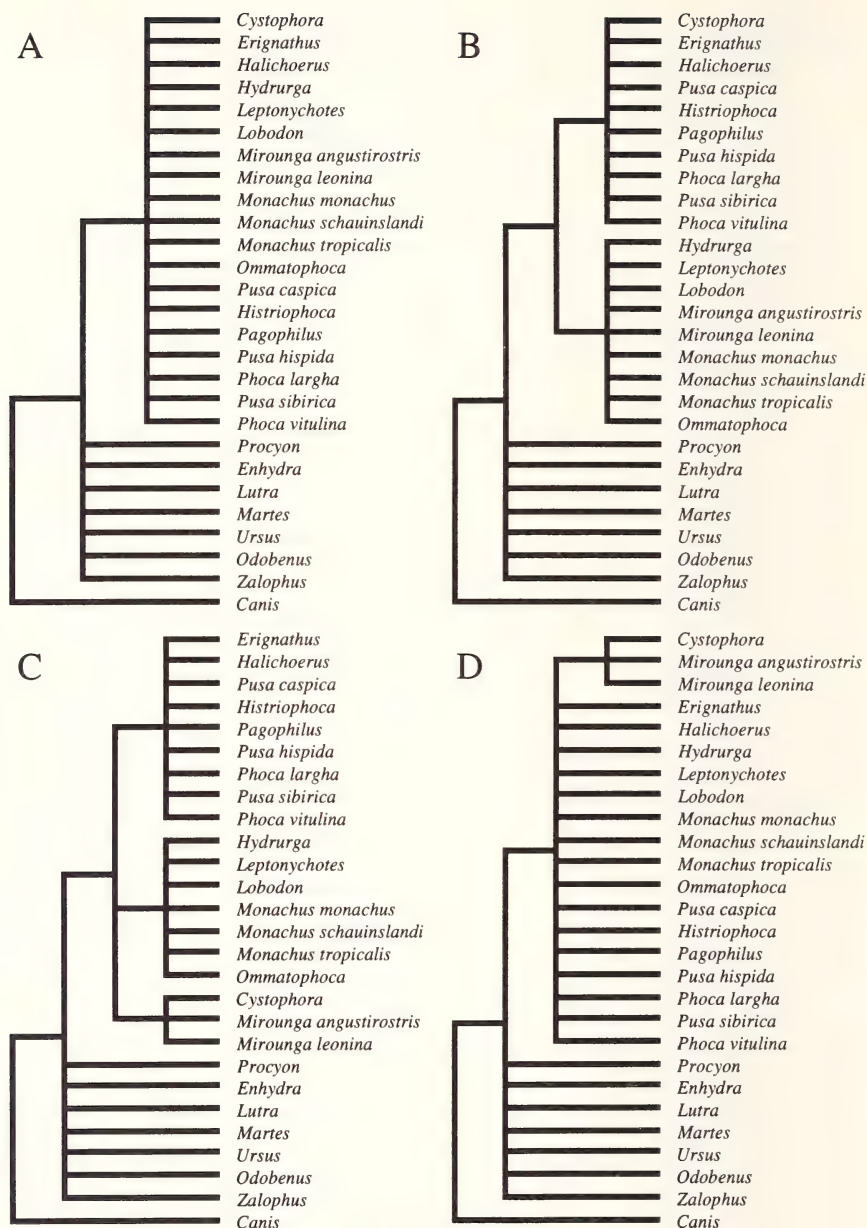


Fig.4A–D: Monophyly constraint trees used to examine various alternative hypotheses of ingroup relationships: (A) (not) phocidae, (B) (not) two subfamilies, (C) three subfamilies, and (D) cystophorinae.

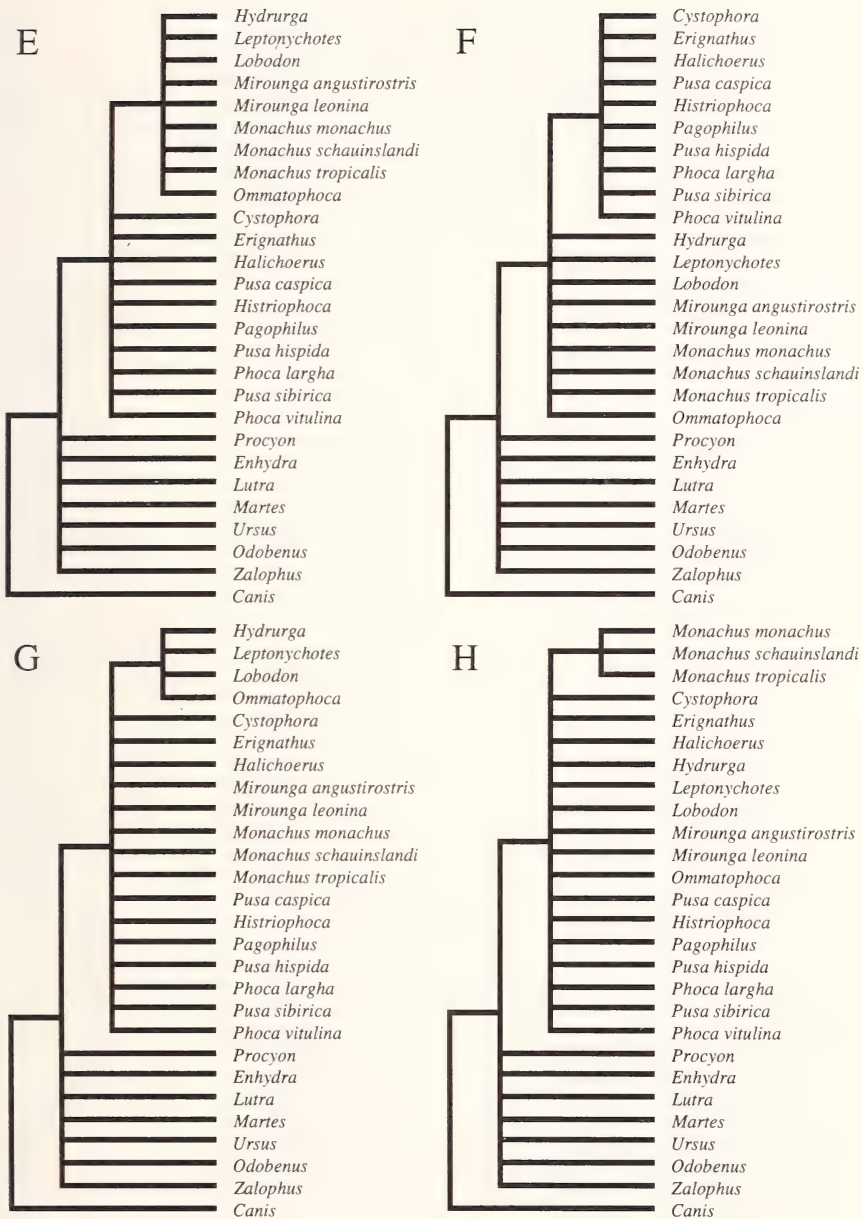


Fig.4E-H: Monophyly constraint trees used to examine various alternative hypotheses of ingroup relationships: (E) (not) monachinae, (F) (not) phocinae, (G) lobodontini, and (H) (not) monachus.

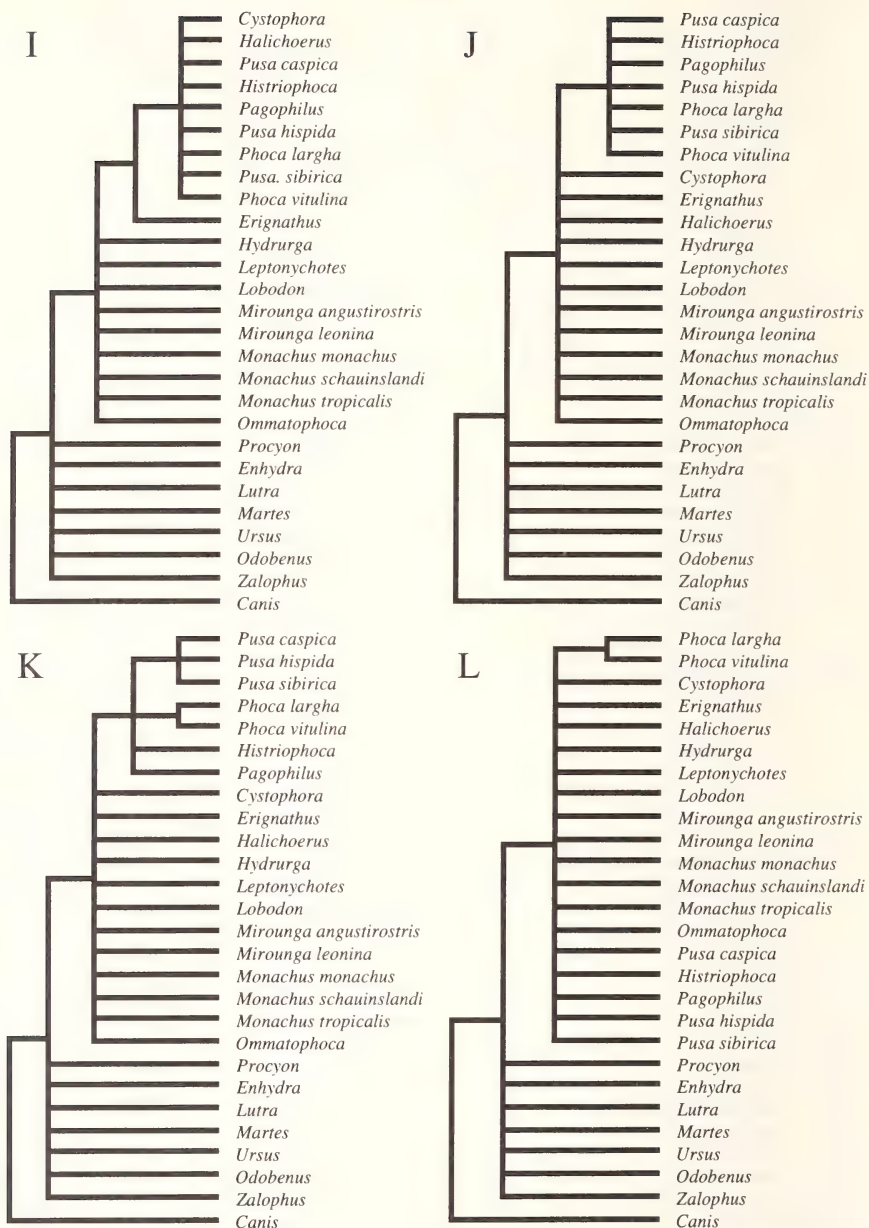


Fig.4I-L: Monophyly constraint trees used to examine various alternative hypotheses of ingroup relationships: (I) erignathus sister, (J) relaxed Burns & Fay, (K) strict Burns & Fay, and (L) phoca.

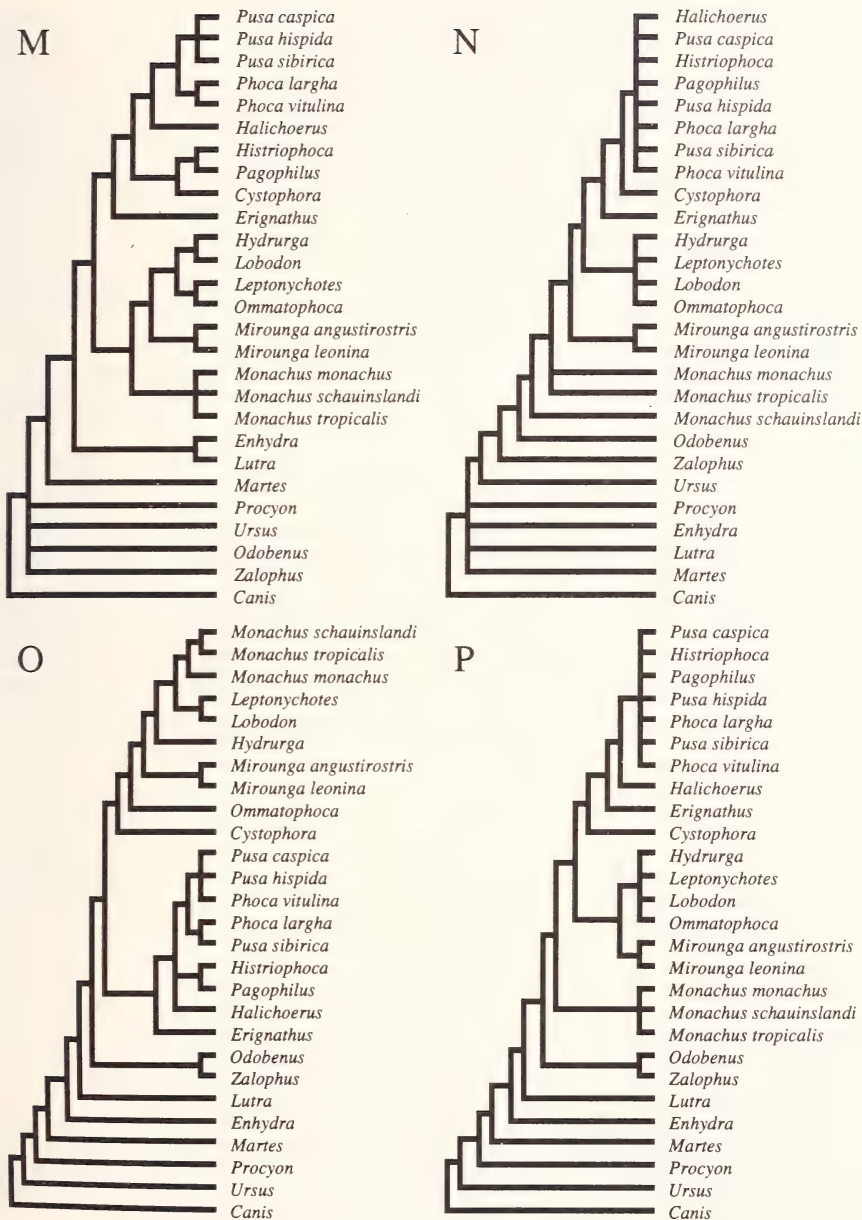


Fig.4M-P: Monophyly constraint trees used to examine various alternative hypotheses of ingroup relationships: (M) de muizon, (N) wyss, (O) unweighted, and (P) condense.

1994). Otherwise, the tribe is almost certainly monophyletic (Wyss 1988:5). To our knowledge, paraphyly of *Mirounga* has never been suggested.

Consensus character states for each higher level taxon were determined from the character states of its constituent species using the same modified majority rule algorithm used to condense specimen observations into the consensus species states (see above; states listed in Appendix B). A heuristic search according to the pattern described above was employed.

Unweighted analysis

The use of inverse weighting for multistate characters is fairly infrequent in phylogenetic systematics (as is the use of multistate characters). Thus, an analysis designed to assess the impact of these different weighting schemes (i.e., inversely versus identically weighted characters) was undertaken. It was performed in exactly the same manner as the overall parsimony analysis except that all characters were unweighted (i.e., each had a weight of 1).

Taxonomic conventions

The ever-changing taxonomy of the carnivores, and especially that within the pinnipeds, reflects the changing opinions on the phylogenetic relationships within this order. Therefore, in order to avoid any confusion, we will refer to the carnivoran taxa as outlined in Tab.1. We will forgo the use of the monotypic phocid tribes Cystophorini (= *Cystophora cristata*), Erignathini (= *Erignathus barbatus*), Miroungini (= *Mirounga* spp.), and Monachini (= *Monachus* spp.) in favour of their constituent taxa. Unless otherwise mentioned, membership of all taxa applies solely to their extant representatives.

Table 1: Indented hierarchy displaying taxonomic conventions employed in this study. Unless otherwise noted, this taxonomy applies only to extant forms. References do not necessarily correspond to the first mention of the group in the literature, but to the manner in which the group is to be recognized here.

- Caniformia (Wyss & Flynn 1993) – canids (*Canis*), ursids (*Ursus*), procyonids (*Procyon*), mustelids (*Martes*, *Enhydra*, and *Lutra*), and Pinnipedia
 - Arctoidea (Wyss & Flynn 1993) – all caniforms above excluding canids
 - Lutrinae (Wozencraft 1993) – otters (*Enhydra* and *Lutra*)
 - Mustelinae (Wozencraft 1993) – weasels, marten (*Martes*), wolverine
 - Pinnipedia (Illiger 1811) – seals, sea lions, fur seals, and walrus
 - Otarioidea (Smirnov 1908) – sea lions, fur seals, and walrus
 - Odobenidae (Allen 1880) – walrus (*Odobenus*)
 - Otariidae (Gill 1866) – sea lions (*Zalophus*) and fur seals
 - Phocidae (Brooks 1828) – phocid seals
 - Monachinae (King 1966) – southern seals (*Mirounga* spp., *Monachus* spp., and the lobodontines)
 - Lobodontini (Scheffer 1958) – *Hydrurga*, *Leptonychotes*, *Lobodon*, and *Ommatophoca*
 - Phocinae (King 1966) – northern seals (*Cystophora*, *Erignathus*, and the Phocini)
 - Phocini (Chapskii 1955a) – *Halichoerus*, *Histiophoca*, *Pagophilus*, *Phoca* spp., and *Pusa* spp.

OVERALL PARSIMONY ANALYSIS

The main goal of this section is to present, and preliminarily discuss the robustness of, the solution to an overall parsimony analysis of the data matrix found in Appendix C. The following two sections will then build on this theme by using a number of techniques to more fully examine the support for this cladistic hypothesis. The morphological description of each character is deferred until the **Character Analysis** section, where it can be combined with a description of their evolutionary pathway (i.e., character reconstruction) as inferred from the phylogeny presented and subsequently analyzed in this and the following two sections.

Incidence of polymorphism (Appendix C)

The characters examined in this study, which are primarily osteological and largely relating to the head skeleton, are characterized by a high degree of intraspecific polymorphism, especially among the phocids. Fully 150 of the 196 characters (76.5%) reveal at least one polymorphic taxon. Of these characters, the vast majority demonstrate taxa that maximally possess a two-state polymorphism (124 or 63.6% of all characters), but three- (24 or 12.2%) and four-state (2 or 1.0%) polymorphisms are also present. These ratios are virtually identical in the 168 characters that were retained for analysis – altogether, 129 displayed polymorphic taxa (76.8%), with the taxa in 106 being maximally two-state polymorphic (63.1%), three-state in 21 (12.5%), and four-state in two (1.2%) – indicating that polymorphic characters do not appear to be inferior to monomorphic ones, and that polymorphism appears to be intrinsic to the morphology of these taxa [as intimated for the pinnipeds at least by Mivart (1885), Doult (1942), Davies (1958b), and Ray (1976b)]. The average number of polymorphic characters for the 27 taxa examined here was 20.8, or roughly 12.4% of the 168 included characters. The range extended from a low of four characters (=2.4%) for *Canis*, to a high of 32 (=19.0%) for both *Leptonychotes* and *Ommatophoca*.

Overall solution (Fig.5)

A parsimony analysis of the 19 extant phocid species (including *Monachus tropicalis*), with eight outgroup taxa, and employing inverse character weighting yielded two equally most parsimonious solutions, each of 69,834 steps (Fig.5A). The differences between these solutions are limited to a subset of the phocines, and arise from the variable placement of *Phoca vitulina* relative to *Erignathus*, *Histiophoca*, *Pagophilus* (which consistently form a monophyletic clade), and *Pusa* spp. One solution holds for *Phoca vitulina* being the sister group of all these taxa (with *Pusa* being monophyletic), while the other has *Phoca vitulina* disrupting *Pusa*, rendering it paraphyletic. However, *Pusa hispida* and *Pusa sibirica* remain as sister taxa in both solutions.

Both the strict and majority rule consensus trees for these equally most parsimonious solutions converge on the same cladogram (Fig.5B) with the conflict between the above taxa being visualized as a polytomy within the phocines. The slightly higher length (70,084 steps) of the consensus tree reflects PAUP's use of hard polytomies (which must satisfy

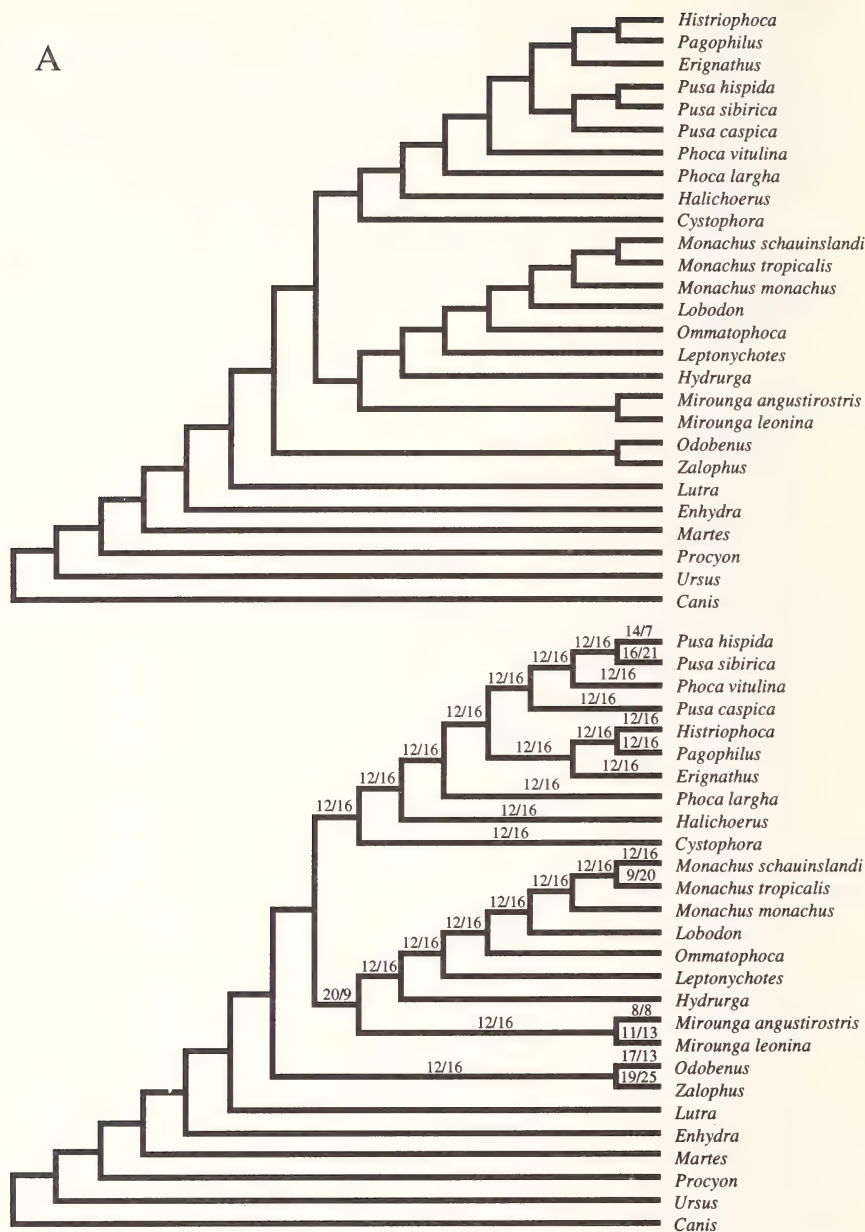


Fig.5A: Cladograms resulting from a parsimony analysis of the inversely weighted data matrix. (A) The two equally most parsimonious solutions (length = 69,834 steps, CI = 0.456, HI = 0.770, RI = 0.629, RC = 0.407).

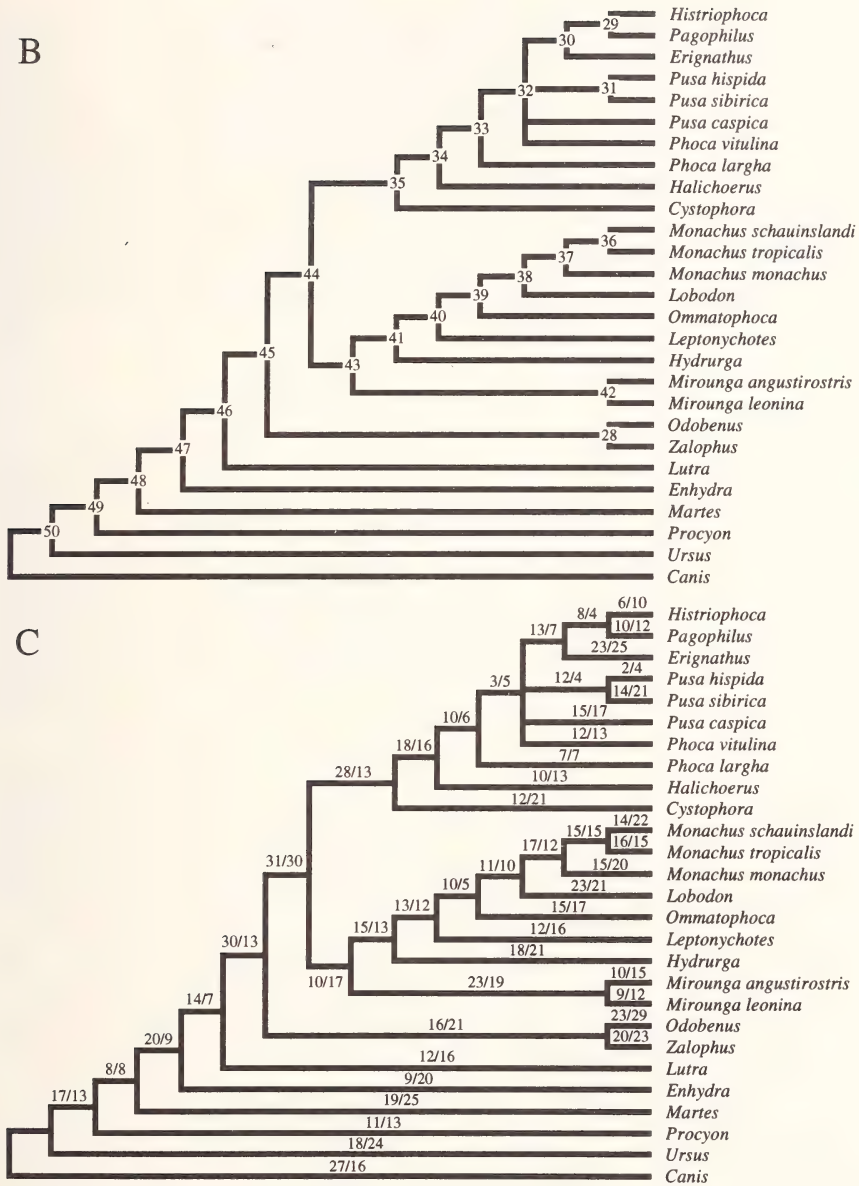


Fig. 5B–C: Cladograms resulting from a parsimony analysis of the inversely weighted data matrix. (B) Consensus tree (identical between strict and majority rule algorithms) for the solutions in (A), with internal nodes numbered. All nodes were found in 100% of the equally most parsimonious solutions. (C) As for (B), but with unweighted branch lengths (presented as accelerated transformation / delayed transformation).

multiple independent speciation events from a polytomy) as a computational aid (Maddison & Maddison 1992; Swofford 1993). Although a consensus tree does not necessarily represent an optimal solution for a given data set (Swofford 1993), and does not here, we will refer to the consensus solution as the overall parsimony solution as we believe it to present the best summary of the data set. The consensus solution reflects the conflict present within the phocines, and its single cladogram provides a more efficient discourse. All tree descriptions (see Appendices D through F) are derived from the consensus solution. However, the optimal tree length will be taken to be that of the two equally most parsimonious solutions (69,834 steps) and the various goodness-of-fit statistics will also refer to the optimal solutions (as will be the case for all other analyses as well), unless specified otherwise.

Outgroup relations (Fig.5C)

This analysis confirms a monophyletic Pinnipedia, with the otarioids forming a monophyletic sister group to the phocids. This is in accordance with the recent upswing in support of a monophyletic Pinnipedia among morphological studies (e.g., Wyss 1987; Flynn et al. 1988; Wolsan 1993; Wyss & Flynn 1993), but contradicts the recent contention of an *Odobenus*-phocid clade (Wyss 1987; Wyss & Flynn 1993; Berta 1991; Berta & Wyss 1994; Vrana et al. 1994). However, a monophyletic Otarioidea is among the most strongly supported of all clades, ranging in support from 16 to 21 unweighted steps, depending upon the optimization criterion employed (see Appendix D for weighted branch lengths; the identities of the synapomorphies supporting each node can be found in Appendix E, and are discussed in the **Character Analysis** section).

A somewhat unexpected result was that of a lutrine affinity for the pinnipeds, with *Lutra* being the immediate sister group and *Enhydra* being the sister group to *Lutra* and the pinnipeds. Although many early workers allied the phocids and the lutrines based on superficial similarities [see references in Taylor (1914)], a lutrine affinity for the phocids based on more robust characters has only been suggested by four workers: Flower (1869), Mivart (1885), McLaren (1960b), and de Muizon (1982a). To our knowledge, however, the equivalent scenario has never been postulated for the pinnipeds as a whole, as the otarioids are typically allied with the ursids under this otherwise diphyletic scenario. Most recent studies advocating a monophyletic Pinnipedia (and including both ursid and mustelid outgroups) conclusively indicate an ursid affinity for the pinnipeds (e.g., Vrana et al. 1994; Lento et al. 1995). Only Wolsan (1993) allies a monophyletic Pinnipedia with the lutrine-like fossil *Potamotherium* (which he considers to be a pinniped) within his Mustelida, but his exclusion of any undisputed lutrines [a lutrine affinity for *Potamotherium* has recently come into question (C.A. Repenning pers. comm.; A.R. Wyss pers. comm.)], plus the lack of an ursid outgroup, precludes any definitive statement on lutrine affinities. However, a *Lutra*-pinniped pairing is generally supported here no less strongly than any other outgroup node and is minimally indicated by seven unequivocal synapomorphies. As well, a lutrine affinity also implies a mustelid affinity for a monophyletic Pinnipedia, which, although still rare, is a somewhat more commonly held hypothesis [e.g., Arnason & Widegren 1986; Miyamoto & Goodman 1986 (albeit as the sister group to a mustelid-procyonid clade); Wolsan 1993].

Interestingly, despite Taylor (1914) noting a high degree of convergence between *Enhydra* (but not *Lutra*) and the phocids due to the constraints of their largely aquatic habitats, it is the apparently less aquatically adapted *Lutra* that forms the immediate sister group to the pinnipeds here. The overall implication of this result is that the relationships advocated herein (and especially the historically unusual lutrine-pinniped pairing) are based more on phylogenetically informative characters than on convergent aquatic features.

If the pinnipeds are momentarily ignored, the fissiped outgroups otherwise fall out as is commonly held for the caniforms. The lutrines form a monophyletic clade within the remaining mustelids (*Martes*), with the procyonids (*Procyon*), ursids (*Ursus*), and canids (*Canis*) forming successive sister taxa to the mustelids (see Tedford 1976; Miyamoto & Goodman 1986; Flynn et al. 1988; Wyss & Flynn 1993). Support for the constituent nodes appears reasonably robust, ranging from eight (Mustelidae under either ACCTRAN or DELTRAN optimization) to 27 (Arctoidea under ACCTRAN optimization) unweighted steps (Fig. 5C; Appendices D and E). It should be noted, however, that this arrangement is dependent on the somewhat subjective placement of the root of the cladogram (which has *Canis* as the ultimate outgroup). This placement was chosen in accordance with the strong agreement for the canids being the most primitive of the extant Caniformia (Tedford 1976; Flynn et al. 1988; Wyss & Flynn 1993; Vrana et al. 1994; but see Wozencraft 1989), but any alternative placement of the root will disrupt the above pattern of sister taxa relationships. Fortunately, however, these alternative placements will not affect the ancestral state assessment used to determine the pattern of ingroup relationships (Maddison et al. 1984).

Ingroup relations (Fig. 5C)

A monophyletic Phocidae enjoys the strongest support of any node in the overall solution, being supported by 30 or 31 synapomorphies (21 of which are unequivocal). However, in contrast to the findings of Wyss (1988a) and Arnason et al. (1995), the overall solution indicates the division of the phocids into two major monophyletic clades: the Monachinae and Phocinae. Support for this arrangement is strong, with the phocines having moderately better support at 13 to 28 unweighted steps (10 of which are unequivocal) versus 10 to 17 (6 of which are unequivocal) for the monachines, depending on the optimization criterion employed (Fig. 5C; Appendices D and E). Although the membership of these subfamilies is as expected (see King 1966), some novel internal relations are indicated in both cases.

Relationships within the Monachinae

With respect to the monachines, the elephant seals (*Mirounga* spp.) are held to be basal, a position traditionally accorded to *Monachus* spp. (Hendey 1972; Repenning & Ray 1977; Repenning et al. 1979; de Muizon 1982a; King 1983; Wyss 1988a; Arnason et al. 1995; Lento et al. 1995). Therefore, coupled with the view that *Monachus* spp. is the most primitive of all extant phocids, as well as a good number of fossil forms (Repenning & Ray 1977; de Muizon 1982a), it is surprising to find the monk seals occupying a terminal position deep within the lobodontines. Overall, the indicated topology for the monachines

also speaks against the contention that *Mirounga* is more closely allied to the lobodontines than either is to *Monachus* (Hendey 1972; King 1983; but see Sarich 1976). However, it appears noteworthy that the similarity between *Monachus* and the lobodontines was recognized long before *Mirounga* was added to the Monachinae (see **Introduction**).

Monophyly of *Monachus* is indicated, again in contrast to the findings of Wyss (1988a). As well, this analysis supports the older contention of a sister group relationship between *M. schauinslandi* and *M. tropicalis* (e.g., King 1956; Kenyon & Rice 1959; King & Harrison 1961; de Muizon 1982a), as opposed to the more recent opinion which holds *M. schauinslandi* to be the most primitive member of the genus (if not the phocids as a whole) (Repenning & Ray 1977; Wyss 1988a). Support for both the terminal position of *Monachus* spp. (as indicated by the strength of the *Lobodon-Monachus* spp. grouping) and their interrelationships are marked by a relatively large number of synapomorphies (Fig. 5C; Appendices D and E).

The terminal placement of *Monachus* spp. now renders the Lobodontini paraphyletic, which has, at best, only been previously hinted at with the inclusion of fossil forms (Hendey 1972; McLaren 1975; Ray 1976a; Berta & Wyss 1994). However, as again estimated by the strength of a *Lobodon-Monachus* spp. alliance, this paraphyly is strongly indicated. As well, novel internal relationships are proposed for the lobodontines. A *Lobodon-Ommatophoca* pairing is indicated (momentarily ignoring *Monachus* spp.), with *Leptonychotes* and *Hydrurga* forming successive sister taxa to this clade, in contrast to the more traditional *Hydrurga-Lobodon*, *Leptonychotes-Ommatophoca* split (Hendey 1972; de Muizon & Hendey 1980; de Muizon 1982a; King 1983). Although some of our lobodontine relations are comparatively weak, they are generally supported by more characters than the traditional pairings, which are based primarily on the larger size and more complex morphology of the postcanines in *Hydrurga* and *Lobodon*, or, equivalently, the reduced nature of the postcanines in *Leptonychotes* and *Ommatophoca* (Hendey 1972; de Muizon & Hendey 1980; de Muizon 1982a; King 1983).

Relationships within the Phocinae

As indicated above, support for this subfamily is reasonably strong. Many of the general themes observed for the monachines were also observed here. Again, a novel suggestion for the most primitive member of the subfamily is obtained, with *Cystophora* adopting the traditional placement of *Erignathus*. Although *Cystophora* is generally agreed to be relatively primitive within the phocines [only de Muizon (1982a), Mouchaty et al. (1995), Perry et al. (1995), and possibly Arnason et al. (1995) depart from this view, embedding *Cystophora* well within the Phocini from its traditional sister taxon status, although this result may be peculiar to phylogenies derived from cytochrome b data in particular], to our knowledge, a basal placement for any taxon besides *Erignathus* is unique. The parallel positions of *Cystophora* and *Mirounga* as the basal members of their respective subfamilies hint that some of the similarities between these members of the now abandoned subfamily Cystophorinae might be based on phocid symplesiomorphies, rather than on convergent features (see King 1966). This contention is strengthened by evidence that similar cystophorine features may have been present in *Allodesmus* (Mitchell 1975), a taxon now

felt to be among the fossil sister taxa of the phocids (Wyss 1987; Berta 1991; Wyss & Flynn 1993; Berta & Wyss 1994).

Instead, *Erignathus* is now embedded within the Phocini (rendering the latter paraphyletic), forming the sister taxon to the clade of *Histiophoca* plus *Pagophilus*. Despite the nearly universal agreement on the primitive, almost monachine, nature of *Erignathus* with respect to the remaining phocines (Chapskii 1955a; King 1966, 1983; Burns & Fay 1970; McLaren 1975; Ray 1976a; Wyss 1988a; Berta & Wyss 1994; Arnason et al. 1995), this clade consistently demonstrates the highest number of synapomorphies within the Phocini: seven under DELTRAN optimization (also the number of unequivocal synapomorphies) and 13 under ACCTRAN optimization.

Paraphyly of the Phocini is an extremely uncommon suggestion, speaking against an apparent host of putative chromosomal and morphological synapomorphies (McLaren 1960a, 1966, 1975; King 1966; Burns & Fay 1970; Arnason 1974, 1977; Arnason et al. 1995). To our knowledge, it has only previously been suggested by de Muizon (1982a), Mouchaty et al. (1995), Perry et al. (1995), and possibly Arnason et al. (1995), with *Cystophora* occupying roughly the same position indicated here for *Erignathus*. Yet, there are hints in the literature that *Erignathus* might not be quite as primitive as it is commonly held to be. Ray (1976a) dismisses suggestions of *Erignathus* possessing monachine tendencies, instead preferring to view it as a conservative, partly aberrant phocine. Chapskii (1955a), who supports a basal placement for *Erignathus*, also notes a number of derived features for this genus (mostly pertaining to the feeding apparatus) with respect to the remaining phocines. As well, *Erignathus* displays a number of karyotypic peculiarities that otherwise contradict its plesiomorphic chromosome number (Arnason 1974, 1977). Wyss (1988a) is entirely correct in regarding these features as being autapomorphic and thus phylogenetically uninformative. Nor do they necessarily indicate a paraphyletic Phocini; however, they do potentially hint at a more derived position for *Erignathus* within the phocines. This latter supposition is tentatively supported here by the relatively large number of character state changes (23 to 25 unweighted steps), very few of which indicate a more primitive placement, in the branch immediately leading to *Erignathus*. Within phocids, five of these changes are autapomorphic, 16 are convergent with other phocids, only three are reversals to the plesiomorphic phocid condition, and one is a reversal convergently found in some other phocids (see Appendix E and **Character Analysis**). Nor does *Erignathus* appear to display an inordinate amount of convergence on the monachine pattern. Most of the convergent characters converge on the states found in selected monachines only, and a good number are convergent on the states found in other phocines. On the basis of this evidence, we would suggest that undue attention has been given to the many unusual and prominent attributes of *Erignathus* [which may stem from an accelerated rate of evolution, as has been postulated at the molecular level for *Pagophilus* (Arnason et al. 1995)], at the expense of its many other similarities with the remaining phocines.

Within the Phocini proper, the paraphyly of a number of taxa is indicated. The new position of *Erignathus* now also disrupts the monophyly of *Phoca* (sensu Burns & Fay 1970). As mentioned previously, paraphyly of this taxon is not a new idea, but it is usually attributed to an intrusion by *Halichoerus* [Chapskii 1955a; de Muizon 1982a; Arnason et al. 1995;

hinted at by Arnason et al. (1993)] which is the sister taxon to the remaining Phocini (plus *Erignathus*) here. *Phoca* (sensu stricto) is also paraphyletic, despite the view of some authors that *Phoca largha* is merely a subspecies of *Phoca vitulina* (Scheffer 1958; Burns 1970; Shaughnessy 1975; Baram et al. 1991). The relatively basal position of *P. largha* initially appears weak, as the taxa internal to it are only united by three to five synapomorphies. However, such a position for *P. largha* (with respect to *P. vitulina* at least) is indicated by McLaren (1975) and possibly by Mouchaty et al. (1995). As well, the low number of synapomorphies may be an artifact of the polytomy in this region. With respect to a strictly dichotomous branching arrangement, the polytomy requires that putative synapomorphies for this node (#32; see Fig. 5B) satisfy an increased number of descendent lineages (four here). Presumably fewer synapomorphies exist to fulfill this more difficult condition, than for dual descendent lineages (e.g., as in node #30) with the possibility of further changes or reversals further along in the tree. In any case, a clade of *P. largha* and *P. vitulina* is not formed in either of the two most parsimonious solutions.

The polytomy within the Phocini also prevents a clear assessment of the status of *Pusa*. The consensus solution is equivocal; however, one of the two equally most parsimonious solutions does reveal a monophyletic *Pusa* (Fig. 5A). At the very least, a sister taxon relationship for *Pusa caspica* is indicated with respect to the remaining *Pusa* spp., as hinted at by Chapskii (1955b). However, the sister taxon status of *Pusa* to the remaining Phocini, as put forth by McLaren (1975), is not supported here.

Histiophoca and *Pagophilus* form a reasonably well supported monophyletic group. This substantiates the long standing, but historically poorly tested claim that the two genera are closely related, or at least very similar to each other (Chapskii 1955a; Davies 1958b; McLaren 1975; de Muizon 1982a; Arnason et al. 1995; Mouchaty et al. 1995). De Muizon's (1982a) hypothesis that any similarity may be exclusively due to symplesiomorphies is not supported.

Summary of ingroup relationships

Overall, the internal relationships of the phocines are comparatively weakly supported in terms of numbers of synapomorphies, especially for those taxa internal to *Halichoerus* (Fig. 5C). In fact, the internal relationships of the monachines are generally much better (and more uniformly) supported, despite the weaker support for the subfamily as a whole.

The new relationships proposed within each subfamily are somewhat difficult to reconcile with previous opinion. This is especially true for the phocines, which have been well studied for the most part, and especially for the novel position of *Erignathus* advocated here. The apparent polytomy within the Phocini (plus *Erignathus* here) is suggested by the numerous conflicting taxonomic assessments and biogeographic or systematic hypotheses for this group (e.g., compare Chapskii 1955a; Davies 1958b; McLaren 1966, 1975; Burns & Fay 1970; Ray 1976a; Repenning et al. 1979; de Muizon 1982a; Arnason et al. 1995; Mouchaty et al. 1995; Perry et al. 1995). This lack of resolution is probably traceable to the rapid adaptive radiation of this group in the post-early Pliocene and/or Pleistocene (Ray 1976a), allowing insufficient time for its members to become clearly differentiated (at least morphologically; see Arnason et al. 1995). Evidence from this study

for this line of reasoning lies in the relatively limited number of synapomorphies supporting most nodes in this region, in addition to the polytomy, which is more typical in regions of a cladogram where speciation has occurred via a rapid adaptive radiation (Wagner 1992). The pattern may also be obscured somewhat by a large amount of parallel evolution within the Phocini.

Although the number of proposed systematic alterations for the monachines is greater than for the phocines, this does not seem to present as great a problem. For the most part, this is because the monachines have not been as well studied, possibly due in large measure to the remoteness of most species with respect to the primarily northern hemisphere population of phocid researchers, combined with the seemingly more intuitive relationships of, and tribal allotment within, this subfamily. This seems to be especially true for the lobodontines, whose internal relationships have never been studied in detail, and whose monophyly (despite their obvious morphological differences) has seemingly never been questioned due to their common and distinctive geographic range, coupled with a similar lack of detailed examination. In the end, the novel monachine relationships advocated here may be a consequence of the freedom allowed all species to form the most parsimonious set of pairings, as opposed to previous studies which tended to constrain the monophyly of one or more of the monachine tribes (see **Condensed analysis** in the **Comparative Tools** section), particularly the Lobodontini.

Finally, in contrast to the assertions of Wyss (1988a) and Berta & Wyss (1994), convergences appear to be much more common than reversals in phocid evolution (see Appendix E and **Character Analysis**), a pattern that holds even under ACCTRAN optimization, where reversals are favoured. Of the homoplastic characters (and excluding within terminal changes), 49 / 85 were convergent (numbers given as ACCTRAN / DELTRAN), 16 / 5 were reversals, and 79 / 55 displayed both. Thus, reversals, when present, were typically found together with convergences (although convergent incidences of reversals only accounted for 45 / 29 characters of this subset). Nor was there a discernible pattern of homoplasy [in contrast to Wyss (1988a) and Berta & Wyss (1994) who indicate a distinct pattern of retrogression for the phocines], with convergences and reversals spread throughout the phocids.

Support for the overall solution

Various indicators point to the “good resolving power” of the data set as a whole (see also **Statistical Tests** and **Comparative Tools** sections). On a purely empirical basis, the data set ran surprisingly “cleanly” (only two solutions) and quickly for such a large matrix (27 taxa and 168 characters). In part, this can be traced to the use of inverse character weighting. While similar runs using unweighted characters (see **Comparative Tools** section) produced only four solutions, analysis times were considerably longer, due to a greater number of slightly less than most parsimonious solutions that needed to be searched through. However, the common perception that a low number of most parsimonious solutions implies a good quality to the data set may be an unsubstantiated claim, as some studies suggest that this number is dependent upon the number of characters (and how many states each possesses) and the number of taxa (Hillis & Huelsenbeck 1992; Lamboy

1994). It is unknown what the extent of this is here, as these factors act in opposition to one another, but it would be prudent to rely on other, more robust, indicators of resolving power.

The relatively high values of selected goodness-of-fit statistics ($CI = 0.456$, $RI = 0.629$, and $RC = 0.407$) likewise point to a high resolving power. Benchmarks for evaluating these statistics are rare, and, as these indices estimate the degree of homoplasy, they may be specific for the group under examination (see **Methods and Materials**). However, in the case of CI , the value obtained here is about on a par with the expected value for 27 taxa, 0.461 (Sanderson & Donoghue 1989). These relatively high values are somewhat surprising, as the phocids as a group, and especially the phocines, have been characterized as possessing a reasonably high number of reversals within a monophyletic pinniped framework (Wyss 1988a; Berta & Wyss 1994). Regardless of whether this apparent preponderance of reversals derives from a singular use of ACCTRAN optimization (see above also), the fairly homoplastic nature of the phocids is reflected by the high value obtained for the HI (0.770). However, this value is likely inflated to an unknown extent due to PAUP's failure to designate polymorphic ancestral nodes (see **Methods and Materials**).

Thus far, we have only presented a preliminary assessment of the support for the overall solution. This will be built upon by the results of specific, statistical tests designed to more objectively quantify the level of support (both for the solution as a whole and for the specific clades within it) and of various comparative tools, which are presented in the following two sections respectively. Although the comparative tools are not tests of support per se, their output very often will indicate the robustness of a solution [= how resistant it is to further change; Maddison et al. (1984)], and can be used to corroborate the findings of the true tests of support.

STATISTICAL TESTS

Interpreting statistical results

While the influx of numerous statistical tests has been a great boon to the practice of phylogenetic analysis, the results of these tests seem to be frequently misinterpreted. The case for both the PTP test and skewness is clear and has been mentioned in the **Methods and Materials** section: the degree of character covariation that these tests really indicate is held to equate with the degree of phylogenetic signal in a given data set. Likewise, analyses such as the bootstrap and Bremer support have been, or could be, taken to provide some form of confidence interval on how well a data matrix estimates the one true phylogeny. In reality, these tests merely indicate how well that data matrix presents its own underlying distribution (= hierarchical pattern of relationships), which may or may not coincide with the real distribution. The extension towards how well this underlying distribution estimates the real phylogeny, again, requires additional assumptions.

Most cladists believe that the one true phylogeny is represented by a pattern of shared derived characteristics in organisms and can be reconstructed by interpreting this pattern through some criterion (e.g., parsimony, maximum likelihood). Thus, we attempt to gather

data sets that include only phylogenetically informative characters (see Sanderson 1989; Kluge & Wolf 1993) that are sufficient in number and adequately distributed to reconstruct all portions of the true phylogeny. Given the view that true homoplasy does not exist [as homoplasy merely represents inadequately or improperly described features (see Hennig 1966)], each set of phylogenetically informative characters should yield the true phylogeny (or at least very close to it) under these ideal conditions.

Ignoring any potential flaws in the logic of the cladistic method, the main problem is that we cannot a priori discriminate between characters that have been shaped by evolution via common descent (i.e., are phylogenetically informative) and those that have been influenced by a host of other processes. The variable inclusion of these latter, phylogenetically misinformative, characters will, when they conflict with the informative characters, deflect us away from the true phylogeny to varying extents. This, undoubtedly, is the cause of the many conflicting systematic hypotheses for a given group present throughout the literature. Thus, our data sets probably possess biased estimates of the actual distribution, and the various tests that aim to place confidence intervals on the distribution implied by the data are, in most cases, placing confidence intervals on this biased distribution (but see Felsenstein & Kishino 1993; Hillis & Bull 1993). This is unwittingly illustrated for the bootstrap in Fig.1 of Hillis & Bull (1993). The bootstrap pseudosamples (= replicates here) are one step too far removed to be able to estimate the true phylogeny (without the additional assumption that all the characters are phylogenetically informative).

Yet, Hillis & Bull (1993) indicate that, under certain circumstances, the bootstrap actually provides a conservative estimate that an indicated group is also found in the known true phylogeny. (The phylogeny was known in this instance as it was computer generated or created in the laboratory using viruses.) But, if this is the case, then how does one explain equally high (and sufficiently high so as to indicate the reality of the clade with some confidence) bootstrap frequencies in conflicting solutions? To illustrate this point, we have run bootstrap analyses equivalent to the one performed here for the "rival" hypotheses of Wyss (1987, 1988a), Wyss & Flynn (1993), and Berta & Wyss (1994). [Where possible, the data matrices were analyzed as indicated in the respective study. The only changes we made were to include all-zero state ancestors for Wyss (1987; 1988a) to polarize the characters, and to change state 9 ("known, but not described") to a question mark for Wyss (1987). This coding more properly reflects that the data are really missing, whereas Wyss's (1987) coding implies that the act of not having a known state described is a putative homology. These changes did not result in a different most parsimonious solution for either study.] In each case, the bootstrap generally supported the findings of the respective conflicting parsimony analyses with bootstrap frequencies about on a par with those observed here (Figs.6 and 8 respectively). This apparently anomalous result of equally (and sufficiently) supported, but highly contrasting solutions supports our contention that at least the bootstrap, and probably most of the remaining tests are merely elucidating how strong the underlying, potentially biased distribution is in each set of characters, and not how well each data matrix estimates the actual phylogeny.

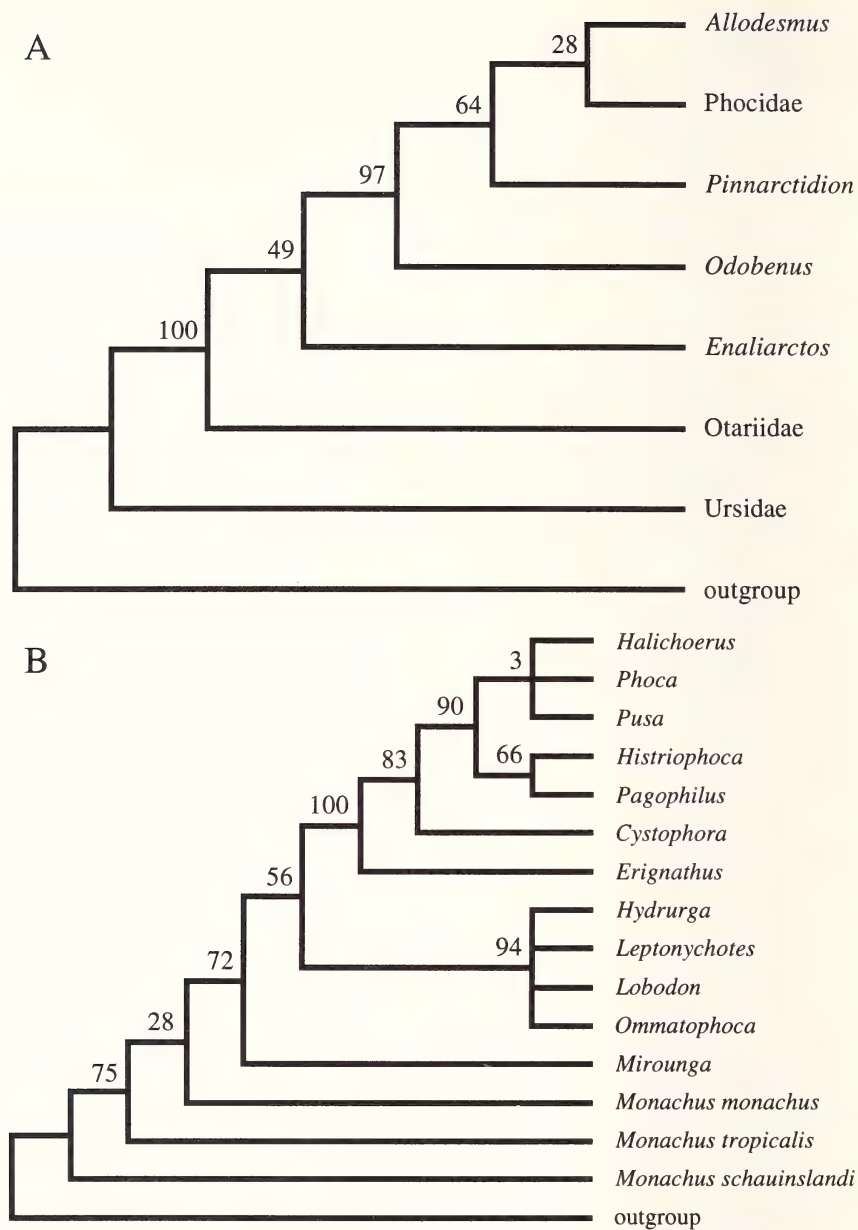


Fig.6A–B: Majority rule consensus solutions with bootstrap frequencies resulting from bootstrap analyses (1,000 replications) of various “rival” data matrices for examining pinniped phylogeny: (A) Wyss (1987) and (B) Wyss (1988a).

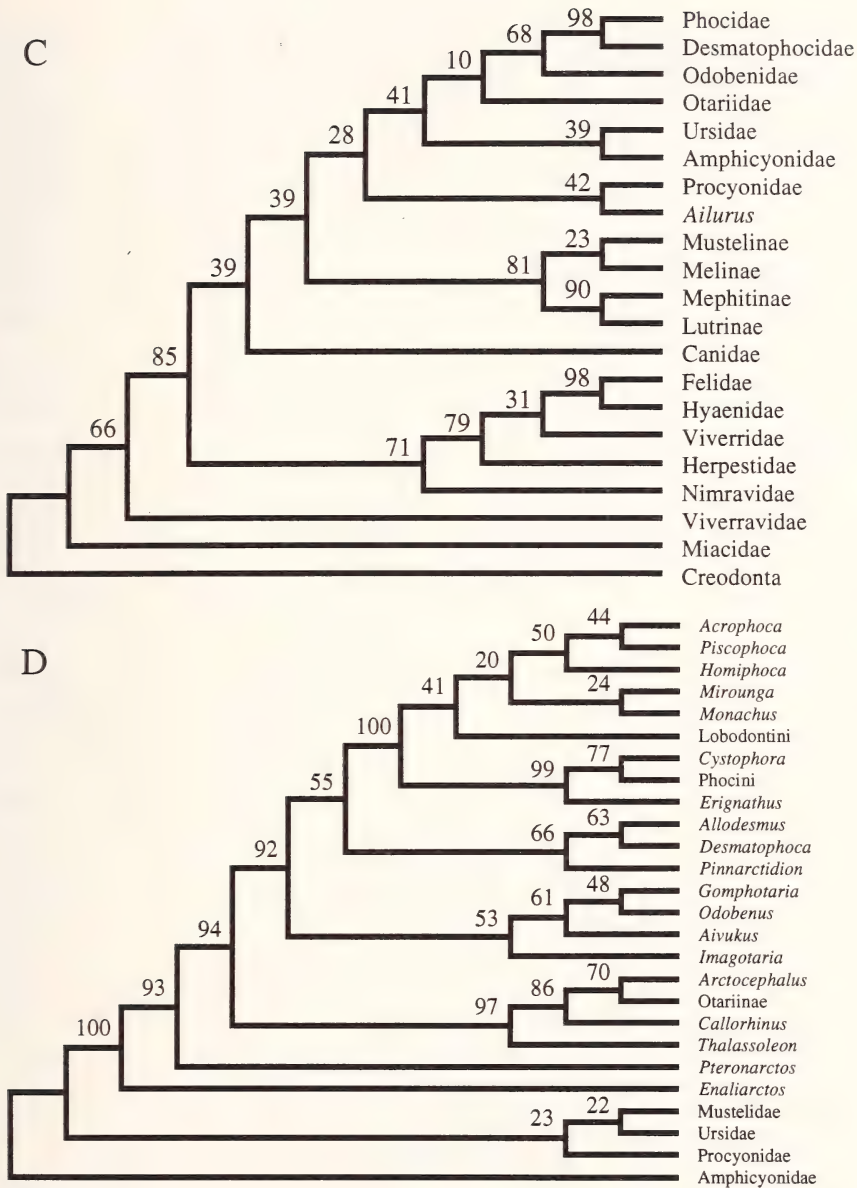


Fig.6C–D: Majority rule consensus solutions with bootstrap frequencies resulting from bootstrap analyses (1,000 replications) of various “rival” data matrices for examining pinniped phylogeny: (C) Wyss & Flynn (1993) and (D) Berta & Wyss (1994).

The solution then seems to be not the accumulation of data matrices with only phylogenetically informative characters (which may be impossible to determine), but of matrices that represent a random sample of the universe of all possible characters. This is based on the assumption that of the many possible signals influencing the form of a character, the phylogenetic signal will be the strongest (otherwise, a systematic analysis based upon phylogenetic principles would appear to be unrealizable). Thus, by taking a random sample, the phylogenetically informative characters will hopefully predominate and point towards the one true phylogeny. As well, in such a case (where the signal within the data matrix closely approximates the true phylogeny), the various statistical tests mentioned above will be more likely to be placing confidence intervals on how well we have reconstructed the true phylogeny.

A simple analogy involves a universe of (scattered) points that roughly indicate a square in space. Through some biased sampling (which emulates the inclusion of increasing numbers of non-phylogenetically determined characters), we could achieve data sets whose underlying distributions are of a straight line and a circle respectively. [Note that this is also possible under random sampling, but should be far less likely to occur. Likewise, biased sampling could also indicate a square (e.g., sample only from the corner regions), but, again, this is unlikely.] By employing tests based on each data matrix, or some sample thereof, we cannot help but observe something along the lines of a line and a circle each time.

Although all of our current tests provide valuable information, they may be erroneously focused. These tests indicate only the signal strength in our samples, with no indication as to the accuracy of that signal. They are similarly hampered by being based, to varying degrees, on the same tree constructing methods (and thus the same potential biases) that were used to generate the cladogram under examination. As stressed by Sanderson (1989), more tests that are independent of the various tree constructing methods are required. Although it is unlikely to ever be developed, what we really require is a statistical test measuring the randomness of our sample of characters, for it is presumably only with a random sample that our data matrices will estimate the true phylogeny to various degrees (which our current tests could then delineate). Unfortunately, even with such a test we would be left with a discrepancy between what it really indicates (randomness of the character set) and what we would interpret it to mean (the potential accuracy of the character set in predicting the true phylogeny). Note that this desired test is subtly, but meaningfully different from our current PTP and skewness tests. In a universe of characters shaped largely by evolution, a random sample thereof should covary significantly, except now this covariation would be primarily due to common descent with modification. The characters need not be completely independent either (and in all likelihood they would not be), merely a random sample. Without such a test for randomness, all that we are left with is a critical examination of the characters used to achieve a given result, something that has, unfortunately, become increasingly rare with the influx of statistics into cladistics.

The total evidence approach, where different data sets are combined into one larger data set (see Kluge 1989; Kluge & Wolf 1993), is one step towards reducing the bias present in our character sets. Disregarding potential problems such as how to combine characters

from very different sources (e.g., morphological versus molecular data), or whether or not one can even justifiably pool data matrices of very different signals (see Bull et al. 1993), total evidence does, in principle, provide the advantage of a more varied data set that presumably provides a better and/or wider representation of the suite of all possible characters. However, we are left with the same dilemma, now only one step further removed. So long as the set of characters is non-random, the tests we currently have will not place confidence intervals on the true phylogeny.

Therefore, we will interpret our results according to what the various tests maximally indicate: character covariation (PTP and skewness tests), or how strongly our data present some underlying distribution which may or may not be the true phylogeny (bootstrap and support analyses, as well as successive approximations and constraint analyses). The true "test" lies in the **Character Analysis** section, where the set of characters producing this distribution are individually presented and described. Implications as to the overall accuracy of our solution (with respect to the one true phylogeny) are not intended. But, since we naturally feel that our data set is one of the best available in terms of taxonomic rank examined, number of taxa (both ingroup and outgroup), range of morphological characters (with the acceptance and inclusion of polymorphic data), and general inclusiveness, we feel that it provides one of the better estimates of the true phylogeny of the phocid seals. However, with no knowledge as to how random our character set is, we make no pretense as to the accuracy of our solution.

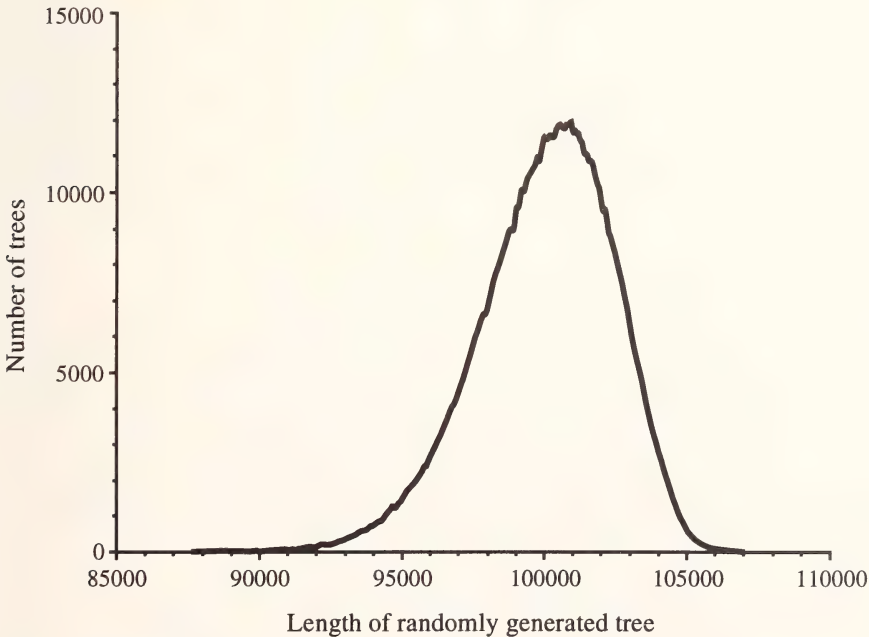


Fig.7: Frequency distribution of tree lengths for a random sample of 1,000,000 trees generated from the inversely weighted data matrix. Skewness statistic (g_1) = -0.503.

Character covariation within the data set

Both the PTP and skewness tests produced highly significant results, indicating very strong character covariation within the data set. Using 99 randomly permuted data matrices, the PTP statistic (or α') was calculated as 0.01. The more accurate estimates proposed by Källersjö et al. (1992) showed even lower values: 6.0×10^{-4} for α'' and 2.2×10^{-18} for α^* . In accordance with Källersjö et al. (1992), this last, lowest value is held to be the best estimate of the level of significance here. The critical PTP length value corresponding to the 0.05 level was determined to be 79,619 steps, some 9,785 steps (142 corrected steps) longer than the overall parsimony solution. The shortest and longest trees derived from the permuted matrices were 79,227 (+ 9,393 steps / 137 corrected steps) and 80,605 steps (+ 10,771 steps / 157 corrected steps) respectively.

Skewness tests echoed the findings of the PTP test. A frequency distribution of tree lengths from a random sample of 1,000,000 trees possessed a value of -0.503 for g_1 (Fig.7). This was judged to be significant at the 0.05 level based on a critical value for g_1 (25 taxa and 250 binary or four-state characters) of -0.08 (Hillis & Huelsenbeck 1992). The shortest random tree obtained, 85,170 steps, was 15,336 steps (223 corrected steps) longer than the overall solution. As suggested by Källersjö et al. (1992), the sample size used here was apparently not sufficient to sample trees from the attenuated left-hand tail of the distribution.

Regional support within the overall solution

While the previous subsection demonstrated significant character covariation throughout the data set as a whole, not all regions within the resultant solution will necessarily be equally supported by this set of covarying characters. The remaining statistical tests show considerable agreement as to the regional localization of stronger and weaker signal within the data set. This more localized signal, it appears, is sufficiently strong and/or widespread to override regions of weak support and be manifested at the level of the entire solution (see above).

Bootstrap analysis (Fig.8)

The majority rule consensus tree obtained from a bootstrap analysis of 1,000 replicates (Fig.8A) agrees quite strongly with the overall parsimony solution. The various goodness-of-fit statistics are virtually identical between the two solutions, and the bootstrap solution at 70,006 steps is only 172 steps (= three corrected steps) longer than the overall solution. Only two major topological differences were observed, one in each phocid subfamily. In the monachines, *Leptonychotes* moved to a more terminal position to form a clade with *Lobodon*. This clade now becomes the sister group to *Monachus* spp. In the phocines, the clade composed of *Erignathus*, *Histriophoca*, and *Pagophilus* moved basally to form the sister group to *Phoca* spp. plus *Pusa* spp. Within this latter clade, *Pusa* is indicated to be monophyletic, with *Pusa caspica* again being held to be basal to the remaining species of the genus. *Phoca* remains paraphyletic and related by sympleiomorphies, with *Phoca largha* maintaining its more basal status within the genus. However, as the bootstrap solution is based on statistical considerations and not parsimonious ones (as well as being

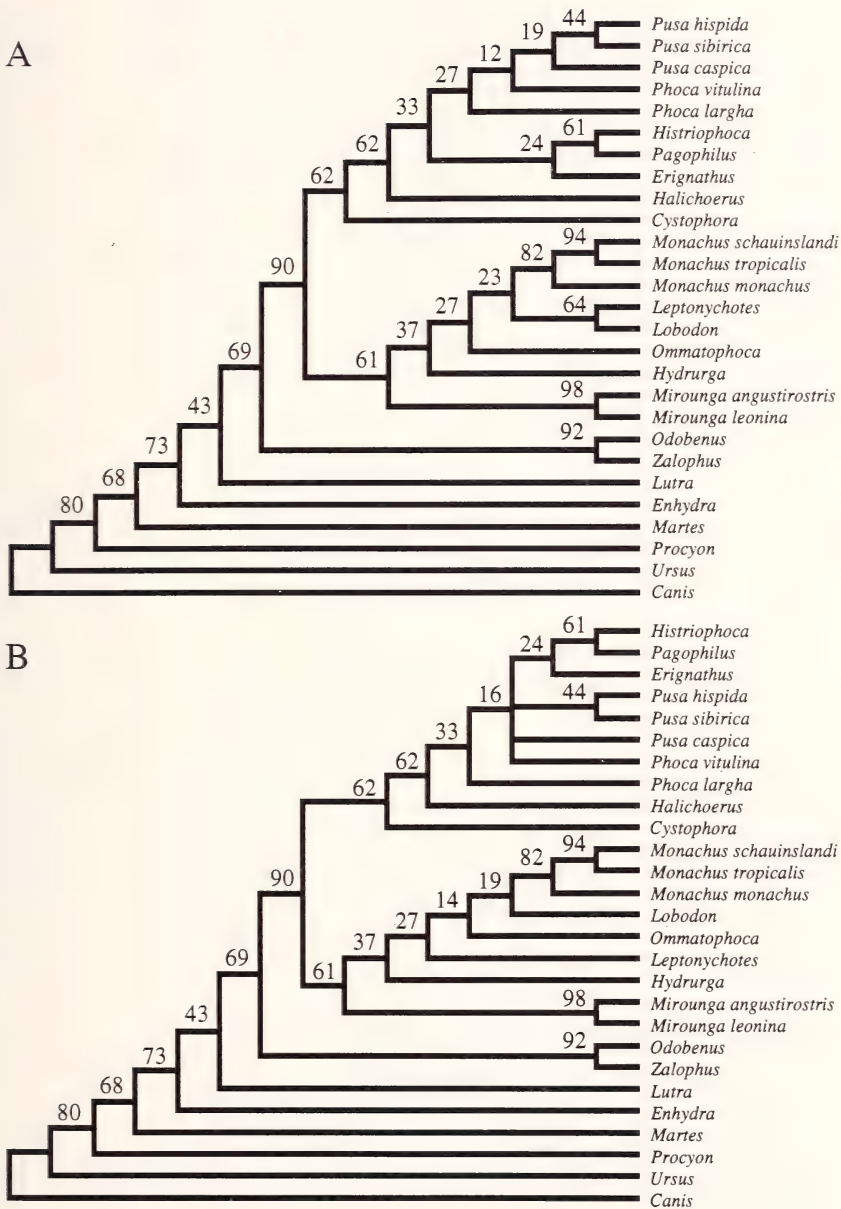


Fig.8: Results from a bootstrap analysis (1,000 replications) of the inversely weighted data matrix. (A) Majority rule consensus tree from bootstrap analysis (length = 70,006 steps, CI = 0.456, HI = 0.770, RI = 0.626, RC = 0.405). (B) Overall parsimony solution with bootstrap frequency of each node.

Table 2: Bootstrap frequencies indicating support within the inversely weighted data matrix for a monophyletic grouping of various outgroup taxa and either the phocids alone or the pinnipeds as a whole. Numbers given as the total number of trees (out of 1000) / percentage of all trees.

Alternative outgroup	For phocids alone	For all pinnipeds
arctoid	< 0.08 / << 1	1000* / 100*
procyonid	1.00 / < 1	1.00 / < 1
ursid	< 0.08 / << 1	21.00 / 2
mustelid (including lutrines)	115.50 / 12	680.50 / 68
musteline	4.00 / < 1	43.67 / 4
lutrine (both <i>Enhydra</i> and <i>Lutra</i>)	219.67 / 22	729.33 / 73
<i>Enhydra</i> alone	11.25 / 1	41.00 / 4
<i>Lutra</i> alone	119.93 / 12	428.67 / 43
otarioid	687.00 / 69	n/a
<i>Odobenus</i> alone	59.00 / 6	n/a
<i>Zalophus</i> alone	24.50 / 2	n/a

* Due to *Canis* being the ultimate outgroup, this arrangement was necessarily found in all bootstrap replicates.

a consensus solution; see **Methods and Materials**), we should look instead to the overall solution.

When bootstrap frequencies are determined for the nodes present in the overall solution (Fig.8B), a clear dichotomy in support can be observed. Outgroup relationships tend to be moderately to strongly supported, with only the node for *Lutra* plus the pinnipeds falling below a bootstrap frequency of 50%. However, this merely reflects an equally strong tendency for the two lutrines to form a monophyletic sister group to the pinnipeds (bootstrap frequency = 39%), in essence a minor alteration. A monophyletic Otarioidea is particularly strongly indicated. Bootstrap frequencies for alternative outgroup arrangements are noticeably smaller, especially for those postulating a diphyletic Pinnipedia (Tab.2).

The monophyly of both the phocids as a whole, and of each of its two subfamilies, show comparable bootstrap frequencies to the outgroup nodes. Beyond this, support for the relationships within each subfamily was distinctly weaker. Only the species clusters of *Histriophoca* plus *Pagophilus*, *Mirounga* spp., and *Monachus* spp. (and *M. schauinslandi* plus *M. tropicalis* within this) display bootstrap frequencies greater than 50%. A monophyletic Phocini (plus *Erignathus*) is also relatively strongly indicated (bootstrap frequency of 62%), giving further support to the basal position of *Cystophora* within the phocines. In fact, *Cystophora* displays an unusually strong tendency to cluster with the monachines (bootstrap frequency of 31%), something that might be expected more of the supposedly more monachine-like *Erignathus*, but was not supported here (bootstrap frequency of <1%).

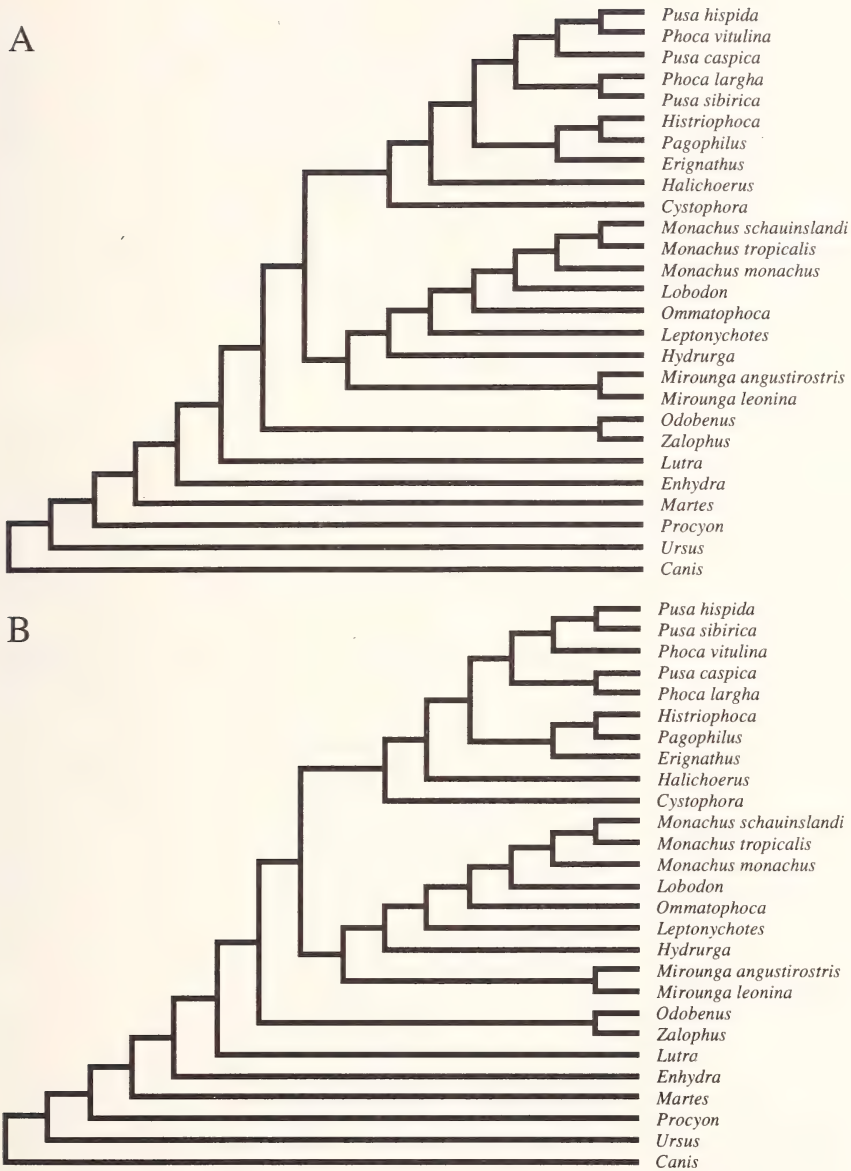


Fig.9: Cladograms resulting from a successive approximations analysis. Characters were reweighted according to their (A) CI and (B) RI or RC from the overall parsimony analysis (with each solution being identical between maximum, minimum, and average fit of the respective goodness-of-fit statistic). Both trees of length = 69,842 steps, CI = 0.456, HI = 0.770, RI = 0.629, RC = 0.407.

Successive approximations (Figs.9 and 10)

The a posteriori weighting of the characters based on one of three goodness-of-fit statistics (CI, RI, or RC) converged on either of two solutions (Fig.9). Each solution, when constrained with the original set of inversely weighted characters, was only very slightly longer than the overall solution at 69,842 steps (= 7 steps / 1 corrected step longer). Topological differences between these two solutions, and between either and the overall solution were found solely within the Phocini (plus *Erignathus*) and limited to the interrelationships between *Phoca* spp. and *Pusa* spp. This conflict is reflected by the strict consensus tree of both solutions [Fig.10A; the majority rule solution (Fig.10B) is the same as that produced by either the RI or RC] where the species of both genera are the sole members of a completely unresolved polytomy.

Support analysis (Fig.11)

Interpreting the results of the support analysis varies according to the form of consensus tree that is viewed, with the strict and majority rule consensus algorithms treating conflicting solutions relatively more severely and more forgivingly respectively (see **Methods and Materials**).

The strict consensus trees show a steady decrease in resolution as increasingly homoplasious solutions are retained. At only one corrected step longer than the most optimal solution (Fig.11A), resolution within the Phocini (plus *Erignathus*) is almost completely lost. Resolution is also lost for the lutrines, reflecting the equally large tendency for these two taxa to form a monophyletic sister group to the pinnipeds (see above). An increase of an additional corrected step (Fig.11B) shows a partial degradation of lobodontine relationships, which becomes complete at the next step (Fig.11C). At this latter step (three corrected steps longer), resolution is completely lost for the Phocini (plus *Erignathus*) as well, and the integrity of the monachines is also lost. Finally, at the limits of the analysis (Fig.11D), almost all structure within the phocids is lost. Only the clades of *Mirounga* spp. and *Monachus* spp. (and within *Monachus*) retain unanimous support. As well, structure is lost for the pinnipeds as a whole, with the otarioids and phocids, although still distinct clades, forming a polytomy with the lutrines. Another polytomy was also formed between *Procyon*, *Martes*, and the lutrine-pinniped clade.

In contrast, the majority rule consensus trees show virtually complete and unaltered resolution, even at the limits of the analysis. Only a progressive degeneration of Phocini (plus *Erignathus*) structure was observed, although the support within the phocids as a whole (as visualized by the percentage of solutions supporting each node) gradually decreased with increasing length (except for most strongly supported species clusters). Among outgroup relationships, only support for the *Lutra*-pinniped and *Martes*-lutrine pairings were observed to decrease, albeit only slightly, with increasing length.

Overall conclusions

Altogether, the findings of these statistical tests largely corroborate those of the parsimony analysis conducted in the previous section. This could be an artifact of all these tests

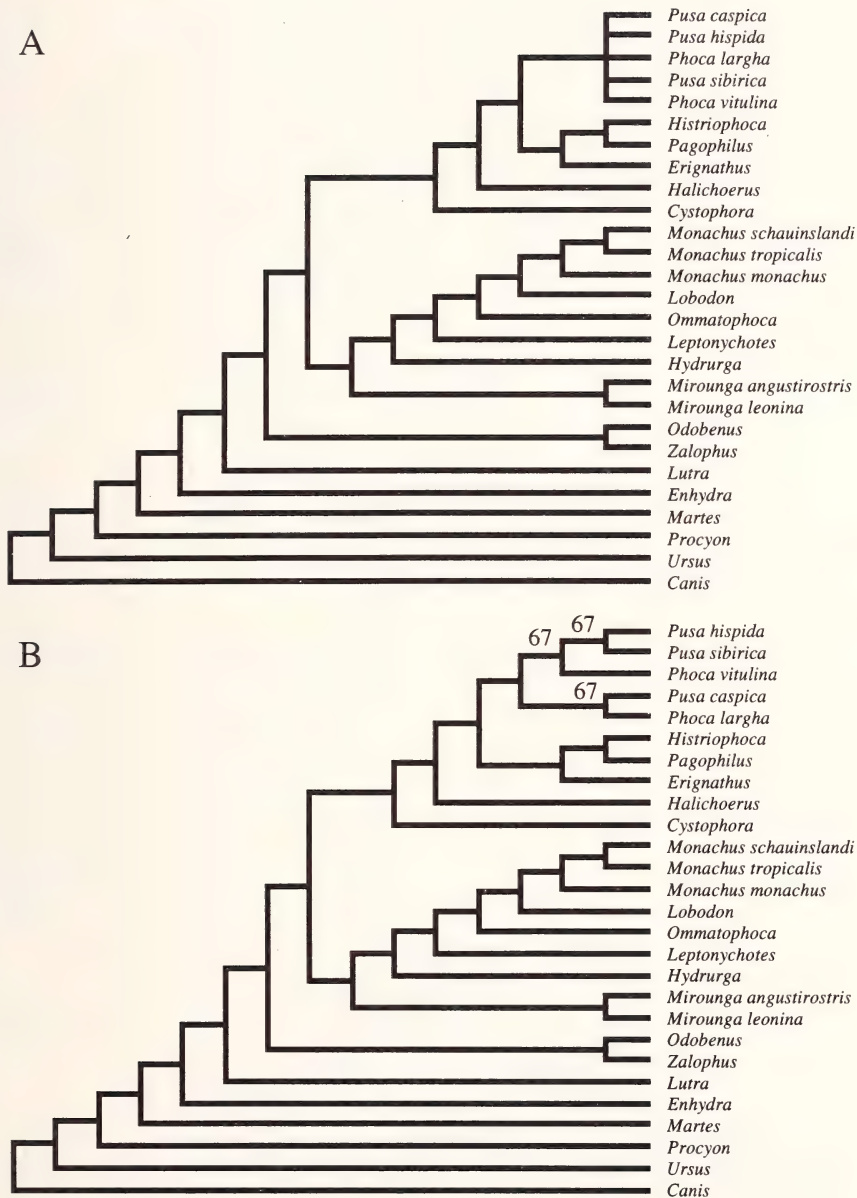


Fig.10: Strict (A) and majority rule (B) consensus solutions for cladograms resulting from successive approximations analyses based upon CI, RI, and RC. Unless otherwise indicated, all nodes in (B) were found in 100% of the equally most parsimonious solutions.

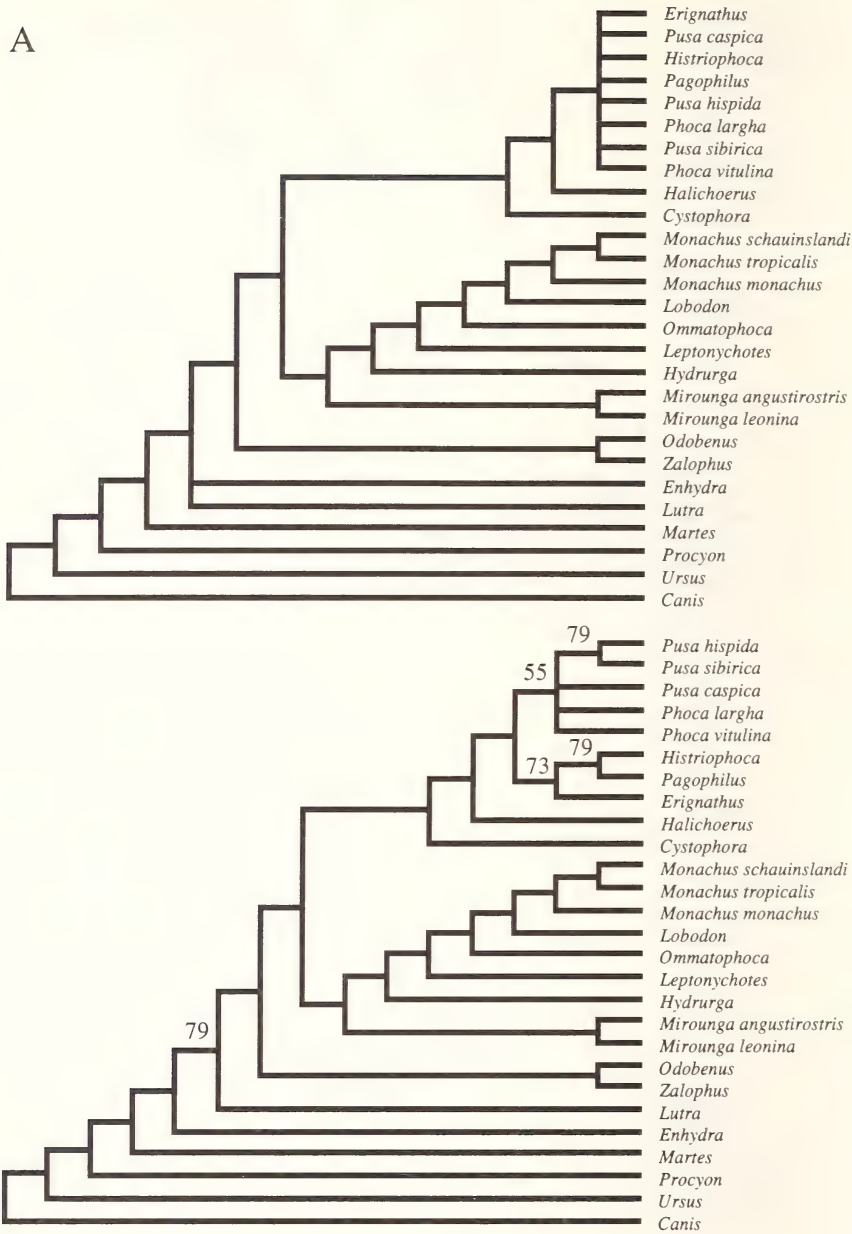


Fig.11A: Strict (top) and majority rule (bottom) consensus solutions resulting from a support analysis of the inversely weighted data matrix. (A) All trees of 69,903 steps or less ($n = 33$).

B

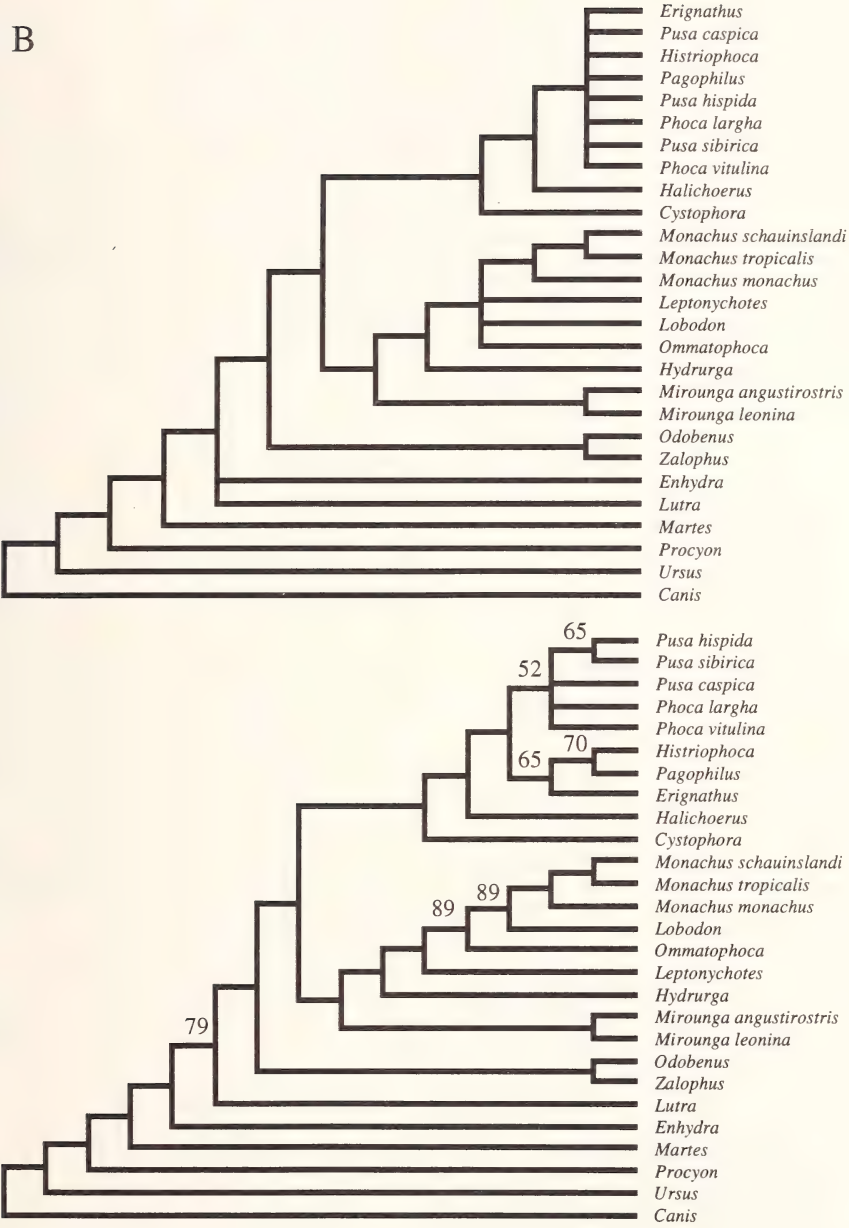


Fig.11B: Strict (top) and majority rule (bottom) consensus solutions resulting from a support analysis of the inversely weighted data matrix. (B) All trees of 69,972 steps or less (n = 187).

C

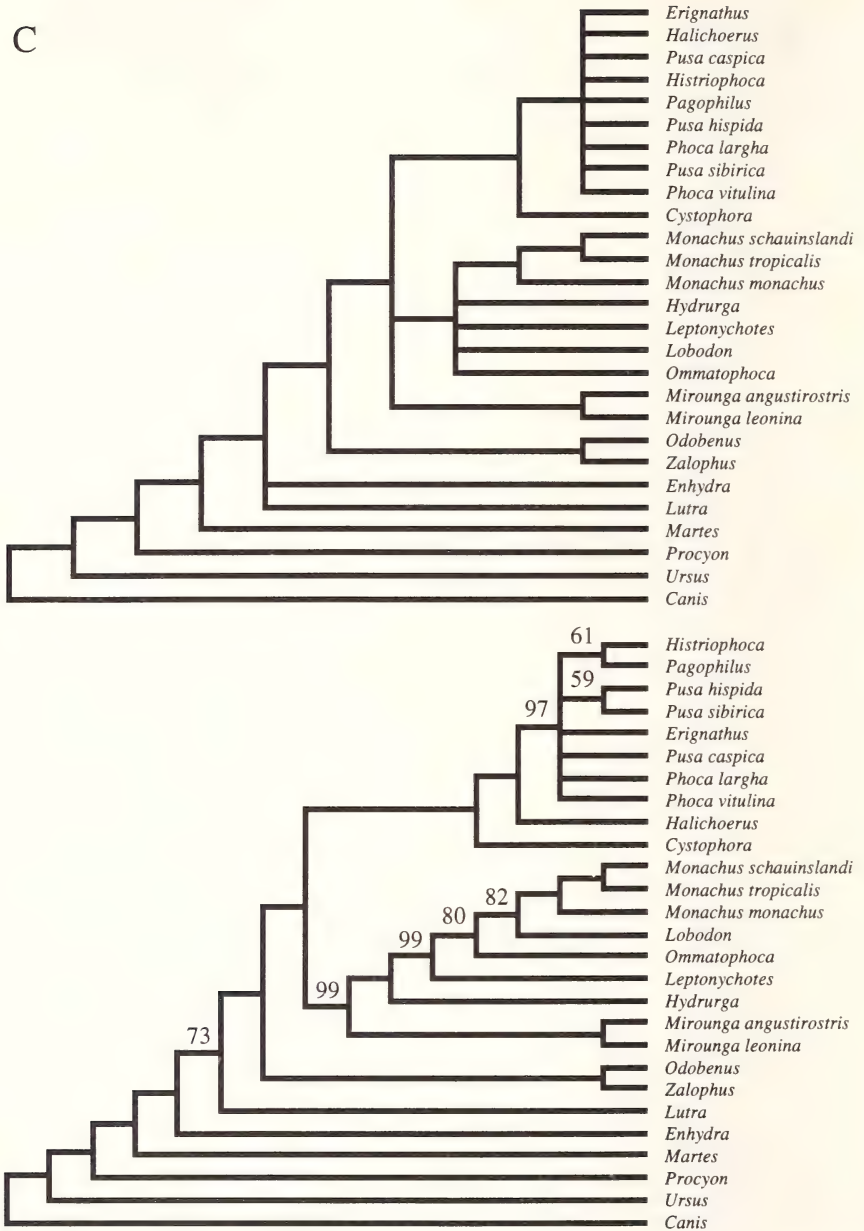


Fig.11C: Strict (top) and majority rule (bottom) consensus solutions resulting from a support analysis of the inversely weighted data matrix. (C) All trees of 70,041 steps or less ($n = 917$).

D

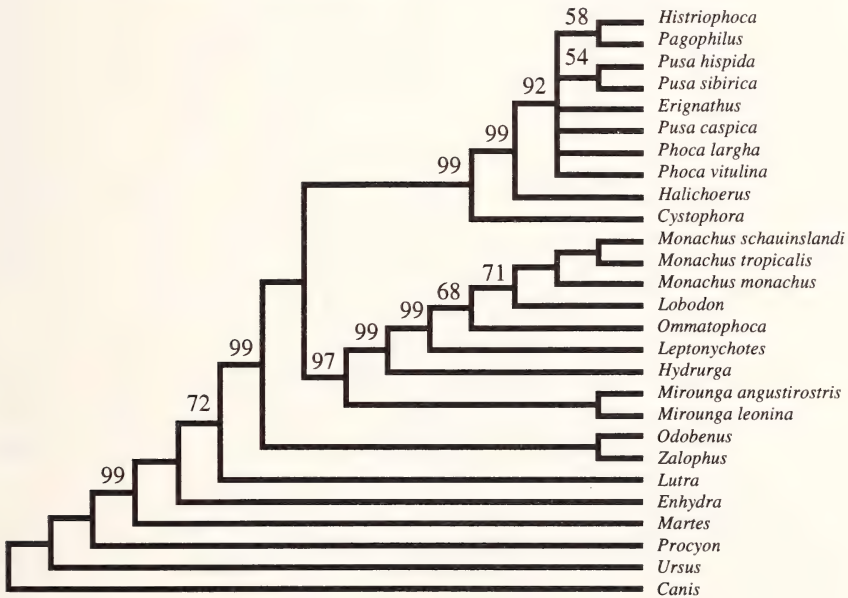
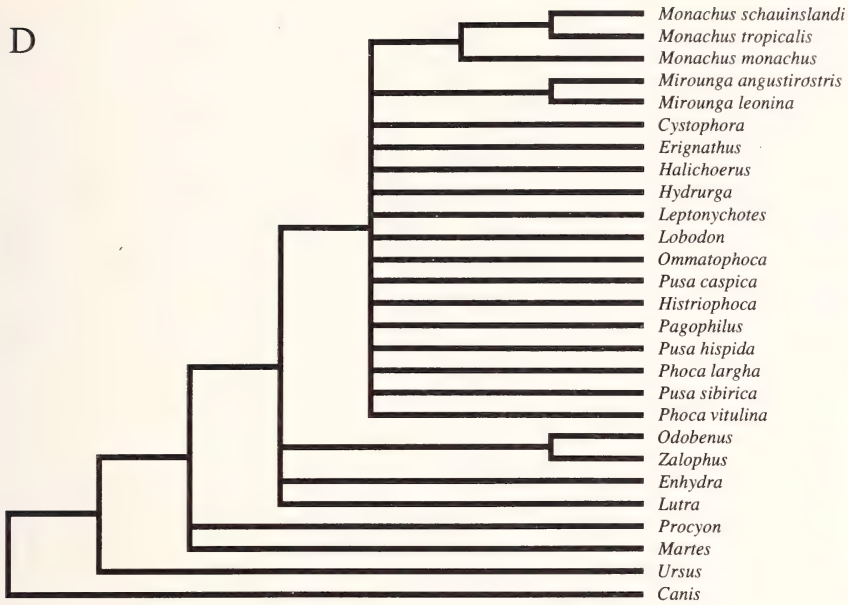


Fig.11D: Strict (top) and majority rule (bottom) consensus solutions resulting from a support analysis of the inversely weighted data matrix. (D) All trees of 70,110 steps or less ($n = 3,409$).

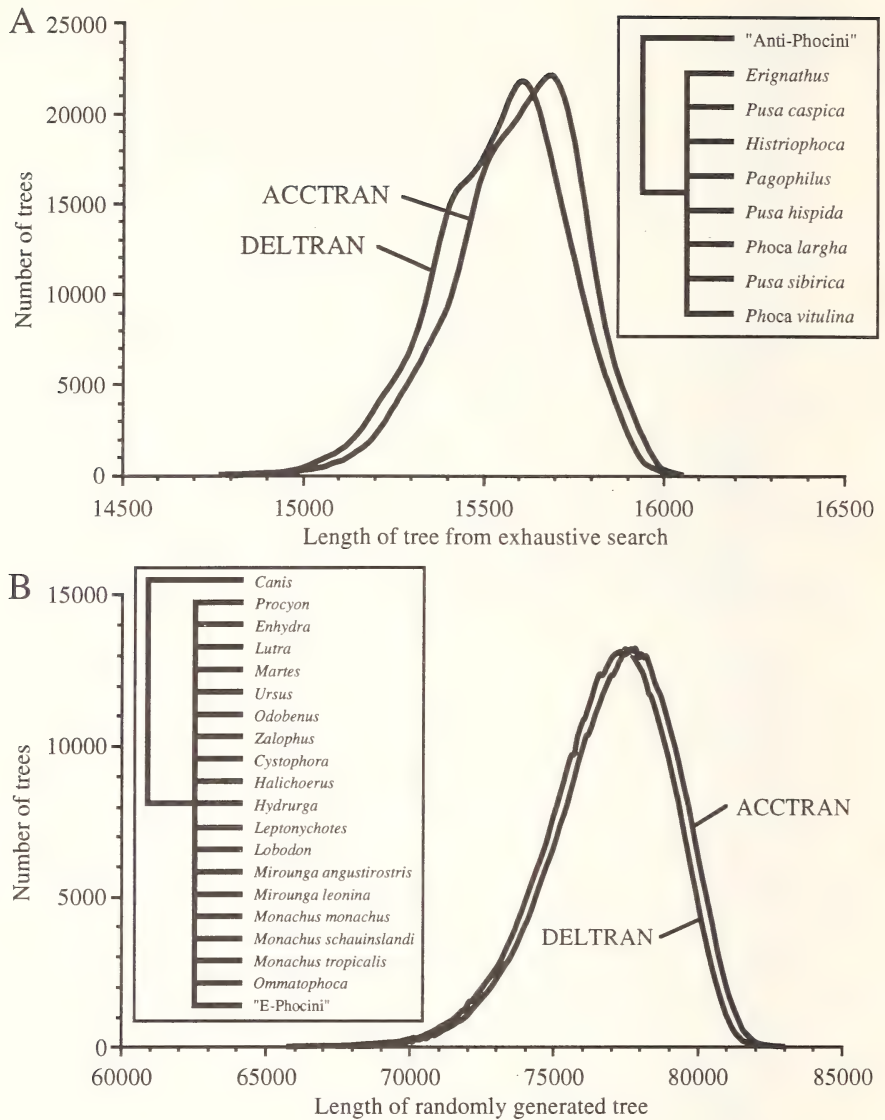


Fig.12: Frequency distributions of tree lengths generated from the inversely weighted data matrix with some regions topologically constrained. (A) Clade "anti-Phocini" collapsed (see insert) according to either accelerated (ACCTRAN; $g_1 = -0.483$) or delayed transformation (DELTRAN; $g_1 = -0.368$) criteria. (B) Clade "E-Phocini" collapsed (see insert) according to either ACCTRAN ($g_1 = -0.540$) or DELTRAN ($g_1 = -0.541$) optimization. Distributions are of either all 135,135 possible trees (A) or of a random sample of 1,000,000 trees (B).

(including the overall parsimony analysis) being based on the same data matrix, or some sample(s) thereof. Combined with all of the procedures using some form of parsimony criterion, it is not too surprising that they all indicate roughly the same solution, as they are merely summarizing the underlying distribution of the matrix in slightly different ways.

As exemplified by the results of the bootstrap analysis, the common finding is for relatively strongly supported outgroup relations, with support dropping off markedly within each phocid subfamily (some fairly robust species pairs therein notwithstanding). However, we would postulate that the region of weaker signal is limited even further to that portion of the cladogram near the polytomy within the Phocini (plus *Erignathus*). Despite the comparably weak bootstrap frequencies generally present in both subfamilies, the pattern advocated in the previous section for the monachines appears to be remarkably robust and survives largely intact in both the support and successive approximations analyses. A monophyletic *Monachus*, in particular, seems to be very robust. In contrast, the pattern within the Phocini (plus *Erignathus*) is more labile, with almost every analysis holding for a slightly different set of relationships. Although the membership of the group in question (*Erignathus*, *Histiophoca*, *Pagophilus*, *Phoca* spp., and *Pusa* spp.) is constant, as is its monophyletic status, only the *Erignathus*, *Histiophoca*, and *Pagophilus* clade appears to have any consistent support. Overall, this set of conclusions could also be reached by merely examining the number of synapomorphies supporting the various nodes within each phocid subfamily (Fig.5C). The nodes within the Monachinae are more strongly supported in this respect than are those within the Phocinae, and especially those within the Phocini (plus *Erignathus*).

Therefore, it was somewhat surprising that a test aimed directly at elucidating this weak region (constrained skewness) did not identify it as such (Fig.12). Constraining the stronger, and therefore supposedly more informative, "anti-Phocini" (Fig.12A) did not eliminate a significant left-hand skew in the distribution as expected [$g_1 = -0.483$ (ACCTRAN) or -0.368 (DELTRAN); critical $g_1 = -0.29$ or -0.22 at the 0.05 level for nine taxa and 250 binary or four-state characters respectively]. Thus, there would appear to be greater support (i.e., character covariation) within the Phocini (plus *Erignathus*) than the remaining tests indicate, as skewness seems to be very sensitive to minute amounts of covariation (Hillis & Huelsenbeck 1992). As well, the g_1 s for the "anti-Phocini" test are approaching their respective critical values to a greater extent than we have ever witnessed in a skewness test, indicating some reduction in the level of character covariation, but not to non-significant levels. Finally, the constrained skewness test does appear to be working properly (within the suspect nature of PAUP's RANDOM TREES subroutine), as the reciprocal constraint of the weaker "E-Phocini" (Fig.12B) produced the expected significantly left-hand skewed distribution [$g_1 = -0.540$ (ACCTRAN) or -0.541 (DELTRAN); critical $g_1 = -0.08$ at the 0.05 level for 25 taxa and 250 binary or four-state characters]. However, in order to more rigorously test this last supposition, random clades of a fair size (say six or seven taxa) should be constrained, and the skewnesses of the resulting distributions analyzed.

COMPARATIVE TOOLS

Constraint analysis**Outgroup constraints** (Figs.3 and 13, and Tab.3)

All outgroup constraints, which forced an alternative set of outgroup relationships to those found in the overall solution, produced cladograms that were longer than the overall solution (Fig.13 and Tab.3). However, in relative terms, these increases were almost negligible, as even the longest solution (from the constraint tree "ursid - diphyly") of 1,388 extra steps (21 corrected steps) only amounts to an increase of 0.77% over the most parsimonious length (of the overall solution) of 69,834 steps. Given such slight increases in length, corresponding bootstrap frequencies for the specific clade(s) under examination were surprisingly low (all below 22%). This might indicate that although very few individual characters directly support the various alternative outgroup relationships, the

Table 3: Summaries of searches of the inversely weighted data matrix with certain topological constraints of outgroup relationships imposed (see Fig.3). MPT = most parsimonious trees. Bootstrap frequencies for the desired monophyletic group are given whenever possible. When a constraint tree imposes multiple monophyletic groups, the bootstrap frequency indicated is that of the least supported major clade (indicated by an asterisk).

Constraint tree	Absolute length	Extra steps relative to overall solution (absolute / corrected)	No. of MPT	Bootstrap analysis frequency	(%)
Pinnipedia					
– monophyly	69834	(+0 / +0)	2	687.00	(69)
– (not) monophyly	70067	(+233 / +4)	3	–	–
– diphyly	70334	(+500 / +8)	2	115.50*	(12)*
Ursidae					
– ursid - monophyly	70374	(+540 / +8)	1	21.00	(2)
– ursid - diphyly	71222	(+1388 / +21)	1	< 0.08	(<< 1)
– ursid - odobenid	70374	(+540 / +8)	1	–	–
Mustelidae					
– mustelid - monophyly	69834	(+0 / +0)	2	680.50	(68)
– mustelid - diphyly	70334	(+500 / +8)	2	115.50	(12)
Mustelinae					
– musteline - monophyly	70225	(+391 / +6)	2	43.67	(4)
– musteline - diphyly	70708	(+874 / +13)	2	4.00	(< 1)
Lutrinae					
– lutrine - monophyly	69834	(+0 / +0)	2	729.33	(73)
– lutrine - diphyly	70067	(+233 / +4)	3	219.67	(22)
Miscellaneous					
– (not) otarioid	70067	(+233 / +4)	3	–	–
– (not) otarioidea	70234	(+400 / +6)	2	–	–
– odobenid	70234	(+400 / +6)	2	59.00	(6)

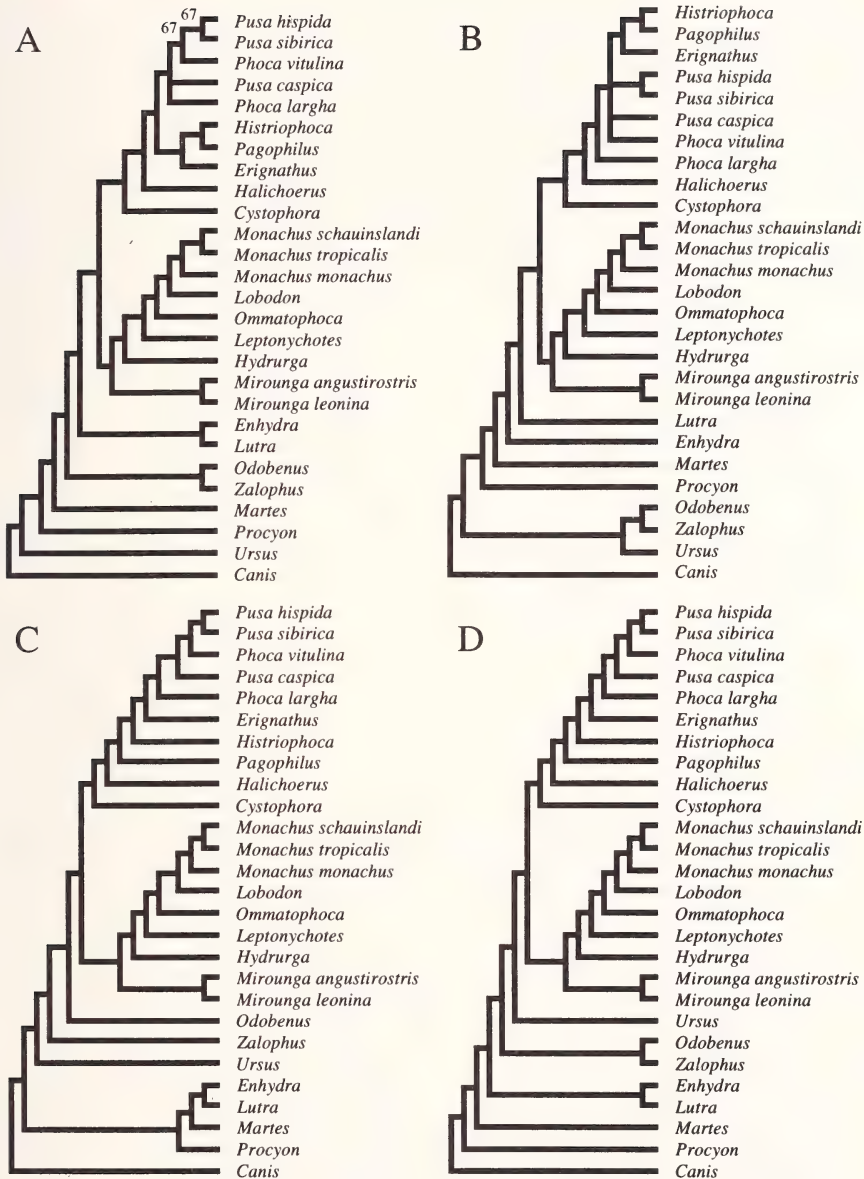


Fig.13A–D: Cladograms resulting from a constraint analysis examining various alternative hypotheses of outgroup relationships: (A) (not) monophyly *, (B) diphyly *, (C) ursid – monophyly, and (D) ursid – diphyly. An asterisk indicates a majority rule consensus solution, where, unless otherwise indicated, all nodes were found in 100% of the equally most parsimonious solutions. See also Fig.3 and Tab.3.

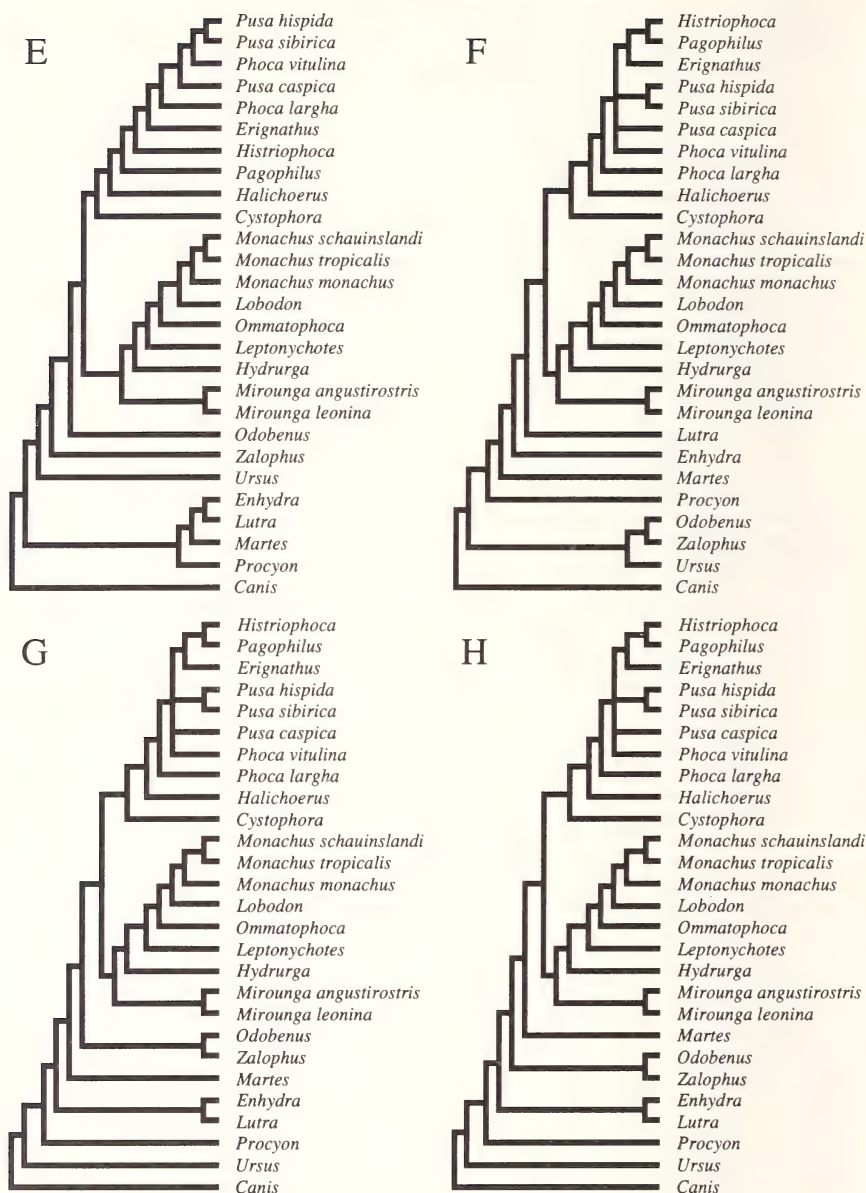


Fig.13E–H: Cladograms resulting from a constraint analysis examining various alternative hypotheses of outgroup relationships: (E) ursid – odobenid, (F) mustelid – diphyly *, (G) musteline – monophyly *, and (H) musteline – diphyly *. An asterisk indicates a majority rule consensus solution, where, unless otherwise indicated, all nodes were found in 100% of the equally most parsimonious solutions. See also Fig.3 and Tab.3.

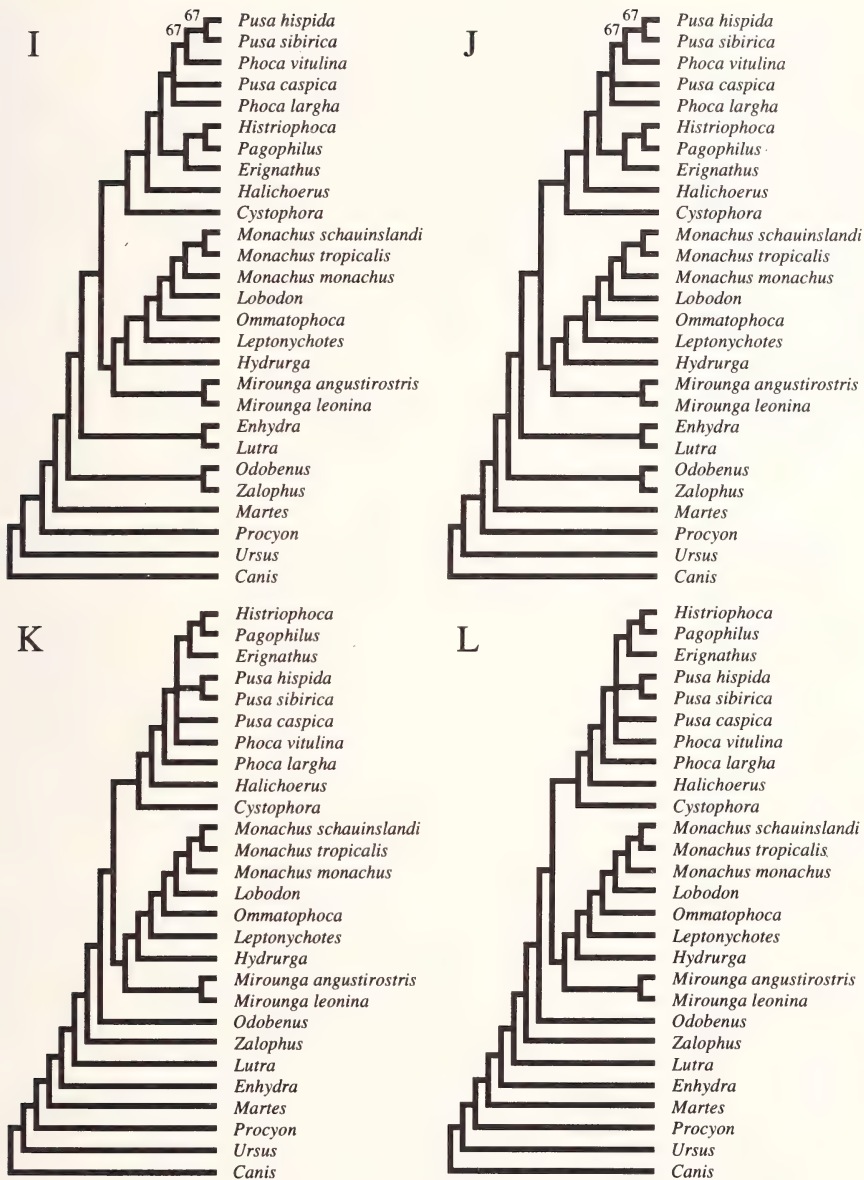


Fig. 13I–L: Cladograms resulting from a constraint analysis examining various alternative hypotheses of outgroup relationships: (I) lutrine – diphyly *, (J) (not) otarioid *, (K) (not) otarioidea *, and (L) odobenid *. An asterisk indicates a majority rule consensus solution, where, unless otherwise indicated, all nodes were found in 100% of the equally most parsimonious solutions. See also Fig. 3 and Tab. 3.

overall matrix can accommodate them with a minimal amount of extra homoplasy (see Overall conclusions – possible effects of polymorphic data below).

Despite these minimal increases in length, some clear patterns did arise in this analysis (Tab.3). Of the paired constraint trees, those advancing a diphyletic Pinnipedia always resulted in a longer and, as measured by the corresponding bootstrap frequency, more weakly supported solution (see also Tab.2). Additional support for a lutrine affinity for the pinnipeds under this data matrix is provided by the observation that the lutrines always form the sister group to the phocids and/or pinnipeds as a whole (Fig.13), unless other sister taxa were specifically constrained for. Numbers of most parsimonious trees were again very low for such a large data set (Tab.3), once again roughly indicative of good resolving power (but see **Overall Parsimony Analysis**; Hillis & Huelsenbeck 1992).

More importantly, relationships within the phocids were identical with those of the overall solution in most cases, or, at most, only slightly altered within the Phocini (plus *Erignathus*). Only those constraint trees supporting an ursid ancestry for the pinnipeds (“ursid - monophyly”, “ursid - diphyletic”, and “ursid - odobenid”) produced major disruptions within the phocids. Again, this was limited to the Phocini (plus *Erignathus*), and amounted to a basal shift of *Histiophoca* and *Pagophilus* to form successive sister taxa to the clade of *Erignathus*, *Phoca* spp., and *Pusa* spp. Thus, the possibility of a symplesiomorphic relationship between *Histiophoca* and *Pagophilus* (see de Muizon 1982a) only appears to arise under the assumption of an ursid affinity for the phocids.

Of the individual solutions (see Fig.13), the constraint of a non-monophyletic Otarioidea – as advocated by Wyss (1987), Berta (1991), Wyss & Flynn (1993), and Berta & Wyss (1994) – converged on the same solution as that resulting from a forced *Odobenus*-phocid pairing. However, while this common solution might point to some affinity between *Odobenus* and the phocids [it only required an extra 400 steps (six corrected steps) over that of the overall solution], such a pairing has very weak support in the data matrix (bootstrap frequency of 6%).

Altogether, the negligible increases in length resulting from the constraint of the various alternative outgroup relationships, coupled with their minimal effects on internal phocid phylogeny point to the potential bias from assuming one outgroup taxon over another for the phocids as being very small. The apparently inherently less stable Phocini (plus *Erignathus*) notwithstanding (see **Statistical Tests** section), the selection of any major arctoid lineage (e.g., lutrines, mustelids, otarioids, or ursids) will apparently all give roughly the same set of internal relationships for the phocids, as was also claimed for the phocines by Perry et al. (1995). This finding might ensue from the early history of the arctoids, whereby the fact that all of these lineages (including the phocids) were diverging at about the same time (Sarich 1976; Wayne et al. 1989; C.A. Repenning, pers. comm.) largely renders the designation of sister taxa as irrelevant, or even erroneous. Thus, the supposition herein of a lutrine affinity for the pinnipeds might be artifactual (i.e., a consequence of this particular biased data set), and an artificial resolution of a real polytomy. Although an intriguing possibility, and preliminarily substantiated by Perry et al. (1995), this question should remain open until more paleontological and/or molecular evidence is accumulated.

Internal constraints (Figs.4 and 14, and Tab.4)

The various alternative ingroup relationships tested in this study likewise all resulted in cladograms that were longer than the overall solution (Tab.4). The increases were again virtually negligible, with most amounting to an increase in length of less than 0.72% (506 extra steps or eight extra corrected steps). The constraints of a monophyletic *Phoca* (both sensu stricto and Burns & Fay 1970) were accommodated with minimal amounts of extra homoplasy in particular. Surprisingly, not even the disruption of one of the most strongly supported nodes in the overall solution, that of a monophyletic Phocidae, produced a tangibly longer solution. Only the very specific constraints of “de muizon” and “wyss” and, to a lesser degree, those requiring a monophyletic Cystophorinae (“three subfamily” and “cystophorinae”) yielded noticeably longer solutions (but still well under a 5%

Table 4: Summaries of searches of the inversely weighted data matrix with certain topological constraints of alternative ingroup relationships imposed (see Fig.4). MPT = most parsimonious trees. Bootstrap frequencies for the desired monophyletic group are given whenever possible. When a constraint tree imposes multiple monophyletic groups, the bootstrap frequency indicated is that of the least supported major clade (indicated by an asterisk).

Constraint tree	Absolute length	Extra steps relative to overall solution (absolute / corrected)	No. of MPT	Bootstrap frequency	analysis (%)
At family level					
– (not) phocidae	70340	(+506 / +8)	2	–	–
At subfamily level					
– (not) two subfamilies	70028	(+194 / +3)	1	–	–
– three subfamilies	70779	(+945 / +14)	4	3.00*	(< 1)*
– cystophorinae	70779	(+945 / +14)	4	3.00	(< 1)
– (not) monachinae	70028	(+194 / +3)	1	–	–
– (not) phocinae	70048	(+214 / +4)	9	–	–
Within Monachinae					
– Lobodontini	70283	(+449 / +7)	1	50.55	(5)
– (not) monachus	70279	(+445 / +7)	2	–	–
Within Phocinae					
– erignathus sister	70140	(+306 / +5)	2	–	–
– relaxed Burns & Fay	69991	(+157 / +3)	3	44.33	(4)
– strict Burns & Fay	70041	(+207 / +3)	1	64.06*	(6)*
– phoca	69892	(+58 / +1)	1	64.06	(6)
Within Phocinae					
– de Muizon	71831	(+1997 / +29)	1	–	–
– Wyss	72406	(+2572 / +38)	1	–	–
Miscellaneous					
– unweighted	70048	(+214 / +4)	2	314.00*	(31)*
– condense	70453	(+619 / +9)	5	44.33*	(4)*

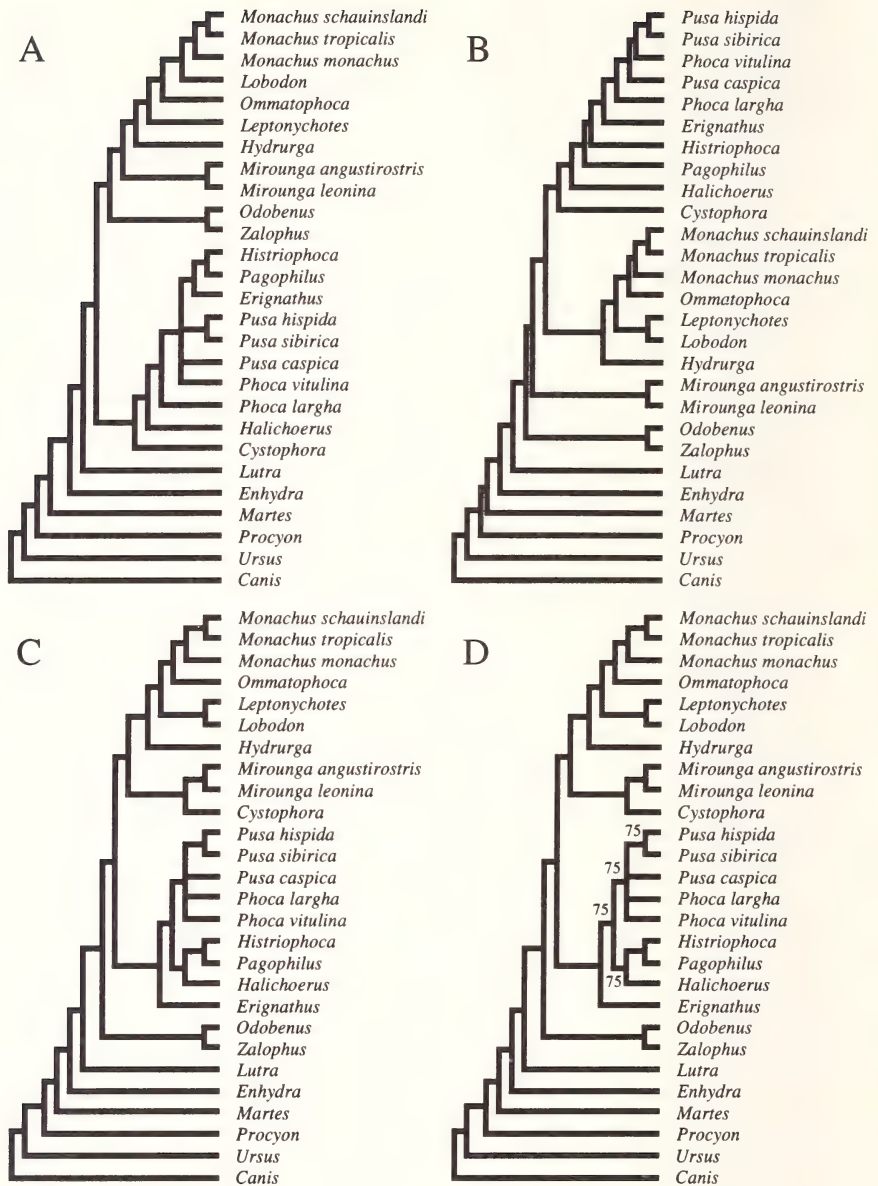


Fig.14A–D: Cladograms resulting from a constraint analysis examining various alternative hypotheses of ingroup relationships: (A) (not) phocidae *, (B) (not) two subfamilies, (C) three subfamilies *, and (D) cystophorinae *. An asterisk indicates a majority rule consensus solution, where, unless otherwise indicated, all nodes were found in 100% of the equally most parsimonious solutions. See also Fig.4 and Tab.4.

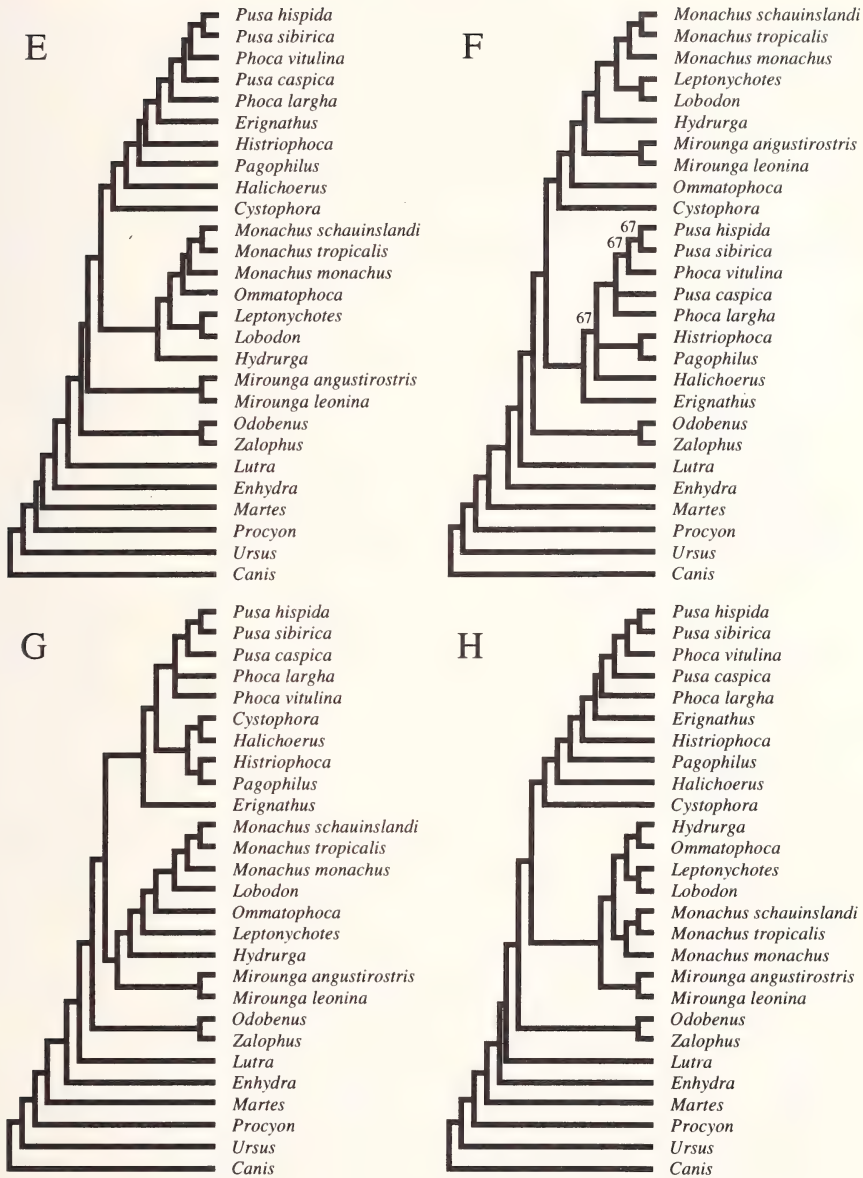


Fig.14E–H: Cladograms resulting from a constraint analysis examining various alternative hypotheses of ingroup relationships: (E) (not) monachinae, (F) (not) phocinae *, (G) erignathus sister *, and (H) lobodontini. An asterisk indicates a majority rule consensus solution, where, unless otherwise indicated, all nodes were found in 100% of the equally most parsimonious solutions. See also Fig.4 and Tab.4.

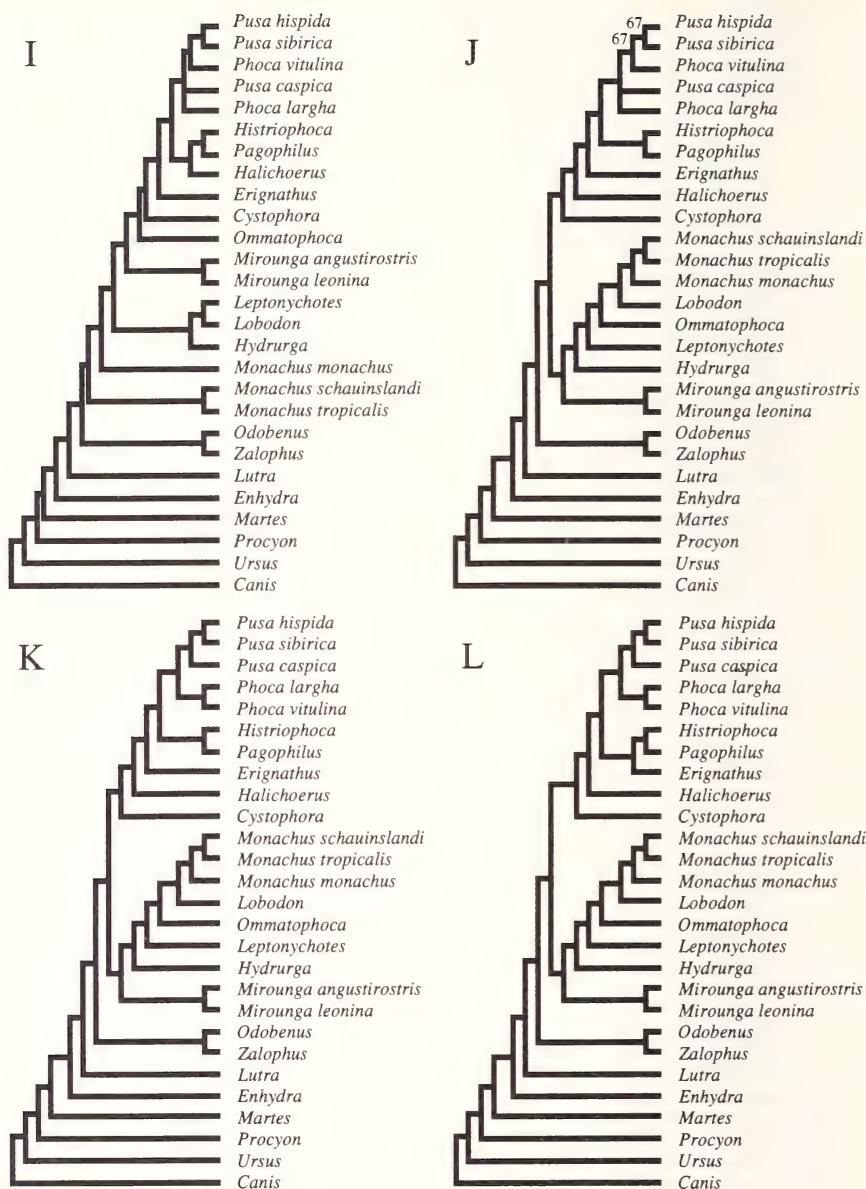


Fig.14I–L: Cladograms resulting from a constraint analysis examining various alternative hypotheses of ingroup relationships: (I) (not) monachus *, (J) relaxed Burns & Fay *, (K) strict Burns & Fay, and (L) phoca. An asterisk indicates a majority rule consensus solution, where, unless otherwise indicated, all nodes were found in 100% of the equally most parsimonious solutions. See also Fig.4 and Tab.4.

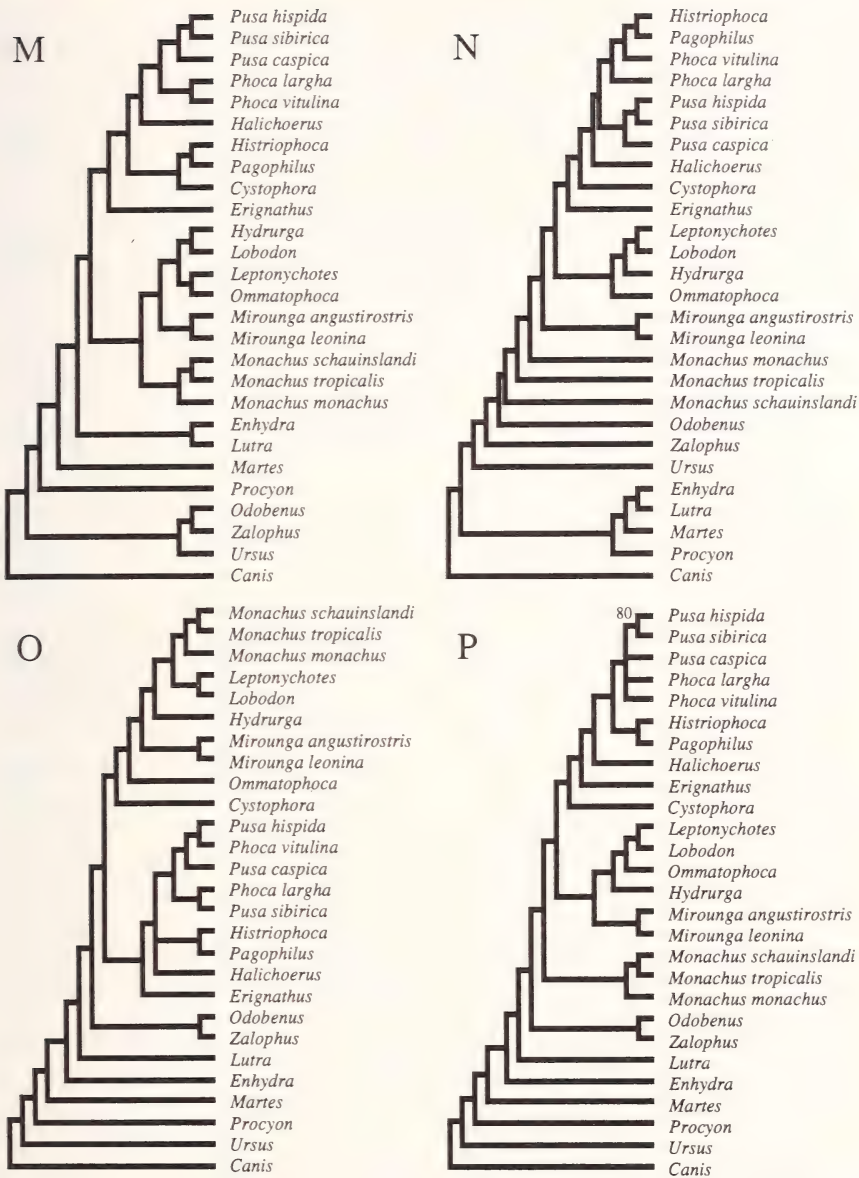


Fig. 14M-P: Cladograms resulting from a constraint analysis examining various alternative hypotheses of ingroup relationships: (M) de muizon, (N) wyss, (O) unweighted *, and (P) condense *. An asterisk indicates a majority rule consensus solution, where, unless otherwise indicated, all nodes were found in 100% of the equally most parsimonious solutions. See also Fig. 4 and Tab. 4.

increase in length). Low bootstrap frequencies (all below 32% and most below 7%) again denote weak support for these alternative groupings, while the small number of most parsimonious solutions likewise hints at good resolving power in the data set.

Of more interest than the magnitude of the increases in length, however, are the topologies resulting from the various constraint conditions (Fig.14). Disruption of a monophyletic Phocidae resulted in the otarioids forming a monophyletic sister group to the monachines, reiterating the late convergence of the latter group on the former (Repenning 1990). Of the two subfamilies, paraphyly of the Monachinae was easier to achieve, as might be expected with the slightly weaker support noted earlier for this entire subfamily (see **Overall Parsimony Analysis** and **Statistical Tests** sections). The constraint of a paraphyletic Phocinae or a monophyletic Cystophorinae, meanwhile, again demonstrates the strong tendency of *Cystophora* to join the monachines. The enforced paraphyly of *Monachus* produced a topology much like that advocated by Wyss (1988a), again demonstrating that a paraphyletic Monachinae is dependent upon a paraphyletic *Monachus* to some degree (Berta & Wyss 1994).

Additional observations support some of the more contentious, non-traditional relationships indicated by the overall solution. Monophyly of *Monachus*, as well as its terminal position within the lobodontines, was extremely robust and was only disrupted when specifically forced to do so. Likewise, paraphyly for the lobodontines was always indicated, even when *Monachus* was disrupted. A more terminal position for *Erignathus* (or, equivalently, a basal position for *Cystophora*) within the phocines was also always observed, when not specifically constrained otherwise. *Erignathus* was typically embedded within the Phocini, but it always clustered internal to *Cystophora* in any case.

Finally, one curious phenomenon was observed in this portion of the analysis. Changes forced within the monachines altered not only the topology elsewhere within this subfamily, as would be expected, but often within the phocines as well. These were largely localized within the Phocini (plus *Erignathus*), and typically amounted to a basal shift of *Histiophoca* and *Pagophilus* to form successive sister taxa to the remaining Phocini (plus *Erignathus*). However, the complete absence of the equivalent reciprocal situation again hints at the comparatively weaker support for the Phocini (plus *Erignathus*) within the phocids (see **Statistical Tests** section). Monachine interrelationships, although comparably weak with respect to a bootstrap analysis (see **Statistical Tests** section), appear to be exceptionally robust by all other indications. Only changes forced directly within the Monachinae seem to be able to disrupt the interrelationships of this subfamily indicated in the overall solution.

Overall conclusions – possible effects of polymorphic data

The fact that no constrained solutions were substantially longer than the overall solution might derive from the high amount of polymorphic data in this analysis (see **Overall Parsimony Analysis**). The flexibility allowed by the alternative states of the polymorphisms likely permitted the very different competing topological hypotheses to be satisfied with a minimal amount of extra homoplasy. In contrast, those data matrices with less polymorphic data (e.g., Berta & Wyss 1994) would presumably be more rigid, and meeting

the requirements of very different topologies would require a larger amount of extra homoplasy. But, in view of the unexpectedly low number of equally most parsimonious solutions (and slightly less than most parsimonious; see skewness analysis in the **Statistical Tests** section) entailed by this supposedly more flexible data matrix, the effects of polymorphic data on parsimony analyses need to be investigated further.

Missing taxa (Fig.15)

The impetus for this analysis initially stemmed from taxonomic considerations within the Phocini (plus *Erignathus*). In a preliminary parsimony analysis, all of the constituent genera except for *Phoca* (sensu stricto) were monophyletic. However, the presence of *Phoca largha* in this study is contingent on the somewhat debatable species status granted it here. Subordinating *P. largha* as a subspecies of *Phoca vitulina* (as advocated by Scheffer 1958; Burns 1970; Shaughnessy 1975; Baram et al. 1991) would effectively render the now monotypic *Phoca* monophyletic. But, as Arnold (1981) suggests that the absence of some taxa might seriously affect the outcome in a low level cladistic analysis, we desired to investigate the effects of the removal of *P. largha* from the analysis. Subsequent analyses also saw the individual removal of *Cystophora*, *Erignathus*, *Lobodon*, and *Ommatophoca* in order to view the effects of their deletion. *Cystophora* was chosen due to its basal position within the phocines, combined with its strong tendency to join the monachines. *Erignathus* was likewise selected due to the novel position indicated for it here, and because of its position within the labile Phocini clade (as with *Phoca largha*). The removal of *Lobodon* provided an insight into the effects of the deletion of a rather topologically unspectacular and undistinguished taxon. Finally, *Ommatophoca* was deleted as it appears to be one the more unstable taxa in the otherwise fairly robust Monachinae (see **Unweighted analysis** below).

As would be expected, the removal of each taxon yielded a shorter solution than that obtained when all taxa were present. Single most parsimonious solutions were the norm, with only the matrix lacking *Erignathus* producing dual equally most parsimonious solutions. However, the degree of shortening in each case was much greater than would be achieved by merely "pruning" the single species branch in question from the tree. For example, the removal of *Phoca largha*, which effected virtually no topological changes, resulted in a solution some 1,452 steps (22 corrected steps) shorter than the overall solution. As the length of the branch leading to *P. largha* was only 383 steps (seven unweighted steps), the removal of taxa must decrease homoplasy elsewhere in the tree. This is demonstrated by the generally reduced branch lengths around the region that the removed taxon formerly occupied (compare Figs.5C and 15 for all removed taxa). Branch lengths within the outgroups were virtually unchanged. As well, the various goodness-of-fit statistics are slightly altered to reflect this decrease in the overall level of homoplasy. Although major changes in topology were generally not evident in this analysis, the removal of taxa again demonstrated how the topology of one region of a tree can affect the topology of another, supposedly distinct region. This was especially evident with the removal of either of the two monachines. The deletion of either *Lobodon* or *Ommatophoca* produced minor, if any, topological changes within the monachines, but generated more substantial changes within the phocines (Figs.15D and E). Again, these latter alterations

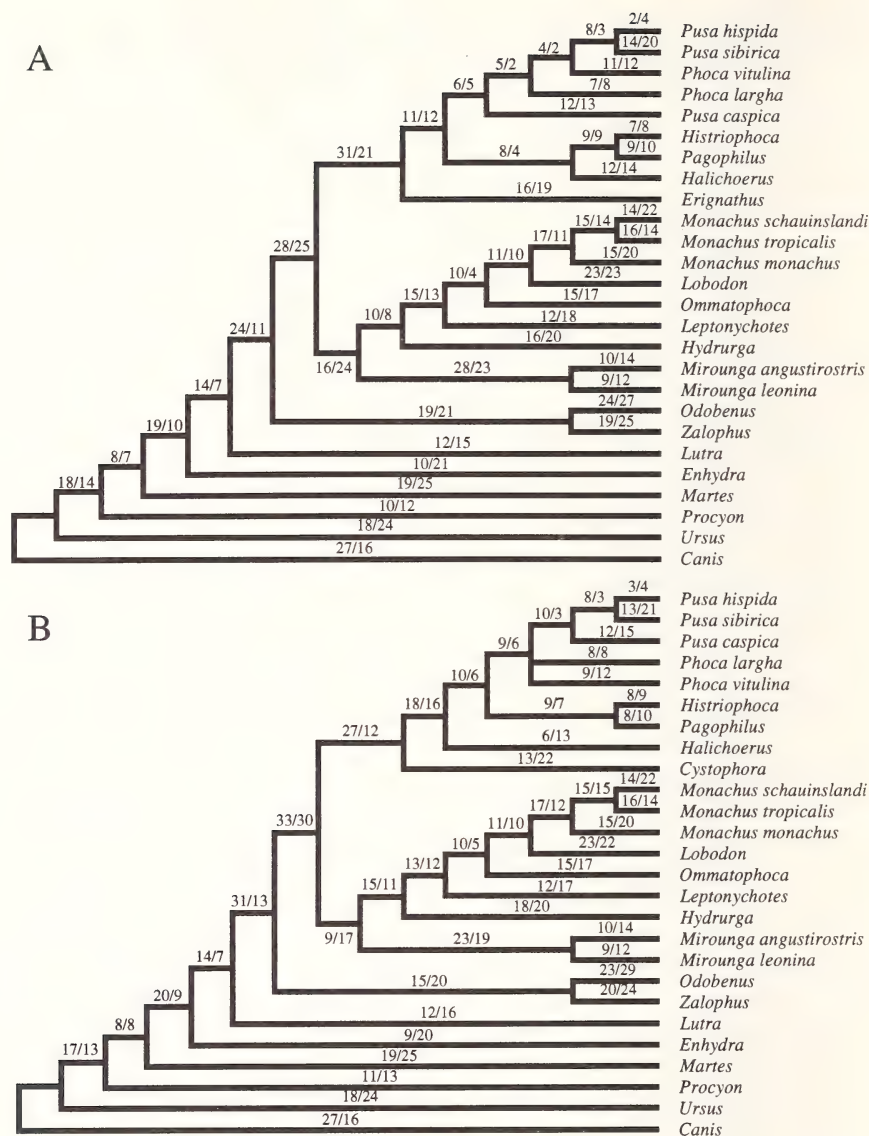


Fig.15A–B: Cladograms resulting from a parsimony analysis of the inversely weighted data matrix with a selected phocid species deleted: (A) *Cystophora* (length = 67,348 steps, CI = 0.461, HI = 0.761, RI = 0.635, RC = 0.414) and (B) *Erignathus* (length = 67,421 steps, CI = 0.462, HI = 0.763, RI = 0.638, RC = 0.419). Unweighted branch lengths presented as accelerated transformation / delayed transformation. Note that (B) is a consensus solution with all nodes found in 100% of the two equally most parsimonious solutions.

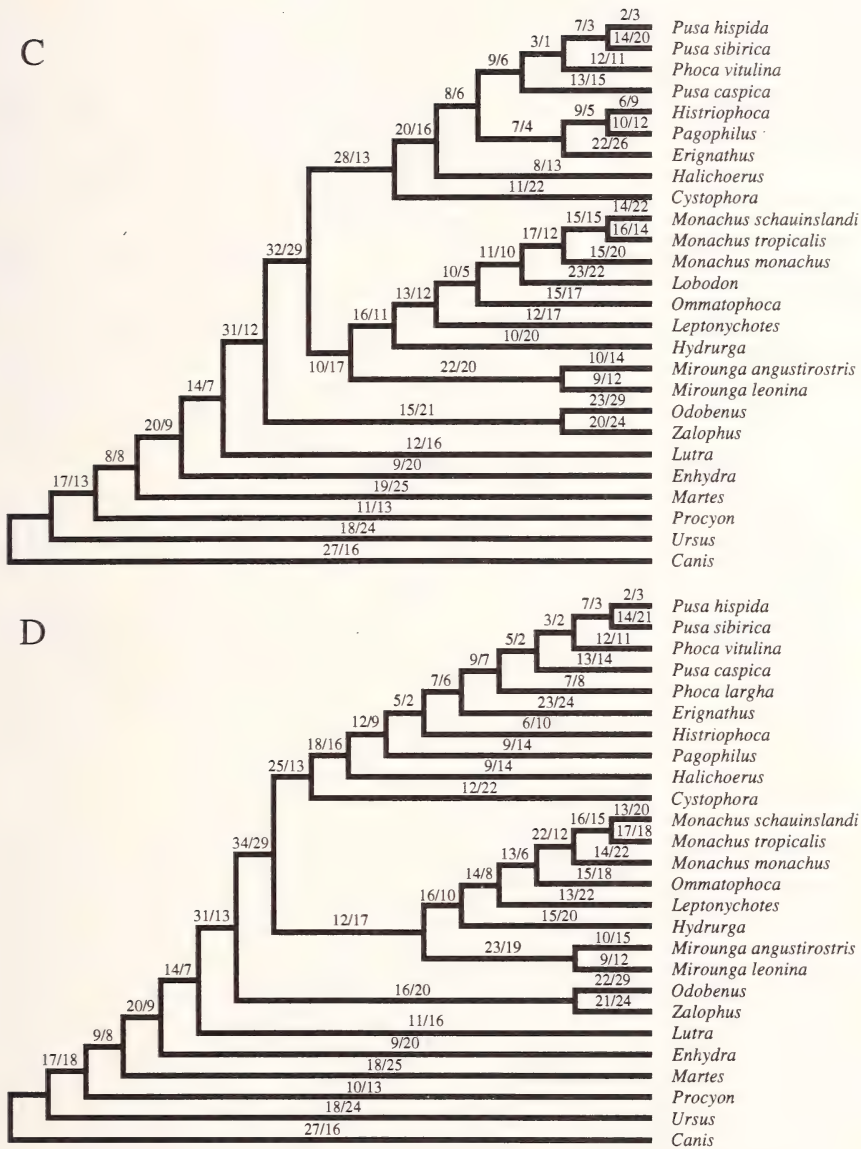


Fig.15C-D: Cladograms resulting from a parsimony analysis of the inversely weighted data matrix with a selected phocid species deleted: (C) *Phoca largha* (length = 68,382 steps, CI = 0.458, HI = 0.765, RI = 0.629, RC = 0.408) and (D) *Lobodon* (length = 67,333 steps, CI = 0.461, HI = 0.763, RI = 0.626, RC = 0.410). Unweighted branch lengths presented as accelerated transformation / delayed transformation.

E

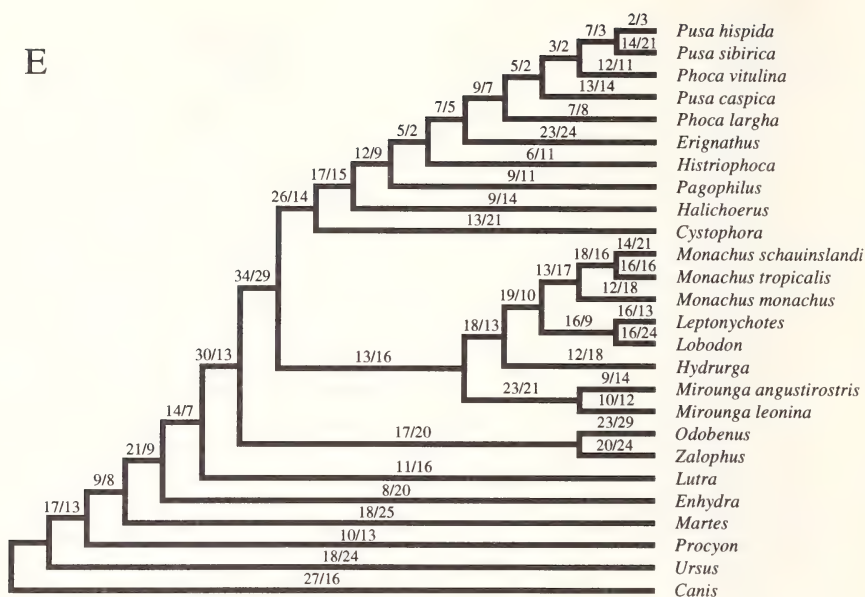


Fig.15E: Cladograms resulting from a parsimony analysis of the inversely weighted data matrix with a selected phocid species deleted: (E) *Ommatophoca* (length = 67,017 steps, CI = 0.460, HI = 0.760, RI = 0.630, RC = 0.409). Unweighted branch lengths presented as accelerated transformation / delayed transformation.

amounted to a basal shift of *Histiophoca* and *Pagophilus* within the Phocini (plus *Erignathus*), so that they became related by sympleisiomorphies. However, like the constraint analyses, the removal of any of the three phocines affected only phocine interrelationships. As mentioned, the removal of *Phoca largha* yielded virtually no changes. In fact, the cladogram obtained (Fig.15C) is identical with one of the two equally most parsimonious solutions (Fig.5A) with *P. largha* merely pruned off. The removal of *Cystophora* caused *Erignathus* to regain its traditional role as the sister taxon to the remaining phocines (Fig.15A). The Phocini, however, remain paraphyletic, as *Halichoerus* now occupies the former position of *Erignathus* (although compared to the overall solution, this analogous clade is shifted basally with respect to the clade composed of *Phoca* spp. and *Pusa* spp.). *Histiophoca* and *Pagophilus* likewise move basally with the absence of *Erignathus* (although they remain as a clade) (Fig.15B), hinting that the supposedly primitive and monachine-like *Erignathus* is responsible for the more terminal position of this clade, and of the other two genera in particular, in the overall solution. This is also substantiated by the constraint analyses, where disruptions to the structure within the Phocini were due primarily to the movement of *Histiophoca* and *Pagophilus*; *Erignathus* generally maintained its relatively terminal position. Again, perhaps too much has been made of some of the more primitive features of *Erignathus* (see **Overall Parsimony**).

Thus, although this analysis into the effects of missing taxa cannot directly indicate the robustness of a given solution, it did indicate results in common with several analyses that could. As in the constraint analyses, the resistance of the monachine topology to changes directed within the phocines again points to the greater stability of this subfamily. As well, this analysis gives further cause to question the historically primitive role typically assigned to *Erignathus*.

“Unweighted” solution (Fig.16)

A parsimony analysis employing identically weighted characters (regardless of the number of character states) was also undertaken, yielding four equally most parsimonious solutions of 1,253 steps each. The consensus solution (identical between strict and majority rule algorithms) is presented in Fig.16.

The outgroup relations for this solution are identical with those of the overall solution; however, large differences are indicated within the phocids. The most striking difference

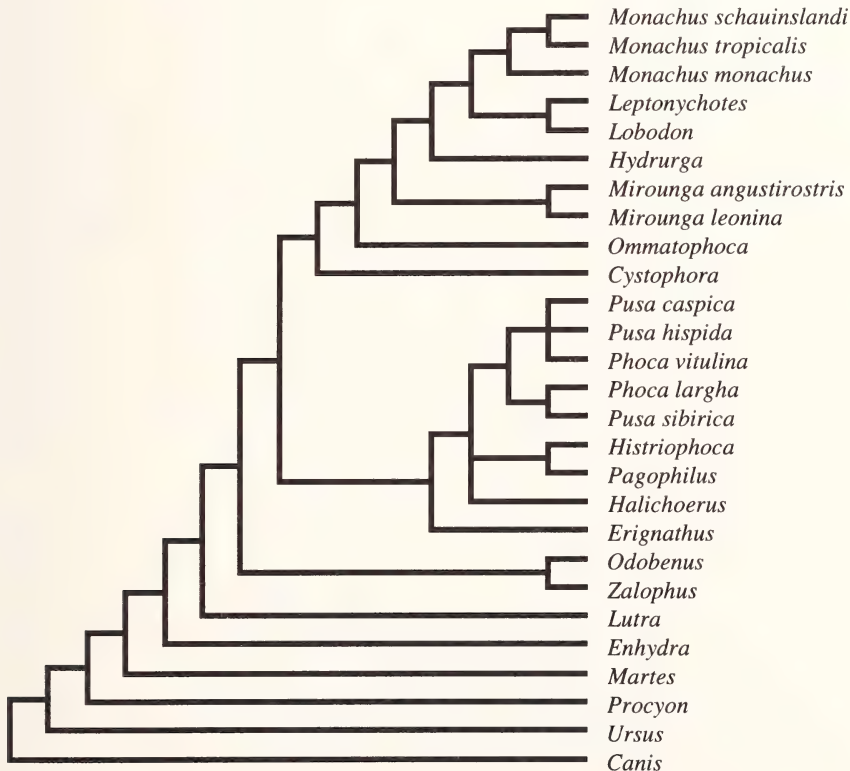


Fig.16: Consensus solution (identical between strict and majority rule algorithms) of four cladograms resulting from a parsimony analysis using identically weighted characters (length = 1,253 steps, CI = 0.460, HI = 0.772, RI = 0.603, RC = 0.396). All nodes were found in 100% of the equally most parsimonious solutions.

is the disruption of the two subfamilies as they are commonly recognized. Two distinct clades are still present, but *Cystophora* is now seen to cluster with the monachines, forming the sister taxon to this subfamily. This result is fairly labile, however, with cladograms of only one additional step finding *Cystophora* back as the sister taxon to the remaining phocines (results not shown). However, as indicated by the bootstrap, *Cystophora* displays a strong tendency to join the monachines even in the inversely weighted data set (bootstrap frequency of 31%).

This tendency on the part of *Cystophora* likely reflects its similarities, be they convergent or symplesiomorphic (with respect to all phocids), with *Mirounga*. The failure of *Mirounga* spp. to show an analogous predisposition (bootstrap frequency of only 2%) relates in turn to a third taxon, *Ommatophoca*. Together, these three genera are uniquely characterized among phocids by nasal processes of the premaxilla that distinctly fail to reach the nasal bones (see **Character Analysis**, character #12). Although this morphology is not as developed in *Ommatophoca*, together with the large number of characters used to describe the nasal region (see **Character Analysis**, characters #5-12), it is apparently sufficient to have all three taxa occupying the basal positions within the one clade. (These same characters, being predominantly multistate, exhibit less of an influence in the inversely weighted data matrix. However, note that even under such ameliorating conditions that *Cystophora* still displays a marked tendency to cluster with the monachines.) In fact, the tendency for all three genera to group together is demonstrated by the inclination for both *Mirounga* spp. and *Ommatophoca* to join the phocines (bootstrap frequency of 9%) being marginally higher than of *Mirounga* spp. alone. This also reflects the surprisingly high tendency of *Ommatophoca* to join the phocines (bootstrap frequency of 14%), presumably to cluster basally with *Cystophora*.

Within the monachines proper, the paraphyly of the lobodontines is even more pronounced with the shift of *Ommatophoca* to its basal position between *Cystophora* and *Mirounga* spp. As well, the traditional lobodontine relationships (i.e., paired *Hydrurga-Lobodon* and *Leptonychotes-Ommatophoca* clades) are contradicted further with *Leptonychotes* and *Lobodon* forming a monophyletic clade. Monophyly of *Monachus* is still indicated, however.

The loss of *Cystophora* to the monachines results in *Erignathus* resuming its traditional sister taxon status to the remaining phocines. Resolution within the now monophyletic Phocini is again limited, but paraphyly of *Phoca* (sensu Burns & Fay 1970), *Phoca* (sensu stricto), and *Pusa* are all indicated, with some novel relationships presented between *Phoca* spp. and *Pusa* spp. *Histiophoca* and *Pagophilus* continue to constitute a clade although, again, it is shifted basally with the loss of *Erignathus*.

This analysis is mentioned primarily as a curiosity into the effects of character "weighting" on this data matrix. As mentioned previously, the uncorrected use of binary and multistate characters will not result in equally weighted characters (as desired here) due to the algorithms used in PAUP (Swofford 1993). However, the results from this analysis do mirror the general conclusions from the analysis of the inversely weighted data set: strongly supported relations for the outgroup taxa and at the level of the phocid subfamilies, and weakly supported/resolved relations within the subfamilies (albeit

apparently somewhat stronger within the monachines). Differences with the overall solution are limited exclusively to within the phocid subfamilies, which demonstrate how labile the relationships at this level are with respect to which characters are used, and/or how they are used. Finally, as demonstrated by a constraint analysis (Fig.14O and Tab.4), the inversely weighted data matrix can accommodate the “unweighted” solution with a minimal amount of extra homoplasy: 214 extra steps (four extra corrected steps). The bootstrap frequency for the least supported major clad of this solution (estimated at 31%) is also remarkably high compared to those of the remaining constraint analyses.

Condensed analysis (Fig.17)

The constrained monophyly of four higher level phocid taxa – *Mirounga*, *Monachus*, *Phoca* (sensu Burns & Fay 1970), and Lobodontini – resulted in some rather major topological changes within each phocid subfamily, with respect to the overall solution.

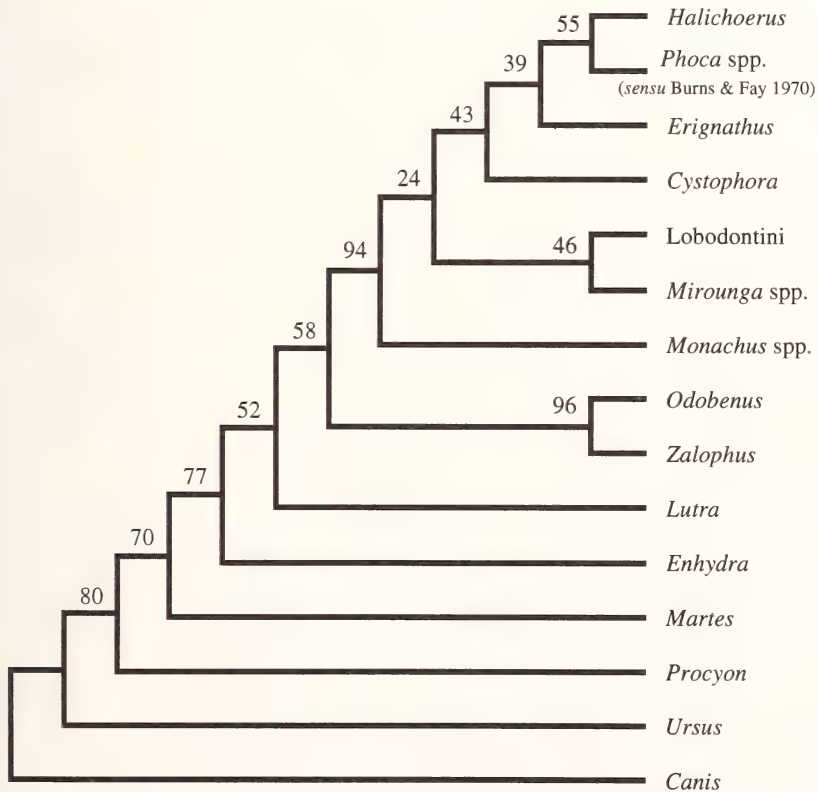


Fig.17: Cladogram resulting from a parsimony analysis of the inversely weighted data matrix with the taxa *Mirounga*, *Monachus*, *Phoca* (sensu Burns & Fay 1970), and Lobodontini collapsed so as to be monophyletic (length = 49,058 steps, CI = 0.518, HI = 0.709, RI = 0.634, RC = 0.483). Numbers represent bootstrap frequencies supporting each node (1,000 replications).

Contrary to most other analyses, the changes were the most severe in the monachines where paraphyly is indicated for the subfamily. This is likely attributable to the improper presumption of a monophyletic Lobodontini, forcing *Monachus* to become the sister taxon to the remaining phocids. This latter scenario has been postulated to be conducive towards obtaining a paraphyletic Monachinae (Berta & Wyss 1994). Moreover, under these conditions of imposed monophyly, the lobodontines and *Mirounga* do form a clade, as suggested by Hendey (1972) and King (1983) (but see Sarich 1976). Within the phocines, the only alteration was the exclusion of *Erignathus* from the Phocini, where it was normally firmly entrenched. *Cystophora*, however, maintains its position as the most basal of the phocines. Overall, the internal phylogeny of the phocids in the condensed solution strongly resembles the solution of Wyss (1988a), which, in effect, included some constrained monophyletic higher taxa. The more traditional appearance of the ingroup relationships (see below also) hints that previous studies into phocid phylogeny probably assumed the monophyly of some higher level taxa to varying degrees as well.

The visualization of the internal phylogeny of the condensed higher level taxa by a constraint analysis of the inversely weighted data matrix (Fig.14P and Tab.4) revealed branching patterns that largely agree with those of the overall solution. Despite their altered placement within the monachines, the internal topology of both *Monachus* and the lobodontines were identical with those of the overall solution. Within *Phoca* (sensu Burns & Fay 1970), a polytomy was again found, indicating uncertainty regarding the relationships in this region. However, *Pusa hispida* and *Pusa sibirica* do continue to form a clade in most solutions. As well, the enforced removal of *Erignathus* again resulted in a more basal shift of the clade of *Histiophoca* plus *Pagophilus* relative to *Phoca* spp. and *Pusa* spp.

The condensed solution is also typified by an increased amount of homoplasy (relative to the overall solution) presumably to account for the constrained monophyly of the otherwise normally paraphyletic higher taxa. This is most clearly indicated by the ensemble CI for the condensed solution (0.518), which although higher than the analogous value of the overall solution, actually falls below the value expected for a study of 15 taxa [0.618; Sanderson & Donoghue (1989)], while that of the overall solution was about on a par with its expected value (see **Overall Parsimony Analysis**). The increased levels of homoplasy present in the condensed solution were also indicated by the constraint analysis, where the constraint of the inversely weighted data matrix to the basic pattern of the condensed solution (see Fig.4P) resulted in one of the larger increases in length of all the constraint analyses, 619 extra steps (nine extra corrected steps) (Tab.4).

The increase in homoplasy for the condensed solution is argued against by several factors, however. Firstly, the ensemble HI is slightly lower (which might arise from the effective removal of nine taxa), while both the ensemble RI and RC are higher than their equivalent values in the overall solution. Another line of evidence originates from the somewhat surprising result that all the bootstrap frequencies for the condensed solution were roughly equivalent to those of the overall solution (compare Figs.8B and 17). While this could have been expected for the outgroup nodes (as their taxa, and thus hopefully their interrelationships, were unchanged), the failure of the bootstrap to reflect the presumably

more homoplasious ingroup topology of the condensed solution is puzzling. Beyond the major limitation that the bootstrap can only indicate signal strength within a data matrix (see **Statistical Tests**), it may also be connected with the reduced number of taxa present in the condensed solution, resulting in fewer reasonable alternative groupings. For instance, one would expect the members of each subfamily to associate with one another whether the subfamily is paraphyletic or not. Thus, the collapsing of the Monachinae to only three taxa in the condensed analysis dramatically reduces the number of alternative pairings, possibly artificially inflating the apparent support for those possibilities that remain.

Finally, it should be stressed that the differences in topology that were obtained in this analysis arose solely from improper assumptions of monophyly, and not because of large scale differences between the data matrices. The consensus character states for each higher level taxon are directly based on the same set of observations that led to the overall solution. Therefore, essentially the same matrix was used in both cases. As well, the altered findings are not dependent on either solution being the correct estimate of the actual (phocid) phylogeny. However, by improperly assuming the monophyly of higher taxa, we may actually be hindering our efforts in systematic biology to uncover the true phylogeny of a group of organisms.

CHARACTER ANALYSIS

The previous two sections dealt largely with the various methods devised to assess the degree of confidence one may have in a specific cladogram (cladistic hypothesis) versus other rival hypotheses. Together with the general misinterpretation of these tests (see **Statistical Tests**), what continually appears to be lost in all this is the realization that any cladistic hypothesis is only as good as the set of characters it is based upon and the underlying hierarchical pattern they indicate. In this regard, this section presents an in-depth analysis of all the characters examined in this study (also listed in Appendix B), with an emphasis on the 168 that were included in the cladistic analysis (excluded characters are marked with an asterisk). Historical notes and descriptions are initially provided for each character, followed by a prose equivalent to the information found in the apomorphy list (Appendix E). This latter feature is limited to the included characters, but reconstructions for the excluded characters may be derived from Appendix E. All reconstructions (including those of the excluded characters) are based on the topology displayed in the overall solution (Fig. 5B). Goodness-of-fit statistics (but now based on the consensus and not the optimal solutions) for all individual characters are presented in Appendix F.

In the following, the citation(s) following each character refer(s) to our source for that character. In many cases, they may not correspond to the initial mention of the feature in the literature, but to the first use of the character in a systematic fashion. Descriptions of characters or character states were often modified from their indicated sources. This was typically done to accommodate the larger range of variation we observed in applying characters initially used to distinguish between a limited distribution of taxa over the fuller set examined here. In other cases, characters were derived from those in the literature

(e.g., character #24 is a derivation of character #23). Typically, this amounted to detailing the various manifestations of a "present" feature that was initially offered in present/absent form only. Finally, although some character states were not represented at the species level (e.g., state 2 for character #51), they did characterize individual specimens and so were retained.

Unfortunately, in attempting to assess the relative size of several characters, an admittedly arbitrary scheme often had to be employed (e.g., small, medium, large, or something equivalent). In such cases, size was determined in relation to the size of the surrounding bone (e.g., the skull as a whole for cranial characters, or the bone in question for post-cranial material), bearing the range of variation observed over the phocids in general in mind.

The use of tendencies for traits (e.g., tendency towards single-rooted postcanines; characters #143 and 144) has occasionally been criticized in cladistic analysis on the basis that characters should be more discretely discernible. However, characters examining tendencies were still employed here as they may be the only way to summarize highly variable morphologies or taxa that show differences between the two optimization criteria used here (accelerated transformation, ACCTRAN; and delayed transformation, DELTRAN).

Unless otherwise noted, anatomical terminology is standardized according to Miller (1962) and/or Davis (1964). Synonyms are given wherever possible. Finally, no polarity is implied by the sequence of character state coding (e.g., zero does not necessarily indicate the plesiomorphic state). In all cases, the polarity of each included character is explicitly stated in the text detailing its phylogenetic reconstruction.

Snout (21 characters)

Clearly the most important feature of the snout deals with the nasal processes of the premaxilla. The morphology of these processes and their relationships to neighbouring elements contain a good deal of useful, and largely untapped, systematic information, as is generally true for the remaining characters as well.

*1) relative position of external nares on snout: 0 = relatively dorsal ("high"); 1 = relatively ventral ("low") (Ridgway 1972).

The dorsal situation of the external nares on the snout has been proposed as a synapomorphy of the Monachinae (Ridgway 1972). However, the examination of both study skins and photographs revealed no appreciable distinction in the placement of the external nares between monachines and phocines. Due to this lack of variation, the character was deleted from the analysis.

*2) relative orientation of external nares on snout: 0 = vertical; 1 = horizontal (Ridgway 1972).

Ridgway (1972) described states 0 and 1 as being synapomorphic for the subfamilies Cystophorinae and Monachinae respectively. However, with the accepted paraphyly of the Cystophorinae (see King 1966), vertically oriented external nares would be better classified as another convergent feature between *Cystophora* and *Mirounga*. Or, as tentatively suggested herein, they might be another feature retained from the primitive phocid ancestor

(see **Overall Parsimony Analysis**). In any case, the distinction between the two states appears to be minor and somewhat arbitrary, with the “horizontal” condition really representing only a slight horizontal shift to a roughly diagonal position. As no unambiguous data for any species could be determined, either from study skins or from photographs, this character was subsequently deleted.

3) shape of anterior margin of premaxilla in dorsal view: 0 = flat, square, or bi-lobed; 1 = tapered and/or rounded (Burns & Fay 1970).

Burns & Fay (1970) used this feature to aid in establishing the systematic relationships of the phocines, and of the genera *Histiophoca*, *Pagophilus*, *Phoca* (all state 0), and *Pusa* (state 1) in particular. During our observations, we noted that some specimens displayed an intermediate morphology that could not be unequivocally assigned to either of the two extreme states. These specimens were coded as being polymorphic for this character.

A tapered or rounded premaxillary margin is primitive within the Caniformia, being found in virtually all outgroup taxa (*Lutra* displays the intermediate condition). The apomorphic state 0 occurs only within the phocids, but with independent origins in each subfamily. In the phocines, this state characterizes the subfamily ancestrally and is retained by all members, including *Pusa* spp. For the monachines, this state is limited to the clade composed of *Lobodon*, *Monachus* spp., and *Ommatophoca*, with *Lobodon* and *Monachus monachus* independently deriving the intermediate condition.

4) triangular lateral extensions of premaxilla into maxilla in dorsal view: 0 = absent; 1 = rudimentary or present (pers. obs.) (Fig.18).

In recording data for the previous character, we noted an unusual morphology for the premaxilla in a number of specimens. In most cases, the premaxilla is bounded laterally for most of its length by the maxilla when viewed dorsally, with the two bones meeting along a smooth curve. However, the antermost portion of the premaxilla occasionally extends laterally as a small right triangle. This extension is not bounded laterally by the maxilla and its roughly right-angled posterior edge disrupts the smooth curve mentioned above. Although occurring sporadically in a wide range of species, this apomorphic condition only appears consistently in *Monachus schauinslandi* and *Monachus tropicalis*, with the polymorphic taxa *Enhydra* and *Ursus* apparently being in the process of independently acquiring this trait.

5) visibility of ventral portion of nasal processes of premaxilla along maxilla in lateral view: 0 = always visible; 1 = not always visible (Wyss 1988a).

As employed by Wyss (1988a), this character was used in conjunction with the next two (characters #6 and 7) to describe the visibility of the nasal processes as a whole. The condition in which the nasal processes were not always visible was felt to be a potential synapomorphy of the monachines among the carnivores, if not most mammals (de Muizon & Hendeby 1980; de Muizon 1982a; Wyss 1988a). However, numerous exceptions to this have been noted, with *Histiophoca* and *Pagophilus* approaching, and *Monachus tropicalis* not displaying, this apparent monachine condition (de Muizon & Hendeby 1980; de Muizon 1982a; Wyss 1988a).

We felt that the above coding was overly restrictive, with the possibility of creating a fair degree of homoplasy as those species sharing the general condition “nasal processes not

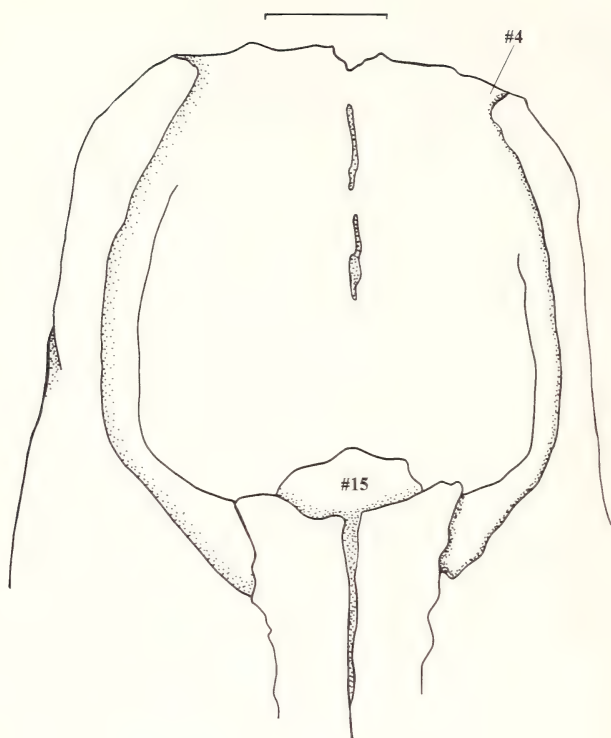


Fig.18: Dorsal view of the snout of *Monachus tropicalis* (USNM 102536) illustrating selected characters (indicated by their number; see **Character Analysis**) of this region. Anterior is towards the top of the page. Scale bar equals 1 cm.

always visible” did not always share the same location for that portion of the process that slips into the nasal aperture. As well, the all-encompassing character is inapplicable for genera such as *Cystophora*, *Mirounga*, and *Ommatophoca*, where the nasal processes are absent dorsally. Therefore, in order to minimize potential homoplasy and to maximize the applicability of this character for all species, we split the nasal processes into three equal portions (dorsal, middle, and ventral) and viewed each separately.

For the ventral portion of the nasal processes, the derived condition (state 1) is limited to only those monachines internal to *Hydrurga*. Within this clade, the polymorphic taxa *Monachus schauinslandi* and *Monachus tropicalis* show partial reversals to the plesiomorphic condition. This likely represents another synapomorphy of these two taxa, although this is not indicated here due to the manner in which PAUP handles polymorphic data (Swofford 1993; see **Methods and Materials**).

6) visibility of middle portion of nasal processes of premaxilla along maxilla in lateral view: 0 = always visible; 1 = not always visible; 9 = n/a – middle portion not present (de Muizon 1982a; Wyss 1988a).

For the suite of characters involving the visibility of the nasal processes of the premaxilla, the middle portion is probably the most important systematically. This middle portion is the one most often identified as defining the monachine condition, whereby the nasal processes are not always visible (Hendey & Repenning 1972; de Muizon & Hendey 1980;

de Muizon 1982a; Wyss 1988a). This is reflected here, with most monachines (with the exception of *Mirounga leonina*, *Monachus tropicalis*, and *Ommatophoca*) sharing the derived condition (state 1). In *Mirounga leonina*, the middle portion of the nasal processes is absent, rendering this character inapplicable (state 9), while *Monachus tropicalis* and *Ommatophoca* independently revert to the primitive condition (state 0). This previously undocumented occurrence in *Ommatophoca* may derive from the failure of the nasal processes to extend fully to the nasals (see character #12). Independent origins of a polymorphic condition occur in *Odobenus*, *Enhydra*, and *Histriophoca*. The presence of the derived state in this last genus (as a synapomorphy with *Pagophilus*) has been noted by de Muizon (1982a) and Wyss (1988a).

7) visibility of dorsal portion of nasal processes of premaxilla along maxilla in lateral view: 0 = always visible; 1 = not always visible; 9 = n/a – dorsal portion not present (Wyss 1988a).

This character apparently contains less systematic information than the other two characters dealing with the visibility of the nasal processes. Most species in this study display the primitive condition (state 0); only *Odobenus* derives the condition whereby the dorsal portion is not visible. Of those taxa where the dorsal portion is not visible due to its absence (*Cystophora*, *Mirounga* spp. and *Ommatophoca*), this condition can only be considered a synapomorphy of the two elephant seals. However, this last state is really more of an unavoidable consequence of character #12.

8) shape of ventral portion of nasal processes of premaxilla along maxilla: 0 = concave; 1 = straight; 2 = convex (Burns & Fay 1970).

The derivation of characters #8 to 10, dealing with the shape of the nasal processes of the premaxilla, in many ways parallels that of the previous suite of characters which examined their visibility from a lateral view. In their more restricted focus on the Phocini, Burns & Fay (1970) initially coded the present suite of characters as “nasal processes concave ventrally and convex dorsally” (for *Phoca* and *Pusa*), or “wholly concave” (for *Histriophoca* and *Pagophilus*). During our observations, we noted that these two states were not sufficient to account for the range of variation observed over the larger set of taxa employed here. As well, such a coding would again exclude those previously mentioned genera that lack the dorsal portion of the nasal processes. Thus, the original character was again subdivided into three sections, which were examined individually.

In the ventral regions, most species retain the primitive condition of a concave shape of the nasal processes. Independent derivations of a straight morphology occur only in *Odobenus*, *Enhydra*, and *Halichoerus*. The convex morphology was never consistently present at the species level.

9) shape of middle portion of nasal processes of premaxilla along maxilla: 0 = concave; 1 = straight; 2 = convex; 9 = n/a – middle portion not present (Burns & Fay 1970).

Again, most species display the primitive condition of a concave shape of the middle portion of the nasal processes. The apomorphic straight morphology occurs intermittently throughout the Caniformia, either by itself (*Enhydra*, *Odobenus*, *Erignathus*, *Halichoerus*, and *Pusa caspica*), or as a polymorphism with state 0 (*Martes*, *Lutra*, *Procyon*, *Lobodon*, and *Pusa sibirica*). This distribution is explained either entirely through independent

origins (DELTRAN optimization), or as a complex series of reversals (ACCTRAN optimization). In this latter case, the straight morphology is a synapomorphy linking *Procyon* through to the lutrines which is lost ancestrally in the pinnipeds, before being regained several times therein. Again, the convex morphology was never consistently present at the species level. State 9 was unique to *Mirounga leonina*.

10) shape of dorsal portion of nasal processes of premaxilla along maxilla: 0 = concave; 1 = straight; 2 = convex; 9 = n/a – dorsal portion not present (Burns & Fay 1970).

Burns & Fay's (1970) initial coding for this group of characters (see character #8) points to the dorsal portion of the nasal processes as perhaps being the key region of variance. However, there does not appear to be a distinct pattern for the distribution of the various states present. The plesiomorphic condition of a convex shape of the dorsal portion of the nasal processes is generally retained throughout the Caniformia (and especially within the monachines), with numerous independent derivations of the remaining apomorphic states. (Again, the distribution of state 9 is more of a consequence of character #12.) Even within the phocines, there does not appear to be a readily discernible pattern of shared derived states; however, the distribution for the more generalized character used by Burns & Fay (1970) is tentatively supported here (but only tentatively; many of the taxa in question are polymorphic for this character and are differentially affected by the optimization criterion used).

11) contact between nasal processes of premaxilla and nasals: 0 = none; 1 = little (less than width of nasal processes); 2 = broad (greater than or equal to width of nasal processes) (Ridgway 1972; Wozencraft 1989).

The plesiomorphic condition among carnivores is for a broad contact between the premaxillary nasal processes and the nasals, with a reduction occurring in the phocids (de Muizon & Hendey 1980; Wozencraft 1989; Wyss & Flynn 1993). Wozencraft (1989) also indicates a reduced contact in lutrines, but Wyss & Flynn (1993) report that this is only true of *Enhydra*. Among phocids, this reduction is generally partial, if any, for the phocines, and full (or virtually so) for the monachines, but with *Monachus* spp. re-obtaining the primitive condition (Mivart 1885; Hendey & Repenning 1972; Ridgway 1972; de Muizon & Hendey 1980). A total lack of contact has been held to be diagnostic for the lobodontines (de Muizon & Hendey 1980). Additionally, *Phoca vitulina* may be naturally dimorphic for this character, with state 0 characterizing Atlantic forms, and state 1 or 2 being typical of Pacific individuals (Allen 1902; Doubt 1942; Chapskii 1955a, 1967). Here, reduced contact is diagnostic of the phocids alone, with the family primitively characterized by state 0. This extreme situation for the hypothetical phocid ancestor could be an artifact associated with character #12, as two of the genera lacking the dorsal portion of the nasal processes (*Cystophora* and *Mirounga*) hold the basal positions within each phocid subfamily. However, it is likely an accurate portrayal, as the monachines generally retain a state of no contact between the nasals and the premaxillary nasal processes. The distribution reported above is generally upheld here. Among the monachines, the lobodontines, exclusive of *Leptonychotes* (state 2), are characterized by state 0, with *Monachus* spp. reverting to re-obtain a broad contact (although *M. monachus* only does so under ACCTRAN optimization). The phocines internal to *Halichoerus* likewise revert

to a broad contact, with *Phoca vitulina* being uniquely characterized among this group by a polymorphic reduced contact (states 0 or 1).

12) length of nasal processes of premaxilla along maxilla: 0 = extend only part way to nasals; 1 = extend fully or virtually fully to nasals (pers. obs.).

The over-reaching effects of this character on all others dealing with the nasal processes of the premaxilla have already been outlined. In association with the previous character, any reduction in contact between the nasal processes and the nasals is held to be apomorphic (de Muizon & Hendey 1980; Wozencraft 1989). However, the important factor here is not the degree of contact between the two, but the degree of extension of the nasal processes. Thus, we consider the situation where the nasal processes do extend to the nasals but fail to contact them (e.g., due to a thin interposing sliver of the maxilla as in *Halichoerus* or *Phoca vitulina*) as a trivial variation of full extension. Therefore, the apomorphic condition is obtained only in the genera *Cystophora*, *Mirounga*, and *Ommatophoca*. It is synapomorphic only for the two elephant seals.

For *Cystophora* and *Mirounga*, the apomorphic condition is likely associated with the convergent morphological changes occurring around the nasal region to allow expansion of the narial opening for extrusion of the inflatable nasal sac (King 1972; Reeves & Ling 1981; Kovacs & Lavigne 1986). Its parallel appearance in *Ommatophoca* is problematic. Although this species is comparatively poorly described, no inflatable nasal appendage has ever been reported for it. However, it should be noted that the nasal processes of *Ommatophoca* do extend much further than they do in either *Cystophora* or *Mirounga*. The apomorphic condition might be expected more for *Halichoerus*, a species with a nasal region very similar in morphology to *Cystophora* and *Mirounga* (King 1972; Reeves & Ling 1981). The similarity is so great that it is often felt that *Halichoerus* should possess a nasal appendage to account for it (King 1972).

13) shape of anterior margin of nasals (ignoring contribution of nasal suture): 0 = flat or broadly indented; 1 = lobular (uni-, bi-, or tri- lobed) (pers. obs.).

Although many authors have commented on various aspects of the morphology of the nasal bones, including their general shape at the anterior end (e.g., Chapskii 1955a; King 1972; Reeves & Ling 1981; Kovacs & Lavigne 1986), very few have examined the potential systematic usefulness of the nasal bones. Our observations revealed two major groups with respect to the shape of the anterior end of the nasals: those with a simple, roughly flat outline, and those with a more complicated lobular appearance. Of these two nasal types, the plesiomorphic lobular condition is distributed throughout the Caniformia, with the apomorphic flattened state represented only among the Otarioids.

Unfortunately, this may be a consequence of the oversimplification of the coding scheme we adopted. As is immediately obvious, the lobular condition encompasses three distinct morphologies [see Fig.7 in King (1956:230)] and numerous derivations thereof. As we found no easy way to homologize these derivations with the major types, we were forced to condense all these forms into the lobular morphology. However, it should be noted that the caniforms nearly universally share a trident-like morphology, consisting of two lateral prongs and a broader medial one. We suggest that this is, in fact, the plesiomorphic condition, with the remaining lobular morphologies being derivations thereof (see the following character).

14) relative lengths of anterior prongs of nasal bones with a trident-shaped (= tri-lobular) morphology: 0 = lateral prongs greater than medial prong; 1 = lateral prongs subequal with medial prong; 2 = lateral prongs less than medial prong; 9 = n/a – nasal bones not trident-shaped (pers. obs.).

One mechanism to account for the numerous derivations of the hypothesized plesiomorphic trident-shaped nasal bones is through the differential expression of the lateral versus medial prongs. In particular, an extreme reduction of the medial prongs could lead to a bi-lobular morphology, that of the lateral prongs to a uni-lobular morphology, and that of both sets of prongs to the flattened morphology of the otarioids (see previous character).

Most of the Caniformia retain the plesiomorphic condition, whereby the lateral prongs are longer than the medial one. The remaining apomorphic states display limited distributions, primarily among the pinnipeds. The condition in which the nasal bones do not possess a trident-shaped morphology occurs only among the otarioids, *Mirounga* spp., and possibly *Cystophora* and *Monachus monachus* (both of which are polymorphic with other states), and may diagnose the pinnipeds ancestrally (ACCTRAN optimization). State 2 occurs unequivocally only in *Ursus* and *Lobodon*, while state 1 is found in *Halichoerus*, *Pagophilus*, and polymorphically with state 0 in *Histriophoca*.

15) visibility of nasal septum in dorsal view: 0 = does not extend beyond nasals (not visible); 1 = extends beyond nasals (visible) (King 1956; pers. obs.) (Fig.18).

Our observations for the previous nasal characters revealed that the nasal septum, which typically lies beneath and is covered by the nasals, was occasionally visible in dorsal view. Typically, when this situation occurred, the septum extended anteriorly to be visible between the prongs of the trident-shaped nasals, although it did extend completely beyond the nasals on some occasions. King (1956) lists these morphologies as a general tendency of *Monachus* spp., occurring to the greatest extent in *M. tropicalis* and the least in *M. schauinslandi*. Its appearance in *M. monachus* seems to be limited to old individuals (King 1956). This condition has also been noted in the fossil lobodontine *Homiphoca capensis* (de Muizon & Hendey 1980). Although we observed this derived condition (state 1) in numerous isolated phocid specimens, it was only consistently present in *Monachus tropicalis*, suggesting that its absence may be an artifact of preparation in some taxa. In any case, the systematic value of this apparently autapomorphic character is limited here.

16) shape of posterior edge of nasals, I: 0 = v-shaped (convergent); 1 = w-shaped (divergent) (Wozencraft 1989).

This character essentially amounts to the relationship between the nasals and the frontals. The divergent morphology is obtained when the frontal bones project between the nasals, while the convergent morphology is obtained by the reverse situation (King 1983). Despite noting the differences between the two taxa for this feature, Wozencraft (1989) proposed the divergent morphology as a synapomorphy of the otarioids. However, this has been criticized by Wyss & Flynn (1993), who note that *Odobenus* really possesses more of a flat termination to the nasals. Under the definition employed above, this would appear to be a modification of the convergent condition. However, despite recognizing the flattened termination, King (1983) still scored *Odobenus* as possessing the divergent morphology.

As well, our observations reveal that *Odobenus* does possess a very subtle divergent morphology, partially disguised by a rounding of the posterior edge of the nasals (see character #17). In any case, the convergent morphology has been repeatedly noted for phocids (Burns & Fay 1970; King 1983; Wozencraft 1989; Wyss & Flynn 1993).

The divergent morphology is present only in a number of the outgroup taxa: *Ursus*, the otarioids, and polymorphically in *Lutra*. Although the phocids share the plesiomorphic convergent morphology with *Canis*, they differ subtly in that the nasals intrude far more deeply between the frontals than in *Canis*, extending posteriorly past the anterior orbital rim. This represents yet another phocid synapomorphy (Wyss & Flynn 1993).

17) shape of posterior edge of nasals, II: 0 = pointed; 1 = rounded (Wozencraft 1989; pers. obs.).

Inclusion of this character follows from observations of the previous character dealing with the nasofrontal suture. Seemingly independent from the nature of the nasofrontal suture was the observation that the nasals either terminated in sharp points or were rounded. A rounded termination is plesiomorphic, characterizing most outgroup taxa except *Martes* and *Zalophus*. Most phocids display the apomorphic pointed morphology, but this condition arises independently within each subfamily: internal to *Cystophora* in the phocines, and in *Mirounga leonina* and internal to *Hydrurga* in the monachines. Among these more terminal taxa, only *Erignathus* and *Monachus schauinslandi* deviate from the typical pattern of their respective subfamilies.

*18) shape of posterior edge of nasals, III: 0 = pointed v-shape; 1 = rounded v-shape; 2 = rounded w-shape; 3 = pointed w-shape (Wozencraft 1989; pers. obs.).

This character is a combination of the previous two characters dealing with the shape of the nasals. However, it is inferior to the previous two in that it is too particular and thus reduces the number of potential synapomorphies in favour of autapomorphies (e.g., only *Zalophus* obtains state 3). It was, therefore, abandoned.

19) distinct caninus fossa: 0 = absent; 1 = present (de Muizon 1982a) (Fig.19).

A well-marked fossa running anteriorly along the alveolar edge of the maxilla from below the infraorbital foramen has been described as a synapomorphy of the phocines, with a convergent appearance in *Mirounga* spp. (de Muizon 1982a). However, there appears to be some confusion centred around the muscle this caninus fossa receives. De Muizon [pers. comm., citing Howell (1928)] states that the caninus muscle is lacking in phocids, so that the fossa serves instead as the origin for the maxillo-naso-labialis. However, such an interpretation is not at all clear from Howell (1928), which, together with other sources (e.g., Miller 1962; Crouch 1969; Bryden 1971), would seem to indicate that the two muscles are merely synonyms for one another. Only Piérard (1971) indicates the two muscles to be distinct entities, thereby voicing an opinion in agreement with de Muizon. Although de Muizon (pers. comm.) indicates that maxillo-naso-labialis fossa would be a more appropriate name for this structure in phocids, we will continue to use the term caninus fossa.

Among outgroup taxa, a distinct fossa was only present for *Canis* rendering the polarity of this character equivocal at the level of the Caniformia. Although the distribution of this character closely matches that of de Muizon (1982a) (we additionally noted the presence

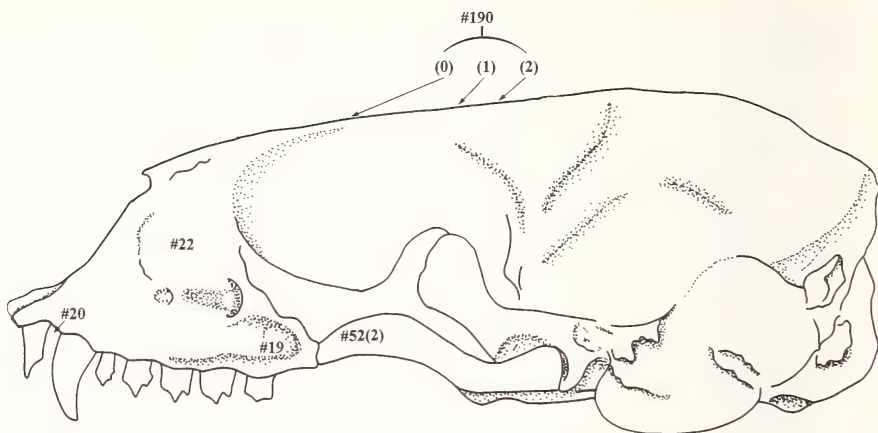


Fig.19: Lateral view of the right side of a phocid skull (*Phoca* sp.) illustrating selected characters (indicated by their number, with specific states presented in parentheses; see **Character Analysis**). Anterior is towards the left of the page. Adapted from Lawlor (1979).

of the fossa in *Hydrurga*), the caninus fossa is indicated here to be a synapomorphy of the whole of the phocids, with a single loss occurring in the ancestor of those monachines internal to *Hydrurga*.

20) depth of unnamed fossa on ventrolateral side of premaxilla: 0 = shallow; 1 = medium; 2 = deep; 9 = absent (pers. obs.) (Fig.19).

Our observations of the snout region revealed a distinct depression located between the last upper incisor and the upper canine in many specimens. This apparently unnamed fossa of the premaxilla provides room for the lower canine when the mouth is closed, and thus essentially relates to the size of the lower canine to some degree.

The general evolutionary trend for this character is for it to decrease in size from its primitive medium depth, often to the point of being entirely absent, in moving towards the pinnipeds. A shallow fossa is a synapomorphy retained from *Procyon* into each phocid subfamily. From there, several independent losses of the fossa occur, most notably in the clade of *Erignathus*, *Histiophoca*, and *Pagophilus*, and in those monachines internal to *Hydrurga*, with *Monachus* spp. showing a tendency to re-develop a shallow fossa. *Mirounga* spp. uniquely derives a deep fossa. Overall, this distribution likely reflects the trend towards homodonty in the pinnipeds, with large canines being secondarily reacquired in the sexually dimorphic *Mirounga* spp. (see also King 1983).

21) anterior opening of infraorbital canal relative to nasolacrimal foramen: 0 = anterior; 1 = ventral (or posterior) (Wozencraft 1989).

Although we are using the character as suggested by Wozencraft (1989), he goes on to suggest that this character may be more accurately recoded as referring to the relative length of the rostrum, noting that those taxa with long rostra also possess an anterior placement of the anterior canal opening. Several phocids are noted for their long rostra [e.g., *Cystophora*, *Hydrurga*, *Lobodon*, and *Mirounga*; King (1972)], but this may only be

in relation to other phocids and not to the Caniformia as a whole. As Wozencraft (1989) gave no criteria for distinguishing long versus short rostra, our observations deal strictly with the placement of the canal opening. These observations and the resulting polarity assessment do coincide with those of Wozencraft (1989). An anterior placement is shared primitively only by *Canis* and *Ursus*, while all remaining taxa are united by the apomorphic ventral (or posterior) placement.

Orbit and zygomatic arch (35 characters)

The orbital region in the pinnipeds, and especially in the phocids, yields a number of diagnostic features. Many of these are correlated with the proportionately narrow interorbital region of the pinnipeds. Although the distribution for most of the characters is well known and well referred to in the literature, very few of these traits have been examined in a systematic context for the phocids.

22) swelling of maxilla anterior to zygomatic arch: 0 = absent; 1 = present (Burns & Fay 1970; King 1972) (Fig.19).

Initially, this character dealt with the formation of a "shoulder" by a dorsolateral projection of the maxilla and jugal in the anterior wall of the orbit. King (1972: her Fig.18) described such a shoulder in *Cystophora* (also Reeves & Ling 1981; Kovacs & Lavigne 1986) and *Mirounga* as a mechanism to displace the eyes laterally to see around the (independently derived) nasal appendages. However, this shoulder was not readily apparent during any of our observations and instead, a swelling of the maxilla anterior to the zygomatic arch was noted for many species. This swelling is noted to be typical of the phocines (Burns & Fay 1970; King 1972), although it is expressed by all phocids to some degree (Burns & Fay 1970). It has been attributed to a lateral expansion of the maxilloturbinals, designed to counteract their constriction by the reduced interorbital region (King 1972) and/or as an adaptation to efficiently warm inspired air in response to the cooling environment of the late Tertiary and current high altitude habitats (de Muizon & Hendey 1980; Mills & Christmas 1990). The lack of a swelling in the lobodontines apparently arises from their accommodation of the expanded maxilloturbinals within a dorsoventrally expanded nasal cavity (de Muizon & Hendey 1980). This likely represents a secondary solution to the problem (the swelling being the first), as certain populations of the fossil lobodontine *Homiphoca capensis* are noted to possess a phocine-like swelling (de Muizon & Hendey 1980).

Here, a truly distinctive swelling (the apomorphic condition) was present only for *Phoca vitulina* and *Pusa* spp., although most phocines are polymorphic for this trait. It also appears in the lutrines, either independently in each (DELTRAN optimization), or as a synapomorphy which is later lost in the pinniped ancestor (ACCTRAN optimization).

*23) distinct preorbital process of maxilla: 0 = absent; 1 = present (Burns & Fay 1970) (Fig.20).

With recoding, this character was included in character #24.

24) size of preorbital process of maxilla: 0 = small; 1 = medium; 2 = large; 9 = absent (Burns & Fay 1970; pers. obs.) (Fig.20).

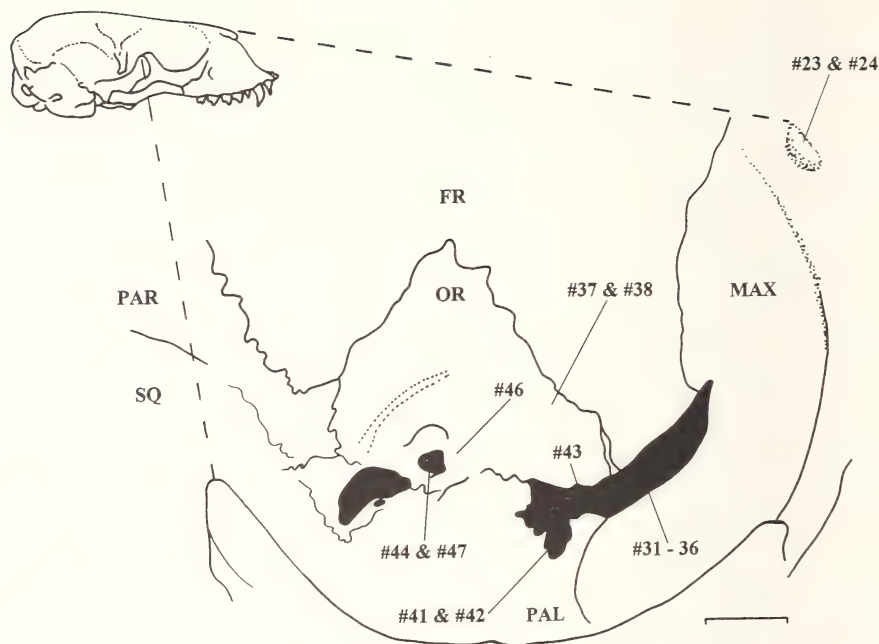


Fig.20: Dorsolateral view of the left interorbital region (see inset) of *Cystophora cristata* (USNM 188914) illustrating selected characters (indicated by their number; see **Character Analysis**) of this region. Anterior is towards the right of the page and dorsal to the top, with the zygomatic arch framing the bottom of the illustration. Abbreviations are as follows: FR = frontal; MAX = maxilla; OR = orbitosphenoid; PAL = palatine; PAR = parietal; and SQ = squamosal. Scale bar equals 1 cm. Inset adapted from Lawlor (1979).

Among pinnipeds, the general distribution of this feature is for it to be present in the otarioids, but only rarely so in the phocids (Mivart 1885), a difference Howell (1928) attributed to details of the orbicularis oculi and possibly the frontalis muscles. Turner (1848) questioned the value of this character for discriminating between the pinnipeds as it was present both throughout the otariids and in representative phocids (e.g., *Hydrurga*). A variable distribution in the pinnipeds is echoed by Hendey & Repenning (1972). Except for *Hydrurga* and *Lobodon*, the preorbital process is generally small in monachines, if not altogether absent, as in *Leptonychotes*, *Monachus schauinslandi*, and *Monachus tropicalis* (Mivart 1885; Hendey & Repenning 1972; de Muizon & Hendey 1980). Among phocines, Burns & Fay (1970) used the size of the preorbital process as one means of distinguishing between the closely related genera *Pagophilus*, *Pusa*, *Histiophoca*, and *Phoca* (listed in descending order of process size). In fissiped carnivores, the process is lacking in all but *Lutra* and *Ursus*, where it is rudimentary (Mivart 1885).

In contrast to the observations of Mivart (1885), we found a distinct preorbital process in all fissiped taxa except *Procyon*. The plesiomorphic condition is for a small process, with an increase to medium size denoting a synapomorphy of the lutrines and the pinnipeds.

This condition is retained for the otarioids (but see character #26 for *Odobenus*) and largely throughout the monachines. *Mirounga* spp. show a tendency to develop a large process, while the process is lost entirely in the clade of *Monachus schauinslandi* and *Monachus tropicalis*. A distinct process is largely lost in the phocines, although many taxa are characterized by a slight ridge or roughening of the maxilla in its former location. Only *Cystophora* (state 1), *Erignathus*, and *Histiophoca* (both state 0) possess distinct preorbital processes.

*25) distinct postorbital process of maxilla: 0 = absent; 1 = present (pers. obs.).

With recoding, this character was included in character #26.

26) size of postorbital process of maxilla: 0 = small; 1 = medium; 2 = large; 9 = absent (pers. obs.).

To date, this feature has been used primarily to elucidate the higher level relationships within the Caniformia. Among the pinnipeds, the presence of the postorbital process has been used to distinguish the otariids from *Odobenus* and the phocids, where it is absent, or, at best, rudimentary (Mivart 1885; Ridgway 1972; King 1983; Wyss 1987). Howell (1928) attributes this absence in the phocids to the lack of an interorbital extension of the temporalis, combined with the larger, more dorsally positioned eyes of this group. However, it may develop with age in phocids as Allen (1887) mentions a distinct frontal (= postorbital?) process in very old individuals of *Monachus tropicalis*. Wozencraft (1989) lists a large postorbital process as being unique for the otariids among caniforms, although Wyss (1987) indicates that it is also present in ursids.

Although *Odobenus* is typically listed as lacking a postorbital process [only Mivart (1885: 497) indicates the presence of one, but he earlier (page 493) contradicts himself], there is cause to doubt these reports. Wozencraft (1989) notes that the strong facial compression characteristic of this taxon has resulted in the confluence of the postorbital process with the lacrimal flange (= preorbital process?) into a single process of questionable homology. Our observations support this finding, although the preorbital process is implicated in the place of the lacrimal flange. However, both the pre- and postorbital processes can be individually differentiated (primarily due to their different bones of origin), and we have chosen to recognize each as being medium in size (state 1).

The general trend within the Caniformia is for a reduction in the size of the postorbital process to its eventual loss ancestrally in the phocids. However, the primitive state for this character is uncertain due to both *Canis* and *Ursus* being polymorphic for this trait (both states 1 and 2). Beyond this, ACCTRAN optimization indicates an initial derivation of a small process for *Procyon*, *Martes*, and *Enhydra*, followed by a medium process uniting *Lutra* and the pinnipeds ancestrally. In contrast, DELTRAN optimization holds for state 1 being a synapomorphy extending from *Martes* to the pinnipeds ancestrally, with *Procyon* and *Enhydra* independently evolving state 0. *Zalophus* always uniquely obtains a large process. The postorbital process is lost ancestrally in the phocids and is never regained within this group. At best, various species possessed a slight ridge, or a roughening of the frontal bone, but nothing that we would term a distinct process.

*27) nasolacrimal (= lacrimal) foramen: 0 = absent; 1 = present (Wozencraft 1989).

With recoding, this character was included in character #28.

28) size of nasolacrimal foramen: 0 = small; 1 = medium or greater; 9 = absent (Wozencraft 1989; pers. obs.).

Among carnivores, the tendency towards the loss of the nasolacrimal foramen may be a synapomorphy of a monophyletic Pinnipedia. The foramen is truly lacking only among phocids, being vestigial in the otariids and often absent in old individuals (King 1983; Wyss 1987; Wozencraft 1989). A gradual loss of the nasolacrimal foramen is indicated here. Primitively, the Caniformia are characterized by a medium-sized foramen (*Canis* and *Ursus*). The foramen either becomes reduced in size for most of the remaining fissiped outgroups (ACCTRAN optimization), or is retained at medium size with some independent derivations of a small foramen (DELTRAN optimization), before becoming lost in the hypothetical pinniped ancestor. The vestigial nature of the foramen noted above by Wozencraft (1989) is not seen in our representative otariid; however, the outright lack of the foramen we observed in *Zalophus* might be artifactual, reflecting the fact that only adult specimens were examined in this study, or that *Zalophus* might not be a typical otariid in this respect. A vestigial foramen is indicated more in *Odobenus*, which is polymorphic for this character (states 1 and 9).

29) location of inferior oblique muscle origin relative to nasolacrimal foramen: 0 = widely separate; 1 = closely adjacent (Wozencraft 1989).

The inferior oblique muscle originates on the skull in the region of the lacrimal bone. The potential fossa denoting this origin, the fossa muscularis, is well developed only in ursids and the pandas, *Ailuropoda* and *Ailurus*, and is completely absent in procyonids and canids (Davis 1964). Our observations indicate that the fossa is also apparently lacking in the pinnipeds, mustelines, and lutrines. Thus, with no reliable indicator for the site of origin, we relied on the data in Wozencraft (1989) for this character. Unfortunately, this character is of limited use here as the closely adjacent morphology is autapomorphic for ursids. Examining for the presence of the fossa muscularis may not be any more informative, as our observations indicate that the presence of the fossa is again autapomorphic for ursids.

30) lacrimal: 0 = absent / not visible; 1 = visible (King 1971; pers. obs.).

The apparent loss of the lacrimal bone has been described for the pinnipeds on a number of occasions (Howell 1928; King 1971, 1983). This loss has been ascribed either to its outright loss, to a posterior displacement and a failure to ossify (Howell 1928), or, more likely, to its fusion with the maxilla during development (King 1971, 1983). In the otarioids, this fusion is age-dependent, with younger animals often displaying a lacrimal (King 1971). No separate lacrimal bone has ever been conclusively reported on a phocid skull of any age (King 1983). The only suspected case involves a tentative assessment for a small unidentified bone fused to the maxilla in a *Mirounga leonina* fetus [Kummer & Neiss 1957 (as cited in Wyss 1987)]. [At one point in our observations, we thought that we had observed the lacrimal in a *Leptonychotes* skull; however, further examination revealed that it was more likely a portion of the maxilloturbinal underlying the widened maxillo-frontal suture (see Howell 1928; character #31).] An age-dependent fusion of the lacrimal to the maxilla has also been noted for mustelines and lutrines (Wozencraft 1989). The disappearance of the lacrimal is limited here to *Martes*, *Enhydra* (which is polymorphic for this trait), and the pinnipeds. This apomorphic loss either arises

independently in *Martes* and the pinnipeds (DELTRAN optimization), or jointly for the mustelids and the pinnipeds, with *Lutra* reversing to the plesiomorphic condition (ACCTRAN optimization).

31) amount of bone reduction along maxillo-frontal suture in interorbital region: 0 = none / irregular perforations; 1 = little – small foramen or narrow fissure; 2 = great – large foramen and/or greatly widened suture (Burns & Fay 1970; pers. obs.) (state 1 – Fig.20).

So-called “defects” in the ossification of phocid skulls are reasonably common and have repeatedly been mentioned (Mivart 1885; Howell 1928; Burns & Fay 1970; King 1972), but have rarely been utilized in a systematic context. Perhaps the largest and most consistently present defect occurs in the interorbital region and corresponds to a widening of the maxillo-frontal suture. This defect (frequently referred to as the orbital vacuity) is irregularly shaped, but roughly crescentic in shape and often confluent with the sphenopalatine foramen of the palate (Burns & Fay 1970; see also character #43). The size of the widened maxillo-frontal suture is quite variable in the phocids, generally large in the otariids, and small or absent in the fissiped carnivores (Howell 1928; Burns & Fay 1970). One potential complicating factor is the report that the size of the suture apparently decreases with age in the lobodontines (de Muizon & Hendeby 1980).

A widened suture is generally absent outside of the phocids, being found only for *Ursus* (state 1 – small foramen located at lacrimo-maxillo-palatine suture) and *Zalophus* (state 2 – large irregularly shaped foramen occupying most of anterior orbital wall together with the broadly confluent sphenopalatine foramen). The two phocid subfamilies are clearly differentiated by this feature, with virtually all phocines (*Pagophilus* being the notable exception) possessing a slightly widened suture (state 1), and virtually all monachines sharing a greatly expanded suture (although the lobodontines are generally polymorphic between states 1 and 2). Together with *Zalophus*, a large amount of bone loss along the maxillo-frontal suture may be a synapomorphy of the pinnipeds as a whole (ACCTRAN optimization), or it may have arisen independently in the otariids and the monachines (DELTRAN optimization).

*32) morphology of bone reduction along maxillo-frontal suture in interorbital region: 0 = none; 1 = irregular perforations; 2 = round / ovoid; 3 = inverse teardrop-shaped; 4 = roughly rectangular; 5 = crescent-shaped (Burns & Fay 1970; pers. obs.) (Fig.20).

Although reasonably reflective of the major shapes for the widened maxillo-frontal sutures of phocids, this character is too particular and was recoded as the more general #31 in an attempt to generate more synapomorphies.

*33) shape of maxillary (anteroventral) edge of widened maxillo-frontal suture: 0 = concave; 1 = straight; 2 = convex; 9 = n/a – maxilla and frontal in contact (pers. obs.) (Fig.20).

This character was abandoned in favour of #31 in an attempt to generate a succinct summary of the widening of the maxillo-frontal suture in phocids.

*34) shape of frontal (posterodorsal) edge of widened maxillo-frontal suture: 0 = concave; 1 = straight; 2 = convex; 9 = n/a – maxilla and frontal in contact (pers. obs.) (Fig.20).

This character was abandoned in favour of #31 in an attempt to generate a succinct summary of the widening of the maxillo-frontal suture in phocids.

*35) degree of invagination of maxillary (anteroventral) edge of widened maxillo-frontal suture: 0 = none to slight; 1 = medium or greater; 9 = n/a – maxilla and frontal in contact (pers. obs.) (Fig.20).

With recoding, this character was included in character #31.

*36) degree of invagination of frontal (posterodorsal) edge of widened maxillo-frontal suture: 0 = none to slight; 1 = medium or greater; 9 = n/a – maxilla and frontal in contact (pers. obs.) (Fig.20).

With recoding, this character was included in character #31.

*37) anterior process of orbitosphenoid: 0 = absent / barely extends onto palatine; 1 = present (pers. obs.) (Fig.20).

With recoding, this character was included in character #38.

38) degree of anterior extension of orbitosphenoid: 0 = extends to distinctly less than one-half length of palatine; 1 = extends to about one-half length of palatine; 2 = extends to distinctly greater than one-half length of palatine; 9 = absent / barely extends onto palatine (Wozencraft 1989; pers. obs.) (Fig.20).

In attempting to determine the relative position and size of the sphenopalatine foramen, we noticed that the length of the orbitosphenoid (with respect to the palatine) varied among, but was more or less constant within the different phocid species. To our knowledge, this has only been reported briefly for the otarioids (Wozencraft 1989), but never fully examined in a systematic context. The primitive condition is one in which the orbitosphenoid extends into the anterior half of the palatine, a condition found in most of the outgroups. (This assessment of state 1 for *Odobenus* is somewhat tentative due to the tremendous compression of the interorbital region that characterizes this genus, obscuring and modifying the exact relationships between the orbitosphenoid and palatine bones.) This plesiomorphic condition is retained primitively in the phocids and characterizes nearly all phocines. In contrast, the monachines derive state 1 ancestrally. The terminal branches of this subfamily (*Lobodon* plus *Monachus* spp.) display a tendency to reduce the orbitosphenoid further, but only *Monachus tropicalis* (and independently in *Erignathus*) essentially lack any anterior extension (state 9).

The above distribution of this character could be related to the length of the interorbital region. A relatively short orbitosphenoid could arise through either a truly shortened orbitosphenoid, a lengthened interorbital region filled in dorsally by the frontal, or a combination of these two factors. The relatively shorter orbitosphenoid of the phocids is due at least in part to their proportionately larger orbits as compared to the remaining caniforms (King 1972). Although this may explain the relatively reduced phocid orbitosphenoid, it does not appear to apply specifically within the phocids, as the phocids with the largest orbits – *Cystophora*, *Leptonychotes*, *Mirounga* spp., and *Ommatophoca* (King 1972) – do not possess the shortest orbitosphenoids. Likewise, *Lobodon*, which possesses a relatively small orbit (King 1972), does not have the predicted relatively long orbitosphenoid.

39) ethmoid / turbinal bones in wall of interorbital region: 0 = absent; 1 = present (pers. obs.).

One manifestation of the numerous defects in ossification mentioned previously for phocid skulls (see character #31) apparently allows for the normally covered ethmoid to form a part of the wall of the interorbital region. Howell (1928) suggests that the visibility of the ethmoturbinals in *Pusa hispida* is due to their crowding by the extremely narrow interorbital region, causing them to force their way through the overlying frontal bones. In any case, this derived condition seems to be independent of the other major defect in the interorbital region, the widened maxillo-frontal suture (character #31), and only occurs consistently for *Zalophus* and *Mirounga angustirostris*. *Lobodon* is polymorphic for this trait, and *Erignathus*, although unrecognized here, also shows a strong tendency towards this trait.

40) approach of palatine to lacrimal region: 0 = does not reach lacrimal region; 1 = reaches or almost reaches lacrimal region (Wozencraft 1989).

In most mammals (but, significantly, excluding the lutrines), the maxilla is restricted to the facial region, causing the anterior orbital wall to be formed by some combination of the lacrimal, frontal, palatine, and jugal (Wyss 1987). However, the unique condition of a reduced lacrimal in pinnipeds allows the maxilla to expand posteriorly to contribute to the medial surface of the anterior orbital wall (Wyss 1987). Together, these two features reduce the contact between the lacrimal (or lacrimal region for those taxa lacking a distinct lacrimal) and either the palatine or jugal (see character #54). Both states of reduced contact have been described as a synapomorphies for a monophyletic Pinnipedia only (Wyss 1987; Wyss & Flynn 1993), although the latter case may characterize the lutrines as well (see character #54).

The above scenario is generally echoed here, with most outgroups displaying the primitive condition, in which the palatine closely approaches or reaches the lacrimal region. The converse of this condition is a synapomorphy of either *Martes*, the lutrines, and the pinnipeds, with a reversal in *Enhydra* (ACCTRAN optimization), or of *Lutra* and the pinnipeds alone, with a parallel appearance in *Martes* (DELTRAN optimization).

41) location of sphenopalatine vacuity: 0 = enclosed in palatine; 1 = not enclosed in palatine (Wozencraft 1989) (Fig.20).

As originally coded by Wozencraft (1989), the derived condition, shared only by the otarioids, was one where the sphenopalatine vacuity was enlarged and eclipsing the orbitosphenoid dorsally. This condition, he further noted, was a function of both the enlargement of the orbital vacuity, including the sphenopalatine foramen (see character #42), and the length of the orbitosphenoid. As we have previously dealt with the relative length of the orbitosphenoid (character #38), we have employed a more generalized coding, asking merely if the sphenopalatine vacuity is limited to the palatine or not.

Even under our modified coding, this character is still a potential synapomorphy of the otarioids. Most of the taxa in this study possess the primitive morphology of an enclosed sphenopalatine vacuity. The derived condition is found only in the otarioids and in most of the monachines. However, there is some uncertainty as to whether this represents convergence between the two groups (DELTRAN optimization), or a synapomorphy, with the phocines reversing to the plesiomorphic condition (ACCTRAN optimization). It seems more likely that the former situation is true. Although the sphenopalatine vacuity in all

pinnipeds (including the phocines) is enlarged as compared to fissiped carnivores (a potential synapomorphy), this expansion is not as great in the phocids. In the otarioids, the expansion is very great and the vacuity eclipses the bone situated dorsal to it (either the frontal or the orbitosphenoid). The monachines secondarily approach the otarioid condition, with the sphenopalatine vacuity generally contacting the margin of the dorsally neighbouring bone, and, in a few isolated cases, eclipsing it, but never to the degree found in the otarioids.

42) relationship of sphenopalatine foramen and pterygopalatine canal: 0 = totally confluent, only single foramen visible; 1 = confluent, but individually distinguishable; 2 = separate (Wozencraft 1989; pers. obs.) (Fig.20).

The enlarged sphenopalatine vacuity of the pinnipeds makes exact identification of foramina in this area difficult. Burns & Fay (1970) state that the vacuity in this region is either homologous with, or includes only a part of, the sphenopalatine foramen. Our observations of an apparent intermediate state (state 1), whereby a single sphenopalatine vacuity is obviously composed of two broadly confluent foramina, hints at the latter. As no one to our knowledge has examined this region in detail for the pinnipeds, the identification of the second foramen cannot be absolute; however, it is likely the pterygopalatine canal. This conjecture is not without precedence, as Davis (1964) describes the confluence of these two cavities into a single foramen in *Ailuropoda* (albeit not enlarged into a vacuity as in the pinnipeds). As well, these two cavities are irregularly confluent throughout the carnivores (Story 1951).

Having the sphenopalatine foramen separate from the pterygopalatine canal is indeed plesiomorphic among the Caniformia, with their total confluence to a single foramen being a synapomorphy of the lutrines plus the pinnipeds. (It should be noted that there is no objective way to discriminate between the confluence of the cavities and merely the loss of one of them.) This state is retained throughout most of the pinnipeds except for the phocines, which display both the primitive pinniped (state 0) and "intermediate" (state 1) states. The intermediate condition unites at least some (DELTRAN optimization), or all (ACCTRAN optimization) of the phocines, with a variable number of reversals accounting for state 0. It should be noted that many phocids were polymorphic for this character, and that these polymorphisms included various combinations of all states, including the plesiomorphic state 2.

43) continuity of sphenopalatine vacuity and widened maxillo-frontal suture: 0 = separate; 1 = confluent; 9 = n/a – widened maxillo-frontal suture absent (Burns & Fay 1970; pers. obs.) (Fig.20).

The expansion of both the maxillo-frontal suture and the sphenopalatine vacuity in the pinnipeds leads to the possibility of their confluence. Burns & Fay (1970) indicate that this is a relatively frequent occurrence among the phocines. The distribution of this character follows the major trends of either of its constituent characters (#31 or 41). The lack of a widened maxillo-frontal suture in most outgroup taxa renders the "inapplicable" condition (state 9) as symplesiomorphic. In phocids, a widened maxillo-frontal suture is almost universally present (missing only in *Pagophilus*), so the distribution of the current character relies more on the morphology of the sphenopalatine vacuity. The more restricted

vacuity of phocines is generally separate from the maxillo-frontal suture, in contrast to the observations of Burns & Fay (1970). This state also defines the ancestral phocid condition. Correspondingly, the more expanded vacuity of monachines is generally confluent with the maxillo-frontal suture, especially in the clade composed of *Lobodon*, *Monachus* spp., and *Ommatophoca*. This condition also arises convergently in *Zalophus*.
 44) relative vertical position of optic foramina: 0 = in lower third of interorbital region; 1 = between lower third and upper two-thirds of interorbital region; 2 = in upper two-thirds of interorbital region (pers. obs.) (Fig.20).

Observations for other characters related to the optic foramina (characters #45-47) revealed that the foramina are not at a constant relative height in the skull. The most common condition was for the foramina to be situated about one-third of the way up the interorbital region (state 1), with displacements to varying degrees occurring both above (state 2) and below (state 0) this apparent demarcation point.

In fact, a ventral displacement of the optic foramina (state 0) is primitive among caniforms, being found in all fissipeds except *Lutra*. *Lutra* instead groups with the pinnipeds in possessing state 1. Three major groups roughly fall out within the pinnipeds. The otarioids are clearly defined by dorsally displaced foramina (state 2), while the phocines (excepting *Cystophora* and *Halichoerus*) revert to the primitive condition. The monachines generally retain the ancestral pinniped morphology (state 1), although *Hydrurga* and *Mirounga leonina* independently obtain the otarioid condition.

45) intracranial openings of optic foramina of orbitosphenoid: 0 = separate; 1 = converging / intermediate; 2 = confluent (Mivart 1885) (Fig.21).

Mivart (1885) initially used a simpler form of this character to distinguish the otarioids (state 2) from the phocids (state 0). Only *Hydrurga*, and possibly *Lobodon*, were noted to deviate from this pattern (Mivart 1885). However, our observations revealed an apparent intermediate condition (state 1) in addition to these two more extreme morphologies. This intermediate state closely resembles state 2, except that each opening is still individually distinguishable despite being reasonably confluent with the other.

Within the Caniformia, any tendency towards confluence of the intracranial openings of the optic foramina is apomorphic. Parallel appearances of the totally confluent morphology (state 2) occur in the otarioids and generally in the monachines internal to *Mirounga* spp. The apparent intermediate condition does not intervene between the two extreme morphologies, but instead occurs independently several times within the Caniformia.

46) interorbital septum anterior to optic foramina: 0 = absent; 1 = present (Wozencraft 1989) (Fig.20).

To some degree, the interorbital septum reflects the narrowness of the interorbital region. This septum is present in those taxa in which the optic foramina possess a common rostral border (Wozencraft 1989), and is formed by the adpression and fusion of the paired wings of the orbitosphenoid anterior to the optic foramina. The septum is typically identified only with the otariids (Turner 1848; Wozencraft 1989). However, the phocids might also be expected to possess an interorbital septum as the pinnipeds as a whole possess a narrower interorbital region than do other carnivores (Howell 1928; see also character

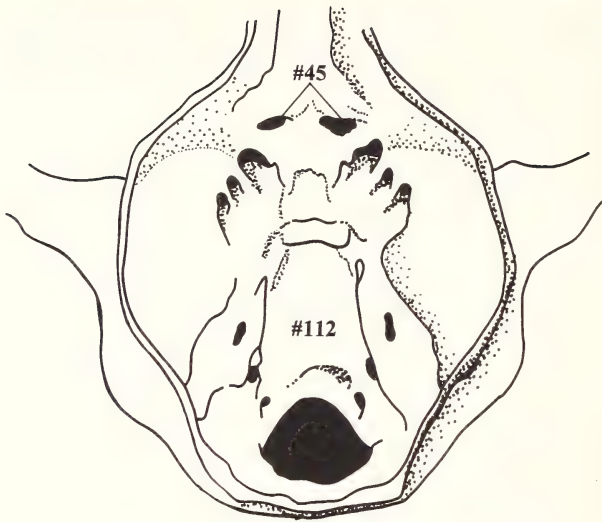


Fig.21: Dorsal view of a frontally-sectioned felid (*Felis domestica*) cranium illustrating selected characters (indicated by their number; see **Character Analysis**) of this region. Anterior is towards the top of the page. Adapted from Gilbert (1968).

#49). This might be especially true for the monachines, as the least interorbital width in this subfamily occurs in the middle or posterior portion of the interorbital region (King 1972; Wyss 1988a), or, in other words, around the region of the orbitosphenoid.

Our observations, however, do not substantiate this line of reasoning. Instead, the apomorphic interorbital septum is an uncommon occurrence, being found in only *Zalophus*, *Monachus monachus*, and *Monachus tropicalis* (the latter of which also possesses an anteriorly located least interorbital width; see character #49). The presence of the septum in the two monk seals might indicate a synapomorphy of the genus as a whole, with a reversal in *Monachus schauinslandi* (ACCTRAN optimization), or simply parallel evolution in each species (DELTRAN optimization).

47) continuity of bilateral optic foramina (interorbital foramen) in interorbital region: 0 = not continuous, no common passage; 1 = continuous, form passage through interorbital region (Mitchell 1975) (Fig.20).

Mitchell (1975) noted that a patent interorbital foramen [i.e., where the left and right optic foramina are continuous medially (either in whole or in part), thereby creating a foramen that pierces the interorbital region] was diagnostic of otariids and of the primitive fossil pinniped *Allodesmus kernensis*. Although we observed that continuity of the foramina is aided by their sharing of a common rostral border, this is not an absolute requirement, as the distribution of this character differs slightly from that of the previous one. Again, the apomorphic continuity of the foramina is uncommon, occurring as expected in *Zalophus*, but also independently in *Martes* and *Monachus monachus*.

48) alisphenoid canal: 0 = absent; 1 = present (Wozencraft 1989).

The distribution of the alisphenoid canal is one of the key characters supporting the diphyletic hypothesis of pinniped ancestry. Along with other evidence, the occurrence of the canal in otarioids together with its lack in phocids has led some workers to ally the

otarioids with ursids and the phocids with mustelids (e.g., Mivart 1885; Tedford 1976; King 1983; Wozencraft 1989). Although suggestive, this character does not resolve the question of pinniped ancestry on its own. Howell (1928) has noted one otariid specimen in which the canal was not bilaterally present, which fuels the contention of other workers that the common absence of the canal in phocids and mustelids is due to convergence (Wyss 1987; Wyss & Flynn 1993).

Although our observations agree with those in the literature, the relationships advocated here indicate a somewhat novel suggestion for the evolution of the alisphenoid canal. The monophyly of the pinnipeds still necessitates homoplasy to explain the distribution of this character; however, the homoplasy now arises from a reversal by the otarioids to re-obtain the primitive condition of possessing the canal as found in *Canis* and *Ursus*.

49) location of least interorbital width: 0 = distinctly anterior to middle of interorbital region; 1 = approximately in the middle of interorbital region; 2 = distinctly posterior to middle of interorbital region (Wyss 1988a).

King (1972, 1983) has argued that the greater reliance of pinnipeds on sight rather than smell has resulted in the lateral compression of the interorbital region (and the underlying turbinal bones) to accommodate larger orbits. This has resulted in a proportionately narrower interorbital region in pinnipeds as compared to fissiped carnivores (Howell 1928), and is the most pronounced in the smaller species (King 1972). The exact nature of this compression is not constant within the pinnipeds, however, with the least interorbital width varying in its location: anterior for the phocines minus *Cystophora* and *Erignathus*, and posterior for all other pinnipeds (Burns & Fay 1970; King 1972; Wyss 1988a).

Unfortunately, the distribution of this character does not lend itself to a simple description. The general tendency is for the phocids to shift the least interorbital width anteriorly from the plesiomorphic posterior placement to the middle of the interorbital region. This also occurs in *Martes* and *Procyon*. The remaining outgroup taxa maintain the plesiomorphic condition. ACCTRAN optimization indicates that state 1 is synapomorphic for both the phocids and the clade of *Martes* and *Procyon*, with two intervening reversals accounting for the lutrines and otarioids. DELTRAN optimization holds for independent origins in *Martes*, *Procyon*, and in each phocid subfamily. However, both optimization schemes indicate that a posterior placement is primitive in the pinnipeds, as Wyss (1988a) suggested. Within the phocids, the distributions mentioned above are only generally supported, with most members retaining a middle placement. The diagnostic anterior and posterior placements only occur for scattered phocines (and also *Monachus tropicalis*) and monachines respectively.

50) location of greatest zygomatic width: 0 = anterior to glenoid fossa (i.e., within zygomatic arch proper); 1 = at level of glenoid fossa (i.e., at squamosal) (pers. obs.).

One mechanism to possibly accommodate the larger eyes and orbits of the phocids is for the zygomatic arches to be bowed outwards and generally broadened (Howell 1928; see character #51). However, we noted some variation in the location of the broadest point of the zygomatic arches. In some forms, the broadest point was located at about the level of

the glenoid fossa, causing the zygomatic arch to take on a roughly triangular form (tapering anteriorly) when viewed dorsally. In the remaining forms, the broadest point was situated anterior to the fossa, causing the arches to take on their typical arched morphology. Of these two forms, the apomorphic state 0 describes a synapomorphy of the mustelids (including the lutrines) and the pinnipeds, with only *Zalophus*, *Erignathus*, and *Lobodon* independently reversing to the primitive condition (state 1).

51) relative position of zygomatic arches: 0 = lower than tooth row; 1 = level with tooth row; 2 = higher than tooth row (Ridgway 1972).

The increase in orbit size noted for phocids (King 1972, 1983) has apparently been achieved with some unique changes involving the zygomatic arch (see the following character also). For instance, simply dropping the zygomatic arches will increase orbit diameter (Howell 1928). An extreme dropping of the zygomatic arches (state 0) has been described as peculiar to *Ommatophoca*, contributing to the proportionately huge (even for a phocid) orbit and eyeballs characteristic of this genus (Mivart 1885; King 1969, 1972, 1983; Ridgway 1972; Ray 1981). However, this extreme condition was never observed consistently in this study, even for *Ommatophoca*. Instead, parallel instances of the apomorphic intermediate condition (a slight dropping of the zygomatic arches – state 1) were found in *Odobenus* and in the monachines internal to *Mirounga* spp., except for *Monachus monachus* which reverted to the plesiomorphic condition (state 2).

52) direction of arch of anterior portion of jugal: 0 = downwards; 1 = flat, no distinct arch; 2 = upwards (Mivart 1885) (state 2 – Fig.19).

In noting the immense orbits of *Ommatophoca*, Mivart (1885) made mention of a distinctive downward arch to the zygomatic arches in this genus. Although most obvious in *Ommatophoca*, this latter feature is common among monachines, and appears to be related to a unique elongation of the maxillo-jugal suture associated with the dropping of the zygomatic arches in this group (see previous character). In most carnivores, the typical morphology of the jugal is of a rather compact bone, with the body being narrower than its articulating ends. Together with the relatively restricted, roughly vertical articulations of the jugal with the squamosal, and especially with the maxilla, this gives the ventral border of the jugal a distinctive upward arch. In those monachines with lowered zygomatic arches, and in *Ommatophoca* in particular, the maxillo-jugal suture is greatly elongated posteriorly, and the jugal tapers anteriorly. As well, the elongation of the suture results in its horizontal rotation, so that the ventral margin of the jugal is now primarily composed of that portion contributing to the suture, and the jugal now possesses a characteristic downward arch (or, at least, is flat, with no arch in either direction). The upward arch, which is associated with the narrower body, remains, but is no longer as obvious, having been shifted posteriorly and diminished in amplitude.

The possible connection between an elongated maxillo-jugal suture and the previous character is supported by their similar distributions. Flat or downward arching jugals (both of which are apomorphic) also diagnose the clade demonstrating the lowered zygomatic arches (lobodontines and *Monachus* spp.). A downwardly arching jugal is limited within this clade to *Lobodon*, *Monachus* spp., and *Ommatophoca*, but with reversals in *Monachus monachus* and *Monachus schauinslandi* to states 2 and 1 respectively. However, a flat

jugal has a wider distribution, characterizing the monachines as a whole (DELTRAN optimization), or possibly all phocids ancestrally (ACCTTRAN optimization). This situation arises from the convergent possession of a flat jugal in *Cystophora*, *Erignathus*, and *Mirounga* spp. from the subset of monachines mentioned above. In these three genera, state 1 results from the increased robustness of the body of the jugal. In no case is the maxillo-jugal suture elongated, nor does the suture contribute to the ventral margin of the jugal.

53) degree of overlap of maxillary and squamosal processes of zygomatic arch on medial surface of zygomatic arch: 0 = little or none; 1 = approach closely – maxilla and squamosal almost or in contact (pers. obs.).

The phocids, and especially the monachines, seem to be characterized by modifications to the sutures in the zygomatic arch (see characters #52 and 56). Generally, these modifications take the form of an elongation of the sutures, and, in the case of the maxillo-jugal suture, a rotation to a more horizontal position. In some cases, this elongation and rotation is sufficient to bring the maxillary and squamosal processes of the zygomatic arch into contact with each other, or at least in very close proximity. Either situation is uncommon in the carnivores. This derived condition (state 1) is not widespread throughout the phocids either, and is found independently in only *Erignathus* and *Leptonychotes*.

54) approach of jugal to lacrimal region: 0 = does not approach lacrimal region; 1 = reaches lacrimal region / almost touches or does touch anterior wall of orbit (Wozencraft 1989; Wyss & Flynn 1993).

Wozencraft (1989) originally employed a more restrictive coding than that used here, examining whether the jugal contacted the lacrimal or not. This resulted in the derived condition (“does not contact lacrimal”) occurring in a wide variety of carnivores, including ursids, mustelines, lutrines, and pinnipeds. However, as pointed out by Wyss & Flynn (1993), the separation between the two bones in many cases is merely due to the intervention of a thin sliver of the maxilla. Recognition of this as a trivial variation of the primitive condition (“jugal and lacrimal in contact”) reduces the distribution of the derived condition (state 0 here) to the pinnipeds alone (and possibly the lutrines; see below). Such a coding also reflects the peculiar contribution of the maxilla to the anterior orbital wall in pinnipeds (Wyss 1987; Wyss & Flynn 1993; see character #40). Although Wyss (1987) indicates that lutrines also possess the derived condition, he discounts this as the configuration of the bones of the anterior orbital wall approximates that of the remaining mustelids more so than that of the pinnipeds. In any case, we too have opted for a less severe coding, partially reflecting our agreement with Wyss & Flynn (1993), and also reflecting the problems caused by the reduced nature of the lacrimal in the pinnipeds.

Yet, despite the failure of the jugal to contact the lacrimal region apparently being a pinniped synapomorphy, an obvious transition sequence for this character occurs within the monachines. In the supposedly primitive *Monachus* spp., the jugal terminates relatively medially [also Allen (1887) for *Monachus tropicalis*], above the centre of the infraorbital foramen. This termination point moves progressively laterally through the intermediate fossil taxon *Homiphoca capensis* to the more derived lobodontines, where it occurs lateral to the infraorbital foramen (Hendey & Repenning 1972; de Muizon & Hendey 1980).

As could be expected, the distribution of this character closely matches that of character #40, which deals with the approach of the palatine to the lacrimal region. Here, the lutrines plus the pinnipeds are united by the derived condition, in which the jugal does not approach the lacrimal. Together, both of these characters, which reflect the unusual contribution of the maxilla to the anterior orbital wall, not only support pinniped monophyly [as in Wyss (1987) and Wyss & Flynn (1993)], but also a lutrine affinity for the pinnipeds. The transition sequence mentioned above was not consistently borne out, although the jugal of *Monachus* spp. was observed to approach the lacrimal to a greater degree than in other phocids.

*55) dorsal process of squamosal process of zygomatic arch: 0 = absent; 1 = present (King 1983; Wozencraft 1989).

With recoding, this character was included in character #56.

56) degree of interlock between jugal and dorsal process of squamosal process of zygomatic arch: 0 = weak; 1 = medium; 2 = strong; 9 = dorsal process of squamosal absent (Wozencraft 1989).

This character stems from the oft-cited observation that the squamosal process of the zygomatic arch and the bifurcated distal end of the jugal form an unusual interlocking or mortised contact in phocids (Mivart 1885; King 1983; Wyss 1987; Wozencraft 1989) and the fossil pinniped genera *Allodesmus*, *Desmatophoca*, and *Pinnarctidion* (Mitchell 1975; Repenning 1975; Wyss 1987; Berta 1991). However, as a similar junction, but of slightly different morphology is also found in sirenians and desmostylians (Barnes 1989), we adopted Wozencraft's (1989) formulation of the character, which focuses on one particular aspect of the junction. The distinct dorsal process of the squamosal process he mentions is found only in phocids (Wozencraft 1989) and most species of *Allodesmus* [see photos and drawings in Mitchell (1975) and Barnes (1979)].

While we affirmed that the presence of the dorsal process is uniquely shared by all phocids among the taxa examined here (see character #55), we also noted that the "strength" of the resulting interlock varies. In some phocids, the jugal merely abuts the dorsal process of the squamosal process (state 0 – weak interlock), while in others, the jugal wraps up and around the dorsal process to varying degrees, thereby increasing the strength of the mortised contact (states 1 and 2). A medium strength interlock is the common morphology for the phocids and characterizes the family primitively. The remaining apomorphic states arise independently on a number of occasions: a weak interlock in *Halichoerus*, *Lobodon*, and *Pusa sibirica*, and a strong interlock in *Cystophora*, *Monachus tropicalis*, and *Pusa caspica*.

Palate and ventral side of snout (18 characters)

Although the palatal region appears to contain a good deal of phylogenetic information, a significant use of palatal characters is primarily limited to Chapskii (1955a) and Ridgway (1972). A primary source of characters is the contours of the hard palate. Chapskii (1955a) indicates this to be a useful source, although the high incidence of intraspecific polymorphism does tend to hinder easy descriptions for some species.

*57) incisive foramina (= palatine fissures / foramina): 0 = absent; 1 = present (pers. obs.).

With recoding, this character was included in characters #58 to 61.

58) size of incisive foramina: 0 = small; 1 = medium; 2 = large; 9 = absent (pers. obs.).

To our knowledge, the incisive foramina have never been used to help resolve phocid phylogeny, despite readily apparent differences in size, general location, and even in their presence or absence. Size, perhaps, is the most obvious character, although the functional significance of any size differences is unknown. We divided the foramina roughly into size classes based on the size of the foramina relative to the size of the anterior end of the hard palate. Increased emphasis for assigning foramina to their appropriate size class was given to their width (rather than their length; see the following character), due to its greater range of variation.

In moving towards the pinnipeds, the general trend is for a stepwise reduction in the size of the incisive foramina. *Canis* and *Ursus* possess the plesiomorphic condition of large foramina, with medium-sized and small foramina describing successive synapomorphies for the remaining fissipeds (excluding *Lutra*) and the pinnipeds respectively. Within the pinnipeds, the otarioids retain small foramina, as do the two phocid subfamilies ancestrally. The phocines are characterized by a reversal back to larger incisive foramina: large foramina for *Halichoerus* and *Phoca largha*, and medium-sized foramina in the remaining species, excluding *Cystophora*. The monachines largely retain small foramina. *Mirounga* spp. (although *M. leonina* is polymorphic for this character) and *Monachus schauinslandi* continue the trend to smaller foramina by losing them outright (see character #61). In contrast, the remaining monk seals show a tendency to revert to larger foramina, as does *Hydrurga*.

59) posterior extension of incisive foramina: 0 = enclosed within premaxilla; 1 = contact premaxillary-maxilla suture; 2 = extend into maxilla; 9 = incisive foramina absent (Chaptskii 1955a).

In some ways, this character overlaps the previous one, as the posterior extension of the foramina is a function of their size. However, whereas the previous character was more a function of their width, this character deals more with their length. Our observations revealed two distinct morphologies (state 0 and 2), with a somewhat arbitrary intermediate (state 1). This latter state is likely not truly intermediary, but rather a modification of one of the two more extreme conditions.

The plesiomorphic state for the Caniformia is uncertain for this character. In most of the basal outgroups the incisive foramina are restricted to the premaxilla, but in *Canis*, the foramina extend well into the maxilla. In any case, the lutrines, otarioids, and the phocids are all united by the possession of foramina that extend into the maxilla to varying degrees. Both phocid subfamilies retain this condition primitively, before showing parallel derivations of foramina that only contact the premaxillary-maxilla suture, again hinting that state 1 is not a true intermediate condition. *Mirounga* spp. and *Monachus schauinslandi* convergently lack incisive foramina, while *Zalophus* and *Cystophora* independently re-obtain state 0.

60) number of incisive foramina: 0 = one; 1 = two; 9 = absent (pers. obs.).

Surprisingly, our observations revealed that the incisive foramina are not always paired (the plesiomorphic condition). Other than those forms that lack the foramina, or show

tendencies thereto (*Mirounga* spp. and *Monachus schauinslandi*), the foramina apparently coalesce in *Odobenus*, leading to the unique possession of a single midline foramen.

61) reduction of incisive foramina: 0 = absent; 1 = present (Allen 1887).

As noted in the previous characters dealing with the incisive foramina, three phocids, *Mirounga angustirostris*, *Mirounga leonina*, and *Monachus schauinslandi*, convergently share (between the two genera) the apomorphic tendency towards the absence of the incisive foramina. This loss appears to be the extreme outcome of another apomorphic tendency: the gradual closing over of the foramina by the bones of the hard palate. This latter tendency is convergently displayed to various degrees in four monachine genera (*Hydrurga*, *Leptonychotes*, *Mirounga*, and *Monachus*). *Hydrurga*, *Leptonychotes* (albeit both are polymorphic for this trait), and *Monachus monachus* display a very early stage in which the foramina are only partially covered over. Allen (1887) described a similar condition in *Monachus tropicalis*, but this was not observed here. In *Mirounga* spp., this process has advanced to the point so that the foramina are completely covered over, with only a pair of depressions laying evidence to their prior existence. Finally, *Monachus schauinslandi* displays the advanced condition where even the depressions are filled in and the foramina can be said to be truly absent. It should be noted that this is not a true developmental series, but isolated glimpses in three parallel ones, as these taxa are not each other's closest relatives.

62) position of major palatine foramen relative to maxillo-palatine suture: 0 = anterior; 1 = on; 2 = posterior (Ridgway 1972).

The plesiomorphic caniform condition for this character is generally agreed to be one where the anterior openings of the major palatine foramen open on, or very closely adjacent to, the maxillo-palatine suture (Wozencraft 1989; Bryant et al. 1993). This plesiomorphic placement is constant within the various carnivoran families, excluding the mustelids (Pocock 1921) and the pinnipeds (Wozencraft 1989). Many independent origins of an apomorphic anterior positioning have been postulated: various mustelines (Pocock 1921; Bryant et al. 1993), the lutrines (and within each of the genera *Lutra* and *Aonyx*) (van Zyll de Jong 1987; Bryant et al. 1993), all monachines except the fossil lobodontine *Homiphoca capensis* (de Muizon & Hendey 1980), and *Pagophilus* (Ridgway 1972). The only specific description of a posterior shift of the foramina is for *Histiophoca* (Ridgway 1972), although a tendency towards this has been noted for *Pusa* spp. in particular (Chapskii 1955a) and most phocines in general (Burns & Fay 1970).

Here, an apomorphic anterior shift of the foramina unites *Lutra* with the pinnipeds. This condition is retained by the hypothetical phocid ancestor and largely throughout the monachines, with only *Ommatophoca* showing a reversal to the primitive condition (state 1). The phocines primitively reverse to the plesiomorphic condition, with *Pagophilus* and *Phoca vitulina* separately redeveloping the anterior shift, and *Erignathus* uniquely deriving the posterior shift.

63) shape of maxillo-palatine suture: 0 = flat / square; 1 = rounded / triangular (Allen 1887).

This and the following two characters deal with the outline of the palatine bones on the palate. In addition to Allen's (1887) observation of a straight transverse suture in *Monachus*

tropicalis, our observations revealed that the anterior edge of the palatines displays other distinct morphologies. This plesiomorphic condition entails the maxillo-palatine suture having a rounded or triangular appearance. The flattening of this suture (manifested as a straight or square anterior edge to the palatines), as in *M. tropicalis*, is a synapomorphy of *Lutra* and the whole of the pinnipeds. Only *Mirounga leonina* and *Pusa sibirica* reverse to re-obtain the primitive condition, although a few other species are polymorphic between the two states.

64) outline of palatine bones in ventral view: 0 = square; 1 = "butterfly-shaped" (Ridgway 1972).

In essence, this character examines the entire ventral outline of the palatines and thus partially overlaps both the preceding and following characters. In contrast to the previous character, however, the different shapes here are determined more by the posterior half of the palatines, rather than the anterior edge. As well, all three characters appear to diagnose synapomorphies at different taxonomic levels. This character is apparently fairly specific, as Ridgway (1972) has used it to distinguish between the genera *Cystophora* (state 0) and *Mirounga* (state 1).

An apomorphic, butterfly-shaped outline to the palatine bones is a purely phocid condition, arising independently within this family on several occasions, and with numerous other species being polymorphic for the trait. It tends to characterize the phocines, existing as a synapomorphy of all members save *Cystophora* (ACCTRAN optimization), or merely for the clade internal to *Phoca largha*, with *Pagophilus* and *Phoca vitulina* independently reversing back to a square outline (DELTRAN optimization). Among monachines, butterfly-shaped palatine bones only exist unequivocally for *Lobodon*, *Mirounga angustirostris*, and *Monachus tropicalis*. The states observed here for *Cystophora* and *Mirounga* generally match those described by Ridgway (1972), except that *Mirounga leonina* obtains the plesiomorphic condition.

65) shape of posterior edge of palatine: 0 = (roughly) triangular; 1 = arched; 2 = straight (de Muizon 1982a).

The final character involving the ventral outline of the palatines deals exclusively with their posterior edge. King (1956) lists *Monachus monachus* as possessing a rounded posterior edge, while *Monachus tropicalis* possesses a pointed morphology (also Allen 1887). *Monachus schauinslandi* may be polymorphic for these two states [Kenyon & Rice 1959; also compare King (1956) and King & Harrison (1961)]. De Muizon (1982a) has pointed to a straight posterior border of the palatines as being a synapomorphy of his Cystophorini (*Cystophora*, *Histiophoca*, and *Pagophilus*), but it may also occur independently in *Erignathus* (Chapksii 1955a). Ridgway (1972) confirms a straight posterior border for *Histiophoca*. However, these observations are partially contradicted by Douthett (1942), who described a rounded "Roman arch" (state 1) in *Histiophoca* and *Pagophilus*. This contradiction for *Histiophoca* may be due to it being polymorphic for this trait (between states 1 and 2), as hinted at by Burns & Fay (1970). Along with *Monachus schauinslandi* (see above), this may also be true for most species in general (Chapksii 1955a). Another complicating factor is our observation that states 1 and 2 lie along a continuum. A straight posterior edge may merely represent a very shallow double

arch. The triangular morphology appears to be independent of this continuum, but may also be an artifact created by a large notch in the posterior edge of the palate (see characters #67 and 68). Thus, the pointed “Gothic arch” described for *Phoca vitulina* and *Pusa hispida* by Doult (1942) may actually be a combination of an arched posterior edge with a large triangular notch.

An arched posterior edge of the palate is both plesiomorphic and common throughout the Caniformia. This primitive condition is retained into both phocid subfamilies, and largely typifies most species. A triangular morphology occurs independently among a few species in both subfamilies: *Phoca* spp. among the phocines, and *Leptonychotes*, *Lobodon*, and *Monachus tropicalis* among the monachines. The other apomorphic state, a straight posterior edge, is found convergently in *Odobenus* and the clade of *Histriophoca* plus *Pagophilus*. In contrast to the observations of Chapkii (1955a), polymorphism was observed to be minimal for this character among the phocids.

66) presence of posteriorly directed process in midline of posterior edge of palatine: 0 = absent; 1 = present (Chapkii 1955a).

In contrast to the notching of the posterior palatal edge present in many phocines (see characters #67 and 68), Chapkii (1955a) noted a small, posteriorly directed process in *Histriophoca*, *Pagophilus*, and occasionally in *Phoca vitulina*. This condition is primitive among caniforms, with the loss of the process being a synapomorphy of *Lutra* and the pinnipeds. But, among this group, only *Mirounga leonina* consistently regained the posteriorly directed process.

67) morphology of notching in posterior edge of palatine: 0 = rounded; 1 = triangular; 2 = incision; 9 = none (Ridgway 1972).

The notching or incision of the posterior edge of the palate has been variously noted for *Phoca* spp. and *Pusa* spp. (Doult 1942; Chapkii 1955a; Burns & Fay 1970; Ridgway 1972). Such a condition does not seem to be typical among the remaining phocines (Doult 1942; Chapkii 1955a; Ridgway 1972; de Muizon 1982a), although Burns & Fay (1970) hint that *Histriophoca* may be polymorphic for this character. King (1956) describes a small incision for *Monachus monachus*, which we would reclassify here as a small triangular notch based on her Fig.7 (page 230).

The primitive condition for the Caniformia as a whole is the lack of any notching. This agrees with the previous character, where a posteriorly directed process is postulated as being plesiomorphic. Notching of any form is reasonably rare and largely restricted to the phocids. The most common form is a triangular shape, occurring consistently in *Mirounga angustirostris* and the clade of *Lobodon* plus *Monachus* spp., but appearing polymorphically (with state 9) in a number of other pinnipeds. *Monachus tropicalis* uniquely derives the incision, while a rounded notch was obtained only for *Histriophoca*, and then only as a species polymorphism with a triangular notch.

68) size of notching in posterior edge of palatine: 0 = small; 1 = medium; 2 = large; 9 = absent (Chapkii 1955a).

The notching present in the posterior edge of the palate of many phocids can have an adverse effect on the determination of the shape of the posterior edge of the palate as a

whole (character #65). Doult (1942) apparently describes a moderate case for *Phoca vitulina* and *Pusa hispida*, where a large triangular notch changed the shape of the posterior edge of the palate from a rounded Roman arch to a pointed Gothic arch. In such cases, there is usually a slight inflection point between the arch and the notch to indicate the two separate morphologies. However, in some specimens, the confluence was so complete that there was no objective way to decide between a triangular posterior edge and a combination of an arched posterior edge with a very large triangular notch. But, despite Chapskii's (1955a) assertion that the palatal contours are generally subject to a fairly high level of intraspecific variation, he still holds this character to be a useful feature for subdividing the phocines.

In keeping with the previous character, the lack of a notch is primitive among the caniforms and is retained into the basal forms of both phocid subfamilies. A small notch is convergently obtained in *Histiophoca* and the clade of *Lobodon* plus *Monachus* spp. Two monk seals go on to derive larger notches – *M. monachus* (state 1) and *M. schauinslandi* (state 2) – as does *Mirounga angustirostris* (state 2). Many species were polymorphic, with the notch being equally present (i.e., one or more of the states 0, 1, or 2) and absent. Yet, somewhat curiously, the “present” state was not necessarily for a small notch, as one would expect if the notch was in the process of being gained, but often for a medium-sized or greater one (as in *Zalophus*, *Hydrurga*, and *Phoca vitulina*).

69) relationship of bony nasal septum to posterior edge of palate: 0 = does not reach posterior edge of palate; 1 = closely approaches / reaches posterior edge of palate (Chapskii 1955a; Ridgway 1972).

Ridgway (1972) used this character to distinguish between the closely related genera *Histiophoca* (state 1 – closely approaches) and *Pagophilus* [state 1 – reaches posterior edge; also Burns & Fay (1970)]. Although useful at the level employed by Ridgway (1972), the distinction between “closely approaching” and “actually reaching” seemed to be fairly minor at the level employed in this study. As well, under such a coding scheme, Burns & Fay (1970) observed that both *Histiophoca* and *Phoca* spp. would be polymorphic for this character. One solution would be to code this character even more finely using the sutures of the hard palate, especially the maxillo-palatine suture (Chapskii 1955a). However, this is often difficult to accurately determine in intact skulls, so we instead propose a more stringent coding of Ridgway's (1972) character: either the bony nasal septum extended posteriorly to approach the posterior edge of the palate, or it distinctly did not.

One exception to this dichotomy was observed fairly consistently in *Mirounga angustirostris*. Here, state 1 was achieved through a combination of a slight posterior extension of the bony nasal septum, a strong notching of the posterior end of the palate (see character #67), and a dorsal arching of the palate in the midline to meet the nasal septum. Together, these factors create a functionally shorter palate, allowing the otherwise slightly elongated nasal septum to reach its posterior end.

The primitive condition, where the bony nasal septum fails to reach the posterior end of the palate, is shared by all the outgroups except *Procyon*. The apomorphic trait is typically associated with the Monachinae (although two parallel reversals occur within the

subfamily), but also appears in two phocines, *Cystophora* and *Pagophilus*. This comes about either as a synapomorphy of the monachines alone, with convergent appearances in the two phocines (DELTRAN optimization), or as a synapomorphy of the phocids as a whole, with an early reversal in the phocines, followed by a re-derivation in *Pagophilus* (ACCTRAN optimization).

70) orientation of pterygoid hamuli: 0 = directed laterally; 1 = in midline; 2 = directed medially (Mivart 1885; Allen 1887; Chapskii 1955a).

The orientation of the pterygoid hamuli appears to be directed by one, and possibly, two factors. The function of the hamuli is to suspend the soft palate over the internal nares. Therefore, the width of the soft palate will directly influence the direction of the hamuli. A second possible influence involves the origin of the pterygoideus externus (= medialis) from the adjacent pterygoid fossa (Davis 1964). Changes in the robustness of this muscle might indirectly affect the hamuli. An increase in robustness (e.g., in those taxa employing a more grinding masticatory motion) may serve to direct the hamuli inwards, whereas a decrease in robustness would cause the orientation to be determined more by the hamuli's primary function. Descriptions of hamular orientation are rare, but laterally directed hamuli have been noted in *Leptonychotes* (Mivart 1885), *Monachus tropicalis* (Allen 1887), and isolated phocines (Chapskii 1955a, 1967). Chapskii (1967) hints at an apparent shift from medially to laterally directed hamuli during the ontogeny of *Phoca largha*. Otherwise, only *Erignathus* has been noted to possess medially directed hamuli (Chapskii 1955a).

All fissiped caniforms are characterized by hamuli situated in the midline, with apomorphic deviations from this occurring only in the pinnipeds. Medially directed hamuli occur convergently in *Mirounga* spp., and either in *Odobenus* alone (DELTRAN optimization), or in the otarioids as a whole (ACCTRAN optimization). However, like all other pinnipeds, none of these taxa are known to employ a grinding style of mastication. Laterally directed hamuli are peculiar to the phocids, appearing independently in *Halichoerus* and the clade of monachines internal to *Hydrurga* (with *Monachus monachus* reversing to the plesiomorphic condition). A relative reduction of the pterygoideus externus has not been described in phocids (see Howell 1928; Bryden 1971; Piérard 1971), and it is not known if these taxa possess a proportionately wider soft palate.

*71) relationship of ethmoid to pterygoid process of basisphenoid on ventral surface of skull: 0 = does not contact pterygoid; 1 = contacts pterygoid (pers. obs.).

With recoding, this character was included in character #72.

72) degree of contact between ethmoid and pterygoid process of basisphenoid: 0 = narrow; 1 = greater than or equal to medium breadth; 9 = none (pers. obs.).

Among the Caniformia, the pterygoid process of the basisphenoid extends to different degrees both anteriorly and posteriorly (see character #73 for the latter). In the anterior direction, we observed two major mechanisms for preventing (or minimizing) contact between the ethmoid and the pterygoid process. Either the two elements did not approach each other closely, or if they did, then contact was prevented by the presence of the pterygoid canal (sensu Burns & Fay 1970). In some cases, the canal was too small to prevent contact absolutely and merely minimized the amount of contact (e.g., changing a potentially broad contact to a narrow one).

The apomorphic condition where the ethmoid and pterygoid process contact one another is generally restricted to the Pinnipedia, being found only in *Procyon* (state 1) and *Martes* (polymorphic between all states) among fissipeds. The early evolution of this character in the pinnipeds is difficult to ascertain due to the polymorphism present in the otarioids. However, the likely scenario is for a narrow contact ancestrally, with the otariids showing a tendency to lose this contact while the phocids and *Odobenus* independently continue to increase its width (as under ACCTRAN optimization). Parallel trends to reducing the contact between the ethmoid and pterygoid are also found in the phocids. A narrow contact is regained in *Phoca largha* and *Pusa* spp., while contact is lost outright in *Phoca vitulina* and the clade of *Lobodon* plus *Monachus* spp.

73) relationship between pterygoid process of basisphenoid and auditory bulla: 0 = does not extend to auditory bulla; 1 = extends to auditory bulla (Burns & Fay 1970).

The posterior extent of the pterygoid process is fairly restricted in most carnivores. Only among *Odobenus* and the phocids does it extend posteriorly to reach the auditory bulla (Burns & Fay 1970). Surprisingly, despite supporting his contention of an *Odobenus*-phocid pairing, this character was not mentioned by Wyss (1987). Our analysis indicates that only the phocids, in parallel with *Lutra* (DELTRAN optimization), unequivocally display the apomorphic condition (state 1); *Odobenus* is polymorphic for this trait. However, the additional polymorphic appearance of this trait in *Enhydra* suggests that this character might be a putative synapomorphy of the lutrines plus the pinnipeds, with the otarioids at least partially reversing to the primitive condition (ACCTRAN optimization).

74) bony constituents of wall of foramen ovale with respect to alisphenoid and squamosal: 0 = alisphenoid only; 1 = both alisphenoid and squamosal; 2 = squamosal only (pers. obs.).

Most anatomical atlases of representative carnivores indicate that the foramen ovale runs solely through the alisphenoid (e.g., Miller 1962; Davis 1964; Crouch 1969). This morphology appears to be fairly consistent throughout the carnivores (see Flower 1869). However, our observations reveal that the squamosal occasionally makes a contribution to the walls of the foramen ovale, and, in some cases, contains the foramen entirely. [A ventral contribution is also occasionally made by the pterygoid in some phocids (pers. obs.), but this is not examined here.]

Any contribution by the squamosal to the foramen ovale represents a derived condition. This is largely diagnostic of, and restricted to, the monachines, with the subfamily characterized ancestrally by a partial squamosal contribution (state 1). This state, which arises independently in *Martes* and *Pusa caspica*, is retained throughout the monachines, with a purely squamosal contribution being found in *Monachus* spp. and convergently in *Cystophora*.

Basiscranial region (43 characters)

The conservative nature of the basiscranial region has rendered it very important historically for elucidating the phylogenetic relationships of various caniform taxa (e.g., Turner 1848; Flower 1869; Pocock 1921; Segall 1943; McLaren 1960b; Hunt 1974). It may be particularly valuable with respect to the phocids, as this region of the skull apparently

shows a lower degree of intergeneric and intraspecific variation than other regions of the skull (King 1966). However, despite its apparent stability, there is still the potential for some homoplasy within this region (see Hunt & Barnes 1994). Important basicranial characters involve such landmarks as the carotid canal [the distinguishing feature of arctoid carnivores (Wyss 1988a)], the auditory bulla, and various other processes and foramina of the region.

75) visibility of the mastoid process in dorsal view: 0 = not visible; 1 = visible (Wyss 1988a).

The condition whereby the mastoid process is visible in dorsal view is unusual among mammals, being restricted primarily to the phocines, with some convergent appearances in the monachines (King 1966; Burns & Fay 1970; Ray 1976b; de Muizon 1982a, Wyss 1988a). Typically, *Monachus* spp. and/or *Ommatophoca* are implicated (King 1966; Ray 1976b; de Muizon 1982a), although Burns & Fay (1970) indicated that it occurred in about half of all the monachine specimens they examined. These convergent appearances can apparently be eliminated if the character is recoded to examine for the presence or absence of a medially curving mastoid crest (de Muizon 1982a), or, equivalently, of a distinct oblique ridge formed by the mastoid process (Burns & Fay 1970). The presence of either of these synonymous features is apparently exclusive to the phocines (Burns & Fay 1970; de Muizon 1982a). We retained the less precise coding in an effort to determine the exact distribution of this character among the Monachinae.

As indicated above, the apomorphic morphology (state 1) is primarily restricted to, and universal among, the phocines. *Pusa caspica* and *Pusa sibirica* appear to be independently losing this trait, primarily due to a reduction in the size of the mastoid process. Convergent appearances of this trait were consistently observed in only two monachines, *Monachus monachus* and *Ommatophoca*, as well as in the fissiped *Procyon*.

76) relative shape of basioccipital-basisphenoid region: 0 = concave; 1 = flat; 2 = convex (Wyss 1988a).

Burns & Fay (1970) noted that all phocines share a relatively flat to convex basioccipital-basisphenoid region, as opposed to the strongly concave form in monachines. Wyss (1988a) extended this last observation to include the otarioids, adding that he believed the concave morphology to be primitive (presumably for the pinnipeds), and therefore not synapomorphic for the monachines. We have modified the coding of this character somewhat by dividing the state "flat to convex" into its two constituent morphologies.

In contrast to Wyss (1988a), our analysis indicates that a flat morphology is primitive for the arctoids (the plesiomorphic state for the caniforms is equivocal), as well as for the pinnipeds. Instead, a concave basioccipital-basisphenoid region is a derived trait, possibly characterizing the monachines ancestrally (ACCTRAN optimization). However, it is only manifested in *Mirounga* spp. among extant species; the remaining monachines largely emulate the supposed phocine condition, displaying either the flat (*Ommatophoca*) or convex morphologies (*Hydrurga*, *Lobodon*, *Monachus* spp.), or both (*Leptonychotes*). The phocines tend towards retention of the flat morphology, with only *Halichoerus* and *Phoca vitulina* developing the convex condition. This latter state also appears convergently in *Canis* and *Enhydra*.

*77) postglenoid (= glenoid) foramen in squamosal: 0 = absent; 1 = present (Wozencraft 1989).

With recoding, this character was included in character #78.

78) size of postglenoid (= glenoid) foramen in squamosal: 0 = small; 1 = medium; 2 = large; 9 = absent (Wozencraft 1989).

The pinnipeds are supposedly unique among the Caniformia in their lack of a postglenoid foramen (Wozencraft 1989), a structure that is present and generally quite conspicuous in all other members of this group (Flower 1869). However, Mivart (1885) has noted the presence of a small postglenoid foramen throughout the pinnipeds, while Berta (1991) considers it to be either vestigial or absent within this group. The form of the foramen appears to be quite variable in *Histiophoca*, from not being universally present to occasionally being shifted laterally so as to be just anterior to the external auditory meatus (Burns & Fay 1970). Our observations corroborate these last two findings, revealing that the postglenoid foramen is not universally absent in pinnipeds, but instead very much reduced and slightly displaced in position. In the phocids, the inflation of the auditory bulla (see characters #80-82), often in combination with an enlargement of the mandibular fossa, virtually eliminates the area between these structures and, as such, the foramen is generally shifted onto the posterior lip of the fossa. Occasionally, we also observed a lateral displacement of the postglenoid foramen equivalent to that noted by Burns & Fay (1970).

Although the postglenoid foramen is common throughout the caniforms (including the pinnipeds), the high degree of polymorphism displayed by this character makes for an uncertain evolutionary pathway, primarily among the outgroup taxa. The plesiomorphic condition is of a large foramen, a state which may persist through to the hypothetical ancestral monachine (DELTRAN optimization). Another scenario holds for a small foramen being a synapomorphy linking *Procyon* through to the phocids (ACCTRAN optimization). Beyond this disparity, there are features in common to the two evolutionary scenarios. A medium-sized foramen is synapomorphic for the phocines (with an independent appearance in *Procyon*), with *Histiophoca* and *Pagophilus* reverting to the plesiomorphic condition. The monachines generally possess a small foramen, as does *Pusa caspica*. Although a number of species were polymorphic for lacking the foramen, only two were consistent for this trait: *Martes* and *Hydrurga*.

79) shape of anterior edge of auditory bulla: 0 = concave; 1 = flat; 2 = convex (Ridgway 1972).

This was another character employed by Ridgway (1972) to distinguish between the genera *Cystophora* (state 1 to 2) and *Mirounga* (state 0). The plesiomorphic state is uncertain due to the autapomorphic appearance of the convex morphology in *Canis*; however, a flat morphology is both primitive and ubiquitous for the arctoids. This state is retained ancestrally in the phocids, with *Lutra*, *Halichoerus*, and the monachines convergently deriving a concave anterior edge. In the monachines, this morphology is often associated with an unusually robust mandibular symphysis which encroaches upon the auditory bulla. *Lobodon* plus *Monachus* spp. revert to the primitive arctoid state.

80) inflation of ectotympanic: 0 = not inflated; 1 = slightly / moderately inflated; 2 = inflated (Wozencraft 1989) (Fig.22).

As with most other carnivores, an inflated auditory bulla is common to all phocids, albeit to varying degrees (Howell 1928; Segall 1943; Hunt 1974). It ranges in size from "large" in *Leptonychotes* to "small" in *Monachus tropicalis* (King 1972). The inflated bulla of

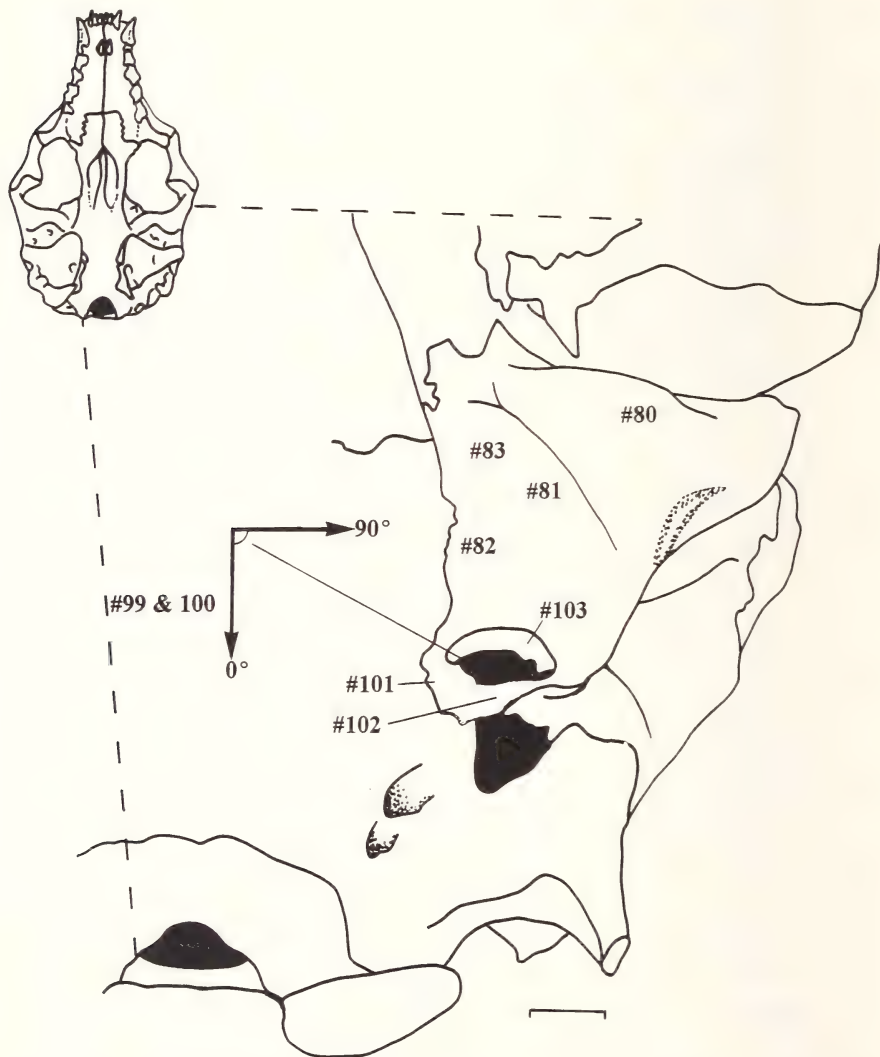


Fig.22: Ventral view of the idealized phocid left basicranial region [but based largely on *Monachus tropicalis* (USNM 102536)] (see inset) illustrating selected characters (indicated by their number; see **Character Analysis**) of this region. Anterior is towards the top of the page and lateral to the right. Scale bar equals 1 cm. Inset adapted from Lawlor (1979).

phocids clearly separates them from the non-inflated bulla of the otarioids (Howell 1928; Repenning 1972; Wyss 1987), a difference that is manifested even during fetal development (Howell 1928). We attempted to elucidate the pattern of bulla inflation using three characters from Wozencraft (1989) that identify different bullar elements. Unfortunately, differentiation between the ectotympanic and entotympanic portions of the auditory bulla is difficult among carnivores due to their high degree of fusion in the adult bulla (Repenning 1972; Hunt 1974). Differentiating between the two regions is aided in some phocids by the presence of a distinct sulcus between them (van der Klaauw 1931; Burns & Fay 1970; see character #83); however, the distinction between this character and the following two remains somewhat arbitrary. Instead, we will use these three characters to represent inflation of respective regions of the bulla (lateral, middle, and medial respectively) rather than of the elements themselves. A further problem is that the inflation of the auditory bulla is best judged internally (see Repenning 1972), but we were limited to an external examination of the bulla in almost all cases.

Despite noting that the ectotympanic forms a large percentage of the bulla in otarioids, Repenning (1972) singles phocids out from the pinnipeds for their enlarged ectotympanic portion. This is corroborated by Wozencraft (1989), who indicates that only the ursids and the otarioids lack an inflated ectotympanic among the carnivores. Again, the plesiomorphic condition for the Caniformia is uncertain; however, it is likely an ectotympanic that is not inflated, as this is the condition shared by all the outgroups except *Canis* and *Martes* (both state 1). These observations are largely in conflict with those of Wozencraft (1989). As expected, an inflated ectotympanic (state 2) is reasonably common among phocids, but more so among phocines where it is ancestral and retained by all members except *Pagophilus* (state 0), and possibly *Histiophoca* (states 0, 1, and 2) and *Phoca vitulina* (states 0 and 1). Among monachines, state 2 characterizes only *Hydrurga* and the clade of *Lobodon* plus *Monachus* spp. In this last clade, a slightly inflated ectotympanic is a synapomorphy of *Monachus schauinslandi* and *Monachus tropicalis*.

81) inflation of caudal entotympanic along anteroposterior axis: 0 = not inflated; 1 = slight / moderate inflation; 2 = inflated (Wozencraft 1989) (Fig.22).

Hunt (1974) indicates that inflation of the caudal entotympanic is primarily responsible for the overall inflation of the carnivoran bulla. Yet, the contribution of the entotympanic to the auditory bulla among the arctoids is quite variable. It is the greatest in some phocines, comprising two-thirds to three-quarters of the bulla (Burns & Fay 1970), but generally comprises about two-thirds of the bulla in most phocids (Repenning 1972). Mustelids display an intermediate ratio, usually comprising more than one-third of the bulla (King 1983), while the entotympanic contributes little more than the formation of the carotid canal in otarioids (Repenning 1972). Among the carnivores, Wozencraft (1989) lists canids, procyonids, mustelids (excluding lutrines and mephitines), and phocids as possessing a caudal entotympanic inflated along the anteroposterior axis. Our observations agree with this distribution, although the polarity is reversed for the caniforms. Here, an inflated entotympanic is plesiomorphic, and its presence in the phocids (except for *Hydrurga* and *Monachus schauinslandi*, which independently obtain state 1) represents a reversal.

82) inflation of medial portion of caudal entotympanic: 0 = not inflated; 1 = slight / moderate inflation; 2 = inflated (Wozencraft 1989) (Fig.22).

According to Wozencraft (1989), the inflation of the medial portion of the entotympanic possesses the same distribution as the previous character: canids, procyonids, mustelids (excluding lutrines and mephitines), and phocids. However, in this case, our observations disagree slightly with those of Wozencraft (1989). Again, the polarity is reversed for the caniforms, with the inflated morphology being primitive. As well, this condition is largely retained throughout the caniforms, with only *Ursus* (state 1), the otarioids (state 0), and the monachines *Hydrurga*, *Monachus* spp., and *Ommatophoca* (states 0 or 1, or both) showing a reduction in the inflation of this portion of the entotympanic.

83) distinct sulcus dividing ectotympanic and entotympanic portions of auditory bulla: 0 = absent; 1 = present (Burns & Fay 1970) (Fig.22).

In discussing the auditory bulla of *Histriophoca*, Burns & Fay (1970) noted the presence of a distinct sulcus dividing the ectotympanic and entotympanic regions in a number of specimens. This sulcus is also very distinct in *Cystophora*, and is apparently present, although less distinct, in other phocids as well (van der Klaauw 1931). Although we observed this sulcus to varying degrees in many phocids (primarily the monachines), these seem to be the sole descriptions of this feature, except for a quick note by Howell (1928) concerning the virtual obliteration of the suture in a fetal *Phoca vitulina*. However, the apomorphic expression of a distinct sulcus is uncommon, being found only in *Martes* and the clade of *Monachus schauinslandi* and *Monachus tropicalis*. Although numerous isolated pinniped specimens possessed rudimentary sulci (coded here as a polymorphism), this morphology was only manifested at the species level for *Odobenus*, *Hydrurga*, and *Leptonychotes*.

84) relationship between auditory bulla and petrosal: 0 = does not cover petrosal; 1 = covers petrosal (King 1966; Wyss 1988a).

King (1966) initially noted the condition whereby the petrosal projects into the posterior lacerate foramen of phocines and *Monachus* spp. (also de Muizon 1982a). As this condition also obtains in *Odobenus* and certain fossil pinnipeds, Wyss (1988a) regarded this morphology as likely being primitive at some level higher than the phocids. As exposure of the petrosal is a mechanism to improve hearing underwater (Repenning 1972; de Muizon 1982a), this condition is, at best, primitive at the level of the lutrines, but more likely the pinnipeds as a whole. De Muizon & Hendey (1980) regarded the converse state (state 1) as diagnostic of the lobodontines. However, Ray (1976b) urged caution in employing both this character and related ones, as the complexity of the general region does not lend itself to being reduced to simple characters. As well, the polymorphic nature of *Leptonychotes* and *Ommatophoca* for this character, and the difficulties in distinguishing between the petrosal and mastoid in this region create additional problems (Ray 1976b).

Our analysis indicates an opposite polarity for this character to that of Wyss (1988a). Here, state 1 is primitive among the Caniformia and the derived condition is found convergently between the lutrines, all phocines, and *Monachus* spp. The occurrence of the derived condition in both *Enhydra* and *Lutra* may represent either convergent evolution

(DELTRAN optimization), or a synapomorphy necessitating a reversal to the plesiomorphic condition ancestrally for the pinnipeds (ACCTRAN optimization).

85) relationship between auditory bulla and paroccipital process: 0 = does not reach process; 1 = reaches (or very closely approaches) process (Wyss 1988a).

In acknowledgement of the limitations of the previous character mentioned by Ray (1976b), Wyss (1988a) proposed this related feature. Wyss (1988a) noted that the condition where the auditory bulla covers the petrosal is coincidental with the bulla extending posteriorly to nearly contact the exoccipital. Through our observations, we have modified this character still further, asking if the bulla contacts (or at least closely approaches) the major process of the exoccipital, the paroccipital process. Naturally, contact with the paroccipital process, or lack thereof, is tied in with inflation of the auditory bulla, particularly the posterior region (Flower 1869). Most fissipeds are noted for a relatively inflated bulla (Segall 1943; Repenning 1972; Hunt 1974), and this is sufficient in *Canis* and *Procyon* to cause contact between it and the paroccipital process (Davis 1964). This condition is also obtained in feloids (Turner 1848; Wozencraft 1989), but not in ursids, where the bulla is relatively flat (Turner 1848; Segall 1943; Davis 1964). However, contact is maintained in the ursids by a bony ridge running between the bulla and the paroccipital process (Segall 1943). In contrast, Flower (1869) holds that the paroccipital process is generally separate from the auditory bulla in most arctoids.

The plesiomorphic state for the Caniformia is inferred to be one where the auditory bulla and paroccipital process are in contact. Together with its occurrence in felids, this suggests that this state is primitive at the level of the carnivores. The derived condition, where contact is lost, describes a synapomorphy linking the lutrines with the pinnipeds. However, this distribution is contingent on our equating of the bony ridge possessed by ursids with the primitive condition, where the auditory bulla and the paroccipital process are directly in contact.

86) groove separating mastoid bulla and petrosal: 0 = absent; 1 = present (King 1972; de Muizon 1982a).

There is some uncertainty on our part as to what feature de Muizon (1982a) was attempting to diagnose with this character. The region around the posterolateral edge of the auditory bulla is punctuated by a number of grooves, pits, and foramina in phocids [see characters #87, 88, 108, and 109; Figs. 6 and 7 in de Muizon (1982a)], and de Muizon's description makes it unclear as to which exact feature he is referring. As de Muizon (1982a) describes the transition of a pit unique to *Histriophoca* and *Pagophilus* into a groove in *Cystophora*, the likely candidate is the "digastric pit" of Burns & Fay (1970: 374). However, as we were unable to find any evidence of either the pit or the groove in the above taxa, we settled instead for a definition synonymous with the stylomastoid groove of King (1972). In other words, the definition we employed is the literal one: is there a groove running between the posterolateral edge of the auditory bulla and the petrosal?

The groove, as we have defined it, is an apomorphic trait found only in *Odobenus* and all phocids. [However, this is dependent upon the assessment of state 0 by PAUP for non-lutrine fissipeds. In these taxa, the plesiomorphic contact between the auditory bulla and the paroccipital process (see previous character) made it impossible to determine the

condition of this character and they were coded as "unknown".] Although this distribution appears to support Wyss's (1987) contention of an *Odobenus*-phocid clade (also Wyss & Flynn 1993), the interpretation of this distribution here is for either parallel origins in each of the two taxa (DELTRAN optimization), or for a synapomorphy of the pinnipeds as a whole, with *Zalophus* reversing to re-obtain the primitive condition (ACCTRAN optimization).

*87) hypomastoid fossa (found along posteroventral edge of the auditory bulla and containing the stylomastoid groove): 0 = absent; 1 = present (Wozencraft 1989).

With recoding, this character was included in character #88.

88) depth of hypomastoid fossa: 0 = shallow; 1 = medium; 2 = deep; 9 = absent (Wozencraft 1989).

The presence of a hypomastoid fossa was employed by Wozencraft (1989) to unite the otarioids with the ursids. Perhaps the key to this outcome is the defining of the fossa so as to be dependent on the presence of a petromastoid ridge running between the paroccipital and mastoid processes (see character #89). However, our observations revealed that these two features are not always coincidental, with many phocids possessing an apparent hypomastoid fossa while lacking the petromastoid ridge. Thus, we modified Wozencraft's (1989) coding of the character so that the two features now appear as separate characters here (see character #89).

The presence of a hypomastoid fossa is primitive among the Caniformia; however, it is difficult to be more specific due to the high incidence of polymorphism in the basal arctoids. *Canis* is characterized by a shallow fossa, while *Procyon* and *Ursus* may share a deep fossa (ACCTRAN optimization only). The apomorphic loss of the fossa unites *Martes*, the lutrines, and the pinnipeds. Several reversals towards a redevelopment of the fossa occur in the pinnipeds, primarily among the otarioids (states 0 or 2) and the monachines. For the monachines, a shallow fossa is regained internal to *Mirounga* spp., and is increased to a deep fossa in *Monachus* spp. Only scattered phocines regain the hypomastoid fossa: *Cystophora* (states 1 and 2), *Erignathus* (states 0 and 1), and possibly *Pagophilus* and *Phoca vitulina* (both states 0 and 9)

89) distinct petromastoid ridge connecting paroccipital and mastoid processes: 0 = absent; 1 = present (Wozencraft 1989).

As mentioned above, this feature rather than the hypomastoid fossa (see character #88) was perhaps the key to Wozencraft (1989) uniting the otarioids (also Mivart 1885; Howell 1928) with the ursids (also Davis 1964). In contrast, de Muizon (1982b) (as cited in Wyss 1987) has used the reduction or outright loss of the petromastoid ridge as an apomorphic trait uniting the mustelids (exclusive of leptarctines and melines, but including lutrines) with the phocids. Wyss (1987) discounts this assessment, noting that the mastoid region in phocids is highly modified, thus rendering the comparison with the mustelid region somewhat dubious. As well, apparent petromastoid ridges have been described for *Leptonychotes*, *Monachus* spp., and *Ommatophoca* (Mivart 1885; Wyss 1987). Complicating all this is the often highly variable form of the petromastoid ridge. We observed that it rarely takes the form of a distinct ridge, but is instead usually fairly low and rounded. As well, in taxa such as *Canis* and *Procyon*, what might be called the

petromastoid ridge is, like the paroccipital processes (see character #85), pressed against the auditory bulla. For our purposes, we required the petromastoid ridge to be separate from the auditory bulla, although not necessarily a prominent, obvious structure.

Our analysis supports Wozencraft (1989), with an apomorphic petromastoid ridge occurring only in *Ursus* and the otarioids, although this is due here to parallel evolution rather than uniting the two groups as a synapomorphy. However, it should be noted that the acceptance of the analogous structure in *Canis* and *Procyon* as a proper petromastoid ridge supports a scenario in keeping with that of de Muizon (1982b), with the loss of the ridge being a synapomorphy linking the mustelines, lutrines, and the pinnipeds as a whole, with the otarioids reversing to re-obtain the plesiomorphic condition.

*90) source of "paroccipital" process: 0 = occipital; 1 = occipital and mastoid; 2 = mastoid (Burns & Fay 1970).

This character reflects the confusion created by having numerous synonyms for a given structure present in the literature. Burns & Fay (1970:375) are entirely correct in saying that the paroccipital processes of phocids should more properly be referred to as the paramastoid processes, as they are "of the occipital and near the mastoid." However, this is also true for all caniforms we have so far examined. It would appear that this process has been historically misnamed (e.g., Turner 1848; Flower 1869; Mivart 1885; Howell 1928; Davis 1964; DeBlase & Martin 1981). Perhaps the least confusing alternative would be to use the non-origin specific synonym "jugular process" (e.g., Miller 1962; Crouch 1969). However, Burns & Fay (1970) suggest that the use of this term be restricted to those instances when the paroccipital and paramastoid processes are confluent or connected by a petromastoid ridge (see character #89). Other than being an unnecessary restriction, this suggestion confuses matters further as it is unclear exactly what the term "paroccipital process" refers to in such a definition (but likely the mastoid process). An overriding complicating factor in all this is that the processes in this general region appear to be distinguished on the basis of which muscles originate from them, rather than on their specific bone of origin. As the paroccipital process serves at least as a partial origin for the digastric muscle (Howell 1928; Miller 1962; Davis 1964; Crouch 1969; Bryden 1971; King 1972), perhaps in one of the early descriptions of this muscle, its process of origin did, in fact, originate on the mastoid, but near the occipital. This character was excluded because of all of this confusion.

91) morphology of paroccipital processes: 0 = absent; 1 = elongated ridges; 2 = bumps / pillars (pers. obs.).

Flower (1869) comments that the general form of the arctoid paroccipital process is one of a roughly triangular bony prominence projecting posterolaterally from the skull which is generally separate from the auditory bulla (but see character #85). Yet, the morphology of the paroccipital process, and its relationships with other structures of the basicranial region, does appear to possess phylogenetically useful variation within the arctoids. Some of this variation is summarized in this and the following three characters.

One immediate observation of the general form of the paroccipital processes (other than simply their presence versus absence) is that they are laterally compressed in some taxa to take on the form of elongated ridges. Among the fissiped caniforms, Turner (1848)

indicates this to be the case solely for the canids. In the phocids, the general pattern is for the paroccipital processes to be poorly developed, if not virtually absent, in the phocines and well developed in the monachines. The exceptions are *Erignathus* and *Mirounga* spp., which take on the characteristics of the opposite subfamily (Bryden 1971; King 1972). The paroccipital processes of the otarioids are well developed, and are confluent with the mastoid process via the petromastoid ridge (Howell 1928; Wozencraft 1989; see character #87).

The lateral compression of the paroccipital processes is a synapomorphy linking the lutrines and the pinnipeds. Several independent reversals to the primitive caniform morphology of rounded processes occur within the pinnipeds: *Zalophus*, *Mirounga angustirostris*, and the phocines internal to *Cystophora* (with *Erignathus* reversing again to re-obtain the primitive pinniped condition). Paroccipital processes were entirely absent only for *Pusa caspica*, although *Pusa sibirica* was polymorphic for this condition.

92) size of paroccipital processes: 0 = small / not prominent; 1 = intermediate; 2 = large / prominent; 9 = processes absent (pers. obs.).

A reduction in the size of the paroccipital processes has only been indicated for the phocines (exclusive of *Erignathus*), *Mirounga* spp., and various mustelids (including the lutrines) among the caniforms (Turner 1848; Flower 1869; Bryden 1971; King 1972). The observation that the paroccipital processes are apparently lost during ontogeny in *Phoca largha* (Chapskii 1967) hints at their former presence in ancestral forms. Our observations largely bear this out. Large processes are plesiomorphic for the Caniformia, before being drastically reduced to state 0 in *Martes*, the lutrines, and the pinnipeds. The monachines, exclusive of *Mirounga* spp., are generally characterized by medium-sized processes. This occurs either as a synapomorphy of the lobodontines plus *Monachus* spp. (ACCTRAN optimization), or only of *Lobodon* plus *Monachus* spp. (DELTRAN optimization). The phocines largely retain small processes except for *Cystophora* and the clade of *Erignathus*, *Histiophoca*, and *Pagophilus*, which independently derive medium-sized processes. Reversals to large processes occurred only in *Zalophus*, *Monachus schauinslandi* plus *Monachus tropicalis*, and possibly *Hydrurga*. Again, paroccipital processes were consistently absent in *Pusa caspica*, and polymorphically so in *Pusa sibirica*.

93) relationship between paroccipital processes and mastoid bone: 0 = separate; 1 = adjacent / continuous; 9 = n/a – paroccipital processes absent (pers. obs.).

In many taxa, we noted that the paroccipital processes were not distinct, isolated structures. Other than contacting the auditory bulla (see character #85), the paroccipital processes often graded into either the mastoid bone anteriorly (more common in forms with small processes such as the Phocini), or the nuchal crest posterodorsally (see the following character). With respect to the mastoid bone, the general distribution is for it to be continuous with the paroccipital processes in *Ursus*, *Martes*, the otarioids, and the phocines internal to *Cystophora* (except *Pusa caspica* which obtains state 9). This could arise through parallel evolution in each of these taxa (DELTRAN optimization). However, the polymorphism of *Procyon* and *Lutra* also allows for the situation whereby state 1 is plesiomorphic for the arcotoids (the condition for the caniforms being equivocal), which the otarioids and phocines (minus *Cystophora*) reverse back to after state 0 arises as a synapomorphy of the lutrines plus the pinnipeds (ACCTRAN optimization).

94) relationship between paroccipital processes and nuchal (= lambdoidal) crest: 0 = separate; 1 = adjacent / continuous; 9 = n/a – paroccipital processes absent (Hendey & Repenning 1972).

Hendey & Repenning (1972) note the tendency of the nuchal crest to become confluent with the enlarged paroccipital processes in *Monachus schauinslandi* and *Monachus tropicalis*. However, at best, this apomorphic feature only arose independently as polymorphisms for *Monachus monachus* and *M. tropicalis*, although we noted it in isolated specimens of *Lobodon*, *Mirounga leonina*, and *Monachus schauinslandi*. Again, processes were consistently absent in *Pusa caspica*, and polymorphically so in *Pusa sibirica*.

95) relative size and shape of posterior lacerate foramen: 0 = not confluent with petrobasilar fissure; 1 = confluent with petrobasilar fissure; 9 = petrobasilar fissure absent (Wyss 1988a).

In most mammals, the posterior lacerate foramen is roughly circular and restricted to an area posteromedial to the auditory bulla. As well, in carnivores, the fissure between the auditory bulla and both the basioccipital and basisphenoid, the petrobasilar fissure, typically disappears during development (Wyss 1988a). However, the phocines, exclusive of *Erignathus*, are peculiar in that the posterior lacerate foramen expands anteromedially to become confluent with the patent petrobasilar fissure (King 1966; Wyss 1988a). We observed that most of the taxa examined here possess at least a crack between the basioccipital and basisphenoid bones and the bulla (see also character #96). Although not a true fissure, we have equated this crack with a reduced petrobasilar fissure. Thus, the state identified by King (1966) and Wyss (1988a) for the phocines is due to the confluence of both an expanded posterior lacerate foramen and an expanded (rather than patent) petrobasilar fissure.

This slight difference in interpretation accounts for state 1 being the most common state here, and primitive at the level of the Arctoidea (the case for the caniforms being equivocal). [The analogous state as defined by King (1966) and Wyss (1988a) was restricted to the phocines minus *Erignathus*.] The converse situation, where the posterior lacerate foramen and petrobasilar fissure are not confluent, is a synapomorphy of the monachines. State 9 was independently obtained for *Martes* and *Erignathus*, due to their parallel outright loss of the petrobasilar fissure [as described by Burns & Fay (1970) for *Erignathus*].

96) relationship between petrobasilar fissure and basioccipital-basisphenoid suture: 0 = in contact, suture unexpanded; 1 = in contact, suture greatly expanded and confluent with fissure; 9 = petrobasilar fissure absent (pers. obs.).

As in the previous character, this character attempts to summarize some of the bone loss occurring in the ventral basicranial region of phocids. In the phocines, numerous perforations are present in this region, most of which display high intraspecific variability (Burns & Fay 1970; King 1972). One of the few features that we observed consistently at the species level is of a medial expansion of the basioccipital-basisphenoid suture away from the auditory bulla. In most cases, this expanded suture was confluent with the expanded petrobasilar fissure, resulting in a great deal of bone loss in the basicranial area. As hinted at by King (1966), this apomorphic condition (state 1) is found only in *Pusa*

spp. However, acceptance of this as a synapomorphy of its members (*P. caspica* and the clade of *P. hispida* and *P. sibirica*) depends on the resolution of the polytomy in this region. Again, state 9 was independently obtained for *Martes* and *Erignathus*.

97) visibility of posterior opening of carotid canal in ventral view: 0 = not visible; 1 = visible; 9 = carotid canal absent (Wyss 1988a).

In concert with character #101, Wyss (1988a) viewed this feature as a synapomorphy of the phocines minus *Erignathus*. Wyss (1988a) tied the apomorphic conditions of both features (state 0 in both) to the characteristic inflated bulla of phocines. However, it is unclear to us why these same conditions would not also occur in most arctoids, which also generally possess inflated bullae (Segall 1943; Repenning 1972; Hunt 1974; see also characters #80-82). Our observations also revealed that the two features (i.e., characters #97 and 101) were not necessarily coincident with one another; thus, they appear separately in this analysis. As well, we were uncertain as to whether the phrase "visibility of the carotid canal" referred to the canal in general, or to the foramen of the canal. Thus, we draw a distinction between these two meanings here, and each appears as a separate character. Visibility of the carotid canal here refers to whether evidence of a carotid canal could be glimpsed in ventral view. Wyss (1988a) implies that the carotid canal is visible in most arctoid carnivores except for the clade mentioned above.

In most taxa, including virtually all phocines, a carotid canal could be ascertained in ventral view; only *Ursus*, *Martes*, *Zalophus*, and *Pusa hispida* failed to demonstrate evidence of the canal in ventral view. [As the carotid canal is diagnostic of arctoid carnivores only (Wyss 1988a), the characters dealing with this feature (#97-104) do not apply to *Canis*.] Unfortunately, the polarity of this character cannot be determined due the occurrence of both states in the basal arctoids, so Wyss's (1988a) assessment of state 0 as the apomorphic trait cannot be verified.

98) visibility of foramen of posterior opening of carotid canal in ventral view: 0 = not visible; 1 = visible; 9 = carotid canal absent (Wyss 1988a).

This variation on the previous character probably provides a more definitive test of Wyss's (1988a) original character. Any inflation of the auditory bulla will tend to overhang and thus obscure the foramen of the carotid canal. The previous character merely examined for any evidence of the carotid canal, which could be as little as a small divot in the posteroventral edge of the bulla.

Unlike the previous character, a polarity assessment is possible here and indicates that state 0 is plesiomorphic among arctoids [in contrast to Wyss (1988a)]. The apomorphic condition, whereby the foramen is visible in ventral view, is limited in distribution to *Enhydra* and *Hydrurga*, although *Procyon*, *Lutra*, *Odobenus*, and *Mirounga angustirostris* are polymorphic for this character.

99) direction of posterior opening of carotid canal, I: 0 = distinctly greater than 45° medially (i.e., roughly medially); 1 = roughly 45° medially; 2 = distinctly less than 45° medially (i.e., roughly posteriorly); 9 = absent (King 1972) (Fig.22).

The direction of the posterior opening of the carotid canal appears to be related to an interaction between the auditory bulla and both the basioccipital and basisphenoid bones. King (1972) notes that there is a tendency in monachines for the basioccipital and

basisphenoid to extend ventrally along the medial edge of the bulla, forcing the opening of the carotid canal posteriorly. In the phocines, this tendency is apparently absent and the carotid canal faces more medially (King 1972). If the lack of this tendency of the basioccipital and basisphenoid bones in the phocines is due to their uniquely expanded petrobasilar fissure (see character #95), then one might predict that the remaining caniforms will approximate the monachine condition.

Among the arctoid carnivores, the primitive condition is for a posteriorly facing carotid canal (the monachine condition) as postulated above. An apomorphic medial shift of the opening of the carotid canal is found universally in the phocines [although it may not characterize them ancestrally (DELTRAN optimization)], and convergently in *Martes* (state 0) and *Lobodon* (state 1). Most phocines (including *Erignathus*, which lacks an expanded petrobasilar fissure) display a medially directed canal. An intermediate shift (state 1) is only found convergently in *Cystophora* and the clade of *Histiophoca* plus *Pagophilus*.

*100) direction of posterior opening of carotid canal, II: 0 = roughly 90° (i.e., medially); 1 = distinctly greater than 45° medially but distinctly less than 90°; 2 = roughly 45° medially; 3 = distinctly less than 45° medially but distinctly greater than 0°; 4 = roughly 0° (i.e., posteriorly); 9 = carotid canal absent (pers. obs.) (Fig.22).

This character represents an inferior coding (with respect to character #99) of the direction of the posterior opening of the carotid canal, as it is too particular and thus limits the number of potential synapomorphies. Therefore, it was abandoned in favour of the previous character.

101) posteromedial bony shelf of auditory bulla extending from aperture of carotid canal to posterior lacerate foramen: 0 = absent; 1 = rudimentary or present; 9 = carotid canal absent (Wyss 1988a) (Fig.22).

As with character #97, Wyss (1988a) described the absence of the bony shelf in phocines, exclusive of *Erignathus* [a distribution echoed by Burns & Fay (1970)], as being an apomorphic trait attributable to the inflated auditory bulla of this group. However, if this is the case, the similar possession of an inflated bulla in most other arctoid carnivores should cause the shelf to be absent in these forms as well, rendering this feature a symplesiomorphy of the group. Our analysis indicates this to be the case, with the apomorphic possession of the shelf being limited to *Erignathus* and the clade of the lobodontines plus *Monachus* spp. Of this latter group, *Monachus monachus* re-obtains the primitive morphology. The shelf may be developing in the polymorphic *Enhydra*.

102) dorsal wall of carotid canal: 0 = open; 1 = closed; 9 = carotid canal absent (pers. obs.) (Fig.22).

Our observations of the basicranial region of the otarioids revealed a peculiar morphology involving the carotid canal and the posterior lacerate foramen. In all the phocids and most other arctoids we examined, the carotid canal is completely encircled by the caudal entotympanic of the auditory bulla, so that its opening is separate from the posterior lacerate foramen. However, in the otarioids, the dorsal wall (which is rotated more medially in *Odobenus* and the phocids *Mirounga* spp. and *Ommatophoca*) of the carotid canal is incomplete, and its foramen is confluent posterodorsally (or posteromedially for

Odobenus) with the posterior lacerate foramen. As this condition also occurs in some basal arctoids (*Martes* and *Ursus*), the primitive state for the arctoids becomes equivocal. However, all reconstructions favour independent origins of this trait between the otarioids (where it is synapomorphic), *Martes*, and *Ursus*.

103) unidentified bone encircling posterior opening of carotid canal: 0 = absent; 1 = present; 9 = carotid canal absent (pers. obs.) (Fig.22).

This character describes a feature peculiar to, and apparently universal among, *Monachus schauinslandi*. In this species, the posterior opening is at least partially encircled (but usually completely so) by a bone distinct from the remainder of the auditory bulla. The identity of this bone is uncertain. It may represent a second caudal entotympanic element, as found in, or postulated for, most of the close phocid relatives advocated here: ursids, otarioids, lutrines, and mephitine mustelids (see Hunt 1974). It has been suggested that a second element may arise during the ontogeny of the Type B bulla possessed by phocids (Wincza 1896; as cited in Hunt 1974). Or, it may merely represent an unfused portion of the single caudal entotympanic. To our knowledge, despite being apparent in some photographs of the basicranial region of *M. schauinslandi* (e.g., King and Kenyon 1961), this feature has never been described before.

104) opening of carotid canal in auditory bulla: 0 = anterior or anteroventral to posterior lacerate foramen; 1 = adjacent to posterior lacerate foramen; 9 = carotid canal absent (Wozencraft 1989).

An anterior opening of the carotid canal relative to the posterior lacerate foramen diagnoses all arctoids except ursids, which uniquely possess an adjacent placement within this group (Wozencraft 1989). This distribution was observed here; however, the basal location of *Ursus* (which possesses state 1 as an autapomorphy) within the arctoids renders the plesiomorphic state of this character equivocal for this group. As well, *Mirounga leonina* and *Ommatophoca* were polymorphic for this character.

*105) median lacerate foramen in auditory bulla: 0 = absent; 1 = present (pers. obs.).

With recoding, this character was included in character #106.

106) size of median lacerate foramen: 0 = small; 1 = medium; 2 = large; 9 = absent (pers. obs.).

The median lacerate foramen (= anterior lacerate foramen, external carotid foramen) appears to be present in most caniforms except *Ailuropoda*, which is polymorphic for this feature (Segall 1943; Story 1951; Davis 1964). Our observations indicate that its apomorphic loss (or perhaps just its lack of distinctiveness from the musculotubular canal lying immediately lateral to it) occurs in *Mirounga* spp. (see character #105). In the remaining caniforms, the foramen is of a variable size. The plesiomorphic condition is for an intermediate size (state 1), as found in *Canis* and *Ursus*, but a small foramen is quickly derived after this. DELTRAN optimization holds that this latter condition is largely retained, with independent derivations of a medium-sized (*Monachus schauinslandi*) or large foramen (otarioids, *Cystophora*, and *Ommatophoca*), and of its outright loss (*Mirounga* spp.). In contrast, ACCTTRAN optimization indicates that a large foramen is synapomorphic for the pinnipeds and retained ancestrally for each phocid subfamily.

Beyond this, independent reversals to state 0 occur within each subfamily (and twice within the monachines), with *Mirounga* spp. again uniquely deriving state 9.

107) mastoid lip in region of external cochlear foramen: 0 = absent; 1 = rudimentary or present (Wyss 1988a).

The presence of a mastoid lip that partially obscures the posterior wall of the auditory bulla and the external cochlear foramen (see the following character) has been noted as being diagnostic of the lobodontines (Repenning & Ray 1977; de Muizon & Hendey 1980; de Muizon 1982a; Wyss 1988a). However, while the mastoid lip is a derived feature, it is not unique to, or indeed universal among, the lobodontines. Instead, it appears convergently in *Leptonychotes*, *Lobodon*, and the clade of *Pusa sibirica* plus *Pusa hispida*, with polymorphic appearances in *Enhydra*, *Lutra*, *Halichoerus*, and *Pusa caspica*.

108) external cochlear foramen: 0 = open; 1 = closed; 9 = absent (de Muizon 1982a).

The external cochlear foramen, first identified and named by Burns & Fay (1970), is unique to phocids, linking the round window to the external surface of the skull to facilitate underwater hearing (Repenning 1972; de Muizon 1982a). Although Repenning (1972) states that the foramen is present in all phocids to various degrees, there is a tendency towards the closure of the foramen in each subfamily to provide the resistance to increased water pressure needed for deep diving (de Muizon 1982a). In the Monachinae, the external cochlear foramen is covered by a mastoid lip in the lobodontines (de Muizon 1982a; Wyss 1988a; but see previous character). In the Phocinae, the closure is accomplished in *Halichoerus*, *Phoca* spp., and *Pusa* spp. by an expansion of the auditory bulla (de Muizon 1982a). However, this closure is less absolute than that of the lobodontines (de Muizon 1982a), so that Burns & Fay (1970) merely note the presence of a reduced foramen in these same phocines.

The external cochlear foramen first arises as a synapomorphy of the phocids. (The assessment of it being missing in the remaining caniforms is a posteriori, as there is no objective way to distinguish between the states "absent" and "closed" based on gross examination of the skull.) The parallel trends towards the closure of the foramen in each phocid subfamily were observed, although the distributions are modified somewhat. In the monachines, it is generally closed in the lobodontines and *Monachus tropicalis*. This latter observation requires either *Monachus monachus* and *Monachus schauinslandi* to convergently re-open the foramen (DELTRAN optimization), or *Monachus tropicalis* to reverse from a state 0 synapomorphy of *Monachus* spp. (ACCTRAN optimization). In the phocines, parallel closure occurs in *Erignathus* and *Pusa sibirica*, the latter possibly as a synapomorphy with *Pusa hispida* (ACCTRAN optimization).

109) relationship between stylomastoid and auricular foramina: 0 = confluent / common; 1 = intermediate; 2 = separate; 9 = auricular foramen absent (de Muizon 1982a).

In noting the "dumbbell-shaped" morphology of the stylomastoid foramen of most phocines, Burns & Fay (1970) realized that this condition actually represents a confluence between the anterior stylomastoid foramen and the posterior auricular foramen, the latter of which is apparently unique to the phocids. These two foramina share a wide range of morphologies, from completely separate to partially confluent, as in the phocines (Burns & Fay 1970), to completely confluent as an auriculostylomastoid foramen in *Mirounga* spp.

(de Muizon 1982a). Our analysis indicates that the auricular foramen first appears ancestrally in the phocids (again, assuming that it is absent in the remaining caniforms), and is separate from the stylomastoid foramen. This condition is retained throughout both subfamilies, with their confluence into a single auriculostylomastoid foramen (state 0) arising in parallel in *Mirounga* spp. and *Pusa sibirica*. This latter observation is another a posteriori assessment, based on the assumption that these phocids still possess the auricular foramen and have not reverted to the primitive condition for the caniforms, in which it is absent.

110) relationship of tympanohyal and stylomastoid foramen: 0 = separated; 1 = closely associated (Wozencraft 1989).

This and the following character deal with the relationship of the tympanohyal to the stylomastoid foramen. As the hyoid apparatus is rarely referred to in the literature, and even more rarely preserved in museum collections (due, in part, to the tympanohyal being cartilaginous), we were forced to rely on the observations of Wozencraft (1989) for both this and the following character. Among the caniforms, a close association between the tympanohyal and the stylomastoid foramen is plesiomorphic. The apomorphic condition, where the two are separated, is a lutrine-pinniped synapomorphy, with an independent origin in the ursids. Observations by Burns & Fay (1970) may contradict this for the phocids; however, the degree of the contradiction depends on the definitions of "closely associated" versus "separated" employed by Wozencraft (1989).

111) location of tympanohyal relative to stylomastoid foramen: 0 = anterior; 1 = posterior (Wozencraft 1989).

An anterior placement of the tympanohyal relative to the stylomastoid foramen is a synapomorphy of the phocids (Wozencraft 1989). This morphology has been corroborated in the phocids by Burns & Fay (1970).

112) position of petrosal relative to intracranial ridges of basioccipital continuous anteriorly with the dorsum sellae: 0 = widely separate; 1 = intermediate; 2 = closely adjacent (Wozencraft 1989) (Fig.21).

As originally coded by Wozencraft (1989), this character dealt with the nature of the petrosal-basioccipital suture, with a note that it was usually not visible from the ventral side of the skull. A wide separation was held to define the clade of the ursids plus the otarioids (Wozencraft 1989). However, the exact nature of this character is elusive, as this character is not apparent from an examination of Wozencraft's (1989) citation for it (van der Klaauw 1931), which appears to refer to either the petrobasilar fissure (see characters #95 and 96), or something analogous to character #84. In any case, in keeping with Wozencraft's (1989) apparent intention (i.e., determining the intracranial approach of the petrosal to the basioccipital), we modified the character slightly to how it now appears above.

The condition where the petrosal and intracranial basioccipital ridges are closely adjacent is plesiomorphic among the caniforms, with any apomorphic separation of the two structures generally characterizing the pinnipeds only (*Ursus* is polymorphic between all three states). This is largely manifested by a wide separation (the ancestral pinniped

condition), with only *Pusa sibirica* obtaining an intermediate separation. Reversals to the plesiomorphic condition occur in both subfamilies: *Pagophilus* and *Phoca vitulina* among phocines, and *Hydrurga* and *Lobodon* among monachines. For the two monachines, this occurs either due to convergence (DELTRAN optimization), or as a synapomorphy followed by a reversal for the remaining, more terminal taxa (ACCTRAN optimization). Thus, with the addition of the phocids, the distribution of our coding largely matches that of Wozencraft (1989). This is due to either the two codings being synonymous (i.e., our coding matches the intent of his original definition) or correlated in some manner.

113) relative size of dorsal region of petrosal: 0 = unexpanded; 1 = intermediate; 2 = expanded (Wyss 1988a).

Several mechanisms allow for the pinnipeds to improve their underwater hearing: creating an external cochlear foramen (see characters #107 and 108), exposing the petrosal externally (see character #84), increasing the size of the promontorium, and/or generally increasing the size of the petrosal (Repenning 1972; Repenning & Ray 1977; de Muizon 1982a). This character and the following one each deal with mechanisms employed by the phocids to increase the size of the petrosal. As defined by Repenning & Ray (1977), the dorsal part of the petrosal is that region above the line extending from the vestibular aqueduct across the top of the cochlear aqueduct to the anterodorsal surface of the petrosal apex. This region is clearly expanded in virtually all known phocids (fossil and Recent), except *Monachus schauinslandi*. The largely unexpanded dorsal region in this phocid (to the exclusion of the other members of *Monachus*) has been used as evidence to support its status as the most primitive of all phocids (Repenning & Ray 1977; Wyss 1988a).

An unexpanded dorsal region of the petrosal is indeed plesiomorphic among the Caniformia. However, our observations reveal that the apomorphic, expanded morphologies (states 1 and 2) have a wider distribution than previously stated, characterizing such non-phocids as *Martes*, *Ursus*, and *Odobenus* [for *Odobenus*, at least, this morphology may be associated with a greatly expanded petrosal apex (Repenning 1975; see following character)]. All three represent convergent evolution (together with the phocids), although ACCTRAN optimization indicates that the expanded condition may be a synapomorphy of the pinnipeds, with *Zalophus* reversing to re-obtain the primitive condition. Among the phocids, an expanded dorsal petrosal is universal except for several monachines: *Ommatophoca*, *Monachus schauinslandi*, *Monachus tropicalis* (all state 0), and *Monachus monachus* (state 1). This may represent a synapomorphy of the group, with a reversal in *Lobodon* and further derivation in *Monachus monachus* (ACCTRAN optimization), or independent evolution in the various clades (DELTRAN optimization).

114) relative size and shape of petrosal apex: 0 = absent / unexpanded and pointed; 1 = intermediate; 2 = dorsoventrally thickened and bulbous (Wyss 1988a).

Overlapping the previous character somewhat, this character specifically examines the very apex of the dorsal region of the petrosal. Wyss (1988a) notes that the phocids exclusive of *Monachus* spp. are united by a massive expansion of the apex, causing it to present a dorsoventrally thickened, bulbous morphology. This morphology has been held to provide a greater sensitivity to sound underwater (Hendey & Repenning 1972), and is in contrast to the condition in most other carnivores and the otarioids, where the apex is unexpanded

and pointed. In *Monachus* spp., the petrosal apex is intermediate between these two extremes (de Muizon 1982a; Wyss 1988a). Wyss (1988a) only employed the two extreme states (homologizing the condition in *Monachus* spp. with the non-phocid condition); however, there is cause to recognize the intermediate state. Only the phocines and *Mirounga* spp. are accurately described as possessing a globular apex. In the lobodontines, the enlarged apex is more of a lower and broader structure (Hendey & Repenning 1972; Ray 1976b).

The distinction between the phocid subfamilies seems to be minimal, however. Despite claims by Repenning (1975), *Odobenus* was not held to possess an expanded apex (but was noted to have an expanded dorsal petrosal region in general; see previous character), and an expanded apex was synapomorphic for the phocids only and generally retained throughout the family. Only *Lobodon* (state 1) and *Monachus* spp. (state 0) showed predispositions towards returning to a plesiomorphic, unexpanded petrosal apex.

115) roof of internal auditory meatus: 0 = reduced; 1 = full internal auditory meatus (Wyss 1988a).

The phocids are distinguished from the remaining pinnipeds (and most other mammals) by the complete reduction of the internal auditory meatus, resulting in separate entrances for the facial and auditory nerves (Gray 1905; Wyss 1988a). Wyss (1988a) further noted that in conjunction with this reduction, the petrosal lip forming the roof of the internal auditory meatus is absent, or, in the case of *Monachus* spp., reduced to a bony spur. We have chosen to separate these two features dealing with the status of the internal auditory meatus and the condition of its former roof (see the following character), as they apparently diagnose synapomorphies of different sets of taxa. For this character, the reduction of the internal auditory meatus is indeed a synapomorphy uniting all phocids.

116) bony spur of roof of internal auditory meatus: 0 = absent; 1 = present (Wyss 1988a).

As indicated under the previous character, the reduction of the internal auditory meatus in phocids typically results in the complete loss of the petrosal lip forming its roof. However, in *Monachus* spp., a bony spur remains and projects medially above the canals of the facial and auditory nerves (Wyss 1988a). Given the typical basal placement of this genus in the phocids, Wyss (1988a) has implicated this morphology as an intermediate stage leading to the complete loss of the petrosal roof. Instead, the possession of a bony spur (or more properly, the incomplete reduction of the petrosal roof) appears to be a synapomorphy linking *Monachus schauinslandi* and *Monachus tropicalis*, although we also noted it in isolated specimens of *Halichoerus*, *Leptonychotes*, *Mirounga leonina*, *Monachus monachus*, *Pusa caspica*, and *Pusa hispida*. The plesiomorphic condition, where the spur is absent, is really a combination of two distinct morphologies. In the remaining phocids, the spur is truly absent and the petrosal lip is typically quite broad, but with virtually no medial expansion. In some taxa (e.g., *Mirounga leonina*), even the lip is lacking entirely. Meanwhile, in non-phocids, the spur is "present", but not visible, as it is subsumed within the complete petrosal roof of the internal auditory meatus.

117) inflation of bullar chamber: 0 = not inflated; 1 = inflated (Wozencraft 1989).

As implied by Repenning (1972), this character provides a truer measure of the inflation of the auditory bulla (see characters #80-82). However, as we were limited in most cases

to a gross external examination of the bulla, we have again relied upon the data in Wozencraft (1989) for this character. Numerous authors have noted the inflated bulla of caniforms (Howell 1928; Repenning 1972; Hunt 1974), and this condition is indicated here to be plesiomorphic and prevalent for the group; only the lutrines and *Zalophus* lack an inflated bullar chamber. This latter situation occurs either convergently in each species (DELTRAN optimization), or as a synapomorphy of the lutrines followed by a reversal to the primitive condition for the pinnipeds, with *Zalophus* independently obtaining state 0 (ACCTRAN optimization).

Bony tentorium and bony falx (5 characters)

Although the bony tentorium and the bony falx are found throughout the carnivores, their potential systematic value has generally been ignored. Using characters from both features, Nojima (1990) argued for a diphyletic origin of the pinnipeds, grouping the otarioids with the ursids and the phocids with the mustelids. However, the common possession of an "A Type II" bony tentorium between ursids, otarioids, and probably all mustelids, to the exclusion of all phocids except *Histiophoca* and *Pagophilus* (Nojima 1990), renders this conclusion somewhat doubtful. As well, Wyss (1987) discounts a phocid-mustelid pairing based on tentorial characters due to the high variability of the bony tentorium throughout the arctoids.

118) contribution of parietal to bony tentorium: 0 = none / processus tentoricus absent; 1 = contributes (Nojima 1990).

The bony tentorium is composed of two main elements projecting from the occipital and from the parietal (processus tentoricus) (Nojima 1990). Among the caniforms, only phocids, possibly exclusive of *Histiophoca* and *Pagophilus*, lack a processus tentoricus, and hence lack a parietal contribution to the bony tentorium (Nojima 1990). Here, the apomorphic lack of a parietal contribution to the bony tentorium is a synapomorphy of the phocids. Furthermore, this condition is universal for the group, including *Histiophoca* and *Pagophilus*.

119) contribution of parietal to bony falx: 0 = none; 1 = contributes; 9 = bony falx absent (Nojima 1990).

As with the bony tentorium, the parietal also occasionally contributes to the bony falx. Of those taxa where the bony falx is present (see character #121), Nojima (1990) indicates a parietal contribution only in the otarioids and the ursids. In phocids, the bony falx is derived exclusively from the occipital (Nojima 1990). This is largely borne out here. A parietal contribution to the bony falx is plesiomorphic in caniforms, characterizing both *Canis* and *Ursus*. Beyond this, the bony falx is initially absent before reappearing, albeit with no contribution from the parietal, as a synapomorphy linking *Lutra* with the pinnipeds. Within this group, a parietal contribution occurs independently in *Zalophus* (possibly the otarioids as a whole; ACCTRAN optimization), *Histiophoca*, and *Mirounga angustirostris* (possibly *Mirounga* spp. as a whole; ACCTRAN optimization).

120) ventral extension of bony tentorium: 0 = does not approach floor of braincase; 1 = approaches dorsal region of petrosal; 2 = approaches or contacts floor of braincase (Nojima 1990).

The morphologies of the bony tentorium and bony falx (see the following character) appear to largely depend on the parietal contribution to each (see characters #118 and 119). In those forms lacking such a contribution (i.e., the phocids generally), both structures are reduced. The bony tentorium, in particular, is reasonably compact in such cases, and fails to reach the floor of the braincase (Nojima 1990). In contrast, the bony tentorium is much expanded in those species with a processus tentoricus, frequently extending to the petrosal apex, or, more commonly, to the floor of the braincase (Wyss 1987; Nojima 1990). However, this relationship is not absolute, as canids obtain state 0 despite possessing a processus tentoricus (Nojima 1990). As well, we noted that a ventral extension to the petrosal apex was only found in the phocids, and not in any forms with a distinct processus tentoricus [although the presence of this structure in *Histriophoca* and *Pagophilus* is unclear (see Nojima 1990)].

The somewhat aberrant morphology of the canids causes the primitive state for the caniforms to be equivocal. However, as Nojima (1990) indicates that all feloids possess state 2, this state is likely plesiomorphic for the caniforms, if not the carnivores as a whole. This condition is retained throughout the caniforms, before the phocids derive state 0 ancestrally. This very much reduced bony tentorium is common to all phocids, with the phocines *Halichoerus* and *Histriophoca* (possibly as a synapomorphy with *Erignathus* and *Pagophilus*; ACCTRAN optimization) independently deriving a tentorium that approaches the petrosal apex.

121) morphology of bony falx proper: 0 = absent; 1 = sail-shaped; 2 = vertical; 3 = inverse sail (Nojima 1990; pers. obs.).

In carnivores, the bony falx is not nearly so ubiquitous as the bony tentorium, being found only in *Ursus* spp. and the pinnipeds (Nojima 1990). Despite this limited distribution, the bony falx does possess several distinct morphologies that our observations reveal are generally dependent on the contribution of the parietal (see character #119). A sail-shaped bony falx, in which the falx arcs posterodorsally from the anterior junction of the two halves of the bony tentorium, is generally restricted to the phocids, which generally lack a parietal contribution to the falx. The contribution of the parietal in the otarioids fills out the bony falx, causing it to extend directly dorsally (state 2) or to arc anterodorsally (state 3). However, these trends are again not absolute, with most phocid specimens obtaining state 2. As well, although the parietal frequently contributes to states 2 and 3, this was not necessarily always the case. In *Ursus*, the bony falx is only partial, despite a parietal contribution, and fails to reach the dorsal wall of the skull (Nojima 1990). We have chosen to distinguish this partial bony falx (see the following character) from the bony falx proper examined here. So, together with the complete lack of a bony falx in the remaining ursids (Nojima 1990), *Ursus* has been scored as lacking the bony falx.

The possession of a bony falx is a derived characteristic within the Caniformia, and is a synapomorphy of *Lutra* and the pinnipeds. For this group, a vertical bony falx is primitive and largely retained throughout. A further derivation to the reduced sail-shaped morphology occurs a number of times within the phocids: *Cystophora*, *Halichoerus*, *Monachus schauinslandi*, *Pusa caspica*, and *Pusa sibirica*. DELTRAN optimization holds these all to be independent derivations, whereas ACCTRAN optimization indicates this

state to be a synapomorphy of the phocines, before a reversal back to the vertical morphology occurs internal to *Halichoerus*. Independent origins of the sail shape in *Monachus schauinslandi* and in each of the two pusids account for the remaining appearances of this state under this latter scenario. The inverse sail morphology never appeared consistently at the species level, being observed only as a polymorphism with state 2 in *Histriophoca* and *Ommatophoca*.

122) partial bony falx: 0 = absent; 1 = present (Nojima 1990; pers. obs.).

The partial bony falx is a small projection originating from the anterodorsal junction of the two halves of the bony tentorium. Although it and the bony falx proper are apparently mutually exclusive (Nojima 1990), we have occasionally noted the simultaneous presence of these two structures. It may be that the partial bony falx indicates the former or future presence of an inverse sail-shaped bony falx, a morphology that was never consistently observed for any species (see previous character). The two structures possess similar orientations and were never observed coincidentally. In any case, we list the partial bony falx as a character separate from the morphology of the bony falx proper. As noted before, Nojima (1990) lists this feature as occurring only in *Ursus*.

Our analysis indicates that the partial bony falx is actually a primitive feature within the Caniformia. It is found in *Canis* and *Ursus* (both of which lack a bony falx proper), before becoming lost in the remaining caniforms (although *Enhydra* and *Erignathus* are polymorphic for this trait).

Dorsal braincase (4 characters)

In carnivores, this region is largely devoid of phylogenetically informative features due to it being almost completely covered by the enlarged temporalis muscle (Davis 1964). Understandably then, most of the few useful characters are associated with this muscle in some manner.

123) shape of fronto-parietal suture: 0 = flat; 1 = unilobe; 2 = bilobed; 3 = trilobed or greater (Burns & Fay 1970).

The fronto-parietal suture is often more than just a simple flat suture. In *Histriophoca* and *Pagophilus*, the suture is usually trilobed, while in *Phoca* and *Pusa* it is bilobed (Burns & Fay 1970). We also noted an additional, unilobular morphology in many species. However, this character is not as straightforward as it would first appear, as the suture rarely appears as a clear-cut example of one of the states listed above. Very often, the lobes are compacted together, and an arbitrary judgment must be made as to what constitutes a main lobe as opposed to an accessory lobe of the main one. As well, individual specimens of *Hydrurga* and *Ommatophoca* confounded this problem still further by having an open anterior fontanelle, something that is apparently quite common in adult *Ommatophoca* (King 1969, 1972, 1983; Ray 1976b). The systematic value of this character is limited still further by the high amount of intraspecific polymorphism.

Despite these numerous problems, a reasonably clear pattern emerged from this character. A flat suture is plesiomorphic, with a unilobular suture diagnosing the mustelids (including the lutrines) plus the pinnipeds. *Zalophus* reverses to the plesiomorphic condition. A multilobed suture is peculiar to the phocids, which are united ancestrally and generally

throughout by a bilobed morphology (albeit polymorphically with states 0 and/or 1 in many species). A unilobular suture is independently regained in *Pusa hispida* (possibly as a synapomorphy with *Pusa sibirica*; ACCTRAN optimization) and the clade of *Monachus schauinslandi* plus *Monachus tropicalis*. The trilobed condition occurs uniquely for the clade of *Histiophoca* plus *Pagophilus*.

*124) separate temporal ridges: 0 = widely spaced; 1 = approximately in midline; 9 = absent (pers. obs.).

During our observations, we noted that in place of a sagittal crest, many specimens possessed distinct paired ridges on either side of the midline. However, this character more properly belongs with characters of the sagittal crest, as separate temporal ridges merely represent incipient crests (Doutt 1942; King 1972). As well, the distance between the ridges appears to be an age-dependent feature (and therefore of questionable systematic value), with the ridges converging on the dorsal midline with increasing age (Doutt 1942). Thus, with recoding, this character was included in character #126.

*125) sagittal crest: 0 = absent; 1 = present (Ridgway 1972).

With recoding, this character was included in character #126.

126) size of sagittal crest: 0 = absent, but separate temporal ridges present; 1 = small; 2 = medium; 3 = large; 9 = absent (Ridgway 1972; pers. obs.).

The sagittal crest is a notoriously labile feature, being subject to both age variation and sexual dimorphism. We tried to minimize the latter problem by scoring a species as possessing a sagittal crest if a crest was consistently present in either sex. The development of sagittal crests in very old individuals from the convergence of the separate temporal ridges has been noted by both Doutt (1942) and King (1972). This potential problem was minimized by examining only adult individuals.

Although reasonably common throughout most of the Carnivora, there are conflicting reports of the manifestation of sagittal crests among the phocids. Ridgway (1972) only mentions distinct crests for *Hydrurga* and *Leptonychotes*, to which Ray (1976b) would apparently add *Mirounga* spp. and *Phoca vitulina* (also Chapskii 1955a). However, de Muizon & Hendeby (1980) indicate reduced crests in *Leptonychotes* and *Lobodon*. King (1972) claims crests of various sizes (but typically small) for all phocids except the three smallest genera (*Histiophoca*, *Pagophilus*, and *Pusa*) which possess widely spaced temporal ridges. *Halichoerus* apparently develops a strong crest with old age (Chapskii 1955a), as does *Monachus tropicalis* (Allen 1887).

This study indicates that sagittal crests are possessed primitively within the Caniformia, before being reduced to separate temporal ridges in going to the pinnipeds. *Canis* is unusual in possessing a large sagittal crest (only found elsewhere in *Zalophus*), with the sagittal crests typically being small in fissiped caniforms. Separate temporal ridges arise as a synapomorphy of the pinnipeds (and possibly *Lutra* as well; ACCTRAN optimization), with a convergent appearance in *Procyon*. Within the phocids, the trend is towards the loss of even this feature. This is limited in the phocines (*Erignathus* and *Pusa sibirica* only), but more widespread in the monachines, diagnosing *Mirounga angustirostris* and the clade of *Lobodon*, *Monachus* spp., and *Ommatophoca*. However, small sagittal crests

are regained in *Monachus monachus*, and as a synapomorphy of *Hydrurga* and *Leptonychotes*, before both the sagittal crests and temporal ridges are lost outright. *Halichoerus* and *Monachus tropicalis* also possessed sagittal crests, albeit as a polymorphism with other states.

Teeth (23 characters)

Despite the great importance attached to teeth by mammalian systematists, they are only infrequently used as a systematic tool within the phocids. Much of this arises from the trend toward homodonty in the pinnipeds, which largely eliminates many potential morphological characters, combined with a high intraspecific variability in the phocids at least (King 1966, 1983; Hillson 1986). Indeed, many studies tend to concentrate on attributes of the dentition as a whole (e.g., tooth formulae), rather than on the morphology of individual teeth (e.g., Burns & Fay 1970; de Muizon 1982a). Additionally, as Chapskii (1955a) has noted for the phocines, the systematic value of phocid teeth may be limited by the high functional demand placed upon them by food specialization within the group and the resultant rapid evolution arising from this (also Davies 1958b). However, teeth characteristics have played a major role in Chapskii's (1955a, 1967) attempts to sort out phocine phylogeny.

127) number of upper incisors in one-half of jaw: 0 = zero; 1 = one; 2 = two; 3 = three (King 1966).

Other than the possession of an inflatable nasal apparatus, the incisor formula was a key character used to support the Cystophorinae, with both *Cystophora* and *Mirounga* possessing a 2/1 pattern, as opposed to the 3/2 pattern of phocines or the 2/2 pattern of monachines (Scheffer 1958; King 1964, 1966; Ridgway 1972). However, beyond the convergent *Cystophora* and *Mirounga* (see King 1966), the incisor formula seems to describe synapomorphies of both phocid subfamilies, although the phocines may retain the ancestral phocid number (McLaren 1975). In an effort to generate synapomorphies with some of the outgroup taxa (which are generally 3/3), we have split the incisor formula into two characters, corresponding to the number of upper and lower incisors respectively.

Only *Odobenus*, *Cystophora*, and the monachines diverge from the plesiomorphic condition of three upper incisors. *Odobenus* uniquely derives one upper incisor (Mivart 1885; Cobb 1933), although it is commonly misidentified as a postcanine due to its position and the unusual pattern of dental succession in this animal (King 1983; see Cobb 1933). The condition of two upper incisors in *Cystophora* and the monachines represents either a case of convergence (DELTRAN optimization), or a synapomorphy of the phocids, with the remaining phocines reversing to re-obtain the primitive condition (ACCTRAN optimization).

128) number of lower incisors in one-half of jaw: 0 = zero; 1 = one; 2 = two; 3 = three (King 1966).

As with the upper incisors (see previous character), three lower incisors are plesiomorphic for the caniforms. However, the reduction to two incisors now occurs either as a synapomorphy of the lutrines plus the pinnipeds, with a reversal to the plesiomorphic

condition in *Lutra* (ACCTAN optimization), or as a synapomorphy of the pinnipeds, with a parallel appearance in *Enhydra* (DELTRAN optimization). Two lower incisors are largely retained throughout the pinnipeds, with further reductions occurring only in *Cystophora*, *Mirounga* spp., and possibly *Leptonychotes* (all convergent origins of state 1), and *Odobenus* (state 0).

*129) morphology of incisors: 0 = peg-like; 1 = unicusate; 2 = caniform; 3 = complex (pers. obs.).

This character was abandoned after numerous unsuccessful attempts to accurately summarize incisor shape in phocids. Any differences between the given states are highly subjective and, as implied by characters #131 and 132, overall incisor morphology is not constant within the series of a given species, causing additional coding difficulties.

130) shape of upper incisors in cross-section: 0 = round; 1 = intermediate; 2 = (strongly) laterally compressed (Wyss 1988a).

Among phocids, the phocines (excluding *Erignathus*) are distinguished by the lateral compression of their upper incisors (Burns & Fay 1970; Wyss 1988a). However, with the additional observations of rounded incisors in the monachines and strongly compressed incisors in the non-phocid carnivores, Wyss (1988a) interpreted the rounded condition as a synapomorphy of the phocids, with the phocines, exclusive of *Erignathus*, reversing to the primitive compressed morphology. *Histiophoca* may be polymorphic for this character (Burns & Fay 1970; but see Scheffer 1960).

Although the above distribution is largely supported for the pinnipeds, only *Martes* and *Enhydra* were observed to possess strongly compressed incisors among the fissipeds. In contrast to Wyss (1988a), this renders rounded incisors as plesiomorphic for the caniforms, and also makes the ancestral state for the phocids equivocal. Under DELTRAN optimization, the primitive rounded incisors are retained through to the phocids, with the laterally compressed incisors typical of the phocines becoming a synapomorphy of most of this group. Meanwhile, ACCTAN optimization holds for sequential reversals between states 0 and 2, so that laterally compressed incisors become ancestral for the phocids, and the trend to rounded incisors describes a synapomorphy of most of the monachines. Other than *Erignathus*, only *Cystophora* (states 0, 1, and 2) and *Phoca vitulina* (state 1) depart from the typical phocine pattern. Among the monachines, truly rounded incisors are only typical of *Lobodon*, *Mirounga* spp. and *Monachus* spp. The remaining taxa possess either state 1 (*Leptonychotes* and *Ommatophoca*) or state 2 (*Hydrurga*).

131) relative size of upper incisors: 0 = outermost incisor about equal in size to remaining incisor(s); 1 = outermost incisor of much greater size than remaining incisor(s); 9 = n/a – only one upper incisor present per quadrant (de Muizon & Hendeby 1980).

In the phocids, the outermost upper incisor is typically larger than the remaining one (King 1983). This is especially true of the lobodontines, where this enlarged tooth, together with the upper canine, aids in opening breathing holes in the sea ice (de Muizon & Hendeby 1980). The lack of an enlarged outermost upper incisor in the fossil lobodontine *Homiphoca* led de Muizon & Hendeby (1980) to postulate this condition as primitive for the monachines. However, our observations indicate that this morphology (i.e., state 0) is

actually apomorphic, and is found in only *Procyon* and *Pagophilus* among extant caniforms. With its single upper incisor, *Odobenus* uniquely obtained state 9.

132) relative size of lower incisors: 0 = outermost incisor about equal in size to remaining incisor(s); 1 = outermost incisor of much greater size than remaining incisor(s); 9 = n/a – one or fewer lower incisors present per quadrant (Scheffer 1960).

In contrast to the previous character, the condition whereby the lower incisors are all of about equal size possesses a much wider distribution and is, in fact, plesiomorphic for the caniforms. State 9 tends to be indicated as a synapomorphy of the pinnipeds due to its presence in *Odobenus*, *Cystophora*, and *Mirounga* spp. However, this is likely due to convergent evolution between the three taxa, as was indicated for the lower incisor formula (see character #128) upon which this character is indirectly based. Instead, in noting that most phocids obtain a larger outermost incisor [as noted in *Histriophoca* by Scheffer (1960) and *Homiphoca* by de Muizon & Hendey (1980)], we propose this state as a synapomorphy of the pinnipeds, with *Zalophus* reversing to the primitive caniform condition. Among phocids, only *Lobodon* and *Pusa sibirica* (possibly as a synapomorphy with *Pusa hispida*; ACCTRAN optimization) likewise reverse to state 0.

133) displacement of incisors (upper or lower): 0 = absent – all in line with one another; 1 = present – incisor series slanted; 9 = n/a – incisors absent or singular (Allen 1887; Hendey & Repenning 1972).

Typically, the incisors are positioned in line with the remaining teeth along the curvilinear tooth row. Presumably, this configuration aids in the efficient dissipation of biting forces. However, a slight posterior displacement of the lower medial incisor relative to the incisor row has been noted in most phocids, including the fossil lobodontine *Homiphoca* (Allen 1887; Hendey & Repenning 1972). Often, this displacement only applies to the roots, with the medial incisors tending to be oriented more horizontally so that their crowns line up with those of the other incisors (Allen 1887). We additionally noted that the equivalent condition can occur in the upper incisors as well, albeit extremely rarely. Although this apomorphic displacement of the incisors is present in individual specimens of most phocid species, it only manifests itself at the species level for a non-phocid, *Lutra*. However, together with *Enhydra*, both *Monachus monachus* and *Monachus schauinslandi* are polymorphic for this trait. This character was inapplicable for *Odobenus* only.

134) procumbency of incisors (upper or lower): 0 = absent; 1 = present; 9 = n/a – upper or lower incisors absent (de Muizon & Hendey 1980).

Several phocid taxa possess the morphology whereby the upper (and less frequently the lower) incisors are angled anteriorly (i.e., are procumbent). This feature is apomorphic and is associated with three of the four lobodontines – *Leptonychotes*, *Lobodon*, and *Ommatophoca* (de Muizon & Hendey 1980) – a distribution supported here. This represents a synapomorphy of these taxa together with *Monachus* spp., which reverts to the primitive condition.

In *Leptonychotes*, this feature together with the large caniform morphology of the incisors (see character #131) and canines function as an ice ream to keep breathing holes open in the winter (Bertram 1940; King 1972; de Muizon & Hendey 1980; Kooyman 1981c). The procumbent incisors of *Lobodon* and *Ommatophoca* are more likely associated with

feeding, as neither taxon is known to actively maintain breathing holes (Bertram 1940).

135) number of upper postcanines: 0 = three; 1 = four; 2 = five; 3 = six (pers. obs.).

The trend to homodonty in the cheek teeth (with the concomitant loss of the carnassial set) of the pinnipeds makes distinguishing within and between the premolars and molars difficult, if not functionally unnecessary. Thus, the cheek teeth are usually collectively referred to as the postcanines. However, differentiating between the postcanines is possible, as four premolars and one molar per quadrant (for a total of five postcanines) have been noted for most phocines, as well as for the monachines *Homiphoca*, *Leptonychotes*, and *Mirounga leonina* (Chapksii 1955a; de Muizon & Hendeby 1980; Burns 1981; Ling & Bryden 1981; Stewart & Stewart 1987). This condition is likely constant (and ancestral) throughout the phocids at least, although Bertram (1940) indicates that the pattern in *Leptonychotes* and *Lobodon* may be one of three premolars and two molars per quadrant. Despite the ease of differentiating between the cheek teeth in fissiped caniforms, we likewise refer to them collectively as postcanines in an effort to identify synapomorphies with the pinnipeds.

The most common condition in the caniforms is for five upper postcanines. *Canis* and *Procyon* obtain state 3, which may be symplesiomorphic (DELTRAN optimization), or independently obtained from an equivocal root for the caniforms (ACCTAN optimization). *Odobenus* and *Enhydra* are autapomorphic for states 0 and 1 respectively. As noted by King (1983), *Zalophus* is polymorphic between states 2 and 3, a condition which is reflective of the otariids when viewed at the family level (King 1983). A sixth upper postcanine (which was interpreted as M²) occurs frequently in *Halichoerus* (Burns & Fay 1970), but this was not supported here.

136) number of lower postcanines: 0 = three; 1 = four; 2 = five; 3 = six; 4 = seven (pers. obs.).

As with the upper postcanines, the assessment of the plesiomorphic condition is again equivocal, being either six (*Martes*, *Procyon*, and possibly *Ursus*) or seven (*Canis* only) postcanines. However, the lutrines plus the pinnipeds are united by a synapomorphic reduction to five postcanines, with *Odobenus* uniquely reducing this further to three postcanines. Four postcanines were never consistently obtained at the species level.

137) morphology of postcanines: 0 = peg-like / unicusate; 1 = triconodont; 2 = multicusate (de Muizon & Hendeby 1980).

The wide variety of postcanine morphologies occurring within the phocids ranges from the heavy, robust postcanines of *Monachus* spp. to the weak, often loosely rooted, ones of *Erignathus* and *Ommatophoca* (King 1983). *Lobodon* is frequently noted for its intricate, sieve-like multicusate postcanines which are used to strain euphausiid shrimp (Bertram 1940; Kooyman 1981a). Yet, despite this range, the postcanines of most phocids can be traced to one form, that of the triconodont morphology, which is typified by a major middle cusp with smaller to subequal cusps flanking it anteriorly and posteriorly. This form is typical of the phocines (Ridgway 1972) and is postulated to be primitive for the phocids, being found in such putative ancestors as *Paragale* and *Potamotherium* (Hendeby & Repenning 1972; de Muizon & Hendeby 1980). The extant phocids are characterized by the modification of this basic triconodont form, either through the loss

of one or both of the accessory cusps, the formation of additional accessory cusps (typically posteriorly), or both (Doutt 1942; Ridgway 1972; de Muizon & Hendey 1972; see characters #138 and 139). In *Erignathus*, the diagnostic tooth wear is so extreme as to frequently obliterate the triconodont morphology of the postcanines (Chapksii 1955a; Burns 1981; King 1983). All these variations on the triconodont theme were still classified as triconodont, so long as such an origin could be reasonably established.

The plesiomorphic condition of multicuspsate postcanines was found in all fissiped outgroups. This is reduced in the pinnipeds, but the ancestral form is equivocal between states 0 and 1. The otarioids largely obtain peg-like or unicuspsate postcanines, although *Zalophus* is polymorphic between states 0 and 1. This latter observation accords with the assessment that accessory cusps represent a derived feature in the otariids (Repenning & Tedford 1977). Most phocids display triconodont postcanines, which develop either ancestrally for the family as a whole (ACCTTRAN optimization), or convergently in each subfamily, with the phocids primitively retaining the equivocal pinniped ancestral state (DELTRAN optimization). Only *Lobodon* (state 2) and *Mirounga leonina* (state 0, possibly as a synapomorphy of *Mirounga* spp.; ACCTTRAN optimization) fail to exhibit triconodont postcanines. The unicuspsate teeth of *M. leonina* appear to develop from the fusion of the individual cusps of a triconodont precursor (pers. obs.).

138) tendency to form additional cusps in triconodont postcanines: 0 = absent; 1 = present; 9 = n/a – postcanines not triconodont (Chapksii 1955a).

As mentioned above, the triconodont morphology tends to show a high degree of variation from the basic (idealized) pattern. In most cases, the exact morphology of the postcanines is associated with prey type (Chapksii 1955a; Davies 1958b). This and the following two characters attempt to diagnose any systematic trends in this variation. The tendency to form additional accessory cusps in triconodont teeth is primarily manifested in the addition of small fourth cusp (and, occasionally, a very small fifth cusp) posteriorly, although an additional anterior cusp is possible. This multicuspsate condition has been implicated in the retention of actively moving prey items (Chapksii 1955a). Additional accessory cusps have been variously noted for most of *Histiophoca*, *Pagophilus*, *Phoca* spp., and *Pusa* spp. (Doutt 1942; Chapksii 1955a). Chapksii (1955a) indicates that an additional cusp may also be formed, albeit very rarely, in *Erignathus*.

This character applies only to three distantly related clades within the phocids: the phocines (with and without the polymorphic *Cystophora*), *Hydrurga*, and *Monachus* spp. [Together with similar distributions in the following two characters, this could be interpreted to support independent origins of the triconodont morphology in each phocid subfamily (see previous character). As well, the indication that the plesiomorphic state 9 is ancestral for the polymorphic *Zalophus* hints at a convergent origin for triconodont postcanines in otariids (also Repenning & Tedford 1977).] The distribution of this character is complicated and shows no clear pattern under either optimization criterion. However, the tendency to gain additional accessory cusps was consistently present in two main groups: *Monachus schauinslandi* (possibly together with *Monachus tropicalis*; ACCTTRAN optimization), and *Phoca* spp. plus *Pusa* spp. Likewise, the lack of the tendency was found in three clades: *Monachus monachus*, *Halichoerus*, and *Erignathus* plus *Histiophoca* plus *Pagophilus*.

139) tendency to lose accessory cusps in triconodont postcanines: 0 = absent; 1 = present; 9 = n/a – postcanines not triconodont (Chapaskii 1955a).

The other variant on the triconodont morphology is to lose some or all of the accessory cusps, a tendency associated with a change in diet to softer foods (Chapaskii 1955a). Occasionally, this loss is so extreme that the tooth appears to be unicusate, as in *Halichoerus* or *Leptonychotes* (Mivart 1885; Chapaskii 1955a; Ridgway 1972). Other taxa noted for the loss of the accessory cusps include *Phoca* spp. (Ridgway 1972) and, to varying degrees of severity, *Histiophoca* (Chapaskii 1955a; Scheffer 1960). State 9 is plesiomorphic for this character. The trend toward losing the accessory cusps is a synapomorphy of the phocines (with and without *Cystophora*), and virtually universal, missing only in *Pusa sibirica* (possibly as a synapomorphy with *Pusa hispida*; ACCTRAN optimization). In those monachines where this character is applicable, the tendency appears only in *Monachus monachus*, and is lacking in *Hydrurga* and *Monachus schauinslandi* (possibly as a synapomorphy with *Monachus tropicalis*; ACCTRAN optimization).

140) size of accessory cusps in triconodont or multicusate postcanines: 0 = small, continuous with major cusp; 1 = larger, distinct from major cusp; 9 = n/a – postcanines not triconodont or multicusate (de Muizon 1982a; pers. obs.).

Triconodont postcanines may occur convergently in both the phocines and monachines (see character #137). This is somewhat corroborated by the different morphologies of the accessory cusps in applicable phocines (state 0), and in *Hydrurga* and *Lobodon* among the monachines (state 1) (de Muizon 1982a). A *Hydrurga-Lobodon* pairing among lobodontines has frequently been advocated on the basis of their distinctive postcanine morphology (Hendey 1972; de Muizon & Hendey 1980; de Muizon 1982a; King 1983). We have limited the distribution of this character to the pinnipeds (automatically rendering state 9 as plesiomorphic), and to those pinnipeds with triconodont or multicusate teeth in particular. Apomorphic, small accessory cusps are universal among the phocines, with and without *Cystophora*. Both apomorphic states are found in the monachines: state 0 for *Monachus* spp. at least, possibly as a synapomorphy of the clade *Lobodon*, *Monachus* spp., plus *Ommatophoca* (ACCTRAN optimization); and state 1 for *Hydrurga* and *Lobodon* only. The convergent possession of state 1 in the latter two taxa speaks against their previous pairing within the lobodontines.

141) relative size of upper postcanines: 0 = all subequal; 1 = #1 (PM¹) noticeably smaller than rest, which are subequal; 2 = #5 (M¹) noticeably smaller than rest, which are subequal; 3 = #1 and #5 noticeably smaller than rest, which are subequal; 4 = #1 and/or #5 noticeably larger than rest, which are subequal; 9 = n/a – postcanine homology uncertain (Allen 1887; Scheffer 1960; de Muizon & Hendey 1980).

The relative sizes of both the upper and lower postcanines appear to contain a good deal of potential systematic information. Unfortunately, any such value is tempered by the problematic nature of both characters. In attempting to summarize the vast amount of variation present throughout the phocids, we concentrated on the first and last postcanine, which appeared to present the clearest and most consistent trends throughout the family (see also Allen 1887; Scheffer 1960). In particular, McLaren (1960a) apparently holds a small last molar to be diagnostic of *Pusa* spp.; however, this reduction of M¹ may be a

trend for all phocids except *Hydrurga* and *Lobodon* (de Muizon & Hendey 1980). Unfortunately, a coding based on the first and last postcanines is limited to the phocids only, due to the generally different homology between the postcanines of the phocids and the outgroups (very few of which possess a 4/1 postcanine formula). Thus, the inapplicability of this and the following character for the outgroups (including the otarioids, in order to avoid biasing the results in favour of a monophyletic Pinnipedia) results in their polarities being determined to some degree by the outgroup relations entailed by the remaining characters.

The primitive condition in phocids is for all upper postcanines to be subequal in size, a state maintained ancestrally in each subfamily. The phocines internal to *Cystophora* are largely characterized by a reduction of the first postcanine only; only *Histiophoca* (state 0) and *Pusa sibirica* (state 3) deviate from this. Among monachines, there exists a tendency to decrease both the first and last postcanines in those taxa internal to *Hydrurga* [as described for *Monachus tropicalis* by Allen (1887)]. *Ommatophoca*, and possibly *Monachus monachus*, retain primitive subequal postcanines. *Mirounga* spp. is uniquely diagnosed by state 4, with the last postcanine typically being the enlarged tooth. A reduction of only the last postcanine was never consistently present at the species level.

142) relative size of lower postcanines: 0 = all subequal; 1 = #1 (PM₁) noticeably smaller than rest, which are subequal; 2 = #5 (M₁) noticeably smaller than rest, which are subequal; 3 = #1 and #5 noticeably smaller than rest, which are subequal; 4 = #1 and/or #5 noticeably larger than rest, which are subequal; 9 = n/a – postcanine homology uncertain (Allen 1887; Scheffer 1960).

This character presents much the same distribution as the previous one [and as indicated by Allen (1887) and Scheffer (1960) for *Monachus tropicalis* and *Histiophoca* respectively]. As with the upper postcanines, subequal lower postcanines represent the ancestral state for the phocids and both subfamilies. The phocines, excluding *Cystophora*, now universally share a reduced first postcanine, as does the clade of *Lobodon* plus *Monachus* spp. among monachines. The reduction of both the first and last postcanines is here limited to *Leptonychotes*, *Mirounga angustirostris* (possibly as a synapomorphy of *Mirounga* spp.; ACCTRAN optimization) and *Monachus tropicalis*. States 2 and 4 never appeared consistently at the species level.

143) tendency to single-rooting of upper postcanines: 0 = absent; 1 = present (de Muizon 1982a).

A tendency towards having single-rooted postcanines was noted exclusively among phocids for *Halichoerus* by de Muizon (1982a). This tendency is also strongly present, and apparently developing, in otariids (Mivart 1885; King 1983). However, this character might have a larger distribution contingent on the definition of the term “tendency”. In phocids, upper postcanine #1 is invariably single-rooted, #5 double-rooted, and #2 to #4 often transitional and variable, a pattern observed in *Histiophoca* by Scheffer (1960). When postcanine #5 is single-rooted, this is more often due to its reduced size (see characters #141 and 142), than to any trend towards single-rootedness of the postcanines. Therefore, if a true tendency to single-rootedness is present, it should affect the inner postcanines, and will be scored as being present if one or more of these postcanines is consistently single-rooted within a species.

The tendency to single-rootedness of the upper postcanines is an apomorphic condition uniting the pinnipeds ancestrally, with a parallel appearance in *Ursus*. This contrasts with the opinion that the otariids possess double-rooted postcanines (except for the first) ancestrally (Repenning & Tedford 1977). However, the single-rooted morphology is only retained in the otarioids, *Cystophora*, *Halichoerus*, and *Mirounga* spp., before reversals to the plesiomorphic morphology occur in each phocid subfamily. The case in which all the upper postcanines were single-rooted was slightly rarer, occurring only among *Zalophus* [although M¹ is double-rooted in a number of other otariids (Repenning & Tedford 1977; King 1983)] and *Mirounga* spp.

144) tendency to single-rooting of lower postcanines: 0 = absent; 1 = present (de Muizon 1982a).

Under ACCTRAN optimization, the distribution of the tendency to single-rooting of the lower postcanines is identical to that of the upper postcanines. However, the polymorphic nature of *Cystophora* leads to another possibility, that of convergent evolution in the otarioids [thereby possibly rescuing Repenning & Tedford's (1977) hypothesis of double-rooted postcanines ancestrally in the otariids], *Halichoerus*, and *Mirounga* spp. (DELTRAN optimization). Again, single-rooting of all lower postcanines was limited to *Zalophus* and *Mirounga* spp.

145) relative size of gap between upper postcanines 4 and 5: 0 = smaller than other gaps; 1 = subequal to other gaps; 2 = larger than other gaps; 9 = n/a – postcanine homology uncertain (Ridgway 1972; pers. obs.).

Ridgway (1972) used the relative size of the gaps between the postcanines (less than versus equal to a tooth width) as a means of distinguishing between the genera *Erignathus* and *Halichoerus*. However, during our observations, we noted that the gaps between the postcanines of a given individual were not of a consistent size. Typically, it was the gap between the last two postcanines that was the discrepant one, and the character was recoded to reflect this observation. A relatively large such gap was noted for *Histriophoca* by Scheffer (1960), and for *Homiphoca* and *Leptonychotes* by de Muizon & Hendeby (1980).

Again, this character was only applied to the phocids due to the difficulties of establishing postcanine homologies between the phocids and the putative outgroups. Primitively, the phocids possess subequal gaps among all the postcanines (state 1). The phocines internal to *Cystophora* largely derive a relatively enlarged gap, with only *Pagophilus* and *Pusa hispida* re-obtaining subequal gaps. Virtually all monachines retain the primitive phocid morphology, with only *Leptonychotes* paralleling the phocine condition.

146) crowding of postcanines (upper and/or lower): 0 = not touching / overlapping; 1 = touching or overlapping (Ridgway 1972).

This character is to some degree an age-dependent one. In phocids, the deciduous dentition is shed or resorbed around the time of birth (Allen 1887; Bertram 1940; Ling & Bryden 1981; King 1983; Stewart & Stewart 1987), causing the adult teeth to initially be crowded and overlapping in the smaller juvenile skull (Doutt 1942; Chapskii 1967). [In most other mammals, such crowding is avoided by having a reduced deciduous dentition associated with the shorter rostrum of immature individuals (Hillson 1986).] As the animal reaches

maturity, the skull grows, allowing the postcanines more room (Doutt 1942), as was clearly demonstrated in an age series of *Phoca largha* (Chapksii 1967).

This character may also be susceptible to the potential case of pedomorphosis in the phocids, and especially in the phocines (see King 1972; Wyss 1994). As it applies to this character, two main skull types have been observed to exist. The skulls of the smaller phocids have been described as possessing a more "juvenile" appearance due to their relatively large crania and relatively small rostra (King 1972). With their smaller rostra, these "juvenile" skulls may demonstrate a higher incidence of postcanine crowding. Conversely, the skulls of the larger phocids present a more "adult" appearance, with relatively smaller crania and longer rostra (King 1972). This skull type might therefore be expected to lack crowding of the postcanines.

Finally, this character has been noted to be sexually dimorphic in *Phoca vitulina* (Allen 1902), but not *Phoca largha* (Chapksii 1967), two otherwise closely related species. Despite these problems, the crowding of the postcanines has been used by Ridgway (1972) to distinguish between the genera *Phoca* (state 1) and *Pusa* (state 0).

As evidenced by the fissipeds observed in this study, the Caniformia are primitively characterized by having the postcanines in contact with one another (but typically merely touching and not overlapping). The converse condition is proposed as a synapomorphy of the Pinnipedia, with reversals in *Monachus monachus*, *M. schauinslandi* (a possible synapomorphy of *Monachus* spp.; ACCTRAN optimization), and *Phoca vitulina*, all of which possess the juvenile skull type. However, numerous other phocines (most notably *Pusa* spp.) with the same skull type do not demonstrate this trait, placing the correlation between skull type and postcanine crowding in some doubt. Bearing this in mind, the observation that the postcanines are not in contact in the phocids primitively may contradict King's (1972) hypothesis that the ancestral phocids possessed a juvenile skull type, while supporting Wyss's (1994) interpretation of it being a secondary derivation.

147) obliqueness of postcanine implantation relative to long axis of tooth row (upper and lower): 0 = straight; 1 = anterior / posterior end of postcanine directed laterally (de Muizon 1982a).

This character is related in many ways to the previous one. In young animals, or those with a juvenile skull type, the relatively short tooth row will crowd the postcanines and push them out of line. With an increase in age (or a change to the adult skull type), the postcanines should fall back into line in the relatively longer tooth row (Doutt 1942; de Muizon 1982a). Apart from those species listed under the previous character, de Muizon (1982a) claimed a tendency towards oblique implantation of the postcanines as a synapomorphy of *Monachus* spp. (but relatively greater in *M. monachus* than in either *M. schauinslandi* or *M. tropicalis*) due to the relative shortness of their tooth rows. King (1972) noted an oblique orientation of the lower teeth of *M. monachus* in particular. This condition may also characterize other phocids with a juvenile skull type. In particular, Chapksii (1955a) comments that *Phoca* spp. is often noted for the obliqueness of its postcanines.

The apomorphic condition, in which the postcanines are obliquely implanted, displays a virtually identical distribution as the previous character: *Monachus* spp. (but including *M.*

tropicalis), *Phoca vitulina*, and possibly *Leptonychotes*. Again, the absence of this trait in other species with a juvenile skull type further weakens any supposed correlation between skull type and postcanine crowding.

148) obliqueness of postcanine implantation (upper and lower) relative to vertical: 0 = straight; 1 = slanted (de Muizon 1982a; pers. obs.).

In addition to angling away from the axis of the tooth row, as in the previous character, the postcanines are also occasionally slanted, typically along the lingual-labial axis. Chapskii (1955a) states that this is virtually universal in *Phoca vitulina*. This condition is likely not associated with postcanine crowding and may, in fact, be enhanced when the postcanines are widely separate, due to their reduced association with each other. However, this apomorphic condition is restricted in distribution to convergent appearances in *Lobodon* (lower postcanines #1 and #2 slanted lingually) and *Mirounga angustirostris* (various postcanines, usually slanted labially).

149) curvature of upper tooth row (postcanines only): 0 = sigmoidal; 1 = arched; 2 = straight; 3 = kinked between PC^{1,2}, otherwise straight; 4 = reverse arch (Ridgway 1972).

A character dealing with the curvature of the upper tooth row was used by Ridgway (1972) to distinguish between the genera *Histiophoca* and *Pagophilus*. *Histiophoca* is often noted for its strongly curved upper tooth row (Scheffer 1958; Burns & Fay 1970), which occasionally approaches a lyrate (= sigmoidal) morphology (Burns & Fay 1970). However, Burns & Fay (1970) do caution that this extreme curvature is not consistent within *Histiophoca*, and that it also occurs within other members of the Phocini, albeit to a lesser extent. Howell (1928) describes an apparently straight tooth row in *Zalophus*.

Our observations revealed that a presence versus absence coding of upper tooth row curvature is too simplistic and does not accurately represent the range of variation present within the phocids. The major recurring patterns were ones where the tooth row arched laterally (state 1), medially (state 4), or laterally anteriorly and medially posteriorly (state 0). The kinked condition (state 3) is obviously an extreme case of one of the other states, but exactly which one is not clear a priori. Thus, this morphology was left as a distinct state.

The plesiomorphic condition is of a sigmoidal upper tooth row, which is possessed by the majority of the non-lutrine fissiped outgroups. The derivation of this character in the lutrines and ancestrally within the pinnipeds is unclear. Either a straight tooth row is synapomorphic for *Lutra* plus the pinnipeds (ACCTRAN optimization), or the ancestral condition for the pinnipeds is equivocal between states 2 and 4, an uncertainty which is preserved into each phocid subfamily (DELTRAN optimization). In any case, the majority of the pinnipeds possess the straight morphology, and, despite its possible ancestral status, a reverse arch is limited to *Cystophora*, *Mirounga* spp., and *Monachus monachus* (where it must appear independently). *Odobenus* obtains a laterally arched tooth row, as does *Enhydra* among the fissipeds. *Erignathus* uniquely reverses to the plesiomorphic sigmoidal tooth row. The kinked morphology was found only in *Monachus schauinslandi* plus *M. tropicalis*, and appears to be a derivative of the straight condition.

Mandible (3 characters)

Although it is frequently mentioned in species descriptions, the mandible exclusive of the teeth has not been a common source of characters in recent systematic studies of the phocids. This has not always been the case. Chapskii (1955a) asserts that the general form of the mandible (and especially of its posterior margins) contains important taxonomic information, a source of information previously exploited primarily by Russian systematists. Another possible character, which was not examined here, deals with the mandibular symphysis which appears to be generally more robust in the monachines than in the phocines (pers. obs.).

150) shape of lingual face of mandible at middle postcanines: 0 = concave; 1 = flat; 2 = convex (Ridgway 1972).

This character has been employed to distinguish between the genera *Phoca* spp. (state 2) and *Pusa* spp. (state 0) (Ridgway 1972). A flat morphology is plesiomorphic among caniforms, with the remaining apomorphic states possessing limited distributions, and among the pinnipeds only. A concave morphology appears independently on a number of occasions: *Odobenus*, *Lobodon*, *Mirounga* spp., and *Monachus tropicalis*. The convex morphology was only noted for *Cystophora* and *Halichoerus*. This arises either as a synapomorphy of the phocines as a whole, with the remaining taxa reversing to the plesiomorphic condition (ACCTRAN optimizations), or independently in the two taxa (DELTRAN optimization). *Phoca* spp. and *Pusa* spp. were not distinguished by this character, as both genera were characterized by a flat morphology.

151) shape of posteroventral edge of mandible: 0 = rounded; 1 = jagged (Ridgway 1972).

In effect, this character deals with the size of the angular process. A rounded posteroventral edge of the mandible (small angular process) has been noted independently for *Hydrurga* (Ridgway 1972) and *Ommatophoca* (Mivart 1885). However, this apomorphic condition generally seems to be a synapomorphy of the monachines minus the elephant seals (*Mirounga* spp.) as a whole. Although a reduction of the angular process seems to characterize all phocids to some degree, a substantial reduction (to the apomorphic condition) occurs only in *Cystophora* and *Erignathus* among phocines.

Taylor (1914) holds the reduction of the angular process to be an aquatic adaptation, with the support provided by the aquatic medium allowing for reduced muscle masses, and therefore reduced muscle attachment points. However, why this would affect the angular process is unclear. The angular process is the posteromost extent of the insertion of the pterygoideus internus (= lateralis) (Davis 1964), but neither a relative reduction, nor a shift in the insertion of this muscle has been described in the phocids (see Howell 1928; Bryden 1971; Piérard 1971). This character may, in fact, be homoplastic as a true reduction of the process (e.g., as in *Leptonychotes*), or an expansion of the angle of the jaw subsuming the process (e.g., as in *Monachus monachus*) will both give the appearance of a reduced angular process.

152) distinct medially directed flange along ventral edge of jaw located posterior to mandibular symphysis and ventral to posterior postcanines: 0 = absent; 1 = present (King 1972).

A mandibular flange (or an elongated symphysis) was noted by King (1972, 1983) for *Odobenus*, *Erignathus*, *Lobodon*, *Pagophilus*, *Phoca* spp., and *Pusa* spp., where the resultant scoop-like mandible was postulated to be an adaptation for a "sucking" mode of feeding [best described for *Odobenus*; see Fay (1982)]. This flange may represent either a vestigial portion, or the precursor of a more robust mandibular symphysis, as this flange was often observed to grade smoothly anteriorly into the symphysis. As well, the flange is generally absent in the monachines, which, on the whole, possess a more robust symphysis (pers. obs.).

The distribution of the flange here closely matches that listed by King (1972, 1983). It appears to be an apomorphic condition shared by all phocines internal to *Halichoerus*, except for *Phoca largha*, but including *Histiophoca*. It was also independently obtained in *Lobodon*, but not consistently in *Odobenus*, which, like *Monachus monachus*, was polymorphic for this trait.

Forelimb (17 characters)

Post-cranial material has only sparingly been used to elucidate the systematics of the phocids. Only King (1966) and Wyss (1988a) have used such material to any degree. This reflects a number of factors. First, the comparative complexity of the mammalian skull yields a disproportionately high number of (obvious) characters. As well, there is a tendency for skins and skulls to be preferentially preserved over post-cranial material for mammals in many museum collections. Often, mammalian taxa are represented only by cranial material, making the inclusion of post-cranial material impossible in a practical sense. Finally, when post-cranial material has been preserved, it is usually disarticulated, making identification of the smaller isolated elements difficult and less desirable for study. Hendey & Repenning (1972) consider many phocine post-cranial features to be primitive, an interpretation also implied by Wyss (1988a). Within the phocids, the generally good diagnostic value of the humerus has been noted (Ray 1976a; de Muizon & Hendey 1980). 153) relative size of scapular spine: 0 = reduced to prominent acromion; 1 = medium; 2 = prominent (King 1966; Wyss 1988a).

The reduction of the scapular spine (both in length and height) in most monachines was initially noted by King (1956, 1966). However, Wyss (1988a) correctly observed that the spine exhibits three morphologies within the phocids: a prominent form in the phocines where it extends virtually the full dorsoventral length of the scapula, the reduction to a knob-like acromion in the lobodontines, and an intermediate condition in *Mirounga* spp. and *Monachus* spp. Although Wyss (1988a) hesitantly equated this intermediate morphology with the phocine pattern, we have chosen to leave it separate. Among the outgroups, a reduced spine occurs only in ursids (Davis 1964) and the otarioids (Wyss 1988a). Wyss (1988a) has taken this distribution to indicate that a reduced spine is primitive for the pinnipeds [assuming an ursid outgroup; see Wyss (1987)].

A prominent scapular spine is plesiomorphic among the Caniformia and largely retained throughout, including *Ursus*. The intermediate condition only appears in *Odobenus*, *Mirounga* spp., and polymorphically with state 2 in *Zalophus*. This could arise through parallel evolution (DELTRAN optimization), but may also indicate a synapomorphy of

the pinnipeds, with subsequent modification in the remaining forms (ACCTRAN optimization). The apomorphic reduction to a prominent acromion unites all monachines except *Mirounga* spp. All phocines possess a prominent scapular spine.

154) relative shape of axillary (= caudal) border of scapula: 0 = straight; 1 = curved (Wyss 1988a; pers. obs.).

This character stems from the following one which was used by Wyss (1988a) to indicate a synapomorphy of the phocids exclusive of *Mirounga* spp. and *Monachus* spp. The shape of the teres major process notwithstanding, we noted that the axillary border of the scapula exhibits one of two distinctive morphologies. In most fissiped carnivores, the axillary border is reasonably straight (Miller 1962; Davis 1964; Crouch 1969). In contrast, the strongly curved border of most pinnipeds appears to be derived from an enlargement of the gleno-vertebral (posterodorsal) portion of the infraspinous region of the scapula (Howell 1928).

The apomorphic curvature of the axillary border presented a more limited distribution here, primarily being a synapomorphy of the phocines (with and without the polymorphic *Cystophora*), with independent origins in *Lutra* and *Ursus* among the outgroups. Among the monachines, only *Monachus monachus* consistently displayed the derived state, although most species were polymorphic for this trait.

155) distinct hook-like teres major process on scapula: 0 = absent; 1 = present (Wyss 1988a).

The teres major process comprises the posterodorsal-most portion of the gleno-vertebral region mentioned by Howell (1928). Wyss (1988a) considered the enlargement of this process (over and above that of the gleno-vertebral region) to form a hook on the axillary border of the scapula a synapomorphy of the phocids exclusive of *Mirounga* spp. and *Monachus* spp. Instead, our analysis indicates that the apomorphic presence of a distinct hook-like teres major process is limited to certain phocines only. It appears as a synapomorphy at the level of either *Phoca largha* (ACCTRAN optimization) or *Phoca vitulina* (DELTRAN optimization), and is maintained for all phocines internal to this, with the exception of *Pusa sibirica* (possibly as a synapomorphy with *Pusa hispida*; ACCTRAN optimization).

*156) supinator (= lateral epicondylar) ridge on humerus: 0 = absent; 1 = present (Wyss 1988a).

With recoding, this character was included in character #157.

157) relative degree of development of supinator (= lateral epicondylar) ridge on humerus: 0 = weak; 1 = medium; 2 = strong; 9 = absent (King 1966; Wyss 1988a).

King (1966) initially used this character to distinguish between the phocines (state 2) and the monachines (state 0). While agreeing with this distribution, Wyss (1988a) added outgroup information. In noting the absence of the supinator ridge in the otarioids (also Howell 1928) and its generally strong development among fissiped carnivores, Wyss (1988a) considered the presence of the ridge in phocines to be a reversal to the primitive (possibly at the level of the carnivores) condition. In contrast, de Muizon & Hendeby (1980) felt the supinator ridge to be a primitive feature among phocids.

The appearance of the supinator ridge among the caniforms appears to be much more complex than indicated by Wyss (1988a). The polarity is equivocal at the level of the Caniformia due to the absence of the ridge in *Canis*. However, a similar absence in the domestic cat, *Felis domestica* (Crouch 1969), increases the likelihood that this is the plesiomorphic condition. The arctoids derive a medium-sized ridge, which the phocids reduce somewhat (state 0). This weak supinator ridge is largely retained for the monachines, with the clade of *Monachus schauinslandi* and *M. tropicalis* losing the ridge completely. A strongly developed ridge is unusual among caniforms, being limited to the phocines exclusive of *Cystophora*, with a parallel appearance in *Procyon*. *Pusa caspica* uniquely derives state 1 among phocids.

*158) deltopectoral crest on humerus: 0 = absent; 1 = present (Wyss 1988a).

With recoding, this character was included in characters #159 and 160.

159) relative length of deltopectoral crest on humerus: 0 = less than or equal to one-half length of humerus; 1 = greater than one-half length of humerus; 9 = absent (Wyss 1988a).

In all pinnipeds, the pectoralis muscle is quite prominent, resulting in a strengthening of its insertion point on the humerus (Howell 1928; Bryden 1971; Hendey & Repenning 1972). Hendey & Repenning (1972) distinguished two main patterns for this strengthening. In phocines, the pectoralis inserts only on the proximal half of the humerus, resulting in a deltopectoral crest that extends towards the enlarged lesser tubercle proximally, and is quite robust at its distal end. The crest extends to slightly less than halfway along the length of the humeral shaft before ending abruptly in a sharp overhang. In contrast, the insertion of the pectoralis in monachines is extended distally on the humerus, resulting in a deltopectoral crest that is two-thirds to three-quarters of the length of the humerus and grades smoothly into its shaft (Hendey & Repenning 1972; Wyss 1988a). *Leptonychotes* apparently shows a disposition towards the phocine pattern (de Muizon 1982a). Otarioids tend towards the monachine pattern (Hendey & Repenning 1972; Wyss 1988a), leading Wyss (1988a) to postulate it as plesiomorphic for the pinnipeds. This character examines one aspect of this morphology, the length of the crest, while the following character looks at the merging of the crest with the humeral shaft.

The current character presents a rather uncertain evolutionary pathway, although the distribution of the states is well marked. The phocine pattern is present in all phocines, with additional appearances in *Canis*, *Procyon*, and *Hydrurga*. Meanwhile, the monachine pattern is found in those monachines internal to *Hydrurga*, *Lutra*, and the otarioids. *Enhydra* and *Mirounga* spp. are polymorphic for these two states. A distinct crest is uniquely absent in *Martes*. However, this distribution has the effect of rendering the polarity at the level of the Caniformia equivocal. This situation may persist through to the phocids, with the different morphologies arising independently within the family (DELTRAN optimization). Another scenario has the monachine pattern as a synapomorphy of the arctoids, before the phocine pattern is derived ancestrally for the phocids and retained into the basal members of each subfamily at least (ACCTRAN optimization).

160) merging of deltopectoral crest to shaft of humerus: 0 = smooth; 1 = abrupt; 9 = absent (Wyss 1988a).

As indicated by Wyss (1988a), the monachine pattern (state 0) represents the plesiomorphic condition, and this extends back to the level of the Caniformia. The phocine pattern, whereby the deltopectoral crest ends abruptly at a virtual right angle to the shaft, is a synapomorphy uniting all phocines, with a parallel appearance in *Leptonychotes*. Again, a distinct crest was uniquely absent in *Martes*.

161) entepicondylar foramen of humerus: 0 = absent; 1 = present (King 1966; Wyss 1988a).

One obvious 'distinguishing characteristic between phocines and monachines is the presence of an entepicondylar foramen in the former and its absence in the latter (King 1966; Wyss 1988a). However, it should be noted that this is a generalization applying primarily to extant forms. Early Pliocene monachines (e.g., *Homiphoca capensis*, various species of *Monotherium*) do possess an entepicondylar foramen (Hendey & Repenning 1972; Ray 1976b; de Muizon & Hendey 1980; de Muizon 1982a; Repenning 1990). Various authors take this to be evidence of a recent loss of the foramen by the monachines (Hendey & Repenning 1972; de Muizon & Hendey 1980; Repenning 1990). As well, we observed phocine specimens in which the foramen was unilaterally (*Pagophilus*, AMNH 180016) or bilaterally absent (*Halichoerus*, USNM 446408), something also infrequently observed in other phocines (King 1966). A polymorphic distribution for this character is also indicated for the Ursidae, where the foramen is generally absent, except for the genera *Ailuropoda* and *Tremarctos* (Davis 1964).

As mentioned by Wyss (1988a), the interpretation of the distribution of this character depends on the outgroup relationships assumed for the phocids. A diphyletic pinniped origin with lutrine affinities for the phocids, as advanced by de Muizon (1982a), yields the monachine pattern as being apomorphic. A monophyletic Pinnipedia with ursid affinities, as postulated by Wyss (1987, 1988a), instead holds the phocine pattern to be apomorphic. Our analysis indicates that the polarity of this character is equivocal at the level of the Pinnipedia. At the level of the Caniformia, however, the possession of an entepicondylar foramen is apomorphic, being found in *Procyon*, *Martes*, *Enhydra*, and *Lutra*, in addition to all phocines. The connection between these fissipeds and the phocines is dependent on the optimization criterion used. With ACCTRAN optimization, the lack of the foramen is a synapomorphy of the pinnipeds, with the phocines homoplastically re-deriving the foramen. Under DELTRAN optimization, the possession of the foramen is synapomorphic for these taxa, with the otarioids and monachines independently reversing to the plesiomorphic condition. Only this latter pattern can account for the proposal whereby the foramen is present in monachines primitively before being lost (see above).

162) distally projecting ledge (palmar process) on cuneiform of carpus: 0 = absent; 1 = present (King 1966; Wyss 1988a).

King (1966) used this character to group *Cystophora* with the phocines (state 1) and *Mirounga* spp. with the monachines (state 0). In noting the absence of the ridge in otarioids, Wyss (1988a) presumed the presence of the ridge to be a phocine synapomorphy at the level of the Pinnipedia. However, such an interpretation is upheld here only under ACCTRAN optimization. Under DELTRAN optimization, the otarioids and monachines independently lose the ridge to match the state found in *Canis*. Otherwise, the palmar

process is a synapomorphy of the arctoids (the polarity being equivocal for the caniforms) and is consistently found in *Ursus*, *Martes*, *Enhydra*, and *Lutra*.

163) general morphology of metacarpal shaft: 0 = no lateral shaft ridges; 1 = lateral shaft ridges (M.A. Cozzuol pers. comm.) (Fig.23).

M.A. Cozzuol (pers. comm.) kindly pointed out that the metacarpals in some phocines are marked by small longitudinal ridges on each side of the distal palmar surface. However, at best, many phocine taxa are only polymorphic for this plesiomorphic caniform feature. The loss of these ridges describes a synapomorphy of *Martes*, the lutrines, and the pinnipeds, with the tendency towards regaining this feature only appearing consistently in *Lutra* and *Pusa caspica*.

164) general morphology of metacarpal head: 0 = smooth; 1 = “palmar” ridges present (King 1966; Wyss 1988a) (Fig.23).

Character #18 of Wyss (1988a) describes a suite of features related to the morphology of the metacarpal-phalangeal articulation. We have chosen to subdivide Wyss’s (1988a) character into its component parts (this character, characters #165 and 166). Wyss (1988a) described his first component, the longitudinal “palmar” ridge, as dividing the distal and palmar surfaces of the metacarpal head (also King 1966). If we have in fact observed the same feature intended by Wyss (1988a), we would amend his definition to something more akin to the keeled heads of Berta & Ray (1990): a longitudinal ridge (or keel) on the distal metacarpal head running between the palmar and anti-palmar surfaces. Among caniforms, this “palmar” ridge is absent only in otarioids and monachines (King 1966; Wyss 1988a), which Wyss (1988a) interprets as a synapomorphy of the pinnipeds, with a reversal to the primitive carnivore condition (state 2) by the phocines. However, our observation of “palmar” ridges among the otarioids renders the outright lack of any such ridges as a synapomorphy solely of the monachines as a whole (ACCTRAN optimization), or of the

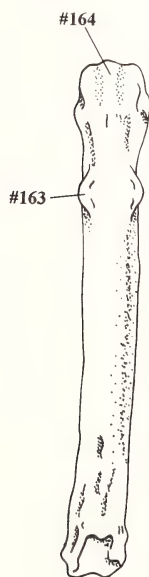


Fig.23: Ventral view of the third metacarpal of a canid (*Canis familiaris*) illustrating selected characters (indicated by their number; see **Character Analysis**) of this element. Distal is towards the top of the page. Adapted from Miller (1962).

monachines less the polymorphic *Mirounga* spp. (DELTRAN optimization). Note, however, that this slight discrepancy may hinge on our definition of this character being different from the one intended by King (1966) and Wyss (1988a).

165) cross-sectional shape of phalanges: 0 = flat; 1 = intermediate; 2 = round (King 1966; Wyss 1988a).

The second of Wyss's (1988a) metacarpal features examined the cross-sectional shape of the phalanges. In the monachines, as in the otarioids, the phalanges are distinctly flattened as opposed to the more rounded morphology of the phocines (Howell 1928; King 1966; Wyss 1988a). However, the phalanges of the phocines are still appreciably flatter than those found in fissiped carnivores (Wyss 1988a), and hence should represent more of an intermediate condition (state 1).

Generally, any apomorphic flattening of the phalanges is limited to the pinnipeds. Strongly flattened phalanges (state 0) arise on at least three main occasions: *Zalophus*, *Phoca vitulina* plus *Pusa* spp. (the two reconstructions indicate a conflicting assortment of independent origins and losses in this general region), and those monachines internal to *Leptonychotes*, minus *Monachus tropicalis* (which regains rounded phalanges). No phocine demonstrated slightly flattened phalanges (state 1). Instead the appearance of this morphology was limited to *Lutra* and *Mirounga leonina*.

166) morphology of proximal phalangeal articular surface: 0 = hinge-like; 1 = trochleated (King 1966; Wyss 1988a).

In most caniforms, the proximal articular surface of the phalanx is strongly trochleated to accommodate the "palmar" ridge of the distal metacarpal head (see character #164). The lack of such a ridge in otarioids and monachines results in a more hinge-like articular surface of the phalanx (King 1966; Wyss 1988a). As with the palmar ridges, Wyss (1988a) interprets this distribution so that a hinge-like articulation is synapomorphic for the pinnipeds, with the phocines reversing to re-obtain the primitive carnivore pattern. While the same distribution of states was observed here, such an interpretation is contingent upon the optimization criterion employed. Wyss's (1988a) scenario is applicable under ACCTRAN optimization, but under DELTRAN optimization, hinge-like articular surfaces are independently obtained in otarioids and monachines.

167) comparative length of metacarpals I and II: 0 = I > II; 1 = I subequal to II; 2 = I < II (King 1966; Wyss 1988a).

Both King (1966) and Wyss (1988a) observed that in phocine seals, as in most carnivores, metacarpals I and II are of approximately equal size. In contrast, the remaining pinnipeds are characterized by an elongated and comparatively thicker first metacarpal (King 1966; Wyss 1988a). This is a generalization, however, as *Cystophora* and *Halichoerus* are approximately intermediate between these extremes (see King 1966: 391). Again, Wyss (1988a) interprets this distribution to indicate a reversal, albeit incomplete (as the first metacarpal is slightly longer than the second in phocines, while the situation is reversed in fissiped carnivores), on the part of the phocines. We divided the original character (relative metacarpal size) into its two component parts: relative metacarpal length and relative metacarpal diameter (= robustness or thickness). As well, we have expanded the

number of character states to account for all permutations of the relative sizes of the two elements.

The plesiomorphic condition is for the second metacarpal to be the longer of the two, a situation found in all fissiped outgroups except for *Enhydra* and *Ursus*, where the metacarpals are subequal in length. The pinnipeds are united by the apomorphic condition whereby the first metacarpal is distinctly longer. As expected, most phocines are diagnosed by having metacarpals of equal length. *Cystophora* retains and *Pusa sibirica* reverts to the primitive pinniped morphology.

168) comparative overall diameter of metacarpals I and II: 0 = I > II; 1 = I subequal to II; 2 = I < II (King 1966; Wyss 1988a).

The comparative robustness of metacarpals I and II follows much the same pattern as their length, except that only scattered phocines reverse towards a more subequal arrangement. An enlarged first metacarpal is a pinniped synapomorphy, with the fissipeds characterized by a second metacarpal of equal (all fissiped arctoids) or greater (*Canis* only) diameter than the first. State 0 is found universally in the otarioids and monachines, and is largely retained throughout the phocines as well. Only *Erignathus*, *Phoca largha*, and *Pusa caspica* independently reverse to obtain the condition where the two elements are roughly equal in diameter.

169) relative degree of development of foreflipper claws: 0 = not well developed or absent; 1 = well developed, prominent (King 1966; Wyss 1988a).

There is the tendency within the pinnipeds (exclusive of the phocines) to reduce both the fore- and hind flipper claws (Wyss 1988a; see character #189). In the otarioids, the foreflipper claws are virtually absent, remaining only as small nodules (Wyss 1988a). Although only *Hydrurga* and *Ommatophoca* possess reduced foreflipper claws among monachines (King 1966), Wyss (1988a) holds them to be reduced for the subfamily, thus describing a pinniped synapomorphy with a reversal occurring in the phocines. For those species where adequate preserved material was lacking, we supplemented our observations with data from King (1966). Here the apomorphic reduction of the foreflipper claws occurred independently in only the otarioids, *Hydrurga*, and *Ommatophoca*.

Pelvis (8 characters)

The general form of the phocid pelvis is very distinctive from that of other carnivores (de Muizon 1982a), lending additional support to the monophyly of the group. However, rather than concentrate on the autapomorphic features of the phocid pelvis, we have attempted to examine characters that clarify either the ingroup (i.e., within the phocids) or outgroup relations of the family.

170) eversion of wing of ilium: 0 = distinctly less than 45°; 1 = roughly 45°; 2 = distinctly greater than 45° (King 1966; Wyss 1988a).

The phocids are uniquely characterized by a laterally everted ilium (King 1966; de Muizon 1982a; Wyss 1988a). The degree of eversion is markedly greater in phocines (exclusive of *Erignathus*) than in monachines, often reaching 90° (Howell 1928; King 1966; Wyss 1988a). In the phocines especially, this eversion benefits the tremendously enlarged iliocostalis portion of the back musculature which originates, at least in part, from the

former medial side of the ilium, as well as the gluteus group extending to the femur (Howell 1928; Bryden 1971; Hendey & Repenning 1972). McLaren (1975) holds that the subfamilial differences arise from the retention of a more primitive muscular arrangement in the monachines, a contention echoed by Hendey & Repenning (1972). The binary coding employed by most authors ("strongly everted or not") disguises the unique form of the ilium in all phocids by grouping the monachines with non-phocids. Therefore, we have subdivided this character more finely, with the categories roughly corresponding to "not everted", "weakly everted", and "strongly everted".

The apomorphic eversion of the ilial wing (states 1 or 2) is largely confined to the phocids, although a weakly everted ilium does occur in *Enhydra* and *Ursus*. As the phocids are characterized ancestrally by state 0, independent eversions of the ilial wing must occur in each subfamily, as implied by Hendey & Repenning (1972). The weakly everted ilium typical of many monachines describes a synapomorphy of those species internal to *Hydrurga*, with *Monachus schauinslandi* (possibly as a synapomorphy with *Monachus tropicalis*; ACCTRAN optimization) reverting to a flat ilium. The strongly everted ilium of the phocines arises ancestrally within this subfamily, with only *Erignathus* (states 0 and 1) largely reversing to the plesiomorphic caniform morphology.

*171) gluteal fossa on wing of ilium: 0 = absent; 1 = present (King 1966; Wyss 1988a). With recoding, this character was included in character #172.

172) depth of gluteal fossa on ilium: 0 = shallow; 1 = medium; 2 = deep; 9 = absent (King 1966; Wyss 1988a).

Apparently associated with the strongly everted phocine (exclusive of *Erignathus*) pelvis is a deep, compact gluteal fossa on the lateral side of the everted ilial wing (King 1966; Wyss 1988a). The majority of this fossa in phocines serves as the origin for the gluteus medius muscle (Howell 1928). The gluteal fossa is apparently absent in the remaining pinnipeds (Wyss 1988a), but exists in *Canis* and *Ursus* as a shallow, elongated trough (Miller 1962; Davis 1964).

A gluteal fossa of shallow or medium depth is found in all fissiped outgroups except possibly *Lutra* (ACCTRAN optimization). A deep fossa unites the phocines ancestrally with only *Erignathus* (state 9) and *Pusa sibirica* (state 1 – possibly as a synapomorphy with *Pusa hispida*; ACCTRAN optimization) deviating from this trend. Beyond this, however, the two optimization criteria used here provide strikingly different pathways for the evolution of this character. ACCTRAN optimization holds for the loss of the fossa uniting *Lutra* plus the pinnipeds with *Leptonychotes*, *Lobodon*, and *Mirounga* spp. independently deriving medium depth fossae. In contrast, DELTRAN optimization indicates that a shallow fossa is a synapomorphy of *Lutra* plus the pinnipeds, with the otarioids, *Hydrurga*, *Monachus* spp. and *Ommatophoca* losing the fossa in parallel. Of these two opposing hypotheses, the latter seems the more likely, as the previous (excluded) character indicates that the loss of the fossa is an apomorphic tendency occurring independently in the taxa mentioned above.

173) relationship of obturator nerve foramen to obturator foramen: 0 = distinctly separate, at least unilaterally; 1 = intermediate – foramina confluent, but individually recognizable; 2 = confluent – obturator nerve foramen not apparent (Wyss 1988a).

Although reasonably common among the otarioids [especially the arctocephaline otariids (the fur seals) and occasionally *Odobenus*], a distinct obturator nerve foramen separate from the obturator foramen is present only in *Monachus schauinslandi* among phocids (King & Harrison 1961; Ray 1976a; Repenning & Ray 1977; Wyss 1988a). Wyss (1988a) has interpreted this feature as being primitive among the pinnipeds, and used the above distribution to justify the sister taxon status of *M. schauinslandi* to the remaining phocids. An identifiable obturator nerve foramen is periodically present in *Cystophora* and *Monachus tropicalis*, but it is confluent with the obturator foramen (state 1), whereas it is displaced towards the cotyloid notch of the acetabulum in *Monachus schauinslandi* (state 0) (King & Harrison 1961; Repenning & Ray 1977; Wyss 1988a; pers. obs.). Any appearance of the obturator nerve foramen (states 0 or 1) is apomorphic among the caniforms. State 0 is only manifested in *Monachus schauinslandi*, while state 1 occurs convergently in the otarioids and *Monachus tropicalis*. *Cystophora* was notably polymorphic for states 1 and 2 for this character.

174) ridges in anterior portion of obturator foramen: 0 = absent; 1 = present (pers. obs.) (Fig.24).

We noted this feature in the pelves of a diverse range of taxa. These ridges may be related to the previous character, as their location closely approximated that of the incompletely separated obturator nerve foramen in species such as *Cystophora* and *Monachus tropicalis* (see previous character). In fact, these ridges may serve to segregate the obturator nerve from various muscles of the hip, most notably the craniad insertions of the obturatorius externus and internus muscles on the obturator membrane (Howell 1928; Miller 1962; Piérard 1971). Admittedly, the term "ridges" is inadequate as the ridges took on many forms, ranging from actual longitudinally oriented ridges that in effect constricted the anterior part of the obturator foramen, to small bony spurs.

In general, the ridges tend to be absent in the fissipeds, although their appearance in *Canis* renders the polarity of this character equivocal at the level of the Caniformia. The ridges mark a synapomorphy of the pinnipeds, with the phocids showing a tendency towards their loss. Ridges are consistently absent in *Monachus* spp. (possibly as a synapomorphy with *Lobodon*; ACCTRAN optimization), *Phoca vitulina*, and the clade of *Pusa hispida* plus *Pusa sibirica*, and polymorphically so in a number of other phocids.

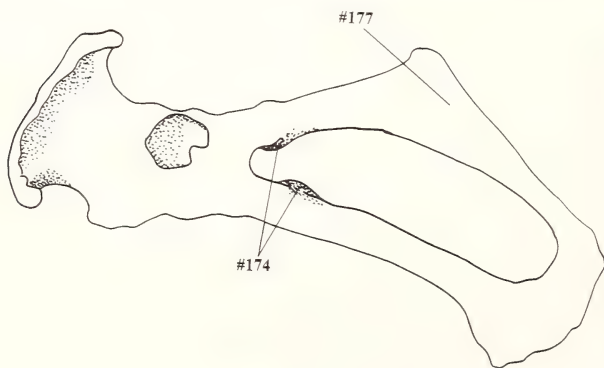


Fig.24: Lateral view of the left pelvic girdle of *Pusa hispida* illustrating selected characters (indicated by their number; see **Character Analysis**) of this element. Anterior is towards the left of the page and dorsal to the top. Adapted from de Muizon (1982a).

175) relative length of post-acetabular region of the pelvis: 0 = shortened (and rounded); 1 = elongated (and narrow) (King 1966; Henzey & Repenning 1972).

Compared with most other carnivores, the post-acetabular region of the pinniped pelvis is characteristically elongated (Howell 1928; de Muizon 1982a; King 1983). The extreme this condition reaches in the phocids (Howell 1928; de Muizon 1982a) is likely related to the lateral eversion of the phocid ilium (see character #170). Yet, even within the phocids, two different pelvis types can be differentiated. Phocines possess a relatively long and narrow post-acetabular region of the pelvis, as opposed to the relatively shorter and rounder form of the monachines (King 1966; Henzey & Repenning 1972). A relatively elongated pelvis is synapomorphic for the mustelids (including the lutrines) plus the pinnipeds. The two phocid subfamilies are clearly divided by this feature. The phocines universally possess an elongated pelvis, while the monachines reverse ancestrally towards a plesiomorphic short pelvis.

176) general curvature of pelvis around long axis: 0 = relatively straight; 1 = distinctly twisted (pers. obs.).

During our observations, we noted a peculiar morphology of the phocine pelvis. In all other caniforms, the pelvis is twisted around its long axis so that when the cranial portion is viewed directly dorsally (i.e., so that the acetabulum points laterally), the medial surfaces of the ischium and pubis are visible. In contrast, the phocine pelvis is reasonably straight, so that the ischium does not deflect appreciably from the long axis of the pelvis. King (1966) does note a lateral bowing of the pubis in female phocids, but this does not refer to the same feature. King's (1966) bowing is more obvious in phocines and involves a medial curvature of the pubis posteriorly so that the innomates are virtually in contact at their posterior ends. As well, we observed the twisting under discussion here in phocines of both sexes. This twisting of the pelvis is a synapomorphy of the phocines, with a parallel appearance in *Lobodon*.

177) relative location of ischiatic spine (= tuber ischiad): 0 = roughly midway along the post-acetabular region; 1 = located in posterior post-acetabular region (pers. obs.) (Fig.24).

In the caniforms, the relative location of the ischiatic spine appears to be associated with the relative length of the pelvis (see character #175). In taxa with relatively short pelvises, the ischiatic spine tends to be located close to the posterior end of the pelvis. The apparent anterior shift of the ischiatic spine in taxa with long pelvises possibly indicates a posterior elongation of the pelvis in these forms. However (compare with the distribution of character #175), an anterior shift of the ischiatic spine is indicated to be a synapomorphy of the pinnipeds, with a reversal in *Odobenus* (ACCTRAN optimization), or of the phocids only with a parallel appearance in *Zalophus* (DELTRAN optimization). This latter scenario accords well with observations of an elongated post-acetabular region in phocids (Howell 1928; de Muizon 1982a). Among phocids, only *Hydrurga* and *Lobodon* revert to the plesiomorphic state (state 1).

There is a possibility that the two states we identified for this character might be an artifact of the sexual dimorphism present in pinniped pelvises. King (1983) states that the posterior outline of the pelvis in male pinnipeds is much more rectangular than the more rounded female morphology [see Fig.36 in King (1969)]. This would result in an apparent posterior

shift of the ischiatic spine in males. However, in noting the fairly consistent anterior shift of the spine throughout the pinnipeds here (in conjunction with our attempts to have an equal representation of males and females), we judge the effect of this potential error to be minimal.

Hind Limb (12 characters)

Certain features of the hind limb have been useful in defining the phocids as a family (e.g., lack of a lesser trochanter on the femur, presence of posterior process on the astragalus) (Howell 1928; de Muizon 1982a), but otherwise, the hind limb (exclusive of the pelvis) has not been used to a great extent to elucidate phocid phylogeny. This might be explained for the femur, at least, by it being assigned a generally low diagnostic value due to its high variability (e.g., Ray 1976a; de Muizon & Hendey 1980).

178) position of greater trochanter on femur: 0 = lower than head; 1 = equal with head; 2 = higher than head (King 1966; de Muizon 1982a).

This character has been briefly mentioned to define either of the phocid subfamilies. King (1966) notes that phocines tend to possess state 2, while de Muizon (1982a) used state 0 to define a synapomorphy of the monachines, a distribution echoed by de Muizon & Hendey (1980). Here, the morphologies whereby the greater trochanter is equal to or higher than the femoral head are apomorphic. State 1 characterizes the phocines ancestrally and is universal within the subfamily except for *Pagophilus*, *Phoca largha*, and *Pusa sibirica*, which independently derive state 2. State 1 also appears in the monachine *Monachus tropicalis* (possibly as a synapomorphy with *Monachus schauinslandi*; ACCTRAN optimization) and the fissipeds *Enhydra*, *Martes*, and possibly *Procyon*, either by convergence (DELTRAN optimization), or as a synapomorphy of the fissiped taxa, with a reversal to the primitive caniform condition in *Lutra* plus the pinnipeds (ACCTRAN optimization).

The slight discrepancy with previous observations (phocines generally possessing state 1 and not state 2) can be related to the fact that our observations of this character were made so that the distal condylar surfaces of the femur were level. However, the autapomorphic development of an epicondylar ridge in phocids causes the distal condylar surfaces to be slightly oblique with respect to the femoral shaft (de Muizon 1982a). Thus, with our technique, the greater trochanter would be shifted to a lower position relative to the femoral head. That this character still indicates a synapomorphy of the phocines speaks for the height to which the greater trochanter is raised in this group.

*179) distinct trochanteric fossa on femur: 0 = absent; 1 = present (King 1966; de Muizon 1982a).

With recoding, this character was included in character #180.

180) depth of trochanteric fossa on femur: 0 = shallow; 1 = medium; 2 = deep; 9 = absent (King 1966; de Muizon 1982a).

As compared to the modern monachines, another distinguishing feature of the phocine femur is the development of a distinct trochanteric fossa (King 1966; de Muizon 1982a). However, the value of this character may be limited by its inconsistent presence in phocines (e.g., it is absent in *Erignathus*) together with its presence in many fossil

monachines as well as *Lobodon* (de Muizon & Hende 1980; de Muizon 1982a). A similar absence of the fossa in the otarioids, combined with its presence throughout the rest of the Carnivora led Wyss (1988a) to suggest that this character indicated yet another reversal on the part of the phocines. In contrast, de Muizon (1982a) held the monachine pattern to be apomorphic for the subfamily.

A deep trochanteric fossa is plesiomorphic among the Caniformia, being found in all major fissiped lineages. The above distribution for this character is largely borne out (with the exception of a shallow fossa in *Zalophus*, *Leptonychotes*, and *Monachus monachus*), but the evolutionary pathway is dependent on the reconstruction technique employed. DELTRAN optimization largely supports de Muizon (1982a), with the plesiomorphic condition being retained by the phocines, and parallel losses or reductions of the fossa occurring in the otarioids and monachines. In contrast, ACCTRAN optimization supports Wyss (1988a), in that the loss of the foramen is synapomorphic for the pinnipeds, with the phocines re-deriving a deep fossa. As expected, *Lobodon* regains a medium depth fossa.

181) lesser trochanter: 0 = absent; 1 = present (de Muizon 1982a).

The phocids are unique among mammals in lacking the lesser trochanter on the femur (Howell 1928; de Muizon 1982a). A slight discrepancy exists as to the resulting new insertion point of the psoas magnus. The majority opinion is that the insertion shifts to the posteroventral ischiatic spine (= pectineal tuberosity) on the ventral edge of the ilium, representing an adaptation to enhance the lateral undulatory movements employed in the phocid swimming style (Miller 1887; Bryden 1971; Piérard 1971; de Muizon & Hende 1980; de Muizon 1981, 1982a). However, Howell (1928) indicates this to be a different muscle, the psoas tertius, and places the insertion of the psoas magnus on the medial tuberosity of tibia, together with the iliocostalis. In any case, the apomorphic loss of the lesser trochanter for the phocids is indicated here.

182) relative width of femur distally: 0 = gracile (less than medium breadth); 1 = robust (greater than or equal to medium breadth) (M.A. Cozzuol pers. comm.).

In conjunction with his research into the possible paraphyletic nature of *Monachus* spp., M.A. Cozzuol kindly pointed out this character to us. He noted that the femur is very robust and broad distally in *M. monachus*, but much more gracile in *M. schauinslandi* and *M. tropicalis*. Additionally, de Muizon & Hende (1980) hint at a wide distal end to the femur in the lobodontines. In applying this character to the other taxa in this study, a comparatively robust femur appears to be a synapomorphy of the monachines, missing only in *Mirounga leonina* and the clade of *Monachus schauinslandi* and *M. tropicalis* (ACCTRAN optimization). However, another possibility holds for independent origins of a wide distal end in *Mirounga angustirostris* and most of the remaining monachines (DELTRAN optimization).

183) proximal fusion of tibia and fibula: 0 = unfused; 1 = rudimentary – not fused all the way around; 2 = totally fused (Wyss 1988a).

The fusion of the proximal epiphysal heads of the pinniped tibia and fibula presumably represents an adaptation to strengthen and decrease the mobility of this region of the leg

to aid in swimming. This condition is obtained in virtually all Recent pinnipeds, the only exceptions being *Odobenus*, where they are rarely fused, and *Monachus schauinslandi*, where they are almost never fused (Ray 1976a; Repenning & Ray 1977; de Muizon & Henzey 1980; de Muizon 1982a; King 1983; Wyss 1988a). Complete fusion is typically observed in later fossil pinnipeds, but not in the earlier basal forms (Repenning & Ray 1977; de Muizon & Henzey 1980; Wyss 1988a), leading to suggestions that the unfused morphology is primitive for phocids (Ray 1976a; de Muizon 1982a). In addition to the two extreme morphologies, we noted that in some specimens, preliminary fusion had occurred between the epiphysal heads (typically in the anterodorsal region), but was incomplete in other regions. In accordance with King's (1956) suggestion that the fusion between the tibia and the fibula may be among the last to occur during ontogeny, this latter condition (state 1) may represent a developmental artifact.

Any fusion of the tibia and fibula is apomorphic within the Caniformia. *Martes* is unique among fissipeds in displaying the rudimentary fusion of these two elements (state 1). At the earliest, complete fusion occurs as a synapomorphy of the pinnipeds (with a reversal in *Odobenus*; ACCTRAN optimization), but for the phocids in any case (with a convergent appearance in *Zalophus*; DELTRAN optimization). Full or partial reversals within the phocids are reasonably limited. Partial reversals occur independently in the phocines *Phoca largha* and *Pusa sibirica* (possibly as a synapomorphy with *Pusa hispida*; ACCTRAN optimization). A full reversal unites the monachines *Lobodon* plus *Monachus* spp., although all species except *Monachus schauinslandi* are polymorphic for states 0 and 1.

184) relative degree of development of the post-tibial (= intercondyloid) fossa of tibia: 0 = weak; 1 = strong (King 1966; Wyss 1988a).

King (1966) distinguished between the phocines and monachines by noting a greater tendency for a more pronounced post-tibial fossa in the former (also de Muizon & Henzey 1980). Other than for a curious tendency towards the phocine condition in the fossil lobodontine *Homiphoca* (Henzey & Repenning 1972; de Muizon & Henzey 1980), this appears to be a unique feature for the phocines, with the fossa being shallow in the otarioids and most fissiped carnivores (Wyss 1988a). However, among the outgroups examined here, only *Canis* demonstrated a weak post-tibial fossa, rendering the polarity of this character equivocal at the level of the Caniformia. The strong fossa typical of fissipeds is largely retained in the pinnipeds, with only *Monachus schauinslandi* plus *Monachus tropicalis*, *Phoca largha*, and *Pusa sibirica* independently deriving a weak fossa. This outcome (plus the high incidence of polymorphism in this character) seriously detracts from the ability of this character to distinguish between the two phocid subfamilies, and may stem from the lack of any substantial difference between the two character states. This, in turn, might relate to the lack of any substantial differences among caniform astragalar trochleae, the structure that articulates with the post-tibial fossa.

*185) robustness of calcaneum: 0 = smaller than or subequal to astragalus; 1 = larger than astragalus (de Muizon 1982a).

The comparative robustness of the calcaneum, when the astragalus is used as a reference, merely reflects the presence or absence of the posterior process on the plantar aspect of the astragalus. As this duplicates character #186, this character was excluded.

186) posterior process on plantar aspect of astragalus: 0 = absent; 1 = present (de Muizon 1982a).

The condition of the phocid astragalus is unique among mammals. Firstly, the astragalus possesses a strong posterior process causing it and the calcaneum to assume roughly equal sizes (Howell 1928; de Muizon 1982a; pers. obs.; see character #185). Secondly, the plantar surface of this posterior process is marked by a distinct groove for the passage of the flexor hallucis longus tendon (see the following character). In phocids, this tendon is better developed than it is in other mammals and plays a key role in their swimming locomotion. In fact, the hypertrophy of this tendon is responsible for another diagnostic feature of the phocids, that of being unable to turn the hind feet forward while on land (Howell 1928; de Muizon 1982a; King 1983). As indicated, the development of a posterior process is synapomorphic for phocids, and is possessed by all extant species (including *Monachus tropicalis*).

187) depth of groove on plantar aspect of posterior process of astragalus: 0 = groove absent; 1 = shallow; 2 = moderate; 3 = deep; 9 = posterior process absent (de Muizon 1982a).

As indicated by the previous character, the groove on the plantar aspect of the astragalus is unique to the phocids (Howell 1928; de Muizon 1982a; King 1983). However, this groove is not equally developed among the phocids, ranging from shallow to deep, and even virtually absent in many monachines (pers. obs.). The differential expression of this feature in the two phocid subfamilies renders the ancestral state for the phocids uncertain. The phocines are characterized ancestrally by a deep groove. This is reduced to a shallow groove in *Phoca* spp. and *Pusa* spp., before the primitive phocine morphology is regained in *Erignathus*, *Histriophoca*, and *Pagophilus*. The monachines are defined by a lack of the groove, although most taxa within this subfamily are polymorphic between this state and states for grooves of various depths.

188) length of metatarsal III relative to remaining metatarsals (shape of posterior flipper margin): 0 = metatarsal III longest; 1 = metatarsal III intermediate; 2 = metatarsal III subequal or slightly shorter; 3 = metatarsal III distinctly shorter (King 1966; Wyss 1988a).

All phocids are characterized by a shortening of the third metatarsal relative to the remaining metatarsals, with the reduction tending to be more extreme in the monachines than in the phocines (King 1966; Wyss 1988a). However, rather than view this as a synapomorphy of the monachines, Wyss (1988a) was more inclined to view shortening as primitive for the phocids, with the phocines partially reversing to approach the typical carnivore pattern (states 0 or 1). This was supported by the observation that *Cystophora* does not group with the phocines, but instead displays a monachine degree of reduction (Wyss 1988a). A reduced third metatarsal is not present in the otarioids, where all metatarsals are of about equal length (Wyss 1988a). Together with the relative reduction of all bones of the third digit of the hind foot (King 1983), the shortening of the third metatarsal also has coincident effects on the shape of the posterior flipper margin as a whole. All phocids possess a concave outline to the posterior flipper to some degree, and, again, it is much more marked in the monachines and the phocines *Cystophora* and *Histriophoca* (King 1983; Wyss 1988a). Phocines, and *Erignathus* in particular, tend

towards a straighter posterior flipper margin (Wyss 1988a). As the outline of the posterior flipper could not be observed directly, we concentrated instead on the relative size of the third metatarsal.

Most fissipeds are characterized by the plesiomorphic state, whereby the third metatarsal is the longest, although *Enhydra* and *Ursus* independently obtain state 1. A shortened third metatarsal is diagnostic of the pinnipeds, with the otarioids generally obtaining state 2 while the phocids derive state 3 ancestrally. No separation between the two phocid subfamilies was obtained here, as virtually all taxa retained a distinctly shortened third metatarsal. Again, this is due, in large measure, to the historically rather arbitrary distinction between the phocine and monachine morphologies ("slightly shorter" versus "distinctly shorter") that was difficult to quantify here. Only *Pusa caspica* [as obtained from Wyss (1988a)] and *Histiophoca* convergently reverse towards the typical fissiped pattern by obtaining state 2. If this observation for *Histiophoca* is accurate, then a severe shortening of the phalanges of the third hind digit must account for the concave posterior flipper margin reported for this genus (see above).

189) relative degree of development of hind flipper claws: 0 = not well developed or absent; 1 = well developed, prominent (King 1966; Wyss 1988a).

As with the foreflippers (see character #169), there exists a tendency towards reduction of the hind flipper claws in the pinnipeds. For the phocids at least, the pattern is more unmistakable. Phocines again have well developed hind flipper claws, while those of all monachines are markedly reduced (King 1966, 1983; Wyss 1988a). The otariids now present something of a categorical problem, as the hind flipper claws are large, but are only present on the middle three digits (Howell 1928; King 1983; Wyss 1988a). *Odobenus* presents less of a problem. Although it likewise possesses the three grooming claws, they are quite small (King 1983; Wyss 1988a). Missing data were again supplemented with observations from King (1966).

The apomorphic reduction of the hind flipper claws occurs independently on three occasions within the Caniformia: *Enhydra*, the otarioids generally (*Zalophus* is regarded here as being polymorphic for this character), and the monachines. This may be a synapomorphy of these taxa, with *Lutra* and the phocines re-obtaining large claws (ACCTRAN optimization), or be the result of parallel evolution (DELTRAN optimization).

Miscellaneous (7 characters)

This section includes hard anatomical characters that did not fall into the other categories and selected soft anatomical features.

190) location of posterior end of cribriform plate: 0 = within interorbital region; 1 = posterior portion of interorbital region; 2 = anterior end of braincase (pers. obs.) (Fig.19).

Perhaps associated with the lateral compression of the interorbital region of the pinnipeds (Howell 1928; King 1972, 1983; see character #49), we noted that the posterior end of the cribriform plate in this group is generally shifted posteriorly. Instead of lying distinctly within the (anterior end of the) interorbital region, as in most caniforms, the plate in all pinnipeds is located within the posterior end of the interorbital region, or, at its most

extreme, at the point where the interorbital region merges with the braincase (pers. obs.). This posterior shift arises somewhere within the lutrines and is retained throughout the pinnipeds. The lutrines and basal monachines generally possess the intermediate condition (state 1), while the remaining pinnipeds are characterized by the more extreme morphology. This shift to the anterior end of the braincase may be a synapomorphy of the pinnipeds, with state 1 being derived ancestrally in the monachines (ACCTTRAN optimization), or the ancestral state for the pinnipeds and phocids may be equivocal between states 1 and 2 (DELTRAN optimization).

191) relative position of vertebrarterial (= intervertebral) foramen of atlas: 0 = visible in dorsal view; 1 = visible in posterior view (King 1966; Wyss 1988a).

Another distinction between the phocid subfamilies concerns the position of the vertebrarterial foramen of the atlas. In phocines, as in most carnivores, the foramen is only visible in posterior view. Only among canids and monachines does the foramen become visible in dorsal view (King 1966; Wyss 1988a). Some problems do exist with this character. *Monachus* spp. more closely approach the typical carnivoran pattern (King 1966; Wyss 1988a). As well, the unusually large size of the foramen in *Odobenus* and *Monachus tropicalis* makes it at least partially visible in both dorsal and posterior views. Here, a dorsally visible vertebrarterial foramen was only present for *Hydrurga* among the monachines, along with a convergent appearance in *Canis*. Although many monachines were polymorphic for this character, this distribution renders both the polarity of this character and its utility for elucidating phocid relationships questionable.

192) claw morphology in cross-section, I: 0 = semicircular; 1 = triangular (Doutt 1942; Ridgway 1972).

Together with the following character, Doutt (1942) used the shape of the claws in cross-section to distinguish between *Phoca vitulina* (state 0) and *Histiophoca*, *Pagophilus*, and *Pusa hispida* (all state 1). Ridgway (1972) applied the same character to distinguish between the genera *Phoca* spp. (state 0) and *Pusa* spp. (state 1). However, observations for both this and the following character were hindered by the general paucity of suitable material. Observations could not be made for *Mirounga angustirostris*, *Phoca largha*, and *Pusa caspica*, and the condition for a number of other specimens could only be estimated from the ungual processes of the terminal phalanges. Bearing this in mind, only *Mirounga leonina* consistently possessed the apomorphic triangular morphology, possibly as a synapomorphy with *Mirounga angustirostris* (ACCTTRAN optimization). A fair number of other pinnipeds were polymorphic for this trait.

193) claw morphology in cross-section, II: 0 = dorsal ridge or annuli absent; 1 = dorsal ridge or annuli present (Doutt 1942; Ridgway 1972).

In combination with the previous character, Doutt (1942) used the presence of a dorsal ridge on the claw to distinguish between *Pusa hispida* (state 1) and *Histiophoca*, *Pagophilus*, and *Phoca vitulina* (all state 0). Again, Ridgway (1972) applied this character to distinguish *Phoca* spp. (state 0) from *Pusa* spp. (state 1). Heeding the problems mentioned under the previous character, an apomorphic dorsal ridge was present only in *Pusa sibirica* and then only polymorphically.

194) mystacial whiskers: 0 = smooth; 1 = beaded (Wyss 1988a).

Systematic differences in the form, distribution, and number of vibrissae are apparent throughout the pinnipeds (see Ling 1977). One striking morphology [although it may be dependent on the thickness of the whisker (Chapskii 1967)] is the apomorphic derivation of beaded mystacial whiskers. This condition, which gives the whisker a wavy outline, is found to varying degrees in all phocids except *Erignathus* and *Monachus* spp., which exhibit the typical carnivoran pattern (also found in the otarioids) of smooth whiskers (King 1983; Wyss 1988a). This distribution has been interpreted to support the primitive position of *Monachus* spp. within the phocids, with a convergent reappearance in *Erignathus* (Wyss 1988a). As suitable material was often lacking to make direct observations, we relied heavily upon the data of Wyss (1988a) to fill in any gaps.

The distribution above is indicated here. Beaded whiskers describe a synapomorphy of the phocids with *Erignathus* and *Monachus* spp. independently reversing to re-obtain the plesiomorphic condition. However, this character does not support a basal position for *Monachus* spp. as supposed by Wyss (1988a). Instead the two genera independently re-obtain smooth mystacial whiskers.

195) secondary hairs: 0 = (largely) absent; 1 = present (Wyss 1988a).

Carnivoran hair occurs in discrete units of a central primary hair surrounded by numerous, smaller secondary hairs (Scheffer 1964; Wyss 1988a). As noted by Wyss (1988a), characters involving either the morphology or the distribution of hair within these units appear to be a potentially valuable, but sadly neglected area of pinniped systematics (see Ling 1978). One interesting variation on the "monotonous" pinniped hair pattern (Scheffer 1964: 299) is the virtual lack of the secondary hairs in *Odobenus*, *Mirounga* spp., and *Monachus* spp. At best, secondary hairs appear in one out of every 10 hair units in these taxa, while some lack secondary hairs altogether (Scheffer 1964; Ling & Bryden 1981; Wyss 1988a). As we could not make direct observations for this character, the data of Wyss (1988a) were used. Parallel apomorphic losses of the secondary hairs in each of the three genera above are indicated.

196) relative overall size of males and females: 0 = females smaller than males; 1 = females subequal to males; 2 = females larger than males (Ralls 1976; Kovacs & Lavigne 1992; McLaren 1993).

Sexual dimorphism in which the male is larger than the female is common throughout the Caniformia. This sexual dimorphism tends to reach an extreme in the otariids, where the male may be four and a half times the size of the female in some species. Phocids exhibit both sexual dimorphism and monomorphism, but are unusual in that females are larger than males in certain species (Ralls 1976; Kovacs & Lavigne 1992). In some phocids, corresponding sexual differences are apparently noticeable with respect to the robustness of the skull (Allen 1887, 1902).

Data for this character were obtained exclusively from the literature. Sources include Bertram (1940), Ralls (1976), Bigg (1981), Bonner (1981), Burns (1981), Frost & Lowry (1981), Kenyon (1981a, 1981b), Kooyman (1981a, 1981b, 1981c), Ling & Bryden (1981), McGinnis & Schusterman (1981), Odell (1981), Ray (1981), Reeves & Ling (1981), Ronald & Healey (1981), King (1983), Nowak (1991), and McLaren (1993). Whenever

possible, preference was given to those sources employing growth curves (e.g., McLaren 1993) or statistics (e.g., Ralls 1976), as they presumably would be less prone to sampling effects than isolated descriptions. As well, lengths were preferentially used to judge size rather than the more commonly used, and often more appropriate, measure of mass. As noted by McLaren (1993), weights are often not recorded for pinnipeds, and the high seasonal variation in pinniped blubber stores makes mass a less reliable criterion for judging size in these animals.

The plesiomorphic condition among the Caniformia is for the male to be larger than the female. This is found universally among all outgroups and is retained into the basal members of each phocid subfamily. Beyond this, the trend within each subfamily is for parallel derivations of monomorphism. This occurs for the phocine clades *Erignathus*, *Histiophoca*, plus *Pagophilus*; and *Pusa hispida* plus *Pusa sibirica*. As well, it characterizes the lobodontines plus *Monachus* spp., with *Hydrurga* and *Ommatophoca* convergently deriving the condition whereby the female is the larger sex.

Summary

Several features of the character set presented above (and, indeed, the data matrix as a whole) need to be stressed. This data matrix is one of the most comprehensive ever compiled (with respect to the number of taxa and morphological characters) to answer the question of phocid phylogeny. To our knowledge, the only other comparable matrix is that of Berta & Wyss (1994). But, beyond its sheer size, another advantageous feature of the matrix lies in the wide range of osteological characters that were employed, originating from virtually all regions of the organism. Most of these characters appear to be phylogenetically informative (but see below), including many of the 28 that were excluded from the analysis. In most cases, these latter characters were excluded as they were deemed to be redundant when considered in the light of other characters. This primarily reflects presence of “character pairs”, where the first character examined for the presence of a feature, while the second detailed the morphology of that feature. However, in some cases, redundant characters reflected an inferior coding scheme (characters #18, 32-36, and 100). Only five characters were excluded a priori because we felt that they were of a dubious nature (characters #1, 2, 90, 124, and 129). However, of those apparently phylogenetically informative characters that remained, many could be improved still further (i.e., have their information content increased) through recoding to remove the apparent a posteriori cases of homoplasy (i.e., non-homologous similarity) within them as advocated by Hennig (1966). (It should be noted that very few characters, discounting within terminal changes, can be seen to possess a “clean” distribution free of any homoplasy.) Largely, this involves a refinement of the coding scheme to distinguish between morphologically very similar, but non-homologous character states (e.g., see character #116).

Several discrepancies can be noted between historical observations of some characters and our observations. No doubt, this can be traced, in part, to the unusually high intraspecific variation among cranial features in pinnipeds. Thus, both sets of observations might well be accurate, but only with respect to the specimen(s) that they were obtained from [and within the bounds of the subjective judgement of different researchers for many qualitative

features (e.g., small versus medium versus large)]. However, another source for any discrepancies might be that we have recorded data for each individual species, whereas many previous studies attempted to describe features that were presumed to apply throughout, or felt to be primitive for, some higher level taxon (e.g., King 1966; Wyss 1988a; Wozencraft 1989; Berta 1991). By examining all phocid species, we believe that we have shown that some of these generalities of phocid (or phocine, or monachine, ...) morphology do not necessarily hold absolutely among all of the concerned species. Finally, some inconsistencies between the inferred evolutionary pathways can also be noted. In most cases, this is due to the pathways being derived from different cladograms. However, in a fair number of other cases [most notably, those arising from Wyss (1988a)], the historical evolutionary pathway was shown to be only one of two equally parsimonious possibilities, corresponding to the singular use of only one optimization criterion available for character reconstruction.

Yet, the most disconcerting contradiction arises when the characters are viewed individually, as opposed to collectively. Together, all of the 168 included characters produced a very clean solution, with a somewhat surprisingly low number of equally most parsimonious (and slightly less than most parsimonious) solutions (see **Overall Parsimony Analysis** and **Statistical Tests**). However, when viewed individually, as in this section, very few characters directly and unequivocally indicate the overall solution that they do as a group (i.e., Fig.5B). This is even more apparent when the entire data matrix is divided into process partitions (sensu Bull et al. 1993; i.e., the characters were roughly divided into distinct anatomical regions) and analyzed separately (Fig.25). (Note that in order to generate character sets of sufficient size to yield reasonable resolution, characters originating from the forelimb, pelvis, hind limb, and atlas were grouped as "post-cranial" characters, while those from the bony falx and tentorium, dorsal braincase, and mandible, and all soft-anatomical features were grouped as "miscellaneous" characters.) Although the resolution is surprisingly good given the very reduced number of characters per taxon (due, in part, to the unusually high number of multistate characters, which can support more putative synapomorphies per character), none of the indicated cladograms really supports a solution comparable to the overall solution. Monophyly of the phocids, one of the strongest nodes in the overall solution, is only indicated in the consensus solutions of the character sets from the basicranial, teeth (which is to some degree an artifact of our coding many teeth characters as being inapplicable for the outgroup taxa, thereby forcing a monophyletic Phocidae), and miscellaneous regions (Fig.25D, E, and G). Monophyly of the phocid subfamilies is even rarer, being indicated only by the basicranial (Phocinae only) and post-cranial (both Monachinae and Phocinae) character sets (Fig.25D and F).

Of the individual results worth noting, the now abandoned Cystophorinae (= *Cystophora* plus *Mirounga* spp.) is clearly supported by both snout and teeth characters (Fig.25A and E). This distribution of support corresponds quite nicely with the major features used to define the Cystophorinae – a 2/1 incisor formula and some form of inflatable nasal proboscis in the adult males, plus some additional minor characteristics from the same regions (see King 1966; Ridgway 1972) – which were based on feeding specializations and sexual selection (McLaren 1975). Additionally, it appears that even the distinctive

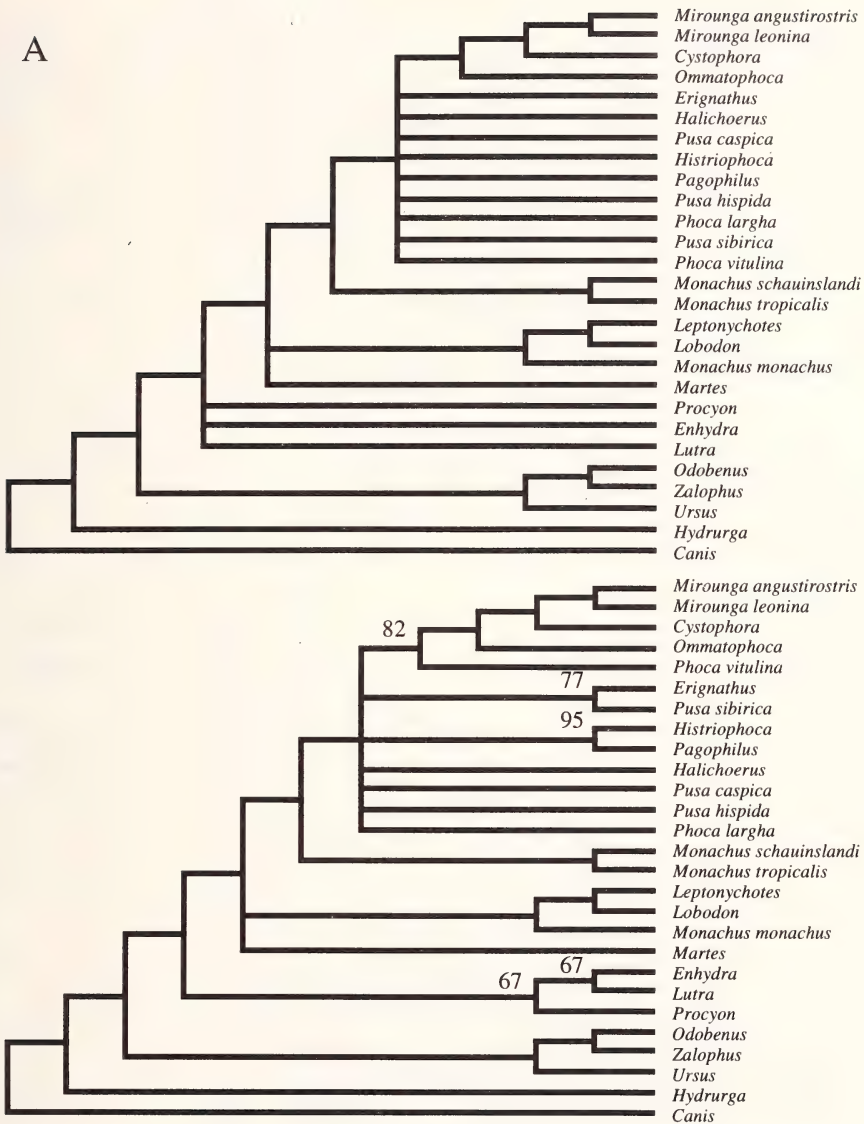


Fig.25A: Consensus solutions (top – strict algorithm; bottom – majority rule algorithm) resulting from a parsimony analysis of the inversely weighted data matrix subdivided according to the region of character origin: (A) snout (18 characters, $n = 66$ trees, length = 5,667 steps, CI = 0.486, HI = 0.710, RI = 0.701, RC = 0.474). Lengths and goodness-of-fit statistics apply only to the majority rule consensus solution, where, unless otherwise indicated, all nodes were found in 100% of the equally most parsimonious solutions.

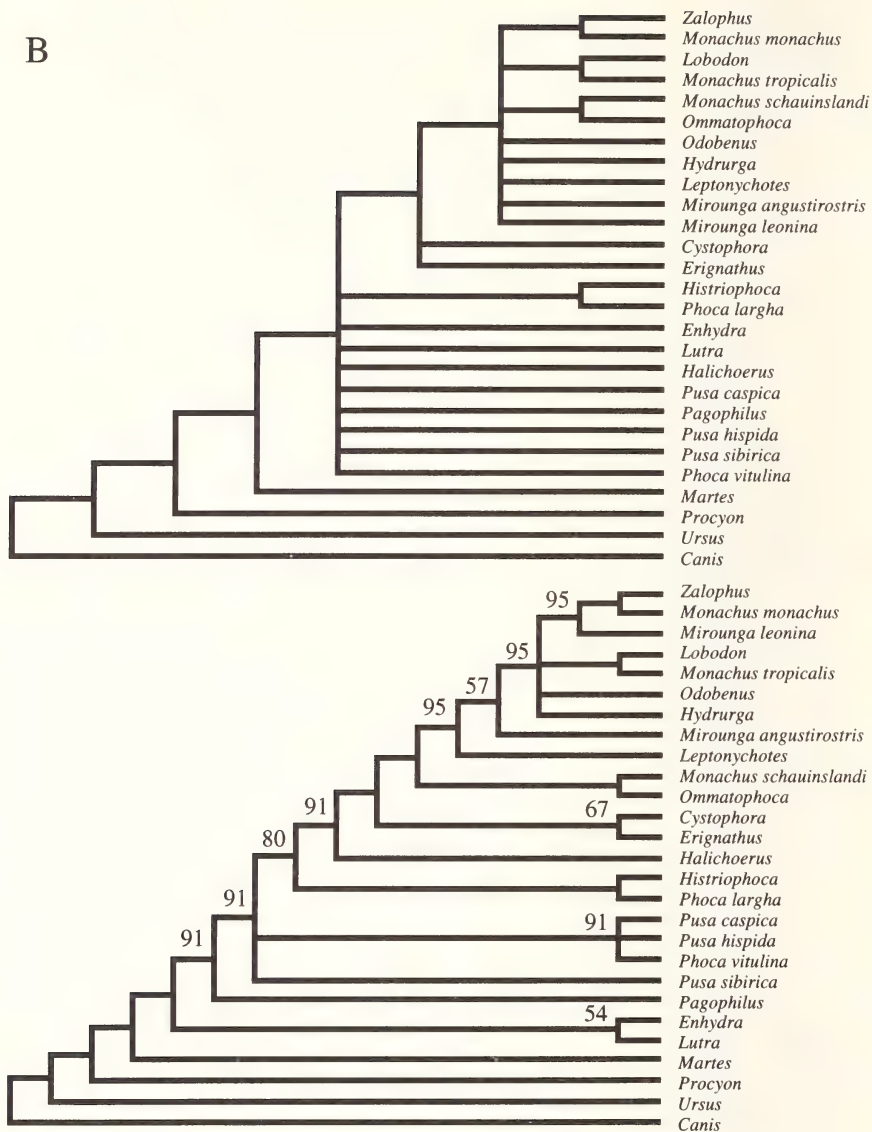


Fig.25B: Consensus solutions (top – strict algorithm; bottom – majority rule algorithm) resulting from a parsimony analysis of the inversely weighted data matrix subdivided according to the region of character origin: (B) orbit (25 characters, n = 334 trees, length = 10,032 steps, CI = 0.477, HI = 0.759, RI = 0.646, RC = 0.449). Lengths and goodness-of-fit statistics apply only to the majority rule consensus solution, where, unless otherwise indicated, all nodes were found in 100% of the equally most parsimonious solutions.

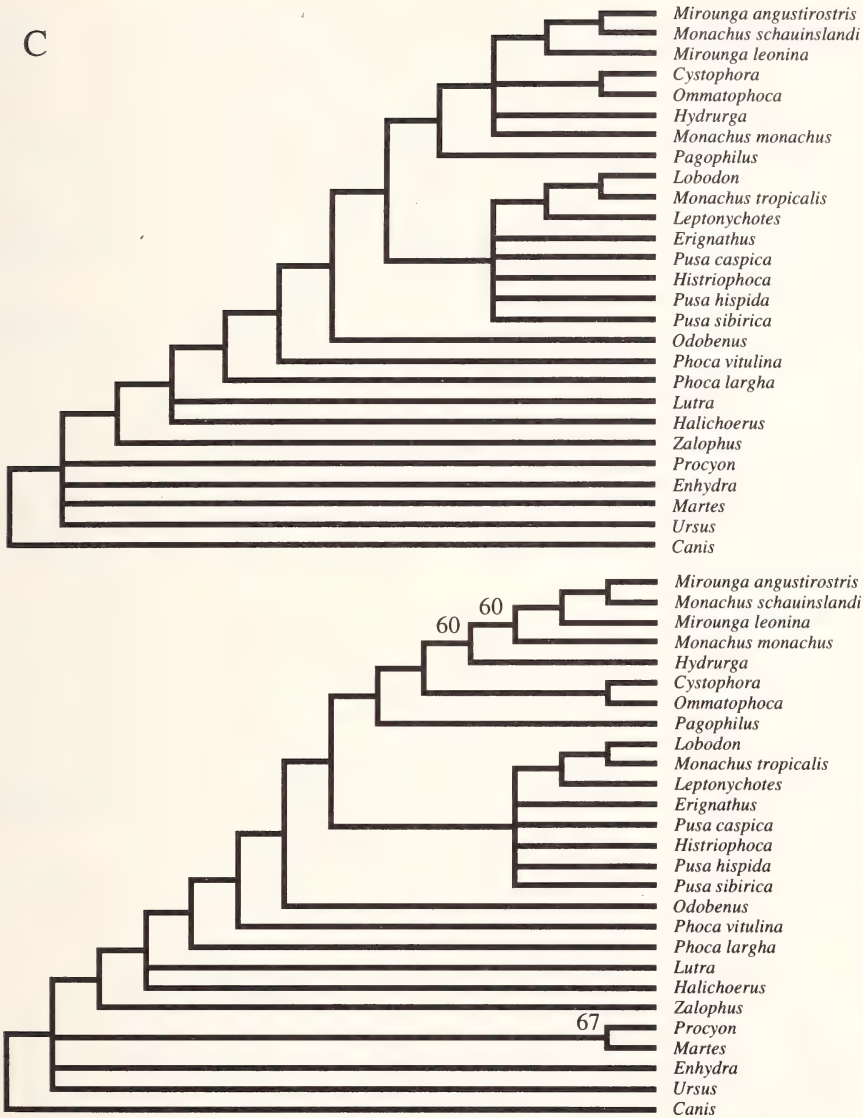


Fig.25C: Consensus solutions (top – strict algorithm; bottom – majority rule algorithm) resulting from a parsimony analysis of the inversely weighted data matrix subdivided according to the region of character origin: (C) palate and ventral side of snout (16 characters, $n = 720$ trees, length = 7,251 steps, $CI = 0.718$, $HI = 0.784$, $RI = 0.664$, $RC = 0.477$). Lengths and goodness-of-fit statistics apply only to the majority rule consensus solution, where, unless otherwise indicated, all nodes were found in 100% of the equally most parsimonious solutions.

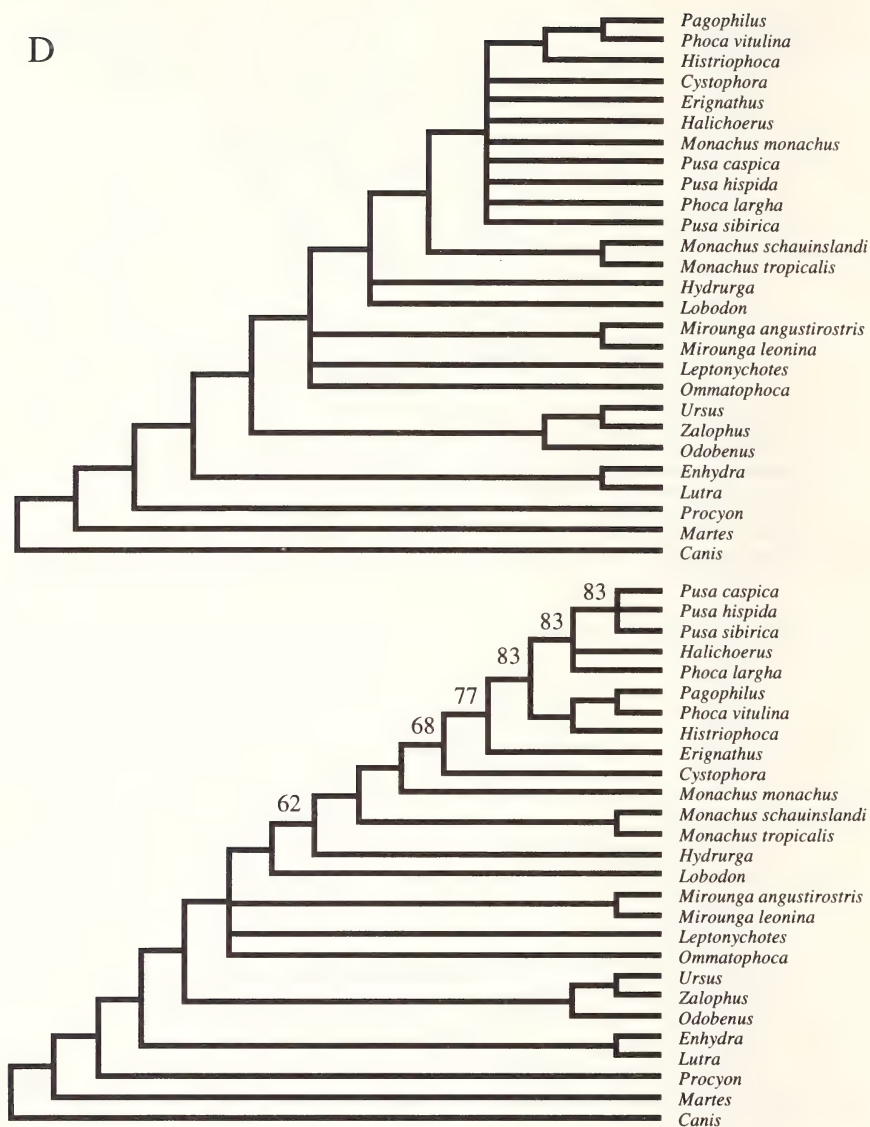


Fig.25D: Consensus solutions (top – strict algorithm; bottom – majority rule algorithm) resulting from a parsimony analysis of the inversely weighted data matrix subdivided according to the region of character origin: (D) basicranial region (38 characters, $n = 195$ trees, length = 12,360 steps, CI = 0.489, HI = 0.705, RI = 0.700, RC = 0.475). Lengths and goodness-of-fit statistics apply only to the majority rule consensus solution, where, unless otherwise indicated, all nodes were found in 100% of the equally most parsimonious solutions.

E

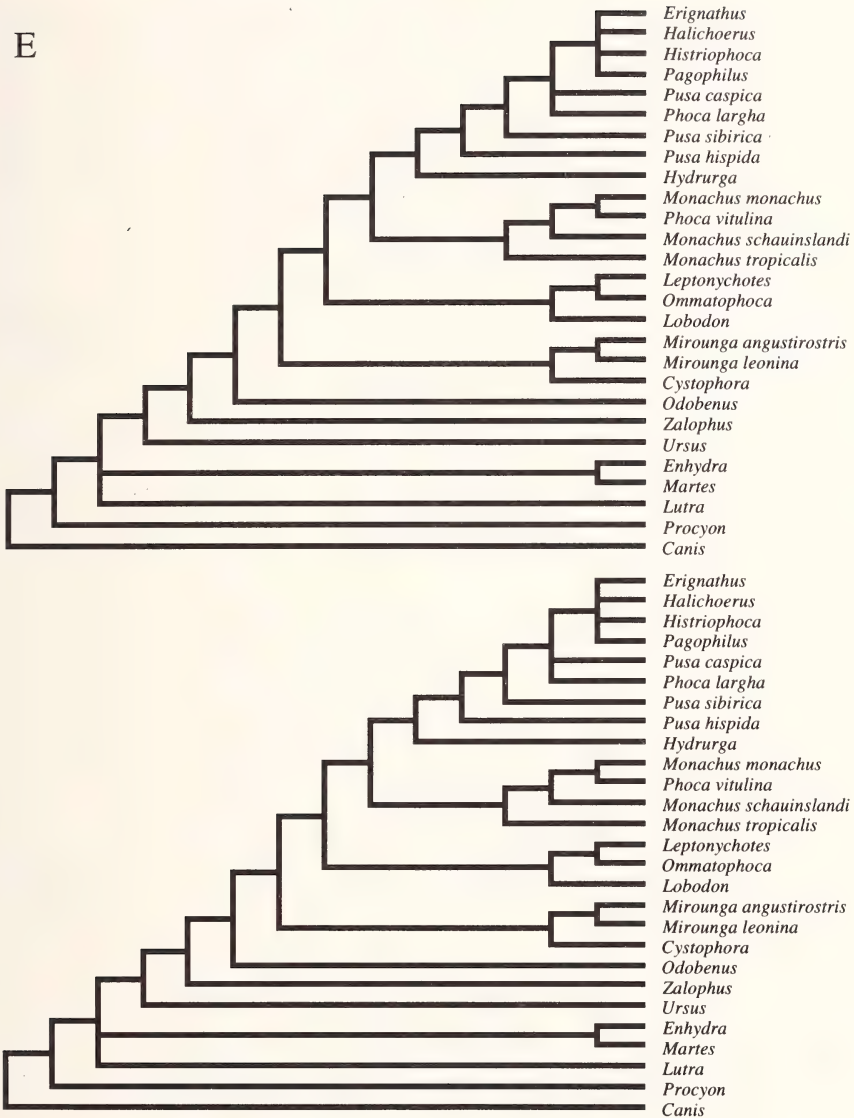


Fig.25E: Consensus solutions (top – strict algorithm; bottom – majority rule algorithm) resulting from a parsimony analysis of the inversely weighted data matrix subdivided according to the region of character origin: (E) teeth (22 characters, $n = 12$ trees, length = 6,912 steps, CI = 0.749, HI = 0.694, RI = 0.762, RC = 0.570). Lengths and goodness-of-fit statistics apply only to the majority rule consensus solution, where all nodes were found in 100% of the equally most parsimonious solutions.

F

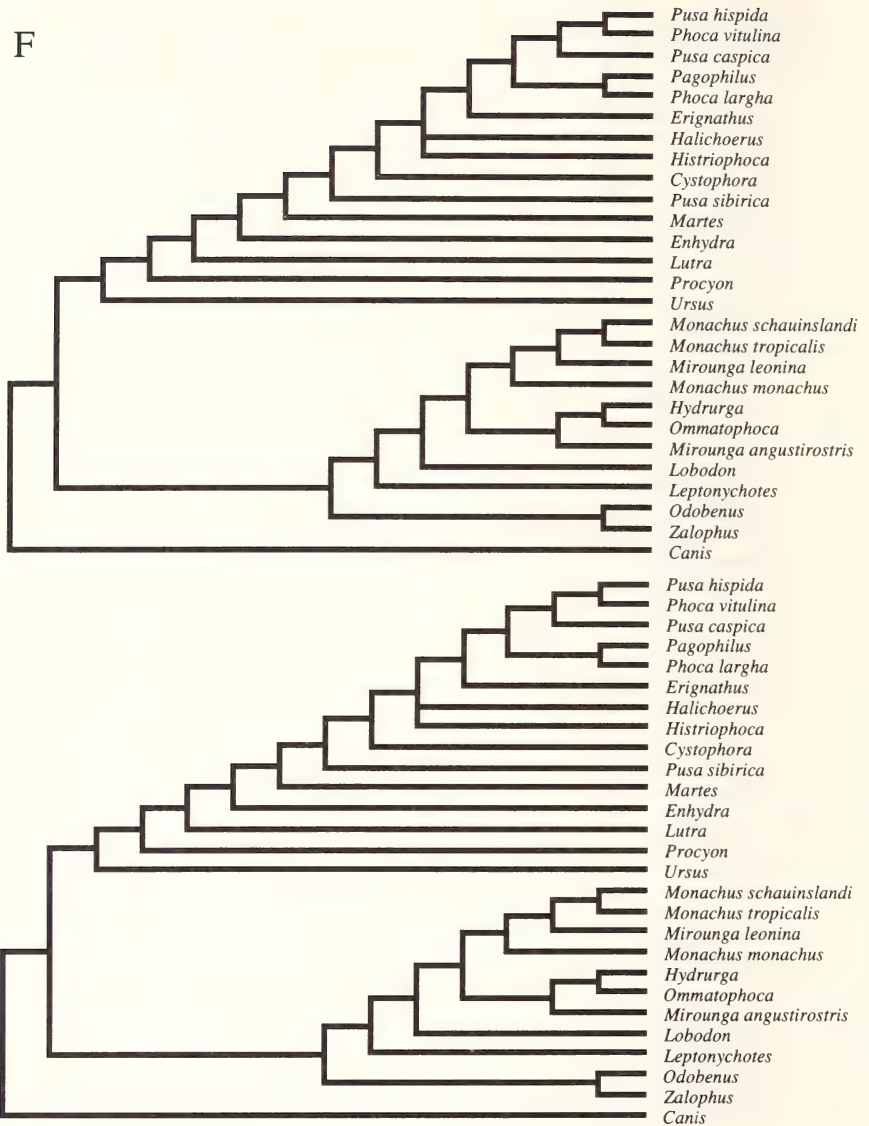


Fig.25F: Consensus solutions (top – strict algorithm; bottom – majority rule algorithm) resulting from a parsimony analysis of the inversely weighted data matrix subdivided according to the region of character origin: (F) postcranial region (32 characters, $n = 3$ trees, length = 14,883 steps, CI = 0.725, HI = 0.787, RI = 0.777, RC = 0.563). Lengths and goodness-of-fit statistics apply only to the majority rule consensus solution, where all nodes were found in 100% of the equally most parsimonious solutions.

G

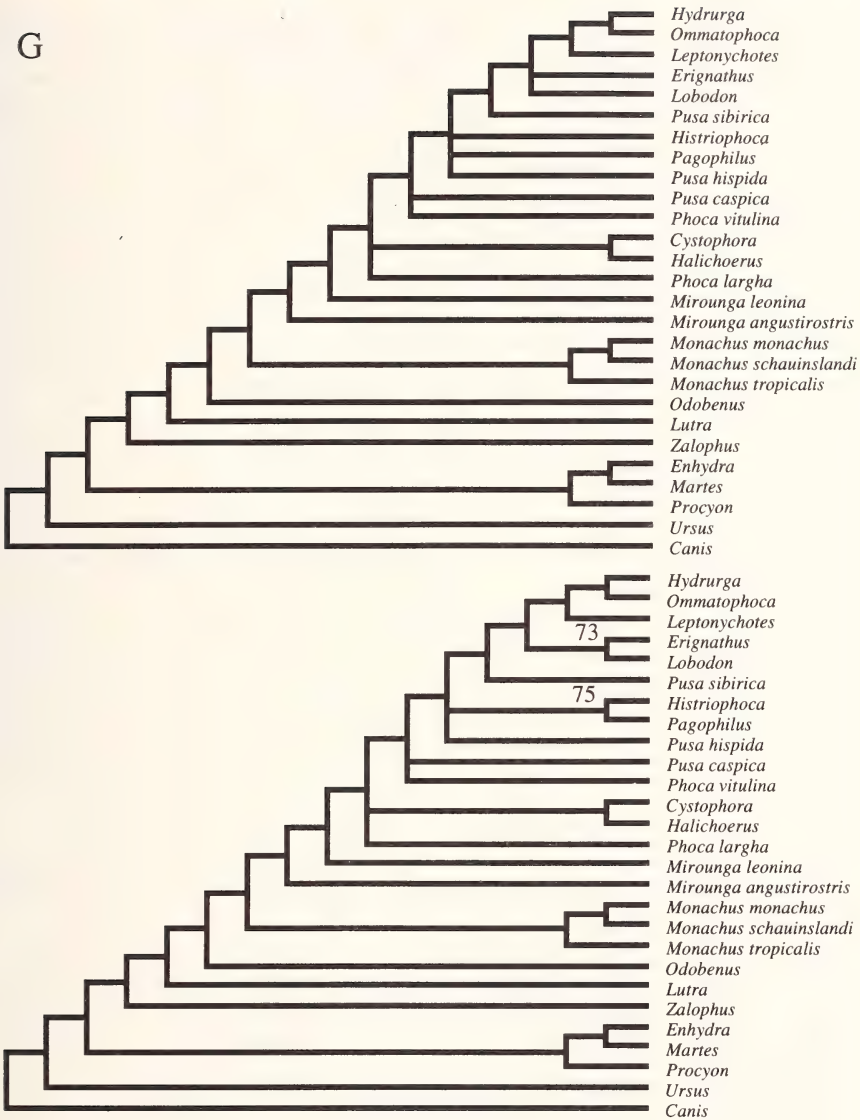


Fig.25G: Consensus solutions (top – strict algorithm; bottom – majority rule algorithm) resulting from a parsimony analysis of the inversely weighted data matrix subdivided according to the region of character origin: (G) miscellaneous features (17 characters, n = 44 trees, length = 6,366 steps, CI = 0.767, HI = 0.758, RI = 0.773, RC = 0.593). Lengths and goodness-of-fit statistics apply only to the majority rule consensus solution, where, unless otherwise indicated, all nodes were found in 100% of the equally most parsimonious solutions.

form of the phocid pelvis (de Muizon 1982a) is not sufficient to assure the monophyly of the phocids over the whole of the post-cranial features (Fig.25F). However, the apparently distinctive nature of the monachine post-cranial morphology as a whole (see Hendey & Repenning 1972; Wyss 1988a) is indicated here, with the monachines, together with the otarioids, being clearly separated from the remaining arctoid carnivores and the phocines. This apparent conflict between the overall and regional solutions, and between the individual regional solutions, can be attributed to one of two causes: 1) sampling error, or 2) the presence of more than one signal within our data set. The potential effects of sampling error have perhaps been underestimated in phylogenetic analysis. It is possible that many competing hypotheses of phylogenetic relationships stem from a biased selection of characters from the universe of all possible characters. With the use of appropriately designed tests, such competing hypotheses may be shown to be statistically equivalent. Such may also be the case here. Although sampling error can never be eliminated, it can be minimized by selecting a random set of characters (or, at least, a wide range of characters) from the universe of all possible characters. The selection of a wide range of characters is the more practical option at this point in time; however, it is susceptible to the second, more serious error source, that of different signals within the process partitions. The possibility of such additional, non-phylogenetic processes being a potential source of character covariation has been mentioned by Faith & Cranston (1992) and Hillis & Huelsenbeck (1992). An obvious example here is for the teeth, where the determining signal is likely a "functional" one, derived from the demands of food specialization within the phocids (see Chapskii 1955a; McLaren 1975). Within the more restricted and more localized regional character sets, these various signals are apparently sufficient to swamp the single (phylogenetic?) signal that predominates at the level of all characters. In all cases, these "regional signals" are also quite strong, indicating a less homoplasious solution (as indicated by the four goodness-of-fit statistics; see Fig.25) than does the "overall signal" (compare with Fig.5). This is especially true of the basicranial, teeth, post-cranial, and miscellaneous data sets. (The dramatic increase in CI for some regions is an artifact of there not being any uninformative characters included in their partitions of the entire data matrix.)

Given such strong "regional signals", we can see how the "overall signal" might have surfaced within the larger data set by examining a closely analogous situation. Wilkinson (1991) suggested that increasing numbers of homoplastic characters (which might be derived from the "regional signals" here) could be accommodated within a data set, so long as they are randomly distributed. Farris (1969) made an even stronger statement in that, given certain conditions (including the random distribution of homoplasy), the number of homoplastic characters could outnumber the number of informative ones (and by a considerable amount) without being detrimental. It would appear then that the various "regional signals" within our data matrix are so localized as to become "insignificant" at the level of the whole matrix. However, the conflicts between these "regional signals", and between each and the "overall signal", are still sufficiently strong to make the overall solution more homoplasious than any of the regional ones. The "overall signal" would appear to be a more widespread, but slightly more dilute signal than the regional ones, which are apparently very strong in certain restricted anatomical regions.

Therefore, if the desired signal in a phylogenetic analysis is the “overall signal” (see **Statistical Tests** section; although the “phylogenetic signal” could equally be one of the “regional signals”), then phylogenies based largely on a set of characters from a single localized region should be avoided. Although the morphologies of any characters obtained from this one region will likely be strongly correlated with one another, this correlation can very often arise from some non-phylogenetic process [e.g., the general resemblance of the snout in *Cystophora* and *Mirounga* spp., which is a manifestation of the morphological requirements of possessing a (convergently derived) inflatable proboscis]. Again, of the two solutions mentioned above, the more practical at this point is to examine a wide range of characters, possibly as a first step towards a total evidence approach. However, this should be done with some caution. The very different signals from the various, supposedly discrete anatomical regions beg the statistical question of whether these separate matrices should have been “pooled” in the first place (see Bull et al. 1993), a major limitation of the total evidence approach. Therefore, one would ideally want to generate a set of randomly distributed characters, as we have argued previously (see **Statistical Tests** section), but it is difficult to fathom how the degree of randomness of such a set could be ascertained. In any case, when properly applied, either method should increase the probability of generating a data matrix where the influence of the various non-phylogenetic signals is minimized, allowing the presumably more widespread phylogenetic signal to dominate and determine the resultant outcome.

It remains then for the final section to present a short summary of the phylogeny of the phocids indicated in this study, including identifying the areas of stronger and weaker support. Various selected implications of this phylogeny will also be examined, as will the lines of research still required in the area of phocid systematics.

DISCUSSION AND CONCLUSIONS

We here recap this study by first presenting an overall summary of the phylogenetic findings in light of the results of the many statistical tests performed and comparative tools employed in the **Statistical Tests** and **Comparative Tools** sections. Possible sources of error affecting the validity of any conclusions thereby reached will be analyzed, before the remainder of this section is given to such miscellaneous topics as the taxonomic implications of our proposed phylogeny of the phocids, concordance of our proposed phylogeny with other lines of evidence (primarily biogeographical and fossil), and, finally, possible future lines of research suggested by this study.

Summary of results

Virtually all of the analyses conducted in the **Overall Parsimony Analysis**, **Statistical Tests** and **Comparative Tools** sections point to a single common pattern, which Faith (1992) would equate with a form of Popperian corroboration. With respect to the overall solution (Fig.5B), outgroup relations clearly possess the strongest support within the cladogram, demonstrating alterations in their topology only when specifically forced to do so. However, as indicated by the constraint analyses (see **Comparative Tools** section),

and as suggested by Sarich (1976), Wayne et al. (1989), Perry et al. (1995), and C.A. Repenning (pers. comm.), the specific pattern advocated here for the outgroup interrelationships might be an unnatural resolution of what should really be a polytomy. Reasonably strong support was also obtained for the phocids as a whole and for each phocid subfamily, but, beyond this, support drops off markedly. Yet, despite relatively weak statistical support, the pattern of monachine interrelationships (and the monophyly of *Monachus* in particular) appears to be exceptionally robust, emerging unaltered in virtually every analysis (again, unless specific changes were imposed upon the subfamily). Relationships within the phocines, and especially within the Phocini (plus *Erignathus*), were demonstrably more labile, showing slightly different patterns with almost every analysis. Topological changes within the Phocini (plus *Erignathus*) could also be effected by imposing changes within the Monachinae. The analogous reverse situation was never observed.

Although many novel, non-traditional relationships are indicated within the phocids by this study, it is worth noting that most studies of phocid phylogeny that employed some form of rigorous methodology (e.g., King 1966; Burns & Fay 1970; Wyss 1988a) have, for their respective times, also advocated some fairly non-traditional relationships. As well, the novel relationships advocated here enjoy reasonable support throughout the many analyses within this study. This is particularly true of the more terminal position within the phocines advocated herein for *Erignathus*. In fact, this historically-regarded "primitive" and "monachine-like" phocine is apparently responsible for causing *Histiophoca* and *Pagophilus* to occupy a more terminal position, and possibly even a relationship based on synapomorphies and not symplesiomorphies, than they might otherwise possess without its influence. The new relationships presented for *Erignathus* likely arise from a fairer appraisal of its overall morphology, without an undue emphasis on some of its (undisputed) more primitive, monachine-like characters. Instead, *Cystophora* is proposed as the sister taxon to the remaining phocines. The similar role played by *Mirounga* within the monachines suggests that the now defunct Cystophorinae may display a large number of phocid symplesiomorphies, especially in features originating from the nasal region. This supposition is strengthened by the appearance of similar features in the fossil pinniped *Allodesmus* (Mitchell 1975), especially with its re-interpreted position as part of the sister group to the phocids (Wyss 1987; Berta 1991; Wyss & Flynn 1993; Berta & Wyss 1994). This distinctive nasal region morphology is also apparently responsible for the moderately strong tendency of *Cystophora* to form the sister taxon of the monachines. The species level approach adopted here permits paraphyly of the lobodontines, a reasonably poorly examined group whose assumed monophyletic status had apparently never been rigorously examined. However, paraphyly of this tribe is dependent on the invasion of the monophyletic *Monachus*. Like *Erignathus*, a more terminal position for *Monachus* may have been hindered historically by a disproportionate emphasis on the (again undisputed) more primitive features of this genus. But, like the other relationships within the monachines, this more terminal position for *Monachus* appears to be fairly robust.

Thus, of the five questions raised in the **Introduction**, we propose the following answers:

1) *Monachus* is monophyletic, with *M. schauinslandi* and *M. tropicalis* sharing a common

ancestor to the exclusion of *M. monachus*; 2) the Phocini are paraphyletic, as are its constituent genera *Phoca* (both sensu stricto and Burns & Fay 1970), and possibly *Pusa*; 3) the Monachinae are monophyletic; 4) the species level relationships of the phocids are as indicated in Fig.5B; and, 5) the pinnipeds are monophyletic, with lutrine affinities.

Potential sources of error

Obviously, the above conclusions must be viewed in the light of a number of qualifying statements. Perhaps the key such qualification is that we have merely presented a summary of one particular data set, using one particular method of tree reconstruction, and whose underlying distribution need not necessarily coincide with the actual phylogeny of the phocids (see also **Statistical Tests** section). Therefore, any judgment as to the accuracy of the results presented herein must ultimately derive from an assessment of the overall quality of the data set, and whether the characters examined in this study constitute a reasonably random sample from the universe of all possible characters. Given these restrictions, however, we believe that both the size and scope of our data matrix give this study several advantages over previous analyses of phocid phylogeny. To our knowledge, this study is the only species level analysis of the entire phocid family. Thus, no potential pairings of species were prevented by the assumed monophyly of any higher level taxa. As well, multiple specimens were examined for each species to attempt to account for the unusually high amount of intraspecific variation within the pinnipeds (Mivart 1885; Dutt 1942; King 1966; Ray 1976b). A wide range of characters, representing most of the osseous skeleton, were also employed, the use of which allowed for a data matrix with very few missing data points. This range of characters, moreover, provided a better overall representation of the suite of all possible characters, the impetus behind the total consensus approach to phylogenetic analysis (see Kluge 1989; Kluge & Wolf 1993). In contrast, the use of sets of characters derived primarily from single anatomical regions yielded solutions even more in conflict with the "traditional wisdom" regarding phocid phylogeny. Finally, simplifying and/or biasing assumptions (e.g., use of only a single outgroup, avoidance of polymorphic data) were avoided, hopefully resulting in a more realistic analysis.

Yet, the sources of information employed in this study still possess inherent limitations. The imposed exclusion of any fossil taxa (due to their general unavailability) could prove detrimental due to the possible effects of the exclusion of any taxa in a low level analysis such as this (Arnold 1981). Be that as it may, the extremely poor fossil record of the pinnipeds, and of the monachines in particular (Hendey & Repenning 1972; Ray 1976a), equates to a high proportion of missing (i.e., undiscovered) fossil taxa. As well, the exclusion of fossil pinniped taxa does not appear to alter the basic topology of pinniped relationships as determined from extant forms only (Flynn et al. 1988; Berta & Wyss 1994). Nonetheless, it would have been interesting at the very least, and informative in any case (particularly with respect to elucidating the evolutionary pathway of certain characters), to have included various fossil pinnipeds and putative fossil pinniped ancestors (e.g., the lutrine-like *Potamotherium*).

Of more concern is the high intraspecific variation characteristic of the pinnipeds mentioned above. This variability is so severe with respect to cranial anatomy in particular,

that Ray (1976b) regards any conclusions based on a limited number of skulls as being extremely tentative (also Davies 1958b). This potential source of error impacts primarily on such species as *Mirounga angustirostris* and *Monachus monachus*, where only a limited number of specimens were available for study (see Appendix A). Fortunately, Kesner (1994) indicates that beyond some minimal number of specimens, it is more advantageous (with respect to error and statistical power) to increase the total number of characters rather than to examine more specimens (to reduce the probability of including an incorrect character state). As well, the modified majority rule algorithm used to determine the consensus character states for each species should reduce the presence of any outright erroneous or trivial states in the data matrix, while hopefully retaining the more important polymorphisms.

As well, the type of data employed in this study might have had some effect on the overall result obtained. The discordance between phylogenies derived from morphological versus biochemical or molecular data has long been noted (see Hillis 1987; Patterson et al. 1993). This conflict has been attributed to the different assumptions and methods of analysis inherent for each data type (Hillis 1987), but may also derive from the fact that morphological and molecular data are apparently the most effective at phylogenetic reconstruction at different taxonomic levels. In assessing attempts to resolve the phylogenetic relationships of the even-toed ungulates (Mammalia: Artiodactyla), Novacek (1993) pointed out that molecular data have produced good resolution for the internal (intra-ordinal) relationships of the group, but not for its outgroup (inter-ordinal) relationships, where morphological data have performed better.

Apparently, molecular data appear to work better at the lower taxonomic levels (see Irwin & Arnason 1994: 53). At progressively higher levels, the accumulation of neutral changes should tend to obscure any phylogenetic signal, being visualized either as a reasonably high amount of homoplasy, or as a general lack of resolution (although conservative molecular regions may be more immune to this potential problem). Conversely, morphological data appear to work better at higher taxonomic levels. As well as being potentially afflicted by some or all of the problems mentioned by Arnold (1981), morphological data do not appear to be discriminatory enough to pick out some of the fine differences required for a species level analysis. Largely, this seems to stem from the traditional use of fairly obvious, but simple morphological characters (e.g., presence or absence of various processes, foramina, ...), which, when combined with the general predisposition towards binary characters, will ignore a vast assemblage of more complex, and potentially more finely discriminating, features (e.g., shape features as elucidated by some form of morphometric analysis). Apart from the increased effort required to acquire these more complex characters, their acceptance has been hindered by the perception that the features are somehow not "real" or discrete, and therefore not subject to natural selection in the same way. This latter point arises from our supposed functional and evolutionary "understanding" of morphological features, allowing us to a priori eliminate potential characters that might be unsuitable for various reasons (e.g., too homoplastic, too trivial).

This conflict between the two data types may have been manifested somewhat in this study with the acknowledgement that the pattern of outgroup relationships was generally

more strongly supported than that of the ingroup relationships. However, reasonable resolution was still found within the phocids, perhaps due to an increased number of more discriminating, non-traditional and/or multistate characters. Increased resolution is still possible, especially within the Phocini (plus *Erignathus*), where even more finely discriminating data are required to dissect the evolutionary pattern out of the rapid adaptive radiation of the group (see below).

Finally, one limitation of cladistic analysis as it applies here, and specifically as it applies to the determination of homologous features, needs to be addressed. The increasing evidence for, and consequent acceptance of pinniped monophyly (e.g., Wyss 1987; Flynn 1988; Flynn et al. 1988; Berta 1991; Cozzuol 1992; Novacek 1992; Wyss & Flynn 1993; Vrana et al. 1994; Arnason et al. 1995; Lento et al. 1995; this study), together with the interpretation that the aquatically related features of the group are homologous, and not convergent (Wyss 1988b), needs to be reconciled with available fossil evidence. Currently, the fossil record of the pinnipeds strongly indicates distinct, if not diphyletic, origins of the otarioids and the phocids, whose first appearances in the fossil record are separated by the North American continent and some seven million years (Repenning et al. 1979). However, assuming for the moment that the known fossil evidence does provide an accurate picture of pinniped origins (but see below for alternative possibilities), note that it does not automatically imply the diphyly of the pinnipeds (as has been held in the past). Granting that the modern pinnipeds all originated from the same ancestral lineage, they would still fit under the strict cladistic definition of a monophyletic group – “a group of species that includes an ancestral species and all of its descendants” (Wiley et al. 1991: 3) – so long as their common ancestor did not also give rise to some other lineage that we would not classify as a pinniped.

Of more concern, however, is that the acceptance of the scenario given above by Repenning et al. (1979) would require us to re-interpret some otherwise apparently homologous features. Even if the pinnipeds are truly (strictly) monophyletic, their separate origins from a presumably terrestrial (or, at best, only partially aquatic) ancestor (as would likely be the case given their geographic separation) would mean that most of their aquatically related characters identified here and elsewhere (e.g., Wyss 1988b) as homologies, would have to have evolved in parallel. The common appearance of such features (and possibly of some non-aquatically related ones as well) would then be a consequence of the adaptational limitations imposed by the inheritance of a common, ancestral body plan (i.e., developmental constraints; see Maynard Smith et al. 1985), possibly based on some key innovation (*sensu* Liem & Osse 1975; see discussion in Russell 1979), combined with the necessity of adapting to an aquatic environment. (Naturally the case for convergent characters due to developmental and functional constraints becomes even more widespread if the Pinnipedia are diphyletic.) An interesting test of this scenario involves the lutrines and the polar bear [*Thalarctos maritimus*; Corbet & Hill (1991)], species becoming increasingly adapted to an aquatic environment. Given their derivation from a reasonably similar arctoid body plan, and a continued tendency towards an increasingly aquatic existence, these species may become indistinguishable from the pinnipeds in a few million years, despite their clearly

independent origin. It is often forgotten that the interpretation of apparent homologies as true homologies in a cladistic analysis is based on parsimony. Given other lines of evidence (which need not necessarily be additional cladistic analyses), such features may turn out to be homoplastic.

We do wish to add that we do not necessarily subscribe to the view that the aquatically related features of pinnipeds are convergently derived. We merely want to point out that the potential paleobiogeographical ramifications of a monophyletic Pinnipedia have largely been ignored to date (see below).

Taxonomic implications

One inescapable consequence of any systematic study is its potential impact on the taxonomy of the group being examined. The many novel relationships posited here for the phocids would argue for a fairly dramatic re-organization of the taxonomy of this group. Although we will outline what some of these changes should be (or at least provide a list of equally acceptable options), we do not intend to propose these changes in a formal manner. They are merely presented as the logical extension of the phylogeny that we have presented.

The monophyly of both *Monachus* and of the Monachinae as a whole allows for these entities to retain their taxonomic status (as a genus and subfamily respectively), without having their names placed in quotation marks (as in Wyss 1988a; Berta & Wyss 1994). The paraphyly of the Lobodontini, meanwhile, argues for one of two solutions. The first has the Monachini (= *Monachus* spp.) subsumed within the Lobodontini, which has priority [see historical review in Scheffer (1958)]. The Miroungini (= *Mirounga* spp.) would remain as a distinct tribe. The second option is for the Lobodontini to be abolished, possibly together with all tribal designations in the monachines as suggested by Hendey & Repenning (1972) and King (1983).

Within the phocines, a similar list of choices is available for the paraphyletic Phocini: either outright abolition or the inclusion of *Erignathus*. The former option seems more tenable, as there appears to be no legitimate reason to exclude only *Cystophora* from the fairly wide range of morphological variation encompassed by such a newly defined Phocini. [Arnason et al. (1995) also indicate that the distinction between *Cystophora* and the Phocini (excluding *Erignathus*) appears to be fairly minor.] The more derived position of *Erignathus* also renders *Phoca* (sensu Burns & Fay 1970) paraphyletic. The elevation of the various subgenera to full generic status, as was done in this study, is not permissible as *Phoca* (sensu stricto), and possibly *Pusa*, would be paraphyletic. This is true regardless of whether *Phoca largha* is granted species status or not. Again, there are two possible solutions to this problem. The first, and the simplest, involves subsuming *Erignathus* as a subgenus within *Phoca* (sensu Burns & Fay). There is some precedence for this, as *Phoca* is the senior synonym for *Erignathus* (as is the case for most phocids) (see Scheffer 1958). A similar procedure has also been advocated for *Halichoerus* by Arnason et al. (1993, 1995). The second solution involves the elevation of all subgenera back to generic status, but with new generic appellations being found for *Phoca largha* and possibly *Pusa caspica*, neither of which possess available generic synonyms.

Other obvious changes are required outside of the phocids (e.g., the pinnipeds should no longer be a carnivoran suborder, but a tribe within the lutrines), but the wholesale alterations to arctoid taxonomy that this would require, even ignoring the difficulties in the application of the term "monophyly" to the pinnipeds (see above), are beyond the scope of this study.

Biogeography and fossil evidence

As a group, the phocids possess one of the more interesting biogeographical distributions among mammals. They are found in both hemispheres, but, excepting *Monachus* spp. which are the only phocids to inhabit tropical climes, are largely limited to the polar and sub-polar regions of each [see Scheffer (1958) and King (1983) for precise species ranges]. This, coupled with a postulated North Atlantic origin for the family (McLaren 1975; Ray 1976a; Repenning et al. 1979), has led to many theories as to the development of the current species distribution. It is not our intent here to develop a new biogeographic hypothesis for the phocids based on the phylogeny advocated herein, but rather to compare this phylogeny with some of the biogeographic hypotheses that have already been put forth.

The basic biogeographic theory for the phocids holds for a North Atlantic origin of the family around the early middle Miocene [15 million years before present (MYBP)]. Fully-fledged representatives of both the monachines and phocines are found in this initial fauna. The remainder of the Miocene saw the isolation of a group of phocines (later to give rise to *Pusa* spp.), and possibly isolated monachines, in the Paratethys Sea, a large ancient sea covering much of what is now eastern Europe. Other phocines and monachines continued to inhabit the North Atlantic at this time, with the monachines being the dominant form, especially on the North American side (Hendey & Repenning 1972; Grigorescu 1976; Ray 1976a; Repenning et al. 1979). Climatic deterioration during the Pliocene evoked different responses on the part of the North Atlantic phocids. The monachines largely retreated southward, retaining their pagophobic habits, while the phocines, although also retreating southward to some degree, responded more by adapting to the cooler climate (Hendey 1972; Ray 1976a).

Within the monachines, *Monachus* spp. (or ancestors thereof) are posited to have remained behind as the remainder of the subfamily continued moving southward. Two competing hypotheses exist as to how the three species of monk seal arose: a progressive westward waif dispersal from the northwest coast of Africa (Hendey 1972; de Muizon 1982a), or the interruption of the gene flow of a wide-ranging North Atlantic population (giving rise to Mediterranean and Caribbean populations), followed by waif dispersal to the Hawaiian islands (Ray 1976a). In either case, *M. schauinslandi* and *M. tropicalis* are held to share a common ancestor to the exclusion of *M. monachus* (in contrast to more recent opinion). The remaining monachines continued their southward migration either on the Pacific side of South America (Repenning et al. 1979), the Atlantic side (Hendey 1972), or on both sides (Ray 1976a; de Muizon 1982a).

Less is known about the phocines, as their poor fossil record combined with a recent post-early Pliocene and/or Pleistocene adaptive radiation (Ray 1976a) largely hinder any detailed description of the dispersal pattern within the subfamily. One theory advocates two separate dispersal movements (McLaren 1975; Ray 1976a; Repenning et al. 1979). The first movement involves an initial northward migration from the *Pusa*-like ancestors of the Paratethys Sea into the Arctic basin, followed by an eastward migration to give rise to modern *Pusa* spp. The land-locked *Pusa caspica* and *Pusa sibirica* are thus apparently remnant populations of this initial Paratethyan stock (although the case is not as clear for *P. sibirica*), rather than migrating in from the Arctic basin during the Pleistocene (see below; also McLaren 1960a; Grigorescu 1976). The second movement involves a westward migration of the remaining phocines from the North Atlantic to their current ranges. Both migrations used the Arctic basin to traverse the North American continent. A second theory (Davies 1958b), although not mentioned per se, apparently holds for a North Atlantic origin for all phocines, with subsequent migrations into the Arctic basin during interglacial periods. Repeated glacial events then divided the different species into their Atlantic and Pacific subspecies, or pushed them away from their original North Atlantic range (as was felt to be the case for *Histriophoca*, *Pusa caspica*, and *Pusa sibirica*). *Pagophilus* and *Histriophoca*, in particular, were posited to be sister species separated by the most recent glaciation event (Davies 1958b).

Altogether, the phylogeny of the phocids presented in this study raises several conflicts with the biogeography of the family as outlined above. These conflicts are present throughout the cladogram. Among outgroup relationships, the potential discrepancy between the increasingly accepted monophyly (likely in a strict cladistic sense) of the pinnipeds, and the separate origins of the otarioids and phocids indicated by the fossil record might be due to the inadequacies of the latter. The most parsimonious solution is for a common origin for all pinnipeds (presumably in the earlier North Pacific site), with our first record of a phocid not being until seven million years later, by which time its ancestors had migrated to the North Atlantic, either northward through the Arctic basin or southward through the Central American Seaway. Surprisingly, to our knowledge, only Costa (1993) has recently suggested such a scenario (and specifically via the southerly route), despite the continual recent allying of the Atlantic phocids with the Pacific desmatophocids (an extinct group of pinnipeds comprised of the genera *Allodesmus*, *Desmatophoca*, and *Pinnarctidion*) within a monophyletic Pinnipedia (Wyss 1987; Berta 1991; Wyss & Flynn 1993; Berta & Wyss 1994). Indeed, the possible biogeographical ramifications of a monophyletic Pinnipedia have been virtually ignored (e.g., see Wyss 1987:25), possibly in light of the strong counter-arguments provided by Ray (1976a: 396-397).

Of the two possible routes to the Atlantic, the southerly route is the more probable. A migration through the Arctic basin does not even appear to be feasible as the Bering land bridge generally blocked access to it from about the late Oligocene to the early Miocene (Hopkins 1967). Some northward migration might have occurred given that modern pinnipeds are capable of migrating surprising distances over land (see Scheffer 1967), something likely even more readily accomplished by their less aquatically adapted

ancestors (see also de Muizon 1982a). As well, the Bering Strait may have been infrequently open around this time (Hopkins 1967). However, a more severe obstacle to a migration through the Arctic basin is its colder climate, which would presumably hinder the progression of the pagophobic phocid ancestors (Scheffer 1967; Ray 1976a). In contrast, the Central American Seaway seems to be a more likely option. By all accounts, it was wide open throughout much of the late Oligocene to early Miocene and beyond (Davies 1958a; Berggren & Hollister 1974; Ray 1976a; de Muizon 1982a), and the use of this route does allow the phocid ancestors to maintain their warm water affinities in agreement with the supposed warm water origin of the phocids in the North Atlantic. Although the utter lack of any phocoid fossils in the reasonably well known Oligocene to Pleistocene fauna of the Pacific coast of North America has been used to argue against a common Pacific origin (Barnes & Mitchell 1975; Ray 1976a), the acceptance of a desmatophocid sister group to the phocids does much to ameliorate this. The various desmatophocid genera are known to have existed around the time of the first appearance of the phocids and their ranges extended at least to south central California for certain species of both *Allodesmus* and *Pinnarctidion* (Mitchell 1975; Repenning 1975; Barnes 1979). Thus, the phocids may represent an offshoot of one of these lineages that migrated through the Central American Seaway into the North Atlantic, as was later also held to have been done by the ancestors of the modern walrus (Repenning 1975; Repenning & Tedford 1977; Repenning et al. 1979).

Within the phocids (accepting the minimal position that the North Atlantic served as the common dispersal site of the family), the terminal position of *Monachus* spp. within the lobodontines demands either a northward re-invasion by this genus from some southern hemisphere locale, or for multiple southward invasions by the lobodontines. There is some precedent for either a northward re-invasion (albeit slight) by, or a more southerly extension of, the *Monachus* lineage. Hendey (1972) holds for a slight northward "re-invasion" by the ancestors of *M. tropicalis*, while *M. monachus* has been reported as far south as Senegal in historical times (Hendey 1972). As well, fossil allies of *Monachus* (i.e., fossil Monachini) have been reported from Peru (de Muizon 1982a), although they more likely represent an unsuccessful colonizing population. The case for *Mirounga* spp. is equivocal here, and does not speak for southward migrations on either the Pacific (e.g., Ray 1976a; de Muizon 1982a) or Atlantic coast (e.g., Hendey 1972) of South America (but see below).

The case for putative northern re-invasions becomes stronger if one examines the timing of parturition among the monachines. Among phocids, parturition typically occurs during the spring of their respective hemispheres (i.e., the beginning versus the end of the calendar year for the northern and southern hemispheres respectively). Curiously, however, the monachines *Mirounga angustirostris*, *Monachus monachus*, and *Monachus tropicalis* possess autumnal pupping times that coincide, in absolute terms, with those of the truly southern hemisphere monachines (Allen 1887; McLaren 1966; Hendey 1972; Bonner 1981; Kenyon 1981b; King 1983; also references in Hayssen et al. 1993). [Most European populations of *Halichoerus* also possess an autumnal pupping time (McLaren 1966; Bonner 1981; King 1983; also references in Hayssen et al. 1993), but this shift has been attributed to competition with *Phoca vitulina* for pupping sites (McLaren 1966).] The

atypical timing of parturition for the above monachines, combined with an apparent lack of alternative explanations such as competition for pupping sites, suggests a southern origin with a northern re-invasion (see Hendey 1972). In the case of *Mirounga angustirostris* in particular, this implies that *Mirounga* (or its ancestors) initially migrated southward along the Atlantic side of South America before rounding Cape Horn and moving northward along the Pacific side, as suggested by Hendey (1972).

Monachus schauinslandi presents several problems for this re-invasion hypothesis. It possesses a normal spring pupping time, although the observation that pupping may begin as early as December for this species (Kenyon 1981b; King 1983; also references in Hayssen et al. 1993) suggests that *M. schauinslandi* has perhaps shifted back towards a normal spring pupping time faster than the remaining northern monachines. Of more concern, however, is the requirement of placing *M. schauinslandi* in the Pacific. Only two routes are possible – through the Central American Seaway, as is universally suggested, or around Cape Horn, as has been postulated for *Mirounga* spp. (Hendey 1972) – and neither is adequate here. Use of the Central American Seaway possesses a time limit, with its closure to marine dispersal occurring at least three and a half to four MYBP (Ray 1976a; de Muizon 1982a). In order to accord with our proposed phylogeny, the northward migration of *Monachus* spp. from the higher southern latitudes (after their derivation from lobodontine stock) would have had to be very rapid indeed. This scenario may well be impossible when allied with the suggestion that the full adaptation of the lobodontines to the high Antarctic latitudes occurred no more than four million years ago (Ray 1976a). However, combined with the suggestion of multiple invasions of the Antarctic continent by the lobodontines (Hendey 1972; McLaren 1975; de Muizon 1982a), it may be that the divergence of the lobodontines and *Monachus* spp. occurred in the middle southern latitudes. The only other possibility, that of an early dispersal of *Monachus schauinslandi* through the Seaway (with little or no previous southward migration), would strongly contradict our cladogram, as it would presumably render this species as the sister group to the remaining monk seals, and very likely to the remaining monachines as well. This is the accepted route however, with the invasion occurring between 8.5 to 13 MYBP (Hendey 1972) or even earlier (Repenning and Ray 1977). Costa (1993) even goes so far to suggest that *M. schauinslandi* did not even migrate through the Central American Seaway with the remaining ancient phocids in the first place. An important point to keep in mind with such early dispersal hypotheses for *M. schauinslandi* is that the main Hawaiian islands are only about six million years old (although the more westerly islands of the chain such as Laysan and Midway do date from 20 to 28 MYBP respectively) (Clague & Dalrymple 1989). Therefore, if such a scenario holds, it is more than likely that the ancestors of *M. schauinslandi* remained tied to the American coast for some time before a founder population reached the Hawaiian islands.

The second route, encircling Cape Horn, is not a viable alternative either. Again, it implies an early separation of *Monachus schauinslandi* from the *Monachus* lineage, leaving *M. monachus* and *M. tropicalis* either as sister taxa, or requiring them to migrate northward in parallel, possibly on either side of the Atlantic. This latter option does have the advantage of agreeing with the current (or historical for *M. tropicalis*) distributions of the

Atlantic *Monachus* spp. However, if *M. schauinslandi* is really the sister group to the remaining monk seals [as advocated by Repenning & Ray (1977) and Wyss (1988a)], then its migration around Cape Horn into the Pacific becomes more plausible, given a terminally placed *Monachus*.

The situation for the phocines is even less clear, with the phylogeny indicated here for this subfamily supporting (or at least not outright contradicting) each of the two major hypotheses presented above. Both do possess problems, however. Monophyly of *Pusa* spp. cannot be assured here, as required for the dual Paratethyan-North Atlantic origin hypothesis, while the relatively basal position of *Phoca largha*, an exclusively western Pacific species, is problematic for a mass origin from the North Atlantic alone. Another possibility might be that only *Cystophora* and *Halichoerus* originated from the North Atlantic, while the remaining, monophyletic forms all arose from the isolated Paratethyan stock. Support for this hypothesis comes from the fact that only *Cystophora* and *Halichoerus*, together with *Pagophilus*, are normally found exclusively in the Atlantic. [The Atlantic-only distribution of *Pagophilus* might have arisen as a result of a recent split in the Arctic basin of an ancestral lineage into the sister species *Histiophoca* and *Pagophilus*, as envisaged by Davies (1958b).] Again, the reasonably basal position of *Phoca largha* is problematic, as this species would presumably be derived from the original *Pusa*-like inhabitants of the Paratethyan, whereas the reverse is indicated here. However, the *Pusa*-like nature of the Paratethyan fauna might be overstated due to the predominance of its fossil material. Other phocine lineages (primarily *Phoca*-like forms) are also represented in the Paratethyan fauna (Grigorescu 1976), and *Phoca largha* (as well as the remaining non-pusids) might have originated from one of them.

Although many of the possible biogeographical options listed here involve long distance migrations for several species, comparable movements for several extant pinniped species are known (see Scheffer 1967; Ray 1976a). These examples include stray individuals that have either been found in presumably less desirable habitats (e.g., too warm for normally pagophilic species, or too cold for the less pagophilic ones), or whose presumed travel route would require traversing such habitats.

Future directions

The study of the evolutionary biology of the phocids faces two major obstacles at the moment. Firstly, the phylogenetic relationships within the Phocini (with or without *Erignathus*) continue to be problematic. In all truth, the pattern that we advocate here is merely one in a long line of hypotheses (e.g., Chapskii 1955a; McLaren 1966, 1975; Burns & Fay 1970; de Muizon 1982a; Arnason et al. 1995; Mouchaty et al. 1995; Perry et al. 1995). More research is needed in this area with techniques better suited to such low level analyses.

One such technique involves the use of molecular data which, paradoxically, has been used more up to now to elucidate the position of the phocids within the pinnipeds (e.g., Sarich 1969a, 1969b, 1975; Arnason 1974, 1977; Haslewood 1978; de Jong 1982; de Jong & Goodman 1982). Instead, the internal phylogeny of the phocid seals has been elucidated largely through the use of (traditional) morphological data. Some initial work

has been performed using molecular data (e.g., Sarich 1976; Arnason & Widegren 1986; Shubin et al. 1990; Baram et al. 1991; Arnason et al. 1993, 1995; Mouchaty et al. 1995; Perry et al. 1995), but only a few biomolecules have been analyzed, and typically only for a very limited number of species. However, the analysis of molecular data seems to hold more promise than does morphological data [but see Cummings et al. (1995) for possible limitations of such data]. As mentioned above, molecular data appear to provide better resolution at the lower taxonomic levels, and therefore might be able to resolve the polytomy within the Phocini. As well, in contrast to their high morphological intraspecific variability, particularly with respect to the skull (Mivart 1885; Doult 1942; Davies 1958b; Ray 1976b), pinnipeds, like most marine mammals, display an unusually low genetic variability (Arnason 1972, 1982; Shubin et al. 1990; Arnason et al. 1993). Presumably, this lower variability would allow for a clearer and stronger signal. Finally, the strong possibility of a molecular clock for some biomolecules (see Thorpe 1982) may allow for the dating of various divergence events, which, in turn, would allow for the examination of such ancillary questions as rates of speciation or extinction (see Harvey & Nee 1993). Yet, resolution at the lower taxonomic levels within the phocids may also be provided by a morphometric analysis of morphological data. Such analyses are commonly used at the specific or intraspecific level to assess differences within or between taxa (e.g., Jolicœur 1975; Thorpe 1975a, 1975b; Youngman 1982). By themselves, morphometric analyses only indicate degrees of similarity between taxa (Albrecht 1980); however, the results of such analyses could easily be transformed into cladistic characters [but see Farris (1990) for potential abuses of this]. This could make a vast suite of additional characters available for cladistic analyses that were previously avoided as their complexity (e.g., shape characters) makes them difficult to obtain and/or to code objectively, or because they were held to be phylogenetically uninformative. However, the phenomenon whereby two characters used in concert may show increased discriminatory power over when either is used in isolation (Lubischew 1962), allows for even seemingly uninformative characters to potentially play some phylogenetic role. As well, morphometric analyses may give us a more objective (i.e., statistical) means to judge the degree of information content in a character. Together, the cladistic analyses of both molecular data and morphological data using morphometric characters should enable a fully-resolved species level solution of the phocids. However, it should be realized that full resolution may not be possible, and that the indicated polytomy within the Phocini (plus *Erignathus* here) does, in fact, describe a real evolutionary event.

The second problem concerns the unusual biogeography of the phocids. The combination of a postulated North Atlantic origin for the phocids, plus the poor paleontological data for the family, has led to much uncertainty in attempts to explain the far-flung pattern of its extant members. These attempts are further hindered by being based largely on a rather superficial view of the phylogenetic relationships of the extant species. Of primary concern here is the tacit assumption of the monophyly of some higher level phocid taxa, the dangers of which are presented in this study. The monophyletic status of some of these taxa has also been called into question (Wyss 1988a; this study). However, with the lack of sufficient fossil evidence, any biogeographic hypothesis must minimally accord with current

systematic opinion. Ideally, the whole area of phocid biogeography needs to be re-examined, with an eye not only to paleontological and systematic data, but also to other historical lines of evidence (e.g., oceanic currents, potential migration routes, glaciation events, competition from other organisms). In the near future, however, any hypotheses will continue to be hindered by the poor fossil record of the family and that of the pinnipeds as a whole. Fortunately, interest in pinniped paleontology has increased in recent years, leading to many new finds, particularly in the southern hemisphere. We would suggest that additional effort should also be focused around the region of Central America to test the hypotheses of the initial eastward migration of the phocid ancestors through the Central American Seaway and the subsequent return migration of the ancestors of *Monachus schauinslandi*. Once all this new material is properly described and analyzed, a more comprehensive attempt at explaining the biogeographic distribution of the phocids can truly be made.

ABSTRACT

The phocid seals present an interesting puzzle within mammalian systematics. The undue attention focused on their contentious ancestral affinities (together with the ongoing debate over pinniped origins) has contributed, in part, to their internal phylogeny remaining reasonably poorly studied. Therefore, a species-level cladistic analysis was undertaken to resolve the overall phylogeny of this family. All recent phocid species were examined (including *Monachus tropicalis*), using representatives of all major extant caniform lineages as outgroups. 168 morphological characters (primarily osteological, and primarily those of the head skeleton) were examined.

A parsimony analysis using PAUP 3.1.1 revealed two equally most parsimonious solutions, each with a consistency index (corrected for uninformative characters) of 0.456. The recent supposition of a monophyletic Pinnipedia was upheld, albeit with lutrine, and not ursid affinities. However, this latter point may be an unnatural resolution of a real polytomy within the evolutionary history of the arctoids. A monophyletic Otarioidea formed the immediate sister group to the phocids. Within the phocids, reasonable support for both traditional subfamilies was found, albeit with novel relationships within each, particularly for their basal taxa. Both *Monachus* spp. and *Erignathus*, which have universally been viewed as the most primitive members of their subfamilies (Monachinae and Phocinae respectively), are held here to hold more derived positions (with strong support for a monophyletic *Monachus* as well), rendering the Antarctic Lobodontini and Arctic Phocini paraphyletic respectively. We suggest that perhaps undue attention has been focussed on the admittedly primitive features of both genera at the expense of other apparently more derived ones. Instead, the basal positions within each subfamily are suggested to be occupied by *Mirounga* spp. and *Cystophora* respectively, leading to the possibility that the diagnostic features of the now abandoned subfamily Cystophorinae may be based, to some degree, on phocid symplesiomorphies. Together with various statistical tests and comparative tools, reasonable support was indicated for this pattern of phylogenetic

relationships, albeit slightly higher among outgroup taxa. Demonstrably weak support (combined with poor resolution) was found only within the Phocini (plus *Erignathus*).

A detailed character analysis is also presented, including historical notes and the evolutionary pathway implied for each character from our cladogram. As well, comments regarding selected areas of cladistic methodology are also made.

LITERATURE CITED

- Albrecht, G.H. (1980): Multivariate analysis and the study of form, with special reference to canonical variate analysis. – *Amer. Zool.* 20:679-693.
- Allen, J.A. (1880): History of the North American pinnipeds: a monograph of walruses, sea-lions, sea-bears and seals of North America. – *Misc. Publ. U.S. Geol. Geogr. Surv. Terr.* 12:1-785.
- (1887): The West Indian seal (*Monachus tropicalis* Gray). – *Bull. Amer. Mus. Natur. Hist.* 2:1-34.
- (1902): The hair seals (family Phocidae) of the North Pacific Ocean and Bering Sea. – *Bull. Amer. Mus. Natur. Hist.* 16:459-499.
- Alroy, J. (1994): Four permutation tests for the presence of phylogenetic structure. – *Syst. Biol.* 43:430-437.
- Anonymous (1992): Convention on International Trade in Endangered Species of Wild Fauna and Flora (CITES), Control List. No. 10. Effective November 19, 1992. Ottawa, Canada: Environment Canada, Canadian Wildlife Service.
- Archie, J.W. (1989): A randomization test for phylogenetic information in systematic data. – *Syst. Zool.* 38:219-252.
- Arnason, U. (1974): Comparative chromosome studies in Pinnipedia. – *Hereditas* 76:179-226.
- (1977): The relationship between the four principal pinniped karyotypes. – *Hereditas* 87:227-242.
- (1982): Karyotype stability in marine mammals. – *Cytogenet. Cell Genet.* 33:274-276.
- Arnason, U., K. Bodin, A. Gullberg, C. Ledje, & S. Mouchaty (1995): A molecular view of pinniped relationships with particular emphasis on the true seals. – *J. Mol. Evol.* 40:78-85.
- Arnason, U., A. Gullberg, E. Johnsson, & C. Ledje (1993): The nucleotide sequence of the mitochondrial DNA molecule of the grey seal, *Halichoerus grypus*, and a comparison with mitochondrial sequences of other true seals. – *J. Mol. Evol.* 37:323-330.
- Arnason, U. & B. Widegren (1986): Pinniped phylogeny enlightened by molecular hybridizations using highly repetitive DNA. – *Mol. Biol. Evol.* 3:356-365.
- Arnold, E.N. (1981): Estimating phylogenies at low taxonomic levels. – *Z. Zool. Syst. Evolutionsforsch.* 19:1-35.
- Atchley, W.R. & B.K. Hall (1991): A model for development and evolution of complex morphological structures. – *Biol. Rev.* 66:101-157.
- Baram, G.I., M.A. Grachev, N.G. Malikov, P.V. Nazimov, & V.V. Shemiakin (1991): Amino acid sequence of myoglobin from seals from Lake Baikal. – *Bioorg. Khim.* 17:1166-1171. [In Russian; only English summary used].
- Barnes, L.G. (1979): Fossil enaliarctine pinnipeds (Mammalia: Otariidae) from Pyramid Hill, Kern County, California. – *Contrib. Sci., Natur. Hist. Mus. Los Angeles County* 318:1-41.
- (1989): A new enaliarctine pinniped from the Astoria Formation, Oregon, and a classification of the Otariidae (Mammalia: Carnivora). – *Contrib. Sci., Natur. Hist. Mus. Los Angeles County* 403:1-26.
- Barnes, L.G. & E.D. Mitchell (1975): Late Cenozoic northeast Pacific Phocidae. – *Rapp. P.-v. Réun. Cons. int. Explor. Mer* 169:34-42.
- Barrett, M., M.J. Donoghue, & E. Sober (1991): Against consensus. – *Syst. Zool.* 40:486-493.

- Berggren, W.A. & C.D. Hollister (1974): Paleogeography, paleobiogeography and the history of circulation in the Atlantic Ocean. In: W.W. Hay (ed.): Studies in Paleo-oceanography: 126-186. Soc. Econ. Paleontol. Mineral. Spec. Publ. 20, Tulsa, Oklahoma.
- Berta, A. (1991): New *Enaliarctos* (Pinnipedimorpha) from the Oligocene and Miocene of Oregon and the role of "enaliarctids" in pinniped phylogeny. – *Smithson. Contrib. Paleobiol.* 69:1-33.
- Berta, A. & C.E. Ray (1990): Skeletal morphology and locomotor capabilities of the archaic pinniped *Enaliarctos melesi*. – *J. Vert. Paleontol.* 10:141-157.
- Berta, A. & A.R. Wyss (1994): Pinniped phylogeny. In: A. Berta & T.A. Deméré (eds.): Contributions in Marine Mammal Paleontology Honoring Frank C. Whitmore, Jr: 33-56. Proc. San Diego Soc. Natur. Hist. 29.
- Bertram, G.C.L. (1940): The biology of the Weddell and crabeater seals: with a study of the comparative behaviour of the Pinnipedia. – *Br. Graham Land Exped., 1934-37 Sci. Rep.* 1:1-139.
- Bigg, M.A. (1981): Harbour seal – *Phoca vitulina* and *P. largha*. In: S.H. Ridgway & R.J. Harrison (eds.): Handbook of Marine Mammals 2:1-28. London: Academic Press.
- Bonner, W.N. (1981): Grey seal – *Halichoerus grypus*. In: S.H. Ridgway & R.J. Harrison (eds.): Handbook of Marine Mammals 2:111-144. London: Academic Press.
- Brookes, J. (1828): A catalogue of the anatomical and zoological museum of Joshua Brookes, Esq., F.R.S. F.L.S. & C. London: Richard Taylor, Fleet Street. 76 pp.
- Bryant, H.N. (1989): An evaluation of cladistic and character analyses as hypothetico-deductive procedures, and the consequences for character weighting. – *Syst. Zool.* 38:214-227.
- Bryant, H.N., A.P. Russell, & W.D. Fitch (1993): Phylogenetic relationships within the extant Mustelidae (Carnivora): appraisal of the cladistic status of the Simpsonian subfamilies. – *Zool. J. Linn. Soc.* 108:301-334.
- Bryden, M.M. (1971): Myology of the southern elephant seal *Mirounga leonina* (L.). – *Antarct. Res. Ser.* 18:109-140.
- Bull, J.J., J.P. Huelsenbeck, C.W. Cunningham, D.L. Swofford, & P.J. Waddell (1993): Partitioning and combining data in phylogenetic analysis. – *Syst. Biol.* 42:384-397.
- Burns, J.J. (1970): Remarks on the distribution and natural history of pagophilic pinnipeds in the Bering and Chukchi seas. – *J. Mammal.* 51:445-454.
- (1981): Bearded seal – *Erignathus barbatus*. In: S.H. Ridgway & R.J. Harrison (eds.): Handbook of Marine Mammals 2:145-170. London: Academic Press.
- Burns, J.J. & F.H. Fay (1970): Comparative morphology of the skull of the Ribbon seal, *Histiophoca fasciata*, with remarks on systematics of Phocidae. – *J. Zool., London* 161:363-394.
- Cavender, J.A. (1978): Taxonomy with confidence. – *Math. Biosci., London* 40:271-280. [Erratum: Vol. 44:308, 1979].
- (1981): Tests of phylogenetic hypotheses under generalized models. – *Math. Biosci., London* 54:217-229.
- Chapksii, K.K. (1955a): An attempt at revision of the systematics and diagnostics of seals of the subfamily Phocinae. – *Trudy Zool. Inst. Akad. Nauk SSSR* 17:160-199. [In Russian. English translation by T.F. Jeletzky, Fish. Res. Board Can. Transl. Ser. Number 114. 1957].
- (1955b): Contribution to the problem of the history of development of the Caspian and Baikal seals. – *Trudy Zool. Inst. Akad. Nauk SSSR* 17:200-216. [In Russian. English translation by the Bureau for Translations, Foreign Language Division, Dept. Secr. State Can. 1958].
- (1967): Morphological-taxonomical nature of the pagetoda form of the Bering sea Largha. – *Trudy Polyar. Nauchno-Issled. Proekt. Inst. Morsk. Ryb. Khoz. Okeanogr. N.M. Knipovicha (PINRO)* 21:147-176. [In Russian. English translation by the Translation Bureau (NKD), Foreign Languages Division, Dept. Secr. State Can. 1968].
- Clague, D.A. & G.B. Dalrymple (1989): Tectonics, geochronology, and the origin of the Hawaiian-Emperor chain. In: E.L. Winterer, D.M. Hussong, & R.W. Decker (eds.): The Geology of North America, Volume N: The Eastern Pacific Ocean and Hawaii: 188-217. Boulder, Colorado: The Geological Society of America.

- Cobb, W.M. (1933): The dentition of the walrus, *Odobenus obesus*. – Proc. zool. Soc. London 1933:645-668.
- Corbet, G.B. & J.E. Hill (1991): A World List of Mammalian Species. Oxford: Oxford University Press.
- Costa, D.P. (1993): The relationship between reproductive and foraging energetics and the evolution of the Pinnipedia. – Symp. zool. Soc. London 66:293-314.
- Cozzuol, M.A. (1992): The oldest seal of the southern hemisphere: implications to phocid phylogeny and dispersal. – J. Vert. Paleontol. 12:25A-26A. [Abstract only].
- Crouch, J.E. (1969): Text-atlas of cat anatomy. Philadelphia: Lea & Febiger.
- Cummings, M.P., S.P. Otto, & J. Wakeley (1995): Sampling properties of DNA sequence data in phylogenetic analysis. – Mol. Biol. Evol. 12:814-822.
- Davies, J.L. (1958a): The Pinnipedia: an essay in zoogeography. – Geogr. Rev. 48:474-493.
- (1958b): Pleistocene geography and the distribution of northern pinnipeds. – Ecology 39:97-113.
- Davis, D.D. (1964): The giant panda: a morphological study of evolutionary mechanisms. – Fieldiana Zool. Mem. 3:1-339.
- DeBlase, A.F. & R.E. Martin (1981): A Manual of Mammalogy with Keys to Families of the World. Dubuque, Iowa: Wm. C. Brown Company Publishers.
- Doutt, J.K. (1942): A review of the genus *Phoca*. – Ann. Carnegie Mus. 29:61-125.
- Ewer, R.F. (1973): The Carnivores. Ithaca, New York: Cornell University Press.
- Faith, D.P. (1991): Cladistic permutation tests for monophyly and nonmonophyly. – Syst. Zool. 40:366-375.
- (1992): On corroboration: a reply to Carpenter. – Cladistics 8:265-273.
- Faith, D.P. & P.S. Cranston (1991): Could a cladogram this short have arisen by chance alone? – Cladistics 7:1-28.
- & – (1992): Probability, parsimony, and Popper. – Syst. Biol. 41:252-257.
- Farris, J.S. (1969): A successive approximations approach to character weighting. – Syst. Zool. 18:374-385.
- (1989): The retention index and the rescaled consistency index. – Cladistics 5:417-419.
- (1990): Phenetics in camouflage. – Cladistics 6:91-100.
- Fay, F.H. (1982): Ecology and biology of the Pacific Walrus, *Odobenus rosmarus divergens* Illiger. – North Amer. Fauna 74:1-279.
- Felsenstein, J. (1985): Confidence limits on phylogenies: an approach using the bootstrap. – Evolution 39:783-791.
- (1993): PHYLIP (Phylogeny Inference Package) Version 3.5c. Distributed by the author. Department of Genetics, University of Washington, Seattle.
- Felsenstein, J. & H. Kishino (1993): Is there something wrong with the bootstrap on phylogenies? A reply to Hillis and Bull. – Syst. Biol. 42:183-200.
- Fitch, W.M. (1979): Cautionary remarks on using gene expression events in parsimony procedures. – Syst. Zool. 28:375-379.
- Flower, W.H. (1869): On the value of the characters of the base of the cranium in the classification of the order Carnivora, and on the systematic position of *Bassaris* and other disputed forms. – Proc. zool. Soc. London 1869:4-37.
- Flynn, J.J. (1988): Ancestry of sea mammals. – Nature 334:383-384.
- Flynn, J.J., N.A. Neff, & R.H. Tedford (1988): Phylogeny of the Carnivora. In: M.J. Benton (ed.): The Phylogeny and Classification of Tetrapods. Vol. 2. Mammals: 73-116. Oxford: Clarendon Press.
- Frost, K.J. & L.F. Lowry (1981): Ringed, Baikal and Caspian seals – *Phoca hispida*, *Phoca sibirica* and *Phoca caspica*. In: S.H. Ridgway & R.J. Harrison (eds.): Handbook of Marine Mammals 2:29-54. London: Academic Press.

- Gauthier, J., A.G. Kluge, & T. Rowe (1988): Amniote phylogeny and the importance of fossils. – *Cladistics* 4:105-209.
- Gilbert, S.C. (1968): *Pictorial Anatomy of the Cat*. Toronto: University of Toronto Press.
- Gill, T. (1866): *Prodrome of a Monograph of the Pinnipedes*. – *Proc. Essex Inst., Salem, Mass., Comm.* 5:3-13. [Not seen by authors].
- Gray, A.A. (1905): Anatomical notes upon the membranous labyrinth of man and of the seal. – *J. Anat. Phys.* 39:349-361.
- Grigorescu, D. (1976): Paratethyan seals. – *Syst. Zool.* 25:407-419.
- Hall, E.R. (1981): *The Mammals of North America*. Second edition. New York: John Wiley & Sons.
- Hall, P. & M.A. Martin. (1988): On bootstrap resampling and iteration. – *Biometrika* 75:661-671.
- Haslewood, G.A.D. (1978): *The Biological Importance of Bile Salts*. New York: North-Holland.
- Harshman, J. (1994): The effect of irrelevant characters on bootstrap values. – *Syst. Biol.* 43:419-424.
- Harvey, P.H. & S. Nee (1993): New uses for new phylogenies. – *Europ. Rev.* 1:11-19.
- Hauser, D.L. & W. Presch (1991): The effect of ordered characters on phylogenetic reconstruction. – *Cladistics* 7:243-265.
- Hayssen, V., A. van Tienhoven, & A. van Tienhoven (1993): *Asdell's Patterns of Mammalian Reproduction: a Compendium of Species-Specific Data*. Ithaca, New York: Cornell University Press.
- Hedges, S.B. (1992): The number of replications needed for accurate estimation of the bootstrap *P* value in phylogenetic studies. – *Mol. Biol. Evol.* 9:366-369.
- Hendey, Q.B. (1972): The evolution and dispersal of the Monachinae (Mammalia: Pinnipedia). – *Ann. S. Afr. Mus.* 59:99-113.
- Hendey, Q.B. & C.A. Repenning (1972): A Pliocene phocid from South Africa. – *Ann. S. Afr. Mus.* 59:71-98.
- Hennig, W. (1966): *Phylogenetic Systematics*. Urbana, Illinois: University of Illinois Press.
- Hillis, D.M. (1987): Molecular versus morphological approaches to systematics. – *Annu. Rev. Ecol. Syst.* 18:23-42.
- Hillis, D.M. & J.J. Bull (1993): An empirical test of bootstrapping as a method for assessing confidence in phylogenetic analysis. – *Syst. Biol.* 42:182-192.
- Hillis, D.M. & J.P. Huelsenbeck (1992): Signal, noise, and reliability in molecular phylogenetic analyses. – *J. Hered.* 83:189-195.
- Hillson, S. (1986): *Teeth*. Cambridge: Cambridge University Press.
- Hopkins, D.M. (1967): The Cenozoic history of Beringia – a synthesis. In: D.M. Hopkins (ed.): *The Bering Land Bridge: 451-484*. Stanford, California: Stanford University Press.
- Howell, A.B. (1928 [1929]): Contribution to the comparative anatomy of the eared and earless seals (genera *Zalophus* and *Phoca*). – *Proc. U.S. Natl. Mus.* 73:1-142.
- Huelsenbeck, J.P. (1991a): Tree-length distribution skewness: an indicator of phylogenetic information. – *Syst. Zool.* 40:257-270.
- (1991b): When are fossils better than extant taxa in phylogenetic analysis? – *Syst. Zool.* 40:458-469.
- Hunt, R.M. Jr. (1974): The auditory bulla in Carnivora: an anatomical basis for reappraisal of carnivore evolution. – *J. Morphol.* 143:21-76.
- Hunt, R.M. Jr. & L.G. Barnes (1994): Basicranial evidence for ursid affinity of the oldest pinnipeds. In: A. Berta & T.A. Deméré (eds.): *Contributions in Marine Mammal Paleontology Honoring Frank C. Whitmore, Jr.* 57-67. *Proc. San Diego Soc. Natur. Hist.* 29.

- Illiger, J.C.W. (1811): *Prodomus Systematis Mammalium et Avium*. Berlin, Germany: C. Salfeld.
[Not seen by authors].
- Irwin, D.M. & U. Arnason (1994): Cytochrome b gene of marine mammals: phylogeny and evolution. – *J. Mammal. Evol.* 2:37-55.
- Jolicœur, P. (1975): Sexual dimorphism and geographical distance as factors of skull variation in the wolf *Canis lupus* L. In: M.W. Fox (ed.): *The Wild Canids*: 54-61. New York: Van Nostrand Reinhold.
- de Jong, W.W. (1982): Eye lens proteins and vertebrate phylogeny. In: M. Goodman (ed.): *Macromolecular Sequences in Systematics and Evolutionary Biology*: 75-114. New York: Plenum Press.
- de Jong, W.W. & M. Goodman (1982): Mammalian phylogeny studied by sequence analysis of the eye lens protein α -crystallin. – *Z. Säugetierkd.* 47:257-276.
- Källersjö, M., J.S. Farris, A.G. Kluge, & C. Bult (1992): Skewness and permutation. – *Cladistics* 8:275-287.
- Kenyon, K.W. (1977): Caribbean monk seal extinct. – *J. Mammal.* 58:97-98.
- (1981a): Sea otter – *Enhydra lutris*. In: S.H. Ridgway & R.J. Harrison (eds.): *Handbook of Marine Mammals* 1:209-223. London: Academic Press.
- (1981b): Monk seals – *Monachus*. In: S.H. Ridgway & R.J. Harrison (eds.): *Handbook of Marine Mammals* 2:195-220. London: Academic Press.
- Kenyon, K.W. & D.W. Rice (1959): Life history of the Hawaiian monk seal. – *Pacif. Sci.* 13:215-252.
- Kesner, M.H. (1994): The impact of morphological variants on a cladistic hypothesis with an example from a myological data set. – *Syst. Biol.* 43:41-57.
- King, J.E. (1956): The monk seals genus *Monachus*. – *Bull. Br. Mus. (Nat. Hist.), Zool.* 3:203-256.
- (1964): *Seals of the World*. London: Trustees of the British Museum (Natural History).
- (1966): Relationships of the Hooded and Elephant seals (genera *Cystophora* and *Mirounga*). – *J. Zool., London* 148:385-398.
- (1968): The Ross and other Antarctic seals. – *Aust. Natur. Hist.* 16(March):29-32.
- (1969): Some aspects of the anatomy of the Ross seal, *Ommatophoca rossi* (Pinnipedia: Phocidae). – *Br. Antarct. Surv. Sci. Rep.* 63: 54 pp.
- (1971): The lacrimal bone in the Otariidae. – *Mammalia* 35:465-470.
- (1972): Observations on phocid skulls. In: R.J. Harrison (ed.): *Functional Anatomy of Marine Mammals* 1:81-115. London: Academic Press.
- (1983): *Seals of the World*, Second edition. Ithaca, New York: Cornell University Press.
- King, J.E. & R.J. Harrison (1961): Some notes on the Hawaiian monk seal. – *Pacif. Sci.* 15:282-293.
- van der Klaauw, C.J. (1931): On the auditory bulla in some fossil mammals, with a general introduction to this region of the skull. – *Bull. Amer. Mus. Natur. Hist.* 62:1-341.
- Kluge, A.G. (1989): A concern for evidence and a phylogenetic hypothesis of relationships among *Epicrates* (Boidae, Serpentes). – *Syst. Zool.* 38:7-25.
- Kluge, A.G. & A.J. Wolf (1993): Cladistics: what's in a word? – *Cladistics* 9:183-199.
- Kooyman, G.L. (1981a): Crabeater seal – *Lobodon carcinophagus*. In: S.H. Ridgway & R.J. Harrison (eds.): *Handbook of Marine Mammals* 2:221-236. London: Academic Press.
- (1981b): Leopard seal – *Hydrurga leptonyx*. In: S.H. Ridgway & R.J. Harrison (eds.): *Handbook of Marine Mammals* 2:261-274. London: Academic Press.
- (1981c): Weddell seal – *Leptonychotes weddelli*. In: S.H. Ridgway & R.J. Harrison (eds.): *Handbook of Marine Mammals* 2:275-296. London: Academic Press.
- Kovacs, K.M. & D.M. Lavigne (1986): *Cystophora cristata*. – *Mamm. Species* 258:1-9.
- & – (1992): Maternal investment in otariid seals and walruses. – *Can. J. Zool.* 70:1953-1964.

- Kummer, B. & S. Neiss (1957): Das Cranium eines 103mm langen Embryos des südlichen See-Elefanten (*Mirounga leonina* L.). – Gegenbaurs Morphol. Jahrb. 98:288-346.
- Lamboy, W.F. (1994): The accuracy of the maximum parsimony method for phylogeny reconstruction with morphological characters. – Syst. Bot. 19:489-505.
- Lawlor, T.E. (1979): Handbook to the Orders and Families of Living Mammals. Eureka, California: Mad River Press Inc.
- Lento, G.M., R.E. Hickson, G.K. Chambers, & D. Penny (1995): Use of spectral analysis to test hypotheses on the origin of pinnipeds. – Mol. Biol. Evol. 12:28-52.
- Li, W.-H. & A. Zharkikh (1994): What is the bootstrap technique? – Syst. Biol. 43:424-430.
- & – (1995): Statistical tests of DNA phylogenies. – Syst. Biol. 44:49-63.
- Liem, K.F. & J.W.M. Osse (1975): Biological versatility, evolution, and food resource exploitation in African cichlid fishes. – Amer. Zool. 15:427-454.
- Ling, J.K. (1977): Vibrissae of marine mammals. In: R.J. Harrison (ed.): Functional Anatomy of Marine Mammals 3:387-415. London: Academic Press.
- (1978): Pelage characteristics and systematic relationships in the Pinnipedia. – Mammalia 42:305-313.
- Ling, J.K. & M.M. Bryden (1981): Southern elephant seal – *Mirounga leonina*. In: S.H. Ridgway & R.J. Harrison (eds.): Handbook of Marine Mammals 2:297-328. London: Academic Press.
- Lubischew, A.A. (1962): On the use of discriminant functions in taxonomy. – Biometrics 18:455-477.
- Maddison, D.R. (1991): The discovery and importance of multiple islands of most-parsimonious trees. – Syst. Zool. 40:315-328.
- Maddison, W.P. (1993): Missing data versus missing characters in phylogenetic analysis. – Syst. Biol. 42:576-581.
- Maddison, W.P., M.J. Donoghue, & D.R. Maddison (1984): Outgroup analysis and parsimony. – Syst. Zool. 33:83-103.
- Maddison, W.P. & D.R. Maddison (1992): MacClade: Analysis of Phylogeny and Character Evolution. Version 3.0. Sunderland, Massachusetts: Sinauer Associates.
- Maynard Smith, J., J.R. Burian, S. Kauffman, P. Alberch, J. Campbell, B. Goodwin, R. Lande, D. Raup, & L. Wolpert (1985): Developmental constraints and evolution. – Quart. Rev. Biol. 60:265-287.
- McDermid, E.M. & W.N. Bonner (1975): Red cell and serum protein systems of grey seals and harbour seals. – Comp. Biochem. Physiol. 50B:97-101.
- McGinnis, S.M. & R.J. Schusterman (1981): Northern elephant seal – *Mirounga angustirostris*. In: S.H. Ridgway & R.J. Harrison (eds.): Handbook of Marine Mammals 2:329-350. London: Academic Press.
- McKenna, M.C. (1969): The origin and early differentiation of therian mammals. – Ann. New York Acad. Sci. 167:217-240.
- McLaren, I.A. (1960a): On the origin of the Caspian and Baikal seals and the paleoclimatological implication. – Amer. J. Sci. 258:47-65.
- (1960b): Are the Pinnipedia biphyletic? – Syst. Zool. 9:18-28.
- (1966): Taxonomy of harbor seals of the western North Pacific and evolution of certain other hair seals. – J. Mammal. 47:466-473.
- (1975): A speculative overview of phocid evolution. – Rapp. P.-v. Réun. Cons. int. Explor. Mer 169:43-48.
- (1993): Growth in pinnipeds. – Biol. Rev. 68:1-79.
- Miller, M.E. (1962): Guide to the Dissection of the Dog. Ithaca, New York: Edward Brothers, Inc.

- Miller, W.C.S. (1887 [1888]): Appendix to the report on seals: the myology of the Pinnipedia. In: The Voyage of the H.M.S. Challenger. Zoology 26(68):139-234.
- Mills, R.P. & H.E. Christmas (1990): Applied comparative anatomy of the nasal turbinates. – Clin. Otolaryngol. 15:553-558.
- Mitchell, E.D. (1967): Controversy over diphyly in pinnipeds. – Syst. Zool. 16:350-351.
- (1975): Parallelism and convergence in the evolution of the Otariidae and Phocidae. – Rapp. P.-v. Réun. Cons. int. Explor. Mer 169:12-26.
- Mitchell, E.D., Jr. & R.H. Tedford (1973): The Enaliarctidae: a new group of extinct Carnivora, and a consideration of the origin of the Otariidae. – Bull. Amer. Mus. Natur. Hist. 151:205-284.
- Mivart, St. G. (1885): Notes on the Pinnipedia. – Proc. zool. Soc. London 1885:484-500.
- Miyamoto, M.M. & M. Goodman (1986): Biomolecular systematics of eutherian mammals: phylogenetic patterns and classification. – Syst. Zool. 35:230-240.
- Mouchaty, S., J.A. Cook, & G.F. Shields (1995): Phylogenetic analysis of northern hair seals based on nucleotide sequences of the mitochondrial cytochrome b gene – J. Mammal. 76:1178-1185.
- de Muizon, Ch. (1981): Une interprétation fonctionnelle et phylogénétique de l'insertion du psos major chez les Phocidae. – C.R. Hebd. Séances. Acad. Sci. (Paris) 292:859-862.
- (1982a): Phocid phylogeny and dispersal. – Ann. S. Afr. Mus. 89:175-213.
- (1982b): Les relations phylogénétiques des Lutrinae (Mustelidae, Mammalia). – Geobios (Lyon), Mém. Spéc. 6:259-277.
- de Muizon, Ch & Q.B. Hendey (1980): Late Tertiary seals of the South Atlantic Ocean. – Ann. S. Afr. Mus. 82:91-128.
- Nojima, T. (1990): A morphological consideration of the relationships of pinnipeds to other carnivorans based on the bony tentorium and bony falx. – Mar. Mamm. Sci. 6:54-74.
- Novacek, M.J. (1991): "All tree histograms" and the evaluation of cladistic evidence: some ambiguities. – Cladistics 7:345-349.
- (1992): Mammalian phylogeny: shaking the tree. – Nature 356:121-125.
- (1993): Reflections on higher mammalian phylogenetics. – J. Mammal. Evol. 1:3-30.
- Nowak, R.M. (1991): Walker's Mammals of the World, Volume II. Fifth edition. Baltimore, Maryland: The Johns Hopkins University Press.
- Odell, D.K. (1981): California sea lion – *Zalophus californianus*. In: S.H. Ridgway & R.J. Harrison (eds.): Handbook of Marine Mammals 1:67-98. London: Academic Press.
- O'Gorman, F. (1963): Observations on terrestrial locomotion in Antarctic seals. – Proc. zool. Soc. London 141:837-850.
- Patterson, C., D.M. Williams, & C.J. Humphries (1993): Congruence between molecular and morphological phylogenies. – Annu. Rev. Ecol. Syst. 24:153-188.
- Perry, E.A., S.M. Carr, S.E. Bartlett, & W.S. Davidson (1995): A phylogenetic perspective on the evolution of reproductive behavior in pagophilic seals of the Northwest Atlantic as indicated by mitochondrial DNA sequences. – J. Mammal. 76:22-31.
- Piérard, J. (1971): Osteology and myology of the Weddell seal *Leptonychotes weddelli* (Lesson, 1826). – Antarct. Res. Ser. 18:53-108.
- Platnick, N.I., C.E. Griswold, & J.A. Coddington (1991): On missing entries in cladistic analysis. – Cladistics 7:337-343.
- Pocock, R.I. (1921): The auditory bulla and other cranial characters in the Mustelidae. – Proc. zool. Soc. London 1921:473-486.
- de Queiroz, K. & M.J. Donoghue (1990): Phylogenetic systematics or Nelson's version of cladistics? – Cladistics 6:61-75.
- Ralls, K. (1976): Mammals in which females are larger than males. – Quart. Rev. Biol. 51:245-276.

- Ray, C.E. (1976a): Geography of phocid evolution. – Syst. Zool. 25:391-406.
- (1976b): *Phoca wymani* and other Tertiary seals (Mammalia: Phocidae) described from the eastern seaboard of North America. – Smithson. Contrib. Paleobiol. 28:1-36.
- Ray, G.C. (1981): Ross seal – *Ommatophoca rossi*. In: S.H. Ridgway & R.J. Harrison (eds.): Handbook of Marine Mammals 2:237-260. London: Academic Press.
- Reeves, R.R. & J.K. Ling (1981): Hooded seal – *Cystophora cristata*. In: S.H. Ridgway & R.J. Harrison (eds.): Handbook of Marine Mammals 2:171-194. London: Academic Press.
- Repenning, C.A. (1972): Underwater hearing in seals: functional morphology. In: R.J. Harrison (ed.): Functional Anatomy of Marine Mammals 1:307-331. London: Academic Press.
- (1975): Otarioid evolution. – Rapp. P.-v. Réun. Cons. int. Explor. Mer 169:27-33.
- (1990): Oldest pinniped. – Science 248:499-500.
- Repenning, C.A. & C.E. Ray (1972): The origin of the Hawaiian monk seal. – Proc. Biol. Soc. Wash. 89(58):667-688.
- Repenning, C.A., C.E. Ray, & D. Grigorescu (1979): Pinniped biogeography. In: J. Gray & A.J. Boucot (eds.): Historical Biogeography, Plate Tectonics, and the Changing Environment: 357-369. Corvallis, Oregon: Oregon State University Press.
- Repenning, C.A. & R.H. Tedford (1977): Otarioid seals of the Neogene: classification, historical zoogeography, and temporal correlation of the sea lions and walruses from the North Pacific region. – U.S. Geol. Surv. Prof. Pap. 992:1-93.
- Ridgway, S.H. (ed.) (1972): Mammals of the Sea: Biology and Medicine. Springfield, Illinois: Charles C. Thomas.
- Rodrigo, A.G. (1993): Calibrating the bootstrap test of monophyly. – Int. J. Parasitol. 23:507-514.
- Ronald, K. & P.J. Healey (1981): Harp seal – *Phoca groenlandica*. In: S.H. Ridgway & R.J. Harrison (eds.): Handbook of Marine Mammals 2:55-88. London: Academic Press.
- Russell, A.P. (1979): Parallelism and integrated design in the foot structure of gekkonine and diplodactyline geckos. – Copeia 1979:1-21.
- Sanderson, M.J. (1989): Confidence limits on phylogenies: the bootstrap revisited. – Cladistics 5:113-129.
- (1990): Flexible phylogeny reconstruction: a review of phylogeny inference packages using parsimony. – Syst. Zool. 39:414-420.
- Sanderson, M.J. & M.J. Donoghue (1989): Patterns of variation in levels of homoplasy. – Evolution 43:1781-1795.
- Sarich, V.M. (1969a): Pinniped origins and the rate of evolution of carnivore albumins. – Syst. Zool. 18:286-295.
- (1969b): Pinniped phylogeny. – Syst. Zool. 18:416-422.
- (1975): Pinniped systematics: immunological comparisons of their albumins and transferins. – Amer. Zool. 15:826. [Abstract only].
- (1976): Transferrin. – Trans. zool. Soc. London. 33:165-171.
- Scheffer, V.B. (1958): Seals, Sea Lions, and Walruses: a Review of the Pinnipedia. Stanford, California: Stanford University Press.
- (1960): Dentition of the ribbon seal. – Proc. zool. Soc., London 135:579-585.
- (1964): Hair patterns in seals (Pinnipedia). – J. Morphol. 115:291-304.
- (1967): Marine mammals and the history of the Bering Strait. In: D.M. Hopkins (ed.): The Bering Land Bridge: 350-363. Stanford, California: Stanford University Press.
- Segall, W. (1943): The auditory region of the arctoid carnivores. – Zool. Ser. Field Mus. Natur. Hist. 29:33-59.
- Shaughnessy, P.D. (1975): Biochemical comparison of the harbour seals *Phoca vitulina richardi* and *P. v. largha*. – Rapp. P.-v. Réun. Cons. int. Explor. Mer 169:70-73.
- Shaughnessy, P.D. & F.H. Fay (1977): A review of the taxonomy and nomenclature of North Pacific Harbour seals. – J. Zool., London 182:385-419.

- Shubin, P.N., T.I. Chelpanova, E.A. Efimtseva, & N.A. Moiseenko (1990): Testing the homozygosity of Baikal seal using data on genetic variability of proteins. – *Genetika* 26:370-373. [In Russian; only English summary used].
- Simpson, G.G. (1945): The principles of classification and a classification of mammals. – *Bull. Amer. Mus. Natur. Hist.* 85:1-350.
- Smirnov, N.A. (1908): Review of the Russian pinnipeds. – *Zap. Akad. nauk Soiuz SSR Otd. fiz.-mat. nauk. VIII ser.* [= *Mem. Acad. Sci. St. Petersburg, Ser. 8 (Phys. Math.)*] 23:1-75. [In Russian. Not seen by authors].
- Sober, E. (1988): *Reconstructing the Past: Parsimony, Evolution, and Inference*. Cambridge, Massachusetts: The Massachusetts Institute of Technology Press.
- Stains, H.J. (1984): Carnivores. In: S. Anderson & J.K. Jones, Jr. (eds.): *Orders and Families of Recent Mammals of the World*. Second edition: 491-521. New York: John Wiley & Sons.
- Stewart, R.E.A. & B.E. Stewart (1987): Dental ontogeny of harp seals, *Phoca groenlandica*. – *Can. J. Zool.* 65:1425-1434.
- Story, H.E. (1951): The carotid arteries in the Procyonidae. – *Fieldiana Zool.* 32:477-557.
- Swofford, D.L. (1993): PAUP: Phylogenetic Analysis Using Parsimony, Version 3.1.1. Computer program distributed by the Illinois Natural History Survey, Champaign, Illinois.
- Taylor, W.P. (1914): The problem of aquatic adaptation in the Carnivora, as illustrated in the osteology and evolution of the sea-otter. – *Univ. Calif. Publ. Geol.* 7:465-495.
- Tedford, R.H. (1976): Relationships of pinnipeds to other carnivores (Mammalia). – *Syst. Zool.* 25:363-374.
- Thorpe, J.P. (1982): The molecular clock hypothesis: biochemical evolution, genetic differentiation and systematics. – *Annu. Rev. Ecol. Syst.* 13:139-168.
- Thorpe, R.S. (1975a): Biometric analysis of incipient speciation in the ringed snake, *Natrix natrix* (L.). – *Experientia* 31:180-181.
- (1975b): Quantitative handling of characters useful in snake systematics with particular reference to intraspecific variation in the ringed snake, *Natrix natrix* (L.). – *Biol. J. Linn. Soc.* 7:24-43.
- Trouessart, E.L. (1897): *Catalogus Mammalium tam Viventium quam Fossilium*, Tomus 1, fascicle 2. Berlin: R. Friedländer und Sohn. [Not seen by authors].
- Turner, H.N. (1848): Observations relating to some of the foramina at the base of the skull in Mammalia, and on the classification of the order Carnivora. – *Proc. zool. Soc. London* 1848:63-88.
- Underwood, G. (1982): Parallel evolution in the context of character analysis. – *Zool. J. Linn. Soc.* 74:245-266.
- Vrana, P. & W. Wheeler (1992): Individual organisms as terminal entities: laying the species problem to rest. – *Cladistics* 8:67-72.
- Vrana, P.B., M.C. Milinkovitch, J.R. Powell, & W.C. Wheeler (1994): Higher level relationships of the arctoid Carnivora based on sequence data and "total evidence". – *Mol. Phylogenet. Evol.* 3:47-58.
- Wagner, P.J. III (1992): Cladograms as tests of speciation patterns. – *Abstr. Programs Geol. Soc. Amer. Annu. Mtg.* 1992 24:A139. [Abstract only].
- Wayne, R.K., R.E. Benveniste, D.N. Janczewski, & S.J. O'Brien (1989): Molecular and biochemical evolution of the Carnivora. In: J.L. Gittleman (ed.): *Carnivore Behavior, Ecology, and Evolution*: 465-494. Ithaca, New York: Cornell University Press.
- Wheeler, Q.D. & K.C. Nixon (1990): Another way of looking at the species problem: a reply to de Queiroz and Donoghue. – *Cladistics* 6:77-81.
- Wiley, E.O. (1981): *Phylogenetics: the Theory and Practice of Phylogenetic Systematics*. New York: John Wiley & Sons, Inc.

- Wiley, E.O., D. Siegel-Causey, D.R. Brooks, & V.A. Funk (1991): The complete cladist: a primer of phylogenetic procedures. – Univ. Kansas Mus. Natur. Hist. Spec. Publ. No.19, Lawrence, Kansas.
- Wilkinson, M. (1991): Homoplasy and parsimony analysis. – Syst. Zool. 40:105-109.
- Wilson, D.E. & D.M. Reeder (eds.) (1993): Mammal Species of the World: a Taxonomic and Geographic Reference. Second edition. Washington, D.C.: Smithsonian Institution Press.
- Wincza, H. (1896): Über einige Entwicklungsveränderungen in der Gegend des Schädelgrundes bei den Säugethieren. – Bull. Int. Acad. Sci., Cracovie 1896:326-337.
- Wolsan, M. (1993): Phylogeny and classification of early European Mustelida (Mammalia: Carnivora). – Acta Theriol. 38:345-384.
- Wozencraft, W.C. (1989): The phylogeny of Recent Carnivora. In: J.L. Gittleman (ed.): Carnivore Behavior, Ecology, and Evolution: 495-535. Ithaca, New York: Cornell University Press.
- (1993): Order Carnivora. In: D.E. Wilson & D.M. Reeder (eds.): Mammal Species of the World: A Taxonomic and Geographic Reference: 279-348. Second edition. Washington, D.C.: Smithsonian Institution Press.
- Wyss, A.R. (1987): The walrus auditory region and the monophyly of pinnipeds. – Amer. Mus. Novitates 2871:1-31.
- (1988a): On “retrogression” in the evolution of the Phocinae and phylogenetic affinities of the monk seals. – Amer. Mus. Novitates 2924:1-38.
- (1988b): Evidence from flipper structure for a single origin of pinnipeds. – Nature 334:427-428.
- (1989): Flippers and pinniped phylogeny: has the problem of convergence been overrated? – Mar. Mamm. Sci. 5:343-360.
- (1994): The evolution of body size in phocids: some ontogenetic and phylogenetic observations. In: A. Berta & T.A. Deméré (eds.): Contributions in Marine Mammal Paleontology Honoring Frank C. Whitmore, Jr: 69-76. Proc. San Diego Soc. Natur. Hist. 29.
- Wyss, A.R. & J.J. Flynn (1993): A phylogenetic analysis and definition of the Carnivora. In: F.S. Szalay, M.J. Novacek, & M.C. McKenna (eds.): Mammal Phylogeny: Placentals: 32-52. New York: Springer-Verlag.
- Yeates, D. (1992): Why remove autapomorphies? – Cladistics 8:387-389.
- Youngman, P.M. (1982): Distribution and systematics of the European mink (*Mustela lutreola*) (Linnaeus, 1761). – Acta Zool. Fenn. 166:1-48.
- van Zyll de Jong, C.G. (1987): A phylogenetic study of the Lutrinae (Carnivora: Mustelidae) using morphological data. – Can. J. Zool. 65:2536-2544.

Authors' addresses:

Olaf R.P. Bininda-Emonds* and Anthony P. Russell Vertebrate Morphology Research Group, Department of Biological Sciences, University of Calgary, Calgary, Alberta T2N 1N4, Canada

E-mail: olaf.bininda@zoology.oxford.ac.uk
arussell@acs.ucalgary.ca

* Current address: Department of Zoology, University of Oxford, South Parks Road, Oxford, OX1 3PS, United Kingdom

APPENDICES

APPENDIX A

Specimen List

A total of 286 specimens were examined. Specimens examined were skulls (including mandible) only, unless followed by: * = skeleton only; ** = skull and skeleton; *** = partial skull; **** = partial skull and skeleton; ***** = skin.

Institutions are abbreviated as follows: AMNH – American Museum of Natural History; ANSP – Academy of Natural Sciences of Philadelphia; BM(NH) – British Museum (Natural History); MCZ – Museum of Comparative Zoology, Harvard; PMA – Provincial Museum of Alberta; UAMZ – University of Alberta Museum of Zoology; UCMZ(M) – University of Calgary Museum of Zoology (Mammalia); USNM – United States National Museum (Smithsonian); UWBM – University of Washington Burke Museum.

Common and Latin names follow Wozencraft (1993) and Corbet & Hill (1991), except for the phocids, which follow Scheffer (1958) with *Phoca vitulina largha* elevated to the full species *Phoca largha*. The number in parentheses following the taxon name refers to the total number of specimens that were examined for that taxon.

Canidae

Canis lupus – grey wolf (8)

UCMZ(M): 1975.185; 1982.94; 1982.95; 1982.97; 1982.100; 1982.103; 1987.16; 1990.35**

Mustelidae

Enhydra lutris – sea otter (6)

AMNH: 215274**; 215275**

UAMZ: “A”**, “2”**, “4”**

USNM: 287288*****

Lutra canadensis – Canadian river otter (8)

AMNH: 135500; 150306**; 184646**

MCZ: 8849***

UCMZ(M): 1975.211**; 1983.5*; 1984.28**; 1993.38**

Martes americana – American pine marten (12)

AMNH: 11421; 11459; 11468; 21544**; 29057**; 29058**

MCZ: 55554***; 55555***

UCMZ(M): 1975.217; 1975.219; 1975.220**; 1992.24*

Odobenidae

Odobenus rosmarus – walrus (8)

AMNH: 15092; 19278**; 70099*

MCZ: 1723***

USNM: 396932*; 500252**; 550409

UWBM: 35215

Otariidae

Zalophus californianus – California sea lion (11)

AMNH: 18066**; 63946*; 73664; 238321*

MCZ: 6164***

Appendix A (continued)

USNM: 23332***; 49425**; 200847**; 504613*****
 UWBM: 34980; 34995

Phocidae*Cystophora cristata* – hooded seal (11)

AMNH: 95; 184659**; 212174***; 212185
 BM(NH): 1890.8.1.4; 1956.11.7.1**
 MCZ: 1084**
 USNM: 188914; 188964; 241360**; 550317**

Erignathus barbatus – bearded seal (14)

AMNH: 28*; 10135; 18165; 18167; 73328***
 BM(NH): 1887.9.28.1**; 1896.9.23.6; 1938.11.26.1
 MCZ: 7679
 USNM: 16116**; 188830; 275046; 288353*****; 396801

Halichoerus grypus – grey seal (10)

AMNH: 69487; 100191**; 125592***; 173535
 BM(NH): 1951.11.28.1
 MCZ: 51488**
 USNM: 19837; 446405; 446408**; 504481

Histiophoca fasciata – ribbon seal (16)

AMNH: 130245**; 130246***; 182746*
 BM(NH): 1965.7.19.7; 1965.7.19.9; 1966.12.7.2****
 MCZ: 6545***; 52239; 52240; 52241**
 USNM: 16484**; 311771***; 399449; 504959**; 504960***; unnumbered*****

Hydrurga leptonyx – leopard seal (13)

AMNH: 34920; 36200**; 77914
 ANSP: 2488
 BM(NH): 1901.1.4.15; 1959.12.17.4**
 MCZ: 51853**
 USNM: 3647***; 14492***; 32564*****; 270326**; 275208*; 550358*

Leptonychotes weddelli – Weddell seal (12)

AMNH: 32450*; 88446; 88548; 212172; 212181***
 BM(NH): 1908.2.20.26**
 MCZ: 51710
 USNM: 269526; 270319*****; 395816***; 504875**; 550075

Lobodon carcinophagus – crabeater seal (12)

AMNH: 85513; 88494; 212179***; "C-2"
 ANSP: 20557
 BM(NH): 1908.2.20.57**; 1935.3.29.2
 MCZ: 51851*; 52287**
 USNM: 269722**; 550078; 550082*****

Mirounga angustirostris – northern elephant seal (7)

AMNH: 32676**; 32677; 32679**
 USNM: 21890**; 38208***; 255975**; 260867**

Appendix A (continued)

Mirounga leonina – southern elephant seal (13)

AMNH: 48153; 48154; 48155; 70240; 77916***; 77925
 BM(NH): 1908.2.20.44****; 1912.9.28.1**; 1951.7.17.1*; 1954.5.20.21
 MCZ: 1178****; 1179****
 USNM: 504927

Monachus monachus – Mediterranean monk seal (8)

AMNH: 73607**; 73608**
 BM(NH): 1863.4.1.1**; 1894.7.27.1**; 1894.7.27.2**; 1894.7.27.3**
 MCZ: 7281**
 USNM: 219059*

Monachus schauinslandi – Hawaiian monk seal (11)

BM(NH): 1958.11.26.1**
 MCZ: 20562; 59230**
 USNM: 181250; 181252*; 243838; 243842; 243845***; 243849; 395991***; 395997***

Monachus tropicalis – West Indian or Caribbean monk seal (10)

AMNH: 10421**; 19600**; 77741**
 ANSP: 4561**; 4616*; 4963**
 BM(NH): 1889.11.5.1
 MCZ: 7264**; 8605**
 USNM: 102536

Ommatophoca rossi – Ross seal (11)

BM(NH): 1901.1.4.12; 1949.2.3.1; 1965.8.2.1*****; 1965.12.20.1*
 MCZ: 51852**; 52305**
 USNM: 270316**; 275206**; 302975**; 339989**; 550088*****

Pagophilus groenlandicus – harp seal (17)

AMNH: 10142; 10155; 100373***; 100377***; 150419; 180016*
 ANSP: 17151***
 BM(NH): 1843.6.23.8; 1938.12.10.4; 1951.11.28.2****
 USNM: 188766*****; 188774; 188816; 188890*****; 257031*; 504476*****; 504477

Phoca largha – spotted or larga seal (9)

AMNH: 15817**; 18169; 19843; 212250
 BM(NH): 1891.12.18.6; 1893.1.27.2*****; 1965.7.19.12; 1965.7.19.14
 MCZ: 11455

Phoca vitulina – harbour seal (11)

AMNH: 183135**; 232391**
 BM(NH): 1867.10.5.4**; 1951.3.2.3*
 MCZ: 5285***; 26861**
 USNM: 140401*****; 188826**; 219876**
 UWBM: 20224; 36047

Pusa caspica – Caspian seal (8)

AMNH: 206593
 BM(NH): 1963.7.19.10; 1963.7.19.11; 1963.7.19.12; 1963.7.19.15
 USNM: 341615**; 341616; 341617

Appendix A (continued)

Pusa hispida – ringed seal (13)

AMNH: 19308; 19310; 73306*
 BM(NH): 1938.11.26.6; 1938.12.10.5**
 MCZ: 6296***; 6297**; 7744***; 11506***
 USNM: 49472*; 230854; 251645**; 305088

Pusa sibirica – Baikal seal (11)

AMNH: 185195; 185595**
 BM(NH): 1963.7.19.8; 1965.9.6.1**; 1965.9.6.2**
 MCZ: 29571
 USNM: 175689****; 504941****; 550028; 550034**; 550037****

Procyonidae*Procyon lotor* – common raccoon (6)

UCMZ(M): 1975.206; 1982.1*; 1985.75**
 PMA: 89.40.2**; 90.34.5**; 90.34.6**

Ursidae*Ursus americanus* – American black bear (10)

MCZ: 675***; 3509***; 56979**; 59938**
 UCMZ(M): 1975.189; 1975.191; 1975.192*; 1975.198; 1984.32
 USNM: 303193*****

APPENDIX B

List of Characters

The following is the complete list of characters (and associated character states) examined in this study. A more detailed discussion of each character is found in the **Character Analysis** section. Excluded characters are preceded by an asterisk.

Snout (21 characters)

- *1) relative position of external nares on snout: 0 = relatively dorsal ("high"); 1 = relatively ventral ("low").
- *2) relative orientation of external nares on snout: 0 = vertical; 1 = horizontal.
- 3) shape of anterior margin of premaxilla in dorsal view: 0 = flat, square, or bi-lobed; 1 = tapered and/or rounded.
- 4) triangular lateral extensions of premaxilla into maxilla in dorsal view: 0 = absent; 1 = rudimentary or present.
- 5) visibility of ventral portion of nasal processes of premaxilla along maxilla in lateral view: 0 = always visible; 1 = not always visible.
- 6) visibility of middle portion of nasal processes of premaxilla along maxilla in lateral view: 0 = always visible; 1 = not always visible; 9 = n/a – middle portion not present.
- 7) visibility of dorsal portion of nasal processes of premaxilla along maxilla in lateral view: 0 = always visible; 1 = not always visible; 9 = n/a – dorsal portion not present.
- 8) shape of ventral portion of nasal processes of premaxilla along maxilla: 0 = concave; 1 = straight; 2 = convex.
- 9) shape of middle portion of nasal processes of premaxilla along maxilla: 0 = concave; 1 = straight; 2 = convex; 9 = n/a – middle portion not present.
- 10) shape of dorsal portion of nasal processes of premaxilla along maxilla: 0 = concave; 1 = straight; 2 = convex; 9 = n/a – dorsal portion not present.
- 11) contact between nasal processes of premaxilla and nasals: 0 = none; 1 = little (less than width of nasal processes); 2 = broad (greater than or equal to width of nasal processes).
- 12) length of nasal processes of premaxilla along maxilla: 0 = extend only part way to nasals; 1 = extend fully or virtually fully to nasals.
- 13) shape of anterior margin of nasals (ignoring contribution of nasal suture): 0 = flat or broadly indented; 1 = lobular (uni-, bi-, or tri-lobed).
- 14) relative lengths of anterior prongs of nasal bones with a trident-shaped (= tri-lobular) morphology: 0 = lateral prongs greater than medial prong; 1 = lateral prongs subequal with medial prong; 2 = lateral prongs less than medial prong; 9 = n/a – nasal bones not trident-shaped.
- 15) visibility of nasal septum in dorsal view: 0 = does not extend beyond nasals (not visible); 1 = extends beyond nasals (visible).
- 16) shape of posterior edge of nasals, I: 0 = v-shaped (convergent); 1 = w-shaped (divergent).
- 17) shape of posterior edge of nasals, II: 0 = pointed; 1 = rounded.
- *18) shape of posterior edge of nasals, III: 0 = pointed v-shape; 1 = rounded v-shape; 2 = rounded w-shape; 3 = pointed w-shape.

- 19) distinct caninus fossa: 0 = absent; 1 = present.
- 20) depth of unnamed fossa on ventrolateral side of premaxilla: 0 = shallow; 1 = medium; 2 = deep; 9 = absent.
- 21) anterior opening of infraorbital canal relative to nasolacrimal foramen: 0 = anterior; 1 = ventral (or posterior).

Orbit and zygomatic arch (35 characters)

- 22) swelling of maxilla anterior to zygomatic arch: 0 = absent; 1 = present.
- *23) distinct preorbital process of maxilla: 0 = absent; 1 = present.
- 24) size of preorbital process of maxilla: 0 = small; 1 = medium; 2 = large; 9 = absent.
- *25) distinct postorbital process of maxilla: 0 = absent; 1 = present.
- 26) size of postorbital process of maxilla: 0 = small; 1 = medium; 2 = large; 9 = absent.
- *27) nasolacrimal (= lacrimal) foramen: 0 = absent; 1 = present.
- 28) size of nasolacrimal foramen: 0 = small; 1 = medium or greater; 9 = absent.
- 29) location of inferior oblique muscle origin relative to nasolacrimal foramen: 0 = widely separate; 1 = closely adjacent.
- 30) lacrimal: 0 = absent / not visible; 1 = visible.
- 31) amount of bone reduction along maxillo-frontal suture in interorbital region: 0 = none / irregular perforations; 1 = little – small foramen or narrow fissure; 2 = great – large foramen and/or greatly widened suture.
- *32) morphology of bone reduction along maxillo-frontal suture in interorbital region: 0 = none; 1 = irregular perforations; 2 = round / ovoid; 3 = inverse teardrop-shaped; 4 = roughly rectangular; 5 = crescent-shaped.
- *33) shape of maxillary (anteroventral) edge of widened maxillo-frontal suture: 0 = concave; 1 = straight; 2 = convex; 9 = n/a – maxilla and frontal in contact.
- *34) shape of frontal edge (posterodorsal) of widened maxillo-frontal suture: 0 = concave; 1 = straight; 2 = convex; 9 = n/a – maxilla and frontal in contact.
- *35) degree of invagination of maxillary edge (anteroventral) of widened maxillo-frontal suture: 0 = none to slight; 1 = medium or greater; 9 = n/a – maxilla and frontal in contact.
- *36) degree of invagination of frontal edge (posterodorsal) of widened maxillo-frontal suture: 0 = none to slight; 1 = medium or greater; 9 = n/a – maxilla and frontal in contact.
- *37) anterior process of orbitosphenoid: 0 = absent / barely extends onto palatine; 1 = present.
- 38) degree of anterior extension of orbitosphenoid: 0 = extends to distinctly less than one-half length of palatine; 1 = extends to about one-half length of palatine; 2 = extends to distinctly greater than one-half length of palatine; 9 = absent / barely extends onto palatine.
- 39) ethmoid / turbinal bones in wall of interorbital region: 0 = absent; 1 = present.
- 40) approach of palatine to lacrimal region: 0 = does not reach lacrimal region; 1 = reaches or almost reaches lacrimal region.
- 41) location of sphenopalatine vacuity: 0 = enclosed in palatine; 1 = not enclosed in palatine.
- 42) relationship of sphenopalatine foramen and pterygopalatine canal: 0 = totally confluent, only single foramen visible; 1 = confluent, but individually distinguishable; 2 = separate.
- 43) continuity of sphenopalatine vacuity and widened maxillo-frontal suture: 0 = separate; 1 = confluent; 9 = n/a – widened maxillo-frontal suture absent.
- 44) relative vertical position of optic foramina: 0 = in lower third of interorbital region; 1 = between lower third and upper two-thirds of interorbital region; 2 = in upper two-thirds of interorbital region.

- 45) intracranial openings of optic foramina of orbitosphenoid: 0 = separate; 1 = converging / intermediate; 2 = confluent.
- 46) interorbital septum anterior to optic foramina: 0 = absent; 1 = present.
- 47) continuity of bilateral optic foramina in interorbital region: 0 = not continuous, no common passage; 1 = continuous, form passage through interorbital region.
- 48) alisphenoid canal: 0 = absent; 1 = present.
- 49) location of least interorbital width: 0 = distinctly anterior to middle of interorbital region; 1 = approximately in the middle of interorbital region; 2 = distinctly posterior to middle of interorbital region.
- 50) location of greatest zygomatic width: 0 = anterior to glenoid fossa (i.e., within zygomatic arch proper); 1 = at level of glenoid fossa (i.e., at squamosal).
- 51) relative position of zygomatic arches: 0 = lower than tooth row; 1 = level with tooth row; 2 = higher than tooth row.
- 52) direction of arch of anterior portion of jugal: 0 = downwards; 1 = flat, no distinct arch; 2 = upwards.
- 53) degree of overlap of maxillary and squamosal processes of zygomatic arch, on medial surface of zygomatic arch: 0 = little or none; 1 = approach closely – maxilla and squamosal almost or in contact.
- 54) approach of jugal to lacrimal region: 0 = does not approach lacrimal region; 1 = reaches lacrimal region / almost touches or does touch anterior wall of orbit.
- *55) dorsal process of squamosal process of zygomatic arch: 0 = absent; 1 = present.
- 56) degree of interlock between jugal and dorsal process of squamosal process of zygomatic arch: 0 = weak; 1 = medium; 2 = strong; 9 = dorsal process of squamosal absent.

Palate and ventral side of snout (18 characters)

- *57) incisive foramina (= palatine fissure / foramen): 0 = absent; 1 = present.
- 58) size of incisive foramina: 0 = small; 1 = medium; 2 = large; 9 = absent.
- 59) posterior extension of incisive foramina: 0 = enclosed within premaxilla; 1 = contact premaxillary-maxilla suture; 2 = extend into maxilla; 9 = incisive foramina absent.
- 60) number of incisive foramina: 0 = one; 1 = two; 9 = absent.
- 61) reduction of incisive foramina: 0 = absent; 1 = present.
- 62) position of major palatine foramen relative to maxillo-palatine suture: 0 = anterior; 1 = on; 2 = posterior.
- 63) shape of maxillo-palatine suture: 0 = flat / square; 1 = rounded / triangular.
- 64) outline of palatine bones in ventral view: 0 = square; 1 = "butterfly-shaped".
- 65) shape of posterior edge of palatine: 0 = (roughly) triangular; 1 = arched; 2 = straight.
- 66) presence of posteriorly directed process in midline of posterior edge of palatine: 0 = absent; 1 = present.
- 67) morphology of notching in posterior edge of palatine: 0 = rounded; 1 = triangular; 2 = incision; 9 = none.
- 68) size of notching in posterior edge of palatine: 0 = small; 1 = medium; 2 = large; 9 = absent.
- 69) relationship of bony nasal septum to posterior edge of palate: 0 = does not reach posterior edge of palate; 1 = closely approaches / reaches posterior edge of palate.
- 70) orientation of pterygoid hamuli: 0 = directed laterally; 1 = in midline; 2 = directed medially.
- *71) relationship of ethmoid to pterygoid on ventral surface of skull: 0 = does not contact pterygoid; 1 = contacts pterygoid.

72) degree of contact between ethmoid and pterygoid process of basisphenoid: 0 = narrow; 1 = greater than or equal to medium breadth; 9 = none.

73) relationship between pterygoid process of basisphenoid and auditory bulla: 0 = does not extend to auditory bulla; 1 = extends to auditory bulla.

74) bony constituents of wall of foramen ovale with respect to alisphenoid and squamosal: 0 = alisphenoid only; 1 = both alisphenoid and squamosal; 2 = squamosal only.

Basicranial region (43 characters)

75) visibility of the mastoid process in dorsal view: 0 = not visible; 1 = visible.

76) relative shape of basioccipital-basisphenoid region: 0 = concave; 1 = flat; 2 = convex.

*77) postglenoid (= glenoid) foramen in squamosal: 0 = absent; 1 = present.

78) size of postglenoid (= glenoid) foramen in squamosal: 0 = small; 1 = medium; 2 = large; 9 = absent.

79) shape of anterior edge of auditory bulla: 0 = concave; 1 = flat; 2 = convex.

80) inflation of ectotympanic: 0 = not inflated; 1 = slightly / moderately inflated; 2 = inflated.

81) inflation of caudal entotympanic along anteroposterior axis: 0 = not inflated; 1 = slight / moderate inflation; 2 = inflated.

82) inflation of medial portion of caudal entotympanic: 0 = not inflated; 1 = slight / moderate inflation; 2 = inflated.

83) distinct sulcus dividing ectotympanic and entotympanic portions of auditory bulla: 0 = absent; 1 = present.

84) relationship between auditory bulla and petrosal: 0 = does not cover petrosal; 1 = covers petrosal.

85) relationship between auditory bulla and paroccipital process: 0 = does not reach process; 1 = reaches (or very closely approaches) process.

86) groove separating mastoid bulla and petrosal: 0 = absent; 1 = present.

*87) hypomastoid fossa (found along posteroventral edge of the auditory bulla and containing the stylomastoid groove): 0 = absent; 1 = present.

88) depth of hypomastoid fossa: 0 = shallow; 1 = medium; 2 = deep; 9 = absent.

89) distinct petromastoid ridge connecting paroccipital and mastoid processes: 0 = absent; 1 = present.

*90) source of "paroccipital" process: 0 = occipital; 1 = occipital and mastoid; 2 = mastoid.

91) morphology of paroccipital processes: 0 = absent; 1 = elongated ridges; 2 = bumps / pillars.

92) size of paroccipital processes: 0 = small / not prominent; 1 = intermediate; 2 = large / prominent; 9 = processes absent.

93) relationship between paroccipital processes and mastoid bone: 0 = separate; 1 = adjacent / continuous; 9 = n/a – paroccipital processes absent.

94) relationship between paroccipital processes and nuchal (= lambdoidal) crest: 0 = separate; 1 = adjacent / continuous; 9 = n/a – paroccipital processes absent.

95) relative size and shape of posterior lacerate foramen: 0 = not confluent with petrobasilar fissure; 1 = confluent with petrobasilar fissure; 9 = petrobasilar fissure absent.

96) relationship between petrobasilar fissure and basioccipital-basisphenoid suture: 0 = in contact, suture unexpanded; 1 = in contact, suture greatly expanded and confluent with fissure; 9 = petrobasilar fissure absent.

- 97) visibility of posterior opening of carotid canal in ventral view: 0 = not visible; 1 = visible; 9 = carotid canal absent.
- 98) visibility of foramen of posterior opening of carotid canal in ventral view: 0 = not visible; 1 = visible; 9 = carotid canal absent.
- 99) direction of posterior opening of carotid canal, I: 0 = distinctly greater than 45° medially (i.e., roughly medially); 1 = roughly 45° medially; 2 = distinctly less than 45° medially (i.e., roughly posteriorly); 9 = absent.
- *100) direction of posterior opening of carotid canal, II: 0 = roughly 90° (i.e., medially); 1 = distinctly greater than 45° medially but distinctly less than 90°; 2 = roughly 45° medially; 3 = distinctly less than 45° medially but distinctly greater than 0°; 4 = roughly 0° (i.e., posteriorly); 9 = carotid canal absent.
- 101) posteromedial bony shelf of auditory bulla extending from aperture of carotid canal to posterior lacerate foramen: 0 = absent; 1 = rudimentary or present; 9 = carotid canal absent.
- 102) dorsal wall of carotid canal: 0 = open; 1 = closed; 9 = carotid canal absent.
- 103) unidentified bone encircling posterior opening of carotid canal: 0 = absent; 1 = present; 9 = carotid canal absent.
- 104) opening of carotid canal in auditory bulla: 0 = anterior or anteroventral to posterior lacerate foramen; 1 = adjacent to posterior lacerate foramen; 9 = carotid canal absent.
- *105) median lacerate foramen in auditory bulla: 0 = absent; 1 = present.
- 106) size of median lacerate foramen: 0 = small; 1 = medium; 2 = large; 9 = absent.
- 107) mastoid lip in region of external cochlear foramen: 0 = absent; 1 = rudimentary or present.
- 108) external cochlear foramen: 0 = open; 1 = closed; 9 = absent.
- 109) relationship between stylomastoid and auricular foramen: 0 = confluent / common; 1 = intermediate; 2 = separate; 9 = auricular foramen absent.
- 110) relationship of tympanohyal and stylomastoid foramen: 0 = separated; 1 = closely associated.
- 111) location of tympanohyal relative to stylomastoid foramen: 0 = anterior; 1 = posterior.
- 112) position of petrosal relative to intracranial ridges of basioccipital continuous anteriorly with the dorsum sellae: 0 = widely separate; 1 = intermediate; 2 = closely adjacent.
- 113) relative size of dorsal region of petrosal: 0 = unexpanded; 1 = intermediate; 2 = expanded.
- 114) relative size and shape of petrosal apex: 0 = absent / unexpanded and pointed; 1 = intermediate; 2 = dorsoventrally thickened and bulbous.
- 115) roof of internal auditory meatus: 0 = reduced; 1 = full internal auditory meatus.
- 116) bony spur of roof of internal auditory meatus: 0 = absent; 1 = present.
- 117) inflation of bullar chamber: 0 = not inflated; 1 = inflated.

Bony tentorium and bony falx (5 characters)

- 118) contribution of parietal to bony tentorium: 0 = none / processus tentoricus absent; 1 = contributes.
- 119) contribution of parietal to bony falx: 0 = none; 1 = contributes; 9 = bony falx absent.
- 120) ventral extension of bony tentorium: 0 = does not approach floor of braincase; 1 = approaches dorsal region of petrosal; 2 = approaches or contacts floor of braincase.
- 121) morphology of bony falx proper: 0 = absent; 1 = sail-shaped; 2 = vertical; 3 = inverse sail.
- 122) partial bony falx: 0 = absent; 1 = present.

Dorsal braincase (4 characters)

123) shape of fronto-parietal suture: 0 = flat; 1 = unilobe; 2 = bi-lobed; 3 = tri-lobed or greater.

*124) separate temporal ridges: 0 = widely spaced; 1 = approximately in midline; 9 = absent.

*125) sagittal crest: 0 = absent; 1 = present.

126) size of sagittal crest: 0 = absent, but separate temporal ridges present; 1 = small; 2 = medium; 3 = large; 9 = absent.

Teeth (23 characters)

127) number of upper incisors in one-half of jaw: 0 = zero; 1 = one; 2 = two; 3 = three.

128) number of lower incisors in one-half of jaw: 0 = zero; 1 = one; 2 = two; 3 = three.

*129) morphology of incisors: 0 = peg-like; 1 = unicusgate; 2 = caniform; 3 = complex; 9 = absent.

130) shape of upper incisors in cross-section: 0 = round; 1 = intermediate; 2 = (strongly) laterally compressed; 9 = absent.

131) relative size of upper incisors: 0 = outermost incisor about equal in size to remaining incisor(s); 1 = outermost incisor of much greater size than remaining incisor(s); 9 = n/a – only one upper incisor present per quadrant.

132) relative size of lower incisors: 0 = outermost incisor about equal in size to remaining incisor(s); 1 = outermost incisor of much greater size than remaining incisor(s); 9 = n/a – one or fewer lower incisors present per quadrant.

133) displacement of incisors (upper or lower): 0 = absent – all in line with one another; 1 = present – incisor series slanted; 9 = n/a – incisors absent or singular.

134) procumbency of incisors (upper or lower): 0 = absent; 1 = present; 9 = n/a – upper or lower incisors absent.

135) number of upper postcanines: 0 = three; 1 = four; 2 = five; 3 = six.

136) number of lower postcanines: 0 = three; 1 = four; 2 = five; 3 = six; 4 = seven.

137) morphology of postcanines: 0 = peg-like / unicusgate; 1 = triconodont; 2 = multicusgate.

138) tendency to form additional cusps in triconodont postcanines: 0 = absent; 1 = present; 9 = n/a – postcanines not triconodont.

139) tendency to lose accessory cusps in triconodont postcanines: 0 = absent; 1 = present; 9 = n/a – postcanines not triconodont.

140) size of accessory cusps in triconodont or multicusgate postcanines: 0 = small, continuous with major cusp; 1 = larger, distinct from major cusp; 9 = n/a – postcanines not triconodont or multicusgate.

141) relative size of upper postcanines: 0 = all subequal; 1 = #1 (PM¹) noticeably smaller than rest, which are subequal; 2 = #5 (M¹) noticeably smaller than rest, which are subequal; 3 = #1 and #5 noticeably smaller than rest, which are subequal; 4 = #1 and/or #5 noticeably larger than rest, which are subequal; 9 = n/a – postcanine homology uncertain.

142) relative size of lower postcanines: 0 = all subequal; 1 = #1 (PM₁) noticeably smaller than rest, which are subequal; 2 = #5 (M₁) noticeably smaller than rest, which are subequal; 3 = #1 and #5 noticeably smaller than rest, which are subequal; 4 = #1 and/or #5 noticeably larger than rest, which are subequal; 9 = n/a – postcanine homology uncertain.

143) tendency to single-rooting of upper postcanines: 0 = absent; 1 = present.

144) tendency to single-rooting of lower postcanines: 0 = absent; 1 = present.

145) relative size of gap between upper postcanines 4 and 5: 0 = smaller than other gaps; 1 = subequal to other gaps; 2 = larger than other gaps; 9 = n/a – postcanine homology uncertain.

146) crowding of postcanines (upper and/or lower): 0 = not touching / overlapping; 1 = touching or overlapping.

147) obliqueness of postcanine implantation relative to long axis of tooth row (upper and lower): 0 = straight; 1 = anterior / posterior end of postcanine directed laterally.

148) obliqueness of postcanine implantation (upper and lower) relative to vertical: 0 = straight; 1 = slanted.

149) curvature of upper tooth row (postcanines only): 0 = sigmoidal; 1 = arched; 2 = straight; 3 = kinked between PC^{1,2}, otherwise straight; 4 = reverse arch.

Mandible (3 characters)

150) shape of lingual face of mandible at middle postcanines: 0 = concave; 1 = flat; 2 = convex.

151) shape of posteroventral edge of mandible: 0 = rounded; 1 = jagged.

152) distinct medially directed flange along ventral edge of jaw located posterior to mandibular symphysis and ventral to posterior postcanines: 0 = absent; 1 = present.

Forelimb (17 characters)

153) relative size of scapular spine: 0 = reduced to prominent acromion; 1 = medium; 2 = prominent.

154) relative shape of axillary (= caudal) border of scapula: 0 = straight; 1 = curved.

155) distinct hook-like teres major process on scapula: 0 = absent; 1 = present.

*156) supinator (= lateral epicondylar) ridge on humerus: 0 = absent; 1 = present.

157) relative degree of development of supinator (= lateral epicondylar) ridge on humerus: 0 = weak; 1 = medium; 2 = strong; 9 = absent.

*158) deltopectoral crest on humerus: 0 = absent; 1 = present.

159) relative length of deltopectoral crest on humerus: 0 = less than or equal to one-half length of humerus; 1 = greater than one-half length of humerus; 9 = absent.

160) merging of deltopectoral crest to shaft of humerus: 0 = smooth; 1 = abrupt; 9 = absent.

161) entepicondylar foramen of humerus: 0 = absent; 1 = present.

162) distally projecting ledge (palmar process) on cuneiform of carpus: 0 = absent; 1 = present.

163) general morphology of metacarpal shaft: 0 = no lateral shaft ridges; 1 = lateral shaft ridges.

164) general morphology of metacarpal head: 0 = smooth; 1 = "palmar" ridges present.

165) cross-sectional shape of phalanges: 0 = flat; 1 = intermediate; 2 = round.

166) morphology of proximal phalangeal articular surface: 0 = hinge-like; 1 = trochleated.

167) comparative length of metacarpals I and II: 0 = I > II; 1 = I subequal to II; 2 = I < II.

168) comparative overall diameter of metacarpals I and II: 0 = I > II; 1 = I subequal to II; 2 = I < II.

169) relative degree of development of foreflipper claws: 0 = not well developed or absent; 1 = well developed, prominent.

Pelvis (8 characters)

170) eversion of wing of ilium: 0 = distinctly less than 45°; 1 = roughly 45°; 2 = distinctly greater than 45°.

*171) gluteal fossa on wing of ilium: 0 = absent; 1 = present.

172) depth of gluteal fossa on ilium: 0 = shallow; 1 = medium; 2 = deep; 9 = absent.

173) relationship of obturator nerve foramen to obturator foramen: 0 = distinctly separate, at least unilaterally; 1 = intermediate – foramina confluent, but individually recognizable; 2 = confluent – obturator nerve foramen not apparent.

174) ridges in anterior portion of obturator foramen: 0 = absent; 1 = present.

175) relative length of post-acetabular region of the pelvis: 0 = shortened (and rounded); 1 = elongated (and narrow).

176) general curvature of pelvis around long axis: 0 = relatively straight; 1 = distinctly twisted.

177) relative location of ischiatic spine (= tuber ischiad): 0 = roughly midway along the post-acetabular region; 1 = located in posterior post-acetabular region.

Hind Limb (12 characters)

178) position of greater trochanter on femur: 0 = lower than head; 1 = equal with head; 2 = higher than head.

*179) distinct trochanteric fossa on femur: 0 = absent; 1 = present.

180) depth of trochanteric fossa on femur: 0 = shallow; 1 = medium; 2 = deep; 9 = absent.

181) lesser trochanter: 0 = absent; 1 = present.

182) relative width of femur distally: 0 = gracile (less than medium breadth); 1 = robust.

183) proximal fusion of tibia and fibula: 0 = unfused; 1 = rudimentary – not fused all the way around; 2 = totally fused.

184) relative degree of development of the post-tibial (= intercondyloid) fossa of tibia: 0 = weak; 1 = strong.

*185) robustness of calcaneum: 0 = smaller than or subequal to astragalus; 1 = larger than astragalus.

186) posterior process on plantar aspect of astragalus: 0 = absent; 1 = present.

187) depth of groove on plantar aspect of posterior process of astragalus: 0 = groove absent; 1 = shallow; 2 = moderate; 3 = deep; 9 = posterior process absent.

188) length of metatarsal III relative to remaining metatarsals (shape of posterior flipper margin): 0 = metatarsal III longest; 1 = metatarsal III intermediate; 2 = metatarsal III subequal or slightly shorter; 3 = metatarsal III distinctly shorter.

189) relative degree of development of hind flipper claws: 0 = not well developed or absent; 1 = well developed, prominent.

Miscellaneous (7 characters)

190) location of posterior end of cribriform plate: 0 = within interorbital region; 1 = posterior portion of interorbital region; 2 = anterior end of braincase.

191) relative position of vertebrarterial (= intervertebral) foramen of atlas: 0 = visible in dorsal view; 1 = visible in posterior view.

192) claw morphology in cross-section, I: 0 = semicircular; 1 = triangular.

193) claw morphology in cross-section, II: 0 = dorsal ridge or annuli absent; 1 = dorsal ridge or annuli present.

194) mystacial whiskers: 0 = smooth; 1 = beaded.

195) secondary hairs: 0 = (largely) absent; 1 = present.

196) relative overall size of males and females: 0 = females smaller than males; 1 = females subequal to males; 2 = females larger than males.

[illegible]

Observations obtained from, or based primarily upon, literature values are indicated in bold face. A question mark indicates a missing observation.

[illegible]

APPENDIX D

Branch lengths and linkages

The information contained in this appendix applies to the overall (consensus) solution presented in Fig.5B. Assigned (inversely weighted) branch lengths are listed according to accelerated transformation / delayed transformation optimization criteria. Outgroup taxa are indicated by an asterisk.

Node	Connected to node	Assigned branch length	Minimum possible length	Maximum possible length
<i>Canis</i> (1)*	50	1448/874	874	1448
<i>Procyon</i> (2)*	49	540/623	391	806
<i>Enhydra</i> (3)*	47	516/1123	416	1306
<i>Lutra</i> (4)*	46	724/1024	400	1390
<i>Martes</i> (5)*	48	1032/1415	799	1465
<i>Ursus</i> (6)*	50	1124/1390	1074	1390
<i>Odobenus</i> (7)*	28	1181/1564	882	2097
<i>Zalophus</i> (8)*	28	1223/1339	857	1755
<i>Cystophora</i> (9)	35	556/1005	498	1088
<i>Erignathus</i> (10)	30	1265/1348	1265	1348
<i>Halichoerus</i> (11)	34	482/665	399	715
<i>Hydrurga</i> (12)	41	965/1115	733	1323
<i>Leptonychotes</i> (13)	40	669/822	586	930
<i>Lobodon</i> (14)	38	1368/1268	1065	1401
<i>Mirounga angustirostris</i> (15)	42	574/844	416	977
<i>Mirounga leonina</i> (16)	42	633/749	533	957
<i>Monachus monachus</i> (17)	37	832/1232	674	1298
<i>Monachus schauinslandi</i> (18)	36	748/1181	615	1281
<i>Monachus tropicalis</i> (19)	36	919/802	536	1102
<i>Ommatophoca</i> (20)	39	844/957	658	1060
<i>Pusa caspica</i> (21)	32	681/831	681	831
<i>Histiophoca</i> (22)	29	202/385	202	385
<i>Pagophilus</i> (23)	29	583/666	550	699
<i>Pusa hispida</i> (24)	31	100/183	100	183
<i>Phoca largha</i> (25)	33	383/383	383	383
<i>Pusa sibirica</i> (26)	31	677/1093	627	1143
<i>Phoca vitulina</i> (27)	32	800/850	800	850
28	45	1066/1432	750	2397
29	30	332/149	149	415
30	32	590/274	274	590
31	32	699/300	300	799
32	33	183/383	133	533
33	34	608/325	275	891
34	35	955/772	356	1413
35	44	1790/791	533	2065
36	37	982/927	749	1243

Node	Connected to node	Assigned branch length	Minimum possible length	Maximum possible length
37	38	1124/816	533	1560
38	39	519/402	286	888
39	40	508/275	250	724
40	41	736/716	533	1018
41	43	874/708	433	1315
42	43	1129/993	685	1495
43	44	633/1141	333	1724
44	45	1780/1855	1272	2521
45	46	2065/766	500	2497
46	47	665/483	383	1048
47	48	1282/541	541	1548
48	49	616/532	366	948
49	50	931/824	549	1239

APPENDIX E

Apomorphy Lists (unweighted)

The information contained in this appendix applies to the overall (consensus) solution presented in Fig.5B. The changes listed are consistent between optimization criteria unless followed by: (A) = accelerated transformation (ACCTRAN) only, or (D) = delayed transformation (DELTRAN) only. Some changes were indicated by PAUP as being equivocal, but were observed to be identical between ACCTRAN and DELTRAN optimizations. The ambiguity arises from a different possible reconstruction under a third optimization criterion (MINF) that wasn't examined here, PAUP listing most within terminal changes as being ambiguous, or because the node immediately preceding the branch was ambiguous. These options are denoted by (F), (?), and (?) respectively.

Note that steps are listed as the number of changes in state for each transition (= unweighted steps). Excluded characters are preceded by an asterisk.

Branch	Character	Steps	CI	Change
<i>Canis</i> ↔ node 50	19	1	0.500	1 ↔ 0
	59	1	0.625	2 ↔ 0
	76	1	0.688	2 ↔ 1
	79	1	0.727	2 ↔ 1
	80	1	0.538	1 ↔ 0
	88	1	0.667	0 ↔ 2 (A)
	93	1	0.625	0 ↔ 1 (A)
	95	1	0.571	0 ↔ 1
	97	1	0.500	9 ↔ 0 (A)
	98	1	0.857	9 ↔ 0
	99	1	0.571	9 ↔ 2
	*100	1	0.556	9 ↔ 4
	101	1	0.667	9 ↔ 0
	102	1	0.500	9 ↔ 0 (A)
	103	1	1.000	9 ↔ 0
	104	1	1.000	9 ↔ 0 (A)
	120	1	0.778	0 ↔ 2
	126	1	0.579	3 ↔ 1
	135	1	0.800	3 ↔ 2 (A)
	136	1	1.000	4 ↔ 3 (A)
	*156	1	0.833	0 ↔ 1
	157	1	0.765	9 ↔ 1
	159	1	0.667	0 ↔ 1 (A)
	162	1	0.600	0 ↔ 1
	168	1	0.571	2 ↔ 1
	172	1	0.625	0 ↔ 1 (A)
	174	1	0.692	1 ↔ 0 (A)
	184	1	0.750	0 ↔ 1 (A)
	191	1	0.833	0 ↔ 1
<i>Canis</i> (within terminal)	*23	1	0.429	1 ⇒ 01 (?)
	24	1	0.571	0 ⇒ 09 (?)
	26	1	0.875	1 ⇒ 12 (?)

Appendix E (continued)

Branch	Character	Steps	CI	Change	
node 50 → <i>Ursus</i>	123	1	0.778	0 ⇒ 01	(?)
	10	1	0.647	2 ⇒ 0	
	14	1	0.538	0 ⇒ 2	
	16	1	0.667	0 ⇒ 1	
	*18	1	0.455	1 ⇒ 2	
	29	1	1.000	0 ⇒ 1	
	31	1	0.636	0 ⇒ 1	
	*32	1	0.643	0 ⇒ 2	
	*33	1	0.667	9 ⇒ 0	
	*34	1	0.750	9 ⇒ 0	
	*35	1	0.692	9 ⇒ 0	
	*36	1	0.500	9 ⇒ 0	
	43	1	0.545	9 ⇒ 0	
	81	1	0.400	2 ⇒ 0	
	82	1	0.500	2 ⇒ 1	
	88	1	0.667	0 → 12	(D)
	89	1	0.500	0 ⇒ 1	
	93	1	0.625	0 → 1	(D)
	97	1	0.500	9 → 0	(D)
	102	1	0.500	9 → 0	(D)
	104	1	1.000	0 → 1	(A)
	104	1	1.000	9 → 1	(D)
	110	1	0.500	1 ⇒ 0	
	113	1	0.375	0 ⇒ 2	
	135	1	0.800	3 → 2	(D)
	143	1	0.250	0 ⇒ 1	
	149	1	0.667	0 ⇒ 12	
	154	1	0.700	0 ⇒ 1	
	159	1	0.667	0 → 1	(D)
	167	1	0.571	2 ⇒ 1	
	170	1	0.636	0 ⇒ 1	
	188	1	0.625	0 ⇒ 1	
<i>Ursus</i> (within terminal)	4	1	1.000	0 ⇒ 01	(?)
	26	1	0.875	1 ⇒ 12	(?)
	44	1	0.636	0 ⇒ 01	(?)
	49	1	0.588	2 ⇒ 02	(?)
	52	1	0.692	2 ⇒ 12	(?)
	88	1	0.667	2 → 12	(A)
	88	1	0.667	1 → 12	(D)
	112	2	0.692	2 ⇒ 012	(?)
	*129	1	0.625	1 ⇒ 12	(?)
	136	2	1.000	3 → 234	(A)
	136	2	1.000	4 → 234	(D)
	144	1	0.600	0 ⇒ 01	(?)
	149	1	0.667	1 ⇒ 12	(?)
	155	1	0.889	0 ⇒ 01	(?)

Appendix E (continued)

Branch	Character	Steps	CI	Change	
node 50 → node 49	172	1	0.625	1 → 01	(A)
	172	1	0.625	0 → 01	(D)
	174	1	0.692	0 → 01	(A)
	174	1	0.692	1 → 01	(D)
	184	1	0.750	1 → 01	(A)
	184	1	0.750	0 → 01	(D)
	9	1	0.583	0 → 1	(A)
	20	1	0.733	1 ⇒ 0	
	21	1	1.000	0 ⇒ 1	
	26	1	0.875	1 → 0	(A)
	28	1	0.800	1 → 0	(A)
	48	1	0.500	1 ⇒ 0	
	49	1	0.588	2 → 1	(A)
	58	1	0.625	2 ⇒ 1	
	78	1	0.682	2 → 0	(A)
	92	1	0.625	2 → 0	(A)
	97	1	0.500	0 → 1	(A)
	97	1	0.500	9 → 1	(D)
	102	1	0.500	0 → 1	(A)
	102	1	0.500	9 → 1	(D)
	104	1	1.000	9 → 0	(D)
	106	1	0.500	1 ⇒ 0	
	119	1	0.786	1 ⇒ 9	
	122	1	1.000	1 ⇒ 0	
	*125	1	0.333	1 → 0	(A)
	136	1	1.000	4 → 3	(D)
	161	1	0.333	0 ⇒ 1	
	178	1	0.643	0 → 1	(A)
	184	1	0.750	0 → 1	(D)
node 49 → <i>Procyon</i>	*23	1	0.429	1 ⇒ 0	
	24	1	0.571	0 ⇒ 9	
	26	1	0.875	1 → 0	(D)
	28	1	0.800	1 → 0	(D)
	49	1	0.588	2 → 1	(D)
	69	1	0.167	0 ⇒ 1	
	*71	1	0.571	0 ⇒ 1	
	72	1	0.667	9 ⇒ 1	
	75	1	0.500	0 ⇒ 1	
	78	1	0.682	0 → 1	(A)
	78	1	0.682	2 → 1	(D)
	92	1	0.625	0 → 1	(A)
	92	1	0.625	2 → 1	(D)
	*124	1	0.692	9 ⇒ 1	
	*125	1	0.333	1 → 0	(D)
	126	1	0.579	1 ⇒ 0	
	131	1	0.833	1 ⇒ 0	
	135	1	0.800	2 → 3	(A)

Appendix E (continued)

Branch	Character	Steps	CI	Change	
	157	1	0.765	1 \Rightarrow 2	
	159	1	0.667	1 \rightarrow 0	(A)
	172	1	0.625	0 \rightarrow 1	(D)
<i>Procyon</i> (within terminal)	9	1	0.583	1 \rightarrow 01	(A)
	9	1	0.583	0 \rightarrow 01	(D)
	45	1	0.500	0 \Rightarrow 01	(?)
	63	1	0.778	1 \Rightarrow 01	(?)
	76	1	0.688	1 \Rightarrow 12	(?)
	79	1	0.727	1 \Rightarrow 12	(?)
	88	1	0.667	2 \rightarrow 02	(A)
	88	1	0.667	0 \rightarrow 02	(D)
	93	1	0.625	1 \rightarrow 01	(A)
	93	1	0.625	0 \rightarrow 01	(D)
	98	1	0.857	0 \Rightarrow 01	(?)
	162	1	0.600	1 \Rightarrow 01	(?)
	174	1	0.692	0 \rightarrow 01	(A)
	174	1	0.692	1 \rightarrow 01	(D)
	178	1	0.643	1 \rightarrow 01	(A)
	178	1	0.643	0 \rightarrow 01	(D)
node 49 \rightarrow node 48	30	1	0.667	1 \rightarrow 0	(A)
	40	1	0.500	1 \rightarrow 0	(A)
	50	1	0.400	1 \Rightarrow 0	
	*87	1	0.500	1 \rightarrow 0	(A)
	88	1	0.667	2 \Rightarrow 9	
	92	1	0.625	2 \rightarrow 0	(D)
	123	1	0.778	0 \Rightarrow 1	
	130	1	0.571	0 \rightarrow 2	(A)
	135	1	0.800	3 \rightarrow 2	(D)
	163	1	0.667	1 \Rightarrow 0	
	174	1	0.692	1 \rightarrow 0	(D)
	175	1	0.750	0 \Rightarrow 1	
node 48 \rightarrow <i>Martes</i>	17	1	0.250	1 \Rightarrow 0	
	*18	1	0.455	1 \Rightarrow 0	
	28	1	0.800	0 \rightarrow 1	(A)
	30	1	0.667	1 \rightarrow 0	(D)
	38	1	0.632	2 \Rightarrow 1	
	40	1	0.500	1 \rightarrow 0	(D)
	45	1	0.500	0 \Rightarrow 1	
	47	1	0.333	0 \Rightarrow 1	
	49	1	0.588	2 \rightarrow 1	(D)
	74	1	0.625	0 \Rightarrow 1	
	*77	1	0.833	1 \Rightarrow 0	
	78	1	0.682	0 \rightarrow 9	(A)
	78	1	0.682	2 \rightarrow 9	(D)
	80	1	0.538	0 \Rightarrow 1	
	83	1	0.800	0 \Rightarrow 1	
	*87	1	0.500	1 \rightarrow 0	(D)

Appendix E (continued)

Branch	Character	Steps	CI	Change	
	93	1	0.625	0 → 1	(D)
	95	1	0.571	1 ⇒ 9	
	96	1	0.500	0 ⇒ 9	
	97	1	0.500	1 ⇒ 0	(?)
	99	1	0.571	2 ⇒ 0	
	*100	1	0.556	4 ⇒ 0	
	102	1	0.500	1 ⇒ 0	(?)
	113	1	0.375	0 ⇒ 12	
	130	1	0.571	0 → 2	(D)
	157	1	0.765	1 ⇒ 0	
	*158	1	1.000	1 ⇒ 0	
	159	1	0.667	1 → 9	(A)
	159	1	0.667	0 → 9	(D)
	160	1	0.667	0 ⇒ 9	
	172	1	0.625	0 → 1	(D)
	178	1	0.643	0 → 1	(D)
	183	1	0.667	0 ⇒ 1	
<i>Martes</i> (within terminal)	9	1	0.583	1 → 01	(A)
	9	1	0.583	0 → 01	(D)
	10	1	0.647	2 ⇒ 02	(?)
	26	1	0.875	0 → 01	(A)
	26	1	0.875	1 → 01	(D)
	58	1	0.625	1 ⇒ 01	(?)
	66	1	0.667	1 ⇒ 01	(?)
	70	1	0.727	1 ⇒ 12	(?)
	*71	1	0.571	0 → 01	(?)
	72	2	0.667	9 ⇒ 019	(?)
	113	1	0.375	1 ⇒ 12	(?)
	*125	1	0.333	0 → 01	(A)
	*125	1	0.333	1 → 01	(D)
	126	1	0.579	1 ⇒ 19	(?)
	132	1	0.714	0 ⇒ 01	(?)
	150	1	0.600	1 → 12	(?)
node 48 → node 47	22	1	0.667	0 → 1	(A)
	24	1	0.571	0 ⇒ 1	
	42	1	0.800	2 ⇒ 0	
	49	1	0.588	1 → 2	(A)
	54	1	1.000	1 ⇒ 0	
	59	1	0.625	0 ⇒ 2	
	73	1	0.750	0 → 1	(A)
	81	1	0.400	2 ⇒ 0	
	84	1	0.400	1 → 0	(A)
	85	1	1.000	1 ⇒ 0	
	91	1	0.556	2 ⇒ 1	
	93	1	0.625	1 → 0	(A)
	110	1	0.500	1 ⇒ 0	
	117	1	0.333	1 → 0	(A)

Appendix E (continued)

Branch	Character	Steps	CI	Change	
node 47 → <i>Enhydra</i>	128	1	0.667	3 → 2	(A)
	*129	1	0.625	1 ⇒ 0	
	136	1	1.000	3 ⇒ 2	
	149	1	0.667	0 → 1	(A)
	172	1	0.625	1 → 0	(A)
	189	1	0.500	1 → 0	(A)
	190	1	0.750	0 → 1	(A)
	8	1	0.333	0 ⇒ 1	
	9	1	0.583	0 → 1	(D)
	22	1	0.667	0 → 1	(D)
	26	1	0.875	1 → 0	(D)
	28	1	0.800	1 → 0	(D)
	40	1	0.500	0 → 1	(A)
	76	1	0.688	1 ⇒ 2	
	78	1	0.682	2 → 09	(D)
	84	1	0.400	1 → 0	(D)
	*87	1	0.500	1 → 0	(D)
	98	1	0.857	0 ⇒ 1	
	117	1	0.333	1 → 0	(D)
	*125	1	0.333	0 → 1	(A)
	128	1	0.667	3 → 2	(D)
	130	1	0.571	0 → 2	(D)
	135	1	0.800	2 ⇒ 1	
	149	1	0.667	0 → 1	(D)
	165	1	0.500	2 ⇒ 0	
	167	1	0.571	2 ⇒ 1	
	170	1	0.636	0 ⇒ 1	
	178	1	0.643	0 → 1	(D)
	188	1	0.625	0 ⇒ 1	
	189	1	0.500	1 → 0	(D)
<i>Enhydra</i> (within terminal)	4	1	1.000	0 ⇒ 01	(?)
	6	1	0.714	0 ⇒ 01	(?)
	10	1	0.647	2 ⇒ 02	(?)
	20	1	0.733	0 ⇒ 09	(?)
	30	1	0.667	0 → 01	(A)
	30	1	0.667	1 → 01	(D)
	38	1	0.632	2 ⇒ 12	(?)
	49	1	0.588	2 ⇒ 12	(?)
	50	1	0.400	0 ⇒ 01	(?)
	64	1	0.545	0 ⇒ 01	(?)
	65	2	0.545	1 ⇒ 012	(?)
	73	1	0.750	1 → 01	(A)
	73	1	0.750	0 → 01	(D)
	*77	1	0.833	1 ⇒ 01	(?)
	78	1	0.682	0 ⇒ 09	(F)
	79	1	0.727	1 ⇒ 01	(?)

Appendix E (continued)

Branch	Character	Steps	CI	Change	
node 47 → node 46	95	1	0.571	1 ⇒ 01	(?)
	101	1	0.667	0 ⇒ 01	(?)
	107	1	0.714	0 ⇒ 01	(?)
	119	1	0.786	9 ⇒ 19	(?)
	121	1	0.600	0 ⇒ 01	(?)
	122	1	1.000	0 ⇒ 01	(?)
	133	1	1.000	0 ⇒ 01	(?)
	157	1	0.765	1 ⇒ 12	(?)
	159	1	0.667	1 → 01	(A)
	159	1	0.667	0 → 01	(D)
	190	1	0.750	1 → 01	(A)
	190	1	0.750	0 → 01	(D)
	26	1	0.875	0 → 1	(A)
	40	1	0.500	1 → 0	(D)
	44	1	0.636	0 → 1	
	58	1	0.625	1 → 0	(A)
	62	1	0.556	1 ⇒ 0	
	63	1	0.778	1 ⇒ 0	
	66	1	0.667	1 ⇒ 0	
	*87	1	0.500	0 → 1	(A)
	119	1	0.786	9 ⇒ 0	
	121	1	0.600	0 ⇒ 2	
	*125	1	0.333	1 → 0	(D)
	126	1	0.579	1 → 0	(A)
	130	1	0.571	2 → 0	(A)
	149	1	0.667	1 → 2	(A)
	172	1	0.625	0 → 9	(A)
	178	1	0.643	1 → 0	(A)
	180	1	0.500	2 → 1	(A)
node 46 → <i>Lutra</i>	9	1	0.583	0 → 12	(D)
	22	1	0.667	0 → 1	(D)
	30	1	0.667	0 → 1	(A)
	58	1	0.625	0 → 2	(A)
	58	1	0.625	1 → 2	(D)
	73	1	0.750	0 → 1	(D)
	78	1	0.682	0 → 12	(A)
	79	1	0.727	1 ⇒ 0	
	84	1	0.400	1 → 0	(D)
	95	1	0.571	1 ⇒ 0	
	117	1	0.333	1 → 0	(D)
	126	1	0.579	0 → 9	(A)
	126	1	0.579	1 → 9	(D)
	128	1	0.667	2 → 3	(A)
	133	1	1.000	0 ⇒ 1	
	154	1	0.700	0 ⇒ 1	
	159	1	0.667	0 → 1	(D)

Appendix E (continued)

Branch	Character	Steps	CI	Change
	163	1	0.667	$0 \Rightarrow 1$
	165	1	0.500	$2 \Rightarrow 1$
	180	1	0.500	$2 \rightarrow 1$ (D)
	189	1	0.500	$0 \rightarrow 1$ (A)
	190	1	0.750	$0 \rightarrow 1$ (D)
<i>Lutra</i> (within terminal)	3	1	0.800	$1 \Rightarrow 01$ (?)
	9	1	0.583	$1 \Rightarrow 12$ (?)
	16	1	0.667	$0 \Rightarrow 01$ (?)
	*18	1	0.455	$1 \Rightarrow 12$ (?)
	20	1	0.733	$0 \Rightarrow 01$ (?)
	24	1	0.571	$1 \Rightarrow 01$ (?)
	28	1	0.800	$0 \rightarrow 01$ (A)
	28	1	0.800	$1 \rightarrow 01$ (D)
	42	1	0.800	$0 \Rightarrow 02$ (?)
	45	1	0.500	$0 \Rightarrow 01$ (?)
	78	1	0.682	$1 \rightarrow 12$ (A)
	78	1	0.682	$2 \rightarrow 12$ (D)
	*87	1	0.500	$1 \Rightarrow 01$ (?)
	88	1	0.667	$9 \Rightarrow 09$ (?)
	92	1	0.625	$0 \Rightarrow 01$ (?)
	93	1	0.625	$0 \Rightarrow 01$ (F)
	98	1	0.857	$0 \Rightarrow 01$ (?)
	107	1	0.714	$0 \Rightarrow 01$ (?)
	130	1	0.571	$0 \Rightarrow 01$ (?)
	132	1	0.714	$0 \Rightarrow 01$ (F)
	149	1	0.667	$2 \rightarrow 02$ (A)
	149	1	0.667	$0 \rightarrow 02$ (D)
	157	1	0.765	$1 \Rightarrow 12$ (?)
	*171	1	0.429	$1 \Rightarrow 01$ (?)
	172	1	0.625	$9 \rightarrow 09$ (A)
	172	1	0.625	$0 \rightarrow 09$ (D)
	178	1	0.643	$0 \Rightarrow 01$ (F)
	184	1	0.750	$1 \Rightarrow 01$ (?)
node 46 \rightarrow node 45	9	1	0.583	$1 \rightarrow 0$ (A)
	14	1	0.538	$0 \rightarrow 9$ (A)
	22	1	0.667	$1 \rightarrow 0$ (A)
	*27	1	1.000	$1 \Rightarrow 0$
	28	1	0.800	$0 \Rightarrow 9$
	30	1	0.667	$1 \rightarrow 0$ (D)
	31	1	0.636	$0 \rightarrow 2$ (A)
	*35	1	0.692	$9 \rightarrow 0$ (A)
	41	1	0.571	$0 \rightarrow 1$ (A)
	58	1	0.625	$1 \rightarrow 0$ (D)
	*71	1	0.571	$0 \Rightarrow 1$
	72	1	0.667	$9 \rightarrow 0$ (A)
	84	1	0.400	$0 \rightarrow 1$ (A)

Appendix E (continued)

Branch	Character	Steps	CI	Change	
	86	1	0.500	0 → 1	(A)
	106	1	0.500	0 → 2	(A)
	112	1	0.692	2 ⇒ 0	
	113	1	0.375	0 → 2	(A)
	117	1	0.333	0 → 1	(A)
	126	1	0.579	1 → 0	(D)
	128	1	0.667	3 → 2	(D)
	132	1	0.714	0 → 9	(A)
	137	1	0.700	2 → 0	(A)
	143	1	0.250	0 ⇒ 1	
	144	1	0.600	0 → 1	(A)
	146	1	0.250	1 ⇒ 0	
	149	1	0.667	0 → 2	(D)
	190	1	0.750	0 → 2	(D)
	153	1	0.833	2 → 1	(A)
	161	1	0.333	1 → 0	(A)
	162	1	0.600	1 → 0	(A)
	166	1	0.500	1 → 0	(A)
	167	1	0.571	2 ⇒ 0	
	168	1	0.571	1 ⇒ 0	
	174	1	0.692	0 ⇒ 1	
	177	1	0.400	1 → 0	(A)
	180	1	0.500	1 → 9	(A)
	183	1	0.667	0 → 2	(A)
	188	1	0.625	0 → 2	(A)
	190	1	0.750	1 → 2	(A)
node 45 → node 28	10	1	0.647	2 → 0	(A)
	13	1	1.000	1 ⇒ 0	
	14	1	0.538	0 → 9	(D)
	16	1	0.667	0 ⇒ 1	
	*18	1	0.455	1 → 2	(A)
	41	1	0.571	0 → 1	(D)
	44	1	0.636	1 ⇒ 2	
	45	1	0.500	0 ⇒ 2	
	48	1	0.500	0 ⇒ 1	
	70	1	0.727	1 → 2	(A)
	73	1	0.750	1 → 0	(A)
	82	1	0.500	2 ⇒ 0	
	88	1	0.667	9 → 0	(A)
	89	1	0.500	0 ⇒ 1	
	93	1	0.625	0 ⇒ 1	(F)
	102	1	0.500	1 ⇒ 0	
	106	1	0.500	0 → 2	(D)
	119	1	0.786	0 → 1	(A)
	137	1	0.700	2 → 0	(D)
	144	1	0.600	0 → 1	(D)

Appendix E (continued)

Branch	Character	Steps	CI	Change	
node 28 → <i>Zalophus</i>	159	1	0.667	0 → 1	(D)
	161	1	0.333	1 → 0	(D)
	166	1	0.500	1 → 0	(D)
	169	1	0.333	1 ⇒ 0	
	*171	1	0.429	1 ⇒ 0	
	172	1	0.625	0 → 9	(D)
	173	1	0.750	2 ⇒ 1	
	188	1	0.625	0 → 2	(D)
	10	1	0.647	2 → 0	(D)
	17	1	0.250	1 ⇒ 0	
	*18	1	0.455	2 → 3	(A)
	*18	1	0.455	1 → 3	(D)
	26	1	0.875	1 ⇒ 2	
	31	1	0.636	0 → 2	(D)
	*32	1	0.643	0 ⇒ 34	
	*33	1	0.667	9 ⇒ 1	
	*34	1	0.750	9 ⇒ 01	
	*35	1	0.692	9 → 0	(D)
	*36	1	0.500	9 ⇒ 1	
	39	1	0.667	0 ⇒ 1	
	43	1	0.545	9 ⇒ 1	
	46	1	0.333	0 ⇒ 1	
	47	1	0.333	0 ⇒ 1	
	50	1	0.400	0 ⇒ 1	
	59	1	0.625	2 ⇒ 0	
	78	1	0.682	2 → 0	(D)
	86	1	0.500	1 → 0	(A)
	88	1	0.667	0 → 2	(A)
	88	1	0.667	9 → 2	(D)
	91	1	0.556	1 ⇒ 2	
	92	1	0.625	0 ⇒ 2	
	97	1	0.500	1 ⇒ 0	
	113	1	0.375	2 → 0	(A)
	117	1	0.333	1 ⇒ 0	(?)
	119	1	0.786	0 → 1	(D)
	123	1	0.778	1 ⇒ 0	
	*125	1	0.333	0 ⇒ 1	
	126	1	0.579	0 ⇒ 3	
	132	1	0.714	9 → 0	(A)
	165	1	0.500	2 ⇒ 0	
	177	1	0.400	1 → 0	(D)
	180	1	0.500	9 → 0	(A)
	180	1	0.500	2 → 0	(D)
	183	1	0.667	0 → 2	(D)
<i>Zalophus</i> (within terminal)	20	2	0.733	0 ⇒ 012	(?)
	*32	1	0.643	3 ⇒ 34	(?)

Appendix E (continued)

Branch	Character	Steps	CI	Change	
	*34	1	0.750	1 \Rightarrow 01	(?)
	67	1	0.778	9 \Rightarrow 19	(?)
	68	1	0.800	9 \Rightarrow 19	(?)
	70	1	0.727	2 \rightarrow 12	(A)
	70	1	0.727	1 \rightarrow 12	(D)
	*71	1	0.571	1 \Rightarrow 01	(?)
	72	1	0.667	0 \rightarrow 09	(A)
	72	1	0.667	9 \rightarrow 09	(D)
	82	1	0.500	0 \Rightarrow 01	(?)
	130	1	0.571	0 \Rightarrow 02	(?)
	135	1	0.800	2 \Rightarrow 23	(?)
	137	1	0.700	0 \Rightarrow 01	(F)
	138	1	0.636	9 \Rightarrow 09	(?)
	139	1	0.750	9 \Rightarrow 19	(?)
	140	1	0.778	9 \Rightarrow 09	(?)
	149	1	0.667	2 \Rightarrow 24	(?)
	153	1	0.833	1 \rightarrow 12	(A)
	153	1	0.833	2 \rightarrow 12	(D)
	155	1	0.889	0 \Rightarrow 01	(?)
	157	1	0.765	1 \Rightarrow 01	(?)
	162	1	0.600	0 \rightarrow 01	(A)
	162	1	0.600	1 \rightarrow 01	(D)
	178	1	0.643	0 \Rightarrow 01	(F)
	184	1	0.750	1 \Rightarrow 01	(?)
	189	1	0.500	0 \rightarrow 01	(A)
	189	1	0.500	1 \rightarrow 01	(D)
	190	1	0.750	2 \Rightarrow 12	(F)
	192	1	1.000	0 \Rightarrow 01	(?)
node 28 \rightarrow <i>Odobenus</i>	7	1	0.500	0 \Rightarrow 1	
	8	1	0.333	0 \Rightarrow 1	
	9	1	0.583	0 \Rightarrow 1	(?)
	10	1	0.647	0 \rightarrow 1	(A)
	10	1	0.647	2 \rightarrow 1	(D)
	*18	1	0.455	1 \rightarrow 2	(D)
	20	1	0.733	0 \Rightarrow 9	
	31	1	0.636	2 \rightarrow 0	(A)
	*35	1	0.692	0 \rightarrow 9	(A)
	38	1	0.632	2 \Rightarrow 19	
	51	1	0.714	2 \Rightarrow 1	
	60	1	0.750	1 \Rightarrow 0	
	65	1	0.545	1 \Rightarrow 2	
	70	1	0.727	1 \rightarrow 2	(D)
	72	1	0.667	9 \rightarrow 01	(D)
	78	1	0.682	0 \rightarrow 29	(A)
	86	1	0.500	0 \rightarrow 1	(D)
	88	1	0.667	9 \rightarrow 0	(D)

Appendix E (continued)

Branch	Character	Steps	CI	Change	
	113	1	0.375	0 → 2	(D)
	127	1	0.667	3 ⇒ 1	
	128	1	0.667	2 ⇒ 0	
	*129	1	0.625	0 ⇒ 9	
	131	1	0.833	1 ⇒ 9	
	132	1	0.714	0 → 9	(D)
	133	1	1.000	0 ⇒ 9	
	134	1	0.667	0 ⇒ 9	
	135	1	0.800	2 ⇒ 0	
	136	1	1.000	2 ⇒ 0	
	149	1	0.667	2 ⇒ 1	
	150	1	0.600	1 ⇒ 0	
	153	1	0.833	2 → 1	(D)
	162	1	0.600	1 → 0	(D)
	177	1	0.400	0 → 1	(A)
	*179	1	0.333	1 ⇒ 0	
	180	1	0.500	2 → 9	(D)
	183	1	0.667	2 → 0	(A)
	189	1	0.500	1 → 0	(D)
	195	1	0.333	1 ⇒ 0	
<i>Odobenus</i> (within terminal)	6	1	0.714	0 ⇒ 01	(?)
	*27	1	1.000	0 ⇒ 01	(?)
	28	1	0.800	9 ⇒ 19	(?)
	*37	1	0.833	1 ⇒ 01	(?)
	38	1	0.632	1 ⇒ 19	(?)
	52	1	0.692	2 ⇒ 12	(?)
	58	1	0.625	0 ⇒ 01	(?)
	63	1	0.778	0 ⇒ 01	(?)
	72	1	0.667	0 → 01	(A)
	72	1	0.667	1 → 01	(D)
	73	1	0.750	0 ⇒ 01	(F)
	*77	1	0.833	1 ⇒ 01	(?)
	78	1	0.682	2 ⇒ 29	(F)
	83	1	0.800	0 ⇒ 01	(?)
	98	1	0.857	0 ⇒ 01	(?)
	112	2	0.692	0 ⇒ 012	(?)
	119	1	0.786	1 → 01	(A)
	119	1	0.786	0 → 01	(D)
	*124	1	0.692	9 ⇒ 19	(?)
	126	1	0.579	0 ⇒ 09	(F)
	152	1	0.750	0 ⇒ 01	(?)
	164	1	1.000	1 ⇒ 01	(?)
	184	1	0.750	1 ⇒ 01	(?)
	188	1	0.625	2 ⇒ 23	(F)
node 45 → node 44	11	1	0.500	2 ⇒ 0	
	19	1	0.500	0 ⇒ 1	

Appendix E (continued)

Branch	Character	Steps	CI	Change
	*25	1	1.000	1 \Rightarrow 0
	26	1	0.875	1 \Rightarrow 9
	*32	1	0.643	0 \Rightarrow 5
	*33	1	0.667	9 \Rightarrow 0
	*34	1	0.750	9 \Rightarrow 2
	*36	1	0.500	9 \Rightarrow 0
	43	1	0.545	9 \Rightarrow 0
	49	1	0.588	2 \rightarrow 1 (A)
	52	1	0.692	2 \rightarrow 1 (A)
	*55	1	1.000	0 \Rightarrow 1
	56	1	0.636	9 \Rightarrow 1
	69	1	0.167	0 \rightarrow 1 (A)
	72	1	0.667	0 \rightarrow 1 (A)
	72	1	0.667	9 \rightarrow 1 (D)
	73	1	0.750	0 \rightarrow 1 (D)
	81	1	0.400	0 \Rightarrow 2
	86	1	0.500	0 \rightarrow 1 (D)
	108	1	0.429	9 \Rightarrow 0
	109	1	0.750	9 \Rightarrow 2
	111	1	1.000	1 \Rightarrow 0
	113	1	0.375	0 \rightarrow 2 (D)
	114	1	0.750	0 \Rightarrow 2
	115	1	1.000	1 \Rightarrow 0
	118	1	1.000	1 \Rightarrow 0
	120	1	0.778	2 \Rightarrow 0
	123	1	0.778	1 \Rightarrow 2
	127	1	0.667	3 \rightarrow 2 (A)
	130	1	0.571	0 \rightarrow 2 (A)
	132	1	0.714	0 \rightarrow 1 (D)
	137	1	0.700	0 \rightarrow 1 (A)
	137	1	0.700	2 \rightarrow 1 (D)
	141	1	0.692	9 \Rightarrow 0
	142	1	0.750	9 \Rightarrow 0
	145	1	0.571	9 \Rightarrow 1
	157	1	0.765	1 \Rightarrow 0
	159	1	0.667	1 \rightarrow 0 (A)
	177	1	0.400	1 \rightarrow 0 (D)
	181	1	1.000	1 \Rightarrow 0
	183	1	0.667	0 \rightarrow 2 (D)
	*185	1	1.000	1 \Rightarrow 0
	186	1	1.000	0 \Rightarrow 1
	187	1	0.913	9 \rightarrow 0 (A)
	188	1	0.625	2 \rightarrow 3 (A)
	188	1	0.625	0 \rightarrow 3 (D)
	194	1	0.333	0 \Rightarrow 1

Appendix E (continued)

Branch	Character	Steps	CI	Change
node 44 → node 43	6	1	0.714	0 ⇒ 1
	31	1	0.636	0 → 2 (D)
	*35	1	0.692	0 → 1 (A)
	*35	1	0.692	9 → 1 (D)
	38	1	0.632	2 ⇒ 1
	41	1	0.571	0 → 1 (D)
	52	1	0.692	2 → 1 (D)
	69	1	0.167	0 → 1 (D)
	74	1	0.625	0 ⇒ 1
	76	1	0.688	1 → 0 (A)
	79	1	0.727	1 ⇒ 0
	95	1	0.571	1 ⇒ 0
	127	1	0.667	3 → 2 (D)
	161	1	0.333	1 → 0 (D)
	162	1	0.600	1 → 0 (D)
	164	1	1.000	1 → 0 (A)
	166	1	0.500	1 → 0 (D)
	175	1	0.750	1 ⇒ 0
	*179	1	0.333	1 → 0 (A)
	180	1	0.500	2 → 9 (D)
	182	1	0.500	0 → 1 (A)
	187	1	0.913	9 → 0 (D)
	189	1	0.500	1 → 0 (D)
	190	1	0.750	2 → 1 (A)
node 43 → node 42	7	1	0.500	0 ⇒ 9
	10	1	0.647	2 ⇒ 9
	12	1	0.333	1 ⇒ 0
	14	1	0.538	0 → 9 (D)
	20	1	0.733	0 ⇒ 2
	24	1	0.571	1 → 2 (A)
	*57	1	0.667	1 → 0 (A)
	58	1	0.625	0 → 9 (A)
	59	1	0.625	2 ⇒ 9
	60	1	0.750	1 → 9 (A)
	61	1	0.600	0 ⇒ 1
	70	1	0.727	1 ⇒ 2
	76	1	0.688	1 → 0 (D)
	*87	1	0.500	1 ⇒ 0 (?)
	*105	1	1.000	1 ⇒ 0
	106	1	0.500	2 ⇒ 9
	109	1	0.750	2 ⇒ 0
	119	1	0.786	0 → 1 (A)
	128	1	0.667	2 ⇒ 1
	130	1	0.571	2 → 0 (A)
	132	1	0.714	1 → 9 (D)
	137	1	0.700	1 → 0 (A)
	141	1	0.692	0 ⇒ 4

Appendix E (continued)

Branch	Character	Steps	CI	Change	
	142	1	0.750	0 → 3	(A)
	144	1	0.600	0 → 1	(D)
	149	1	0.667	2 ⇒ 4	(?)
	150	1	0.600	1 ⇒ 0	
	153	1	0.833	2 → 1	(D)
	172	1	0.625	9 → 0	(A)
	*179	1	0.333	1 → 0	(D)
	192	1	1.000	0 → 1	(A)
	195	1	0.333	1 ⇒ 0	
node 42 → <i>Mirounga leonina</i>	6	1	0.714	1 ⇒ 9	
	9	1	0.583	0 ⇒ 9	
	17	1	0.250	1 ⇒ 0	
	*18	1	0.455	1 ⇒ 0	
	24	1	0.571	1 → 2	(D)
	43	1	0.545	0 ⇒ 1	
	44	1	0.636	1 ⇒ 2	
	49	1	0.588	2 → 1	(D)
	63	1	0.778	0 ⇒ 1	
	66	1	0.667	0 ⇒ 1	
	78	1	0.682	2 → 0	(D)
	*124	1	0.692	9 ⇒ 1	
	*129	1	0.625	0 ⇒ 2	
	165	1	0.500	2 ⇒ 1	
	182	1	0.500	1 → 0	(A)
	192	1	1.000	0 → 1	(D)
<i>Mirounga leonina</i> (within terminal)	*34	1	0.750	2 ⇒ 12	(?)
	42	1	0.800	0 ⇒ 01	(?)
	*57	1	0.667	0 → 01	(A)
	*57	1	0.667	1 → 01	(D)
	58	1	0.625	9 → 09	(A)
	58	1	0.625	0 → 09	(D)
	59	2	0.625	9 ⇒ 019	(?)
	60	1	0.750	9 → 19	(A)
	60	1	0.750	1 → 19	(D)
	74	1	0.625	1 ⇒ 01	(?)
	80	2	0.538	0 ⇒ 012	(?)
	97	1	0.500	1 ⇒ 01	(?)
	104	1	1.000	0 ⇒ 01	(?)
	119	1	0.786	1 → 01	(A)
	119	1	0.786	0 → 01	(D)
	123	1	0.778	2 ⇒ 12	(?)
	137	1	0.700	0 → 01	(A)
	137	1	0.700	1 → 01	(D)
	138	1	0.636	9 ⇒ 09	(?)
	139	1	0.750	9 → 09	(?)
	140	1	0.778	9 ⇒ 09	(?)

Appendix E (continued)

Branch	Character	Steps	CI	Change	
	142	3	0.750	3 → 0234	(A)
	142	3	0.750	0 → 0234	(D)
	151	1	0.500	1 ⇒ 01	(?)
	153	1	0.833	1 ⇒ 01	(?)
	154	1	0.700	0 ⇒ 01	(?)
	*156	1	0.833	1 ⇒ 01	(?)
	157	1	0.765	0 ⇒ 09	(?)
	159	1	0.667	0 ⇒ 01	(F)
	164	1	1.000	0 → 01	(A)
	164	1	1.000	1 → 01	(D)
	170	1	0.636	0 ⇒ 01	(?)
	174	1	0.692	1 ⇒ 01	(?)
	183	1	0.667	2 ⇒ 02	(?)
	187	2	0.913	0 ⇒ 013	(?)
	190	1	0.750	1 → 12	(A)
	190	1	0.750	2 → 12	(D)
node 42 → <i>Mirounga angustirostris</i>	31	1	0.636	2 ⇒ 1	(?)
	39	1	0.667	0 ⇒ 1	
	49	1	0.588	1 → 2	(A)
	*57	1	0.667	1 → 0	(D)
	58	1	0.625	0 → 9	(D)
	60	1	0.750	1 → 9	(D)
	64	1	0.545	0 ⇒ 1	
	67	1	0.778	9 ⇒ 1	
	68	1	0.800	9 ⇒ 2	
	78	1	0.682	0 → 12	(A)
	91	1	0.556	1 ⇒ 2	
	119	1	0.786	0 → 1	(D)
	126	1	0.579	0 ⇒ 9	(F)
	137	1	0.700	1 → 0	(D)
	142	1	0.750	0 → 3	(D)
	148	1	0.500	0 ⇒ 1	
	182	1	0.500	0 → 1	(D)
	190	1	0.750	2 → 1	(D)
<i>Mirounga angustirostris</i> (within terminal)	24	1	0.571	2 → 12	(A)
	24	1	0.571	1 → 12	(D)
	*34	1	0.750	2 ⇒ 02	(?)
	*35	1	0.692	1 ⇒ 01	(?)
	*36	1	0.500	0 ⇒ 01	(?)
	51	1	0.714	2 ⇒ 12	(?)
	52	1	0.692	1 ⇒ 12	(?)
	78	1	0.682	1 → 12	(A)
	78	1	0.682	2 → 12	(D)
	92	1	0.625	0 ⇒ 01	(?)
	98	1	0.857	0 ⇒ 01	(?)
	120	1	0.778	0 ⇒ 01	(?)

Appendix E (continued)

Branch	Character	Steps	CI	Change	
	131	1	0.833	1 \Rightarrow 01	(?)
	136	2	1.000	2 \Rightarrow 123	(?)
	141	1	0.692	4 \Rightarrow 24	(?)
	*156	1	0.833	1 \Rightarrow 01	(?)
	157	1	0.765	0 \Rightarrow 09	(?)
	159	1	0.667	0 \Rightarrow 01	(F)
	164	1	1.000	0 \rightarrow 01	(A)
	164	1	1.000	1 \rightarrow 01	(D)
	165	1	0.500	2 \Rightarrow 02	(?)
	170	1	0.636	0 \Rightarrow 01	(?)
	*171	1	0.429	1 \Rightarrow 01	(?)
	172	1	0.625	0 \Rightarrow 09	(F)
	174	1	0.692	1 \Rightarrow 01	(?)
	184	1	0.750	1 \Rightarrow 01	(?)
node 43 \rightarrow node 41	14	1	0.538	9 \rightarrow 0	(A)
	45	1	0.500	0 \Rightarrow 2	
	51	1	0.714	2 \Rightarrow 1	
	76	1	0.688	0 \rightarrow 2	(A)
	88	1	0.667	9 \Rightarrow 0	
	92	1	0.625	0 \rightarrow 1	(A)
	101	1	0.667	0 \Rightarrow 1	
	112	1	0.692	0 \rightarrow 2	(A)
	*125	1	0.333	0 \rightarrow 1	(A)
	126	1	0.579	0 \Rightarrow 1	(F)
	132	1	0.714	9 \rightarrow 1	(A)
	143	1	0.250	1 \Rightarrow 0	
	144	1	0.600	1 \rightarrow 0	(A)
	151	1	0.500	1 \Rightarrow 0	
	153	1	0.833	1 \rightarrow 0	(A)
	153	1	0.833	2 \rightarrow 0	(D)
	164	1	1.000	1 \rightarrow 0	(D)
	*171	1	0.429	1 \rightarrow 0	(A)
	182	1	0.500	0 \rightarrow 1	(D)
	196	1	0.500	0 \rightarrow 1	(A)
node 41 \rightarrow <i>Hydrurga</i>	44	1	0.636	1 \Rightarrow 2	
	49	1	0.588	1 \rightarrow 2	(A)
	58	1	0.625	0 \Rightarrow 12	(?)
	76	1	0.688	1 \rightarrow 2	(D)
	*77	1	0.833	1 \Rightarrow 0	
	78	1	0.682	0 \rightarrow 9	(A)
	78	1	0.682	2 \rightarrow 9	(D)
	80	1	0.538	0 \Rightarrow 2	
	81	1	0.400	2 \Rightarrow 1	
	82	1	0.500	2 \Rightarrow 0	
	92	1	0.625	1 \rightarrow 2	(A)
	92	1	0.625	0 \rightarrow 2	(D)

Appendix E (continued)

Branch	Character	Steps	CI	Change	
	98	1	0.857	0 \Rightarrow 1	
	106	1	0.500	2 \rightarrow 0	(A)
	112	1	0.692	0 \rightarrow 2	(D)
	123	1	0.778	2 \Rightarrow 01	
	*125	1	0.333	0 \rightarrow 1	(D)
	*129	1	0.625	0 \Rightarrow 2	
	130	1	0.571	0 \rightarrow 2	(D)
	138	1	0.636	9 \Rightarrow 0	
	139	1	0.750	9 \Rightarrow 0	
	140	1	0.778	9 \Rightarrow 1	
	169	1	0.333	1 \Rightarrow 0	
	*171	1	0.429	1 \rightarrow 0	(D)
	172	1	0.625	0 \rightarrow 9	(D)
	177	1	0.400	0 \Rightarrow 1	
	*179	1	0.333	1 \rightarrow 0	(D)
	190	1	0.750	2 \rightarrow 1	(D)
	191	1	0.833	1 \Rightarrow 0	
	196	1	0.500	1 \rightarrow 2	(A)
	196	1	0.500	0 \rightarrow 2	(D)
<i>Hydrurga</i> (within terminal)	20	1	0.733	0 \Rightarrow 01	(?)
	24	1	0.571	1 \Rightarrow 12	(?)
	31	1	0.636	2 \Rightarrow 12	(?)
	*35	1	0.692	1 \Rightarrow 01	(?)
	*37	1	0.833	1 \Rightarrow 01	(?)
	38	2	0.632	1 \Rightarrow 019	(?)
	58	1	0.625	1 \Rightarrow 12	(?)
	61	1	0.600	0 \Rightarrow 01	(?)
	64	1	0.545	0 \Rightarrow 01	(?)
	67	1	0.778	9 \Rightarrow 19	(?)
	68	1	0.800	9 \Rightarrow 29	(?)
	83	1	0.800	0 \Rightarrow 01	(?)
	88	1	0.667	0 \Rightarrow 01	(?)
	123	1	0.778	1 \Rightarrow 01	(?)
	131	1	0.833	1 \Rightarrow 01	(?)
	154	1	0.700	0 \Rightarrow 01	(?)
	155	1	0.889	0 \Rightarrow 01	(?)
	*156	1	0.833	1 \Rightarrow 01	(?)
	157	1	0.765	0 \Rightarrow 09	(?)
	165	1	0.500	2 \Rightarrow 02	(?)
	187	1	0.913	0 \Rightarrow 02	(?)
node 41 \rightarrow node 40	5	1	1.000	0 \Rightarrow 1	
	17	1	0.250	1 \Rightarrow 0	
	*18	1	0.455	1 \Rightarrow 0	
	19	1	0.500	1 \Rightarrow 0	
	20	1	0.733	0 \Rightarrow 9	
	*32	1	0.643	5 \Rightarrow 4	

Appendix E (continued)

Branch	Character	Steps	CI	Change	
	*34	1	0.750	2 \Rightarrow 0	
	49	1	0.588	2 \rightarrow 1	(D)
	59	1	0.625	2 \rightarrow 1	(A)
	70	1	0.727	1 \Rightarrow 0	
	78	1	0.682	2 \rightarrow 0	(D)
	108	1	0.429	0 \Rightarrow 1	
	130	1	0.571	2 \rightarrow 1	(A)
	134	1	0.667	0 \Rightarrow 1	
	141	1	0.692	0 \rightarrow 3	(A)
	159	1	0.667	0 \Rightarrow 1	(F)
	170	1	0.636	0 \Rightarrow 1	
	*179	1	0.333	0 \rightarrow 1	(A)
	190	1	0.750	1 \rightarrow 2	(A)
	196	1	0.500	0 \rightarrow 1	(D)
node 40 \rightarrow <i>Leptonychotes</i>	11	1	0.500	0 \Rightarrow 2	
	24	1	0.571	1 \Rightarrow 0	
	53	1	0.500	0 \Rightarrow 1	
	59	1	0.625	2 \rightarrow 1	(D)
	65	1	0.545	1 \Rightarrow 0	
	69	1	0.167	1 \Rightarrow 0	
	106	1	0.500	0 \rightarrow 12	(D)
	107	1	0.714	0 \Rightarrow 1	
	112	1	0.692	0 \rightarrow 2	(D)
	*125	1	0.333	0 \rightarrow 1	(D)
	130	1	0.571	0 \rightarrow 1	(D)
	137	1	0.700	1 \Rightarrow 0	(?)
	141	1	0.692	0 \rightarrow 3	(D)
	142	1	0.750	0 \Rightarrow 3	
	145	1	0.571	1 \Rightarrow 2	
	160	1	0.667	0 \Rightarrow 1	
	*171	1	0.429	0 \rightarrow 1	(A)
	172	1	0.625	9 \rightarrow 0	(A)
	180	1	0.500	9 \Rightarrow 0	
<i>Leptonychotes</i> (within terminal)	10	1	0.647	2 \Rightarrow 02	(?)
	31	1	0.636	2 \Rightarrow 12	(?)
	*32	1	0.643	4 \Rightarrow 34	(?)
	*35	1	0.692	1 \Rightarrow 01	(?)
	*36	1	0.500	0 \Rightarrow 01	(?)
	42	1	0.800	0 \Rightarrow 01	(?)
	61	1	0.600	0 \Rightarrow 01	(?)
	64	1	0.545	0 \Rightarrow 01	(?)
	72	1	0.667	1 \Rightarrow 01	(?)
	76	1	0.688	2 \rightarrow 12	(A)
	76	1	0.688	1 \rightarrow 12	(D)
	79	1	0.727	0 \Rightarrow 01	(?)
	83	1	0.800	0 \Rightarrow 01	(?)
	88	1	0.667	0 \Rightarrow 01	(?)

Appendix E (continued)

Branch	Character	Steps	CI	Change	
	92	1	0.625	1 → 01	(A)
	92	1	0.625	0 → 01	(D)
	101	1	0.667	1 ⇒ 01	(?)
	106	1	0.500	2 → 12	(A)
	106	1	0.500	1 → 12	(D)
	114	1	0.750	2 ⇒ 12	(?)
	123	2	0.778	2 ⇒ 012	(?)
	128	1	0.667	2 ⇒ 12	(?)
	*129	1	0.625	0 ⇒ 02	(?)
	132	1	0.714	1 ⇒ 19	(?)
	147	1	0.667	0 ⇒ 01	(?)
	150	1	0.600	1 ⇒ 12	(?)
	154	1	0.700	0 ⇒ 01	(?)
	157	1	0.765	0 ⇒ 01	(?)
	174	1	0.692	1 ⇒ 01	(?)
	175	1	0.750	0 ⇒ 01	(?)
	176	1	0.800	1 ⇒ 01	(?)
	177	1	0.400	0 ⇒ 01	(?)
	178	1	0.643	0 ⇒ 01	(?)
	187	1	0.913	0 ⇒ 03	(?)
	190	1	0.750	2 ⇒ 12	(F)
node 40 → node 39	3	1	0.800	1 ⇒ 0	
	38	1	0.632	1 → 0	(A)
	43	1	0.545	0 ⇒ 1	
	52	1	0.692	1 ⇒ 0	
	82	1	0.500	2 → 1	(A)
	112	1	0.692	2 → 0	(A)
	113	1	0.375	2 → 0	(A)
	*125	1	0.333	1 → 0	(A)
	126	1	0.579	1 ⇒ 9	(F)
	140	1	0.778	9 → 0	(A)
	165	1	0.500	2 ⇒ 0	
node 39 → <i>Ommatophoca</i>	6	1	0.714	1 ⇒ 0	
	7	1	0.500	0 ⇒ 9	
	10	1	0.647	2 ⇒ 9	
	12	1	0.333	1 ⇒ 0	
	38	1	0.632	0 → 2	(A)
	38	1	0.632	1 → 2	(D)
	41	1	0.571	1 ⇒ 0	
	45	1	0.500	2 ⇒ 1	
	59	1	0.625	1 → 02	(A)
	62	1	0.556	0 ⇒ 1	
	75	1	0.500	0 ⇒ 1	
	76	1	0.688	2 → 1	(A)
	82	1	0.500	2 → 1	(D)
	106	1	0.500	0 → 2	(D)
	113	1	0.375	2 → 0	(D)

Appendix E (continued)

Branch	Character	Steps	CI	Change	
	130	1	0.571	0 → 1	(D)
	141	1	0.692	3 → 0	(A)
	169	1	0.333	1 ⇒ 0	
	*171	1	0.429	1 → 0	(D)
	172	1	0.625	0 → 9	(D)
	*179	1	0.333	1 ⇒ 0	(?)
	187	1	0.913	0 ⇒ 123	
	196	1	0.500	1 ⇒ 2	(?)
<i>Ommatophoca</i> (within terminal)	19	1	0.500	0 ⇒ 01	(?)
	31	1	0.636	2 ⇒ 12	(?)
	54	1	1.000	0 → 01	(A)
	54	1	1.000	0 → 01	(D)
	58	1	0.625	0 ⇒ 01	(?)
	59	1	0.625	0 → 02	(A)
	59	1	0.625	2 → 02	(D)
	63	1	0.778	0 ⇒ 01	(?)
	70	1	0.727	0 ⇒ 01	(?)
	72	1	0.667	1 ⇒ 01	(?)
	74	1	0.625	1 ⇒ 01	(?)
	88	1	0.667	0 ⇒ 01	(?)
	92	1	0.625	1 → 01	(A)
	92	1	0.625	0 → 01	(D)
	104	1	1.000	0 ⇒ 01	(?)
	109	1	0.750	2 ⇒ 02	(?)
	119	1	0.786	0 ⇒ 01	(?)
	121	1	0.600	2 ⇒ 23	(?)
	123	1	0.778	2 ⇒ 12	(?)
	*124	1	0.692	9 ⇒ 19	(?)
	126	1	0.579	9 ⇒ 09	(?)
	137	1	0.700	1 ⇒ 01	(?)
	138	1	0.636	9 ⇒ 09	(?)
	139	1	0.750	9 ⇒ 19	(?)
	140	1	0.778	0 → 09	(A)
	140	1	0.778	9 → 09	(D)
	149	1	0.667	2 ⇒ 23	(?)
	150	2	0.600	1 ⇒ 012	(?)
	154	1	0.700	0 ⇒ 01	(?)
	*156	1	0.833	1 ⇒ 01	(?)
	157	1	0.765	0 ⇒ 09	(?)
	159	1	0.667	1 ⇒ 01	(?)
	176	1	0.800	1 ⇒ 01	(?)
	183	1	0.667	2 ⇒ 12	(?)
	187	2	0.913	1 ⇒ 123	(?)
	191	1	0.833	1 ⇒ 01	(?)
node 39 → node 38	*32	1	0.643	4 ⇒ 2	
	*36	1	0.500	0 → 1	(A)
	59	1	0.625	2 → 1	(D)

Appendix E (continued)

Branch	Character	Steps	CI	Change
node 38 → <i>Lobodon</i>	67	1	0.778	9 ⇒ 1
	68	1	0.800	9 ⇒ 0
	*71	1	0.571	1 ⇒ 0
	72	1	0.667	1 ⇒ 9
	76	1	0.688	1 → 2 (D)
	79	1	0.727	0 ⇒ 1
	80	1	0.538	0 ⇒ 2
	92	1	0.625	0 → 1 (D)
	106	1	0.500	2 → 0 (A)
	114	1	0.750	2 → 0 (A)
	130	1	0.571	1 → 0 (A)
	142	1	0.750	0 ⇒ 1
	174	1	0.692	1 → 0 (A)
	183	1	0.667	2 ⇒ 0
	14	1	0.538	0 ⇒ 2
	24	1	0.571	1 ⇒ 0
	*36	1	0.500	0 → 1 (D)
	38	1	0.632	1 → 02 (D)
	49	1	0.588	1 ⇒ 2
	50	1	0.400	0 ⇒ 1
	56	1	0.636	1 ⇒ 0
	64	1	0.545	0 ⇒ 1
	65	1	0.545	1 ⇒ 0
	82	1	0.500	1 → 2 (A)
	99	1	0.571	2 ⇒ 1
	*100	1	0.556	4 ⇒ 2
	107	1	0.714	0 ⇒ 1
	113	1	0.375	0 → 2 (A)
	114	1	0.750	0 → 1 (A)
	114	1	0.750	2 → 1 (D)
	*129	1	0.625	0 ⇒ 2
	132	1	0.714	1 ⇒ 0
	137	1	0.700	1 ⇒ 2 (?)
	140	1	0.778	0 → 1 (A)
	140	1	0.778	9 → 1 (D)
	141	1	0.692	3 → 1 (A)
	141	1	0.692	0 → 1 (D)
	148	1	0.500	0 ⇒ 1
	150	1	0.600	1 ⇒ 0
	152	1	0.750	0 ⇒ 1
	*171	1	0.429	0 → 1 (A)
	172	1	0.625	9 → 0 (A)
	176	1	0.800	1 ⇒ 0
	177	1	0.400	0 ⇒ 1
	180	1	0.500	9 ⇒ 1

Appendix E (continued)

Branch	Character	Steps	CI	Change	
<i>Lobodon</i> (within terminal)	3	1	0.800	0 \Rightarrow 01	(?)
	9	1	0.583	0 \Rightarrow 01	(?)
	38	1	0.632	0 \Rightarrow 02	(?)
	39	1	0.667	0 \Rightarrow 01	(?)
	44	1	0.636	1 \Rightarrow 12	(?)
	63	1	0.778	0 \Rightarrow 01	(?)
	92	1	0.625	1 \Rightarrow 12	(?)
	119	1	0.786	0 \Rightarrow 01	(?)
	154	1	0.700	0 \Rightarrow 01	(?)
	164	1	1.000	0 \Rightarrow 01	(?)
	174	1	0.692	0 \rightarrow 01	(A)
	174	1	0.692	1 \rightarrow 01	(D)
	178	1	0.643	0 \Rightarrow 01	(?)
	183	1	0.667	0 \Rightarrow 01	(?)
	187	3	0.913	0 \Rightarrow 0123	(?)
	191	1	0.833	1 \Rightarrow 01	(?)
node 38 \rightarrow node 37	11	1	0.500	0 \rightarrow 2	(A)
	20	1	0.733	9 \rightarrow 0	(A)
	46	1	0.333	0 \rightarrow 1	(A)
	58	1	0.625	0 \rightarrow 1	(A)
	61	1	0.600	0 \rightarrow 1	(A)
	74	1	0.625	1 \Rightarrow 2	
	82	1	0.500	2 \rightarrow 0	(D)
	84	1	0.400	1 \Rightarrow 0	
	88	1	0.667	0 \Rightarrow 2	
	108	1	0.429	1 \rightarrow 0	(A)
	114	1	0.750	2 \rightarrow 0	(D)
	134	1	0.667	1 \Rightarrow 0	
	138	1	0.636	9 \rightarrow 0	(A)
	139	1	0.750	9 \rightarrow 0	(A)
	140	1	0.778	9 \rightarrow 0	(D)
	146	1	0.250	0 \rightarrow 1	(A)
	147	1	0.667	0 \Rightarrow 1	
	149	1	0.667	2 \rightarrow 3	(A)
	*171	1	0.429	1 \rightarrow 0	(D)
	172	1	0.625	0 \rightarrow 9	(D)
node 37 \rightarrow <i>Monachus monachus</i>	174	1	0.692	1 \rightarrow 0	(D)
	194	1	0.333	1 \Rightarrow 0	
	195	1	0.333	1 \Rightarrow 0	
	14	1	0.538	0 \Rightarrow 9	
	20	1	0.733	9 \rightarrow 0	(D)
	*36	1	0.500	0 \rightarrow 1	(D)
	38	1	0.632	0 \rightarrow 1	(A)
	46	1	0.333	0 \rightarrow 1	(D)
	47	1	0.333	0 \Rightarrow 1	
	51	1	0.714	1 \Rightarrow 2	
	52	1	0.692	0 \Rightarrow 2	

Appendix E (continued)

Branch	Character	Steps	CI	Change	
	61	1	0.600	0 → 1	(D)
	68	1	0.800	0 ⇒ 1	
	70	1	0.727	0 ⇒ 1	
	75	1	0.500	0 ⇒ 1	
	101	1	0.667	1 ⇒ 0	
	108	1	0.429	1 → 0	(D)
	113	1	0.375	0 → 1	(A)
	113	1	0.375	2 → 1	(D)
	*125	1	0.333	0 ⇒ 1	
	126	1	0.579	9 ⇒ 1	
	*129	1	0.625	0 ⇒ 1	
	138	1	0.636	9 → 0	(D)
	139	1	0.750	0 → 1	(A)
	139	1	0.750	9 → 1	(D)
	146	1	0.250	0 → 1	(D)
	149	1	0.667	3 → 4	(A)
	149	1	0.667	2 → 4	(D)
	154	1	0.700	0 ⇒ 1	
	180	1	0.500	9 ⇒ 0	
<i>Monachus monachus</i> (within terminal)	3	1	0.800	0 ⇒ 01	(?)
	11	2	0.500	2 → 012	(A)
	11	2	0.500	0 → 012	(D)
	*32	1	0.643	2 ⇒ 25	(?)
	41	1	0.571	1 ⇒ 01	(?)
	42	1	0.800	0 ⇒ 01	(?)
	58	1	0.625	1 → 01	(A)
	58	1	0.625	0 → 01	(D)
	63	1	0.778	0 ⇒ 01	(?)
	78	1	0.682	0 ⇒ 01	(?)
	79	1	0.727	1 ⇒ 01	(?)
	82	1	0.500	1 → 01	(A)
	82	1	0.500	0 → 01	(D)
	94	1	1.000	0 ⇒ 01	(?)
	95	1	0.571	0 ⇒ 01	(?)
	121	1	0.600	2 ⇒ 12	(?)
	123	1	0.778	2 ⇒ 02	(?)
	133	1	1.000	0 ⇒ 01	(?)
	141	1	0.692	3 → 03	(A)
	141	1	0.692	0 → 03	(D)
	142	1	0.750	1 ⇒ 01	(?)
	152	1	0.750	0 ⇒ 01	(?)
	167	1	0.571	0 ⇒ 01	(?)
	168	1	0.571	0 ⇒ 01	(?)
	183	1	0.667	0 ⇒ 01	(?)
	196	1	0.500	1 ⇒ 12	(?)

Appendix E (continued)

Branch	Character	Steps	CI	Change	
node 37 → node 36	4	1	1.000	0 ⇒ 1	
	11	1	0.500	0 → 2	(D)
	*23	1	0.429	1 → 0	(A)
	24	1	0.571	1 ⇒ 9	
	*36	1	0.500	1 → 0	(A)
	69	1	0.167	1 ⇒ 0	
	80	1	0.538	2 ⇒ 1	
	83	1	0.800	0 ⇒ 1	
	92	1	0.625	1 ⇒ 2	(?)
	113	1	0.375	2 → 0	(D)
	116	1	1.000	0 ⇒ 1	
	123	1	0.778	2 ⇒ 1	
	138	1	0.636	0 → 1	(A)
	141	1	0.692	0 → 3	(D)
	149	1	0.667	2 → 3	(D)
	*156	1	0.833	1 ⇒ 0	
	157	1	0.765	0 ⇒ 9	
	170	1	0.636	1 → 0	(A)
	173	1	0.750	2 → 0	(A)
	178	1	0.643	0 → 1	(A)
	*179	1	0.333	1 → 0	(A)
	182	1	0.500	1 ⇒ 0	
	184	1	0.750	1 → 0	
node 36 → <i>Monachus tropicalis</i>	6	1	0.714	1 ⇒ 0	
	15	1	1.000	0 ⇒ 1	
	*37	1	0.833	1 ⇒ 0	
	38	1	0.632	0 → 9	(A)
	38	1	0.632	1 → 9	(D)
	46	1	0.333	0 → 1	(D)
	49	1	0.588	1 ⇒ 0	
	56	1	0.636	1 ⇒ 2	
	58	1	0.625	0 → 1	(D)
	61	1	0.600	1 → 0	(A)
	64	1	0.545	0 ⇒ 1	
	65	1	0.545	1 ⇒ 0	
	67	1	0.778	1 ⇒ 2	
	82	1	0.500	1 → 0	(A)
	108	1	0.429	0 → 1	(A)
	142	1	0.750	1 ⇒ 3	
	146	1	0.250	1 → 0	(A)
	150	1	0.600	1 ⇒ 0	
	165	1	0.500	0 ⇒ 2	
	173	1	0.750	0 → 1	(A)
	173	1	0.750	2 → 1	(D)
	178	1	0.643	0 → 1	(D)
	*179	1	0.333	1 → 0	(D)

Appendix E (continued)

Branch	Character	Steps	CI	Change	
<i>Monachus tropicalis</i> (within terminal)	5	1	1.000	1 \Rightarrow 01	(?)
	20	1	0.733	0 \rightarrow 09	(A)
	20	1	0.733	9 \rightarrow 09	(D)
	*23	1	0.429	0 \rightarrow 01	(A)
	*23	1	0.429	1 \rightarrow 01	(D)
	24	1	0.571	9 \Rightarrow 09	(?)
	42	1	0.800	0 \Rightarrow 01	(?)
	44	2	0.636	1 \Rightarrow 012	(?)
	59	1	0.625	1 \Rightarrow 12	(?)
	62	1	0.556	0 \Rightarrow 01	(?)
	74	1	0.625	2 \Rightarrow 12	(?)
	76	1	0.688	2 \Rightarrow 12	(?)
	*77	1	0.833	1 \Rightarrow 01	(?)
	78	1	0.682	0 \Rightarrow 09	(?)
	84	1	0.400	0 \Rightarrow 01	(?)
	91	1	0.556	1 \Rightarrow 12	(?)
	94	1	1.000	0 \Rightarrow 01	(?)
	*124	1	0.692	9 \Rightarrow 19	(?)
	*125	1	0.333	0 \Rightarrow 01	(?)
	126	2	0.579	9 \Rightarrow 019	(?)
	137	1	0.700	1 \Rightarrow 01	(?)
	138	1	0.636	1 \rightarrow 19	(A)
	138	1	0.636	9 \rightarrow 19	(D)
	139	2	0.750	0 \rightarrow 019	(A)
	139	2	0.750	9 \rightarrow 019	(D)
	140	1	0.778	0 \Rightarrow 09	(?)
	153	1	0.833	0 \Rightarrow 01	(?)
	155	1	0.889	0 \Rightarrow 01	(?)
	164	1	1.000	0 \Rightarrow 01	(?)
	170	1	0.636	0 \rightarrow 01	(A)
	170	1	0.636	1 \rightarrow 01	(D)
	183	1	0.667	0 \Rightarrow 01	(?)
	187	1	0.913	0 \Rightarrow 02	(?)
	192	1	1.000	0 \Rightarrow 01	(?)
node 36 \rightarrow <i>Monachus schauinslandi</i>	14	1	0.538	0 \Rightarrow 1	
	17	1	0.250	0 \Rightarrow 1	
	*18	1	0.455	0 \Rightarrow 1	
	*23	1	0.429	1 \rightarrow 0	(D)
	*32	1	0.643	2 \Rightarrow 4	
	*34	1	0.750	0 \Rightarrow 2	
	38	1	0.632	1 \rightarrow 0	(D)
	41	1	0.571	1 \Rightarrow 0	
	45	1	0.500	2 \Rightarrow 1	
	46	1	0.333	1 \rightarrow 0	(A)
	52	1	0.692	0 \Rightarrow 1	
	*57	1	0.667	1 \Rightarrow 0	
	58	1	0.625	1 \rightarrow 9	(A)

Appendix E (continued)

Branch	Character	Steps	CI	Change	
	58	1	0.625	0 → 9	(D)
	59	1	0.625	1 ⇒ 9	
	60	1	0.750	1 ⇒ 9	
	61	1	0.600	0 → 1	(D)
	68	1	0.800	0 ⇒ 2	
	81	1	0.400	2 ⇒ 1	
	82	1	0.500	0 → 1	(D)
	103	1	1.000	0 ⇒ 1	
	106	1	0.500	0 ⇒ 1	
	108	1	0.429	1 → 0	(D)
	121	1	0.600	2 ⇒ 1	
	138	1	0.636	9 → 1	(D)
	139	1	0.750	9 → 0	(D)
	146	1	0.250	0 → 1	(D)
	170	1	0.636	1 → 0	(D)
	173	1	0.750	2 → 0	(D)
<i>Monachus schauinslandi</i> (within terminal)	5	1	1.000	1 ⇒ 01	(?)
	20	1	0.733	0 → 09	(A)
	20	1	0.733	9 → 09	(D)
	31	1	0.636	2 ⇒ 12	(?)
	*33	2	0.667	0 ⇒ 012	(?)
	*35	1	0.692	1 ⇒ 01	(?)
	44	1	0.636	1 ⇒ 01	(?)
	62	1	0.556	0 ⇒ 01	(?)
	76	1	0.688	2 ⇒ 12	(?)
	*77	1	0.833	1 ⇒ 01	(?)
	78	1	0.682	0 ⇒ 09	(?)
	91	1	0.556	1 ⇒ 12	(?)
	*124	1	0.692	9 ⇒ 09	(?)
	126	1	0.579	9 ⇒ 09	(?)
	132	1	0.714	1 ⇒ 01	(?)
	133	1	1.000	0 ⇒ 01	(?)
	145	1	0.571	1 ⇒ 12	(?)
	175	1	0.750	0 ⇒ 01	(?)
	178	1	0.643	1 → 01	(A)
	178	1	0.643	0 → 01	(D)
	*179	1	0.333	0 → 01	(A)
	*179	1	0.333	1 → 01	(D)
	180	1	0.500	9 ⇒ 09	(?)
	191	1	0.833	1 ⇒ 01	(?)
node 44 → node 35	3	1	0.800	1 ⇒ 0	
	31	1	0.636	2 → 1	(A)
	31	1	0.636	0 → 1	(D)
	*35	1	0.692	9 → 0	(D)
	41	1	0.571	1 → 0	(A)
	42	1	0.800	0 → 1	(A)
	62	1	0.556	0 ⇒ 1	

Appendix E (continued)

Branch	Character	Steps	CI	Change	
	75	1	0.500	0 \Rightarrow 1	
	78	1	0.682	0 \rightarrow 1	(A)
	78	1	0.682	2 \rightarrow 1	(D)
	80	1	0.538	0 \Rightarrow 2	
	84	1	0.400	1 \Rightarrow 0	(?)
	99	1	0.571	2 \rightarrow 0	(A)
	*100	1	0.556	4 \rightarrow 1	(A)
	121	1	0.600	2 \rightarrow 1	(A)
	138	1	0.636	9 \rightarrow 0	(A)
	139	1	0.750	9 \rightarrow 1	(A)
	140	1	0.778	9 \rightarrow 0	(A)
	150	1	0.600	1 \rightarrow 2	(A)
	153	1	0.833	1 \rightarrow 2	(A)
	154	1	0.700	0 \rightarrow 1	(A)
	160	1	0.667	0 \Rightarrow 1	
	161	1	0.333	0 \rightarrow 1	(A)
	162	1	0.600	0 \rightarrow 1	(A)
	166	1	0.500	0 \rightarrow 1	(A)
	170	1	0.636	0 \Rightarrow 2	
	172	1	0.625	9 \Rightarrow 2	
	176	1	0.800	1 \Rightarrow 0	
	178	1	0.643	0 \Rightarrow 1	(F)
	180	1	0.500	9 \rightarrow 2	(A)
	187	1	0.913	0 \rightarrow 3	(A)
	187	1	0.913	9 \rightarrow 3	(D)
	189	1	0.500	0 \rightarrow 1	(A)
node 35 \rightarrow <i>Cystophora</i>	7	1	0.500	0 \Rightarrow 9	
	10	1	0.647	2 \Rightarrow 9	
	12	1	0.333	1 \Rightarrow 0	
	14	1	0.538	0 \rightarrow 29	(D)
	*34	1	0.750	2 \Rightarrow 1	
	42	1	0.800	0 \rightarrow 12	(D)
	52	1	0.692	2 \rightarrow 1	(D)
	56	1	0.636	1 \Rightarrow 2	
	59	1	0.625	2 \Rightarrow 0	
	69	1	0.167	0 \rightarrow 1	(D)
	74	1	0.625	0 \Rightarrow 2	
	88	1	0.667	9 \Rightarrow 12	
	92	1	0.625	0 \Rightarrow 1	
	99	1	0.571	0 \rightarrow 1	(A)
	99	1	0.571	2 \rightarrow 1	(D)
	*100	1	0.556	1 \rightarrow 2	(A)
	*100	1	0.556	4 \rightarrow 2	(D)
	106	1	0.500	0 \rightarrow 2	(D)
	121	1	0.600	2 \rightarrow 1	(D)
	*124	1	0.692	9 \Rightarrow 1	
	127	1	0.667	3 \rightarrow 2	(D)

Appendix E (continued)

Branch	Character	Steps	CI	Change	
<i>Cystophora</i> (within terminal)	128	1	0.667	2 \Rightarrow 1	
	132	1	0.714	1 \rightarrow 9	(D)
	149	1	0.667	2 \Rightarrow 4	(?)
	150	1	0.600	1 \rightarrow 2	(D)
	151	1	0.500	1 \Rightarrow 0	
	14	1	0.538	9 \rightarrow 29	(A)
	14	1	0.538	2 \rightarrow 29	(D)
	*25	1	1.000	0 \Rightarrow 01	(?)
	26	1	0.875	9 \Rightarrow 09	(?)
	42	1	0.800	1 \Rightarrow 12	(?)
	49	2	0.588	1 \rightarrow 012	(A)
	49	2	0.588	2 \rightarrow 012	(D)
	65	1	0.545	1 \Rightarrow 12	(?)
	70	1	0.727	1 \Rightarrow 12	(?)
	88	1	0.667	2 \Rightarrow 12	(?)
	112	1	0.692	0 \Rightarrow 01	(?)
	130	2	0.571	2 \rightarrow 012	(A)
	130	2	0.571	0 \rightarrow 012	(D)
	137	1	0.700	1 \Rightarrow 01	(?)
	138	1	0.636	0 \rightarrow 09	(A)
	138	1	0.636	9 \rightarrow 09	(D)
	139	1	0.750	1 \rightarrow 19	(A)
	139	1	0.750	9 \rightarrow 19	(D)
	140	1	0.778	0 \rightarrow 09	(A)
	140	1	0.778	9 \rightarrow 09	(D)
	144	1	0.600	1 \rightarrow 01	(A)
	144	1	0.600	0 \rightarrow 01	(D)
	154	1	0.700	1 \rightarrow 01	(A)
	154	1	0.700	0 \rightarrow 01	(D)
	163	1	0.667	0 \Rightarrow 01	(?)
	165	1	0.500	2 \Rightarrow 02	(?)
	170	1	0.636	2 \Rightarrow 12	(?)
	172	1	0.625	2 \Rightarrow 12	(?)
	173	1	0.750	2 \Rightarrow 12	(?)
	180	1	0.500	2 \Rightarrow 12	(?)
	184	1	0.750	1 \Rightarrow 01	(?)
node 35 \rightarrow node 34	14	1	0.538	9 \rightarrow 0	(A)
	17	1	0.250	1 \Rightarrow 0	
	*18	1	0.455	1 \Rightarrow 0	
	22	1	0.667	0 \rightarrow 1	(A)
	*23	1	0.429	1 \Rightarrow 0	
	24	1	0.571	1 \Rightarrow 9	
	49	1	0.588	2 \rightarrow 1	(D)
	52	1	0.692	1 \rightarrow 2	(A)
	58	1	0.625	0 \Rightarrow 2	(F)
	64	1	0.545	0 \rightarrow 1	(A)
	69	1	0.167	1 \rightarrow 0	(A)

Appendix E (continued)

Branch	Character	Steps	CI	Change	
	*87	1	0.500	1 \Rightarrow 0	(?)
	91	1	0.556	1 \Rightarrow 2	
	93	1	0.625	0 \Rightarrow 1	(F)
	99	1	0.571	2 \rightarrow 0	(D)
	*100	1	0.556	4 \rightarrow 1	(D)
	106	1	0.500	2 \rightarrow 0	(A)
	127	1	0.667	2 \rightarrow 3	(A)
	130	1	0.571	0 \rightarrow 2	(D)
	132	1	0.714	9 \rightarrow 1	(A)
	139	1	0.750	9 \rightarrow 1	(D)
	140	1	0.778	9 \rightarrow 0	(D)
	141	1	0.692	0 \Rightarrow 1	
	142	1	0.750	0 \Rightarrow 1	
	145	1	0.571	1 \Rightarrow 2	
	154	1	0.700	0 \rightarrow 1	(D)
	157	1	0.765	0 \Rightarrow 2	
	167	1	0.571	0 \Rightarrow 1	
node 34 \rightarrow <i>Halichoerus</i>	8	1	0.333	0 \Rightarrow 1	
	9	1	0.583	0 \Rightarrow 1	
	10	1	0.647	2 \Rightarrow 0	
	14	1	0.538	0 \Rightarrow 1	(?)
	42	1	0.800	1 \rightarrow 0	(A)
	56	1	0.636	1 \Rightarrow 0	
	70	1	0.727	1 \Rightarrow 0	
	76	1	0.688	1 \Rightarrow 2	
	79	1	0.727	1 \Rightarrow 0	
	120	1	0.778	0 \Rightarrow 1	
	121	1	0.600	2 \rightarrow 1	(D)
	*125	1	0.333	0 \Rightarrow 1	
	138	1	0.636	9 \rightarrow 0	(D)
	144	1	0.600	0 \rightarrow 1	(D)
	150	1	0.600	1 \rightarrow 2	(D)
<i>Halichoerus</i> (within terminal)	22	1	0.667	1 \rightarrow 01	(A)
	22	1	0.667	0 \rightarrow 01	(D)
	*34	1	0.750	2 \Rightarrow 12	(?)
	*35	1	0.692	0 \Rightarrow 01	(?)
	*37	1	0.833	1 \Rightarrow 01	(?)
	38	1	0.632	2 \Rightarrow 29	(?)
	41	1	0.571	0 \Rightarrow 01	(?)
	43	1	0.545	0 \Rightarrow 01	(?)
	64	1	0.545	1 \rightarrow 01	(A)
	64	1	0.545	0 \rightarrow 01	(D)
	*71	1	0.571	1 \Rightarrow 01	(?)
	72	1	0.667	1 \Rightarrow 19	(?)
	78	2	0.682	1 \Rightarrow 012	(?)
	107	1	0.714	0 \Rightarrow 01	(?)
	123	2	0.778	2 \Rightarrow 023	(?)

Appendix E (continued)

Branch	Character	Steps	CI	Change	
	126	1	0.579	0 \Rightarrow 02	(?)
	132	1	0.714	1 \Rightarrow 01	(?)
	141	1	0.692	1 \Rightarrow 13	(?)
	142	1	0.750	1 \Rightarrow 13	(?)
	149	1	0.667	2 \Rightarrow 02	(?)
	157	1	0.765	2 \Rightarrow 12	(?)
	182	1	0.500	0 \Rightarrow 01	(?)
	188	1	0.625	3 \Rightarrow 23	(?)
node 34 \rightarrow node 33	11	1	0.500	0 \Rightarrow 2	
	44	1	0.636	1 \Rightarrow 0	
	72	1	0.667	1 \Rightarrow 0	
	121	1	0.600	1 \rightarrow 2	(A)
	138	1	0.636	0 \rightarrow 1	(A)
	138	1	0.636	9 \rightarrow 1	(D)
	143	1	0.250	1 \Rightarrow 0	
	144	1	0.600	1 \rightarrow 0	(A)
	150	1	0.600	2 \rightarrow 1	(A)
	155	1	0.889	0 \rightarrow 1	(A)
	187	1	0.913	3 \Rightarrow 1	
node 33 \rightarrow <i>Phoca largha</i>	38	1	0.632	2 \Rightarrow 1	
	49	1	0.588	1 \Rightarrow 0	
	65	1	0.545	1 \Rightarrow 0	
	168	1	0.571	0 \Rightarrow 1	
	178	1	0.643	1 \Rightarrow 2	
	183	1	0.667	2 \Rightarrow 1	
	184	1	0.750	1 \Rightarrow 0	
<i>Phoca largha</i> (within terminal)	20	1	0.733	0 \Rightarrow 01	(?)
	22	1	0.667	1 \rightarrow 01	(A)
	22	1	0.667	0 \rightarrow 01	(D)
	*34	1	0.750	2 \Rightarrow 02	(?)
	41	1	0.571	0 \Rightarrow 01	(?)
	42	1	0.800	1 \rightarrow 01	(A)
	42	1	0.800	0 \rightarrow 01	(D)
	43	1	0.545	0 \Rightarrow 01	(?)
	52	1	0.692	2 \Rightarrow 12	(?)
	62	1	0.556	1 \Rightarrow 01	(?)
	64	1	0.545	1 \rightarrow 01	(A)
	64	1	0.545	0 \rightarrow 01	(D)
	70	1	0.727	1 \Rightarrow 01	(?)
	76	1	0.688	1 \Rightarrow 12	(?)
	99	1	0.571	0 \Rightarrow 01	(?)
	*100	1	0.556	1 \Rightarrow 12	(?)
	119	1	0.786	0 \Rightarrow 01	(?)
	*124	1	0.692	9 \Rightarrow 19	(?)
	126	1	0.579	0 \Rightarrow 09	(?)
	141	1	0.692	1 \Rightarrow 13	(?)

Appendix E (continued)

Branch	Character	Steps	CI	Change	
node 33 → node 32	145	1	0.571	2 ⇒ 12	(?)
	155	1	0.889	1 → 01	(A)
	155	1	0.889	0 → 01	(D)
	172	1	0.625	2 ⇒ 12	(?)
	42	1	0.800	0 → 1	(D)
	58	1	0.625	2 ⇒ 1	
	64	1	0.545	0 → 1	(D)
	*124	1	0.692	9 ⇒ 0	
	152	1	0.750	0 ⇒ 1	
	155	1	0.889	0 → 1	(D)
	165	1	0.500	2 → 0	(A)
	11	1	0.500	2 ⇒ 01	
node 32 → <i>Phoca vitulina</i>	*35	1	0.692	0 ⇒ 1	
	62	1	0.556	1 ⇒ 0	
	64	1	0.545	1 ⇒ 0	
	65	1	0.545	1 ⇒ 0	
	*71	1	0.571	1 ⇒ 0	
	72	1	0.667	0 ⇒ 9	
	76	1	0.688	1 ⇒ 2	
	80	1	0.538	2 ⇒ 01	
	112	1	0.692	0 ⇒ 2	
	130	1	0.571	2 ⇒ 1	
	146	1	0.250	0 ⇒ 1	
	147	1	0.667	0 ⇒ 1	
<i>Phoca vitulina</i> (within terminal)	165	1	0.500	2 → 0	(D)
	174	1	0.692	1 ⇒ 0	
	11	1	0.500	1 ⇒ 01	(?)
	22	1	0.667	1 → 01	(A)
	22	1	0.667	0 → 01	(D)
	31	1	0.636	1 ⇒ 12	(?)
	*34	1	0.750	2 ⇒ 12	(?)
	42	1	0.800	1 ⇒ 12	(?)
	49	1	0.588	1 ⇒ 01	(?)
	52	1	0.692	2 ⇒ 12	(?)
	56	1	0.636	1 ⇒ 01	(?)
	67	1	0.778	9 ⇒ 19	(?)
	68	2	0.800	9 ⇒ 019	(?)
	78	1	0.682	1 ⇒ 12	(?)
	79	1	0.727	1 ⇒ 01	(?)
	80	1	0.538	1 ⇒ 01	(?)
	*87	1	0.500	0 ⇒ 01	(?)
	88	1	0.667	9 ⇒ 09	(?)
	119	1	0.786	0 ⇒ 01	(?)
	123	1	0.778	2 ⇒ 12	(?)
	*124	1	0.692	0 ⇒ 01	(?)
	136	1	1.000	2 ⇒ 23	(?)
	172	1	0.625	2 ⇒ 12	(?)

Appendix E (continued)

Branch	Character	Steps	CI	Change	
node 32 → <i>Pusa caspica</i>	187	1	0.913	1 ⇒ 01	(?)
	192	1	1.000	0 ⇒ 01	(?)
	9	1	0.583	0 ⇒ 1	
	22	1	0.667	0 → 1	(D)
	43	1	0.545	0 ⇒ 1	
	56	1	0.636	1 ⇒ 2	
	74	1	0.625	0 ⇒ 1	
	78	1	0.682	1 ⇒ 0	
	91	1	0.556	2 ⇒ 0	
	92	1	0.625	0 ⇒ 9	
	93	1	0.625	1 ⇒ 9	
	94	1	1.000	0 ⇒ 9	
	96	1	0.500	0 ⇒ 1	
	*100	1	0.556	1 ⇒ 0	
	121	1	0.600	2 ⇒ 1	
	157	1	0.765	2 ⇒ 1	
	163	1	0.667	0 ⇒ 1	
	165	1	0.500	2 → 0	(D)
	168	1	0.571	0 ⇒ 1	
	188	1	0.625	3 ⇒ 2	
<i>Pusa caspica</i> (within terminal)	14	1	0.538	0 ⇒ 01	(?)
	*37	1	0.833	1 ⇒ 01	(?)
	38	2	0.632	2 ⇒ 129	(?)
	49	1	0.588	1 ⇒ 01	(?)
	59	1	0.625	2 ⇒ 12	(?)
	63	1	0.778	0 ⇒ 01	(?)
	75	1	0.500	1 ⇒ 01	(?)
	107	1	0.714	0 ⇒ 01	(?)
	112	1	0.692	0 ⇒ 02	(?)
	120	1	0.778	0 ⇒ 01	(?)
	*124	1	0.692	0 ⇒ 01	(?)
	131	1	0.833	1 ⇒ 01	(?)
	132	1	0.714	1 ⇒ 01	(?)
	178	1	0.643	1 ⇒ 12	(?)
	184	1	0.750	1 ⇒ 01	(?)
	187	1	0.913	1 ⇒ 12	(?)
node 32 → node 31	10	1	0.647	2 → 1	(A)
	96	1	0.500	0 ⇒ 1	
	107	1	0.714	0 ⇒ 1	
	108	1	0.429	0 → 1	(A)
	123	1	0.778	2 → 1	(A)
	132	1	0.714	1 → 0	(A)
	139	1	0.750	1 → 0	(A)
	155	1	0.889	1 → 0	(A)
	172	1	0.625	2 → 1	(A)
	174	1	0.692	1 ⇒ 0	
	183	1	0.667	2 → 1	(A)

Appendix E (continued)

Branch	Character	Steps	CI	Change	
node 31 → <i>Pusa sibirica</i>	196	1	0.500	0 ⇒ 1	
	10	1	0.647	2 → 1	(D)
	20	1	0.733	0 ⇒ 9	
	22	1	0.667	0 → 1	(D)
	42	1	0.800	1 ⇒ 0	
	56	1	0.636	1 ⇒ 0	
	63	1	0.778	0 ⇒ 1	
	108	1	0.429	0 → 1	(D)
	109	1	0.750	2 ⇒ 0	
	112	1	0.692	0 ⇒ 1	
	121	1	0.600	2 ⇒ 1	
	*124	1	0.692	0 ⇒ 9	
	126	1	0.579	0 ⇒ 9	
	132	1	0.714	1 → 0	(D)
	139	1	0.750	1 → 0	(D)
	141	1	0.692	1 ⇒ 3	
	155	1	0.889	1 → 0	(D)
	165	1	0.500	0 → 12	(A)
	167	1	0.571	1 ⇒ 0	
	172	1	0.625	2 → 1	(D)
	178	1	0.643	1 ⇒ 2	
	180	1	0.500	2 ⇒ 1	
	183	1	0.667	2 → 1	(D)
	184	1	0.750	1 ⇒ 0	
<i>Pusa sibirica</i> (within terminal)	9	1	0.583	0 ⇒ 01	(?)
	*35	1	0.692	0 ⇒ 01	(?)
	43	1	0.545	0 ⇒ 01	(?)
	51	1	0.714	2 ⇒ 12	(?)
	59	1	0.625	2 ⇒ 12	(?)
	67	1	0.778	9 ⇒ 19	(?)
	68	1	0.800	9 ⇒ 09	(?)
	75	1	0.500	1 ⇒ 01	(?)
	78	1	0.682	1 ⇒ 01	(?)
	91	1	0.556	2 ⇒ 02	(?)
	92	1	0.625	0 ⇒ 09	(?)
	93	1	0.625	1 ⇒ 19	(?)
	94	1	1.000	0 ⇒ 09	(?)
	120	1	0.778	0 ⇒ 01	(?)
	123	1	0.778	1 → 12	(A)
	123	1	0.778	2 → 12	(D)
	130	1	0.571	2 ⇒ 12	(?)
	165	1	0.500	1 → 12	(A)
	165	1	0.500	2 → 12	(D)
	187	2	0.913	1 ⇒ 123	(?)
	191	1	0.833	1 ⇒ 01	(?)
	192	1	1.000	0 ⇒ 01	(?)
	193	1	1.000	0 ⇒ 01	(?)

Appendix E (continued)

Branch	Character	Steps	CI	Change	
node 31 → <i>Pusa hispida</i>	97	1	0.500	1 ⇒ 0	
	123	1	0.778	2 → 1	(D)
	145	1	0.571	2 ⇒ 1	
	165	1	0.500	2 → 0	(D)
<i>Pusa hispida</i> (within terminal)	10	2	0.647	1 → 012	(A)
	10	2	0.647	2 → 012	(D)
	14	1	0.538	0 ⇒ 01	(?)
	22	1	0.667	1 → 01	(A)
	22	1	0.667	0 → 01	(D)
	38	1	0.632	2 ⇒ 12	(?)
	43	1	0.545	0 ⇒ 01	(?)
	49	1	0.588	1 ⇒ 01	(?)
	51	1	0.714	2 ⇒ 12	(?)
	59	1	0.625	2 ⇒ 12	(?)
	65	1	0.545	1 ⇒ 01	(?)
	72	1	0.667	0 ⇒ 01	(?)
	76	1	0.688	1 ⇒ 12	(?)
	108	1	0.429	1 → 01	(A)
	108	1	0.429	0 → 01	(D)
	119	1	0.786	0 ⇒ 01	(?)
	132	1	0.714	0 → 01	(A)
	132	1	0.714	1 → 01	(D)
	139	1	0.750	0 → 01	(A)
	139	1	0.750	1 → 01	(D)
	155	1	0.889	0 → 01	(A)
	155	1	0.889	1 → 01	(D)
	163	1	0.667	0 ⇒ 01	(?)
	172	1	0.625	1 → 12	(A)
	172	1	0.625	2 → 12	(D)
	183	1	0.667	1 → 12	(A)
	183	1	0.667	2 → 12	(D)
node 32 → node 30	10	1	0.647	2 → 0	(A)
	20	1	0.733	0 ⇒ 9	
	22	1	0.667	1 → 0	(A)
	*23	1	0.429	0 → 1	(A)
	24	1	0.571	9 → 0	(A)
	*32	1	0.643	5 → 4	(A)
	52	1	0.692	2 → 1	(A)
	59	1	0.625	2 ⇒ 1	
	72	1	0.667	0 ⇒ 1	
	92	1	0.625	0 ⇒ 1	
	*100	1	0.556	1 → 0	(A)
	120	1	0.778	0 → 1	(A)
	138	1	0.636	1 ⇒ 0	
	165	1	0.500	0 → 2	(A)
	187	1	0.913	1 ⇒ 3	
	196	1	0.500	0 ⇒ 1	

Appendix E (continued)

Branch	Character	Steps	CI	Change	
node 30 → <i>Erignathus</i>	9	1	0.583	0 ⇒ 1	
	17	1	0.250	0 ⇒ 1	
	*18	1	0.455	0 ⇒ 1	
	*23	1	0.429	0 → 1	(D)
	24	1	0.571	9 → 0	(D)
	*32	1	0.643	5 → 234	(D)
	*37	1	0.833	1 ⇒ 0	
	38	1	0.632	2 ⇒ 9	
	44	1	0.636	0 ⇒ 2	
	45	1	0.500	0 ⇒ 1	
	50	1	0.400	0 ⇒ 1	
	52	1	0.692	2 → 1	(D)
	53	1	0.500	0 ⇒ 1	
	62	1	0.556	1 ⇒ 2	
	*87	1	0.500	0 ⇒ 1	
	88	1	0.667	9 ⇒ 01	
	91	1	0.556	2 ⇒ 1	
	95	1	0.571	1 ⇒ 9	
	96	1	0.500	0 ⇒ 9	
	*100	1	0.556	1 → 0	(D)
	101	1	0.667	0 ⇒ 1	
	108	1	0.429	0 ⇒ 1	
	*124	1	0.692	0 ⇒ 9	
	126	1	0.579	0 ⇒ 9	
	130	1	0.571	2 ⇒ 0	
	149	1	0.667	2 ⇒ 0	
	151	1	0.500	1 ⇒ 0	
	168	1	0.571	0 ⇒ 1	
	170	1	0.636	2 ⇒ 01	
	*171	1	0.429	1 ⇒ 0	
	172	1	0.625	2 ⇒ 9	
	180	1	0.500	2 ⇒ 0	
	194	1	0.333	1 ⇒ 0	
<i>Erignathus</i> (within terminal)	10	2	0.647	0 → 012	(A)
	10	2	0.647	2 → 012	(D)
	*32	2	0.643	4 ⇒ 234	(?)
	*34	2	0.750	2 ⇒ 012	(?)
	*35	1	0.692	0 ⇒ 01	(?)
	76	1	0.688	1 ⇒ 12	(?)
	78	1	0.682	1 ⇒ 01	(?)
	79	1	0.727	1 ⇒ 12	(?)
	88	1	0.667	1 ⇒ 01	(?)
	112	1	0.692	0 ⇒ 01	(?)
	119	1	0.786	0 ⇒ 01	(?)
	120	1	0.778	1 → 01	(A)
	120	1	0.778	0 → 01	(D)
	122	1	1.000	0 ⇒ 01	(?)

Appendix E (continued)

Branch	Character	Steps	CI	Change	
	132	1	0.714	1 \Rightarrow 01	(?)
	157	1	0.765	2 \Rightarrow 12	(?)
	170	1	0.636	1 \Rightarrow 01	(?)
	174	1	0.692	1 \Rightarrow 01	(?)
	176	1	0.800	0 \Rightarrow 01	(?)
	187	1	0.913	3 \Rightarrow 23	(?)
	192	1	1.000	0 \Rightarrow 01	(?)
node 30 \rightarrow node 29	14	1	0.538	0 \rightarrow 1	(A)
	42	1	0.800	1 \rightarrow 0	(A)
	49	1	0.588	1 \rightarrow 0	(A)
	65	1	0.545	1 \Rightarrow 2	
	78	1	0.682	1 \Rightarrow 2	
	80	1	0.538	2 \rightarrow 0	(A)
	99	1	0.571	0 \Rightarrow 1	
	*100	1	0.556	0 \rightarrow 2	(A)
	*100	1	0.556	1 \rightarrow 2	(D)
	123	1	0.778	2 \Rightarrow 3	
node 29 \rightarrow <i>Pagophilus</i>	10	1	0.647	2 \rightarrow 0	(D)
	14	1	0.538	0 \rightarrow 1	(D)
	*23	1	0.429	1 \rightarrow 0	(A)
	24	1	0.571	0 \rightarrow 9	(A)
	31	1	0.636	1 \Rightarrow 0	
	*32	1	0.643	4 \Rightarrow 0	
	*33	1	0.667	0 \Rightarrow 9	
	*34	1	0.750	2 \Rightarrow 9	
	*35	1	0.692	0 \Rightarrow 9	
	*36	1	0.500	0 \Rightarrow 9	
	43	1	0.545	0 \Rightarrow 9	
	62	1	0.556	1 \Rightarrow 0	
	64	1	0.545	1 \Rightarrow 0	
	69	1	0.167	0 \Rightarrow 1	
	80	1	0.538	2 \rightarrow 0	(D)
	112	1	0.692	0 \Rightarrow 2	
	131	1	0.833	1 \Rightarrow 0	
	145	1	0.571	2 \Rightarrow 1	
	178	1	0.643	1 \Rightarrow 2	
<i>Pagophilus</i> (within terminal)	17	1	0.250	0 \Rightarrow 01	(?)
	*18	1	0.455	0 \Rightarrow 01	(?)
	22	1	0.667	0 \Rightarrow 01	(?)
	42	2	0.800	0 \rightarrow 012	(A)
	42	2	0.800	1 \rightarrow 012	(D)
	49	1	0.588	0 \rightarrow 01	(A)
	49	1	0.588	1 \rightarrow 01	(D)
	51	1	0.714	2 \Rightarrow 12	(?)
	52	1	0.692	1 \rightarrow 12	(A)
	52	1	0.692	2 \rightarrow 12	(D)
	56	1	0.636	1 \Rightarrow 01	(?)

Appendix E (continued)

Branch	Character	Steps	CI	Change	
	58	1	0.625	1 \Rightarrow 12	(?)
	76	1	0.688	1 \Rightarrow 12	(?)
	*87	1	0.500	0 \Rightarrow 01	(?)
	88	1	0.667	9 \Rightarrow 09	(?)
	120	1	0.778	1 \rightarrow 01	(A)
	120	1	0.778	0 \rightarrow 01	(D)
	141	1	0.692	1 \Rightarrow 13	(?)
	163	1	0.667	0 \Rightarrow 01	(?)
	165	1	0.500	2 \Rightarrow 02	(?)
	167	1	0.571	1 \Rightarrow 01	(?)
	168	1	0.571	0 \Rightarrow 01	(?)
	180	1	0.500	2 \Rightarrow 12	(?)
	184	1	0.750	1 \Rightarrow 01	(?)
	187	3	0.913	3 \Rightarrow 0123	(?)
node 29 \rightarrow <i>Histriophoca</i>	*23	1	0.429	0 \rightarrow 1	(D)
	24	1	0.571	9 \rightarrow 0	(D)
	38	1	0.632	2 \Rightarrow 1	
	42	1	0.800	1 \rightarrow 0	(D)
	49	1	0.588	1 \rightarrow 0	(D)
	67	1	0.778	9 \Rightarrow 01	
	68	1	0.800	9 \Rightarrow 0	
	119	1	0.786	0 \Rightarrow 1	
	120	1	0.778	0 \rightarrow 1	(D)
	141	1	0.692	1 \Rightarrow 0	
	188	1	0.625	3 \Rightarrow 2	
<i>Histriophoca</i> (within terminal)	6	1	0.714	0 \Rightarrow 01	(?)
	10	1	0.647	0 \rightarrow 02	(A)
	10	1	0.647	2 \rightarrow 02	(D)
	14	1	0.538	1 \rightarrow 01	(A)
	14	1	0.538	0 \rightarrow 01	(D)
	*32	1	0.643	4 \rightarrow 45	(A)
	*32	1	0.643	5 \rightarrow 45	(D)
	*34	1	0.750	2 \Rightarrow 12	(?)
	52	1	0.692	1 \rightarrow 12	(A)
	52	1	0.692	2 \rightarrow 12	(D)
	56	2	0.636	1 \Rightarrow 012	(?)
	67	1	0.778	1 \Rightarrow 01	(?)
	70	1	0.727	1 \Rightarrow 01	(?)
	76	1	0.688	1 \Rightarrow 12	(?)
	80	2	0.538	0 \rightarrow 012	(A)
	80	2	0.538	2 \rightarrow 012	(D)
	92	1	0.625	1 \Rightarrow 12	(?)
	121	1	0.600	2 \Rightarrow 23	(?)
	130	1	0.571	2 \Rightarrow 12	(?)
	142	1	0.750	1 \Rightarrow 14	(?)
	149	1	0.667	2 \Rightarrow 02	(?)
	155	1	0.889	1 \Rightarrow 01	(?)
	174	1	0.692	1 \Rightarrow 01	(?)

APPENDIX F

Character Diagnostics (unweighted)

The information contained in this appendix applies to the overall (consensus) solution presented in Fig.5B. Note that steps are listed as the number of changes in state for each character (= unweighted steps). Excluded characters are preceded by an asterisk.

Charac. No.	Min. Steps	Tree Steps	Max. Steps	CI	HI	RI	RC
*1	-	-	-	-	-	-	-
*2	-	-	-	-	-	-	-
3	4	5	4	0.800	0.800	0.900	0.720
4	3	3	4	1.000	0.667	1.000	1.000
5	3	3	6	1.000	0.667	1.000	1.000
6	5	7	10	0.714	0.714	0.600	0.429
7	2	4	5	0.500	0.500	0.333	0.167
8	1	3	3	0.333	0.667	0.000	0.000
9	7	12	12	0.583	0.750	0.000	0.000
10	11	17	18	0.647	0.824	0.143	0.092
11	4	8	11	0.500	0.750	0.429	0.214
12	1	3	4	0.333	0.667	0.333	0.111
13	1	1	2	1.000	0.000	1.000	1.000
14	7	13	15	0.538	0.769	0.250	0.135
15	1	1	1	1.000	0.000	0/0	0/0
16	2	3	4	0.667	0.667	0.500	0.333
17	2	8	12	0.250	0.875	0.400	0.100
*18	5	11	14	0.455	0.727	0.333	0.152
19	2	4	13	0.500	0.750	0.818	0.409
20	11	15	20	0.733	0.800	0.556	0.407
21	1	1	2	1.000	0.000	1.000	1.000
22	6	9	9	0.667	0.889	0.000	0.000
*23	3	7	11	0.429	0.857	0.500	0.214
24	8	14	21	0.571	0.786	0.538	0.308
*25	2	2	9	1.000	0.500	1.000	1.000
26	7	8	12	0.875	0.625	0.800	0.700
*27	2	2	7	1.000	0.500	1.000	1.000
28	4	5	8	0.800	0.600	0.750	0.600
29	1	1	1	1.000	0.000	0/0	0/0
30	2	3	5	0.667	0.667	0.667	0.444
31	7	11	17	0.636	0.818	0.600	0.382
*32	9	14	21	0.643	0.714	0.583	0.375
*33	4	6	10	0.667	0.500	0.667	0.444
*34	12	16	24	0.750	0.812	0.667	0.500
*35	9	13	20	0.692	0.846	0.636	0.441
*36	4	8	12	0.500	0.750	0.500	0.250
*37	5	6	6	0.833	0.833	0.000	0.000
38	12	19	21	0.632	0.842	0.222	0.140

Appendix F (continued)

Charac. No.	Min. Steps	Tree Steps	Max. Steps	CI	HI	RI	RC
39	2	3	3	0.667	0.667	0.000	0.000
40	1	2	4	0.500	0.500	0.667	0.333
41	4	7	11	0.571	0.857	0.571	0.327
42	12	15	19	0.800	0.867	0.571	0.457
43	6	11	19	0.545	0.818	0.615	0.336
44	7	11	18	0.636	0.818	0.636	0.405
45	4	8	13	0.500	0.750	0.556	0.278
46	1	3	3	0.333	0.667	0.000	0.000
47	1	3	3	0.333	0.667	0.000	0.000
48	1	2	4	0.500	0.500	0.667	0.333
49	10	17	19	0.588	0.882	0.222	0.131
50	2	5	7	0.400	0.800	0.400	0.160
51	5	7	11	0.714	0.857	0.667	0.476
52	9	13	16	0.692	0.846	0.429	0.297
53	1	2	2	0.500	0.500	0.000	0.000
54	2	2	5	1.000	0.500	1.000	1.000
*55	1	1	8	1.000	0.000	1.000	1.000
56	7	11	18	0.636	0.727	0.636	0.405
*57	2	3	3	0.667	0.667	0.000	0.000
58	10	16	19	0.625	0.812	0.333	0.208
59	10	16	21	0.625	0.812	0.455	0.284
60	3	4	4	0.750	0.500	0.000	0.000
61	3	5	6	0.600	0.800	0.333	0.200
62	5	9	15	0.556	0.778	0.600	0.333
63	7	9	12	0.778	0.889	0.600	0.467
64	6	11	13	0.545	0.909	0.286	0.156
65	6	11	12	0.545	0.818	0.167	0.091
66	2	3	6	0.667	0.667	0.750	0.500
67	7	9	11	0.778	0.667	0.500	0.389
68	8	10	11	0.800	0.700	0.333	0.267
69	1	6	9	0.167	0.833	0.375	0.062
70	8	11	14	0.727	0.818	0.500	0.364
*71	4	7	12	0.571	0.857	0.625	0.357
72	10	15	21	0.667	0.867	0.545	0.364
73	3	4	7	0.750	0.750	0.750	0.562
74	5	8	13	0.625	0.750	0.625	0.391
75	3	6	13	0.500	0.833	0.700	0.350
76	11	16	18	0.688	0.875	0.286	0.196
*77	5	6	6	0.833	0.833	0.000	0.000
78	15	22	26	0.682	0.864	0.364	0.248
79	8	11	13	0.727	0.818	0.400	0.291
80	7	13	19	0.538	0.846	0.500	0.269
81	2	5	7	0.400	0.600	0.400	0.160
82	4	8	10	0.500	0.750	0.333	0.167

Appendix F (continued)

Charac. No.	Min. Steps	Tree Steps	Max. Steps	CI	HI	RI	RC
83	4	5	6	0.800	0.800	0.500	0.400
84	2	5	13	0.400	0.800	0.727	0.291
85	1	1	4	1.000	0.000	1.000	1.000
86	1	2	3	0.500	0.500	0.500	0.250
*87	4	8	13	0.500	0.875	0.556	0.278
88	12	18	24	0.667	0.833	0.500	0.333
89	1	2	3	0.500	0.500	0.500	0.250
*90	-	-	-	-	-	-	-
91	5	9	15	0.556	0.778	0.600	0.333
92	10	16	21	0.625	0.812	0.455	0.284
93	5	8	16	0.625	0.750	0.727	0.455
94	4	4	4	1.000	0.500	0/0	0/0
95	4	7	14	0.571	0.714	0.700	0.400
96	2	4	5	0.500	0.500	0.333	0.167
97	3	6	6	0.500	0.667	0.000	0.000
98	6	7	7	0.857	0.714	0.000	0.000
99	4	7	14	0.571	0.571	0.700	0.400
*100	5	9	14	0.556	0.556	0.556	0.309
101	4	6	9	0.667	0.667	0.600	0.400
102	2	4	5	0.500	0.500	0.333	0.167
103	2	2	2	1.000	0.000	0/0	0/0
104	4	4	4	1.000	0.500	0/0	0/0
*105	1	1	2	1.000	0.000	1.000	1.000
106	4	8	11	0.500	0.625	0.429	0.214
107	5	7	8	0.714	0.857	0.333	0.238
108	3	7	15	0.429	0.714	0.667	0.286
109	3	4	12	0.750	0.500	0.889	0.667
110	1	2	3	0.500	0.500	0.500	0.250
111	1	1	8	1.000	0.000	1.000	1.000
112	9	13	17	0.692	0.846	0.500	0.346
113	3	8	10	0.375	0.750	0.286	0.107
114	3	4	13	0.750	0.500	0.900	0.675
115	1	1	8	1.000	0.000	1.000	1.000
116	1	1	2	1.000	0.000	1.000	1.000
117	1	3	3	0.333	0.667	0.000	0.000
118	1	1	8	1.000	0.000	1.000	1.000
119	11	14	17	0.786	0.857	0.500	0.393
120	7	9	14	0.778	0.778	0.714	0.556
121	6	10	14	0.600	0.700	0.500	0.300
122	3	3	4	1.000	0.667	1.000	1.000
123	14	18	23	0.778	0.833	0.556	0.432
*124	9	13	15	0.692	0.846	0.333	0.231
*125	3	9	10	0.333	0.889	0.143	0.048

Appendix F (continued)

Charac. No.	Min. Steps	Tree Steps	Max. Steps	CI	HI	RI	RC
126	11	19	21	0.579	0.789	0.200	0.116
127	2	3	11	0.667	0.333	0.889	0.593
128	4	6	10	0.667	0.500	0.667	0.444
*129	5	8	11	0.625	0.625	0.500	0.312
130	8	14	19	0.571	0.857	0.455	0.260
131	5	6	6	0.833	0.667	0.000	0.000
132	10	14	19	0.714	0.857	0.556	0.397
133	5	5	5	1.000	0.600	0/0	0/0
134	2	3	4	0.667	0.333	0.500	0.333
135	4	5	5	0.800	0.400	0.000	0.000
136	8	8	9	1.000	0.500	1.000	1.000
137	7	10	15	0.700	0.800	0.625	0.438
138	7	11	17	0.636	0.818	0.600	0.382
139	9	12	19	0.750	0.833	0.700	0.525
140	7	9	16	0.778	0.778	0.778	0.605
141	9	13	24	0.692	0.615	0.733	0.508
142	9	12	21	0.750	0.583	0.750	0.562
143	1	4	7	0.250	0.750	0.500	0.125
144	3	5	7	0.600	0.800	0.500	0.300
145	4	7	17	0.571	0.714	0.769	0.440
146	1	4	9	0.250	0.750	0.625	0.156
147	2	3	5	0.667	0.667	0.667	0.444
148	1	2	2	0.500	0.500	0.000	0.000
149	10	15	18	0.667	0.733	0.375	0.250
150	6	10	11	0.600	0.800	0.200	0.120
151	2	4	10	0.500	0.750	0.750	0.375
152	3	4	10	0.750	0.750	0.857	0.643
153	5	6	13	0.833	0.667	0.875	0.729
154	7	10	15	0.700	0.900	0.625	0.438
155	8	9	11	0.889	0.889	0.667	0.593
*156	5	6	7	0.833	0.833	0.500	0.417
157	13	17	26	0.765	0.824	0.692	0.529
*158	1	1	1	1.000	0.000	0/0	0/0
159	6	9	14	0.667	0.778	0.625	0.417
160	2	3	12	0.667	0.333	0.900	0.600
161	1	3	13	0.333	0.667	0.833	0.278
162	3	5	13	0.600	0.800	0.800	0.480
163	4	6	8	0.667	0.833	0.500	0.333
164	6	6	10	1.000	0.833	1.000	1.000
165	7	14	16	0.500	0.857	0.222	0.111
166	1	2	11	0.500	0.500	0.900	0.450
167	4	7	15	0.571	0.714	0.727	0.416
168	4	7	11	0.571	0.714	0.571	0.327
169	1	3	4	0.333	0.667	0.333	0.111
170	7	11	20	0.636	0.818	0.692	0.441

Appendix F (continued)

Charac. No.	Min. Steps	Tree Steps	Max. Steps	CI	HI	RI	RC
*171	3	7	10	0.429	0.857	0.429	0.184
172	10	16	24	0.625	0.812	0.571	0.357
173	3	4	5	0.750	0.500	0.500	0.375
174	9	13	17	0.692	0.923	0.500	0.346
175	3	4	12	0.750	0.750	0.889	0.667
176	4	5	13	0.800	0.800	0.889	0.711
177	2	5	10	0.400	0.800	0.625	0.250
178	9	14	18	0.643	0.857	0.444	0.286
*179	2	6	7	0.333	0.833	0.200	0.067
180	6	12	17	0.500	0.750	0.455	0.227
181	1	1	8	1.000	0.000	1.000	1.000
182	2	4	7	0.500	0.750	0.600	0.300
183	8	12	19	0.667	0.833	0.636	0.424
184	9	12	13	0.750	0.917	0.250	0.188
*185	1	1	8	1.000	0.000	1.000	1.000
186	1	1	8	1.000	0.000	1.000	1.000
187	21	23	35	0.913	0.826	0.857	0.783
188	5	8	11	0.625	0.625	0.500	0.312
189	2	4	12	0.500	0.750	0.800	0.400
190	6	8	12	0.750	0.750	0.667	0.500
191	5	6	6	0.833	0.833	0.000	0.000
192	6	6	6	1.000	0.833	0/0	0/0
193	1	1	1	1.000	0.000	0/0	0/0
194	1	3	12	0.333	0.667	0.818	0.273
195	1	3	6	0.333	0.667	0.600	0.200
196	3	6	13	0.500	0.667	0.700	0.350

In der Serie BONNER ZOOLOGISCHE MONOGRAPHIEN sind erschienen:

1. Naumann, C.M.: Untersuchungen zur Systematik und Phylogenese der holarktischen Sesiiden (Insecta, Lepidoptera), 1971, 190 S., DM 48,—
2. Ziswiler, V., H.R. Güttinger & H. Bregulla: Monographie der Gattung *Erythrura* Swainson, 1837 (Aves, Passeres, Estrildidae). 1972, 158 S., 2 Tafeln, DM 40,—
3. Eisentraut, M.: Die Wirbeltierfauna von Fernando Poo und Westkamerun. Unter besonderer Berücksichtigung der Bedeutung der pleistozänen Klimaschwankungen für die heutige Faunenverteilung. 1973, 428 S., 5 Tafeln, DM 106,—
4. Herrlinger, E.: Die Wiedereinbürgerung des Uhus *Bubo bubo* in der Bundesrepublik Deutschland. 1973, 151 S., DM 38,—
5. Ulrich, H.: Das Hypopygium der Dolichopodiden (Diptera): Homologie und Grundplanmerkmale. 1974, 60 S., DM 15,—
6. Jost, O.: Zur Ökologie der Wasseramsel (*Cinclus cinclus*) mit besonderer Berücksichtigung ihrer Ernährung. 1975, 183 S., DM 46,—
7. Haffer, J.: Avifauna of northwestern Colombia, South America. 1975, 182 S., DM 46,—
8. Eisentraut, M.: Das Gaumenfaltenmuster der Säugetiere und seine Bedeutung für stammesgeschichtliche und taxonomische Untersuchungen. 1976, 214 S., DM 54,—
9. Rath, P., & E. Kulzer: Physiology of hibernation and related lethargic states in mammals and birds. 1976, 93 S., 1 Tafel, DM 23,—
10. Haffer, J.: Secondary contact zones of birds in northern Iran. 1977, 64 S., 1 Falttafel, DM 16,—
11. Guibé, J.: Les batraciens de Madagascar. 1978, 144 S., 82 Tafeln, DM 36,—
12. Thaler, E.: Das Aktionssystem von Winter- und Sommergoldhähnchen (*Regulus regulus*, *R. ignicapillus*) und deren ethologische Differenzierung. 1979, 151 S., DM 38,—
13. Homberger, D.G.: Funktionell-morphologische Untersuchungen zur Radiation der Ernährungs- und Trinkmethoden der Papageien (Psittaci). 1980, 192 S., DM 48,—
14. Kullander, S.O.: A taxonomical study of the genus *Apistogramma* Regan, with a revision of Brazilian and Peruvian species (Teleostei: Percoidei: Cichlidae). 1980, 152 S., DM 38,—
15. Scherzinger, W.: Zur Ethologie der Fortpflanzung und Jugendentwicklung des Habichtskauzes (*Strix uralensis*) mit Vergleichen zum Waldkauz (*Strix aluco*). 1980, 66 S., DM 17,—
16. Salvador, A.: A revision of the lizards of the genus *Acanthodactylus* (Sauria: Lacertidae). 1982, 167 S., DM 42,—
17. Marsch, E.: Experimentelle Analyse des Verhaltens von *Scarabaeus sacer* L. beim Nahrungserwerb. 1982, 79 S., DM 20,—
18. Hutterer, R., & D.C.D. Happold: The shrews of Nigeria (Mammalia: Soricidae). 1983, 79 S., DM 20,—
19. Rheinwald, G. (Hrsg.): Die Wirbeltiersammlungen des Museums Alexander Koenig. 1984, 239 S., DM 60,—
20. Nilson, G., & C. Andrén: The Mountain Vipers of the Middle East — the *Vipera xanthina* complex (Reptilia, Viperidae). 1986, 90 S., DM 23,—
21. Kumerloeve, H.: Bibliographie der Säugetiere und Vögel der Türkei. 1986, 132 S., DM 33,—
22. Klaver, C., & W. Böhme: Phylogeny and Classification of the Chamaeleonidae (Sauria) with Special Reference to Hemipenis Morphology. 1986, 64 S., DM 16,—

23. Bublitz, J.: Untersuchungen zur Systematik der rezenten Caenolestidae Trouessart, 1898 — unter Verwendung craniometrischer Methoden. 1987, 96 S., DM 24,—
24. Arratia, G.: Description of the primitive family Diplomystidae (Siluriformes, Teleostei, Pisces): Morphology, taxonomy and phylogenetic implications. 1987, 120 S., DM 30,—
25. Nikolaus, G.: Distribution atlas of Sudan's birds with notes on habitat and status. 1987, 322 S., DM 81,—
26. Löhrl, H.: Etho-ökologische Untersuchungen an verschiedenen Kleiberarten (Sitidae) — eine vergleichende Zusammenstellung. 1988, 208 S., DM 52,—
27. Böhme, W.: Zur Genitalmorphologie der Sauria: Funktionelle und stammesgeschichtliche Aspekte. 1988, 175 S., DM 44,—
28. Lang, M.: Phylogenetic and biogeographic patterns of Basiliscine Iguanians (Reptilia: Squamata: "Iguanidae"). 1989, 172 S., DM 43,—
29. Hoi-Leitner, M.: Zur Veränderung der Säugetierfauna des Neusiedlersee-Gebietes im Verlauf der letzten drei Jahrzehnte. 1989, 104 S., DM 26,—
30. Bauer, A. M.: Phylogenetic systematics and Biogeography of the Carphodactylini (Reptilia: Gekkonidae). 1990, 220 S., DM 55,—
31. Fiedler, K.: Systematic, evolutionary, and ecological implications of myrmecophily within the Lycaenidae (Insecta: Lepidoptera: Papilionoidea). 1991, 210 S., DM 53,—
32. Arratia, G.: Development and variation of the suspensorium of primitive Catfishes (Teleostei: Ostariophysi) and their phylogenetic relationships. 1992, 148 S., DM 37,—
33. Kotrba, M.: Das Reproduktionssystem von *Cyrtodiopsis whitei* Curran (Diptera, Diptera) unter besonderer Berücksichtigung der inneren weiblichen Geschlechtsorgane: 1993, 115 S., DM 32,—
34. Blaschke-Berthold, U.: Anatomie und Phylogenie der Bibionomorpha (Insecta, Diptera). 1993, 206 S., DM 52,—
35. Hallermann, J.: Zur Morphologie der Ethmoidalregion der Iguania (Squamata) — eine vergleichend-anatomische Untersuchung. 1994, 133 S., DM 33,—
36. Arratia, G., & L. Huaquin: Morphology of the lateral line system and of the skin of Diplomystid and certain primitive Loricarioid Catfishes and systematic and ecological considerations. 1995, 110 S., DM 28,—
37. Hille, A.: Enzymelektrophoretische Untersuchung zur genetischen Populationsstruktur und geographischen Variation im *Zygaena-transalpina*-Superspezies-Komplex (Insecta, Lepidoptera, Zygaenidae). 1995, 224 S., DM 56,—
38. Martens, J., & S. Eck: Towards an Ornithology of the Himalayas: Systematics, ecology and vocalizations of Nepal birds. 1995, 448 S., 3 Farbtafeln, DM 112,—
39. Chen, X.: Morphology, phylogeny, biogeography and systematics of *Phoxinus* (Pisces: Cyprinidae). 1996, 227 S., DM 57,—
40. Browne, D. J., & C. H. Scholtz: The morphology of the hind wing articulation and wing base of the Scarabaeoidea (Coleoptera) with some phylogenetic implications. 1996, 200 S., DM 50,—
41. Bininda-Emonds, O. R. P., & A. P. Russell: A morphological perspective on the phylogenetic relationships of the extant phocid seals (Mammalia: Carnivora: Phocidae). 1996, 256 S., DM 64,—

Seit Nr. 30 werden die Monographien ausschließlich über die Konvertierung von Disketten-texten hergestellt. Dies ergibt neben einer Kosten- und Zeitersparnis auch eine deutlich geringere Fehlerquote im Endprodukt. Dazu müssen einige Voraussetzungen erfüllt sein: IBM-kompatibel, Betriebssystem MS-DOS, 3,5- oder 5,25-Zoll-Diskette, „endlos“ beschrieben, ASCII oder wordperfect. Wer sich für Einzelheiten interessiert, wende sich bitte an den Schriftleiter.

Wegen der Gestaltung der Manuskripte, insbesondere des Literaturverzeichnisses, werden die Autoren auf die letzten erschienenen Monographien verwiesen.



HECKMAN
BINDERY, INC.
Bound-To-Please®

MAY 00

N. MANCHESTER, INDIANA 46962

SMITHSONIAN INSTITUTION LIBRARIES



3 9088 01206 9894